Reza N. Jazar

# Vehicle Dynamics

## Theory and Application

# Vehicle Dynamics:
# Theory and Application

Reza N. Jazar

Vehicle Dynamics:
Theory and Applications

Reza N. Jazar
Dept. of Mechanical Engineering
Manhattan College
Riverdale, NY  10471

Printed on acid-free paper.

9  8  7  6  5  4  3  2  1

springer.com

Dedicated to
my son, *Kavosh,*
my daughter, *Vazan,*
and my wife, *Mojgan.*

Happiness is when you win a race against yourself.

# Preface

This text is for engineering students. It introduces the fundamental knowledge used in *vehicle dynamics*. This knowledge can be utilized to develop computer programs for analyzing the ride, handling, and optimization of road vehicles.

Vehicle dynamics has been in the engineering curriculum for more than a hundred years. Books on the subject are available, but most of them are written for specialists and are not suitable for a classroom application. A new student, engineer, or researcher would not know where and how to start learning vehicle dynamics. So, there is a need for a textbook for beginners. This textbook presents the fundamentals with a perspective on future trends.

The study of classical vehicle dynamics has its roots in the work of great scientists of the past four centuries and creative engineers in the past century who established the methodology of dynamic systems. The development of vehicle dynamics has moved toward modeling, analysis, and optimization of multi-body dynamics supported by some compliant members. Therefore, merging dynamics with optimization theory was an expected development. The fast-growing capability of accurate positioning, sensing, and calculations, along with intelligent computer programming are the other important developments in vehicle dynamics. So, a textbook help the reader to make a computer model of vehicles, which this book does.

### Level of the Book

This book has evolved from nearly a decade of research in nonlinear dynamic systems and teaching courses in vehicle dynamics. It is addressed primarily to the last year of undergraduate study and the first year graduate student in engineering. Hence, it is an intermediate textbook. It provides both fundamental and advanced topics. The whole book can be covered in two successive courses, however, it is possible to jump over some sections and cover the book in one course. Students are required to know the fundamentals of kinematics and dynamics, as well as a basic knowledge of numerical methods.

The contents of the book have been kept at a fairly theoretical-practical level. Many concepts are deeply explained and their application emphasized, and most of the related theories and formal proofs have been explained. The book places a strong emphasis on the physical meaning and applications of the concepts. Topics that have been selected are of high interest in the field. An attempt has been made to expose students to a

broad range of topics and approaches.

There are four special chapters that are indirectly related to vehicle dynamics: *Applied Kinematics*, *Applied Mechanisms*, *Applied Dynamics*, and *Applied Vibrations*. These chapters provide the related background to understand vehicle dynamics and its subsystems.

### Organization of the Book

The text is organized so it can be used for teaching or for self-study. Chapter 1 "Fundamentals," contains general preliminaries about tire and rim with a brief review of road vehicle classifications.

Part *I* "One Dimensional Vehicle Dynamics," presents forward vehicle dynamics, tire dynamics, and driveline dynamics. Forward dynamics refers to weight transfer, accelerating, braking, engine performance, and gear ratio design.

Part *II* "Vehicle Kinematics," presents a detailed discussion of vehicle mechanical subsystems such as steering and suspensions.

Part *III* "Vehicle Dynamics," employs Newton and Lagrange methods to develop the maneuvering dynamics of vehicles.

Part *IV* "Vehicle Vibrations," presents a detailed discussion of vehicle vibrations. An attempt is made to review the basic approaches and demonstrate how a vehicle can be modeled as a vibrating multiple degree-of-freedom system. The concepts of the Newton-Euler dynamics and Lagrangian method are used equally for derivation of equations of motion. The RMS optimization technique for suspension design of vehicles is introduced and applied to vehicle suspensions. The outcome of the optimization technique is the optimal stiffness and damping for a car or suspended equipment.

### Method of Presentation

This book uses a "*fact-reason-application*" structure. The "fact" is the main subject we introduce in each section. Then the reason is given as a "proof." The application of the fact is examined in some "examples." The "examples" are a very important part of the book because they show how to implement the "facts." They also cover some other facts that are needed to expand the subject.

### Prerequisites

Since the book is written for senior undergraduate and first-year graduate-level students of engineering, the assumption is that users are familiar with matrix algebra as well as basic dynamics. Prerequisites are the fundamentals of kinematics, dynamics, vector analysis, and matrix theory. These basics are usually taught in the first three undergraduate years.

### Unit System

The system of units adopted in this book is, unless otherwise stated, the international system of units (SI). The units of degree (deg) or radian ( rad) are utilized for variables representing angular quantities.

### Symbols

- Lowercase bold letters indicate a vector. Vectors may be expressed in an $n$ dimensional Euclidian space. Example:

$$\mathbf{r} \quad , \quad \mathbf{s} \quad , \quad \mathbf{d} \quad , \quad \mathbf{a} \quad , \quad \mathbf{b} \quad , \quad \mathbf{c}$$
$$\mathbf{p} \quad , \quad \mathbf{q} \quad , \quad \mathbf{v} \quad , \quad \mathbf{w} \quad , \quad \mathbf{y} \quad , \quad \mathbf{z}$$
$$\boldsymbol{\omega} \quad , \quad \boldsymbol{\alpha} \quad , \quad \boldsymbol{\epsilon} \quad , \quad \boldsymbol{\theta} \quad , \quad \boldsymbol{\delta} \quad , \quad \boldsymbol{\phi}$$

- Uppercase bold letters indicate a dynamic vector or a dynamic matrix, such as force and moment. Example:

$$\mathbf{F} \quad , \quad \mathbf{M}$$

- Lowercase letters with a hat indicate a unit vector. Unit vectors are not bolded. Example:

$$\hat{i} \quad , \quad \hat{j} \quad , \quad \hat{k} \quad , \quad \hat{e} \quad , \quad \hat{u} \quad , \quad \hat{n}$$
$$\hat{I} \quad , \quad \hat{J} \quad , \quad \hat{K} \quad , \quad \hat{e}_\theta \quad , \quad \hat{e}_\varphi \quad , \quad \hat{e}_\psi$$

- Lowercase letters with a tilde indicate a $3 \times 3$ skew symmetric matrix associated to a vector. Example:

$$\tilde{a} = \begin{bmatrix} 0 & -a_3 & a_2 \\ a_3 & 0 & -a_1 \\ -a_2 & a_1 & 0 \end{bmatrix} \quad , \quad \mathbf{a} = \begin{bmatrix} a_1 \\ a_2 \\ a_3 \end{bmatrix}$$

- An arrow above two uppercase letters indicates the start and end points of a position vector. Example:

$$\overrightarrow{ON} = \text{a position vector from point } O \text{ to point } N$$

- The length of a vector is indicated by a non-bold lowercase letter. Example:

$$r = |\mathbf{r}| \quad , \quad a = |\mathbf{a}| \quad , \quad b = |\mathbf{b}| \quad , \quad s = |\mathbf{s}|$$

- Capital letter $B$ is utilized to denote a body coordinate frame. Example:

$$B(oxyz) \quad , \quad B(Oxyz) \quad , \quad B_1(o_1x_1y_1z_1)$$

- Capital letter $G$ is utilized to denote a global, inertial, or fixed coordinate frame. Example:

$$G \quad , \quad G(XYZ) \quad , \quad G(OXYZ)$$

- Right subscript on a transformation matrix indicates the *departure* frames. Example:

$$R_B = \text{transformation matrix from frame } B(oxyz)$$

- Left superscript on a transformation matrix indicates the *destination* frame. Example:

$$
\begin{aligned}
{}^G R_B &= \text{transformation matrix from frame } B(oxyz) \\
&\quad \text{to frame } G(OXYZ)
\end{aligned}
$$

- Capital letter $R$ indicates rotation or a transformation matrix, if it shows the beginning and destination coordinate frames. Example:

$${}^G R_B = \begin{bmatrix} \cos\alpha & -\sin\alpha & 0 \\ \sin\alpha & \cos\alpha & 0 \\ 0 & 0 & 1 \end{bmatrix}$$

- Whenever there is no sub or superscript, the matrices are shown in a bracket. Example:

$$[T] = \begin{bmatrix} \cos\alpha & -\sin\alpha & 0 \\ \sin\alpha & \cos\alpha & 0 \\ 0 & 0 & 1 \end{bmatrix}$$

- Left superscript on a vector denotes the frame in which the vector is expressed. That superscript indicates the frame that the vector belongs to; so the vector is expressed using the unit vectors of that frame. Example:

$${}^G \mathbf{r} = \text{position vector expressed in frame } G(OXYZ)$$

- Right subscript on a vector denotes the tip point that the vector is referred to. Example:

$$
\begin{aligned}
{}^G \mathbf{r}_P &= \text{position vector of point } P \\
&\quad \text{expressed in coordinate frame } G(OXYZ)
\end{aligned}
$$

- Right subscript on an angular velocity vector indicates the frame that the angular vector is referred to. Example:

$$\boldsymbol{\omega}_B = \text{angular velocity of the body coordinate frame } B(oxyz)$$

- Left subscript on an angular velocity vector indicates the frame that the angular vector is measured with respect to. Example:

$$_G\boldsymbol{\omega}_B \quad = \quad \text{angular velocity of the body coordinate frame } B(oxyz)$$
$$\text{with respect to the global coordinate frame } G(OXYZ)$$

- Left superscript on an angular velocity vector denotes the frame in which the angular velocity is expressed. Example:

$$_G^{B_2}\boldsymbol{\omega}_{B_1} \quad = \quad \text{angular velocity of the body coordinate frame } B_1$$
$$\text{with respect to the global coordinate frame } G,$$
$$\text{and expressed in body coordinate frame } B_2$$

Whenever the subscript and superscript of an angular velocity are the same, we usually drop the left superscript. Example:

$$_G\boldsymbol{\omega}_B \equiv {}_G^G\boldsymbol{\omega}_B$$

Also for position, velocity, and acceleration vectors, we drop the left subscripts if it is the same as the left superscript. Example:

$$_B^B\mathbf{v}_P \equiv {}^B\mathbf{v}_P$$

- Left superscript on derivative operators indicates the frame in which the derivative of a variable is taken. Example:

$$\frac{^Gd}{dt}x \quad , \quad \frac{^Gd}{dt}{}^B\mathbf{r}_P \quad , \quad \frac{^Bd}{dt}{}_B^G\mathbf{r}_P$$

If the variable is a vector function, and also the frame in which the vector is defined is the same frame in which a time derivative is taken, we may use the following short notation,

$$\frac{^Gd}{dt}{}^G\mathbf{r}_P = {}^G\dot{\mathbf{r}}_P \quad , \quad \frac{^Bd}{dt}{}_o^B\mathbf{r}_P = {}_o^B\dot{\mathbf{r}}_P$$

and write equations simpler. Example:

$$^G\mathbf{v} = \frac{^Gd}{dt}{}^G\mathbf{r}(t) = {}^G\dot{\mathbf{r}}$$

- If followed by angles, lowercase $c$ and $s$ denote $cos$ and $sin$ functions in mathematical equations. Example:

$$c\alpha = \cos\alpha \quad , \quad s\varphi = \sin\varphi$$

- Capital bold letter **I** indicates a unit matrix, which, depending on the dimension of the matrix equation, could be a $3 \times 3$ or a $4 \times 4$ unit matrix. $\mathbf{I}_3$ or $\mathbf{I}_4$ are also being used to clarify the dimension of **I**. Example:

$$\mathbf{I} = \mathbf{I}_3 = \begin{bmatrix} 1 & 0 & 0 \\ 0 & 1 & 0 \\ 0 & 0 & 1 \end{bmatrix}$$

- An asterisk ★ indicates a more advanced subject or example that is not designed for undergraduate teaching and can be dropped in the first reading.

# Contents

# 1

# Tire and Rim Fundamentals

We introduce and review some topics about tires, wheels, roads, vehicles, and their interactions. These subjects are needed to understand vehicle dynamics better.

## 1.1   Tires and Sidewall Information

Pneumatic tires are the only means to transfer forces between the road and the vehicle. Tires are required to produce the forces necessary to control the vehicle, and hence, they are an important component of a vehicle.

Figure 1.1 illustrates a cross section view of a tire on a rim to show the dimension parameters that are used to standard tires.



FIGURE 1.1. Cross section of a tire on a rim to show tire height and width.

The *section height*, *tire height*, or simply *height*, $h_T$, is a number that must be added to the rim radius to make the wheel radius. The *section width*, or *tire width*, $w_T$, is the widest dimension of a tire when the tire is not loaded.

Tires are required to have certain information printed on the tire *sidewall*. Figure 1.2 illustrates a side view of a sample tire to show the important information printed on a tire sidewall.

# 1

# Tire and Rim Fundamentals

We introduce and review some topics about tires, wheels, roads, vehicles, and their interactions. These subjects are needed to understand vehicle dynamics better.

## 1.1 Tires and Sidewall Information

Pneumatic tires are the only means to transfer forces between the road and the vehicle. Tires are required to produce the forces necessary to control the vehicle, and hence, they are an important component of a vehicle.

Figure 1.1 illustrates a cross section view of a tire on a rim to show the dimension parameters that are used to standard tires.



FIGURE 1.1. Cross section of a tire on a rim to show tire height and width.

The *section height*, *tire height*, or simply *height*, $h_T$, is a number that must be added to the rim radius to make the wheel radius. The *section width*, or *tire width*, $w_T$, is the widest dimension of a tire when the tire is not loaded.

Tires are required to have certain information printed on the tire *sidewall*. Figure 1.2 illustrates a side view of a sample tire to show the important information printed on a tire sidewall.

FIGURE 1.2. Side view of a tire and the most important information printed on a tire sidewall.

The codes in Figure 1.2 are:

| 1 | Size number. |
| 2 | Maximum allowed inflation pressure. |
| 3 | Type of tire construction. |
| 4 | M&S denotes a tire for mud and snow. |
| 5 | E-Mark is the Europe type approval mark and number. |
| 6 | US Department of Transport (DOT) identification numbers. |
| 7 | Country of manufacture. |
| 8 | Manufacturers, brand name, or commercial name. |

The most important information on the sidewall of a tire is the *size number*, indicated by [ 1 ]. To see the format of the size number, an example is shown in Figure 1.3 and their definitions are explained as follows.

[ P ] *Tire type.* The first letter indicates the proper type of car that the tire is made for. [ P ] stands for passenger car. The first letter can also be [ ST ] for special trailer, [ T ] for temporary, and [ LT ] for light truck.

[ 215 ] *Tire width.* This three-number code is the width of the unloaded tire from sidewall to sidewall measured in [ mm ].

## P  215 / 60 R 15  96 H

| P | Passenger car |
| 215 | Tire width [mm] |
| 60 | Aspect ratio [%] |
| R | Radial |
| 15 | Rim diameter [in] |
| 96 | Load rating |
| H | Speed rating |

FIGURE 1.3. A sample of a tire size number and its meaning.

$\boxed{60}$ *Aspect ratio.* This two-number code is the ratio of the tire section height to tire width, expressed as a percentage. Aspect ratio is shown by $s_T$.

$$s_T = \frac{h_T}{w_T} \times 100 \tag{1.1}$$

Generally speaking, tire aspect ratios range from 35, for race car tires, to 75 for tires used on utility vehicles.

$\boxed{R}$ *Tire construction type.* The letter $\boxed{R}$ indicates that the tire has a radial construction. It may also be $\boxed{B}$ for bias belt or bias ply, and $\boxed{D}$ for diagonal.

$\boxed{15}$ *Rim diameter.* This is a number in [ in] to indicate diameter of the rim that the tire is designed to fit on.

$\boxed{96}$ *Load rate or load index.* Many tires come with a service description at the end of the tire size. The service description is made of a two-digit number (load index) and a letter (speed rating). The load index is a representation of the maximum load each tire is designed to support.

Table 1.1 shows some of the most common load indices and their load-carrying capacities. The load index is generally valid for speeds under $210 \, \mathrm{km/ \, h} \; (\approx 130 \, \mathrm{mi/ \, h})$.

$\boxed{H}$ *Speed rate.* Speed rate indicates the maximum speed that the tire can sustain for a ten minute endurance without breaking down.

Table 1.2 shows the most common speed rate indices and their meanings.

**Example 1** *Weight of a car and load index of its tire.*

*For a car that weighs $2 \, tons = 2000 \, \mathrm{kg}$, we need a tire with a load index higher than 84. This is because we have about $500 \, \mathrm{kg}$ per tire and it is in a load index of 84.*

Table 1.1 - Maximum load-carrying capacity tire index.

| Index | Maximum load | Index | Maximum load |
|-------|--------------|-------|--------------|
| 0 | $45\,\text{kg} \approx 99\,\text{lbf}$ | | |
| $\cdots$ | $\cdots$ | 100 | $800\,\text{kg} \approx 1764\,\text{lbf}$ |
| 71 | $345\,\text{kg} \approx 761\,\text{lbf}$ | 101 | $825\,\text{kg} \approx 1819\,\text{lbf}$ |
| 72 | $355\,\text{kg} \approx 783\,\text{lbf}$ | 102 | $850\,\text{kg} \approx 1874\,\text{lbf}$ |
| 73 | $365\,\text{kg} \approx 805\,\text{lbf}$ | 103 | $875\,\text{kg} \approx 1929\,\text{lbf}$ |
| 74 | $375\,\text{kg} \approx 827\,\text{lbf}$ | 104 | $900\,\text{kg} \approx 1984\,\text{lbf}$ |
| 75 | $387\,\text{kg} \approx 853\,\text{lbf}$ | 105 | $925\,\text{kg} \approx 2039\,\text{lbf}$ |
| 76 | $400\,\text{kg} \approx 882\,\text{lbf}$ | 106 | $950\,\text{kg} \approx 2094\,\text{lbf}$ |
| 77 | $412\,\text{kg} \approx 908\,\text{lbf}$ | 107 | $975\,\text{kg} \approx 2149\,\text{lbf}$ |
| 78 | $425\,\text{kg} \approx 937\,\text{lbf}$ | 108 | $1000\,\text{kg} \approx 2205\,\text{lbf}$ |
| 79 | $437\,\text{kg} \approx 963\,\text{lbf}$ | 109 | $1030\,\text{kg} \approx 2271\,\text{lbf}$ |
| 80 | $450\,\text{kg} \approx 992\,\text{lbf}$ | 110 | $1060\,\text{kg} \approx 2337\,\text{lbf}$ |
| 81 | $462\,\text{kg} \approx 1019\,\text{lbf}$ | 111 | $1090\,\text{kg} \approx 2403\,\text{lbf}$ |
| 82 | $475\,\text{kg} \approx 1047\,\text{lbf}$ | 113 | $1120\,\text{kg} \approx 2469\,\text{lbf}$ |
| 83 | $487\,\text{kg} \approx 1074\,\text{lbf}$ | 113 | $1150\,\text{kg} \approx 2581\,\text{lbf}$ |
| 84 | $500\,\text{kg} \approx 1102\,\text{lbf}$ | 114 | $1180\,\text{kg} \approx 2601\,\text{lbf}$ |
| 85 | $515\,\text{kg} \approx 1135\,\text{lbf}$ | 115 | $1215\,\text{kg} \approx 2679\,\text{lbf}$ |
| 86 | $530\,\text{kg} \approx 1163\,\text{lbf}$ | 116 | $1250\,\text{kg} \approx 2806\,\text{lbf}$ |
| 87 | $545\,\text{kg} \approx 1201\,\text{lbf}$ | 117 | $1285\,\text{kg} \approx 2833\,\text{lbf}$ |
| 88 | $560\,\text{kg} \approx 1235\,\text{lbf}$ | 118 | $1320\,\text{kg} \approx 2910\,\text{lbf}$ |
| 89 | $580\,\text{kg} \approx 1279\,\text{lbf}$ | 119 | $1360\,\text{kg} \approx 3074\,\text{lbf}$ |
| 90 | $600\,\text{kg} \approx 1323\,\text{lbf}$ | 120 | $1400\,\text{kg} \approx 3086\,\text{lbf}$ |
| 91 | $615\,\text{kg} \approx 1356\,\text{lbf}$ | 121 | $1450\,\text{kg} \approx 3197\,\text{lbf}$ |
| 92 | $630\,\text{kg} \approx 1389\,\text{lbf}$ | 122 | $1500\,\text{kg} \approx 3368\,\text{lbf}$ |
| 93 | $650\,\text{kg} \approx 1433\,\text{lbf}$ | 123 | $1550\,\text{kg} \approx 3417\,\text{lbf}$ |
| 94 | $670\,\text{kg} \approx 1477\,\text{lbf}$ | 124 | $1600\,\text{kg} \approx 3527\,\text{lbf}$ |
| 95 | $690\,\text{kg} \approx 1521\,\text{lbf}$ | 125 | $1650\,\text{kg} \approx 3690\,\text{lbf}$ |
| 96 | $710\,\text{kg} \approx 1565\,\text{lbf}$ | 126 | $1700\,\text{kg} \approx 3748\,\text{lbf}$ |
| 97 | $730\,\text{kg} \approx 1609\,\text{lbf}$ | 127 | $1750\,\text{kg} \approx 3858\,\text{lbf}$ |
| 98 | $750\,\text{kg} \approx 1653\,\text{lbf}$ | 128 | $1800\,\text{kg} \approx 3968\,\text{lbf}$ |
| 99 | $775\,\text{kg} \approx 1709\,\text{lbf}$ | $\cdots$ | $\cdots$ |
| | | 199 | $13600\,\text{kg} \approx 30000\,\text{lbf}$ |

**Example 2** *Height of a tire based on tire numbers.*

*A tire has the size number P215/60R15 96H. The aspect ratio 60 means the height of the tire is equal to 60% of the tire width. To calculate the tire height in* [mm], *we should multiply the first number* (215) *by the second number* (60) *and divide by* 100.

$$h_T = 215 \times \frac{60}{100} = 129\,\text{mm} \qquad (1.2)$$

*This is the tire height from rim to tread.*

Table 1.2 - Maximum speed tire index.

| Index | Maximum speed | Index | Maximum speed |
|-------|---------------|-------|---------------|
| $B$ | $50\,\mathrm{km/h} \approx 31\,\mathrm{mi/h}$ | $P$ | $150\,\mathrm{km/h} \approx 93\,\mathrm{mi/h}$ |
| $C$ | $60\,\mathrm{km/h} \approx 37\,\mathrm{mi/h}$ | $Q$ | $160\,\mathrm{km/h} \approx 100\,\mathrm{mi/h}$ |
| $D$ | $65\,\mathrm{km/h} \approx 40\,\mathrm{mi/h}$ | $R$ | $170\,\mathrm{km/h} \approx 106\,\mathrm{mi/h}$ |
| $E$ | $70\,\mathrm{km/h} \approx 43\,\mathrm{mi/h}$ | $S$ | $180\,\mathrm{km/h} \approx 112\,\mathrm{mi/h}$ |
| $F$ | $80\,\mathrm{km/h} \approx 50\,\mathrm{mi/h}$ | $T$ | $190\,\mathrm{km/h} \approx 118\,\mathrm{mi/h}$ |
| $G$ | $90\,\mathrm{km/h} \approx 56\,\mathrm{mi/h}$ | $U$ | $200\,\mathrm{km/h} \approx 124\,\mathrm{mi/h}$ |
| $J$ | $100\,\mathrm{km/h} \approx 62\,\mathrm{mi/h}$ | $H$ | $210\,\mathrm{km/h} \approx 130\,\mathrm{mi/h}$ |
| $K$ | $110\,\mathrm{km/h} \approx 68\,\mathrm{mi/h}$ | $V$ | $240\,\mathrm{km/h} \approx 150\,\mathrm{mi/h}$ |
| $L$ | $120\,\mathrm{km/h} \approx 75\,\mathrm{mi/h}$ | $W$ | $270\,\mathrm{km/h} \approx 168\,\mathrm{mi/h}$ |
| $M$ | $130\,\mathrm{km/h} \approx 81\,\mathrm{mi/h}$ | $Y$ | $300\,\mathrm{km/h} \approx 188\,\mathrm{mi/h}$ |
| $N$ | $140\,\mathrm{km/h} \approx 87\,\mathrm{mi/h}$ | $Z$ | $+240\,\mathrm{km/h} \approx +149\,\mathrm{mi/h}$ |

**Example 3** *Alternative tire size indication.*

*If the load index is not indicated on the tire, then a tire with a size number such as $255/50R17\ 100V$ may also be numbered by $255/50V\,R17$.*

**Example 4** *Tire and rim widths.*

*The dimensions of a tire are dependent on the rim on which it is mounted. For tires with an aspect ratio of 50 and above, the rim width is approximately 70% of the tire's width, rounded to the nearest 0.5 in. As an example, a $P255/50R16$ tire has a design width of $255\,\mathrm{mm} = 10.04\,\mathrm{in}$ however, 70% of $10.04\,\mathrm{in}$ is $7.028\,\mathrm{in}$, which rounded to the nearest 0.5 in, is 7 in. Therefore, a $P255/50R16$ tire should be mounted on a $7 \times 16$ rim.*

*For tires with aspect ratio 45 and below, the rim width is 85% of the tire's section width, rounded to the nearest 0.5 in. For example, a $P255/45R17$ tire with a section width of $255\,\mathrm{mm} = 10.04\,\mathrm{in}$, needs an 8.5 in rim because 85% of $10.04\,\mathrm{in}$ is $8.534\,\mathrm{in} \approx 8.5\,\mathrm{in}$. Therefore, a $P255/45R17$ tire should be mounted on an $8\frac{1}{2} \times 17$ rim.*

**Example 5** *Calculating tire diameter and radius.*

*We are able to calculate the overall diameter of a tire using the tire size numbers. By multiplying the tire width and the aspect ratio, we get the tire height. As an example, we use tire number $P235/75R15$.*

$$
\begin{aligned}
h_T &= 235 \times 75\% \\
&= 176.25\,\mathrm{mm} \approx 6.94\,\mathrm{in}
\end{aligned} \tag{1.3}
$$

*Then, we add twice the tire height $h_T$ to the rim diameter to determine the*

*tire's unloaded diameter $D = 2R$ and radius $R$.*

$$
\begin{aligned}
D &= 2 \times 6.94 + 15 \\
  &= 28.88\,\text{in} \approx 733.8\,\text{mm} \qquad\qquad (1.4) \\
R &= D/2 = 366.9\,\text{mm} \qquad\qquad\qquad (1.5)
\end{aligned}
$$

**Example 6** *Speed rating code.*

*Two similar tires are coded as $P235/70HR15$ and $P235/70R15\ 100H$. Both tires have code $H \equiv 210\,\text{km/ h}$ for speed rating. However, the second tire can sustain the coded speed only when it is loaded less than the specified load index, so it states $100H \equiv 800\,\text{kg}\ 210\,\text{km/ h}$.*

*Speed ratings generally depend on the type of tire. Off road vehicles usually use Q-rated tires, passenger cars usually use R-rated tires for typical street cars or T-rated for performance cars.*

**Example 7** *Tire weight.*

*The average weight of a tire for passenger cars is $10 - 12\,\text{kg}$. The weight of a tire for light trucks is $14 - 16\,\text{kg}$, and the average weight of commercial truck tires is $135 - 180\,\text{kg}$.*

**Example 8** *Effects of aspect ratio.*

*A higher aspect ratio provides a softer ride and an increase in deflection under the load of the vehicle. However, lower aspect ratio tires are normally used for higher performance vehicles. They have a wider road contact area and a faster response. This results in less deflection under load, causing a rougher ride to the vehicle.*

*Changing to a tire with a different aspect ratio will result in a different contact area, therefore changing the load capacity of the tire.*

**Example 9** ★ *BMW tire size code.*

*BMW, a European car, uses the metric system for sizing its tires. As an example, $TD230/55ZR390$ is a metric tire size code. $TD$ indicates the BMW TD model, $230$ is the section width in $[\,\text{mm}\,]$, $55$ is the aspect ratio in percent, $Z$ is the speed rating, $R$ means radial, and $390$ is the rim diameter in $[\,\text{mm}\,]$.*

**Example 10** ★ *"MS," "M + S," "M/S," and "M&S" signs.*

*The sign "MS," and "M + S," and "M/S," and "M&S" indicate that the tire has some mud and snow capability. Most radial tires have one of these signs.*

**Example 11** ★ *U.S. DOT tire identification number.*

*The US tire identification number is in the format "DOT DNZE ABCD 1309." It begins with the letters DOT to indicate that the tire meets US federal standards. DOT stands for Department of Transportation. The next two characters, $DN$, after DOT is the plant code, which refers to the manufacturer and the factory location at which the tire was made.*

*The next two characters, ZE, are a letter-number combination that refers to the specific mold used for forming the tire. It is an internal factory code and is not usually a useful code for customers.*

*The last four numbers, 1309, represents the week and year the tire was built. The other numbers, ABCD, are marketing codes used by the manufacturer or at the manufacturer's instruction. An example is shown in Figure 1.4.*

$$DOT \quad DNZE \quad ABCD \quad 1309$$

FIGURE 1.4. An example of a US DOT tire identification number.

*DN is the plant code for Goodyear-Dunlop Tire located in Wittlich, Germany. ZE is the tire's mold size, ABCD is the compound structure code, 13 indicates the 13th week of the year, and 09 indicates year 2009. So, the tire is manufactured in the 13th week of 2009 at Goodyear-Dunlop Tire in Wittlich, Germany.*

**Example 12 ★** *Canadian tires identification number.*
*In Canada, all tires should have an identification number on the sidewall. An example is shown in Figure 1.5.*

$$DOT \quad B3CD \quad E52X \quad 2112 \quad \text{🇨🇦}$$

FIGURE 1.5. An example of a Canadian DOT tire identification number.

*This identification number provides the manufacturer, time, and place that the tire was made. The first two characters following DOT indicate the manufacturer and plant code. In this case, B3 indicates Group Michelin located at Bridgewater, Nova Scotia, Canada. The third and fourth characters, CD, are the tire's mold size code. The fifth, sixth, seventh, and eighth characters, E52X, are optional and are used by the manufacturer. The final four numbers, 2112, indicates the manufacturing date. For example, 2112 indicate the twenty first week of year 2012. Finally, the maple leaf sign or the flag sign following the identification number indicates that the tire is manufactured in Canada. It also certifies that the tire meets Transport Canada requirements.*

**Example 13 ★** *E-Mark and international codes.*
*All tires sold in Europe after July 1997 must carry an E-mark. An example is shown by* $\boxed{5}$ *in Figure 1.2. The mark itself is either an upper or lower case "E" followed by a number in a circle or rectangle, followed by a further number. An "E" indicates that the tire is certified to comply with the dimensional, performance and marking requirements of ECE*

*regulation. ECE or UNECE stands for the united nations economic commission for Europe. The number in the circle or rectangle is the country code. Example: 11 is the UK. The first two digits outside the circle or rectangle indicate the regulation series under which the tire was approved. Example: "02" is for ECE regulation 30 governing passenger tires, and "00" is for ECE regulation 54 governing commercial vehicle tires. The remaining numbers represent the ECE mark type approval numbers. Tires may have also been tested and met the required noise limits. These tires may have a second ECE branding followed by an "−s" for sound.*

*Table 1.3 indicates the European country codes for tire manufacturing.*

*Besides the DOT and ECE codes for US and Europe, we may also see the other country codes such as: ISO−9001 for international standards organization, C.C.C for China compulsory product certification, JIS D 4230 for Japanese industrial standard.*

*Table 1.3 - European county codes for tire manufacturing.*

| Code | Country | Code | Country |
|------|---------|------|---------|
| E1 | Germany | E14 | Switzerland |
| E2 | France | E15 | Norway |
| E3 | Italy | E16 | Finland |
| E4 | Netherlands | E17 | Denmark |
| E5 | Sweden | E18 | Romania |
| E6 | Belgium | E19 | Poland |
| E7 | Hungary | E20 | Portugal |
| E8 | Czech Republic | E21 | Russia |
| E9 | Spain | E22 | Greece |
| E10 | Yugoslavia | E23 | Ireland |
| E11 | United Kingdom | E24 | Croatia |
| E12 | Austria | E25 | Slovenia |
| E13 | Luxembourg | E26 | Slovakia |

**Example 14 ★** *Light truck tires.*

*The tire sizes for a light truck may be shown in two formats:*

$$LT245/70R16$$

*or*

$$32 \times 11.50R16LT$$

*In the first format, LT ≡light truck, 245 ≡tire width in millimeters, 70 ≡aspect ratio in percent, R ≡radial structure, and 16 ≡rim diameter in inches.*

*In the second format, 32 ≡tire diameter in inches, 11.50 ≡tire width in inches, R ≡radial structure, 16 ≡rim diameter in inches, and LT ≡light truck.*

**Example 15 ★** *UTQG ratings.*

Tire manufacturers may put some other symbols, numbers, and letters on their tires supposedly rating their products for wear, wet traction, and heat resistance. These characters are referred to as UTQG (Uniform Tire Quality Grading), although there is no uniformity and standard in how they appear. There is an index for wear to show the average wearing life time in mileage. The higher the wear number, the longer the tire lifetime. An index of 100 is equivalent to approximately 20000 miles or 30000 km. Other numbers are indicated in Table 1.4.

Table 1.4 - Tread wear rating index.

| Index | Life (Approximate) | |
|-------|-----------|-----------|
| 100 | 32000 km | 20000 mi |
| 150 | 48000 km | 30000 mi |
| 200 | 64000 km | 40000 mi |
| 250 | 80000 km | 50000 mi |
| 300 | 96000 km | 60000 mi |
| 400 | 129000 km | 80000 mi |
| 500 | 161000 km | 100000 mi |

The UTQG also rates tires for wet traction and heat resistance. These are rated in letters between "A" to "C," where "A" is the best, "B" is intermediate and "C" is acceptable. An "A" wet traction rating is typically an indication that the tire has a deep open tread pattern with lots of sipping, which are the fine lines in the tread blocks.

An "A" heat resistance rating indicates two things: First, low rolling resistance due to stiffer tread belts, stiffer sidewalls, or harder compounds; second, thinner sidewalls, more stable blocks in the tread pattern. Temperature rating is also indicated by a letter between "A" to "CM," where "A" is the best, "B" is intermediate, and "C" is acceptable.

There might also be a traction rating to indicate how well a tire grips the road surface. This is an overall rating for both dry and wet conditions. Tires are rated as: "AA" for the best, "A" for better, "B" for good, and "C" for acceptable.

**Example 16 ★** *Tire sidewall additional marks.*

$TL \equiv$ Tubeless

$TT \equiv$ Tube type, tire with an inner-tube

Made in Country $\equiv$ Name of the manufacturing country

$C \equiv$ Commercial tires made for commercial trucks; Example: $185R14C$

$B \equiv$ Bias ply

$SFI \equiv$ Side facing inwards

$SFO \equiv$ Side facing outwards

$TWI \equiv$ Tire wear index

It is an indicator in the main tire profile, which shows when the tire is worn down and needs to be replaced.
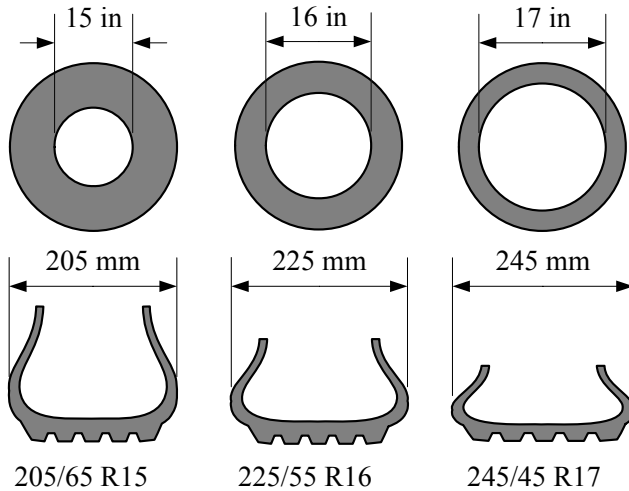
FIGURE 1.6. The plus one (+1) concept is a rule to find the tire to a rim with a 1 inch increase in diameter.

$SL \equiv$ *Standard load; Tire for normal usage and loads*
$XL \equiv$ *Extra load; Tire for heavy loads*
$rf \equiv$ *Reinforced tires*
*Arrow $\equiv$ Direction of rotation*
*Some tread patterns are designed to perform better when driven in a specific direction. Such tires will have an arrow showing which way the tire should rotate when the vehicle is moving forwards.*

**Example 17** ★ *Plus one (+1) concept.*
*The plus one (+1) concept describes the sizing up of a rim and matching it to a proper tire. Generally speaking, each time we add 1 in to the rim diameter, we should add 20 mm to the tire width and subtract 10% from the aspect ratio. This compensates the increases in rim width and diameter, and provides the same overall tire radius. Figure 1.6 illustrates the idea.*

*By using a tire with a shorter sidewall, we get a quicker steering response and better lateral stability. However, we will have a stiffer ride.*

**Example 18** ★ *Under- and over-inflated tire.*
*Overheat caused by improper inflation of tires is a common tire failure. An under-inflated tire will support less of the vehicle weight with the air pressure in the tire; therefore, more of the vehicle weight will be supported by the tire. This tire load increase causes the tire to have a larger tireprint that creates more friction and more heat.*

*In an over-inflated tire, too much of the vehicle weight is supported by the tire air pressure. The vehicle will be bouncy and hard to steer because the tireprint is small and only the center portion of the tireprint is contacting*
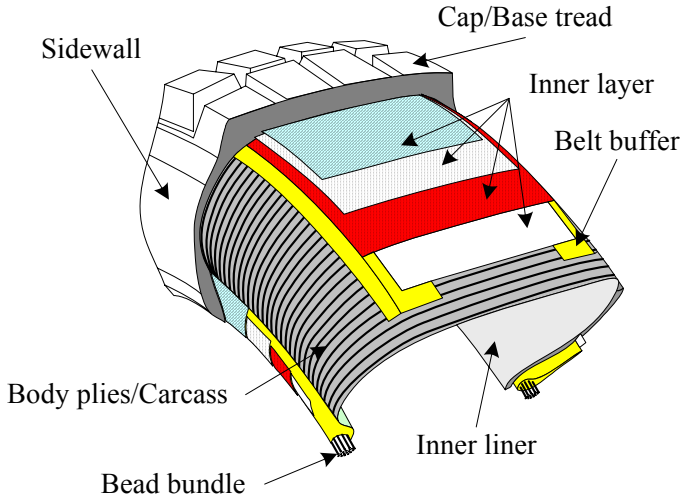
FIGURE 1.7. Illustration of a sample radial tire interior components and arrangement.

*the road surface.*

*In a properly-inflated tire, approximately* 95% *of the vehicle weight is supported by the air pressure in the tire and* 5% *is supported by the tire wall.*

## 1.2 Tire Components

A tire is an advanced engineering product made of rubber and a series of synthetic materials cooked together. Fiber, textile, and steel cords are some of the components that go into the tire's inner liner, body plies, bead bundle, belts, sidewalls, and tread. Figure 1.7 illustrates a sample of tire interior components and their arrangement.

The main components of a tire are explained below.

*Bead* or *bead bundle* is a loop of high strength steel cable coated with rubber. It gives the tire the strength it needs to stay seated on the wheel rim and to transfer the tire forces to the rim.

*Inner layers* are made up of different fabrics, called plies. The most common ply fabric is polyester cord. The top layers are also called cap plies. *Cap plies* are polyesteric fabric that help hold everything in place. Cap plies are not found on all tires; they are mostly used on tires with higher speed ratings to help all the components stay in place at high speeds.

An *inner liner* is a specially compounded rubber that forms the inside of a tubeless tire. It inhibits loss of air pressure.

*Belts* or belt buffers are one or more rubber-coated layers of steel, polyester, nylon, Kevlar or other materials running circumferentially around the tire under the tread. They are designed to reinforce body plies to hold the tread flat on the road and make the best contact with the road. Belts reduce squirm to improve tread wear and resist damage from impacts and penetration.

The *carcass* or *body plies* are the main part in supporting the tension forces generated by tire air pressure. The carcass is made of rubber-coated steel or other high strength cords tied to bead bundles. The cords in a radial tire, as shown in Figure 1.7, run perpendicular to the tread. The plies are coated with rubber to help them bond with the other components and to seal in the air.

A tire's strength is often described by the number of carcass plies. Most car tires have two carcass plies. By comparison, large commercial jetliners often have tires with 30 or more carcass plies.

The *sidewall* provides lateral stability for the tire, protects the body plies, and helps to keep the air from escaping from the tire. It may contain additional components to help increase the lateral stability.

The *tread* is the portion of the tire that comes in contact with the road. Tread designs vary widely depending on the specific purpose of the tire. The tread is made from a mixture of different kinds of natural and synthetic rubbers. The outer perimeter of a tire is also called the *crown*.

The *tread groove* is the space or area between two tread rows or blocks. The tread groove gives the tire traction and is especially useful during rain or snow.

**Example 19** *Tire rubber main material.*

*There are two major ingredients in a rubber compound: the rubber and the filler. They are combined in such a way to achieve different objectives. The objective may be performance optimization, traction maximization, or better rolling resistance. The most common fillers are different types of carbon black and silica. The other tire ingredients are antioxidants, antiozonant, and anti-aging agents.*

*Tires are combined with several components and cooked with a heat treatment. The components must be formed, combined, assembled, and cured together. Tire quality depends on the ability to blend all of the separate components into a cohesive product that satisfies the driver's needs. A modern tire is a mixture of steel, fabric, and rubber. Generally speaking, the weight percentage of the components of a tire are:*

1— *Reinforcements: steel, rayon, nylon,* 16%
2— *Rubber: natural/synthetic,* 38%
3— *Compounds: carbon, silica, chalk,* 30%
4— *Softener: oil, resin,* 10%
5— *Vulcanization: sulfur, zinc oxide,* 4%
6— *Miscellaneous,* 2%

**Example 20**  *Tire cords.*

Because tires have to carry heavy loads, steel and fabric cords are used in their construction to reinforce the rubber compound and provide strength. The most common materials suitable for the tire application are cotton, rayon, polyester, steel, fiberglass, and aramid.

**Example 21**  *Bead components and preparation.*

The bead component of tires is a non-extensible composite loop that anchors the carcass and locks the tire into the rim. The tire bead components include the steel wire loop and apex or bead filler. The bead wire loop is made from a steel wire covered by rubber and wound around the tire with several continuous loops. The bead filler is made from a very hard rubber compound, which is extruded to form a wedge.

**Example 22**  *Tire ply construction.*

The number of plies and cords indicates the number of layers of rubber-coated fabric or steel cords in the tire. In general, the greater the number of plies, the more weight a tire can support. Tire manufacturers also indicate the number and type of cords used in the tire.

**Example 23** ★ *Tire tread extrusion.*

Tire tread, or the portion of the tire that comes in contact with the road, consists of the tread, tread shoulder, and tread base. Since there are at least three different rubber compounds used in forming the tread profile, three rubber compounds are extruded simultaneously into a shared extruder head.

**Example 24** ★ *Different rubber types used in tires.*

There are five major rubbers used in tire production: natural rubber, styrene-butadiene rubber (SBR), polybutadiene rubber (BR), butyl rubber, and halogenated butyl rubber. The first three are primarily used for tread and sidewall compounds, while butyl rubber and halogenated butyl rubber are primarily used for the inner liner and the inside portion that holds the compressed air inside the tire.

**Example 25** ★ *History of rubber.*

About 2500 years ago, people living in Central and South America used the sap and latex of a local tree to waterproof their shoes, and clothes. This material was introduced to the first pilgrim travelers in the 17th century. The first application of this new material was discovered by the English as an eraser. This application supports the name **rubber**, because it was used for rubbing out pencil marks. The rubber pneumatic tires were invented in 1845 and its production began in 1888.

The natural rubber is a mixture of polymers and isomers. The main rubber isomer is shown in Figure 1.8 and is called **isoprene**. The natural rubber may be vulcanized to make longer and stronger polyisopren, suitable for tire production. Vulcanization is usually done by sulfur as cross-links. Figure 1.9 illustrates a vulcanized rubber polymer.

$$
\begin{array}{ccccccc}
 & & H & & & & \\
 & & | & & & & \\
 & H- & C & -H & & & \\
 H & & | & & & H & \\
 | & & | & & & | & \\
 - C & - & C & = C & - & C & - \\
 | & & & & | & | & \\
 H & & & & H & H &
\end{array}
$$
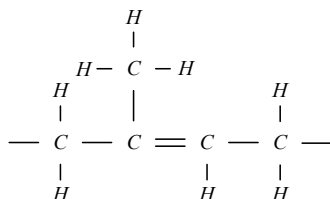
FIGURE 1.8. Illustration of the monomer unit of natural rubber.

$$
\begin{array}{ccccccc}
 & & H & & & & \\
 & & | & & & & \\
 & H- & C & -H & & & \\
 H & & | & & & H & \\
 | & & | & & & | & \\
 - C & - & C & - C & - & C & - \\
 | & & | & & | & | & \\
 H & & | & & H & H & \\
 & & S & & & & \\
 & & | & & & & \\
 & & S & & & & \\
 H & & | & & & H & \\
 | & & | & & & | & \\
 - C & - & C & - C & - & C & - \\
 | & & | & & | & | & \\
 H & & H- & C & -H & H & \\
 & & & | & & & \\
 & & & H & & &
\end{array}
$$
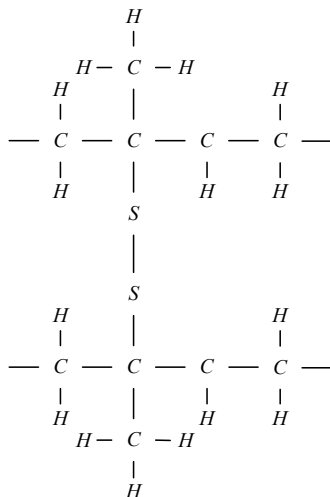
FIGURE 1.9. Illustration of a vulcanized rubber.

**Example 26** ★ *A world without rubber.*

   *Rubber is the main material used to make a tire compliant. A compliant tire can stick to the road surface while it goes out of shape and provides distortion to move in another direction. The elastic characteristic of a tire allows the tire to be pointed in a direction different than the direction the car is pointed. There is no way for a vehicle to turn without rubber tires, unless it moves at a very low speed. If vehicles were equipped with only noncompliant wheels then trains moving on railroads would be the main travelling vehicles. People could not live too far from the railways and there would not be much use for bicycles and motorcycles.*

## 1.3  Radial and Non-Radial Tires

Tires are divided in two classes: *radial* and *non-radial*, depending on the angle between carcass metallic cords and the tire-plane. Each type of tire

Sidewall

Cap/Base tread

Inner layer

Belt buffer

Body plies/Carcass

Bead bundle

Inner liner
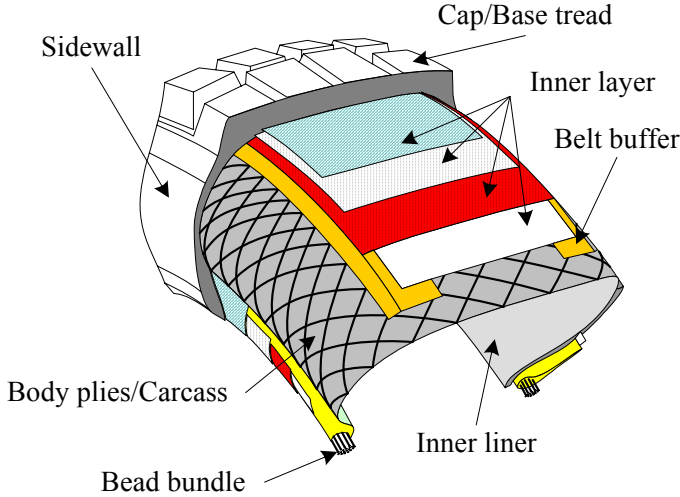
FIGURE 1.10. Examples of a non-radial tire's interior components and arrangement.

construction has its own set of characteristics that are the key to its performance.

The radial tire is constructed with reinforcing steel cable belts that are assembled in parallel and run side to side, from one bead to another bead at an angle of 90 deg to the circumferential centerline of the tire. This makes the tire more flexible radially, which reduces rolling resistance and improves cornering capability. Figure 1.7 shows the interior structure and the carcass arrangement of a radial tire.

The non-radial tires are also called *bias-ply* and *cross-ply* tires. The plies are layered diagonal from one bead to the other bead at about a 30 deg angle, although any other angles may also be applied. One ply is set on a bias in one direction as succeeding plies are set alternately in opposing directions as they cross each other. The ends of the plies are wrapped around the bead wires, anchoring them to the rim of the wheel. Figure 1.10 shows the interior structure and the carcass arrangement of a non-radial tire.

The most important difference in the dynamics of radial and non-radial tires is their different ground sticking behavior when a lateral force is applied on the wheel. This behavior is shown in Figure 1.11. The radial tire, shown in Figure 1.11(a), flexes mostly in the sidewall and keeps the tread flat on the road. The bias-ply tire, shown in Figure 1.11(b) has less contact with the road as both tread and sidewalls distort under a lateral load.

The radial arrangement of carcass in a radial tire allows the tread and sidewall act independently. The sidewall flexes more easily under the weight

(a) Radial tire          (b) Non-Radial tire
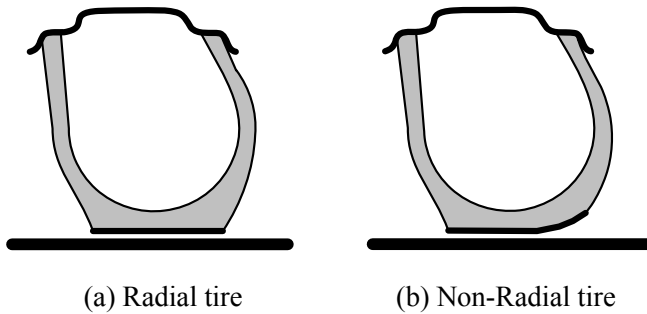
FIGURE 1.11. Ground-sticking behavior of radial and non-radial tires in the presence of a lateral force.

of the vehicle. So, more vertical deflection is achieved with radial tires. As the sidewall flexes under the load, the belts hold the tread firmly and evenly on the ground and reduces tread scrub. In a cornering maneuver, the independent action of the tread and sidewalls keeps the tread flat on the road. This allows the tire to hold its path. Radial tires are the preferred tire in most applications today.

The cross arrangement of carcass in bias-ply tires allows it act as a unit. When the sidewalls deflect or bend under load, the tread squeezes in and distorts. This distortion affects the tireprint and decrease traction. Because of the bias-ply inherent construction, sidewall strength is less than that of a radial tire's construction and cornering is less effective.

**Example 27** *Increasing the strength of tires.*

*The strength of bias-ply tires increases by increasing the number of plies and bead wires. However, more plies means more mass, which increases heat and reduces tire life. To increase a radial tire's strength, larger diameter steel cables are used in the tire's carcass.*

**Example 28** *Tubeless and tube-type tire construction.*

*A tubeless tire is similar in construction to a tube-type tire, except that a thin layer of air and moisture-resistant rubber is used on the inside of the tubeless tire from bead to bead to obtain an internal seal of the casing. This eliminates the need for a tube and flap. Both tires, in equivalent sizes, can carry the same load at the same inflation pressure.*

**Example 29** ★ *New shallow tires.*

*Low aspect ratio tires are radial tubeless tires that have a section width wider than their section height. The aspect ratio of these tires is between 50% to 30%. Therefore, shallow tires have shorter sidewall heights and wider tread widths. This feature improves stability and handling from a higher lateral spring rates.*

**Example 30** ★ *Tire function.*

*A tire is a pneumatic system to support a vehicle's load. Tires support a vehicle's load by using compressed air to create tension in the carcass plies. Tire carcass are a series of cords that have a high tension strength, and almost no compression strength. So, it is the air pressure that creates tension in the carcass and carries the load. In an inflated and unloaded tire, the cords pull equally on the bead wire all around the tire. When the tire is loaded, the tension in the cords between the rim and the ground is relieved while the tension in other cords is unchanged. Therefore, the cords opposite the ground pull the bead upwards. This is how pressure is transmitted from the ground to the rim.*

*Besides vertical load carrying, a tire must transmit acceleration, braking, and cornering forces to the road. These forces are transmitted to the rim in a similar manner. Acceleration and braking forces also depend on the friction between the rim and the bead. A tire also acts as a spring between the rim and the road.*

## 1.4  Tread

The tread pattern is made up of tread *lugs* and tread *voids*. The lugs are the sections of rubber that make contact with the road and voids are the spaces that are located between the lugs. Lugs are also called *slots* or *blocks*, and voids are also called *grooves*. The tire tread pattern of block-groove configurations affect the tire's traction and noise level. Wide and straight grooves running circumferentially have a lower noise level and high lateral friction. More lateral grooves running from side to side increase traction and noise levels. A sample of a tire tread is shown in Figure 1.12.

Tires need both circumferential and lateral grooves. The water on the road is compressed into the grooves by the vehicle's weight and is evacuated from the tireprint region, providing better traction at the tireprint contact. Without such grooves, the water would not be able to escape out to the sides of the wheel. This would causes a thin layer of water to remain between the road and the tire, which causes a loss of friction with the road surface. Therefore, the grooves in the tread provide an escape path for water.

On a dry road, the tire treads reduce grip because they reduce the contact area between the rubber and the road. This is the reason for using treadless or slick tires at smooth and dry race tracks.

The mud-terrain tire pattern is characterized by large lugs and large voids. The large lugs provide large bites in poor traction conditions and the large voids allow the tire to clean itself by releasing and expelling the mud and dirt. The all-terrain tire pattern is characterized by smaller voids and lugs when compared to the mud terrain tire. A denser pattern of lugs and smaller voids make all-terrain tires quieter on the street. However,
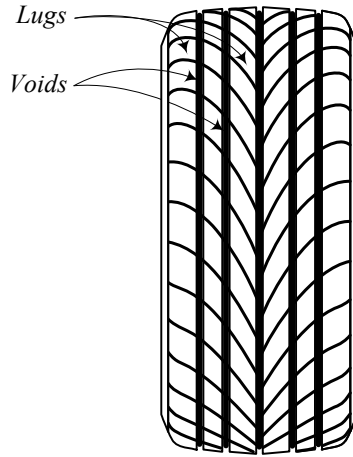
Lugs

Voids

FIGURE 1.12. A sample of tire tread to show lugs and voids.

smaller voids cannot clean themselves easily and if the voids fill up with mud, the tire loses some of it's traction. The all-terrain tire is good for highway driving.

**Example 31** *Asymmetrical and directional tread design.*
*The design of the tread pattern may be asymmetric and change from one side to the other. Asymmetric patterns are designed to have two or more different functions and provide a better overall performance.*

*A directional tire is designed to rotate in only one direction for maximum performance. Directional tread pattern is especially designed for driving on wet, snowy, or muddy roads. A non-directional tread pattern is designed to rotate in either direction without sacrificing in performance.*

**Example 32** *Self-cleaning.*
*Self-cleaning is the ability of a tire's tread pattern to release mud or material from the voids of tread. This ability provides good bite on every rotation of the tire. A better mud tire releases the mud or material easily from the tread voids.*

## 1.5  ★ Hydroplaning

*Hydroplaning* is sliding of a tire on a film of water. Hydroplaning can occur when a car drives through standing water and the water cannot totally escape out from under the tire. This causes the tire to lift off the ground and slide on the water. The hydroplaning tire will have little traction and therefore, the car will not obey the driver's command.
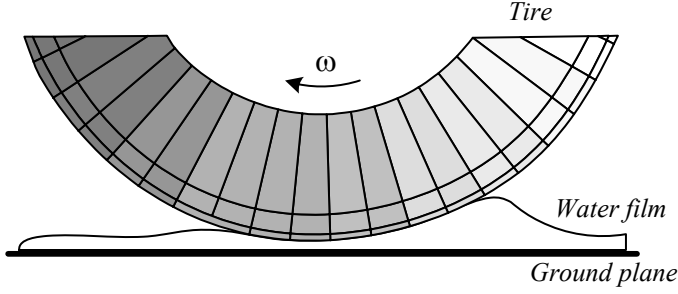
FIGURE 1.13. Illustration of hydroplaning phnomena.

Deep grooves running from the center front edge of the tireprint to the corners of the back edges, along with a wide central channel help water to escape from under the tire. Figure 1.13 illustrates the hydroplaning phenomena when the tire is riding over a water layer.

There are three types of hydroplaning: dynamic, viscous, and rubber hydroplaning. *Dynamic hydroplaning* occurs when standing water on a wet road is not displaced from under the tires fast enough to allow the tire to make pavement contact over the total tireprint. The tire rides on a wedge of water and loses its contact with the road. The speed at which hydroplaning happens is called *hydroplaning speed*.

*Viscous hydroplaning* occurs when the wet road is covered with a layer of oil, grease, or dust. Viscous hydroplaning happens with less water depth and at a lower speed than dynamic hydroplaning.

*Rubber hydroplaning* is generated by superheated steam at high pressure in the tireprint, which is caused by the friction-generated heat in a hard braking.

**Example 33** *Aeronautic hydroplaning speed.*

*In aerospace engineering the hydroplaning speed is estimated in* [*knots*] *by*

$$v_H = 9\sqrt{p} \tag{1.6}$$

*where, p is tire inflation pressure in* [*psi*].

*For main wheels of a B757 aircraft, the hydroplaning speed would be*

$$\begin{aligned} v_H &= 9\sqrt{144} \\ &= 108\,knots \approx 55.5\,\mathrm{m/s}. \end{aligned}$$

*Equation (1.6) for a metric system would be*

$$v_x = 5.5753 \times 10^{-2}\sqrt{p} \tag{1.7}$$

*where $v_x$ is in* [m/s] *and p is in* [Pa]. *As an example, the hydroplaning*
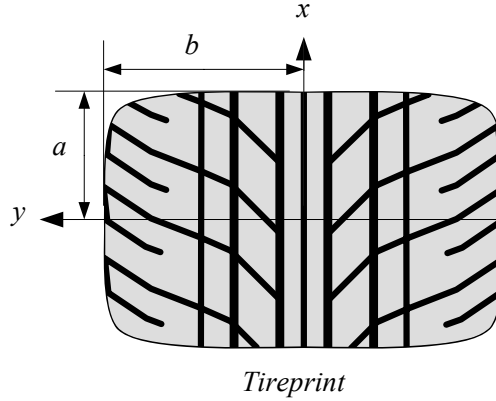
*Tireprint*

FIGURE 1.14. A tireprint.

*speed of a car using tires with pressure* $28psi \approx 193053\,\mathrm{Pa}$ *is*

$$\begin{aligned}
v_x &= 5.5753 \times 10^{-2}\sqrt{193053} \\
&\approx 24.5\,\mathrm{m/s} \\
&\approx 47.6knots \approx 88.2\,\mathrm{km/h} \approx 54.8\,\mathrm{mi/h}.
\end{aligned} \tag{1.8}$$

## 1.6   Tireprint

The contact area between a tire and the road is called the *tireprint* and is shown by $A_P$. At any point of a tireprint, the normal and friction forces are transmitted between the road and tire. The effect of the contact forces can be described by a resulting force system including force and torque vectors applied at the center of the tireprint.

The tireprint is also called *contact patch*, *contact region*, or *tire footprint*. A simplified model of tireprint is shown in Figure 1.14.

The area of the tireprint is inversely proportional to the tire pressure. Lowering the tire pressure is a technique used for off-road vehicles in sandy, muddy, or snowy areas, and for drag racing. Decreasing the tire pressure causes the tire to slump so more of the tire is in contact with the surface, giving better traction in low friction conditions. It also helps the tire grip small obstacles as the tire conforms more to the shape of the obstacle, and makes contact with the object in more places. Low tire pressure increases fuel consumption, tire wear, and tire temperature.

**Example 34**  *Uneven wear in front and rear tires.*

*In most vehicles, the front and rear tires will wear at different rates. So, it is advised to swap the front and rear tires as they wear down to even out the wear patterns. This is called rotating the tires.*
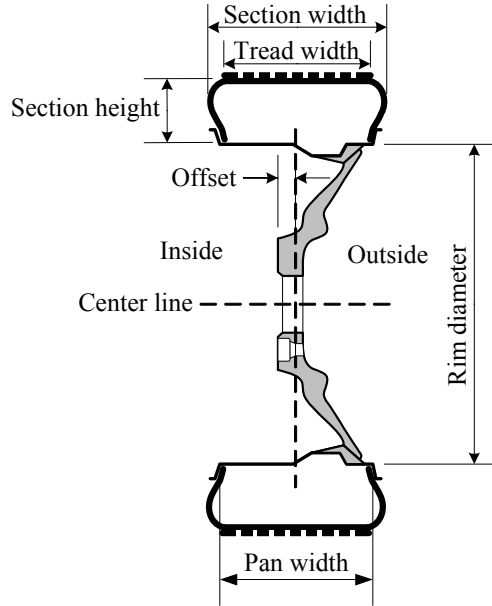
FIGURE 1.15. Illustration of a wheel and its dimensions.

*Front tires, especially on front-wheel drive vehicles, wear out more quickly than rear tires.*

## 1.7   Wheel and Rim

When a tire is installed on a rim and is inflated, it is called a wheel. A *wheel* is a combined tire and *rim*. The rim is the metallic cylindrical part where the tire is installed. Most passenger cars are equipped with steel rims. The steel rim is made by welding a disk to a shell. However, light alloy rims made with light metals such as aluminium and magnesium are also popular. Figure 1.15 illustrates a wheel and the most important dimensional names.

A rim has two main parts: *flange* and *spider*. The flange or *hub* is the ring or shell on which the tire is mounted. The spider or *center section* is the disc section that is attached to the hub. The rim width is also called pan width and measured from inside to inside of the bead seats of the flange. Flange provides lateral support to the tire. A flange has two *bead seats* providing radial support to the tire. The *well* is the middle part between the bead seats with sufficient depth and width to enable the tire beads to be mounted and demounted on the rim. The *rim hole* or *valve aperture* is the hole or slot in the rim that accommodates the valve for tire inflation.

There are two main rim shapes: 1− drop center rim (*DC*) and, 2− wide
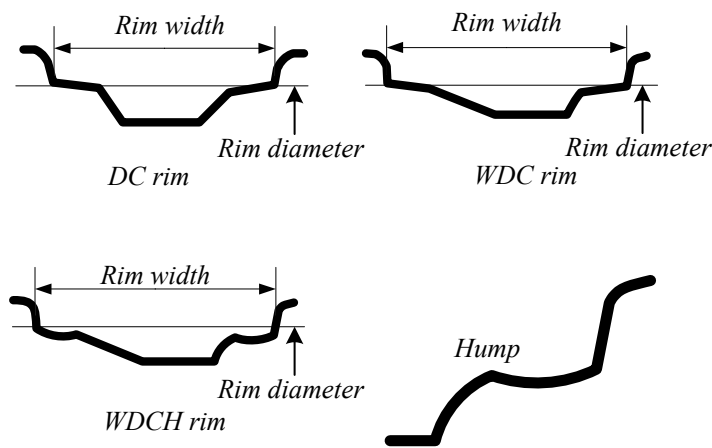
FIGURE 1.16. Illustration of DC, WDC, and WDCH rims and their geometry.



FIGURE 1.17. A sample rim number.

drop center rim ($WDC$). The $WDC$ may also come with a *hump*. The humped $WDC$ may be called $WDCH$. Their cross sections are illustrated in Figure 1.16.

Drop center (DC) rims usually are symmetric with a well between the bead seats. The well is built to make mounting and demounting the tire easy. The bead seats are around 5 deg tapered. Wide drop center rims ($WDC$) are wider than $DC$ rims and are built for low aspect ratio tires. The well of $WDC$ rims are shallower and wider. Today, most passenger cars are equipped with $WDC$ rims. The $WDC$ rims may be manufactured with a hump behind the bead seat area to prevent the bead from slipping down.

A sample of rim numbering and its meaning is shown in Figure 1.17. Rim width, rim diameter, and offset are shown in Figure 1.15. Offset is
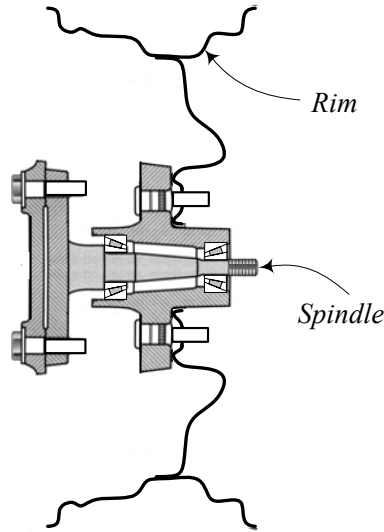
FIGURE 1.18. Illustration of a wheel attched to the spindle axle.

the distance between the inner plane and the center plane of the rim. A rim may be designed with a negative, zero, or positive offset. A rim has a positive offset if the spider is outward from the center plane.

The flange shape code signifies the tire-side profile of the rim and can be $B$, $C$, $D$, $E$, $F$, $G$, $J$, $JJ$, $JK$, and $K$. Usually the profile code follows the nominal rim width but different arrangements are also used. Figure 1.18 illustrates how a wheel is attached to the spindle axle.

**Example 35** *Wire spoke wheel.*

*A rim that uses wires to connect the center part to the exterior flange is called a wire spoke wheel, or simply a wire wheel. The wires are called spokes. This type of wheel is usually used on classic vehicles. The high-power cars do not use wire wheels because of safety. Figure 1.19 depicts two examples of wire spoke wheels.*

**Example 36** *Light alloy rim material.*

*Metal is the main material for manufacturing, rims, however, new composite materials are also used for rims occasionally. Composite material rims are usually thermoplastic resin with glass fiber reinforcement, developed mainly for low weight. Their strength and heat resistance still need improvement before being a proper substitute for metallic rims.*

*Other than steel and composite materials, light alloys such as aluminum, magnesium, and titanium are used for manufacturing rims.*

*Aluminum is very good for its weight, thermal conductivity, corrosion resistance, easy casting, low temperature, easy machine processing, and recy-*

Center line                Center line
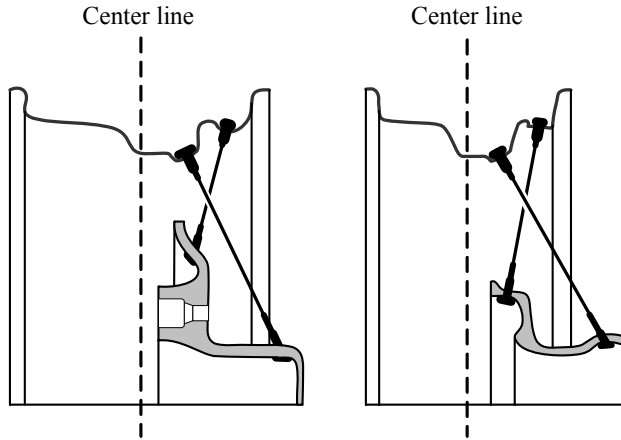


FIGURE 1.19. Two samples of wire spoke wheel.



*Ground plane   Magnesium rim   Aluminum rim        Steel rim*
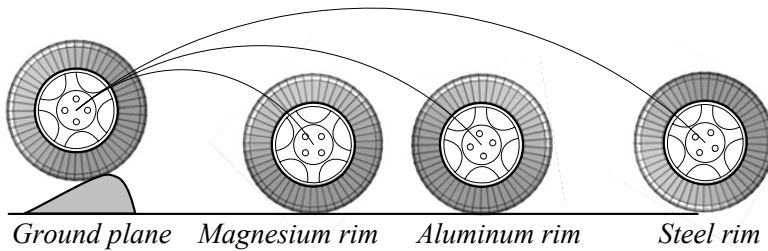
FIGURE 1.20. The difference between aluminum, magnesium, and steel rims in regaining road contact after a jump.

*cling. Magnesium is about* 30% *lighter than aluminum, and is excellent for size stability and impact resistance. However, magnesium is more expensive and it is used mainly for luxury or racing cars. The corrosion resistance of magnesium is not as good as aluminum. Titanium is much stronger than aluminum with excellent corrosion resistance. However, titanium is expensive and hard to be machine processed.*

*The difference between aluminum, magnesium, and steel rims is illustrated in Figure 1.20. Light weight wheels regain contact with the ground quicker than heavier wheels.*

**Example 37** *Spare tire.*

*Road vehicles typically carry a spare tire, which is already mounted on a rim ready to use in the event of flat tire. After* 1980, *some cars have been equipped with spare tires that are smaller than normal size. These spare tires are called doughnuts or space-saver spare tires. Although the doughnut spare tire is not very useful or popular, it can help to save a little space,*

*weight, cost, and gas mileage. Doughnut spare tires can not be driven far or fast.*

**Example 38** *Wheel history.*

*Stone and wooden wheels were invented and used somewhere in the Middle East about* 5000 *years ago. Hard wheels have some inefficient characteristics namely poor traction, low friction, harsh ride, and poor load carrying capacity.*

*Solid rubber tires and air tube tires began to be used in the late nineteen and early twentieth century.*

# 1.8   Vehicle Classifications

Road vehicles are usually classified based on their size and number of axles. Although there is no standard or universally accepted classification method, there are a few important and applied vehicle classifications.

## 1.8.1   ISO and FHWA Classification

ISO3833 classifies ground vehicles in 7 groups:

1— Motorcycles
2— Passenger cars
3— Busses
4— Trucks
5— Agricultural tractors
6— Passenger cars with trailer
7— Truck trailer/semi trailer road trains

The Federal Highway Administration (FHWA) classifies road vehicles based on size and application. All road vehicles are classified in 13 classes as described below:

1— Motorcycles
2— Passenger cars, including cars with a one-axle or two-axle trailer
3— Other two-axle vehicles, including: pickups, and vans, with a one-axle or two-axle trailer
4— Buses
5— Two axle, six-tire single units
6— Three-axle single units
7— Four or more axle single units
8— Four or fewer axle single trailers
9— Five-axle single trailers
10— Six or more axle single trailers
11— Five or less axle multi-trailers

12— Six-axle multi-trailers

13— Seven or more axle multi-trailers

Figure 1.21 illustrates the FHWA classification. The definition of FHWA classes follow.

*Motorcycles*: Any motorvehicle having a seat or saddle and no more than three wheels that touch the ground is a motorcycle. Motorcycles, motor scooters, mopeds, motor-powered or motor-assisted bicycles, and three-wheel motorcycles are in this class. Motorcycles are usually, but not necessarily, steered by handlebars. Figure 1.22 depicts a three-wheel motorcycle.

*Passenger Cars*: Street cars, including sedans, coupes, and station wagons manufactured primarily for carrying passengers, are in this class. Figure 1.23 illustrates a two-door passenger car. Passenger cars are also called street cars, *automobiles*, or *autos*.

*Other Two-Axle, Four-Tire Single-Unit Vehicles*: All two-axle, four-tire vehicles other than passenger cars make up this class. This class includes pickups, panels, vans, campers, motor homes, ambulances, hearses, carryalls, and minibuses. Other two-axle, four-tire single-unit vehicles pulling recreational or light trailers are also included in this class. Distinguishing class 3 from class 2 is not clear, so these two classes may sometimes be combined into class 2.

*Buses*: A motor vehicle able to carry more than ten persons is a bus. Buses are manufactured as traditional passenger-carrying vehicles with two axles and six tires. However, buses with three or more axles are also manufactured.

*Two-Axle, Six-Tire, Single-Unit Trucks*: Vehicles on a single frame including trucks, camping and recreational vehicles, motor homes with two axles, and dual rear wheels are in this class.

*Three-Axle Single-Unit Trucks*: Vehicles having a single frame including trucks, camping, recreational vehicles, and motor homes with three axles are in this class.

*Four-or-More-Axle-Single-Unit Trucks*: All trucks on a single frame with four or more axles make up this class.

*Four-or-Fewer-Axle Single-Trailer Trucks*: Vehicles with four or fewer axles consisting of two units, one of which is a tractor or straight truck power unit, are in this class.

*Five-Axle Single-Trailer Trucks*: Five-axle vehicles consisting of two units, one of which is a tractor or straight truck power unit, are in this class.

*Six-or-More-Axle Single-Trailer Trucks*: Vehicles with six or more axles consisting of two units, one of which is a tractor or straight truck power unit, are in this class.

*Five-or-Fewer-Axle Multi-Trailer Trucks*: Vehicles with five or fewer axles consisting of three or more units, one of which is a tractor or straight truck power unit, are in this class.
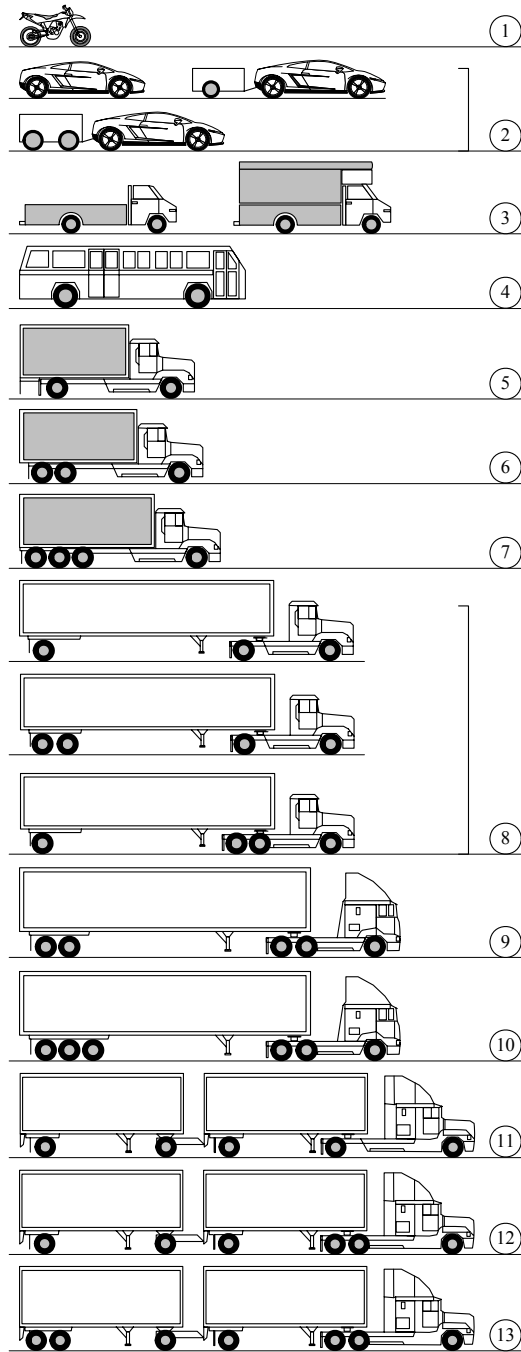
FIGURE 1.21. The FHWA vehicle classification.
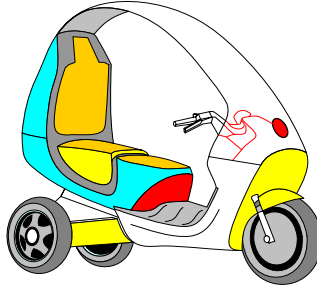
FIGURE 1.22. A three-wheel motorcycle.
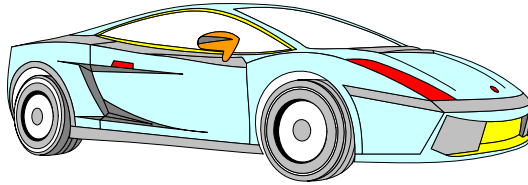


FIGURE 1.23. A two-door passenger car.

*Six-Axle Multi-Trailer Trucks*: Six-axle vehicles consisting of three or more units, one of which is a tractor or straight truck power unit, are in this class.

*Seven or More Axle Multi-Trailer Trucks*: Vehicles with seven or more axles consisting of three or more units, one of which is a tractor or straight truck power unit are in this class.

The classes 6 to 13 are also called truck. A *truck* is a motor vehicle designed primarily for carrying load and/or property.

## 1.8.2   Passenger Car Classifications

A passenger car or automobile is a motorvehicle designed for carrying ten or fewer persons. Automobiles may be classified based on their size and weight. Size classification is based on wheelbase, the distance between front and rear axles. Weight classification is based on curb weight, the weight of an automobile with standard equipment, and a full complement of fuel and other fluids, but with no load, persons, or property. The wheelbase is rounded to the nearest inch and the curb weight to the nearest $100 \, \text{lb} \approx 50 \, \text{kg}$ before classification.

For a size classification, passenger car may be classified as a *small*, *midsize*, and *large* car. *Small cars* have a wheelbase of less than $99 \, \text{in} \approx 2.5 \, \text{m}$, *midsize cars* have a wheelbase of less than $109 \, \text{in} \approx 2.8 \, \text{m}$ and greater than $100 \, \text{in} \approx 2.5 \, \text{m}$, and *large cars* have a wheelbase of more than $110 \, \text{in} \approx 2.8 \, \text{m}$.

Each class may also be divided further.

For a weight classification, passenger car may be classified as *light*, *midweight*, and *heavy*. *Light weight cars* have a curb weight of less than $2400\,\text{lb} \approx 1100\,\text{kg}$, *midweight cars* have a curb weight of less than $3400\,\text{lb} \approx 1550\,\text{kg}$ and more than $2500\,\text{lb} \approx 1150\,\text{kg}$, and *heavy cars* have a curb weight of more than $3500\,\text{lb} \approx 1600\,\text{kg}$. Each class may also be divided in some subdivisions.

Dynamically, passenger cars may be classified by their type of suspension, engine, driveline arrangement, weight distribution, or any other parameters that affect the dynamics of a car. However, in the market, passenger cars are usually divided into the following classes according to the number of passengers and load capacity.

1— Economy
2— Compact
3— Intermediate
4— Standard Size
5— Full Size
6— Premium Luxury
7— Convertible Premium
8— Convertible
9— Minivan
10— Midsize
11— SUV

In another classification, cars are divided according to size and shape. However, using size and shape to classify passenger cars is not clear-cut; many vehicles fall in between classes. Also, not all are sold in all countries, and sometimes their names differ between countries. Common entries in the shape classification are the *sedan*, *coupe*, *convertible*, *minivan/van*, *wagon*, and *SUV*.

A *sedan* is a car with a four-door body configuration and a conventional trunk or a sloping back with a hinged rear cargo hatch that opens upward.

A *coupe* is a two-door car.

A *convertible* is a car with a removable or retractable top.

A *minivan/van* is a vehicle with a box-shaped body enclosing a large cargo or passenger area. The identified gross weight of a van is less than $10\,000\,\text{lb} \approx 4\,500\,\text{kg}$. Vans can be identifiable by their enclosed cargo or passenger area, short hood, and box shape. Vans can be divided into *mini van*, *small van*, *midsize van*, *full-size van*, and *large van*. The van subdivision has the same specifications as SUV subdivisions.

A *wagon* is a car with an extended body and a roofline that extends past the rear doors.

An *SUV* (sport utility vehicle) is a vehicle with off-road capability. SUV is designed for carrying ten or fewer persons, and generally considered a multi-purpose vehicle. Most SUVs are four-wheel-drive with and increased

ground clearance. The SUV is also known as 4-by-4, $4WD$, $4 \times 4$ or $4x4$. SUVs can be divided into *mini, small, midsize, full-size*, and *large SUV*.

Mini SUVs are those with a wheelbase of less than or equal to 88 in $\approx$ 224 cm. A mini SUV is typically a microcar with a high clearance, and off-road capability. Small SUVs have a wheelbase of greater than 88 in $\approx$ 224 cm with an overall width of less than 66 in $\approx$ 168 cm. Small SUVs are short and narrow $4 \times 4$ multi-purpose vehicles. Midsize SUVs have a wheelbase of greater than 88 in $\approx$ 224 cm with an overall width greater than 66 in $\approx$ 168 cm, but less than 75 in $\approx$ 190 cm. Midsize SUVs are $4 \times 4$ multi-purpose vehicles designed around a shortened pickup truck chassis. Full-size SUVs are made with a wheelbase greater than 88 in $\approx$ 224 cm and a width between 75 in $\approx$ 190 cm and 80 in $\approx$ 203 cm. Full-size SUVs are $4 \times 4$ multi-purpose vehicles designed around an enlarged pickup truck chassis. Large SUVs are made with a wheelbase of greater than 88 in $\approx$ 224 cm and a width more than 80 in $\approx$ 203 cm.

Because of better performance, the vehicle manufacturing companies are going to make more cars four-wheel-drive. So, four-wheel-drive does not refer to a specific class of cars anymore.

A *truck* is a vehicle with two or four doors and an exposed cargo box. A light truck has a gross weight of less than 10 000 lb $\approx$ 4 500 kg. A medium truck has a gross weight from 10 000 lb $\approx$ 4 500 kg to 26 000 lb $\approx$ 12 000 kg. A heavy truck is a truck with a gross weight of more than 26 000 lb $\approx$ 12 000 kg.

### 1.8.3  Passenger Car Body Styles

Passenger cars are manufactured in so many different styles and shapes. Not all of those classes are made today, and some have new shapes and still carry the same old names. Some of them are as follows:

*Convertible* or *cabriolet* cars are automobiles with removable or retractable rooves. There are also the subdivisions *cabrio coach* or *semi-convertible* with partially retractable rooves.

*Coupé* or *coupe* are two-door automobiles with two or four seats and a fixed roof. In cases where the rear seats are smaller than regular size, it is called a two-plus-two or $2 + 2$. Coupé cars may also be convertible.

*Crossover SUV* or *XUV* cars are smaller sport utility vehicles based on a car platform rather than truck chassis. Crossover cars are a mix of SUV, minivan, and wagon to encompass some of the advantages of each.

*Estate car* or just *estate* is the British/English term for what North Americans call a station wagon.

*Hardtop* cars are those having a removable solid roof on a convertible car. However, today a fixed-roof car whose doors have no fixed window frame are also called a hardtops.

*Hatchback* cars are identified by a rear door, including the back window that opens to access a storage area that is not separated from the rest of

the passenger compartment. A hatchback car may have two or four doors and two or four seats. They are also called three-door, or five-door cars. A hatchback car is called a *liftback* when the opening area is very sloped and is lifted up to open.

A *limousine* is a chauffeur-driven car with a glass-window dividing the front seats from the rear. Limousines are usually an extended version of a luxury car.

*Minivans* are boxy wagon cars usually containing three rows of seats, with a capacity of six or more passengers and extra luggage space.

An *MPV* (*multi-purpose vehicle*) is designed as large cars or small buses having off-road capability and easy loading of goods. However, the idea for a car with a multi-purpose application can be seen in other classes, especially SUVs.

*Notchback* cars are something between the hatchback and sedan. Notchback is a sedan with a separate trunk compartment.

A *pickup truck* (or simply *pickup*) is a small or medium-sized truck with a separate cabin and rear cargo area. Pickups are made to act as a personal truck, however they might also be used as light commercial vehicles.

*Sedan* is the most common body style that are cars with four or more seats and a fixed roof that is full-height up to the rear window. Sedans can have two or four doors.

*Station wagon* or wagon is a car with a full-height body all the way to the rear; the load-carrying space created is accessed via a rear door or doors.

## 1.9    Summary

Tires are the only component of a vehicle to transfer forces between the road and the vehicle. Tire classification parameters are indicated on the sidewall, such as dimensions, maximum load-carrying capacity, and maximum speed index. A sample of tire size and performance code is shown in Figure 1.24 and their definitions are explained as follows:

$$\textbf{P  215 / 60 R 15  96 H}$$

FIGURE 1.24. A sample of tire size.

$\boxed{P}$ stands for passenger car. $\boxed{215}$ is the unloaded tire width, in [mm]. $\boxed{60}$ is the aspect ratio of the tire, $s_T = \frac{h_T}{w_T} \times 100$, which is the section height to tire width, expressed as a percentage. $\boxed{R}$ stands for radial. $\boxed{15}$ is the rim diameter that the tire is designed to fit in [in]. $\boxed{96}$ is the load index, and $\boxed{H}$ is the speed rate index.

Road vehicles are usually classified based on their size and number of axles. There is no universally accepted standard classification, however, ISO and FHWA present two important classifications in North America. ISO3833 classifies ground vehicles into seven groups:

1- Motorcycles
2- Passenger cars
3- Busses
4- Trucks
5- Agricultural tractors
6- Passenger cars with trailer
7- Truck trailer/semitrailer road trains

FHWA classifies all road vehicles into 13 classes:Motorcycles

1- Motorcycles
2- Passenger cars with one or two axles trailer
3- Other two-axle four-wheel single units
4- Buses
5- Two-axle six-wheel single units
6- Three-axle single units
7- Four-or-more-axle single units
8-Four-or-less-axle single trailers
9-Five-axle single trailers
10-Six-or-more-axle single trailers
11-Five-or-less-axle multi-trailers
12-Six-axle-multi-trailers
13-Seven-or-more-axle multi-trailers

# 1.10   Key Symbols

| | |
|---|---|
| $A_P$ | tireprint area |
| $B$ | bias ply tire |
| $D$ | tire diameter |
| $D$ | diagonal |
| $DC$ | drop center rim |
| $DOT$ | Department of Transportation |
| $FHWA$ | Federal Highway Administration |
| $h_T$ | section height |
| $H$ | speed rate |
| $WDCH$ | humped wide drop center rim |
| $LT$ | light truck |
| $M\&S$ | mud and snow |
| $p$ | tire inflation pressure |
| $P$ | passenger car |
| $R$ | radial tire |
| $s_T$ | aspect ratio |
| $ST$ | special trailer |
| $T$ | temporary tire |
| $v_H$ | hydroplaning speed |
| $v, v_x$ | forward velocity of vehicle |
| $w_T$ | tire width |
| $WDC$ | wide drop center rim |

# Exercises

1. Problem of tire beads.

   Explain what would be the possible problem for a tire that has tight or loose beads.

2. Tire size codes.

   Explain the meaning of the following tire size codes:

   (a)
   $$10.00R20\ 14(G)$$

   (b)
   $$18.4R46$$

   (c)
   $$480/80R46155A8$$

   (d)
   $$18.4 - 38(10)$$

   (e)
   $$76 \times 50.00B32 = 1250/45B32$$

   (f)
   $$LT255/85B16$$

   (g)
   $$33x12.50R15LT$$

3. Tire height and diameter.

   Find the tire height $h_T$ and diameter $D$ for the following tires.

   (a)
   $$480/80R46\ 155A8$$

   (b)
   $$P215/65R15\ 96H$$

4. ★ Plus one.

   Increase 1 in to the diameter of the rim of the following tires and find a proper tire for the new rim.

   $$P215/65R15\ 96H$$
   $$P215/60R15\ 96H$$

5. Tire of Porsche 911 turbo$^{TM}$.

   A model of Porsche 911 turbo$^{TM}$ uses the following tires.

$$\begin{array}{ll} front & 235/35ZR19 \\ rear & 305/30ZR19 \end{array}$$

   Determine and compare $h_T$, and $D$ for the front and rear tires.

6. Tire of Porsche Cayenne turbo$^{TM}$.

   A model of Porsche Cayenne turbo$^{TM}$ is an all-wheel-drive that uses the following tire.

$$255/55R18$$

   What is the angular velocity of its tires when it is moving at the top speed $v = 171\,\mathrm{mi/\,h} \approx 275\,\mathrm{km/\,h}$?

7. Tire of Ferrari P 4/5 by Pininfarina$^{TM}$.

   A model of Ferrari P 4/5 by Pininfarina$^{TM}$ is a rear-wheel-drive sport car that uses the following tires.

$$\begin{array}{ll} front & 255/35ZR20 \\ rear & 335/30ZR20 \end{array}$$

   What is the angular velocity of its tires when it is moving at the top speed $v = 225\,\mathrm{mi/\,h} \approx 362\,\mathrm{km/\,h}$?

8. Tire of Mercedes-Benz SLR 722 Edition$^{TM}$.

   A model of Mercedes-Benz SLR 722 Edition$^{TM}$ uses the following tires.

$$\begin{array}{ll} front & 255/35R19 \\ rear & 295/30R19 \end{array}$$

   What is the speed of this car if its rear tires are turning at

$$\omega = 2000\ rmp.$$

   At that speed, what would be the angular velocity of the front tires?

9. Tire of Chevrolet Corvette Z06$^{TM}$.

   A model of Chevrolet Corvette Z06$^{TM}$ uses the following tires.

$$\begin{array}{ll} front & 275/35ZR18 \\ rear & 325/30ZR19 \end{array}$$

   What is the speed of this car if its rear tires are turning at

$$\omega = 2000\ rmp.$$

   At that speed, what would be the angular velocity of the front tires?

10. Tire of Koenigsegg CCX$^{TM}$.

    Koenigsegg CCX$^{TM}$ is a sport car, equipped with the following tires.

    $$\begin{array}{ll} front & 255/35R19 \\ rear & 335/30R20 \end{array}$$

    What is the angular speed ratio of the rear tire to the front tire?

# Part I

# One-Dimensional Vehicle Dynamics

# 2

# Forward Vehicle Dynamics

Straight motion of an ideal rigid vehicle is the subject of this chapter. We ignore air friction and examine the load variation under the tires to determine the vehicle's limits of acceleration, road grade, and kinematic capabilities.

## 2.1   Parked Car on a Level Road

When a car is parked on level pavement, the normal force, $F_z$, under each of the front and rear wheels, $F_{z_1}$, $F_{z_2}$, are

$$F_{z_1} = \frac{1}{2}mg\frac{a_2}{l} \tag{2.1}$$

$$F_{z_2} = \frac{1}{2}mg\frac{a_1}{l} \tag{2.2}$$

where, $a_1$ is the distance of the car's mass center, $C$, from the front axle, $a_2$ is the distance of $C$ from the rear axle, and $l$ is the wheel base.

$$l = a_1 + a_2 \tag{2.3}$$
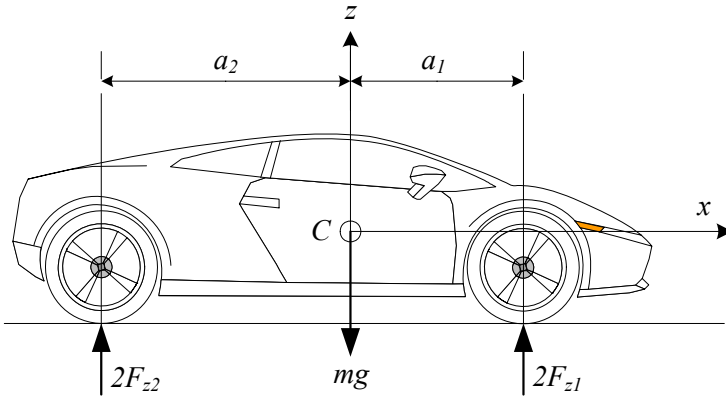


FIGURE 2.1. A parked car on level pavement.

**Proof.** Consider a longitudinally symmetrical car as shown in Figure 2.1. It can be modeled as a two-axel vehicle. A symmetric two-axel vehicle is equivalent to a rigid beam having two supports. The vertical force under the front and rear wheels can be determined using planar static equilibrium equations.

$$\sum F_z = 0 \qquad (2.4)$$

$$\sum M_y = 0 \qquad (2.5)$$

Applying the equilibrium equations

$$2F_{z_1} + 2F_{z_2} - mg = 0 \qquad (2.6)$$
$$-2F_{z_1}a_1 + 2F_{z_2}a_2 = 0 \qquad (2.7)$$

provide the reaction forces under the front and rear tires.

$$F_{z_1} = \frac{1}{2}mg\frac{a_2}{a_1 + a_2}$$
$$= \frac{1}{2}mg\frac{a_2}{l} \qquad (2.8)$$
$$F_{z_2} = \frac{1}{2}mg\frac{a_1}{a_1 + a_2}$$
$$= \frac{1}{2}mg\frac{a_1}{l} \qquad (2.9)$$

■

**Example 39** *Reaction forces under wheels.*
*A car has 890 kg mass. Its mass center, C, is 78 cm behind the front wheel axis, and it has a 235 cm wheel base.*

$$a_1 = 0.78\,\mathrm{m} \qquad (2.10)$$
$$l = 2.35\,\mathrm{m} \qquad (2.11)$$
$$m = 890\,\mathrm{kg} \qquad (2.12)$$

*The force under each front wheel is*

$$F_{z_1} = \frac{1}{2}mg\frac{a_2}{l}$$
$$= \frac{1}{2}890 \times 9.81 \times \frac{2.35 - 0.78}{2.35} = 2916.5\,\mathrm{N} \qquad (2.13)$$

*and the force under each rear wheel is*

$$F_{z_2} = \frac{1}{2}mg\frac{a_1}{l}$$
$$= \frac{1}{2}890 \times 9.81 \times \frac{0.78}{2.35} = 1449\,\mathrm{N}. \qquad (2.14)$$

**Example 40** *Mass center position.*
   *Equations (2.1) and (2.2) can be rearranged to calculate the position of
mass center.*

$$a_1 = \frac{2l}{mg} F_{z_2} \tag{2.15}$$

$$a_2 = \frac{2l}{mg} F_{z_1} \tag{2.16}$$

*Reaction forces under the front and rear wheels of a horizontally parked
car, with a wheel base $l = 2.34\,\mathrm{m}$, are:*

$$F_{z_1} = 2000\,\mathrm{N} \tag{2.17}$$
$$F_{z_2} = 1800\,\mathrm{N} \tag{2.18}$$

*Therefore, the longitudinal position of the car's mass center is at*

$$a_1 = \frac{2l}{mg} F_{z_2}$$
$$= 2\frac{2.34}{2\,(2000 + 1800)} \times 1800 = 1.1084\,\mathrm{m} \tag{2.19}$$

$$a_2 = \frac{2l}{mg} F_{z_1}$$
$$= 2\frac{2.34}{2\,(2000 + 1800)} \times 2000 = 1.2316\,\mathrm{m}. \tag{2.20}$$

**Example 41** *Longitudinal mass center determination.*
   *The position of mass center $C$ can be determined experimentally. To
determine the longitudinal position of $C$, we should measure the total weight
of the car as well as the force under the front or the rear wheels. Figure 2.2
illustrates a situation in which we measure the force under the front wheels.*

   *Assuming the force under the front wheels is $2F_{z_1}$, the position of the
mass center is calculated by static equilibrium conditions*

$$\sum F_z = 0 \tag{2.21}$$
$$\sum M_y = 0. \tag{2.22}$$

*Applying the equilibrium equations*

$$2F_{z_1} + 2F_{z_2} - mg = 0 \tag{2.23}$$
$$-2F_{z_1}a_1 + 2F_{z_2}a_2 = 0 \tag{2.24}$$
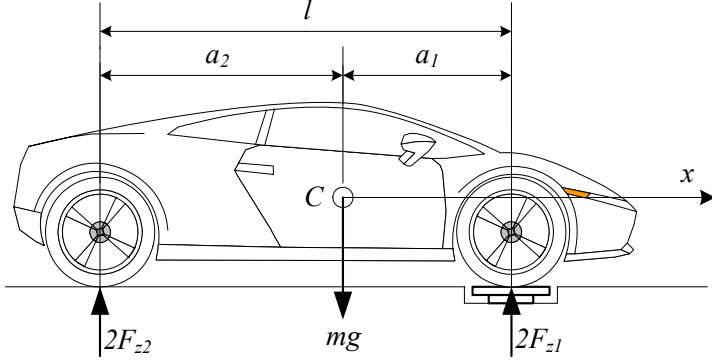
FIGURE 2.2. Measuring the force under the front wheels.

provide the longitudinal position of $C$ and the reaction forces under the rear wheels.

$$a_1 = \frac{2l}{mg} F_{z_2}$$

$$= \frac{2l}{mg} \left( mg - 2F_{z_1} \right) \tag{2.25}$$

$$F_{z_2} = \frac{1}{2} \left( mg - 2F_{z_1} \right) \tag{2.26}$$

**Example 42** *Lateral mass center determination.*

Most cars are approximately symmetrical about the longitudinal center plane passing the middle of the wheels, and therefore, the lateral position of the mass center $C$ is close to the center plane. However, the lateral position of $C$ may be calculated by weighing one side of the car.

**Example 43** *Height mass center determination.*

To determine the height of mass center $C$, we should measure the force under the front or rear wheels while the car is on an inclined surface. Experimentally, we use a device such as is shown in Figure 2.3. The car is parked on a level surface such that the front wheels are on a scale jack. The front wheels will be locked and anchored to the jack, while the rear wheels will be left free to turn. The jack lifts the front wheels and the required vertical force applied by the jacks is measured by a load cell.

Assume that we have the longitudinal position of $C$ and the jack is lifted such that the car makes an angle $\phi$ with the horizontal plane. The slope angle $\phi$ is measurable using level meters. Assuming the force under the front wheels is $2F_{z_1}$, the height of the mass center can be calculated by
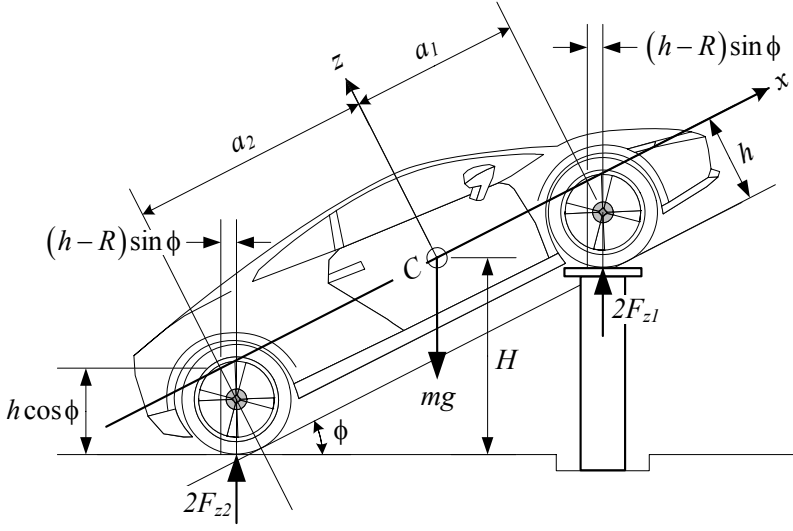
FIGURE 2.3. Measuring the force under the wheels to find the height of the mass center.

*static equilibrium conditions*

$$\sum F_Z = 0 \tag{2.27}$$

$$\sum M_y = 0. \tag{2.28}$$

*Applying the equilibrium equations*

$$2F_{z_1} + 2F_{z_2} - mg \quad = \quad 0 \tag{2.29}$$

$$\begin{aligned} -2F_{z_1}\left(a_1 \cos\phi - (h-R)\sin\phi\right) \\ +2F_{z_2}\left(a_2 \cos\phi + (h-R)\sin\phi\right) \quad = \quad 0 \end{aligned} \tag{2.30}$$

*provides the vertical position of $C$ and the reaction forces under the rear wheels.*

$$F_{z_2} = \frac{1}{2}mg - F_{z_1} \tag{2.31}$$

$$h = \frac{F_{z_1}\left(R\sin\phi + a_1\cos\phi\right) + F_{z_2}\left(R\sin\phi - a_2\cos\phi\right)}{mg\sin\phi}$$

$$= R + \frac{a_1 F_{z_1} - a_2 F_{z_2}}{mg}\cot\phi$$

$$= R + \left(2\frac{F_{z_1}}{mg}l - a_2\right)\cot\phi \tag{2.32}$$

*A car with the following specifications*

$$
\begin{aligned}
m &= 2000\,\mathrm{kg} \\
2F_{z_1} &= 18000\,\mathrm{N} \\
\phi &= 30\,\mathrm{deg} \approx 0.5236\,\mathrm{rad} \\
a_1 &= 110\,\mathrm{cm} \\
l &= 230\,\mathrm{cm} \\
R &= 30\,\mathrm{cm}
\end{aligned}
\tag{2.33}
$$

*has a C at height h.*

$$
h = 34\,\mathrm{cm}
\tag{2.34}
$$

*There are three assumptions in this calculation: 1— the tires are assumed to be rigid disks with radius R, 2— fluid shift, such as fuel, coolant, and oil, are ignored, and 3— suspension deflections are assumed to be zero.*

*Suspension deflection generates the maximum effect on height determination error. To eliminate the suspension deflection, we should lock the suspension, usually by replacing the shock absorbers with rigid rods to keep the vehicle at its ride height.*

**Example 44** *Different front and rear tires.*

*Depending on the application, it is sometimes necessary to use different type of tires and wheels for front and rear axles. When the longitudinal position of C for a symmetric vehicle is determined, we can find the height of C by measuring the load on only one axle. As an example, consider the motorcycle in Figure 2.4. It has different front and rear tires.*

*Assume the load under the rear wheel of the motorcycle $F_z$ is known. The height h of C can be found by taking a moment of the forces about the tireprint of the front tire.*

$$
h = \frac{F_{z_2}\,(a_1 + a_2)}{mg} - a_1 \cos\left(\sin^{-1}\frac{H}{a_1 + a_2}\right) + \frac{R_f + R_r}{2}
\tag{2.35}
$$

**Example 45** *Statically indeterminate.*

*A vehicle with more than three wheels is statically indeterminate. To determine the vertical force under each tire, we need to know the mechanical properties and conditions of the tires, such as the value of deflection at the center of the tire, and its vertical stiffness.*

## 2.2   Parked Car on an Inclined Road

When a car is parked on an inclined pavement as shown in Figure 2.5, the normal force, $F_z$, under each of the front and rear wheels, $F_{z_1}$, $F_{z_2}$, is:
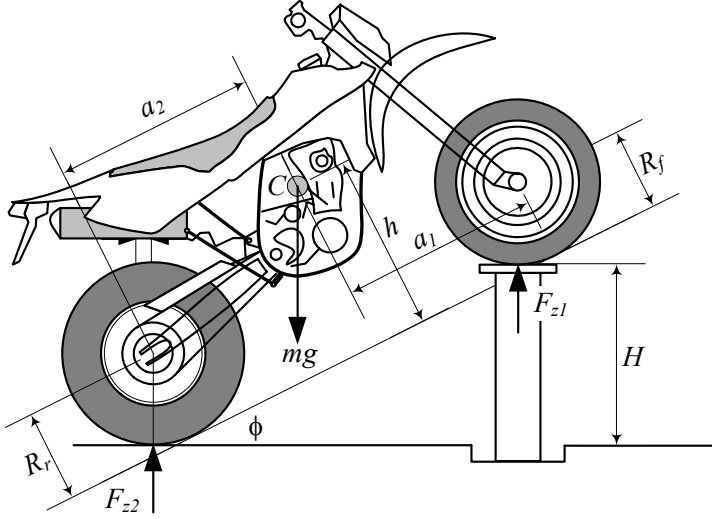
FIGURE 2.4. A motorcycle with different front and rear tires.

$$F_{z_1} = \frac{1}{2}mg\frac{a_2}{l}\cos\phi + \frac{1}{2}mg\frac{h}{l}\sin\phi \qquad (2.36)$$

$$F_{z_2} = \frac{1}{2}mg\frac{a_1}{l}\cos\phi - \frac{1}{2}mg\frac{h}{l}\sin\phi \qquad (2.37)$$

$$l = a_1 + a_2$$

where, $\phi$ is the angle of the road with the horizon. The horizon is perpendicular to the gravitational acceleration **g**.

**Proof.** Consider the car shown in Figure 2.5. Let us assume the parking brake forces are applied on only the rear tires. It means the front tires are free to spin. Applying the planar static equilibrium equations

$$\sum F_x = 0 \qquad (2.38)$$

$$\sum F_z = 0 \qquad (2.39)$$

$$\sum M_y = 0 \qquad (2.40)$$

shows that

$$2F_{x_2} - mg\sin\phi = 0 \qquad (2.41)$$

$$2F_{z_1} + 2F_{z_2} - mg\cos\phi = 0 \qquad (2.42)$$

$$-2F_{z_1}a_1 + 2F_{z_2}a_2 - 2F_{x_2}h = 0. \qquad (2.43)$$
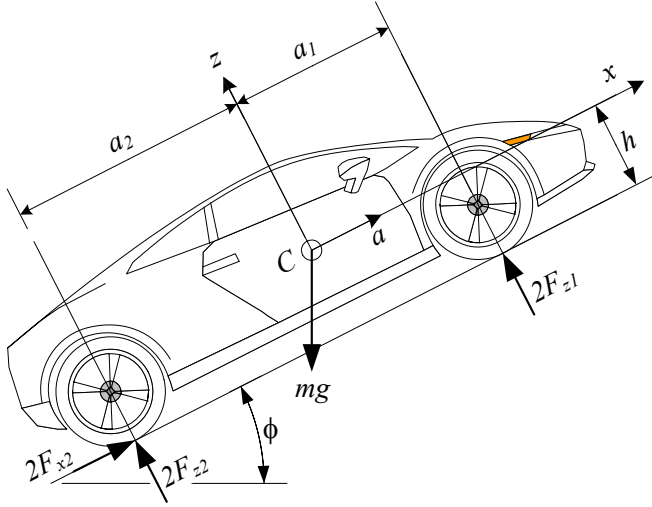
FIGURE 2.5. A parked car on inclined pavement.

These equations provide the brake force and reaction forces under the front and rear tires.

$$F_{z_1} = \frac{1}{2}mg\frac{a_2}{l}\cos\phi - \frac{1}{2}mg\frac{h}{l}\sin\phi \qquad (2.44)$$

$$F_{z_2} = \frac{1}{2}mg\frac{a_1}{l}\cos\phi + \frac{1}{2}mg\frac{h}{l}\sin\phi \qquad (2.45)$$

$$F_{x_2} = \frac{1}{2}mg\sin\phi \qquad (2.46)$$

∎

**Example 46** *Increasing the inclination angle.*

When $\phi = 0$, Equations (2.36) and (2.37) reduce to (2.1) and (2.2). By increasing the inclination angle, the normal force under the front tires of a parked car decreases and the normal force and braking force under the rear tires increase. The limit for increasing $\phi$ is where the weight vector m**g** goes through the contact point of the rear tire with the ground. Such an angle is called a **tilting angle**.

**Example 47** *Maximum inclination angle.*

The required braking force $F_{x_2}$ increases by the inclination angle. Because $F_{x_2}$ is equal to the friction force between the tire and pavement, its maximum depends on the tire and pavement conditions. There is a specific angle $\phi_M$ at which the braking force $F_{x_2}$ will saturate and cannot increase any more. At this maximum angle, the braking force is proportional to the normal force $F_{z_2}$

$$F_{x_2} = \mu_{x_2}F_{z_2} \qquad (2.47)$$

*where, the coefficient $\mu_{x_2}$ is the x-direction friction coefficient for the rear wheel. At $\phi = \phi_M$, the equilibrium equations will reduce to*

$$2\mu_{x_2}F_{z_2} - mg\sin\phi_M = 0 \tag{2.48}$$

$$2F_{z_1} + 2F_{z_2} - mg\cos\phi_M = 0 \tag{2.49}$$

$$2F_{z_1}a_1 - 2F_{z_2}a_2 + 2\mu_{x_2}F_{z_2}h = 0. \tag{2.50}$$

*These equations provide*

$$F_{z_1} = \frac{1}{2}mg\frac{a_2}{l}\cos\phi_M - \frac{1}{2}mg\frac{h}{l}\sin\phi_M \tag{2.51}$$

$$F_{z_2} = \frac{1}{2}mg\frac{a_1}{l}\cos\phi_M + \frac{1}{2}mg\frac{h}{l}\sin\phi_M \tag{2.52}$$

$$\tan\phi_M = \frac{a_1\mu_{x_2}}{l - \mu_{x_2}h} \tag{2.53}$$

*showing that there is a relation between the friction coefficient $\mu_{x_2}$, maximum inclination $\phi_M$, and the geometrical position of the mass center $C$. The angle $\phi_M$ increases by decreasing h.*

*For a car having the specifications*

$$
\begin{aligned}
\mu_{x_2} &= 1 \\
a_1 &= 110\,\text{cm} \\
l &= 230\,\text{cm} \\
h &= 35\,\text{cm}
\end{aligned}
\tag{2.54}
$$

*the tilting angle is*

$$\phi_M \approx 0.514\,\text{rad} \approx 29.43\,\text{deg}. \tag{2.55}$$

**Example 48** *Front wheel braking.*

*When the front wheels are the only braking wheels $F_{x_2} = 0$ and $F_{x_1} \neq 0$. In this case, the equilibrium equations will be*

$$2F_{x_1} - mg\sin\phi = 0 \tag{2.56}$$

$$2F_{z_1} + 2F_{z_2} - mg\cos\phi = 0 \tag{2.57}$$

$$-2F_{z_1}a_1 + 2F_{z_2}a_2 - 2F_{x_1}h = 0. \tag{2.58}$$

*These equations provide the brake force and reaction forces under the front and rear tires.*

$$F_{z_1} = \frac{1}{2}mg\frac{a_2}{l}\cos\phi - \frac{1}{2}mg\frac{h}{l}\sin\phi \tag{2.59}$$

$$F_{z_2} = \frac{1}{2}mg\frac{a_1}{l}\cos\phi + \frac{1}{2}mg\frac{h}{l}\sin\phi \tag{2.60}$$

$$F_{x_1} = \frac{1}{2}mg\sin\phi \tag{2.61}$$

*At the ultimate angle $\phi = \phi_M$*

$$F_{x_1} = \mu_{x_1} F_{z_1} \qquad (2.62)$$

*and*

$$2\mu_{x_1} F_{z_1} - mg \sin \phi_M = 0 \qquad (2.63)$$
$$2F_{z_1} + 2F_{z_2} - mg \cos \phi_M = 0 \qquad (2.64)$$
$$2F_{z_1} a_1 - 2F_{z_2} a_2 + 2\mu_{x_1} F_{z_1} h = 0. \qquad (2.65)$$

*These equations provide*

$$F_{z_1} = \frac{1}{2} mg \frac{a_2}{l} \cos \phi_M - \frac{1}{2} mg \frac{h}{l} \sin \phi_M \qquad (2.66)$$

$$F_{z_2} = \frac{1}{2} mg \frac{a_1}{l} \cos \phi_M + \frac{1}{2} mg \frac{h}{l} \sin \phi_M \qquad (2.67)$$

$$\tan \phi_M = \frac{a_2 \mu_{x_1}}{l - \mu_{x_1} h}. \qquad (2.68)$$

*Let's name the ultimate angle for the front wheel brake in Equation (2.53) as $\phi_{M_f}$, and the ultimate angle for the rear wheel brake in Equation (2.68) as $\phi_{M_r}$. Comparing $\phi_{M_f}$ and $\phi_{M_r}$ shows that*

$$\frac{\phi_{M_f}}{\phi_{M_r}} = \frac{a_1 \mu_{x_2} \left( l - \mu_{x_1} h \right)}{a_2 \mu_{x_1} \left( l - \mu_{x_2} h \right)}. \qquad (2.69)$$

*We may assume the front and rear tires are the same and so,*

$$\mu_{x_1} = \mu_{x_2} \qquad (2.70)$$

*therefore,*

$$\frac{\phi_{M_f}}{\phi_{M_r}} = \frac{a_1}{a_2}. \qquad (2.71)$$

Hence, if $a_1 < a_2$ then $\phi_{M_f} < \phi_{M_r}$ and therefore, a rear brake is more effective than a front brake on uphill parking as long as $\phi_{M_r}$ is less than the tilting angle, $\phi_{M_r} < \tan^{-1} \frac{a_2}{h}$. At the tilting angle, the weight vector passes through the contact point of the rear wheel with the ground.

Similarly we may conclude that when parked on a downhill road, the front brake is more effective than the rear brake.

**Example 49** *Four-wheel braking.*

Consider a four-wheel brake car, parked uphill as shown in Figure 2.6. In these conditions, there will be two brake forces $F_{x_1}$ on the front wheels and two brake forces $F_{x_1}$ on the rear wheels.
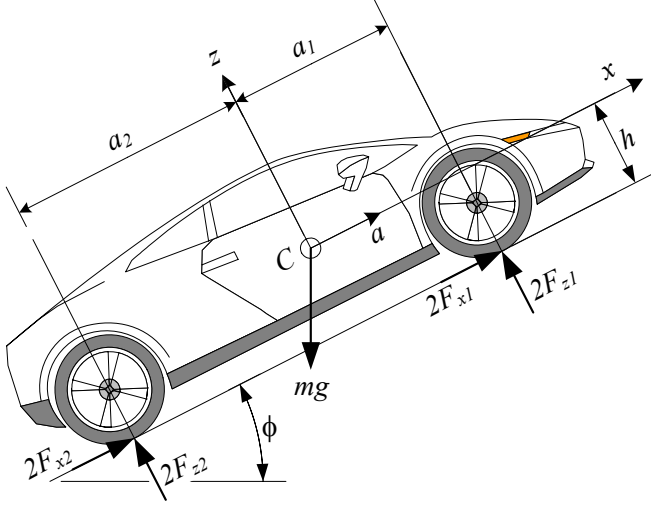
FIGURE 2.6. A four wheel brake car, parked uphill.

*The equilibrium equations for this car are*

$$2F_{x_1} + 2F_{x_2} - mg\sin\phi = 0 \tag{2.72}$$

$$2F_{z_1} + 2F_{z_2} - mg\cos\phi = 0 \tag{2.73}$$

$$-2F_{z_1}a_1 + 2F_{z_2}a_2 - (2F_{x_1} + 2F_{x_2})h = 0. \tag{2.74}$$

*These equations provide the brake force and reaction forces under the front and rear tires.*

$$F_{z_1} = \frac{1}{2}mg\frac{a_2}{l}\cos\phi - \frac{1}{2}mg\frac{h}{l}\sin\phi \tag{2.75}$$

$$F_{z_2} = \frac{1}{2}mg\frac{a_1}{l}\cos\phi + \frac{1}{2}mg\frac{h}{l}\sin\phi \tag{2.76}$$

$$F_{x_1} + F_{x_2} = \frac{1}{2}mg\sin\phi \tag{2.77}$$

*At the ultimate angle $\phi = \phi_M$, all wheels will begin to slide simultaneously and therefore,*

$$F_{x_1} = \mu_{x_1}F_{z_1} \tag{2.78}$$

$$F_{x_2} = \mu_{x_2}F_{z_2}. \tag{2.79}$$

*The equilibrium equations show that*

$$2\mu_{x_1}F_{z_1} + 2\mu_{x_2}F_{z_2} - mg\sin\phi_M = 0 \tag{2.80}$$

$$2F_{z_1} + 2F_{z_2} - mg\cos\phi_M = 0 \tag{2.81}$$

$$-2F_{z_1}a_1 + 2F_{z_2}a_2 - (2\mu_{x_1}F_{z_1} + 2\mu_{x_2}F_{z_2})h = 0. \tag{2.82}$$
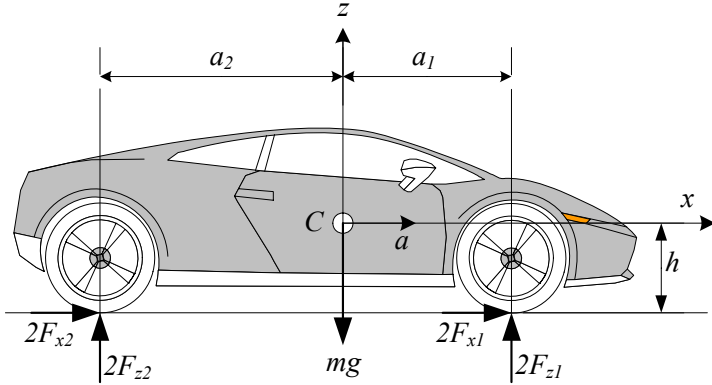
FIGURE 2.7. An accelerating car on a level pavement.

*Assuming*

$$\mu_{x_1} = \mu_{x_2} = \mu_x \tag{2.83}$$

*will provide*

$$F_{z_1} = \frac{1}{2}mg\frac{a_2}{l}\cos\phi_M - \frac{1}{2}mg\frac{h}{l}\sin\phi_M \tag{2.84}$$

$$F_{z_2} = \frac{1}{2}mg\frac{a_1}{l}\cos\phi_M + \frac{1}{2}mg\frac{h}{l}\sin\phi_M \tag{2.85}$$

$$\tan\phi_M = \mu_x. \tag{2.86}$$

## 2.3   Accelerating Car on a Level Road

When a car is speeding with acceleration $a$ on a level road as shown in Figure 2.7, the vertical forces under the front and rear wheels are

$$F_{z_1} = \frac{1}{2}mg\frac{a_2}{l} - \frac{1}{2}mg\frac{h}{l}\frac{a}{g} \tag{2.87}$$

$$F_{z_2} = \frac{1}{2}mg\frac{a_1}{l} + \frac{1}{2}mg\frac{h}{l}\frac{a}{g}. \tag{2.88}$$

The first terms, $\frac{1}{2}mg\frac{a_2}{l}$ and $\frac{1}{2}mg\frac{a_1}{l}$, are called *static parts*, and the second terms $\pm\frac{1}{2}mg\frac{h}{l}\frac{a}{g}$ are called *dynamic parts* of the normal forces.

**Proof.** The vehicle is considered as a rigid body that moves along a horizontal road. The force at the tireprint of each tire may be decomposed to a normal and a longitudinal force. The equations of motion for the accelerating car come from Newton's equation in $x$-direction and two static

equilibrium equations.

$$\sum F_x = ma \tag{2.89}$$

$$\sum F_z = 0 \tag{2.90}$$

$$\sum M_y = 0. \tag{2.91}$$

Expanding the equations of motion produces three equations for four unknowns $F_{x_1}$, $F_{x_2}$, $F_{z_1}$, $F_{z_2}$.

$$2F_{x_1} + 2F_{x_2} = ma \tag{2.92}$$

$$2F_{z_1} + 2F_{z_2} - mg = 0 \tag{2.93}$$

$$-2F_{z_1}a_1 + 2F_{z_2}a_2 - 2\left(F_{x_1} + F_{x_2}\right)h = 0 \tag{2.94}$$

However, it is possible to eliminate $(F_{x_1} + F_{x_2})$ between the first and third equations, and solve for the normal forces $F_{z_1}$, $F_{z_2}$.

$$
\begin{aligned}
F_{z_1} &= \left(F_{z_1}\right)_{st} + \left(F_{z_1}\right)_{dyn} \\
&= \frac{1}{2}mg\frac{a_2}{l} - \frac{1}{2}mg\frac{h}{l}\frac{a}{g}
\end{aligned} \tag{2.95}
$$

$$
\begin{aligned}
F_{z_2} &= \left(F_{z_2}\right)_{st} + \left(F_{z_2}\right)_{dyn} \\
&= \frac{1}{2}mg\frac{a_1}{l} + \frac{1}{2}mg\frac{h}{l}\frac{a}{g}
\end{aligned} \tag{2.96}
$$

The static parts

$$\left(F_{z_1}\right)_{st} = \frac{1}{2}mg\frac{a_2}{l} \tag{2.97}$$

$$\left(F_{z_2}\right)_{st} = \frac{1}{2}mg\frac{a_1}{l} \tag{2.98}$$

are weight distribution for a stationary car and depend on the horizontal position of the mass center. However, the dynamic parts

$$\left(F_{z_1}\right)_{dyn} = -\frac{1}{2}mg\frac{h}{l}\frac{a}{g} \tag{2.99}$$

$$\left(F_{z_2}\right)_{dyn} = \frac{1}{2}mg\frac{h}{l}\frac{a}{g} \tag{2.100}$$

indicate the weight distribution according to horizontal acceleration, and depend on the vertical position of the mass center.

When accelerating $a > 0$, the normal forces under the front tires are less than the static load, and under the rear tires are more than the static load.

∎

**Example 50** *Front-wheel-drive accelerating on a level road.*
When the car is front-wheel-drive, $F_{x_2} = 0$. Equations (2.92) to (2.88) will provide the same vertical tireprint forces as (2.87) and (2.88). However, the required horizontal force to achieve the same acceleration, a, must be provided by solely the front wheels.

**Example 51** *Rear-wheel drive accelerating on a level road.*
If a car is rear-wheel drive then, $F_{x_1} = 0$ and the required force to achieve the acceleration, a, must be provided only by the rear wheels. The vertical force under the wheels will still be the same as (2.87) and (2.88).

**Example 52** *Maximum acceleration on a level road.*
The maximum acceleration of a car is proportional to the friction under its tires. We assume the friction coefficients at the front and rear tires are equal and all tires reach their maximum tractions at the same time.

$$F_{x_1} = \pm\mu_x F_{z_1} \tag{2.101}$$

$$F_{x_2} = \pm\mu_x F_{z_2} \tag{2.102}$$

Newton's equation (2.92) can now be written as

$$ma = \pm 2\mu_x \left( F_{z_1} + F_{z_2} \right). \tag{2.103}$$

Substituting $F_{z_1}$ and $F_{z_2}$ from (2.93) and (2.94) results in

$$a = \pm\mu_x g. \tag{2.104}$$

Therefore, the maximum acceleration and deceleration depend directly on the friction coefficient.

**Example 53** *Maximum acceleration for a single-axle drive car.*
The maximum acceleration $a_{rwd}$ for a rear-wheel-drive car is achieved when we substitute $F_{x_1} = 0$, $F_{x_2} = \mu_x F_{z_2}$ in Equation (2.92) and use Equation (2.88)

$$\mu_x mg \left( \frac{a_1}{l} + \frac{h}{l} \frac{a_{rwd}}{g} \right) = ma_{rwd} \tag{2.105}$$

and therefore,

$$\frac{a_{rwd}}{g} = \frac{a_1 \mu_x}{l - h\mu_x}$$

$$= \frac{\mu_x}{1 - \mu_x \dfrac{h}{l}} \frac{a_1}{l}. \tag{2.106}$$

The front wheels can leave the ground when $F_{z_1} = 0$. Substituting $F_{z_1} = 0$ in Equation (2.88) provides the maximum acceleration at which the front wheels are still on the road.

$$\frac{a_{rwd}}{g} \leq \frac{a_2}{h} \tag{2.107}$$
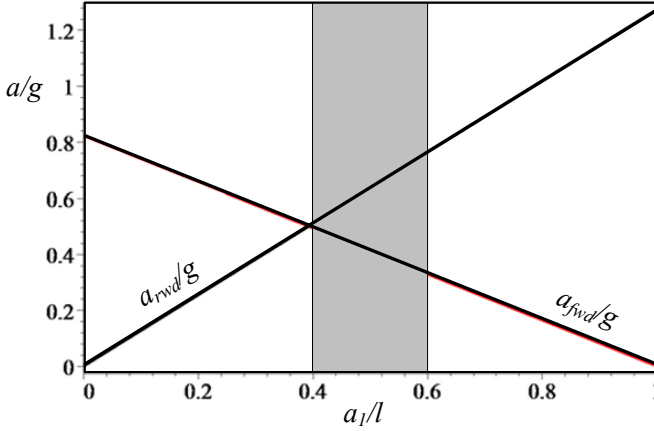
FIGURE 2.8. Effect of mass center position on the maximum achievable acceleration of a front- and a rear-wheel drive car.

*Therefore, the maximum attainable acceleration would be the less value of Equation (2.106) or (2.107).*

*Similarly, the maximum acceleration $a_{fwd}$ for a front-wheel drive car is achieved when we substitute $F_{x_2} = 0$, $F_{x_1} = \mu_x F_{z_1}$ in Equation (2.92) and use Equation (2.87).*

$$
\begin{aligned}
\frac{a_{fwd}}{g} &= \frac{a_2 \mu_x}{l + h\mu_x} \\
&= \frac{\mu_x}{1 + \mu_x \dfrac{h}{l}} \left( 1 - \frac{a_1}{l} \right)
\end{aligned} \qquad (2.108)
$$

*To see the effect of changing the position of mass center on the maximum achievable acceleration, we plot Figure 2.8 for a sample car with*

$$
\begin{aligned}
\mu_x &= 1 \\
h &= 0.56\,\mathrm{m} \\
l &= 2.6\,\mathrm{m}.
\end{aligned} \qquad (2.109)
$$

*Passenger cars are usually in the range $0.4 < (a_1/g) < 0.6$, with $(a_1/g) \to 0.4$ for front-wheel-drive cars, and $(a_1/g) \to 0.6$ for rear-wheel-drive cars. In this range, $(a_{rwd}/g) > (a_{fwd}/g)$ and therefore rear-wheel-drive cars can reach higher forward acceleration than front-wheel-drive cars. It is an important applied fact, especially for race cars.*

*The maximum acceleration may also be limited by the tilting condition*

$$
\frac{a_M}{g} \leq \frac{a_2}{h}. \qquad (2.110)
$$

**Example 54** *Minimum time for* $0 - 100 \, \text{km/h}$ *on a level road.*
   *Consider a car with the following characteristics:*

$$
\begin{aligned}
length &= 4245 \, \text{mm} \\
width &= 1795 \, \text{mm} \\
height &= 1285 \, \text{mm} \\
wheel\ base &= 2272 \, \text{mm} \\
front\ track &= 1411 \, \text{mm} \\
rear\ track &= 1504 \, \text{mm} \\
net\ weight &= 1500 \, \text{kg} \\
h &= 220 \, \text{mm} \\
\mu_x &= 1 \\
a_1 &= a_2
\end{aligned}
\tag{2.111}
$$

*Assume the car is rear-wheel-drive and its engine can provide the maximum traction supported by friction. Equation (2.88) determines the load on the rear wheels and therefore, the forward equation of motion is*

$$
\begin{aligned}
2F_{x_2} &= 2\mu_x F_{z_2} \\
&= \mu_x mg \frac{a_1}{l} + \mu_x mg \frac{h}{l} \frac{1}{g} a \\
&= m\,a.
\end{aligned}
\tag{2.112}
$$

*Rearrangement provides the following differential equation to calculate velocity and displacement:*

$$
\begin{aligned}
a = \ddot{x} &= \frac{\mu_x g \dfrac{a_1}{l}}{1 - \mu_x g \dfrac{h}{l}\dfrac{1}{g}} \\
&= g\mu_x \frac{a_1}{l - h\mu_x}
\end{aligned}
\tag{2.113}
$$

*Taking an integral*

$$
\int_0^{27.78} dv = \int_0^t a\, dt
\tag{2.114}
$$

*between* $v = 0$ *and* $v = 100 \, \text{km/h} \approx 27.78 \, \text{m/s}$ *shows that the minimum time for* $0 - 100 \, \text{km/h}$ *on a level road is*

$$
t = \frac{27.78}{g\mu_x \dfrac{a_1}{l - h\mu_x}} \approx 5.11 \, \text{s}
\tag{2.115}
$$

*If the same car was front-wheel-drive, then the traction force would be*

$$
\begin{aligned}
2F_{x_1} &= 2\mu_x F_{z_1} \\
&= \mu_x mg \frac{a_2}{l} - \mu_x mg \frac{h}{l}\frac{1}{g}a \\
&= ma.
\end{aligned}
\tag{2.116}
$$

*and the equation of motion would reduce to*

$$
\begin{aligned}
a = \ddot{x} &= \frac{\mu_x g \dfrac{a_2}{l}}{1 + \mu_x g \dfrac{h}{l}\dfrac{1}{g}} \\
&= g\mu_x \frac{a_2}{l + h\mu_x}.
\end{aligned}
\tag{2.117}
$$

*The minimum time for* $0 - 100 \,\text{km/h}$ *on a level road for this front-wheel-drive car is*

$$
t = \frac{27.78}{g\mu_x \dfrac{a_2}{l + h\mu_x}} \approx 6.\,21\,\text{s}.
\tag{2.118}
$$

*Now consider the same car to be four-wheel-drive. Then, the traction force is*

$$
\begin{aligned}
2F_{x_1} + 2F_{x_2} &= 2\mu_x \left(F_{z_1} + F_{z_2}\right) \\
&= \frac{g}{l}m\left(a_1 + a_2\right) \\
&= ma.
\end{aligned}
\tag{2.119}
$$

*and the minimum time for* $0 - 100 \,\text{km/h}$ *on a level road for this four-wheel-drive car can theoretically be reduced to*

$$
t = \frac{27.78}{g} \approx 2.83\,\text{s}.
\tag{2.120}
$$

## 2.4  Accelerating Car on an Inclined Road

When a car is accelerating on an inclined pavement with angle $\phi$ as shown in Figure 2.9, the normal force under each of the front and rear wheels, $F_{z_1}$, $F_{z_2}$, would be:

$$
F_{z_1} = \frac{1}{2}mg\left(\frac{a_2}{l}\cos\phi - \frac{h}{l}\sin\phi\right) - \frac{1}{2}ma\frac{h}{l}
\tag{2.121}
$$

$$
F_{z_2} = \frac{1}{2}mg\left(\frac{a_1}{l}\cos\phi + \frac{h}{l}\sin\phi\right) + \frac{1}{2}ma\frac{h}{l}
\tag{2.122}
$$

$$
l = a_1 + a_2
$$
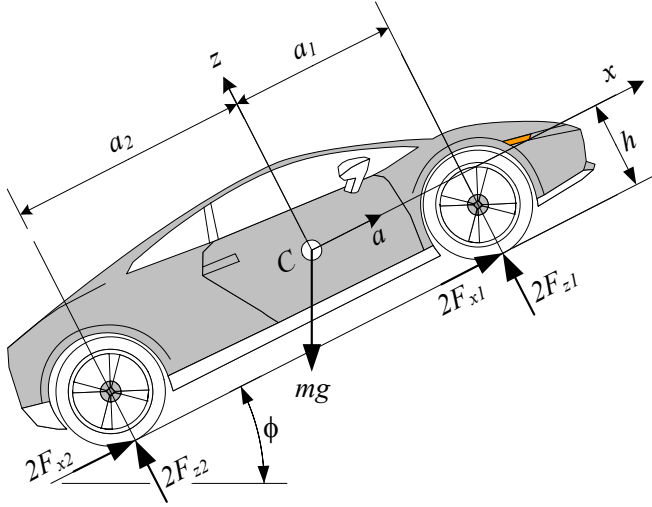
FIGURE 2.9. An accelerating car on inclined pavement.

The dynamic parts, $\pm\frac{1}{2}mg\frac{h}{l}\frac{a}{g}$, depend on acceleration $a$ and height $h$ of mass center $C$ and remain unchanged, while the static parts are influenced by the slope angle $\phi$ and height $h$ of mass center.

**Proof.** The Newton's equation in $x$-direction and two static equilibrium equations, must be examined to find the equation of motion and ground reaction forces.

$$\sum F_x = ma \tag{2.123}$$

$$\sum F_z = 0 \tag{2.124}$$

$$\sum M_y = 0. \tag{2.125}$$

Expanding these equations produces three equations for four unknowns $F_{x_1}$, $F_{x_2}$, $F_{z_1}$, $F_{z_2}$.

$$2F_{x_1} + 2F_{x_2} - mg\sin\phi = ma \tag{2.126}$$

$$2F_{z_1} + 2F_{z_2} - mg\cos\phi = 0 \tag{2.127}$$

$$2F_{z_1}a_1 - 2F_{z_2}a_2 + 2\left(F_{x_1} + F_{x_2}\right)h = 0 \tag{2.128}$$

It is possible to eliminate $\left(F_{x_1} + F_{x_2}\right)$ between the first and third equations, and solve for the normal forces $F_{z_1}$, $F_{z_2}$.

$$
\begin{aligned}
F_{z_1} &= \left(F_{z_1}\right)_{st} + \left(F_{z_1}\right)_{dyn} \\
&= \frac{1}{2}mg\left(\frac{a_2}{l}\cos\phi - \frac{h}{l}\sin\phi\right) - \frac{1}{2}ma\frac{h}{l} \tag{2.129}
\end{aligned}
$$

$$F_{z_2} = (F_{z_2})_{st} + (F_{z_2})_{dyn}$$

$$= \frac{1}{2}mg\left(\frac{a_1}{l}\cos\phi + \frac{h}{l}\sin\phi\right) + \frac{1}{2}ma\frac{h}{l} \qquad (2.130)$$

∎

**Example 55** *Front-wheel-drive car, accelerating on inclined road.*
For a front-wheel-drive car, we may substitute $F_{x_1} = 0$ in Equations (2.126) and (2.128) to have the governing equations. However, it does not affect the ground reaction forces under the tires (2.129 and 2.130) as long as the car is driven under its limit conditions.

**Example 56** *Rear-wheel-drive car, accelerating on inclined road.*
Substituting $F_{x_2} = 0$ in Equations (2.126) and (2.128) and solving for the normal reaction forces under each tire provides the same results as (2.129) and (2.130). Hence, the normal forces applied on the tires do not sense if the car is front-, rear-, or all-wheel drive. As long as we drive in a straight path at low acceleration, the drive wheels can be the front or the rear ones. However, the advantages and disadvantages of front-, rear-, or all-wheel drive cars appear in maneuvering, slippery roads, or when the maximum acceleration is required.

**Example 57** *Maximum acceleration on an inclined road.*
The maximum acceleration depends on the friction under the tires. Let's assume the friction coefficients at the front and rear tires are equal. Then, the front and rear traction forces are

$$F_{x_1} \leq \mu_x F_{z_1} \qquad (2.131)$$

$$F_{x_2} \leq \mu_x F_{z_2}. \qquad (2.132)$$

If we assume the front and rear wheels reach their traction limits at the same time, then

$$F_{x_1} = \pm\mu_x F_{z_1} \qquad (2.133)$$

$$F_{x_2} = \pm\mu_x F_{z_2} \qquad (2.134)$$

and we may rewrite Newton's equation (2.123) as

$$ma_M = \pm 2\mu_x\left(F_{z_1} + F_{z_2}\right) - mg\sin\phi \qquad (2.135)$$

where, $a_M$ is the maximum achievable acceleration.
Now substituting $F_{z_1}$ and $F_{z_2}$ from (2.129) and (2.130) results in

$$\frac{a_M}{g} = \pm\mu_x\cos\phi - \sin\phi. \qquad (2.136)$$

Accelerating on an uphill road $(a > 0, \phi > 0)$ and braking on a downhill road $(a < 0, \phi < 0)$ are the extreme cases in which the car can stall. In these cases, the car can move as long as

$$\mu_x \geq |\tan\phi|. \qquad (2.137)$$

**Example 58** *Limits of acceleration and inclination angle.*
   *Assuming $F_{z_1} > 0$ and $F_{z_2} > 0$, we can write Equations (2.121) and (2.122) as*

$$\frac{a}{g} \leq \frac{a_2}{h} \cos\phi - \sin\phi \tag{2.138}$$

$$\frac{a}{g} \geq -\frac{a_1}{h} \cos\phi - \sin\phi. \tag{2.139}$$

*Hence, the maximum achievable acceleration $(a > 0)$ is limited by $a_2$, $h$, $\phi$; while the maximum deceleration $(a < 0)$ is limited by $a_1$, $h$, $\phi$. These two equations can be combined to result in*

$$-\frac{a_1}{h} \cos\phi \leq \frac{a}{g} + \sin\phi \leq \frac{a_2}{h} \cos\phi. \tag{2.140}$$

   *If $a \to 0$, then the limits of the inclination angle would be*

$$-\frac{a_1}{h} \leq \tan\phi \leq \frac{a_2}{h}. \tag{2.141}$$

*This is the maximum and minimum road inclination angles that the car can stay on without tilting and falling.*

**Example 59** *Maximum deceleration for a single-axle-brake car.*
   *We can find the maximum braking deceleration $a_{fwb}$ of a front-wheel-brake car on a horizontal road by substituting $\phi = 0$, $F_{x_2} = 0$, $F_{x_1} = -\mu_x F_{z_1}$ in Equation (2.126) and using Equation (2.121)*

$$-\mu_x mg \left( \frac{a_2}{l} - \frac{h}{l} \frac{a_{rwb}}{g} \right) = m a_{fwb} \tag{2.142}$$

*therefore,*

$$\frac{a_{fwb}}{g} = -\frac{\mu_x}{1 - \mu_x \dfrac{h}{l}} \left( 1 - \frac{a_1}{l} \right). \tag{2.143}$$

*Similarly, the maximum braking deceleration $a_{rwb}$ of a front-wheel-brake car can be achieved when we substitute $F_{x_2} = 0$, $F_{x_1} = \mu_x F_{z_1}$.*

$$\frac{a_{rwb}}{g} = -\frac{\mu_x}{1 + \mu_x \dfrac{h}{l}} \frac{a_1}{l} \tag{2.144}$$

*The effect of changing the position of the mass center on the maximum achievable braking deceleration is shown in Figure 2.10 for a sample car with*

$$\begin{aligned} \mu_x &= 1 \\ h &= 0.56\,\mathrm{m} \\ l &= 2.6\,\mathrm{m}. \end{aligned} \tag{2.145}$$
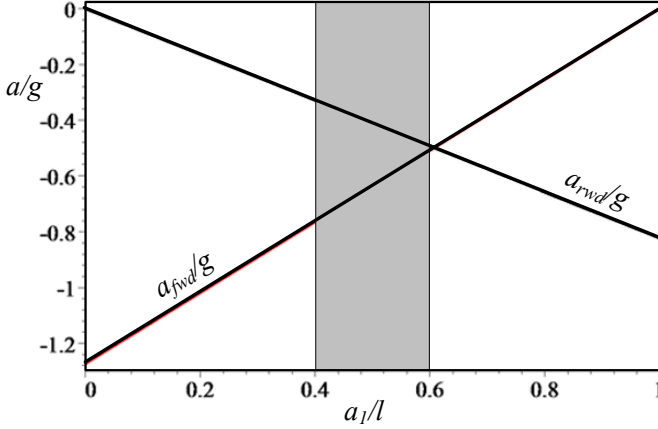
FIGURE 2.10. Effect of mass center position on the maximum achievable deccel-
eration of a front-wheel and a rear-wheel-drive car.

Passenger cars are usually in the range $0.4 < (a_1/l) < 0.6$. In this range,
$(a_{fwb}/g) < (a_{rwb}/g)$ and therefore, front-wheel-brake cars can reach better
forward deceleration than rear-wheel-brake cars. Hence, front brakes are
much more important than the rear brakes.

**Example 60 ★** *A car with a trailer.*
Figure 2.11 depicts a car moving on an inclined road and pulling a trailer.
To analyze the car-trailer motion, we need to separate the car and trailer
to see the forces at the hinge, as shown in Figure 2.12. We assume the
mass center of the trailer $C_t$ is at distance $b_3$ in front of the only axle of
the trailer. If $C_t$ is behind the trailer axle, then $b_3$ should be negative in the
following equations.
For an ideal hinge between a car and a trailer moving in a straight path,
there must be a horizontal force $F_{x_t}$ and a vertical force $F_{z_t}$.
Writing the Newton's equation in $x$-direction and two static equilibrium
equations for both the trailer and the vehicle

$$\sum F_x = m_t a \tag{2.146}$$

$$\sum F_z = 0 \tag{2.147}$$

$$\sum M_y = 0 \tag{2.148}$$

we find the following set of equations:

$$F_{x_t} - m_t\, g \sin \phi = m_t\, a \tag{2.149}$$

$$2F_{z_3} - F_{z_t} - m_t\, g \cos \phi = 0 \tag{2.150}$$

$$2F_{z_3} b_3 - F_{z_t} b_2 - F_{x_t}\, (h_2 - h_1) = 0 \tag{2.151}$$
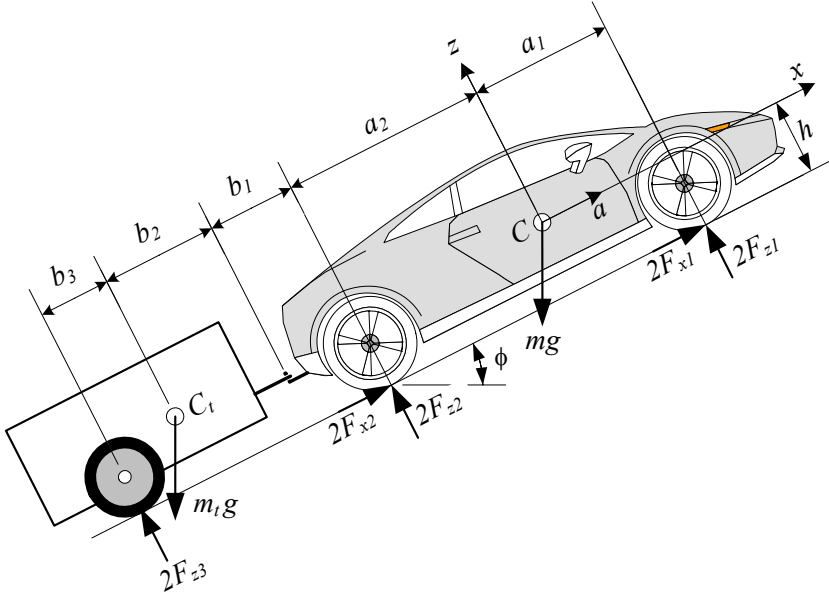
FIGURE 2.11. A car moving on an inclined road and pulling a trailer.

$$2F_{x_1} + 2F_{x_2} - F_{x_t} - mg \sin \phi = ma \qquad (2.152)$$

$$2F_{z_1} + 2F_{z_2} - F_{z_t} - mg \cos \phi = 0 \qquad (2.153)$$

$$2F_{z_1} a_1 - 2F_{z_2} a_2 + 2 \left( F_{x_1} + F_{x_2} \right) h$$
$$-F_{x_t} \left( h - h_1 \right) + F_{z_t} \left( b_1 + a_2 \right) = 0 \qquad (2.154)$$

*If the value of traction forces $F_{x_1}$ and $F_{x_2}$ are given, then these are six equations for six unknowns: $a$, $F_{x_t}$, $F_{z_t}$, $F_{z_1}$, $F_{z_2}$, $F_{z_3}$. Solving these equations provide the following solutions:*

$$a = \frac{2}{m + m_t} \left( F_{x_1} + F_{x_2} \right) - g \sin \phi \qquad (2.155)$$

$$F_{x_t} = \frac{2m_t}{m + m_t} \left( F_{x_1} + F_{x_2} \right) \qquad (2.156)$$

$$F_{z_t} = \frac{h_1 - h_2}{b_2 - b_3} \frac{2m_t}{m + m_t} \left( F_{x_1} + F_{x_2} \right) + \frac{b_3}{b_2 - b_3} m_t \, g \cos \phi \qquad (2.157)$$

$$F_{z_1} = \frac{b_3}{2l} \left( \frac{2a_2 - b_1}{b_2 - b_3} m_t + \frac{a_2}{b_3} m \right) g \cos \phi$$
$$+ \left[ \frac{2a_2 - b_1}{b_2 - b_3} \left( h_1 - h_2 \right) m_t - h_1 m_t - hm \right] \frac{F_{x_1} + F_{x_2}}{l \left( m + m_t \right)} \qquad (2.158)$$
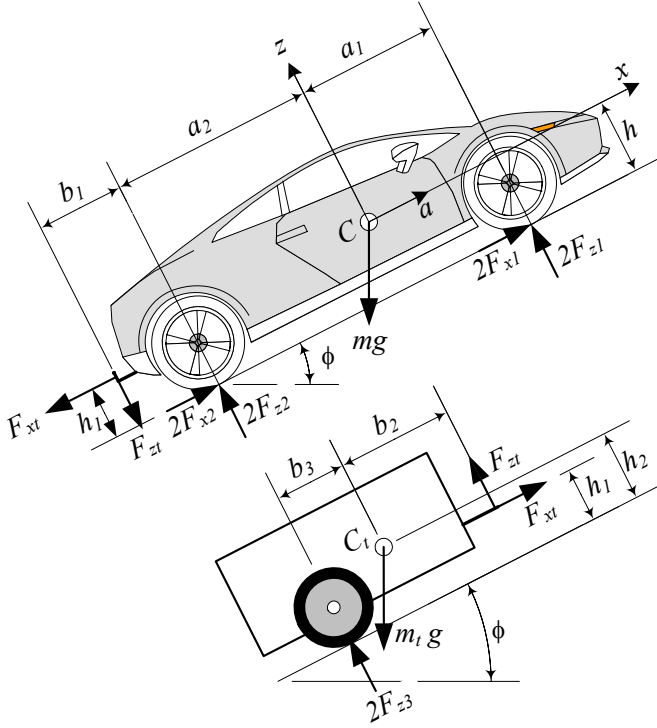
FIGURE 2.12. Free-body-diagram of a car and the trailer when moving on an uphill road.

$$F_{z_2} = \frac{b_3}{2l}\left(\frac{a_1 - a_2 + b_1}{b_2 - b_3}m_t + \frac{a_1}{b_3}m\right)g\cos\phi$$

$$+ \left[\frac{a_1 - a_2 + b_1}{b_2 - b_3}(h_1 - h_2)m_t + h_1 m_t + hm\right]\frac{F_{x_1} + F_{x_2}}{l(m + m_t)} \quad (2.159)$$

$$F_{z_3} = \frac{1}{2}\frac{b_2}{b_2 - b_3}m_t g\cos\phi + \frac{h_1 - h_2}{b_2 - b_3}\frac{m_t}{m + m_t}(F_{x_1} + F_{x_2}) \quad (2.160)$$

$$l = a_1 + a_2. \quad (2.161)$$

However, if the value of acceleration $a$ is known, then unknowns are: $F_{x_1} + F_{x_2}$, $F_{x_t}$, $F_{z_t}$, $F_{z_1}$, $F_{z_2}$, $F_{z_3}$.

$$F_{x_1} + F_{x_2} = \frac{1}{2}(m + m_t)(a + g\sin\phi) \quad (2.162)$$

$$F_{x_t} = m_t(a + g\sin\phi) \quad (2.163)$$

$$F_{z_t} = \frac{h_1 - h_2}{b_2 - b_3}m_t(a + g\sin\phi) + \frac{b_3}{b_2 - b_3}m_t g\cos\phi \quad (2.164)$$

$$F_{z_1} = \frac{b_3}{2l}\left(\frac{2a_2 - b_1}{b_2 - b_3}m_t + \frac{a_2}{b_3}m\right)g\cos\phi \tag{2.165}$$

$$+\frac{1}{2l}\left[\frac{2a_2 - b_1}{b_2 - b_3}(h_1 - h_2)m_t - h_1 m_t - hm\right](a + g\sin\phi)$$

$$F_{z_2} = \frac{b_3}{2l}\left(\frac{a_1 - a_2 + b_1}{b_2 - b_3}m_t + \frac{a_1}{b_3}m\right)g\cos\phi \tag{2.166}$$

$$+\frac{1}{2l}\left[\frac{a_1 - a_2 + b_1}{b_2 - b_3}(h_1 - h_2)m_t + h_1 m_t + hm\right](a + g\sin\phi)$$

$$F_{z_3} = \frac{1}{2}\frac{m_t}{b_2 - b_3}(b_2\,g\cos\phi + (h_1 - h_2)(a + g\sin\phi)) \tag{2.167}$$

$$l = a_1 + a_2.$$

**Example 61** ★ *Maximum inclination angle for a car with a trailer.*
*For a car and trailer as shown in Figure 2.11, the maximum inclina-
tion angle $\phi_M$ is the angle at which the car cannot accelerate the vehicle.
Substituting $a = 0$ and $\phi = \phi_M$ in Equation (2.155) shows that*

$$\sin\phi_M = \frac{2}{(m + m_t)\,g}(F_{x_1} + F_{x_2}). \tag{2.168}$$

*The value of maximum inclination angle $\phi_M$ increases by decreasing the
total weight of the vehicle and trailer $(m + m_t)\,g$ or increasing the traction
force $F_{x_1} + F_{x_2}$.*
*The traction force is limited by the maximum torque on the drive wheel
and the friction under the drive tire. Let's assume the vehicle is four-wheel-
drive and friction coefficients at the front and rear tires are equal. Then,
the front and rear traction forces are*

$$F_{x_1} \leq \mu_x F_{z_1} \tag{2.169}$$

$$F_{x_2} \leq \mu_x F_{z_2}. \tag{2.170}$$

*If we assume the front and rear wheels reach their traction limits at the
same time, then*

$$F_{x_1} = \mu_x F_{z_1} \tag{2.171}$$

$$F_{x_2} = \mu_x F_{z_2} \tag{2.172}$$

*and we may rewrite the Equation (2.168) as*

$$\sin\phi_M = \frac{2\mu_x}{(m + m_t)\,g}(F_{z_1} + F_{z_2}). \tag{2.173}$$

*Now substituting $F_{z_1}$ and $F_{z_2}$ from (2.158) and (2.159) results in*

$$(mb_3 - mb_2 - m_t b_3)\,\mu_x\cos\phi_M + (b_2 - b_3)(m + m_t)\sin\phi_M$$
$$= 2\mu_x\frac{m_t(h_1 - h_2)}{m + m_t}(F_{x_1} + F_{x_2}). \tag{2.174}$$

*If we arrange Equation (2.174) as*

$$A \cos \phi_M + B \sin \phi_M = C \tag{2.175}$$

*then*

$$\phi_M = \text{atan2}(\frac{C}{\sqrt{A^2 + B^2}}, \pm\sqrt{1 - \frac{C^2}{A^2 + B^2}}) - \text{atan2}(A, B) \tag{2.176}$$

*and*

$$\phi_M = \text{atan2}(\frac{C}{\sqrt{A^2 + B^2}}, \pm\sqrt{A^2 + B^2 - C^2}) - \text{atan2}(A, B) \tag{2.177}$$

*where*

$$
\begin{aligned}
A &= (mb_3 - mb_2 - m_t b_3)\, \mu_x & (2.178) \\
B &= (b_2 - b_3)(m + m_t) & (2.179) \\
C &= 2\mu_x \frac{m_t(h_1 - h_2)}{m + m_t}(F_{x_1} + F_{x_2}). & (2.180)
\end{aligned}
$$

*For a rear-wheel-drive car pulling a trailer with the following character-istics:*

$$
\begin{aligned}
l &= 2272\,\text{mm} \\
w &= 1457\,\text{mm} \\
h &= 230\,\text{mm} \\
a_1 &= a_2 \\
h_1 &= 310\,\text{mm} \\
b_1 &= 680\,\text{mm} \\
b_2 &= 610\,\text{mm} \\
b_3 &= 120\,\text{mm} & (2.181) \\
h_2 &= 560\,\text{mm} \\
m &= 1500\,\text{kg} \\
m_t &= 150\,\text{kg} \\
\mu_x &= 1 \\
\phi &= 10\,\text{deg} \\
a &= 1\,\text{m/s}^2
\end{aligned}
$$

*we find*

$$
\begin{aligned}
F_{z_1} &= 3441.78\,\text{N} \\
F_{z_2} &= 3877.93\,\text{N} \\
F_{z_3} &= 798.57\,\text{N} \\
F_{z_t} &= 147.99\,\text{N} & (2.182) \\
F_{x_t} &= 405.52\,\text{N} \\
F_{x_2} &= 2230.37\,\text{N}.
\end{aligned}
$$

*To check if the required traction force $F_{x_2}$ is applicable, we should compare it to the maximum available friction force $\mu F_{z_2}$ and it must be*

$$F_{x_2} \le \mu F_{z_2}. \tag{2.183}$$

**Example 62** ★ *Solution of equation $a\cos\theta + b\sin\theta = c$.*
   *The first type of trigonometric equation is*

$$a\cos\theta + b\sin\theta = c. \tag{2.184}$$

*It can be solved by introducing two new variables $r$ and $\eta$ such that*

$$a = r\sin\eta \tag{2.185}$$
$$b = r\cos\eta \tag{2.186}$$

*and therefore,*

$$r = \sqrt{a^2 + b^2} \tag{2.187}$$
$$\eta = \operatorname{atan2}(a, b). \tag{2.188}$$

*Substituting the new variables show that*

$$\sin(\eta + \theta) = \frac{c}{r} \tag{2.189}$$

$$\cos(\eta + \theta) = \pm\sqrt{1 - \frac{c^2}{r^2}}. \tag{2.190}$$

*Hence, the solutions of the problem are*

$$\theta = \operatorname{atan2}(\frac{c}{r}, \pm\sqrt{1 - \frac{c^2}{r^2}}) - \operatorname{atan2}(a, b) \tag{2.191}$$

*and*

$$\theta = \operatorname{atan2}(\frac{c}{r}, \pm\sqrt{r^2 - c^2}) - \operatorname{atan2}(a, b). \tag{2.192}$$

   *Therefore, the equation $a\cos\theta + b\sin\theta = c$ has two solutions if $r^2 = a^2 + b^2 > c^2$, one solution if $r^2 = c^2$, and no solution if $r^2 < c^2$.*

**Example 63** ★ *The function $\tan_2^{-1}\frac{y}{x} = \operatorname{atan2}(y, x)$.*
   *There are many situations in kinematics calculation in which we need to find an angle based on the $\sin$ and $\cos$ functions of an angle. However, $\tan^{-1}$ cannot show the effect of the individual sign for the numerator and denominator. It always represents an angle in the first or fourth quadrant. To overcome this problem and determine the angle in the correct quadrant, the $\operatorname{atan2}$ function is introduced as below.*

$$\operatorname{atan2}(y, x) = \begin{cases} \tan^{-1}\dfrac{y}{x} & if \quad y > 0 \\ \tan^{-1}\dfrac{y}{x} + \pi\operatorname{sign} y & if \quad y < 0 \\ \dfrac{\pi}{2}\operatorname{sign} x & if \quad y = 0 \end{cases} \tag{2.193}$$

*In this text, whether it has been mentioned or not, wherever $\tan^{-1}\frac{y}{x}$ is used, it must be calculated based on $\operatorname{atan2}(y, x)$.*

**Example 64** *Zero vertical force at the hinge.*
*We can make the vertical force at the hinge equal to zero by examining Equation (2.157) for the hinge vertical force $F_{z_t}$.*

$$F_{z_t} = \frac{h_1 - h_2}{b_2 - b_3} \frac{2m_t}{m + m_t} (F_{x_1} + F_{x_2}) + \frac{b_3}{b_2 - b_3} m_t\, g \cos\phi \qquad (2.194)$$

*To make $F_{z_t} = 0$, it is enough to adjust the position of trailer mass center $C_t$ exactly on top of the trailer axle and at the same height as the hinge. In these conditions we have*

$$h_1 \;=\; h_2 \qquad\qquad (2.195)$$
$$b_3 \;=\; 0 \qquad\qquad (2.196)$$

*that makes*

$$F_{z_t} = 0. \qquad\qquad (2.197)$$

*However, to increase safety, the load should be distributed evenly throughout the trailer. Heavy items should be loaded as low as possible, mainly over the axle. Bulkier and lighter items should be distributed to give a little positive $b_3$. Such a trailer is called nose weight at the towing coupling.*

## 2.5   Parked Car on a Banked Road

Figure 2.13 depicts the effect of a bank angle $\phi$ on the load distribution of a vehicle. A bank causes the load on the lower tires to increase, and the load on the upper tires to decrease. The tire reaction forces are:

$$F_{z_1} = \frac{1}{2}\frac{mg}{w}\left(b_2 \cos\phi - h \sin\phi\right) \qquad\qquad (2.198)$$

$$F_{z_2} = \frac{1}{2}\frac{mg}{w}\left(b_1 \cos\phi + h \sin\phi\right) \qquad\qquad (2.199)$$

$$w = b_1 + b_2 \qquad\qquad (2.200)$$

**Proof.** Starting with equilibrium equations

$$\sum F_y = 0 \qquad\qquad (2.201)$$

$$\sum F_z = 0 \qquad\qquad (2.202)$$

$$\sum M_x = 0. \qquad\qquad (2.203)$$
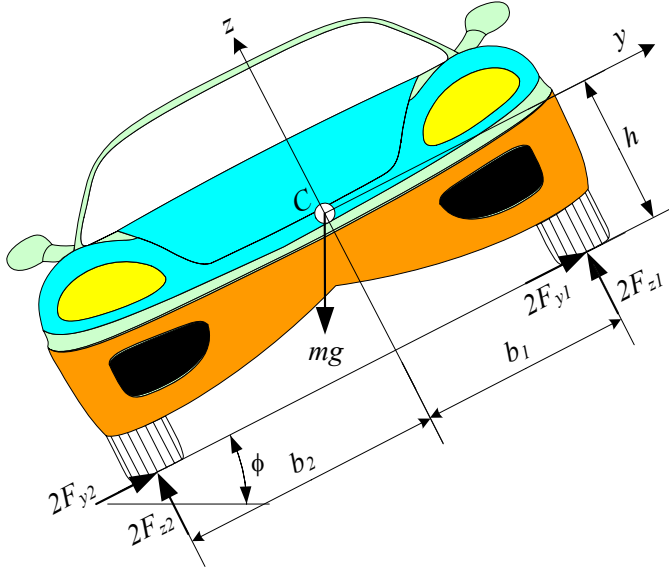
FIGURE 2.13. Normal force under the uphill and downhill tires of a vehicle, parked on banked road.

we can write

$$2F_{y_1} + 2F_{y_2} - mg\sin\phi = 0 \qquad (2.204)$$

$$2F_{z_1} + 2F_{z_2} - mg\cos\phi = 0 \qquad (2.205)$$

$$2F_{z_1}b_1 - 2F_{z_2}b_2 + 2\left(F_{y_1} + F_{y_2}\right)h = 0. \qquad (2.206)$$

We assumed the force under the lower tires, front and rear, are equal, and also the forces under the upper tires, front and rear are equal. To calculate the reaction forces under each tire, we may assume the overall lateral force $F_{y_1} + F_{y_2}$ as an unknown. The solution of these equations provide the lateral and reaction forces under the upper and lower tires.

$$F_{z_1} = \frac{1}{2}mg\frac{b_2}{w}\cos\phi - \frac{1}{2}mg\frac{h}{w}\sin\phi \qquad (2.207)$$

$$F_{z_2} = \frac{1}{2}mg\frac{b_1}{w}\cos\phi + \frac{1}{2}mg\frac{h}{w}\sin\phi \qquad (2.208)$$

$$F_{y_1} + F_{y_2} = \frac{1}{2}mg\sin\phi \qquad (2.209)$$

At the ultimate angle $\phi = \phi_M$, all wheels will begin to slide simultaneously and therefore,

$$F_{y_1} = \mu_{y_1}F_{z_1} \qquad (2.210)$$

$$F_{y_2} = \mu_{y_2}F_{z_2}. \qquad (2.211)$$

The equilibrium equations show that

$$2\mu_{y_1} F_{z_1} + 2\mu_{y_2} F_{z_2} - mg\sin\phi = 0 \tag{2.212}$$

$$2F_{z_1} + 2F_{z_2} - mg\cos\phi = 0 \tag{2.213}$$

$$2F_{z_1} b_1 - 2F_{z_2} b_2 + 2\left(\mu_{y_1} F_{z_1} + \mu_{y_2} F_{z_2}\right) h = 0. \tag{2.214}$$

Assuming

$$\mu_{y_1} = \mu_{y_2} = \mu_y \tag{2.215}$$

will provide

$$F_{z_1} = \frac{1}{2} mg \frac{b_2}{w} \cos\phi_M - \frac{1}{2} mg \frac{h}{w} \sin\phi_M \tag{2.216}$$

$$F_{z_2} = \frac{1}{2} mg \frac{b_1}{w} \cos\phi_M + \frac{1}{2} mg \frac{h}{w} \sin\phi_M \tag{2.217}$$

$$\tan\phi_M = \mu_y. \tag{2.218}$$

These calculations are correct as long as

$$\tan\phi_M \quad \leq \quad \frac{b_2}{h} \tag{2.219}$$

$$\mu_y \quad \leq \quad \frac{b_2}{h}. \tag{2.220}$$

If the lateral friction $\mu_y$ is higher than $b_2/h$ then the car will roll downhill. To increase the capability of a car moving on a banked road, the car should be as wide as possible with a mass center as low as possible. ∎

**Example 65** *Tire forces of a parked car in a banked road.*
   *A car having*

$$
\begin{aligned}
m &= 980\,\text{kg} \\
h &= 0.6\,\text{m} \\
w &= 1.52\,\text{m} \\
b_1 &= b_2
\end{aligned}
\tag{2.221}
$$

*is parked on a banked road with $\phi = 4\deg$. The forces under the lower and upper tires of the car are:*

$$
\begin{aligned}
F_{z_1} &= 2265.2\,\text{N} \\
F_{z_2} &= 2529.9\,\text{N} \\
F_{y_1} + F_{y_2} &= 335.3\,\text{N}
\end{aligned}
\tag{2.222}
$$

   *The ratio of the uphill force $F_{z_1}$ to downhill force $F_{z_2}$ depends on only the mass center position.*

$$\frac{F_{z_1}}{F_{z_2}} = \frac{b_2\cos\phi - h\sin\phi}{b_1\cos\phi + h\sin\phi} \tag{2.223}$$
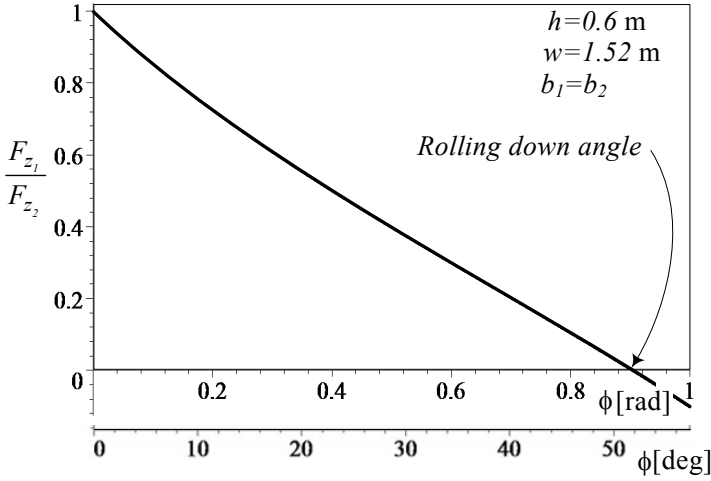
FIGURE 2.14. Illustration of the force ratio $F_{z_1}/F_{z_2}$ as a function of road bank angle $\phi$.

*Assuming a symmetric car with $b_1 = b_2 = w/2$ simplifies the equation to*

$$\frac{F_{z_1}}{F_{z_2}} = \frac{w\cos\phi - 2h\sin\phi}{w\cos\phi + 2h\sin\phi}. \tag{2.224}$$

*Figure 2.14 illustrates the behavior of force ratio $F_{z_1}/F_{z_2}$ as a function of $\phi$ for $h = 0.6$ m and $w = 1.52$ m. The rolling down angle $\phi_M = \tan^{-1}(b_2/h) = 51.71$ deg indicates the bank angle at which the force under the uphill wheels become zero and the car rolls down. The negative part of the curve indicates the required force to keep the car on the road, which is not applicable in real situations.*

## 2.6  ★ Optimal Drive and Brake Force Distribution

A certain acceleration $a$ can be achieved by adjusting and controlling the longitudinal forces $F_{x_1}$ and $F_{x_2}$. The optimal longitudinal forces under the front and rear tires to achieve the maximum acceleration are

$$
\begin{aligned}
\frac{F_{x_1}}{mg} &= -\frac{1}{2}\frac{h}{l}\left(\frac{a}{g}\right)^2 + \frac{1}{2}\frac{a_2}{l}\frac{a}{g} \\
&= -\frac{1}{2}\mu_x^2\frac{h}{l} + \frac{1}{2}\mu_x\frac{a_2}{l}
\end{aligned}
\tag{2.225}
$$

$$\frac{F_{x_2}}{mg} = \frac{1}{2}\frac{h}{l}\left(\frac{a}{g}\right)^2 + \frac{1}{2}\frac{a_1}{l}\frac{a}{g}$$

$$= \frac{1}{2}\mu_x^2\frac{h}{l} + \frac{1}{2}\mu_x\frac{a_1}{l}. \tag{2.226}$$

**Proof.** The longitudinal equation of motion for a car on a horizontal road is

$$2F_{x_1} + 2F_{x_2} = ma \tag{2.227}$$

and the maximum traction forces under each tire is a function of normal force and the friction coefficient.

$$F_{x_1} \leq \pm\mu_x F_{z_1} \tag{2.228}$$

$$F_{x_2} \leq \pm\mu_x F_{z_2} \tag{2.229}$$

However, the normal forces are a function of the car's acceleration and geometry.

$$F_{z_1} = \frac{1}{2}mg\frac{a_2}{l} - \frac{1}{2}mg\frac{h}{l}\frac{a}{g} \tag{2.230}$$

$$F_{z_2} = \frac{1}{2}mg\frac{a_1}{l} + \frac{1}{2}mg\frac{h}{l}\frac{a}{g} \tag{2.231}$$

We may generalize the equations by making them dimensionless. Under the best conditions, we should adjust the traction forces to their maximum

$$\frac{F_{x_1}}{mg} = \frac{1}{2}\mu_x\left(\frac{a_2}{l} - \frac{h}{l}\frac{a}{g}\right) \tag{2.232}$$

$$\frac{F_{x_2}}{mg} = \frac{1}{2}\mu_x\left(\frac{a_1}{l} + \frac{h}{l}\frac{a}{g}\right) \tag{2.233}$$

and therefore, the longitudinal equation of motion (2.227) becomes

$$\frac{a}{g} = \mu_x. \tag{2.234}$$

Substituting this result back into Equations (2.232) and (2.233) shows that

$$\frac{F_{x_1}}{mg} = -\frac{1}{2}\frac{h}{l}\left(\frac{a}{g}\right)^2 + \frac{1}{2}\frac{a_2}{l}\frac{a}{g} \tag{2.235}$$

$$\frac{F_{x_2}}{mg} = \frac{1}{2}\frac{h}{l}\left(\frac{a}{g}\right)^2 + \frac{1}{2}\frac{a_1}{l}\frac{a}{g}. \tag{2.236}$$

Depending on the geometry of the car $(h, a_1, a_2)$, and the acceleration $a > 0$, these two equations determine how much the front and rear driving forces must be. The same equations are applied for deceleration $a < 0$, to
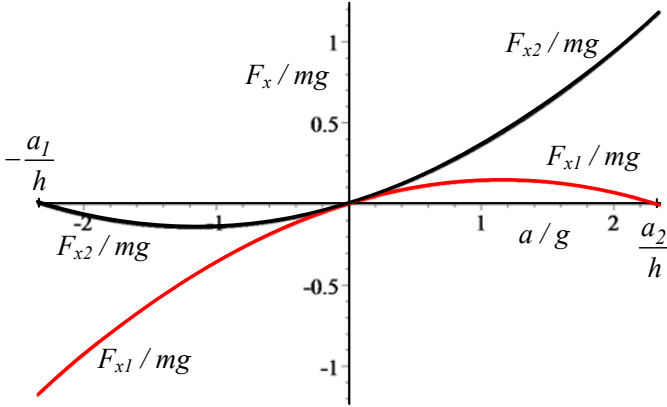
FIGURE 2.15. Optimal driving and braking forces for a sample car.

determine the value of optimal front and rear braking forces. Figure 2.15 represents a graphical illustration of the optimal driving and braking forces for a sample car using the following data:

$$
\begin{aligned}
\mu_x &= 1 \\
\frac{h}{l} &= \frac{0.56}{2.6} = 0.21538 \\
\frac{a_1}{l} &= \frac{a_2}{l} = \frac{1}{2}.
\end{aligned}
\tag{2.237}
$$

When accelerating $a > 0$, the optimal driving force on the rear tire grows rapidly while the optimal driving force on the front tire drops after a maximum. The value $(a/g) = (a_2/h)$ is the maximum possible acceleration at which the front tires lose their contact with the ground. The acceleration at which front (or rear) tires lose their ground contact is called *tilting acceleration*.

The opposite phenomenon happens when decelerating. For $a < 0$, the optimal front brake force increases rapidly and the rear brake force goes to zero after a minimum. The deceleration $(a/g) = -(a_1/h)$ is the maximum possible deceleration at which the rear tires lose their ground contact.

The graphical representation of the optimal driving and braking forces can be shown better by plotting $F_{x_1}/(mg)$ versus $F_{x_2}/(mg)$ using $(a/g)$ as a parameter.

$$
F_{x_1} = \frac{a_2 - \dfrac{a}{g}h}{a_1 + \dfrac{a}{g}h} F_{x_2}
\tag{2.238}
$$

$$
\frac{F_{x_1}}{F_{x_2}} = \frac{a_2 - \mu_x h}{a_1 + \mu_x h}
\tag{2.239}
$$
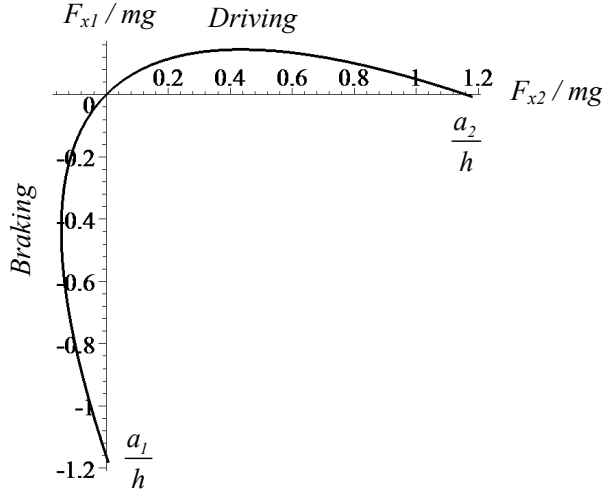
FIGURE 2.16. Optimal traction and braking force distribution between the front and rear wheels.

Such a plot is shown in Figure 2.16. This is a design curve describing the relationship between forces under the front and rear wheels to achieve the maximum acceleration or deceleration.

Adjusting the optimal force distribution is not an automatic procedure and needs a force distributor control system to measure and adjust the forces. ∎

**Example 66** ★ *Slope at zero.*

*The initial optimal traction force distribution is the slope of the optimal curve* $(F_{x_1}/(mg), F_{x_2}/(mg))$ *at zero.*

$$\frac{d\dfrac{F_{x_1}}{mg}}{d\dfrac{F_{x_2}}{mg}} = \lim_{a \to 0} \frac{-\dfrac{1}{2}\dfrac{h}{l}\left(\dfrac{a}{g}\right)^2 + \dfrac{1}{2}\dfrac{a_2}{l}\dfrac{a}{g}}{\dfrac{1}{2}\dfrac{h}{l}\left(\dfrac{a}{g}\right)^2 + \dfrac{1}{2}\dfrac{a_1}{l}\dfrac{a}{g}}$$

$$= \frac{a_2}{a_1} \tag{2.240}$$

*Therefore, the initial traction force distribution depends on only the position of mass center C.*

**Example 67** ★ *Brake balance and ABS.*

*When braking, a car is stable if the rear wheels do not lock. Thus, the rear brake forces must be less than the maximum possible braking force at all time. This means the brake force distribution should always be in the shaded area of Figure 2.17, and below the optimal curve. This restricts the*

FIGURE 2.17. Optimal braking force distribution between the front and rear wheels, along with a thre-line under estimation.

*achievable deceleration, especially at low friction values, but increases the stability of the car.*

*Whenever it is easier for a force distributor to follow a line, the optimal brake curve is underestimated using two or three lines, and a control system adjusts the force ratio $F_{x_1}/F_{x_2}$. A sample of three-line approximation is shown in Figure 2.17.*

*Distribution of the brake force between the front and rear wheels is called* **brake balance***. Brake balance varies with deceleration. The higher the stop, the more load will transfer to the front wheels and the more braking effort they can support. Meanwhile the rear wheels are unloaded and they must have less braking force.*

**Example 68 ★** *Best race car.*

*Racecars always work at the maximum achievable acceleration to finish their race in minimum time. They are usually designed with rear-wheel-drive and all-wheel-brake. However, if an all-wheel-drive race car is reasonable to build, then a force distributor, to follow the curve shown in Figure 2.18, is what it needs to race better.*

**Example 69 ★** *Effect of $C$ location on braking.*

*Load is transferred from the rear wheels to the front when the brakes are applied. The higher the $C$, the more load transfer. So, to improve braking, the mass center $C$ should be as low as possible and as back as possible. This is not feasible for every vehicle, especially for forward-wheel drive street cars. However, this fact should be taken into account when a car is*

$F_{x1} / mg$


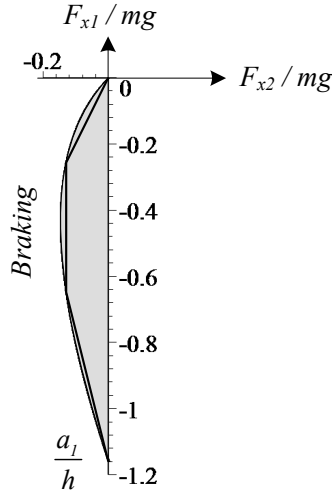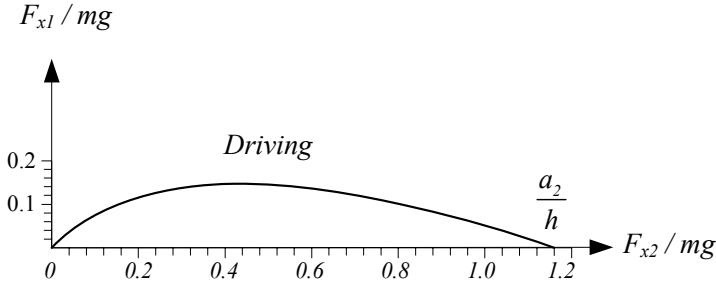
FIGURE 2.18. Optimal traction force distribution between the front and rear wheels.
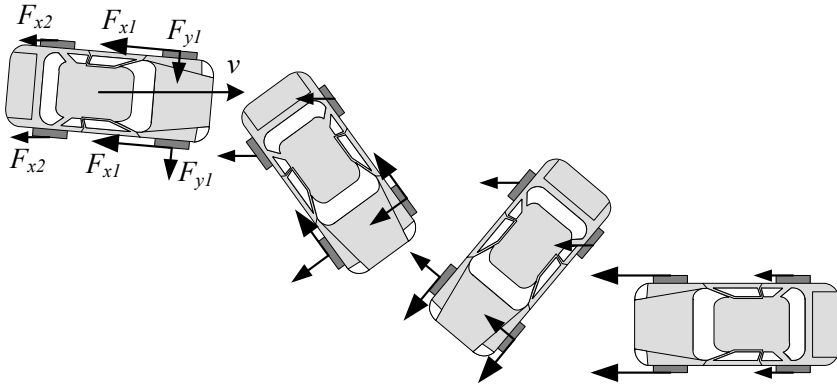


FIGURE 2.19. 180 deg sliding rotation of a rear-wheel-locked car.

being designed for better braking performance.

**Example 70 ★** *Front and rear wheel locking.*

*The optimal brake force distribution is according to Equation (2.239) for an ideal $F_{x_1}/F_{x_2}$ ratio. However, if the brake force distribution is not ideal, then either the front or the rear wheels will lock up first. Locking the rear wheels makes the vehicle unstable, and it loses directional stability. When the rear wheels lock, they slide on the road and they lose their capacity to support lateral force. The resultant shear force at the tireprint of the rear wheels reduces to a dynamic friction force in the opposite direction of the sliding.*

*A slight lateral motion of the rear wheels, by any disturbance, develops a yaw motion because of unbalanced lateral forces on the front and rear wheels. The yaw moment turns the vehicle about the z-axis until the rear end leads the front end and the vehicle turns 180 deg. Figure 2.19 illustrates a 180 deg sliding rotation of a rear-wheel-locked car.*

*The lock-up of the front tires does not cause a directional instability, although the car would not be steerable and the driver would lose control.*


## 2.7 ★ Vehicles With More Than Two Axles

If a vehicle has more than two axles, such as the three-axle car shown in Figure 2.20, then the vehicle will be statically indeterminate and the normal forces under the tires cannot be determined by static equilibrium equations. We need to consider the suspensions' deflection to determine their applied forces.

The $n$ normal forces $F_{z_i}$ under the tires can be calculated using the following $n$ algebraic equations.

$$2\sum_{i=1}^{n} F_{z_i} - mg\cos\phi = 0 \tag{2.241}$$

$$2\sum_{i=1}^{n} F_{z_i}x_i + h\left(a + mg\sin\phi\right) = 0 \tag{2.242}$$

$$\frac{F_{z_i}}{k_i} - \frac{x_i - x_1}{x_n - x_1}\left(\frac{F_{z_n}}{k_n} - \frac{F_{z_1}}{k_1}\right) - \frac{F_{z_1}}{k_1} = 0 \text{ for } i = 2, 3, \cdots, n-1 \tag{2.243}$$

where $F_{x_i}$ and $F_{z_i}$ are the longitudinal and normal forces under the tires attached to the axle number $i$, and $x_i$ is the distance of mass center $C$ from the axle number $i$. The distance $x_i$ is positive for axles in front of $C$, and is negative for the axles in back of $C$. The parameter $k_i$ is the vertical stiffness of the suspension at axle $i$.

**Proof.** For a multiple-axle vehicle, the following equations

$$\sum F_x = ma \tag{2.244}$$

$$\sum F_z = 0 \tag{2.245}$$

$$\sum M_y = 0 \tag{2.246}$$

provide the same sort of equations as (2.126)-(2.128). However, if the total number of axles are $n$, then the individual forces can be substituted by a summation.

$$2\sum_{i=1}^{n} F_{x_i} - mg\sin\phi = ma \tag{2.247}$$

$$2\sum_{i=1}^{n} F_{z_i} - mg\cos\phi = 0 \tag{2.248}$$
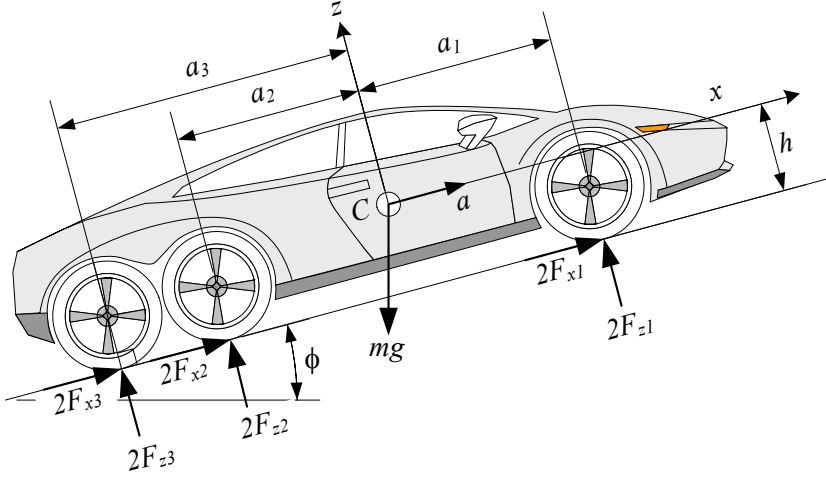
FIGURE 2.20. A three-axle car moving on an inclined road.

$$2\sum_{i=1}^{n} F_{z_i} x_i + 2h \sum_{i=1}^{n} F_{x_i} = 0 \tag{2.249}$$

The overall forward force $F_x = 2\sum_{i=1}^{n} F_{x_i}$ can be eliminated between Equations (2.247) and (2.249) to make Equation (2.242). Then, there remain two equations (2.241) and (2.242) for $n$ unknowns $F_{z_i}$, $i = 1, 2, \cdots, n$. Hence, we need $n - 2$ extra equations to be able to find the wheel loads. The extra equations come from the compatibility among the suspensions' deflection.

We ignore the tires' compliance, and use $z$ to indicate the static vertical displacement of the car at $C$. Then, if $z_i$ is the suspension deflection at the center of axle $i$, and $k_i$ is the vertical stiffness of the suspension at axle $i$, the deflections are

$$z_i = \frac{F_{z_i}}{k_i}. \tag{2.250}$$

For a flat road, and a rigid vehicle, we must have

$$\frac{z_i - z_1}{x_i - x_1} = \frac{z_n - z_1}{x_n - x_1} \quad \text{for} \quad i = 2, 3, \cdots, n-1 \tag{2.251}$$

which, after substituting with (2.250), reduces to Equation (2.243). The $n - 2$ equations (2.251) along with the two equations (2.241) and (2.242) are enough to calculate the normal load under each tire. The resultant set of equations is linear and may be arranged in a matrix form

$$[A][X] = [B] \tag{2.252}$$

where

$$[X] = \begin{bmatrix} F_{z_1} & F_{z_2} & F_{z_3} & \cdots & F_{z_n} \end{bmatrix}^T \qquad (2.253)$$

$$[A] = \begin{bmatrix} 2 & 2 & \cdots & \cdots & \cdots & \cdots & 2 \\ 2x_1 & 2x_2 & \cdots & \cdots & \cdots & \cdots & 2x_n \\ \dfrac{x_n - x_2}{k_1 l} & \dfrac{1}{k_2} & \cdots & \cdots & \cdots & \cdots & \dfrac{x_2 - x_1}{k_n l} \\ \cdots & \cdots & \cdots & \cdots & \cdots & & \cdots \\ \dfrac{x_n - x_i}{k_1 l} & \cdots & \cdots & \dfrac{1}{k_i} & \cdots & \cdots & \dfrac{x_i - x_1}{k_n l} \\ \cdots & \cdots & \cdots & \cdots & \cdots & \cdots & \cdots \\ \dfrac{x_n - x_{n-1}}{k_1 l} & \cdots & \cdots & \cdots & \cdots & \dfrac{1}{k_{n-1}} & \dfrac{x_{n-1} - x_1}{k_n l} \end{bmatrix} \qquad (2.254)$$

$$l = x_1 - x_n \qquad (2.255)$$

$$[B] = \begin{bmatrix} mg\cos\phi & -h\left(a + mg\sin\phi\right) & 0 & \cdots & 0 \end{bmatrix}^T. \qquad (2.256)$$

∎

**Example 71 ★** *Wheel reactions for a three-axle car.*

*Figure 2.20 illustrates a three-axle car moving on an inclined road. We start counting the axles of a multiple-axle vehicle from the front axle as axle-1, and move sequentially to the back as shown in the figure.*

*The set of equations for the three-axle car, as seen in Figure 2.20, is*

$$2F_{x_1} + 2F_{x_2} + 2F_{x_3} - mg\sin\phi = ma \qquad (2.257)$$

$$2F_{z_1} + 2F_{z_2} + 2F_{z_3} - mg\cos\phi = 0 \qquad (2.258)$$

$$2F_{z_1} x_1 + 2F_{z_2} x_2 + 2F_{z_3} x_3 + 2h\left(F_{x_1} + F_{x_2} + F_{x_3}\right) = 0 \qquad (2.259)$$

$$\frac{1}{x_2 - x_1}\left(\frac{F_{z_2}}{k_2} - \frac{F_{z_1}}{k_1}\right) - \frac{1}{x_3 - x_1}\left(\frac{F_{z_3}}{k_3} - \frac{F_{z_1}}{k_1}\right) = 0 \qquad (2.260)$$

*which can be simplified to*

$$2F_{z_1} + 2F_{z_2} + 2F_{z_3} - mg\cos\phi = 0 \qquad (2.261)$$

$$2F_{z_1} x_1 + 2F_{z_2} x_2 + 2F_{z_3} x_3 + hm\left(a + g\sin\phi\right) = 0 \qquad (2.262)$$

$$\left(x_2 k_2 k_3 - x_3 k_2 k_3\right) F_{z_1} + \left(x_1 k_1 k_2 - x_2 k_1 k_2\right) F_{z_3}$$
$$- \left(x_1 k_1 k_3 - x_3 k_1 k_3\right) F_{z_2} = 0. \qquad (2.263)$$

*The set of equations for wheel loads is linear and may be rearranged in a matrix form*

$$[A]\,[X] = [B] \qquad (2.264)$$

*where*

$$[A] = \begin{bmatrix} 2 & 2 & 2 \\ 2x_1 & 2x_2 & 2x_3 \\ k_2k_3(x_2 - x_3) & k_1k_3(x_3 - x_1) & k_1k_2(x_1 - x_2) \end{bmatrix} \qquad (2.265)$$

$$[X] = \begin{bmatrix} F_{z_1} \\ F_{z_2} \\ F_{z_3} \end{bmatrix} \qquad (2.266)$$

$$[B] = \begin{bmatrix} mg\cos\phi \\ -hm(a + g\sin\phi) \\ 0 \end{bmatrix}. \qquad (2.267)$$

*The unknown vector may be found using matrix inversion*

$$[X] = [A]^{-1}[B]. \qquad (2.268)$$

*The solution of the equations are*

$$\frac{1}{k_1 m} F_{z_1} = \frac{Z_1}{Z_0} \qquad (2.269)$$

$$\frac{1}{k_2 m} F_{z_2} = \frac{Z_2}{Z_0} \qquad (2.270)$$

$$\frac{1}{k_2 m} F_{z_3} = \frac{Z_3}{Z_0} \qquad (2.271)$$

*where,*

$$Z_0 = -4k_1k_2(x_1 - x_2)^2 - 4k_2k_3(x_2 - x_3)^2 - 4k_1k_3(x_3 - x_1)^2 \qquad (2.272)$$

$$\begin{aligned} Z_1 = \; & g(x_2k_2 - x_1k_3 - x_1k_2 + x_3k_3)h\sin\phi \\ & + a(x_2k_2 - x_1k_3 - x_1k_2 + x_3k_3)h \\ & + g(k_2x_2^2 - x_1k_2x_2 + k_3x_3^2 - x_1k_3x_3)\cos\phi \qquad (2.273) \end{aligned}$$

$$\begin{aligned} Z_2 = \; & g(x_1k_1 - x_2k_1 - x_2k_3 + x_3k_3)h\sin\phi \\ & + a(x_1k_1 - x_2k_1 - x_2k_3 + x_3k_3)h \\ & + g(k_1x_1^2 - x_2k_1x_1 + k_3x_3^2 - x_2k_3x_3)\cos\phi \qquad (2.274) \end{aligned}$$

$$\begin{aligned} Z_3 = \; & g(x_1k_1 + x_2k_2 - x_3k_1 - x_3k_2)h\sin\phi \\ & + a(x_1k_1 + x_2k_2 - x_3k_1 - x_3k_2)h \\ & + g(k_1x_1^2 - x_3k_1x_1 + k_2x_2^2 - x_3k_2x_2)\cos\phi \qquad (2.275) \end{aligned}$$

$$x_1 = a_1 \qquad (2.276)$$

$$x_2 = -a_2 \qquad (2.277)$$

$$x_3 = -a_3. \qquad (2.278)$$
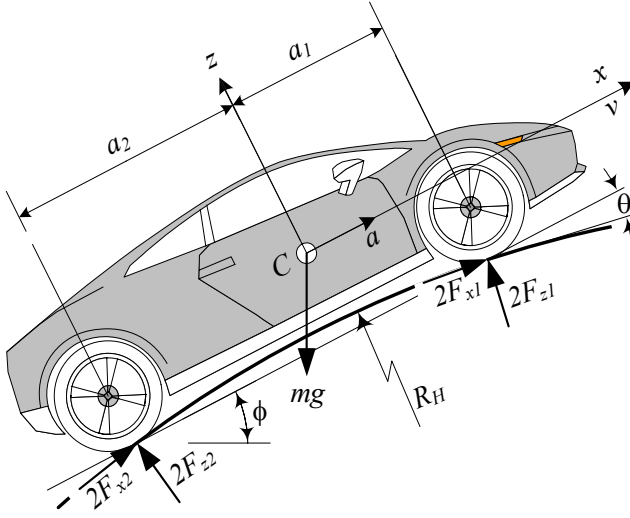
FIGURE 2.21. A cresting vehicle at a point where the hill has a radius of curvature $R_h$.

## 2.8 ★ Vehicles on a Crest and Dip

When a road has an outward or inward curvature, we call the road is a crest or a dip. The curvature can decrease or increase the normal forces under the wheels.

### 2.8.1 ★ Vehicles on a Crest

Moving on the convex curve of a hill is called *cresting*. The normal force under the wheels of a cresting vehicle is less than the force on a flat inclined road with the same slope, because of the developed centrifugal force $mv^2/R_H$ in the $-z$-direction.

Figure 2.21 illustrates a cresting vehicle at the point on the hill with a radius of curvature $R_H$. The traction and normal forces under its tires are approximately equal to

$$F_{x_1} + F_{x_2} \approx \frac{1}{2}m\left(a + g\sin\phi\right) \tag{2.279}$$

$$F_{z_1} \approx \frac{1}{2}mg\left[\left(\frac{a_2}{l}\cos\phi + \frac{h}{l}\sin\phi\right)\right]$$
$$-\frac{1}{2}ma\frac{h}{l} - \frac{1}{2}m\frac{v^2}{R_H}\frac{a_2}{l} \tag{2.280}$$

$$F_{z_2} \approx \frac{1}{2}mg\left[\left(\frac{a_1}{l}\cos\phi - \frac{h}{l}\sin\phi\right)\right]$$
$$+\frac{1}{2}ma\frac{h}{l} - \frac{1}{2}m\frac{v^2}{R_H}\frac{a_1}{l} \tag{2.281}$$

$$l = a_1 + a_2. \tag{2.282}$$

**Proof.** For the cresting car shown in Figure 2.21, the normal and tangential directions are equivalent to the $-z$ and $x$ directions respectively. Hence, the governing equation of motion for the car is

$$\sum F_x = ma \tag{2.283}$$

$$-\sum F_z = m\frac{v^2}{R_H} \tag{2.284}$$

$$\sum M_y = 0. \tag{2.285}$$

Expanding these equations produces the following equations:

$$2F_{x_1}\cos\theta + 2F_{x_2}\cos\theta - mg\sin\phi = ma \tag{2.286}$$

$$-2F_{z_1}\cos\theta - 2F_{z_2}\cos\theta + mg\cos\phi = m\frac{v^2}{R_H} \tag{2.287}$$

$$2F_{z_1}a_1\cos\theta - 2F_{z_2}a_2\cos\theta + 2\left(F_{x_1}+F_{x_2}\right)h\cos\theta$$
$$+2F_{z_1}a_1\sin\theta - 2F_{z_2}a_2\sin\theta - 2\left(F_{x_1}+F_{x_2}\right)h\sin\theta = 0. \tag{2.288}$$

We may eliminate $\left(F_{x_1}+F_{x_2}\right)$ between the first and third equations, and solve for the total traction force $F_{x_1}+F_{x_2}$ and wheel normal forces $F_{z_1}$, $F_{z_2}$.

$$F_{x_1}+F_{x_2} = \frac{ma + mg\sin\phi}{2\cos\theta} \tag{2.289}$$

$$F_{z_1} = \frac{1}{2}mg\left[\left(\frac{a_2}{l\cos\theta}\cos\phi + \frac{h\left(1-\sin 2\theta\right)}{l\cos\theta\cos 2\theta}\sin\phi\right)\right]$$
$$-\frac{1}{2}ma\frac{h\left(1-\sin 2\theta\right)}{l\cos\theta\cos 2\theta} - \frac{1}{2}m\frac{v^2}{R_H}\frac{a_2}{l\cos\theta} \tag{2.290}$$

$$F_{z_2} = \frac{1}{2}mg\left[\left(\frac{a_1}{l\cos\theta}\cos\phi - \frac{h\left(1-\sin 2\theta\right)}{l\cos\theta\cos 2\theta}\sin\phi\right)\right]$$
$$+\frac{1}{2}ma\frac{h\left(1-\sin 2\theta\right)}{l\cos\theta\cos 2\theta} - \frac{1}{2}m\frac{v^2}{R_H}\frac{a_1}{l\cos\theta\cos\theta} \tag{2.291}$$

If the car's wheel base is much smaller than the radius of curvature, $l \ll R_H$, then the slope angle $\theta$ is too small, and we may use the following trigonometric approximations.

$$\cos\theta \approx \cos 2\theta \approx 1 \tag{2.292}$$

$$\sin\theta \approx \sin 2\theta \approx 0 \tag{2.293}$$

Substituting these approximations in Equations (2.289)-(2.291) produces the following approximate results:

$$F_{x_1} + F_{x_2} \approx \frac{1}{2}m\left(a + g\sin\phi\right) \tag{2.294}$$

$$F_{z_1} \approx \frac{1}{2}mg\left[\left(\frac{a_2}{l}\cos\phi + \frac{h}{l}\sin\phi\right)\right]$$
$$-\frac{1}{2}ma\frac{h}{l} - \frac{1}{2}m\frac{v^2}{R_H}\frac{a_2}{l} \tag{2.295}$$

$$F_{z_2} \approx \frac{1}{2}mg\left[\left(\frac{a_1}{l}\cos\phi - \frac{h}{l}\sin\phi\right)\right]$$
$$+\frac{1}{2}ma\frac{h}{l} - \frac{1}{2}m\frac{v^2}{R_H}\frac{a_1}{l} \tag{2.296}$$

■

**Example 72 ★** *Wheel loads of a cresting car.*
  *Consider a car with the following specifications:*

$$
\begin{aligned}
l &= 2272\,\text{mm} \\
w &= 1457\,\text{mm} \\
m &= 1500\,\text{kg} \\
h &= 230\,\text{mm} \\
a_1 &= a_2 \\
v &= 15\,\text{m/s} \\
a &= 1\,\text{m/s}^2
\end{aligned}
\tag{2.297}
$$

*which is cresting a hill at a point where the road has*

$$
\begin{aligned}
R_H &= 40\,\text{m} \\
\phi &= 30\,\text{deg} \\
\theta &= 2.5\,\text{deg}.
\end{aligned}
\tag{2.298}
$$

*The force information on the car is:*

$$
\begin{aligned}
F_{x_1} + F_{x_2} &= 4432.97\,\text{N} \\
F_{z_1} &= 666.33\,\text{N} \\
F_{z_2} &= 1488.75\,\text{N} \\
mg &= 14715\,\text{N} \\
F_{z_1} + F_{z_2} &= 2155.08\,\text{N} \\
m\frac{v^2}{R_H} &= 8437.5\,\text{N}
\end{aligned}
\tag{2.299}
$$

*If we simplifying the results by assuming small $\theta$, the approximate values of the forces are*

$$
\begin{aligned}
F_{x_1} + F_{x_2} &= 4428.75\,\text{N} \\
F_{z_1} &\approx 628.18\,\text{N} \\
F_{z_2} &\approx 1524.85\,\text{N} \\
mg &= 14715\,\text{N} \\
F_{z_1} + F_{z_2} &\approx 2153.03\,\text{N} \\
m\frac{v^2}{R_H} &= 8437.5\,\text{N}.
\end{aligned}
\tag{2.300}
$$

**Example 73 ★** *Losing the road contact in a crest.*

When a car goes too fast, it can lose its road contact. Such a car is called a **flying car**. The condition to have a flying car is $F_{z_1} = 0$ and $F_{z_2} = 0$.

Assuming a symmetric car $a_1 = a_2 = l/2$ with no acceleration, and using the approximate Equations (2.280) and (2.281)

$$
\frac{1}{2}mg\left[\left(\frac{a_2}{l}\cos\phi + \frac{h}{l}\sin\phi\right)\right] - \frac{1}{2}m\frac{v^2}{R_H}\frac{a_2}{l} = 0 \tag{2.301}
$$

$$
\frac{1}{2}mg\left[\left(\frac{a_1}{l}\cos\phi - \frac{h}{l}\sin\phi\right)\right] - \frac{1}{2}m\frac{v^2}{R_H}\frac{a_1}{l} = 0 \tag{2.302}
$$

we can find the critical minimum speed $v_c$ to start flying. There are two critical speeds $v_{c_1}$ and $v_{c_2}$ for losing the contact of the front and rear wheels respectively.

$$
v_{c_1} = \sqrt{2gR_H\left(\frac{h}{l}\sin\phi + \frac{1}{2}\cos\phi\right)} \tag{2.303}
$$

$$
v_{c_2} = \sqrt{-2gR_H\left(\frac{h}{l}\sin\phi - \frac{1}{2}\cos\phi\right)} \tag{2.304}
$$

For any car, the critical speeds $v_{c_1}$ and $v_{c_2}$ are functions of the hill's radius of curvature $R_H$ and the angular position on the hill, indicated by $\phi$. The angle $\phi$ cannot be out of the tilting angles given by Equation (2.141).

$$
-\frac{a_1}{h} \leq \tan\phi \leq \frac{a_2}{h} \tag{2.305}
$$

Figure 2.22 illustrates a cresting car over a circular hill, and Figure 2.23 depicts the critical speeds $v_{c_1}$ and $v_{c_2}$ at a different angle $\phi$ for $-1.371\,\text{rad} \leq$
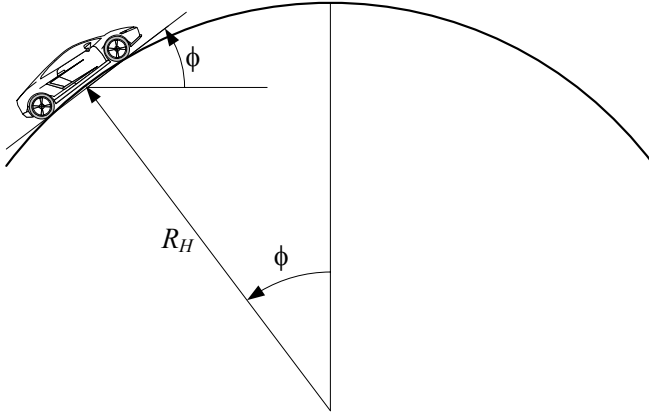
FIGURE 2.22. A cresting car over a circular hill.

$\phi \leq 1.371$ rad. *The specifications of the car and the hill are:*

$$
\begin{aligned}
l &= 2272\,\text{mm} \\
h &= 230\,\text{mm} \\
a_1 &= a_2 \\
a &= 0\,\text{m/s}^2 \\
R_H &= 100\,\text{m.}
\end{aligned}
$$

*At the maximum uphill slope $\phi = 1.371$ rad $\approx 78.5$ deg, the front wheels can leave the ground at zero speed while the rear wheels are on the ground. When the car moves over the hill and reaches the maximum downhill slope $\phi = -1.371$ rad $\approx -78.5$ deg the rear wheels can leave the ground at zero speed while the front wheels are on the ground. As long as the car is moving uphill, the front wheels can leave the ground at a lower speed while going downhill the rear wheels leave the ground at a lower speed. Hence, at each slope angle $\phi$ the lower curve determines the critical speed $v_c$.*

*To have a general image of the critical speed, we may plot the lower values of $v_c$ as a function of $\phi$ using $R_H$ or $h/l$ as a parameter. Figure 2.24 shows the effect of hill radius of curvature $R_H$ on the critical speed $v_c$ for a car with $h/l = 0.10123$ mm/mm and Figure 2.25 shows the effect of a car's high factor $h/l$ on the critical speed $v_c$ for a circular hill with $R_H = 100$ m.*

## 2.8.2  ★ Vehicles on a Dip

Moving on the concave curve of a hill is called *dipping*. The normal force under the wheels of a dipping vehicle is more than the force on a flat inclined road with the same slope, because of the developed centrifugal
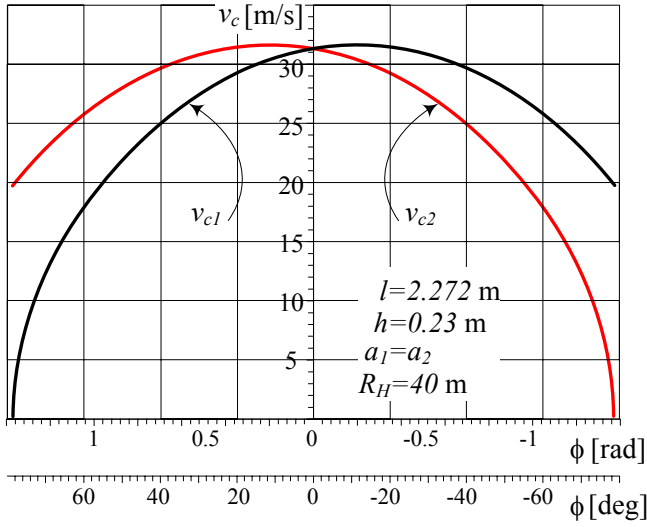
FIGURE 2.23. Critical speeds $v_{c_1}$ and $v_{c_2}$ at different angle $\phi$ for a specific car and hill.
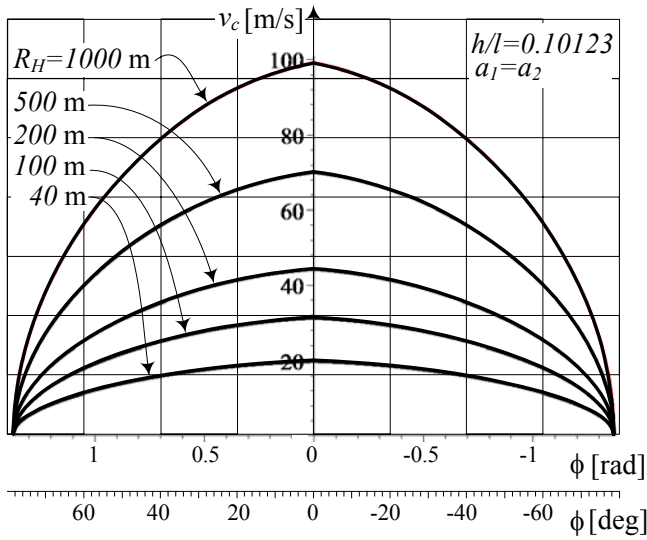


FIGURE 2.24. Effect of hill radius of curvature $R_h$ on the critical speed $v_c$ for a car.
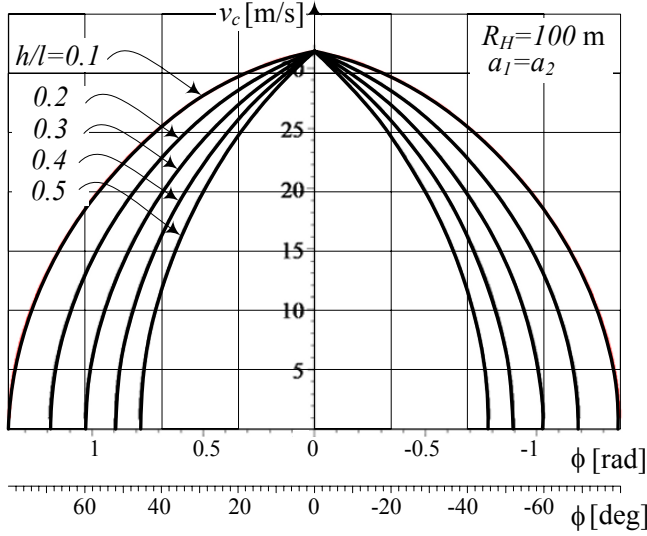
FIGURE 2.25. Effect of a car's height factor $h/l$ on the critical speed $v_c$ for a circular hill.

force $mv^2/R_H$ in the $z$-direction.

Figure 2.26 illustrates a dipping vehicle at a point where the hill has a radius of curvature $R_H$. The traction and normal forces under the tires of the vehicle are approximately equal to

$$F_{x_1} + F_{x_2} \approx \frac{1}{2}m\left(a + g\sin\phi\right) \qquad (2.306)$$

$$F_{z_1} \approx \frac{1}{2}mg\left[\left(\frac{a_2}{l}\cos\phi + \frac{h}{l}\sin\phi\right)\right]$$
$$-\frac{1}{2}ma\frac{h}{l} + \frac{1}{2}m\frac{v^2}{R_H}\frac{a_2}{l} \qquad (2.307)$$

$$F_{z_2} \approx \frac{1}{2}mg\left[\left(\frac{a_1}{l}\cos\phi - \frac{h}{l}\sin\phi\right)\right]$$
$$+\frac{1}{2}ma\frac{h}{l} + \frac{1}{2}m\frac{v^2}{R_H}\frac{a_1}{l} \qquad (2.308)$$

$$l = a_1 + a_2. \qquad (2.309)$$

**Proof.** To develop the equations for the traction and normal forces under the tires of a dipping car, we follow the same procedure as a cresting car. The normal and tangential directions of a dipping car, shown in Figure 2.21, are equivalent to the $z$ and $x$ directions respectively. Hence, the governing
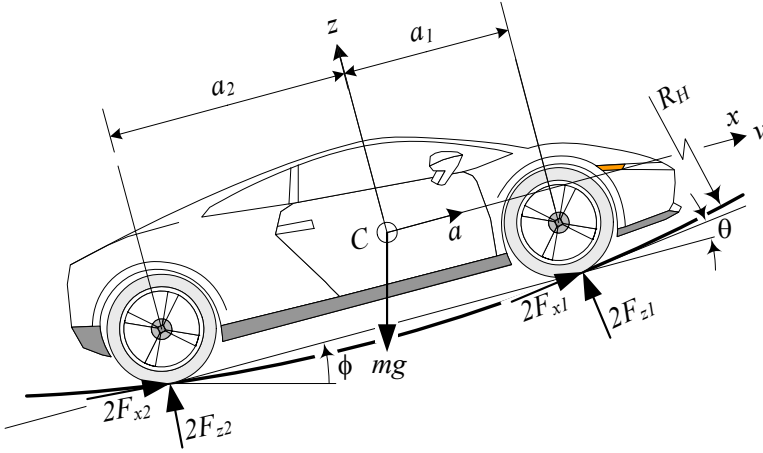
FIGURE 2.26. A dipping vehicle at a point where the hill has a radius of curvature $R_h$.

equations of motion for the car are

$$\sum F_x = ma \tag{2.310}$$

$$\sum F_z = m\frac{v^2}{R_H} \tag{2.311}$$

$$\sum M_y = 0. \tag{2.312}$$

Expanding these equations produces the following equations:

$$2F_{x_1}\cos\theta + 2F_{x_2}\cos\theta - mg\sin\phi = ma \tag{2.313}$$

$$-2F_{z_1}\cos\theta - 2F_{z_2}\cos\theta + mg\cos\phi = m\frac{v^2}{R_H} \tag{2.314}$$

$$2F_{z_1}a_1\cos\theta - 2F_{z_2}a_2\cos\theta + 2\left(F_{x_1} + F_{x_2}\right)h\cos\theta$$
$$+2F_{z_1}a_1\sin\theta - 2F_{z_2}a_2\sin\theta - 2\left(F_{x_1} + F_{x_2}\right)h\sin\theta = 0. \tag{2.315}$$

The total traction force $(F_{x_1} + F_{x_2})$ may be eliminated between the first and third equations. Then, the resultant equations provide the following forces for the total traction force $F_{x_1} + F_{x_2}$ and wheel normal forces $F_{z_1}$, $F_{z_2}$:

$$F_{x_1} + F_{x_2} = \frac{ma + mg\sin\phi}{2\cos\theta} \tag{2.316}$$

$$F_{z_1} = \frac{1}{2}mg\left[\left(\frac{a_2}{l\cos\theta}\cos\phi + \frac{h\,(1-\sin2\theta)}{l\cos\theta\cos2\theta}\sin\phi\right)\right]$$
$$-\frac{1}{2}ma\frac{h\,(1-\sin2\theta)}{l\cos\theta\cos2\theta} + \frac{1}{2}m\frac{v^2}{R_H}\frac{a_2}{l\cos\theta} \tag{2.317}$$

$$F_{z_2} = \frac{1}{2}mg\left[\left(\frac{a_1}{l\cos\theta}\cos\phi - \frac{h\,(1-\sin2\theta)}{l\cos\theta\cos2\theta}\sin\phi\right)\right]$$
$$+\frac{1}{2}ma\frac{h\,(1-\sin2\theta)}{l\cos\theta\cos2\theta} + \frac{1}{2}m\frac{v^2}{R_H}\frac{a_1}{l\cos\theta\cos\theta} \tag{2.318}$$

Assuming $\theta \ll 1$, these forces can be approximated to

$$F_{x_1} + F_{x_2} \approx \frac{1}{2}m\,(a + g\sin\phi) \tag{2.319}$$

$$F_{z_1} \approx \frac{1}{2}mg\left[\left(\frac{a_2}{l}\cos\phi + \frac{h}{l}\sin\phi\right)\right]$$
$$-\frac{1}{2}ma\frac{h}{l} + \frac{1}{2}m\frac{v^2}{R_H}\frac{a_2}{l} \tag{2.320}$$

$$F_{z_2} \approx \frac{1}{2}mg\left[\left(\frac{a_1}{l}\cos\phi - \frac{h}{l}\sin\phi\right)\right]$$
$$+\frac{1}{2}ma\frac{h}{l} + \frac{1}{2}m\frac{v^2}{R_H}\frac{a_1}{l}. \tag{2.321}$$

■

**Example 74 ★** *Wheel loads of a dipping car.*
*Consider a car with the following specifications:*

$$
\begin{aligned}
l &= 2272\,\text{mm} \\
w &= 1457\,\text{mm} \\
m &= 1500\,\text{kg} \\
h &= 230\,\text{mm} \\
a_1 &= a_2 \\
v &= 15\,\text{m/s} \\
a &= 1\,\text{m/s}^2
\end{aligned}
\tag{2.322}
$$

*that is dipping on a hill at a point where the road has*

$$
\begin{aligned}
R_H &= 40\,\text{m} \\
\phi &= 30\,\text{deg} \\
\theta &= 2.5\,\text{deg}.
\end{aligned}
\tag{2.323}
$$

*The force information of the car is:*

$$
\begin{aligned}
F_{x_1} + F_{x_2} &= 4432.97\,\text{N} \\
F_{z_1} &= 4889.1\,\text{N} \\
F_{z_2} &= 5711.52\,\text{N} \\
mg &= 14715\,\text{N} \\
F_{z_1} + F_{z_2} &= 10600.62\,\text{N} \\
m\frac{v^2}{R_H} &= 8437.5\,\text{N}
\end{aligned}
\qquad (2.324)
$$

*If we ignore the effect of θ by assuming θ ≪ 1, then the approximate value of the forces are*

$$
\begin{aligned}
F_{x_1} + F_{x_2} &= 4428.75\,\text{N} \\
F_{z_1} &\approx 4846.93\,\text{N} \\
F_{z_2} &\approx 1524.85\,\text{N} \\
mg &= 5743.6\,\text{N} \\
F_{z_1} + F_{z_2} &\approx 10590.53\,\text{N} \\
m\frac{v^2}{R_H} &= 8437.5\,\text{N}.
\end{aligned}
\qquad (2.325)
$$

## 2.9  Summary

For straight motion of a symmetric rigid vehicle, we may assume the forces on the left wheel are equal to the forces on the right wheel, and simplify the tire force calculation.

When a car is accelerating on an inclined road with angle $\phi$, the normal forces under the front and rear wheels, $F_{z_1}$, $F_{z_2}$, are:

$$
F_{z_1} = \frac{1}{2}mg\left(\frac{a_2}{l}\cos\phi - \frac{h}{l}\sin\phi\right) - \frac{1}{2}ma\frac{h}{l} \qquad (2.326)
$$

$$
F_{z_2} = \frac{1}{2}mg\left(\frac{a_1}{l}\cos\phi + \frac{h}{l}\sin\phi\right) + \frac{1}{2}ma\frac{h}{l} \qquad (2.327)
$$

$$
l = a_1 + a_2 \qquad (2.328)
$$

where, $\frac{1}{2}mg\left(\frac{a_1}{l}\cos\phi \pm \frac{h}{l}\sin\phi\right)$ is the static part and $\pm\frac{1}{2}mg\frac{h}{l}\frac{a}{g}$ is the dynamic part, because it depends on the acceleration $a$.

## 2.10   Key Symbols

| | |
|---|---|
| $a \equiv \ddot{x}$ | acceleration |
| $a_{fwd}$ | front wheel drive acceleration |
| $a_{rwd}$ | rear wheel drive acceleration |
| $a_1$ | distance of first axle from mass center |
| $a_2$ | distance of second axle from mass center |
| $a_i$ | distance of axle number $i$ from mass center |
| $a_M$ | maximum acceleration |
| $a, b$ | arguments for $atan2(a, b)$ |
| $A, B, C$ | constant parameters |
| $b_1$ | distance of left wheels from mass center |
| $b_1$ | distance of hinge point from rear axle |
| $b_2$ | distance of right wheels from mass center |
| $b_2$ | distance of hinge point from trailer mass center |
| $b_3$ | distance of trailer axle from trailer mass center |
| $C$ | mass center of vehicle |
| $C_t$ | mass center of trailer |
| $F$ | force |
| $F_x$ | traction or brake force under a wheel |
| $F_{x_1}$ | traction or brake force under front wheels |
| $F_{x_2}$ | traction or brake force under rear wheels |
| $F_{x_t}$ | horizontal force at hinge |
| $F_z$ | normal force under a wheel |
| $F_{z_1}$ | normal force under front wheels |
| $F_{z_2}$ | normal force under rear wheels |
| $F_{z_3}$ | normal force under trailer wheels |
| $F_{z_t}$ | normal force at hinge |
| $g, \mathbf{g}$ | gravitational acceleration |
| $h$ | height of $C$ |
| $H$ | height |
| $I$ | mass moment of inertia |
| $k_i$ | vertical stiffness of suspension at axle number $i$ |
| $l$ | wheel base |
| $m$ | car mass |
| $m_t$ | trailer mass |
| $M$ | moment |
| $R$ | tire radius |
| $R_f$ | front tire radius |
| $R_r$ | rear tire radius |
| $R_H$ | radius of curvature |
| $t$ | time |
| $v \equiv \dot{x}, \mathbf{v}$ | velocity |
| $v_c$ | critical velocity |

| | |
|---|---|
| $w$ | track |
| $z_i$ | deflection of axil number $i$ |
| $x, y, z$ | vehicle coordinate axes |
| $X, Y, Z$ | global coordinate axes |
| | |
| $\theta$ | road slope |
| $\phi$ | road angle with horizon |
| $\phi_M$ | maximum slope angle |
| $\mu$ | friction coefficient |

Subscriptions

| | |
|---|---|
| $dyn$ | dynamic |
| $f$ | front |
| $fwd$ | front-wheel-drive |
| $M$ | maximum |
| $r$ | rear |
| $rwd$ | rear-wheel-drive |
| $st$ | statics |

# Exercises

1. Axle load.

   Consider a car with the following specifications that is parked on a level road. Find the load on the front and rear axles.

$$
\begin{aligned}
m &= 1765\,\mathrm{kg} \\
l &= 2.84\,\mathrm{m} \\
a_1 &= 1.22\,\mathrm{m} \\
a_2 &= 1.62\,\mathrm{m}
\end{aligned}
$$

2. Axle load.

   Consider a car with the following specification, and find the axles load.

$$
\begin{aligned}
m &= 1245\,\mathrm{kg} \\
a_1 &= 1100\,\mathrm{mm} \\
a_2 &= 1323\,\mathrm{mm}
\end{aligned}
$$

3. Mass center distance ratio.

   Peugeot 907 Concept$^{TM}$ approximately has the following specifications.

$$
\begin{aligned}
m &= 1400\,\mathrm{kg} \\
l &= 97.5\,\mathrm{in}
\end{aligned}
$$

   Assume $a_1/a_2 \approx 1.131$ and determine the axles load.

4. Axle load ratio.

   Jeep Commander XK$^{TM}$ approximately has the following specifications.

$$
\begin{aligned}
mg &= 5091\,\mathrm{lb} \\
l &= 109.5\,\mathrm{in}
\end{aligned}
$$

   Assume $F_{z_1}/F_{z_2} \approx 1.22$ and determine the axles load.

5. Axle load and mass center distance ratio.

   The wheelbase of the 1981 DeLorean Sportscar$^{TM}$ is

$$
l = 94.89\,\mathrm{in}.
$$

   Find the axles load if we assume

$$
\begin{aligned}
a_1/a_2 &\approx 0.831 \\
mg &= 3000\,\mathrm{lb}.
\end{aligned}
$$

6. Mass center height.

   McLaren SLR 722 Sportscar$^{TM}$ has the following specifications.

   $$front\ tire \quad 255/35ZR19$$
   $$rear\ tire \quad 295/30ZR19$$

   $$m = 1649\,\text{kg}$$
   $$l = 2700\,\text{mm}$$

   When the front axle is lifted $H = 540\,\text{mm}$, assume that

   $$a_1 = a_2$$
   $$F_{z_2} = 0.68mg.$$

   What is the height $h$ of the mass center?

7. A parked car on an uphill road.

   Specifications of Lamborghini Gallardo$^{TM}$ are

   $$m = 1430\,\text{kg}$$
   $$l = 2560\,\text{mm}.$$

   Assume

   $$a_1 = a_2$$
   $$h = 520\,\text{mm}$$

   and determine the forces $F_{z_1}$, $F_{z_2}$, and $F_{x_2}$ if the car is parked on an uphill with $\phi = 30\,\text{deg}$ and the hand brake is connected to the rear wheels.

   What would be the maximum road grade $\phi_M$, that the car can be parked, if $\mu_{x_2} = 1$.

8. Parked on an uphill road.

   Rolls-Royce Phantom$^{TM}$ has the following specifications

   $$m = 2495\,\text{kg}$$
   $$l = 3570\,\text{mm}$$
   $$F_{z_2} = 0.499mg.$$

   Assume the car is parked on an uphill road and

   $$a_1 = a_2$$
   $$h = 670\,\text{mm}$$
   $$\phi = 30\,\text{deg}.$$

   Determine the forces under the wheels if the car is

    (a) front wheel braking

    (b) rear wheel braking

    (c) four wheel braking.

9. A parked car on an downhill road.

   Solve Exercise 7 if the car is parked on a downhill road.

10. Maximum acceleration.

   Honda CR-V$^{TM}$ is a midsize SUV car with the following specifications.

$$
\begin{aligned}
m &= 1550\,\mathrm{kg} \\
l &= 2620\,\mathrm{mm}
\end{aligned}
$$

   Assume

$$
\begin{aligned}
a_1 &= a_2 \\
h &= 720\,\mathrm{mm} \\
\mu_x &= 0.8
\end{aligned}
$$

   and determine the maximum acceleration of the car if

    (a) the car is rear-wheel drive

    (b) the car is front-wheel drive

    (c) the car is four-wheel drive.

11. Minimum time for $0 - 100\,\mathrm{km/h}$.

   RoadRazer$^{TM}$ is a light weight rear-wheel drive sportscar with

$$
\begin{aligned}
m &= 300\,\mathrm{kg} \\
l &= 2286\,\mathrm{mm} \\
h &= 260\,\mathrm{mm.}
\end{aligned}
$$

   Assume $a_1 = a_2$. If the car can reach the speed $0 - 100\,\mathrm{km/h}$ in $t = 3.2\,\mathrm{s}$, what would be the minimum friction coefficient?

12. Axle load of an all-wheel drive car.

   Acura Courage$^{TM}$ is an all-wheel drive car with

$$
\begin{aligned}
m &= 2058.9\,\mathrm{kg} \\
l &= 2750.8\,\mathrm{mm.}
\end{aligned}
$$

   Assume $a_1 = a_2$ and $h = 760\,\mathrm{mm}$. Determine the axles load if the car is accelerating at $a = 1.7\,\mathrm{m/s^2}$.

13. A car with a trailer.

    Volkswagen Touareg$^{TM}$ is an all-wheel drive car with

    $$
    \begin{aligned}
    m &= 2268\,\text{kg} \\
    l &= 2855\,\text{mm.}
    \end{aligned}
    $$

    Assume $a_1 = a_2$ and the car is pulling a trailer with

    $$
    \begin{aligned}
    m_t &= 600\,\text{kg} \\
    b_1 &= 855\,\text{mm} \\
    b_2 &= 1350\,\text{mm} \\
    b_3 &= 150\,\text{mm} \\
    h_1 &= h_2.
    \end{aligned}
    $$

    If the car is accelerating on a level road with acceleration $a = 2\,\text{m/s}^2$, what would be the forces at the hinge.

14. A parked car on a banked road.

    Cadillac Escalade$^{TM}$ is a SUV car with

    $$
    \begin{aligned}
    m &= 2569.6\,\text{kg} \\
    l &= 2946.4\,\text{mm} \\
    w_f &= 1732.3\,\text{mm} \\
    w_r &= 1701.8\,\text{mm.}
    \end{aligned}
    $$

    Assume $b_1 = b_2$, $h = 940\,\text{mm}$, and use an average track to determine the wheels load when the car is parked on a banked road with $\phi = 12\,\text{deg.}$

15. ★ A parked car on a banked road with $w_f \neq w_r$.

    Determine the wheels load of a parked car on a banked road, if the front and rear tracks of the car are different.

16. Optimal traction force.

    Mitsubishi Outlander$^{TM}$ is an all-wheel drive SUV car with the following specifications.

    $$
    \begin{aligned}
    m &= 1599.8\,\text{kg} \\
    l &= 2669.6\,\text{mm} \\
    w &= 1539.3\,\text{mm.}
    \end{aligned}
    $$

    Assume

    $$
    \begin{aligned}
    a_1 &= a_2 \\
    h &= 760\,\text{mm} \\
    \mu_x &= 0.75
    \end{aligned}
    $$

and find the optimal traction force ratio $F_{x_1}/F_{x_2}$ to reach the maximum acceleration.

17. ★ A three-axle car.

    Citroën Cruise Crosser$^{TM}$ is a three-axle off-road pick-up car. Assume

$$
\begin{aligned}
m &= 1800\,\mathrm{kg} \\
a_1 &= 1100\,\mathrm{mm} \\
a_2 &= 1240\,\mathrm{mm} \\
a_3 &= 1500\,\mathrm{mm} \\
k_1 &= 12800\,\mathrm{N/m} \\
k_2 &= 14000\,\mathrm{N/m} \\
k_3 &= 14000\,\mathrm{N/m}
\end{aligned}
$$

and find the axles load on a level road when the car is moving with no acceleration.

# 3

# Tire Dynamics

The tire is the main component interacting with the road. The performance of a vehicle is mainly influenced by the characteristics of its tires. Tires affect a vehicle's handling, traction, ride comfort, and fuel consumption. To understand its importance, it is enough to remember that a vehicle can maneuver only by longitudinal, vertical, and lateral force systems generated under the tires.
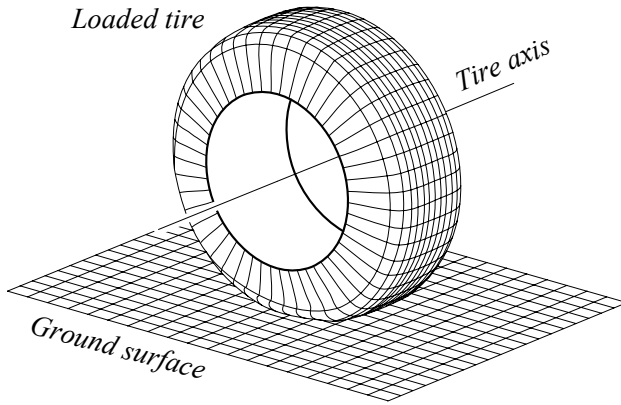


FIGURE 3.1. A vertically loaded stationary tire.

Figure 3.1 illustrates a model of a vertically loaded stationary tire. To model the tire-road interactions, we determine the tireprint and describe the forces distributed on the tireprint.

## 3.1 Tire Coordinate Frame and Tire Force System

To describe the tire-road interaction and force system, we attach a Cartesian coordinate frame at the center of the tireprint, as shown in Figure 3.2, assuming a flat and horizontal ground. The $x$-axis is along the intersection line of the tire-plane and the ground. *Tire plane* is the plane made by narrowing the tire to a flat disk. The $z$-axis is perpendicular to the ground, opposite to the gravitational acceleration $\mathbf{g}$, and the $y$-axis makes the coordinate system a right-hand triad.

To show the tire orientation, we use two angles: camber angle $\gamma$ and sideslip angle $\alpha$. The *camber angle* is the angle between the tire-plane and
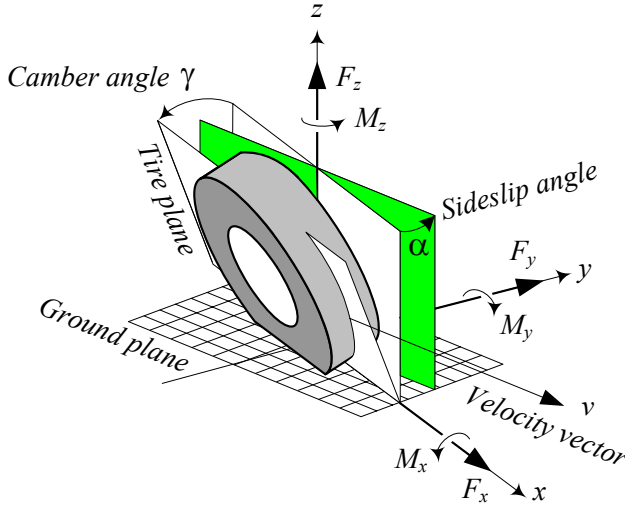
FIGURE 3.2. Tire coordinate system.

the vertical plane measured about the $x$-axis. The camber angle can be recognized better in a front view as shown in Figure 3.3. The *sideslip angle* $\alpha$, or simply *sideslip*, is the angle between the velocity vector $\mathbf{v}$ and the $x$-axis measured about the $z$-axis. The sideslip can be recognized better in a top view, as shown in Figure 3.4.

The force system that a tire receives from the ground is assumed to be located at the center of the tireprint and can be decomposed along $x$, $y$, and $z$ axes. Therefore, the interaction of a tire with the road generates a 3D force system including three forces and three moments, as shown in Figure 3.2.

1. *Longitudinal force $F_x$.* It is a force acting along the $x$-axis. The resultant longitudinal force $F_x > 0$ if the car is accelerating, and $F_x < 0$ if the car is braking. Longitudinal force is also called *forward force.*

2. *Normal force $F_z$.* It is a vertical force, normal to the ground plane. The resultant normal force $F_z > 0$ if it is upward. Normal force is also called *vertical force* or *wheel load.*

3. *Lateral force $F_y$.* It is a force, tangent to the ground and orthogonal to both $F_x$ and $F_z$. The resultant lateral force $F_y > 0$ if it is in the $y$-direction.

4. *Roll moment $M_x$.* It is a longitudinal moment about the $x$-axis. The resultant roll moment $M_x > 0$ if it tends to turn the tire about the $x$-axis. The roll moment is also called the *bank moment, tilting torque,* or *overturning moment.*
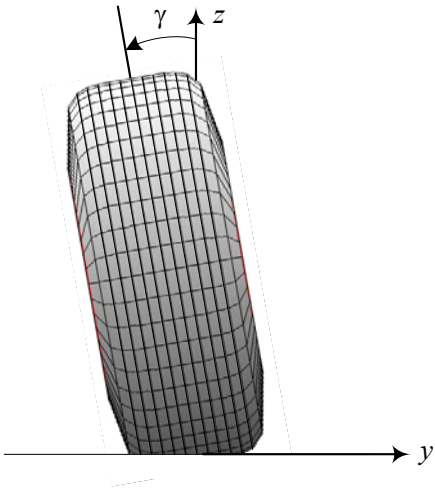
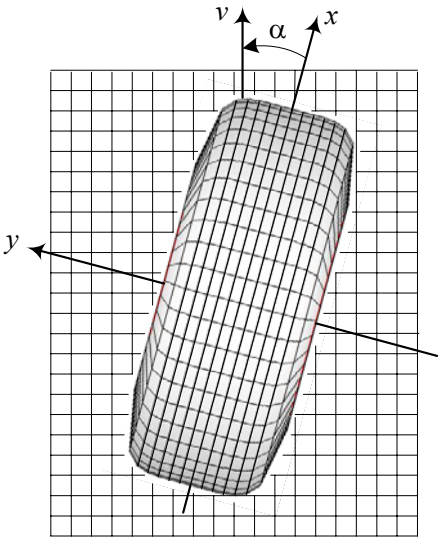FIGURE 3.3. Front view of a tire and measurment of the camber angle.



FIGURE 3.4. Top view of a tire and measurment of the side slip angle.

5.  *Pitch moment $M_y$.* It is a lateral moment about the $y$-axis. The resultant pitch moment $M_y > 0$ if it tends to turn the tire about the $y$-axis and move forward. The pitch moment is also called *rolling resistance torque.*

6.  *Yaw moment $M_z$.* It is an upward moment about the $z$-axis. The resultant yaw moment $M_z > 0$ if it tends to turn the tire about the $z$-axis. The yaw moment is also called the *aligning moment, self aligning moment,* or *bore torque.*

The moment applied to the tire from the vehicle about the tire axis is called *wheel torque $T$.*

**Example 75** *Origin of tire coordinate frame.*
For a cambered tire, it is not always possible to find or define a center point for the tireprint to be used as the origin of the tire coordinate frame. It is more practical to set the origin of the tire coordinate frame at the center of the intersection line between the tire-plane and the ground. So, the origin of the tire coordinate frame is at the center of the tireprint when the tire is standing upright and stationary on a flat road.

**Example 76** *SAE tire coordinate system.*
The tire coordinate system adopted by the Society of Automotive Engineers (SAE) is shown in Figure 3.5. The origin of the coordinate system is at the center of the tireprint when the tire is standing stationary. The $x$-axis is at the intersection of the tire-plane and the ground plane. The $z$-axis is downward and perpendicular to the tireprint. The $y$-axis is on the ground plane and goes to the right to make the coordinate frame a right-hand frame.
The sideslip angle $\alpha$ is considered positive if the tire is slipping to the right, and the camber angle $\gamma$ is positive when the tire leans to the right.
The SAE coordinate system is as good as the coordinate system in Figure 3.2 and may be used alternatively. However, having the $z$-axis directed downward is sometimes inefficient and confusing. Furthermore, in SAE convention, the camber angle for the left and right tires of a vehicle have opposite signs. So, the camber angle of the left tire is positive when the tire leans to the right and the camber angle of the right tire is positive when the tire leans to the left.

## 3.2   Tire Stiffness

As an applied approximation, the vertical tire force $F_z$ can be calculated as a linear function of the normal tire deflection $\triangle z$ measured at the tire center.
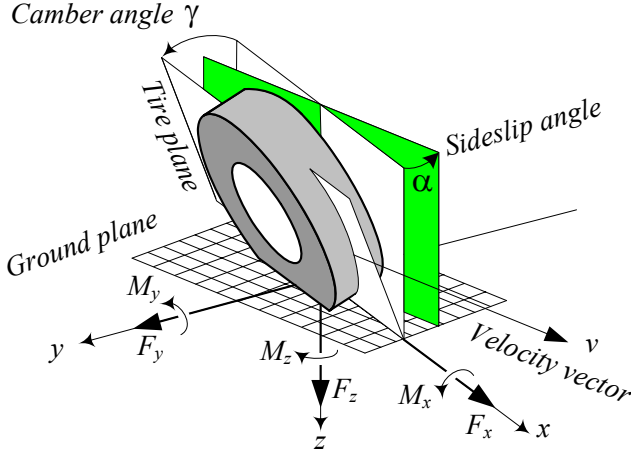
$$F_z = k_z \triangle z \tag{3.1}$$

FIGURE 3.5. SAE tire coordinate system.

The coefficient $k_z$ is called *tire stiffness* in the $z$-direction. Similarly, the reaction of a tire to a lateral and a longitudinal force can be approximated by

$$F_x = k_x \triangle x \tag{3.2}$$
$$F_y = k_y \triangle y \tag{3.3}$$

where the coefficient $k_x$ and $k_y$ are called *tire stiffness* in the $x$ and $y$ directions.

**Proof.** The deformation behavior of tires to the applied forces in any three directions $x$, $y$, and $z$ are the first important tire characteristics in tire dynamics. Calculating the tire stiffness is generally based on experiment and therefore, they are dependent on the tire's mechanical properties, as well as environmental characteristics.

Consider a vertically loaded tire on a stiff and flat ground as shown in Figure 3.6. The tire will deflect under the load and generate a pressurized contact area to balance the vertical load.

Figure 3.7 depicts a sample of experimental stiffness curve in the $(F_z, \triangle z)$ plane. The curve can be expressed by a mathematical function

$$F_z = f(\triangle z) \tag{3.4}$$

however, we may use a linear approximation for the range of the usual application.

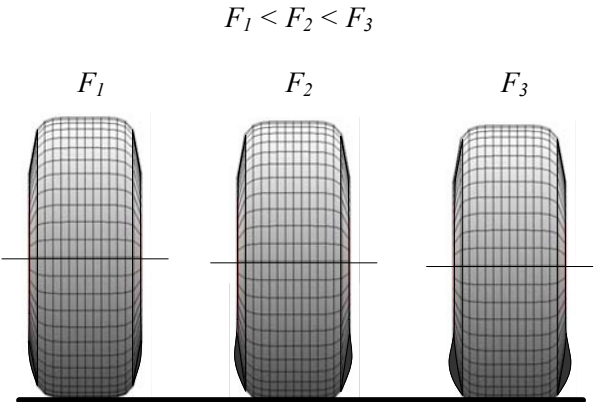$$F_z = \frac{\partial f}{\partial (\triangle z)} \triangle z \tag{3.5}$$

$$F_1 < F_2 < F_3$$

$F_1$          $F_2$          $F_3$

FIGURE 3.6. Vertically loaded tire at zero camber.
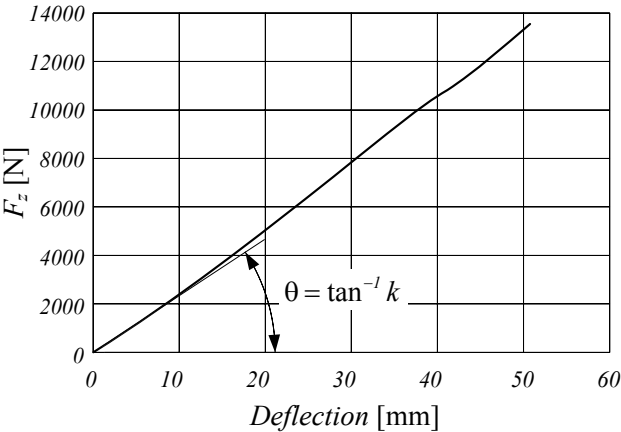
$\theta = \tan^{-1} k$

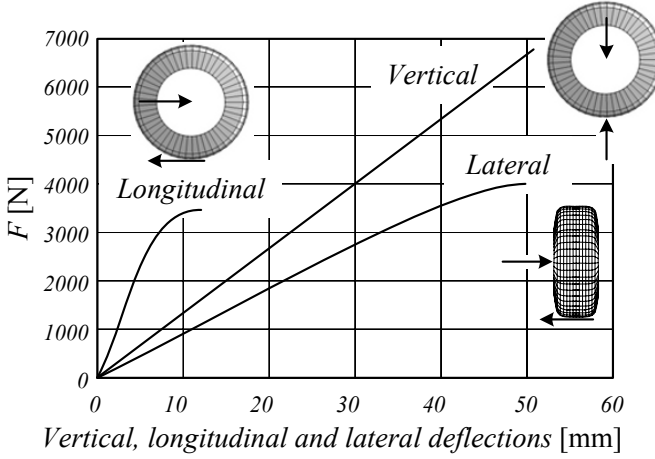FIGURE 3.7. A sample tire vertical stiffness curve.

FIGURE 3.8. Vertical, longitudinal, and lateral stiffness curves.

The coefficient $\frac{\partial f}{\partial(\triangle z)}$ is the slope of the experimental stiffness curve at zero and is shown by a stiffness coefficient $k_z$

$$k_z = \tan\theta = \lim_{\triangle z \to 0} \frac{\partial f}{\partial(\triangle z)}. \tag{3.6}$$

Therefore, the normal tire deflection $\triangle z$ remains proportional to the vertical tire force $F_z$.

$$F_z = k_z \triangle z \tag{3.7}$$

The tire can apply only pressure forces to the road, so normal force is restricted to $F_z > 0$.

The stiffness curve can be influenced by many parameters. The most effective one is the tire inflation pressure.

Lateral and longitudinal force/deflection behavior is also determined experimentally by applying a force in the appropriate direction. The lateral and longitudinal forces are limited by the sliding force when the tire is vertically loaded. Figure 3.8 depicts a sample of longitudinal and lateral stiffness curves compared to a vertical stiffness curve.

The practical part of a tire's longitudinal and lateral stiffness curves is the linear part and may be estimated by linear equations.

$$F_x = k_x \triangle x \tag{3.8}$$
$$F_y = k_y \triangle y \tag{3.9}$$

The coefficients $k_x$ and $k_y$ are called the *tire stiffness* in the $x$ and $y$ directions. They are measured by the slope of the experimental stiffness curves
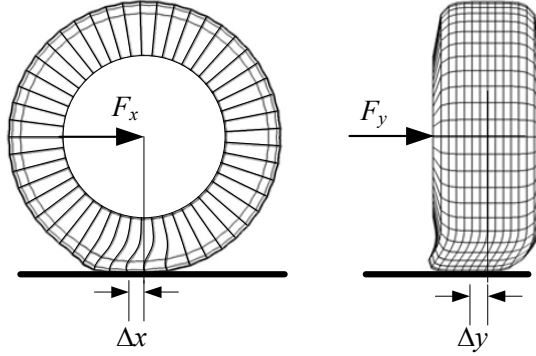
FIGURE 3.9. Illustration of laterally and longitudinally tire deformation.

in the $(F_x, \triangle x)$ and $(F_y, \triangle y)$ planes.

$$k_x = \lim_{\triangle x \to 0} \frac{\partial f}{\partial (\triangle x)} \tag{3.10}$$

$$k_y = \lim_{\triangle y \to 0} \frac{\partial f}{\partial (\triangle y)} \tag{3.11}$$

When the longitudinal and lateral forces increase, parts of the tireprint creep and slide on the ground until the whole tireprint starts sliding. At this point, the applied force saturates and reaches its maximum supportable value.

Generally, a tire is most stiff in the longitudinal direction and least stiff in the lateral direction.

$$k_x > k_z > k_y \tag{3.12}$$

Figure 3.9 illustrates tire deformation under a lateral and a longitudinal force.  ■

**Example 77 ★** *Nonlinear tire stiffness.*

*In a better modeling, the vertical tire force $F_z$ is a function of the normal tire deflection $\triangle z$, and deflection velocity $\triangle \dot{z}$.*

$$F_z = F_z (\triangle z, \triangle \dot{z}) \tag{3.13}$$

$$= F_{z_s} + F_{z_d} \tag{3.14}$$

*In a first approximation we may assume $F_z$ is a combination of a static and a dynamic part. The static part is a nonlinear function of the vertical tire deflection and the dynamic part is proportional to the vertical speed of the tire.*

$$F_{z_s} = k_1 \triangle z + k_2 (\triangle z)^2 \tag{3.15}$$

$$F_{z_d} = k_3 \dot{z} \tag{3.16}$$

*The constants $k_1$ and $k_2$ are calculated from the first and second slopes of the experimental stiffness curve in the $(F_z, \triangle z)$ plane, and $k_3$ is the first slope of the curve in the $(F_z, \dot{z})$ plane, which indicates the tire damping.*

$$k_1 \;=\; \left. \frac{\partial \, F_z}{\partial \, \triangle z} \right|_{\triangle z = 0} \tag{3.17}$$

$$k_2 \;=\; \left. \frac{1}{2} \, \frac{\partial^2 \, F_z}{\partial \, (\triangle z)^2} \right|_{\triangle z = 0} \tag{3.18}$$

$$k_3 \;=\; \left. \frac{\partial \, F_z}{\partial \, \dot{z}} \right|_{\dot{z} = 0} \tag{3.19}$$

*The value of $k_1 = 200000 \, \mathrm{N/\,m}$ is a good approximation for a $205/50R15$ passenger car tire, and $k_1 = 1200000 \, \mathrm{N/\,m}$ is a good approximation for a $X31580R22.5$ truck tire.*

*Tires with a larger number of plies have higher damping, because the plies' internal friction generates the damping. Tire damping decreases by increasing speeds.*

**Example 78** ★ *Hysteresis effect.*

*Because tires are made from rubber, which is a viscoelastic material, the loading and unloading stiffness curves are not exactly the same. They are similar to those in Figure 3.10, which make a loop with the unloading curve below the loading. The area within the loop is the amount of dissipated energy during loading and unloading. As a tire rotates under the weight of a vehicle, it experiences repeated cycles of deformation and recovery, and it dissipates energy loss as heat. Such a behavior is a common property of hysteretic material and is called hysteresis. So, **hysteresis** is a characteristic of a deformable material such as rubber, that the energy of deformation is greater than the energy of recovery. The amount of dissipated energy depends on the mechanical characteristics of the tire. Hysteretic energy loss in rubber decreases as temperature increases.*

*The hysteresis effect causes a loaded rubber not to rebound fully after load removal. Consider a high hysteresis race car tire turning over road irregularities. The deformed tire recovers slowly, and therefore, it cannot push the tireprint tail on the road as hard as the tireprint head. The difference in head and tail pressures causes a resistance force, which is called rolling resistance.*

*Race cars have high hysteresis tires to increase friction and limit traction. Street cars have low hysteresis tires to reduce the rolling resistance and low operating temperature. Hysteresis level of tires inversely affect the stopping distance. A high hysteresis tire makes the stopping shorter, however, it wears rapidly and has a shorter life time.*
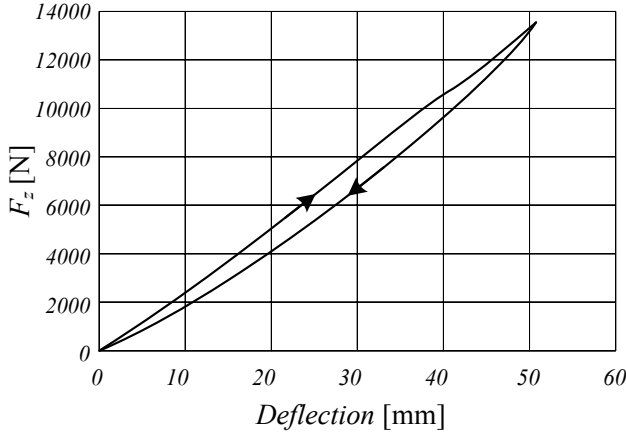
FIGURE 3.10. Histeresis loop in a vertically loading and unloading tire.

## 3.3    Tireprint Forces

The force per unit area applied on a tire in a tireprint can be decomposed into a component normal to the ground and a tangential component on the ground. The normal component is the contact pressure $\sigma_z$, while the tangential component can be further decomposed in the $x$ and $y$ directions to make the longitudinal and lateral shear stresses $\tau_x$ and $\tau_y$. For a stationary tire under normal load, the tireprint is symmetrical. Due to equilibrium conditions, the overall integral of the normal stress over the tireprint area $A_P$ must be equal to the normal load $F_z$, and the integral of shear stresses must be equal to zero.

$$\int_{A_P} \sigma_z(x, y)\, dA = F_z \tag{3.20}$$

$$\int_{A_P} \tau_x(x, y)\, dA = 0 \tag{3.21}$$

$$\int_{A_P} \tau_y(x, y)\, dA = 0 \tag{3.22}$$

### 3.3.1    Static Tire, Normal Stress

Figure 3.11 illustrates a stationary tire under a normal load $F_z$ along with the generated normal stress $\sigma_z$ applied on the ground. The applied loads on the tire are illustrated in the side view shown in Figure 3.12. For a stationary tire, the shape of normal stress $\sigma_z(x, y)$ over the tireprint area depends on tire and load conditions, however its distribution over the tireprint is generally in the shape shown in Figure 3.13.
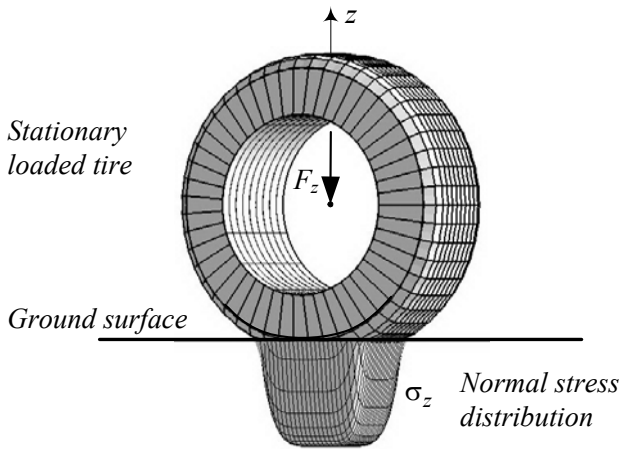
FIGURE 3.11. Normal stress $\sigma_z$ applied on the round because of a stationary tire under a normal load $F_z$.
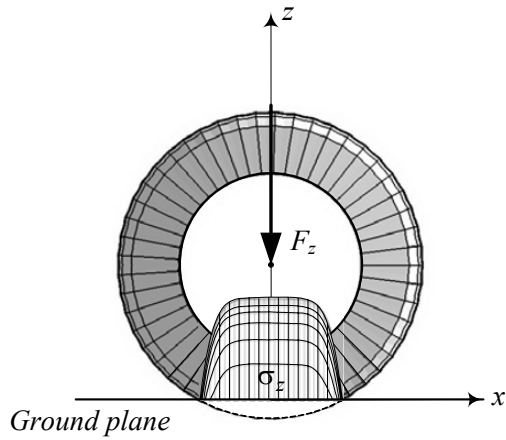


FIGURE 3.12. Side view of a normal force $F_z$ and stress $\sigma_z$ applied on a stationary tire.
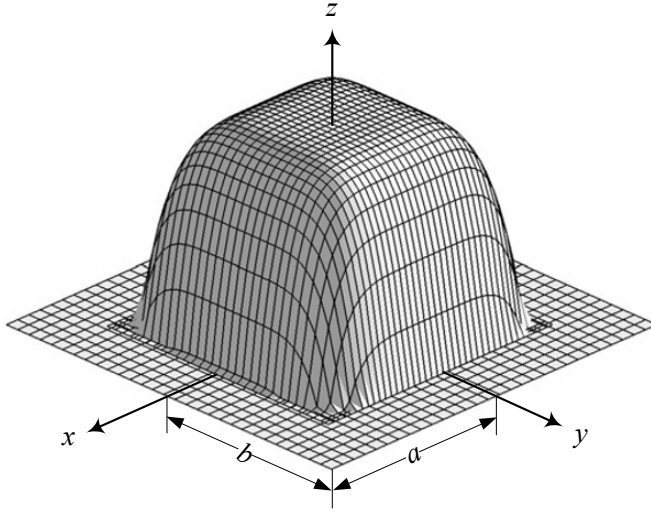
FIGURE 3.13. A model of normal stress $\sigma_z(x, y)$ in the tireprint area for a stationary tire.

The normal stress $\sigma_z(x, y)$ may be approximated by the function

$$\sigma_z(x, y) = \sigma_{z_M} \left( 1 - \frac{x^6}{a^6} - \frac{y^6}{b^6} \right) \tag{3.23}$$

where $a$ and $b$ indicate the dimensions of the tireprint, as shown in Figure 3.14. The tireprints may approximately be modeled by a mathematical function

$$\frac{x^{2n}}{a^{2n}} + \frac{y^{2n}}{b^{2n}} = 1 \qquad n \in N. \tag{3.24}$$

For radial tires, $n = 3$ or $n = 2$ may be used,

$$\frac{x^6}{a^6} + \frac{y^6}{b^6} = 1 \tag{3.25}$$

while for non-radial tires $n = 1$ is a better approximation.

$$\frac{x^2}{a^2} = \frac{y^2}{b^2} = 1. \tag{3.26}$$

**Example 79** *Normal stress in tireprint.*
*A car weighs* 800 kg. *If the tireprint of each radial tire is* $A_P = 4 \times a \times b = 4 \times 5\,\text{cm} \times 12\,\text{cm}$, *then the normal stress distribution under each tire,* $\sigma_z$,
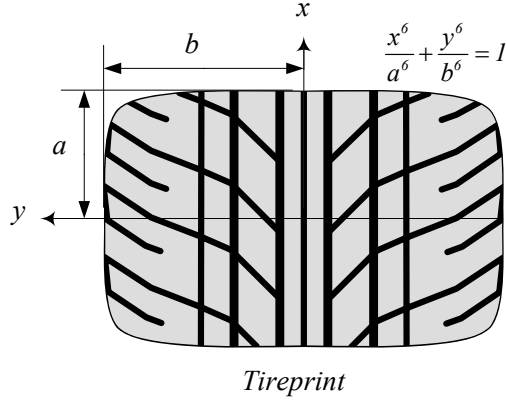
*Tireprint*

FIGURE 3.14. A mode for tireprint of stationary radial tires under normal load.

*must satisfy the equilibrium equation.*

$$F_z = \frac{1}{4} 800 \times 9.81$$

$$= \int_{A_P} \sigma_z(x, y) \, dA$$

$$= \int_{-0.05}^{0.05} \int_{-0.12}^{0.12} \sigma_{z_M} \left( 1 - \frac{x^6}{0.05^6} - \frac{y^6}{0.12^6} \right) dy \, dx$$

$$= 1.7143 \times 10^{-2} \sigma_{z_M} \tag{3.27}$$

*Therefore, the maximum normal stress is*

$$\sigma_{z_M} = \frac{F_z}{1.7143 \times 10^{-2}} = 1.1445 \times 10^5 \, \text{Pa} \tag{3.28}$$

*and the stress distribution over the tireprint is*

$$\sigma_z(x, y) = 1.1445 \times 10^5 \left( 1 - \frac{x^6}{0.05^6} - \frac{y^6}{0.12^6} \right) \text{Pa.} \tag{3.29}$$

**Example 80** *Normal stress in tireprint for $n = 2$.*

  *The maximum normal stress $\sigma_{z_M}$ for an $800 \, \text{kg}$ car having an $A_P = 4 \times a \times b = 4 \times 5 \, \text{cm} \times 12 \, \text{cm}$, can be found for $n = 2$ as*

$$F_z = \frac{1}{4} 800 \times 9.81$$

$$= \int_{A_P} \sigma_z(x, y) \, dA$$

$$= \int_{-0.05}^{0.05} \int_{-0.12}^{0.12} \sigma_{z_M} \left( 1 - \frac{x^4}{0.05^4} - \frac{y^4}{0.12^4} \right) dy \, dx$$

$$= 1.44 \times 10^{-2} \sigma_{z_M} \tag{3.30}$$

FIGURE 3.15. Direction of tangential stresses on the tireprint of a stationary vertically loaded tire.

$$\sigma_{z_M} = \frac{F_z}{1.44 \times 10^{-2}} = 1.3625 \times 10^5 \text{ Pa}. \tag{3.31}$$
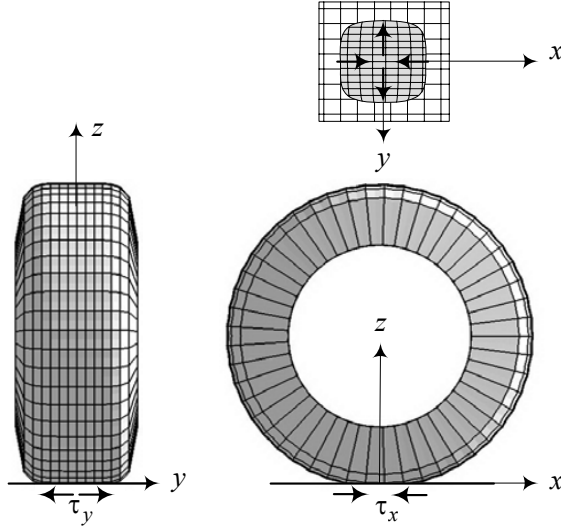
*Comparing $\sigma_{z_M} = 1.3625 \times 10^5$ Pa for $n = 2$ to $\sigma_{z_M} = 1.1445 \times 10^5$ Pa for $n = 3$ shows that maximum stress for $n = 2$ is $\left(1 - \frac{1.1445}{1.3625}\right) \times 100 = 16\%$ more than $n = 3$.*

### 3.3.2    Static Tire, Tangential Stresses

Because of geometry changes to a circular tire in contact with the ground, a three-dimensional stress distribution will appear in the tireprint even for a stationary tire. The *tangential stress* $\tau$ on the tireprint can be decomposed in $x$ and $y$ directions. The tangential stress is also called *shear stress* or *friction stress*.

The tangential stress on a tire is inward in $x$ direction and outward in $y$ direction. Hence, the tire tries to stretch the ground in the $x$-axis and compact the ground on the $y$-axis. Figure 3.15 depicts the shear stresses on a vertically loaded stationary tire. The force distribution on the tireprint is not constant and is influenced by tire structure, load, inflation pressure, and environmental conditions:

The tangential stress $\tau_x$ in the $x$-direction may be modeled by the following equation.

$$\tau_x(x, y) = -\tau_{x_M} \left(\frac{x^{2n+1}}{a^{2n+1}}\right) \sin^2\left(\frac{x}{a}\pi\right) \cos\left(\frac{y}{2b}\pi\right) \qquad n \in N \qquad (3.32)$$
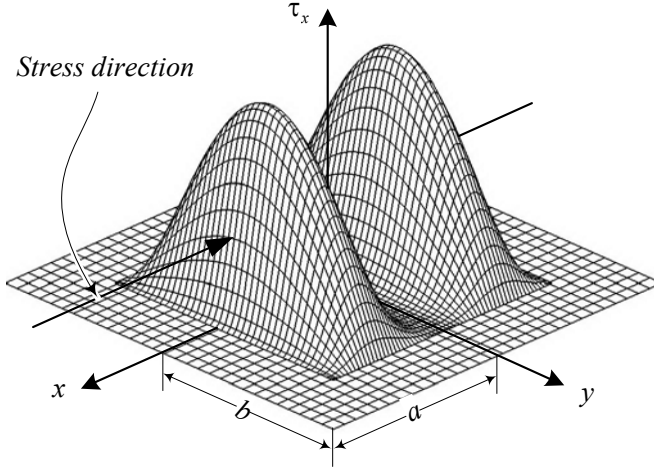
FIGURE 3.16. Absolute value of a $\tau_x$ distribution model for $n = 1$.

$\tau_x$ is negative for $x > 0$ and is positive for $x < 0$, showing an inward longitudinal stress. Figure 3.16 illustrates the absolute value of a $\tau_x$ distribution for $n = 1$.

The $y$-direction tangential stress $\tau_y$ may be modeled by the equation

$$\tau_y(x, y) = -\tau_{y_M}\left(\frac{x^{2n}}{a^{2n}} - 1\right)\sin\left(\frac{y}{b}\pi\right) \qquad n \in N \qquad (3.33)$$

where $\tau_y$ is positive for $y > 0$ and negative for $y < 0$, showing an outward lateral stress. Figure 3.17 illustrates the absolute value of a $\tau_y$ distribution for $n = 1$.

## 3.4   Effective Radius

Consider a vertically loaded wheel that is turning on a flat surface as shown in Figure 3.18. The *effective radius* of the wheel $R_w$, which is also called a *rolling radius*, is defined by

$$R_w = \frac{v_x}{\omega_w} \qquad (3.34)$$

where, $v_x$ is the forward velocity, and $\omega_w$ is the angular velocity of the wheel. The effective radius $R_w$ is approximately equal to

$$R_w \approx R_g - \frac{R_g - R_h}{3} \qquad (3.35)$$

and is a number between the unloaded or *geometric radius* $R_g$ and the *loaded height* $R_h$.

$$R_h < R_w < R_g \qquad (3.36)$$
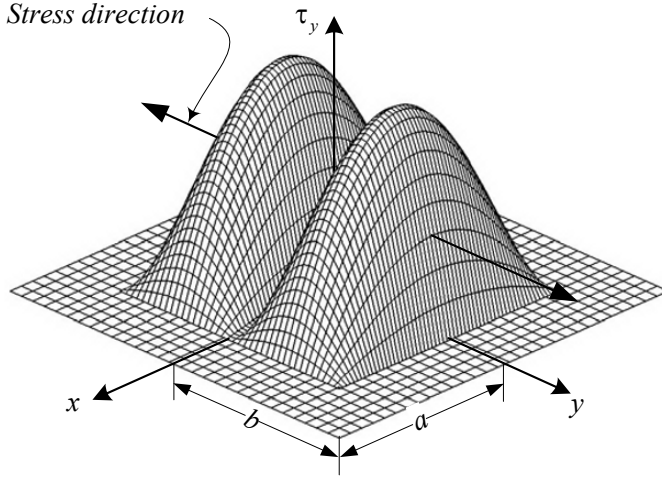
FIGURE 3.17. Absolute value of a $\tau_y$ distribution model for $n = 1$.

**Proof.** An effective radius $R_w = v_x/\omega_w$ is defined by measuring a wheel's angular velocity $\omega_w$ and forward velocity $v_x$. As the tire turns forward, each part of the circumference is flattened as it passes through the contact area. A practical estimate of the effective radius can be made by substituting the arc with the straight length of tireprint. The tire vertical deflection is

$$R_g - R_h = R_g \left(1 - \cos\varphi\right) \tag{3.37}$$

and therefore

$$R_h = R_g \cos\varphi \tag{3.38}$$

$$a = R_g \sin\varphi. \tag{3.39}$$

If the motion of the tire is compared to the rolling of a rigid disk with radius $R_w$, then the tire must move a distance $a = R_w\varphi$ for an angular rotation $\varphi$.

$$a = R_g \sin\varphi = R_w\varphi \tag{3.40}$$

Hence,

$$R_w = \frac{R_g \sin\varphi}{\varphi}. \tag{3.41}$$

Expanding $\frac{\sin\varphi}{\varphi}$ in a Taylor series show that

$$R_w = R_g \left(1 - \frac{1}{6}\varphi^2 + O\left(\varphi^4\right)\right). \tag{3.42}$$
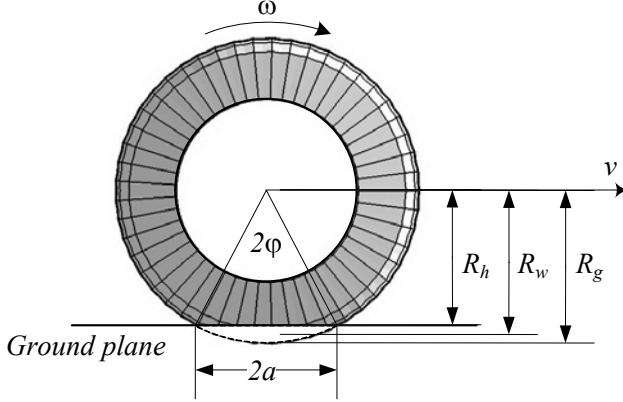
FIGURE 3.18. Effective radius $R_w$ compared to tire radius $R_g$ and loaded height $R_h$.

Using Equation (3.37) we may approximate

$$\cos\varphi \quad \approx \quad 1 - \frac{1}{2}\varphi^2 \tag{3.43}$$

$$\varphi^2 \quad \approx \quad 2\left(1 - \cos\varphi\right)$$

$$\approx \quad 2\left(1 - \frac{R_h}{R_g}\right) \tag{3.44}$$

and therefore,

$$R_w \quad \approx \quad R_g\left(1 - \frac{1}{3}\left(1 - \frac{R_h}{R_g}\right)\right)$$

$$= \quad \frac{2}{3}R_g + \frac{1}{3}R_h. \tag{3.45}$$

Because $R_h$ is a function of tire load $F_z$,

$$R_h \quad = \quad R_h\left(F_z\right)$$

$$= \quad R_g - \frac{F_z}{k_z} \tag{3.46}$$

the effective radius $R_w$ is also a function of the tire load. The angle $\varphi$ is called *tireprint angle* or *tire contact angle*.

The vertical stiffness of radial tires is less than non-radial tires under the same conditions. So, the loaded height of radial tires, $R_h$, is less than the non-radials'. However, the effective radius of radial tires $R_w$, is closer to their unloaded radius $R_g$. As a good estimate, for a non-radial tire, $R_w \approx 0.96R_g$, and $R_h \approx 0.94R_g$, while for a radial tire, $R_w \approx 0.98R_g$, and $R_h \approx 0.92R_g$.

Generally speaking, the effective radius $R_w$ depends on the type of tire, stiffness, load conditions, inflation pressure, and wheel's forward velocity. ∎

**Example 81** *Compression and expansion of tires in the tireprint zone.*

*Because of longitudinal deformation, the peripheral velocity of any point of the tread varies periodically. When it gets close to the starting point of the tireprint, it slows down and a circumferential compression results. The tire treads are compressed in the first half of the tireprint and gradually expanded in the second half. The treads in the tireprint contact zone almost stick to the ground, and therefore their circumferential velocity is close to the forward velocity of the tire center $v_x$. The treads regain their initial circumferential velocity $R_g\omega_w$ after expanding and leaving the contact zone.*

**Example 82** *Tire rotation.*
*The geometric radius of a tire $P235/75R15$ is $R_g = 366.9\,\mathrm{mm}$, because*

$$
\begin{aligned}
h_T &= 235 \times 75\% \\
&= 176.25\,\mathrm{mm} \approx 6.94\,\mathrm{in} 
\end{aligned}
\tag{3.47}
$$

*and therefore,*

$$
\begin{aligned}
R_g &= \frac{2h_T + 15}{2} \\
&= \frac{2 \times 6.94 + 15}{2} \\
&= 14.44\,\mathrm{in} \approx 366.9\,\mathrm{mm}.
\end{aligned}
\tag{3.48}
$$

*Consider a vehicle with such a tire is traveling at a high speed such as $v = 50\,\mathrm{m/s} = 180\,\mathrm{km/h} \approx 111.8\,\mathrm{mi/h}$. The tire is radial, and therefore the effective tire radius $R_w$ is approximately equal to*

$$
R_w \approx 0.98 R_g \approx 359.6\,\mathrm{mm}.
\tag{3.49}
$$

*After moving a distance $d = 100\,\mathrm{km}$, this tire must have been turned $n_1 = 44259$ times because*

$$
\begin{aligned}
n_1 &= \frac{d}{\pi D} \\
&= \frac{100 \times 10^3}{2\pi \times 359.6 \times 10^{-3}} = 44259.
\end{aligned}
\tag{3.50}
$$

*Now assume the vehicle travels the same distance $d = 100\,\mathrm{km}$ at a low inflation pressure, such that the effective radius of the tire remained close to at the loaded radius*

$$
\begin{aligned}
R_w &\approx R_h \approx 0.92 R_g \\
&= 330.8\,\mathrm{mm}.
\end{aligned}
\tag{3.51}
$$
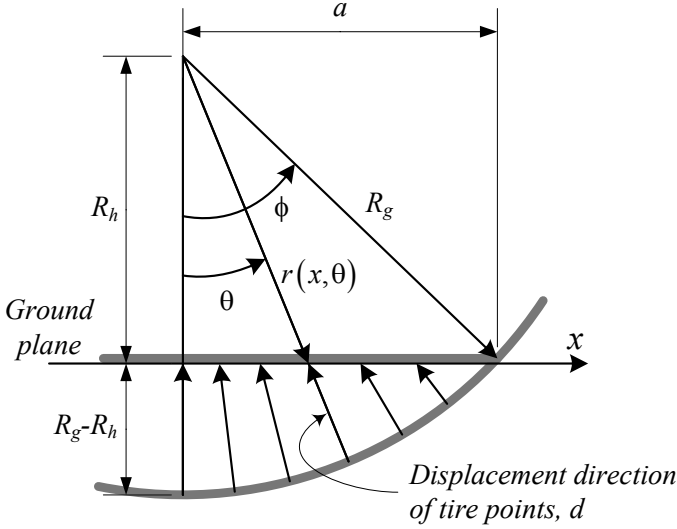
FIGURE 3.19. Radial motion of the tire peripheral points in the contact area.

*This tire must turn $n_2 = 48112$ times to travel $d = 100\,\mathrm{km}$, because,*

$$
\begin{aligned}
n_2 &= \frac{d}{\pi D} \\
&= \frac{100 \times 10^3}{2\pi \times 330.8 \times 10^{-3}} = 48112.
\end{aligned}
\tag{3.52}
$$

**Example 83 ★** *Radial motion of tire's peripheral points in the tireprint.*
   *The radial displacement of a tire's peripheral points during road contact may be modeled by a function*

$$
d = d(x, \theta).
\tag{3.53}
$$

*We assume that a peripheral point of the tire moves along only the radial direction during contact with the ground, as shown in Figure 3.19.*
   *Let's show a radius at an angle $\theta$, by $r = r(x, \theta)$. Knowing that*

$$
\cos \theta = \frac{R_h}{r}
\tag{3.54}
$$

$$
\cos \phi = \frac{R_h}{R_g}
\tag{3.55}
$$

*we can find*

$$
r = R_g \frac{\cos \phi}{\cos \theta}.
\tag{3.56}
$$

*Thus, the displacement function is*

$$
\begin{aligned}
d &= R_g - r(x, \theta) \\
&= R_g \left( 1 - \frac{R_h}{R_g \cos\theta} \right) \qquad -\phi < \theta < \phi. \qquad (3.57)
\end{aligned}
$$

**Example 84** *Tread travel.*

*Let's follow a piece of tire tread in its travel around the spin axis when the vehicle moves forward at a constant speed. Although the wheel is turning at constant angular velocity $\omega_w$, the tread does not travel at constant speed. At the top of the tire, the radius is equal to the unloaded radius $R_g$ and the speed of the tread is $R_g\omega_w$ relative to the wheel center. As the tire turns, the tread approaches the leading edge of tireprint, and slows down. The tread is compacted radially, and gets squeezed in the heading part of the tireprint area. Then, it is stretched out and unpacked in the tail part of the tireprint as it moves to the tail edge. In the middle of the tireprint, the tread speed is $R_h\omega_w$ relative to the wheel center.*

*The variable radius of a tire during the motion through the tireprint is*

$$
r = R_g \frac{\cos\phi}{\cos\theta} \qquad -\phi < \theta < \phi \qquad (3.58)
$$

*where $\phi$ is the half of the contact angle, and $\theta$ is the angular rotation of the tire, as shown in Figure 3.19. The angular velocity of the tire is $\omega_w = \dot{\theta}$ and is assumed to be constant. Then, the radial velocity $\dot{r}$ and acceleration $\ddot{r}$ of the tread with respect to the wheel center are*

$$
\dot{r} = R_g\omega_w \cos\phi \frac{\sin\theta}{\cos^2\theta} \qquad\qquad (3.59)
$$

$$
\ddot{r} = \frac{1}{2} R_g\omega_w^2 \frac{\cos\phi}{\cos^3\theta} (3 - \cos 2\theta). \qquad (3.60)
$$

*Figure 3.20 depicts $r$, $\dot{r}$, and $\ddot{r}$ for a sample car with the following data:*

$$
\begin{aligned}
R_g &= 0.5\,\mathrm{m} & (3.61) \\
\phi &= 15\,\mathrm{deg} & (3.62) \\
\omega_w &= 60\,\mathrm{rad/s} & (3.63)
\end{aligned}
$$

## 3.5   Rolling Resistance

A turning tire on the ground generates a longitudinal force called *rolling resistance*. The force is opposite to the direction of motion and is proportional to the normal force on the tireprint.

$$
\begin{aligned}
\mathbf{F}_r &= -F_r \,\hat{\imath} & (3.64) \\
F_r &= \mu_r F_z & (3.65)
\end{aligned}
$$
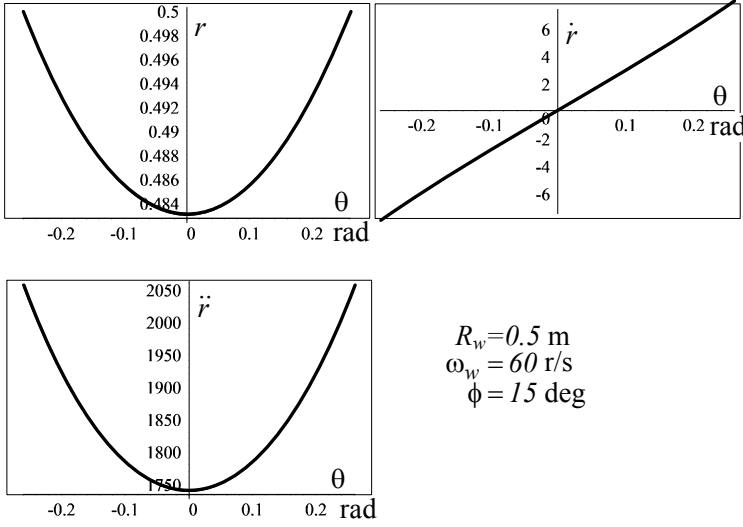
FIGURE 3.20. Radial displacement, velocity, and acceleration of tire treads in the tireprint.

The parameter $\mu_r$ is called the *rolling friction coefficient*. $\mu_r$ is not constant and mainly depends on tire speed, inflation pressure, sideslip and camber angles. It also depends on mechanical properties, speed, wear, temperature, load, size, driving and braking forces, and road condition.

**Proof.** When a tire is turning on the road, that portion of the tire's circumference that passes over the pavement undergoes a deflection. Part of the energy that is spent in deformation will not be restored in the following relaxation. Hence, a change in the distribution of the contact pressure makes normal stress $\sigma_z$ in the heading part of the tireprint be higher than the tailing part. The dissipated energy and stress distortion cause the rolling resistance.

Figures 3.21 and 3.22 illustrate a model of normal stress distribution across the tireprint and their resultant force $F_z$ for a turning tire.

Because of higher normal stress in the front part of the tireprint, the resultant normal force moves forward. Forward shift of the normal force makes a resistance moment in the $-y$ direction, opposing the forward rotation.

$$\mathbf{M}_r \quad = \quad -M_r\,\hat{j} \qquad\qquad (3.66)$$
$$M_r \quad = \quad F_z\,\Delta x \qquad\qquad (3.67)$$

The rolling resistance moment $\mathbf{M}_r$ can be substituted by a rolling resistance

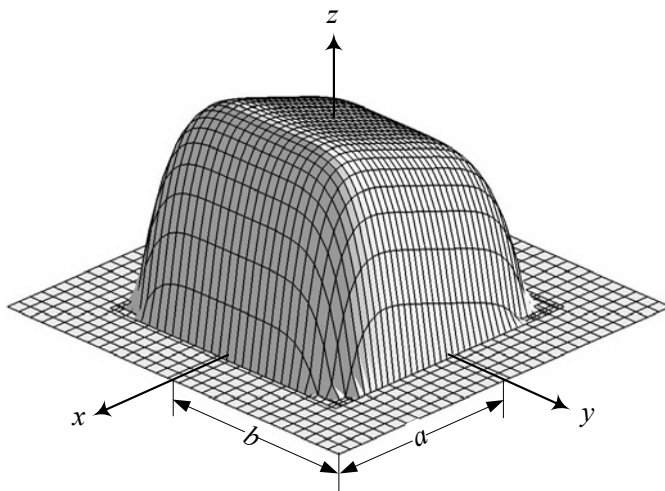FIGURE 3.21. A model of normal stress $\sigma_z(x, y)$ in the tireprint area for a rolling tire.
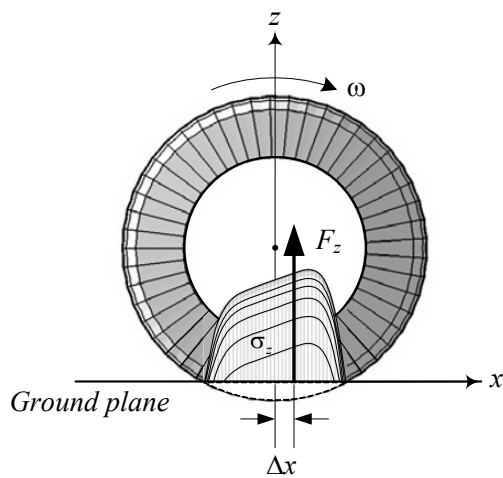


FIGURE 3.22. Side view of a normal stress $\sigma_z$ distribution and its resultant force $F_z$ on a rolling tire.

force $\mathbf{F}_r$ parallel to the $x$-axis.

$$\mathbf{F}_r = -F_r\,\hat{\imath} \tag{3.68}$$

$$F_r = \frac{1}{R_h}M_r = \frac{\Delta x}{R_h}F_z \tag{3.69}$$

Practically the rolling resistance force can be defined using a rolling friction coefficient $\mu_r$.

$$F_r = \mu_r\,F_z \tag{3.70}$$

■

**Example 85** *A model for normal stress of a turning tire.*
*We may assume that the normal stress of a turning tire is expressed by*

$$\sigma_z = \sigma_{z_m}\left(1 - \frac{x^{2n}}{a^{2n}} - \frac{y^{2n}}{b^{2n}} + \frac{x}{4a}\right) \tag{3.71}$$

*where $n = 3$ or $n = 2$ for radial tires and $n = 1$ for non-radial tires. We may determine the stress mean value $\sigma_{z_m}$ by knowing the total load on the tire. As an example, using $n = 3$ for an $800\,\mathrm{kg}$ car with a tireprint $A_P = 4 \times a \times b = 4 \times 5\,\mathrm{cm} \times 12\,\mathrm{cm}$, we have*

$$
\begin{aligned}
F_z &= \frac{1}{4}800 \times 9.81 \\
&= \int_{A_P} \sigma_z(x,y)\,dA \\
&= \int_{-0.05}^{0.05}\int_{-0.12}^{0.12} \sigma_{z_m}\left(1 - \frac{x^6}{0.05^6} - \frac{y^6}{0.12^6} + \frac{x}{4 \times 0.05}\right) dy\,dx \\
&= 1.7143 \times 10^{-2}\sigma_{z_m} \tag{3.72}
\end{aligned}
$$

*and therefore,*

$$\sigma_{z_m} = \frac{F_z}{1.7143 \times 10^{-2}} = 1.1445 \times 10^5\,\mathrm{Pa} \tag{3.73}$$

**Example 86** *Deformation and rolling resistance.*
*The distortion of stress distribution is proportional to the tire-road deformation that is the reason for shifting the resultant force forward. Hence, the rolling resistance increases with increasing deformation. A high pressure tire on concrete has lower rolling resistance than a low pressure tire on soil.*

*To model the mechanism of dissipation energy for a turning tire, we assume there are many small dampers and springs in the tire structure. Pairs of parallel dampers and springs are installed radially and circumstantially. Figures 3.23 and 3.24 illustrate the damping and spring structure of a tire.*
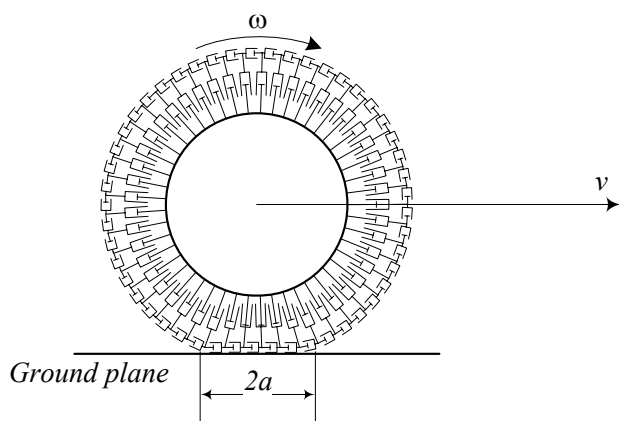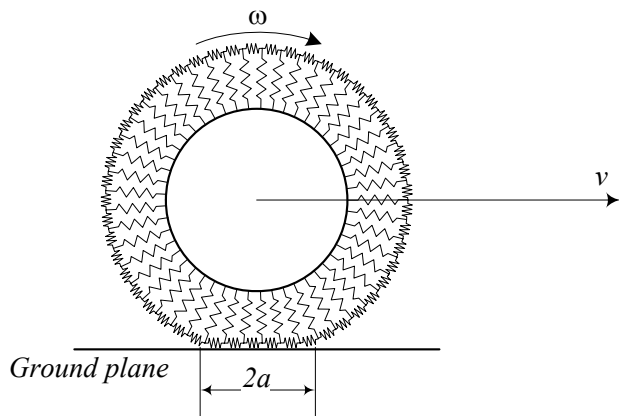
FIGURE 3.23. Damping structure of a tire.



FIGURE 3.24. Spring structure of a tire.

### 3.5.1   ★ Effect of Speed on the Rolling Friction Coefficient

The rolling friction coefficient $\mu_r$ increases with a second degree of speed. It is possible to express $\mu_r = \mu_r(v_x)$ by the function

$$\mu_r = \mu_0 + \mu_1\, v_x^2. \tag{3.74}$$

**Proof.** The rolling friction coefficient increases by increasing speed experimentally. We can use a polynomial function

$$\mu_r = \sum_{i=0}^{n} \mu_i\, v_x^i \tag{3.75}$$

to fit the experimental data. Practically, two or three terms of the polynomial would be enough. The function

$$\mu_r = \mu_0 + \mu_1\, v_x^2 \tag{3.76}$$

is simple and good enough for representing experimental data and analytic calculation. The values of

$$\mu_0 \quad = \quad 0.015 \tag{3.77}$$
$$\mu_1 \quad = \quad 7 \times 10^{-6}\, \mathrm{s^2/m^2} \tag{3.78}$$

are reasonable values for most passenger car tires. However, $\mu_0$ and $\mu_1$ should be determined experimentally for any individual tire. Figure 3.25 depicts a comparison between Equation (3.74) and experimental data for a radial tire.

Generally speaking, the rolling friction coefficient of radial tires show to be less than non-radials. Figure 3.26 illustrates a sample comparison.

Equation (3.74) is applied when the speed is below the tire's critical speed. *Critical speed* is the speed at which standing circumferential waves appear and the rolling friction increases rapidly. The wavelength of the standing waves are close to the length of the tireprint. Above the critical speed, overheating happens and tire fails very soon. Figure 3.27 illustrates the circumferential waves in a rolling tire at its critical speed. ∎

**Example 87** *Rolling resistance force and vehicle velocity.*

*For computer simulation purposes, a fourth degree equation is presented to evaluate the rolling resistance force $F_r$*

$$F_r = C_0 + C_1\, v_x + C_2\, v_x^4. \tag{3.79}$$

*The coefficients $C_i$ are dependent on the tire characteristics, however, the following values can be used for a typical raided passenger car tire:*

$$C_0 \quad = \quad 9.91 \times 10^{-3}$$
$$C_1 \quad = \quad 1.95 \times 10^{-5} \tag{3.80}$$
$$C_2 \quad = \quad 1.76 \times 10^{-9}$$
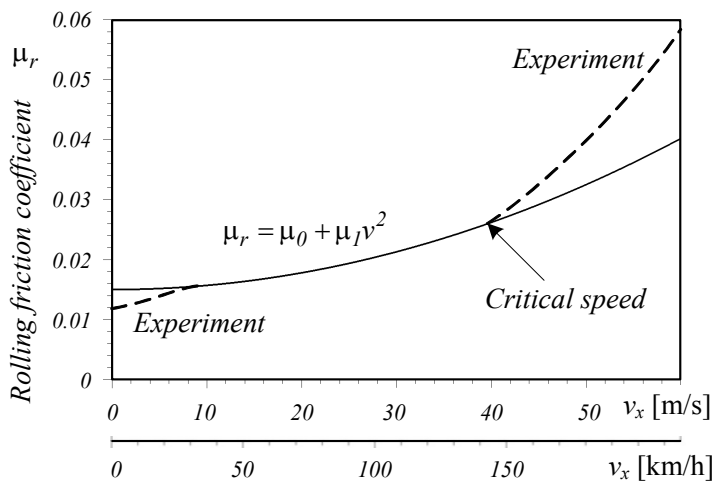
FIGURE 3.25. Comparison between the analytic equation and experimental data for the rolling friction coefficient of a radial tire.
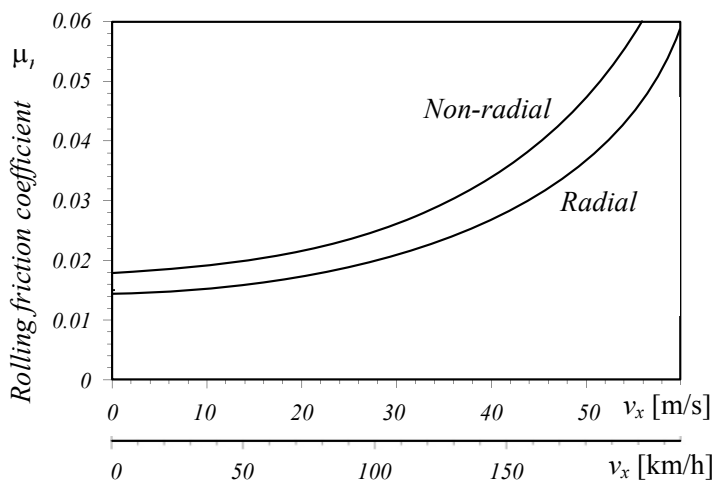


FIGURE 3.26. Comparison of the rolling friction coefficient between radial and non-radial tires.
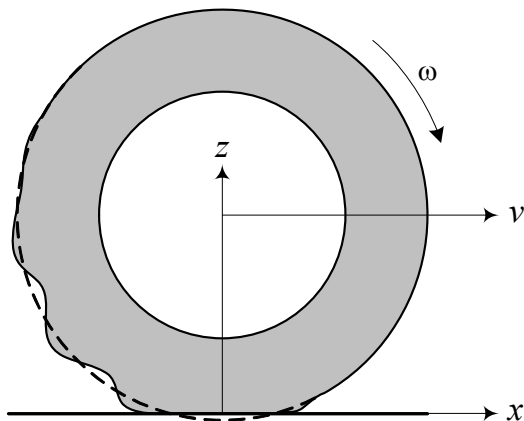
FIGURE 3.27. Illustration of circumferential waves in a rolling tire at its critical speed.

**Example 88** *Road pavement and rolling resistance.*
    *The effect of the pavement and road condition is introduced by assigning a value for $\mu_0$ in equation $\mu_r = \mu_0 + \mu_1 v_x^2$. Table 3.1 is a good reference.*

*Table 3.1 - The value of $\mu_0$  on different pavements.*

| Road and pavement condition | $\mu_0$ |
|---|---|
| Very good concrete | $0.008 - 0.1$ |
| Very good tarmac | $0.01 - 0.0125$ |
| Average concrete | $0.01 - 0.015$ |
| Very good pavement | $0.015$ |
| Very good macadam | $0.013 - 0.016$ |
| Average tarmac | $0.018$ |
| Concrete in poor condition | $0.02$ |
| Good block paving | $0.02$ |
| Average macadam | $0.018 - 0.023$ |
| Tarmac in poor condition | $0.23$ |
| Dusty macadam | $0.023 - 0.028$ |
| Good stone paving | $0.033 - 0.055$ |
| Good natural paving | $0.045$ |
| Stone pavement in poor condition | $0.085$ |
| Snow shallow ($5\,\mathrm{cm}$) | $0.025$ |
| Snow thick ($10\,\mathrm{cm}$) | $0.037$ |
| Unmaintained natural road | $0.08 - 0.16$ |
| Sand | $0.15 - 0.3$ |

**Example 89** *Tire information tips.*

*A new front tire with a worn rear tire can cause instability.*

*Tires stored in direct sunlight for long periods of time will harden and age more quickly than those kept in a dark area.*

*Prolonged contact with oil or gasoline causes contamination of the rubber compound, making the tire life short.*

**Example 90 ★** *Wave occurrence justification.*

*The normal stress will move forward when the tire is turning on a road. By increasing the speed, the normal stress will shift more and concentrate in the first half of the tireprint, causing low stress in the second half of the tireprint. High stress in the first half along with no stress in the second half is similar to hammering the tire repeatedly.*

**Example 91 ★** *Race car tires.*

*Racecars have very smooth tires, known as* **slicks**. *Smooth tires reduce the rolling friction and maximize straight line speed. The slick racing tires are also pumped up to high pressure. High pressure reduces the tireprint area. Hence, the normal stress shift reduces and the rolling resistance decreases.*

**Example 92 ★** *Effect of tire structure, size, wear, and temperature on the rolling friction coefficient.*

*The tire material and the arrangement of tire plies affect the rolling friction coefficient and the critical speed. Radial tires have around* 20% *lower* $\mu_r$, *and* 20% *higher critical speed.*

*Tire radius* $R_g$ *and aspect ratio* $h_T/w_T$ *are the two size parameters that affect the rolling resistance coefficient. A tire with larger* $R_g$ *and smaller* $h_T/w_T$ *has lower rolling resistance and higher critical speed.*

*Generally speaking, the rolling friction coefficient decreases with wear in both radial and non-radial tires, and increases by increasing temperature.*

### 3.5.2    ★ Effect of Inflation Pressure and Load on the Rolling Friction Coefficient

The rolling friction coefficient $\mu_r$ decreases by increasing the inflation pressure $p$. The effect of increasing pressure is equivalent to decreasing normal load $F_z$.

The following empirical equation has been suggested to show the effects of both pressure $p$ and load $F_z$ on the rolling friction coefficient.

$$\mu_r = \frac{K}{1000}\left(5.1 + \frac{5.5 \times 10^5 + 90F_z}{p} + \frac{1100 + 0.0388F_z}{p}v_x^2\right) \qquad (3.81)$$

The parameter $K$ is equal to 0.8 for radial tires, and is equal to 1.0 for non-radial tires. The value of $F_z$, $p$, and $v_x$ must be in [N], [Pa], and [m/s] respectively.
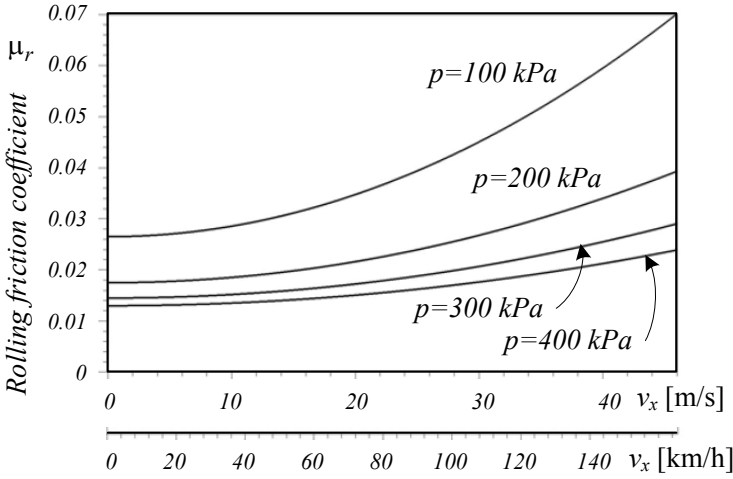
FIGURE 3.28. Motorcycle rolling friction coefficient.

**Example 93** *Motorcycle rolling friction coefficient.*

*The following equations are suggested for calculating rolling friction coefficient $\mu_r$ applicable to motorcycles. They can be only used as a rough lower estimate for passenger cars. The equations consider the inflation pressure and forward velocity of the motorcycle.*

$$\mu_r = \begin{cases} 0.0085 + \dfrac{1800}{p} + \dfrac{2.0606}{p}\, v_x^2 & v_x \leq 46\,\mathrm{m/s}\,(\approx 165\,\mathrm{km/h}) \\[4mm] \dfrac{1800}{p} + \dfrac{3.7714}{p}\, v_x^2 & v_x > 46\,\mathrm{m/s}\,(\approx 165\,\mathrm{km/h}) \end{cases} \tag{3.82}$$

*The speed $v_x$ must be expressed in $\mathrm{m/s}$ and the pressure $p$ must be in Pa. Figure 3.28 illustrates this equation for $v_x \leq 46\,\mathrm{m/s}\,(\approx 165\,\mathrm{km/h})$.*

*Increasing the inflation pressure $p$ decreases the rolling friction coefficient $\mu_r$.*

**Example 94** *Dissipated power because of rolling friction.*

*Rolling friction reduces the vehicle's power. The dissipated power because of rolling friction is equal to the rolling friction force $F_r$ times the forward velocity $v_x$. Using Equation (3.81), the rolling resistance power is*

$$\begin{aligned} P &= F_r\, v_x \\ &= -\mu_r\, v_x\, F_z \\ &= \frac{-K\, v_x}{1000}\left(5.1 + \frac{5.5 \times 10^5 + 90 F_z}{p} + \frac{1100 + 0.0388 F_z}{p}\, v_x^2\right) F_z. \tag{3.83} \end{aligned}$$

*The resultant power $P$ is in $[\mathrm{W}]$ when the normal force $F_z$ is expressed in $[\mathrm{N}]$, velocity $v_x$ in $[\mathrm{m/s}]$, and pressure $p$ in $[\mathrm{Pa}]$.*

*The rolling resistance dissipated power for motorcycles can be found based on Equation (3.82).*

$$P = \begin{cases} \left(0.0085 + \dfrac{1800}{p} + \dfrac{2.0606}{p}v_x^2\right)v_x F_z & v_x \le 46\,\mathrm{m/s}\,(\approx 165\,\mathrm{km/h}) \\[2ex] \left(\dfrac{1800}{p} + \dfrac{3.7714}{p}v_x^2\right)v_x F_z & v_x > 46\,\mathrm{m/s}\,(\approx 165\,\mathrm{km/h}) \end{cases}$$
$$(3.84)$$

**Example 95** *Rolling resistance dissipated power.*

*If a vehicle is moving at $100\,\mathrm{km/h} \approx 27.78\,\mathrm{m/s} \approx 62\,\mathrm{mi/h}$ and each radial tire of the vehicle is pressurized up to $220\,\mathrm{kPa} \approx 32\,\mathrm{psi}$ and loaded by $220\,\mathrm{kg}$, then the dissipated power, because of rolling resistance, is*

$$\begin{aligned} P &= 4 \times \frac{K v_x}{1000}\left(5.1 + \frac{5.5 \times 10^5 + 90F_z}{p} + \frac{1100 + 0.0388F_z}{p}v_x^2\right)F_z \\ &= 2424.1\,\mathrm{W} \approx 2.4\,\mathrm{kW}. \end{aligned} \quad (3.85)$$

*To compare the given equations, assume the vehicle has motorcycle tires with power loss given by Equation (3.84).*

$$\begin{aligned} P &= \left(0.0085 + \frac{1800}{p} + \frac{2.0606}{p}v_x^2\right)v_x F_z \\ &= 5734.1\,\mathrm{W} \approx 5.7\,\mathrm{kW}. \end{aligned} \quad (3.86)$$

*It shows that if the vehicle uses motorcycle tires, it dissipates more power.*

**Example 96** *Effects of improper inflation pressure.*

*High inflation pressure increases stiffness, which reduces ride comfort and generates vibration. Tireprint and traction are reduced when tires are over inflated. Over-inflation causes the tire to transmit shock loads to the suspension, and reduces the tire's ability to support the required load for cornerability, braking, and acceleration.*

*Under-inflation results in cracking and tire component separation. It also increases sidewall flexing and rolling resistance that causes heat and mechanical failure. A tire's load capacity is largely determined by its inflation pressure. Therefore, under-inflation results in an overloaded tire that operates at high deflection with a low fuel economy, and low handling.*

*Figure 3.29 illustrates the effect of over and under inflation on tire-road contact compared to a proper inflated tire.*

*Proper inflation pressure is necessary for optimum tire performance, safety, and fuel economy. Correct inflation is especially significant to the endurance and performance of radial tires because it may not be possible to find a $5\,\mathrm{psi} \approx 35\,\mathrm{kPa}$ under-inflation in a radial tire just by looking.*
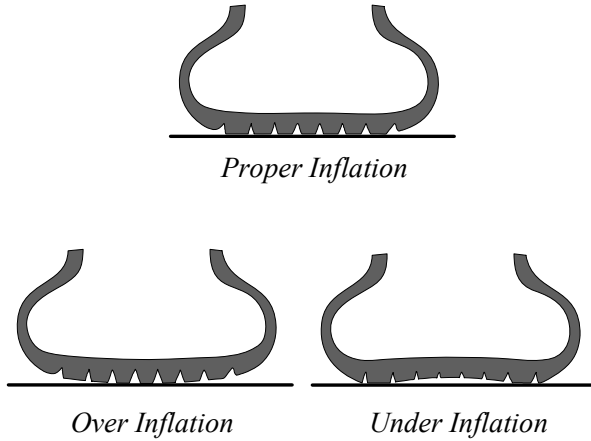
FIGURE 3.29. Tire-road contact of an over- and under-inflated tire compared to a properly inflated tire.

*However, under-inflation of* $5 \, \text{psi} \approx 35 \, \text{kPa}$ *can reduce up to 25% of the tire performance and life.*

*A tire may lose* $1$ *to* $2 \, \text{psi}$ *(*$\approx 7$ *to* $14 \, \text{kPa}$*) every month. The inflation pressure can also change by* $1 \, \text{psi} \approx 7 \, \text{kPa}$ *for every* $10 \, °\text{F} \approx 5 \, °\text{C}$ *of temperature change. As an example, if a tire is inflated to* $35 \, \text{psi} \approx 240 \, \text{kPa}$ *on an* $80 \, °\text{F} \approx 26 \, °\text{C}$ *summer day, it could have an inflation pressure of* $23 \, \text{psi} \approx 160 \, \text{kPa}$ *on a* $20 \, °\text{F} \approx -6 \, °\text{C}$ *day in winter. This represents a normal loss of* $6 \, \text{psi} \approx 40 \, \text{kPa}$ *over the six months and an additional loss of* $6 \, \text{psi} \approx 40 \, \text{kPa}$ *due to the* $60 \, °\text{F} \approx 30 \, °\text{C}$ *change. At* $23 \, \text{psi} \approx 160 \, \text{kPa}$*, this tire is functioning under-inflated.*

**Example 97** *Small / large and soft / hard tires.*

*If the driving tires are small, the vehicle becomes twitchy with low traction and low top speed. However, when the driving tires are big, then the vehicle has slow steering response and high tire distortion in turns, decreasing the stability.*

*Softer front tires show more steerability, less stability, and more wear while hard front tires show the opposite. Soft rear tires have more rear traction, but they make the vehicle less steerable, more bouncy, and less stable. Hard rear tires have less rear traction, but they make the vehicle more steerable, less bouncy, and more stable.*

### 3.5.3   ★ *Effect of Sideslip Angle on Rolling Resistance*

When a tire is turning on the road with a sideslip angle $\alpha$, a significant increase in rolling resistance occurs. The rolling resistance force $F_r$ would
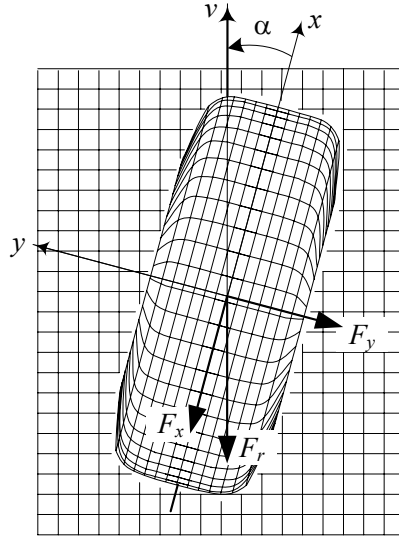
FIGURE 3.30. Effect of sideslip angle $\alpha$ on rolling resistance force $F_r$.

then be

$$F_r = F_x \cos\alpha + F_y \sin\alpha \qquad (3.87)$$
$$\approx F_x - C_\alpha \alpha^2 \qquad (3.88)$$

where, $F_x$ is the longitudinal force opposing the motion, and $F_y$ is the lateral force.

**Proof.** Figure 3.30 illustrates the top view of a turning tire on the ground under a sideslip angle $\alpha$. The rolling resistance force is defined as the force opposite to the velocity vector of the tire, which has angle $\alpha$ with the $x$-axis. Assume a longitudinal force $F_x$ in $-x$-direction is applied on the tire. Sideslip $\alpha$ increases $F_x$ and generates a lateral force $F_y$. The sum of the components of the longitudinal force $F_x$ and the lateral force $F_y$ makes the rolling resistance force $F_r$.

$$F_r = F_x \cos\alpha + F_y \sin\alpha \qquad (3.89)$$

For small values of the sideslip $\alpha$, the lateral force is proportional to $-\alpha$ and therefore,

$$F_r \approx F_x - C_\alpha \alpha^2. \qquad (3.90)$$

■

### 3.5.4  ★ *Effect of Camber Angle on Rolling Resistance*

When a tire travels with a camber angle $\gamma$, the component of rolling moment $\mathbf{M}_r$ on rolling resistance $\mathbf{F}_r$ will be reduced, however, a component of aligning moment $M_z$ on rolling resistance will appear.

$$\mathbf{F}_r = -F_r\,\hat{\imath} \tag{3.91}$$

$$F_r = \frac{1}{R_h}M_r\cos\gamma + \frac{1}{R_h}M_z\sin\gamma \tag{3.92}$$

**Proof.** Rolling moment $M_r$ appears when the normal force $F_z$ shifts forward. However, only the component $M_r\cos\gamma$ is perpendicular to the tire-plane and prevents the tire's spin. Furthermore, when a moment in $z$-direction is applied on the tire, only the component $M_z\sin\gamma$ will prevent the tire's spin. Therefore, the camber angle $\gamma$ will affect the rolling resistance according to

$$\mathbf{F}_r = -F_r\,\hat{\imath}$$

$$F_r = \frac{1}{h}M_r\cos\gamma\frac{1}{h}M_z\sin\gamma \tag{3.93}$$

where $M_r$ may be substituted by Equation (3.66) to show the effect of normal force $F_z$.

$$F_r = \frac{\Delta x}{h}F_z\cos\gamma\frac{1}{h}M_z\sin\gamma \tag{3.94}$$

∎

## 3.6  Longitudinal Force

The *longitudinal slip ratio* of a tire is

$$s = \frac{R_g\omega_w}{v_x} - 1 \tag{3.95}$$

where, $R_g$ is the tire's geometric and unloaded radius, $\omega_w$ is the tire's angular velocity, and $v_x$ is the tire's forward velocity. Slip ratio is positive for driving and is negative for braking.

To accelerate or brake a vehicle, longitudinal forces must develop between the tire and the ground. When a moment is applied to the spin axis of the tire, slip ratio occurs and a longitudinal force $F_x$ is generated at the tireprint. The force $F_x$ is proportional to the normal force,

$$\mathbf{F}_x = F_x\,\hat{\imath} \tag{3.96}$$

$$F_x = \mu_x\left(s\right)F_z \tag{3.97}$$

where the coefficient $\mu_x\left(s\right)$ is called the *longitudinal friction coefficient* and is a function of slip ratio $s$ as shown in Figure 3.31. The friction coefficient
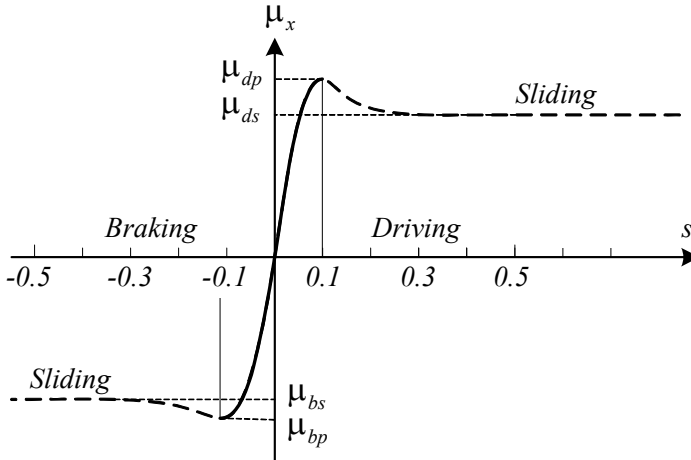
FIGURE 3.31. Longitudinal friction coefficient as a function of slip ratio $s$, in driving and braking.

reaches a driving peak value $\mu_{dp}$ at $s \approx 0.1$, before dropping to an almost steady-state value $\mu_{ds}$. The friction coefficient $\mu_x(s)$ may be assumed proportional to $s$ when $s$ is very small

$$\mu_x(s) = C_s\, s \qquad s << 1 \tag{3.98}$$

where $C_s$ is called the *longitudinal slip coefficient*.

The tire will spin when $s \gtrsim 0.1$ and the friction coefficient remains almost constant. The same phenomena happens in braking at the values $\mu_{bp}$ and $\mu_{bs}$.

**Proof.** Slip ratio, or simply *slip*, is defined as the difference between the actual speed of the tire $v_x$ and the equivalent tire speeds $R_w \omega_w$. Figure 3.32 illustrates a turning tire on the ground. The ideal distance that the tire would freely travel with no slip is denoted by $d_F$, while the actual distance the tire travels is denoted by $d_A$. Thus, for a slipping tire, $d_A > d_F$, and for a spinning tire, $d_A < d_F$.

The difference $d_F - d_A$ is the tire slip and therefore, the slip ratio of the tire is

$$s = \frac{d_F - d_A}{d_A}. \tag{3.99}$$

To have the instant value of $s$, we must measure the travel distances in an infinitesimal time length, and therefore,

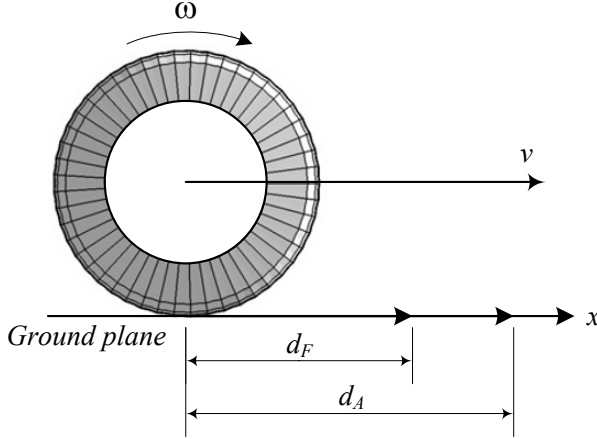$$s \equiv \frac{\dot{d}_F - \dot{d}_A}{\dot{d}_A}. \tag{3.100}$$

FIGURE 3.32. A turning tire on the ground to show the no slip travel distance $d_F$, and the actual travel distance $d_A$.

If the angular velocity of the tire is $\omega_w$ then, $\dot{d}_F = R_g \omega_w$ and $\dot{d}_A = R_w \omega_w$ where, $R_g$ is the geometric tire radius and $R_w$ is the effective radius. Therefore, the slip ratio $s$ can be defined based on the actual speed $v_x = R_w \omega_w$, and the free speed $R_g \omega_w$

$$
\begin{aligned}
s &= \frac{R_g \omega_w - R_w \omega_w}{R_w \omega_w} \\
&= \frac{R_g \omega_w}{v_x} - 1
\end{aligned}
\tag{3.101}
$$

A tire can exert longitudinal force only if a longitudinal slip is present. Longitudinal slip is also called *circumferential* or *tangential slip*. During acceleration, the actual velocity $v_x$ is less than the free velocity $R_g \omega_w$, and therefore, $s > 0$. However, during braking, the actual velocity $v_x$ is higher than the free velocity $R_g \omega_w$ and therefore, $s < 0$.

The frictional force $F_x$ between a tire and the road surface is a function of normal load $F_z$, vehicle speed $v_x$, and wheel angular speed $\omega_w$. In addition to these variables there are a number of parameters that affect $F_x$, such as tire pressure, tread design, wear, and road surface. It has been determined empirically that a contact friction of the form $F_x = \mu_x(\omega_w, v_x) F_z$ can model experimental measurements obtained with constant $v_x$, $\omega_w$. ∎

**Example 98** *Slip ratio based on equivalent angular velocity $\omega_{eq}$.*

*It is possible to define an effective angular velocity $\omega_{eq}$ as an equivalent angular velocity for a tire with radius $R_g$ to proceed with the actual speed $v_x = R_g \omega_{eq}$. Using $\omega_{eq}$ we have*

$$
v_x = R_g \omega_{eq} = R_w \omega_w
\tag{3.102}
$$

*and therefore,*

$$s = \frac{R_g\omega_w - R_g\omega_{eq}}{R_g\omega_{eq}}$$
$$= \frac{\omega_w}{\omega_{eq}} - 1. \tag{3.103}$$

**Example 99** *Slip ratio is $-1 < s < 0$ in braking.*

*When we brake, a braking moment is applied to the wheel axis. The tread of the tire will be stretched circumstantially in the tireprint zone. Hence, the tire is moving faster than a free tire*

$$R_w\omega_w > R_g\omega_w \tag{3.104}$$

*and therefore, $s < 0$. The equivalent radius for a braking tire is more than the free radius*

$$R_w > R_g. \tag{3.105}$$

*Equivalently, we may express the condition using the equivalent angular velocity $\omega_e$ and deduce that a braking tire turns slower than a free tire*

$$R_g\omega_{eq} > R_g\omega_w. \tag{3.106}$$

*The brake moment can be high enough to lock the tire. In this case $\omega_w = 0$ and therefore, $s = -1$. It shows that the longitudinal slip would be between $-1 < s < 0$ when braking.*

$$-1 < s < 0 \quad for \quad a < 0 \tag{3.107}$$

**Example 100** *Slip ratio is $0 < s < \infty$ in driving.*

*When we drive, a driving moment is applied to the tire axis. The tread of the tire will be compressed circumstantially in the tireprint zone. Hence, the tire is moving slower than a free tire*

$$R_w\omega_w < R_g\omega_w \tag{3.108}$$

*and therefore $s > 0$. The equivalent radius for a driving tire is less than the free radius*

$$R_w < R_g. \tag{3.109}$$

*Equivalently, we may express the condition using the equivalent angular velocity $\omega_e$ and deduce that a driving tire turns faster than a free tire*

$$R_g\omega_{eq} < R_g\omega_w. \tag{3.110}$$

*The driving moment can be high enough to overcome the friction and turn the tire on pavement while the car is not moving. In this case $v_x = 0$*

*and therefore, $s = \infty$. It shows that the longitudinal slip would be between $0 < s < \infty$ when accelerating.*

$$0 < s < \infty \quad for \quad a > 0 \tag{3.111}$$

*The tire speed $R_w \omega_w$ equals vehicle speed $v_x$ only if acceleration is zero. In this case, the normal force acting on the tire and the size of the tireprint are constant in time. No element of the tireprint is slipping on the road.*

**Example 101** *Power and maximum velocity.*

*Consider a moving car with power $P = 100\,\text{kW} \approx 134\,\text{hp}$ can attain $279\,\text{km}/\,\text{h} \approx 77.5\,\text{m}/\,\text{s} \approx 173.3\,\text{mi}/\,\text{h}$. The total driving force must be*

$$F_x = \frac{P}{v_x} = \frac{100 \times 10^3}{77.5} = 1290.3\,\text{N}. \tag{3.112}$$

*If we assume that the car is rear-wheel-drive and the rear wheels are driving at the maximum traction under the load $1600\,\text{N}$, then the longitudinal friction coefficient $\mu_x$ is*

$$\mu_x = \frac{F_x}{F_z} = \frac{1290.3}{1600} \approx 0.806. \tag{3.113}$$

**Example 102** *Slip of hard tire on hard road.*

*A tire with no slip cannot create any tangential force. Assume a toy car equipped with steel tires is moving on a glass table. Such a car cannot accelerate or steer easily. If the car can steer at very low speeds, it is because there is sufficient microscopic slip to generate forces to steer or drive. The glass table and the small contact area of the small metallic tires deform and stretch each other, although such a deformation is very small. If there is any friction between the tire and the surface, there must be slip to maneuver.*

**Example 103** *Samples for longitudinal friction coefficients $\mu_{dp}$ and $\mu_{ds}$.*

*Table 3.2 shows the average values of longitudinal friction coefficients $\mu_{dp}$ and $\mu_{ds}$ for a passenger car tire $215/65R15$. It is practical to assume $\mu_{dp} = \mu_{bp}$, and $\mu_{ds} = \mu_{bs}$.*

Table 3.2 - Average of longitudinal friction coefficients.

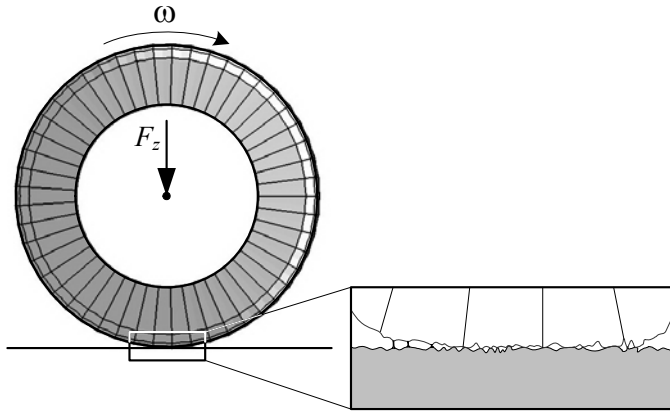| Road surface | Peak value, $\mu_{dp}$ | Sliding value, $\mu_{ds}$ |
|---|---|---|
| Asphalt, dry | $0.8 - 0.9$ | 0.75 |
| Concrete, dry | $0.8 - 0.9$ | 0.76 |
| Asphalt, wet | $0.5 - 0.7$ | $0.45 - 0.6$ |
| Concrete, wet | 0.8 | 0.7 |
| Gravel | 0.6 | 0.55 |
| Snow, packed | 0.2 | 0.15 |
| Ice | 0.1 | 0.07 |

FIGURE 3.33. The molecular binding between the tire and road surfaces.

**Example 104** *Friction mechanisms.*

*Rubber tires generate friction in three mechanisms: 1− adhesion, 2− deformation, and 3− wear.*

$$F_x = F_{ad} + F_{de} + F_{we}. \tag{3.114}$$

**Adhesion** *friction is equivalent to sticking. The rubber resists sliding on the road because adhesion causes it stick to the road surface. Adhesion occurs as a result of molecular binding between the rubber and surfaces. Because the real contact area is much less than the observed contact area, high local pressure make molecular binding, as shown in Figure 3.33. Bound occurs at the points of contact and welds the surfaces together. The adhesion friction is equal to the required force to break these molecular bounds and separate the surfaces. The adhesion is also called* **cold welding** *and is attributed to pressure rather than heat. Higher load increases the contact area, makes more bounds, and increases the friction force. So the adhesion friction confirms the friction equation*

$$F_x = \mu_x\left(s\right)\,F_z. \tag{3.115}$$

*The main contribution to tire traction force on a dry road is the adhesion friction. The adhesion friction decreases considerably on a road covered by water, ice, dust, or lubricant. Water on a wet road prevents direct contact between the tire and road and reduces the formation of adhesion friction. The main contribution to tire friction when it slides on a road surface is the viscoelastic energy dissipation in the tireprint area. This dissipative energy is velocity and is time-history dependent.*

**Deformation friction** *is the result of deforming rubber and filling the microscopic irregularities on the road surface. The surface of the road has many peaks and valleys called* **asperities**. *Movement of a tire on a rough*

*surface results in the deformation of the rubber by peaks and high points on the surface. A load on the tire causes the peaks of irregularities to penetrate the tire and the tire drapes over the peaks. The deformation friction force, needed to move the irregularities in the rubber, comes from the local high pressure across the irregularities. Higher load increases the penetration of the irregularities in the tire and therefore increases the friction force. So the deformation friction confirms the friction equation (3.115).*

*The main contribution to the tire traction force on a wet road is the deformation friction. The adhesion friction decreases considerably on a road covered by water, ice, dust, or lubricant.*

*Deformation friction exists in relative movement between any contacted surfaces. No matter how much care is taken to form a smooth surface, the surfaces are irregular with microscopic peaks and valleys. Opposite peaks interact with each other and cause damage to both surfaces.*

***Wear friction*** *is the result of excessive local stress over the tensile strength of the rubber. High local stresses deform the structure of the tire surface past the elastic point. The polymer bonds break, and the tire surface tears in microscopic scale. This tearing makes the wear friction mechanism. Wear results in separation of material. Higher load eases the tire wear and therefore increases the wear friction force. So the wear friction confirms the friction equation (3.115).*

**Example 105** *Empirical slip models.*

*Based on experimental data and curve fitting methods, some mathematical equations are presented to simulate the longitudinal tire force as a function of longitudinal slip s. Most of these models are too complicated to be useful in vehicle dynamics. However, a few of them are simple and accurate enough to be applied.*

*The Pacejka model, which was presented in 1991, has the form*

$$F_x\left(s\right) = c_1 \sin\left(c_2 \tan^{-1}\left(c_3 s - c_4\left(c_3 s - \tan^{-1}\left(c_3 s\right)\right)\right)\right) \qquad (3.116)$$

*where $c_1$, $c_2$, and $c_3$ are three constants based on the tire experimental data.*

*The 1987 Burckhardt model is a simpler equation that needs three numbers.*

$$F_x\left(s\right) = c_1\left(1 - e^{-c_2 s}\right) - c_3 s \qquad (3.117)$$

*There is another Burckhardt model that includes the velocity dependency.*

$$F_x\left(s\right) = \left(c_1\left(1 - e^{-c_2 s}\right) - c_3 s\right) e^{-c_4 v} \qquad (3.118)$$

*This model needs four numbers to be measured from experiment.*

*By expanding and approximating the 1987 Burckhardt model, the simpler model by Kiencke and Daviss was suggested in 1994. This model is*

$$F_x\left(s\right) = k_s \frac{s}{1 + c_1 s + c_2 s^2} \qquad (3.119)$$

*where $k_s$ is the slope of $F_x(s)$ versus $s$ at $s = 0$*

$$k_s = \lim_{s \to 0} \frac{\triangle F_s}{\triangle s} \tag{3.120}$$

*and $c_1$, $c_2$ are two experimental numbers.*
   *Another simple model is the 2002 De-Wit model*

$$F_x(s) = c_1\sqrt{s} - c_2 s \tag{3.121}$$

*that is based on two numbers $c_1$, $c_2$.*
   *In either case, we need at least one experimental curve such as shown in Figure 3.31 to find the constant numbers $c_i$. The constants $c_i$ are the numbers that best fit the associated equation with the experimental curve. The 1997 Burckhardt model (3.118) needs at least two similar tests at two different speeds.*

**Example 106** ★ *Alternative slip ratio.*
   *An alternative method for defining the slip ratio is*

$$s = \begin{cases} 1 - \dfrac{v_x}{R_g \omega_w} & R_g \omega_w > v_x \quad driving \\[2mm] \dfrac{R_g \omega_w}{v_x} - 1 & R_g \omega_w < v_x \quad braking \end{cases} \tag{3.122}$$

*where $v_x$ is the speed of the wheel center, $\omega_w$ is the angular velocity of the wheel, and $R_g$ is the tire radius.*
   *In another alternative definition, the following equation is used for longitudinal slip:*

$$\begin{aligned} s &= 1 - \left(\frac{R_g \omega_w}{v_x}\right)^n \quad where \quad n = \begin{cases} +1 & R_g \omega_w \le v_x \\ -1 & R_g \omega_w > v_x \end{cases} \tag{3.123} \\ s &\in [0,1] \end{aligned}$$

*In this definition $s$ is always between zero and one. When $s = 1$, then the tire is either locked while the car is sliding, or the tire is spinning while the car is not moving.*

**Example 107** ★ *Tire on soft sand.*
   *Figure 3.34 illustrates a tire turning on sand. The sand will be packed when the tire passes. The applied stresses from the sand on the tire are developed during the angle $\theta_1 < \theta < \theta_2$ measured counterclockwise from vertical direction.*
   *It is possible to define a relationship between the normal stress $\sigma$ and tangential stress $\tau$ under the tire*

$$\tau = (c + \sigma \tan\theta)\left(1 - e^{\frac{r}{k}[\theta_1 - \theta + (1-s)(\sin\theta) - \sin\theta_1]}\right) \tag{3.124}$$
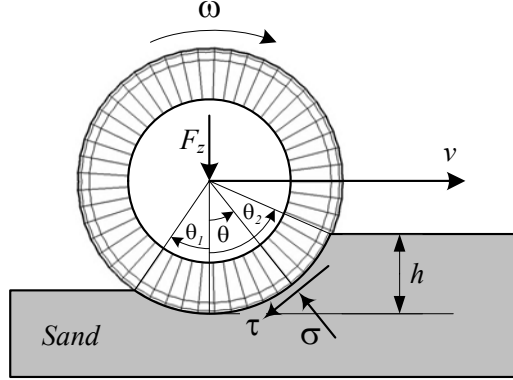
FIGURE 3.34. A tire turning on sand.

*where s is the slip ratio defined in Equation (3.122), and*

$$\tau_M = c + \sigma \tan \theta \qquad (3.125)$$

*is the maximum shear stress in the sand applied on the tire. In this equation, c is the cohesion stress of the sand, and k is a constant.*

**Example 108 ★** *Lateral slip ratio.*

*Analytical expressions can be established for the force contributions in x and y directions using adhesive and sliding concept by defining longitudinal and lateral slip ratios $s_x$ and $s_y$*

$$s_x = \frac{R_g \omega_w}{v_x} - 1 \qquad (3.126)$$

$$s_y = \frac{R_g \omega_w}{v_y} \qquad (3.127)$$

*where $v_x$ is the longitudinal speed of the wheel and $v_y$ is the lateral speed of the wheel. The unloaded geometric radius of the tire is denoted by $R_g$ and $\omega_w$ is the rotation velocity of the wheel.*

*At very low slips, the resulting tire forces are proportional to the slip*

$$F_x = C_{s_x} s_x \qquad (3.128)$$

$$F_y = C_{s_y} s_y \qquad (3.129)$$

*where $C_{s_x}$ is the longitudinal slip coefficient and $C_{s_y}$ is the lateral slip coefficient.*

## 3.7 Lateral Force

When a turning tire is under a vertical force $F_z$ and a lateral force $F_y$, its path of motion makes an angle $\alpha$ with respect to the tire-plane. The angle
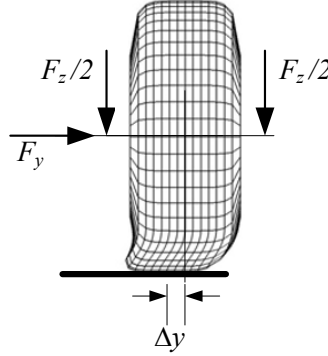
FIGURE 3.35. Front view of a laterally deflected tire.

is called *sideslip* angle and is proportional to the *lateral force*

$$\mathbf{F}_y = F_y \hat{\jmath} \tag{3.130}$$
$$F_y = -C_\alpha \, \alpha \tag{3.131}$$

where $C_\alpha$ is called the *cornering stiffness* of the tire.

$$
\begin{aligned}
C_\alpha &= \lim_{\alpha \to 0} \frac{\partial \left(-F_y\right)}{\partial \alpha} \\
&= \left| \lim_{\alpha \to 0} \frac{\partial F_y}{\partial \alpha} \right| \tag{3.132}
\end{aligned}
$$

The lateral force $\mathbf{F}_y$ is at a distance $a_{x_\alpha}$ behind the centerline of the tireprint and makes a moment $\mathbf{M}_z$ called *aligning moment*.

$$\mathbf{M}_z = M_z \, \hat{k} \tag{3.133}$$
$$M_z = F_y \, a_{x_\alpha} \tag{3.134}$$

For small $\alpha$, the aligning moment $\mathbf{M}_z$ tends to turn the tire about the $z$-axis and make the $x$-axis align with the velocity vector $\mathbf{v}$. The aligning moment always tends to reduce $\alpha$.

**Proof.** When a wheel is under a constant load $F_z$ and then a lateral force is applied on the rim, the tire will deflect laterally as shown in Figure 3.35. The tire acts as a linear spring under small lateral forces

$$F_y = k_y \, \Delta y \tag{3.135}$$

with a lateral stiffness $k_y$.

The wheel will start sliding laterally when the lateral force reaches a maximum value $F_{y_M}$. At this point, the lateral force approximately remains constant and is proportional to the vertical load

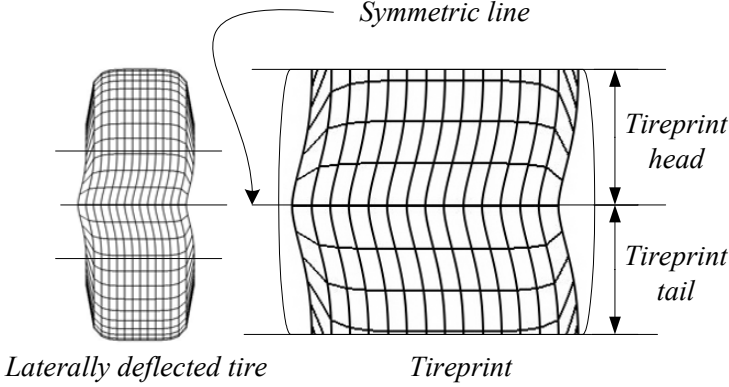$$F_{y_M} = \mu_y \, F_z \tag{3.136}$$

FIGURE 3.36. Bottom view of a laterally deflected tire.

where, $\mu_y$ is the tire friction coefficient in the $y$-direction. A bottom view of the tireprint of a laterally deflected tire is shown in Figure 3.36.

If the laterally deflected tire is turning forward on the road, the tireprint will also flex longitudinally. A bottom view of the tireprint for such a laterally deflected and turning tire is shown in Figure 3.37. Although the tire-plane remains perpendicular to the road, the path of the wheel makes an angle $\alpha$ with tire-plane. As the wheel turns forward, undeflected treads enter the tireprint region and deflect laterally as well as longitudinally. When a tread moves toward the end of the tireprint, its lateral deflection increases until it approaches the tailing edge of the tireprint. The normal load decreases at the tail of the tireprint, so the friction force is lessened and the tread can slide back to its original position when leaving the tireprint region. The point where the laterally deflected tread slides back is called *sliding line*.

A turning tire under lateral force and the associated *sideslip angle* $\alpha$ are shown in Figure 3.38. Lateral distortion of the tire treads is a result of a tangential stress distribution $\tau_y$ over the tireprint. Assuming that the tangential stress $\tau_y$ is proportional to the distortion, the resultant lateral force $F_y$

$$F_y = \int_{A_P} \tau_y \, dA_p \qquad (3.137)$$

is at a distance $a_{x_\alpha}$ behind the center line.

$$a_{x_\alpha} = \frac{1}{F_y} \int_{A_P} x \, \tau_y \, dA_p \qquad (3.138)$$

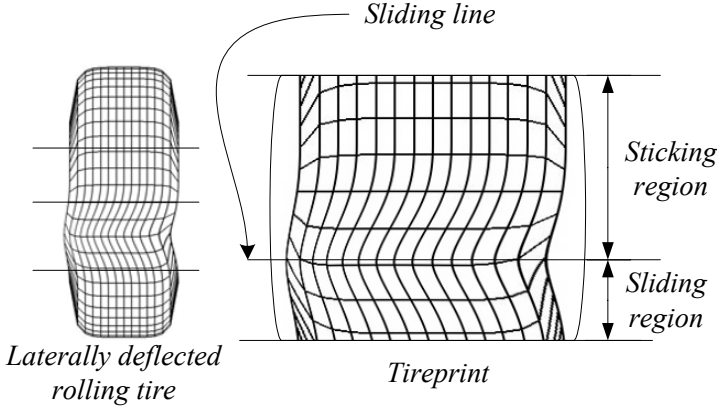The distance $a_{x_\alpha}$ is called the *pneumatic trail*, and the resultant moment

FIGURE 3.37. Bottom view of a laterally deflected and turning tire.

$\mathbf{M}_z$ is called the aligning moment.

$$\mathbf{M}_z = M_z \,\hat{k} \tag{3.139}$$

$$M_z = F_y \, a_{x_\alpha} \tag{3.140}$$

The aligning moment tends to turn the tire about the $z$-axis and make it align with the direction of tire velocity vector $\mathbf{v}$. A stress distribution $\tau_y$, the resultant lateral force $F_y$, and the pneumatic trail $a_{x_\alpha}$ are illustrated in Figure 3.38.

There is also a lateral shift in the tire vertical force $F_z$ because of slip angle $\alpha$, which generates a *slip moment* $M_x$ about the forward $x$-axis.

$$\mathbf{M}_x = -M_x \,\hat{i} \tag{3.141}$$

$$M_x = F_z \, a_{y_\alpha} \tag{3.142}$$

The slip angle $\alpha$ always increases by increasing the lateral force $F_y$. However, the sliding line moves toward the tail at first and then moves forward by increasing the lateral force $F_y$. Slip angle $\alpha$ and lateral force $F_y$ work as action and reaction. A lateral force generates a slip angle, and a slip angle generates a lateral force. Hence, we can steer the tires of a car to make a slip angle and produce a lateral force to turn the car. Steering causes a slip angle in the tires and creates a lateral force. The slip angle $\alpha > 0$ if the tire should be turned about the $z$-axis to be aligned with the velocity vector $\mathbf{v}$. A positive slip angle $\alpha$ generates a negative lateral force $F_y$. Hence, steering to the right about the $-z$-axis makes a positive slip angle and produces a negative lateral force to move the tire to the right.

A sample of measured lateral force $F_y$ as a function of slip angle $\alpha$ for a constant vertical load is plotted in Figure 3.39. The lateral force $F_y$ is linear for small slip angles, however the rate of increasing $F_y$ decreases
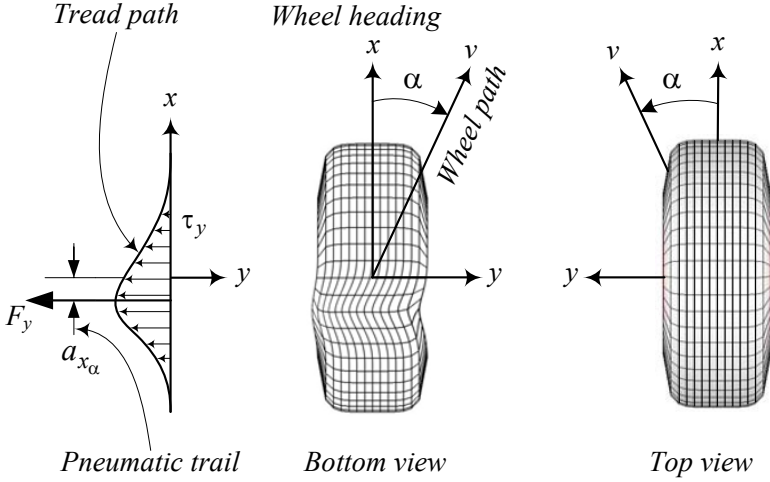
*Tread path*      *Wheel heading*

*Pneumatic trail*     *Bottom view*        *Top view*

FIGURE 3.38. The stress distribution $\tau_y$, the resultant lateral force $F_y$, and the pneumatic trail $a_y$ for a turning tire going on a positive slip angle $\alpha$.

for higher $\alpha$. The lateral force remains constant or drops slightly when $\alpha$ reaches a critical value at which the tire slides on the road. Therefore, we may assume the lateral force $F_y$ is proportional to the slip angle $\alpha$ for low values of $\alpha$.

$$F_y = -C_\alpha \, \alpha \qquad (3.143)$$

$$C_\alpha = \lim_{\alpha \to 0} \frac{\partial \left(-F_y\right)}{\partial \alpha} \qquad (3.144)$$

The cornering stiffness $C_\alpha$ of radial tires are higher than $C_\alpha$ for non-radial tires. This is because radial tires need a smaller slip angle $\alpha$ to produce the same amount of lateral force $F_y$.

Examples of aligning moments for radial and non-radial tires are illustrated in Figure 3.40. The pneumatic trail $a_{x_\alpha}$ increases for small slip angles up to a maximum value, and decreases to zero and even negative values for high slip angles. Therefore, the behavior of aligning moment $\mathbf{M}_z$ is similar to what is shown in Figure 3.40.

The lateral force $F_y = -C_\alpha \, \alpha$ can be decomposed to $F_y \cos \alpha$, parallel to the path of motion $v$, and $F_y \sin \alpha$, perpendicular to $v$ as shown in Figure 3.41. The component $F_y \cos \alpha$, normal to the path of motion, is called *cornering force*, and the component $F_y \sin \alpha$, along the path of motion, is called *drag force*.

Lateral force $F_y$ is also called *side force* or *grip*. We may combine the lateral forces of all a vehicle's tires and have them acting at the car's mass center $C$. ∎
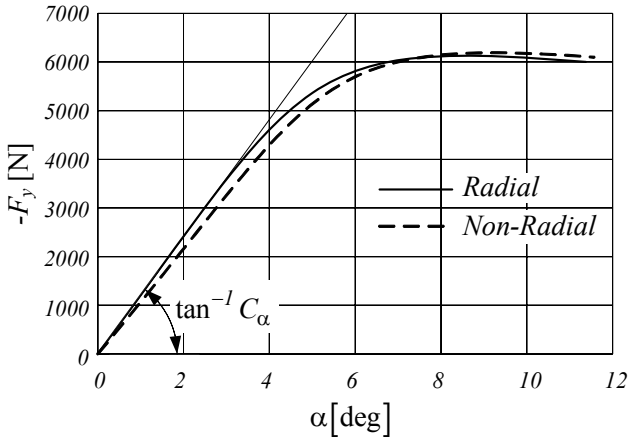
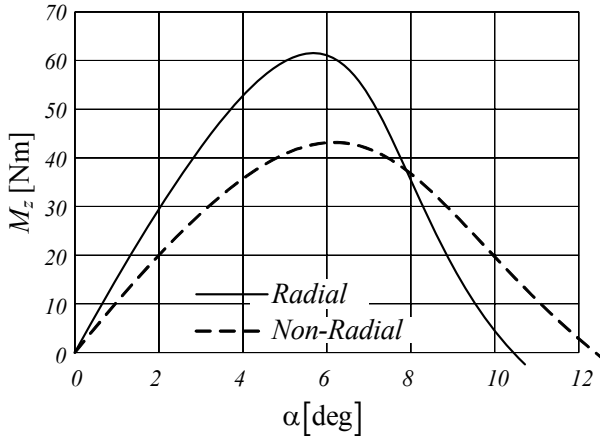FIGURE 3.39. Lateral force $F_y$ as a function of slip angle $\alpha$ for a constant vertical load.

FIGURE 3.40. Aligning moment $M_z$ as a function of slip angle $\alpha$ for a constant vertical load.
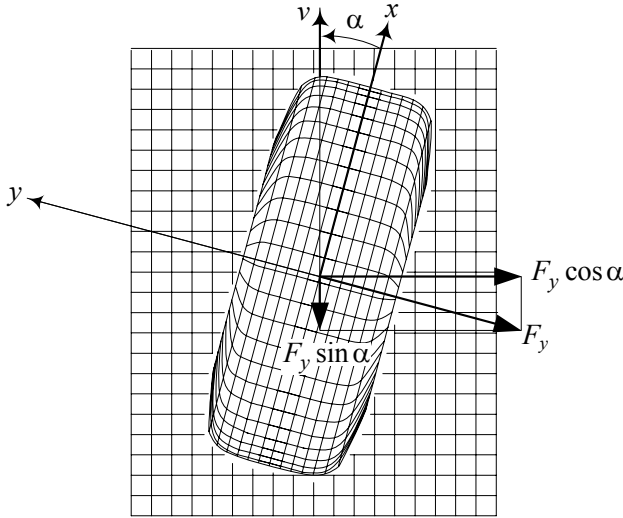
FIGURE 3.41. The cornering and drag components of a lateral force $F_y$.

**Example 109** *Effect of tire load on lateral force curve.*

When the wheel load $F_z$ increases, the tire treads can stick to the road better. Hence, the lateral force increases at a constant slip angle $\alpha$, and the slippage occurs at the higher slip angles. Figure 3.42 illustrates the lateral force behavior of a sample tire for different normal loads.

Increasing the load not only increases the maximum attainable lateral force, it also pushes the maximum of the lateral force to higher slip angles.

Sometimes the effect of load on lateral force is presented in a dimensionless variable to make it more practical. Figure 3.43 depicts a sample.

**Example 110** *Gough diagram.*

The slip angle $\alpha$ is the main affective parameter on the lateral force $F_y$ and aligning moment $M_z = F_y a_{x_\alpha}$. However, $F_z$ and $M_z$ depend on many other parameters such as speed $v$, pressure $p$, temperature, humidity, and road conditions. A better method to show $F_z$ and $M_z$ is to plot them versus each other for a set of parameters. Such a graph is called a **Gough diagram**. Figure 3.44 depicts a sample Gough diagram for a radial passenger car tire. Every tire has its own Gough diagram, although we may use an average diagram for radial or non-radial tires.

**Example 111** *Effect of velocity.*

The curve of lateral force as a function of the slip angle $F_y(\alpha)$ decreases as velocity increases. Hence, we need to increase the sideslip angle at higher velocities to generate the same lateral force. Sideslip angle increases by
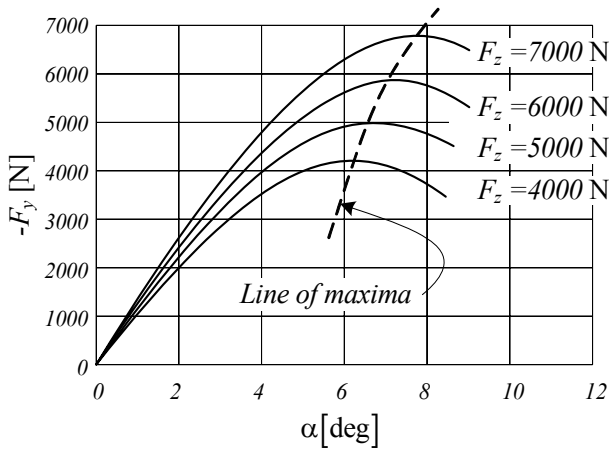
FIGURE 3.42. Lateral force behavior of a sample tire for different normal loads as a function of slip angle $\alpha$.
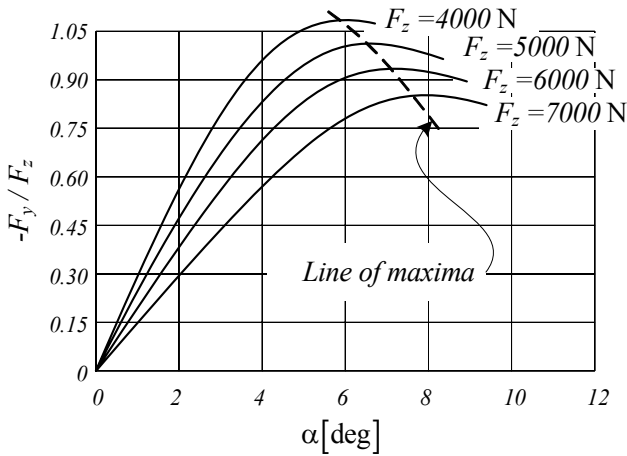


FIGURE 3.43. Effect of load on lateral force as a function of slip angle $\alpha$ presented in a dimensionless fashion.
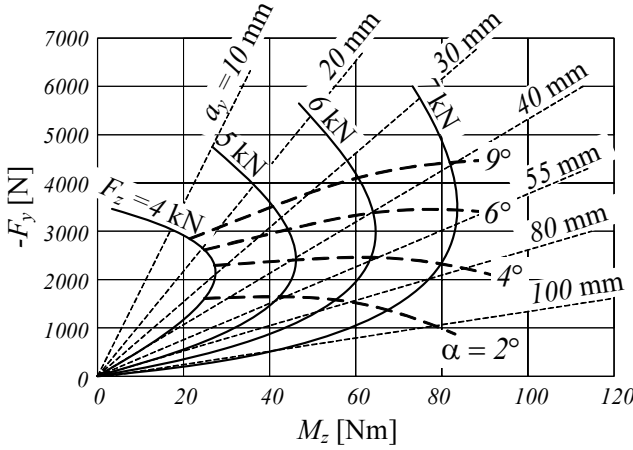
FIGURE 3.44. Gough diagram for a radial passenger car tire.

increasing the steer angle. Figure 3.45 illustrates the effect of velocity on $F_y$ for a radial passenger tire. Because of this behavior, a fixed steer angle, the curvature of a one-wheel-car trajectory, increases by increasing the driving speed.

**Example 112 ★** *A model for lateral force.*

When the sideslip angle is not small, the linear approximation (3.131) cannot model the tire behavior. Based on a parabolic normal stress distribution on the tireprint, the following third-degree function was presented in the 1950s to calculate the lateral force at high sideslips

$$F_y = -C_\alpha \, \alpha \left( 1 - \frac{1}{3} \left| \frac{C_\alpha \, \alpha}{F_{y_M}} \right| + \frac{1}{27} \left( \frac{C_\alpha \, \alpha}{F_{y_M}} \right)^2 \right) \qquad (3.145)$$

where $F_{y_M}$ is the maximum lateral force that the tire can support. $F_{y_M}$ is set by the tire load and the lateral friction coefficient $\mu_y$. Let's show the sideslip angle at which the lateral force $F_y$ reaches its maximum value $F_{y_M}$ by $\alpha_M$. Equation (3.145) shows that

$$\alpha_M = \frac{3 F_{y_M}}{C_\alpha} \qquad (3.146)$$

and therefore,

$$F_y = -C_\alpha \, \alpha \left( 1 - \frac{\alpha}{\alpha_M} + \frac{1}{3} \left( \frac{\alpha}{\alpha_M} \right)^2 \right) \qquad (3.147)$$

$$\frac{F_y}{F_{y_M}} = \frac{3\alpha}{\alpha_M} \left( 1 - \frac{\alpha}{\alpha_M} + \frac{1}{3} \left( \frac{\alpha}{\alpha_M} \right)^2 \right). \qquad (3.148)$$
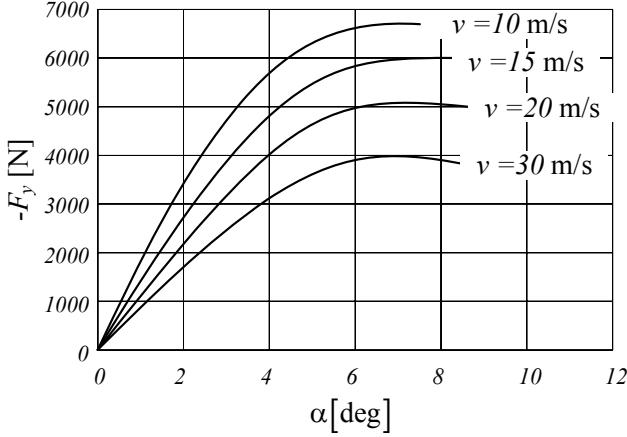
FIGURE 3.45. Effect of velocity on $F_y$ and $M_z$ for a radial tire.

*Figure 3.46 shows the cubic curve model for lateral force as a function of the sideslip angle. The Equation is applicable only for $0 \leq \alpha \leq \alpha_M$.*

**Example 113 ★** *A model for lateral stress.*

*Consider a tire turning on a dry road at a low sideslip angle $\alpha$. Assume the developed lateral stress on tireprint can be expressed by the following equation:*

$$\tau_y(x, y) = c\tau_{yM} \left(1 - \frac{x}{a}\right) \left(1 - \frac{x^3}{a^3}\right) \cos^2\left(\frac{y}{2b}\pi\right) \tag{3.149}$$

*The coefficient $c$ is proportional to the tire load $F_z$ sideslip $\alpha$, and longitudinal slip $s$. If the tireprint $A_P = 4 \times a \times b = 4 \times 5\,\text{cm} \times 12\,\text{cm}$, then the lateral force under the tire, $F_y$, for $c = 1$ is*

$$
\begin{aligned}
F_y &= \int_{A_P} \tau_y(x, y)\, dA \\
&= \int_{-0.05}^{0.05} \int_{-0.12}^{0.12} \tau_{yM} \left(1 - \frac{x}{0.05}\right)\left(1 - \frac{x^3}{0.05^3}\right) \cos^2\left(\frac{y\pi}{0.24}\right) dy\, dx \\
&= 0.0144\tau_{yM}.
\end{aligned}
\tag{3.150}
$$

*If we calculate the lateral force $F_y = 1000\,\text{N}$ by measuring the lateral acceleration, then the maximum lateral stress is*

$$\tau_{yM} = \frac{F_z}{0.014\,4} = 69444\,\text{Pa} \tag{3.151}$$

*and the lateral stress distribution over the tireprint is*

$$\tau_y(x, y) = 69444 \left(1 - \frac{x}{0.05}\right)\left(1 - \frac{x^3}{0.05^3}\right) \cos^2\left(\frac{y\pi}{0.24}\right) \text{Pa}. \tag{3.152}$$
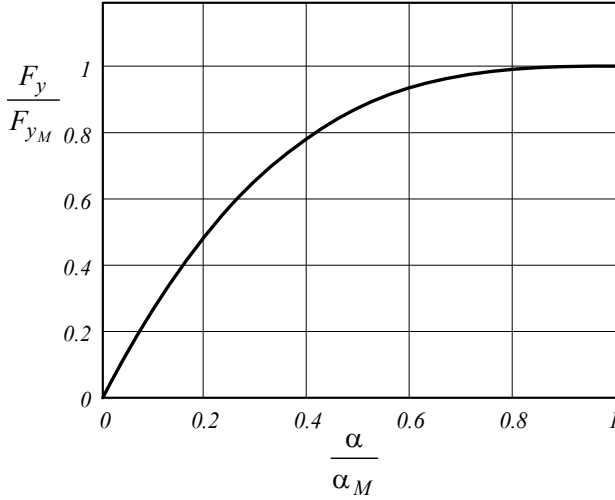
FIGURE 3.46. A cubic curve model for lateral force as a function of the sideslip angle.

## 3.8  Camber Force

Camber angle $\gamma$ is the tilting angle of tire about the longitudinal $x$-axis. Camber angle generates a lateral force $F_y$ called *camber trust* or *camber force*. Figure 3.47 illustrates a front view of a cambered tire and the generated camber force $F_y$. Camber angle is assumed positive $\gamma > 0$, when it is in the positive direction of the $x$-axis, measured from the $z$-axis to the tire. A positive camber angle generates a camber force along the $-y$-axis.

The camber force is proportional to $\gamma$ at low camber angles, and depends directly on the wheel load $F_z$. Therefore,

$$\mathbf{F}_y = F_y\,\hat{\jmath} \tag{3.153}$$
$$F_y = -C_\gamma\,\gamma \tag{3.154}$$

where $C_\gamma$ is called the *camber stiffness* of tire.

$$C_\gamma = \lim_{\gamma \to 0} \frac{\partial\,(-F_y)}{\partial\gamma} \tag{3.155}$$

In presence of both, camber $\gamma$ and sideslip $\alpha$, the overall lateral force $F_y$ on a tire is a superposition of the corner force and camber trust.

$$F_y = -C_\gamma\,\gamma - C_\alpha\,\alpha \tag{3.156}$$

**Proof.** When a wheel is under a constant load and then a camber angle is applied on the rim, the tire will deflect laterally such that it is longer in
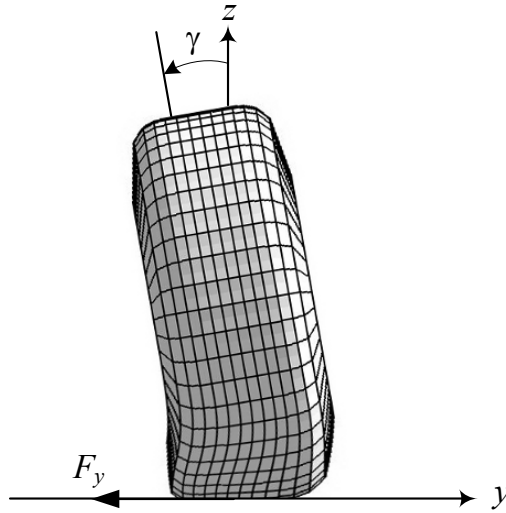
FIGURE 3.47. A front view of a cambered tire and the generated camber force.

the cambered side and shorter in the other side. Figure 3.48 compares the tireprint of a straight and a cambered tire, turning slowly on a flat road. As the wheel turns forward, undeflected treads enter the tireprint region and deflect laterally as well as longitudinally. However, because of the shape of the tireprint, the treads entering the tireprint closer to the cambered side, have more time to be stretched laterally. Because the developed lateral stress is proportional to the lateral stretch, the nonuniform tread stretching generates an asymmetric stress distribution and more lateral stress will be developed on the cambered side. The result of the nonuniform lateral stress distribution over the tireprint of a cambered tire produces the camber trust $F_y$ in the cambered direction.

$$\mathbf{F}_y \quad = \quad F_y\,\hat{\jmath} \tag{3.157}$$

$$F_y \quad = \quad \int_{A_P} \tau_y\,dA \tag{3.158}$$

The camber trust is proportional to the camber angle for small angles.

$$F_y = -C_\gamma\,\gamma \tag{3.159}$$

The camber trust $F_y$ shifts a distance $a_{x_\gamma}$ forward when the cambered tire turns on the road. The resultant moment

$$\mathbf{M}_z \quad = \quad M_z\,\hat{k} \tag{3.160}$$

$$M_z \quad = \quad F_y\,a_{x_\gamma} \tag{3.161}$$
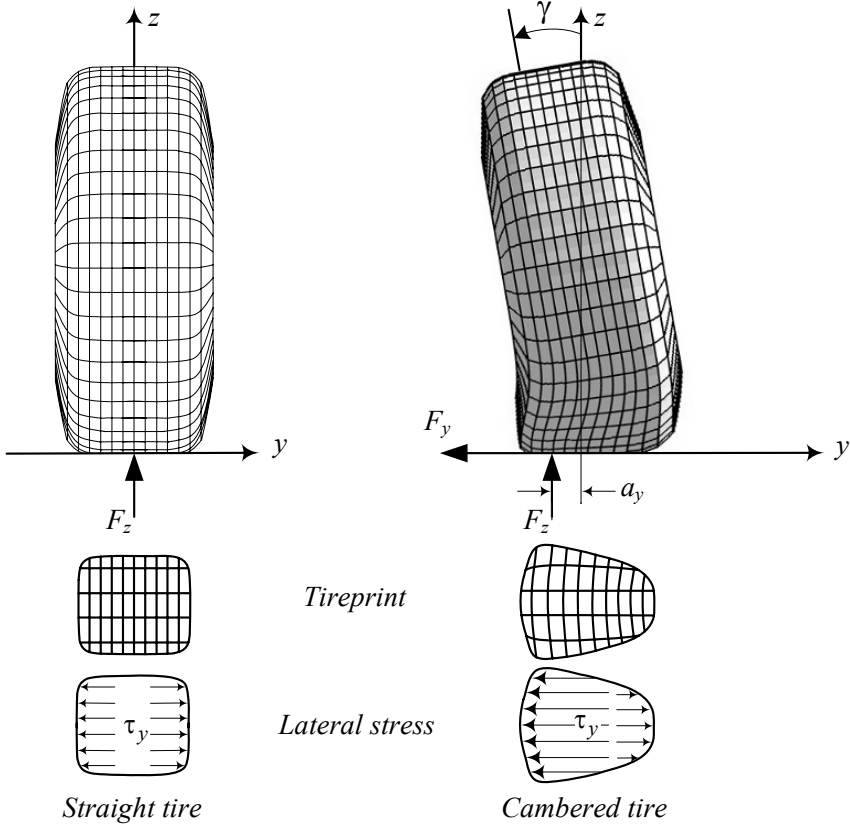
FIGURE 3.48. The tireprint of a straight and a cambered tire, turning slowly on a flat road.

is called *camber torque*, and the distance $a_{x_\gamma}$ is called *camber trail*. Camber trail is usually very small and hence, the camber torque can be ignored in linear analysis of vehicle dynamics.

Because the tireprint of a cambered tire deforms to be longer in the cambered side, the resultant vertical force $F_z$

$$F_z = \int_{A_P} \sigma_z \, dA \qquad (3.162)$$

that supports the wheel load, shifts laterally to a distance $a_{y_\gamma}$ from the center of the tireprint.

$$a_{y_\gamma} = \frac{1}{F_z} \int_{A_P} y \, \sigma_z \, dA_p \qquad (3.163)$$

The distance $a_{y_\gamma}$ is called the *camber arm*, and the resultant moment $\mathbf{M}_x$
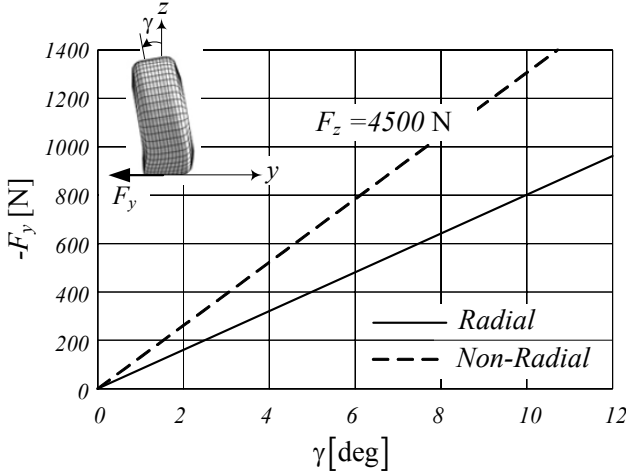
FIGURE 3.49. The camber force $F_y$ for different camber angle $\gamma$ at a constant tire load.

is called the *camber moment*.

$$\mathbf{M}_x = M_x\,\hat{k} \tag{3.164}$$
$$M_x = -F_z\,a_{y_\gamma} \tag{3.165}$$

The camber moment tends to turn the tire about the $x$-axis and make the tire-plane align with the $z$-axis. The camber arm $a_{y_\gamma}$ is proportional to the camber angle $\gamma$ for small angles.

$$a_{y_\gamma} = C_{y_\gamma}\,\gamma \tag{3.166}$$

Figure 3.49 shows the camber force $F_y$ for different camber angle $\gamma$ at a constant tire load $F_z = 4500\,\text{N}$. Radial tires generate lower camber force due to their higher flexibility.

It is better to illustrate the effect of $F_z$ graphically to visualize the camber force. Figure 3.50 depicts the variation of camber force $F_y$ as a function of normal load $F_z$ at different camber angles for a sample radial tire.

If we apply a slip angle $\alpha$ to a turning cambered tire, the tireprint will distort similar to the shape in Figure 3.51 and the path of treads become more complicated. The resultant lateral force would be at a distance $a_{x_\gamma}$ and $a_{y_\gamma}$ from the center of the tireprint. Both distances $a_{x_\gamma}$ and $a_{y_\gamma}$ are functions of angles $\alpha$ and $\gamma$. Camber force due to $\gamma$, along with the corner force due to $\alpha$, give the total lateral force applied on a tire. Therefore, the lateral force can be calculated as

$$F_y = -C_\alpha\,\alpha - C_\gamma\,\gamma \tag{3.167}$$

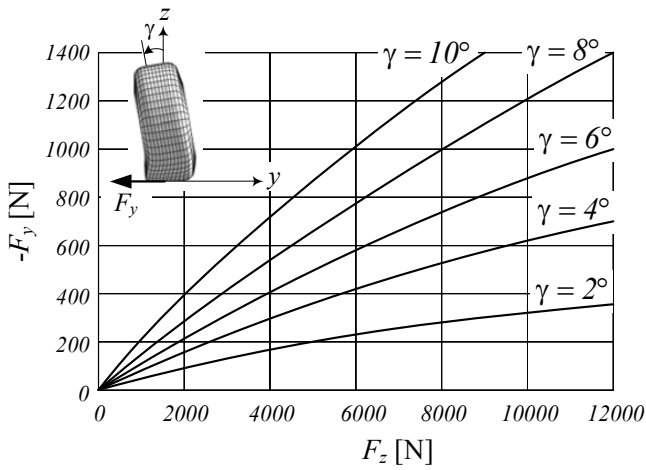FIGURE 3.50. The variation of camber force $F_y$ as a function of normal load $F_z$ at different camber angles for a sample radial tire.
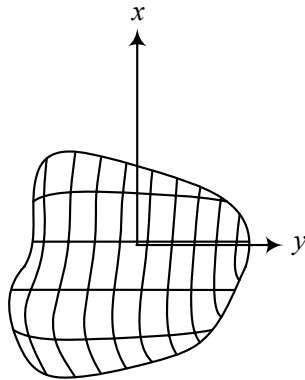


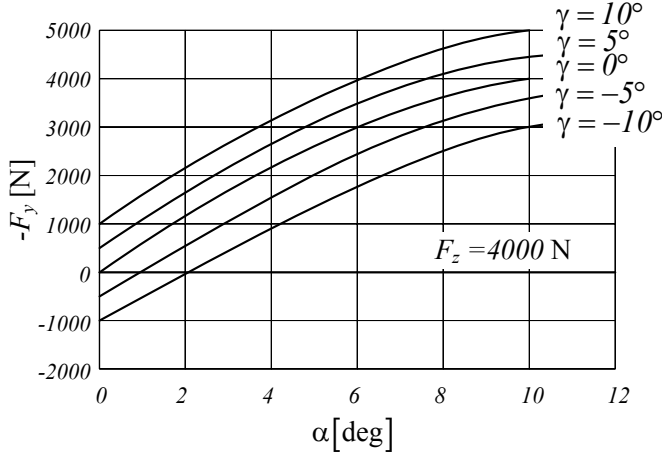FIGURE 3.51. Tireprint of a cambered tire under a sideslip.

FIGURE 3.52. An example for lateral force as a function of $\gamma$ and $\alpha$ at a constant load $F_z = 4000\,\mathrm{N}$.

that is acceptable for $\gamma \lesssim 10\,\mathrm{deg}$ and $\alpha \lesssim 5\,\mathrm{deg}$. Presence of both camber angle $\gamma$ and slip angle $\alpha$ makes the situation interesting because the total lateral force can be positive or negative. Figure 3.52 illustrates an example of lateral force as a function of $\gamma$ and $\alpha$ at a constant load $F_z = 4000\,\mathrm{N}$. Similar to lateral force, the aligning moment $M_z$ can be approximated as a combination of the slip and camber angle effects

$$M_z = C_{M_\alpha}\,\alpha + C_{M_\gamma}\,\gamma. \tag{3.168}$$

For a radial tire, $C_{M_\alpha} \approx 0.013\,\mathrm{N\,m/\,deg}$ and $C_{M_\gamma} \approx 0.0003\,\mathrm{N\,m/\,deg}$, while for a non-radial tire, $C_{M_\alpha} \approx 0.01\,\mathrm{N\,m/\,deg}$ and $C_{M_\gamma} \approx 0.001\,\mathrm{N\,m/\,deg}$. ■

**Example 114** *Banked road.*

*Consider a vehicle moving on a road with a transversal slope $\beta$, while its tires remain vertical. There is a downhill component of weight, $F_1 = mg\sin\beta$, that pulls the vehicle down. There is also an uphill camber force due to camber $\gamma \approx \beta$ of tires with respect to the road $F_2 = C_\gamma\gamma$. The resultant lateral force $F_y = C_\gamma\gamma - mg\sin\beta$ depends on camber stiffness $C_\gamma$ and determines if the vehicle goes uphill or downhill. Since the camber stiffness $C_\gamma$ is higher for non-radial tires, it is more possible for a radial tire to go downhill and a non-radial uphill.*

*The effects of cambering are particularly important for motorcycles that produce a large part of the cornering force by cambering. For cars and trucks, the cambering angles are much smaller and in many applications their effect can be negligible. However, some suspensions are designed to make the wheels camber when the axle load varies.*

**Example 115** *Camber importance and tireprint model.*

*Cambering of a tire creates a lateral force, even though there is no sideslip. The effects of cambering are particularly important for motorcycles that produce a large part of the lateral force by camber. The following equations are presented to model the lateral deviation of a cambered tireprint from the straight tireprint, and expressing the lateral stress $\tau_y$ due to camber*

$$y = -\sin\gamma \left( \sqrt{R_g^2 - x^2} - \sqrt{R_g^2 - a^2} \right) \tag{3.169}$$

$$\tau_y = -\gamma k \left( a^2 - x^2 \right) \tag{3.170}$$

*where $k$ is chosen such that the average camber defection is correct in the tireprint*

$$\int_{-a}^{a} \tau_y \, dx = \int_{-a}^{a} y \, dx. \tag{3.171}$$

*Therefore,*

$$k = \frac{3\sin\gamma}{4a^3\gamma} \left( -a\sqrt{R_g^2 - a^2} + R_g^2 \sin^{-1} \frac{a}{R_g} \right) \tag{3.172}$$

$$\approx \frac{3}{4} \frac{R_g \sqrt{R_g^2 - a^2}}{a^2} \tag{3.173}$$

*and*

$$\tau_y = -\frac{3}{4}\gamma \frac{R_g \sqrt{R_g^2 - a^2}}{a^2} \left( a^2 - x^2 \right). \tag{3.174}$$

## 3.9  Tire Force

Tires may be considered as a force generator with two major outputs: forward force $F_x$, lateral force $F_y$, and three minor outputs: aligning moment $M_z$, roll moment $M_x$, and pitch moment $M_y$. The input of the force generator is the tire load $F_z$, sideslip $\alpha$, longitudinal slip $s$, and the camber angle $\gamma$.

$$F_x = F_x (F_z, \alpha, s, \gamma) \tag{3.175}$$

$$F_y = F_y (F_z, \alpha, s, \gamma) \tag{3.176}$$

$$M_x = M_x (F_z, \alpha, s, \gamma) \tag{3.177}$$

$$M_y = M_y (F_z, \alpha, s, \gamma) \tag{3.178}$$

$$M_z = M_z (F_z, \alpha, s, \gamma) \tag{3.179}$$

Ignoring the rolling resistance and aerodynamic force, and when the tire is under a load $F_z$ plus only one more of the inputs $\alpha$, $s$, or $\gamma$, the major

output forces can be approximated by a set of linear equations

$$F_x = \mu_x(s)\,F_z \tag{3.180}$$
$$\mu_x(s) = C_s\,s$$
$$F_y = -C_\alpha\,\alpha \tag{3.181}$$
$$F_y = -C_\gamma\,\gamma \tag{3.182}$$

where, $C_s$ is the longitudinal slip coefficient, $C_\alpha$ is the lateral stiffness, and $C_\gamma$ is the camber stiffness.

When the tire has a combination of tire inputs, the tire forces are called *tire combined force*. The most important tire combined force is the shear force because of longitudinal and sideslips. However, as long as the angles and slips are within the linear range of tire behavior, a superposition can be utilized to estimate the output forces.

Driving and braking forces change the lateral force $F_y$ generated at any sideslip angle $\alpha$. This is because the longitudinal force pulls the tireprint in the direction of the driving or braking force and hence, the length of lateral displacement of the tireprint will also change.

Figure 3.53 illustrates how a sideslip $\alpha$ affects the longitudinal force ratio $F_x/F_z$ as a function of slip ratio $s$. Figure 3.54 illustrates the effect of sideslip $\alpha$ on the lateral force ratio $F_y/F_z$ as a function of slip ratio $s$. Figure 3.55 and 3.56 illustrate the same force ratios as Figures 3.53 and 3.54 when the slip ratio $s$ is a parameter.

**Proof.** Consider a turning tire under a sideslip angle $\alpha$. The tire develops a lateral force $F_y = -C_\alpha\,\alpha$. Applying a driving or braking force on this tire will reduce the lateral force while developing a longitudinal force $F_x = \mu_x(s)\,F_z$. Experimental data shows that the reduction in lateral force in presence of a slip ratio $s$ is similar to Figure 3.54. Now assume the sideslip $\alpha$ is reduced to zero. Reduction $\alpha$ will increase the longitudinal force while decreasing the lateral force. Increasing the longitudinal force is experimentally similar to Figure 3.55.

A turning tire under a slip ratio $s$ develops a longitudinal force $F_x = \mu_x(s)\,F_z$. Applying a sideslip angle $\alpha$ will reduce the longitudinal force while developing a lateral force. Experimental data shows that the reduction in longitudinal force in presence of a sideslip $\alpha$ is similar to Figure 3.53. Now assume the slip ratio $s$ and hence, the driving or breaking force is reduced to zero. Reduction $s$ will increase the lateral force while decreasing the longitudinal force. Increasing the lateral force is similar to Figure 3.54. ∎

**Example 116** *Pacejka model.*
*An approximate equation is presented to describe force Equations (3.175)*
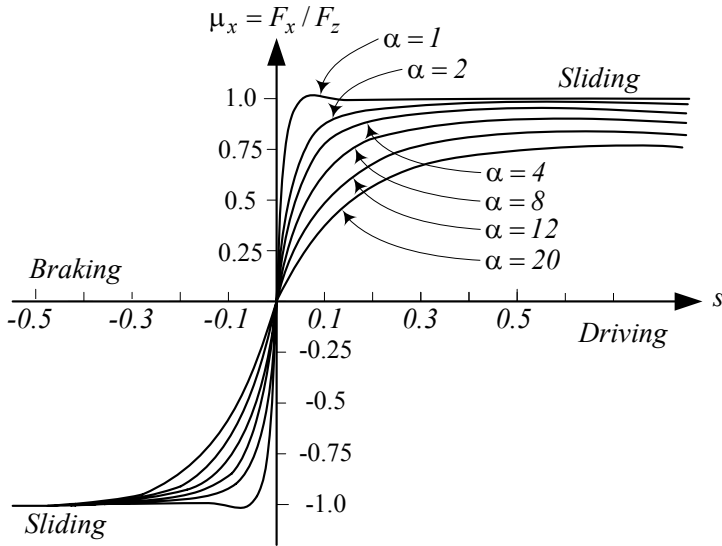
FIGURE 3.53. Longitudinal force ratio $F_x/F_z$ as a function of slip ratio $s$ for different sideslip $\alpha$.



FIGURE 3.54. Lateral force ratio $F_y/F_z$ as a function of slip ratio $s$ for different sideslip $\alpha$.
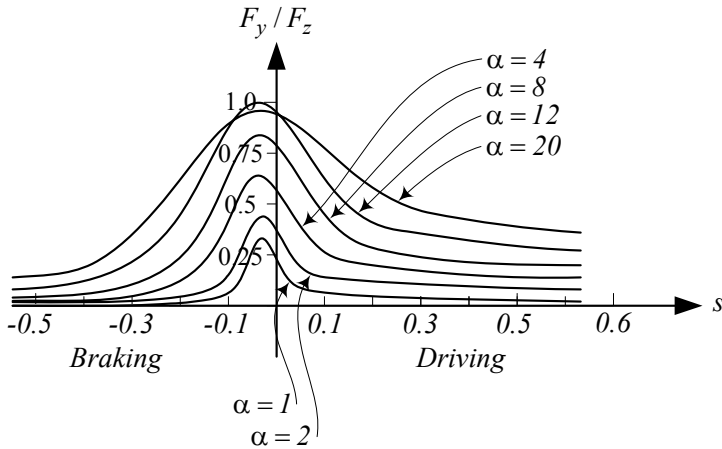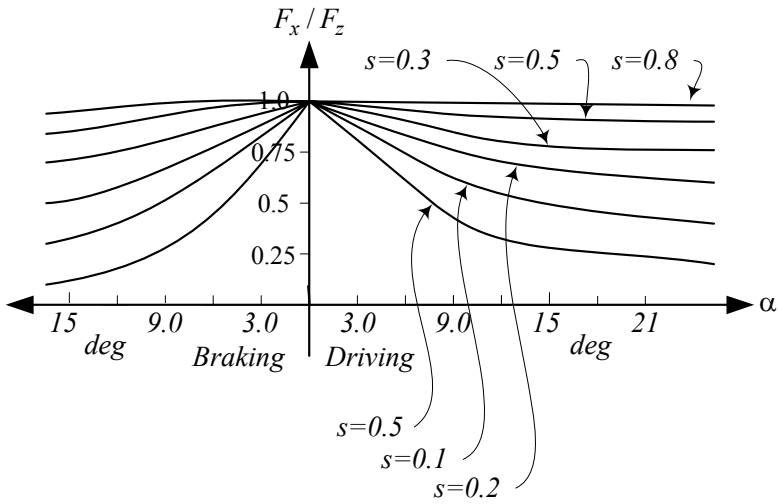
FIGURE 3.55. Longitudinal force ratio $F_x/F_z$ as a function of sideslip $\alpha$ for different slip ratio $s$.
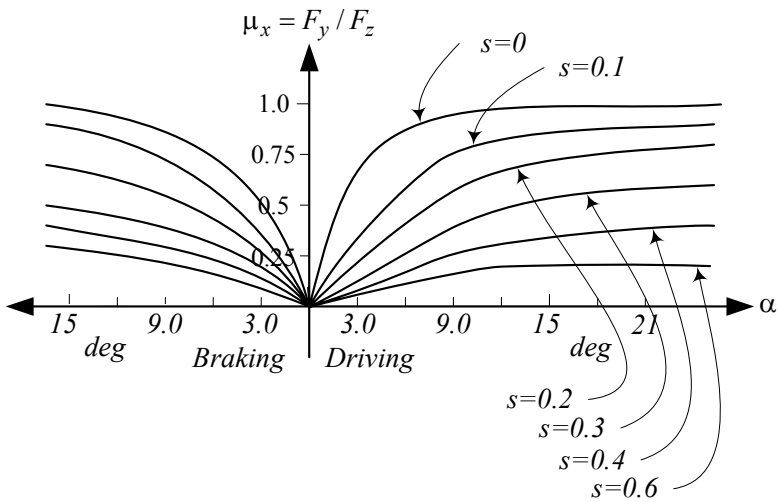


FIGURE 3.56. Lateral force ratio $F_y/F_z$ as a function of sideslip $\alpha$ for different slip ratio $s$.
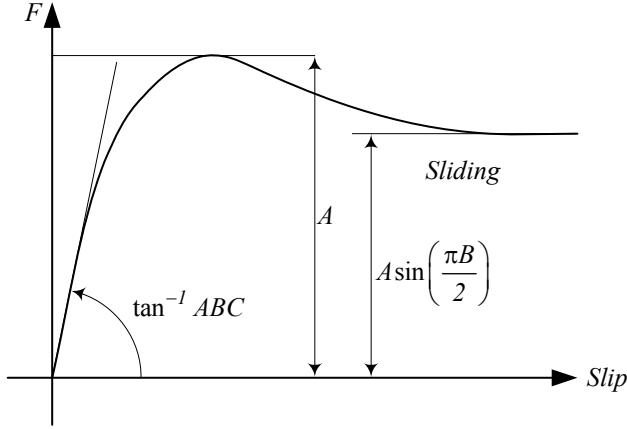
FIGURE 3.57. Parameters $A$, $B$, $C$, $D$ and a tire experimental curve.

or (3.176). This equation is called the Pacejka model.

$$F = A\sin\left\{B\tan^{-1}\left[Cx - D\left(Cx - \tan^{-1}(Cx)\right)\right]\right\} \quad (3.183)$$

$$A = \mu F_z \quad (3.184)$$

$$C = \frac{C_\alpha}{AB} \quad (3.185)$$

$$B, D = shape\ factors \quad (3.186)$$

The Pacejka model is substantially empirical. However, when the parameters $A$, $B$, $C$, $D$, $C_1$, and $C_2$ are determined for a tire, the equation expresses the tire behavior well enough. Figure 3.57 illustrates how the parameters can be determined from a test force-slip experimental result.

**Example 117** *Friction ellipse.*

*When the tire is under both longitudinal and sideslips, the tire is under combined slip. The shear force on the tireprint of a tire under a combined slip can approximately be found using a friction ellipse model.*

$$\left(\frac{F_y}{F_{y_M}}\right)^2 + \left(\frac{F_x}{F_{x_M}}\right)^2 = 1 \quad (3.187)$$

*A friction ellipse is shown in Figure 3.58.*

**Proof.** *The shear force* $\mathbf{F}_{shear}$*, applied on the tire at tireprint, parallel to the ground surface, has two components: the longitudinal force* $F_x$ *and the lateral force* $F_y$*.*

$$\mathbf{F}_{shear} = F_x\,\hat{\imath} + F_y\,\hat{\jmath} \quad (3.188)$$

$$F_x = C_s\,s\,F_z \quad (3.189)$$

$$F_y = -C_\alpha\,\alpha \quad (3.190)$$

FIGURE 3.58. Friction ellipse.

*These forces cannot exceed their maximum values $F_{y_M}$ and $F_{x_M}$.*

$$
\begin{aligned}
F_{y_M} &= \mu_y\, F_z \\
F_{x_M} &= \mu_x\, F_z
\end{aligned}
$$

*The tire shown in Figure 3.58 is moving along the velocity vector $v$ at a sideslip angle $\alpha$. The $x$-axis indicates the tire-plane. When there is no sideslip, the maximum longitudinal force is $F_{x_M} = \mu_x\, F_z = \overrightarrow{OA}$. Now, if a sideslip angle $\alpha$ is applied, a lateral force $F_y = \overrightarrow{OE}$ is generated, and the longitudinal force reduces to $F_x = \overrightarrow{OB}$. The maximum lateral force would be $F_{y_M} = \mu_y\, F_z = \overrightarrow{OD}$ when there is no longitudinal slip.*

*In presence of the longitudinal and lateral forces, we may assume that the tip point of the maximum shear force vector is on the following friction ellipse:*

$$
\left( \frac{F_y}{F_{y_M}} \right)^2 + \left( \frac{F_x}{F_{x_M}} \right)^2 = 1 \tag{3.191}
$$

*When $\mu_x = \mu_y = \mu$, the friction ellipse would be a circle and*

$$
F_{shear} = \mu\, F_z. \tag{3.192}
$$

∎

**Example 118** *Wide tires.*

A wide tire has a shorter tireprint than a narrow tire. Assuming the same vehicle and same tire pressure, the area of tireprint would be equal in both tires. The shorter tireprint at the same sideslip has more of its length stuck to the road than longer tireprint. So, a wider tireprint generates more lateral force than a narrower tireprint for the same tire load and sideslip.

Generally speaking, tire performance and maximum force capability decrease with increasing speed in both wide and narrow tires.

**Example 119** sin *tire forces model.*

A few decades ago, a series of applied sine functions were developed based on experimental data to model tire forces. The sine functions, which are explained below, may be used to model tire forces, especially for computer purposes, effectively.

The lateral force of a tire is

$$F_y = A \sin \left\{ B \tan^{-1} (C\Phi) \right\} \tag{3.193}$$

$$\Phi = (1 - E)(\alpha + \delta)\mu F_z \tag{3.194}$$

$$C = \frac{C_\alpha}{AB} \tag{3.195}$$

$$C_\alpha = C_1 \sin \left( 2 \tan^{-1} \frac{F_z}{C_2} \right) \tag{3.196}$$

$$A, B = Shape\ factors \tag{3.197}$$

$$C_1 = Maximum\ cornering\ stiffness \tag{3.198}$$

$$C_2 = Tire\ load\ at\ maximum\ cornerin\ stiffness \tag{3.199}$$

## 3.10 Summary

We attach a coordinate frame $(oxyz)$ to the tire at the center of the tireprint, called the tire frame. The $x$-axis is along the intersection line of the tire-plane and the ground. The $z$-axis is perpendicular to the ground, and the $y$-axis makes the coordinate system right-hand. We show the tire orientation using two angles: camber angle $\gamma$ and sideslip angle $\alpha$. The camber angle is the angle between the tire-plane and the vertical plane measured about the $x$-axis, and the sideslip angle $\alpha$ is the angle between the velocity vector $\mathbf{v}$ and the $x$-axis measured about the $z$-axis.

A vertically loaded wheel turning on a flat surface has an effective radius $R_w$, called rolling radius

$$R_w = \frac{v_x}{\omega_w} \tag{3.200}$$

where $v_x$ is the forward velocity, and $\omega_w$ is the angular velocity of the

wheel. The effective radius $R_w$ is approximately equal to

$$R_w \approx R_g - \frac{R_g - R_h}{3} \tag{3.201}$$

and is a number between the unloaded or geometric radius $R_g$ and the loaded height $R_h$.

$$R_h < R_w < R_g \tag{3.202}$$

A turning tire on the ground generates a longitudinal force called rolling resistance. The force is opposite to the direction of motion and is proportional to the normal force on the tireprint.

$$F_r = \mu_r F_z \tag{3.203}$$

The parameter $\mu_r$ is called the rolling friction coefficient and is a function of tire mechanical properties, speed, wear, temperature, load, size, driving and braking forces, and road condition.

The tire force in the $x$-direction is a combination of the longitudinal force $F_x$ and the roll resistance $F_r$. The longitudinal force is

$$F_x = \mu_x(s) F_z \tag{3.204}$$

where $s$ is the longitudinal slip ratio of the tire

$$s = \frac{R_g \omega_w}{v_x} - 1 \tag{3.205}$$

$$\mu_x(s) = C_s s \qquad s \ll 1 \tag{3.206}$$

The wheel force in the tire $y$-direction, $F_y$, is a combination of the lateral force and the tire roll resistance $F_r$. The lateral force is

$$F_y = -C_\gamma \gamma - C_\alpha \alpha \tag{3.207}$$

where $-C_\gamma \gamma$ is called the camber trust and $C_\alpha \alpha$ is called the sideslip force.

# 3.11   Key Symbols

| | |
|---|---|
| $a \equiv \ddot{x}$ | acceleration |
| $a, b$ | semiaxes of $A_P$ |
| $a_{x_\alpha}$ | |
| $a_{x_\gamma}$ | camber trail |
| $a_{y_\gamma}$ | camber arm |
| $A_P$ | tireprint area |
| $c_1, c_2, c_3, c_4$ | coefficients of the function $F_x = F_x(s)$ |
| $C_0, C_1, C_2$ | coefficients of the polynomial function $F_r = F_r(v_x)$ |
| $C_s$ | longitudinal slip coefficient |
| $C_{s_x}, C_{s_y}$ | longitudinal and lateral slip coefficients |
| $C_\alpha$ | sideslip coefficient |
| $C_\gamma$ | camber stiffness |
| $d$ | distance of tire travel |
| $d_F$ | no slip tire travel |
| $d_A$ | actual tire travel |
| $D$ | tire diameter |
| $E$ | Young modulus |
| $f$ | function |
| $f_k$ | spring force |
| $F_r \; \mathbf{F}_r$ | rolling resistance force |
| $F_x$ | longitudinal force, forward force |
| $F_y$ | lateral force |
| $F_{y_M}$ | pneumatic trail |
| $F_z$ | normal force, vertical force, wheel load |
| $g \; \mathbf{g}$ | gravitational acceleration |
| $k$ | stiffness |
| $k_1, k_2, k_3$ | nonlinear tire stiffness coefficients |
| $k_{eq}$ | equivalent stiffness |
| $k_s$ | slope of $F_x(s)$ versus $s$ at $s = 0$ |
| $k_x$ | tire stiffness in the $x$-direction |
| $k_y$ | tire stiffness in the $y$-direction |
| $k_z$ | tire stiffness in the $z$-direction |
| $K$ | radial and non-radial tires parameter in $\mu_r = \mu_r(p, v_x)$ |
| $m$ | mass |
| $M_r \; \mathbf{M}_r$ | rolling resistance moment |
| $M_x, \; \mathbf{M}_x$ | roll moment, bank moment, tilting torque, |
| $M_y$ | pitch moment, rolling resistance torque |
| $M_z$ | yaw moment, aligning moment, self aligning moment, bore torque |
| $n$ | exponent for shape and stress distribution of $A_P$ |
| $n_1$ | number of tire rotations |
| $p$ | tire inflation pressure |
| $P$ | rolling resistance power |

| | |
|---|---|
| $r$ | radial position of tire periphery |
| $r = \omega/\omega_n$ | frequency ratio |
| $R_g$ | geometric radius |
| $R_h$ | loaded height |
| $R_w$ | rolling radius |
| $s$ | longitudinal slip |
| $s_y$ | lateral slip |
| $T$ | wheel torque |
| $v \equiv \dot{x}$, $\mathbf{v}$ | velocity |
| $x, y, z$, $\mathbf{x}$ | displacement |
| $x, y, z$ | coordinate axes |
| $\triangle x$ | tire deflection in the $x$-direction, rolling resistance arm |
| $\triangle y$ | tire deflection in the $y$-direction |
| $\triangle z$ | tire deflection in the $z$-direction |
| $\dot{z}$ | tire deflection rate in the $z$-direction |
| | |
| $\alpha$ | sideslip angle |
| $\alpha_M$ | maximum sideslip angle |
| $\beta$ | transversal slope |
| $\gamma$ | camber angle |
| $\delta$ | deflection |
| $\triangle x$ | tire deflection in the $x$-direction, rolling resistance arm |
| $\triangle y$ | tire deflection in the $y$-direction |
| $\triangle z$ | tire deflection in the $z$-direction |
| $\theta$ | tire angular rotation |
| $\mu_0, \mu_1$ | nonlinear rolling friction coefficient |
| $\mu_r$ | rolling friction coefficient |
| $\mu_x(s)$ | longitudinal friction coefficient |
| $\mu_{dp}$ | friction coefficient driving peak value |
| $\mu_{ds}$ | friction coefficient steady-state value |
| $\sigma_{z_M}$ | maximum normal stress |
| $\sigma_z(x, y)$ | normal stress over the tireprint |
| $\sigma_{z_m}$ | normal stress mean value |
| $\tau_x(x, y), \tau_y(x, y)$ | shear stresses over the tireprint |
| $\tau_{x_M}, \tau_{y_M}$ | maximum shear stresses |
| $\varphi$ | contact angle, angular length of $A_P$ |
| $\omega_{eq}$ | equivalent tire angular velocity |
| $\omega_w$ | angular velocity of a wheel |
| $\omega_w$ | actual tire angular velocity |

# Exercises

1. Tireprint size and average normal stress.

   The curb weight of a model of Land Rover $LR3^{TM}$ is

   $$m = 2461 \,\text{kg} \approx 5426 \,\text{lb}$$

   while the gross vehicle weight can be

   $$m = 3230 \,\text{kg} \approx 7121 \,\text{lb}.$$

   Assume a front to rear load ratio

   $$\frac{F_{z_f}}{F_{z_r}} = \frac{1450 \,\text{kg}}{1875 \,\text{kg}}$$

   and use the following data

   $$
   \begin{aligned}
   l &= 2885 \,\text{mm} \approx 113.6 \,\text{in} \\
   Tires &= 255/55R19
   \end{aligned}
   $$

   to determine the the size parameters of the tireprints $a$, and $b$, for the front and rear tires. Assume a uniform normal stress on tireprints.

2. Tireprint size, radial tire.

   Holden TK Barina$^{TM}$ is a hatchback car with the following characteristics.

   $$
   \begin{aligned}
   m &= 2461 \,\text{kg} \approx 5426 \,\text{lb} \\
   l &= 2480 \,\text{mm} \\
   Tires &= 185/55R15 \ 82V
   \end{aligned}
   $$

   Assume

   $$
   \begin{aligned}
   m &= 860 \,\text{kg} \\
   \frac{a_1}{a_2} &= 1.1
   \end{aligned}
   $$

   and determine the size of its tireprints for $n = 3$.

3. Rolling resistance coefficient.

   Alfa Romeo Spider$^{TM}$ has the following characteristics.

   $$
   \begin{aligned}
   m &= 1690 \,\text{kg} \approx 3725.8 \,\text{lb} \\
   l &= 2530 \,\text{mm} \approx 99.6 \,\text{in} \\
   Tires &= P225/50R17
   \end{aligned}
   $$

Determine the rolling resistance coefficient $\mu_r$ for the front and rear tires of the car at zero and at top speed $v_M$.

$$v_M = 235.0 \, \text{km/h} \approx 146.0 \, \text{mi/h}$$

Assume $a_1/a_2 = 1.2$ and use $p = 27 \, psi$.

4. Rolling resistance power.

   A model of Mitsubishi Galant$^{TM}$ has the following specifications.

$$
\begin{aligned}
m &= 1,700 \, \text{kg} \\
l &= 2750 \, \text{mm} \\
Tires &= P235/45R18 \\
v_M &\approx 190 \, \text{km/h}
\end{aligned}
$$

   Assume $a_1/a_2 = 1.2$ and $p = 27 \, psi$ to find the rolling resistance power at the maximum speed.

5. Longitudinal slip.

   (a) Determine the longitudinal slip $s$ for the tire $P225/50R17$ if $R_w = 0.98R_g$.

   (b) If the speed of the wheel is $v_x = 100 \, \text{km/h}$, what would be the angular velocity $\omega_w$ and equivalent angular velocity $\omega_{eq}$ of the tire.

6. Cornering and drag force on a tire.

   Consider the tire for which we have estimated the lateral force behavior shown in Figure 3.42. If the sideslip angle $\alpha$ is $4 \, \text{deg}$ and $F_z = 5000 \, \text{N}$, calculate the cornering and drag force on the tire.

7. Required camber angle.

   Consider the tire for which we have estimated the behavior shown in Figure 3.52. Assume $F_z = 4000 \, \text{N}$ and we need a lateral force $F_y = -3000 \, \text{N}$. If $\alpha = 4 \, \text{deg}$, what would be the required camber angle $\gamma$? Estimate the coefficients $C_\alpha$ and $C_\gamma$.

8. High camber angle.

   Consider a tire with $C_\gamma = 300 \, \text{N/deg}$ and $C_\alpha = 700 \, \text{N/deg}$. If the camber angle is $\gamma = 18 \, \text{deg}$ how much lateral force will develop for a zero sideslip angle? How much sideslip angle is needed to reduce the value of the lateral force to $F_y = -3000 \, \text{N}$?

9. Sideslip and longitudinal slip.

   Consider the tire for which we have estimated the behavior shown in Figure 3.54. Assume a vehicle with that tire is turning with a constant speed on a circle such that $\alpha = 4\,\text{deg}$. What should be the sideslip angle $\alpha$ if we accelerate the vehicle such that $s = 0.05$, or decelerate the vehicle such that $s = -0.05$?

10. ★ Motion of the air in tire.

    What do you think about the motion of the pressurized air within the tires, when the vehicle moves with constant velocity or constant acceleration?

# 4

# Driveline Dynamics

The maximum achievable acceleration of a vehicle is limited by two factors: maximum torque at driving wheels, and maximum traction force at tireprints. The first one depends on engine and transmission performance, and the second one depends on tire-road friction. In this chapter, we examine engine and transmission performance.

## 4.1  Engine Dynamics

The maximum attainable power $P_e$ of an internal combustion engine is a function of the engine angular velocity $\omega_e$. This function must be determined experimentally, however, the function $P_e = P_e(\omega_e)$, which is called the *power performance function*, can be estimated by a third-order polynomial
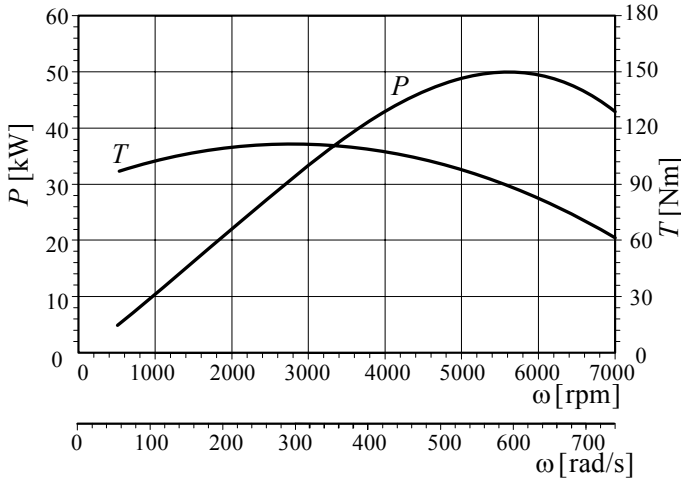


FIGURE 4.1. A sample of power and torque performances for a spark ignition engine.

$$
\begin{aligned}
P_e &= \sum_{i=1}^{3} P_i \, \omega_e^i \\
&= P_1 \, \omega_e + P_2 \, \omega_e^2 + P_3 \, \omega_e^3.
\end{aligned} \tag{4.1}
$$

If we use $\omega_M$ to indicate the angular velocity, measured in $[\text{rad}/\text{s}]$, at which the engine power reaches the maximum value $P_M$, measured in $[\text{W} = \text{N\,m}/\text{s}]$, then for spark ignition engines we use

$$P_1 = \frac{P_M}{\omega_M} \tag{4.2}$$

$$P_2 = \frac{P_M}{\omega_M^2} \tag{4.3}$$

$$P_3 = -\frac{P_M}{\omega_M^3}. \tag{4.4}$$

Figure 4.1 illustrates a sample for power performance of a spark ignition engine that provides $P_M = 50\,\text{kW}$ at $\omega_M = 586\,\text{rad}/\text{s} \approx 5600\,\text{rpm}$. The curve begins at an angular velocity at which the engine starts running smoothly.

For indirect injection Diesel engines we use

$$P_1 = 0.6\frac{P_M}{\omega_M} \tag{4.5}$$

$$P_2 = 1.4\frac{P_M}{\omega_M^2} \tag{4.6}$$

$$P_3 = -\frac{P_M}{\omega_M^3} \tag{4.7}$$

and for direct injection Diesel engines we use

$$P_1 = 0.87\frac{P_M}{\omega_M} \tag{4.8}$$

$$P_2 = 1.13\frac{P_M}{\omega_M^2} \tag{4.9}$$

$$P_3 = -\frac{P_M}{\omega_M^3}. \tag{4.10}$$

The driving torque of the engine $T_e$ is the torque that provides $P_e$

$$\begin{aligned}
T_e &= \frac{P_e}{\omega_e} \\
&= P_1 + P_2\,\omega_e + P_3\,\omega_e^2. \tag{4.11}
\end{aligned}$$

**Example 120** *Porsche* $911^{TM}$ *and Corvette* $Z06^{TM}$ *engines.*

*A model of Porsche 911 turbo has a flat-6 cylinder, twin-turbo engine with* $3596\,\text{cm}^3 \approx 220\,\text{in}^3$ *total displacement. The engine provides a maximum power* $P_M = 353\,\text{kW} \approx 480\,\text{hp}$ *at* $\omega_M = 6000\,\text{rpm} \approx 628\,\text{rad}/\text{s}$, *and a maximum torque* $T_M = 620\,\text{N\,m} \approx 457\,\text{lb\,ft}$ *at* $\omega_e = 5000\,\text{rpm} \approx 523\,\text{rad}/\text{s}$. *The car weighs around* $1585\,\text{kg} \approx 3494\,\text{lb}$ *and can move from 0 to* $96\,\text{km}/\text{h} \approx 60\,\text{mi}/\text{h}$ *in 3.7 s. Porsche 911 has a top speed of* $310\,\text{km}/\text{h} \approx 193\,\text{mi}/\text{h}$.

*The power performance equation for the Porsche 911 engine has the co-efficients*

$$P_1 = \frac{P_M}{\omega_M} = \frac{353000}{628} = 562.1 \,\mathrm{W/s} \tag{4.12}$$

$$P_2 = \frac{P_M}{\omega_M^2} = \frac{353000}{628^2} = 0.89507 \,\mathrm{W/s^2} \tag{4.13}$$

$$P_3 = -\frac{P_M}{\omega_M^3} = -\frac{353000}{628^3} = -1.4253 \times 10^{-3} \,\mathrm{W/s^3} \tag{4.14}$$

*and, its power performance function is*

$$P_e = 562.1\,\omega_e + 0.89507\,\omega_e^2 - 1.4253 \times 10^{-3}\,\omega_e^3. \tag{4.15}$$

A model of Corvette Z06 uses a V8 engine with $6997\,\mathrm{cm^3} \approx 427\,\mathrm{in^3}$ total displacement. The engine provides a maximum power $P_M = 377\,\mathrm{kW} \approx 512\,\mathrm{hp}$ at $\omega_M = 6300\,\mathrm{rpm} \approx 660\,\mathrm{rad/s}$, and a maximum torque $T_M = 637\,\mathrm{N\,m} \approx 470\,\mathrm{lb\,ft}$ at $\omega_e = 4800\,\mathrm{rpm} \approx 502\,\mathrm{rad/s}$. The Corvette weighs around $1418\,\mathrm{kg} \approx 3126\,\mathrm{lb}$ and can move from $0$ to $100\,\mathrm{km/h} \approx 62\,\mathrm{mi/h}$ in $3.9\,\mathrm{s}$ in first gear. Its top speed is $320\,\mathrm{km/h} \approx 198\,\mathrm{mi/h}$.

The power performance equation for the engine of Corvette Z06 has the coefficients

$$P_1 = \frac{P_M}{\omega_M} = \frac{377000}{660} = 571.2 \,\mathrm{W/s} \tag{4.16}$$

$$P_2 = \frac{P_M}{\omega_M^2} = \frac{377000}{660^2} = 0.86547 \,\mathrm{W/s^2} \tag{4.17}$$

$$P_3 = -\frac{P_M}{\omega_M^3} = -\frac{377000}{660^3} = -1.3113 \times 10^{-3} \,\mathrm{W/s^3} \tag{4.18}$$

*and, its power performance function is*

$$P_e = 571.2\,\omega_e + 0.86547\,\omega_e^2 - 1.3113 \times 10^{-3}\,\omega_e^3. \tag{4.19}$$

*The power performance curves for the Porsche 911 and Corvette Z06 are plotted in Figure 4.2.*

Although there is almost no limit for developing a powerful engine, any engine with power around $100\,\mathrm{hp}$ would be enough for street cars with normal applications. It seems that engines with $600\,\mathrm{hp}$ reach the limit of application for street cars. However, race cars may have higher power depending on the race regulations. As an example, formula 1 regulations dictates the type of engine permitted. It must be a four-stroke engine, less than $3000\,\mathrm{cm^3}$ swept volume, no more than ten cylinders, and no more than five valves per cylinder, but there is no limit for power.
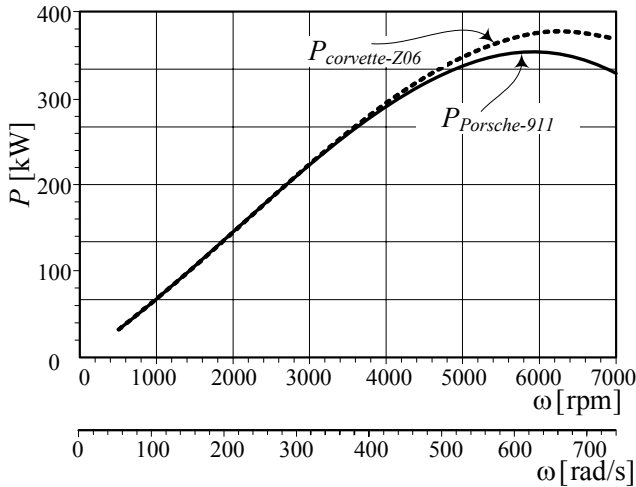
FIGURE 4.2. Power performance curves for the Porsche 911 and Corvette Z06.

**Example 121** *Below the curves $P_e = P_e(\omega_e)$ and $T_e = T_e(\omega_e)$.*

An engine can theoretically work at any point under the performance curve $P_e = P_e(\omega_e)$. Assume the angular velocity of an engine is kept constant by applying a braking force. Then, by opening the throttle, we produce more power until the throttle is wide open, and the maximum power at that angular velocity is gained.

Power rises with $\omega_e$, and continues to climb until a maximum power $P_M$, and then starts decreasing. The torque $T_e = P_e/\omega_e$ also increases with $\omega_e$ but reaches a maximum point before the maximum power. Hence, the torque starts decreasing sooner than the power. When the power starts decreasing, the torque is very far from its peak value.

Drivers usually cannot feel the engine power, however they may feel the engine torque.

**Example 122** *Engine efficiency curves.*

Engines are supposed to convert the chemical energy, embedded in the fuel, into mechanical energy at the engine output shaft. Depending on the working conditions, this conversion happens at a specific efficiency. The constant efficiency contours can be added to the performance map of the engine to show the efficiency at an operating condition. Hence, every point under the curve $P_e = P_e(\omega_e)$ can be an operating condition at a specific efficiency. The maximum efficiency usually happens around the angular velocity corresponding to the maximum torque when the throttle is almost wide open. A sample of power performance of a spark ignition engine with constant efficiency contours is shown in Figure 4.3.
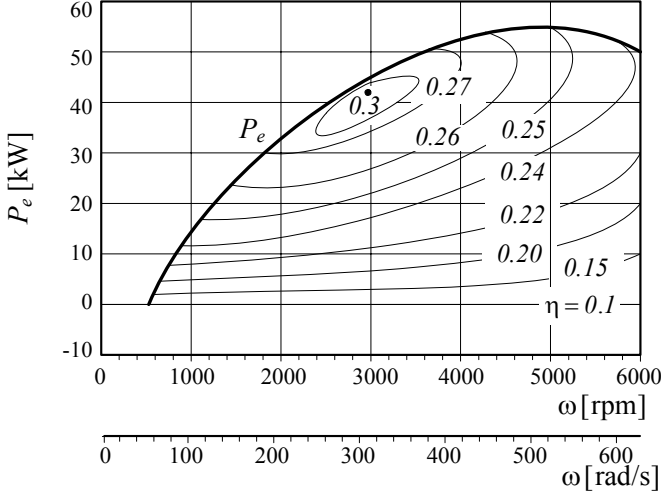
FIGURE 4.3. An example of power performance in a spark ignition engine with constant efficiency contours.

**Example 123** *Power units.*

There are many different units for expressing power. The metric unit for power is Watt [W].

$$1\,\mathrm{W} = \frac{1\,\mathrm{J}}{1\,\mathrm{s}} = \frac{1\,\mathrm{N\,m}}{1\,\mathrm{s}} \tag{4.20}$$

*Horsepower* [hp] *is also used in vehicle dynamics.*

$$1\,\mathrm{W} = 0.001341\,\mathrm{hp} \tag{4.21}$$
$$1\,\mathrm{hp} = 745.699872\,\mathrm{W} \tag{4.22}$$

There are four definitions for horsepower: international, metric, water, and electric. They slightly differ.

$$1\,\mathrm{hp}(international) = 745.699872\,\mathrm{W} \tag{4.23}$$
$$1\,\mathrm{hp}(electrical) = 746\,\mathrm{W} \tag{4.24}$$
$$1\,\mathrm{hp}(water) = 746.043\,\mathrm{W} \tag{4.25}$$
$$1\,\mathrm{hp}(metric) = 735.4988\,\mathrm{W} \tag{4.26}$$

Depending on the application, other units may also be useful.

$$1\,\mathrm{W} = 0.239006\,\mathrm{cal/\,s} \tag{4.27}$$
$$1\,\mathrm{W} = 0.000948\,\mathrm{Btu/\,s} \tag{4.28}$$
$$1\,\mathrm{W} = 0.737561\,\mathrm{ft\,lb}/s \tag{4.29}$$

*James Watt* $(1736 - 1819)$ *experimented and concluded that a horse can lift a weight of* $550\,\mathrm{lb}$ *for one foot in one second. It means the horse performs work at the rate of* $550\,\mathrm{ft\,lb/\,s} \approx 745.701\,\mathrm{W}$, *or* $33000\,\mathrm{ft\,lb/\,min}$. *Watt then stated that 33000-foot-pounds per minute of work was equivalent to the power of one horse, or, one horsepower. He said that* $33000\,\mathrm{ft\,lb/\,min}$ *is equivalent to one horsepower. The following formulas apply for calculating horsepower from a torque measurement in the English unit system:*

$$P[\mathrm{hp}] = \frac{T[\mathrm{ft\,lb}]\,\omega[\mathrm{rpm}]}{5252} \qquad (4.30)$$

$$P[\mathrm{hp}] = \frac{F[\mathrm{lb}]\,v_x[\mathrm{mi/\,h}]}{374} \qquad (4.31)$$

**Example 124** *Fuel consumption at constant speed.*

*Consider a vehicle moving straight at a constant speed* $v_x$. *The energy required to travel can be calculated by multiplying the power at the drive wheels by time*

$$
\begin{aligned}
E &= Pt \\
&= P\frac{d}{v_x} \qquad (4.32)
\end{aligned}
$$

*where* $d$ *is the distance traveled and* $E$ *is the needed energy to turn the wheels. To find the actual energy needed to run the whole vehicle, we should include the coefficients of efficiencies. We use* $\eta_e$ *for engine efficiency,* $H$ *for thermal value of fuel, and* $\rho_f$ *for density of the fuel. When the vehicle moves at constant speed, the traction force* $F_x$ *is equal to the resistance forces. Therefore, the fuel consumption per unit distance,* $q$, *is*

$$q = \frac{F_x}{\eta_e\,\eta_t\,\rho_f\,H}. \qquad (4.33)$$

*The dimension of* $q$ *in SI is* $\left[\,\mathrm{m^3/\,m}\,\right]$, *however, liter per* $100\,\mathrm{km}$ *is more common. In the United States, the fuel consumption of vehicles is called by* $[\,\mathrm{mi/\,gal}\,]$.

**Example 125** ★ *Changing the curve* $P_e = P_e\,(\omega_e)$.

*The whole power performance curve moves up when the engine's compression ratio increases. The angular velocity at which the engine's peak torque happens can be moved by changing the cam, header lengths, and intake manifold runner lengths.*

*The wheel power curve, or the power delivered to the ground, may have a different shape and a different peak* $\omega_e$, *because of transmission losses. The best result is obtained from a power curve measured by a chassis dynamometer.*

**Example 126** ★ *Power peak versus torque peak.*

When the engine is operating at its torque peak (say $P_e = 173.4\,\mathrm{kW} \approx 232.5\,\mathrm{hp}$ *at* $\omega_e = 3600\,\mathrm{rpm}$) *in a gear, it is generating some level of torque (say* $T_M = 460\,\mathrm{N\,m} \approx 340\,\mathrm{ft\,lb}$ *times the overall gearing ratio) at the drive wheels. This is the best performance in that gear. By changing the gear and making the engine to operate at the power peak (say* $P_e = 209\,\mathrm{kW} \approx 280\,\mathrm{hp}$ *at* $\omega_e = 5000\,\mathrm{rpm}$), *it delivers less torque* $T_e = 400\,\mathrm{N\,m} \approx 295\,\mathrm{ft\,lbf}$. *However, it will deliver more torque to the drive wheels, at the same car speed. This is because we gear it up by nearly* $39\%(\approx [5000 - 3600]\,/3600)$, *while the engine torque is dropped by* $13\%(\approx [460 - 400]\,/460)$. *Hence, we gain* $26\%$ *in drive wheel torque at the power peak versus the torque peak, at a given car speed.*

As long as the performance curves of engines are similar to those in Figure 4.1, any engine speed, other than the power peak speed $\omega_M$, at a given car speed will provide a lower torque value at the drive wheels. Therefore, theoretically the best top speed will always occur when the vehicle is operating at its power peak.

A car running at its power peak can accelerate no faster at the same vehicle speed. There is no better gear to choose, even if another gear would place the engine closer to its torque peak. A car running at peak power at a given vehicle speed is delivering the maximum possible torque to the tires, although the engine may not be running at its torque peak. The transmission amplifies the torque coming from the engine by a factor equal to the gear ratio.

**Example 127** ★ *Ideal engine performance.*

It is said that an ideal engine is one that produces a constant power regardless of speed. For this kind of ideal engine we have

$$P_e \;=\; P_0 \tag{4.34}$$

$$T_e \;=\; \frac{P_0}{\omega_e}. \tag{4.35}$$

Figure 4.4 depicts a sample of the power and torque performance curves for an ideal engine having $P_0 = 50\,\mathrm{kW}$.

In vehicle dynamics, we introduce a gearbox to keep the engine running at the maximum power or in a working range around the maximum power. So, practically we keep the power of the engine, and therefore, the power at wheels constant at the maximum value. Hence, the torque at the wheels should be similar to the torque of an ideal engine. A constant power performance is an applied approximation for electrical motors.

Another ideal engine would generate a linear torque-speed relationship. For such an ideal engine we have

$$T_e \;=\; C_e\,\omega_e \tag{4.36}$$

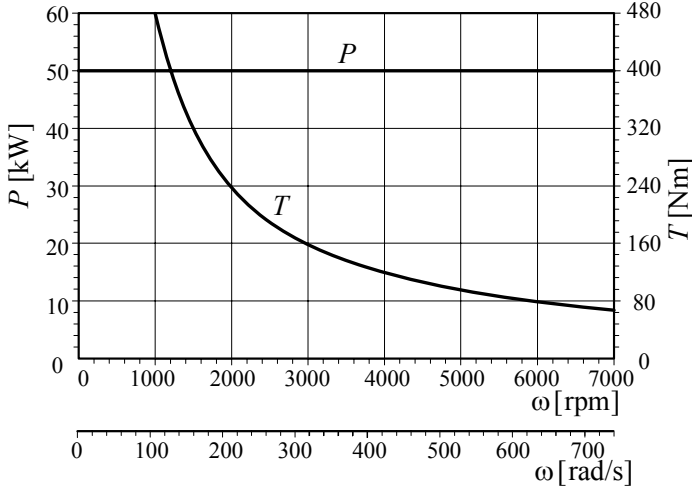$$P_e \;=\; C_e\,\omega_e^2. \tag{4.37}$$

FIGURE 4.4. Power and torque performance curves for an ideal engine.

*However, internal combustion engines do not work like this ideal engine. Figure 4.5 illustrates such an ideal performance for $C_e = 0.14539$.*

**Example 128** ★ *Maximum power and torque at the same $\omega_M$.*

*Ideal performance for an engine would be having maximum power and maximum torque at the same angular velocity $\omega_M$. However, it is impossible to have such an engine because the maximum torque $T_M$ of a spark ignition engine occurs at*

$$\frac{dT_e}{d\omega_e} = P_2 + 2P_3\,\omega_e = 0 \tag{4.38}$$

$$\omega_e = \frac{-P_2}{2P_3} = \frac{\dfrac{P_M}{\omega_M^2}}{2\dfrac{P_M}{\omega_M^3}} = \frac{1}{2}\omega_M \tag{4.39}$$

*that is half of the speed at which the power is maximum.*

*When the torque is maximum, the power is at*

$$P_e = P_1\frac{\omega_M}{2} + P_2\left(\frac{\omega_M}{2}\right)^2 + P_3\left(\frac{\omega_M}{2}\right)^3$$

$$= \frac{5}{8}P_M. \tag{4.40}$$

*However, when the power is maximum at $\omega_e = \omega_M$, the torque is*

$$T_e = \frac{1}{\omega_M}P_M. \tag{4.41}$$
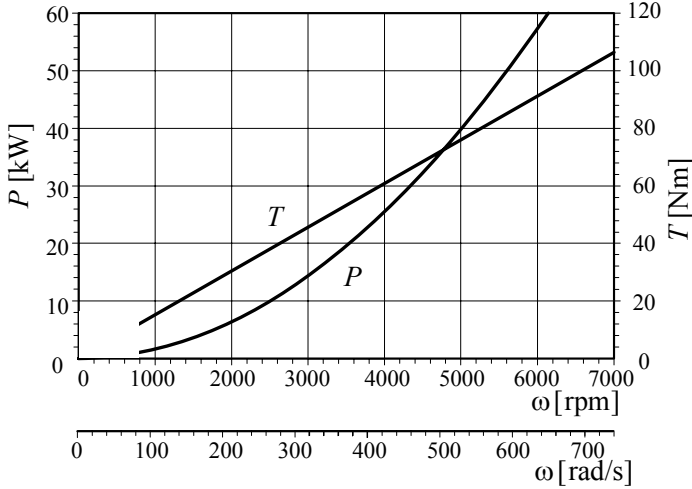
FIGURE 4.5. Performance curves of an ideal engine having a linear torque-speed relationship $T_e = 0.14539\,\omega_e$.

## 4.2   Driveline and Efficiency

We use the word *driveline*, equivalent to transmission, to call the systems and devices that transfer torque and power from the engine to the drive wheels of a vehicle. Most vehicles use one of two common transmission types: manual gear transmission, and automatic transmission with torque convertor. A driveline includes the engine, clutch, gearbox, propeller shaft, differential, drive shafts, and drive wheels. Figure 4.6 illustrates how the driveline for a rear-wheel-drive vehicle is assembled.

The *engine* is the power source in the driveline. The output from the engine is an engine torque $T_e$, at an associated engine speed $\omega_e$.

The *clutch* connects and disconnects the engine to the rest of the driveline when the vehicle is equipped with a manual gearbox.

The *gearbox* can be used to change the transmission ratio between the engine and the drive wheels.

The *propeller shaft* connects the gearbox to the differential. The propeller shaft does not exist in front-engined front-wheel-drive and rear-engined rear-wheel-drive vehicles. In those vehicles, the differential is integrated with the gearbox in a unit that is called the *transaxle*.

The *differential* is a constant transmission ratio gearbox that allows the drive wheels to have different speeds. So, they can handle the car in a curve.

The *drive shafts* connect the differential to the drive wheels.

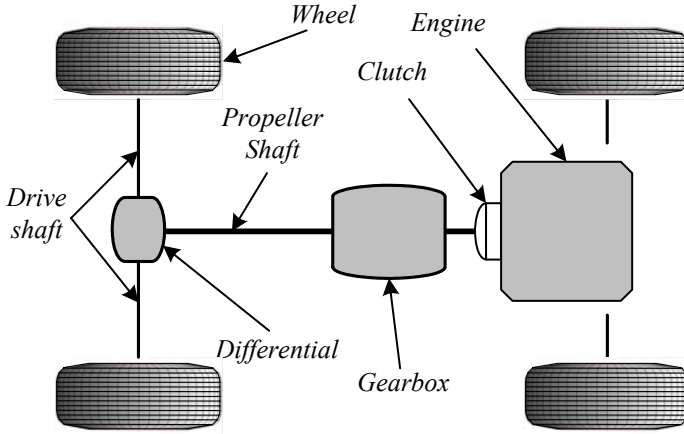The *drive wheels* transform the engine torque to a traction force on the

FIGURE 4.6. Driveline components of a rear wheel drive vehicle.

road.

The input and output torque and angular velocity for each device in a driveline are indicated in Figure 4.7.

The available power at the drive wheels is

$$P_w = \eta P_e \tag{4.42}$$

where $\eta < 1$ indicates the *overall efficiency* between the engine and the drive wheels

$$\eta = \eta_c\, \eta_t. \tag{4.43}$$

$\eta_c < 1$ is the *convertor efficiency* and $\eta_t < 1$ is the *transmission efficiency*.

The relationship between the angular velocity of the engine and the velocity of the vehicle is

$$v_x = \frac{R_w\, \omega_e}{n_g\, n_d} \tag{4.44}$$

where $n_g$ is the transmission ratio of the gearbox, $n_d$ is the transmission ratio of the differential, $\omega_e$ is the engine angular velocity, and $R_w$ is the effective tire radius.

*Transmission ratio* or *gear reduction ratio* of a gearing device, $n$, is the ratio of the input velocity to the output velocity

$$n = \frac{\omega_{in}}{\omega_{out}} \tag{4.45}$$

while the *speed ratio* $\omega_r$ is the ratio of the output velocity to the input velocity.

$$\omega_r = \frac{\omega_{out}}{\omega_{in}} \tag{4.46}$$
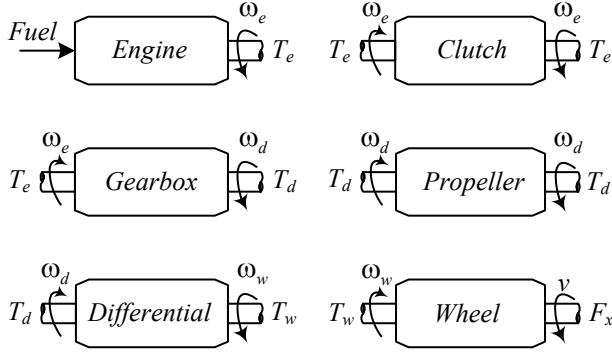
FIGURE 4.7. The input and output torque and angular velocity of each driveline component.

**Proof.** The engine is connected to the drive wheels through a *driveline.* Because of friction in the driveline, especially in the gearbox and torque convertor, the power at the drive wheels is always less than the power at the engine output shaft. The ratio of output power to input power is a number called *efficiency*

$$\eta = \frac{P_{out}}{P_{in}}. \tag{4.47}$$

If we show the efficiency of transmission by $\eta_t$ and the efficiency of torque convertor by $\eta_c$, then the overall efficiency of the driveline is $\eta = \eta_c \, \eta_t$. The power at the wheel is the output power of driveline $P_{out} = P_w$ and the engine power is the input power to the driveline $P_{in} = P_e$. Therefore,

$$P_w = \eta P_e. \tag{4.48}$$

Figure 4.8 illustrates a driving wheel with radius $R_w$ that is turning with angular velocity $\omega_w$ on the ground and moving with velocity $v_x$.

$$v_x = R_w \, \omega_w \tag{4.49}$$

There are two gearing devices between the engine and the drive wheel: gearbox and differential. Assigning $n_g$ for the transmission ratio of the gearbox and $n_d$ for the transmission ratio of the differential, the overall transmission ratio of the driveline is

$$n = n_g \, n_d. \tag{4.50}$$

So, the angular velocity of the engine $\omega_e$ is $n$ times of the angular velocity of the drive wheel $\omega_w$.

$$\begin{aligned} \omega_e &= n \, \omega_w \\ &= n_g \, n_d \, \omega_w \end{aligned} \tag{4.51}$$
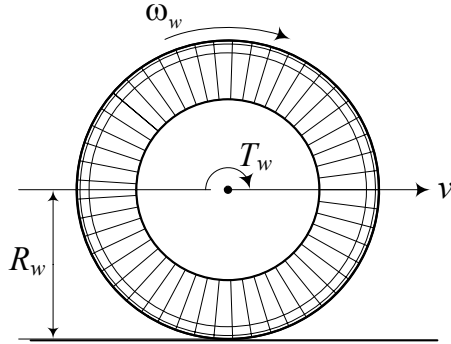
FIGURE 4.8. A tire with radius $R_w$ rolling on the ground and moving with velocity $v$ and angular velocity $\omega_w$.

Therefore,

$$v_x = \frac{R_w \, \omega_e}{n_g \, n_d}. \tag{4.52}$$

∎

**Example 129** *Front and rear-engined, front and rear drive.*

The engine may be installed in the front or back of a car. They are called front-engined and rear-engined vehicle respectively. The driving wheels may also be the front, the rear, or all wheels. Therefore, there are six possible combinations. Out of those six combinations, the front-engined front-wheel-drive, front-engined rear-wheel-drive, and front-engined all-wheel-drive vehicles are the most common. There are only a few manufacturers that make cars with rear-engined rear-wheel-drive. However, there is no rear-engined front-wheel-drive vehicle.

**Example 130** *Torque at the wheel.*

The power at the wheel is $P_w = \eta P_e$, and the angular velocity at the wheel is $\omega_w = \omega_e / (n_g \, n_d)$. Knowing $P = T\omega$, we find out that the available torque at the wheel, $T_w$, is

$$
\begin{aligned}
T_w &= \frac{P_w}{\omega_w} = \eta \, n_g \, n_d \, \frac{P_e}{\omega_e} \\
&= \eta \, n_g \, n_d \, T_e. \tag{4.53}
\end{aligned}
$$

**Example 131** *Power law.*

For any mechanical device in the driveline of a car, there is a simple law to remember.

$$
\begin{aligned}
Power \ in &= Power \ out \ minus \ losses \\
P_{in} &= P_{out} - P_{loss} \tag{4.54}
\end{aligned}
$$

*Also, because of*

$$Power \quad = \quad Torque \times \ angular \ velocity$$
$$P \quad = \quad T\omega \tag{4.55}$$

*any gearing device in the driveline of a car can reduce or increase the input torque in by increasing or decreasing the angular velocity.*

**Example 132 ★** *Volumetric, thermal, and mechanical efficiencies.*

*There is an efficiency between the attainable power in fuel and the power available at the engine's output shaft.*

$$\eta' = \eta_V \, \eta_T \, \eta_M. \tag{4.56}$$

$\eta_V$ *is the engine* **volumetric efficiency**, $\eta_T$ *is the* **thermal efficiency**, *and* $\eta_M$ *is the* **mechanical efficiency**.

**Volumetric efficiency** $\eta_V$ *identifies how much fueled air gets into the cylinder.*

*The fueled air mixture that fills the cylinder volume in the intake stroke is what will be used to create the power. Volumetric efficiency $\eta_V$ indicates the amount of fueled air in the cylinder relative to atmospheric air. If the cylinder is filled with fueled air at atmospheric pressure, then the engine has 100% volumetric efficiency. Super and turbo chargers increase the pressure entering the cylinder, giving the engine a volumetric efficiency greater than 100%. However, if the cylinder is filled with less than the atmospheric pressure, then the engine has less than 100% volumetric efficiency. Engines typically run between 80% and 100% of $\eta_V$.*

*Volumetric efficiency $\eta_V$ can be changed by any occurrence that affects the fueled air flow into the cylinder. The power of an engine is proportionally dependent on the mass ratio of fuel/air that gets into the cylinders of the engine.*

**Thermal efficiency** $\eta_T$ *identifies how much of the fuel is converted to usable power.*

*Although having more fueled air into the cylinder means more fuel energy is available to make power, not all of the available energy converts to mechanical energy. The best engines can convert only about 1/3 of the chemical energy to mechanical energy.*

*Thermal efficiency is changed by the compression ratio, ignition timing, plug location, and chamber design. Low compression engines may have an $\eta_T \approx 0.26$. A high compression racing engine may have an $\eta_T \approx 0.34$. Therefore, racing engines may produce about 30% more power because of their higher $\eta_T$.*

*Any improvement in the thermal efficiency $\eta_T$ significantly improves the final power that the engine produces. Therefore, a huge investment is expended in research to improve $\eta_T$.*

**Mechanical efficiency** $\eta_M$ *identifies how much power is consumed by the engine to run itself.*

*Some of the produced power is consumed by the engine's moving parts. It takes power to overcome the friction between parts and to run engine accessories. So, depending on how much fuel goes into the cylinder and how much converts to power, some of this power is used by the engine to run itself. The leftover power is what we can measure on an engine dynamometer. The difference between the engine output power and the generated power in the cylinders is the mechanical efficiency $\eta_M$.*

*Mechanical efficiency is affected by mechanical components of the engine or the devices attached to the engine. It also depends on the engine speed. The greater the speed, the more power it takes to turn the engine. This means the $\eta_M$ drops with speed. The mechanical efficiency $\eta_M$ is also called* **friction power** *because it indicates how much power is needed to overcome the engine friction.*

*The engine power performance curve supplied by a car manufacturer is usually the gross engine performance and does not include the mechanical efficiency. Therefore, the effective engine power available at the transmission input shaft is reduced by the power needed for accessories such as the fan, electric alternator, power steering pump, water pump, braking system, and air conditioning compressor.*

## 4.3   Gearbox and Clutch Dynamics

The internal combustion engine cannot operate below a minimum engine speed $\omega_{min}$. Consequently, the vehicle cannot move slower than a minimum speed $v_{min}$ while the engine is connected to the drive wheels.

$$v_{min} = \frac{R_w \, \omega_{min}}{n_g \, n_d} \tag{4.57}$$

At starting and stopping stages of motion, the vehicle needs to have speeds less than $v_{min}$. A clutch or a torque converter must be used for starting, stopping, and gear shifting.

Consider a vehicle with only one drive wheel. Then, the forward velocity $v_x$ of the vehicle is proportional to the angular velocity of the engine $\omega_e$, and the tire *traction force* $F_x$ is proportional to the engine torque $T_e$

$$\omega_e = \frac{n_i \, n_d}{R_w} v_x \tag{4.58}$$

$$T_e = \frac{1}{\eta} \frac{R_w}{n_i n_d} F_x \tag{4.59}$$

where $R_w$ is the effective tire radius, $n_d$ is the differential transmission ratio, $n_i$ is the gearbox transmission ratio in gear number $i$, and $\eta$ is the overall driveline efficiency. Equation (4.58) is called the *speed equation*, and Equation (4.59) is called the *traction equation*.

**Proof.** The froward velocity $v_x$ of a driving wheel with radius $R_w$ is

$$v_x = R_w \, \omega_w \tag{4.60}$$

and the traction force $F_x$ on the driving wheel is

$$F_x = \frac{T_w}{R_w}. \tag{4.61}$$

$T_w$ is the applied spin torque on the wheel, and $\omega_w$ is the wheel angular velocity.

The wheel inputs $T_w$ and $\omega_w$ are the output torque and angular velocity of differential. The differential input torque $T_d$ and angular velocity $\omega_d$ are

$$T_d \;=\; \frac{1}{\eta_d \, n_d} T_w \tag{4.62}$$

$$\omega_d \;=\; n_d \, \omega_w \tag{4.63}$$

where $n_d$ is the differential transmission ratio and $\eta_d$ is the differential efficiency.

The differential inputs $T_d$ and $\omega_d$ are the output torque and angular velocity of the vehicle's gearbox. The engine's torque $T_e$ and angular velocity $\omega_e$ are the inputs of the gearbox. The input-output relationships for a gearbox depend on the engaged gear ratio $n_i$.

$$T_e \;=\; \frac{1}{\eta_g \, n_i} T_d \tag{4.64}$$

$$\omega_e \;=\; n_i \, \omega_d \tag{4.65}$$

$\eta_g$ is the gearbox efficiency, and $n_i$ is the gear reduction ratio in the gear number $i$. Therefore, the forward velocity of a driving wheel $v_x$, is proportional to the engine angular velocity $\omega_e$, and the tire traction force $F_x$ is proportional to the engine torque $T_e$, when the driveline is engaged to the engine.

$$\omega_e \;=\; \frac{n_i \, n_d}{R_w} v_x \tag{4.66}$$

$$T_e \;=\; \frac{1}{\eta_g \eta_d} \frac{1}{n_i n_d} T_w$$

$$\;=\; \frac{1}{\eta_g \eta_d} \frac{R_w}{n_i n_d} F_x$$

$$\;=\; \frac{1}{\eta} \frac{R_w}{n_i n_d} F_x \tag{4.67}$$

Having the torque performance function $T_e = T_e \left( \omega_e \right)$ enables us to determine the wheel torque $T_w$ as a function of vehicle speed $v_x$ at each gear ratio $n_i$.

$$T_w = \eta \, n_i n_d \, T_e \left( \omega_e \right) \tag{4.68}$$

Using the approximate equation (4.11) for $T_e$ provides

$$
\begin{aligned}
T_w &= \eta\, n_i n_d \left( P_1 + P_2 \left( \frac{n_i\, n_d}{R_w} v_x \right) + P_3 \left( \frac{n_i\, n_d}{R_w} v_x \right)^2 \right) \\
&= \eta \left( P_1 n_d n_i + \eta \frac{P_2}{R_w} n_d^2 n_i^2 v_x + \eta \frac{P_3}{R_w^2} n_d^3 n_i^3 v_x^2 \right).
\end{aligned}
\tag{4.69}
$$

■

**Example 133** *A six-gear gearbox.*

  *Consider a inefficient passenger car with the following specifications:*

$$
\begin{aligned}
m &= 1550\,\text{kg} \\
R_w &= 0.326\,\text{m} \\
\eta &= 0.24 \\
torque &= 392\,\text{N m}\ \ at\ 4400\,\text{rpm} \approx 460.7\,\text{rad/s} \\
power &= 206000\,\text{W}\ \ at\ 6800\,\text{rpm} \approx 712.1\,\text{rad/s} \\
1st\ gear\ ratio &= n_1 = 3.827 \\
2nd\ gear\ ratio &= n_2 = 2.36 \\
3rd\ gear\ ratio &= n_3 = 1.685 \\
4th\ gear\ ratio &= n_4 = 1.312 \\
5th\ gear\ ratio &= n_5 = 1 \\
6th\ gear\ ratio &= n_6 = 0.793 \\
reverse\ gear\ ratio &= n_r = 3.28 \\
final\ drive\ ratio &= n_d = 3.5451
\end{aligned}
\tag{4.70}
$$

*Based on the speed equation (4.58),*

$$
\begin{aligned}
\omega_e &= \frac{n_i\, n_d}{R_w} v_x \\
&= \frac{3.5451 n_i}{0.326} v_x \\
&= 10.875 n_i\, v_x
\end{aligned}
\tag{4.71}
$$

*we can find the gear-speed plot that is shown in Figure 4.9. The angular velocities associated to maximum power and maximum torque are indicated by dashed lines.*

  *The power and torque performance equations for the engine can be approximated by*

$$
\begin{aligned}
P_e &= 289.29\,\omega_e + 0.40624\,\omega_e^2 - 5.7049 \times 10^{-4}\,\omega_e^3 \tag{4.72} \\
T_e &= 289.29 + 0.406\,24 \omega_e - 5.704\,9 \times 10^{-4}\omega_e^2 \tag{4.73}
\end{aligned}
$$
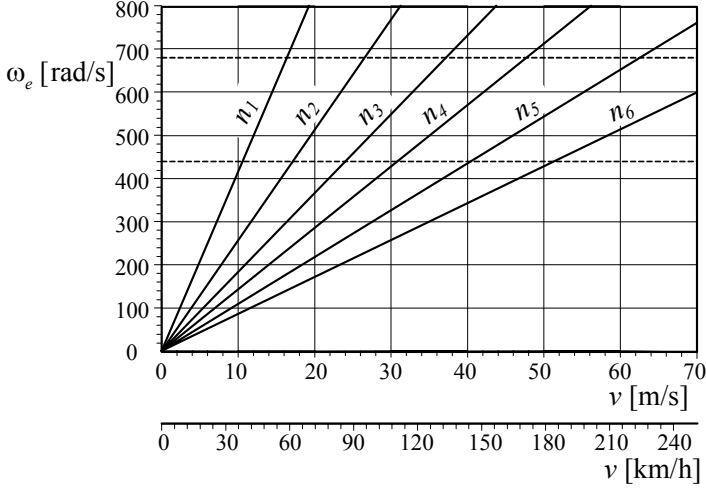
FIGURE 4.9. A sample of a gear-speed plot for a gearbox.

*because*

$$P_1 = \frac{P_M}{\omega_M} = \frac{206000}{712.1} = 289.29 \,\mathrm{W/\,s} \tag{4.74}$$

$$P_2 = \frac{P_M}{\omega_M^2} = \frac{206000}{712.1^2} = 0.40624 \,\mathrm{W/\,s^2} \tag{4.75}$$

$$P_3 = -\frac{P_M}{\omega_M^3} = -\frac{206000}{712.1^3} = -5.7049 \times 10^{-4} \,\mathrm{W/\,s^3}. \tag{4.76}$$

*Using the torque equation (4.73) and the traction equation (4.71), we can plot the wheel torque as a function of vehicle speed at different gears.*

$$
\begin{aligned}
T_w &= \eta \, n_i n_d \, T_e \\
&= \eta \, n_i n_d \left( 289.29 + 0.406\,24\omega_e - 5.704\,9 \times 10^{-4}\omega_e^2 \right) \\
&= -5.7405 \times 10^{-2} n_i^3 v_x^2 + 3.758\,8 n_i^2 v_x + 246.13 n_i \tag{4.77}
\end{aligned}
$$

*Figure 4.10 shows the wheel torque-speed Equation (4.77) at each gear $n_i$. The envelope curve for the series of torque-speed equations is similar to the torque curve of a constant power ideal engine.*

**Example 134 ★** *Envelope curve for torque-speed family.*
   *Assume the torque-speed equation of a car is similar to Equation (4.77) that is a second degree of speed having the gear ratio $n = n_i$ as a parameter.*

$$T = an^3 v^2 + bn^2 v + cn \tag{4.78}$$

*A variation of the parameter generates a series of curves called family. An envelope is a curve tangent to all members of the family. To find the envelope of a family, we should eliminate the parameter between the equation of*
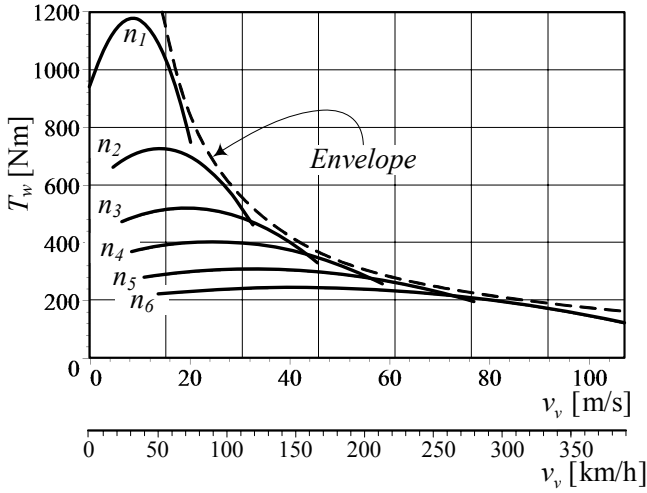
FIGURE 4.10. Wheel torque-speed Equation (4.77) at each gear $n_i$ of a gearbox, and the envelope curve simulating an ideal engine behavior.

*the family and its derivative with respect to the parameter. The derivative of the family (4.78) with respect to the parameter n*

$$\frac{\partial T}{\partial n} = 3an^2v^2 + 2bnv + c = 0 \tag{4.79}$$

*leads to*

$$n = \frac{-b \pm \sqrt{b^2 - 3ac}}{3av}. \tag{4.80}$$

*Substituting the parameter back into the equation of the family provides the equation of the envelop analytically.*

$$T = \frac{b}{27a^2v} \left( b - \sqrt{b^2 - 3ac} \right) \left( b - \sqrt{b^2 - 3ac} - \frac{6ac}{b} \right) \tag{4.81}$$

*The equation of envelope for the wheel torque-speed family at different gears is equivalent to*

$$T \equiv \frac{C}{v} \tag{4.82}$$

*where $C$ is a constant. Such a torque equation belongs to an ideal constant power device introduced in Example 127.*

**Example 135** *Mechanical and hydraulic clutches.*

  *Mechanical clutches are widely used in passenger cars and are normally in the form of a dry single-disk clutch. The adhesion between input and output shafts is produced by circular disks that rub against each other.*

*Engagement begins with the engine running at $\omega_e = \omega_{min}$ and the clutch being released gradually from time $t = 0$ to $t = t_1$ such that the transmitted torque $T_c$ from the engine to the gearbox increases almost linearly in time from $T_c = 0$ to the maximum value $T_c = T_{c_1}$ that can be handled in slipping mode. The transmitted torque remains constant until the input and output disks stick together and a speed equality is achieved. At this time, the clutch is rigid and $T_c = T_e$.*

*The transmitted torque $T_c$ should overcome the resistance force and the vehicle should accelerate sometime in $0 < t \le t_1$. The magnitude of the transferable torque depends on the applied force between the disks, the frictional coefficient between clutch disks, the effective frictional area, and the number of frictional pairs. The axial force is generally produced by a preloaded spring. The driver can control the spring force by using the clutch pedal, and adjust the transferred torque.*

*The hydraulic clutch consists of a pump wheel connected to the engine and a clutch-ended turbine that is equipped with radial vanes. A torque is transferred between the pump wheel and the turbine over a fluid, which is accelerated by the pump and decelerated in the turbine. The hydraulic clutch is also called Foettinger clutch.*

*The transferred torque can be calculated according to the Foettinger's law*

$$T_c = C_c \rho \omega_p^2 D^2 \tag{4.83}$$

*where $C_c$ is slip factor, $\rho$ is the oil density, $\omega_p$ is the pump angular velocity, and $D$ is the clutch diameter.*

**Example 136** *Acceleration capacity at different speed.*

*Assume an engine is working at speed $\omega_M$ associated to the maximum power $P_M$.*

$$
\begin{aligned}
P_M &= T_e \, \omega_M \\
&= \frac{1}{\eta} F_x \, v_x \tag{4.84}
\end{aligned}
$$

*Substituting*

$$F_x = m a_x \tag{4.85}$$

*indicates that*

$$P_M = \frac{m}{\eta} a_x \, v_x \tag{4.86}$$

*and therefore,*

$$a_x = P_M \frac{\eta}{m} \frac{1}{v_x}. \tag{4.87}$$

*Equation (4.87) is called* **acceleration capacity** *and expresses the achievable acceleration of a vehicle at speed $v_x$. The acceleration capacity decreases by increasing velocity. As an example, Figure 4.11 depicts the acceleration capacity $a_x$ as a function of the forward speed $v_x$ for a vehicle*
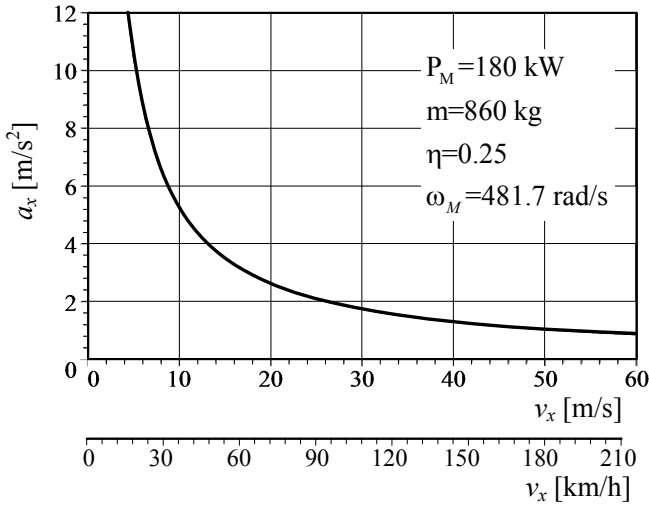
FIGURE 4.11. An example for the acceleration capacity $a_x$ as a fucntion of forward speed $v_x$.

with mass $m = 860\,\mathrm{kg}$, maximum power $P_M = 180\,\mathrm{kW} \approx 241.4\,\mathrm{hp}$ at $\omega_M = 4600\,\mathrm{rpm} \approx 481.7\,\mathrm{rad/\,s}$, and efficiency $\eta = 0.25$.

**Example 137** *Power-limited and traction-limited accelerations.*

Acceleration capacity is power-limited acceleration and is based on the assumption that the driving force does not reach the tire traction limit. Therefore, the vehicle reaches its peak acceleration because the engine cannot deliver any more power.

The traction-limited acceleration happens when the engine delivers more power, but vehicle acceleration is limited because the tires cannot transmit any more driving force to the ground. Equation $F_x = \mu_x F_z$ gives the maximum transmittable force. If more driving torque is applied to the wheel, the tire slips and enters the dynamic friction regime where the coefficient of friction, and hence the traction force, are less.

**Example 138** ★ *Gearbox stability condition.*

Consider a vehicle moving at speed $v_x$ when the gearbox is engaged in gear number $i$ with transmission ratio $n_i$. To be safe, we have to select the transmission ratios such that when the engine reaches the maximum torque it can shift to a lower gear $n_{i-1}$ without reaching the maximum permissible engine speed. The maximum permissible engine speed is usually indicated by a red line or red region.

Let's show the engine speed for the maximum torque $T_M$ by $\omega_e = \omega_T$.

*The speed of the vehicle at $\omega_e = \omega_T$ is*

$$v_x = \frac{R_w}{n_i \, n_d} \omega_T. \tag{4.88}$$

*When we shift the gear to $n_{i-1}$ the engine speed $\omega_e$ jumps to a higher speed $\omega_e = \omega_{i-1} > \omega_T$ at the same vehicle speed*

$$\omega_{i-1} = \frac{n_{i-1} \, n_d}{R_w} v_x. \tag{4.89}$$

*The stability condition requires that $\omega_{i-1}$ be less than the maximum permissible engine speed $\omega_{Max}$*

$$\omega_{i-1} \leq \omega_{Max}. \tag{4.90}$$

*Using Equations (4.88) and (4.89), we may define the following condition between transmission ratios at two successive gears and the engine speed:*

$$\frac{\omega_{i-1}}{\omega_i} = \frac{\omega_{Max}}{\omega_T} = \frac{n_{i-1}}{n_i} \tag{4.91}$$

*A constant relative gear ratio, at a constant vehicle speed, can be a simple rule for a stable gearbox design*

$$\frac{n_{i-1}}{n_i} = c_g. \tag{4.92}$$

**Example 139** *Transmission ratios and stability condition.*
*Consider a passenger car with the following gearbox transmission ratios:*

$$
\begin{aligned}
\text{1st gear ratio} \quad &= \quad n_1 = 3.827 \\
\text{2nd gear ratio} \quad &= \quad n_2 = 2.36 \\
\text{3rd gear ratio} \quad &= \quad n_3 = 1.685 \\
\text{4th gear ratio} \quad &= \quad n_4 = 1.312 \\
\text{5th gear ratio} \quad &= \quad n_5 = 1 \\
\text{6th gear ratio} \quad &= \quad n_6 = 0.793 \\
\text{final drive ratio} \quad &= \quad n_d = 3.5451
\end{aligned}
\tag{4.93}
$$

*The stability condition requires that $n_{i-1}/n_i = cte$. We examine the gear ratios and find out that the relative gear ratios are not constant.*

$$\frac{n_5}{n_6} = \frac{1}{0.793} = 1.261$$

$$\frac{n_4}{n_5} = \frac{1.312}{1} = 1.312$$

$$\frac{n_3}{n_4} = \frac{1.685}{1.312} = 1.284\,3$$

$$\frac{n_2}{n_3} = \frac{2.36}{1.685} = 1.4$$

$$\frac{n_1}{n_2} = \frac{3.827}{2.36} = 1.621\,6 \tag{4.94}$$

*We may change the gear ratios to have* $n_{i-1}/n_i = cte$. *Let's start from the higher gear and find the lower gears using* $c_g = n_6/n_5 = 1.261$.

$$n_6 = 0.793$$

$$n_5 = 1$$

$$n_4 = c_g n_5 = 1.261$$

$$n_3 = c_g n_4 = 1.261 \times 1.261 = 1.59$$

$$n_2 = c_g n_3 = 1.261 \times 1.59 = 2$$

$$n_1 = c_g n_2 = 1.261 \times 2 = 2.522 \tag{4.95}$$

*We may also start from the first two gears and find the higher gears using* $c_g = n_1/n_2 = 3.827/2.36 = 1.6216$.

$$n_1 = 3.827$$

$$n_2 = 2.36$$

$$n_3 = \frac{n_2}{c_g} = \frac{2.36}{1.6216} = 1.455$$

$$n_4 = \frac{n_3}{c_g} = \frac{1.455}{1.6216} = 0.897$$

$$n_5 = \frac{n_4}{c_g} = \frac{0.897}{1.6216} = 0.553$$

$$n_6 = \frac{n_5}{c_g} = \frac{0.553}{1.6216} = 0.341 \tag{4.96}$$

*None of these two sets shows a practical design. The best way to apply a constant relative ratio is to use the first and final gears and fit four intermittent gears such that* $n_{i-1}/n_i = cte$. *Using* $n_1$ *and* $n_6$ *we have,*

$$\frac{n_1}{n_6} = \frac{3.827}{0.793}$$

$$= \frac{n_1}{n_2}\frac{n_2}{n_3}\frac{n_3}{n_4}\frac{n_4}{n_5}\frac{n_5}{n_6}$$

$$= c_g^5 \tag{4.97}$$

*and therefore,*

$$c_g = 1.37. \tag{4.98}$$

*Now we are able to find the gear ratios.*

$$
\begin{aligned}
n_1 &= 3.827 \\
n_2 &= \frac{n_1}{c_g} = \frac{3.827}{1.37} = 2.793 \\
n_3 &= \frac{n_2}{c_g} = \frac{2.793}{1.37} = 2.039 \\
n_4 &= \frac{n_3}{c_g} = \frac{2.039}{1.37} = 1.488 \\
n_5 &= \frac{n_4}{c_g} = \frac{1.488}{1.37} = 1.086 \\
n_6 &= 0.793
\end{aligned}
\tag{4.99}
$$

## 4.4   Gearbox Design

The speed and traction equations (4.58) and (4.59) can be used to calculate the gear ratios of a gearbox as well as vehicle performance. Theoretically the engine should work at its maximum power to have the best performance. However, to control the speed of the vehicle, we need to vary the engine's angular velocity. Hence, we pick an angular velocity range $(\omega_1, \omega_2)$ around $\omega_M$, which is associated to the maximum power $P_M$, and sweep the range repeatedly at different gears. The range $(\omega_1, \omega_2)$ is called the engine's *working range*.

As a general guideline, we may use the following recommendations to design the transmission ratios of a vehicle gearbox:

1. We may design the differential transmission ratio $n_d$ and the final gear $n_n$ such that the final gear $n_n$ is a direct gear, $n_n = 1$, when the vehicle is moving at the moderate highway speed. Using $n_n = 1$ implies that the input and output of the gearbox are directly connected with each other. Direct engagement maximizes the mechanical efficiency of the gearbox.

2. We may design the differential transmission ratio $n_d$ and the final gear $n_n$ such that the final gear $n_n$ is a direct gear, $n_n = 1$, when the vehicle is moving at the maximum attainable speed.

3. The first gear $n_1$ may be designed by the maximum desired torque at driving wheels. Maximum torque is determined by the slope of a desired climbing road.

4. We can find the intermediate gears using the gear stability condition. Stability condition provides that the engine speed must not exceed the maximum permissible speed if we gear down from $n_i$ to $n_{i-1}$, when the engine is working at the maximum torque in $n_i$.
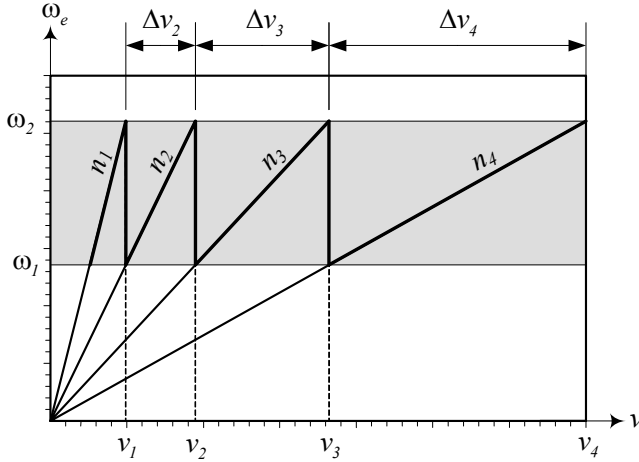
FIGURE 4.12. A gear-speed plot for a geometric gearbox design.

5. The value of $c_g$ for relative gear ratios

$$\frac{n_{i-1}}{n_i} = c_g \qquad (4.100)$$

can be chosen in the range.

$$1 \leq c_g \leq 2 \qquad (4.101)$$

To determine the middle gear ratios, there are two recommended methods:

1— Geometric ratios
2— Progressive ratios

### 4.4.1  Geometric Ratio Gearbox Design

When the jump of engine speed in any two successive gears is constant at a vehicle speed, we call the gearbox *geometric*. The design condition for a geometric gearbox is

$$n_i = \frac{n_{i-1}}{c_g} \qquad (4.102)$$

where $c_g$ is the constant relative gear ratio and is called *step jump*.

**Proof.** A geometric gearbox has constant engine speed jump in any gear shift. So, a geometric gearbox must have a gear-speed plot such as that shown in Figure 4.12.

The engine working range is defined by two speeds $(\omega_1, \omega_2)$

$$\{(\omega_1, \omega_2), \omega_1 < \omega_M < \omega_2\}. \tag{4.103}$$

When the engine reaches the maximum speed $\omega_2$ in the gear number $i$ with ratio $n_i$, we gear up to $n_{i+1}$ to jump the engine speed down to $\omega_1$. The engine's speed jump is kept constant for any gear change from $n_i$ to $n_{i+1}$. Employing the speed equation (4.58), we have

$$
\begin{aligned}
\triangle\omega &= \omega_2 - \omega_1 \\
&= \frac{n_{i-1}\, n_d}{R_w} v_x - \frac{n_i\, n_d}{R_w} v_x \\
&= (n_{i-1} - n_i) \frac{n_d}{R_w} v_x
\end{aligned}
\tag{4.104}
$$

and therefore,

$$
\begin{aligned}
\frac{\omega_2 - \omega_1}{\omega_1} &= \frac{n_{i-1} - n_i}{n_i} \\
\frac{\omega_2}{\omega_1} - 1 &= \frac{n_{i-1}}{n_i} - 1 \\
\frac{\omega_2}{\omega_1} &= \frac{n_{i-1}}{n_i} = cte.
\end{aligned}
\tag{4.105}
$$

Let's indicate the maximum vehicle speed in gear $n_i$ by $v_i$ and in gear $n_{i-1}$ by $v_{i-1}$, then,

$$
\begin{aligned}
\omega_2 &= \frac{n_i\, n_d}{R_w} v_i \\
&= \frac{n_{i-1}\, n_d}{R_w} v_{i-1}
\end{aligned}
\tag{4.106}
$$

and therefore, the maximum speed in gear $i$ to the maximum speed in gear $i-1$ is inverse of the gear ratios

$$c_g = \frac{n_{i-1}}{n_i} = \frac{v_i}{v_{i-1}}. \tag{4.107}$$

The change in vehicle speed between gear $n_{i-1}$ and $n_i$ is indicated by

$$\triangle v_i = v_i - v_{i-1} \tag{4.108}$$

and is called *speed span*.

Having the step jump $c_g$, and knowing the maximum speed $v_i$ of the vehicle in gear $n_i$, are enough to find the maximum velocity of the car in the other gears

$$
\begin{aligned}
v_i &= c_g\, v_{i-1} \\
v_{i-1} &= \frac{1}{c_g} v_i \\
v_{i+1} &= c_g\, v_i.
\end{aligned}
$$

$$v_i = c_g\, v_{i-1} \tag{4.109}$$

$$v_{i-1} = \frac{1}{c_g} v_i \tag{4.110}$$

$$v_{i+1} = c_g\, v_i. \tag{4.111}$$

■
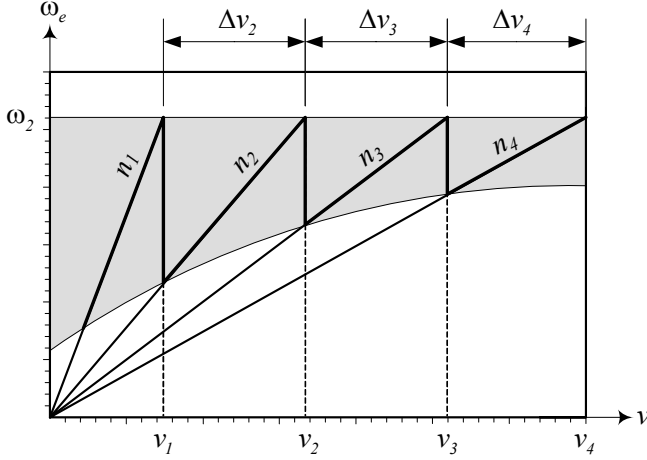
FIGURE 4.13. A gear-speed plot for a progressive gearbox design.

## 4.4.2  ★ Progressive Ratio Gearbox Design

When the speed span of a vehicle in any two successive gears is kept constant, we call the gearbox *progressive*. The design condition for a progressive gearbox is

$$n_{i+1} = \frac{n_i n_{i-1}}{2n_{i-1} - n_i} \tag{4.112}$$

where $n_{i-1}$, $n_i$, and $n_{i+1}$ are the transmission ratios of three successive gears.

**Proof.** A progressive gearbox has constant vehicle speed span in any gear. So, a progressive gearbox must have a gear-speed plot such as that shown in Figure 4.13.

Indicating the maximum vehicle speed in gear $n_i$ by $v_i$, in gear $n_{i-1}$ by $v_{i-1}$, and in gear $n_{i+1}$ by $v_{i+1}$, we have

$$
\begin{aligned}
\omega_2 &= \frac{n_i\, n_d}{R_w}\, v_i \\
&= \frac{n_{i-1}\, n_d}{R_w}\, v_{i-1} \\
&= \frac{n_{i+1}\, n_d}{R_w}\, v_{i+1}.
\end{aligned} \tag{4.113}
$$

The difference in vehicle speed at maximum engine speed is

$$
\begin{aligned}
\triangle v &= v_i - v_{i-1} \\
&= v_{i+1} - v_i
\end{aligned} \tag{4.114}
$$

and therefore,

$$v_{i+1} + v_{i-1} = 2v_i \tag{4.115}$$

$$\frac{v_{i+1}}{v_i} + \frac{v_{i-1}}{v_i} = 2 \tag{4.116}$$

$$\frac{n_i}{n_{i+1}} + \frac{n_i}{n_{i-1}} = 2 \tag{4.117}$$

$$n_{i+1} = \frac{n_i n_{i-1}}{2n_{i-1} - n_i}. \tag{4.118}$$

The step jump of a progressive gearbox decreases in higher gears. If the step jump $c_{g_i}$ between $n_i$ and $n_{i+1}$ is

$$\frac{n_i}{n_{i+1}} = c_{g_i} \tag{4.119}$$

then,

$$c_{g_i} = 2 - \frac{1}{c_{g_{i-1}}}. \tag{4.120}$$

■

**Example 140** *A gearbox with three gears.*
*Consider an $m = 860\,\mathrm{kg}$ car having an engine with $\eta = \eta_d\,\eta_g = 0.84$ and the power-speed relationship*

$$P_e = 100 - \frac{100}{398^2}\left(\omega_e - 398\right)^2 \ \mathrm{kW} \tag{4.121}$$

*where $\omega_e$ is in $[\mathrm{rad/\,s}]$. We define the working range for the engine*

$$272\,\mathrm{rad/\,s}\,(\approx 2600\,\mathrm{rpm}) \le \omega_e \le 524\,\mathrm{rad/s}\,(\approx 5000\,\mathrm{rpm}) \tag{4.122}$$

*when the power is $100\,\mathrm{kW} \ge P_e \ge 90\,\mathrm{kW}$. The power performance curve (4.121) is illustrated in Figure 4.14 and the working range is shaded.*
*The differential of the vehicle uses $n_d = 4$, and the effective tire radius is $R_w = 0.326\,\mathrm{m}$. We like to design a three-gear geometric gearbox to have the minimum time required to reach the speed $v_x = 100\,\mathrm{km/\,h} \approx 27.78\,\mathrm{m/\,s} \approx 62\,\mathrm{mi/\,h}$. We assume that the total resistance force is constant, and the engine cannot accelerate the car at $v_x = 180\,\mathrm{km/\,h} = 50\,\mathrm{m/\,s} \approx 112\,\mathrm{mi/\,h}$ anymore. Assume that every gear change takes $0.47\,\mathrm{s}$ and we need $t_0 = 2.58\,\mathrm{s}$ to adjust the engine speed with the car speed in first gear.*
*Using the speed equation (4.58), the relationship between vehicle and engine speeds is*

$$\begin{aligned} v_x &= \frac{R_w}{n_d\,n_i}\omega_e \\ &= \frac{0.326}{4\,n_i}\omega_e. \end{aligned} \tag{4.123}$$
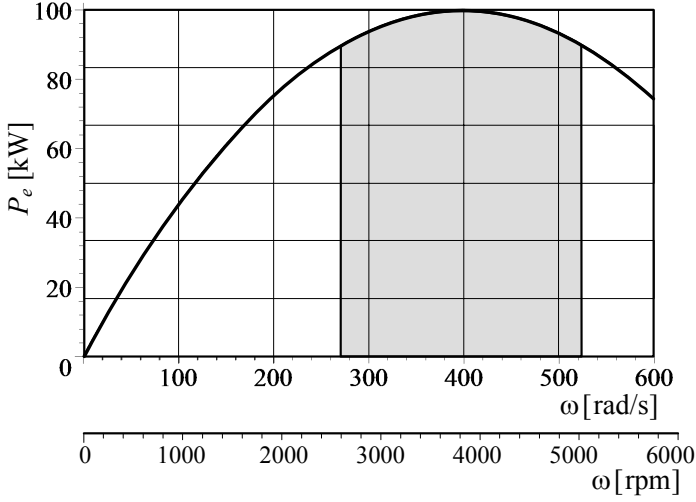
FIGURE 4.14. The power performance curve (4.121) and its working range.

*At the maximum speed $v_x = 50\,\mathrm{m/\,s}$, the engine is rotating at the upper limit of the working range $\omega_e = 524\,\mathrm{rad/\,s}$ and the gearbox is operating in third gear. Therefore, Equation (4.123) provides that*

$$
\begin{aligned}
n_3 &= \frac{0.326}{4}\frac{\omega_e}{v_x} \\
&= \frac{0.326}{4}\frac{524}{50} = 0.85412. 
\end{aligned}
\tag{4.124}
$$

*The speed equation*

$$
v_x = \frac{0.326}{4 \times 0.85412}\omega_e
\tag{4.125}
$$

*is applied as long as the gearbox is operating in third gear $n_i = n_3$, and $\omega_e$ is in the working range. By decreasing $\omega_e$ and sweeping down over the working range, the speed of the car will reduce. At the lower range $\omega_e = 272\,\mathrm{rad/\,s}$, the vehicle speed is*

$$
\begin{aligned}
v_x &= \frac{0.326}{4 \times 0.85412} \times 272 \\
&= 25.95\,\mathrm{m/\,s} \\
&\approx 93.43\,\mathrm{km/\,h} \approx 58\,\mathrm{mi/\,h}.
\end{aligned}
\tag{4.126}
$$

*At this speed we should gear down to $n_2$ and jump to the higher range*

$\omega_e = 524\,\mathrm{rad/s}$. *This provides that*

$$
\begin{aligned}
n_2 &= \frac{0.326}{4}\frac{\omega_e}{v_x} \\
&= \frac{0.326}{4}\frac{524}{25.95} = 1.6457.
\end{aligned}
\tag{4.127}
$$

*Therefore, the engine and vehicle speed relationship in second gear is*

$$
v_x = \frac{0.326}{4 \times 1.6457}\omega_e
\tag{4.128}
$$

*that is applicable as long as* $n_i = n_2$, *and* $\omega_e$ *is in the working range. Sweeping down the engine's angular velocity reduces the vehicle speed to*

$$
\begin{aligned}
v_x &= \frac{0.326}{4 \times 1.6457} \times 272 \\
&= 13.47\,\mathrm{m/s} \\
&\approx 48.49\,\mathrm{km/h} \approx 30.1\,\mathrm{mi/h}.
\end{aligned}
\tag{4.129}
$$

*At this speed we should gear down to* $n_1$ *and jump again to the higher range* $\omega_e = 524\,\mathrm{rad/s}$. *This provides that*

$$
\begin{aligned}
n_1 &= \frac{0.326}{4}\frac{\omega_e}{v_x} \\
&= \frac{0.326}{4}\frac{524}{13.47} = 3.1705
\end{aligned}
\tag{4.130}
$$

*and therefore, the speed equation for the first gear is*

$$
v_x = \frac{0.326}{4 \times 3.1705}\omega_e.
\tag{4.131}
$$

*At the lower range of the engine's speed in the first gear* $n_i = n_1$, *the speed of the vehicle is*

$$
\begin{aligned}
v_x &= \frac{0.326}{4 \times 3.1705} \times 272 \\
&= 7\,\mathrm{m/s} \\
&\approx 25.2\,\mathrm{km/h} \approx 15.6\,\mathrm{mi/h}.
\end{aligned}
\tag{4.132}
$$

*Therefore, the three-gear gearbox uses the following gear ratios:*

$$
\begin{aligned}
n_1 &= 3.1705 \\
n_2 &= 1.6457 \\
n_3 &= 0.85412
\end{aligned}
\tag{4.133}
$$

The speed equations for the three gears are plotted in Figure 4.15. Such a plot is called a **gear-speed** plot. Figure 4.15 also shows the gear switching
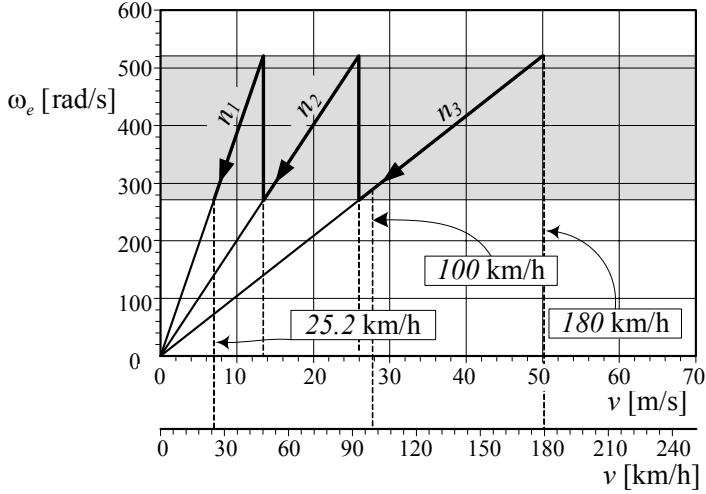
FIGURE 4.15. The gear-speed plot for a three-gear gearbox.

*points and how the vehicle speed is reducing from $v_x = 50\,\text{m/s}$ to $v_x = 7\,\text{m/s}$.*

*To evaluate the required time to reach the desired speed, we need to find the traction force $F_x$ from the traction equation and integrate.*

$$
\begin{aligned}
F_x &= \eta \frac{n_i n_d}{R_w} \frac{P_e}{\omega_e} \\
&= \frac{\eta}{\omega_e} \frac{n_i n_d}{R_w} \left( 100 - \frac{100}{398^2} \left( \omega_e - 398 \right)^2 \right) \\
&= \frac{25}{39\,601} \frac{\eta}{R_w^2} n_d n_i \left( 796 R_w - n_d n_i v_x \right) \text{ kN.} \qquad (4.134)
\end{aligned}
$$

*At the maximum speed, the gearbox is in the third gear and the traction force $F_x$ is equal to the total resistance force $F_R$.*

$$
\begin{aligned}
F_x &= F_R = \frac{\eta P_e}{v_x} \\
&= \frac{0.84 \times 90}{50} = 1.512\,\text{kN} \qquad (4.135)
\end{aligned}
$$

*Therefore, the traction force in the first gear is*

$$
\begin{aligned}
F_x &= \frac{25}{39601} \frac{\eta}{R_w^2} n_d n_1 \left( 796 R_w - n_d n_1 v_x \right) \\
&= \frac{25}{39601} \frac{0.84}{0.326^2} \times 4 \times 3.1705 \left( 796 \times 0.326 - 4 \times 3.1705 v_x \right) \\
&= 16.421 - 0.80252 v_x \text{ kN.} \qquad (4.136)
\end{aligned}
$$

*Based on Newton's equation of motion*

$$F_x - F_R = m\frac{dv_x}{dt} \tag{4.137}$$

*we can evaluate the required time to sweep the velocity from zero to $v_x = 13.47\,\mathrm{m/s}$*

$$
\begin{aligned}
t_1 &= m\int_0^{13.47} \frac{1}{F_x - F_R} dv_x \\
&= 860\int_0^{13.47} \frac{10^{-3}}{16.421 - 0.80252v_x - 1.512} dv_x \\
&= 1.3837\,\mathrm{s}.
\end{aligned}
\tag{4.138}
$$

*In second gear, we have*

$$
\begin{aligned}
F_x &= \frac{25}{39601}\frac{\eta}{R_w^2} n_d n_2 \left(796 R_w - n_d n_2 v_x\right) \\
&= \frac{25}{39601}\frac{0.84}{0.326^2} \times 4 \times 1.6457 \left(796 \times 0.326 - 4 \times 1.6457 v_x\right) \\
&= 8.5235 - 0.21622 v_x\ \mathrm{kN}
\end{aligned}
\tag{4.139}
$$

*and therefore, the sweep time in the second gear is*

$$
\begin{aligned}
t_2 &= m\int_{13.47}^{25.95} \frac{1}{F_x - F_R} dv_x \\
&= 860\int_{13.47}^{25.95} \frac{10^{-3}}{8.5235 - 0.21622 v_x - 1.512} dv_x \\
&= 4.2712\,\mathrm{s}.
\end{aligned}
\tag{4.140}
$$

*Finally, the traction equation in the third gear is*

$$
\begin{aligned}
F_x &= \frac{25}{39601}\frac{\eta}{R_w^2} n_d n_3 \left(796 R_w - n_d n_3 v_x\right) \\
&= \frac{25}{39601}\frac{0.84}{0.326^2} \times 4 \times 0.85412 \left(796 \times 0.326 - 4 \times 0.85412 v_x\right) \\
&= 4.4237 - 5.8242 \times 10^{-2} v_x\ \mathrm{kN}
\end{aligned}
\tag{4.141}
$$

*and the sweep time is*

$$
\begin{aligned}
t_3 &= m\int_{25.95}^{27.78} \frac{1}{F_x - F_R} dv_x \\
&= 860\int_{25.95}^{27.78} \frac{10^{-3}}{4.4237 - 5.8242 \times 10^{-2} v_x - 1.512} dv_x \\
&= 1.169\,\mathrm{s}.
\end{aligned}
\tag{4.142}
$$

*The total time to reach the speed $v_x = 100\,\mathrm{km/h} \approx 27.78\,\mathrm{m/s}$ is then equal to*

$$
\begin{aligned}
t &= t_0 + t_1 + t_2 + t_3 + 3 \times 0.47 \\
&= 2.58 + 1.3837 + 4.2712 + 1.169 + 3 \times 0.47 \\
&= 10.814\,\mathrm{s} \quad\quad\quad\quad\quad\quad (4.143)
\end{aligned}
$$

**Example 141** *Better performance with a four-gear gearbox.*
*A car equipped with a small engine has the following specifications:*

$$
\begin{aligned}
m &= 860\,\mathrm{kg} \\
R_w &= 0.326\,\mathrm{m} \\
\eta &= 0.84 \\
n_d &= 4 \quad\quad\quad\quad\quad\quad (4.144)
\end{aligned}
$$

*and the engine operates based on the following performance equation:*

$$
P_e = 100 - \frac{100}{398^2}(\omega_e - 398)^2\ \mathrm{kW} \quad\quad\quad\quad (4.145)
$$

*where $\omega_e$ is in $[\mathrm{rad/s}]$. Assuming the engine works well in the range*

$$
272\,\mathrm{rad/s}\,(\approx 2600\,\mathrm{rpm}) \le \omega_e \le 524\,\mathrm{rad/s}\,(\approx 5000\,\mathrm{rpm}) \quad\quad (4.146)
$$

*when the power is $100\,\mathrm{kW} \ge P_e \ge 90\,\mathrm{kW}$. We would like to design a gearbox to minimize the time to reach $v_x = 100\,\mathrm{km/h} \approx 27.78\,\mathrm{m/s} \approx 62\,\mathrm{mi/h}$.*
*The power performance equation (4.145) is illustrated in Figure 4.14 and the working range is shaded. To make this example comparable to Example 140 we assume that the total resistance force is constant, and the engine cannot accelerate the car at $v_x = 180\,\mathrm{km/h}$. Furthermore, we assume that every gear change takes $0.47\,\mathrm{s}$ and a time $t_0 = 2.58\,\mathrm{s}$ is needed to adjust the engine speed need in first gear.*
*Let's design a four-gear gearbox and set the third gear such that we reach the desired speed $v_x = 27.78\,\mathrm{m/s}$ at the higher limit of working range $\omega_e = 524\,\mathrm{rad/s}$. The gear-speed plot for such a design is plotted in Figure 4.16.*
*Using the speed equation (4.58), the relationship between vehicle and engine speeds is*

$$
\begin{aligned}
v_x &= \frac{R_w}{n_d\,n_i}\omega_e \\
&= \frac{0.326}{4\,n_i}\omega_e. \quad\quad\quad\quad\quad\quad (4.147)
\end{aligned}
$$

*At the speed $v_x = 100\,\mathrm{km/h} \approx 27.78\,\mathrm{m/s}$, the engine is rotating at the upper limit of the working range $\omega_e = 524\,\mathrm{rad/s}$ and the gearbox is operating*
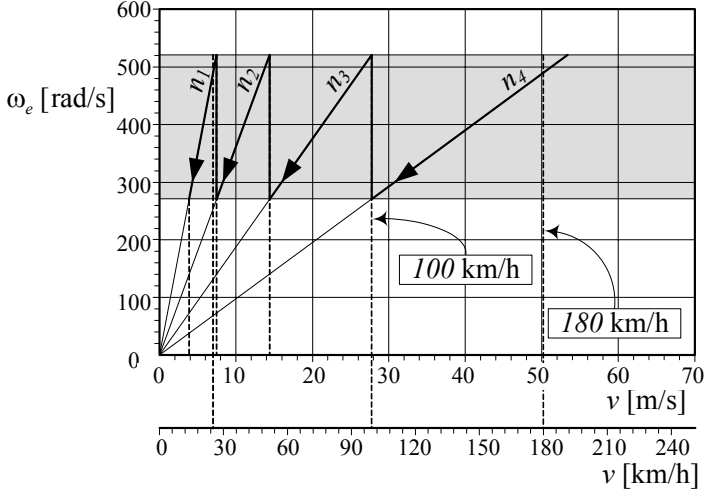
FIGURE 4.16. The gear-speed plot for Example 141.

*in third gear $n_i = n_3$. Therefore,*

$$
\begin{aligned}
n_3 &= \frac{0.326}{4}\frac{\omega_e}{v_x} \\
&= \frac{0.326}{4}\frac{524}{27.78} = 1.5373
\end{aligned}
\tag{4.148}
$$

*and the speed equation in the third gear $n_i = n_3$ is*

$$
v_x = \frac{0.326}{4 \times 1.5373}\omega_e
\tag{4.149}
$$

*while $\omega_e$ is in the working range. By sweeping down to the lower limit of the working range $\omega_e = 272\,\mathrm{rad/s}$, the speed of the car will reduce to*

$$
\begin{aligned}
v_x &= \frac{0.326}{4 \times 1.5373} \times 272 \\
&= 14.42\,\mathrm{m/s} \\
&\approx 51.91\,\mathrm{km/h} \approx 32.25\,\mathrm{mi/h}.
\end{aligned}
\tag{4.150}
$$

*At this speed we should gear down to $n_2$ and jump to the higher range $\omega_e = 524\,\mathrm{rad/s}$. This provides that*

$$
\begin{aligned}
n_2 &= \frac{0.326}{4}\frac{\omega_e}{v_x} \\
&= \frac{0.326}{4}\frac{524}{14.42} = 2.9616.
\end{aligned}
\tag{4.151}
$$

*Therefore, the gear-speed relationship in second gear $n_i = n_2$ is*

$$v_x = \frac{0.326}{4 \times 2.9616} \omega_e. \qquad (4.152)$$

*Sweeping down the engine's angular velocity to $\omega_e = 272\,\text{rad/s}$, reduces the vehicle speed to*

$$
\begin{aligned}
v_x &= \frac{0.326}{4 \times 2.9616} \times 272 \\
&= 7.48\,\text{m/s} \qquad (4.153) \\
&\approx 26.9\,\text{km/h} \approx 16.7\,\text{mi/h}.
\end{aligned}
$$

*At this speed, we gear down to $n_1$ and jump again to the higher range $\omega_e = 524\,\text{rad/s}$. This provides that*

$$
\begin{aligned}
n_1 &= \frac{0.326}{4} \frac{\omega_e}{v_x} \\
&= \frac{0.326}{4} \frac{524}{7.48} = 5.7055 \qquad (4.154)
\end{aligned}
$$

*and therefore the speed equation for first gear is*

$$v_x = \frac{0.326}{4 \times 5.7055} \omega_e. \qquad (4.155)$$

*In first gear, $n_i = n_1$, and the vehicle's speed at the lower range of the engine's speed is*

$$
\begin{aligned}
v_x &= \frac{0.326}{4 \times 5.7055} \times 272 \\
&= 3.88\,\text{m/s} \qquad (4.156) \\
&\approx 14\,\text{km/h} \approx 8.7\,\text{mi/h}.
\end{aligned}
$$

*To calculate the fourth gear $n_i = n_4$ we may use the gear-speed equation and set the engine speed to the lower limit $\omega_e = 272\,\text{rad/s}$ while the car is moving at the maximum speed in third gear. Therefore,*

$$
\begin{aligned}
n_4 &= \frac{0.326}{4} \frac{\omega_e}{v_x} \\
&= \frac{0.326}{4} \frac{272}{27.78} = 0.79798. \qquad (4.157)
\end{aligned}
$$

*The four-gear gearbox uses the following ratios:*

$$
\begin{aligned}
n_1 &= 5.7055 \\
n_2 &= 2.9616 \\
n_3 &= 1.5373 \\
n_4 &= 0.79798 \qquad (4.158)
\end{aligned}
$$

*To calculate the required time to reach the desired speed $v_x = 100\,\mathrm{km/h} \approx 27.78\,\mathrm{m/s}$, we need to use the traction equations and find the traction force $F_x$*

$$\begin{aligned} F_x &= \eta \frac{n_i n_d}{R_w} \frac{P_e}{\omega_e} \\ &= \frac{\eta}{\omega_e} \frac{n_i n_d}{R_w} \left(100 - \frac{100}{398^2}(\omega_e - 398)^2\right) \\ &= \frac{25}{39\,601} \frac{\eta}{R_w^2} n_d n_i (796 R_w - n_d n_i v_x)\ \mathrm{kN}. \end{aligned} \qquad (4.159)$$

*At the maximum speed, the gearbox is in fourth gear and the traction force $F_x$ is equal to the total resistance force $F_R$.*

$$\begin{aligned} F_x &= F_R = \frac{\eta P_e}{v_x} \\ &= \frac{0.84 \times 90}{50} = 1.512\,\mathrm{kN} \end{aligned} \qquad (4.160)$$

*Therefore, the traction force in the first gear is*

$$\begin{aligned} F_x &= \frac{25}{39601} \frac{\eta}{R_w^2} n_d n_1 (796 R_w - n_d n_1 v_x) \\ &= \frac{25}{39601} \frac{0.84}{0.326^2} \times 4 \times 5.7055\,(796 \times 0.326 - 4 \times 5.7055 v_x) \\ &= 29.55 - 2.5989 v_x\ \mathrm{kN}. \end{aligned} \qquad (4.161)$$

*Using Newton's equation of motion*

$$F_x - F_R = m\frac{dv_x}{dt} \qquad (4.162)$$

*we can evaluate the required time to reach the velocity $v_x = 7.48\,\mathrm{m/s}$*

$$\begin{aligned} t_1 &= m \int_0^{7.48} \frac{1}{F_x - F_R}\,dv_x \\ &= 860 \int_0^{7.48} \frac{10^{-3}}{29.55 - 2.5989 v_x - 1.512}\,dv_x \\ &= 0.39114\,\mathrm{s}. \end{aligned} \qquad (4.163)$$

*In second gear we have*

$$\begin{aligned} F_x &= \frac{25}{39601} \frac{\eta}{R_w^2} n_d n_2 (796 R_w - n_d n_2 v_x) \\ &= \frac{25}{39601} \frac{0.84}{0.326^2} \times 4 \times 2.9616\,(796 \times 0.326 - 4 \times 2.9616 v_x) \\ &= 15.339 - 0.70025 v_x\ \mathrm{kN} \end{aligned} \qquad (4.164)$$

*and therefore, the sweep time in second gear is*

$$
\begin{aligned}
t_2 &= m \int_{7.48}^{14.42} \frac{1}{F_x - F_R} dv_x \\
&= 860 \int_{7.48}^{14.42} \frac{10^{-3}}{15.339 - 0.70025 v_x - 1.512} dv_x \\
&= 1.0246 \, \text{s}. 
\end{aligned} \tag{4.165}
$$

*The traction equation in third gear is*

$$
\begin{aligned}
F_x &= \frac{25}{39601} \frac{\eta}{R_w^2} n_d n_3 \left( 796 R_w - n_d n_3 v_x \right) \\
&= \frac{25}{39601} \frac{0.84}{0.326^2} \times 4 \times 1.5373 \left( 796 \times 0.326 - 4 \times 1.5373 v_x \right) \\
&= 7.9621 - 0.18868 v_x \, \text{kN} 
\end{aligned} \tag{4.166}
$$

*and the sweep time is*

$$
\begin{aligned}
t_3 &= m \int_{14.42}^{27.78} \frac{1}{F_x - F_R} dv_x \\
&= 860 \int_{14.42}^{27.78} \frac{10^{-3}}{7.9621 - 0.18868 v_x - 1.512} dv_x \\
&= 5.1359 \, \text{s}. 
\end{aligned} \tag{4.167}
$$

*The total time to reach the speed $v_x = 100 \, \text{km/h} \approx 27.78 \, \text{m/s}$ is then equal to*

$$
\begin{aligned}
t &= t_0 + t_1 + t_2 + t_3 + 3 \times 0.07 \\
&= 2.58 + 0.39114 + 1.0246 + 5.1359 + 3 \times 0.47 \\
&= 10.542 \, \text{s} 
\end{aligned} \tag{4.168}
$$

**Example 142** *Working range.*
   *Consider that a car equipped with a small engine has the following specifications:*

$$
\begin{aligned}
m &= 860 \, \text{kg} \\
R_w &= 0.326 \, \text{m} \\
\eta &= 0.84 \\
n_d &= 4.
\end{aligned} \tag{4.169}
$$

*The performance equation of the engine is*

$$
P_e = 100 - \frac{100}{398^2} \left( \omega_e - 398 \right)^2 \, \text{kW} \tag{4.170}
$$

*where $\omega_e$ is in $[\mathrm{rad/s}]$. The engine provides a maximum power $P_M =$
$100\,\mathrm{kW}$ at $\omega_M = 400\,\mathrm{rad/s}$.*

*The total resistance force is assumed to be constant, and the maximum
attainable speed is assumed to be $v_x = 180\,\mathrm{km/h}$. Furthermore, we assume
that every gear change takes $0.07\,\mathrm{s}$ and a minimum time $t_0 = 0.18\,\mathrm{s}$ is
needed to adjust the engine speed with that car speed in the first gear.*

*We would like to design a four-gear gearbox to minimize the time to reach
$v_x = 100\,\mathrm{km/h} \approx 27.78\,\mathrm{m/s}$.*

*To find the best working range for the engine, we set third gear to reach
the desired speed $v_x = 100\,\mathrm{km/h}$ at the upper limit of the working range.
Therefore, fourth gear starts with the lower limit of the working range when
we gear up. If fourth gear is set such that the car reaches the maximum speed
$v_x = 180\,\mathrm{km/h} \approx 50\,\mathrm{m/s}$ at the upper limit of the working range, then the
gear-speed equation*

$$\omega_e = \frac{n_i\,n_d}{R_w}\,v_x \tag{4.171}$$

*provides*

$$\omega_{Max} = \frac{4n_4}{0.326} \times 50 \tag{4.172}$$

$$\omega_{min} = \frac{4n_4}{0.326} \times 27.78. \tag{4.173}$$

*By setting $\omega_{min}$ and $\omega_{Max}$ to an equal distance from $\omega_M = 400\,\mathrm{rad/s}$,*

$$\frac{\omega_{Max} + \omega_{min}}{2} = 400 \tag{4.174}$$

*we find*

$$n_4 = 0.83826 \tag{4.175}$$
$$\omega_{min} = 285.73\,\mathrm{rad/s} \tag{4.176}$$
$$\omega_{Max} = 514.27\,\mathrm{rad/s}. \tag{4.177}$$

*We are designing a gearbox such that the ratio $\omega_e/v_x$ is kept constant in
each gear. The engine speed jumps up from $\omega_{min}$ to $\omega_{Max}$ when we gear
down from $n_4$ to $n_3$ at $\omega_{min}$, hence,*

$$\omega_{Max} = \frac{4n_3}{0.326} \times 27.78 = 514.27 \tag{4.178}$$
$$n_3 = 1.5087. \tag{4.179}$$

*Therefore, the speed of the car in third gear at the lower limit of the engine
speed is*

$$v_x = 27.78\frac{\omega_{min}}{\omega_{Max}}$$
$$= 27.78 \times \frac{27.78}{50} = 15.435\,\mathrm{m/s}. \tag{4.180}$$

*The engine's speed jumps again to $\omega_{Max}$ when we gear it down from $n_3$ to $n_2$, hence,*

$$\omega_{Max} = \frac{4n_2}{0.326} \times 15.435 = 514.27 \tag{4.181}$$

$$n_2 = 2.715\,5. \tag{4.182}$$

*Finally the speed of the car in second gear at the lower limit of the engine speed is*

$$v_x = 15.435\frac{\omega_{min}}{\omega_{Max}}$$
$$= 15.435 \times \frac{27.78}{50} = 8.5757\,\text{m/s}. \tag{4.183}$$

*that provides the following gear ratio in first gear*

$$\omega_{Max} = \frac{4n_1}{0.326} \times 8.5757 = 514.27 \tag{4.184}$$

$$n_1 = 4.8874. \tag{4.185}$$

*The speed of the car in first gear at the lower limit of the engine speed is then equal to*

$$v_x = 8.5757\frac{\omega_{min}}{\omega_{Max}}$$
$$= 8.5757 \times \frac{27.78}{50} = 4.7647\,\text{m/s}. \tag{4.186}$$

*Therefore, the four gears of the gearbox have the following ratios:*

$$n_1 = 4.8874$$
$$n_2 = 2.7155$$
$$n_3 = 1.5087$$
$$n_4 = 0.83826 \tag{4.187}$$

*and the working range for the engine is*

$$285.73\,\text{rad/s}\,(\approx 2730\,\text{rpm}) \le \omega_e \le 514.27\,\text{rad/s}\,(\approx 4911\,\text{rpm})\,. \tag{4.188}$$

*The power performance curve (4.170) is illustrated in Figure 4.17 and the working range is shaded. The gear-speed plot of this design is also plotted in Figure 4.18.*

*Balance of the traction force $F_x$ and the total resistance force $F_R$ at the maximum speed provides*

$$F_x = F_R = \frac{\eta P_e}{v_x}$$
$$= \frac{0.84 \times 90}{50} = 1.512\,\text{kN}. \tag{4.189}$$
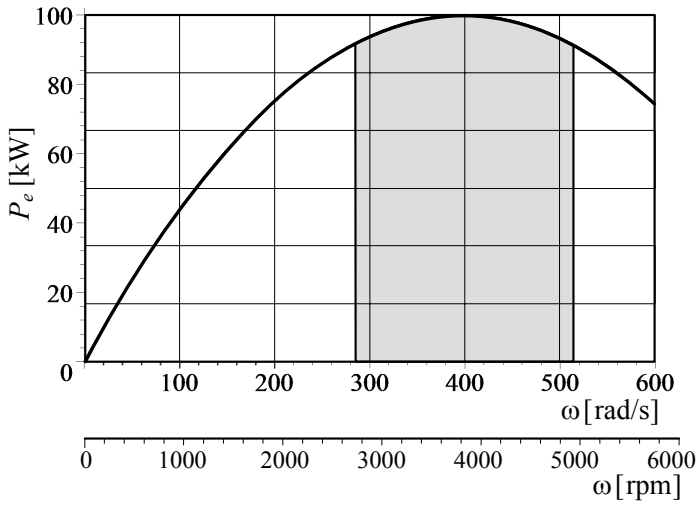
FIGURE 4.17. The power performance curve (4.170) and its working range.
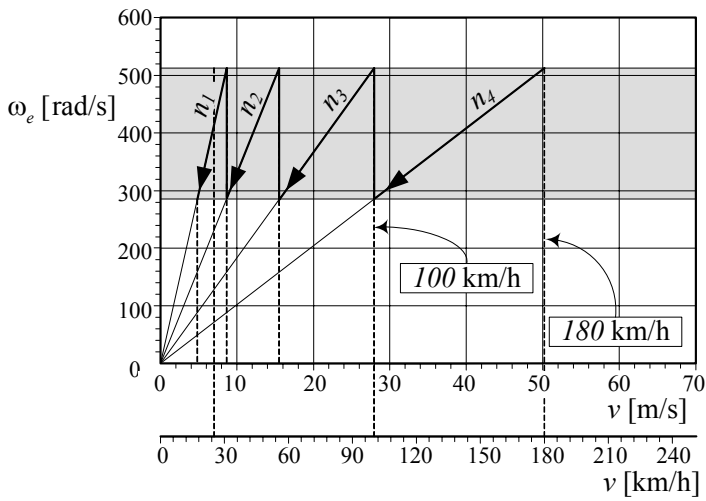


FIGURE 4.18. The gear-speed plot for Example 142.

*The traction force in first gear is*

$$
\begin{aligned}
F_x &= \frac{25}{39601} \frac{\eta}{R_w^2} n_d n_1 \left(796 R_w - n_d n_1 v_x\right) \\
&= \frac{25}{39601} \frac{0.84}{0.326^2} \times 4 \times 4.8874 \left(796 \times 0.326 - 4 \times 4.8874 v_x\right) \\
&= 25.313 - 1.907 v_x \text{ kN}. \tag{4.190}
\end{aligned}
$$

*The time in first gear $n_1$ can be calculated by integrating Newton's equation of motion*

$$
F_x - F_R = m \frac{dv_x}{dt} \tag{4.191}
$$

*and sweep the velocity from $v_x = 0$ to $v_x = 8.5757 \text{ m/s}$*

$$
\begin{aligned}
t_1 &= m \int_0^{8.5757} \frac{1}{F_x - F_R} dv_x \\
&= 860 \int_0^{8.5757} \frac{10^{-3}}{25.313 - 1.907 v_x - 1.512} dv_x \\
&= 0.52398 \text{ s}. \tag{4.192}
\end{aligned}
$$

*In second gear, the traction force is*

$$
\begin{aligned}
F_x &= \frac{25}{39601} \frac{\eta}{R_w^2} n_d n_2 \left(796 R_w - n_d n_2 v_x\right) \\
&= \frac{25}{39601} \frac{0.84}{0.326^2} \times 4 \times 2.7155 \left(796 \times 0.326 - 4 \times 2.7155 v_x\right) \\
&= 14.064 - 0.5887 v_x \text{ kN} \tag{4.193}
\end{aligned}
$$

*and therefore, the sweep time in second gear is*

$$
\begin{aligned}
t_2 &= m \int_{8.5757}^{15.435} \frac{1}{F_x - F_R} dv_x \\
&= 860 \int_{8.5757}^{15.435} \frac{10^{-3}}{14.064 - 0.5887 v_x - 1.512} dv_x \\
&= 1.1286 \text{ s}. \tag{4.194}
\end{aligned}
$$

*In third gear, the traction force is*

$$
\begin{aligned}
F_x &= \frac{25}{39601} \frac{\eta}{R_w^2} n_d n_3 \left(796 R_w - n_d n_3 v_x\right) \\
&= \frac{25}{39601} \frac{0.84}{0.326^2} \times 4 \times 1.5087 \left(796 \times 0.326 - 4 \times 1.5087 v_x\right) \\
&= 7.814 - 0.18172 v_x \text{ kN} \tag{4.195}
\end{aligned}
$$

*and the third sweep time is*

$$
\begin{aligned}
t_3 &= m \int_{15.435}^{27.78} \frac{1}{F_x - F_R} dv_x \\
&= 860 \int_{15.435}^{27.78} \frac{10^{-3}}{7.814 - 0.18172 v_x - 1.512} dv_x \\
&= 4.8544\,\text{s}.
\end{aligned}
\tag{4.196}
$$

*The total time to reach the speed* $v_x = 100\,\text{km/h} \approx 27.78\,\text{m/s}$ *is then equal to*

$$
\begin{aligned}
t &= t_0 + t_1 + t_2 + t_3 + 3 \times 0.07 \\
&= 2.58 + 0.52398 + 1.1286 + 4.8544 + 3 \times 0.47 \\
&= 10.497\,\text{s}
\end{aligned}
\tag{4.197}
$$

## 4.5  Summary

The maximum attainable power $P_e$ of an internal combustion engine is a function of the engine angular velocity $\omega_e$. This function must be determined by experiment however, the function $P_e = P_e(\omega_e)$, which is called the *power performance*, can be estimated by a mathematical function such as

$$
P_e = P_1 \omega_e + P_2 \omega_e^2 + P_3 \omega_e^3
\tag{4.198}
$$

where,

$$
P_1 = \frac{P_M}{\omega_M}
\tag{4.199}
$$

$$
P_2 = \frac{P_M}{\omega_M^2}
\tag{4.200}
$$

$$
P_3 = -\frac{P_M}{\omega_M^3}.
\tag{4.201}
$$

$\omega_M$ is the angular velocity, measured in $[\text{rad/s}]$, at which the engine power reaches the maximum value $P_M$, measured in $[\text{W} = \text{N m/s}]$.

The engine torque $T_e$ is the torque that provides $P_e$

$$
\begin{aligned}
T_e &= \frac{P_e}{\omega_e} \\
&= P_1 + P_2 \omega_e + P_3 \omega_e^2.
\end{aligned}
\tag{4.202}
$$

An ideal engine is the one that produces a constant power regardless of speed. For the ideal engine, we have

$$
P_e = P_0
\tag{4.203}
$$

$$
T_e = \frac{P_0}{\omega_e}.
\tag{4.204}
$$

We use a gearbox to make the engine approximately work at a constant power close to the $P_M$. To design a gearbox we use two equations: the speed equation

$$\omega_e = \frac{n_i\, n_d}{R_w} v_x \tag{4.205}$$

and the traction equation

$$T_e = \frac{1}{\eta} \frac{R_w}{n_i n_d} F_x \tag{4.206}$$

These equations state that the forward velocity $v_x$ of a vehicle is proportional to the angular velocity of the engine $\omega_e$, and the tire *traction force* $F_x$ is proportional to the engine torque $T_e$, where, $R_w$ is the effective tire radius, $n_d$ is the differential transmission ratio, $n_i$ is the gearbox transmission ratio in gear number $i$, and $\eta$ is the overall driveline efficiency.

# 4.6   Key Symbols

| | |
|---|---|
| $a \equiv \ddot{x}$ | acceleration |
| $a_i, i = 0, \cdots, 6$ | coefficients of function $T_e = T_e\left(\omega_e\right)$ |
| $a_x$ | acceleration capacity |
| $AWD$ | all-wheel-drive |
| $c_g$ | constant relative gear ratio |
| $C_c$ | slip factor |
| $d$ | distance traveled |
| $D$ | clutch diameter |
| $E$ | energy |
| $F_x$ | traction force |
| $FWD$ | front-wheel-drive |
| $H$ | thermal value of fuel |
| $m$ | vehicle mass |
| $n = \omega_{in}/\omega_{out}$ | gear reduction ratio |
| $n_i$ | gearbox transmission ratio in gear number $i$ |
| $n_d$ | transmission ratio |
| $n_g$ | overall transmission ratio |
| $P$ | power |
| $P_0$ | ideal engine constant power |
| $P_1, P_2, P_3$ | coefficients of the power performance function |
| $P_e$ | maximum attainable power of an engine |
| $P_e = P_e\left(\omega_e\right)$ | power performance function |
| $P_M$ | maximum power |
| $q$ | fuel consumption per unit distance |
| $r = \omega/\omega_n$ | frequency ratio |
| $RWD$ | rear-wheel-drive |
| $T_d$ | differential input torque |
| $T_e$ | engine torque |
| $T_M$ | maximum torque |
| $T_w$ | wheel torque |
| $v \equiv \dot{x},\ \mathbf{v}$ | velocity |
| $v_{min}$ | minimum vehicle speed corresponding to $\omega_{min}$ |
| $\triangle v$ | difference in maximum vehicle speed at two different gears |
| $x, y, z,\ \mathbf{x}$ | displacement |
| | |
| $\eta$ | overall efficiency |
| $\eta_c$ | convertor efficiency |
| $\eta_e$ | engine efficiency |
| $\eta_M$ | mechanical efficiency |
| $\eta_t$ | transmission efficiency |
| $\eta_t$ | thermal efficiency |
| $\eta_T$ | thermal efficiency |

| | |
|---|---|
| $\eta_V$ | volumetric efficiency |
| $\mu_x$ | traction coefficient |
| $\rho$ | oil density |
| $\rho_f$ | fuel density |
| $\phi$ | slope of the road |
| $\omega_d$ | differential input angular velocity |
| $\omega_e$ | engine angular velocity |
| $\omega_{min}$ | minimum engine speed |
| $\omega_M$ | engine angular velocity at maximum power |
| $\omega_{Max}$ | maximum engine speed |
| $\omega_p$ | pump angular velocity |
| $\omega_r = \frac{\omega_{out}}{\omega_{in}}$ | speed ratio |

## Exercises

1. Power performance.

   Audi $R8^{TM}$ with $m = 1558\,\mathrm{kg}$, has a $V8$ engine with

   $$P_M = 313\,\mathrm{kW} \approx 420\,\mathrm{hp} \ at \ \omega_M = 7800 \ rpm$$

   and Audi $TT$ Coupe$^{TM}$ with $m = 1430\,\mathrm{kg}$, has a $V6$ engine with

   $$P_M = 184\,\mathrm{kW} \approx 250\,\mathrm{hp} \ at \ \omega_M = 6300 \ rpm.$$

   Determine the power performance equations of their engines and compare the power mass ratio, $P_M/m$ of the cars.

2. Power and torque performance.

   A model of Nissan $NISMO$ $350Z$ with $m = 1522\,\mathrm{kg}$, has a $V6$ engine with

   $$\begin{aligned} P_M &= 228\,\mathrm{kW} \approx 306\,\mathrm{hp} \ at \ \omega_M = 6800 \ rpm \\ T_M &= 363\,\mathrm{N\,m} \approx 268\,\mathrm{lb\,ft} \ at \ \omega = 4800 \ rpm. \end{aligned}$$

   Determine the power and torque performance equations, and compare $T_M$ from the torque equation with the above reported number.

3. Fuel consumption conversion.

   A model of Subaru Impreza $WRX$ STI$^{TM}$ with $m = 1521\,\mathrm{kg}$, has a turbocharged flat-4 engine with

   $$P_M = 219\,\mathrm{kW} \approx 293\,\mathrm{hp} \ at \ \omega_M = 6000 \ rpm.$$

   Fuel consumption of the car is 19 mi/ gal in city and 25 mi/ gal in highway. Determine the fuel consumption in liter per 100 km.

4. Fuel consumption conversion.

   A model of Mercedes-Benz $SLR$ $722$ Edition$^{TM}$ with $m = 1724\,\mathrm{kg}$, has a supercharged $V8$ engine with

   $$P_M = 485\,\mathrm{kW} \approx 650\,\mathrm{hp} \ at \ \omega_M = 6500 \ rpm.$$

   The maximum speed of the car is

   $$v_M = 337\,\mathrm{km/h} \approx 209\,\mathrm{mi/h}.$$

   Assume the maximum speed happens at the maximum power and use an overall efficiency $\eta = 0.75$ to determine the traction force at the maximum speed.

5. **Car speed and engine speed.**

   A model of Toyota Camry$^{TM}$ has a 3.5-liter, 6-cylinder engine with

   $$P_M = 268\,\text{hp } at \ \omega_M = 6200 \ rpm.$$

   The car uses transaxle/front-wheel drive and is equipped with a six-speed ECT-i automatic transmission.

   $$
   \begin{aligned}
   1st \text{ gear ratio} \ &= \ n_1 = 3.300 \\
   2nd \text{ gear ratio} \ &= \ n_2 = 1.900 \\
   3rd \text{ gear ratio} \ &= \ n_3 = 1.420 \\
   4th \text{ gear ratio} \ &= \ n_4 = 1.000 \\
   5th \text{ gear ratio} \ &= \ n_5 = 0.713 \\
   6th \text{ gear ratio} \ &= \ n_6 = 0.609 \\
   \text{reverse gear ratio} \ &= \ n_r = 4.148 \\
   \text{final drive ratio} \ &= \ n_d = 3.685
   \end{aligned}
   $$

   Determine the speed of the car at each gear, when the engine is running at $\omega_M$, and it is equipped with

   (a) $P215/55R17$ tires
   (b) $P215/60R16$ tires.

6. **Geer-speed equations.**

   A model of Ford Mondeo$^{TM}$ is equipped with a 2.0-liter, which has

   $$T_M = 185\,\text{N m } at \ \omega_e = 4500 \ rpm.$$

   It has a manual five-speed gearbox.

   $$
   \begin{aligned}
   1st \text{ gear ratio} \ &= \ n_1 = 3.42 \\
   2nd \text{ gear ratio} \ &= \ n_2 = 2.14 \\
   3rd \text{ gear ratio} \ &= \ n_3 = 1.45 \\
   4th \text{ gear ratio} \ &= \ n_4 = 1.03 \\
   5th \text{ gear ratio} \ &= \ n_5 = 0.81 \\
   \text{reverse gear ratio} \ &= \ n_r = 3.46 \\
   \text{final drive ratio} \ &= \ n_d = 4.06
   \end{aligned}
   $$

   If the tires of the car are $205/55R16$, determine the gear-speed equations for each gear.

7. Final drive and gear ratios.

A model of Renault/Dacia Logan$^{TM}$ with $m = 1115\,\mathrm{kg}$, has a four-cylinder engine with

$$
\begin{aligned}
P_M &= 77\,\mathrm{kW} \approx 105\,\mathrm{hp}\ at\ \omega_M = 5750\ rpm \\
T_M &= 148\,\mathrm{N\,m}\ at\ \omega_e = 3750\ rpm \\
v_M &= 183\,\mathrm{km/\,h} \\
Tires &= 185/65R15.
\end{aligned}
$$

It has a five-speed gearbox. When the engine is running at $1000\ rpm$ the speed of the car at each gear is as follow.

$$
\begin{aligned}
1st\ \text{gear ratio} &= n_1 = 7.25\,\mathrm{km/\,h} \\
2nd\ \text{gear ratio} &= n_2 = 13.18\,\mathrm{km/\,h} \\
3rd\ \text{gear ratio} &= n_3 = 19.37\,\mathrm{km/\,h} \\
4th\ \text{gear ratio} &= n_4 = 26.21\,\mathrm{km/\,h} \\
5th\ \text{gear ratio} &= n_5 = 33.94\,\mathrm{km/\,h}
\end{aligned}
$$

Assume that the top speed happens when the car is in the final gear and the engine is at the maximum power. Evaluate the final drive ratio, $n_d$ and gear ratios $n_i, i = 1, 2, \cdots 5$.

8. Traction equation.

A model of Jeep Wrangler$^{TM}$ is equipped with a $V6$ engine and has the following specifications.

$$
\begin{aligned}
P_M &= 153\,\mathrm{kW} \approx 205\,\mathrm{hp}\ at\ \omega_M = 5200\ rpm \\
T_M &= 325\,\mathrm{N\,m} \approx 240\,\mathrm{lb\,ft}\ at\ \omega_e = 4000\ rpm
\end{aligned}
$$

A model of the car may have a six-speed manual transmission with the following gear ratios

$$
\begin{aligned}
1st\ \text{gear ratio} &= n_1 = 4.46 \\
2nd\ \text{gear ratio} &= n_2 = 2.61 \\
3rd\ \text{gear ratio} &= n_3 = 1.72 \\
4th\ \text{gear ratio} &= n_4 = 1.25 \\
5th\ \text{gear ratio} &= n_5 = 1.00 \\
6th\ \text{gear ratio} &= n_6 = 0.84 \\
\text{reverse gear ratio} &= n_r = 4.06 \\
\text{final drive ratio} &= n_d = 3.21
\end{aligned}
$$

or a four-speed automatic transmission with the following gear ratios.

$$1st \text{ gear ratio} = n_1 = 2.84$$
$$2nd \text{ gear ratio} = n_2 = 1.57$$
$$3rd \text{ gear ratio} = n_3 = 1.0$$
$$4th \text{ gear ratio} = n_4 = 0.69$$
$$\text{reverse gear ratio} = n_r = 2.21$$
$$\text{final drive ratio} = n_d = 4.10$$

Assume

$$\eta = 0.8$$
$$Tires = 245/75R16$$

and determine the traction equation for the two models.

9. Acceleration capacity.

Lamborghini Murcielago$^{TM}$ is equipped with a 6.2-liter $V12$ engine and has the following specifications.

$$P_M = 631 \text{ hp } at \ \omega_M = 8000 \ rpm$$
$$T_M = 487 \text{ lb ft } at \ \omega_e = 6000 \ rpm$$

$$m = 3638 \text{ lb}$$
$$Front \ tire = P245/35ZR18$$
$$Rear \ tire = P335/30ZR18$$

The gearbox of the car uses ratios close to the following values.

$$1st \text{ gear ratio} = n_1 = 2.94$$
$$2nd \text{ gear ratio} = n_2 = 2.056$$
$$3rd \text{ gear ratio} = n_3 = 1.520$$
$$4th \text{ gear ratio} = n_4 = 1.179$$
$$5th \text{ gear ratio} = n_5 = 1.030$$
$$6th \text{ gear ratio} = n_6 = 0.914$$
$$\text{reverse gear ratio} = n_r = 2.529$$
$$\text{final drive ratio} = n_d = 3.42$$

If $\eta = 0.8$, then

(a) determine the wheel torque function at each gear
(b) determine the acceleration capacity of the car.

10. ★ Gearbox stability.

A model of Jaguar $XJ^{TM}$ is a rear-wheel drive car with a 4.2-liter $V8$ engine. Some of the car's specifications are close to the following values.

$$
\begin{aligned}
m &= 3638\,\text{lb} \\
l &= 119.4\,\text{in} \\
Front\ tire &= P235/50R18 \\
Rear\ tire &= P235/50R18 \\
P_M &= 300\,\text{hp}\ at\ \omega_M = 6000\ rpm
\end{aligned}
$$

If gear ratios of the car's gearbox are

$$
\begin{aligned}
1st\ \text{gear ratio} &= n_1 = 4.17 \\
2nd\ \text{gear ratio} &= n_2 = 2.34 \\
3rd\ \text{gear ratio} &= n_3 = 1.52 \\
4th\ \text{gear ratio} &= n_4 = 1.14 \\
5th\ \text{gear ratio} &= n_5 = 0.87 \\
6th\ \text{gear ratio} &= n_6 = 0.69 \\
\text{reverse gear ratio} &= n_r = 3.40 \\
\text{final drive ratio} &= n_d = 2.87
\end{aligned}
$$

check the gearbox stability condition. In case the relative gear ratio is not constant, determine the new gear ratios using the relative ratio of the first two gears.

11. ★ Geometric gearbox design.

Lamborghini Diablo$^{TM}$ is a rear-wheel drive car that was built in years $1990 - 2000$. The car is equipped with a 5.7-liter $V12$ engine. Some of the car's specifications are given.

$$
\begin{aligned}
P_M &= 492\,\text{hp}\ at\ \omega_M = 7000\ rpm \\
T_M &= 580\,\text{N}\,\text{m} \approx 428\,\text{lb}\,\text{ft}\ at\ \omega_e = 5200\ rpm \\
v_M &= 328\,\text{km/h} \approx 203\,\text{mi/h}
\end{aligned}
$$

$$
\begin{aligned}
m &= 1576\,\text{kg} \approx 3474\,\text{lb} \\
l &= 2650\,\text{mm} \approx 104\,\text{in} \\
w_f &= 1540\,\text{mm} \approx 60.6\,\text{in} \\
w_r &= 1640\,\text{mm} \approx 64.6\,\text{in}
\end{aligned}
$$

$$
\begin{aligned}
Front\ tire &= 245/40ZR17 \\
Rear\ tire &= 335/35ZR17
\end{aligned}
$$

The gear ratios of the car's gearbox are close to the following values.

$$
\begin{aligned}
1st \text{ gear ratio} &= n_1 = 2.31 & v_M &= 97.3\,\mathrm{km/h} \approx 60.5\,\mathrm{mi/h} \\
2nd \text{ gear ratio} &= n_2 = 1.52 & v_M &= 147.7\,\mathrm{km/h} \approx 91.8\,\mathrm{mi/h} \\
3rd \text{ gear ratio} &= n_3 = 1.12 & v_M &= 200.2\,\mathrm{km/h} \approx 124\,\mathrm{mi/h} \\
4th \text{ gear ratio} &= n_4 = 0.88 & v_M &= 254.8\,\mathrm{km/h} \approx 158.4\,\mathrm{mi/h} \\
5th \text{ gear ratio} &= n_5 = 0.68 & v_M &= 325\,\mathrm{km/h} \approx 202\,\mathrm{mi/h} \\
\text{reverse gear ratio} &= n_r = 2.12 & v_M &= 105.7\,\mathrm{km/h} \approx 65.7\,\mathrm{mi/h} \\
\text{final drive ratio} &= n_d = 2.41 &&
\end{aligned}
$$

Assume $\eta = 0.9$ and

(a) Determine the step jump $c_g$ for each gear change.

(b) Determine the speed span for each gear change.

(c) Determine the engine speed at the maximum car speed for each gear.

(d) Determine the power performance equation and find the engine power at the maximum car speed for each gear.

(e) There is a difference between the car's top speed and the maximum speed in the $5th$ gear. Find the engine power at the car's top speed. Based on the top speed, determine the overall resistance forces.

(f) Accept the $1st$ gear data and assume a symmetric working range around the maximum power. Determine the other gear ratios based on a geometric design.

12. Manual and auto transmission comparison.

A model of Nissan $U12$ Pintara$^{TM}$ may come with manual or auto transmission. A model with a manual transmission has gear ratios and characteristics close to the following values

$$
\begin{aligned}
1st \text{ gear ratio} &= n_1 = 3.285 \\
2nd \text{ gear ratio} &= n_2 = 1.850 \\
3rd \text{ gear ratio} &= n_3 = 1.272 \\
4th \text{ gear ratio} &= n_4 = 0.954 \\
5th \text{ gear ratio} &= n_5 = 0.740 \\
\text{reverse gear ratio} &= n_r = 3.428 \\
\text{final drive ratio} &= n_d = 3.895
\end{aligned}
$$

and the model with an auto transmission has gear ratios close to the following values.

$$
\begin{aligned}
1st \text{ gear ratio} &= n_1 = 2.785 \\
2nd \text{ gear ratio} &= n_2 = 1.545 \\
3rd \text{ gear ratio} &= n_3 = 1.000 \\
4th \text{ gear ratio} &= n_4 = 0.694 \\
\text{reverse gear ratio} &= n_r = 2.272 \\
\text{final drive ratio} &= n_d = 3.876
\end{aligned}
$$

Compare the transmissions according to geometric design condition and determine which one has the maximum deviation.

13. ★ Progressive and geometric gearbox design.

An all wheel drive model of Hyundai Santa Fe$^{TM}$ has specifications close to the following numbers.

$$
\begin{aligned}
P_M &= 242 \,\text{hp } at \ \omega_M = 6000 \ rpm \\
T_M &= 226 \,\text{lb ft } at \ \omega_e = 4500 \ rpm \\
m &= 1724 \,\text{kg} \approx 4022 \,\text{lb} \\
l &= 2700 \,\text{mm} \approx 106.3 \,\text{in} \\
Tires &= P235/70R16
\end{aligned}
$$

$$
\begin{aligned}
1st \text{ gear ratio} &= n_1 = 3.79 \\
2nd \text{ gear ratio} &= n_2 = 2.06 \\
3rd \text{ gear ratio} &= n_3 = 1.42 \\
4th \text{ gear ratio} &= n_4 = 1.03 \\
5th \text{ gear ratio} &= n_5 = 0.73 \\
\text{reverse gear ratio} &= n_r = 3.81 \\
\text{final drive ratio} &= n_d = 3.68
\end{aligned}
$$

Assume that the car can reach a speed $v = 200.2 \,\text{km/ h} \approx 124 \,\text{mi/ h}$ at the maximum power $P_M$ in the final gear $n_5 = 0.73$. Accept $n_5$ and redesign the gear ratios based on a progressive and a geometric gearbox.

14. ★ Engine performance estimation.

Consider a $RWD$ vehicle with the following specifications.

$$
\begin{aligned}
m &= 6300 \,\text{lb} \\
l &= 153 \,\text{in} \\
F_{z_1}/F_{z_2} &= 4410/6000 \\
Tires &= 245/75R16
\end{aligned}
$$

If an experiment shows that

$$v_M = 62.6 \, \text{mi}/\text{h} \quad at \quad 3\% \; slope$$
$$v_M = 52.1 \, \text{mi}/\text{h} \quad at \quad 6\% \; slope$$
$$v_M = 0 \quad\quad\quad\quad at \quad 33.2\% \; slope$$

estimate the maximum power of the vehicle. Assume $\eta = 0.85$.

Hint: assume that when the vehicle is stuck on a road with the maximum slope, the engine is working at the maximum torque. However, when the vehicle is moving on a slope at the maximum speed, the engine is working at the maximum power. Slope 3% means the angle of the road with horizon is

$$\phi = \tan^{-1} \frac{3}{100}.$$

15. ★ Gearbox design.

Consider a $RWD$ vehicle with the following specifications.

$$P_M \;\; = \;\; 141 \, \text{kW} \approx 189 \, \text{hp} \; at \; \omega_M = 7800 \; rpm$$
$$T_M \;\; = \;\; 181 \, \text{N m} \approx 133 \, \text{lb ft} \; at \; \omega_e = 6800 \; rpm$$
$$v_M \;\; = \;\; 237 \, \text{km}/\text{h} \approx 147 \, \text{mi}/\text{h}$$
$$\eta \;\; = \;\; 0.90$$

$$m \;\; = \;\; 875 \, \text{kg}$$
$$l \;\; = \;\; 2300 \, \text{mm}$$
$$Front \; tirest \;\; = \;\; 195/50R16$$
$$Rear \; tirest \;\; = \;\; 225/45R17$$

$$1st \; \text{gear ratio} \;\; = \;\; n_1 = 3.116$$
$$2nd \; \text{gear ratio} \;\; = \;\; n_2 = 2.050$$
$$3rd \; \text{gear ratio} \;\; = \;\; n_3 = 1.481$$
$$4th \; \text{gear ratio} \;\; = \;\; n_4 = 1.166$$
$$5th \; \text{gear ratio} \;\; = \;\; n_5 = 0.916$$
$$6th \; \text{gear ratio} \;\; = \;\; n_6 = 0.815$$
$$\text{reverse gear ratio} \;\; = \;\; n_r = 3.250$$
$$\text{final drive ratio} \;\; = \;\; n_d = 4.529$$

(a) Based on the maximum velocity at the $6th$ gear $n_6$, redesign the gear ratios. Use $\pm 20\%$ around the maximum power for the working range.

(b) Assume the car is supposed to be able to run on a 28% slope with zero acceleration, and redesign the gear ratios.

# Part II

# Vehicle Kinematics

# 5

# Applied Kinematics

Position, velocity, and acceleration are called kinematics information. Rotational position analysis is the key to calculate kinematics of relatively moving rigid bodies. In this chapter, we review kinematics and show applied methods to calculate the relative kinematic information of rigid bodies. A vehicle has many moving sub-systems such as suspensions, and the vehicle can be treated as a moving rigid body in an inertia coordinate frame.

## 5.1 Rotation About Global Cartesian Axes

Consider a Cartesian coordinate frame $Oxyz$ fixed to a rigid body $B$ that is attached to the ground $G$ at the origin point $O$. The orientation of the rigid body $B$ with respect to the global coordinate frame $OXYZ$ fixed to the ground is known when the orientation of $Oxyz$ with respect to $OXYZ$ is determined. Figure 5.1 illustrates a body coordinate $B$ rotating about point $O$ in global coordinate frame $G$.
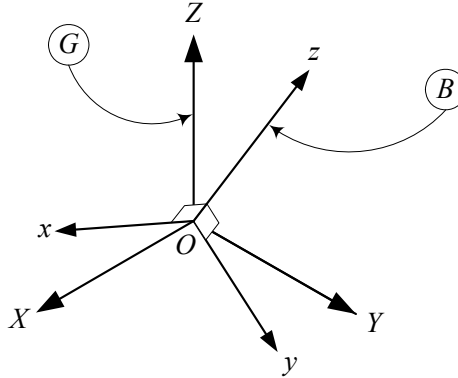


FIGURE 5.1. A body coordinate $B$ rotating about point $O$ in global coordinate frame $G$.

If the rigid body, $B$ rotates $\alpha$ degrees about the $Z$-axis of the global coordinate frame, then coordinates of any point $P$ of the rigid body in the local and global coordinate frames are related by the equation

$$^{G}\mathbf{r} = R_{Z,\alpha} \, ^{B}\mathbf{r} \tag{5.1}$$

where

$$R_{Z,\alpha} = \begin{bmatrix} \cos\alpha & -\sin\alpha & 0 \\ \sin\alpha & \cos\alpha & 0 \\ 0 & 0 & 1 \end{bmatrix} \tag{5.2}$$

and

$$^G\mathbf{r} = \begin{bmatrix} X \\ Y \\ Z \end{bmatrix} \tag{5.3}$$

$$^B\mathbf{r} = \begin{bmatrix} x \\ y \\ z \end{bmatrix}. \tag{5.4}$$

Similarly, rotation $\beta$ degrees about the $Y$-axis, and $\gamma$ degrees about the $X$-axis of the global frame relate the local and global coordinates of point $P$ by the following equations:

$$^G\mathbf{r} = R_{Y,\beta}\,^B\mathbf{r} \tag{5.5}$$
$$^G\mathbf{r} = R_{X,\gamma}\,^B\mathbf{r} \tag{5.6}$$

where

$$R_{Y,\beta} = \begin{bmatrix} \cos\beta & 0 & \sin\beta \\ 0 & 1 & 0 \\ -\sin\beta & 0 & \cos\beta \end{bmatrix} \tag{5.7}$$

$$R_{X,\gamma} = \begin{bmatrix} 1 & 0 & 0 \\ 0 & \cos\gamma & -\sin\gamma \\ 0 & \sin\gamma & \cos\gamma \end{bmatrix}. \tag{5.8}$$

**Proof.** Let $(\hat{i}, \hat{j}, \hat{k})$ and $(\hat{I}, \hat{J}, \hat{K})$ be the unit vectors along the coordinate axes of $Oxyz$ and $OXYZ$ respectively. The rigid body has a space fixed point at $O$, which is the common origin of $Oxyz$ and $OXYZ$. The dashed lines in Figure 5.2 illustrate the top view of the coordinate frames at initial position.

The initial position of a body point $P$ is indicated by $P_1$. The position vector $\mathbf{r}_1$ of $P_1$ can be expressed in body and global coordinate frames by

$$^B\mathbf{r}_1 = x_1\hat{i} + y_1\hat{j} + z_1\hat{k} \tag{5.9}$$
$$^G\mathbf{r}_1 = X_1\hat{I} + Y_1\hat{J} + Z_1\hat{K} \tag{5.10}$$

where $^B\mathbf{r}_1$ refers to the position vector $\mathbf{r}_1$ expressed in the body coordinate frame $B$, and $^G\mathbf{r}_1$ refers to the position vector $\mathbf{r}_1$ expressed in the global coordinate frame $G$.

If the rigid body undergoes a rotation $\alpha$ about the $Z$-axis, then the local frame $Oxyz$, and point $P$ will be seen in a second position, as shown by
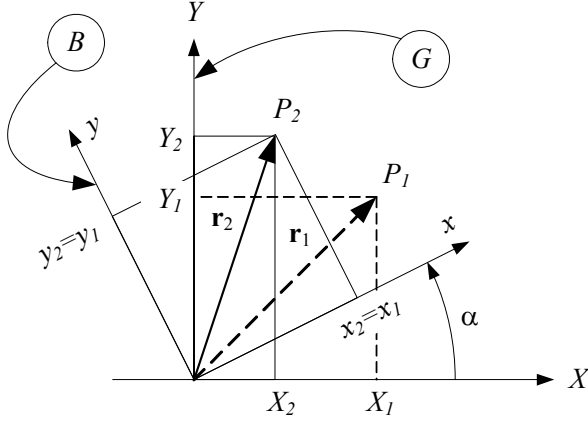
FIGURE 5.2. Position vectors of point $P$ before and after the rotation of the local frame about the $Z$-axis of the global frame.

the solid lines in Figure 5.2. Now the position vector $\mathbf{r}_2$ of $P_2$ is expressed in both coordinate frames by

$$
\begin{aligned}
{}^B\mathbf{r}_2 &= x_2\hat{\imath} + y_2\hat{\jmath} + z_2\hat{k} & (5.11)\\
{}^G\mathbf{r}_2 &= X_2\hat{I} + Y_2\hat{J} + Z_2\hat{K}. & (5.12)
\end{aligned}
$$

Using Equation (5.11) and the definition of the inner product, we may write

$$
\begin{aligned}
X_2 &= \hat{I} \cdot \mathbf{r}_2 \\
&= \hat{I} \cdot x_2\hat{\imath} + \hat{I} \cdot y_2\hat{\jmath} + \hat{I} \cdot z_2\hat{k} & (5.13)\\
Y_2 &= \hat{J} \cdot \mathbf{r}_2 \\
&= \hat{J} \cdot x_2\hat{\imath} + \hat{J} \cdot y_2\hat{\jmath} + \hat{J} \cdot z_2\hat{k} & (5.14)\\
Z_2 &= \hat{K} \cdot \mathbf{r}_2 \\
&= \hat{K} \cdot x_2\hat{\imath} + \hat{K} \cdot y_2\hat{\jmath} + \hat{K} \cdot z_2\hat{k} & (5.15)
\end{aligned}
$$

or equivalently

$$
\begin{bmatrix} X_2 \\ Y_2 \\ Z_2 \end{bmatrix} = \begin{bmatrix} \hat{I} \cdot \hat{\imath} & \hat{I} \cdot \hat{\jmath} & \hat{I} \cdot \hat{k} \\ \hat{J} \cdot \hat{\imath} & \hat{J} \cdot \hat{\jmath} & \hat{J} \cdot \hat{k} \\ \hat{K} \cdot \hat{\imath} & \hat{K} \cdot \hat{\jmath} & \hat{K} \cdot \hat{k} \end{bmatrix} \begin{bmatrix} x_2 \\ y_2 \\ z_2 \end{bmatrix}. \qquad (5.16)
$$

The elements of the *Z-rotation matrix*, $R_{Z,\alpha}$, are called the *direction cosines* of ${}^B\mathbf{r}_2$ with respect to $OXYZ$. Figure 5.2 shows the top view of the initial and final configurations of $\mathbf{r}$ in both coordinate systems $Oxyz$

and $OXYZ$. Analyzing Figure 5.2 indicates that

$$
\begin{array}{lll}
\hat{I} \cdot \hat{\imath} = \cos\alpha, & \hat{I} \cdot \hat{\jmath} = -\sin\alpha, & \hat{I} \cdot \hat{k} = 0 \\
\hat{J} \cdot \hat{\imath} = \sin\alpha, & \hat{J} \cdot \hat{\jmath} = \cos\alpha, & \hat{J} \cdot \hat{k} = 0 \\
\hat{K} \cdot \hat{\imath} = 0, & \hat{K} \cdot \hat{\jmath} = 0, & \hat{K} \cdot \hat{k} = 1.
\end{array}
\tag{5.17}
$$

Combining Equations (5.16) and (5.17) shows that

$$
\begin{bmatrix} X_2 \\ Y_2 \\ Z_2 \end{bmatrix} = \begin{bmatrix} \cos\alpha & -\sin\alpha & 0 \\ \sin\alpha & \cos\alpha & 0 \\ 0 & 0 & 1 \end{bmatrix} \begin{bmatrix} x_2 \\ y_2 \\ z_2 \end{bmatrix}
\tag{5.18}
$$

which can also be shown in the following short notation:

$$
{}^{G}\mathbf{r}_2 = R_{Z,\alpha}\,{}^{B}\mathbf{r}_2
\tag{5.19}
$$

$$
R_{Z,\alpha} = \begin{bmatrix} \cos\alpha & -\sin\alpha & 0 \\ \sin\alpha & \cos\alpha & 0 \\ 0 & 0 & 1 \end{bmatrix}.
\tag{5.20}
$$

Equation (5.19) states that the vector $\mathbf{r}$ at the second position in the global coordinate frame is equal to $R_Z$ times the position vector in the local coordinate frame. Hence, we are able to find the global coordinates of a point of a rigid body after rotation about the $Z$-axis, if we have its local coordinates.

Similarly, rotation $\beta$ about the $Y$-axis and rotation $\gamma$ about the $X$-axis are described by the $Y$-*rotation matrix* $R_{Y,\beta}$ and the $X$-*rotation matrix* $R_{X,\gamma}$ respectively.

$$
R_{Y,\beta} = \begin{bmatrix} \cos\beta & 0 & \sin\beta \\ 0 & 1 & 0 \\ -\sin\beta & 0 & \cos\beta \end{bmatrix}
\tag{5.21}
$$

$$
R_{X,\gamma} = \begin{bmatrix} 1 & 0 & 0 \\ 0 & \cos\gamma & -\sin\gamma \\ 0 & \sin\gamma & \cos\gamma \end{bmatrix}
\tag{5.22}
$$

The rotation matrices $R_{Z,\alpha}$, $R_{Y,\beta}$, and $R_{X,\gamma}$ are called *basic global rotation matrices*. We usually refer to the first, second, and third rotations about the axes of the global coordinate frame by $\alpha$, $\beta$, and $\gamma$ respectively.
∎

**Example 143** *Successive rotation about global axes.*
*The final position of the point $P(1, 2, 3)$ after a 30 deg rotation about the $Z$-axis, followed by 30 deg about the $X$-axis, and then 90 deg about the $Y$-axis can be found by first multiplying $R_{Z,30}$ by $[1, 2, 3]^T$ to get the new global position after first rotation*

$$
\begin{bmatrix} X_2 \\ Y_2 \\ Z_2 \end{bmatrix} = \begin{bmatrix} \cos 30 & -\sin 30 & 0 \\ \sin 30 & \cos 30 & 0 \\ 0 & 0 & 1 \end{bmatrix} \begin{bmatrix} 1 \\ 2 \\ 3 \end{bmatrix} = \begin{bmatrix} -0.134 \\ 2.23 \\ 3 \end{bmatrix}
\tag{5.23}
$$

*and then multiplying* $R_{X,30}$ *by* $[-0.134, 2.23, 3]^T$ *to get the position of* $P$ *after the second rotation*

$$
\begin{bmatrix} X_3 \\ Y_3 \\ Z_3 \end{bmatrix} = \begin{bmatrix} 1 & 0 & 0 \\ 0 & \cos 30 & -\sin 30 \\ 0 & \sin 30 & \cos 30 \end{bmatrix} \begin{bmatrix} -0.134 \\ 2.23 \\ 3 \end{bmatrix} = \begin{bmatrix} -0.134 \\ 0.433 \\ 3.714 \end{bmatrix}
$$
(5.24)

*and finally multiplying* $R_{Y,90}$ *by* $[-0.134, 0.433, 3.714]^T$ *to get the final position of* $P$ *after the third rotation.*

$$
\begin{bmatrix} X_4 \\ Y_4 \\ Z_4 \end{bmatrix} = \begin{bmatrix} \cos 90 & 0 & \sin 90 \\ 0 & 1 & 0 \\ -\sin 90 & 0 & \cos 90 \end{bmatrix} \begin{bmatrix} -0.134 \\ 0.433 \\ 3.714 \end{bmatrix} = \begin{bmatrix} 3.714 \\ 0.433 \\ 0.134 \end{bmatrix}
$$
(5.25)

**Example 144** *Global rotation, local position.*

If a point $P$ is moved to ${}^G\mathbf{r}_2 = [2, 3, 2]^T$ *after a* $60 \deg$ *rotation about the* $Z$-*axis, its position in the local coordinate is*

$$
{}^B\mathbf{r}_2 = R_{Z,60}^{-1}\, {}^G\mathbf{r}_2
$$

$$
\begin{bmatrix} x_2 \\ y_2 \\ z_2 \end{bmatrix} = \begin{bmatrix} \cos 60 & -\sin 60 & 0 \\ \sin 60 & \cos 60 & 0 \\ 0 & 0 & 1 \end{bmatrix}^{-1} \begin{bmatrix} 2 \\ 3 \\ 2 \end{bmatrix} = \begin{bmatrix} 3.6 \\ -0.23 \\ 2 \end{bmatrix}.
$$
(5.26)

The local coordinate frame was coincident with the global coordinate frame before rotation, thus the global coordinates of $P$ before rotation was also ${}^G\mathbf{r}_1 = [3.6, -0.23, 2]^T$.

## 5.2 Successive Rotation About Global Cartesian Axes

The final global position of a point $P$ in a rigid body $B$ with position vector $\mathbf{r}$, after a sequence of rotations $R_1$, $R_2$, $R_3$, ..., $R_n$ about the global axes can be found by

$$
{}^G\mathbf{r} = {}^GR_B\, {}^B\mathbf{r}
$$
(5.27)

where,

$$
{}^GR_B = R_n \cdots R_3 R_2 R_1
$$
(5.28)

and ${}^G\mathbf{r}$ and ${}^B\mathbf{r}$ indicate the position vector $\mathbf{r}$ expressed in the global and local coordinate frames. ${}^GR_B$ is called the *global rotation matrix*. It maps the local coordinates to their corresponding global coordinates.

Because matrix multiplications do not commute, the sequence of performing rotations is important. A rotation matrix is *orthogonal* that means

its transpose $R^T$ is equal to its inverse $R^{-1}$.

$$R^T = R^{-1} \tag{5.29}$$

**Example 145** *Successive global rotation matrix.*

*The global rotation matrix after a rotation $R_{Z,\alpha}$ followed by $R_{Y,\beta}$ and then $R_{X,\gamma}$ is*

$$
\begin{aligned}
{}^G R_B &= R_{X,\gamma} R_{Y,\beta} R_{Z,\alpha} \\
&= \begin{bmatrix} c\alpha c\beta & -c\beta s\alpha & s\beta \\ c\gamma s\alpha + c\alpha s\beta s\gamma & c\alpha c\gamma - s\alpha s\beta s\gamma & -c\beta s\gamma \\ s\alpha s\gamma - c\alpha c\gamma s\beta & c\alpha s\gamma + c\gamma s\alpha s\beta & c\beta c\gamma \end{bmatrix}.
\end{aligned} \tag{5.30}
$$

**Example 146** *Successive global rotations, global position.*

*The point $P$ of a rigid body that is attached to the global frame at $O$ is located at*

$$\begin{bmatrix} X_1 \\ Y_1 \\ Z_1 \end{bmatrix} = \begin{bmatrix} 0.0 \\ 0.26 \\ 0.97 \end{bmatrix}. \tag{5.31}$$

*The rotation matrix to find the new position of the point after a $-29\deg$ rotation about the $X$-axis, followed by $30\deg$ about the $Z$-axis, and again $132\deg$ about the $X$-axis is*

$$
\begin{aligned}
{}^G R_B &= R_{X,132} R_{Z,30} R_{X,-29} \\
&= \begin{bmatrix} 0.87 & -0.44 & -0.24 \\ -0.33 & -0.15 & -0.93 \\ 0.37 & 0.89 & -0.27 \end{bmatrix}.
\end{aligned} \tag{5.32}
$$

*Therefore, its new position is at*

$$
\begin{bmatrix} X_2 \\ Y_2 \\ Z_2 \end{bmatrix} = \begin{bmatrix} 0.87 & -0.44 & -0.24 \\ -0.33 & -0.15 & -0.93 \\ 0.37 & 0.89 & -0.27 \end{bmatrix} \begin{bmatrix} 0.0 \\ 0.26 \\ 0.97 \end{bmatrix} = \begin{bmatrix} -0.35 \\ -0.94 \\ -0.031 \end{bmatrix}. \tag{5.33}
$$

**Example 147** *Order of rotation, and order of matrix multiplication.*

*Changing the order of global rotation matrices is equivalent to changing the order of rotations.*

*The position of a point $P$ of a rigid body $B$ is located at ${}^B\mathbf{r}_P = \begin{bmatrix} 1 & 2 & 3 \end{bmatrix}^T$. Its global position after rotation $30\deg$ about the $X$-axis and then $45\deg$ about the $Y$-axis is at*

$$
\begin{aligned}
\left({}^G\mathbf{r}_P\right)_1 &= R_{Y,45} R_{X,30} \, {}^B\mathbf{r}_P \\
&= \begin{bmatrix} 0.53 & -0.84 & 0.13 \\ 0.0 & 0.15 & 0.99 \\ -0.85 & -0.52 & 0.081 \end{bmatrix} \begin{bmatrix} 1 \\ 2 \\ 3 \end{bmatrix} = \begin{bmatrix} -0.76 \\ 3.27 \\ -1.64 \end{bmatrix} \tag{5.34}
\end{aligned}
$$

*and if we change the order of rotations, then its position would be at*

$$\left({}^{G}\mathbf{r}_{P}\right)_{2} = R_{X,30}\,R_{Y,45}\,{}^{B}\mathbf{r}_{P}$$

$$= \begin{bmatrix} 0.53 & 0.0 & 0.85 \\ -0.84 & 0.15 & 0.52 \\ -0.13 & -0.99 & 0.081 \end{bmatrix} \begin{bmatrix} 1 \\ 2 \\ 3 \end{bmatrix} = \begin{bmatrix} 3.08 \\ 1.02 \\ -1.86 \end{bmatrix}. \quad (5.35)$$

*These two final positions of $P$ are $d = \left|\left({}^{G}\mathbf{r}_{P}\right)_{1} - \left({}^{G}\mathbf{r}_{P}\right)_{2}\right| = 4.456$ apart.*

**Example 148** *Global roll-pitch-yaw angles.*

*The rotation about the $X$-axis of the global coordinate frame is called* **roll**, *the rotation about the $Y$-axis of the global coordinate frame is called* **pitch**, *and the rotation about the $Z$-axis of the global coordinate frame is called* **yaw**. *The global roll-pitch-yaw rotation matrix is*

$$\begin{aligned}{}^{G}R_{B} &= R_{Z,\gamma}R_{Y,\beta}R_{X,\alpha} \\ &= \begin{bmatrix} c\beta c\gamma & -c\alpha s\gamma + c\gamma s\alpha s\beta & s\alpha s\gamma + c\alpha c\gamma s\beta \\ c\beta s\gamma & c\alpha c\gamma + s\alpha s\beta s\gamma & -c\gamma s\alpha + c\alpha s\beta s\gamma \\ -s\beta & c\beta s\alpha & c\alpha c\beta \end{bmatrix}. \quad (5.36)\end{aligned}$$

*Given the roll, pitch, and yaw angles, we can compute the overall rotation matrix using Equation (5.36). Also, we are able to compute the equivalent roll, pitch, and yaw angles when a rotation matrix is given. Suppose that $r_{ij}$ indicates the element of row $i$ and column $j$ of the roll-pitch-yaw rotation matrix (5.36), then the roll angle is*

$$\alpha = \tan^{-1}\left(\frac{r_{32}}{r_{33}}\right) \quad (5.37)$$

*and the pitch angle is*

$$\beta = -\sin^{-1}\left(r_{31}\right) \quad (5.38)$$

*and the yaw angle is*

$$\gamma = \tan^{-1}\left(\frac{r_{21}}{r_{11}}\right) \quad (5.39)$$

*provided that $\cos\beta \neq 0$.*

## 5.3  Rotation About Local Cartesian Axes

Consider a rigid body $B$ with a space-fixed point at point $O$. The local body coordinate frame $B(Oxyz)$ is coincident with a global coordinate frame $G(OXYZ)$, where the origin of both frames are on the fixed point $O$. If the body undergoes a rotation $\varphi$ about the $z$-axis of its local coordinate frame, as can be seen in the top view shown in Figure 5.3, then coordinates

of any point of the rigid body in the local and global coordinate frames are related by the equation

$$^B\mathbf{r} = R_{z,\varphi}\,^G\mathbf{r}. \tag{5.40}$$

The vectors $^G\mathbf{r}$ and $^B\mathbf{r}$ are the position vectors of the point in the global and local frames respectively

$$^G\mathbf{r} = \begin{bmatrix} X & Y & Z \end{bmatrix}^T \tag{5.41}$$

$$^B\mathbf{r} = \begin{bmatrix} x & y & z \end{bmatrix}^T \tag{5.42}$$

and $R_{z,\varphi}$ is the *z-rotation matrix*

$$R_{z,\varphi} = \begin{bmatrix} \cos\varphi & \sin\varphi & 0 \\ -\sin\varphi & \cos\varphi & 0 \\ 0 & 0 & 1 \end{bmatrix}. \tag{5.43}$$

Similarly, rotation $\theta$ about the $y$-axis and rotation $\psi$ about the $x$-axis are described by the *y-rotation matrix* $R_{y,\theta}$ and the *x-rotation matrix* $R_{x,\psi}$ respectively.

$$R_{y,\theta} = \begin{bmatrix} \cos\theta & 0 & -\sin\theta \\ 0 & 1 & 0 \\ \sin\theta & 0 & \cos\theta \end{bmatrix} \tag{5.44}$$

$$R_{x,\psi} = \begin{bmatrix} 1 & 0 & 0 \\ 0 & \cos\psi & \sin\psi \\ 0 & -\sin\psi & \cos\psi \end{bmatrix} \tag{5.45}$$

**Proof.** Vector $\mathbf{r}$ indicates the position of a point $P$ of the rigid body $B$ where it is initially at $P_1$. Using the unit vectors $(\hat{\imath}, \hat{\jmath}, \hat{k})$ along the axes of local coordinate frame $B(Oxyz)$, and $(\hat{I}, \hat{J}, \hat{K})$ along the axes of global coordinate frame $B(OXYZ)$, the initial and final position vectors $\mathbf{r}_1$ and $\mathbf{r}_2$ in both coordinate frames can be expressed by

$$^B\mathbf{r}_1 = x_1\hat{\imath} + y_1\hat{\jmath} + z_1\hat{k} \tag{5.46}$$

$$^G\mathbf{r}_1 = X_1\hat{I} + Y_1\hat{J} + Z_1\hat{K} \tag{5.47}$$

$$^B\mathbf{r}_2 = x_2\hat{\imath} + y_2\hat{\jmath} + z_2\hat{k} \tag{5.48}$$

$$^G\mathbf{r}_2 = X_2\hat{I} + Y_2\hat{J} + Z_2\hat{K}. \tag{5.49}$$

The vectors $^B\mathbf{r}_1$ and $^B\mathbf{r}_2$ are the initial and final positions of the vector $\mathbf{r}$ expressed in body coordinate frame $Oxyz$, and $^G\mathbf{r}_1$ and $^G\mathbf{r}_2$ are the initial and final positions of the vector $\mathbf{r}$ expressed in the global coordinate frame $OXYZ$.
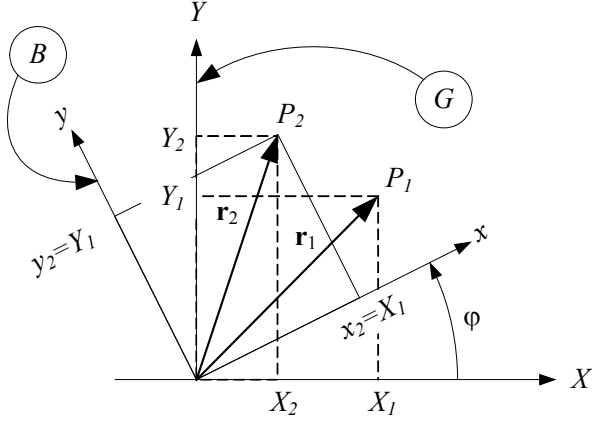
FIGURE 5.3. Position vectors of point $P$ before and after rotation of the local frame about the $z$-axis of the local frame.

The components of $^B\mathbf{r}_2$ can be found if we have the components of $^G\mathbf{r}_2$. Using Equation (5.49) and the definition of the inner product, we may write

$$x_2 = \hat{\imath} \cdot \mathbf{r}_2 = \hat{\imath} \cdot X_2\hat{I} + \hat{\imath} \cdot Y_2\hat{J} + \hat{\imath} \cdot Z_2\hat{K} \tag{5.50}$$

$$y_2 = \hat{\jmath} \cdot \mathbf{r}_2 = \hat{\jmath} \cdot X_2\hat{I} + \hat{\jmath} \cdot Y_2\hat{J} + \hat{\jmath} \cdot Z_2\hat{K} \tag{5.51}$$

$$z_2 = \hat{k} \cdot \mathbf{r}_2 = \hat{k} \cdot X_2\hat{I} + \hat{k} \cdot Y_2\hat{J} + \hat{k} \cdot Z_2\hat{K} \tag{5.52}$$

or equivalently

$$\begin{bmatrix} x_2 \\ y_2 \\ z_2 \end{bmatrix} = \begin{bmatrix} \hat{\imath} \cdot \hat{I} & \hat{\imath} \cdot \hat{J} & \hat{\imath} \cdot \hat{K} \\ \hat{\jmath} \cdot \hat{I} & \hat{\jmath} \cdot \hat{J} & \hat{\jmath} \cdot \hat{K} \\ \hat{k} \cdot \hat{I} & \hat{k} \cdot \hat{J} & \hat{k} \cdot \hat{K} \end{bmatrix} \begin{bmatrix} X_2 \\ Y_2 \\ Z_2 \end{bmatrix}. \tag{5.53}$$

The elements of the $z$-rotation matrix $R_{z,\varphi}$ are the *direction cosines* of $^G\mathbf{r}_2$ with respect to $Oxyz$. So, the elements of the matrix in Equation (5.53) are

$$\begin{aligned} \hat{\imath} \cdot \hat{I} &= \cos\varphi, & \hat{\imath} \cdot \hat{J} &= \sin\varphi, & \hat{\imath} \cdot \hat{K} &= 0 \\ \hat{\jmath} \cdot \hat{I} &= -\sin\varphi, & \hat{\jmath} \cdot \hat{J} &= \cos\varphi, & \hat{\jmath} \cdot \hat{K} &= 0 \\ \hat{k} \cdot \hat{I} &= 0, & \hat{k} \cdot \hat{J} &= 0, & \hat{k} \cdot \hat{K} &= 1 \end{aligned} \tag{5.54}$$

Combining Equations (5.53) and (5.54), we can find the components of $^B\mathbf{r}_2$ by multiplying $z$-rotation matrix $R_{z,\varphi}$ and vector $^G\mathbf{r}_2$.

$$\begin{bmatrix} x_2 \\ y_2 \\ z_2 \end{bmatrix} = \begin{bmatrix} \cos\varphi & \sin\varphi & 0 \\ -\sin\varphi & \cos\varphi & 0 \\ 0 & 0 & 1 \end{bmatrix} \begin{bmatrix} X_2 \\ Y_2 \\ Z_2 \end{bmatrix}. \tag{5.55}$$

It can also be shown in the following short form:

$$^{B}\mathbf{r}_2 = R_{z,\varphi}\,^{G}\mathbf{r}_2 \tag{5.56}$$

where

$$R_{z,\varphi} = \begin{bmatrix} \cos\varphi & \sin\varphi & 0 \\ -\sin\varphi & \cos\varphi & 0 \\ 0 & 0 & 1 \end{bmatrix}. \tag{5.57}$$

Equation (5.56) says that after rotation about the $z$-axis of the local coordinate frame, the position vector in the local frame is equal to $R_{z,\varphi}$ times the position vector in the global frame. Hence, after rotation about the $z$-axis, we are able to find the coordinates of any point of a rigid body in a local coordinate frame, if we have its coordinates in the global frame.

Similarly, rotation $\theta$ about the $y$-axis and rotation $\psi$ about the $x$-axis are described by the $y$-rotation matrix $R_{y,\theta}$ and the $x$-rotation matrix $R_{x,\psi}$ respectively.

$$R_{y,\theta} = \begin{bmatrix} \cos\theta & 0 & -\sin\theta \\ 0 & 1 & 0 \\ \sin\theta & 0 & \cos\theta \end{bmatrix} \tag{5.58}$$

$$R_{x,\psi} = \begin{bmatrix} 1 & 0 & 0 \\ 0 & \cos\psi & \sin\psi \\ 0 & -\sin\psi & \cos\psi \end{bmatrix} \tag{5.59}$$

We indicate the first, second, and third rotations about the local axes by $\varphi$, $\theta$, and $\psi$ respectively. ∎

**Example 149** *Local rotation, local position.*

*If a local coordinate frame $Oxyz$ has been rotated 60 deg about the $z$-axis and a point $P$ in the global coordinate frame $OXYZ$ is at $(4,3,2)$, its coordinates in the local coordinate frame $Oxyz$ are*

$$\begin{bmatrix} x \\ y \\ z \end{bmatrix} = \begin{bmatrix} \cos 60 & \sin 60 & 0 \\ -\sin 60 & \cos 60 & 0 \\ 0 & 0 & 1 \end{bmatrix} \begin{bmatrix} 4 \\ 3 \\ 2 \end{bmatrix} = \begin{bmatrix} 4.60 \\ -1.97 \\ 2.0 \end{bmatrix}. \tag{5.60}$$

**Example 150** *Local rotation, global position.*

*If a local coordinate frame $Oxyz$ has been rotated 60 deg about the $z$-axis and a point $P$ in the local coordinate frame $Oxyz$ is at $(4,3,2)$, its position in the global coordinate frame $OXYZ$ is at*

$$\begin{bmatrix} X \\ Y \\ Z \end{bmatrix} = \begin{bmatrix} \cos 60 & \sin 60 & 0 \\ -\sin 60 & \cos 60 & 0 \\ 0 & 0 & 1 \end{bmatrix}^{T} \begin{bmatrix} 4 \\ 3 \\ 2 \end{bmatrix} = \begin{bmatrix} -0.60 \\ 4.96 \\ 2.0 \end{bmatrix}. \tag{5.61}$$

**Example 151** *Successive local rotation, global position.*
*First we turn a rigid body* $-90 \deg$ *about the y-axis and then* $90 \deg$ *about the x-axis. If a body point P is at* $^B\mathbf{r}_P = \begin{bmatrix} 9.5 & -10.1 & 10.1 \end{bmatrix}^T$, *then its position in the global coordinate frame is at*

$$
\begin{aligned}
^G\mathbf{r}_2 &= [R_{x,90} R_{y,-90}]^{-1} \, ^B\mathbf{r}_P \\
&= R_{y,-90}^{-1} R_{x,90}^{-1} \, ^B\mathbf{r}_P \\
&= R_{y,-90}^{T} R_{x,90}^{T} \, ^B\mathbf{r}_P \\
&= \begin{bmatrix} 10.1 \\ -10.1 \\ 9.5 \end{bmatrix}.
\end{aligned}
\tag{5.62}
$$

**Example 152** *Global position and postmultiplication of rotation matrix.*
*The local position of a point P after rotation is at* $^B\mathbf{r} = \begin{bmatrix} 1 & 2 & 3 \end{bmatrix}^T$. *If the local rotation matrix to transform* $^G\mathbf{r}$ *to* $^B\mathbf{r}$ *is given as*

$$
^B R_{z,\varphi} = \begin{bmatrix} \cos\varphi & \sin\varphi & 0 \\ -\sin\varphi & \cos\varphi & 0 \\ 0 & 0 & 1 \end{bmatrix} = \begin{bmatrix} \cos 30 & \sin 30 & 0 \\ -\sin 30 & \cos 30 & 0 \\ 0 & 0 & 1 \end{bmatrix}
\tag{5.63}
$$

*then we may find the global position vector* $^G\mathbf{r}$ *by postmultiplication* $^B R_{z,\varphi}$ *by the local position vector* $^B\mathbf{r}^T$,

$$
\begin{aligned}
^G\mathbf{r}^T &= \, ^B\mathbf{r}^T \, ^B R_{z,\varphi} \\
&= \begin{bmatrix} 1 & 2 & 3 \end{bmatrix} \begin{bmatrix} \cos 30 & \sin 30 & 0 \\ -\sin 30 & \cos 30 & 0 \\ 0 & 0 & 1 \end{bmatrix} \\
&= \begin{bmatrix} -0.13 & 2.23 & 3.0 \end{bmatrix}
\end{aligned}
\tag{5.64}
$$

*instead of premultiplication of* $^B R_{z,\varphi}^{-1}$ *by* $^B\mathbf{r}$.

$$
\begin{aligned}
^G\mathbf{r} &= \, ^B R_{z,\varphi}^{-1} \, ^B\mathbf{r} \\
&= \begin{bmatrix} \cos 30 & -\sin 30 & 0 \\ \sin 30 & \cos 30 & 0 \\ 0 & 0 & 1 \end{bmatrix} \begin{bmatrix} 1 \\ 2 \\ 3 \end{bmatrix} = \begin{bmatrix} -0.13 \\ 2.23 \\ 3 \end{bmatrix}
\end{aligned}
\tag{5.65}
$$

## 5.4   Successive Rotation About Local Cartesian Axes

The final global position of a point $P$ in a rigid body $B$ with position vector $\mathbf{r}$, after some rotations $R_1$, $R_2$, $R_3$, ..., $R_n$ about the local axes, can be found by

$$
^B\mathbf{r} = \, ^B R_G \, ^G\mathbf{r}
\tag{5.66}
$$

where

$$^BR_G = R_n \cdots R_3 R_2 R_1. \tag{5.67}$$

$^BR_G$ is called the *local rotation matrix* and it maps the global coordinates to their corresponding local coordinates.

**Example 153** *Successive local rotation, local position.*

A local coordinate frame $B(Oxyz)$ that initially is coincident with a global coordinate frame $G(OXYZ)$ undergoes a rotation $\varphi = 30\deg$ about the z-axis, then $\theta = 30\deg$ about the x-axis, and then $\psi = 30\deg$ about the y-axis. The local coordinates of a point $P$ located at $X = 5$, $Y = 30$, $Z = 10$ can be found by $\begin{bmatrix} x & y & z \end{bmatrix}^T = R_{y,\psi} R_{x,\theta} R_{z,\varphi} \begin{bmatrix} 5 & 30 & 10 \end{bmatrix}^T$. The local rotation matrix is

$$^BR_G = R_{y,30} R_{x,30} R_{z,30} = \begin{bmatrix} 0.63 & 0.65 & -0.43 \\ -0.43 & 0.75 & 0.50 \\ 0.65 & -0.125 & 0.75 \end{bmatrix} \tag{5.68}$$

and coordinates of $P$ in the local frame are

$$\begin{bmatrix} x \\ y \\ z \end{bmatrix} = \begin{bmatrix} 0.63 & 0.65 & -0.43 \\ -0.43 & 0.75 & 0.50 \\ 0.65 & -0.125 & 0.75 \end{bmatrix} \begin{bmatrix} 5 \\ 30 \\ 10 \end{bmatrix} = \begin{bmatrix} 18.35 \\ 25.35 \\ 7.0 \end{bmatrix}. \tag{5.69}$$

**Example 154** *Successive local rotation.*

The rotation matrix for a body point $P(x,y,z)$ after rotation $R_{z,\varphi}$ followed by $R_{x,\theta}$ and $R_{y,\psi}$ is

$$
\begin{aligned}
^BR_G &= R_{y,\psi} R_{x,\theta} R_{z,\varphi} \\
&= \begin{bmatrix} c\varphi c\psi - s\theta s\varphi s\psi & c\psi s\varphi + c\varphi s\theta s\psi & -c\theta s\psi \\ -c\theta s\varphi & c\theta c\varphi & s\theta \\ c\varphi s\psi + s\theta c\psi s\varphi & s\varphi s\psi - c\varphi s\theta c\psi & c\theta c\psi \end{bmatrix}.
\end{aligned} \tag{5.70}
$$

**Example 155** *Local roll-pitch-yaw angles*

Rotation about the x-axis of the local frame is called **roll** or **bank**, rotation about y-axis of the local frame is called **pitch** or **attitude**, and rotation about the z-axis of the local frame is called **yaw**, **spin**, or **heading**. The local roll-pitch-yaw angles are shown in Figure 5.4.

The local roll-pitch-yaw rotation matrix is

$$
\begin{aligned}
^BR_G &= R_{z,\psi} R_{y,\theta} R_{x,\varphi} \\
&= \begin{bmatrix} c\theta c\psi & c\varphi s\psi + s\theta c\psi s\varphi & s\varphi s\psi - c\varphi s\theta c\psi \\ -c\theta s\psi & c\varphi c\psi - s\theta s\varphi s\psi & c\psi s\varphi + c\varphi s\theta s\psi \\ s\theta & -c\theta s\varphi & c\theta c\varphi \end{bmatrix}.
\end{aligned} \tag{5.71}
$$

Note the difference between roll-pitch-yaw and Euler angles, although we show both utilizing $\varphi$, $\theta$, and $\psi$.
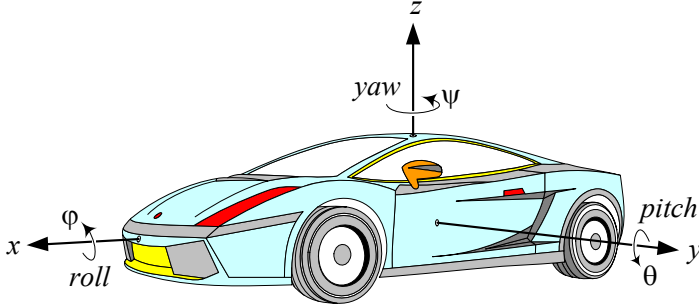
FIGURE 5.4. Local roll-pitch-yaw angles.

## 5.5  ★ Euler Angles

The rotation about the $Z$-axis of the global coordinate is called *precession*, the rotation about the $x$-axis of the local coordinate is called *nutation*, and the rotation about the $z$-axis of the local coordinate is called *spin*. The *precession-nutation-spin rotation* angles are also called *Euler angles*. Rotation matrix based on Euler angles has application in rigid body kinematics. To find the Euler angles rotation matrix to go from the global frame $G(OXYZ)$ to the final body frame $B(Oxyz)$, we employ a body frame $B'(Ox'y'z')$ as shown in Figure 5.5 that before the first rotation coincides with the global frame. Let there be at first a rotation $\varphi$ about the $z'$-axis. Because $Z$-axis and $z'$-axis are coincident, by our theory

$$^{B'}\mathbf{r} = {}^{B'}R_G {}^G\mathbf{r} \tag{5.72}$$

$$^{B'}R_G = R_{z,\varphi} = \begin{bmatrix} \cos\varphi & \sin\varphi & 0 \\ -\sin\varphi & \cos\varphi & 0 \\ 0 & 0 & 1 \end{bmatrix}. \tag{5.73}$$

Next we consider the $B'(Ox'y'z')$ frame as a new fixed global frame and introduce a new body frame $B''(Ox''y''z'')$. Before the second rotation, the two frames coincide. Then, we execute a $\theta$ rotation about $x''$-axis as shown in Figure 5.6. The transformation between $B'(Ox'y'z')$ and $B''(Ox''y''z'')$ is

$$^{B''}\mathbf{r} = {}^{B''}R_{B'} {}^{B'}\mathbf{r} \tag{5.74}$$

$$^{B''}R_{B'} = R_{x,\theta} = \begin{bmatrix} 1 & 0 & 0 \\ 0 & \cos\theta & \sin\theta \\ 0 & -\sin\theta & \cos\theta \end{bmatrix}. \tag{5.75}$$

Finally, we consider the $B''(Ox''y''z'')$ frame as a new fixed global frame and consider the final body frame $B(Oxyz)$ to coincide with $B''$ before the third rotation. We now execute a $\psi$ rotation about the $z''$-axis as shown in
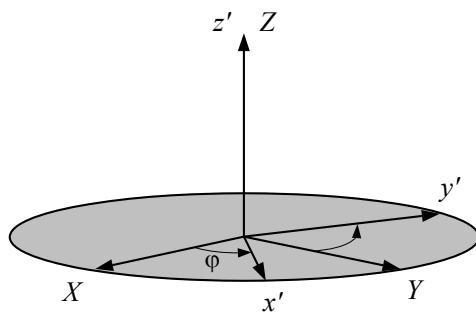
FIGURE 5.5. First Euler angle.
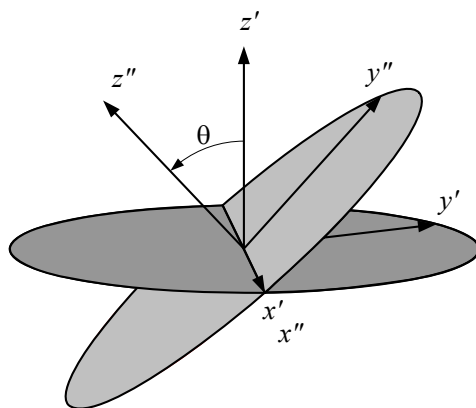


FIGURE 5.6. Second Euler angle.
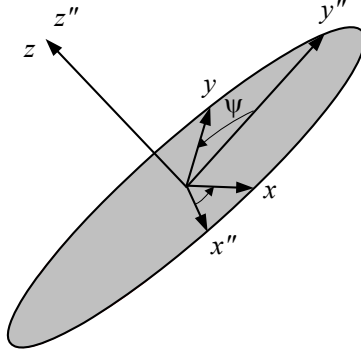
FIGURE 5.7. Third Euler angle.

Figure 5.7. The transformation between $B''(Ox''y''z'')$ and $B(Oxyz)$ is

$$^B\mathbf{r} \;=\; ^B R_{B''}\, ^{B''}\mathbf{r} \tag{5.76}$$

$$^B R_{B''} \;=\; R_{z,\psi} = \begin{bmatrix} \cos\psi & \sin\psi & 0 \\ -\sin\psi & \cos\psi & 0 \\ 0 & 0 & 1 \end{bmatrix}. \tag{5.77}$$

By the rule of composition of rotations, the transformation from $G(OXYZ)$ to $B(Oxyz)$ is

$$^B\mathbf{r} = {}^B R_G\, {}^G\mathbf{r} \tag{5.78}$$

where

$$
\begin{aligned}
^B R_G &= R_{z,\psi} R_{x,\theta} R_{z,\varphi} \\
&= \begin{bmatrix}
c\varphi c\psi - c\theta s\varphi s\psi & c\psi s\varphi + c\theta c\varphi s\psi & s\theta s\psi \\
-c\varphi s\psi - c\theta c\psi s\varphi & -s\varphi s\psi + c\theta c\varphi c\psi & s\theta c\psi \\
s\theta s\varphi & -c\varphi s\theta & c\theta
\end{bmatrix}
\end{aligned} \tag{5.79}
$$

and therefore,

$$
\begin{aligned}
^B R_G^{-1} &= {}^B R_G^T = {}^G R_B = [R_{z,\psi} R_{x,\theta} R_{z,\varphi}]^T \\
&= \begin{bmatrix}
c\varphi c\psi - c\theta s\varphi s\psi & -c\varphi s\psi - c\theta c\psi s\varphi & s\theta s\varphi \\
c\psi s\varphi + c\theta c\varphi s\psi & -s\varphi s\psi + c\theta c\varphi c\psi & -c\varphi s\theta \\
s\theta s\psi & s\theta c\psi & c\theta
\end{bmatrix}.
\end{aligned} \tag{5.80}
$$

Given the angles of precession $\varphi$, nutation $\theta$, and spin $\psi$, we can compute the overall rotation matrix using Equation (5.79). Also we are able to compute the equivalent precession, nutation, and spin angles when a rotation matrix is given.

If $r_{ij}$ indicates the element of row $i$ and column $j$ of the precession-nutation-spin rotation matrix, then,

$$\theta = \cos^{-1}(r_{33}) \tag{5.81}$$

$$\varphi = -\tan^{-1}\left(\frac{r_{31}}{r_{32}}\right) \tag{5.82}$$

$$\psi = \tan^{-1}\left(\frac{r_{13}}{r_{23}}\right) \tag{5.83}$$

provided that $\sin\theta \neq 0$.

**Example 156 ★** *Euler angle rotation matrix.*

The Euler or precession-nutation-spin rotation matrix for $\varphi = 79.15\,\text{deg}$, $\theta = 41.41\,\text{deg}$, and $\psi = -40.7\,\text{deg}$ *would be found by substituting* $\varphi$, $\theta$, *and* $\psi$ *in Equation (5.79).*

$$
\begin{aligned}
{}^B R_G &= R_{z,-40.7}R_{x,41.41}R_{z,79.15} \tag{5.84}\\
&= \begin{bmatrix} 0.63 & 0.65 & -0.43 \\ -0.43 & 0.75 & 0.50 \\ 0.65 & -0.125 & 0.75 \end{bmatrix}
\end{aligned}
$$

**Example 157 ★** *Euler angles of a local rotation matrix.*

The local rotation matrix after a rotation $30\,\text{deg}$ *about the z-axis,* $30\,\text{deg}$ *about the x-axis, and* $30\,\text{deg}$ *about the y-axis is*

$$
\begin{aligned}
{}^B R_G &= R_{y,30}R_{x,30}R_{z,30}\\
&= \begin{bmatrix} 0.63 & 0.65 & -0.43 \\ -0.43 & 0.75 & 0.50 \\ 0.65 & -0.125 & 0.75 \end{bmatrix} \tag{5.85}
\end{aligned}
$$

*and therefore, the local coordinates of a sample point at* $X = 5$, $Y = 30$, *and* $Z = 10$ *are*

$$
\begin{bmatrix} x \\ y \\ z \end{bmatrix} = \begin{bmatrix} 0.63 & 0.65 & -0.43 \\ -0.43 & 0.75 & 0.50 \\ 0.65 & -0.125 & 0.75 \end{bmatrix} \begin{bmatrix} 5 \\ 30 \\ 10 \end{bmatrix} = \begin{bmatrix} 18.35 \\ 25.35 \\ 7.0 \end{bmatrix}. \tag{5.86}
$$

*The Euler angles of the corresponding precession-nutation-spin rotation matrix are*

$$
\begin{aligned}
\theta &= \cos^{-1}(0.75) = 41.41\,\text{deg} \tag{5.87}\\
\varphi &= -\tan^{-1}\left(\frac{0.65}{-0.125}\right) = 79.15\,\text{deg} \tag{5.88}\\
\psi &= \tan^{-1}\left(\frac{-0.43}{0.50}\right) = -40.7\,\text{deg}. \tag{5.89}
\end{aligned}
$$

*Hence,* $R_{y,30}R_{x,30}R_{z,30} = R_{z,\psi}R_{x,\theta}R_{z,\varphi}$ *when* $\varphi = 79.15\,\text{deg}$, $\theta = 41.41\,\text{deg}$, *and* $\psi = -40.7\,\text{deg}$. *In other words, the rigid body attached to the local frame moves to the final configuration by undergoing either three consecutive rotations* $\varphi = 79.15\,\text{deg}$, $\theta = 41.41\,\text{deg}$, *and* $\psi = -40.7\,\text{deg}$ *about the* $z$, $x$, *and* $z$ *axes respectively, or three consecutive rotations* $30\,\text{deg}$, $30\,\text{deg}$, *and* $30\,\text{deg}$ *about the* $z$, $x$, *and* $y$ *axes.*

**Example 158 ★** *Relative rotation matrix of two bodies.*

*Consider a rigid body $B_1$ with an orientation matrix $^{B_1}R_G$ made by Euler angles $\varphi = 30\,\text{deg}$, $\theta = -45\,\text{deg}$, $\psi = 60\,\text{deg}$, and another rigid body $B_2$ having $\varphi = 10\,\text{deg}$, $\theta = 25\,\text{deg}$, $\psi = -15\,\text{deg}$, with respect to the global frame. To find the relative rotation matrix $^{B_1}R_{B_2}$ to map the coordinates of the second body frame $B_2$ to the first body frame $B_1$, we need to find the individual rotation matrices first.*

$$
\begin{aligned}
^{B_1}R_G &= R_{z,60}R_{x,-45}R_{z,30} \\
&= \begin{bmatrix} 0.127 & 0.78 & -0.612 \\ -0.927 & -0.127 & -0.354 \\ -0.354 & 0.612 & 0.707 \end{bmatrix}
\end{aligned} \tag{5.90}
$$

$$
\begin{aligned}
^{B_2}R_G &= R_{z,10}R_{x,25}R_{z,-15} \\
&= \begin{bmatrix} 0.992 & -6.33 \times 10^{-2} & -0.109 \\ 0.103 & 0.907 & 0.408 \\ 7.34 \times 10^{-2} & -0.416 & 0.906 \end{bmatrix}
\end{aligned} \tag{5.91}
$$

*The desired rotation matrix $^{B_1}R_{B_2}$ may be found by*

$$
^{B_1}R_{B_2} = {}^{B_1}R_G\,{}^{G}R_{B_2} \tag{5.92}
$$

*which is equal to*

$$
\begin{aligned}
^{B_1}R_{B_2} &= {}^{B_1}R_G\,{}^{B_2}R_G^T \\
&= \begin{bmatrix} 0.992 & 0.103 & 7.34 \times 10^{-2} \\ -6.33 \times 10^{-2} & 0.907 & -0.416 \\ -0.109 & 0.408 & 0.906 \end{bmatrix}.
\end{aligned} \tag{5.93}
$$

**Example 159 ★** *Euler angles rotation matrix for small angles.*

*The Euler rotation matrix $^{B}R_G = R_{z,\psi}R_{x,\theta}R_{z,\varphi}$ for very small Euler angles $\varphi, \theta,$ and $\psi$ is approximated by*

$$
^{B}R_G = \begin{bmatrix} 1 & \gamma & 0 \\ -\gamma & 1 & \theta \\ 0 & -\theta & 1 \end{bmatrix} \tag{5.94}
$$

*where*

$$
\gamma = \varphi + \psi. \tag{5.95}
$$

*Therefore, wen the angles of rotation are small, the angles $\varphi$ and $\psi$ are indistinguishable.*
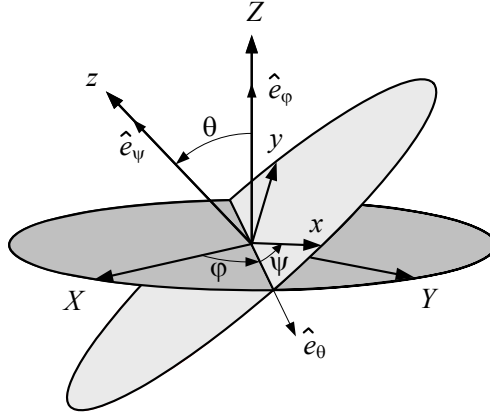
FIGURE 5.8. Euler angles frame $\hat{e}_\varphi, \hat{e}_\theta, \hat{e}_\psi$.

**Example 160** ★ *Small second Euler angle.*

   *If $\theta \to 0$ then the Euler rotation matrix $^B R_G = R_{z,\psi} R_{x,\theta} R_{z,\varphi}$ approaches to*

$$
^B R_G = \begin{bmatrix} c\varphi c\psi - s\varphi s\psi & c\psi s\varphi + c\varphi s\psi & 0 \\ -c\varphi s\psi - c\psi s\varphi & -s\varphi s\psi + c\varphi c\psi & 0 \\ 0 & 0 & 1 \end{bmatrix}
$$

$$
= \begin{bmatrix} \cos(\varphi + \psi) & \sin(\varphi + \psi) & 0 \\ -\sin(\varphi + \psi) & \cos(\varphi + \psi) & 0 \\ 0 & 0 & 1 \end{bmatrix} \tag{5.96}
$$

*and therefore, the angles $\varphi$ and $\psi$ are indistinguishable even if the value of $\varphi$ and $\psi$ are finite. Hence, the Euler set of angles in rotation matrix (5.79) is not unique when $\theta = 0$.*

**Example 161** ★ *Angular velocity vector in terms of Euler frequencies.*

   *A Eulerian local frame $E(o, \hat{e}_\varphi, \hat{e}_\theta, \hat{e}_\psi)$ can be introduced by defining unit vectors $\hat{e}_\varphi$, $\hat{e}_\theta$, and $\hat{e}_\psi$ as shown in Figure 5.8. Although the Eulerian frame is not necessarily orthogonal, it is very useful in rigid body kinematic analysis.*

   *The angular velocity vector $_G\boldsymbol{\omega}_B$ of the body frame $B(Oxyz)$ with respect to the global frame $G(OXYZ)$ can be written in Euler angles frame $E$ as the sum of three Euler angle rate vectors:*

$$
_G^E\boldsymbol{\omega}_B = \dot{\varphi}\hat{e}_\varphi + \dot{\theta}\hat{e}_\theta + \dot{\psi}\hat{e}_\psi. \tag{5.97}
$$

*where the rate of Euler angles, $\dot{\varphi}$, $\dot{\theta}$, and $\dot{\psi}$ are called Euler frequencies.*

   *To find $_G\boldsymbol{\omega}_B$ in the body frame we must express the unit vectors $\hat{e}_\varphi$, $\hat{e}_\theta$, and $\hat{e}_\psi$ shown in Figure 5.8, in the body frame. The unit vector $\hat{e}_\varphi =$*

$\begin{bmatrix} 0 & 0 & 1 \end{bmatrix}^T = \hat{K}$ *is in the global frame and can be transformed to the body frame after three rotations*

$$
\begin{aligned}
{}^B\hat{e}_\varphi &= {}^B R_G \hat{K} \\
&= R_{z,\psi} R_{x,\theta} R_{z,\varphi} \hat{K} \\
&= \begin{bmatrix} \sin\theta \sin\psi \\ \sin\theta \cos\psi \\ \cos\theta \end{bmatrix}.
\end{aligned}
\qquad (5.98)
$$

*The unit vector* $\hat{e}_\theta = \begin{bmatrix} 1 & 0 & 0 \end{bmatrix}^T = \hat{i}'$ *is in the intermediate frame* $Ox'y'z'$ *and needs to get two rotations* $R_{x,\theta}$ *and* $R_{z,\psi}$ *to be transformed to the body frame*

$$
\begin{aligned}
{}^B\hat{e}_\theta &= {}^B R_{Ox'y'z'} \hat{i}' \\
&= R_{z,\psi} R_{x,\theta} \hat{i}' \\
&= \begin{bmatrix} \cos\psi \\ -\sin\psi \\ 0 \end{bmatrix}.
\end{aligned}
\qquad (5.99)
$$

*The unit vector* $\hat{e}_\psi$ *is already in the body frame,* $\hat{e}_\psi = \begin{bmatrix} 0 & 0 & 1 \end{bmatrix}^T = \hat{k}$. *Therefore,* ${}_G\boldsymbol{\omega}_B$ *is expressed in the body coordinate frame as*

$$
\begin{aligned}
{}^B_G\boldsymbol{\omega}_B &= \dot{\varphi} \begin{bmatrix} \sin\theta \sin\psi \\ \sin\theta \cos\psi \\ \cos\theta \end{bmatrix} + \dot{\theta} \begin{bmatrix} \cos\psi \\ -\sin\psi \\ 0 \end{bmatrix} + \dot{\psi} \begin{bmatrix} 0 \\ 0 \\ 1 \end{bmatrix} \\
&= \left( \dot{\varphi} \sin\theta \sin\psi + \dot{\theta} \cos\psi \right) \hat{i} \\
&\quad + \left( \dot{\varphi} \sin\theta \cos\psi - \dot{\theta} \sin\psi \right) \hat{j} \\
&\quad + \left( \dot{\varphi} \cos\theta + \dot{\psi} \right) \hat{k}
\end{aligned}
\qquad (5.100)
$$

*and therefore, components of* ${}_G\boldsymbol{\omega}_B$ *in body frame* $Oxyz$ *are related to the Euler angle frame* $O\varphi\theta\psi$ *by the following relationship:*

$$
{}^B_G\boldsymbol{\omega}_B = {}^B R_E \, {}^E_G\boldsymbol{\omega}_B
\qquad (5.101)
$$

$$
\begin{bmatrix} \omega_x \\ \omega_y \\ \omega_z \end{bmatrix} = \begin{bmatrix} \sin\theta \sin\psi & \cos\psi & 0 \\ \sin\theta \cos\psi & -\sin\psi & 0 \\ \cos\theta & 0 & 1 \end{bmatrix} \begin{bmatrix} \dot{\varphi} \\ \dot{\theta} \\ \dot{\psi} \end{bmatrix}.
\qquad (5.102)
$$

*Then,* ${}_G\boldsymbol{\omega}_B$ *can be expressed in the global frame using an inverse transfor-*

*mation of Euler rotation matrix (5.79)*

$$\begin{aligned}
{}^G_G\boldsymbol{\omega}_B &= {}^B R_G^{-1}\,{}^B_G\boldsymbol{\omega}_B \\[2mm]
&= {}^B R_G^{-1} \begin{bmatrix} \dot{\varphi}\sin\theta\sin\psi + \dot{\theta}\cos\psi \\ \dot{\varphi}\sin\theta\cos\psi - \dot{\theta}\sin\psi \\ \dot{\varphi}\cos\theta + \dot{\psi} \end{bmatrix} \tag{5.103} \\[2mm]
&= \left(\dot{\theta}\cos\varphi + \dot{\psi}\sin\theta\sin\varphi\right)\hat{I} \\
&\quad + \left(\dot{\theta}\sin\varphi - \dot{\psi}\cos\varphi\sin\theta\right)\hat{J} \\
&\quad + \left(\dot{\varphi} + \dot{\psi}\cos\theta\right)\hat{K} \tag{5.104}
\end{aligned}$$

*and hence, components of $_G\boldsymbol{\omega}_B$ in global coordinate frame $OXYZ$ are related to the Euler angle coordinate frame $O\varphi\theta\psi$ by the following relationship:*

$$\begin{aligned}
{}^G_G\boldsymbol{\omega}_B &= {}^G R_E\,{}^E_G\boldsymbol{\omega}_B \tag{5.105}
\end{aligned}$$

$$\begin{bmatrix} \omega_X \\ \omega_Y \\ \omega_Z \end{bmatrix} = \begin{bmatrix} 0 & \cos\varphi & \sin\theta\sin\varphi \\ 0 & \sin\varphi & -\cos\varphi\sin\theta \\ 1 & 0 & \cos\theta \end{bmatrix} \begin{bmatrix} \dot{\varphi} \\ \dot{\theta} \\ \dot{\psi} \end{bmatrix}. \tag{5.106}$$

**Example 162 ★** *Euler frequencies based on a Cartesian angular velocity vector.*

*The vector $^B_G\boldsymbol{\omega}_B$, that indicates the angular velocity of a rigid body $B$ with respect to the global frame $G$ written in frame $B$, is related to the Euler frequencies by*

$$\begin{aligned}
{}^B_G\boldsymbol{\omega}_B &= {}^B R_E\,{}^E_G\boldsymbol{\omega}_B \\[2mm]
{}^B_G\boldsymbol{\omega}_B &= \begin{bmatrix} \omega_x \\ \omega_y \\ \omega_z \end{bmatrix} = \begin{bmatrix} \sin\theta\sin\psi & \cos\psi & 0 \\ \sin\theta\cos\psi & -\sin\psi & 0 \\ \cos\theta & 0 & 1 \end{bmatrix} \begin{bmatrix} \dot{\varphi} \\ \dot{\theta} \\ \dot{\psi} \end{bmatrix}. \tag{5.107}
\end{aligned}$$

*The matrix of coefficients is not an orthogonal matrix because,*

$$^B R_E^T \neq\; ^B R_E^{-1} \tag{5.108}$$

$$^B R_E^T = \begin{bmatrix} \sin\theta\sin\psi & \sin\theta\cos\psi & \cos\theta \\ \cos\psi & -\sin\psi & 0 \\ 0 & 0 & 1 \end{bmatrix} \tag{5.109}$$

$$^B R_E^{-1} = \frac{1}{\sin\theta} \begin{bmatrix} \sin\psi & \cos\psi & 0 \\ \sin\theta\cos\psi & -\sin\theta\sin\psi & 0 \\ -\cos\theta\sin\psi & -\cos\theta\cos\psi & 1 \end{bmatrix}. \tag{5.110}$$

*It is because the Euler angles coordinate frame $O\varphi\theta\psi$ is not an orthogonal frame. For the same reason, the matrix of coefficients that relates the Euler*

*frequencies and the components of* $_G^G\boldsymbol{\omega}_B$

$$_G^G\boldsymbol{\omega}_B \quad = \quad {}^GR_E\, _G^E\boldsymbol{\omega}_B \tag{5.111}$$

$$_G^G\boldsymbol{\omega}_B \quad = \quad \begin{bmatrix} \omega_X \\ \omega_Y \\ \omega_Z \end{bmatrix} = \begin{bmatrix} 0 & \cos\varphi & \sin\theta\sin\varphi \\ 0 & \sin\varphi & -\cos\varphi\sin\theta \\ 1 & 0 & \cos\theta \end{bmatrix} \begin{bmatrix} \dot\varphi \\ \dot\theta \\ \dot\psi \end{bmatrix} \tag{5.112}$$

*is not an orthogonal matrix. Therefore, the Euler frequencies based on local and global decomposition of the angular velocity vector* $_G\boldsymbol{\omega}_B$ *must solely be found by the inverse of coefficient matrices*

$$_G^E\boldsymbol{\omega}_B \quad = \quad {}^BR_E^{-1}\, _G^B\boldsymbol{\omega}_B \tag{5.113}$$

$$\begin{bmatrix} \dot\varphi \\ \dot\theta \\ \dot\psi \end{bmatrix} = \frac{1}{\sin\theta} \begin{bmatrix} \sin\psi & \cos\psi & 0 \\ \sin\theta\cos\psi & -\sin\theta\sin\psi & 0 \\ -\cos\theta\sin\psi & -\cos\theta\cos\psi & 1 \end{bmatrix} \begin{bmatrix} \omega_x \\ \omega_y \\ \omega_z \end{bmatrix} \tag{5.114}$$

*and*

$$_G^E\boldsymbol{\omega}_B \quad = \quad {}^GR_E^{-1}\, _G^G\boldsymbol{\omega}_B \tag{5.115}$$

$$\begin{bmatrix} \dot\varphi \\ \dot\theta \\ \dot\psi \end{bmatrix} = \frac{1}{\sin\theta} \begin{bmatrix} -\cos\theta\sin\varphi & \cos\theta\cos\varphi & 1 \\ \sin\theta\cos\varphi & \sin\theta\sin\varphi & 0 \\ \sin\varphi & -\cos\varphi & 0 \end{bmatrix} \begin{bmatrix} \omega_X \\ \omega_Y \\ \omega_Z \end{bmatrix}. \tag{5.116}$$

*Using (5.113) and (5.115), it can be verified that the transformation matrix* ${}^BR_G = {}^BR_E\, {}^GR_E^{-1}$ *would be the same as Euler transformation matrix (5.79).*

The angular velocity vector can thus be expressed as

$$\begin{aligned}
_G\boldsymbol{\omega}_B \quad &= \quad \begin{bmatrix} \hat\imath & \hat\jmath & \hat k \end{bmatrix} \begin{bmatrix} \omega_x \\ \omega_y \\ \omega_z \end{bmatrix} \\[2mm]
&= \quad \begin{bmatrix} \hat I & \hat J & \hat K \end{bmatrix} \begin{bmatrix} \omega_X \\ \omega_Y \\ \omega_Z \end{bmatrix} \\[2mm]
&= \quad \begin{bmatrix} \hat K & \hat e_\theta & \hat k \end{bmatrix} \begin{bmatrix} \dot\varphi \\ \dot\theta \\ \dot\psi \end{bmatrix}.
\end{aligned} \tag{5.117}$$

**Example 163** ★ *Angular velocity and local roll-pitch-yaw rate.*
    *Using the roll-pitch-yaw frequencies, the angular velocity of a body $B$ with respect to the global reference frame is*

$$\begin{aligned}
_G\boldsymbol{\omega}_B \quad &= \quad \omega_x\hat\imath + \omega_y\hat\jmath + \omega_z\hat k \\
&= \quad \dot\varphi\hat e_\varphi + \dot\theta\hat e_\theta + \dot\psi\hat e_\psi.
\end{aligned} \tag{5.118}$$

*Relationships between the components of $_G\boldsymbol{\omega}_B$ in body frame and roll-pitch-yaw components are found when the local roll unit vector $\hat{e}_\varphi$ and pitch unit vector $\hat{e}_\theta$ are transformed to the body frame. The roll unit vector $\hat{e}_\varphi = \begin{bmatrix} 1 & 0 & 0 \end{bmatrix}^T$ transforms to the body frame after rotation $\theta$ and then rotation $\psi$*

$$^B\hat{e}_\varphi = R_{z,\psi} R_{y,\theta} \begin{bmatrix} 1 \\ 0 \\ 0 \end{bmatrix} = \begin{bmatrix} \cos\theta \cos\psi \\ -\cos\theta \sin\psi \\ \sin\theta \end{bmatrix}. \tag{5.119}$$

*The pitch unit vector $\hat{e}_\theta = \begin{bmatrix} 0 & 1 & 0 \end{bmatrix}^T$ transforms to the body frame after rotation $\psi$*

$$^B\hat{e}_\theta = R_{z,\psi} \begin{bmatrix} 0 \\ 1 \\ 0 \end{bmatrix} = \begin{bmatrix} \sin\psi \\ \cos\psi \\ 0 \end{bmatrix}. \tag{5.120}$$

*The yaw unit vector $\hat{e}_\psi = \begin{bmatrix} 0 & 0 & 1 \end{bmatrix}^T$ is already along the local z-axis. Hence, $_G\boldsymbol{\omega}_B$ can be expressed in body frame $Oxyz$ as*

$$
\begin{aligned}
{}^B_G\boldsymbol{\omega}_B &= \begin{bmatrix} \omega_x \\ \omega_y \\ \omega_z \end{bmatrix} \\
&= \dot{\varphi} \begin{bmatrix} \cos\theta \cos\psi \\ -\cos\theta \sin\psi \\ \sin\theta \end{bmatrix} + \dot{\theta} \begin{bmatrix} \sin\psi \\ \cos\psi \\ 0 \end{bmatrix} + \dot{\psi} \begin{bmatrix} 0 \\ 0 \\ 1 \end{bmatrix} \\
&= \begin{bmatrix} \cos\theta \cos\psi & \sin\psi & 0 \\ -\cos\theta \sin\psi & \cos\psi & 0 \\ \sin\theta & 0 & 1 \end{bmatrix} \begin{bmatrix} \dot{\varphi} \\ \dot{\theta} \\ \dot{\psi} \end{bmatrix}
\end{aligned} \tag{5.121}
$$

*and therefore, $_G\boldsymbol{\omega}_B$ in global frame $OXYZ$ in terms of local roll-pitch-yaw frequencies is*

$$
\begin{aligned}
{}^G_G\boldsymbol{\omega}_B &= \begin{bmatrix} \omega_X \\ \omega_Y \\ \omega_Z \end{bmatrix} = {}^B R_G^{-1} \begin{bmatrix} \omega_x \\ \omega_y \\ \omega_z \end{bmatrix} \\
&= {}^B R_G^{-1} \begin{bmatrix} \dot{\theta} \sin\psi + \dot{\varphi} \cos\theta \cos\psi \\ \dot{\theta} \cos\psi - \dot{\varphi} \cos\theta \sin\psi \\ \dot{\psi} + \dot{\varphi} \sin\theta \end{bmatrix} \\
&= \begin{bmatrix} \dot{\varphi} + \dot{\psi} \sin\theta \\ \dot{\theta} \cos\varphi - \dot{\psi} \cos\theta \sin\varphi \\ \dot{\theta} \sin\varphi + \dot{\psi} \cos\theta \cos\varphi \end{bmatrix} \\
&= \begin{bmatrix} 1 & 0 & \sin\theta \\ 0 & \cos\varphi & -\cos\theta \sin\varphi \\ 0 & \sin\varphi & \cos\theta \cos\varphi \end{bmatrix} \begin{bmatrix} \dot{\varphi} \\ \dot{\theta} \\ \dot{\psi} \end{bmatrix}.
\end{aligned} \tag{5.122}
$$

## 5.6   General Transformation

Consider a general situation in which two coordinate frames, $G(OXYZ)$ and $B(Oxyz)$ with a common origin $O$, are employed to express the components of a vector $\mathbf{r}$. There is always a *transformation matrix* $^GR_B$ to map the components of $\mathbf{r}$ from the reference frame $B(Oxyz)$ to the other reference frame $G(OXYZ)$.

$$^G\mathbf{r} = {}^GR_B\,{}^B\mathbf{r} \tag{5.123}$$

In addition, the inverse map, $^B\mathbf{r} = {}^GR_B^{-1}\,{}^G\mathbf{r}$, can be done by $^BR_G$

$$^B\mathbf{r} = {}^BR_G\,{}^G\mathbf{r} \tag{5.124}$$

where,

$$\left|{}^GR_B\right| = \left|{}^BR_G\right| = 1 \tag{5.125}$$

and

$$^BR_G = {}^GR_B^{-1} = {}^GR_B^{T}. \tag{5.126}$$

**Proof.** Decomposition of the unit vectors of $G(OXYZ)$ along the axes of $B(Oxyz)$

$$\hat{I} = (\hat{I}\cdot\hat{\imath})\hat{\imath} + (\hat{I}\cdot\hat{\jmath})\hat{\jmath} + (\hat{I}\cdot\hat{k})\hat{k} \tag{5.127}$$

$$\hat{J} = (\hat{J}\cdot\hat{\imath})\hat{\imath} + (\hat{J}\cdot\hat{\jmath})\hat{\jmath} + (\hat{J}\cdot\hat{k})\hat{k} \tag{5.128}$$

$$\hat{K} = (\hat{K}\cdot\hat{\imath})\hat{\imath} + (\hat{K}\cdot\hat{\jmath})\hat{\jmath} + (\hat{K}\cdot\hat{k})\hat{k} \tag{5.129}$$

introduces the transformation matrix $^GR_B$ to map the local frame to the global frame

$$\begin{bmatrix} \hat{I} \\ \hat{J} \\ \hat{K} \end{bmatrix} = \begin{bmatrix} \hat{I}\cdot\hat{\imath} & \hat{I}\cdot\hat{\jmath} & \hat{I}\cdot\hat{k} \\ \hat{J}\cdot\hat{\imath} & \hat{J}\cdot\hat{\jmath} & \hat{J}\cdot\hat{k} \\ \hat{K}\cdot\hat{\imath} & \hat{K}\cdot\hat{\jmath} & \hat{K}\cdot\hat{k} \end{bmatrix} \begin{bmatrix} \hat{\imath} \\ \hat{\jmath} \\ \hat{k} \end{bmatrix} = {}^GR_B \begin{bmatrix} \hat{\imath} \\ \hat{\jmath} \\ \hat{k} \end{bmatrix} \tag{5.130}$$

where

$$
\begin{aligned}
^GR_B &= \begin{bmatrix} \hat{I}\cdot\hat{\imath} & \hat{I}\cdot\hat{\jmath} & \hat{I}\cdot\hat{k} \\ \hat{J}\cdot\hat{\imath} & \hat{J}\cdot\hat{\jmath} & \hat{J}\cdot\hat{k} \\ \hat{K}\cdot\hat{\imath} & \hat{K}\cdot\hat{\jmath} & \hat{K}\cdot\hat{k} \end{bmatrix} \\
&= \begin{bmatrix} \cos(\hat{I},\hat{\imath}) & \cos(\hat{I},\hat{\jmath}) & \cos(\hat{I},\hat{k}) \\ \cos(\hat{J},\hat{\imath}) & \cos(\hat{J},\hat{\jmath}) & \cos(\hat{J},\hat{k}) \\ \cos(\hat{K},\hat{\imath}) & \cos(\hat{K},\hat{\jmath}) & \cos(\hat{K},\hat{k}) \end{bmatrix}.
\end{aligned}
\tag{5.131}
$$

The elements of $^GR_B$ are direction cosines of the axes of $G(OXYZ)$ in frame $B(Oxyz)$. This set of nine direction cosines then completely specifies the orientation of the frame $B(Oxyz)$ in the frame $G(OXYZ)$, and can

be used to map the coordinates of any point $(x, y, z)$ to its corresponding coordinates $(X, Y, Z)$.

Alternatively, using the method of unit vector decomposition to develop the matrix $^B R_G$ leads to

$$^B\mathbf{r} = {}^B R_G\, {}^G\mathbf{r} = {}^G R_B^{-1}\, {}^G\mathbf{r}$$

$$^B R_G = \begin{bmatrix} \hat{\imath} \cdot \hat{I} & \hat{\imath} \cdot \hat{J} & \hat{\imath} \cdot \hat{K} \\ \hat{\jmath} \cdot \hat{I} & \hat{\jmath} \cdot \hat{J} & \hat{\jmath} \cdot \hat{K} \\ \hat{k} \cdot \hat{I} & \hat{k} \cdot \hat{J} & \hat{k} \cdot \hat{K} \end{bmatrix}$$

$$= \begin{bmatrix} \cos(\hat{\imath}, \hat{I}) & \cos(\hat{\imath}, \hat{J}) & \cos(\hat{\imath}, \hat{K}) \\ \cos(\hat{\jmath}, \hat{I}) & \cos(\hat{\jmath}, \hat{J}) & \cos(\hat{\jmath}, \hat{K}) \\ \cos(\hat{k}, \hat{I}) & \cos(\hat{k}, \hat{J}) & \cos(\hat{k}, \hat{K}) \end{bmatrix} \tag{5.132}$$

and shows that the inverse of a transformation matrix is equal to the transpose of the transformation matrix,

$$^G R_B^{-1} = {}^G R_B^T. \tag{5.133}$$

A matrix with condition (5.133) is called *orthogonal*. Orthogonality of $R$ comes from the fact that it maps an orthogonal coordinate frame to another orthogonal coordinate frame.

The transformation matrix $R$ has only three *independent* elements. The constraint equations among the elements of $R$ will be found by applying the orthogonality condition (5.133).

$$^G R_B \cdot {}^G R_B^T = I \tag{5.134}$$

$$\begin{bmatrix} r_{11} & r_{12} & r_{13} \\ r_{21} & r_{22} & r_{23} \\ r_{31} & r_{32} & r_{33} \end{bmatrix} \begin{bmatrix} r_{11} & r_{21} & r_{31} \\ r_{12} & r_{22} & r_{32} \\ r_{13} & r_{23} & r_{33} \end{bmatrix} = \begin{bmatrix} 1 & 0 & 0 \\ 0 & 1 & 0 \\ 0 & 0 & 1 \end{bmatrix}. \tag{5.135}$$

Therefore, the dot product of any two different rows of $^G R_B$ is zero, and the dot product of any row of $^G R_B$ with the same row is one.

$$\begin{aligned} r_{11}^2 + r_{12}^2 + r_{13}^2 &= 1 \\ r_{21}^2 + r_{22}^2 + r_{23}^2 &= 1 \\ r_{31}^2 + r_{32}^2 + r_{33}^2 &= 1 \\ r_{11} r_{21} + r_{12} r_{22} + r_{13} r_{23} &= 0 \\ r_{11} r_{31} + r_{12} r_{32} + r_{13} r_{33} &= 0 \\ r_{21} r_{31} + r_{22} r_{32} + r_{23} r_{33} &= 0 \end{aligned} \tag{5.136}$$

These relations are also true for columns of $^G R_B$, and evidently for rows and columns of $^B R_G$. The orthogonality condition can be summarized in the following equation:

$$\hat{\mathbf{r}}_{H_i} \cdot \hat{\mathbf{r}}_{H_j} = \hat{\mathbf{r}}_{H_i}^T\, \hat{\mathbf{r}}_{H_j} = \sum_{i=1}^{3} r_{ij} r_{ik} = \delta_{jk} \qquad (j, k = 1, 2, 3) \tag{5.137}$$

where $r_{ij}$ is the element of row $i$ and column $j$ of the transformation matrix $R$, and $\delta_{jk}$ is the *Kronecker's delta*

$$\delta_{jk} = 1 \text{ if } j = k, \text{ and } \delta_{jk} = 0 \text{ if } j \neq k. \tag{5.138}$$

Equation (5.137) gives six independent relations satisfied by nine direction cosines. It follows that there are only three independent direction cosines. The independent elements of the matrix $R$ cannot obviously be in the same row or column, or any diagonal.

The determinant of a transformation matrix is equal to one,

$$\left|{}^{G}R_{B}\right| = 1 \tag{5.139}$$

because of Equation (5.134), and noting that

$$
\begin{aligned}
\left|{}^{G}R_{B} \cdot {}^{G}R_{B}^{T}\right| &= \left|{}^{G}R_{B}\right| \cdot \left|{}^{G}R_{B}^{T}\right| \\
&= \left|{}^{G}R_{B}\right| \cdot \left|{}^{G}R_{B}\right| \\
&= \left|{}^{G}R_{B}\right|^{2} = 1.
\end{aligned} \tag{5.140}
$$

Using linear algebra and row vectors $\hat{\mathbf{r}}_{H_1}, \hat{\mathbf{r}}_{H_2}$, and $\hat{\mathbf{r}}_{H_3}$ of ${}^{G}R_{B}$, we know that

$$\left|{}^{G}R_{B}\right| = \hat{\mathbf{r}}_{H_1}^{T} \cdot (\hat{\mathbf{r}}_{H_2} \times \hat{\mathbf{r}}_{H_3}) \tag{5.141}$$

and because the coordinate system is right handed, we have $\hat{\mathbf{r}}_{H_2} \times \hat{\mathbf{r}}_{H_3} = \hat{\mathbf{r}}_{H_1}$ so $\left|{}^{G}R_{B}\right| = \hat{\mathbf{r}}_{H_1}^{T} \cdot \hat{\mathbf{r}}_{H_1} = 1.$ ∎

**Example 164** *Elements of the transformation matrix.*

*The position vector* $\mathbf{r}$ *of a point* $P$ *may be expressed in terms of its components with respect to either* $G\,(OXYZ)$ *or* $B\,(Oxyz)$ *frames. If* ${}^{G}\mathbf{r} = 100\hat{I} - 50\hat{J} + 150\hat{K}$, *and we are looking for components of* $\mathbf{r}$ *in the* $Oxyz$ *frame, then we have to find the proper rotation matrix* ${}^{B}R_{G}$ *first. Assume that the angle between the* $x$ *and* $X$ *axes is* $40\,\deg$, *and the angle between the* $y$ *and* $Y$ *axes is* $60\,\deg$.

*The row elements of* ${}^{B}R_{G}$ *are the direction cosines of the* $Oxyz$ *axes in the* $OXYZ$ *coordinate frame. The* $x$*-axis lies in the* $XZ$ *plane at* $40\,\deg$ *from the* $X$*-axis, and the angle between* $y$ *and* $Y$ *is* $60\,\deg$. *Therefore,*

$$
\begin{aligned}
{}^{B}R_{G} &= \begin{bmatrix} \hat{i} \cdot \hat{I} & \hat{i} \cdot \hat{J} & \hat{i} \cdot \hat{K} \\ \hat{j} \cdot \hat{I} & \hat{j} \cdot \hat{J} & \hat{j} \cdot \hat{K} \\ \hat{k} \cdot \hat{I} & \hat{k} \cdot \hat{J} & \hat{k} \cdot \hat{K} \end{bmatrix} \\[2mm]
&= \begin{bmatrix} \cos 40 & 0 & \sin 40 \\ \hat{j} \cdot \hat{I} & \cos 60 & \hat{j} \cdot \hat{K} \\ \hat{k} \cdot \hat{I} & \hat{k} \cdot \hat{J} & \hat{k} \cdot \hat{K} \end{bmatrix} \\[2mm]
&= \begin{bmatrix} 0.766 & 0 & 0.643 \\ \hat{j} \cdot \hat{I} & 0.5 & \hat{j} \cdot \hat{K} \\ \hat{k} \cdot \hat{I} & \hat{k} \cdot \hat{J} & \hat{k} \cdot \hat{K} \end{bmatrix}
\end{aligned} \tag{5.142}
$$

*and by using* $^B R_G \, ^G R_B = \, ^B R_G \, ^B R_G^T = I$

$$
\begin{bmatrix}
0.766 & 0 & 0.643 \\
r_{21} & 0.5 & r_{23} \\
r_{31} & r_{32} & r_{33}
\end{bmatrix}
\begin{bmatrix}
0.766 & r_{21} & r_{31} \\
0 & 0.5 & r_{32} \\
0.643 & r_{23} & r_{33}
\end{bmatrix}
=
\begin{bmatrix}
1 & 0 & 0 \\
0 & 1 & 0 \\
0 & 0 & 1
\end{bmatrix}
\tag{5.143}
$$

*we obtain a set of equations to find the missing elements.*

$$
\begin{aligned}
0.766 \, r_{21} + 0.643 \, r_{23} &= 0 \\
0.766 \, r_{31} + 0.643 \, r_{33} &= 0 \\
r_{21}^2 + r_{23}^2 + 0.25 &= 1 \\
r_{21} r_{31} + 0.5 r_{32} + r_{23} r_{33} &= 0 \\
r_{31}^2 + r_{32}^2 + r_{33}^2 &= 1
\end{aligned}
\tag{5.144}
$$

*Solving these equations provides the following transformation matrix:*

$$
^B R_G =
\begin{bmatrix}
0.766 & 0 & 0.643 \\
0.557 & 0.5 & -0.663 \\
-0.322 & 0.866 & 0.383
\end{bmatrix}
\tag{5.145}
$$

*and then we can find the components of* $^B \mathbf{r}$.

$$
\begin{aligned}
^B \mathbf{r} &= \, ^B R_G \, ^G \mathbf{r} \\
&=
\begin{bmatrix}
0.766 & 0 & 0.643 \\
0.557 & 0.5 & -0.663 \\
-0.322 & 0.866 & 0.383
\end{bmatrix}
\begin{bmatrix}
100 \\
-50 \\
150
\end{bmatrix} \\
&=
\begin{bmatrix}
173.05 \\
-68.75 \\
-18.05
\end{bmatrix}
\end{aligned}
\tag{5.146}
$$

**Example 165** *Global position, using* $^B \mathbf{r}$ *and* $^B R_G$.
   *The position vector* $\mathbf{r}$ *of a point* $P$ *may be described in either* $G\,(OXYZ)$ *or* $B\,(Oxyz)$ *frames. If* $^B \mathbf{r} = 100 \hat{\imath} - 50 \hat{\jmath} + 150 \hat{k}$, *and the following* $^B R_G$ *is the transformation matrix to map* $^G \mathbf{r}$ *to* $^B \mathbf{r}$

$$
\begin{aligned}
^B \mathbf{r} &= \, ^B R_G \, ^G \mathbf{r} \\
&=
\begin{bmatrix}
0.766 & 0 & 0.643 \\
0.557 & 0.5 & -0.663 \\
-0.322 & 0.866 & 0.383
\end{bmatrix}
\, ^G \mathbf{r}
\end{aligned}
\tag{5.147}
$$

*then the components of $^G\mathbf{r}$ in $G\,(OXYZ)$ would be*

$$
\begin{aligned}
^G\mathbf{r} &= {}^G R_B\,{}^B\mathbf{r} \\
&= {}^B R_G^T\,{}^B\mathbf{r} \\
&= \begin{bmatrix} 0.766 & 0.557 & -0.322 \\ 0 & 0.5 & 0.866 \\ 0.643 & -0.663 & 0.383 \end{bmatrix} \begin{bmatrix} 100 \\ -50 \\ 150 \end{bmatrix} \\
&= \begin{bmatrix} 0.45 \\ 104.9 \\ 154.9 \end{bmatrix} .
\end{aligned}
\tag{5.148}
$$

**Example 166** *Two points transformation matrix.*

*The global position vector of two points, $P_1$ and $P_2$, of a rigid body $B$ are*

$$
^G\mathbf{r}_{P_1} = \begin{bmatrix} 1.077 \\ 1.365 \\ 2.666 \end{bmatrix}
\tag{5.149}
$$

$$
^G\mathbf{r}_{P_2} = \begin{bmatrix} -0.473 \\ 2.239 \\ -0.959 \end{bmatrix} .
\tag{5.150}
$$

*The origin of the body $B\,(Oxyz)$ is fixed on the origin of $G\,(OXYZ)$, and the points $P_1$ and $P_2$ are lying on the local x-axis and y-axis respectively.*

*To find $^G R_B$, we use the local unit vectors $^G\hat{\imath}$ and $^G\hat{\jmath}$*

$$
^G\hat{\imath} = \frac{^G\mathbf{r}_{P_1}}{|^G\mathbf{r}_{P_1}|} = \begin{bmatrix} 0.338 \\ 0.429 \\ 0.838 \end{bmatrix}
\tag{5.151}
$$

$$
^G\hat{\jmath} = \frac{^G\mathbf{r}_{P_2}}{|^G\mathbf{r}_{P_2}|} = \begin{bmatrix} -0.191 \\ 0.902 \\ -0.387 \end{bmatrix}
\tag{5.152}
$$

*to obtain $^G\hat{k}$*

$$
\begin{aligned}
^G\hat{k} &= \hat{\imath} \times \hat{\jmath} = \tilde{\imath}\,\hat{\jmath} \\
&= \begin{bmatrix} 0 & -0.838 & 0.429 \\ 0.838 & 0 & -0.338 \\ -0.429 & 0.338 & 0 \end{bmatrix} \begin{bmatrix} -0.191 \\ 0.902 \\ -0.387 \end{bmatrix} \\
&= \begin{bmatrix} -0.922 \\ -0.029 \\ 0.387 \end{bmatrix}
\end{aligned}
\tag{5.153}
$$

*where $\tilde{\imath}$ is the skew-symmetric matrix corresponding to $\hat{\imath}$, and $\tilde{\imath}\,\hat{\jmath}$ is an alternative for $\hat{\imath} \times \hat{\jmath}$.*

Hence, the transformation matrix using the coordinates of two points $^G\mathbf{r}_{P_1}$ and $^G\mathbf{r}_{P_2}$ would be

$$
\begin{aligned}
^GR_B &= \begin{bmatrix} ^G\hat{\imath} & ^G\hat{\jmath} & ^G\hat{k} \end{bmatrix} \\
&= \begin{bmatrix} 0.338 & -0.191 & -0.922 \\ 0.429 & 0.902 & -0.029 \\ 0.838 & -0.387 & 0.387 \end{bmatrix}.
\end{aligned}
\tag{5.154}
$$

**Example 167** *Length invariant of a position vector.*
*Describing a vector in different frames utilizing rotation matrices does not affect the length and direction properties of the vector. Therefore, the length of a vector is an invariant*

$$
|\mathbf{r}| = \left|^G\mathbf{r}\right| = \left|^B\mathbf{r}\right|.
\tag{5.155}
$$

*The length invariant property can be shown by*

$$
\begin{aligned}
|\mathbf{r}|^2 &= {}^G\mathbf{r}^T\,{}^G\mathbf{r} \\
&= \left[^GR_B\,{}^B\mathbf{r}\right]^T\,{}^GR_B\,{}^B\mathbf{r} \\
&= {}^B\mathbf{r}^T\,{}^GR_B^T\,{}^GR_B\,{}^B\mathbf{r} \\
&= {}^B\mathbf{r}^T\,{}^B\mathbf{r}.
\end{aligned}
\tag{5.156}
$$

**Example 168** ★ *Skew symmetric matrices for $\hat{\imath}$, $\hat{\jmath}$, and $\hat{k}$.*
*The definition of skew symmetric matrix $\tilde{a}$ corresponding to a vector $\mathbf{a}$ is defined by*

$$
\tilde{a} = \begin{bmatrix} 0 & -a_3 & a_2 \\ a_3 & 0 & -a_1 \\ -a_2 & a_1 & 0 \end{bmatrix}.
\tag{5.157}
$$

*Hence,*

$$
\tilde{\imath} = \begin{bmatrix} 0 & 0 & 0 \\ 0 & 0 & -1 \\ 0 & 1 & 0 \end{bmatrix}
\tag{5.158}
$$

$$
\tilde{\jmath} = \begin{bmatrix} 0 & 0 & 1 \\ 0 & 0 & 0 \\ -1 & 0 & 0 \end{bmatrix}
\tag{5.159}
$$

$$
\tilde{k} = \begin{bmatrix} 0 & -1 & 0 \\ 1 & 0 & 0 \\ 0 & 0 & 0 \end{bmatrix}.
\tag{5.160}
$$

**Example 169** *Inverse of Euler angles rotation matrix.*
*Precession-nutation-spin or Euler angle rotation matrix (5.79)*

$$
\begin{aligned}
{}^{B}R_{G} &= R_{z,\psi}R_{x,\theta}R_{z,\varphi} \\
&= \begin{bmatrix} c\varphi c\psi - c\theta s\varphi s\psi & c\psi s\varphi + c\theta c\varphi s\psi & s\theta s\psi \\ -c\varphi s\psi - c\theta c\psi s\varphi & -s\varphi s\psi + c\theta c\varphi c\psi & s\theta c\psi \\ s\theta s\varphi & -c\varphi s\theta & c\theta \end{bmatrix}
\end{aligned}
\quad (5.161)
$$

*must be inverted to be a transformation matrix to map body coordinates to global coordinates.*

$$
\begin{aligned}
{}^{G}R_{B} &= {}^{B}R_{G}^{-1} = R_{z,\varphi}^{T}R_{x,\theta}^{T}R_{z,\psi}^{T} \\
&= \begin{bmatrix} c\varphi c\psi - c\theta s\varphi s\psi & -c\varphi s\psi - c\theta c\psi s\varphi & s\theta s\varphi \\ c\psi s\varphi + c\theta c\varphi s\psi & -s\varphi s\psi + c\theta c\varphi c\psi & -c\varphi s\theta \\ s\theta s\psi & s\theta c\psi & c\theta \end{bmatrix}
\end{aligned}
\quad (5.162)
$$

*The transformation matrix (5.161) is called a local Euler rotation matrix, and (5.162) is called a global Euler rotation matrix.*

**Example 170 ★** *Alternative proof for transformation matrix.*
  *Starting with an identity*

$$
\begin{bmatrix} \hat{\imath} & \hat{\jmath} & \hat{k} \end{bmatrix} \begin{bmatrix} \hat{\imath} \\ \hat{\jmath} \\ \hat{k} \end{bmatrix} = 1
\quad (5.163)
$$

*we may write*

$$
\begin{bmatrix} \hat{I} \\ \hat{J} \\ \hat{K} \end{bmatrix} = \begin{bmatrix} \hat{I} \\ \hat{J} \\ \hat{K} \end{bmatrix} \begin{bmatrix} \hat{\imath} & \hat{\jmath} & \hat{k} \end{bmatrix} \begin{bmatrix} \hat{\imath} \\ \hat{\jmath} \\ \hat{k} \end{bmatrix} .
\quad (5.164)
$$

*Since matrix multiplication can be performed in any order, we find*

$$
\begin{aligned}
\begin{bmatrix} \hat{I} \\ \hat{J} \\ \hat{K} \end{bmatrix} &= \begin{bmatrix} \hat{I} \cdot \hat{\imath} & \hat{I} \cdot \hat{\jmath} & \hat{I} \cdot \hat{k} \\ \hat{J} \cdot \hat{\imath} & \hat{J} \cdot \hat{\jmath} & \hat{J} \cdot \hat{k} \\ \hat{K} \cdot \hat{\imath} & \hat{K} \cdot \hat{\jmath} & \hat{K} \cdot \hat{k} \end{bmatrix} \begin{bmatrix} \hat{\imath} \\ \hat{\jmath} \\ \hat{k} \end{bmatrix} \\
&= {}^{G}R_{B} \begin{bmatrix} \hat{\imath} \\ \hat{\jmath} \\ \hat{k} \end{bmatrix}
\end{aligned}
\quad (5.165)
$$

*where,*

$$
{}^{G}R_{B} = \begin{bmatrix} \hat{I} \\ \hat{J} \\ \hat{K} \end{bmatrix} \begin{bmatrix} \hat{\imath} & \hat{\jmath} & \hat{k} \end{bmatrix} .
\quad (5.166)
$$

*Following the same method we can show that*

$$
{}^{B}R_{G} = \begin{bmatrix} \hat{\imath} \\ \hat{\jmath} \\ \hat{k} \end{bmatrix} \begin{bmatrix} \hat{I} & \hat{J} & \hat{K} \end{bmatrix} .
\quad (5.167)
$$
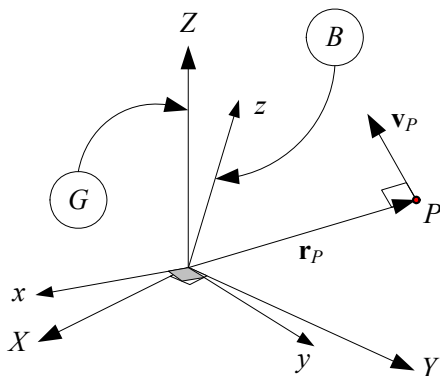
FIGURE 5.9. A rotating rigid body $B(Oxyz)$ with a fixed point $O$ in a global frame $G(OXYZ)$.

## 5.7 Angular Velocity

Consider a rotating rigid body $B(Oxyz)$ with a fixed point $O$ in a reference frame $G(OXYZ)$ as shown in Figure 5.9. The motion of the body can be described by a time varying rotation transformation matrix between the global and body frames to map the instantaneous coordinates of any fixed point in body frame $B$ into their coordinates in the global frame $G$

$$^{G}\mathbf{r}(t) = {}^{G}R_B(t)\,{}^{B}\mathbf{r}. \tag{5.168}$$

The velocity of a body point in the global frame is

$$
\begin{aligned}
{}^{G}\dot{\mathbf{r}}(t) &= {}^{G}\mathbf{v}(t) && (5.169)\\
&= {}^{G}\dot{R}_B(t)\,{}^{B}\mathbf{r} && (5.170)\\
&= {}_{G}\tilde{\omega}_B\,{}^{G}\mathbf{r}(t) && (5.171)\\
&= {}_{G}\boldsymbol{\omega}_B \times {}^{G}\mathbf{r}(t) && (5.172)
\end{aligned}
$$

where ${}_{G}\boldsymbol{\omega}_B$ is the *angular velocity vector* of $B$ with respect to $G$. It is equal to a rotation with *angular rate* $\dot{\phi}$ about an *instantaneous axis of rotation* $\hat{u}$.

$$\boldsymbol{\omega} = \begin{bmatrix} \omega_1 \\ \omega_2 \\ \omega_3 \end{bmatrix} = \dot{\phi}\,\hat{u} \tag{5.173}$$

The angular velocity vector is associated with a skew symmetric matrix

$_G\tilde{\omega}_B$ called the *angular velocity matrix*

$$\tilde{\omega} = \begin{bmatrix} 0 & -\omega_3 & \omega_2 \\ \omega_3 & 0 & -\omega_1 \\ -\omega_2 & \omega_1 & 0 \end{bmatrix} \qquad (5.174)$$

where

$$\begin{aligned} _G\tilde{\omega}_B &= {}^G\dot{R}_B \, {}^G R_B^T & (5.175) \\ &= \dot{\phi}\,\tilde{u}. & (5.176) \end{aligned}$$

**Proof.** Consider a rigid body with a fixed point $O$ and an attached frame $B(Oxyz)$ as shown in Figure 5.9. The body frame $B$ is initially coincident with the global frame $G$. Therefore, the position vector of a body point $P$ is

$$^G\mathbf{r}(t_0) = {}^B\mathbf{r}. \qquad (5.177)$$

The global time derivative of $^G\mathbf{r}$ is

$$\begin{aligned} ^G\mathbf{v} &= {}^G\dot{\mathbf{r}} \\ &= \frac{^Gd}{dt}\,{}^G\mathbf{r}(t) \\ &= \frac{^Gd}{dt}\,[{}^G R_B(t)\,{}^B\mathbf{r}] \\ &= \frac{^Gd}{dt}\,[{}^G R_B(t)\,{}^G\mathbf{r}(t_0)] \\ &= {}^G\dot{R}_B(t)\,{}^B\mathbf{r}. & (5.178) \end{aligned}$$

Eliminating $^B\mathbf{r}$ between (5.168) and (5.178) determines the velocity of the point in global frame

$$^G\mathbf{v} = {}^G\dot{R}_B(t)\,{}^G R_B^T(t)\,{}^G\mathbf{r}(t). \qquad (5.179)$$

We denote the coefficient of $^G\mathbf{r}(t)$ by $\tilde{\omega}$

$$_G\tilde{\omega}_B = {}^G\dot{R}_B \, {}^G R_B^T \qquad (5.180)$$

and write Equation (5.179) as

$$^G\mathbf{v} = {}_G\tilde{\omega}_B \, {}^G\mathbf{r}(t) \qquad (5.181)$$

or as

$$^G\mathbf{v} = {}_G\boldsymbol{\omega}_B \times {}^G\mathbf{r}(t). \qquad (5.182)$$

The time derivative of the orthogonality condition, $^G R_B\,{}^G R_B^T = \mathbf{I}$, introduces an important identity

$$^G\dot{R}_B \, {}^G R_B^T + {}^G R_B \, {}^G\dot{R}_B^T = 0 \qquad (5.183)$$

which can be utilized to show that $_G\tilde{\omega}_B = [^G\dot{R}_B\,^GR_B^T]$ is a skew-symmetric matrix because

$$^GR_B\,^G\dot{R}_B^T = \left[^G\dot{R}_B\,^GR_B^T\right]^T. \tag{5.184}$$

The vector $_G^G\boldsymbol{\omega}_B$ is called the *instantaneous angular velocity* of the body $B$ relative to the global frame $G$ as seen from the $G$ frame.

Since a vectorial equation can be expressed in any coordinate frame, we may use any of the following expressions for the velocity of a body point in body or global frames

$$^G_G\mathbf{v}_P \;=\; ^G_G\boldsymbol{\omega}_B \times {}^G\mathbf{r}_P \tag{5.185}$$

$$^B_G\mathbf{v}_P \;=\; ^B_G\boldsymbol{\omega}_B \times {}^B\mathbf{r}_P \tag{5.186}$$

where $^G_G\mathbf{v}_P$ is the global velocity of point $P$ expressed in the global frame and $^B_G\mathbf{v}_P$ is the global velocity of point $P$ expressed in the body frame.

$$\begin{aligned}
^G_G\mathbf{v}_P \;&=\; ^GR_B\,^B_G\mathbf{v}_P \\
&=\; ^GR_B\left(^B_G\boldsymbol{\omega}_B \times {}^B\mathbf{r}_P\right) \tag{5.187}
\end{aligned}$$

$^G_G\mathbf{v}_P$ and $^B_G\mathbf{v}_P$ can be converted to each other using a rotation matrix

$$\begin{aligned}
^B_G\mathbf{v}_P \;&=\; ^GR_B^T\,^G_G\mathbf{v}_P \tag{5.188}\\
&=\; ^GR_B^T\,_G\tilde{\omega}_B\,^G_G\mathbf{r}_P \\
&=\; ^GR_B^T\,^G\dot{R}_B\,^GR_B^T\,^G_G\mathbf{r}_P \\
&=\; ^GR_B^T\,^G\dot{R}_B\,^B_G\mathbf{r}_P. \tag{5.189}
\end{aligned}$$

showing that

$$^B_G\tilde{\omega}_B = ^GR_B^T\,^G\dot{R}_B \tag{5.190}$$

which is called the *instantaneous angular velocity* of $B$ relative to the global frame $G$ as seen from the $B$ frame. From the definitions of $_G\tilde{\omega}_B$ and $^B_G\tilde{\omega}_B$ we are able to transform the two angular velocity matrices by

$$_G\tilde{\omega}_B = ^GR_B\,^B_G\tilde{\omega}_B\,^GR_B^T \tag{5.191}$$

$$^B_G\tilde{\omega}_B = ^GR_B^T\,_G\tilde{\omega}_B\,^GR_B \tag{5.192}$$

or equivalently

$$^G\dot{R}_B = {}_G\tilde{\omega}_B\,^GR_B \tag{5.193}$$

$$^G\dot{R}_B = ^GR_B\,^B_G\tilde{\omega}_B \tag{5.194}$$

$$_G\tilde{\omega}_B\,^GR_B = ^GR_B\,^B_G\tilde{\omega}_B. \tag{5.195}$$

The angular velocity of $B$ in $G$ is negative of the angular velocity of $G$ in $B$ if both are expressed in the same coordinate frame.

$$^G_G\tilde{\omega}_B \;=\; -^G_B\tilde{\omega}_G \tag{5.196}$$

$$^B_G\tilde{\omega}_B \;=\; -^B_B\tilde{\omega}_G. \tag{5.197}$$

$_G\omega_B$ and can always be expressed in the form

$$_G\boldsymbol{\omega}_B = \omega\hat{u} \tag{5.198}$$

where $\hat{u}$ is a unit vector parallel to $_G\omega_B$ and indicates the *instantaneous axis of rotation.* ■

**Example 171** *Rotation of a body point about a global axis.*
    *Consider a rigid body is turning about the $Z$-axis with $\dot{\alpha} = 10\deg/s$. The global velocity of a point $P(5, 30, 10)$, when the body is turned $\alpha = 30\deg$, is*

$$
\begin{aligned}
^G\mathbf{v}_P &= {}^G\dot{R}_B(t)\,{}^B\mathbf{r}_P \\[4pt]
&= \frac{^Gd}{dt}\left(\begin{bmatrix} \cos\alpha & -\sin\alpha & 0 \\ \sin\alpha & \cos\alpha & 0 \\ 0 & 0 & 1 \end{bmatrix}\right)\begin{bmatrix} 5 \\ 30 \\ 10 \end{bmatrix} \\[4pt]
&= \dot{\alpha}\begin{bmatrix} -\sin\alpha & -\cos\alpha & 0 \\ \cos\alpha & -\sin\alpha & 0 \\ 0 & 0 & 0 \end{bmatrix}\begin{bmatrix} 5 \\ 30 \\ 10 \end{bmatrix} \\[4pt]
&= \frac{10\pi}{180}\begin{bmatrix} -\sin\frac{\pi}{6} & -\cos\frac{\pi}{6} & 0 \\ \cos\frac{\pi}{6} & -\sin\frac{\pi}{6} & 0 \\ 0 & 0 & 0 \end{bmatrix}\begin{bmatrix} 5 \\ 30 \\ 10 \end{bmatrix} = \begin{bmatrix} -4.97 \\ -1.86 \\ 0 \end{bmatrix}
\end{aligned}
\tag{5.199}
$$

*at this moment, point $P$ is at*

$$
\begin{aligned}
^G\mathbf{r}_P &= {}^GR_B\,{}^B\mathbf{r}_P \\[4pt]
&= \begin{bmatrix} \cos\frac{\pi}{6} & -\sin\frac{\pi}{6} & 0 \\ \sin\frac{\pi}{6} & \cos\frac{\pi}{6} & 0 \\ 0 & 0 & 1 \end{bmatrix}\begin{bmatrix} 5 \\ 30 \\ 10 \end{bmatrix} = \begin{bmatrix} -10.67 \\ 28.48 \\ 10 \end{bmatrix}.
\end{aligned}
\tag{5.200}
$$

**Example 172** *Rotation of a global point about a global axis.*
    *A point $P$ of a rigid body is at $^B\mathbf{r}_P = \begin{bmatrix} 5 & 30 & 10 \end{bmatrix}^T$. When it is turned $\alpha = 30\deg$ about the $Z$-axis, the global position of $P$ is*

$$
\begin{aligned}
^G\mathbf{r}_P &= {}^GR_B\,{}^B\mathbf{r}_P \\[4pt]
&= \begin{bmatrix} \cos\frac{\pi}{6} & -\sin\frac{\pi}{6} & 0 \\ \sin\frac{\pi}{6} & \cos\frac{\pi}{6} & 0 \\ 0 & 0 & 1 \end{bmatrix}\begin{bmatrix} 5 \\ 30 \\ 10 \end{bmatrix} = \begin{bmatrix} -10.67 \\ 28.48 \\ 10 \end{bmatrix}.
\end{aligned}
\tag{5.201}
$$

*If the body is turning with $\dot{\alpha} = 10\deg/s$, the global velocity of the point $P$*

*would be*

$$
{}^G\mathbf{v}_P = {}^G\dot{R}_B\,{}^GR_B^T\,{}^G\mathbf{r}_P \tag{5.202}
$$

$$
= \frac{10\pi}{180}
\begin{bmatrix}
-s\frac{\pi}{6} & -c\frac{\pi}{6} & 0 \\
c\frac{\pi}{6} & -s\frac{\pi}{6} & 0 \\
0 & 0 & 0
\end{bmatrix}
\begin{bmatrix}
c\frac{\pi}{6} & -s\frac{\pi}{6} & 0 \\
s\frac{\pi}{6} & c\frac{\pi}{6} & 0 \\
0 & 0 & 1
\end{bmatrix}^T
\begin{bmatrix}
-10.67 \\
28.48 \\
10
\end{bmatrix}
$$

$$
=
\begin{bmatrix}
-4.97 \\
-1.86 \\
0
\end{bmatrix}.
$$

**Example 173 ★** *Principal angular velocities.*

 The principal rotational matrices about the axes $X$, $Y$, and $Z$ are

$$
R_{X,\gamma} =
\begin{bmatrix}
1 & 0 & 0 \\
0 & \cos\gamma & -\sin\gamma \\
0 & \sin\gamma & \cos\gamma
\end{bmatrix} \tag{5.203}
$$

$$
R_{Y,\beta} =
\begin{bmatrix}
\cos\beta & 0 & \sin\beta \\
0 & 1 & 0 \\
-\sin\beta & 0 & \cos\beta
\end{bmatrix} \tag{5.204}
$$

$$
R_{Z,\alpha} =
\begin{bmatrix}
\cos\alpha & -\sin\alpha & 0 \\
\sin\alpha & \cos\alpha & 0 \\
0 & 0 & 1
\end{bmatrix}. \tag{5.205}
$$

*and hence, their time derivatives are*

$$
\dot{R}_{X,\gamma} = \dot{\gamma}
\begin{bmatrix}
0 & 0 & 0 \\
0 & -\sin\gamma & -\cos\gamma \\
0 & \cos\gamma & -\sin\gamma
\end{bmatrix} \tag{5.206}
$$

$$
\dot{R}_{Y,\beta} = \dot{\beta}
\begin{bmatrix}
-\sin\beta & 0 & \cos\beta \\
0 & 0 & 0 \\
-\cos\beta & 0 & -\sin\beta
\end{bmatrix} \tag{5.207}
$$

$$
\dot{R}_{Z,\alpha} = \dot{\alpha}
\begin{bmatrix}
-\sin\alpha & -\cos\alpha & 0 \\
\cos\alpha & -\sin\alpha & 0 \\
0 & 0 & 0
\end{bmatrix}. \tag{5.208}
$$

*Therefore, the principal angular velocity matrices about axes $X$, $Y$, and $Z$ are*

$$
{}_G\tilde{\omega}_X = \dot{R}_{X,\gamma}R_{X,\gamma}^T = \dot{\gamma}
\begin{bmatrix}
0 & 0 & 0 \\
0 & 0 & -1 \\
0 & 1 & 0
\end{bmatrix} \tag{5.209}
$$

$$
{}_G\tilde{\omega}_Y = \dot{R}_{Y,\beta}R_{Y,\beta}^T = \dot{\beta}
\begin{bmatrix}
0 & 0 & 1 \\
0 & 0 & 0 \\
-1 & 0 & 0
\end{bmatrix} \tag{5.210}
$$

$$_G\tilde{\omega}_Z = \dot{R}_{Z,\alpha}R_{Z,\alpha}^T = \dot{\alpha}\begin{bmatrix} 0 & -1 & 0 \\ 1 & 0 & 0 \\ 0 & 0 & 0 \end{bmatrix} \tag{5.211}$$

which are equivalent to

$$_G\tilde{\omega}_X = \dot{\gamma}\tilde{I} \tag{5.212}$$
$$_G\tilde{\omega}_Y = \dot{\beta}\tilde{J} \tag{5.213}$$
$$_G\tilde{\omega}_Z = \dot{\alpha}\tilde{K} \tag{5.214}$$

and therefore, the principal angular velocity vectors are

$$_G\boldsymbol{\omega}_X = \omega_X\hat{I} = \dot{\gamma}\hat{I} \tag{5.215}$$
$$_G\boldsymbol{\omega}_Y = \omega_Y\hat{J} = \dot{\beta}\hat{J} \tag{5.216}$$
$$_G\boldsymbol{\omega}_Z = \omega_Z\hat{K} = \dot{\alpha}\hat{K}. \tag{5.217}$$

Utilizing the same technique, we can find the following principal angular velocity matrices about the local axes:

$$_G^B\tilde{\omega}_x = R_{x,\psi}^T\dot{R}_{x,\psi} = \dot{\psi}\begin{bmatrix} 0 & 0 & 0 \\ 0 & 0 & -1 \\ 0 & 1 & 0 \end{bmatrix} = \dot{\psi}\tilde{\imath} \tag{5.218}$$

$$_G^B\tilde{\omega}_y = R_{y,\theta}^T\dot{R}_{y,\theta} = \dot{\theta}\begin{bmatrix} 0 & 0 & 1 \\ 0 & 0 & 0 \\ -1 & 0 & 0 \end{bmatrix} = \dot{\theta}\tilde{\jmath} \tag{5.219}$$

$$_G^B\tilde{\omega}_z = R_{z,\varphi}^T\dot{R}_{z,\varphi} = \dot{\varphi}\begin{bmatrix} 0 & -1 & 0 \\ 1 & 0 & 0 \\ 0 & 0 & 0 \end{bmatrix} = \dot{\varphi}\tilde{k} \tag{5.220}$$

**Example 174** *Decomposition of an angular velocity vector.*
Every angular velocity vector can be decomposed to three principal angular velocity vectors.

$$\begin{aligned} _G\boldsymbol{\omega}_B &= \left(_G\boldsymbol{\omega}_B \cdot \hat{I}\right)\hat{I} + \left(_G\boldsymbol{\omega}_B \cdot \hat{J}\right)\hat{J} + \left(_G\boldsymbol{\omega}_B \cdot \hat{K}\right)\hat{K} \tag{5.221} \\ &= \omega_X\hat{I} + \omega_Y\hat{J} + \omega_Z\hat{K} \\ &= \dot{\gamma}\hat{I} + \dot{\beta}\hat{J} + \dot{\alpha}\hat{K} \\ &= \boldsymbol{\omega}_X + \boldsymbol{\omega}_Y + \boldsymbol{\omega}_Z \end{aligned}$$

**Example 175** *Combination of angular velocities.*
Starting from a combination of rotations

$$^0R_2 = {}^0R_1\,{}^1R_2 \tag{5.222}$$

and taking a time derivative, we find

$$^0\dot{R}_2 = {}^0\dot{R}_1\,{}^1R_2 + {}^0R_1\,{}^1\dot{R}_2. \tag{5.223}$$

*Now, substituting the derivative of rotation matrices with*

$$
\begin{aligned}
{}^{0}\dot{R}_2 &= {}_{0}\tilde{\omega}_2 \, {}^{0}R_2 && (5.224) \\
{}^{0}\dot{R}_1 &= {}_{0}\tilde{\omega}_1 \, {}^{0}R_1 && (5.225) \\
{}^{1}\dot{R}_2 &= {}_{1}\tilde{\omega}_2 \, {}^{1}R_2 && (5.226)
\end{aligned}
$$

*results in*

$$
\begin{aligned}
{}_{0}\tilde{\omega}_2 \, {}^{0}R_2 &= {}_{0}\tilde{\omega}_1 \, {}^{0}R_1 \, {}^{1}R_2 + {}^{0}R_1 \, {}_{1}\tilde{\omega}_2 \, {}^{1}R_2 \\
&= {}_{0}\tilde{\omega}_1 \, {}^{0}R_2 + {}^{0}R_1 \, {}_{1}\tilde{\omega}_2 \, {}^{0}R_1^T \, {}^{0}R_1 \, {}^{1}R_2 \\
&= {}_{0}\tilde{\omega}_1 \, {}^{0}R_2 + {}_{1}^{0}\tilde{\omega}_2 \, {}^{0}R_2 && (5.227)
\end{aligned}
$$

*where*

$$
{}^{0}R_1 \, {}_{1}\tilde{\omega}_2 \, {}^{0}R_1^T = {}_{1}^{0}\tilde{\omega}_2. \qquad (5.228)
$$

*Therefore, we find*

$$
{}_{0}\tilde{\omega}_2 = {}_{0}\tilde{\omega}_1 + {}_{1}^{0}\tilde{\omega}_2 \qquad (5.229)
$$

*which indicates that the angular velocities may be added relatively:*

$$
{}_{0}\boldsymbol{\omega}_2 = {}_{0}\boldsymbol{\omega}_1 + {}_{1}^{0}\boldsymbol{\omega}_2 \qquad (5.230)
$$

*This result also holds for any number of angular velocities*

$$
\begin{aligned}
{}_{0}\boldsymbol{\omega}_n &= {}_{0}\boldsymbol{\omega}_1 + {}_{1}^{0}\boldsymbol{\omega}_2 + {}_{2}^{0}\boldsymbol{\omega}_3 + \cdots + {}_{n-1}^{0}\boldsymbol{\omega}_n && (5.231) \\
&= \sum_{i=1}^{n} {}_{i-1}^{0}\boldsymbol{\omega}_i.
\end{aligned}
$$

**Example 176 ★** *Angular velocity in terms of Euler frequencies.*
   *The angular velocity vector can be expressed by Euler frequencies. There-fore,*

$$
\begin{aligned}
{}_{G}^{B}\boldsymbol{\omega}_B &= \omega_x \hat{\imath} + \omega_y \hat{\jmath} + \omega_z \hat{k} \\
&= \dot{\varphi}\hat{e}_\varphi + \dot{\theta}\hat{e}_\theta + \dot{\psi}\hat{e}_\psi \\
&= \dot{\varphi}\begin{bmatrix} \sin\theta\sin\psi \\ \sin\theta\cos\psi \\ \cos\theta \end{bmatrix} + \dot{\theta}\begin{bmatrix} \cos\psi \\ -\sin\psi \\ 0 \end{bmatrix} + \dot{\psi}\begin{bmatrix} 0 \\ 0 \\ 1 \end{bmatrix} \\
&= \begin{bmatrix} \sin\theta\sin\psi & \cos\psi & 0 \\ \sin\theta\cos\psi & -\sin\psi & 0 \\ \cos\theta & 0 & 1 \end{bmatrix}\begin{bmatrix} \dot{\varphi} \\ \dot{\theta} \\ \dot{\psi} \end{bmatrix} && (5.232)
\end{aligned}
$$

*and*

$$
\begin{aligned}
{}^{G}_{G}\boldsymbol{\omega}_B &= {}^{B}R_G^{-1}\, {}^{B}_{G}\boldsymbol{\omega}_B \\[4pt]
&= {}^{B}R_G^{-1}
\begin{bmatrix}
\dot\varphi \sin\theta \sin\psi + \dot\theta \cos\psi \\
\dot\varphi \sin\theta \cos\psi - \dot\theta \sin\psi \\
\dot\varphi \cos\theta + \dot\psi
\end{bmatrix} \\[4pt]
&=
\begin{bmatrix}
0 & \cos\varphi & \sin\theta \sin\varphi \\
0 & \sin\varphi & -\cos\varphi \sin\theta \\
1 & 0 & \cos\theta
\end{bmatrix}
\begin{bmatrix}
\dot\varphi \\
\dot\theta \\
\dot\psi
\end{bmatrix}
\end{aligned}
\tag{5.233}
$$

*where the inverse of the Euler transformation matrix is*

$$
{}^{B}R_G^{-1} =
\begin{bmatrix}
c\varphi c\psi - c\theta s\varphi s\psi & -c\varphi s\psi - c\theta c\psi s\varphi & s\theta s\varphi \\
c\psi s\varphi + c\theta c\varphi s\psi & -s\varphi s\psi + c\theta c\varphi c\psi & -c\varphi s\theta \\
s\theta s\psi & s\theta c\psi & c\theta
\end{bmatrix}.
\tag{5.234}
$$

**Example 177** ★ *Angular velocity in terms of rotation frequencies.*
   *Consider the Euler angles transformation matrix:*

$$
{}^{B}R_G = R_{z,\psi} R_{x,\theta} R_{z,\varphi}
\tag{5.235}
$$

*The angular velocity matrix is then equal to*

$$
\begin{aligned}
{}_{B}\tilde\omega_G &= {}^{B}\dot R_G \, {}^{B}R_G^{T} \\[4pt]
&= \left( \dot\varphi\, R_{z,\psi} R_{x,\theta} \frac{dR_{z,\varphi}}{dt} + \dot\theta\, R_{z,\psi} \frac{dR_{x,\theta}}{dt} R_{z,\varphi} + \dot\psi\, \frac{dR_{z,\psi}}{dt} R_{x,\theta} R_{z,\varphi} \right) \\
&\quad \times \left( R_{z,\psi} R_{x,\theta} R_{z,\varphi} \right)^{T} \\[4pt]
&= \dot\varphi\, R_{z,\psi} R_{x,\theta} \frac{dR_{z,\varphi}}{dt} R_{z,\varphi}^{T} R_{x,\theta}^{T} R_{z,\psi}^{T} \\
&\quad + \dot\theta\, R_{z,\psi} \frac{dR_{x,\theta}}{dt} R_{x,\theta}^{T} R_{z,\psi}^{T} \\
&\quad + \dot\psi\, \frac{dR_{z,\psi}}{dt} R_{z,\psi}^{T}
\end{aligned}
\tag{5.236}
$$

*which, in matrix form, is*

$$
\begin{aligned}
{}_{B}\tilde\omega_G &= \dot\varphi
\begin{bmatrix}
0 & \cos\theta & -\sin\theta \cos\psi \\
-\cos\theta & 0 & \sin\theta \sin\psi \\
\sin\theta \cos\psi & -\sin\theta \sin\psi & 0
\end{bmatrix} \\[4pt]
&\quad + \dot\theta
\begin{bmatrix}
0 & 0 & \sin\psi \\
0 & 0 & \cos\psi \\
-\sin\psi & -\cos\psi & 0
\end{bmatrix}
+ \dot\psi
\begin{bmatrix}
0 & 1 & 0 \\
-1 & 0 & 0 \\
0 & 0 & 0
\end{bmatrix}
\end{aligned}
\tag{5.237}
$$

*or*

$$
{}_{B}\tilde\omega_G =
\begin{bmatrix}
0 & \dot\psi + \dot\varphi c\theta & \dot\theta s\psi - \dot\varphi s\theta c\psi \\
-\dot\psi - \dot\varphi c\theta & 0 & \dot\theta c\psi + \dot\varphi s\theta s\psi \\
-\dot\theta s\psi + \dot\varphi s\theta c\psi & -\dot\theta c\psi - \dot\varphi s\theta s\psi & 0
\end{bmatrix}.
\tag{5.238}
$$

*The corresponding angular velocity vector is*

$$_B\boldsymbol{\omega}_G = -\begin{bmatrix} \dot{\theta}c\psi + \dot{\varphi}s\theta s\psi \\ -\dot{\theta}s\psi + \dot{\varphi}s\theta c\psi \\ \dot{\psi} + \dot{\varphi}c\theta \end{bmatrix}$$

$$= -\begin{bmatrix} \sin\theta\sin\psi & \cos\psi & 0 \\ \sin\theta\cos\psi & -\sin\psi & 0 \\ \cos\theta & 0 & 1 \end{bmatrix}\begin{bmatrix} \dot{\varphi} \\ \dot{\theta} \\ \dot{\psi} \end{bmatrix}. \qquad (5.239)$$

*However,*

$$_B^B\tilde{\omega}_G = -_G^B\tilde{\omega}_B \qquad (5.240)$$

$$_B^B\boldsymbol{\omega}_G = -_G^B\boldsymbol{\omega}_B \qquad (5.241)$$

*and therefore,*

$$_G^B\boldsymbol{\omega}_B = \begin{bmatrix} \sin\theta\sin\psi & \cos\psi & 0 \\ \sin\theta\cos\psi & -\sin\psi & 0 \\ \cos\theta & 0 & 1 \end{bmatrix}\begin{bmatrix} \dot{\varphi} \\ \dot{\theta} \\ \dot{\psi} \end{bmatrix}. \qquad (5.242)$$

**Example 178 ★** *Coordinate transformation of angular velocity.*

*Angular velocity $_1\boldsymbol{\omega}_2$ of coordinate frame $B_2$ with respect to $B_1$ and expressed in $B_1$ can be expressed in base coordinate frame $B_0$ according to*

$$^0R_1\, _1\tilde{\omega}_2\, ^0R_1^T = {}_1^0\tilde{\omega}_2. \qquad (5.243)$$

*To show this equation, it is enough to apply both sides on an arbitrary vector $^0\mathbf{r}$. Therefore, the left-hand side would be*

$$\begin{aligned}
^0R_1\, _1\tilde{\omega}_2\, ^0R_1^T\, ^0\mathbf{r} &= {}^0R_1\, _1\tilde{\omega}_2\, ^1R_0\, ^0\mathbf{r} \\
&= {}^0R_1\, _1\tilde{\omega}_2\, ^1\mathbf{r} \\
&= {}^0R_1\left(_1\boldsymbol{\omega}_2 \times {}^1\mathbf{r}\right) \\
&= {}^0R_1\, _1\boldsymbol{\omega}_2 \times {}^0R_1\, ^1\mathbf{r} \\
&= {}_1^0\boldsymbol{\omega}_2 \times {}^0\mathbf{r} \qquad (5.244)
\end{aligned}$$

*which is equal to the right-hand side after applying on the vector $^0\mathbf{r}$*

$$_1^0\tilde{\omega}_2\, ^0\mathbf{r} = {}_1^0\boldsymbol{\omega}_2 \times {}^0\mathbf{r}. \qquad (5.245)$$

**Example 179 ★** *Time derivative of unit vectors.*

*Using Equation (5.186) we can define the time derivative of unit vectors of a body coordinate frame $B(\hat{\imath}, \hat{\jmath}, \hat{k})$, rotating in the global coordinate frame $G(\hat{I}, \hat{J}, \hat{K})$*

$$\frac{^Gd\hat{\imath}}{dt} = {}_G^B\boldsymbol{\omega}_B \times \hat{\imath} \qquad (5.246)$$

$$\frac{^Gd\hat{\jmath}}{dt} = {}_G^B\boldsymbol{\omega}_B \times \hat{\jmath} \qquad (5.247)$$

$$\frac{^Gd\hat{k}}{dt} = {}_G^B\boldsymbol{\omega}_B \times \hat{k}. \qquad (5.248)$$

**Example 180 ★** *Elements of the angular velocity matrix.*
   *Utilizing the **permutation symbol***

$$\epsilon_{ijk} = \frac{1}{2}(i-j)(j-k)(k-i) \quad , \quad i,j,k = 1,2,3 \tag{5.249}$$

*allows us to find the elements of the angular velocity matrix, $\tilde{\omega}$, when the angular velocity vector, $\boldsymbol{\omega} = \begin{bmatrix} \omega_1 & \omega_2 & \omega_3 \end{bmatrix}^T$, is given.*

$$\tilde{\omega}_{ij} = \epsilon_{ijk}\,\omega_k \tag{5.250}$$

*We may verify that following relationship between permutation symbol $\epsilon_{ijk}$ and Kronecker's delta $\delta_{mn}$.*

$$\epsilon_{ijk}\epsilon_{imn} = \delta_{jm}\delta_{kn} - \delta_{jn}\delta_{km} \tag{5.251}$$

# 5.8  ★ Time Derivative and Coordinate Frames

The time derivative of a vector depends on the coordinate frame in which we are taking the derivative. The time derivative of a vector $\mathbf{r}$ in the global frame is called the *G-derivative* and is denoted by

$$\frac{^G d}{dt}\mathbf{r}$$

while the time derivative of the vector in the body frame is called the *B-derivative* and is denoted by

$$\frac{^B d}{dt}\mathbf{r}.$$

The left superscript on the derivative symbol indicates the frame in which the derivative is taken, and hence, its unit vectors are considered constant.
   Time derivative is straightforward if the vector is expressed in the same coordinate frame that we are taking the derivative, because the unit vectors are constant and scalar coefficients are the only time variables. The derivatives of $^B\mathbf{r}_P$ in $B$ and $^G\mathbf{r}_P$ in $G$ are

$$\frac{^B d}{dt}\,^B\mathbf{r}_P \quad = \quad ^B\dot{\mathbf{r}}_P = \,^B\mathbf{v}_P = \dot{x}\,\hat{\imath} + \dot{y}\,\hat{\jmath} + \dot{z}\,\hat{k} \tag{5.252}$$

$$\frac{^G d}{dt}\,^G\mathbf{r}_P \quad = \quad ^G\dot{\mathbf{r}}_P = \,^G\mathbf{v}_P = \dot{X}\,\hat{I} + \dot{Y}\,\hat{J} + \dot{Z}\,\hat{K}. \tag{5.253}$$

It is also possible to find the *G*-derivative of $^B\mathbf{r}_P$ and the *B*-derivative of $^G\mathbf{r}_P$. We define the *G*-derivative of a body vector $^B\mathbf{r}_P$ by

$$^B_G\mathbf{v}_P = \frac{^G d}{dt}\,^B\mathbf{r}_P \tag{5.254}$$

and similarly, a $B$-derivative of a global vector $^G\mathbf{r}_P$ by

$$_B^G\mathbf{v}_P = \frac{^Bd}{dt} {}^G\mathbf{r}_P. \tag{5.255}$$

When point $P$ is moving in frame $B$ while $B$ is rotating in $G$, the $G$-derivative of $^B\mathbf{r}_P(t)$ is defined by

$$
\begin{aligned}
\frac{^Gd}{dt} {}^B\mathbf{r}_P(t) &= {}^B\dot{\mathbf{r}}_P + {}_G^B\boldsymbol{\omega}_B \times {}^B\mathbf{r}_P \\
&= {}_G^B\dot{\mathbf{r}}_P \tag{5.256}
\end{aligned}
$$

and the $B$-derivative of $^G\mathbf{r}_P$ is defined by

$$
\begin{aligned}
\frac{^Bd}{dt} {}^G\mathbf{r}_P(t) &= {}^G\dot{\mathbf{r}}_P - {}_G\boldsymbol{\omega}_B \times {}^G\mathbf{r}_P \\
&= {}_B^G\dot{\mathbf{r}}_P. \tag{5.257}
\end{aligned}
$$

**Proof.** Let $G(OXYZ)$ with unit vectors $\hat{I}$, $\hat{J}$, and $\hat{K}$ be the global coordinate frame, and let $B(Oxyz)$ with unit vectors $\hat{i}$, $\hat{j}$, and $\hat{k}$ be a body coordinate frame. The position vector of a moving point $P$, as shown in Figure 5.10, can be expressed in the body and global frames

$$
\begin{aligned}
^B\mathbf{r}_P(t) &= x(t)\,\hat{i} + y(t)\,\hat{j} + z(t)\,\hat{k} \tag{5.258} \\
^G\mathbf{r}_P(t) &= X(t)\,\hat{I} + Y(t)\,\hat{J} + Z(t)\,\hat{K}. \tag{5.259}
\end{aligned}
$$

The time derivative of $^B\mathbf{r}_P$ in $B$ and $^G\mathbf{r}_P$ in $G$ are

$$
\frac{^Bd}{dt} {}^B\mathbf{r}_P = {}^B\dot{\mathbf{r}}_P = {}^B\mathbf{v}_P = \dot{x}\,\hat{i} + \dot{y}\,\hat{j} + \dot{z}\,\hat{k} \tag{5.260}
$$

$$
\frac{^Gd}{dt} {}^G\mathbf{r}_P = {}^G\dot{\mathbf{r}}_P = {}^G\mathbf{v}_P = \dot{X}\,\hat{I} + \dot{Y}\,\hat{J} + \dot{Z}\,\hat{K} \tag{5.261}
$$

because the unit vectors of $B$ in Equation (5.258) and the unit vectors of $G$ in Equation (5.259) are considered constant.

Using Equation (5.186) for the global velocity of a body fixed point $P$, expressed in body frame

$$
\begin{aligned}
_G^B\mathbf{v}_P &= {}_G^B\boldsymbol{\omega}_B \times {}^B\mathbf{r}_P \\
&= \frac{^Gd}{dt} {}^B\mathbf{r}_P \tag{5.262}
\end{aligned}
$$

and definition (5.254), we can find the $G$-derivative of the position vector
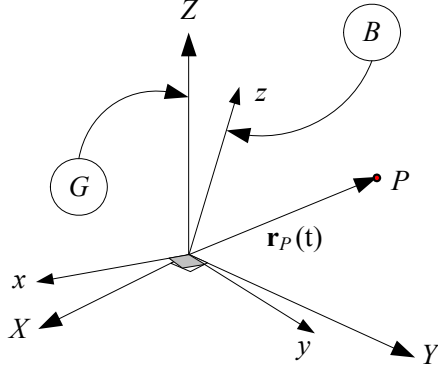
FIGURE 5.10. A moving body point $P$ at $^B\mathbf{r}(t)$ in the rotating body frame $B$.

$^B\mathbf{r}_P$ as

$$
\begin{aligned}
\frac{^Gd}{dt}\,^B\mathbf{r}_P &= \frac{^Gd}{dt}\left(x\hat{\imath} + y\hat{\jmath} + z\hat{k}\right) \\
&= \dot{x}\,\hat{\imath} + \dot{y}\,\hat{\jmath} + \dot{z}\,\hat{k} + x\frac{^Gd\hat{\imath}}{dt} + y\frac{^Gd\hat{\jmath}}{dt} + z\frac{^Gd\hat{k}}{dt} \\
&= {}^B\dot{\mathbf{r}}_P + x\,_G^B\boldsymbol{\omega}_B \times \hat{\imath} + y\,_G^B\boldsymbol{\omega}_B \times \hat{\jmath} + z\,_G^B\boldsymbol{\omega}_B \times \hat{k} \\
&= {}^B\dot{\mathbf{r}}_P + {}_G^B\boldsymbol{\omega}_B \times \left(x\hat{\imath} + y\hat{\jmath} + z\hat{k}\right) \\
&= {}^B\dot{\mathbf{r}}_P + {}_G^B\boldsymbol{\omega}_B \times {}^B\mathbf{r}_P \\
&= \frac{^Bd}{dt}\,^B\mathbf{r}_P + {}_G^B\boldsymbol{\omega}_B \times {}^B\mathbf{r}_P.
\end{aligned}
\tag{5.263}
$$

We achieved this result because the $x$, $y$, and $z$ components of $^B\mathbf{r}_P$ are scalar. Scalars are invariant with respect to frame transformations. Therefore, if $x$ is a scalar then,

$$
\frac{^Gd}{dt}x = \frac{^Bd}{dt}x = \dot{x}.
\tag{5.264}
$$

The $B$-derivative of $^G\mathbf{r}_P$ can be found similarly

$$
\begin{aligned}
\frac{^Bd}{dt}\,^G\mathbf{r}_P &= \frac{^Bd}{dt}\left(X\hat{I} + Y\hat{J} + Z\hat{K}\right) \\
&= \dot{X}\,\hat{I} + \dot{Y}\,\hat{J} + \dot{Z}\,\hat{K} + X\frac{^Bd\hat{I}}{dt} + Y\frac{^Bd\hat{J}}{dt} + Z\frac{^Bd\hat{K}}{dt} \\
&= {}^G\dot{\mathbf{r}}_P + {}_B^G\boldsymbol{\omega}_G \times {}^G\mathbf{r}_P
\end{aligned}
\tag{5.265}
$$

and therefore,

$$
\frac{^Bd}{dt}\,^G\mathbf{r}_P = {}^G\dot{\mathbf{r}}_P - {}_G\boldsymbol{\omega}_B \times {}^G\mathbf{r}_P.
\tag{5.266}
$$

The angular velocity of $B$ relative to $G$ is a vector quantity and can be expressed in either frames.

$$\begin{aligned}
{}_{G}^{G}\boldsymbol{\omega}_B &= \omega_X \hat{I} + \omega_Y \hat{J} + \omega_Z \hat{K} & (5.267)\\
{}_{G}^{B}\boldsymbol{\omega}_B &= \omega_x \hat{i} + \omega_y \hat{j} + \omega_z \hat{k}. & (5.268)
\end{aligned}$$

∎

**Example 181 ★** *Time derivative of a moving point in B.*
*Consider a local frame $B$, rotating in $G$ by $\dot\alpha$ about the $Z$-axis, and a moving point at ${}^{B}\mathbf{r}_P(t) = t\hat{i}$ . Therefore,*

$$\begin{aligned}
{}^{G}\mathbf{r}_P &= {}^{G}R_B\,{}^{B}\mathbf{r}_P = R_{Z,\alpha}(t)\,{}^{B}\mathbf{r}_P\\
&= \begin{bmatrix} \cos\alpha & -\sin\alpha & 0 \\ \sin\alpha & \cos\alpha & 0 \\ 0 & 0 & 1 \end{bmatrix} \begin{bmatrix} t \\ 0 \\ 0 \end{bmatrix}\\
&= t\cos\alpha\hat{I} + t\sin\alpha\hat{J}. & (5.269)
\end{aligned}$$

*The angular velocity matrix is*

$$\begin{aligned}
{}_{G}\tilde{\omega}_B &= {}^{G}\dot{R}_B\,{}^{G}R_B^{T}\\
&= \dot\alpha\hat{K} & (5.270)
\end{aligned}$$

*that gives*

$$_{G}\boldsymbol{\omega}_B = \dot\alpha\hat{K}. \qquad (5.271)$$

*It can also be verified that*

$$\begin{aligned}
{}_{G}^{B}\tilde{\omega}_B &= {}^{G}R_B^{T}\,{}_{G}^{G}\tilde{\omega}_B\,{}^{G}R_B\\
&= \dot\alpha\tilde{k} & (5.272)
\end{aligned}$$

*and therefore,*

$$_{G}^{B}\boldsymbol{\omega}_B = \dot\alpha\hat{k}. \qquad (5.273)$$

*Now we can find the following derivatives:*

$$\begin{aligned}
\frac{{}^{B}d}{dt}\,{}^{B}\mathbf{r}_P &= {}^{B}\dot{\mathbf{r}}_P\\
&= \hat{i} & (5.274)
\end{aligned}$$

$$\begin{aligned}
\frac{{}^{G}d}{dt}\,{}^{G}\mathbf{r}_P &= {}^{G}\dot{\mathbf{r}}_P\\
&= (\cos\alpha - t\dot\alpha\sin\alpha)\,\hat{I} + (\sin\alpha + t\dot\alpha\cos\alpha)\,\hat{J}. & (5.275)
\end{aligned}$$

*For the mixed derivatives, we start with*

$$
\begin{aligned}
\frac{{}^{G}d}{dt}\,{}^{B}\mathbf{r}_P &= \frac{{}^{B}d}{dt}\,{}^{B}\mathbf{r}_P + {}^{B}_{G}\boldsymbol{\omega}_B \times {}^{B}\mathbf{r}_P \\[2mm]
&= \begin{bmatrix} 1 \\ 0 \\ 0 \end{bmatrix} + \dot{\alpha} \begin{bmatrix} 0 \\ 0 \\ 1 \end{bmatrix} \times \begin{bmatrix} t \\ 0 \\ 0 \end{bmatrix} \\[2mm]
&= \begin{bmatrix} 1 \\ t\dot{\alpha} \\ 0 \end{bmatrix} = \hat{\imath} + t\dot{\alpha}\hat{\jmath} = {}^{B}_{G}\dot{\mathbf{r}}_P
\end{aligned}
\tag{5.276}
$$

*which is the global velocity of $P$ expressed in $B$. We may, however, transform ${}^{B}_{G}\dot{\mathbf{r}}_P$ to the global frame and find the global velocity expressed in $G$.*

$$
\begin{aligned}
{}^{G}\dot{\mathbf{r}}_P &= {}^{G}R_B\,{}^{B}_{G}\dot{\mathbf{r}}_P \\[2mm]
&= \begin{bmatrix} \cos\alpha & -\sin\alpha & 0 \\ \sin\alpha & \cos\alpha & 0 \\ 0 & 0 & 1 \end{bmatrix} \begin{bmatrix} 1 \\ t\dot{\alpha} \\ 0 \end{bmatrix} \\[2mm]
&= \begin{bmatrix} \cos\alpha - t\dot{\alpha}\sin\alpha \\ \sin\alpha + t\dot{\alpha}\cos\alpha \\ 0 \end{bmatrix} \\[2mm]
&= (\cos\alpha - t\dot{\alpha}\sin\alpha)\,\hat{I} + (\sin\alpha + t\dot{\alpha}\cos\alpha)\,\hat{J}
\end{aligned}
\tag{5.277}
$$

*The next derivative is*

$$
\begin{aligned}
\frac{{}^{B}d}{dt}\,{}^{G}\mathbf{r}_P &= {}^{G}\dot{\mathbf{r}}_P - {}_{G}\boldsymbol{\omega}_B \times {}^{G}\mathbf{r}_P \\[2mm]
&= \begin{bmatrix} \cos\alpha - t\dot{\alpha}\sin\alpha \\ \sin\alpha + t\dot{\alpha}\cos\alpha \\ 0 \end{bmatrix} - \dot{\alpha}\begin{bmatrix} 0 \\ 0 \\ 1 \end{bmatrix} \times \begin{bmatrix} t\cos\alpha \\ t\sin\alpha \\ 0 \end{bmatrix} \\[2mm]
&= \begin{bmatrix} \cos\alpha \\ \sin\alpha \\ 0 \end{bmatrix} = (\cos\alpha)\,\hat{I} + (\sin\alpha)\,\hat{J} \\[2mm]
&= {}^{G}_{B}\dot{\mathbf{r}}_P
\end{aligned}
\tag{5.278}
$$

*which is the velocity of $P$ relative to $B$ and expressed in $G$. To express this velocity in $B$ we apply a frame transformation*

$$
\begin{aligned}
{}^{B}\dot{\mathbf{r}}_P &= {}^{G}R_B^{T}\,{}^{G}_{B}\dot{\mathbf{r}}_P \\[2mm]
&= \begin{bmatrix} \cos\alpha & -\sin\alpha & 0 \\ \sin\alpha & \cos\alpha & 0 \\ 0 & 0 & 1 \end{bmatrix}^{T} \begin{bmatrix} \cos\alpha \\ \sin\alpha \\ 0 \end{bmatrix} \\[2mm]
&= \begin{bmatrix} 1 \\ 0 \\ 0 \end{bmatrix} = \hat{\imath}.
\end{aligned}
\tag{5.279}
$$

*Sometimes it is more applied if we transform the vector to the same frame in which we are taking the derivative and then apply the differential operator. Therefore,*

$$\frac{^Gd}{dt}\,^B\mathbf{r}_P \quad = \quad \frac{^Gd}{dt}\left(^GR_B\,^B\mathbf{r}_P\right) = \frac{^Gd}{dt}\begin{bmatrix} t\cos\alpha \\ t\sin\alpha \\ 0 \end{bmatrix}$$

$$= \quad \begin{bmatrix} \cos\alpha - t\dot\alpha\sin\alpha \\ \sin\alpha + t\dot\alpha\cos\alpha \\ 0 \end{bmatrix} \tag{5.280}$$

*and*

$$\frac{^Bd}{dt}\,^G\mathbf{r}_P \quad = \quad \frac{^Bd}{dt}\left(^GR_B^T\,^G\mathbf{r}_P\right)$$

$$= \quad \frac{^Bd}{dt}\begin{bmatrix} t \\ 0 \\ 0 \end{bmatrix} = \begin{bmatrix} 1 \\ 0 \\ 0 \end{bmatrix}. \tag{5.281}$$

**Example 182 ★** *Orthogonality of position and velocity vectors.*
   *If the position vector of a body point in global frame is denoted by* $\mathbf{r}$ *then*

$$\frac{d\mathbf{r}}{dt}\cdot\mathbf{r} = 0. \tag{5.282}$$

*To show this property we may take a derivative from*

$$\mathbf{r}\cdot\mathbf{r} = r^2 \tag{5.283}$$

*and find*

$$\frac{d}{dt}(\mathbf{r}\cdot\mathbf{r}) \quad = \quad \frac{d\mathbf{r}}{dt}\cdot\mathbf{r} + \mathbf{r}\cdot\frac{d\mathbf{r}}{dt}$$

$$= \quad 2\frac{d\mathbf{r}}{dt}\cdot\mathbf{r}$$

$$= \quad 0. \tag{5.284}$$

*Equation (5.282) is correct in every coordinate frame and for every constant length vector, as long as the vector and the derivative are expressed in the same coordinate frame.*

**Example 183 ★** *Derivative transformation formula.*
   *The global velocity of a fixed point in the body coordinate frame* $B\,(Oxyz)$ *can be found by Equation (5.172). Now consider a point* $P$ *that can move in* $B\,(Oxyz)$. *In this case, the body position vector* $^B\mathbf{r}_P$ *is not constant, and therefore, the global velocity of such a point expressed in* $B$ *is*

$$\frac{^Gd}{dt}\,^B\mathbf{r}_P \quad = \quad \frac{^Bd}{dt}\,^B\mathbf{r}_P + \,_G^B\boldsymbol{\omega}_B \times\,^B\mathbf{r}_P \tag{5.285}$$

$$= \quad \,_G^B\dot{\mathbf{r}}_P. \tag{5.286}$$

*Sometimes the result of Equation (5.285) is utilized to define transformation of the differential operator from a body to a global coordinate frame*

$$\frac{{}^Gd}{dt}\Box \quad = \quad \frac{{}^Bd}{dt}\Box + {}^B_G\boldsymbol{\omega}_B \times {}^B\Box \tag{5.287}$$

$$= \quad {}^B_G\dot{\Box} \tag{5.288}$$

*however, special attention must be paid to the coordinate frame in which the vector $\Box$ and the final result are expressed. The final result is ${}^B_G\dot{\Box}$ showing the global $(G)$ time derivative expressed in body frame $(B)$. The vector $\Box$ might be any vector such as position, velocity, angular velocity, momentum, angular velocity, or even a time-varying force vector.*

*Equation (5.287) is called the **derivative transformation formula** and relates the time derivative of a vector as it would be seen from frame $G$ to its derivative as seen in frame $B$. The derivative transformation formula (5.287) is more general and can be applied to every vector for derivative transformation between every two relatively moving coordinate frames.*

**Example 184 ★** *Differential equation for rotation matrix.*

*Equation (5.175) for defining the angular velocity matrix may be written as a first-order differential equation*

$$\frac{d}{dt}{}^GR_B - {}^GR_B\,{}_G\tilde{\omega}_B = 0. \tag{5.289}$$

*The solution of the equation confirms the exponential definition of the rotation matrix as*

$$^GR_B = e^{\tilde{\omega}t} \tag{5.290}$$

*or*

$$\tilde{\omega}t \quad = \quad \dot{\phi}\tilde{u}$$
$$= \quad \ln\left({}^GR_B\right). \tag{5.291}$$

**Example 185 ★** *Acceleration of a body point in the global frame.*

*The angular acceleration vector of a rigid body $B(Oxyz)$ in the global frame $G(OXYZ)$ is denoted by ${}_G\boldsymbol{\alpha}_B$ and is defined as the global time derivative of ${}_G\boldsymbol{\omega}_B$.*

$$_G\boldsymbol{\alpha}_B = \frac{{}^Gd}{dt}\,{}_G\boldsymbol{\omega}_B \tag{5.292}$$

*Using this definition, the acceleration of a fixed body point in the global frame is*

$$^G\mathbf{a}_P \quad = \quad \frac{{}^Gd}{dt}\left({}_G\boldsymbol{\omega}_B \times {}^G\mathbf{r}_P\right)$$
$$= \quad {}_G\boldsymbol{\alpha}_B \times {}^G\mathbf{r}_P + {}_G\boldsymbol{\omega}_B \times \left({}_G\boldsymbol{\omega}_B \times {}^G\mathbf{r}_P\right). \tag{5.293}$$
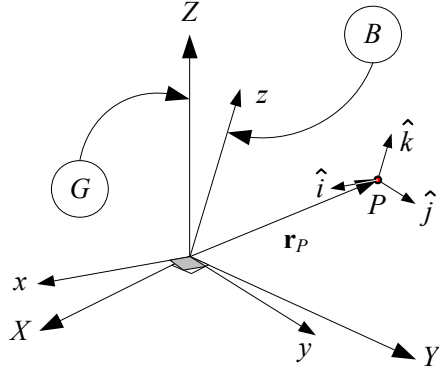
FIGURE 5.11. A body coordinate frame moving with a fixed point in the global coordinate frame.

**Example 186 ★** *Alternative definition of angular velocity vector.*
    *The angular velocity vector of a rigid body $B(\hat{\imath}, \hat{\jmath}, \hat{k})$ in global frame $G(\hat{I}, \hat{J}, \hat{K})$ can also be defined by*

$$
{}_{G}^{B}\boldsymbol{\omega}_B = \hat{\imath}(\frac{{}^G d\hat{\jmath}}{dt} \cdot \hat{k}) + \hat{\jmath}(\frac{{}^G d\hat{k}}{dt} \cdot \hat{\imath}) + \hat{k}(\frac{{}^G d\hat{\imath}}{dt} \cdot \hat{\jmath}). \tag{5.294}
$$

**Proof.** *Consider a body coordinate frame $B$ moving with a fixed point in the global coordinate frame $G$. The fixed point of the body is taken as the origin of both coordinate frames, as shown in Figure 5.11. To describe the motion of the body, it is sufficient to describe the motion of the local unit vectors $\hat{\imath}$, $\hat{\jmath}$, $\hat{k}$ . Let $\mathbf{r}_P$ be the position vector of a body point $P$. Then, ${}^B\mathbf{r}_P$ is a vector with constant components.*

$$
{}^B\mathbf{r}_P = x\hat{\imath} + y\hat{\jmath} + z\hat{k} \tag{5.295}
$$

*When the body moves, it is only the unit vectors $\hat{\imath}$, $\hat{\jmath}$, and $\hat{k}$ that vary relative to the global coordinate frame. Therefore, the vector of differential displacement is*

$$
d\mathbf{r}_P = x \, d\hat{\imath} + y \, d\hat{\jmath} + z \, d\hat{k} \tag{5.296}
$$

*which can also be expressed by*

$$
d\mathbf{r}_P = (d\mathbf{r}_P \cdot \hat{\imath}) \, \hat{\imath} + (d\mathbf{r}_P \cdot \hat{\jmath}) \, \hat{\jmath} + \left(d\mathbf{r}_P \cdot \hat{k}\right) \hat{k}. \tag{5.297}
$$

*Substituting (5.296) in the right-hand side of (5.297) results in*

$$
\begin{aligned}
d\mathbf{r}_P &= \left(x\hat{\imath} \cdot d\hat{\imath} + y\hat{\imath} \cdot d\hat{\jmath} + z\hat{\imath} \cdot d\hat{k}\right) \hat{\imath} \\
&\quad + \left(x\hat{\jmath} \cdot d\hat{\imath} + y\hat{\jmath} \cdot d\hat{\jmath} + z\hat{\jmath} \cdot d\hat{k}\right) \hat{\jmath} \\
&\quad + \left(x\hat{k} \cdot d\hat{\imath} + y\hat{k} \cdot d\hat{\jmath} + z\hat{k} \cdot d\hat{k}\right) \hat{k}.
\end{aligned} \tag{5.298}
$$

*Utilizing the unit vectors' relationships*

$$\hat{j} \cdot d\hat{i} = -\hat{i} \cdot d\hat{j} \tag{5.299}$$

$$\hat{k} \cdot d\hat{j} = -\hat{j} \cdot d\hat{k} \tag{5.300}$$

$$\hat{i} \cdot d\hat{k} = -\hat{k} \cdot d\hat{i} \tag{5.301}$$

$$\hat{i} \cdot d\hat{i} = \hat{j} \cdot d\hat{j} = \hat{k} \cdot d\hat{k} = 0 \tag{5.302}$$

$$\hat{i} \cdot \hat{j} = \hat{j} \cdot \hat{k} = \hat{k} \cdot \hat{i} = 0 \tag{5.303}$$

$$\hat{i} \cdot \hat{i} = \hat{j} \cdot \hat{j} = \hat{k} \cdot \hat{k} = 1 \tag{5.304}$$

*the $d\mathbf{r}_P$ reduces to*

$$\begin{aligned} d\mathbf{r}_P = & \left( z\hat{i} \cdot d\hat{k} - y\hat{j} \cdot d\hat{i} \right) \hat{i} \\ & + \left( x\hat{j} \cdot d\hat{i} - z\hat{k} \cdot d\hat{j} \right) \hat{j} \\ & + \left( y\hat{k} \cdot d\hat{j} - x\hat{i} \cdot d\hat{k} \right) \hat{k}. \end{aligned} \tag{5.305}$$

*This equation can be rearranged to be expressed as a vector product*

$$d\mathbf{r}_P = \left( (\hat{k} \cdot d\hat{j})\hat{i} + (\hat{i} \cdot d\hat{k})\hat{j} + (\hat{j} \cdot d\hat{i})\hat{k} \right) \times \left( x\hat{i} + y\hat{j} + z\hat{k} \right) \tag{5.306}$$

*or*

$$_G^B \dot{\mathbf{r}}_P = \left( (\hat{k} \cdot \frac{^G d\hat{j}}{dt})\hat{i} + (\hat{i} \cdot \frac{^G d\hat{k}}{dt})\hat{j} + (\hat{j} \cdot \frac{^G d\hat{i}}{dt})\hat{k} \right) \times \left( x\hat{i} + y\hat{j} + z\hat{k} \right). \tag{5.307}$$

*Comparing this result with*

$$\dot{\mathbf{r}}_P = {}_G\boldsymbol{\omega}_B \times \mathbf{r}_P \tag{5.308}$$

*shows that*

$$_G^B \boldsymbol{\omega}_B = \hat{i} \left( \frac{^G d\hat{j}}{dt} \cdot \hat{k} \right) + \hat{j} \left( \frac{^G d\hat{k}}{dt} \cdot \hat{i} \right) + \hat{k} \left( \frac{^G d\hat{i}}{dt} \cdot \hat{j} \right). \tag{5.309}$$

■

**Example 187** ★ *Alternative proof for angular velocity definition (5.294).*

*The angular velocity definition presented in Equation (5.294) can also be shown by direct substitution for $^G R_B$ in the angular velocity matrix $_G^B \tilde{\omega}_B$*

$$_G^B \tilde{\omega}_B = {}^G R_B^T \, {}^G \dot{R}_B. \tag{5.310}$$

*Therefore,*

$$
{}^B_G\tilde{\omega}_B = 
\begin{bmatrix}
\hat{i}\cdot\hat{I} & \hat{i}\cdot\hat{J} & \hat{i}\cdot\hat{K} \\
\hat{j}\cdot\hat{I} & \hat{j}\cdot\hat{J} & \hat{j}\cdot\hat{K} \\
\hat{k}\cdot\hat{I} & \hat{k}\cdot\hat{J} & \hat{k}\cdot\hat{K}
\end{bmatrix}
\cdot \frac{{}^Gd}{dt}
\begin{bmatrix}
\hat{I}\cdot\hat{i} & \hat{I}\cdot\hat{j} & \hat{I}\cdot\hat{k} \\
\hat{J}\cdot\hat{i} & \hat{J}\cdot\hat{j} & \hat{J}\cdot\hat{k} \\
\hat{K}\cdot\hat{i} & \hat{K}\cdot\hat{j} & \hat{K}\cdot\hat{k}
\end{bmatrix}
$$

$$
=
\begin{bmatrix}
\left(\hat{i}\cdot\dfrac{{}^Gd\hat{i}}{dt}\right) & \left(\hat{i}\cdot\dfrac{{}^Gd\hat{j}}{dt}\right) & \left(\hat{i}\cdot\dfrac{{}^Gd\hat{k}}{dt}\right) \\[4mm]
\left(\hat{j}\cdot\dfrac{{}^Gd\hat{i}}{dt}\right) & \left(\hat{j}\cdot\dfrac{{}^Gd\hat{j}}{dt}\right) & \left(\hat{j}\cdot\dfrac{{}^Gd\hat{k}}{dt}\right) \\[4mm]
\left(\hat{k}\cdot\dfrac{{}^Gd\hat{i}}{dt}\right) & \left(\hat{k}\cdot\dfrac{{}^Gd\hat{j}}{dt}\right) & \left(\hat{k}\cdot\dfrac{{}^Gd\hat{k}}{dt}\right)
\end{bmatrix}
\tag{5.311}
$$

*which shows that*

$$
{}^B_G\boldsymbol{\omega}_B =
\begin{bmatrix}
\left(\dfrac{{}^Gd\hat{j}}{dt}\cdot\hat{k}\right) \\[4mm]
\left(\dfrac{{}^Gd\hat{k}}{dt}\cdot\hat{i}\right) \\[4mm]
\left(\dfrac{{}^Gd\hat{i}}{dt}\cdot\hat{j}\right)
\end{bmatrix}.
\tag{5.312}
$$

**Example 188 ★** *Second derivative.*
   In general, ${}^Gd\mathbf{r}/dt$ *is a variable vector in* $G(OXYZ)$ *and in any other coordinate frame such as* $B\,(oxyz)$. *Therefore, it can be differentiated in either coordinate frames* $G$ *or* $B$. *However, the order of differentiating is important. In general,*

$$
\frac{{}^Bd}{dt}\frac{{}^Gd\mathbf{r}}{dt} \neq \frac{{}^Gd}{dt}\frac{{}^Bd\mathbf{r}}{dt}.
\tag{5.313}
$$

*As an example, consider a rotating body coordinate frame about the* $Z$*-axis, and a variable vector as*

$$
{}^G\mathbf{r} = t\hat{I}.
\tag{5.314}
$$

*Therefore,*

$$
\frac{{}^Gd\mathbf{r}}{dt} = {}^G\dot{\mathbf{r}} = \hat{I}
\tag{5.315}
$$

*and hence,*

$$
\begin{aligned}
{}^B\left(\frac{{}^Gd\mathbf{r}}{dt}\right) &= {}^B_G\dot{\mathbf{r}} = R^T_{Z,\varphi}\left[\hat{I}\right] \\
&=
\begin{bmatrix}
\cos\varphi & \sin\varphi & 0 \\
-\sin\varphi & \cos\varphi & 0 \\
0 & 0 & 1
\end{bmatrix}
\begin{bmatrix}
1 \\ 0 \\ 0
\end{bmatrix} \\
&= \cos\varphi\hat{i} - \sin\varphi\hat{j}
\end{aligned}
\tag{5.316}
$$

*which provides*

$$\frac{{}^B d}{dt}\frac{{}^G d\mathbf{r}}{dt} = -\dot\varphi \sin\varphi\hat{\imath} - \dot\varphi\cos\varphi\hat{\jmath} \tag{5.317}$$

*and*

$$G\left(\frac{{}^B d}{dt}\frac{{}^G d\mathbf{r}}{dt}\right) = -\dot\varphi\hat{J}. \tag{5.318}$$

*Now*

$$^B\mathbf{r} = R_{Z,\varphi}^T\left[t\hat{I}\right] = t\cos\varphi\hat{\imath} - t\sin\varphi\hat{\jmath} \tag{5.319}$$

*that provides*

$$\frac{{}^B d\mathbf{r}}{dt} = \left(-t\dot\varphi\sin\varphi + \cos\varphi\right)\hat{\imath} - \left(\sin\varphi + t\dot\varphi\cos\varphi\right)\hat{\jmath} \tag{5.320}$$

*and*

$$\begin{aligned}
G\left(\frac{{}^B d\mathbf{r}}{dt}\right) &= {}^G_B\dot{\mathbf{r}} \\
&= R_{Z,\varphi}\left(\left(-t\dot\varphi\sin\varphi + \cos\varphi\right)\hat{\imath} - \left(\sin\varphi + t\dot\varphi\cos\varphi\right)\hat{\jmath}\right) \\
&= \begin{bmatrix} \cos\varphi & -\sin\varphi & 0 \\ \sin\varphi & \cos\varphi & 0 \\ 0 & 0 & 1 \end{bmatrix}\begin{bmatrix} -t\dot\varphi\sin\varphi + \cos\varphi \\ -\sin\varphi - t\dot\varphi\cos\varphi \\ 0 \end{bmatrix} \\
&= \hat{I} - t\dot\varphi\hat{J} \tag{5.321}
\end{aligned}$$

*which shows*

$$\begin{aligned}
\frac{{}^G d}{dt}\frac{{}^B d\mathbf{r}}{dt} &= -\left(\dot\varphi + t\ddot\varphi\right)\hat{J} \tag{5.322} \\
&\neq \frac{{}^B d}{dt}\frac{{}^G d\mathbf{r}}{dt}.
\end{aligned}$$

## 5.9   Rigid Body Velocity

Consider a rigid body with an attached local coordinate frame $B\,(oxyz)$ moving freely in a fixed global coordinate frame $G(OXYZ)$, as shown in Figure 5.12. The rigid body can rotate in the global frame, while the origin of the body frame $B$ can translate relative to the origin of $G$. The coordinates of a body point $P$ in local and global frames are related by the following equation:

$$^G\mathbf{r}_P = {}^GR_B\,{}^B\mathbf{r}_P + {}^G\mathbf{d}_B \tag{5.323}$$

where ${}^G\mathbf{d}_B$ indicates the position of the moving origin $o$ relative to the fixed origin $O$.
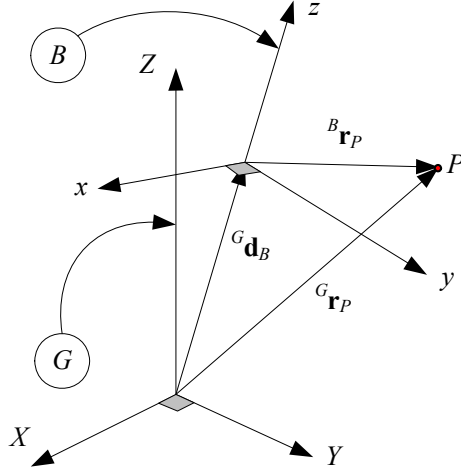
FIGURE 5.12. A rigid body with an attached coordinate frame $B\,(oxyz)$ moving freely in a global coordinate frame $G(OXYZ)$.

The velocity of the point $P$ in $G$ is

$$
\begin{aligned}
{}^G\mathbf{v}_P \;&=\; {}^G\dot{\mathbf{r}}_P \\
&=\; {}^G\dot{R}_B\,{}^B\mathbf{r}_P + {}^G\dot{\mathbf{d}}_B \\
&=\; {}_G\tilde{\omega}_B\,{}^G_B\mathbf{r}_P + {}^G\dot{\mathbf{d}}_B \\
&=\; {}_G\tilde{\omega}_B\left({}^G\mathbf{r}_P - {}^G\mathbf{d}_B\right) + {}^G\dot{\mathbf{d}}_B \\
&=\; {}_G\boldsymbol{\omega}_B \times \left({}^G\mathbf{r}_P - {}^G\mathbf{d}_B\right) + {}^G\dot{\mathbf{d}}_B.
\end{aligned}
\tag{5.324}
$$

**Proof.** Direct differentiating shows

$$
\begin{aligned}
{}^G\mathbf{v}_P \;&=\; \frac{{}^Gd}{dt}\,{}^G\mathbf{r}_P = {}^G\dot{\mathbf{r}}_P \\
&=\; \frac{{}^Gd}{dt}\left({}^GR_B\,{}^B\mathbf{r}_P + {}^G\mathbf{d}_B\right) \\
&=\; {}^G\dot{R}_B\,{}^B\mathbf{r}_P + {}^G\dot{\mathbf{d}}_B.
\end{aligned}
\tag{5.325}
$$

The local position vector ${}^B\mathbf{r}_P$ can be substituted from (5.323) to obtain

$$
\begin{aligned}
{}^G\mathbf{v}_P \;&=\; {}^G\dot{R}_B\,{}^GR_B^T\left({}^G\mathbf{r}_P - {}^G\mathbf{d}_B\right) + {}^G\dot{\mathbf{d}}_B \\
&=\; {}_G\tilde{\omega}_B\left({}^G\mathbf{r}_P - {}^G\mathbf{d}_B\right) + {}^G\dot{\mathbf{d}}_B \\
&=\; {}_G\boldsymbol{\omega}_B \times \left({}^G\mathbf{r}_P - {}^G\mathbf{d}_B\right) + {}^G\dot{\mathbf{d}}_B.
\end{aligned}
\tag{5.326}
$$

It may also be written using relative position vector

$$
{}^G\mathbf{v}_P = {}_G\boldsymbol{\omega}_B \times {}^G_B\mathbf{r}_P + {}^G\dot{\mathbf{d}}_B.
\tag{5.327}
$$

∎
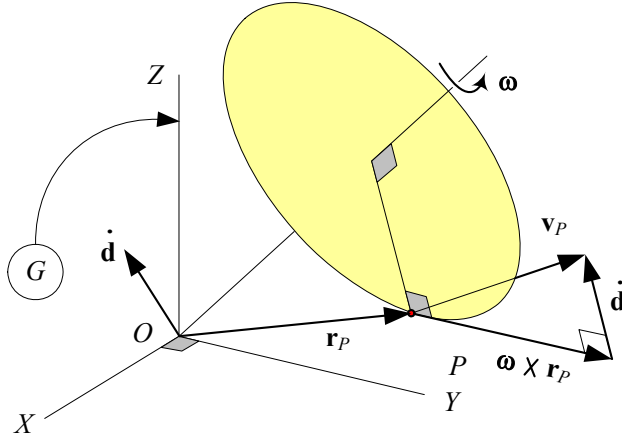
FIGURE 5.13. Geometric interpretation of rigid body velocity.

**Example 189** *Geometric interpretation of rigid body velocity.*

*Figure 5.13 illustrates a body point $P$ of a moving rigid body. The global velocity of point $P$*

$$^G\mathbf{v}_P = {}_G\boldsymbol{\omega}_B \times {}_B^G\mathbf{r}_P + {}^G\dot{\mathbf{d}}_B$$

*is a vector addition of rotational and translational velocities, both expressed in the global frame. At the moment, the body frame is assumed to be coincident with the global frame, and the body frame has a velocity $^G\dot{\mathbf{d}}_B$ with respect to the global frame. The translational velocity $^G\dot{\mathbf{d}}_B$ is a common property for every point of the body, but the rotational velocity ${}_G\boldsymbol{\omega}_B \times {}_B^G\mathbf{r}_P$ differs for different points of the body.*

**Example 190** *Velocity of a moving point in a moving body frame.*

*Assume that point $P$ in Figure 5.12 is moving in frame $B$, indicated by time varying position vector $^B\mathbf{r}_P(t)$. The global velocity of $P$ is a composition of the velocity of $P$ in $B$, rotation of $B$ relative to $G$, and velocity of $B$ relative to $G$.*

$$
\begin{aligned}
\frac{^Gd}{dt}\, {}^G\mathbf{r}_P &= \frac{^Gd}{dt}\left({}^G\mathbf{d}_B + {}^G R_B\, {}^B\mathbf{r}_P\right) \\
&= \frac{^Gd}{dt}\, {}^G\mathbf{d}_B + \frac{^Gd}{dt}\left({}^G R_B\, {}^B\mathbf{r}_P\right) \\
&= {}^G\dot{\mathbf{d}}_B + {}_B^G\dot{\mathbf{r}}_P + {}_G\boldsymbol{\omega}_B \times {}_B^G\mathbf{r}_P \qquad (5.328)
\end{aligned}
$$

**Example 191** *Velocity of a body point in multiple coordinate frames.*

*Consider three frames, $B_0$, $B_1$ and $B_2$, as shown in Figure 5.14. The velocity of point $P$ should be measured and expressed in a coordinate frame. If the point is stationary in a frame, say $B_2$, then the time derivative of $^2\mathbf{r}_P$ in $B_2$ is zero. If frame $B_2$ is moving relative to frame $B_1$, then, the*
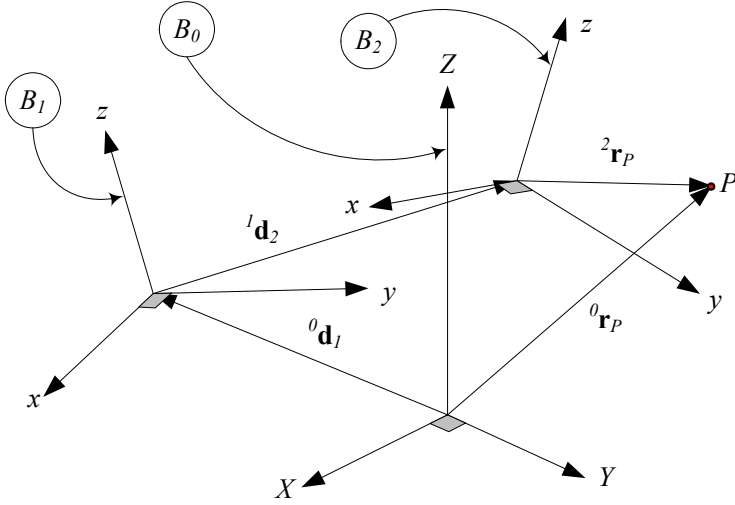
FIGURE 5.14. A rigid body coordinate frame $B_2$ is moving in a frame $B_1$ that is moving in the base coordinate frame $B_0$.

*time derivative of $^1\mathbf{r}_P$ is a combination of the rotational component due to rotation of $B_2$ relative to $B_1$ and the velocity of $B_2$ relative to $B_1$. In forward velocity kinematics, the velocities must be measured in the base frame $B_0$. Therefore, the velocity of point $P$ in the base frame is a combination of the velocity of $B_2$ relative to $B_1$ and the velocity of $B_1$ relative to $B_0$.*

*The global coordinate of the body point $P$ is*

$$
\begin{aligned}
^0\mathbf{r}_P &= \quad ^0\mathbf{d}_1 + {}^0_1\mathbf{d}_2 + {}^0_2\mathbf{r}_P & (5.329)\\
&= \quad ^0\mathbf{d}_1 + {}^0R_1\,{}^1\mathbf{d}_2 + {}^0R_2\,{}^2\mathbf{r}_P. & (5.330)
\end{aligned}
$$

*Therefore, the velocity of point $P$ can be found by combining the relative velocities*

$$
\begin{aligned}
^0\dot{\mathbf{r}}_P &= \quad ^0\dot{\mathbf{d}}_1 + ({}^0\dot{R}_1\,{}^1\mathbf{d}_2 + {}^0R_1\,{}^1\dot{\mathbf{d}}_2) + {}^0\dot{R}_2\,{}^2\mathbf{r}_P \\
&= \quad ^0\dot{\mathbf{d}}_1 + {}^0_0\boldsymbol{\omega}_1 \times {}^0_1\mathbf{d}_2 + {}^0R_1\,{}^1\dot{\mathbf{d}}_2 + {}^0_0\boldsymbol{\omega}_2 \times {}^0_2\mathbf{r}_P & (5.331)
\end{aligned}
$$

*Most of the time, it is better to use a relative velocity method and write*

$$
^0_0\mathbf{v}_P = {}^0_0\mathbf{v}_1 + {}^0_1\mathbf{v}_2 + {}^0_2\mathbf{v}_P \tag{5.332}
$$

*because*

$$
\begin{aligned}
^0_0\mathbf{v}_1 &= {}^0_0\dot{\mathbf{d}}_1 & (5.333)\\
^0_1\mathbf{v}_2 &= {}^0_0\boldsymbol{\omega}_1 \times {}^0_1\mathbf{d}_2 + {}^0R_1\,{}^1\dot{\mathbf{d}}_2 & (5.334)\\
^0_2\mathbf{v}_P &= {}^0_0\boldsymbol{\omega}_2 \times {}^0_2\mathbf{r}_P & (5.335)
\end{aligned}
$$

*and therefore,*

$$^0\mathbf{v}_P = {}^0\dot{\mathbf{d}}_1 + {}^0_0\boldsymbol{\omega}_1 \times {}^0_1\mathbf{d}_2 + {}^0R_1 \, {}^1\dot{\mathbf{d}}_2 + {}^0_0\boldsymbol{\omega}_2 \times {}^0_2\mathbf{r}_P. \tag{5.336}$$

**Example 192** *Velocity vectors are free vectors.*

Velocity vectors are free, so to express them in different coordinate frames we need only to premultiply them by a rotation matrix. Hence, considering ${}^k_j\mathbf{v}_i$ as the velocity of the origin of the $B_i$ coordinate frame with respect to the origin of frame $B_j$ expressed in frame $B_k$, we can write

$$^k_j\mathbf{v}_i = -{}^k_i\mathbf{v}_j \tag{5.337}$$

*and*

$$^k_j\mathbf{v}_i = {}^kR_m \, {}^m_j\mathbf{v}_i \tag{5.338}$$

*and therefore,*

$$\frac{{}^id}{dt} \, {}^i_i\mathbf{r}_P = {}^i\mathbf{v}_P = {}^i_j\mathbf{v}_P + {}^i_i\boldsymbol{\omega}_j \times {}^i_j\mathbf{r}_P. \tag{5.339}$$

**Example 193** ★ *Zero velocity points.*

To answer whether there is a point with zero velocity at each time, we may utilize Equation (5.324) and write

$$_G\tilde{\omega}_B \left( {}^G\mathbf{r}_0 - {}^G\mathbf{d}_B \right) + {}^G\dot{\mathbf{d}}_B = 0 \tag{5.340}$$

to search for ${}^G\mathbf{r}_0$ which refers to a point with zero velocity

$$^G\mathbf{r}_0 = {}^G\mathbf{d}_B - {}_G\tilde{\omega}_B^{-1} \, {}^G\dot{\mathbf{d}}_B \tag{5.341}$$

*however, the skew symmetric matrix* $_G\tilde{\omega}_B$ *is singular and has no inverse. In other words, there is no general solution for Equation (5.340).*

If we restrict ourselves to planar motions, say $XY$-plane, then $_G\boldsymbol{\omega}_B = \omega\hat{K}$ and $_G\tilde{\omega}_B^{-1} = 1/\omega$. Hence, in 2D space there is a point at any time with zero velocity at position ${}^G\mathbf{r}_0$ given by

$$^G\mathbf{r}_0(t) = {}^G\mathbf{d}_B(t) - \frac{1}{\omega} \, {}^G\dot{\mathbf{d}}_B(t). \tag{5.342}$$

The zero velocity point is called the **pole** or **instantaneous center of rotation**. The position of the pole is generally a function of time and the path of its motion is called a **centroid**.

**Example 194** ★ *Eulerian and Lagrangian view points.*

When a variable quantity is measured within the stationary global coordinate frame, it is called absolute or the **Lagrangian** viewpoint. When the variable is measured within a moving body coordinate frame, it is called relative or the **Eulerian** viewpoint.

In 2D planar motion of a rigid body, there is always a pole of zero velocity at

$$^G\mathbf{r}_0 = {}^G\mathbf{d}_B - \frac{1}{\omega} \, {}^G\dot{\mathbf{d}}_B. \tag{5.343}$$
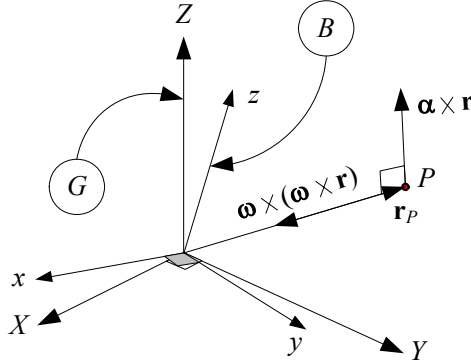
FIGURE 5.15. A rotating rigid body $B(Oxyz)$ with a fixed point $O$ in a reference frame $G(OXYZ)$.

*The position of the pole in the body coordinate frame can be found by substituting for $^G\mathbf{r}$ from (5.323)*

$$^G R_B \, ^B\mathbf{r}_0 + {}^G\mathbf{d}_B = {}^G\mathbf{d}_B - {}_G\tilde{\omega}_B^{-1} \, {}^G\dot{\mathbf{d}}_B \qquad (5.344)$$

*and solving for the position of the zero velocity point in the body coordinate frame $^B\mathbf{r}_0$.*

$$
\begin{aligned}
^B\mathbf{r}_0 &= -\,{}^G R_B^T \, {}_G\tilde{\omega}_B^{-1} \, {}^G\dot{\mathbf{d}}_B \\
&= -\,{}^G R_B^T \left[ {}^G\dot{R}_B \, {}^G R_B^T \right]^{-1} {}^G\dot{\mathbf{d}}_B \\
&= -\,{}^G R_B^T \left[ {}^G R_B \, {}^G\dot{R}_B^{-1} \right] {}^G\dot{\mathbf{d}}_B \\
&= -\,{}^G\dot{R}_B^{-1} \, {}^G\dot{\mathbf{d}}_B \qquad (5.345)
\end{aligned}
$$

   *Therefore, $^G\mathbf{r}_0$ indicates the path of motion of the pole in the global frame, while $^B\mathbf{r}_0$ indicates the same path in the body frame. The $^G\mathbf{r}_0$ refers to the Lagrangian centroid and $^B\mathbf{r}_0$ refers to the Eulerian centroid.*

## 5.10   Angular Acceleration

Consider a rotating rigid body $B(Oxyz)$ with a fixed point $O$ in a reference frame $G(OXYZ)$ as shown in Figure 5.15.

   Equation (5.172), for the velocity vector of a point in a fixed origin body frame,

$$
\begin{aligned}
^G\dot{\mathbf{r}}(t) &= {}^G\mathbf{v}(t) \\
&= {}_G\tilde{\omega}_B \, {}^G\mathbf{r}(t) \\
&= {}_G\boldsymbol{\omega}_B \times {}^G\mathbf{r}(t) \qquad (5.346)
\end{aligned}
$$

can be utilized to find the acceleration vector of the body point

$$
\begin{aligned}
{}^{G}\ddot{\mathbf{r}} \;&=\; \frac{{}^{G}d}{dt}\,{}^{G}\dot{\mathbf{r}}(t) \\
&=\; {}_{G}\boldsymbol{\alpha}_{B} \times {}^{G}\mathbf{r} + {}_{G}\boldsymbol{\omega}_{B} \times \left( {}_{G}\boldsymbol{\omega}_{B} \times {}^{G}\mathbf{r} \right) &(5.347) \\
&=\; \left( \ddot{\phi}\hat{u} + \dot{\phi}\dot{\hat{\mathbf{u}}} \right) \times {}^{G}\mathbf{r} + \dot{\phi}^{2}\,\hat{u} \times \left( \hat{u} \times {}^{G}\mathbf{r} \right). &(5.348)
\end{aligned}
$$

${}_{G}\boldsymbol{\alpha}_{B}$ is the *angular acceleration vector* of the body with respect to the $G$ frame.

$$
{}_{G}\boldsymbol{\alpha}_{B} = \frac{{}^{G}d}{dt}\,{}_{G}\boldsymbol{\omega}_{B} \tag{5.349}
$$

**Proof.** Differentiating Equation (5.346) gives

$$
\begin{aligned}
{}^{G}\ddot{\mathbf{r}} \;&=\; {}_{G}\dot{\boldsymbol{\omega}}_{B} \times {}^{G}\mathbf{r} + {}_{G}\boldsymbol{\omega}_{B} \times {}^{G}\dot{\mathbf{r}} \\
&=\; {}_{G}\boldsymbol{\alpha}_{B} \times {}^{G}\mathbf{r} + {}_{G}\boldsymbol{\omega}_{B} \times \left( {}_{G}\boldsymbol{\omega}_{B} \times {}^{G}\mathbf{r} \right) &(5.350)
\end{aligned}
$$

and because

$$
\begin{aligned}
\boldsymbol{\omega} &= \dot{\phi}\hat{u} &(5.351) \\
\boldsymbol{\alpha} &= \ddot{\phi}\hat{u} + \dot{\phi}\dot{\hat{\mathbf{u}}} &(5.352)
\end{aligned}
$$

we derive Equation (5.348). Therefore, the position, velocity, and acceleration vectors of a body point are

$$
{}^{B}\mathbf{r}_{P} = x\hat{\imath} + y\hat{\jmath} + z\hat{k} \tag{5.353}
$$

$$
\begin{aligned}
{}^{G}\mathbf{v}_{P} \;&=\; {}^{G}\dot{\mathbf{r}}_{P} = \frac{{}^{G}d}{dt}\,{}^{B}\mathbf{r}_{P} \\
&=\; {}_{G}\boldsymbol{\omega}_{B} \times {}^{G}\mathbf{r} &(5.354)
\end{aligned}
$$

$$
\begin{aligned}
{}^{G}\mathbf{a}_{P} \;&=\; {}^{G}\dot{\mathbf{v}}_{P} = {}^{G}\ddot{\mathbf{r}}_{P} = \frac{{}^{G}d^{2}}{dt^{2}}\,{}^{B}\mathbf{r}_{P} \\
&=\; {}_{G}\boldsymbol{\alpha}_{B} \times {}^{G}\mathbf{r} + {}_{G}\boldsymbol{\omega}_{B} \times {}^{G}\dot{\mathbf{r}} \\
&=\; {}_{G}\boldsymbol{\alpha}_{B} \times {}^{G}\mathbf{r} + {}_{G}\boldsymbol{\omega}_{B} \times \left( {}_{G}\boldsymbol{\omega}_{B} \times {}^{G}\mathbf{r} \right). &(5.355)
\end{aligned}
$$

The angular acceleration expressed in the body frame is the body derivative of the angular velocity vector. To show this, we use the derivative transport formula (5.287)

$$
\begin{aligned}
{}^{B}_{G}\boldsymbol{\alpha}_{B} \;&=\; \frac{{}^{G}d}{dt}\,{}^{B}_{G}\boldsymbol{\omega}_{B} \\
&=\; \frac{{}^{B}d}{dt}\,{}^{B}_{G}\boldsymbol{\omega}_{B} + {}^{B}_{G}\boldsymbol{\omega}_{B} \times {}^{B}_{G}\boldsymbol{\omega}_{B} \\
&=\; \frac{{}^{B}d}{dt}\,{}^{B}_{G}\boldsymbol{\omega}_{B} \\
&=\; {}^{B}_{G}\dot{\boldsymbol{\omega}}_{B}. &(5.356)
\end{aligned}
$$
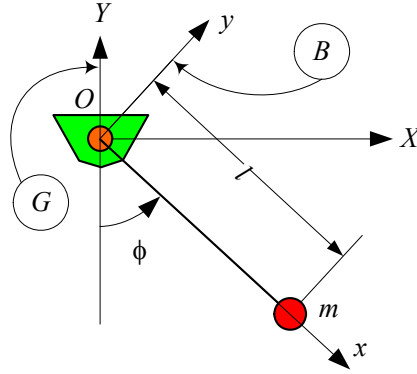
FIGURE 5.16. Illustration of a simple pendulum.

The angular acceleration of $B$ in $G$ can always be expressed in the form

$$_G\boldsymbol{\alpha}_B = {}_G\alpha_B \, \hat{u}_\alpha \tag{5.357}$$

where $\hat{u}_\alpha$ is a unit vector parallel to $_G\boldsymbol{\alpha}_B$. The angular velocity and angular acceleration vectors are not parallel in general, and therefore,

$$\hat{u}_\alpha \quad \neq \quad \hat{u}_\omega \tag{5.358}$$

$$_G\alpha_B \quad \neq \quad {}_G\dot{\omega}_B. \tag{5.359}$$

However, the only special case is when the axis of rotation is fixed in both $G$ and $B$ frames. In this case

$$_G\boldsymbol{\alpha}_B = \alpha \, \hat{u} = \dot{\omega} \, \hat{u} = \ddot{\phi} \, \hat{u}. \tag{5.360}$$

∎

**Example 195** *Velocity and acceleration of a simple pendulum.*

*A point mass attached to a massless rod and hanging from a revolute joint is called a simple pendulum. Figure 5.16 illustrates a simple pendulum. A local coordinate frame $B$ is attached to the pendulum that rotates in a global frame $G$. The position vector of the bob and the angular velocity vector $_G\boldsymbol{\omega}_B$ are*

$$^B\mathbf{r} \quad = \quad l\hat{\imath} \tag{5.361}$$

$$^G\mathbf{r} \quad = \quad {}^GR_B \, {}^B\mathbf{r} = \begin{bmatrix} l\sin\phi \\ -l\cos\phi \\ 0 \end{bmatrix} \tag{5.362}$$

$$^B_G\boldsymbol{\omega}_B \quad = \quad \dot{\phi}\hat{k} \tag{5.363}$$

$$_G\boldsymbol{\omega}_B \quad = \quad {}^GR_B^T \, {}^B_G\boldsymbol{\omega}_B = \dot{\phi} \, \hat{K}. \tag{5.364}$$

$$^{G}R_{B} = \begin{bmatrix} \cos\left(\frac{3}{2}\pi + \phi\right) & -\sin\left(\frac{3}{2}\pi + \phi\right) & 0 \\ \sin\left(\frac{3}{2}\pi + \phi\right) & \cos\left(\frac{3}{2}\pi + \phi\right) & 0 \\ 0 & 0 & 1 \end{bmatrix}$$

$$= \begin{bmatrix} \sin\phi & \cos\phi & 0 \\ -\cos\phi & \sin\phi & 0 \\ 0 & 0 & 1 \end{bmatrix} \tag{5.365}$$

*Its velocity is therefore given by*

$$\begin{aligned} ^{B}_{G}\mathbf{v} &= {}^{B}\dot{\mathbf{r}} + {}^{B}_{G}\boldsymbol{\omega}_{B} \times {}^{B}_{G}\mathbf{r} \\ &= 0 + \dot{\phi}\hat{k} \times l\hat{\imath} \\ &= l\dot{\phi}\hat{\jmath} \end{aligned} \tag{5.366}$$

$$^{G}\mathbf{v} = {}^{G}R_{B}{}^{B}\mathbf{v} = \begin{bmatrix} l\dot{\phi}\cos\phi \\ l\dot{\phi}\sin\phi \\ 0 \end{bmatrix}. \tag{5.367}$$

*The acceleration of the bob is then equal to*

$$\begin{aligned} ^{B}_{G}\mathbf{a} &= {}^{B}_{G}\dot{\mathbf{v}} + {}^{B}_{G}\boldsymbol{\omega}_{B} \times {}^{B}_{G}\mathbf{v} \\ &= l\ddot{\phi}\hat{\jmath} + \dot{\phi}\hat{k} \times l\dot{\phi}\hat{\jmath} \\ &= l\ddot{\phi}\hat{\jmath} - l\dot{\phi}^{2}\hat{\imath} \end{aligned} \tag{5.368}$$

$$^{G}\mathbf{a} = {}^{G}R_{B}{}^{B}\mathbf{a} = \begin{bmatrix} l\ddot{\phi}\cos\phi - l\dot{\phi}^{2}\sin\phi \\ l\ddot{\phi}\sin\phi + l\dot{\phi}^{2}\cos\phi \\ 0 \end{bmatrix}. \tag{5.369}$$

**Example 196** *Motion of a vehicle on the Earth.*

*Consider the motion of a vehicle on the Earth at latitude* 30 deg *and heading north, as shown in Figure 5.17. The vehicle has the velocity* $v = {}^{B}_{E}\dot{\mathbf{r}} = 80$ km/h $= 22.22$ m/s *and acceleration* $a = {}^{B}_{E}\ddot{\mathbf{r}} = 0.1$ m/s$^{2}$, *both with respect to the road. The radius of the Earth is* $R$, *and hence, the vehicle's kinematics are*

$$\begin{aligned} ^{B}_{E}\mathbf{r} &= R\hat{k} \text{ m} & (5.370) \\ ^{B}_{E}\dot{\mathbf{r}} &= 22.22\hat{\imath} \text{ m/s} & (5.371) \\ ^{B}_{E}\ddot{\mathbf{r}} &= 0.1\hat{\imath} \text{ m/s}^{2} & (5.372) \\ \dot{\theta} &= \frac{v}{R} \text{ rad/s} & (5.373) \\ \ddot{\theta} &= \frac{a}{R} \text{ rad/s}^{2}. & (5.374) \end{aligned}$$

*There are three coordinate frames involved. A body coordinate frame* $B$ *is attached to the vehicle as shown in the figure. A global coordinate* $G$ *is set up at the center of the Earth. Another local coordinate frame* $E$ *is rigidly*
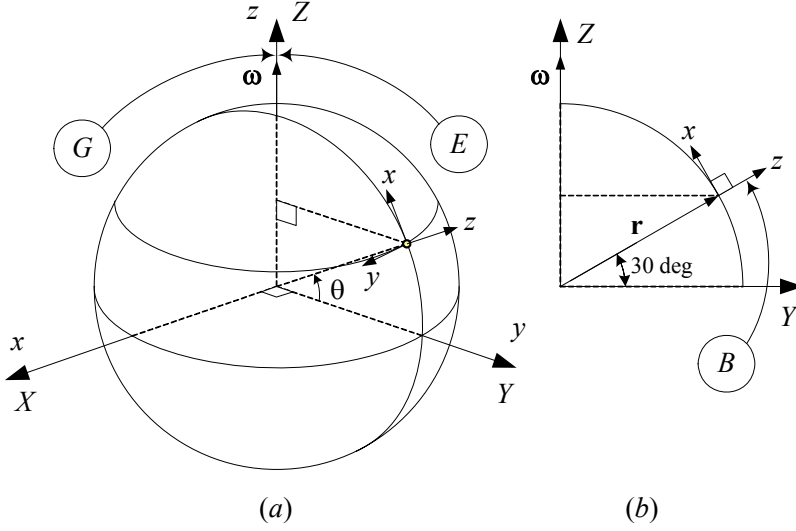
FIGURE 5.17. The motion of a vehicle at $30\,\mathrm{deg}$ latitude and heading north on the Earth.

*attached to the Earth and turns with the Earth. The frames $E$ and $G$ are assumed coincident at the moment. The angular velocity of $B$ is*

$$
\begin{aligned}
{}^{B}_{G}\boldsymbol{\omega}_{B} &= {}_{G}\boldsymbol{\omega}_{E} + {}^{G}_{E}\boldsymbol{\omega}_{B} \\
&= {}^{B}R_{G}\left(\omega_{E}\,\hat{K} + \dot{\theta}\hat{I}\right) \\
&= \left(\omega_{E}\cos\theta\right)\hat{\imath} + \left(\omega_{E}\sin\theta\right)\hat{k} + \dot{\theta}\hat{\jmath} \\
&= \left(\omega_{E}\cos\theta\right)\hat{\imath} + \left(\omega_{E}\sin\theta\right)\hat{k} + \frac{v}{R}\hat{\jmath}.
\end{aligned}
\qquad (5.375)
$$

*Therefore, the velocity and acceleration of the vehicle are*

$$
\begin{aligned}
{}^{B}_{G}\mathbf{v} &= {}^{B}\dot{\mathbf{r}} + {}^{B}_{G}\boldsymbol{\omega}_{B} \times {}^{B}_{G}\mathbf{r} \\
&= 0 + {}^{B}_{G}\boldsymbol{\omega}_{B} \times R\hat{k} \\
&= v\hat{\imath} - \left(R\omega_{E}\cos\theta\right)\hat{\jmath}
\end{aligned}
\qquad (5.376)
$$

$$
\begin{aligned}
{}^{B}_{G}\mathbf{a} \;=\;& {}^{B}_{G}\dot{\mathbf{v}} + {}^{B}_{G}\boldsymbol{\omega}_B \times {}^{B}_{G}\mathbf{v}\\[2mm]
=\;& a\hat{\imath} + \left(R\omega_E\,\dot{\theta}\sin\theta\right)\hat{\jmath} +
\begin{bmatrix}\omega_E\cos\theta\\[1mm] \dfrac{v}{R}\\[1mm] \omega_E\sin\theta\end{bmatrix}
\times
\begin{bmatrix} v\\ -R\omega_E\cos\theta\\ 0\end{bmatrix}\\[2mm]
=\;& a\hat{\imath} + \left(R\omega_E\,\dot{\theta}\sin\theta\right)\hat{\jmath} +
\begin{bmatrix} R\omega_E^2\,\cos\theta\sin\theta\\ v\omega_E\sin\theta\\ -\frac{1}{R}v^2 - R\omega_E^2\cos^2\theta\end{bmatrix}\\[2mm]
=\;&
\begin{bmatrix} a + R\omega_E^2\,\cos\theta\sin\theta\\ 2R\omega_E\,\dot{\theta}\sin\theta\\ -\frac{1}{R}v^2 - R\omega_E^2\cos^2\theta\end{bmatrix}.
\end{aligned}
\tag{5.377}
$$

The term $a\hat{\imath}$ is the acceleration relative to Earth, $(2R\omega_E\,\dot{\theta}\sin\theta)\hat{\jmath}$ is the Coriolis acceleration, $-\frac{v^2}{R}\hat{k}$ is the centrifugal acceleration due to traveling, and $-(R\omega_E^2\cos^2\theta)$ is the centrifugal acceleration due to Earth's rotation.

Substituting the numerical values and accepting $R = 6.3677\times10^6$ m provides

$$
\begin{aligned}
{}^{B}_{G}\mathbf{v} \;=\;& 22.22\hat{\imath} - 6.3677\times10^6\left(\frac{2\pi}{24\times3600}\frac{366.25}{365.25}\right)\cos\frac{\pi}{6}\hat{\jmath}\\[2mm]
=\;& 22.22\hat{\imath} - 402.13\hat{\jmath}\ \mathrm{m/s}
\end{aligned}
\tag{5.378}
$$

$$
{}^{B}_{G}\mathbf{a} = 1.5662\times10^{-2}\hat{\imath} + 1.6203\times10^{-3}\hat{\jmath} - 2.5473\times10^{-2}\hat{k}\ \mathrm{m/s^2}. \tag{5.379}
$$

**Example 197 ★** *Combination of angular accelerations.*

It is shown that the angular velocity of several bodies rotating relative to each other can be related according to (5.231)

$$
{}_{0}\boldsymbol{\omega}_n = {}_{0}\boldsymbol{\omega}_1 + {}_{1}^{0}\boldsymbol{\omega}_2 + {}_{2}^{0}\boldsymbol{\omega}_3 + \cdots + {}_{n-1}^{0}\boldsymbol{\omega}_n. \tag{5.380}
$$

However, in general, there is no such equation for angular accelerations

$$
{}_{0}\boldsymbol{\alpha}_n \neq {}_{0}\boldsymbol{\alpha}_1 + {}_{1}^{0}\boldsymbol{\alpha}_2 + {}_{2}^{0}\boldsymbol{\alpha}_3 + \cdots + {}_{n-1}^{0}\boldsymbol{\alpha}_n. \tag{5.381}
$$

To show this, consider a pair of rigid links connected by revolute joints. The angular velocities of the links are

$$
\begin{aligned}
{}_{0}\boldsymbol{\omega}_1 \;=\;& \dot{\theta}_1\,{}^{0}\hat{k}_0 \tag{5.382}\\[2mm]
{}_{1}^{0}\boldsymbol{\omega}_2 \;=\;& \dot{\theta}_2\,{}^{0}\hat{k}_1 \tag{5.383}
\end{aligned}
$$

$$
\begin{aligned}
{}_{0}\boldsymbol{\omega}_2 \;=\;& {}_{0}\boldsymbol{\omega}_1 + {}_{1}^{0}\boldsymbol{\omega}_2\\[1mm]
=\;& \dot{\theta}_1\,{}^{0}\hat{k}_0 + \dot{\theta}_2\,{}^{0}\hat{k}_1\\[1mm]
=\;& \dot{\theta}_1\,{}^{0}\hat{k}_0 + \dot{\theta}_2\,{}^{0}R_1\,{}^{1}\hat{k}_1 \tag{5.384}
\end{aligned}
$$

*however, the angular accelerations show that*

$$_0\boldsymbol{\alpha}_1 = \frac{^0 d}{dt}\,_0\boldsymbol{\omega}_1 = \,_0\dot{\omega}_1\,^0\hat{k}_0 \tag{5.385}$$

$$
\begin{aligned}
_0\boldsymbol{\alpha}_2 &= \frac{^0 d}{dt}\,_0\boldsymbol{\omega}_2 = \frac{^0 d}{dt}\left(\dot{\theta}_1\,^0\hat{k}_0 + \dot{\theta}_2\,^0 R_1\,^1\hat{k}_1\right) \\
&= \ddot{\theta}_1\,^0\hat{k}_0 + \ddot{\theta}_2\,^0 R_1\,^1\hat{k}_1 + \,_0\boldsymbol{\omega}_1 \times \dot{\theta}_2\,^0 R_1\,^1\hat{k}_1 \\
&= \ddot{\theta}_1\,^0\hat{k}_0 + \ddot{\theta}_2\,^0\hat{k}_1 + \dot{\theta}_1\,\dot{\theta}_2\,^0\hat{k}_0 \times \,^0\hat{k}_1 \\
&= \,_0\boldsymbol{\alpha}_1 + \,_1^0\boldsymbol{\alpha}_2 + \,_0\boldsymbol{\omega}_1 \times \,_1^0\boldsymbol{\omega}_2
\end{aligned}
\tag{5.386}
$$

*and therefore,*

$$_0\boldsymbol{\alpha}_2 \neq \,_0\boldsymbol{\alpha}_1 + \,_1^0\boldsymbol{\alpha}_2. \tag{5.387}$$

Equation (5.386) is the relative acceleration equation. It expresses the relative accelerations for connected rigid bodies.

**Example 198 ★** *Angular acceleration and Euler angles.*
The angular velocity $_G^B\boldsymbol{\omega}_B$ in terms of Euler angles is

$$
\begin{aligned}
_G^G\boldsymbol{\omega}_B &=
\begin{bmatrix} \omega_X \\ \omega_Y \\ \omega_Z \end{bmatrix}
=
\begin{bmatrix}
0 & \cos\varphi & \sin\theta\sin\varphi \\
0 & \sin\varphi & -\cos\varphi\sin\theta \\
1 & 0 & \cos\theta
\end{bmatrix}
\begin{bmatrix} \dot{\varphi} \\ \dot{\theta} \\ \dot{\psi} \end{bmatrix} \\
&=
\begin{bmatrix}
\dot{\theta}\cos\varphi + \dot{\psi}\sin\theta\sin\varphi \\
\dot{\theta}\sin\varphi - \dot{\psi}\cos\varphi\sin\theta \\
\dot{\varphi} + \dot{\psi}\cos\theta
\end{bmatrix}.
\end{aligned}
\tag{5.388}
$$

*The angular acceleration is then equal to*

$$_G^G\boldsymbol{\alpha}_B = \frac{^G d}{dt}\,_G^G\boldsymbol{\omega}_B \tag{5.389}$$

$$
=
\begin{bmatrix}
\cos\varphi\left(\ddot{\theta} + \dot{\varphi}\dot{\psi}\sin\theta\right) + \sin\varphi\left(\ddot{\psi}\sin\theta + \dot{\theta}\dot{\psi}\cos\theta - \dot{\theta}\dot{\varphi}\right) \\
\sin\varphi\left(\ddot{\theta} + \dot{\varphi}\dot{\psi}\sin\theta\right) + \cos\varphi\left(\dot{\theta}\dot{\varphi} - \ddot{\psi}\sin\theta - \dot{\theta}\dot{\psi}\cos\theta\right) \\
\ddot{\varphi} + \ddot{\psi}\cos\theta - \dot{\theta}\dot{\psi}\sin\theta
\end{bmatrix}.
$$

The angular acceleration vector in the body coordinate frame is then equal to

$$_G^B\boldsymbol{\alpha}_B = \,^G R_B^T\,_G^G\boldsymbol{\alpha}_B \tag{5.390}$$

$$
=
\begin{bmatrix}
c\varphi c\psi - c\theta s\varphi s\psi & c\psi s\varphi + c\theta c\varphi s\psi & s\theta s\psi \\
-c\varphi s\psi - c\theta c\psi s\varphi & -s\varphi s\psi + c\theta c\varphi c\psi & s\theta c\psi \\
s\theta s\varphi & -c\varphi s\theta & c\theta
\end{bmatrix}
\,_G^G\boldsymbol{\alpha}_B
$$

$$
=
\begin{bmatrix}
\cos\psi\left(\ddot{\theta} + \dot{\varphi}\dot{\psi}\sin\theta\right) + \sin\psi\left(\varphi''\sin\theta + \dot{\theta}\dot{\varphi}\cos\theta - \dot{\theta}\dot{\psi}\right) \\
\cos\psi\left(\ddot{\varphi}\sin\theta + \dot{\theta}\dot{\varphi}\cos\theta - \dot{\theta}\dot{\psi}\right) - \sin\psi\left(\ddot{\theta} + \dot{\varphi}\dot{\psi}\sin\theta\right) \\
\ddot{\varphi}\cos\theta - \ddot{\psi} - \dot{\theta}\dot{\varphi}\sin\theta
\end{bmatrix}.
$$
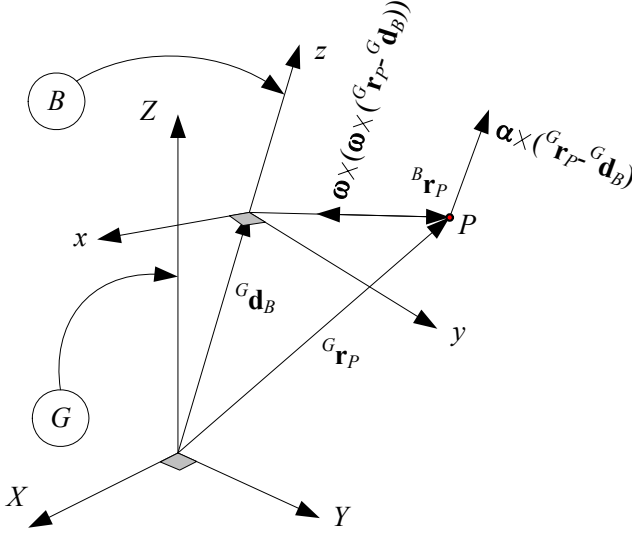
FIGURE 5.18. A rigid body with coordinate frame $B\,(oxyz)$ moving freely in a fixed global coordinate frame $G(OXYZ)$.

## 5.11   Rigid Body Acceleration

Consider a rigid body with an attached local coordinate frame $B\,(oxyz)$ moving freely in a fixed global coordinate frame $G(OXYZ)$. The rigid body can rotate in the global frame, while the origin of the body frame $B$ can translate relative to the origin of $G$. The coordinates of a body point $P$ in local and global frames, as shown in Figure 5.18, are related by the equation

$$ {}^G\mathbf{r}_P = {}^G R_B \,{}^B\mathbf{r}_P + {}^G\mathbf{d}_B \tag{5.391} $$

where ${}^G\mathbf{d}_B$ indicates the position of the moving origin $o$ relative to the fixed origin $O$.

The acceleration of point $P$ in $G$ is

$$
\begin{aligned}
{}^G\mathbf{a}_P &= {}^G\dot{\mathbf{v}}_P = {}^G\ddot{\mathbf{r}}_P \\
&= {}_G\boldsymbol{\alpha}_B \times \left({}^G\mathbf{r}_P - {}^G\mathbf{d}_B\right) \\
&\quad + {}_G\boldsymbol{\omega}_B \times \left({}_G\boldsymbol{\omega}_B \times \left({}^G\mathbf{r}_P - {}^G\mathbf{d}_B\right)\right) + {}^G\ddot{\mathbf{d}}_B. \tag{5.392}
\end{aligned}
$$

**Proof.** The acceleration of point $P$ is a consequence of differentiating the

velocity equation (5.326) or (5.327).

$$
\begin{aligned}
{}^G\mathbf{a}_P &= \frac{{}^Gd}{dt}\,{}^G\mathbf{v}_P \\
&= {}_G\boldsymbol{\alpha}_B \times {}_B^G\mathbf{r}_P + {}_G\boldsymbol{\omega}_B \times {}_B^G\dot{\mathbf{r}}_P + {}^G\ddot{\mathbf{d}}_B \\
&= {}_G\boldsymbol{\alpha}_B \times {}_B^G\mathbf{r}_P + {}_G\boldsymbol{\omega}_B \times \left({}_G\boldsymbol{\omega}_B \times {}_B^G\mathbf{r}_P\right) + {}^G\ddot{\mathbf{d}}_B \\
&= {}_G\boldsymbol{\alpha}_B \times \left({}^G\mathbf{r}_P - {}^G\mathbf{d}_B\right) \\
&\quad + {}_G\boldsymbol{\omega}_B \times \left({}_G\boldsymbol{\omega}_B \times \left({}^G\mathbf{r}_P - {}^G\mathbf{d}_B\right)\right) + {}^G\ddot{\mathbf{d}}_B.
\end{aligned} \tag{5.393}
$$

The term ${}_G\boldsymbol{\omega}_B \times \left({}_G\boldsymbol{\omega}_B \times {}_B^G\mathbf{r}_P\right)$ is called *centripetal acceleration* and is independent of the angular acceleration. The term ${}_G\boldsymbol{\alpha}_B \times {}_B^G\mathbf{r}_P$ is called *tangential acceleration* and is perpendicular to ${}_B^G\mathbf{r}_P$. ∎

**Example 199** *Acceleration of joint 2 of a 2R planar manipulator.*

   *A 2R planar manipulator is illustrated in Figure 5.19. The elbow joint has a circular motion about the base joint. Knowing that*

$$
{}_0\boldsymbol{\omega}_1 = \dot{\theta}_1\,{}^0\hat{k}_0 \tag{5.394}
$$

*we can write*

$$
\begin{aligned}
{}_0\boldsymbol{\alpha}_1 &= {}_0\dot{\boldsymbol{\omega}}_1 = \ddot{\theta}_1\,{}^0\hat{k}_0 \tag{5.395} \\
{}_0\dot{\boldsymbol{\omega}}_1 \times {}^0\mathbf{r}_1 &= \ddot{\theta}_1\,{}^0\hat{k}_0 \times {}^0\mathbf{r}_1 \\
&= \ddot{\theta}_1\,R_{Z,\theta+90}\,{}^0\mathbf{r}_1 \tag{5.396} \\
{}_0\boldsymbol{\omega}_1 \times \left({}_0\boldsymbol{\omega}_1 \times {}^0\mathbf{r}_1\right) &= -\dot{\theta}_1^2\,{}^0\mathbf{r}_1 \tag{5.397}
\end{aligned}
$$

*and calculate the acceleration of the elbow joint*

$$
{}^0\ddot{\mathbf{r}}_1 = \ddot{\theta}_1\,R_{Z,\theta+90}\,{}^0\mathbf{r}_1 - \dot{\theta}_1^2\,{}^0\mathbf{r}_1. \tag{5.398}
$$

**Example 200** *Acceleration of a moving point in a moving body frame.*

   *Assume the point P in Figure 5.18 is indicated by a time varying local position vector* ${}^B\mathbf{r}_P(t)$. *Then, the velocity and acceleration of P can be found by applying the derivative transformation formula (5.287).*

$$
\begin{aligned}
{}^G\mathbf{v}_P &= {}^G\dot{\mathbf{d}}_B + {}^B\dot{\mathbf{r}}_P + {}_G^B\boldsymbol{\omega}_B \times {}^B\mathbf{r}_P \\
&= {}^G\dot{\mathbf{d}}_B + {}^B\mathbf{v}_P + {}_G^B\boldsymbol{\omega}_B \times {}^B\mathbf{r}_P
\end{aligned} \tag{5.399}
$$

$$
\begin{aligned}
{}^G\mathbf{a}_P &= {}^G\ddot{\mathbf{d}}_B + {}^B\ddot{\mathbf{r}}_P + {}_G^B\boldsymbol{\omega}_B \times {}^B\dot{\mathbf{r}}_P + {}_G^B\dot{\boldsymbol{\omega}}_B \times {}^B\mathbf{r}_P \\
&\quad + {}_G^B\boldsymbol{\omega}_B \times \left({}^B\dot{\mathbf{r}}_P + {}_G^B\boldsymbol{\omega}_B \times {}^B\mathbf{r}_P\right) \\
&= {}^G\ddot{\mathbf{d}}_B + {}^B\mathbf{a}_P + 2{}_G^B\boldsymbol{\omega}_B \times {}^B\mathbf{v}_P + {}_G^B\dot{\boldsymbol{\omega}}_B \times {}^B\mathbf{r}_P \\
&\quad + {}_G^B\boldsymbol{\omega}_B \times \left({}_G^B\boldsymbol{\omega}_B \times {}^B\mathbf{r}_P\right). 
\end{aligned} \tag{5.400}
$$

FIGURE 5.19. A 2R planar manipulator.

*It is also possible to take the derivative from Equation (5.323) with the assumption* $^B\dot{\mathbf{r}}_P \neq 0$ *and find the acceleration of* $P$.

$$^G\mathbf{r}_P = {}^G R_B \, {}^B\mathbf{r}_P + {}^G\mathbf{d}_B \tag{5.401}$$

$$\begin{aligned} ^G\dot{\mathbf{r}}_P &= {}^G\dot{R}_B \, {}^B\mathbf{r}_P + {}^G R_B \, {}^B\dot{\mathbf{r}}_P + {}^G\dot{\mathbf{d}}_B \\ &= {}_G\boldsymbol{\omega}_B \times {}^G R_B \, {}^B\mathbf{r}_P + {}^G R_B \, {}^B\dot{\mathbf{r}}_P + {}^G\dot{\mathbf{d}}_B \end{aligned} \tag{5.402}$$

$$\begin{aligned} ^G\ddot{\mathbf{r}}_P &= {}_G\dot{\boldsymbol{\omega}}_B \times {}^G R_B \, {}^B\mathbf{r}_P + {}_G\boldsymbol{\omega}_B \times {}^G\dot{R}_B \, {}^B\mathbf{r}_P + {}_G\boldsymbol{\omega}_B \times {}^G R_B \, {}^B\dot{\mathbf{r}}_P \\ &\quad + {}^G\dot{R}_B \, {}^B\dot{\mathbf{r}}_P + {}^G R_B \, {}^B\ddot{\mathbf{r}}_P + {}^G\ddot{\mathbf{d}}_B \\ &= {}_G\dot{\boldsymbol{\omega}}_B \times {}^G_B\mathbf{r}_P + {}_G\boldsymbol{\omega}_B \times \left({}_G\boldsymbol{\omega}_B \times {}^G\mathbf{r}_P\right) + 2\,{}_G\boldsymbol{\omega}_B \times {}^G_B\dot{\mathbf{r}}_P \\ &\quad + {}^G_B\ddot{\mathbf{r}}_P + {}^G\ddot{\mathbf{d}}_B \end{aligned} \tag{5.403}$$

*The third term on the right-hand side is called the* **Coriolis acceleration**. *The Coriolis acceleration is perpendicular to both* $_G\boldsymbol{\omega}_B$ *and* $^B\dot{\mathbf{r}}_P$.

**Example 201** ★ *Acceleration of a body point.*
   *Consider a rigid body is moving and rotating in a global frame. The acceleration of a body point can be found by taking twice the time derivative of its position vector*

$$^G\mathbf{r}_P = {}^G R_B \, {}^B\mathbf{r}_P + {}^G\mathbf{d}_B \tag{5.404}$$

$$^G\dot{\mathbf{r}}_P = {}^G\dot{R}_B \, {}^B\mathbf{r}_P + {}^G\dot{\mathbf{d}}_B \tag{5.405}$$

$$
\begin{aligned}
{}^{G}\ddot{\mathbf{r}}_P &= {}^{G}\ddot{R}_B \, {}^{B}\mathbf{r}_P + {}^{G}\ddot{\mathbf{d}}_B \\
&= {}^{G}\ddot{R}_B \, {}^{G}R_B^T \left({}^{G}\mathbf{r}_P - {}^{G}\mathbf{d}_B\right) + {}^{G}\ddot{\mathbf{d}}_B.
\end{aligned}
\tag{5.406}
$$

*Differentiating the angular velocity matrix*

$$
{}_{G}\tilde{\omega}_B = {}^{G}\dot{R}_B \, {}^{G}R_B^T
\tag{5.407}
$$

*shows that*

$$
\begin{aligned}
{}_{G}\dot{\tilde{\omega}}_B &= \frac{{}^{G}d}{dt} {}_{G}\tilde{\omega}_B = {}^{G}\ddot{R}_B \, {}^{G}R_B^T + {}^{G}\dot{R}_B \, {}^{G}\dot{R}_B^T \\
&= {}^{G}\ddot{R}_B \, {}^{G}R_B^T + {}_{G}\tilde{\omega}_B \, {}_{G}\tilde{\omega}_B^T
\end{aligned}
\tag{5.408}
$$

*and therefore,*

$$
{}^{G}\ddot{R}_B \, {}^{G}R_B^T = {}_{G}\dot{\tilde{\omega}}_B - {}_{G}\tilde{\omega}_B \, {}_{G}\tilde{\omega}_B^T.
\tag{5.409}
$$

*Hence, the acceleration vector of the body point becomes*

$$
{}^{G}\ddot{\mathbf{r}}_P = \left({}_{G}\dot{\tilde{\omega}}_B - {}_{G}\tilde{\omega}_B \, {}_{G}\tilde{\omega}_B^T\right)\left({}^{G}\mathbf{r}_P - {}^{G}\mathbf{d}_B\right) + {}^{G}\ddot{\mathbf{d}}_B
\tag{5.410}
$$

*where*

$$
{}_{G}\dot{\tilde{\omega}}_B = {}_{G}\tilde{\alpha}_B = \begin{bmatrix} 0 & -\dot{\omega}_3 & \dot{\omega}_2 \\ \dot{\omega}_3 & 0 & -\dot{\omega}_1 \\ -\dot{\omega}_2 & \dot{\omega}_1 & 0 \end{bmatrix}
\tag{5.411}
$$

*and*

$$
{}_{G}\tilde{\omega}_B \, {}_{G}\tilde{\omega}_B^T = \begin{bmatrix} \omega_2^2 + \omega_3^2 & -\omega_1\omega_2 & -\omega_1\omega_3 \\ -\omega_1\omega_2 & \omega_1^2 + \omega_3^2 & -\omega_2\omega_3 \\ -\omega_1\omega_3 & -\omega_2\omega_3 & \omega_1^2 + \omega_2^2 \end{bmatrix}.
\tag{5.412}
$$

## 5.12   ★ Axis-angle Rotation

When the rotation is about an arbitrary axis going through the origin, two parameters are necessary to define the direction of the line through $O$ and one is necessary to define the amount of rotation of the rigid body about this line. Let the body frame $B(Oxyz)$ rotate $\phi$ about a line indicated by a unit vector $\hat{u}$ with direction cosines $u_1, u_2, u_3$,

$$
\hat{u} = u_1\hat{I} + u_2\hat{J} + u_3\hat{K}
\tag{5.413}
$$

$$
\sqrt{u_1^2 + u_2^2 + u_3^2} = 1.
\tag{5.414}
$$

This is called *axis-angle* representation of a rotation.

A transformation matrix ${}^{G}R_B$ that maps the coordinates in the local frame $B(Oxyz)$ to the corresponding coordinates in the global frame $G(OXYZ)$,

$$
{}^{G}\mathbf{r} = {}^{G}R_B \, {}^{B}\mathbf{r}
\tag{5.415}
$$

FIGURE 5.20. Axis of rotation $\hat{u}$ when it is coincident with the local $z$-axis.

is

$$^{G}R_{B} = R_{\hat{u},\phi} = \mathbf{I}\cos\phi + \hat{u}\hat{u}^{T}\operatorname{vers}\phi + \tilde{u}\sin\phi \qquad (5.416)$$

$$^{G}R_{B} = \begin{bmatrix} u_{1}^{2}\operatorname{vers}\phi + c\phi & u_{1}u_{2}\operatorname{vers}\phi - u_{3}s\phi & u_{1}u_{3}\operatorname{vers}\phi + u_{2}s\phi \\ u_{1}u_{2}\operatorname{vers}\phi + u_{3}s\phi & u_{2}^{2}\operatorname{vers}\phi + c\phi & u_{2}u_{3}\operatorname{vers}\phi - u_{1}s\phi \\ u_{1}u_{3}\operatorname{vers}\phi - u_{2}s\phi & u_{2}u_{3}\operatorname{vers}\phi + u_{1}s\phi & u_{3}^{2}\operatorname{vers}\phi + c\phi \end{bmatrix}$$
$$(5.417)$$

where

$$\begin{aligned} \operatorname{vers}\phi &= versine\,\phi \\ &= 1 - \cos\phi \qquad\qquad (5.418) \\ &= 2\sin^{2}\frac{\phi}{2} \end{aligned}$$

and $\tilde{u}$ is the skew-symmetric matrix corresponding to the vector $\hat{u}$

$$\tilde{u} = \begin{bmatrix} 0 & -u_{3} & u_{2} \\ u_{3} & 0 & -u_{1} \\ -u_{2} & u_{1} & 0 \end{bmatrix}. \qquad (5.419)$$

A matrix $\tilde{u}$ is *skew-symmetric* if

$$\tilde{u}^{T} = -\tilde{u}. \qquad (5.420)$$

The transformation matrix (5.417) is the most general rotation matrix for a local frame rotating with respect to a global frame. If the axis of rotation (5.413) coincides with a global coordinate axis, then the Equations (5.20), (5.21), or (5.22) will be reproduced.

**Proof.** Interestingly, the effect of rotation $\phi$ about an axis $\hat{u}$ is equivalent to a sequence of rotations about the axes of a local frame in which the

local frame is first rotated to bring one of its axes, say the $z$-axis, into coincidence with the rotation axis $\hat{u}$, followed by a rotation $\phi$ about that local axis, then the reverse of the first sequence of rotations.

Figure 5.20 illustrates an axis of rotation $\hat{u} = u_1 \hat{I} + u_2 \hat{J} + u_3 \hat{K}$ , the global frame $G\,(OXYZ)$, and the rotated local frame $B\,(Oxyz)$ when the local $z$-axis is coincident with $\hat{u}$. Based on Figure 5.20, the local frame $B\,(Oxyz)$ undergoes a sequence of rotations $\varphi$ about the $z$-axis and $\theta$ about the $y$-axis to bring the local $z$-axis into coincidence with the rotation axis $\hat{u}$, followed by rotation $\phi$ about $\hat{u}$, and then perform the sequence backward. Therefore, the rotation matrix $^{G}R_{B}$ to map coordinates in local frame to their coordinates in global frame after rotation $\phi$ about $\hat{u}$ is

$$
\begin{aligned}
^{G}R_{B} \;&=\; {}^{B}R_{G}^{-1} = {}^{B}R_{G}^{T} = R_{\hat{u},\phi} \\
&=\; [R_{z,-\varphi}\,R_{y,-\theta}\,R_{z,\phi}\,R_{y,\theta}\,R_{z,\varphi}]^{T} \\
&=\; R_{z,\varphi}^{T}\,R_{y,\theta}^{T}\,R_{z,\phi}^{T}\,R_{y,-\theta}^{T}\,R_{z,-\varphi}^{T}
\end{aligned}
\tag{5.421}
$$

but

$$
\sin\varphi \;=\; \frac{u_2}{\sqrt{u_1^2 + u_2^2}}
\tag{5.422}
$$

$$
\cos\varphi \;=\; \frac{u_1}{\sqrt{u_1^2 + u_2^2}}
\tag{5.423}
$$

$$
\sin\theta \;=\; \sqrt{u_1^2 + u_2^2}
\tag{5.424}
$$

$$
\cos\theta \;=\; u_3
\tag{5.425}
$$

$$
\sin\theta\sin\varphi \;=\; u_2
\tag{5.426}
$$

$$
\sin\theta\cos\varphi \;=\; u_1
\tag{5.427}
$$

and hence,

$$
^{G}R_{B} = R_{\hat{u},\phi}
\tag{5.428}
$$

$$
= \begin{bmatrix}
u_1^2 \operatorname{vers}\phi + c\phi & u_1 u_2 \operatorname{vers}\phi - u_3 s\phi & u_1 u_3 \operatorname{vers}\phi + u_2 s\phi \\
u_1 u_2 \operatorname{vers}\phi + u_3 s\phi & u_2^2 \operatorname{vers}\phi + c\phi & u_2 u_3 \operatorname{vers}\phi - u_1 s\phi \\
u_1 u_3 \operatorname{vers}\phi - u_2 s\phi & u_2 u_3 \operatorname{vers}\phi + u_1 s\phi & u_3^2 \operatorname{vers}\phi + c\phi
\end{bmatrix}.
$$

The matrix (5.428) can be decomposed to

$$
\begin{aligned}
R_{\hat{u},\phi} \;=\;& \cos\phi \begin{bmatrix} 1 & 0 & 0 \\ 0 & 1 & 0 \\ 0 & 0 & 1 \end{bmatrix} \\
&+ (1 - \cos\phi) \begin{bmatrix} u_1 \\ u_2 \\ u_3 \end{bmatrix} \begin{bmatrix} u_1 & u_2 & u_3 \end{bmatrix} \\
&+ \sin\phi \begin{bmatrix} 0 & -u_3 & u_2 \\ u_3 & 0 & -u_1 \\ -u_2 & u_1 & 0 \end{bmatrix}
\end{aligned}
\tag{5.429}
$$

to be equal to

$$^G R_B = R_{\hat{u},\phi} = \mathbf{I}\cos\phi + \hat{u}\hat{u}^T \operatorname{vers}\phi + \tilde{u}\sin\phi. \tag{5.430}$$

Equation (5.416) is called the *Rodriguez rotation formula* (or the *Euler-Lexell-Rodriguez formula*). It is sometimes reported in literature as the following equivalent forms:

$$\begin{aligned}
R_{\hat{u},\phi} &= \mathbf{I} + (\sin\phi)\,\tilde{u} + (\operatorname{vers}\phi)\,\tilde{u}^2 & (5.431)\\
R_{\hat{u},\phi} &= \left[\mathbf{I} - \hat{u}\hat{u}^T\right]\cos\phi + \tilde{u}\sin\phi + \hat{u}\hat{u}^T & (5.432)\\
R_{\hat{u},\phi} &= -\tilde{u}^2\cos\phi + \tilde{u}\sin\phi + \tilde{u}^2 + \mathbf{I} & (5.433)
\end{aligned}$$

The *inverse of an angle-axis rotation* is

$$\begin{aligned}
^B R_G &= {}^G R_B^T = R_{\hat{u},-\phi}\\
&= \mathbf{I}\cos\phi + \hat{u}\hat{u}^T \operatorname{vers}\phi - \tilde{u}\sin\phi. & (5.434)
\end{aligned}$$

It means orientation of $B$ in $G$, when $B$ is rotated $\phi$ about $\hat{u}$, is the same as the orientation of $G$ in $B$, when $B$ is rotated $-\phi$ about $\hat{u}$. We can verify that

$$\begin{aligned}
\tilde{u}\hat{u} &= 0 & (5.435)\\
\mathbf{I} - \hat{u}\hat{u}^T &= \tilde{u}^2 & (5.436)\\
\mathbf{r}^T\tilde{u}\mathbf{r} &= 0 & (5.437)\\
\hat{u} \times \mathbf{r} &= \tilde{u}\mathbf{r} = -\tilde{r}\hat{u} = -\mathbf{r} \times \hat{u}. & (5.438)
\end{aligned}$$

■

**Example 202** ★ *Axis-angle rotation when $\hat{u} = \hat{K}$.*
  If the local frame $B\,(Oxyz)$ rotates about the $Z$-axis, then

$$\hat{u} = \hat{K} \tag{5.439}$$

*and the transformation matrix (5.417) reduces to*

$$\begin{aligned}
^G R_B &= \begin{bmatrix}
0\operatorname{vers}\phi + \cos\phi & 0\operatorname{vers}\phi - 1\sin\phi & 0\operatorname{vers}\phi + 0\sin\phi\\
0\operatorname{vers}\phi + 1\sin\phi & 0\operatorname{vers}\phi + \cos\phi & 0\operatorname{vers}\phi - 0\sin\phi\\
0\operatorname{vers}\phi - 0\sin\phi & 0\operatorname{vers}\phi + 0\sin\phi & 1\operatorname{vers}\phi + \cos\phi
\end{bmatrix}\\
&= \begin{bmatrix}
\cos\phi & -\sin\phi & 0\\
\sin\phi & \cos\phi & 0\\
0 & 0 & 1
\end{bmatrix} & (5.440)
\end{aligned}$$

*which is equivalent to the rotation matrix about the $Z$-axis of global frame in (5.20).*

**Example 203** ★ *Rotation about a rotated local axis.*

*If the body coordinate frame $Oxyz$ rotates $\varphi$ deg about the global $Z$-axis, then the $x$-axis would be along*

$$\hat{u}_x = {}^G R_{Z,\varphi}\, \hat{i} = \begin{bmatrix} \cos\varphi & -\sin\varphi & 0 \\ \sin\varphi & \cos\varphi & 0 \\ 0 & 0 & 1 \end{bmatrix} \begin{bmatrix} 1 \\ 0 \\ 0 \end{bmatrix}$$

$$= \begin{bmatrix} \cos\varphi \\ \sin\varphi \\ 0 \end{bmatrix}. \tag{5.441}$$

*Rotation $\theta$ about $\hat{u}_x = (\cos\varphi)\,\hat{I} + (\sin\varphi)\,\hat{J}$ is defined by Rodriguez's formula (5.417)*

$$ {}^G R_{\hat{u}_x,\theta} = \begin{bmatrix} \cos^2\varphi\,\mathrm{vers}\,\theta + \cos\theta & \cos\varphi\sin\varphi\,\mathrm{vers}\,\theta & \sin\varphi\sin\theta \\ \cos\varphi\sin\varphi\,\mathrm{vers}\,\theta & \sin^2\varphi\,\mathrm{vers}\,\theta + \cos\theta & -\cos\varphi\sin\theta \\ -\sin\varphi\sin\theta & \cos\varphi\sin\theta & \cos\theta \end{bmatrix}. $$

*Now, rotation $\varphi$ about the global $Z$-axis followed by rotation $\theta$ about the local $x$-axis is transformed by*

$$\begin{aligned} {}^G R_B &= {}^G R_{\hat{u}_x,\theta}\, {}^G R_{Z,\varphi} \\ &= \begin{bmatrix} \cos\varphi & -\cos\theta\sin\varphi & \sin\theta\sin\varphi \\ \sin\varphi & \cos\theta\cos\varphi & -\cos\varphi\sin\theta \\ 0 & \sin\theta & \cos\theta \end{bmatrix} \end{aligned} \tag{5.442}$$

*that must be equal to $[R_{x,\theta}\, R_{z,\varphi}]^{-1} = R_{z,\varphi}^T\, R_{x,\theta}^T$.*

**Example 204** ★ *Axis and angle of rotation.*

*Given a transformation matrix ${}^G R_B$ we may obtain the axis $\hat{u}$ and angle $\phi$ of the rotation by considering that*

$$\tilde{u} = \frac{1}{2\sin\phi}\left( {}^G R_B - {}^G R_B^T \right) \tag{5.443}$$

$$\cos\phi = \frac{1}{2}\left( \mathrm{tr}\left( {}^G R_B \right) - 1 \right) \tag{5.444}$$

*because*

$$\begin{aligned} {}^G R_B - {}^G R_B^T &= \begin{bmatrix} 0 & -2(\sin\phi)\,u_3 & 2(\sin\phi)\,u_2 \\ 2(\sin\phi)\,u_3 & 0 & -2(\sin\phi)\,u_1 \\ -2(\sin\phi)\,u_2 & 2(\sin\phi)\,u_1 & 0 \end{bmatrix} \\ &= 2\sin\phi \begin{bmatrix} 0 & -u_3 & u_2 \\ u_3 & 0 & -u_1 \\ -u_2 & u_1 & 0 \end{bmatrix} \\ &= 2\tilde{u}\sin\phi \end{aligned} \tag{5.445}$$

*and*

$$
\begin{aligned}
\mathrm{tr}\left({}^{G}R_{B}\right) &= r_{11} + r_{22} + r_{33} \\
&= 3\cos\phi + u_1^2\left(1-\cos\phi\right) + u_2^2\left(1-\cos\phi\right) + u_3^2\left(1-\cos\phi\right) \\
&= 3\cos\phi + u_1^2 + u_2^2 + u_3^2 - \left(u_1^2 + u_2^2 + u_3^2\right)\cos\phi \\
&= 2\cos\phi + 1.
\end{aligned} \tag{5.446}
$$

**Example 205 ★** *Axis and angle of a rotation matrix.*

*A body coordinate frame, B, undergoes three Euler rotations $(\varphi, \theta, \psi) = (30, 45, 60)\,\mathrm{deg}$ with respect to a global frame G. The rotation matrix to transform coordinates of B to G is*

$$
\begin{aligned}
{}^{G}R_{B} &= {}^{B}R_{G}^{T} = [R_{z,\psi}R_{x,\theta}R_{z,\varphi}]^{T} \\
&= R_{z,\varphi}^{T}R_{x,\theta}^{T}R_{z,\psi}^{T} \\
&= \begin{bmatrix} 0.126\,83 & -0.926\,78 & 0.353\,55 \\ 0.780\,33 & -0.126\,83 & -0.612\,37 \\ 0.612\,37 & 0.353\,55 & 0.707\,11 \end{bmatrix}.
\end{aligned} \tag{5.447}
$$

*The unique angle-axis of rotation for this rotation matrix can then be found by Equations (5.443) and (5.444).*

$$
\begin{aligned}
\phi &= \cos^{-1}\left(\frac{1}{2}\left(\mathrm{tr}\left({}^{G}R_{B}\right)-1\right)\right) \\
&= \cos^{-1}\left(-0.146\,45\right) = 98\,\mathrm{deg}
\end{aligned} \tag{5.448}
$$

$$
\begin{aligned}
\tilde{u} &= \frac{1}{2\sin\phi}\left({}^{G}R_{B} - {}^{G}R_{B}^{T}\right) \\
&= \begin{bmatrix} 0.0 & -0.862\,85 & -0.130\,82 \\ 0.862\,85 & 0.0 & -0.488\,22 \\ 0.130\,82 & 0.488\,22 & 0.0 \end{bmatrix}
\end{aligned} \tag{5.449}
$$

$$
\hat{u} = \begin{bmatrix} 0.488\,22 \\ -0.130\,82 \\ 0.862\,85 \end{bmatrix} \tag{5.450}
$$

*As a double check, we may verify the angle-axis rotation formula and derive the same rotation matrix.*

$$
\begin{aligned}
{}^{G}R_{B} &= R_{\hat{u},\phi} = \mathbf{I}\cos\phi + \hat{u}\hat{u}^{T}\,\mathrm{vers}\,\phi + \tilde{u}\sin\phi \\
&= \begin{bmatrix} 0.126\,82 & -0.926\,77 & 0.353\,54 \\ 0.780\,32 & -0.126\,83 & -0.612\,37 \\ 0.612\,36 & 0.353\,55 & 0.707\,09 \end{bmatrix}
\end{aligned} \tag{5.451}
$$
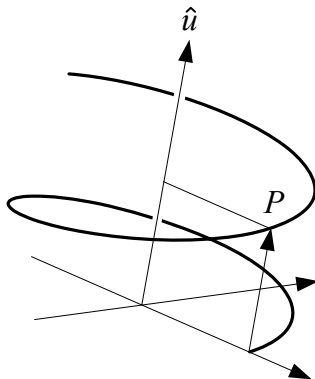
FIGURE 5.21. A screw motion is translation along a line combined with a rotation about the line.

## 5.13   ★ Screw Motion

Any rigid body motion can be produced by a single translation along an axis combined with a unique rotation about that axis. This is called *Chasles theorem*. Such a motion is called *screw*. Consider the *screw* motion illustrated in Figure 5.21. Point $P$ rotates about the screw axis indicated by $\hat{u}$ and simultaneously translates along the same axis. Hence, any point on the *screw axis* moves along the axis, while any point off the axis moves along a *helix*.

The angular rotation of the rigid body about the screw is called *twist*. *Pitch* of a screw, $p$, is the ratio of *translation*, $h$, to *rotation*, $\phi$.

$$p = \frac{h}{\phi} \tag{5.452}$$

So, pitch is the rectilinear distance through which the rigid body translates parallel to the axis of screw for a unit rotation. If $p > 0$, then the screw is *right-handed*, and if $p < 0$, it is *left-handed*.

A screw is shown by $\check{s}(h, \phi, \hat{u}, \mathbf{s})$ and is indicated by a unit vector $\hat{u}$, a *location* vector $\mathbf{s}$, a twist angle $\phi$, and a translation $h$ (or pitch $p$). The location vector $\mathbf{s}$ indicates the global position of a point on the screw axis. The twist angle $\phi$, the twist axis $\hat{u}$, and the pitch $p$ (or translation $h$) are called *screw parameters*.

The screw is another transformation method to describe the motion of a rigid body. A linear displacement along an axis combined with an angular displacement about the same axis arises in steering kinematics of vehicles. If $^B\mathbf{r}_P$ indicates the position vector of a body point, its position vector in the global frame after a screw motion is

$$^G\mathbf{r}_P = \check{s}(h, \phi, \hat{u}, \mathbf{s})\, ^B\mathbf{r}_P \tag{5.453}$$

that is equivalent to a translation $^G\mathbf{d}_B$ along with a rotation $^GR_B$.

$$^G\mathbf{r}_P = {}^GR_B \; {}^B\mathbf{r}_P + {}^G\mathbf{d}_B \tag{5.454}$$

We may introduce a $4\times4$ matrix $[T]$, that is called the *homogeneous matrix*,

$$^GT_B = \left[ \begin{array}{cc} {}^GR_B & {}^G\mathbf{d} \\ 0 & 1 \end{array} \right] \tag{5.455}$$

and combine the translation and rotation to express the motion with only a matrix multiplication

$$^G\mathbf{r}_P = {}^GT_B \; {}^B\mathbf{r}_P \tag{5.456}$$

where, $^G\mathbf{r}_P$ and $^B\mathbf{r}_P$ are expanded with an extra zero element to be consistent with the $4 \times 4$ matrix $[T]$.

$$^G\mathbf{r}_P = \left[ \begin{array}{c} X \\ Y \\ Z \\ 0 \end{array} \right] \tag{5.457}$$

$$^B\mathbf{r}_P = \left[ \begin{array}{c} x \\ y \\ z \\ 0 \end{array} \right]. \tag{5.458}$$

Homogeneous matrix representation can be used for screw transformations to combine the screw rotation and screw translation about the screw axis.

If $\hat{u}$ passes through the origin of the coordinate frame, then $\mathbf{s} = 0$ and the screw motion is called *central screw* $\check{s}(h, \phi, \hat{u})$. For a central screw we have

$$^G\check{s}_B(h, \phi, \hat{u}) = D_{\hat{u},h} \; R_{\hat{u},\phi} \tag{5.459}$$

where,

$$D_{\hat{u},h} = \left[ \begin{array}{cccc} 1 & 0 & 0 & hu_1 \\ 0 & 1 & 0 & hu_2 \\ 0 & 0 & 1 & hu_3 \\ 0 & 0 & 0 & 1 \end{array} \right] \tag{5.460}$$

$$R_{\hat{u},\phi} = \left[ \begin{array}{cccc} u_1^2 \operatorname{vers} \phi + c\phi & u_1 u_2 \operatorname{vers} \phi - u_3 s\phi & u_1 u_3 \operatorname{vers} \phi + u_2 s\phi & 0 \\ u_1 u_2 \operatorname{vers} \phi + u_3 s\phi & u_2^2 \operatorname{vers} \phi + c\phi & u_2 u_3 \operatorname{vers} \phi - u_1 s\phi & 0 \\ u_1 u_3 \operatorname{vers} \phi - u_2 s\phi & u_2 u_3 \operatorname{vers} \phi + u_1 s\phi & u_3^2 \operatorname{vers} \phi + c\phi & 0 \\ 0 & 0 & 0 & 1 \end{array} \right] \tag{5.461}$$

and hence,

$$
{}^{G}\check{s}_B(h, \phi, \hat{u}) = \begin{bmatrix} {}^{G}R_B & {}^{G}\mathbf{d} \\ 0 & 1 \end{bmatrix} =
$$
$$
\begin{bmatrix}
u_1^2 \text{ vers } \phi + c\phi & u_1 u_2 \text{ vers } \phi - u_3 s\phi & u_1 u_3 \text{ vers } \phi + u_2 s\phi & h u_1 \\
u_1 u_2 \text{ vers } \phi + u_3 s\phi & u_2^2 \text{ vers } \phi + c\phi & u_2 u_3 \text{ vers } \phi - u_1 s\phi & h u_2 \\
u_1 u_3 \text{ vers } \phi - u_2 s\phi & u_2 u_3 \text{ vers } \phi + u_1 s\phi & u_3^2 \text{ vers } \phi + c\phi & h u_3 \\
0 & 0 & 0 & 1
\end{bmatrix}.
$$
$$(5.462)$$

As a result, a central screw transformation matrix includes the pure or fundamental translations and rotations as special cases because a pure translation corresponds to $\phi = 0$, and a pure rotation corresponds to $h = 0$ (or $p = \infty$).

When the screw is not central and $\hat{u}$ is not passing through the origin, a screw motion to move $\mathbf{p}$ to $\mathbf{p}''$ is denoted by

$$
\begin{aligned}
\mathbf{p}'' &= (\mathbf{p} - \mathbf{s}) \cos \phi + (1 - \cos \phi) (\hat{u} \cdot (\mathbf{p} - \mathbf{s})) \hat{u} \\
&+ (\hat{u} \times (\mathbf{p} - \mathbf{s})) \sin \phi + \mathbf{s} + h \hat{u}
\end{aligned}
$$
$$(5.463)$$

or

$$
\begin{aligned}
\mathbf{p}'' &= {}^{G}R_B (\mathbf{p} - \mathbf{s}) + \mathbf{s} + h\hat{u} \\
&= {}^{G}R_B \mathbf{p} + \mathbf{s} - {}^{G}R_B \mathbf{s} + h\hat{u}
\end{aligned}
$$
$$(5.464)$$

and therefore,

$$
\mathbf{p}'' = \check{s}(h, \phi, \hat{u}, \mathbf{s})\mathbf{p} = [T]\,\mathbf{p}
$$
$$(5.465)$$

where

$$
\begin{aligned}
[T] &= \begin{bmatrix} {}^{G}R_B & {}^{G}\mathbf{s} - {}^{G}R_B\,{}^{G}\mathbf{s} + h\hat{u} \\ 0 & 1 \end{bmatrix} \\
&= \begin{bmatrix} {}^{G}R_B & {}^{G}\mathbf{d} \\ 0 & 1 \end{bmatrix}.
\end{aligned}
$$
$$(5.466)$$

The vector ${}^{G}\mathbf{s}$, called *location vector,* is the global position of the body frame before screw motion. The vectors $\mathbf{p}''$ and $\mathbf{p}$ are global positions of a point $P$ after and before screw, as shown in Figure 5.22.

The screw axis is indicated by the unit vector $\hat{u}$. Now a body point $P$ moves from its first position to its second position $P'$ by a rotation about $\hat{u}$. Then it moves to $P''$ by a translation $h$ parallel to $\hat{u}$. The initial position of $P$ is pointed by $\mathbf{p}$ and its final position is pointed by $\mathbf{p}''$.

A screw motion is a four variable function $\check{s}(h, \phi, \hat{u}, \mathbf{s})$. A screw has a line of action $\hat{u}$ at ${}^{G}\mathbf{s}$, a twist $\phi$, and a translation $h$.

The instantaneous screw axis was first used by Mozzi $(1730 - 1813)$ in 1763 although Chasles $(1793 - 1880)$ is credited with this discovery.
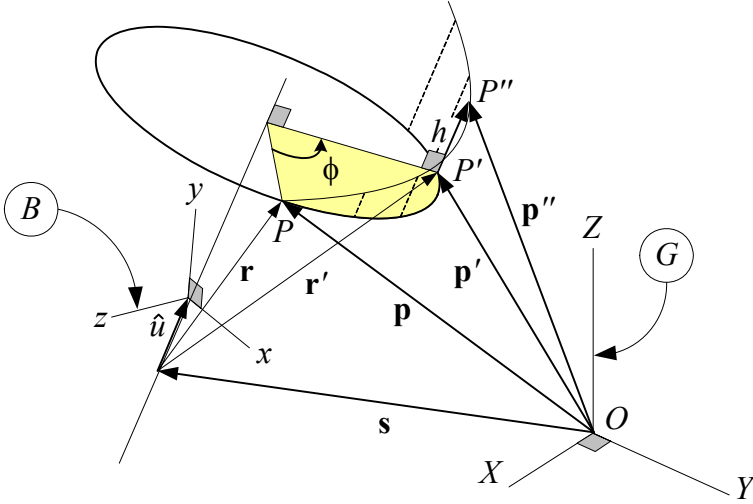
FIGURE 5.22. Screw motion of a rigid body.

**Proof.** The angle-axis rotation formula (5.416) relates $\mathbf{r}'$ and $\mathbf{r}$, which are position vectors of $P$ after and before rotation $\phi$ about $\hat{u}$ when $\mathbf{s} = 0$, $h = 0$.

$$\mathbf{r}' = \mathbf{r}\cos\phi + (1 - \cos\phi)(\hat{u} \cdot \mathbf{r})\,\hat{u} + (\hat{u} \times \mathbf{r})\sin\phi \qquad (5.467)$$

However, when the screw axis does not pass through the origin of $G(OXYZ)$, then $\mathbf{r}'$ and $\mathbf{r}$ must accordingly be substituted with the following equations:

$$\mathbf{r} \;=\; \mathbf{p} - \mathbf{s} \qquad\qquad (5.468)$$
$$\mathbf{r}' \;=\; \mathbf{p}'' - \mathbf{s} - h\hat{u} \qquad\qquad (5.469)$$

where $\mathbf{r}'$ is a vector after rotation and hence in $G$ coordinate frame, and $\mathbf{r}$ is a vector before rotation and hence in $B$ coordinate frame.

Therefore, the relationship between the new and old positions of the body point $P$ after a screw motion is

$$
\begin{aligned}
\mathbf{p}'' \;=\; & (\mathbf{p} - \mathbf{s})\cos\phi + (1 - \cos\phi)(\hat{u} \cdot (\mathbf{p} - \mathbf{s}))\,\hat{u} \\
& + (\hat{u} \times (\mathbf{p} - \mathbf{s}))\sin\phi + (\mathbf{s} + h\hat{u}). 
\end{aligned} \qquad (5.470)
$$

Equation (5.470) is the *Rodriguez formula* for the most general rigid body motion. Defining new notations $^{G}\mathbf{p} = \mathbf{p}''$ and $^{B}\mathbf{p} = \mathbf{p}$ and also noting that $\mathbf{s}$ indicates a point on the rotation axis and therefore rotation does not affect $\mathbf{s}$, we may factor out $^{B}\mathbf{p}$ and write the Rodriguez formula in the following form

$$
\begin{aligned}
^{G}\mathbf{p} \;=\; & \left(\mathbf{I}\cos\phi + \hat{u}\hat{u}^{T}(1 - \cos\phi) + \tilde{u}\sin\phi\right)\,{}^{B}\mathbf{p} \\
& - \left(\mathbf{I}\cos\phi + \hat{u}\hat{u}^{T}(1 - \cos\phi) + \tilde{u}\sin\phi\right)\,{}^{G}\mathbf{s} + {}^{G}\mathbf{s} + h\hat{u} \quad (5.471)
\end{aligned}
$$

which can be rearranged to show that a screw can be represented by a homogeneous transformation

$$
\begin{aligned}
{}^{G}\mathbf{p} &= {}^{G}R_{B}\,{}^{B}\mathbf{p} + {}^{G}\mathbf{s} - {}^{G}R_{B}\,{}^{G}\mathbf{s} + h\hat{u} \tag{5.472}\\
&= {}^{G}R_{B}\,{}^{B}\mathbf{p} + {}^{G}\mathbf{d} \\
&= {}^{G}T_{B}\,{}^{B}\mathbf{p}
\end{aligned}
$$

$$
\begin{aligned}
{}^{G}T_{B} &= {}^{G}\check{s}_{B}(h, \phi, \hat{u}, \mathbf{s}) \tag{5.473}\\
&= \left[ \begin{array}{cc} {}^{G}R_{B} & {}^{G}\mathbf{s} - {}^{G}R_{B}\,{}^{G}\mathbf{s} + h\hat{u} \\ 0 & 1 \end{array} \right] = \left[ \begin{array}{cc} {}^{G}R_{B} & {}^{G}\mathbf{d} \\ 0 & 1 \end{array} \right]
\end{aligned}
$$

where,

$$
\begin{aligned}
{}^{G}R_{B} &= \mathbf{I}\cos\phi + \hat{u}\hat{u}^{T}(1 - \cos\phi) + \tilde{u}\sin\phi \tag{5.474}\\
{}^{G}\mathbf{d} &= \left( (\mathbf{I} - \hat{u}\hat{u}^{T})(1 - \cos\phi) - \tilde{u}\sin\phi \right) {}^{G}\mathbf{s} + h\hat{u}. \tag{5.475}
\end{aligned}
$$

Direct substitution shows that:

$$
{}^{G}R_{B} = \left[ \begin{array}{ccc} u_{1}^{2}\operatorname{vers}\phi + c\phi & u_{1}u_{2}\operatorname{vers}\phi - u_{3}s\phi & u_{1}u_{3}\operatorname{vers}\phi + u_{2}s\phi \\ u_{1}u_{2}\operatorname{vers}\phi + u_{3}s\phi & u_{2}^{2}\operatorname{vers}\phi + c\phi & u_{2}u_{3}\operatorname{vers}\phi - u_{1}s\phi \\ u_{1}u_{3}\operatorname{vers}\phi - u_{2}s\phi & u_{2}u_{3}\operatorname{vers}\phi + u_{1}s\phi & u_{3}^{2}\operatorname{vers}\phi + c\phi \end{array} \right]
\tag{5.476}
$$

$$
{}^{G}\mathbf{d} = \left[ \begin{array}{c} hu_{1} + (s_{1} - u_{1}(s_{3}u_{3} + s_{2}u_{2} + s_{1}u_{1}))\operatorname{vers}\phi + (s_{2}u_{3} - s_{3}u_{2})s\phi \\ hu_{2} + (s_{2} - u_{2}(s_{3}u_{3} + s_{2}u_{2} + s_{1}u_{1}))\operatorname{vers}\phi + (s_{3}u_{1} - s_{1}u_{3})s\phi \\ hu_{3} + (s_{3} - u_{3}(s_{3}u_{3} + s_{2}u_{2} + s_{1}u_{1}))\operatorname{vers}\phi + (s_{1}u_{2} - s_{2}u_{1})s\phi \end{array} \right]
\tag{5.477}
$$

This representation of a rigid motion requires six independent parameters, namely one for rotation angle $\phi$, one for translation $h$, two for screw axis $\hat{u}$, and two for location vector ${}^{G}\mathbf{s}$. It is because three components of $\hat{u}$ are related to each other according to

$$
\hat{u}^{T}\hat{u} = 1 \tag{5.478}
$$

and the location vector ${}^{G}\mathbf{s}$ can locate any arbitrary point on the screw axis. It is convenient to choose the point where it has the minimum distance from $O$ to make ${}^{G}\mathbf{s}$ perpendicular to $\hat{u}$. Let us indicate the *shortest location vector* by ${}^{G}\mathbf{s}_{0}$, then there is a constraint among the components of the location vector

$$
{}^{G}\mathbf{s}_{0}^{T}\,\hat{u} = 0. \tag{5.479}
$$

If $\mathbf{s} = 0$ then the screw axis passes through the origin of $G$ and (5.473) reduces to (5.462).

The screw parameters $\phi$ and $h$, together with the screw axis $\hat{u}$ and location vector ${}^{G}\mathbf{s}$, completely define a rigid motion of $B(oxyz)$ in $G(OXYZ)$. Having the screw parameters and screw axis, we can find the elements of

the transformation matrix by Equations (5.476) and (5.477). So, given the transformation matrix $^GT_B$, we can find the screw angle and axis by

$$
\begin{aligned}
\cos\phi &= \frac{1}{2}\left(\operatorname{tr}\left(^GR_B\right)-1\right)\\
&= \frac{1}{2}\left(\operatorname{tr}\left(^GT_B\right)-2\right)\\
&= \frac{1}{2}\left(r_{11}+r_{22}+r_{33}-1\right)
\end{aligned}
\tag{5.480}
$$

$$
\tilde{u}=\frac{1}{2\sin\phi}\left(^GR_B-\,^GR_B^T\right)
\tag{5.481}
$$

hence,

$$
\hat{u}=\frac{1}{2\sin\phi}\begin{bmatrix} r_{32}-r_{23} \\ r_{13}-r_{31} \\ r_{21}-r_{12} \end{bmatrix}.
\tag{5.482}
$$

To find all the required screw parameters, we must also find $h$ and co-ordinates of one point on the screw axis. Because the points on the screw axis are invariant under the rotation, we must have

$$
\begin{bmatrix} r_{11} & r_{12} & r_{13} & r_{14} \\ r_{21} & r_{22} & r_{23} & r_{24} \\ r_{31} & r_{32} & r_{33} & r_{34} \\ 0 & 0 & 0 & 1 \end{bmatrix}\begin{bmatrix} X \\ Y \\ Z \\ 1 \end{bmatrix}=\begin{bmatrix} 1 & 0 & 0 & hu_1 \\ 0 & 1 & 0 & hu_2 \\ 0 & 0 & 1 & hu_3 \\ 0 & 0 & 0 & 1 \end{bmatrix}\begin{bmatrix} X \\ Y \\ Z \\ 1 \end{bmatrix}
\tag{5.483}
$$

where $(X,Y,Z)$ are coordinates of points on the screw axis.

As a sample point, we may find the intersection point of the screw line with $YZ$-plane, by setting $X_s=0$ and searching for $\mathbf{s}=\begin{bmatrix} 0 & Y_s & Z_s \end{bmatrix}^T$. Therefore,

$$
\begin{bmatrix} r_{11}-1 & r_{12} & r_{13} & r_{14}-hu_1 \\ r_{21} & r_{22}-1 & r_{23} & r_{24}-hu_2 \\ r_{31} & r_{32} & r_{33}-1 & r_{34}-hu_3 \\ 0 & 0 & 0 & 0 \end{bmatrix}\begin{bmatrix} 0 \\ Y_s \\ Z_s \\ 1 \end{bmatrix}=\begin{bmatrix} 0 \\ 0 \\ 0 \\ 0 \end{bmatrix}
\tag{5.484}
$$

which generates three equations to be solved for $Y_s$, $Z_s$, and $h$.

$$
\begin{bmatrix} h \\ Y_s \\ Z_s \end{bmatrix}=\begin{bmatrix} u_1 & -r_{12} & -r_{13} \\ u_2 & 1-r_{22} & -r_{23} \\ u_3 & -r_{32} & 1-r_{33} \end{bmatrix}^{-1}\begin{bmatrix} r_{14} \\ r_{24} \\ r_{34} \end{bmatrix}
\tag{5.485}
$$

Now we can find the shortest location vector $^G\mathbf{s}_0$ by

$$
^G\mathbf{s}_0=\mathbf{s}-(\mathbf{s}\cdot\hat{u})\hat{u}.
\tag{5.486}
$$

■

**Example 206** ★ *Central screw transformation of a base unit vector.*

*Consider two initially coincident frames $G(OXYZ)$ and $B(oxyz)$. The body performs a screw motion along the $Y$-axis for $h = 2$ and $\phi = 90\deg$. The position of a body point at $\begin{bmatrix} 1 & 0 & 0 & 1 \end{bmatrix}^T$ can be found by applying the central screw transformation.*

$$\check{s}(h, \phi, \hat{u}) = \check{s}(2, \frac{\pi}{2}, \hat{J}) \tag{5.487}$$

$$= D(2\hat{J}) R(\hat{J}, \frac{\pi}{2})$$

$$= \begin{bmatrix} 1 & 0 & 0 & 0 \\ 0 & 1 & 0 & 2 \\ 0 & 0 & 1 & 0 \\ 0 & 0 & 0 & 1 \end{bmatrix} \begin{bmatrix} 0 & 0 & 1 & 0 \\ 0 & 1 & 0 & 0 \\ -1 & 0 & 0 & 0 \\ 0 & 0 & 0 & 1 \end{bmatrix}$$

$$= \begin{bmatrix} 0 & 0 & 1 & 0 \\ 0 & 1 & 0 & 2 \\ -1 & 0 & 0 & 0 \\ 0 & 0 & 0 & 1 \end{bmatrix}$$

*Therefore,*

$$^G\hat{i} = \check{s}(2, \frac{\pi}{2}, \hat{J})\, ^B\hat{i} \tag{5.488}$$

$$= \begin{bmatrix} 0 & 0 & 1 & 0 \\ 0 & 1 & 0 & 2 \\ -1 & 0 & 0 & 0 \\ 0 & 0 & 0 & 1 \end{bmatrix} \begin{bmatrix} 1 \\ 0 \\ 0 \\ 1 \end{bmatrix}$$

$$= \begin{bmatrix} 0 & 2 & -1 & 1 \end{bmatrix}^T.$$

*The pitch of this screw is*

$$p = \frac{h}{\phi} = \frac{2}{\frac{\pi}{2}} = \frac{4}{\pi} = 1.2732 \quad unit/rad. \tag{5.489}$$

**Example 207** ★ *Screw transformation of a point.*

*Consider two initially parallel frames $G(OXYZ)$ and $B(oxyz)$. The body performs a screw motion along $X = 2$ and parallel to the $Y$-axis for $h = 2$ and $\phi = 90\deg$. Therefore, the body coordinate frame is at location $\mathbf{s} = \begin{bmatrix} 2 & 0 & 0 \end{bmatrix}^T$. The position of a body point at $^B\mathbf{r} = \begin{bmatrix} 3 & 0 & 0 & 1 \end{bmatrix}^T$ can be found by applying the screw transformation, which is*

$$^G T_B = \begin{bmatrix} ^G R_B & \mathbf{s} - {}^G R_B\,\mathbf{s} + h\hat{u} \\ 0 & 1 \end{bmatrix} \tag{5.490}$$

$$= \begin{bmatrix} 0 & 0 & 1 & 2 \\ 0 & 1 & 0 & 2 \\ -1 & 0 & 0 & 2 \\ 0 & 0 & 0 & 1 \end{bmatrix}$$

*because,*

$$^{G}R_{B} = \begin{bmatrix} 0 & 0 & 1 \\ 0 & 1 & 0 \\ -1 & 0 & 0 \end{bmatrix} \tag{5.491}$$

$$\mathbf{s} = \begin{bmatrix} 2 \\ 0 \\ 0 \end{bmatrix} \tag{5.492}$$

$$\hat{u} = \begin{bmatrix} 0 \\ 1 \\ 0 \end{bmatrix}. \tag{5.493}$$

*Therefore, the position vector of $^{G}\mathbf{r}$ would then be*

$$
\begin{aligned}
^{G}\mathbf{r} &= {}^{G}T_{B}\,{}^{B}\mathbf{r} \\
&= \begin{bmatrix} 0 & 0 & 1 & 2 \\ 0 & 1 & 0 & 2 \\ -1 & 0 & 0 & 2 \\ 0 & 0 & 0 & 1 \end{bmatrix} \begin{bmatrix} 3 \\ 0 \\ 0 \\ 1 \end{bmatrix} = \begin{bmatrix} 2 \\ 2 \\ -1 \\ 1 \end{bmatrix}.
\end{aligned} \tag{5.494}
$$

**Example 208** ★ *Rotation of a vector.*

*Transformation equation $^{G}\mathbf{r} = {}^{G}R_{B}\,{}^{B}\mathbf{r}$ and Rodriguez rotation formula (5.416) describe the rotation of any vector fixed in a rigid body. However, the vector can conveniently be described in terms of two points fixed in the body to derive the screw equation.*

*A reference point $P_1$ with position vector $\mathbf{r}_1$ at the tail, and a point $P_2$ with position vector $\mathbf{r}_2$ at the head, define a vector in the rigid body. Then the transformation equation between body and global frames can be written as*

$$^{G}(\mathbf{r}_2 - \mathbf{r}_1) = {}^{G}R_{B}\,{}^{B}(\mathbf{r}_2 - \mathbf{r}_1). \tag{5.495}$$

*Assume the original and final positions of the reference point $P_1$ are along the rotation axis. Equation (5.495) can then be rearranged in a form suitable for calculating coordinates of the new position of point $P_2$ in a transformation matrix form*

$$
\begin{aligned}
^{G}\mathbf{r}_2 &= {}^{G}R_{B}\,{}^{B}(\mathbf{r}_2 - \mathbf{r}_1) + {}^{G}\mathbf{r}_1 \\
&= {}^{G}R_{B}\,{}^{B}\mathbf{r}_2 + {}^{G}\mathbf{r}_1 - {}^{G}R_{B}\,{}^{B}\mathbf{r}_1 \\
&= {}^{G}T_{B}\,{}^{B}\mathbf{r}_2
\end{aligned} \tag{5.496}
$$

*where*

$$^{G}T_{B} = \begin{bmatrix} {}^{G}R_{B} & {}^{G}\mathbf{r}_1 - {}^{G}R_{B}\,{}^{B}\mathbf{r}_1 \\ 0 & 1 \end{bmatrix}. \tag{5.497}$$

*It is compatible with screw motion (5.473) for $h = 0$.*
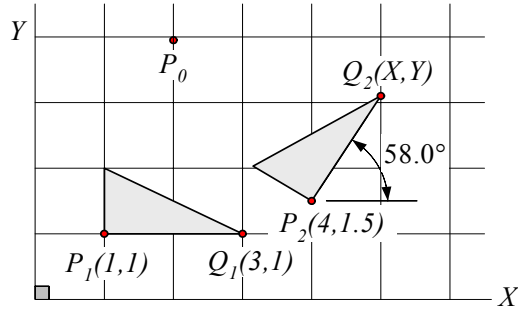
FIGURE 5.23. Motion in a plane.

**Example 209** ★ *Special cases for screw determination.*

*There are two special cases for screws. The first one occurs when $r_{11} = r_{22} = r_{33} = 1$, then, $\phi = 0$ and the motion is a pure translation $h$ parallel to $\hat{u}$, where,*

$$\hat{u} = \frac{r_{14} - s_1}{h}\hat{I} + \frac{r_{24} - s_2}{h}\hat{J} + \frac{r_{34} - s_3}{h}\hat{K}. \qquad (5.498)$$

*Since there is no unique screw axis in this case, we cannot locate any specific point on the screw axis.*

*The second special case occurs when $\phi = 180 \deg$. In this case*

$$\hat{u} = \begin{bmatrix} \sqrt{\frac{1}{2}(r_{11} + 1)} \\ \sqrt{\frac{1}{2}(r_{22} + 1)} \\ \sqrt{\frac{1}{2}(r_{33} + 1)} \end{bmatrix} \qquad (5.499)$$

*however, $h$ and $(X, Y, Z)$ can again be calculated from (5.485).*

**Example 210** ★ *Rotation and translation in a plane.*

*Assume a plane is displaced from position 1 to position 2 according to Figure 5.23. New coordinates of $Q_2$ are*

$$
\begin{aligned}
\mathbf{r}_{Q_2} &= {}^2R_1\,(\mathbf{r}_{Q_1} - \mathbf{r}_{P_1}) + \mathbf{r}_{P_2} & (5.500) \\
&= \begin{bmatrix} \cos 58 & -\sin 58 & 0 \\ \sin 58 & \cos 58 & 0 \\ 0 & 0 & 1 \end{bmatrix} \left( \begin{bmatrix} 3 \\ 1 \\ 0 \end{bmatrix} - \begin{bmatrix} 1 \\ 1 \\ 0 \end{bmatrix} \right) + \begin{bmatrix} 4 \\ 1.5 \\ 0 \end{bmatrix} \\
&= \begin{bmatrix} 1.06 \\ 1.696 \\ 0 \end{bmatrix} + \begin{bmatrix} 4 \\ 1.5 \\ 0 \end{bmatrix} = \begin{bmatrix} 5.06 \\ 3.196 \\ 0.0 \end{bmatrix}
\end{aligned}
$$

*or equivalently*

$$\mathbf{r}_{Q_2} = {}^2T_1 \, \mathbf{r}_{Q_1} \tag{5.501}$$

$$= \begin{bmatrix} {}^2R_1 & \mathbf{r}_{P_2} - {}^2R_1 \mathbf{r}_{P_1} \\ 0 & 1 \end{bmatrix} \mathbf{r}_{Q_1}$$

$$= \begin{bmatrix} \cos 58 & -\sin 58 & 0 & 4.318 \\ \sin 58 & \cos 58 & 0 & 0.122 \\ 0 & 0 & 1 & 0 \\ 0 & 0 & 0 & 1 \end{bmatrix} \begin{bmatrix} 3 \\ 1 \\ 0 \\ 1 \end{bmatrix}$$

$$= \begin{bmatrix} 5.06 \\ 3.196 \\ 0 \\ 1 \end{bmatrix}.$$

**Example 211 ★** *Pole of planar motion.*

In the planar motion of a rigid body, going from position 1 to position 2, there is always one point in the plane of motion that does not change its position. Hence, the body can be considered as having rotated about this point, which is known as the finite rotation pole. The transformation matrix can be used to locate the pole. Figure 5.23 depicts a planar motion of a triangle. To locate the pole of motion $P_0(X_0, Y_0)$ we need the transformation of the motion. Using the data given in Figure 5.23 we have

$$
{}^2T_1 = \begin{bmatrix} {}^2R_1 & \mathbf{r}_{P_2} - {}^2R_1 \mathbf{r}_{P_1} \\ 0 & 1 \end{bmatrix} \tag{5.502}
$$

$$
= \begin{bmatrix} c\alpha & -s\alpha & 0 & -c\alpha + s\alpha + 4 \\ s\alpha & c\alpha & 0 & -c\alpha - s\alpha + 3.5 \\ 0 & 0 & 1 & 0 \\ 0 & 0 & 0 & 1 \end{bmatrix}.
$$

*The pole would be conserved under the transformation. Therefore,*

$$
\mathbf{r}_{P_0} = {}^2T_1 \, \mathbf{r}_{P_0} \tag{5.503}
$$

$$
\begin{bmatrix} X_0 \\ Y_0 \\ 0 \\ 1 \end{bmatrix} = \begin{bmatrix} \cos\alpha & -\sin\alpha & 0 & -\cos\alpha + \sin\alpha + 4 \\ \sin\alpha & \cos\alpha & 0 & -\cos\alpha - \sin\alpha + 1.5 \\ 0 & 0 & 1 & 0 \\ 0 & 0 & 0 & 1 \end{bmatrix} \begin{bmatrix} X_0 \\ Y_0 \\ 0 \\ 1 \end{bmatrix}
$$

*which for $\alpha = 58 \deg$ provides*

$$
X_0 = -1.5\sin\alpha + 1 - 4\cos\alpha = 2.049
$$
$$
Y_0 = 4\sin\alpha + 1 - 1.5\cos\alpha = 3.956.
$$

**Example 212 ★** *Determination of screw parameters.*

We are able to determine screw parameters when we have the original and final position of three non-colinear points of a rigid body. Assume $\mathbf{p}_0$,

$\mathbf{q}_0$, and $\mathbf{r}_0$ denote the position of points $P$, $Q$, and $R$ before the screw motion, and $\mathbf{p}_1$, $\mathbf{q}_1$, and $\mathbf{r}_1$ denote their positions after the screw motion.

To determine screw parameters, $\phi$, $\hat{u}$, $h$, and $\mathbf{s}$, we should solve the following three simultaneous Rodriguez equations:

$$\mathbf{p}_1 - \mathbf{p}_0 = \tan\frac{\phi}{2}\hat{u} \times (\mathbf{p}_1 + \mathbf{p}_0 - 2\mathbf{s}) + h\hat{u} \tag{5.504}$$

$$\mathbf{q}_1 - \mathbf{q}_0 = \tan\frac{\phi}{2}\hat{u} \times (\mathbf{q}_1 + \mathbf{q}_0 - 2\mathbf{s}) + h\hat{u} \tag{5.505}$$

$$\mathbf{r}_1 - \mathbf{r}_0 = \tan\frac{\phi}{2}\hat{u} \times (\mathbf{r}_1 + \mathbf{r}_0 - 2\mathbf{s}) + h\hat{u} \tag{5.506}$$

We start with subtracting Equation (5.506) from (5.504) and (5.505).

$$(\mathbf{p}_1 - \mathbf{p}_0) - (\mathbf{r}_1 - \mathbf{r}_0) = \tan\frac{\phi}{2}\hat{u} \times [(\mathbf{p}_1 + \mathbf{p}_0) - (\mathbf{r}_1 - \mathbf{r}_0)] \tag{5.507}$$

$$(\mathbf{q}_1 - \mathbf{q}_0) - (\mathbf{r}_1 - \mathbf{r}_0) = \tan\frac{\phi}{2}\hat{u} \times [(\mathbf{q}_1 + \mathbf{q}_0) - (\mathbf{r}_1 - \mathbf{r}_0)] \tag{5.508}$$

Now multiplying both sides of (5.507) by $[(\mathbf{q}_1 - \mathbf{q}_0) - (\mathbf{r}_1 - \mathbf{r}_0)]$ which is perpendicular to $\hat{u}$

$$\begin{aligned}&[(\mathbf{q}_1 - \mathbf{q}_0) - (\mathbf{r}_1 - \mathbf{r}_0)] \times [(\mathbf{p}_1 - \mathbf{p}_0) - (\mathbf{r}_1 - \mathbf{r}_0)]\\&= \tan\tfrac{\phi}{2}[(\mathbf{q}_1 - \mathbf{q}_0) - (\mathbf{r}_1 - \mathbf{r}_0)] \times \{\hat{u} \times [(\mathbf{p}_1 + \mathbf{p}_0) - (\mathbf{r}_1 - \mathbf{r}_0)]\}\end{aligned} \tag{5.509}$$

gives us

$$\begin{aligned}&[(\mathbf{q}_1 - \mathbf{q}_0) - (\mathbf{r}_1 - \mathbf{r}_0)] \times [(\mathbf{p}_1 + \mathbf{p}_0) - (\mathbf{r}_1 - \mathbf{r}_0)]\\&= \tan\tfrac{\phi}{2}[(\mathbf{q}_1 - \mathbf{q}_0) - (\mathbf{r}_1 - \mathbf{r}_0)] \cdot [(\mathbf{p}_1 + \mathbf{p}_0) - (\mathbf{r}_1 - \mathbf{r}_0)]\,\hat{u}\end{aligned} \tag{5.510}$$

and therefore, the rotation angle can be found by equating $\tan\frac{\phi}{2}$ and the norm of the right-hand side of the following equation:

$$\tan\frac{\phi}{2}\hat{u} = \frac{[(\mathbf{q}_1 - \mathbf{q}_0) - (\mathbf{r}_1 - \mathbf{r}_0)] \times (\mathbf{p}_1 + \mathbf{p}_0) - (\mathbf{r}_1 - \mathbf{r}_0)}{[(\mathbf{q}_1 - \mathbf{q}_0) - (\mathbf{r}_1 - \mathbf{r}_0)] \cdot (\mathbf{p}_1 + \mathbf{p}_0) - (\mathbf{r}_1 - \mathbf{r}_0)} \tag{5.511}$$

To find $\mathbf{s}$, we may start with the cross product of $\hat{u}$ with Equation (5.504).

$$\begin{aligned}\hat{u} \times (\mathbf{p}_1 - \mathbf{p}_0) &= \hat{u} \times \left[\tan\frac{\phi}{2}\hat{u} \times (\mathbf{p}_1 + \mathbf{p}_0 - 2\mathbf{s}) + h\hat{u}\right] \tag{5.512}\\&= \tan\frac{\phi}{2}\{[\hat{u} \cdot (\mathbf{p}_1 + \mathbf{p}_0)]\,\hat{u} - (\mathbf{p}_1 + \mathbf{p}_0) + 2[\mathbf{s} - (\hat{u} \cdot \mathbf{s})\,\hat{u}]\}\end{aligned}$$

Note that $\mathbf{s} - (\hat{u} \cdot \mathbf{s})\,\hat{u}$ is the component of $\mathbf{s}$ perpendicular to $\hat{u}$, where $\mathbf{s}$ is a vector from the origin of the global frame $G(OXYZ)$ to an arbitrary point on the screw axis. This perpendicular component indicates a vector

*with the shortest distance between $O$ and $\hat{u}$. Let's assume $\mathbf{s}_0$ is the name of the shortest $\mathbf{s}$. Therefore,*

$$
\begin{aligned}
\mathbf{s}_0 &= \mathbf{s} - (\hat{u} \cdot \mathbf{s})\,\hat{u} \\
&= \frac{1}{2}\left[ \frac{\hat{u} \times \mathbf{p}_1 - \mathbf{p}_0}{\tan \frac{\phi}{2}} - [\hat{u} \cdot (\mathbf{p}_1 + \mathbf{p}_0)]\,\hat{u} + \mathbf{p}_1 + \mathbf{p}_0 \right]. \qquad (5.513)
\end{aligned}
$$

*The last parameter of the screw is the pitch $h$, which can be found from any one of the Equations (5.504), (5.505), or (5.506).*

$$
\begin{aligned}
h &= \hat{u} \cdot (\mathbf{p}_1 - \mathbf{p}_0) \\
&= \hat{u} \cdot (\mathbf{q}_1 - \mathbf{q}_0) \\
&= \hat{u} \cdot (\mathbf{r}_1 - \mathbf{r}_0) \qquad (5.514)
\end{aligned}
$$

**Example 213** ★ *Alternative derivation of screw transformation.*

   *Assume the screw axis does not pass through the origin of $G$. If $^G\mathbf{s}$ is the position vector of some point on the axis $\hat{u}$, then we can derive the matrix representation of screw $\check{s}(h, \phi, \hat{u}, \mathbf{s})$ by translating the screw axis back to the origin, performing the central screw motion, and translating the line back to its original position.*

$$
\begin{aligned}
\check{s}(h, \phi, \hat{u}, \mathbf{s}) &= D(^G\mathbf{s})\,\check{s}(h, \phi, \hat{u})\,D(-\,^G\mathbf{s}) \\
&= D(^G\mathbf{s})\,D(h\hat{u})\,R(\hat{u}, \phi)\,D(-\,^G\mathbf{s}) \\
&= \begin{bmatrix} \mathbf{I} & ^G\mathbf{s} \\ 0 & 1 \end{bmatrix} \begin{bmatrix} ^GR_B & h\hat{u} \\ 0 & 1 \end{bmatrix} \begin{bmatrix} \mathbf{I} & -\,^G\mathbf{s} \\ 0 & 1 \end{bmatrix} \\
&= \begin{bmatrix} ^GR_B & ^G\mathbf{s} - ^GR_B\,^G\mathbf{s} + h\hat{u} \\ 0 & 1 \end{bmatrix} \qquad (5.515)
\end{aligned}
$$

**Example 214** ★ *Rotation about an off-center axis.*

   *Rotation of a rigid body about an axis indicated by $\hat{u}$ and passing through a point at $^G\mathbf{s}$, where $^G\mathbf{s} \times \hat{u} \neq 0$ is a rotation about an off-center axis. The transformation matrix associated with an off-center rotation can be obtained from the screw transformation by setting $h = 0$. Therefore, an off-center rotation transformation is*

$$
^GT_B = \begin{bmatrix} ^GR_B & ^G\mathbf{s} - ^GR_B\,^G\mathbf{s} \\ 0 & 1 \end{bmatrix}. \qquad (5.516)
$$

**Example 215** ★ *Principal central screw.*

   *There are three principal central screws, namely the x-screw, y-screw, and z-screw, which are*

$$
\check{s}(h_Z, \alpha, \hat{K}) = \begin{bmatrix} \cos\alpha & -\sin\alpha & 0 & 0 \\ \sin\alpha & \cos\alpha & 0 & 0 \\ 0 & 0 & 1 & p_Z\,\alpha \\ 0 & 0 & 0 & 1 \end{bmatrix} \qquad (5.517)
$$

$$\check{s}(h_Y, \beta, \hat{J}) = \begin{bmatrix} \cos\beta & 0 & \sin\beta & 0 \\ 0 & 1 & 0 & p_Y\beta \\ -\sin\beta & 0 & \cos\beta & 0 \\ 0 & 0 & 0 & 1 \end{bmatrix} \tag{5.518}$$

$$\check{s}(h_X, \gamma, \hat{I}) = \begin{bmatrix} 1 & 0 & 0 & p_X\gamma \\ 0 & \cos\gamma & -\sin\gamma & 0 \\ 0 & \sin\gamma & \cos\gamma & 0 \\ 0 & 0 & 0 & 1 \end{bmatrix}. \tag{5.519}$$

**Example 216 ★** *Proof of Chasles theorem.*

*Let $[T]$ be an arbitrary spatial displacement, and decompose it into a rotation $R$ about $\hat{u}$ and a translation $D$.*

$$[T] = [D][R] \tag{5.520}$$

*We may also decompose the translation $[D]$ into two components $[D_\parallel]$ and $[D_\perp]$, parallel and perpendicular to $\hat{u}$, respectively.*

$$[T] = [D_\parallel][D_\perp][R] \tag{5.521}$$

*Now $[D_\perp][R]$ is a planar motion, and is therefore equivalent to some rotation $[R'] = [D_\perp][R]$ about an axis parallel to the rotation axis $\hat{u}$. This yields the decomposition $[T] = [D_\parallel][R']$. This decomposition completes the proof, since the axis of $[D_\parallel]$ can be taken equal to $\hat{u}$.*

**Example 217 ★** *Every rigid motion is a screw.*

*To show that any proper rigid motion can be considered as a screw motion, we must show that a homogeneous transformation matrix*

$$^GT_B = \begin{bmatrix} ^GR_B & ^G\mathbf{d} \\ 0 & 1 \end{bmatrix} \tag{5.522}$$

*can be written in the form*

$$^GT_B = \begin{bmatrix} ^GR_B & (\mathbf{I} - {}^GR_B)\,\mathbf{s} + h\hat{u} \\ 0 & 1 \end{bmatrix}. \tag{5.523}$$

*This problem is then equivalent to the following equation to find $h$ and $\hat{u}$.*

$$^G\mathbf{d} = (\mathbf{I} - {}^GR_B)\,\mathbf{s} + h\hat{u} \tag{5.524}$$

*The matrix $[\mathbf{I} - {}^GR_B]$ is singular because $^GR_B$ always has 1 as an eigenvalue. This eigenvalue corresponds to $\hat{u}$ as eigenvector. Therefore,*

$$[\mathbf{I} - {}^GR_B]\hat{u} = [\mathbf{I} - {}^GR_B^T]\hat{u} = 0 \tag{5.525}$$

*and an inner product shows that*

$$\begin{aligned} \hat{u} \cdot {}^G\mathbf{d} &= \hat{u} \cdot \big[\mathbf{I} - {}^GR_B\big]\,\mathbf{s} + \hat{u} \cdot h\hat{u} \\ &= \big[\mathbf{I} - {}^GR_B\big]\hat{u} \cdot \mathbf{s} + \hat{u} \cdot h\hat{u} \end{aligned}$$

*which leads to*

$$h = \hat{u} \cdot {}^{G}\mathbf{d}. \tag{5.526}$$

*Now we may use h to find* $\mathbf{s}$

$$\mathbf{s} = \left[\mathbf{I} - {}^{G}R_B\right]^{-1} \left({}^{G}\mathbf{d} - h\hat{u}\right). \tag{5.527}$$

## 5.14   Summary

To analyze the relative motion of rigid bodies, we instal a body coordinate frame at the mass center of each body. The relative motion of the bodies can be expressed by the relative motion of the frames.

Coordinates of a point in two Cartesian coordinate frames with a common origin are convertible based on nine directional cosines of the three axes of a frame in the other. The conversion of coordinates in the two frames can be cast in matrix transformation

$$
{}^{G}\mathbf{r} = {}^{G}R_B \, {}^{B}\mathbf{r} \tag{5.528}
$$

$$
\begin{bmatrix} X_2 \\ Y_2 \\ Z_2 \end{bmatrix} = \begin{bmatrix} \hat{I}\cdot\hat{\imath} & \hat{I}\cdot\hat{\jmath} & \hat{I}\cdot\hat{k} \\ \hat{J}\cdot\hat{\imath} & \hat{J}\cdot\hat{\jmath} & \hat{J}\cdot\hat{k} \\ \hat{K}\cdot\hat{\imath} & \hat{K}\cdot\hat{\jmath} & \hat{K}\cdot\hat{k} \end{bmatrix} \begin{bmatrix} x_2 \\ y_2 \\ z_2 \end{bmatrix} \tag{5.529}
$$

where,

$$
{}^{G}R_B = \begin{bmatrix} \cos(\hat{I},\hat{\imath}) & \cos(\hat{I},\hat{\jmath}) & \cos(\hat{I},\hat{k}) \\ \cos(\hat{J},\hat{\imath}) & \cos(\hat{J},\hat{\jmath}) & \cos(\hat{J},\hat{k}) \\ \cos(\hat{K},\hat{\imath}) & \cos(\hat{K},\hat{\jmath}) & \cos(\hat{K},\hat{k}) \end{bmatrix}. \tag{5.530}
$$

The transformation matrix ${}^{G}R_B$ is orthogonal and therefore its inverse is equal to its transpose.

$$
{}^{G}R_B^{-1} = {}^{G}R_B^{T} \tag{5.531}
$$

When a body coordinate frame $B$ and a global frame $G$ have a common origin and frame $B$ rotates continuously with respect to frame $G$, the rotation matrix ${}^{G}R_B$ is time dependent.

$$
{}^{G}\mathbf{r}(t) = {}^{G}R_B(t) \, {}^{B}\mathbf{r} \tag{5.532}
$$

Then, the global velocity of a point in $B$ is

$$
\begin{aligned}
{}^{G}\dot{\mathbf{r}}(t) &= {}^{G}\mathbf{v}(t) \\
&= {}^{G}\dot{R}_B(t) \, {}^{B}\mathbf{r} \\
&= {}_{G}\tilde{\omega}_B \, {}^{G}\mathbf{r}(t)
\end{aligned} \tag{5.533}
$$

where $_G\tilde{\omega}_B$ is the skew symmetric angular velocity matrix

$$_G\tilde{\omega}_B = {}^G\dot{R}_B {}^G R_B^T \tag{5.534}$$

$$_G\tilde{\omega}_B = \begin{bmatrix} 0 & -\omega_3 & \omega_2 \\ \omega_3 & 0 & -\omega_1 \\ -\omega_2 & \omega_1 & 0 \end{bmatrix}. \tag{5.535}$$

The matrix $_G\tilde{\omega}_B$ is associated with the angular velocity vector $_G\omega_B = \dot{\phi}\,\hat{u}$, which is equal to an angular rate $\dot{\phi}$ about the instantaneous axis of rotation $\hat{u}$.

Angular velocities of connected rigid bodies may be added relatively to find the angular velocity of the $n$th body in the base coordinate frame

$$_0\omega_n = {}_0\omega_1 + {}_1^0\omega_2 + {}_2^0\omega_3 + \cdots + {}_{n-1}^0\omega_n = \sum_{i=1}^{n} {}_{i-1}^0\omega_i. \tag{5.536}$$

Relative time derivatives between the global and a coordinate frames attached to a moving rigid body must be taken according to the following rules.

$$\frac{^B d}{dt} {}^B\mathbf{r}_P = {}^B\dot{\mathbf{r}}_P = {}^B\mathbf{v}_P = \dot{x}\,\hat{\imath} + \dot{y}\,\hat{\jmath} + \dot{z}\,\hat{k} \tag{5.537}$$

$$\frac{^G d}{dt} {}^G\mathbf{r}_P = {}^G\dot{\mathbf{r}}_P = {}^G\mathbf{v}_P = \dot{X}\,\hat{I} + \dot{Y}\,\hat{J} + \dot{Z}\,\hat{K} \tag{5.538}$$

$$\frac{^G d}{dt} {}^B\mathbf{r}_P\,(t) = {}^B\dot{\mathbf{r}}_P + {}^B_G\omega_B \times {}^B\mathbf{r}_P = {}^B_G\dot{\mathbf{r}}_P \tag{5.539}$$

$$\frac{^B d}{dt} {}^G\mathbf{r}_P\,(t) = {}^G\dot{\mathbf{r}}_P - {}_G\omega_B \times {}^G\mathbf{r}_P = {}^G_B\dot{\mathbf{r}}_P. \tag{5.540}$$

The global velocity of a point $P$ in a moving frame $B$ at

$$^G\mathbf{r}_P = {}^G R_B\,{}^B\mathbf{r}_P + {}^G\mathbf{d}_B$$

is

$$\begin{aligned}
^G\mathbf{v}_P &= {}^G\dot{\mathbf{r}}_P \\
&= {}_G\tilde{\omega}_B \left({}^G\mathbf{r}_P - {}^G\mathbf{d}_B\right) + {}^G\dot{\mathbf{d}}_B \\
&= {}_G\omega_B \times \left({}^G\mathbf{r}_P - {}^G\mathbf{d}_B\right) + {}^G\dot{\mathbf{d}}_B.
\end{aligned} \tag{5.541}$$

When a body coordinate frame $B$ and a global frame $G$ have a common origin, the global acceleration of a point $P$ in frame $B$ is

$$\begin{aligned}
^G\ddot{\mathbf{r}} &= \frac{^G d}{dt} {}^G\mathbf{v}_P \\
&= {}_G\alpha_B \times {}^G\mathbf{r} + {}_G\omega_B \times \left({}_G\omega_B \times {}^G\mathbf{r}\right)
\end{aligned} \tag{5.542}$$

where, $_G\boldsymbol{\alpha}_B$ is the angular acceleration of $B$ with respect to $G$

$$_G\boldsymbol{\alpha}_B = \frac{^Gd}{dt} \, _G\boldsymbol{\omega}_B. \tag{5.543}$$

However, when the body coordinate frame $B$ has a rigid motion with respect to $G$, then

$$
\begin{aligned}
^G\mathbf{a}_P &= \frac{^Gd}{dt} \, ^G\mathbf{v}_P \\
&= \, _G\boldsymbol{\alpha}_B \times \left( ^G\mathbf{r}_P - \, ^G\mathbf{d}_B \right) \\
&\quad + \, _G\boldsymbol{\omega}_B \times \left( _G\boldsymbol{\omega}_B \times \left( ^G\mathbf{r}_P - \, ^G\mathbf{d}_B \right) \right) + \, ^G\ddot{\mathbf{d}}_B \tag{5.544}
\end{aligned}
$$

where $^G\mathbf{d}_B$ indicates the position of the origin of $B$ with respect to the origin of $G$.

Angular accelerations of two connected rigid bodies are related according to

$$_0\boldsymbol{\alpha}_2 = \, _0\boldsymbol{\alpha}_1 + \, _1^0\boldsymbol{\alpha}_2 + \, _0\boldsymbol{\omega}_1 \times \, _1^0\boldsymbol{\omega}_2. \tag{5.545}$$

# 5.15   Key Symbols

| | |
|---|---|
| $B,\ Oxyz$ | body Cartesian coordinate frame |
| $^G\mathbf{d}_B$ | position vector of body coordinate frame $B$ in $G$ |
| $^0_1\mathbf{d}_2$ | position of frame $B_2$ respect to $B_1$ expressed in $B_0$ |
| $\hat{e}_\varphi, \hat{e}_\theta, \hat{e}_\psi$ | Euler angle coordinate frame unit vectors |
| $G,\ OXYZ$ | global Cartesian coordinate frame |
| $\hat{\imath}, \hat{\jmath}, \hat{k}$ | body coordinate frame unit vectors |
| $\tilde{\imath}, \tilde{\jmath}, \tilde{k}$ | skew symmetric matrix associated to $\hat{\imath}, \hat{\jmath}, \hat{k}$ |
| $\hat{I}, \hat{J}, \hat{K}$ | global coordinate frame unit vectors |
| $p = h/\phi$ | pitch of screw |
| $P$ | point |
| $^G\mathbf{r}$ | position vector in global coordinate frame |
| $^B\mathbf{r}$ | position vector in body coordinate frame |
| $\hat{\mathbf{r}}_{H_1}, \hat{\mathbf{r}}_{H_2}, \hat{\mathbf{r}}_{H_3}$ | row vectors of a rotation matrix |
| $R_Z$ | rotation matrix about the global $Z$-axis |
| $R_Y$ | rotation matrix about the global $Y$-axis |
| $R_X$ | rotation matrix about the global $X$-axis |
| $\dot{R}$ | time derivative of a rotation matrix $R$ |
| $^GR_B$ | rotation matrix from local frame to global frame |
| $R^T$ | transpose of a rotation matrix |
| $R^{-1}$ | inverse of a rotation matrix |
| $R_Z$ | rotation matrix about the body $z$-axis |
| $R_Y$ | rotation matrix about the body $y$-axis |
| $R_X$ | rotation matrix about the body $x$-axis |
| $^{B_1}R_{B_2}$ | rotation matrix from coordinate frame $B_1$ to $B_2$ |
| $^BR_G$ | rotation matrix from global to local coordinate frame |
| $\check{s}(h, \phi, \hat{u}, \mathbf{s})$ | screw motion |
| $t$ | time |
| $\hat{u}, \phi$ | axis and angle of rotation |
| $\hat{u}_\alpha$ | instant angular acceleration axis |
| $\hat{u}_\omega$ | instant angular velocity axis |
| $x, y, z$ | body coordinates of a point |
| $X, Y, Z$ | body coordinates of a point |
| $x, y, z,\ \mathbf{x}$ | displacement |
| | |
| | |
| $_G\boldsymbol{\alpha}_B$ | angular acceleration of body $B$ expressed in $G$ |
| $\delta_{jk}$ | Kronecker's delta |
| $\epsilon_{ijk}$ | permutation symbol |
| $\dot{\varphi}, \dot{\theta}, \dot{\psi}$ | Euler frequencies |
| $_G\boldsymbol{\omega}_B$ | angular velocity of rigid body $B$ expressed in $G$ |
| $\tilde{\omega}$ | skew symmetric matrix associated to $\omega$ |

## Exercises

1. Body point and global rotations.

   The point $P$ is at $\mathbf{r}_P = (1, 2, 1)$ in a body coordinate $B(Oxyz)$. Find the final global position of $P$ after a rotation of $30\deg$ about the $X$-axis, followed by a $45\deg$ rotation about the $Z$-axis.

2. Body point after global rotation.

   Find the position of a point $P$ in the local coordinate, if it is moved to $^G\mathbf{r}_P = [1, 3, 2]^T$ after a $60\deg$ rotation about the $Z$-axis.

3. Invariant of a vector.

   A point was at $^B\mathbf{r}_P = [1, 2, z]^T$. After a rotation of $60\deg$ about the $X$-axis, followed by a $30\deg$ rotation about the $Z$-axis, it is at

   $$^G\mathbf{r}_P = \begin{bmatrix} X \\ Y \\ 2.933 \end{bmatrix}.$$

   Find $z$, $X$, and $Y$.

4. ★ Constant length vector.

   Show that the length of a vector will not change by rotation.

   $$\left|^G\mathbf{r}\right| = \left|^G R_B \, ^B\mathbf{r}\right|$$

   Show that the distance between two body points will not change by rotation.

   $$\left|^B\mathbf{p}_1 - {}^B\mathbf{p}_2\right| = \left|^G R_B \, ^B\mathbf{p}_1 - {}^G R_B \, ^B\mathbf{p}_2\right|$$

5. Global roll-pitch-yaw rotation angles.

   Calculate the role, pitch, and yaw angles for the following rotation matrix:

   $$^B R_G = \begin{bmatrix} 0.53 & -0.84 & 0.13 \\ 0.0 & 0.15 & 0.99 \\ -0.85 & -0.52 & 0.081 \end{bmatrix}$$

6. Body point, local rotation.

   What is the global coordinates of a body point at $^B\mathbf{r}_P = [2, 2, 3]^T$, after a rotation of $60\deg$ about the $x$-axis?

7. Two local rotations.

   Find the global coordinates of a body point at $^B\mathbf{r}_P = [2, 2, 3]^T$ after a rotation of $60\deg$ about the $x$-axis followed by $60\deg$ about the $z$-axis.

8. Combination of local and global rotations.

   Find the final global position of a body point at $^B\mathbf{r}_P = [10, 10, -10]^T$ after a rotation of $45 \deg$ about the $x$-axis followed by $60 \deg$ about the $Z$-axis.

9. Combination of global and local rotations.

   Find the final global position of a body point at $^B\mathbf{r}_P = [10, 10, -10]^T$ after a rotation of $45 \deg$ about the $X$-axis followed by $60 \deg$ about the $z$-axis.

10. ★ Euler angles from rotation matrix.

    Find the Euler angles for the following rotation matrix:

    $$^B R_G = \begin{bmatrix} 0.53 & -0.84 & 0.13 \\ 0.0 & 0.15 & 0.99 \\ -0.85 & -0.52 & 0.081 \end{bmatrix}$$

11. ★ Equivalent Euler angles to two rotations.

    Find the Euler angles corresponding to the rotation matrix $^B R_G = A_{y,45} A_{x,30}$.

12. ★ Equivalent Euler angles to three rotations.

    Find the Euler angles corresponding to the rotation matrix $^B R_G = A_{z,60} A_{y,45} A_{x,30}$.

13. ★ Local and global positions, Euler angles.

    Find the conditions between the Euler angles to transform $^G\mathbf{r}_P = [1, 1, 0]^T$ to $^B\mathbf{r}_P = [0, 1, 1]^T$.

14. Elements of rotation matrix.

    The elements of rotation matrix $^G R_B$ are

    $$^G R_B = \begin{bmatrix} \cos(\hat{I}, \hat{\imath}) & \cos(\hat{I}, \hat{\jmath}) & \cos(\hat{I}, \hat{k}) \\ \cos(\hat{J}, \hat{\imath}) & \cos(\hat{J}, \hat{\jmath}) & \cos(\hat{J}, \hat{k}) \\ \cos(\hat{K}, \hat{\imath}) & \cos(\hat{K}, \hat{\jmath}) & \cos(\hat{K}, \hat{k}) \end{bmatrix}.$$

    Find $^G R_B$ if $^G\mathbf{r}_{P_1} = (0.7071, -1.2247, 1.4142)$ is a point on the $x$-axis, and $^G\mathbf{r}_{P_2} = (2.7803, 0.38049, -1.0607)$ is a point on the $y$-axis.

15. Local position, global velocity.

    A body is turning about the $Z$-axis at a constant angular rate $\dot{\alpha} = 2 \, \mathrm{rad/sec}$. Find the global velocity of a point at

    $$^B\mathbf{r} = \begin{bmatrix} 5 \\ 30 \\ 10 \end{bmatrix}.$$

16. Global position, constant angular velocity.

A body is turning about the $Z$-axis at a constant angular rate $\dot{\alpha} = 2 \, \mathrm{rad/s}$. Find the global position of a point at

$$
{}^B\mathbf{r} = \begin{bmatrix} 5 \\ 30 \\ 10 \end{bmatrix}
$$

after $t = 3 \, \mathrm{sec}$ if the body and global coordinate frames were coincident at $t = 0 \, \mathrm{sec}$.

17. Turning about $x$-axis.

Find the angular velocity matrix when the body coordinate frame is turning $35 \, \mathrm{deg/sec}$ at $45 \, \mathrm{deg}$ about the $x$-axis.

18. Combined rotation and angular velocity.

Find the rotation matrix for a body frame after $30 \, \mathrm{deg}$ rotation about the $Z$-axis, followed by $30 \, \mathrm{deg}$ about the $X$-axis, and then $90 \, \mathrm{deg}$ about the $Y$-axis. Then calculate the angular velocity of the body if it is turning with $\dot{\alpha} = 20 \, \mathrm{deg/sec}$, $\dot{\beta} = -40 \, \mathrm{deg/sec}$, and $\dot{\gamma} = 55 \, \mathrm{deg/sec}$ about the $Z$, $Y$, and $X$ axes respectively.

19. Angular velocity, expressed in body frame.

The point $P$ is at $\mathbf{r}_P = (1, 2, 1)$ in a body coordinate $B(Oxyz)$. Find ${}^B_G\tilde{\omega}_B$ when the body frame is turned $30 \, \mathrm{deg}$ about the $X$-axis at a rate $\dot{\gamma} = 75 \, \mathrm{deg/sec}$, followed by $45 \, \mathrm{deg}$ about the $Z$-axis at a rate $\dot{\alpha} = 25 \, \mathrm{deg/sec}$.

20. Global roll-pitch-yaw angular velocity.

Calculate the angular velocity for a global roll-pitch-yaw rotation of $\alpha = 30 \, \mathrm{deg}$, $\beta = 30 \, \mathrm{deg}$, and $\gamma = 30 \, \mathrm{deg}$ with $\dot{\alpha} = 20 \, \mathrm{deg/sec}$, $\dot{\beta} = -20 \, \mathrm{deg/sec}$, and $\dot{\gamma} = 20 \, \mathrm{deg/sec}$.

21. Roll-pitch-yaw angular velocity.

Find ${}^B_G\tilde{\omega}_B$ and ${}_G\tilde{\omega}_B$ for the role, pitch, and yaw rates equal to $\dot{\alpha} = 20 \, \mathrm{deg/sec}$, $\dot{\beta} = -20 \, \mathrm{deg/sec}$, and $\dot{\gamma} = 20 \, \mathrm{deg/sec}$ respectively, and having the following rotation matrix:

$$
{}^B R_G = \begin{bmatrix} 0.53 & -0.84 & 0.13 \\ 0.0 & 0.15 & 0.99 \\ -0.85 & -0.52 & 0.081 \end{bmatrix}
$$

22. ★ Differentiating in local and global frames.

Consider a local point at ${}^B\mathbf{r}_P = t\hat{\imath} + \hat{\jmath}$. The local frame $B$ is rotating in $G$ by $\dot{\alpha}$ about the $Z$-axis. Calculate $\frac{{}^B d}{dt}{}^B\mathbf{r}_P$, $\frac{{}^G d}{dt}{}^G\mathbf{r}_P$, $\frac{{}^B d}{dt}{}^G\mathbf{r}_P$, and $\frac{{}^G d}{dt}{}^B\mathbf{r}_P$.

23. ★ Transformation of angular velocity exponents.

   Show that
   $$_G^B\tilde{\omega}_B^n = {}^GR_B^T \, _G\tilde{\omega}_B^n \, {}^GR_B.$$

24. Local position, global acceleration.

   A body is turning about the $Z$-axis at a constant angular accel-
   eration $\ddot{\alpha} = 2\,\text{rad}/\sec^2$. Find the global velocity of a point, when
   $\dot{\alpha} = 2\,\text{rad}/\sec$, $\alpha = \pi/3\,\text{rad}$ and

   $$^B\mathbf{r} = \begin{bmatrix} 5 \\ 30 \\ 10 \end{bmatrix}.$$

25. Global position, constant angular acceleration.

   A body is turning about the $Z$-axis at a constant angular acceleration
   $\ddot{\alpha} = 2\,\text{rad}/\sec^2$. Find the global position of a point at

   $$^B\mathbf{r} = \begin{bmatrix} 5 \\ 30 \\ 10 \end{bmatrix}$$

   after $t = 3\,\sec$ if the body and global coordinate frames were coinci-
   dent at $t = 0\,\sec$.

26. Turning about $x$-axis.

   Find the angular acceleration matrix when the body coordinate frame
   is turning $-5\,\deg/\sec^2$, $35\,\deg/\sec$ at $45\,\deg$ about the $x$-axis.

27. Angular acceleration and Euler angles.

   Calculate the angular velocity and acceleration vectors in body and
   global coordinate frames if the Euler angles and their derivatives are:

   $$\begin{array}{lll}
   \varphi = .25\,\text{rad} & \dot{\varphi} = 2.5\,\text{rad}/\sec & \ddot{\varphi} = 25\,\text{rad}/\sec^2 \\
   \theta = -.25\,\text{rad} & \dot{\theta} = -4.5\,\text{rad}/\sec & \ddot{\theta} = 35\,\text{rad}/\sec^2 \\
   \psi = .5\,\text{rad} & \dot{\psi} = 3\,\text{rad}/\sec & \ddot{\psi} = 25\,\text{rad}/\sec^2
   \end{array}$$

28. Combined rotation and angular acceleration.

   Find the rotation matrix for a body frame after $30\,\deg$ rotation about
   the $Z$-axis, followed by $30\,\deg$ about the $X$-axis, and then $90\,\deg$
   about the $Y$-axis. Then calculate the angular velocity of the body
   if it is turning with $\dot{\alpha} = 20\,\deg/\sec$, $\dot{\beta} = -40\,\deg/\sec$, and $\dot{\gamma} =
   55\,\deg/\sec$ about the $Z$, $Y$, and $X$ axes respectively. Finally, cal-
   culate the angular acceleration of the body if it is turning with
   $\ddot{\alpha} = 2\,\deg/\sec^2$, $\ddot{\beta} = 4\,\deg/\sec^2$, and $\ddot{\gamma} = -6\,\deg/\sec^2$ about the
   $Z$, $Y$, and $X$ axes.

# 6

# Applied Mechanisms

Most of the mechanisms used in vehicle subsystems are made of four-bar linkages. Double $A$-arm for independent suspension, and trapezoidal steering are two examples of mechanisms in vehicle subsystems. In this chapter, we review the analysis and design methods for such mechanisms.

## 6.1  Four-Bar Linkage

An individual rigid member that can have relative motion with respect to all other members is called a *link*. A link may also be called a *bar*, *body*, *arm*, or a *member*. Any two or more links connected together, such that no relative motion can occur among them, are considered a single link.

*Axis of joint*     *Axis of joint*

*Revolute*          *Prismatic*
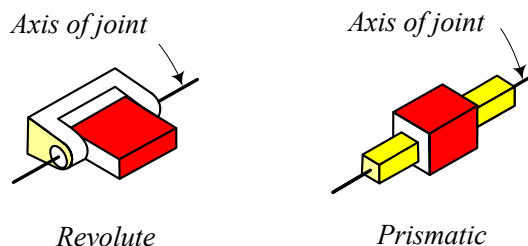
FIGURE 6.1. A revolute and a prismatic joint.

Two links are connected by a *joint* where their relative motion can be expressed by a single coordinate. Joints are typically *revolute* (rotary) or *prismatic* (translatory). Figure 6.1 illustrates a geometric form for a revolute and a prismatic joint. A *revolute joint* (R), is like a hinge that allows relative rotation between the two connected links. A *prismatic joint* (P), allows a relative translation between the two connected links.

Relative rotation or translation, between two connected links by a revolute or prismatic joint, occurs about a line called *axis of joint*. The value of the single variable describing the relative position of two connected links at a joint is called the *joint coordinate* or *joint variable*. It is an *angle* for a revolute joint, and a *distance* for a prismatic joint.

A set of connecting links to do a function is called a *mechanism*. A *linkage* is made by attaching, and fixing, one link of a mechanism to the ground. The fixed link is called the *ground link*. There are two types of linkages,
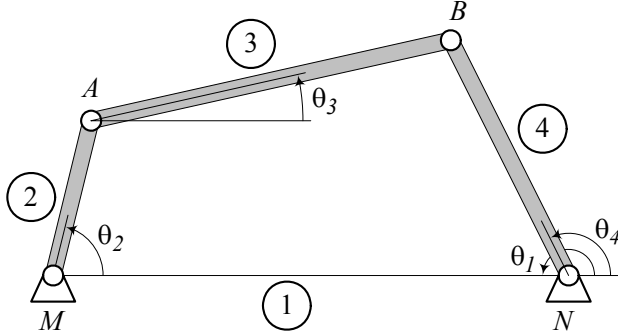
FIGURE 6.2. A four-bar linkage.

*closed loop* or *parallel*, and *open loop* or *serial*. In vehicle subsystems we usually use closed-loop linkages. Open-loop linkages are used in robotic systems where an actuator controls the joint variable at each joint.

A four-bar linkage is shown in Figure 6.2. Link number 1 is the ground link $MN$. The ground link is the base and used as a reference link. We measure all the variables with respect to the ground link. Link number $2 \equiv MA$ is usually the *input link* which is controlled by the *input angle* $\theta_2$. Link number $4 \equiv NB$ is usually the *output link* with angular position $\theta_4$, and link number $3 \equiv AB$ is the *coupler link* with angular position $\theta_3$ that connects the input and output links together.

The angular position of the output and coupler links, $\theta_4$ and $\theta_3$, are functions of the links' length and the value of the *input variable* $\theta_2$. The angles $\theta_4$ and $\theta_3$ can be calculated by the following functions

$$\theta_4 \quad = \quad 2\tan^{-1}\left(\frac{-B \pm \sqrt{B^2 - 4AC}}{2A}\right) \tag{6.1}$$

$$\theta_3 \quad = \quad 2\tan^{-1}\left(\frac{-E \pm \sqrt{E^2 - 4DF}}{2D}\right) \tag{6.2}$$

where,

$$A \quad = \quad J_3 - J_1 + (1 - J_2)\cos\theta_2 \tag{6.3}$$
$$B \quad = \quad -2\sin\theta_2 \tag{6.4}$$
$$C \quad = \quad J_1 + J_3 - (1 + J_2)\cos\theta_2 \tag{6.5}$$

$$D \quad = \quad J_5 - J_1 + (1 + J_4)\cos\theta_2 \tag{6.6}$$
$$E \quad = \quad -2\sin\theta_2 \tag{6.7}$$
$$F \quad = \quad J_5 + J_1 - (1 - J_4)\cos\theta_2 \tag{6.8}$$
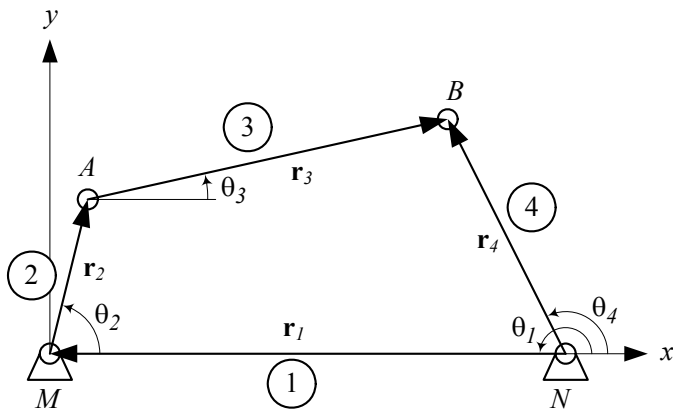
FIGURE 6.3. Expressing a four-bar linkage with a vector loop.

and

$$J_1 = \frac{d}{a} \qquad (6.9)$$

$$J_2 = \frac{d}{c} \qquad (6.10)$$

$$J_3 = \frac{a^2 - b^2 + c^2 + d^2}{2ac} \qquad (6.11)$$

$$J_4 = \frac{d}{b} \qquad (6.12)$$

$$J_5 = \frac{c^2 - d^2 - a^2 - b^2}{2ab}. \qquad (6.13)$$

**Proof.** We may show a closed loop, four-bar linkage by a vector loop as shown in Figure 6.3. The direction of each vector is arbitrary. However, the angle of each vector should be measured with respect to the positive direction of the $x$-axis. The vector expression of each link is shown in Table 6.1.

Table 6.1 - Vector representation of the four-bar linkage
shown in Figure 6.3.

| Link | Name | Vector | Length | Angle | Variable |
|------|---------|-----------|--------|----------------------|------------|
| 1 | Ground | $\mathbf{r}_1$ | $d$ | $\theta_1 = 180\,\mathrm{deg}$ | $-$ |
| 2 | Input | $\mathbf{r}_2$ | $a$ | $\theta_2$ | $\theta_2$ |
| 3 | Coupler | $\mathbf{r}_3$ | $b$ | $\theta_3$ | $\theta_3$ |
| 4 | Output | $\mathbf{r}_4$ | $c$ | $\theta_4$ | $\theta_4$ |

The vector loop in global coordinate frame $G$ is

$$^G\mathbf{r_4} + {}^G\mathbf{r_1} + {}^G\mathbf{r_2} - {}^G\mathbf{r_3} = \mathbf{0} \tag{6.14}$$

where,

$$
\begin{aligned}
{}^G\mathbf{r_1} &= -d\,\hat{\imath} &\tag{6.15}\\
{}^G\mathbf{r_2} &= a\,(\cos\theta_2\,\hat{\imath} + \sin\theta_2\,\hat{\jmath}) &\tag{6.16}\\
{}^G\mathbf{r_3} &= b\,(\cos\theta_3\,\hat{\imath} + \sin\theta_3\,\hat{\jmath}) &\tag{6.17}\\
{}^G\mathbf{r_4} &= c\,(\cos\theta_4\,\hat{\imath} + \sin\theta_4\,\hat{\jmath}) &\tag{6.18}
\end{aligned}
$$

and the left superscript $G$ reminds that the vectors are expressed in the global coordinate frame attached to the ground link. Substituting the Cartesian expressions for the planar vectors in Equation (6.14) results in

$$
\begin{aligned}
-d\,\hat{\imath} + a\,(\cos\theta_2\,\hat{\imath} + \sin\theta_2\,\hat{\jmath}) + b\,(\cos\theta_3\,\hat{\imath} + \sin\theta_3\,\hat{\jmath}) \\
-c\,(\cos\theta_4\,\hat{\imath} + \sin\theta_4\,\hat{\jmath}) &= 0. \tag{6.19}
\end{aligned}
$$

We may decompose Equation (6.19) into sin and cos components.

$$
\begin{aligned}
a\sin\theta_2 + b\sin\theta_3 - c\sin\theta_4 &= 0 \tag{6.20}\\
-d + a\cos\theta_2 + b\cos\theta_3 - c\cos\theta_4 &= 0 \tag{6.21}
\end{aligned}
$$

To derive the relationship between the input angle $\theta_2$ and the output angle $\theta_4$, the coupler angle $\theta_3$ must be eliminated between Equations (6.20) and (6.21). Transferring the terms not containing $\theta_3$ to the other side of the equations, and squaring both sides, provides the following equations:

$$
\begin{aligned}
(b\sin\theta_3)^2 &= (-a\sin\theta_2 + c\sin\theta_4)^2 \tag{6.22}\\
(b\cos\theta_3)^2 &= (-a\cos\theta_2 + c\cos\theta_4 + d)^2 \tag{6.23}
\end{aligned}
$$

By adding Equations (6.22) and (6.23), and simplifying, we derive the following equation:

$$J_1\cos\theta_4 - J_2\cos\theta_2 + J_3 = \cos(\theta_4 - \theta_2) \tag{6.24}$$

where

$$J_1 = \frac{d}{a} \tag{6.25}$$

$$J_2 = \frac{d}{c} \tag{6.26}$$

$$J_3 = \frac{a^2 - b^2 + c^2 + d^2}{2ac}. \tag{6.27}$$

Equation (6.24) is called *Freudenstein's equation*. The Freudenstein's equation may be expanded by using trigonometry

$$\sin\theta_4 = \frac{2\tan\dfrac{\theta_4}{2}}{1 + \tan^2\dfrac{\theta_4}{2}} \tag{6.28}$$

$$\cos\theta_4 = \frac{1 - \tan^2\dfrac{\theta_4}{2}}{1 + \tan^2\dfrac{\theta_4}{2}} \tag{6.29}$$

to provide a more practical equation

$$A\tan^2\frac{\theta_4}{2} + B\tan\frac{\theta_4}{2} + C = 0 \tag{6.30}$$

where $A$, $B$, and $C$ are functions of the input variable.

$$
\begin{aligned}
A &= J_3 - J_1 + (1 - J_2)\cos\theta_2 & \text{(6.31)}\\
B &= -2\sin\theta_2 & \text{(6.32)}\\
C &= J_1 + J_3 - (1 + J_2)\cos\theta_2 & \text{(6.33)}
\end{aligned}
$$

Equation (6.30) is a quadratic in $\tan(\theta_4/2)$ and can be used to find the output angle $\theta_4$.

$$\theta_4 = 2\tan^{-1}\left(\frac{-B \pm \sqrt{B^2 - 4AC}}{2A}\right) \tag{6.34}$$

To find the relationship between the input angle $\theta_2$ and the coupler angle $\theta_3$, the output angle $\theta_4$ must be eliminated between Equations (6.20) and (6.21). Transferring the terms not containing $\theta_4$ to the right-hand side of the equations, and squaring both sides, provides

$$
\begin{aligned}
(c\sin\theta_4)^2 &= (a\sin\theta_2 + b\sin\theta_3)^2 & \text{(6.35)}\\
(c\cos\theta_4)^2 &= (a\cos\theta_2 + b\cos\theta_3 - d)^2. & \text{(6.36)}
\end{aligned}
$$

By adding Equations (6.35) and (6.36), and simplifying, we derive the equation:

$$J_1\cos\theta_3 + J_4\cos\theta_2 + J_5 = \cos(\theta_3 - \theta_2) \tag{6.37}$$

where

$$J_4 = \frac{d}{b} \tag{6.38}$$

$$J_5 = \frac{c^2 - d^2 - a^2 - b^2}{2ab}. \tag{6.39}$$

Equation (6.37) may be expanded and transformed to

$$D\tan^2\frac{\theta_3}{2} + E\tan\frac{\theta_3}{2} + F = 0 \tag{6.40}$$

where $D$, $E$, and $F$ are functions of the input variable.

$$
\begin{aligned}
D &= J_5 - J_1 + (1 + J_4)\cos\theta_2 & \text{(6.41)}\\
E &= -2\sin\theta_2 & \text{(6.42)}\\
F &= J_5 + J_1 - (1 - J_4)\cos\theta_2 & \text{(6.43)}
\end{aligned}
$$

Equation (6.40) is a quadratic in $\tan(\theta_3/2)$ and can be used to find the coupler angle $\theta_3$.

$$\theta_3 = 2\tan^{-1}\left(\frac{-E \pm \sqrt{E^2 - 4DF}}{2D}\right) \qquad (6.44)$$

Equations (6.34) and (6.44) can be used to calculate the output and coupler angles $\theta_4$ and $\theta_3$ as two functions of the input angle $\theta_2$, provided the lengths $a$, $b$, $c$, and $d$ are given. ∎

**Example 218** *Two possible configurations for a four-bar linkage.*
*At any angle $\theta_2$, and for suitable values of a, b, c, and d, Equations (6.1) and (6.2) provide two values for the output and coupler angles, $\theta_4$ and $\theta_3$. Both solutions are possible and provide two different configurations for each input angle $\theta_2$.*
*A suitable set of (a, b, c, d) is the numbers that make the radicals in Equations (6.1) and (6.2) real.*
*As an example, consider a linkage with the following lengths:*

$$
\begin{aligned}
a &= 1 \\
b &= 2 \\
c &= 2.5 \\
d &= 3. \qquad (6.45)
\end{aligned}
$$

The $J_i, i = 1, 2, 3, 4, 5$ are functions of the links' length and are equal to

$$
\begin{aligned}
J_1 &= \frac{d}{a} = 3 \\
J_2 &= \frac{d}{c} = \frac{3}{2.5} = 1.2 \\
J_3 &= \frac{a^2 - b^2 + c^2 + d^2}{2ac} = 2.45 \\
J_4 &= \frac{d}{b} = 1.5 \\
J_5 &= \frac{c^2 - d^2 - a^2 - b^2}{2ab} = -1.9375. \qquad (6.46)
\end{aligned}
$$

The coefficients of the quadratic equations are then calculated.

$$
\begin{aligned}
A &= -0.6914213562 \\
B &= -1.414213562 \\
C &= 3.894365082 \\
D &= -3.169733048 \\
E &= -1.414213562 \\
F &= 1.416053390 \qquad (6.47)
\end{aligned}
$$
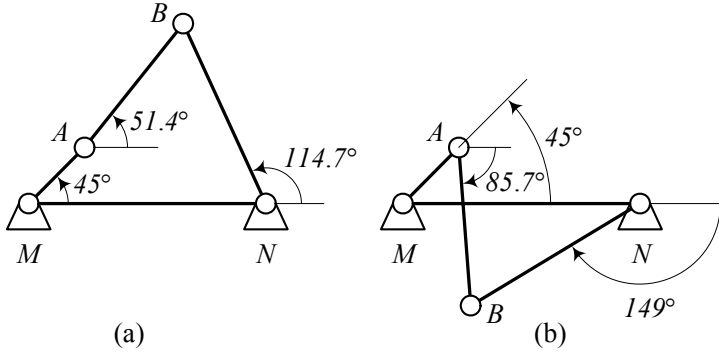
FIGURE 6.4. Two possible configuration of a four-bar linkage having the same input angle $\theta_2$.

*Using the minus sign, the output and coupler angles at $\theta_2 = \pi/4\,\text{rad} = 45\,\text{deg}$ are*

$$
\begin{aligned}
\theta_4 &\approx 2\,\text{rad} \approx 114.73\,\text{deg} \\
\theta_3 &\approx 0.897\,\text{rad} \approx 51.42\,\text{deg}
\end{aligned} \tag{6.48}
$$

*and using the plus sign, they are*

$$
\begin{aligned}
\theta_4 &\approx -2.6\,\text{rad} \approx -149\,\text{deg} \\
\theta_3 &\approx -1.495\,\text{rad} \approx -85.7\,\text{deg}\,.
\end{aligned} \tag{6.49}
$$

*Figure 6.4 depicts the two possible configurations of the linkage for $\theta_2 = 45\,\text{deg}$. The configuration in Figure 6.4(a) is called **convex**, **non-crossed**, or **elbow-up**, and the configuration in Figure 6.4(b) is called **concave**, **crossed**, or **elbow-down**.*

**Example 219** *Velocity analysis of a four-bar linkage.*

*The velocity analysis of a four-bar linkage is possible by taking a time derivative of Equations (6.20) and (6.21),*

$$
\begin{aligned}
&\frac{d}{dt}\left(a\sin\theta_2 + b\sin\theta_3 - c\sin\theta_4\right) \\
&= a\,\omega_2\cos\theta_2 + b\,\omega_3\cos\theta_3 - c\,\omega_4\cos\theta_4 = 0
\end{aligned} \tag{6.50}
$$

$$
\begin{aligned}
&\frac{d}{dt}\left(-d + a\cos\theta_2 + b\cos\theta_3 - c\cos\theta_4\right) \\
&= -a\,\omega_2\sin\theta_2 - b\,\omega_3\sin\theta_3 + c\,\omega_4\sin\theta_4 = 0
\end{aligned} \tag{6.51}
$$

*where*

$$
\begin{aligned}
\omega_2 &= \dot{\theta}_2 \\
\omega_3 &= \dot{\theta}_3 \\
\omega_4 &= \dot{\theta}_4.
\end{aligned} \tag{6.52}
$$

Assuming $\theta_2$ and $\omega_2$ are given values, and $\theta_3$, $\theta_4$ are known from Equations (6.1) and (6.2), we may solve Equations (6.50) and (6.51), for $\omega_3$ and $\omega_4$.

$$\omega_4 = \frac{a \sin (\theta_2 - \theta_3)}{c \sin (\theta_4 - \theta_3)} \omega_2 \tag{6.53}$$

$$\omega_3 = \frac{a \sin (\theta_2 - \theta_4)}{b \sin (\theta_4 - \theta_3)} \omega_2 \tag{6.54}$$

**Example 220** *Velocity of moving joints for a four-bar linkage.*

Having the coordinates $\theta_2$, $\theta_3$, $\theta_4$ and velocities $\omega_2$, $\omega_3$, $\omega_4$ enables us to calculate the absolute and relative velocities of points $A$ and $B$ shown in Figure 6.3. The absolute velocity is referred to the ground link, and relative velocity refers to a moving point.

The absolute velocity of points $A$ and $B$ are

$$
\begin{aligned}
{}^G\mathbf{v}_A &= {}_G\boldsymbol{\omega}_2 \times {}^G\mathbf{r}_2 \\
&= \begin{bmatrix} 0 \\ 0 \\ \omega_2 \end{bmatrix} \times \begin{bmatrix} a \cos \theta_2 \\ a \sin \theta_2 \\ 0 \end{bmatrix} = \begin{bmatrix} -a\omega_2 \sin \theta_2 \\ a\omega_2 \cos \theta_2 \\ 0 \end{bmatrix}
\end{aligned} \tag{6.55}
$$

$$
\begin{aligned}
{}^G\mathbf{v}_B &= {}_G\boldsymbol{\omega}_4 \times {}^G\mathbf{r}_4 \\
&= \begin{bmatrix} 0 \\ 0 \\ \omega_4 \end{bmatrix} \times \begin{bmatrix} c \cos \theta_4 \\ c \sin \theta_4 \\ 0 \end{bmatrix} = \begin{bmatrix} -c\omega_4 \sin \theta_4 \\ c\omega_4 \cos \theta_4 \\ 0 \end{bmatrix}
\end{aligned} \tag{6.56}
$$

and the velocity of point $B$ with respect to point $A$ is

$$
\begin{aligned}
{}^G\mathbf{v}_{B/A} &= {}^G\mathbf{v}_B - {}^G\mathbf{v}_A \\
&= \begin{bmatrix} -c\omega_4 \sin \theta_4 \\ c\omega_4 \cos \theta_4 \\ 0 \end{bmatrix} - \begin{bmatrix} -a\omega_2 \sin \theta_2 \\ a\omega_2 \cos \theta_2 \\ 0 \end{bmatrix} \\
&= \begin{bmatrix} a\omega_2 \sin \theta_2 - c\omega_4 \sin \theta_4 \\ c\omega_4 \cos \theta_4 - a\omega_2 \cos \theta_2 \\ 0 \end{bmatrix}.
\end{aligned} \tag{6.57}
$$

The velocity of point $B$ with respect to $A$ can also be found as

$$
\begin{aligned}
{}^G\mathbf{v}_{B/A} &= {}^GR_2 \, {}^2\mathbf{v}_B \\
&= {}^GR_2 \, {}^2\mathbf{v}_B \\
&= {}^GR_2 \left( {}_2\boldsymbol{\omega}_3 \times {}^2\mathbf{r}_3 \right) \\
&= {}_G\boldsymbol{\omega}_3 \times {}^G\mathbf{r}_3 \\
&= \begin{bmatrix} 0 \\ 0 \\ \omega_3 \end{bmatrix} \times \begin{bmatrix} b \cos \theta_3 \\ b \sin \theta_3 \\ 0 \end{bmatrix} = \begin{bmatrix} -b\omega_3 \sin \theta_3 \\ b\omega_3 \cos \theta_3 \\ 0 \end{bmatrix}.
\end{aligned} \tag{6.58}
$$

*Equations (6.57) and (6.58) are both correct and convertible to each other.*

**Example 221** *Acceleration analysis of a four-bar linkage.*
   *The acceleration analysis of a four-bar linkage is possible by taking a time derivative from Equations (6.50) and (6.51),*

$$\frac{d}{dt} \left( a\,\omega_2 \cos\theta_2 + b\,\omega_3 \cos\theta_3 - c\,\omega_4 \cos\theta_4 \right)$$
$$= \quad a\alpha_2 \cos\theta_2 + b\alpha_3 \cos\theta_3 - c\alpha_4 \cos\theta_4$$
$$-a\omega_2^2 \sin\theta_2 - b\omega_3^2 \sin\theta_3 + c\omega_4^2 \sin\theta_4$$
$$= \quad 0 \tag{6.59}$$

$$\frac{d}{dt} \left( -a\,\omega_2 \sin\theta_2 - b\,\omega_3 \sin\theta_3 + c\,\omega_4 \sin\theta_4 \right)$$
$$= \quad -a\alpha_2 \sin\theta_2 - b\alpha_3 \sin\theta_3 + c\alpha_4 \sin\theta_4$$
$$-a\omega_2^2 \cos\theta_2 - b\omega_3^2 \cos\theta_3 + c\omega_4^2 \cos\theta_4$$
$$= \quad 0 \tag{6.60}$$

*where*

$$\alpha_2 = \dot{\omega}_2$$
$$\alpha_3 = \dot{\omega}_3$$
$$\alpha_4 = \dot{\omega}_4. \tag{6.61}$$

*Assuming $\theta_2$, $\omega_2$, and $\alpha_2$ are given values as the kinematics of the input link, $\theta_3$, $\theta_4$ are known from Equations (6.1) and (6.2), and $\omega_3$, $\omega_4$ are known from Equations (6.53) and (6.54), we may solve Equations (6.59) and (6.60), for $\alpha_3$ and $\alpha_4$.*

$$\alpha_4 = \frac{C_3 C_4 - C_1 C_6}{C_1 C_5 - C_2 C_4} \tag{6.62}$$
$$\alpha_3 = \frac{C_3 C_5 - C_2 C_6}{C_1 C_5 - C_2 C_4} \tag{6.63}$$

*where*

$$C_1 = c\sin\theta_4$$
$$C_2 = b\sin\theta_3$$
$$C_3 = a\alpha_2 \sin\theta_2 + a\omega_2^2 \cos\theta_2 + b\omega_3^2 \cos\theta_3 - c\omega_4^2 \cos\theta_4$$
$$C_4 = c\cos\theta_4$$
$$C_5 = b\cos\theta_3$$
$$C_6 = a\alpha_2 \cos\theta_2 - a\omega_2^2 \sin\theta_2 - b\omega_3^2 \sin\theta_3 + c\omega_4^2 \sin\theta_4. \tag{6.64}$$

**Example 222** *Acceleration of moving joints for a four-bar linkage.*
  *Having the angular kinematics of a four-bar linkage $\theta_2$, $\theta_3$, $\theta_4$, $\omega_2$, $\omega_3$, $\omega_4$, $\alpha_2$, $\alpha_3$, and $\alpha_4$ is necessary and enough to calculate the absolute and relative accelerations of points A and B shown in Figure 6.3. The absolute acceleration is referred to as the ground link, and the relative acceleration refers to a moving point.*
  *The absolute acceleration of points A and B are*

$$
\begin{aligned}
{}^{G}\mathbf{a}_A &= {}_{G}\boldsymbol{\alpha}_2 \times {}^{G}\mathbf{r}_2 + {}_{G}\boldsymbol{\omega}_2 \times \left({}_{G}\boldsymbol{\omega}_2 \times {}^{G}\mathbf{r}_2\right) \\
&= \begin{bmatrix} -a\alpha_2 \sin\theta_2 - a\omega_2^2 \cos\theta_2 \\ a\alpha_2 \cos\theta_2 - a\omega_2^2 \sin\theta_2 \\ 0 \end{bmatrix}
\end{aligned} \tag{6.65}
$$

$$
\begin{aligned}
{}^{G}\mathbf{a}_B &= {}_{G}\boldsymbol{\alpha}_4 \times {}^{G}\mathbf{r}_4 + {}_{G}\boldsymbol{\omega}_4 \times \left({}_{G}\boldsymbol{\omega}_4 \times {}^{G}\mathbf{r}_4\right) \\
&= \begin{bmatrix} -c\alpha_4 \sin\theta_4 - c\omega_4^2 \cos\theta_4 \\ c\alpha_4 \cos\theta_4 - c\omega_4^2 \sin\theta_4 \\ 0 \end{bmatrix}
\end{aligned} \tag{6.66}
$$

*where*

$$
{}^{G}\mathbf{r}_2 = \begin{bmatrix} a\cos\theta_2 \\ a\sin\theta_2 \\ 0 \end{bmatrix} \tag{6.67}
$$

$$
{}^{G}\mathbf{r}_4 = \begin{bmatrix} c\cos\theta_4 \\ c\sin\theta_4 \\ 0 \end{bmatrix} \tag{6.68}
$$

$$
{}_{G}\boldsymbol{\omega}_2 = \begin{bmatrix} 0 \\ 0 \\ \omega_2 \end{bmatrix} \tag{6.69}
$$

$$
{}_{G}\boldsymbol{\omega}_4 = \begin{bmatrix} 0 \\ 0 \\ \omega_4 \end{bmatrix} \tag{6.70}
$$

$$
{}_{G}\boldsymbol{\alpha}_2 = \begin{bmatrix} 0 \\ 0 \\ \alpha_2 \end{bmatrix} \tag{6.71}
$$

$$
{}_{G}\boldsymbol{\alpha}_4 = \begin{bmatrix} 0 \\ 0 \\ \alpha_4 \end{bmatrix}. \tag{6.72}
$$

*The acceleration of point B with respect to point A is*

$$
\begin{aligned}
{}^{G}\mathbf{a}_{B/A} &= {}_{G}\boldsymbol{\alpha}_3 \times {}^{G}\mathbf{r}_3 + {}_{G}\boldsymbol{\omega}_3 \times \left( {}_{G}\boldsymbol{\omega}_3 \times {}^{G}\mathbf{r}_3 \right) \\
&= \begin{bmatrix} -b\alpha_3 \sin\theta_3 - b\omega_3^2 \cos\theta_3 \\ b\alpha_3 \cos\theta_3 - b\omega_3^2 \sin\theta_3 \\ 0 \end{bmatrix}
\end{aligned}
\tag{6.73}
$$

*where*

$$
{}^{G}\mathbf{r}_3 = \begin{bmatrix} b\cos\theta_3 \\ b\sin\theta_3 \\ 0 \end{bmatrix}
\tag{6.74}
$$

$$
{}_{G}\boldsymbol{\omega}_3 = \begin{bmatrix} 0 \\ 0 \\ \omega_3 \end{bmatrix}
\tag{6.75}
$$

$$
{}_{G}\boldsymbol{\alpha}_3 = \begin{bmatrix} 0 \\ 0 \\ \alpha_3 \end{bmatrix}.
\tag{6.76}
$$

**Example 223** *Grashoff criterion.*

*The ability of a four-bar linkage to have a rotary link is determined by Grashoff criterion. Assume the four links have the lengths s, l, p, and q, where*

$$
\begin{aligned}
l &= \textit{longest link} \\
s &= \textit{shortest link} \\
p, q &= \textit{the other two links}
\end{aligned}
$$

*then, the* **Grashoff criterion** *states that the linkage can have a rotary link if*

$$
l + s < p + q.
\tag{6.77}
$$

*Different types of a Grashoff mechanism are:*

1− *Shortest link is the input link, then the mechanism is a crank-rocker.*
2− *Shortest link is the ground link, and the mechanism is a crank-crank.*
3− *At all other conditions, the mechanism is a rocker-rocker.*

*A crank-crank mechanism is also called a drag-link.*

**Example 224** *Limit positions for a four-bar linkage.*

*When the output link of a four-bar linkage stops while the input link can turn, we say the linkage is at a* **limit position**. *It happens when the angle between the input and coupler links is either 180 deg or 360 deg. Limit positions of a four-bar linkage, if there are any, must be determined by the designer to make sure the linkage is designed properly. A limit position for a four-bar linkage is shown in Figure 6.5.*
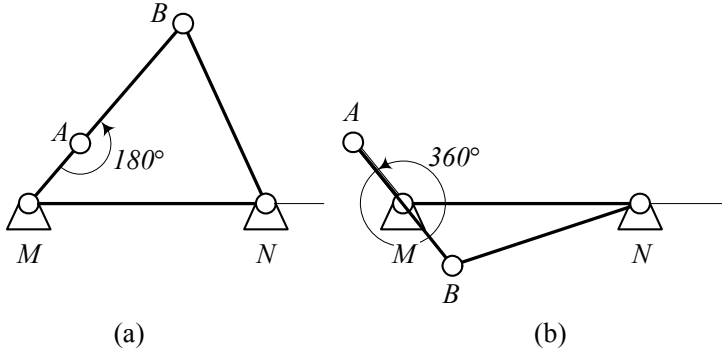
FIGURE 6.5. Limit position for a four-bar linkage.

*We show the limit angle of the output link by $\theta_{4_{L1}}$, $\theta_{4_{L2}}$, and the corresponding input angles by $\theta_{2_{L1}}$, $\theta_{2_{L2}}$. They can be calculated by the following equations:*

$$\theta_{2_{L1}} = \cos^{-1}\left[\frac{(a+b)^2 + d^2 - c^2}{2d(a+b)}\right] \tag{6.78}$$

$$\theta_{4_{L1}} = \cos^{-1}\left[\frac{(a+b)^2 - d^2 - c^2}{2cd}\right] \tag{6.79}$$

$$\theta_{2_{L2}} = \cos^{-1}\left[\frac{(b-a)^2 + d^2 - c^2}{2d(b-a)}\right] \tag{6.80}$$

$$\theta_{4_{L2}} = \cos^{-1}\left[\frac{(b-a)^2 - d^2 - c^2}{2cd}\right] \tag{6.81}$$

*The sweep angle of the output link would be*

$$\phi = \theta_{4_{L2}} - \theta_{4_{L1}}. \tag{6.82}$$

**Example 225** *Dead positions for a four-bar linkage.*

*When the input link of a four-bar linkage locks, we say the linkage is at a* **dead position**. *It happens when the angle between the output and coupler links is either 180 deg or 360 deg. Limit positions of a four-bar linkage, if there are any, must be determined by the designer to make sure the linkage is never stuck in a dead position. A dead position for a four-bar linkage is shown in Figure 6.6.*

*We show the dead angle of the output link by $\theta_{4_{D1}}$, $\theta_{4_{D2}}$, and the corresponding input angles by $\theta_{2_{D1}}$, $\theta_{2_{D2}}$. They can be calculated by the following*
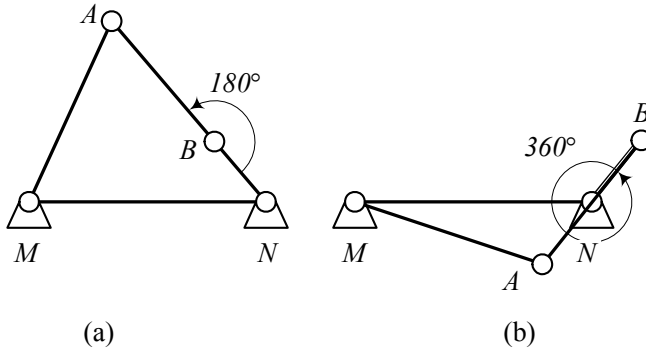
FIGURE 6.6. Dead position for a four-bar linkage.

equations:

$$\theta_{2_{D1}} = \cos^{-1}\left[\frac{a^2 + d^2 - (b+c)^2}{2ad}\right] \tag{6.83}$$

$$\theta_{4_{D1}} = \cos^{-1}\left[\frac{a^2 - d^2 - (b+c)^2}{2(b+c)d}\right] \tag{6.84}$$

$$\theta_{2_{D2}} = \cos^{-1}\left[\frac{a^2 + d^2 - (b-c)^2}{2ad}\right] \tag{6.85}$$

$$\theta_{4_{D2}} = \cos^{-1}\left[\frac{a^2 - d^2 - (b-c)^2}{2ad}\right] \tag{6.86}$$

**Example 226 ★** *Designing a four-bar linkage using Freudenstein's equation.*

*Designing a mechanism can be thought of as determining the required lengths of the links to accomplish a specific task.*

*Freudenstein's equation (6.24)*

$$J_1 \cos\theta_4 - J_2 \cos\theta_2 + J_3 = \cos(\theta_4 - \theta_2) \tag{6.87}$$

$$J_1 = \frac{d}{a} \tag{6.88}$$

$$J_2 = \frac{d}{c} \tag{6.89}$$

$$J_3 = \frac{a^2 - b^2 + c^2 + d^2}{2ac} \tag{6.90}$$

*determines the input-output relationship of a four-bar linkage. This equation can be utilized to design a four-bar linkage for three associated input-output angles.*
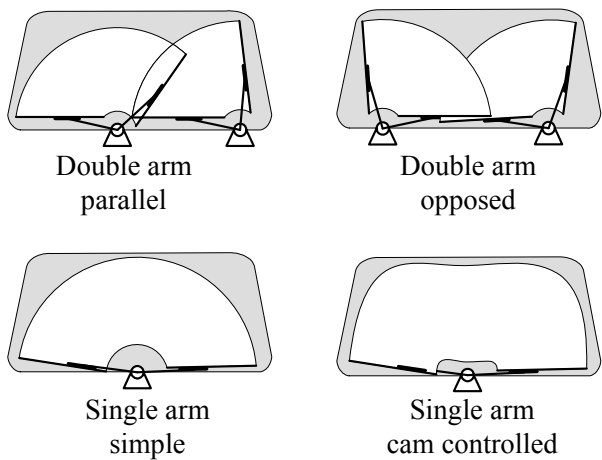
FIGURE 6.7. Four popular windshield wiper systems.

Figure 6.7 illustrates the four popular windshield wiper systems. Double-arm parallel method is the most popular wiping system that serves more than 90% of passenger cars. The double-arm opposing method has been used been using since last century, however, it was never very popular. The single-arm simple method is not very efficient, so the controlled single-arm is designed to maximize the wiped area.

Wipers are used on windshields, and headlights. Figure 6.8 illustrates a sample of double-arm parallel windshield wiper mechanism. A four-bar linkage makes the main mechanism match the angular positions of the left and right wipers. A **dyad** or a two-link connects the driving motor to the main four-bar linkage and converts the rotational output of the motor into the back-and-forth motion of the wipers.

The input and output links of the main four-bar linkage at three different positions are shown in Figure 6.9. We show the beginning and the end angles for the input link by $\theta_{21}$ and $\theta_{23}$, and for the output link by $\theta_{41}$ and $\theta_{43}$ respectively. To design the mechanism we must match the angular positions of the left and right blades at the beginning and at the end positions. Let's add another match point approximately in the middle of the total sweep angles and design a four-bar linkage to match the angles indicated in Table 6.2.

Table 6.2 - Matching angles for a four-bar linkage of the double-arm parallel mechanism shown in Figure 6.9.

| Matching | Input angle | Output angle |
|---|---|---|
| 1 | $\theta_{21} = 157.6 \deg \approx 2.75 \, \mathrm{rad}$ | $\theta_{41} = 157.2 \deg \approx 2.74 \, \mathrm{rad}$ |
| 2 | $\theta_{22} = 113.1 \deg \approx 1.97 \, \mathrm{rad}$ | $\theta_{42} = 97.5 \deg \approx 1.7 \, \mathrm{rad}$ |
| 3 | $\theta_{23} = 69.5 \deg \approx 1.213 \, \mathrm{rad}$ | $\theta_{43} = 26.8 \deg \approx 0.468 \, \mathrm{rad}$ |

FIGURE 6.8. A sample of double-arm parallel windshield wiper mechanism.
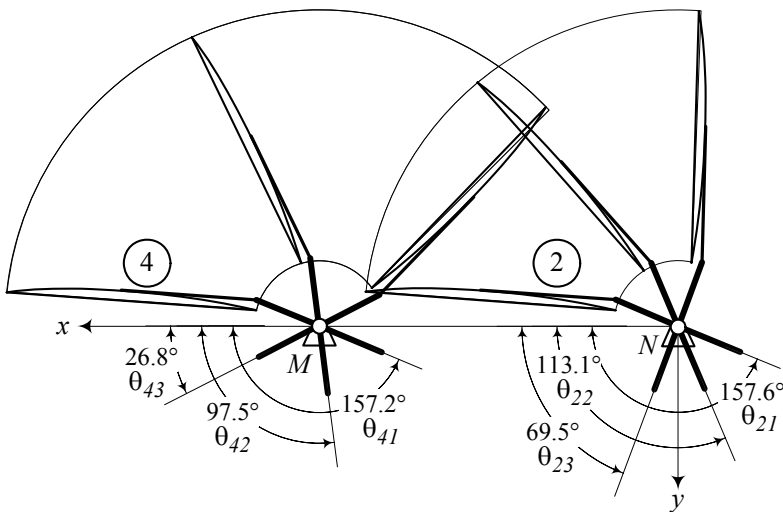


FIGURE 6.9. The input and output links of the main four-bar linkage of a windshield wiper at three different positions.

*Substituting the input and output angles in Freudenstein's equation (6.24)*

$$J_1 \cos\theta_{41} - J_2 \cos\theta_{21} + J_3 = \cos(\theta_{41} - \theta_{21})$$
$$J_1 \cos\theta_{42} - J_2 \cos\theta_{22} + J_3 = \cos(\theta_{42} - \theta_{22}) \qquad (6.91)$$
$$J_1 \cos\theta_{43} - J_2 \cos\theta_{23} + J_3 = \cos(\theta_{43} - \theta_{23})$$

*provides the following set of three equations:*

$$J_1 \cos 2.74 - J_2 \cos 2.75 + J_3 = \cos(2.74 - 2.75)$$
$$J_1 \cos 1.7 - J_2 \cos 1.97 + J_3 = \cos(1.7 - 1.97) \qquad (6.92)$$
$$J_1 \cos 0.468 - J_2 \cos 1.213 + J_3 = \cos(0.468 - 1.213)$$

*The set of equations (6.92) is linear for the unknowns $J_1$, $J_2$, and $J_3$*

$$\begin{bmatrix} -0.92044 & 0.9243 & 1 \\ -0.12884 & 0.38868 & 1 \\ 0.89247 & -0.35021 & 1 \end{bmatrix} \begin{bmatrix} J_1 \\ J_2 \\ J_3 \end{bmatrix} = \begin{bmatrix} 0.99995 \\ 0.96377 \\ 0.73509 \end{bmatrix} \qquad (6.93)$$

*with the following solution:*

$$\begin{bmatrix} J_1 \\ J_2 \\ J_3 \end{bmatrix} = \begin{bmatrix} 2.5284 \\ 3.8043 \\ -0.18911 \end{bmatrix} \qquad (6.94)$$

The three factors $J_1$, $J_2$, $J_3$ should be used to find four numbers for the links' length.

$$J_1 = \frac{d}{a} \qquad (6.95)$$

$$J_2 = \frac{d}{c} \qquad (6.96)$$

$$J_3 = \frac{a^2 - b^2 + c^2 + d^2}{2ac} \qquad (6.97)$$

*So, we may preset the length of one of the links, based on the physical situation. Traditionally, we use $a = 1$ and find the remaining lengths. Then, the designed mechanism can be magnified or shrunk to fit the required geometry. In this example, we find*

$$a = 1$$
$$b = 2.8436$$
$$c = 0.66462$$
$$d = 2.5284. \qquad (6.98)$$

*Assuming a distance $d = 75\,\mathrm{cm} \approx 29.5\,\mathrm{in}$ for a real passenger car, between*
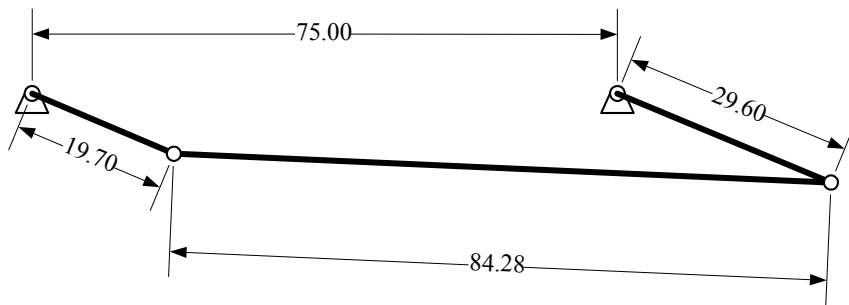
FIGURE 6.10. The main four-bar linkage of the windshield wiper at the initial position measured in [cm].

the left and right fixed joints $M$ and $N$, we find the following dimensions:

$$
\begin{aligned}
a &= 296\,\text{mm} \\
b &= 843\,\text{mm} \\
c &= 197\,\text{mm} \\
d &= 750\,\text{mm}
\end{aligned}
\tag{6.99}
$$

Such a mechanism is shown in Figure 6.10 at the initial position.

**Example 227 ★** *Equal sweep angles for input and output links.*
    Let's place the second matching point of the windshield wiper mechanism in Example 226 exactly in the middle of the total sweep angles

$$
\theta_{22} = \frac{157.6 + 69.5}{2} = 113.55 \deg \approx 1.982\,\text{rad}
$$
$$
\theta_{42} = \frac{157.2 + 26.8}{2} = 92 \deg \approx 1.605\,\text{rad}.
\tag{6.100}
$$

The first and second sweep angles for such matching points would be equal. Having equal sweep angles makes the motion of the wipers more uniform, although it cannot guarantee that the angular speed ratio of the left and right blades remains constant.
    The matching points for the main four-bar linkage of the windshield wiper with equal sweep angles are indicated in Table 6.3.

Table 6.3 - Equal sweep angle matching points for the four-bar linkage of the double-arm parallel mechanism shown in Figure 6.9.

| Matching | Input angle | Output angle |
|---|---|---|
| 1 | $\theta_{21} = 157.6 \deg \approx 2.75\,\text{rad}$ | $\theta_{41} = 157.2 \deg \approx 2.74\,\text{rad}$ |
| 2 | $\theta_{22} = 113.55 \deg \approx 1.982\,\text{rad}$ | $\theta_{42} = 92 \deg \approx 1.605\,\text{rad}$ |
| 3 | $\theta_{23} = 69.5 \deg \approx 1.213\,\text{rad}$ | $\theta_{43} = 26.8 \deg \approx 0.468\,\text{rad}$ |

Substituting the angles in Freudenstein's equation (6.24) provides the following set of three equations:

$$\begin{aligned} J_1 \cos 2.74 - J_2 \cos 2.75 + J_3 &= \cos(2.74 - 2.75) \\ J_1 \cos 1.605 - J_2 \cos 1.982 + J_3 &= \cos(1.605 - 1.982) \\ J_1 \cos 0.468 - J_2 \cos 1.213 + J_3 &= \cos(0.468 - 1.213) \end{aligned} \quad (6.101)$$

The set of equations can be written in a matrix form for the three unknowns $J_1$, $J_2$, and $J_3$

$$\begin{bmatrix} -0.920\,44 & 0.924\,3 & 1 \\ -.0332 & .3993 & 1 \\ 0.892\,47 & -0.350\,21 & 1 \end{bmatrix} \begin{bmatrix} J_1 \\ J_2 \\ J_3 \end{bmatrix} = \begin{bmatrix} 0.999\,95 \\ .929589 \\ 0.735\,09 \end{bmatrix} \quad (6.102)$$

with the solution.

$$\begin{bmatrix} J_1 \\ J_2 \\ J_3 \end{bmatrix} = \begin{bmatrix} 0.276 \\ 0.6 \\ 0.699 \end{bmatrix} \quad (6.103)$$

Using $a = 1$ and the three factors $J_1$, $J_2$, and $J_3$

$$J_1 = \frac{d}{a} \quad (6.104)$$

$$J_2 = \frac{d}{c} \quad (6.105)$$

$$J_3 = \frac{a^2 - b^2 + c^2 + d^2}{2ac}, \quad (6.106)$$

we can find the links' length.

$$\begin{aligned} a &= 1 \\ b &= 0.803 \\ c &= 0.46 \\ d &= 0.276. \end{aligned} \quad (6.107)$$

Assuming a distance $d = 75\,\text{cm} \approx 29.5\,\text{in}$ between the left and right fixed joint $M$ and $N$, we find the following dimensions for a real passenger car:

$$\begin{aligned} a &= 2717\,\text{mm} \\ b &= 2182\,\text{mm} \\ c &= 1250\,\text{mm} \\ d &= 750\,\text{mm} \end{aligned} \quad (6.108)$$

These dimensions do not show a practical design because the links' length may be longer than the width of the vehicle. It shows that the designed mechanism is highly dependent on the second match point. So, it might be possible to design a desirable mechanism by choosing a suitable second match point.

**Example 228 ★** *Second match point and link's length.*

To see how the design of the windshield wiper mechanism in Example 226 is dependent on the second match point, let's set

$$\theta_{22} = \frac{157.6 + 69.5}{2} = 113.55 \deg \approx 1.982 \, \text{rad} \tag{6.109}$$

and make $\theta_{42}$ a variable. The three matching points for the main four-bar linkage of the windshield wiper are indicated in Table 6.4.

Table 6.4 - *Variable second match point for the four-bar linkage of the double-arm parallel mechanism shown in Figure 6.9.*

| Matching | Input angle | Output angle |
|:---:|:---|:---|
| 1 | $\theta_{21} = 157.6 \deg \approx 2.75 \, \text{rad}$ | $\theta_{41} = 157.2 \deg \approx 2.74 \, \text{rad}$ |
| 2 | $\theta_{22} = 113.55 \deg \approx 1.982 \, \text{rad}$ | $\theta_{42}$ |
| 3 | $\theta_{23} = 69.5 \deg \approx 1.213 \, \text{rad}$ | $\theta_{43} = 26.8 \deg \approx 0.468 \, \text{rad}$ |

The Freudenstein's equation (6.24) provides the following set of equations:

$$\begin{aligned}
J_1 \cos 2.74 - J_2 \cos 2.75 + J_3 &= \cos(2.74 - 2.75) \\
J_1 \cos\theta_{42} - J_2 \cos 1.982 + J_3 &= \cos(\theta_{42} - 1.982) \\
J_1 \cos 0.468 - J_2 \cos 1.213 + J_3 &= \cos(0.468 - 1.213)
\end{aligned} \tag{6.110}$$

The set of equations gives the following solutions:

$$\begin{aligned}
J_1 &= \frac{79.657 \cos(\theta_{42} - 1.9815) - 70.96}{79.657 \cos\theta_{42} + 13.828} \\
J_2 &= \frac{93.642 \cos(\theta_{42} - 1.981) + 13.681 \cos\theta_{42} - 81.045}{65.832 \cos\theta_{42} + 11.428} \\
J_3 &= \frac{32.357 - 25.959 \cos(\theta_{42} - 1.981) + 53.184 \cos(\theta_{42})}{11.428 + 65.83 \cos(\theta_{42})}
\end{aligned} \tag{6.111}$$

Having $d = 75 \, \text{cm} \approx 29.5 \, \text{in}$ between the left and right fixed joint $M$ and $N$ as a ground link, and using the factors $J_1$, $J_2$, and $J_3$

$$J_1 = \frac{d}{a} \tag{6.112}$$

$$J_2 = \frac{d}{c} \tag{6.113}$$

$$J_3 = \frac{a^2 - b^2 + c^2 + d^2}{2ac}, \tag{6.114}$$

we can find the length of the other links $a$, $b$, and $c$ as functions of $\theta_{42}$. Figure 6.11 illustrates how the angle $\theta_{42}$ affects the lengths of the links.
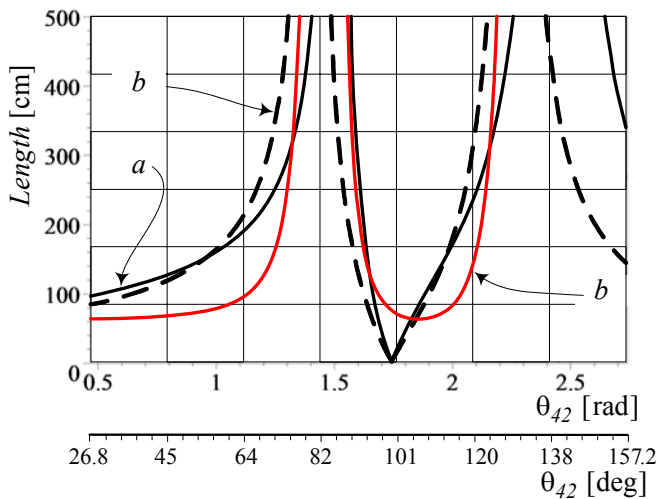
FIGURE 6.11. The length of links $a$, $b$, and $c$ as functions of $\theta_{42}$.
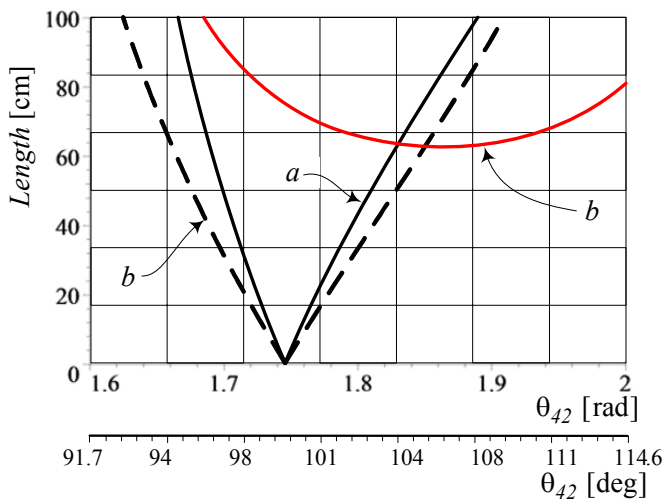


FIGURE 6.12. Maginification of the plot for the length of links $a$, $b$, and $c$ as functions of $\theta_{42}$, around the optimal design.
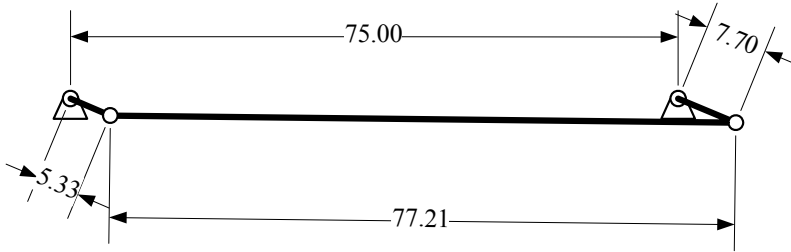
FIGURE 6.13. The finalized main four-bar linkage of the windshield wiper at the initial position measured in [cm].

To hide the mechanism under the hood in a small space, we need to have the lengths $a$ and $c$ much shorter than the ground $d$. Based on Figure 6.11, a possible solution would be around $\theta_{42} = 100 \deg$. Figure 6.12 illustrates a magnified view around $\theta_{42} = 100 \deg$.

To have the length of $a$ and $c$ less than $100\,\text{mm} \approx 3.94\,\text{in}$ we pick $\theta_{43} = 99.52\deg \approx 1.737\,\text{rad}$. Then the factors $J_1$, $J_2$, and $J_3$ are

$$\begin{bmatrix} J_1 \\ J_2 \\ J_3 \end{bmatrix} = \begin{bmatrix} 9.740208376 \\ 14.06262379 \\ -3.032892944 \end{bmatrix} \tag{6.115}$$

and the links' length for $d = 75\,\text{cm} \approx 29.5\,\text{in}$ are equal to

$$\begin{aligned} a &= 77\,\text{mm} \\ b &= 772\,\text{mm} \\ c &= 53.3\,\text{mm} \\ d &= 750\,\text{mm}. \end{aligned} \tag{6.116}$$

These numbers show a compact and reasonable mechanism. Figure 6.13 illustrates the finalized four-bar linkage of the windshield wiper at the initial position.

**Example 229** ★ *Designing a dyad to attach a motor.*

The main four-bar linkage of a windshield wiper is a rocker-rocker mechanism because both the input and the output links must oscillate between two specific limits. To run the wipers and lock them at the limits, a two-link dyad can be designed. First we set the point of installing a rotary motor according to the physical conditions. Let point $P$, as shown in Figure 6.14, be the point at which we install the electric motor to run the mechanism. The next step would be to select a point on the input link to attach the second link of the dyad. Although joint $B$ is usually the best choice, we select a point on the extension of the input link, indicated by $D$. There must be a dyad between joints $D$ and $P$ with lengths $p$ and $q$. When the mechanism

is at the initial position, joint $D$ is at the longest distance form the motor $P$, and when it is at the final position, joint $D$ is at the shortest distance form the motor $P$. Let's show the longest distance between $P$ and $D$ by $l$ and the shortest distance by $s$.

$$
\begin{aligned}
l &= \text{longest distance between } P \text{ and } D \\
s &= \text{shortest distance between } P \text{ and } D \\
p, q &= \text{dyad lengths between } P \text{ and } D
\end{aligned}
$$

When $P$ and $D$ are at the maximum distance, the two-link dyad must be along each other, and when $P$ and $D$ are at the minimum distance, the two-link dyad must be on top of each other. Therefore,

$$
\begin{aligned}
l &= q + p & (6.117) \\
s &= q - p & (6.118)
\end{aligned}
$$

where $p$ is the shortest link, and $q$ is the longest link of the dyad. Solving Equations (6.117) and (6.118) for $p$ and $q$ provides

$$
p = \frac{l - s}{2} \tag{6.119}
$$

$$
q = \frac{l + s}{2}. \tag{6.120}
$$

In this example we measure

$$
\begin{aligned}
l &= 453.8 \, \text{mm} \\
s &= 312.1 \, \text{mm}
\end{aligned} \tag{6.121}
$$

and calculate for $p$ and $q$

$$
\begin{aligned}
p &= 70.8 \, \text{mm} \\
q &= 382.9 \, \text{mm}.
\end{aligned} \tag{6.122}
$$

The final design of the windshield mechanism and the running motor is shown in Figure 6.14 at the initial and final positions. The shorter link of the running dyad, $p$, must be attached to the motor at $P$, and the larger link, $q$, connects joint $D$ to the shorter link at $C$. The motor will turn the shorter link, $PC$ continuously at an angular speed $\omega$, while the longer link, $CD$, will run the mechanism and protect the wiper links to go beyond the initial and final angles.

**Example 230** *Application of four-bar linkage in a vehicle.*

The **double A arm** suspension is a very popular mechanism for independent suspension of street cars. Figure 6.15 illustrates a double A arm suspension and its equivalent kinematic model. We attach the wheel to a coupler point at $C$. The double A arm is also called **double wishbone** suspension.
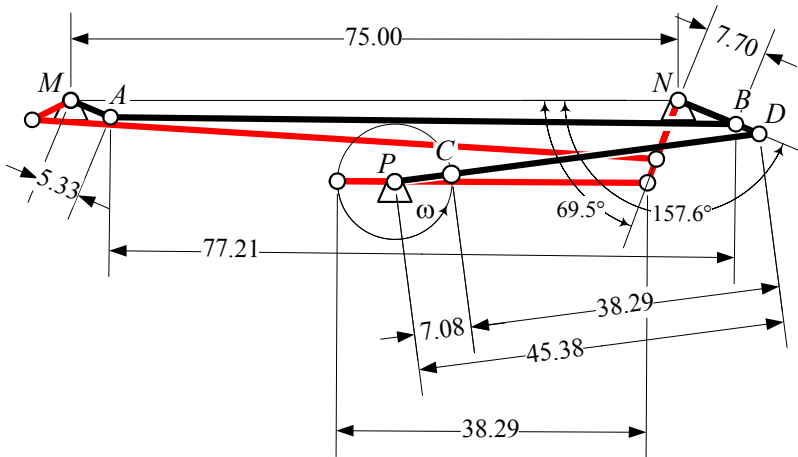
FIGURE 6.14. The final design of the windshield mechanism at the initial and final positions.
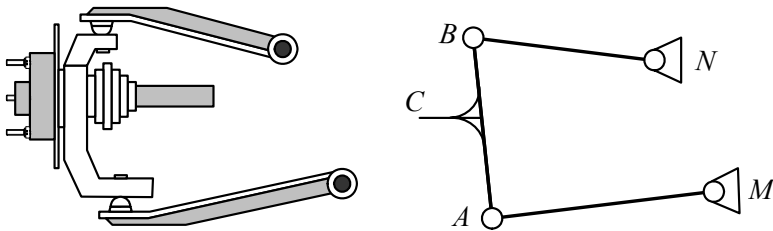


FIGURE 6.15. Double A arm suspension in a four-bar linkage mechanism.
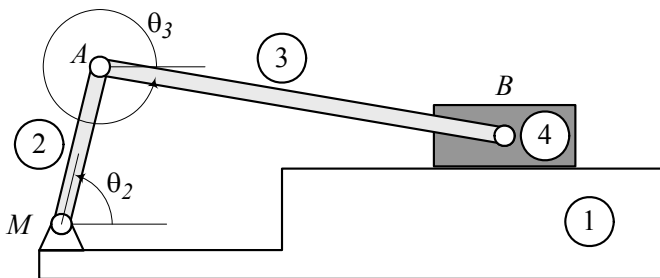
FIGURE 6.16. A slider-crank mechanism.

## 6.2   Slider-Crank Mechanism

A *slider-crank mechanism* is shown in Figure 6.16. A slider-crank mechanism is a four-bar linkage. Link number 1 is the ground, which is the base and reference link. Link number $2 \equiv MA$ is usually the input link, which is controlled by the input angle $\theta_2$. Link number 4 is the slider link that is usually considered as the output link. The output variable is the horizontal distance $s$ between the slider and a fixed point on the ground, which is usually the revolute joint at $M$. If the slider slides on a flat surface, we define the horizon by a straight line parallel to the flat surface and passing through $M$. The link number $3 \equiv AB$ is the coupler link with angular position $\theta_3$, which connects the input link to the output slider. This mechanism is called the slider-crank because in most applications, the input link is a crank link that rotates $360 \deg$, and the output is a slider.

The position of the output slider, $s$, and the angular position of the coupler link, $\theta_3$, are functions of the link's length and the value of the input variable $\theta_2$. The functions are

$$s \quad = \quad \frac{-G \pm \sqrt{G^2 - 4H}}{2} \tag{6.123}$$

$$\theta_3 \quad = \quad \sin^{-1}\left(\frac{e - a\sin\theta_2}{-b}\right) \tag{6.124}$$

where

$$G \quad = \quad -2a\cos\theta_2 \tag{6.125}$$

$$H \quad = \quad a^2 + e^2 - b^2 - 2ae\sin\theta_2. \tag{6.126}$$

**Proof.** We show the slider-crank mechanism by a vector loop, as shown in Figure 6.17. The direction of each vector is arbitrary, however the angles should be associated to the vector's direction and be measured with the positive direction of the $x$-axis. The links and their expression vectors are shown in Table 6.5.
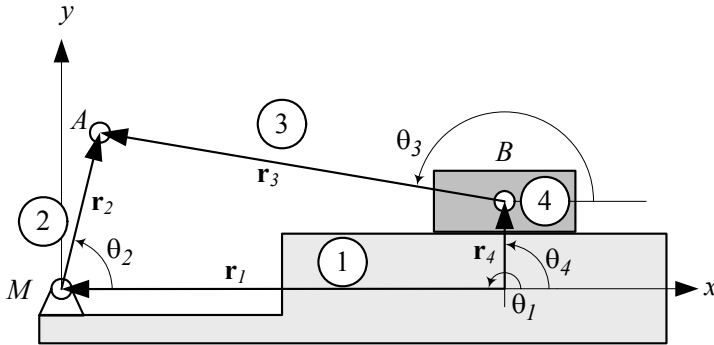
FIGURE 6.17. Expressing a slider-crank mechanism by a vector loop.

Table 6.5 - Vector representation of the slider-crank mechanism
shown in Figure 6.17.

| Link | Vector | Length | Angle | Variable |
|------|--------|--------|-------|----------|
| 1 | $^{G}\mathbf{r}_1$ | $s$ | $\theta_1 = 180 \deg$ | $s$ |
| 2 | $^{G}\mathbf{r}_2$ | $a$ | $\theta_2$ | $\theta_2$ |
| 3 | $^{G}\mathbf{r}_3$ | $b$ | $\theta_3$ | $\theta_3$ |
| 4 | $^{G}\mathbf{r}_4$ | $e$ | $\theta_4 = 90 \deg$ | $-$ |

The vector loop is

$$^{G}\mathbf{r}_1 + {^{G}\mathbf{r}_2} - {^{G}\mathbf{r}_3} - {^{G}\mathbf{r}_4} = \mathbf{0} \tag{6.127}$$

and we may decompose the vector equation (6.127) into sin and cos components.

$$a \sin \theta_2 - b \sin \theta_3 - e \;\; = \;\; 0 \tag{6.128}$$
$$a \cos \theta_2 - b \cos \theta_3 - s \;\; = \;\; 0 \tag{6.129}$$

To derive the relationship between the input angle $\theta_2$ and the output position $s$, the coupler angle $\theta_3$ must be eliminated between Equations (6.128) and (6.129). Transferring the terms containing $\theta_3$ to the other side of the equations, and squaring both sides, we get

$$(b \sin \theta_3)^2 \;\; = \;\; (a \sin \theta_2 - e)^2 \tag{6.130}$$
$$(b \cos \theta_3)^2 \;\; = \;\; (a \cos \theta_2 - s)^2 . \tag{6.131}$$

By adding Equations (6.130) and (6.131), we derive the following equation:

$$s^2 - 2as \cos \theta_2 + a^2 + e^2 - b^2 - 2ae \sin \theta_2 = 0 \tag{6.132}$$

or

$$s^2 + Gs + H = 0 \tag{6.133}$$

where

$$G = -2a \cos \theta_2 \tag{6.134}$$
$$H = a^2 + e^2 - b^2 - 2ae \sin \theta_2. \tag{6.135}$$

Equation (6.133) is a quadratic in $s$ and provides the following solution:

$$s = \frac{-G \pm \sqrt{G^2 - 4H}}{2} \tag{6.136}$$

To find the relationship between the input angle $\theta_2$ and the coupler angle $\theta_3$, we can use Equations (6.128) or (6.129) to solve for $\theta_3$.

$$\theta_3 = \sin^{-1}\left(\frac{e - a\sin\theta_2}{-b}\right) \tag{6.137}$$

$$\theta_3 = \cos^{-1}\left(\frac{s - a\cos\theta_2}{-b}\right) \tag{6.138}$$

Equations (6.34) and (6.44) can be used to calculate the output and coupler variables $s$ and $\theta_3$ as functions of the input angle $\theta_2$, provided the lengths $a$, $b$, and $e$ are given. ■

**Example 231** *Two possible configurations for a slider-crank mechanism.*
*At any angle $\theta_2$, and for suitable values of a, b, and e, Equation (6.136) provides two values for the output variable s. Both solutions are possible and provide two different configurations for the mechanism. A suitable set of (a, b, e) is the numbers that make the radical in Equations (6.136) real.*
*As an example, consider a slider-crank mechanism at $\theta_2 = \pi/4 \,\mathrm{rad} = 45 \deg$ with the lengths*

$$a = 1$$
$$b = 2$$
$$e = 0.5. \tag{6.139}$$

*To solve the possible configurations, we start by calculating the coefficients of the quadratic equation (6.133)*

$$G = -2a \cos \theta_2$$
$$= -1.4142 \tag{6.140}$$
$$H = a^2 + e^2 - b^2 - 2ae \sin \theta_2$$
$$= -3.4571. \tag{6.141}$$

*Employing Equation (6.136) provides*

$$s = \frac{-G \pm \sqrt{G^2 - 4H}}{2} = \begin{cases} 2.696 \\ -1.282 \end{cases}. \tag{6.142}$$
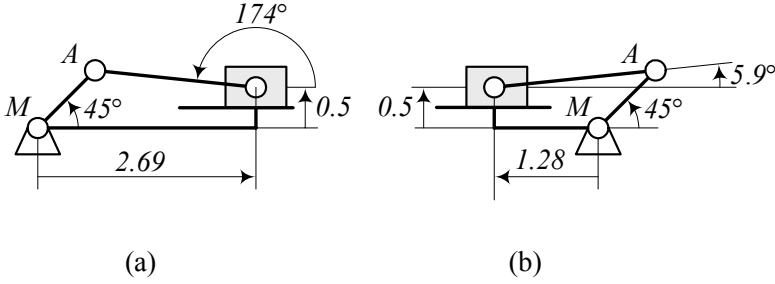
FIGURE 6.18. Two possible configurations of a slider-crank mechanism having the same input angle $\theta_2$.

*The corresponding coupler angle $\theta_3$ can be calculated form either Equation (6.137) or (6.138).*

$$\theta_3 = \sin^{-1}\left(\frac{e - a\sin\theta_2}{-b}\right) = \cos^{-1}\left(\frac{s - a\cos\theta_2}{-b}\right)$$

$$\approx \begin{cases} 3.037\,\mathrm{rad} \approx 174\,\mathrm{deg} \\ 0.103\,\mathrm{rad} \approx 5.9\,\mathrm{deg} \end{cases} \tag{6.143}$$

*Figure 6.18 depicts the two possible configurations of the mechanism for $\theta_2 = 45\,\mathrm{deg}$.*

**Example 232** *Velocity analysis of a slider-crank mechanism.*

*The velocity analysis of a slider-crank mechanism is possible by taking a time derivative of Equations (6.128) and (6.129),*

$$\frac{d}{dt}(a\sin\theta_2 - b\sin\theta_3 - e)$$
$$= a\omega_2\cos\theta_2 - b\omega_3\cos\theta_3 = 0 \tag{6.144}$$

$$\frac{d}{dt}(a\cos\theta_2 - b\cos\theta_3 - s)$$
$$= -a\omega_2\sin\theta_2 + b\omega_3\sin\theta_3 - \dot{s} = 0 \tag{6.145}$$

*where*

$$\omega_2 = \dot{\theta}_2$$
$$\omega_3 = \dot{\theta}_3. \tag{6.146}$$

*Assuming $\theta_2$ and $\omega_2$ are given values, and $s$, $\theta_3$ are known from Equations (6.123) and (6.124), we may solve Equations (6.144) and (6.145) for $\dot{s}$ and $\omega_3$.*

$$\dot{s} = \frac{\sin(\theta_3 - \theta_2)}{\cos\theta_3}a\omega_2 \tag{6.147}$$

$$\omega_3 = \frac{\cos\theta_2}{\cos\theta_3}\frac{a}{b}\omega_2 \tag{6.148}$$

**Example 233** *Velocity of moving joints for a slider-crank mechanism.*

*Having the coordinates $\theta_2$, $\theta_3$, $s$ and velocities $\omega_2$, $\omega_3$, $\dot{s}$ enables us to calculate the absolute and relative velocities of points $A$ and $B$ shown in Figure 6.17. The absolute velocities of points $A$ and $B$ are*

$$
\begin{aligned}
{}^{G}\mathbf{v}_A \;&=\; {}_{G}\boldsymbol{\omega}_2 \times {}^{G}\mathbf{r}_2 \\
&= \begin{bmatrix} 0 \\ 0 \\ \omega_2 \end{bmatrix} \times \begin{bmatrix} a\cos\theta_2 \\ a\sin\theta_2 \\ 0 \end{bmatrix} = \begin{bmatrix} -a\omega_2\sin\theta_2 \\ a\omega_2\cos\theta_2 \\ 0 \end{bmatrix}
\end{aligned}
\tag{6.149}
$$

$$
\begin{aligned}
{}^{G}\mathbf{v}_B \;&=\; \dot{s}\,\hat{\imath} \\
&= \begin{bmatrix} \dfrac{\sin(\theta_3-\theta_2)}{\cos\theta_3}\,a\omega_2 \\ 0 \\ 0 \end{bmatrix}
\end{aligned}
\tag{6.150}
$$

*and the velocity of point $B$ with respect to point $A$ is*

$$
\begin{aligned}
{}^{G}\mathbf{v}_{B/A} \;&=\; {}^{G}\mathbf{v}_B - {}^{G}\mathbf{v}_A \\
&= \begin{bmatrix} \dfrac{\sin(\theta_3-\theta_2)}{\cos\theta_3}\,a\omega_2 \\ 0 \\ 0 \end{bmatrix} - \begin{bmatrix} -a\omega_2\sin\theta_2 \\ a\omega_2\cos\theta_2 \\ 0 \end{bmatrix} \\
&= \begin{bmatrix} a\omega_2\sin\theta_2 + a\dfrac{\omega_2}{\cos\theta_3}\sin(\theta_3-\theta_2) \\ -a\omega_2\cos\theta_2 \\ 0 \end{bmatrix}.
\end{aligned}
\tag{6.151}
$$

*The velocity of point $B$ with respect to $A$ can also be found as*

$$
\begin{aligned}
{}^{G}\mathbf{v}_{B/A} \;&=\; {}^{G}R_2\,{}^{2}\mathbf{v}_B \\
&= {}^{G}R_2\,{}^{2}\mathbf{v}_B \\
&= {}^{G}R_2\left( {}_{2}\boldsymbol{\omega}_3 \times {}^{2}\mathbf{r}_3 \right) \\
&= {}_{G}\boldsymbol{\omega}_3 \times {}^{G}\mathbf{r}_3 \\
&= \begin{bmatrix} 0 \\ 0 \\ \omega_3 \end{bmatrix} \times \begin{bmatrix} b\cos\theta_3 \\ b\sin\theta_3 \\ 0 \end{bmatrix} = \begin{bmatrix} -b\omega_3\sin\theta_3 \\ b\omega_3\cos\theta_3 \\ 0 \end{bmatrix}.
\end{aligned}
\tag{6.152}
$$

*Equations (6.151) and (6.152) are both correct and convertible to each other.*

**Example 234** *Acceleration analysis of a slider-crank mechanism.*

The acceleration analysis of a slider-crank mechanism is possible by taking another time derivative from Equations (6.144) and (6.145),

$$\frac{d}{dt}\left(a\,\omega_2\cos\theta_2 - b\,\omega_3\cos\theta_3\right)$$
$$= a\alpha_2\cos\theta_2 - b\alpha_3\cos\theta_3 - a\omega_2^2\sin\theta_2 + b\omega_3^2\sin\theta_3$$
$$= 0 \tag{6.153}$$

$$\frac{d}{dt}\left(-a\,\omega_2\sin\theta_2 + b\,\omega_3\sin\theta_3 - \dot{s}\right)$$
$$= -a\alpha_2\sin\theta_2 - b\alpha_3\sin\theta_3 + a\omega_2^2\cos\theta_2 + b\omega_3^2\cos\theta_3 - \ddot{s}$$
$$= 0 \tag{6.154}$$

where,

$$\alpha_2 = \dot{\omega}_2$$
$$\alpha_3 = \dot{\omega}_3. \tag{6.155}$$

Assuming $\theta_2$, $\omega_2$, and $\alpha_2$ are given values as the kinematics of the input link, $s$, $\theta_3$, are known from Equations (6.123) and (6.124), and $\dot{s}$, $\omega_3$ are known from Equations (6.147) and (6.148), we may solve Equations (6.153) and (6.154) for $\ddot{s}$ and $\alpha_3$.

$$\ddot{s} = \frac{-a\alpha_2\sin(\theta_2 + \theta_3) + b\omega_3^2\cos 2\theta_3 + a\omega_2^2\cos(\theta_2 - \theta_3)}{\cos\theta_3} \tag{6.156}$$

$$\alpha_3 = \frac{a\alpha_2\cos\theta_2 - a\omega_2^2\sin\theta_2 + b\omega_3^2\sin\theta_3}{b\cos\theta_3} \tag{6.157}$$

**Example 235** *Acceleration of moving joints of a slider-crank mechanism.*

Having the angular kinematics of a slider-crank mechanism $\theta_2$, $\theta_3$, $s$, $\omega_2$, $\omega_3$, $\dot{s}$, $\alpha_2$, $\alpha_3$, and $\ddot{s}$ are necessary and enough to calculate the absolute and relative accelerations of points $A$ and $B$, shown in Figure 6.17.

The absolute acceleration of points $A$ and $B$ are

$$^G\mathbf{a}_A = {}_G\boldsymbol{\alpha}_2 \times {}^G\mathbf{r}_2 + {}_G\boldsymbol{\omega}_2 \times \left({}_G\boldsymbol{\omega}_2 \times {}^G\mathbf{r}_2\right)$$
$$= \begin{bmatrix} -a\alpha_2\sin\theta_2 - a\omega_2^2\cos\theta_2 \\ a\alpha_2\cos\theta_2 - a\omega_2^2\sin\theta_2 \\ 0 \end{bmatrix} \tag{6.158}$$

$$^G\mathbf{a}_B = \ddot{s}\,\hat{\imath}$$
$$= \begin{bmatrix} \dfrac{-a\alpha_2\sin(\theta_2 + \theta_3) + b\omega_3^2\cos 2\theta_3 + a\omega_2^2\cos(\theta_2 - \theta_3)}{\cos\theta_3} \\ 0 \\ 0 \end{bmatrix}. \tag{6.159}$$

FIGURE 6.19. Limit position for a slider-crank mechanism.

*The acceleration of point B with respect to point A is*

$$
{}^G\mathbf{a}_{B/A} = {}_G\boldsymbol{\alpha}_3 \times {}^G\mathbf{r}_3 + {}_G\boldsymbol{\omega}_3 \times \left( {}_G\boldsymbol{\omega}_3 \times {}^G\mathbf{r}_3 \right)
$$

$$
= \begin{bmatrix} -b\alpha_3 \sin\theta_3 - b\omega_3^2 \cos\theta_3 \\ b\alpha_3 \cos\theta_3 - b\omega_3^2 \sin\theta_3 \\ 0 \end{bmatrix}. \tag{6.160}
$$

**Example 236** *Limit positions for a slider-crank mechanism.*

*When the output slider of a slider-crank mechanism stops while the input link can turn, we say the slider is at a* **limit position***. It happens when the angle between the input and coupler links is either* 180 deg *or* 360 deg*. Limit positions of a slider-crank mechanism are usually dictated by the design requirements. A limit position for a slider-crank mechanism is shown in Figure 6.19.*

*We show the limit angle of the input link by* $\theta_{2_{L1}}$, $\theta_{2_{L2}}$, *and the corresponding horizontal distance of the slider by* $s_{Max}$, $s_{min}$. *They can be calculated by the following equations:*

$$
\theta_{2_{L1}} = \sin^{-1}\left[\frac{e}{b+a}\right] \tag{6.161}
$$

$$
s_{Max} = \sqrt{(b+a)^2 - e^2} \tag{6.162}
$$

$$
\theta_{2_{L2}} = \sin^{-1}\left[\frac{e}{b-a}\right] \tag{6.163}
$$

$$
s_{min} = \sqrt{(b-a)^2 - e^2} \tag{6.164}
$$

*The length of stroke that the slider travels repeatedly would be*

$$
\begin{aligned}
s &= s_{Max} - s_{min} \\
&= \sqrt{(b+a)^2 - e^2} - \sqrt{(b-a)^2 - e^2}. \tag{6.165}
\end{aligned}
$$

**Example 237 ★** *Quick return slider-crank mechanism.*

*Consider a slider-crank with a rotating input link at a constant angular velocity $\omega_2$. The required time for the slider to move from $s_{min}$ to $s_{Max}$ is*

$$t_1 = \frac{\theta_{2_{L2}} - \theta_{2_{L1}}}{\omega_2}$$

$$= \frac{1}{\omega_2}\left(\sin^{-1}\left[\frac{e}{b-a}\right] - \sin^{-1}\left[\frac{e}{b+a}\right]\right) \qquad (6.166)$$

*and the required time for returning from $s_{Max}$ to $s_{min}$ is*

$$t_2 = \frac{\theta_{2_{L1}} - \theta_{2_{L2}}}{\omega_2}$$

$$= \frac{1}{\omega_2}\left(\sin^{-1}\left[\frac{e}{b+a}\right] - \sin^{-1}\left[\frac{e}{b-a}\right]\right). \qquad (6.167)$$

*If $e = 0$, then*

$$\theta_{2_{L1}} = 0 \qquad (6.168)$$
$$\theta_{2_{L2}} = 180 \deg \qquad (6.169)$$

*and therefore,*

$$t_1 = t_2 = \frac{\pi}{\omega_2}. \qquad (6.170)$$

*However, when $e < 0$ then,*

$$t_2 < t_1 \qquad (6.171)$$

*and the slider returns to $s_{min}$ faster. Such a mechanism is called **quick return**.*

## 6.3   Inverted Slider-Crank Mechanism

An *inverted slider-crank mechanism* is shown in Figure 6.20. It is a four-link mechanism. Link number 1 is the ground link, which is the base and reference link. Link number $2 \equiv MA$ is usually the input link, which is controlled by the input angle $\theta_2$. Link number 4 is the slider link and is usually considered as the output link. The slider link has a revolute joint with the ground and a prismatic joint with the coupler link $3 \equiv AB$. The output variable can be the angle of the slider with the horizon, or the length $AB$. The link number $3 \equiv AB$ is the coupler link with angular position $\theta_3$.

If we attach the coupler link of a slider-crank mechanism to the ground, an inverted slider-crank mechanism is made. Changing the grounded link produces a new mechanism that is called an *inversion* of the previous mechanism. Hence, the inverted slider-crank is an inversion of a slider-crank mechanism.
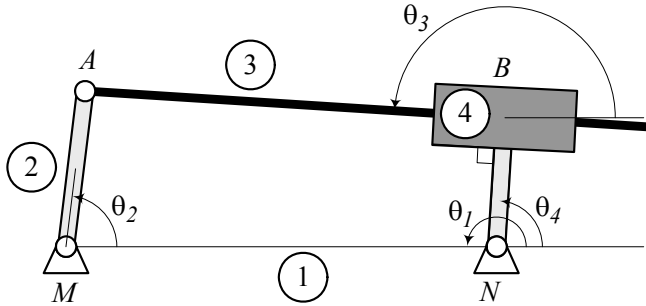
FIGURE 6.20. An inverted slider-crank mechanism.

The angular position of the output slider $\theta_4$ and the length of the coupler link $b$ are functions of the lengths of the links and the value of the input variable $\theta_2$. These variables are:

$$b = \pm\sqrt{a^2 + d^2 - e^2 - 2ad\cos\theta_2} \qquad (6.172)$$

$$\theta_4 = \theta_3 + \frac{\pi}{2}$$

$$= 2\tan^{-1}\left(\frac{-H \pm \sqrt{H^2 - 4GI}}{2G}\right) \qquad (6.173)$$

where

$$G = d - e - a\cos\theta_2 \qquad (6.174)$$

$$H = 2a\sin\theta_2 \qquad (6.175)$$

$$I = a\cos\theta_2 - d - e. \qquad (6.176)$$

**Proof.** We show the inverted slider-crank mechanism by a vector loop as shown in Figure 6.21. The direction of each vector is arbitrary, however, the angles should be associated to the vector's direction and be measured with positive direction of the $x$-axis. The links and their expression vectors are shown in Table 6.6.

Table 6.6 - Vector representation of the inverted slider-crank mechanism shown in Figure 6.21.

| Link | Vector | Length | Angle | Variable |
|------|--------|--------|-------|----------|
| 1 | $^G\mathbf{r}_1$ | $d$ | $\theta_1 = 180\,\text{deg}$ | $d$ |
| 2 | $^G\mathbf{r}_2$ | $a$ | $\theta_2$ | $\theta_2$ |
| 3 | $^G\mathbf{r}_3$ | $b$ | $\theta_3$ | $\theta_3$ or $\theta_4$ |
| 4 | $^G\mathbf{r}_4$ | $e$ | $\theta_4 = \theta_3 + 90\,\text{deg}$ | $-$ |

The vector loop is

$$^G\mathbf{r}_1 + {}^G\mathbf{r}_2 - {}^G\mathbf{r}_3 - {}^G\mathbf{r}_4 = \mathbf{0} \qquad (6.177)$$
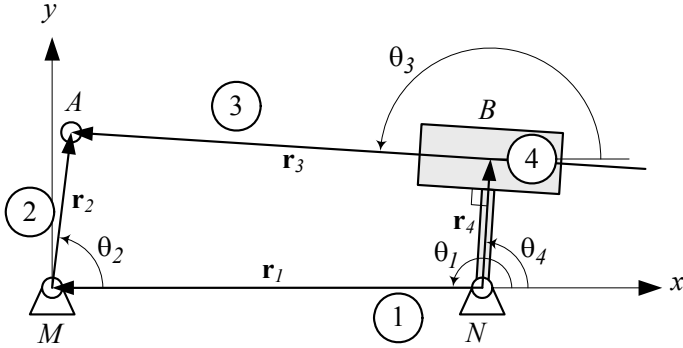
FIGURE 6.21. Kinematic model of an inverted slider-crank mechanism.

which can be decomposed into sin and cos components.

$$a \sin \theta_2 - b \sin \left( \theta_4 - \frac{\pi}{2} \right) - e \sin \theta_4 \quad = \quad 0 \qquad (6.178)$$

$$-d + a \cos \theta_2 - b \sin \left( \theta_4 - \frac{\pi}{2} \right) - e \cos \theta_4 \quad = \quad 0 \qquad (6.179)$$

To derive the relationship between the input angle $\theta_2$ and the output $\theta_4$, we eliminate $b$ between Equations (6.178) and (6.179) and find

$$(a \cos \theta_2 - d) \cos \theta_4 + a \sin \theta_2 \sin \theta_4 - e = 0. \qquad (6.180)$$

The have a better expression suitable for computer programming, we may use trigonometric equations

$$\sin \theta_4 \quad = \quad 2 \frac{2 \tan \dfrac{\theta_4}{2}}{1 + \tan^2 \dfrac{\theta_4}{2}} \qquad (6.181)$$

$$\cos \theta_4 \quad = \quad \frac{1 + \tan^2 \dfrac{\theta_4}{2}}{1 + \tan^2 \dfrac{\theta_4}{2}} \qquad (6.182)$$

to transform Equation (6.180) to a more useful equation

$$G \tan^2 \frac{\theta_4}{2} + H \tan \frac{\theta_4}{2} + I = 0 \qquad (6.183)$$

where, $I$, $J$, and $K$ are functions of the input variable.

$$G \quad = \quad d - e - a \cos \theta_2 \qquad (6.184)$$
$$H \quad = \quad 2a \sin \theta_2 \qquad (6.185)$$
$$I \quad = \quad a \cos \theta_2 - d - e \qquad (6.186)$$

Equation (6.183) is a quadratic in $\tan(\theta_4/2)$ and can be used to find the output angle $\theta_4$.

$$\theta_4 = 2\tan^{-1}\left(\frac{-H \pm \sqrt{H^2 - 4GI}}{2G}\right) \tag{6.187}$$

To find the relationship between the input angle $\theta_2$ and the coupler length $b$, we may solve Equations (6.178) and (6.179) for $\sin\theta_4$ and $\cos\theta_4$

$$\sin\theta_4 \quad = \quad \frac{ab\cos\theta_2 - ae\sin\theta_2 + bd}{b^2 + e^2} \tag{6.188}$$

$$\cos\theta_4 \quad = \quad -\frac{ab\sin\theta_2 - ae\cos\theta_2 + ed}{b^2 + e^2} \tag{6.189}$$

or substitute (6.187) in (6.180) and solve for $b$. By squaring and adding Equations (6.188) and (6.189), we find the following equation:

$$a^2 - b^2 + d^2 - e^2 - 2ad\cos\theta_2 = 0 \tag{6.190}$$

which must be solved for $b$.

$$b = \pm\sqrt{a^2 + d^2 - e^2 - 2ad\cos\theta_2} \tag{6.191}$$

∎

**Example 238** *Two possible configurations for an inverted slider-crank mechanism.*

*At any angle $\theta_2$, and for suitable values of $a$, $d$, and $e$, Equations (6.172) and (6.173) provide two values for the output $b$ and coupler angles $\theta_4$. Both solutions are possible and provide two different configurations for the mechanism. A suitable set of $(a, d, e)$ are the numbers that make the radicals in Equations (6.172) and (6.173) real.*

*For example, consider an inverted slider-crank mechanism at $\theta_2 = \pi/4\,\mathrm{rad} = 45\,\mathrm{deg}$ with the lengths*

$$\begin{aligned} a &= 1 \\ e &= 0.5 \\ d &= 3. \end{aligned} \tag{6.192}$$

*The parameters of Equation (6.172) are equal to*

$$\begin{aligned} G &= d - e - a\cos\theta_2 = 1.7929 \\ H &= 2a\sin\theta_2 = 1.4142 \\ I &= a\cos\theta_2 - d - e = -2.7929 \end{aligned} \tag{6.193}$$

*Now, Equation (6.183) gives two real values for $\theta_4$*

$$\theta_4 \approx \begin{cases} 1.48\,\mathrm{rad} \approx 84.8\,\mathrm{deg} \\ -2.08\,\mathrm{rad} \approx -120\,\mathrm{deg} \end{cases}. \tag{6.194}$$
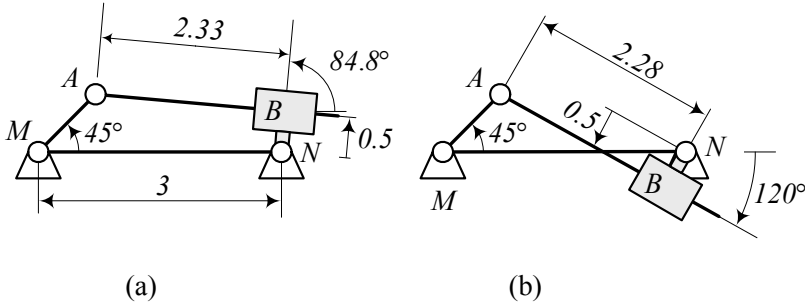
FIGURE 6.22. Two configurations of an inverted slider crank mechanism for $\theta_2 = 45 \deg$.

Using the known values and for $\theta_4 = 1.48 \, \text{rad}$, Equations (6.188) will provide

$$b \approx 2.33. \tag{6.195}$$

When $\theta_4 = -1.732 \, \text{rad}$ we get

$$b = -2.28. \tag{6.196}$$

Figure 6.22 depicts the two configurations of the mechanism for $\theta_2 = 45 \deg$.

**Example 239** *Velocity analysis of an inverted slider-crank mechanism.*

The velocity analysis of a slider-crank mechanism can be found by taking a time derivative of Equations (6.178) and (6.179),

$$\frac{d}{dt} \left( a \sin \theta_2 + b \cos \theta_4 - e \sin \theta_4 \right)$$

$$= a \omega_2 \cos \theta_2 - b \omega_4 \sin \theta_4 + \dot{b} \cos \theta_4 - e \omega_4 \cos \theta_4 = 0 \tag{6.197}$$

$$\frac{d}{dt} \left( a \cos \theta_2 + b \cos \theta_4 - e \cos \theta_4 - d \right)$$

$$= -a \omega_2 \sin \theta_2 - b \omega_4 \sin \theta_4 + \dot{b} \cos \theta_4 + e \omega_4 \sin \theta_4 = 0 \tag{6.198}$$

where

$$\omega_2 = \dot{\theta}_2$$
$$\omega_4 = \omega_3 = \dot{\theta}_4. \tag{6.199}$$

Assuming $\theta_2$ and $\omega_2$ are given values, and b, $\theta_4$ are known from Equations (6.172) and (6.173), we may solve Equations (6.197) and (6.198) for $\dot{b}$ and $\omega_4$.

$$\dot{b} = \frac{a}{b} \omega_2 \left[ b \cos (\theta_4 - \theta_2) - e \sin (\theta_4 - \theta_2) \right] \tag{6.200}$$

$$\omega_4 = \omega_3 = \frac{a}{b} \omega_2 \sin (\theta_2 - \theta_4) \tag{6.201}$$

**Example 240** *Velocity of moving joints for an inverted slider-crank mechanism.*

*Having the coordinates $\theta_2$, $\theta_4$, $b$ and velocities $\omega_2$, $\omega_4$, $\dot{b}$ enables us to calculate the absolute and relative velocities of points $A$ and $B$ shown in Figure 6.21. The absolute and relative velocities of points $A$ and $B$ are*

$$
\begin{aligned}
{}^G\mathbf{v}_A &= {}^G\boldsymbol{\omega}_2 \times {}^G\mathbf{r}_2 \\
&= \begin{bmatrix} 0 \\ 0 \\ \omega_2 \end{bmatrix} \times \begin{bmatrix} a\cos\theta_2 \\ a\sin\theta_2 \\ 0 \end{bmatrix} = \begin{bmatrix} -a\omega_2\sin\theta_2 \\ a\omega_2\cos\theta_2 \\ 0 \end{bmatrix}
\end{aligned} \tag{6.202}
$$

$$
\begin{aligned}
{}^G\mathbf{v}_{B_4} &= {}^G\boldsymbol{\omega}_4 \times {}^G\mathbf{r}_4 \\
&= \begin{bmatrix} 0 \\ 0 \\ \omega_4 \end{bmatrix} \times \begin{bmatrix} e\cos\theta_4 \\ e\sin\theta_4 \\ 0 \end{bmatrix} = \begin{bmatrix} -e\omega_4\sin\theta_4 \\ e\omega_4\cos\theta_4 \\ 0 \end{bmatrix}
\end{aligned} \tag{6.203}
$$

$$
\begin{aligned}
{}^G\mathbf{v}_{B_3/A} &= {}^G\boldsymbol{\omega}_3 \times \left(-{}^G\mathbf{r}_3\right) \\
&= \begin{bmatrix} 0 \\ 0 \\ \omega_4 \end{bmatrix} \times \begin{bmatrix} -b\cos\theta_4 \\ -b\sin\theta_4 \\ 0 \end{bmatrix} = \begin{bmatrix} b\omega_4\sin\theta_4 \\ -b\omega_4\cos\theta_4 \\ 0 \end{bmatrix}
\end{aligned} \tag{6.204}
$$

$$
\begin{aligned}
{}^G\mathbf{v}_{B_3} &= {}^G\mathbf{v}_{B_3/A} + {}^G\mathbf{v}_A \\
&= \begin{bmatrix} b\omega_4\sin\theta_4 \\ -b\omega_4\cos\theta_4 \\ 0 \end{bmatrix} + \begin{bmatrix} -a\omega_2\sin\theta_2 \\ a\omega_2\cos\theta_2 \\ 0 \end{bmatrix} \\
&= \begin{bmatrix} b\omega_4\sin\theta_4 - a\omega_2\sin\theta_2 \\ a\omega_2\cos\theta_2 - b\omega_4\cos\theta_4 \\ 0 \end{bmatrix}
\end{aligned} \tag{6.205}
$$

$$
\begin{aligned}
{}^G\mathbf{v}_{B_3/B_4} &= {}^G\mathbf{v}_{B_3} - {}^G\mathbf{v}_{B_4} \\
&= \begin{bmatrix} b\omega_4\sin\theta_4 - a\omega_2\sin\theta_2 \\ a\omega_2\cos\theta_2 - b\omega_4\cos\theta_4 \\ 0 \end{bmatrix} - \begin{bmatrix} -e\omega_4\sin\theta_4 \\ e\omega_4\cos\theta_4 \\ 0 \end{bmatrix} \\
&= \begin{bmatrix} \omega_4 e\sin\theta_4 - a\omega_2\sin\theta_2 + b\omega_4\sin\theta_4 \\ a\omega_2\cos\theta_2 - \omega_4 e\cos\theta_4 - b\omega_4\cos\theta_4 \\ 0 \end{bmatrix}.
\end{aligned} \tag{6.206}
$$

**Example 241** *Acceleration analysis of an inverted slider-crank mechanism.*

The acceleration analysis of an inverted slider-crank mechanism can be found by taking another time derivative from Equations (6.197) and (6.198),

$$
\frac{d}{dt}\left(a\,\omega_2\cos\theta_2 - b\,\omega_4\sin\theta_4 + \dot{b}\cos\theta_4 - e\,\omega_4\cos\theta_4\right)
$$
$$
= \quad a\alpha_2\cos\theta_2 - a\omega_2^2\sin\theta_2 - b\alpha_4\sin\theta_4 + b\omega_4^2\cos\theta_4
$$
$$
+\ddot{b}\cos\theta_4 - \dot{b}\omega_4\sin\theta_4 - e\alpha_4\cos\theta_4 + e\omega_4^2\sin\theta_4
$$
$$
= \quad 0 \tag{6.207}
$$

$$
\frac{d}{dt}\left(-a\,\omega_2\sin\theta_2 - b\,\omega_4\sin\theta_4 + \dot{b}\cos\theta_4 + e\,\omega_4\sin\theta_4\right)
$$
$$
= \quad -a\alpha_2\sin\theta_2 + a\omega_2^2\cos\theta_2 - b\alpha_4\sin\theta_4 - b\omega_4^2\cos\theta_4
$$
$$
+\ddot{b}\cos\theta_4 - \dot{b}\omega_4\sin\theta_4 + e\alpha_4\sin\theta_4 + e\omega_4^2\cos\theta_4
$$
$$
= \quad 0 \tag{6.208}
$$

where

$$
\alpha_2 = \dot{\omega}_2
$$
$$
\alpha_4 = \alpha_3 = \dot{\omega}_4 = \dot{\omega}_3. \tag{6.209}
$$

Assuming $\theta_2$, $\omega_2$, and $\alpha_4$ are given values as the kinematics of the input link, $b$, $\theta_4$, are known from Equations (6.172) and (6.173), and $\dot{b}$, $\omega_4$ are known from Equations (6.200) and (6.201), we may solve Equations (6.207) and (6.208), for $\ddot{b}$ and $\alpha_4$

$$
\ddot{b} = \frac{C_7 C_{12} - C_9 C_{10}}{C_7 C_{11} - C_8 C_{10}} \tag{6.210}
$$
$$
\alpha_4 = \frac{C_9 C_{11} - C_8 C_{12}}{C_7 C_{11} - C_8 C_{10}} \tag{6.211}
$$

where,

$$
C_7 = \sin\theta_4
$$
$$
C_8 = b\cos\theta_4 + e\sin\theta_4
$$
$$
C_9 = a\alpha_2\sin\theta_2 + a\omega_2^2\cos\theta_2 - 2\dot{b}\omega_4\cos\theta_4
$$
$$
+b\omega_4^2\sin\theta_4 - e\omega_4^2\cos\theta_4
$$
$$
C_{10} = \cos\theta_4
$$
$$
C_{11} = -b\sin\theta_4 + e\cos\theta_4
$$
$$
C_{12} = a\alpha_2\cos\theta_2 - a\omega_2^2\sin\theta_2 + 2\dot{b}\omega_4\sin\theta_4
$$
$$
+b\omega_4^2\cos\theta_4 + e\omega_4^2\sin\theta_4. \tag{6.212}
$$
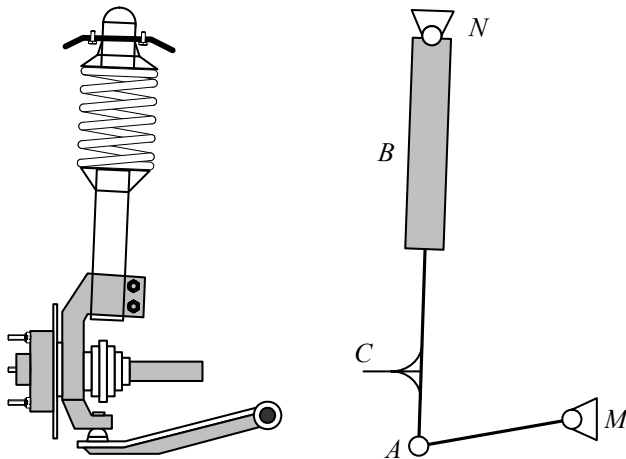
FIGURE 6.23. The McPherson strut suspension is an inverted slider mechanism.

**Example 242** *Application of inverted slider mechanism in vehicles.*

The McPherson strut suspension is a very popular mechanism for independent front suspension of street cars. Figure 6.23 illustrates a McPherson strut suspension and its equivalent kinematic model. We attach the wheel to a coupler point at $C$.

The piston rod of the shock absorber serves as a kingpin axis at the top of the strut. At the bottom, the shock absorber pivots on a ball joint on a single lower arm. The McPherson strut, also called the Chapman strut, was invented by Earl McPherson in the 1940s. It was first introduced on the 1949 Ford Vedette, and also adopted in the 1951 Ford Consul, and then become one of the dominating suspension systems because it's compactness and has a low cost.

## 6.4   Instant Center of Rotation

In a general plane motion of a rigid body, at a given instant, the velocities of various points of the body can be expressed as the result of a rotation about an axis perpendicular to the plane. This axis intersects the plane at a point called the *instantaneous center of rotation* of the body with respect to the ground. The instantaneous center of rotation is also called *instant center*, *centro*, and *pole*.

If the directions of the velocities of two different body points $A$ and $B$ are known, the instant center of rotation $I$ is at the intersection of the lines perpendicular to the velocity vectors $\mathbf{v}_A$ and $\mathbf{v}_B$. Such a situation is shown in Figure 6.24(a).

If the velocity vectors $\mathbf{v}_A$ and $\mathbf{v}_B$ are perpendicular to the line $AB$ and
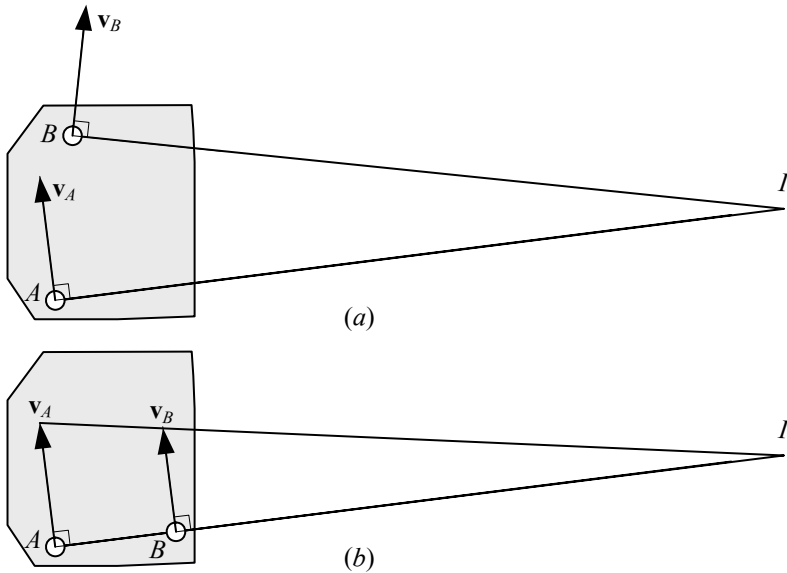
FIGURE 6.24. Determination of the instantaneous center of rotation $I$ for a moving rigid body.

if their magnitudes are known, the instantaneous center of rotation $I$ is at the intersection of $AB$ with the line joining the extremities of the velocity vectors. Such a situation is shown in Figure 6.24(b).

There is an instant center of rotation between every two links moving with respect to each other. The instant center is a point common to both bodies that has the same velocity in each body coordinate frame.

The three instant centers , $I_{12}$, $I_{23}$, and $I_{13}$ between three links numbered 1, 2, and 3 lie on a straight line. This statement is called the *Kennedy theorem* for three instant centers.

**Proof.** Consider the two bodies shown in Figure 6.25. The ground is link number 1, links number 2 and 3 are pivoted to the ground at points $M$ and $N$, and are rotating with angular velocities $\omega_2$ and $\omega_3$. The two links are contacted at point $C$. The revolute joint at $M$ is the instant center $I_{12}$ and the revolute joint at $N$ is the instant center $I_{13}$.

The velocity of point $C$ as a point of link 2 is $\mathbf{v}_{C_2}$, perpendicular to the radius $MC$. Similarly, the velocity of point $C$ as a point of link 3 is $\mathbf{v}_{C_2}$, perpendicular to the radius $NC$. The instant center of rotation $I_{13}$ must be a common point with the same velocity in both bodies. Let's draw the normal line $n - n$, and tangential line $t - t$ to the curves of links 2 and 3, at the contact point $C$.

Point $C$ is a common point between the two bodies. The normal components of $\mathbf{v}_{C_2}$ and $\mathbf{v}_{C_3}$ must be equal to keep contact, so the only difference
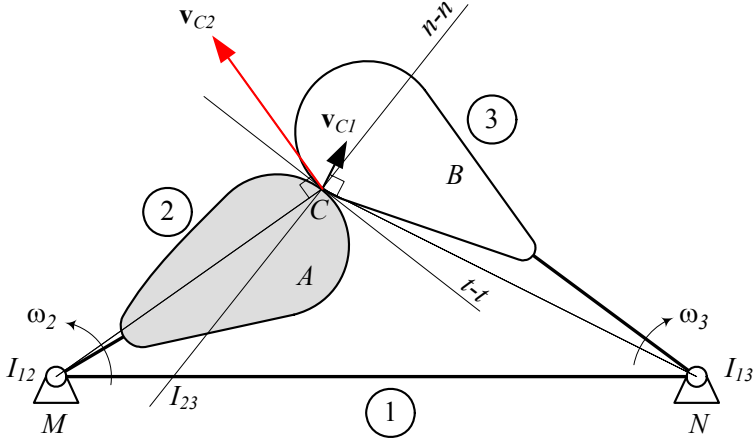
FIGURE 6.25. A 3-link mechanism with the ground as link number 1, and two moving links, numbers 2 and 3.

between the velocity of the common point can be in the tangent components. So, the instant center of rotation $I_{13}$ must be at a position where the relative velocity of points $C_2$ and $C_3$ with respect to $I_{13}$ are equal and are on the line $t - t$. Hence, it must be on the normal line $n - n$, and the intersection of the normal line $n - n$ with the center line $MN$ is the only possible point for the instant center of rotation $I_{13}$.

Let's define

$$I_{12}I_{23} = l_2 \qquad (6.213)$$

$$I_{13}I_{23} = l_3 \qquad (6.214)$$

then, because the velocities of the two bodies must be equal at the common instant center of rotation, we have

$$l_2\omega_2 = l_3\omega_3 \qquad (6.215)$$

or

$$\frac{\omega_2}{\omega_3} = \frac{l_3}{l_2}$$

$$= \frac{1}{1 + \dfrac{d}{l_2}} \qquad (6.216)$$

where, $d$ is the length of the ground link $MN$.  ■
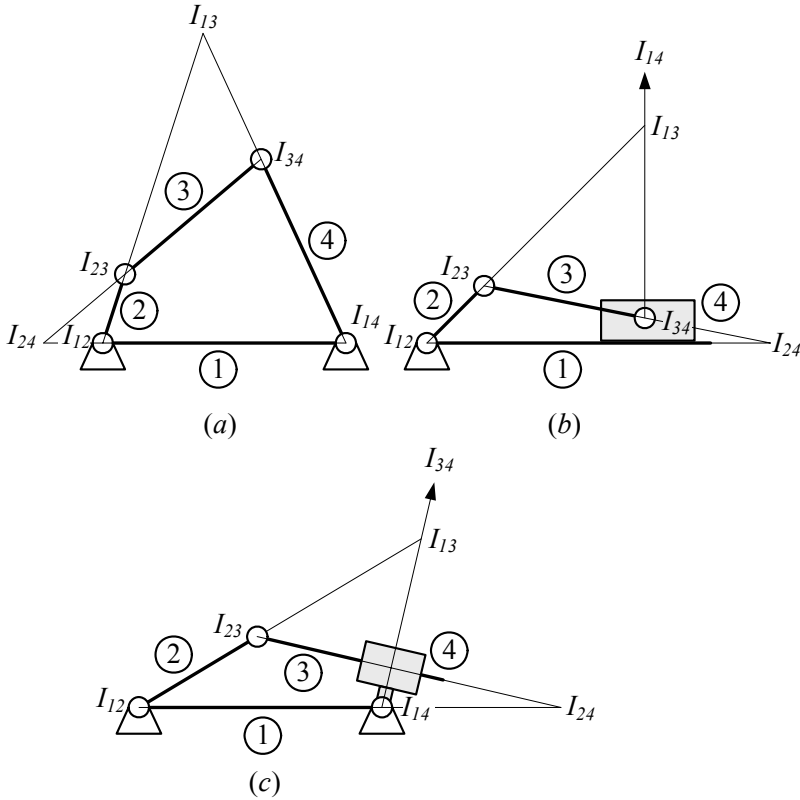
FIGURE 6.26. The instant centers of rotation for a four-bar linkage, a slider-crank, and an inverted slider-crank mechanism.

**Example 243** *Number of instant centers.*

   *There is one instant center between every two relatively moving bodies. So, there are three instant centers between three bodies. The number $N$ of instant centers between $n$ relatively moving bodies is*

$$N = \frac{n(n-1)}{2}. \qquad (6.217)$$

*Thus, a four-bar linkage has six instant centers, $I_{12}$, $I_{13}$, $I_{14}$, $I_{23}$, $I_{24}$, $I_{34}$. The symbol $I_{ij}$ indicates the instant center of rotation between kinks $i$ and $j$. Because two links have only one instant center, we have*

$$I_{ij} = I_{ji}. \qquad (6.218)$$

   *The four instant centers of rotation for a four-bar linkage, a slider-crank, and an inverted slider-crank mechanisms are shown in Figure 6.26. The instant center of rotation for two links that slide on each other is at infinity,*
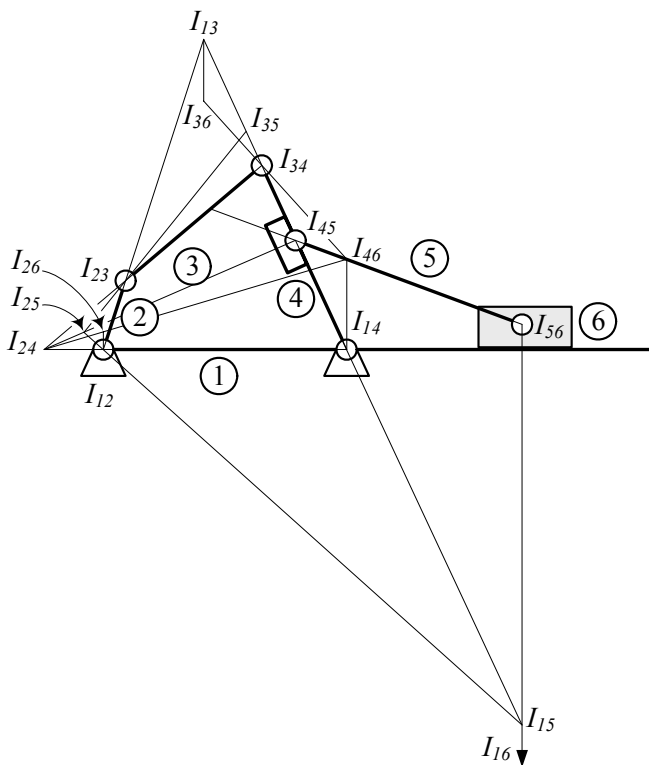
FIGURE 6.27. Fifteen instant center of rotations for a 6-link mechanism.

on a line normal to the common tangent. So, $I_{14}$ in Figure 6.26(b) is on a line perpendicular to the ground, and $I_{34}$ in Figure 6.26(c) is on perpendicular to the link 3.

Figure 6.27 depicts the 15 instant centers for a six-link mechanism.

**Example 244** *Application of instant center of rotation in vehicles.*

Figure 6.28 illustrates a double A-arm suspension and its equivalent kinematic model. The wheel will be fastened to the coupler link AB, witch connects the upper A-arm BN to the lower A-arm AN. The A-arms are connected to the body with two revolute joints at N and M. The body of the vehicle acts as the ground link for the suspension mechanism, which is a four-bar linkage.

Points N and M are, respectively, the instant centers of rotation for the upper and lower arms with respect to the body. The intersection point of the extension line for the upper and lower A-arms indicates the instant center of rotation for the coupler with respect to the body. When the suspension moves, the wheel will rotate about point I with respect to the body. Point I is called the **roll center** of the wheel and body.
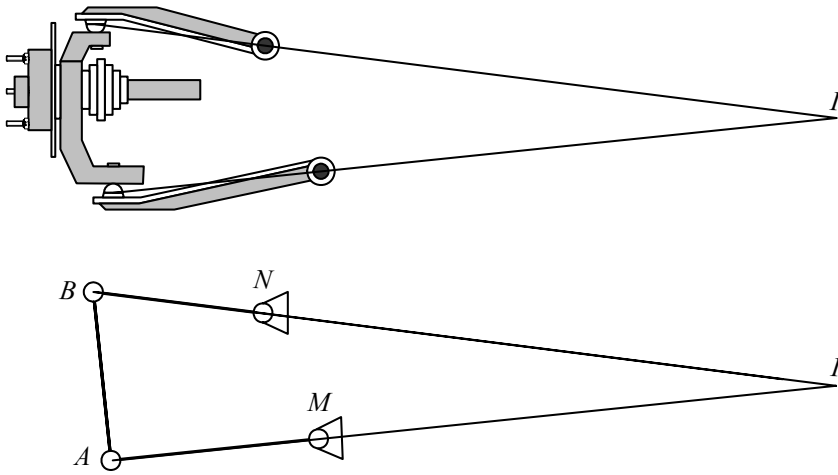
FIGURE 6.28. The roll center of a double A-arm suspension and its equivalent kinematic model.

**Example 245** *The instant centers of rotation may not be stationary.*

When a mechanism moves, the instant centers of rotation may move, if they are not at a fixed joint with the ground. Figure 6.29 illustrates a four-bar linkage at a few different positions and shows the instant centers of rotation for the coupler with respect to the ground $I_{13}$. Point $I_{13}$ will move when the linkage moves, and traces a path shown in the figure.

**Example 246** *Sliding a slender on the wall.*

Figure 6.30 illustrates a slender bar $AB$ sliding at points $A$ and $C$. We have the velocity axis of two points $A$ and $C$, and therefore, we can find the instant center of rotation $I$.

The coordinates of point $I$ are a function of the parameter $\theta$ as follows:

$$x_I = h \cot \theta \qquad (6.219)$$
$$y_I = h + x_I \cot \theta$$
$$= h \left(1 + \cot^2 \theta\right). \qquad (6.220)$$

Eliminating $\theta$ between $x$ and $y$, generates the path of motion for $I$.

$$y_I = h \left(1 + \frac{x_I^2}{h^2}\right) \qquad (6.221)$$

**Example 247 ★** *Plane motion of a rigid body.*

The plane motion of a rigid body is such that all points of the body move only in parallel planes. So, to study the motion of the body, it is enough to examine the motion of points in just one plane.
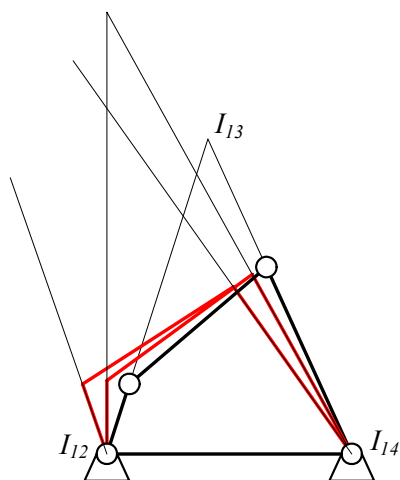
FIGURE 6.29. Path of motion for the instant center of rotation $I_{13}$.
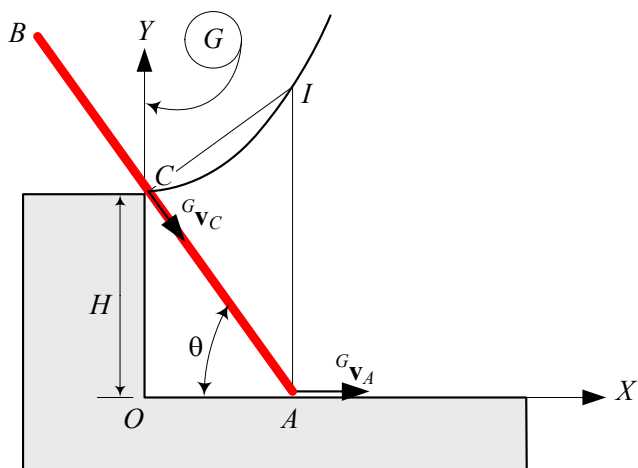


FIGURE 6.30. A slender bar $AB$ sliding at points $A$ and $C$.
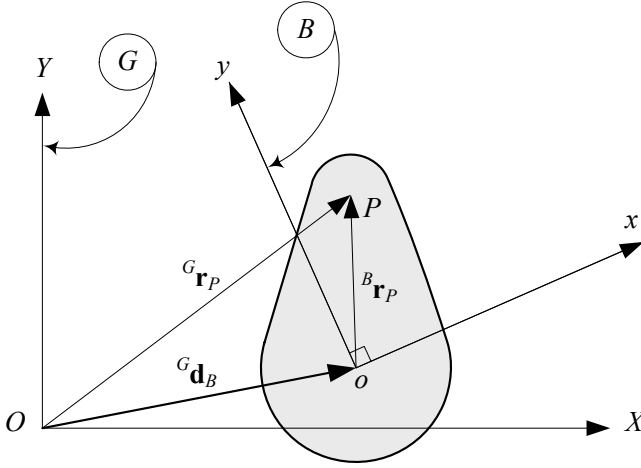
FIGURE 6.31. A rigid body in a planar motion.

*Figure 6.31 illustrates a rigid body in a planar motion and the correspond-ing coordinate frames. The position, velocity, and acceleration of body point P are:*

$$
\begin{aligned}
{}^{G}\mathbf{r}_P &= {}^{G}\mathbf{d}_B + {}^{G}R_B\,{}^{B}\mathbf{r}_P \\
&= {}^{G}\mathbf{d}_B + {}^{G}_{B}\mathbf{r}_P
\end{aligned}
\tag{6.222}
$$

$$
\begin{aligned}
{}^{G}\mathbf{v}_P &= {}^{G}\dot{\mathbf{d}}_B + {}_{G}\boldsymbol{\omega}_B \times \left({}^{G}\mathbf{r}_P - {}^{G}\mathbf{d}_B\right) \\
&= {}^{G}\dot{\mathbf{d}}_B + {}_{G}\boldsymbol{\omega}_B \times {}^{G}_{B}\mathbf{r}_P
\end{aligned}
\tag{6.223}
$$

*where, ${}^{G}\mathbf{d}_B$ indicates the position of the moving origin o relative to the fixed origin O. The term ${}^{G}\dot{\mathbf{d}}_B$ is the velocity of point o and, ${}_{G}\boldsymbol{\omega}_B \times {}^{G}_{B}\mathbf{r}_P$ is the velocity of point P relative to o.*

$$
{}^{G}\mathbf{v}_{P/o} = {}_{G}\boldsymbol{\omega}_B \times {}^{G}_{B}\mathbf{r}_P
\tag{6.224}
$$

*Although it is not a correct view, it might sometimes help if we interpret ${}^{G}\dot{\mathbf{d}}_B$ as the translational velocity and ${}_{G}\boldsymbol{\omega}_B \times {}^{G}_{B}\mathbf{r}_P$ as the rotational velocity components of ${}^{G}\mathbf{v}_P$. Then, the velocity of any point P of a rigid body is a superposition of the velocity ${}^{G}\dot{\mathbf{d}}_B$ of another arbitrary point o and the angular velocity ${}_{G}\boldsymbol{\omega}_B \times {}^{G}_{B}\mathbf{r}_P$ of the points P around o.*

*The relative velocity vector ${}^{G}\mathbf{v}_{P/o}$ is perpendicular to the relative position vector ${}^{G}_{B}\mathbf{r}_P$. Employing the same concept we can say that the velocity of points P and o with respect to another point Q are perpendicular to ${}^{G}_{B}\mathbf{r}_{P/Q}$ and ${}^{G}_{B}\mathbf{r}_{o/Q}$ respectively. We may search for a point Q, as the instantaneous center of rotation, at which the velocity is zero. Points o, P, and Q are shown in Figure 6.32.*
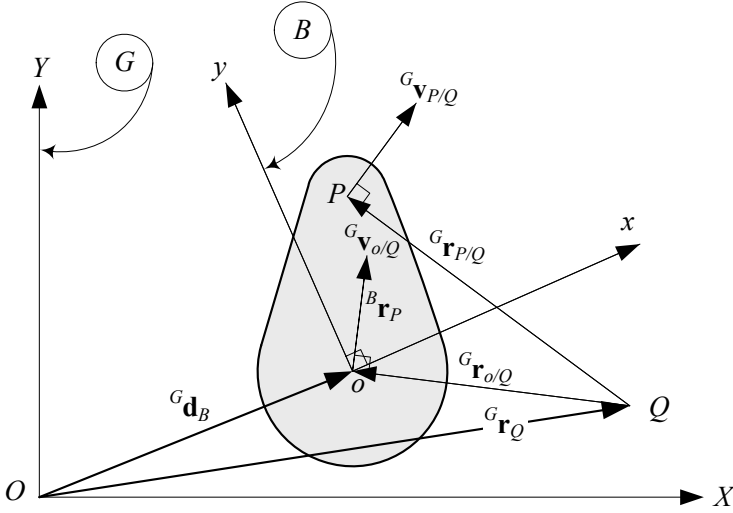
FIGURE 6.32. Instant center of rotation $Q$, for planar motion of a rigid body.

*Assuming a position vector ${}^G\mathbf{r}_{o/Q}$ for the instant center point $Q$, let's define*

$$
{}^G\mathbf{r}_{o/Q} = a_Q \, {}^G\dot{\mathbf{d}}_B + b_Q \, {}_G\boldsymbol{\omega}_B \times {}^G\dot{\mathbf{d}}_B \tag{6.225}
$$

*then, following (6.223), the velocity of point $Q$ can be expressed by*

$$
\begin{aligned}
{}^G\mathbf{v}_Q &= {}^G\dot{\mathbf{d}}_B + {}_G\boldsymbol{\omega}_B \times {}^G\mathbf{r}_{Q/o} \\
&= {}^G\dot{\mathbf{d}}_B - {}_G\boldsymbol{\omega}_B \times {}^G\mathbf{r}_{o/Q} \\
&= {}^G\dot{\mathbf{d}}_B - {}_G\boldsymbol{\omega}_B \times \left( a_Q \, {}^G\dot{\mathbf{d}}_B + b_Q \, {}_G\boldsymbol{\omega}_B \times {}^G\dot{\mathbf{d}}_B \right) \\
&= {}^G\dot{\mathbf{d}}_B - a_Q \, {}_G\boldsymbol{\omega}_B \times {}^G\dot{\mathbf{d}}_B - b_Q \, {}_G\boldsymbol{\omega}_B \times \left( {}_G\boldsymbol{\omega}_B \times {}^G\dot{\mathbf{d}}_B \right) \\
&= 0.
\end{aligned} \tag{6.226}
$$
$$\tag{6.227}$$

*Now, using the following equations*

$$
\begin{aligned}
{}_G\boldsymbol{\omega}_B &= \omega \hat{K} \tag{6.228} \\
{}_G\boldsymbol{\omega}_B \times \left( {}_G\boldsymbol{\omega}_B \times {}^G\dot{\mathbf{d}}_B \right) &= \left( {}_G\boldsymbol{\omega}_B \cdot {}^G\dot{\mathbf{d}}_B \right) {}_G\boldsymbol{\omega}_B - \omega^2 \, {}^G\dot{\mathbf{d}}_B \tag{6.229} \\
{}_G\boldsymbol{\omega}_B \cdot {}^G\dot{\mathbf{d}}_B &= 0 \tag{6.230}
\end{aligned}
$$

*we find*

$$
\left( 1 + b_Q \, \omega^2 \right) {}^G\dot{\mathbf{d}}_B - a_Q \, {}_G\boldsymbol{\omega}_B \times {}^G\dot{\mathbf{d}}_B = 0. \tag{6.231}
$$

*Because ${}^G\dot{\mathbf{d}}_B$ and ${}_G\boldsymbol{\omega}_B \times {}^G\dot{\mathbf{d}}_B$ must be perpendicular, Equation (6.231)*

*provides*

$$1 + b_Q\,\omega^2 = 0 \tag{6.232}$$

$$a_Q = 0 \tag{6.233}$$

*and therefore,*

$${}^G\mathbf{r}_{Q/o} = \frac{1}{\omega^2}\left({}_G\boldsymbol{\omega}_B \times {}^G\dot{\mathbf{d}}_B\right). \tag{6.234}$$

**Example 248 ★** *Instantaneous center of acceleration.*

   *For planar motions of rigid bodies, it is possible to find a body point with zero acceleration. Such a point may be called the instantaneous center of acceleration. When a rigid body is in a planar motion, we can be express the acceleration of a body point $P$, such as shown in Figure 6.32, as*

$$
\begin{aligned}
{}^G\mathbf{a}_P &= {}^G\ddot{\mathbf{d}}_B + {}_G\boldsymbol{\alpha}_B \times \left({}^G\mathbf{r}_P - {}^G\mathbf{d}_B\right) \\
&\quad + {}_G\boldsymbol{\omega}_B \times \left({}_G\boldsymbol{\omega}_B \times \left({}^G\mathbf{r}_P - {}^G\mathbf{d}_B\right)\right) \\
&= {}^G\ddot{\mathbf{d}}_B + {}_G\boldsymbol{\alpha}_B \times {}^G_B\mathbf{r}_P + {}_G\boldsymbol{\omega}_B \times \left({}_G\boldsymbol{\omega}_B \times {}^G_B\mathbf{r}_P\right). \tag{6.235}
\end{aligned}
$$

*The term ${}_G\boldsymbol{\omega}_B \times \left({}_G\boldsymbol{\omega}_B \times {}^G_B\mathbf{r}_P\right)$ is the centripetal acceleration, and the term ${}_G\boldsymbol{\alpha}_B \times {}^G_B\mathbf{r}_P$ is the tangential acceleration and is perpendicular to ${}^G_B\mathbf{r}_P$. Because the motion is planar, the angular velocity vector is always in parallel to $\hat{k}$ and $\hat{K}$ unit vectors.*

$${}_G\boldsymbol{\omega}_B = \omega\hat{K} \tag{6.236}$$

$${}_G\boldsymbol{\alpha}_B = \alpha\hat{K} \tag{6.237}$$

*Therefore, the velocity ${}^G\mathbf{v}_P$ and acceleration ${}^G\mathbf{a}_P$ can be simplified to*

$${}^G\mathbf{a}_P = {}^G\ddot{\mathbf{d}}_B + {}_G\boldsymbol{\alpha}_B \times {}^G_B\mathbf{r}_P - \omega^2\, {}^G_B\mathbf{r}_P. \tag{6.238}$$

*We now look for a zero acceleration point $S$ and express its position vector by*

$${}^G\mathbf{r}_{S/o} = a_S\, {}^G\ddot{\mathbf{d}}_B + b_S\, {}_G\boldsymbol{\alpha}_B \times {}^G\ddot{\mathbf{d}}_B \tag{6.239}$$

*and based on (6.238) we have,*

$$
\begin{aligned}
{}^G\mathbf{a}_S &= {}^G\ddot{\mathbf{d}}_B + {}_G\boldsymbol{\alpha}_B \times {}^G_B\mathbf{r}_S - \omega^2\, {}^G_B\mathbf{r}_S \\
&= {}^G\ddot{\mathbf{d}}_B + {}_G\boldsymbol{\alpha}_B \times {}^G\mathbf{r}_{S/o} - \omega^2\, {}^G\mathbf{r}_{S/o} \\
&= {}^G\ddot{\mathbf{d}}_B + {}_G\boldsymbol{\alpha}_B \times \left(a_S\, {}^G\ddot{\mathbf{d}}_B + b_S\, {}_G\boldsymbol{\alpha}_B \times {}^G\ddot{\mathbf{d}}_B\right) \\
&\quad - \omega^2\left(a_S\, {}^G\ddot{\mathbf{d}}_B + b_S\, {}_G\boldsymbol{\alpha}_B \times {}^G\ddot{\mathbf{d}}_B\right) \\
&= {}^G\ddot{\mathbf{d}}_B + a_S\, {}_G\boldsymbol{\alpha}_B \times {}^G\ddot{\mathbf{d}}_B + b_S\, {}_G\boldsymbol{\alpha}_B \times \left({}_G\boldsymbol{\alpha}_B \times {}^G\ddot{\mathbf{d}}_B\right) \\
&\quad - a_S\,\omega^2\, {}^G\ddot{\mathbf{d}}_B - b_S\,\omega^2\, {}_G\boldsymbol{\alpha}_B \times {}^G\ddot{\mathbf{d}}_B \\
&= 0. \tag{6.240}
\end{aligned}
$$

*Simplifying results in*

$$\left(1 - a_S\,\omega^2 - b_S\,\alpha^2\right)\,{}^G\ddot{\mathbf{d}}_B + \left(a_S - b_S\,\omega^2\right)\,{}_G\boldsymbol{\alpha}_B \times {}^G\ddot{\mathbf{d}}_B = 0 \qquad (6.241)$$

*and because* ${}^G\ddot{\mathbf{d}}_B$ *and* ${}_G\boldsymbol{\alpha}_B \times {}^G\ddot{\mathbf{d}}_B$ *are perpendicular, we must have*

$$1 - a_S\,\omega^2 - b_S\,\alpha^2 \;=\; 0 \qquad (6.242)$$
$$a_S - b_S\,\omega^2 \;=\; 0 \qquad (6.243)$$

*and hence,*

$$a_S \;=\; \frac{\omega^2}{\omega^2 + \alpha^2} \qquad (6.244)$$

$$b_S \;=\; \frac{1}{\omega^2 + \alpha^2}. \qquad (6.245)$$

*The position vector of the instant center of acceleration is then equal to*

$$ {}^G\mathbf{r}_{S/o} = \frac{1}{\omega^2 + \alpha^2}\left(\omega^2\,{}^G\ddot{\mathbf{d}}_B + {}_G\boldsymbol{\alpha}_B \times {}^G\ddot{\mathbf{d}}_B\right) \qquad (6.246)$$

## 6.5   Coupler Point Curve

The most common independent suspension systems are double $A$-arm and inverted slider-crank mechanisms. The wheel of the vehicle will be attached to a point of the coupler link of the mechanism, which is attached to the body of the vehicle.

### 6.5.1   Coupler Point Curve for Four-Bar Linkages

Figure 6.33 illustrates a four-bar linkage $MNAB$ and a coupler point at $C$. When the mechanism moves, the coupler point $C$ will move on a path.

The path of the coupler point is called the *coupler point curve*. Considering $\theta_2$ as the input of the mechanism, the parametric coordinates of the coupler point curve $(x_C, y_C)$ are

$$x_C \;=\; a\cos\theta_2 + e\cos\left(\beta - \gamma + \alpha\right) \qquad (6.247)$$
$$y_C \;=\; a\sin\theta_2 + e\sin\left(\beta - \gamma + \alpha\right) \qquad (6.248)$$

where,

$$\gamma \;=\; \tan^{-1}\frac{a\sin\theta_2}{d - a\cos\theta_2} \qquad (6.249)$$

$$\beta \;=\; \tan^{-1}\frac{\sqrt{4b^2 f^2 - \left(b^2 + f^2 - c^2\right)^2}}{b^2 + f^2 - c^2} \qquad (6.250)$$

$$f \;=\; \sqrt{a^2 + d^2 - 2ad\cos\theta_2}. \qquad (6.251)$$
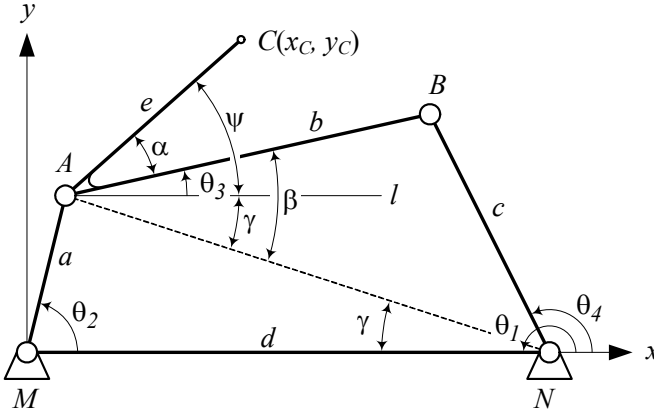
FIGURE 6.33. A four-bar linkage $MNAB$ and a coupler point at $C$.

**Proof.** The position of the coupler point $C$ in Figure 6.33 is defined by the polar coordinates length $e$ and angle $\alpha$ in a coordinate frame attached to the coupler link, and by $(x_C, y_C)$ in the Cartesian coordinate frame attached to the ground. The length of the links are indicated by $MA = a$, $AB = b$, $NB = c$, and $MN = d$. We show the angle $\angle ANM$ by $\gamma$ and $\angle BAN$ by $\beta$. Let's draw a line $l$ through $A$ and parallel to the ground link $MN$, then,

$$\angle NAl \quad = \quad \angle ANM = \gamma \qquad\qquad (6.252)$$

$$\angle CAl \quad = \quad \psi \qquad\qquad (6.253)$$

$$\psi \quad = \quad \beta - \gamma + \alpha. \qquad\qquad (6.254)$$

The global coordinates of point $C$ are

$$x_C \quad = \quad a \cos \theta_2 + e \cos \psi \qquad\qquad (6.255)$$

$$y_C \quad = \quad a \sin \theta_2 + e \sin \psi \qquad\qquad (6.256)$$

where, $\psi$ comes from Equation (6.254). The angle $\beta$ can be calculated from the cosine law in $\triangle BAN$,

$$\cos \beta = \frac{b^2 + f^2 - c^2}{2bf} \qquad\qquad (6.257)$$

where, $f = AN$. Applying the cosine law in $\triangle AMN$ shows that $f$ is equal to

$$f = \sqrt{a^2 + d^2 - 2ad \cos \theta_2} \qquad\qquad (6.258)$$

given by Equation (6.251).
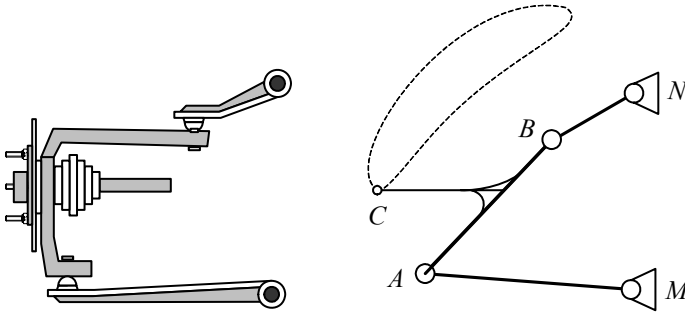
FIGURE 6.34. A double A arm suspension mechanism and its equivalent four-bar linkage kinematic model.

For computer calculation ease, it is better to find $\beta$ from the trigonometric equation

$$\tan^2 \beta = \sec^2 \beta - 1 \tag{6.259}$$

after we substitute $\sec \beta$ from Equation (6.257).

$$\beta = \tan^{-1} \frac{\sqrt{4b^2 f^2 - (b^2 + f^2 - c^2)^2}}{b^2 + f^2 - c^2} \tag{6.260}$$

The angle $\gamma$ can be found from a tan equation based on the vertical distance of point $A$ from the ground link $MN$.

$$\gamma = \tan^{-1} \frac{a \sin \theta_2}{d - a \cos \theta_2} \tag{6.261}$$

Therefore, the coordinates $x_C$ and $y_C$ can be calculated as two parametric functions of $\theta_2$ for a given set of $a$, $b$, $c$, $d$, $e$, and $\alpha$. ∎

**Example 249** *A poorly designed double A arm suspension mechanism.*

*Figure 6.34 illustrates a double A arm suspension mechanism and its equivalent four-bar linkage kinematic model. Points $M$ and $N$ are fixed joints on the body, and points $A$ and $B$ are moving joints attached to the wheel supporting coupler link. Point $C$ is on the spindle and supposed to be the wheel center. When the wheel moves up and down, the wheel center moves on a the couple point curve shown in the figure. The wheel's center of proper suspension mechanism is supposed to move vertically, however, the wheel center of the suspension moves on a high curvature path and generates an undesired camber.*

*A small motion of the kinematic model of suspension is shown in Figure 6.35, and the actual suspension and wheel configurations are shown in Figure 6.36.*
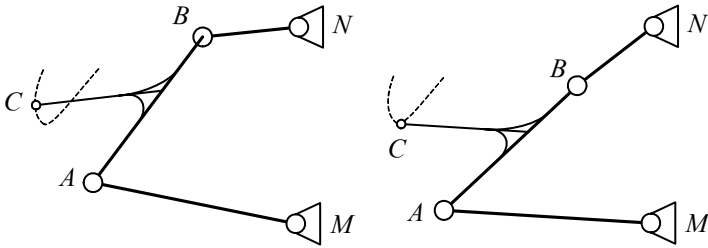
FIGURE 6.35. A small motion of the kinematic model.
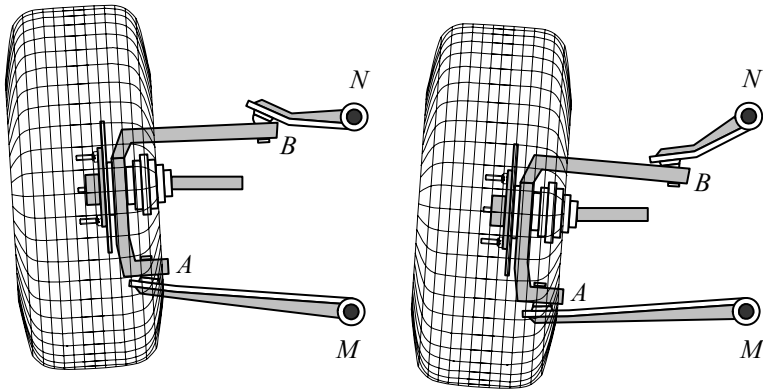


FIGURE 6.36. A small motion of the actual suspension and wheel configurations.
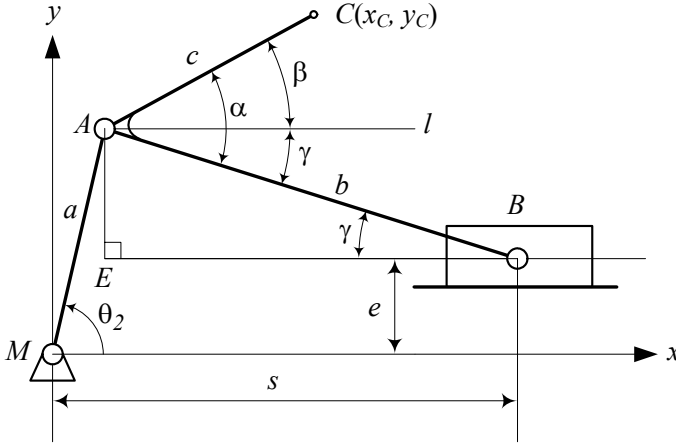
FIGURE 6.37. A slider-crank mechanism and a coupler point at $C$.

### 6.5.2  Coupler Point Curve for a Slider-Crank Mechanism

Figure 6.37 illustrates a slider-crank mechanism and a coupler point at $C$. When the mechanism moves, coupler point $C$ will move on a coupler point curve with the following parametric equation:

$$
\begin{aligned}
x_C &= a\cos\theta_2 + c\cos(\alpha - \gamma) & (6.262)\\
y_C &= a\sin\theta_2 + c\sin(\alpha - \gamma) & (6.263)
\end{aligned}
$$

The angle $\theta_2$ is the input angle and acts as a parameter, and angle $\gamma$ can be calculated from the following equation.

$$
\gamma = \sin^{-1}\frac{a\sin\theta_2 - e}{b} \qquad (6.264)
$$

**Proof.** We attach a planar Cartesian coordinate frame to the ground link at $M$. The $x$-axis is parallel to the ground indicated by the sliding surface, as shown in Figure 6.37. Drawing a line $l$ through $A$ and parallel to the ground shows that

$$
\beta = \alpha - \gamma \qquad (6.265)
$$

where $\gamma$ is the angle between the coupler link and the ground.

The coordinates $(x_C, y_C)$ for point $C$ are

$$
\begin{aligned}
x_C &= a\cos\theta_2 + c\cos\beta & (6.266)\\
y_C &= a\sin\theta_2 + c\sin\beta. & (6.267)
\end{aligned}
$$
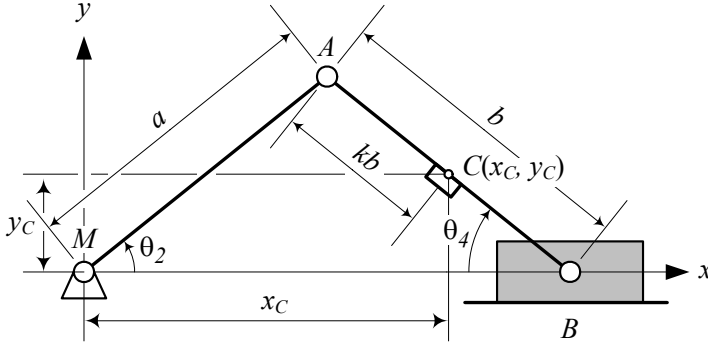
FIGURE 6.38. A centric and symmetric slider-crank mechanism.

To calculate the angle $\gamma$, we examine $\triangle AEB$ and find

$$
\begin{aligned}
\sin \gamma &= \frac{AE}{AB} \\
&= \frac{a \sin \theta_2 - e}{b}
\end{aligned}
\tag{6.268}
$$

that finishes Equation (6.264).

Therefore, the coordinates $x_C$ and $y_C$ can be calculated as two parametric functions of $\theta_2$ for a given set of $a$, $b$, $c$, $e$, and $\alpha$. ∎

**Example 250** *A centric and symmetric slider-crank mechanism.*

*Point $C\left(x_C, y_C\right)$ is the coupler point of a centric and symmetric slider-crank mechanism shown in Figure 6.38. It is centric because $e = 0$, and is symmetric because $a = b$, and therefore, $\theta_2 = \theta_4$. Point $C$ is on the coupler link $AB$ and is at a distance $kb$ from $A$, where $0 < k < 1$.*

*The coordinates of point $C$ are*

$$
\begin{aligned}
x_C &= a \cos \theta_2 + ka \cos \theta_2 \\
&= a\left(1 + k\right) \cos \theta_2
\end{aligned}
\tag{6.269}
$$

$$
\begin{aligned}
y_C &= a \sin \theta_2 - ka \sin \theta_2 \\
&= a\left(1 - k\right) \sin \theta_2
\end{aligned}
\tag{6.270}
$$

*and therefore,*

$$
\cos \theta_2 = \frac{x_C}{a\left(1 + k\right)}
\tag{6.271}
$$

$$
\sin \theta_2 = \frac{y_C}{a\left(1 - k\right)}.
\tag{6.272}
$$

*Using $\cos^2 \theta_2 + \sin^2 \theta_2 = 1$, we can show that the coupler point $C$ will*
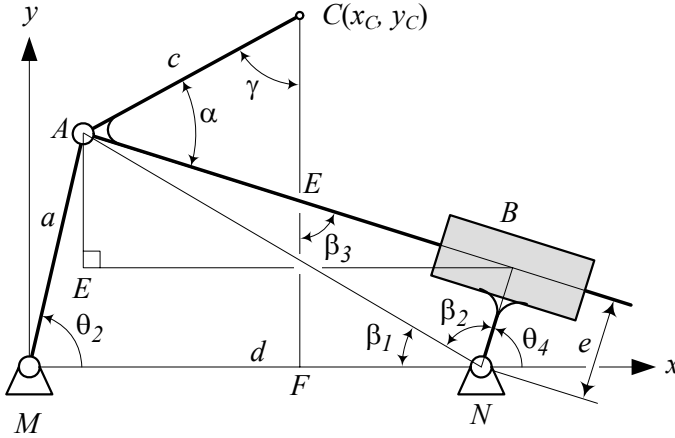
FIGURE 6.39. An inverted slider-crank mechanism and a coupler point at $C$.

*move on an ellipse.*

$$\frac{x_C^2}{a^2\left(1+k\right)^2} + \frac{y_C^2}{a^2\left(1-k\right)^2} = 1 \tag{6.273}$$

## 6.5.3 Coupler Point Curve for Inverted Slider-Crank Mechanism

Figure 6.39 illustrates an inverted slider-crank mechanism and a coupler point at $C$. When the mechanism moves, the coupler point $C$ will move on a coupler point curve with the following parametric equation:

$$x_C = a\cos\theta_2 + c\cos\left(\pi - \alpha - \theta_4\right) \tag{6.274}$$
$$y_C = a\sin\theta_2 + c\sin\left(\pi - \alpha - \theta_4\right) \tag{6.275}$$

The angle $\theta_2$ is the input angle and acts as a parameter, and $\theta_4$ is the angle of the output link, given by Equation (6.173).

$$\theta_4 = 2\tan^{-1}\left(\frac{-H \pm \sqrt{H^2 - 4GI}}{2G}\right) \tag{6.276}$$

$$G = d - e - a\cos\theta_2 \tag{6.277}$$
$$H = 2a\sin\theta_2 \tag{6.278}$$
$$I = a\cos\theta_2 - d - e. \tag{6.279}$$

**Proof.** We attach a planar Cartesian coordinate frame to the ground link at $MN$. Drawing a vertical line through $C$ defines the variable angle $\gamma = \angle ACF$ as shown in Figure 6.39. We also define three angles $\beta_1 = \angle ANM$,

$\beta_2 = \angle ANB$, and $\beta_3 = \angle BEF$, to simplify the calculations. From $\triangle ACE$, we find

$$\gamma = \pi - \beta_3 - \alpha \tag{6.280}$$

and from quadrilateral $\square EFNB$, we find

$$\beta_3 + \angle EFN + \beta_2 + \beta_1 + \angle EBN = 2\pi. \tag{6.281}$$

However,

$$\angle EBN = \frac{\pi}{2} \tag{6.282}$$

$$\angle EFN = \frac{\pi}{2} \tag{6.283}$$

and therefore,

$$\beta_3 + \beta_2 + \beta_1 = \pi. \tag{6.284}$$

The output angle $\theta_4$ is equal to

$$\theta_4 = \pi - (\beta_2 + \beta_1), \tag{6.285}$$

and thus,

$$\theta_4 = \beta_3. \tag{6.286}$$

Now the angle $\gamma$ may be written as

$$\gamma = \pi - \theta_4 - \alpha \tag{6.287}$$

where $\theta_4$ is the output angle, found in Equation (6.173).

Therefore, the coordinates $x_C$ and $y_C$ can be calculated as two parametric functions of $\theta_2$ for a given set of $a$, $d$, $c$, $e$, and $\alpha$. ∎

## 6.6  ★ Universal Joint Dynamics

The *universal joint* shown in Figure 6.40 is a mechanism used to connect rotating shafts that intersect in an angle $\varphi$. The universal joint is also known as *Hook's coupling, Hook joint, Cardan joint,* or *yoke joint.*

Figure 6.41 illustrates a universal joint. There are four links in a universal joint: link number 1 is the ground, which has a revolute joint with the input link 2 and the output link 4. The input and the output links are connected with a cross-link 3. The universal joint is a three-dimensional four-bar linkage for which the cross-link acts as a coupler link.

The driver and driven shafts make a complete revolution at the same time, but the velocity ratio is not constant throughout the revolution. The angular velocity of the output shaft 4 relative to the input shaft 2 is called
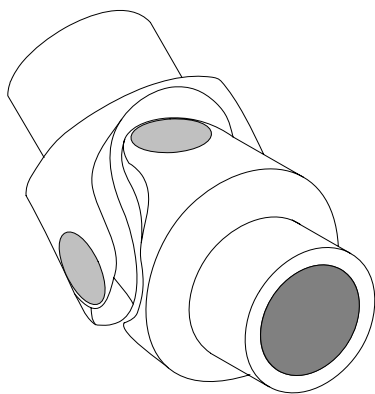
FIGURE 6.40. A universal joint.
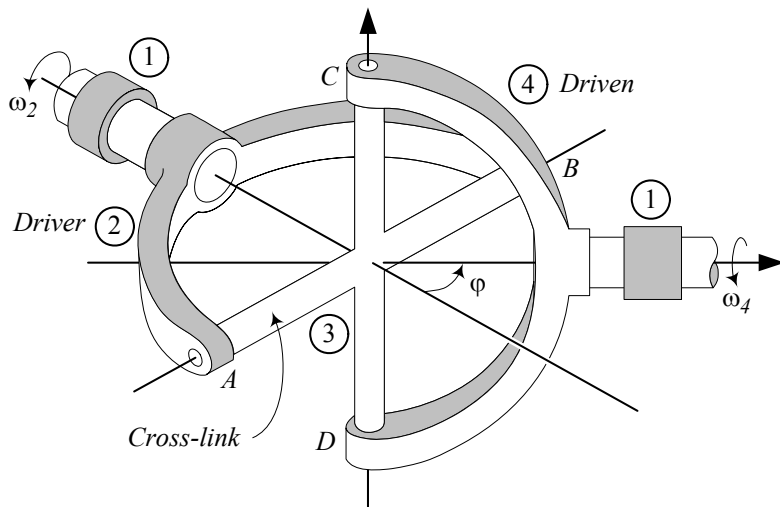


FIGURE 6.41. A universal joint with four links: link 1 is the ground, link 2 is the input, link 4 is the output, and the cross-link 3 is a coupler link.
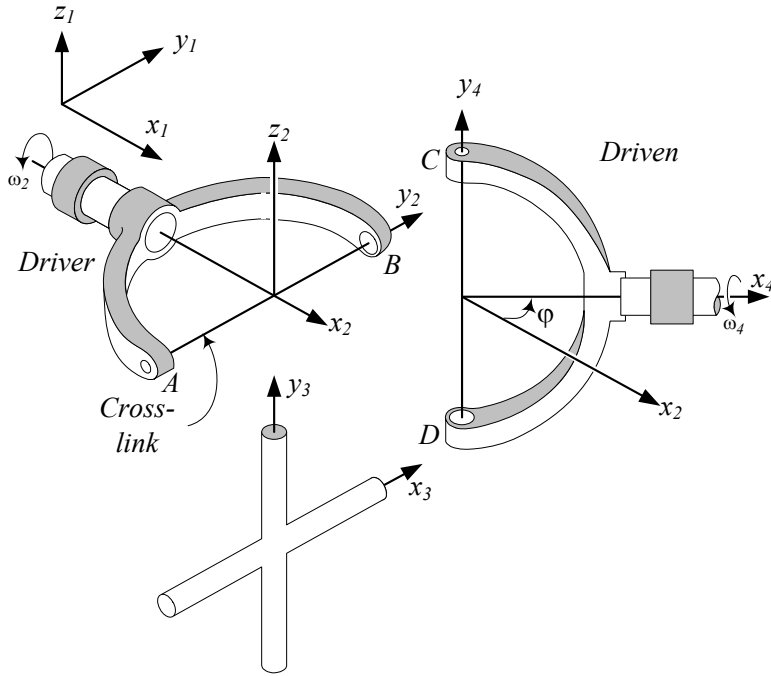
FIGURE 6.42. A separate illustration of the input, output, and the cross links for a universal joint.

*speed ratio* $\Omega$ and is a function of the angular position of the input shaft $\theta$, and the angle between the shafts $\varphi$.

$$\Omega = \frac{\omega_4}{\omega_2} = \frac{\cos\varphi}{1 - \sin^2\varphi\cos^2\theta} \tag{6.288}$$

**Proof.** A universal joint may appear in many shapes, however, regardless of how it is constructed, it has essentially the form shown in Figure 6.41. Each connecting shaft ends in a $U$-shaped yoke. The yokes are connected by a rigid cross-link. The ends of the cross-link are set in bearings in the yokes. When the driver yoke turns, the cross-link rotates relative to the yoke about its axis $AB$. Similarly, the cross-link rotates about the axis $CD$ and relative to the driven yoke.

Although the driver and driven shafts make a complete revolution at the same time, the velocity ratio is not constant throughout the revolution. A separate illustration of the input, output, and the cross links are shown in Figure 6.42.

The angular velocity of the cross-link may be shown by

$$\begin{aligned} {}_1\boldsymbol{\omega}_3 &= {}_1\boldsymbol{\omega}_2 + \tfrac{1}{2}\boldsymbol{\omega}_3 \\ &= {}_1\boldsymbol{\omega}_4 + \tfrac{1}{4}\boldsymbol{\omega}_3 \end{aligned} \tag{6.289}$$
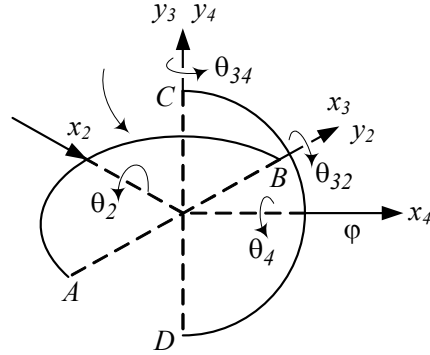
FIGURE 6.43. A kinematic model for a universal joint.

where, $_1\boldsymbol{\omega}_2$ is the angular velocity of the driver yoke about the $x_2$-axis and $_2^1\boldsymbol{\omega}_3$ is the angular velocity of the cross-link about the axis $AB$ relative to the drive yoke expressed in the ground coordinate frame.

Figure 6.43 shows that the unit vectors $\hat{\jmath}_2$ and $\hat{\jmath}_3$ are along the arms of the cross link, and the unit vectors $\hat{\imath}_2$ and $\hat{\imath}_4$ are along the shafts. Having the angular velocity vectors,

$$_1\boldsymbol{\omega}_2 = \begin{bmatrix} \omega_{21}\,\hat{\imath}_1 \\ \hat{\jmath}_1 \\ \hat{k}_1 \end{bmatrix} = \begin{bmatrix} \omega_{21} \\ 0 \\ 0 \end{bmatrix} \tag{6.290}$$

$$_1\boldsymbol{\omega}_4 = \begin{bmatrix} \omega_{41}\,\hat{\imath}_4 \\ \hat{\jmath}_4 \\ \hat{k}_4 \end{bmatrix} = \begin{bmatrix} \omega_{41} \\ 0 \\ 0 \end{bmatrix} \tag{6.291}$$

$$_2\boldsymbol{\omega}_3 = \begin{bmatrix} \hat{\imath}_2 \\ \omega_{32}\,\hat{\jmath}_2 \\ \hat{k}_2 \end{bmatrix} \tag{6.292}$$

$$_2^3\boldsymbol{\omega}_3 = \begin{bmatrix} \omega_{32}\,\hat{\imath}_3 \\ \hat{\jmath}_3 \\ \hat{k}_3 \end{bmatrix} \tag{6.293}$$

$$_4\boldsymbol{\omega}_3 = \begin{bmatrix} \hat{\imath}_4 \\ \omega_{34}\,\hat{\jmath}_4 \\ \hat{k}_4 \end{bmatrix} \tag{6.294}$$

$$_4^3\boldsymbol{\omega}_3 = \begin{bmatrix} \hat{\imath}_3 \\ \omega_{34}\,\hat{\jmath}_3 \\ \hat{k}_3 \end{bmatrix} \tag{6.295}$$

we can simplify Equation (6.289) to

$$\omega_{32}\,\hat{\imath}_3 + \omega_{21}\,\hat{\imath}_2 = \omega_{41}\,\hat{\imath}_4 + \omega_{34}\,\hat{\jmath}_3. \tag{6.296}$$

However, because the cross-link coordinate frame is right-handed, we have

$$\hat{\imath}_3 \times \hat{\jmath}_3 = \hat{k}_3 \tag{6.297}$$

and therefore,

$$(\omega_{32}\,\hat{\imath}_3 + \omega_{21}\,\hat{\imath}_2) \cdot \hat{k}_3 = (\omega_{41}\,\hat{\imath}_4 + \omega_{34}\,\hat{\jmath}_3) \cdot \hat{k}_3 \tag{6.298}$$

that results in the following equation:

$$\omega_{21}\,\hat{\imath}_2 \cdot \hat{k}_3 = \omega_{41}\,\hat{\imath}_4 \cdot \hat{k}_3 \tag{6.299}$$

Now the required equation for the speed ratio $\Omega = \omega_{41}/\omega_{21}$ is

$$
\begin{aligned}
\Omega &= \frac{\omega_{41}}{\omega_{21}} \\
&= \frac{\hat{\imath}_3 \times \hat{\jmath}_3 \cdot \hat{\imath}_2}{\hat{\imath}_3 \times \hat{\jmath}_3 \cdot \hat{\imath}_4}.
\end{aligned} \tag{6.300}
$$

The unit vector $\hat{\jmath}_3$ is perpendicular to $\hat{\imath}_3$ and $\hat{\imath}_4$, we may write

$$\hat{\jmath}_3 = a\hat{\imath}_4 \times \hat{\imath}_3 \tag{6.301}$$

where $a$ is a coefficient. Now

$$
\begin{aligned}
\hat{\imath}_3 \times \hat{\jmath}_3 &= \hat{\imath}_3 \times (a\hat{\imath}_4 \times \hat{\imath}_3) \\
&= a\left[\hat{\imath}_4 - (\hat{\imath}_3 \cdot \hat{\imath}_4)\,\hat{\imath}_3\right]
\end{aligned} \tag{6.302}
$$

and because

$$\hat{\imath}_3 \cdot \hat{\imath}_2 = 0 \tag{6.303}$$

we find

$$
\begin{aligned}
\Omega &= \frac{\omega_{41}}{\omega_{21}} \\
&= \frac{\hat{\imath}_2 \cdot a\left[\hat{\imath}_4 - (\hat{\imath}_3 \cdot \hat{\imath}_4)\,\hat{\imath}_3\right]}{\hat{\imath}_3 \cdot a\left[\hat{\imath}_4 - (\hat{\imath}_3 \cdot \hat{\imath}_4)\,\hat{\imath}_3\right]} \\
&= \frac{\hat{\imath}_2 \cdot \hat{\imath}_4}{1 - (\hat{\imath}_3 \cdot \hat{\imath}_4)^2} \\
&= \frac{\cos\varphi}{1 - (\hat{\imath}_3 \cdot \hat{\imath}_4)^2}.
\end{aligned} \tag{6.304}
$$

If we show the angular position of the input yoke by $\theta$, then

$$
\begin{aligned}
\hat{\imath}_3 &= \cos\theta\,\hat{\jmath}_1 + \sin\theta\,\hat{k}_1 \tag{6.305} \\
\hat{\imath}_4 &= \cos\varphi\,\hat{\imath}_1 - \sin\varphi\,\hat{\jmath}_1 \tag{6.306}
\end{aligned}
$$
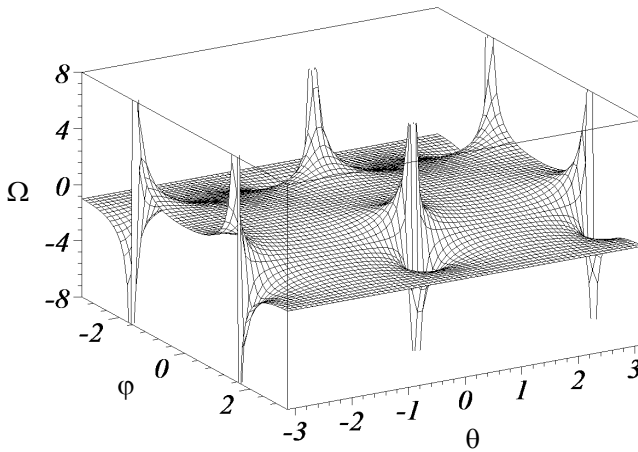
FIGURE 6.44. A three-dimensional plot for the speed ratio of a universal joint, $\Omega$ as a function of the input angle $\theta$ and the angle between input and output shafts $\varphi$.

and the final equation for the speed ratio is found as

$$
\begin{aligned}
\Omega &= \frac{\omega_{41}}{\omega_{21}} \\
&= \frac{\cos \varphi}{1 - \sin^2 \varphi \cos^2 \theta}.
\end{aligned}
\tag{6.307}
$$

This formula shows that although both shafts complete one revolution at the same time, the ratio of their angular speed varies with the angle of rotation $\theta(t)$ of the driver and is a function also of the shaft angle $\varphi$. Thus, even if the angular speed $\omega_{21}$ of the drive shaft is constant, the angular speed $\omega_{41}$ of a driven shaft will not be uniform. ∎

**Example 251 ★** *Graphical illustration of the universal joint speed ratio* $\Omega$.

*Figure 6.44 depicts a three-dimensional plot for* $\Omega$. *The* $\Omega$-*surface is plotted for one revolution of the drive shaft and every possible angle between the two shafts.*

$$
\begin{aligned}
-\pi &< \theta < \pi \\
-\pi &< \varphi < \pi
\end{aligned}
$$

*A two-dimensional view for* $\Omega$ *is depicted in Figure 6.45. When* $\varphi \lessgtr 10 \deg$ *there is not much fluctuation in speed ratio, however, when the angle*
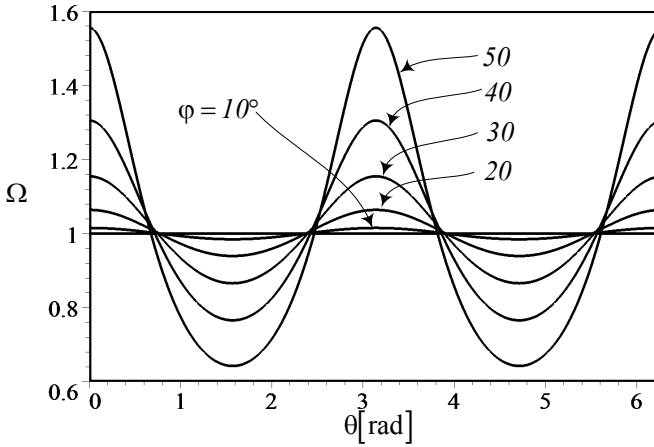
FIGURE 6.45. A two-dimensional view of $\Omega$ as a function of the input angle $\theta$ and the angle between input and output shafts $\varphi$.

*between the two shafts is more than* $10 \deg$ *then the speed ratio* $\Omega$ *cannot be assumed constant. The universal joint stuck when* $\varphi = 90 \deg$, *because theoretically*

$$\lim_{\varphi \to 90} \Omega = indefinite. \tag{6.308}$$

*The behavior of* $\Omega$ *as a function of* $\theta$ *and* $\varphi$ *can be better viewed in a polar coordinate, as shown in Figure 6.46.*

**Example 252 ★** *Maximum and minimum of* $\omega_{41}$ *in one revolution.*
   *The maximum value of* $\Omega$ *is*

$$\Omega_M = \frac{1}{\cos \varphi} \tag{6.309}$$

*at*

$$\theta = 0, \pi \tag{6.310}$$

*and the minimum value of* $\Omega$ *is*

$$\Omega_m = \cos \varphi \tag{6.311}$$

*at*

$$\theta = \frac{\pi}{2}, \frac{3\pi}{2}. \tag{6.312}$$

**Example 253 ★** *History of the universal joint.*
   *The need to transmit a rotary motion from one shaft to another, which are intersecting at an angle, was a problem for installing clocktowers in*
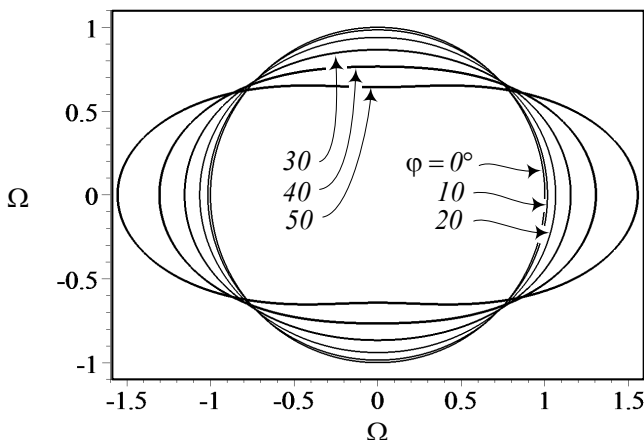
FIGURE 6.46. The behavior of speed ratio $\Omega$ as a function of $\theta$ and $\varphi$ in a polar coordinate.

*the* 1300*s. The transmission of the rotation to the hands should be displaced because of tower construction. Cardano* (1501 − 1576) *in* 1550, *Hook* (1635 − 1703) *in* 1663, *and Schott* (1608 − 1666) *in* 1664 *used the joint for transferring rotary motion. Hook was the first man who said that the rotary motion between the input and output shafts is not uniform. However, Monge* (1746 − 1818) *is the first person to publish the mathematical principles of the joint in* 1794, *and later by Poncelet (*1788 − 1867*) in* 1822.

**Example 254 ★** *Double universal joint.*

   *To eliminate the non-uniform speed ratio between the input and output shafts, connected by a universal joint, we can connect a second joint to make the intermediate shaft have a variable speed ratio with respect to both the input and the output shafts in such a way that the overall speed ratio between the input and output shafts remain equal to one.*

**Example 255 ★** *Alternative proof for universal joint equation.*

   *Consider a universal joint such as that shown in Figure 6.41. Looking along the axis of the input shaft, we see points A and B moving in a circle and points C and D moving in an ellipse as shown in Figure 6.47(a). This is because A and B trace a circle in a normal plane, and C and D trace a circle in a rotated plane by the angle $\varphi$. Assume the universal joint starts rotating when the axis CD of the cross link is at the intersection of the planes of motion CD and AB, as shown in Figure 6.47(a). If the axis AB turns an angle $\theta$, then the projection of the axis CD will turn the same angle, as can be seen in Figure 6.47(b). However, the angle of rotation CD is $\theta_4$ different than $\theta$ when we look at the axis CD along the output shaft.*

(a)                    (b)
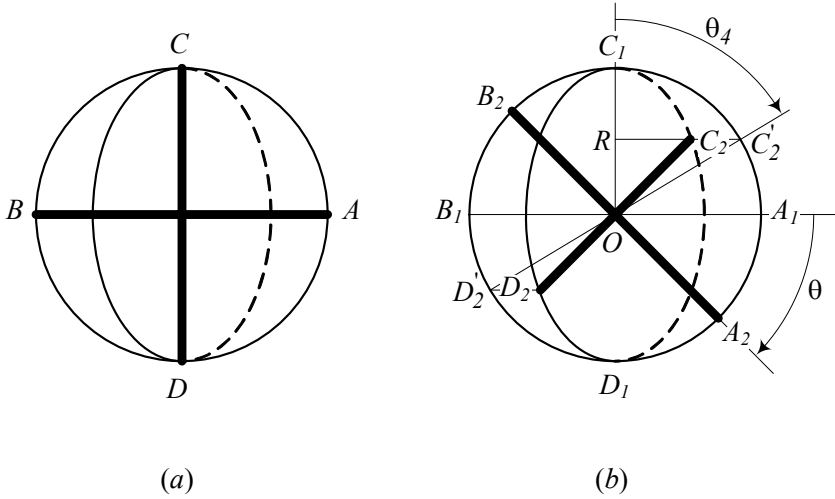
FIGURE 6.47. Rotation of the cross link from a viewpoint along the input shaft.

*Looking along the input shaft, the axis $AB$ starts from $A_1 B_1$ and moves to $A_2 B_2$ after rotation $\varphi$. From the same viewpoint, the axis $CD$ starts from $C_1 D_1$ and moves to $C_2 D_2$, however, $CD$ would be at $C_2' D_2'$, if it were looking along the output shaft. The geometric relationship between the angles are*

$$\frac{C_2' R}{OR} = \tan \theta_4 \tag{6.313}$$

$$\frac{C_2 R}{OR} = \tan \theta \tag{6.314}$$

$$\frac{C_2 R}{C_2' R} = \cos \varphi. \tag{6.315}$$

*Therefore,*

$$\tan \theta = \tan \theta_4 \cos \varphi \tag{6.316}$$

*which after differentiation becomes*

$$\frac{\omega_2}{\csc^2 \theta} = \frac{\omega_4}{\csc^2 \theta_4} \cos \varphi \tag{6.317}$$

*Eliminating $\theta_4$ between (6.316) and (6.317), we find the relationship between the input and output shafts' angular velocities.*

$$\omega_4 = \frac{\cos \varphi}{\sin^2 \theta + \cos^2 \theta \cos^2 \varphi} \omega_2 \tag{6.318}$$

*The speed ratio would then be the same as (6.288).*

$$\Omega \;=\; \frac{\omega_4}{\omega_2} = \frac{\cos\varphi}{\sin^2\theta + \cos^2\theta\cos^2\varphi} \tag{6.319}$$

$$=\; \frac{\cos\varphi}{1 - \sin^2\varphi\cos^2\theta} \tag{6.320}$$

**Example 256** ★ *Alternative proof for the universal joint speed ratio equation.*

*Poncelet (1788 − 1867) in 1824 used spherical trigonometry to find the universal joint speed ratio equation.*

*The universal joint can be used to transfer torque at larger angles than flexible couplings. One universal joint may be used to transmit power up to a $\varphi = 15\deg$ depending on the application. Universal joints are available in a wide variety of torque capacities.*

## 6.7    Summary

Every movable component of a vehicle, such as the doors, hoods, windshield wipers, axles, wheels, and suspensions, are connected to the vehicle body using some mechanisms. The four-bar linkage and inverted slider-crank mechanism are the two common mechanisms that we use to connect wheels of independent suspensions to the vehicle's body. There are analytic equations for determining position of the all links of a mechanism with respect to one of the links that we call the input link.

The wheels are installed on a spindle, which is rigidly attached to the coupler link of the mechanisms. The center of the wheel will move on a coupler point curve, which depends on the links' length.

# 6.8   Key Symbols

| | |
|---|---|
| $a \equiv \ddot{x}$ | acceleration |
| $a, b, c, \cdots$ | links' length of a linkage |
| $\mathbf{a}$ | acceleration vector |
| $A, B, \cdots$ | coefficients of quadratic equations |
| $b$ | relative position of an inverted slider |
| $\dot{b}$ | relative speed of a slider |
| $\ddot{b}$ | relative acceleration of a slider |
| $C_1, C_2, \cdots$ | link acceleration parameters of linkages |
| $\mathbf{d}$ | position vector of a moving frame |
| $f = 1/T$ | cyclic frequency [Hz] |
| $g$ | gravitational acceleration |
| $\hat{\imath}, \hat{\jmath}, \hat{k}$ | unit vectors of Cartesian coordinate frames |
| $I$ | instant center of rotation |
| $J_1, J_2, \cdots$ | link position parameters of linkages |
| $l$ | length |
| $l$ | length of the longest link |
| $n$ | number of links |
| $N$ | number of instant center of rotations |
| $p, q$ | length of the middle links |
| $\mathbf{r}$ | joint relative position vector |
| $s$ | displacement position of an slider |
| $s$ | length of the shortest link |
| $\dot{s}$ | speed of a slider |
| $\ddot{s}$ | acceleration of a slider |
| $t$ | time |
| $T$ | period |
| $x, y, z, \ \mathbf{x}$ | displacement |
| $x, y, z$ | Cartesian coordinates |
| $x_C, y_C$ | coupler point coordinates |
| $\mathbf{v}$ | velocity vector |
| | |
| $\boldsymbol{\alpha}$ | angular acceleration vector |
| $\alpha_i$ | angular acceleration of link number $i$ |
| $\theta_i$ | angular position of link number $i$ |
| $\theta$ | angular position of input and output axles of a universal joint |
| $\varphi$ | angle between the input and output axles of a universal joint |
| $\boldsymbol{\omega}$ | angular velocity vector |
| $\omega_i$ | angular velocity of link number $i$ |
| $\Omega$ | angular velocity ratio |

# Exercises

1. Two possible configurations for a four-bar linkage.

   Consider a four-bar linkage with the following links.

$$
\begin{aligned}
a &= 10\,\text{cm} \\
b &= 25\,\text{cm} \\
c &= 30\,\text{cm} \\
d &= 25\,\text{cm}
\end{aligned}
$$

   If $\theta_2 = 30\,\text{deg}$ what would be the angles $\theta_3$ and $\theta_4$ for a convex configuration?

2. Angular velocity of a four-bar linkage output link.

   Consider a four-bar linkage with the following links.

$$
\begin{aligned}
a &= 10\,\text{cm} \\
b &= 25\,\text{cm} \\
c &= 30\,\text{cm} \\
d &= 25\,\text{cm}
\end{aligned}
$$

   Determine the angular velocity of the output link $\omega_4$ at $\theta_2 = 30\,\text{deg}$ if $\omega_2 = 2\pi\,\text{rad}/\text{s}$.

3. Angular acceleration of a four-bar linkage output link.

   Consider a four-bar linkage with the following links.

$$
\begin{aligned}
a &= 10\,\text{cm} \\
b &= 25\,\text{cm} \\
c &= 30\,\text{cm} \\
d &= 25\,\text{cm}
\end{aligned}
$$

   Determine the angular acceleration of the output link $\alpha_4$ at $\theta_2 = 30\,\text{deg}$ if $\alpha_2 = 0.2\pi\,\text{rad}/\text{s}^2$ and $\omega_2 = 2\pi\,\text{rad}/\text{s}$.

4. Grashoff criterion.

   Consider a four-bar linkage with the following links.

$$
\begin{aligned}
a &= 10\,\text{cm} \\
b &= 25\,\text{cm} \\
c &= 30\,\text{cm}
\end{aligned}
$$

   Determine the limit values of the length $d$ to satisfy the Grashoff criterion.

5. Limit and dead positions.

   Consider a four-bar linkage with the following links.

$$a = 10\,\text{cm}$$
$$b = 25\,\text{cm}$$
$$c = 30\,\text{cm}$$
$$d = 25\,\text{cm}$$

   Determine if there is any limit or dead positions for the linkage.

6. ★ Limit position determination.

   Explain how we may be able to determine the limit positions of a four-bar linkage by the following condition.

$$\frac{d\theta}{dt} = 0$$

7. Two possible configurations for a slider-crank mechanism.

   Consider a slider-crank mechanism with the following links.

$$a = 10\,\text{cm}$$
$$b = 45\,\text{cm}$$
$$e = 0$$

   If $\theta_2 = 30\,\text{deg}$ what would be angle $\theta_3$ and position of the slides $s$ for a convex configuration?

8. Angular velocity and acceleration of the slider of a slider-crank mechanism.

   Consider a slider-crank mechanism with the following links.

$$a = 10\,\text{cm}$$
$$b = 45\,\text{cm}$$
$$e = 0$$

   Determine the angular velocity and acceleration of the slider at $\theta_2 = 30\,\text{deg}$ if $\omega_2 = 2\pi\,\text{rad/s}$ and $\alpha_2 = 0.2\pi\,\text{rad/s}^2$.

9. Quick return time.

   Consider a slider-crank mechanism with the following links.

$$a = 10\,\text{cm}$$
$$b = 45\,\text{cm}$$
$$e = 3\,\text{cm}$$

   Determine the difference time between go and return half cycle of the slider motion if $\omega_2 = 2\pi\,\text{rad/s}$.

10. Two possible configurations for an inverted slider-crank mechanism.

    Consider an inverted slider-crank mechanism with the following links.

$$a = 10\,\text{cm}$$
$$d = 45\,\text{cm}$$
$$e = 5\,\text{cm}$$

    If $\theta_2 = 30\,\text{deg}$, what would be the angle $\theta_3$ and position of the slides $b$?

11. Instant center of rotation.

    Find the instant center of rotations for the 6-bar linkage shown in Figure 6.48.
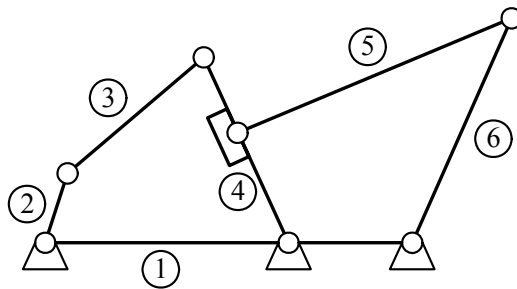


FIGURE 6.48. A 6-bar linkage.

12. A coupler point of a four-bar linkage.

    Consider a four-bar linkage with the following links

$$a = 10\,\text{cm}$$
$$b = 25\,\text{cm}$$
$$c = 30\,\text{cm}$$
$$d = 25\,\text{cm}$$

    and a coupler point with the following parameters.

$$e = 10\,\text{cm}$$
$$\alpha = 30\,\text{deg}$$

    Determine the coordinates of the coupler point if $\theta_2 = 30\,\text{deg}$.

13. A coupler point of a slider-crank mechanism.

Consider a slider-crank mechanism with the following parameters.

$$
\begin{aligned}
a &= 10\,\mathrm{cm} \\
b &= 45\,\mathrm{cm} \\
e &= 3\,\mathrm{cm} \\
c &= 10\,\mathrm{cm} \\
\alpha &= 30\,\mathrm{deg}
\end{aligned}
$$

Determine the coordinates of the coupler point.

14. A coupler point of an inverted slider-crank mechanism if $\theta_2 = 30\,\mathrm{deg}$. Consider an inverted slider-crank mechanism with the following parameters.

$$
\begin{aligned}
a &= 10\,\mathrm{cm} \\
d &= 45\,\mathrm{cm} \\
e &= 5\,\mathrm{cm} \\
c &= 10\,\mathrm{cm} \\
\alpha &= 30\,\mathrm{deg}
\end{aligned}
$$

Determine the coordinates of the coupler point if $\theta_2 = 30\,\mathrm{deg}$.

# 7

# Steering Dynamics

To maneuver a vehicle we need a steering mechanism to turn wheels. Steering dynamics which we review in this chapter, introduces new requirements and challenges.

## 7.1 Kinematic Steering

Consider a front-wheel-steering $4WS$ vehicle that is turning to the left, as shown in Figure 7.1. When the vehicle is moving very slowly, there is a kinematic condition between the inner and outer wheels that allows them to turn slip-free. The condition is called the *Ackerman condition* and is expressed by

$$\cot \delta_o - \cot \delta_i = \frac{w}{l} \tag{7.1}$$

where, $\delta_i$ is the steer angle of the *inner wheel*, and $\delta_o$ is the steer angle of the *outer wheel*. The inner and outer wheels are defined based on the turning center $O$.
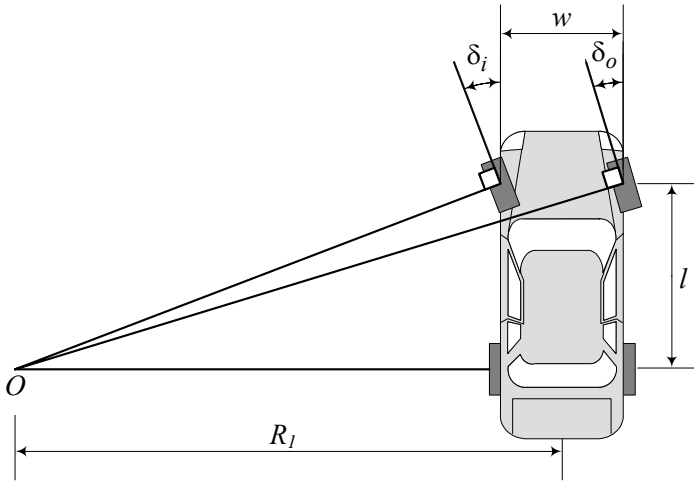


FIGURE 7.1. A front-wheel-steering vehicle and the Ackerman condition.

The distance between the steer axes of the steerable wheels is called the *track* and is shown by $w$. The distance between the front and real axles
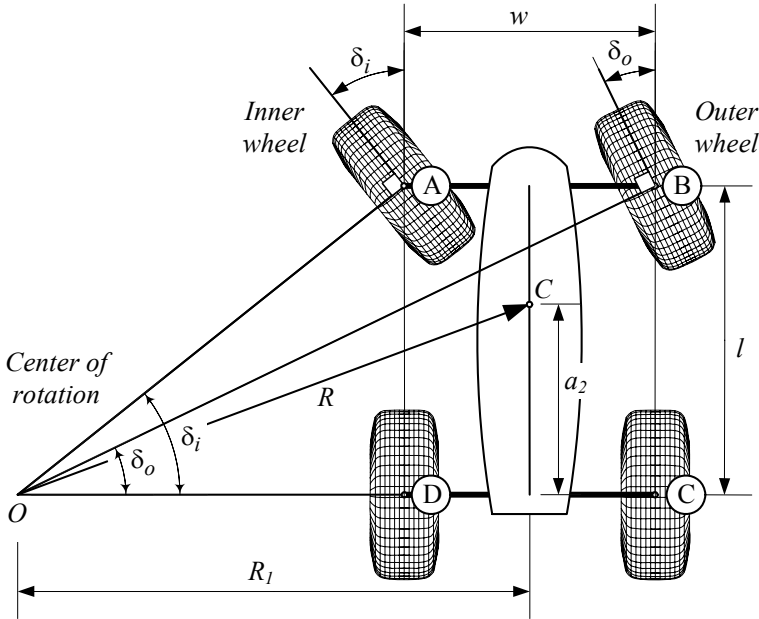
FIGURE 7.2. A front-wheel-steering vehicle and steer angles of the inner and outer wheels.

is called the *wheelbase* and is shown by $l$. Track $w$ and wheelbase $l$ are considered as kinematic width and length of the vehicle.

The mass center of a steered vehicle will turn on a circle with radius $R$,

$$R = \sqrt{a_2^2 + l^2 \cot^2 \delta} \tag{7.2}$$

where $\delta$ is the cot-average of the inner and outer steer angles.

$$\cot \delta = \frac{\cot \delta_o + \cot \delta_i}{2}. \tag{7.3}$$

The angle $\delta$ is the equivalent steer angle of a bicycle having the same wheelbase $l$ and radius of rotation $R$.

**Proof.** To have all wheels turning freely on a curved road, the normal line to the center of each tire-plane must intersect at a common point. This is the Ackerman condition.

Figure 7.2 illustrates a vehicle turning left. So, the turning center $O$ is on the left, and the inner wheels are the left wheels that are closer to the center of rotation. The inner and outer steer angles $\delta_i$ and $\delta_o$ may be calculated

from the triangles $\triangle OAD$ and $\triangle OBC$ as follows:

$$\tan \delta_i \quad = \quad \frac{l}{R_1 - \dfrac{w}{2}} \tag{7.4}$$

$$\tan \delta_o \quad = \quad \frac{l}{R_1 + \dfrac{w}{2}} \tag{7.5}$$

Eliminating $R_1$

$$R_1 \quad = \quad \frac{1}{2}w + \frac{l}{\tan \delta_i}$$
$$= \quad -\frac{1}{2}w + \frac{l}{\tan \delta_o} \tag{7.6}$$

provides the Ackerman condition (7.1), which is a direct relationship between $\delta_i$ and $\delta_o$.

$$\cot \delta_o - \cot \delta_i = \frac{w}{l} \tag{7.7}$$

To find the vehicle's turning radius $R$, we define an equivalent bicycle model, as shown in Figure 7.3. The radius of rotation $R$ is perpendicular to the vehicle's velocity vector $\mathbf{v}$ at the mass center $C$. Using the geometry shown in the bicycle model, we have

$$R^2 \quad = \quad a_2^2 + R_1^2 \tag{7.8}$$

$$\cot \delta \quad = \quad \frac{R_1}{l}$$
$$= \quad \frac{1}{2}\left(\cot \delta_i + \cot \delta_o\right) \tag{7.9}$$

and therefore,

$$R = \sqrt{a_2^2 + l^2 \cot^2 \delta}. \tag{7.10}$$

The Ackerman condition is needed when the speed of the vehicle is too small, and slip angles are zero. There is no lateral force and no centrifugal force to balance each other. The Ackerman steering condition is also called the *kinematic steering condition*, because it is a static condition at zero velocity.

A device that provides steering according to the Ackerman condition (7.1) is called *Ackerman steering*, *Ackerman mechanism*, or *Ackerman geometry*. There is no four-bar linkage steering mechanism that can provide the Ackerman condition perfectly. However, we may design a multi-bar linkages to work close to the condition and be exact at a few angles.

Figure 7.4 illustrates the Ackerman condition for different values of $w/l$. The inner and outer steer angles get closer to each other by decreasing $w/l$.

∎
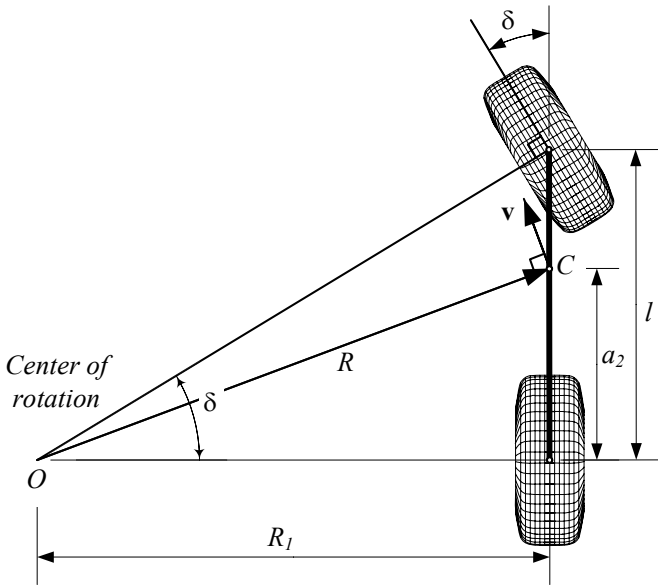
FIGURE 7.3. Equivalent bicycle model for a front-wheel-steering vehicle.
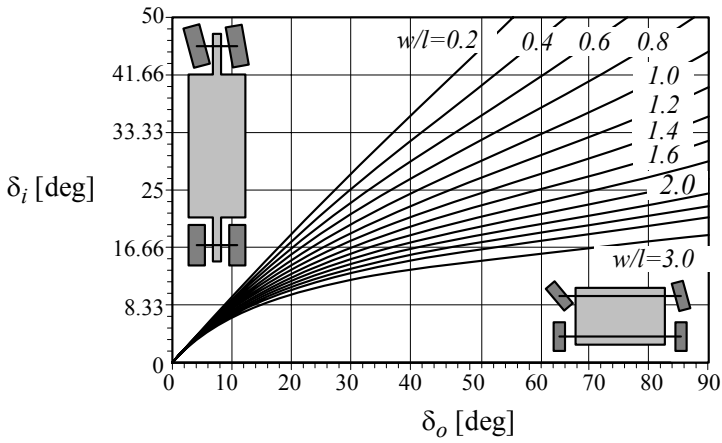


FIGURE 7.4. Effect of $w/l$ on the Ackerman condition for front-wheel-steering vehicles.

**Example 257** *Turning radius, or radius of rotation.*
    *Consider a vehicle with the following dimensions and steer angle:*

$$
\begin{aligned}
l &= 103.1 \,\text{in} \approx 2.619 \,\text{m} \\
w &= 61.6 \,\text{in} \approx 1.565 \,\text{m} \\
a_2 &= 60 \,\text{in} \approx 1.524 \,\text{m} \\
\delta_i &= 12 \,\text{deg} \approx 0.209 \,\text{rad}
\end{aligned} \tag{7.11}
$$

*The kinematic steering characteristics of the vehicle would be*

$$
\begin{aligned}
\delta_o &= \cot^{-1}\left(\frac{w}{l} + \cot\delta_i\right) \\
&= 0.186 \,\text{rad} \approx 10.661 \,\text{deg}
\end{aligned} \tag{7.12}
$$

$$
\begin{aligned}
R_1 &= l\cot\delta_i + \frac{1}{2}w \\
&= 516.9 \,\text{in} \approx 13.129 \,\text{m}
\end{aligned} \tag{7.13}
$$

$$
\begin{aligned}
\delta &= \cot^{-1}\left(\frac{\cot\delta_o + \cot\delta_i}{2}\right) \\
&= 0.19684 \,\text{rad} \approx 11.278 \,\text{deg}
\end{aligned} \tag{7.14}
$$

$$
\begin{aligned}
R &= \sqrt{a_2^2 + l^2\cot^2\delta} \\
&= 520.46 \,\text{in} \approx 13.219 \,\text{m}.
\end{aligned} \tag{7.15}
$$

**Example 258** $w$ *is the front track.*
    *Most cars have different tracks in front and rear. The track $w$ in the kinematic condition (7.1) refers to the front track $w_f$. The rear track has no effect on the kinematic condition of a front-wheel-steering vehicle. The rear track $w_r$ of a $FWS$ vehicle can be zero with the same kinematic steering condition (7.1).*

**Example 259** *Space requirement.*
    *The kinematic steering condition can be used to calculate the space requirement of a vehicle during a turn. Consider the front wheels of a two-axle vehicle, steered according to the Ackerman geometry as shown in Figure 7.5.*

    *The outer point of the front of the vehicle will run on the maximum radius $R_{Max}$, whereas a point on the inner side of the vehicle at the location of the rear axle will run on the minimum radius $R_{min}$. The front outer point has an overhang distance $g$ from the front axle. The maximum radius $R_{Max}$ is*

$$
R_{Max} = \sqrt{(R_{min} + w)^2 + (l + g)^2}. \tag{7.16}
$$
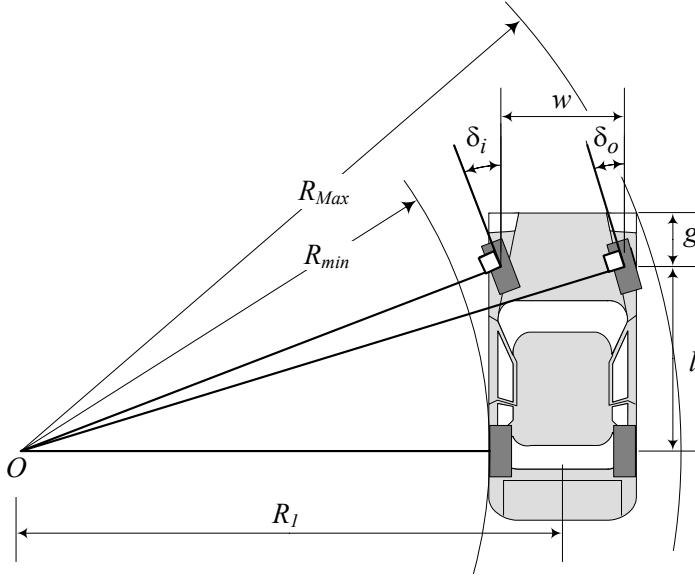
FIGURE 7.5. The required space for a turning two-axle vehicle.

*Therefore, the required space for turning is a ring with a width $\triangle R$, which is a function of the vehicle's geometry.*

$$
\begin{aligned}
\triangle R &= R_{Max} - R_{min} \\
&= \sqrt{(R_{min} + w)^2 + (l + g)^2} - R_{min} \quad (7.17)
\end{aligned}
$$

*The required space $\triangle R$ can be calculated based on the steer angle by substituting $R_{min}$*

$$
\begin{aligned}
R_{min} &= R_1 - \frac{1}{2}w \\
&= \frac{l}{\tan \delta_i} \quad (7.18) \\
&= \frac{l}{\tan \delta_o} - w \quad (7.19)
\end{aligned}
$$

*and getting*

$$
\begin{aligned}
\triangle R &= \sqrt{\left(\frac{l}{\tan \delta_i} + 2w\right)^2 + (l + g)^2} - \frac{l}{\tan \delta_i} \quad (7.20) \\
&= \sqrt{\left(\frac{l}{\tan \delta_o} + w\right)^2 + (l + g)^2} - \frac{l}{\tan \delta_o} + w. \quad (7.21)
\end{aligned}
$$
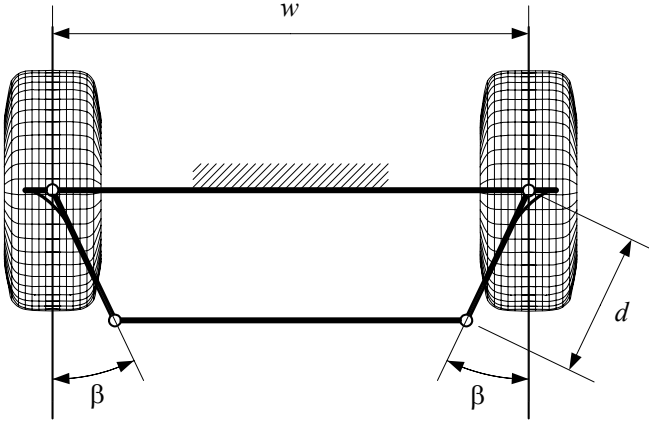
FIGURE 7.6. A trapezoidal steering mechanism.

In this example the width of the car $w_v$ and the track $w$ are assumed to be equal. The width of vehicles are always greater than their track.

$$w_v > w \tag{7.22}$$

**Example 260** *Trapezoidal steering mechanism.*
*Figure 7.6 illustrates a symmetric four-bar linkage, called a **trapezoidal steering mechanism**, that has been used for more than* $100$ *years. The mechanism has two characteristic parameters: angle* $\beta$ *and offset arm length* $d$. *A steered position of the trapezoidal mechanism is shown in Figure 7.7 to illustrate the inner and outer steer angles* $\delta_i$ *and* $\delta_o$.
*The relationship between the inner and outer steer angles of a trapezoidal steering mechanism is*

$$\sin\left(\beta + \delta_i\right) + \sin\left(\beta - \delta_o\right)$$
$$= \frac{w}{d} + \sqrt{\left(\frac{w}{d} - 2\sin\beta\right)^2 - \left(\cos\left(\beta - \delta_o\right) - \cos\left(\beta + \delta_i\right)\right)^2}. \tag{7.23}$$

*To prove this equation, we examine Figure 7.8. In the triangle* $\triangle ABC$ *we can write*

$$\begin{aligned}\left(w - 2d\sin\beta\right)^2 &= \left(w - d\sin\left(\beta + \delta_i\right) - d\sin\left(\beta - \delta_o\right)\right)^2 \\ &\quad + \left(d\cos\left(\beta - \delta_o\right) - d\cos\left(\beta + \delta_i\right)\right)^2\end{aligned} \tag{7.24}$$

*and derive Equation (7.23) with some manipulation.*
*The functionality of a trapezoidal steering mechanism, compared to the associated Ackerman condition, is shown in Figure 7.9 for* $x = 2.4\,\mathrm{m} \approx 7.87\,\mathrm{ft}$ *and* $d = 0.4\,\mathrm{m} \approx 1.3\,\mathrm{ft}$. *The horizontal axis shows the inner steer angle and the vertical axis shows the outer steer angle. It depicts that for*
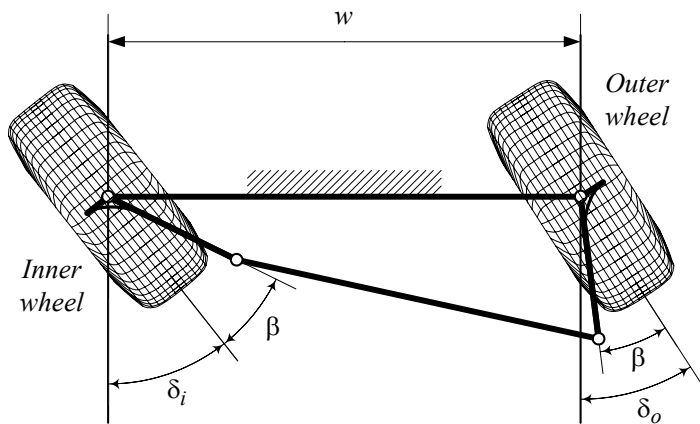
FIGURE 7.7. Steered configuration of a trapezoidal steering mechanism.
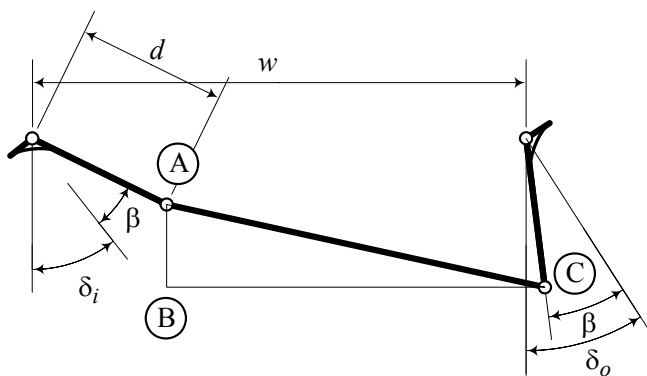


FIGURE 7.8. Trapezoidal steering triangle $ABC$.
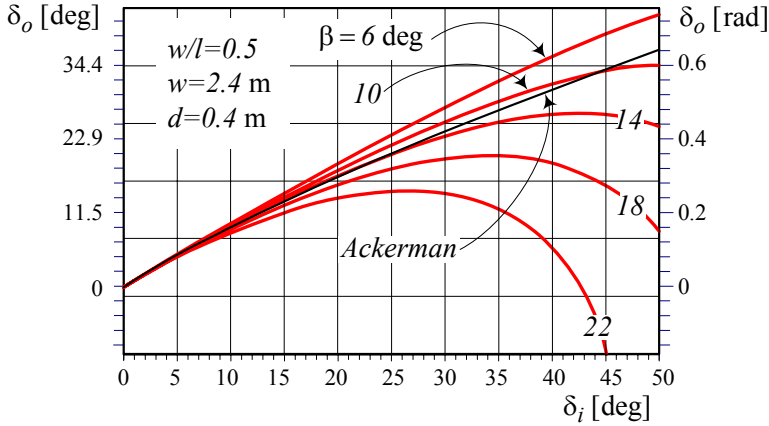
FIGURE 7.9. Behavior of a trapezoidal steering mechanism, compared to the associated Ackerman mechanism.

*a given l and w, a mechanism with $\beta \approx 10$ deg is the best simulator of an Ackerman mechanism if $\delta_i < 50$ deg.*

*To examine the trapezoidal steering mechanism and compare it with the Ackerman condition, we define an error parameter $e = \delta_{D_o} - \delta_{A_o}$. The error e is the difference between the outer steer angles calculated by the trapezoidal mechanism and the Ackerman condition at the same inner steer angle $\delta_i$.*

$$e = \Delta\delta_o$$
$$= \delta_{D_o} - \delta_{A_o} \tag{7.25}$$

*Figure 7.10 depicts the error e for a sample steering mechanism using the angle $\beta$ as a parameter.*

**Example 261 ★** *Locked rear axle.*

*Sometimes in a simple design of vehicles, we eliminate the differential and use a locked rear axle in which no relative rotation between the left and right wheels is possible. Such a simple design is usually used in toy cars, or small off-road vehicles such as a mini Baja.*

*Consider the vehicle shown in Figure 7.2. In a slow left turn, the speed of the inner rear wheel should be*

$$v_{ri} = \left(R_1 - \frac{w}{2}\right)r = R_w\omega_{ri} \tag{7.26}$$

*and the speed of the outer rear wheel should be*

$$v_{ro} = \left(R_1 + \frac{w}{2}\right)r = R_w\omega_{ro} \tag{7.27}$$

*where, r is the yaw velocity of the vehicle, $R_w$ is rear wheels radius, and $\omega_{ri}$, $\omega_{ro}$ should be the angular velocity of the rear inner and outer wheels*
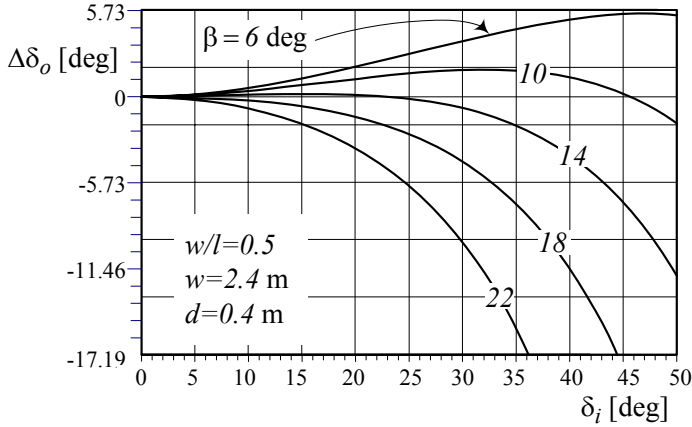
FIGURE 7.10. The error parameter $e = \delta_{D_o} - \delta_{A_o}$ for a sample trapezoidal steering mechanism.

*about their common axle. If the rear axle is locked, we have*

$$\omega_{ri} = \omega_{ro} = \omega \tag{7.28}$$

*however,*

$$\left(R_1 - \frac{w}{2}\right) \neq \left(R_1 + \frac{w}{2}\right) \tag{7.29}$$

*which shows it is impossible to have a locked axle for a nonzero w.*

*Turning with a locked rear axle reduces the load on the inner wheels and makes the rear inner wheel overcome the friction force and spin. Hence, the traction of the inner wheel drops to the maximum friction force under a reduced load. However, the load on the outer wheels increases and hence, the friction limit of the outer wheel helps to have higher traction force on the outer rear wheel.*

*Eliminating the differential and using a locked drive axle is an impractical design for street cars. However, it can be an acceptable design for small and light cars moving on dirt or slippery surfaces. It reduces the cost and simplifies the design significantly.*

*In a conventional two-wheel-drive motor vehicle, the rear wheels are driven using a differential, and the vehicle is steered by changing the direction of the front wheels. With an ideal differential, equal torque is delivered to each drive wheel. The rotational speed of the drive wheels are determined by the differential and the tire-road characteristics. However, a vehicle using a differential has disadvantages when one wheel has lower traction. Differences in traction characteristics of each of the drive wheels may come from different tire-road characteristics or weight distribution. Because a differential delivers equal torque, the wheel with greater tractive*
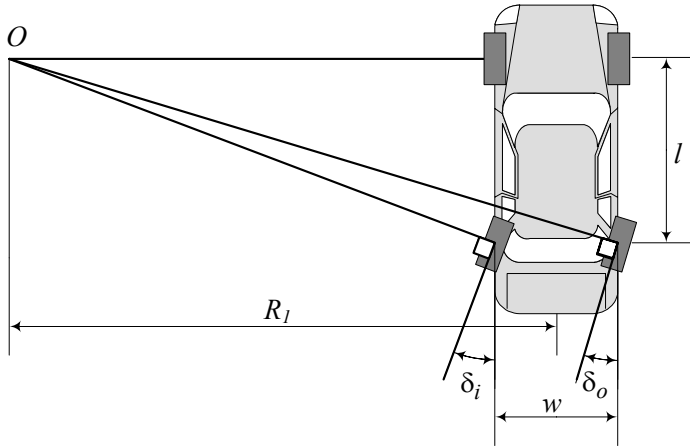
FIGURE 7.11. A rear-wheel-steering vehicle.

*ability can deliver only the same amount of torque as the wheel with the lower traction. The steering behavior of a vehicle with a differential is relatively stable under changing tire-road conditions. However, the total thrust may be reduced when the traction conditions are different for each drive wheel.*

**Example 262** ★ *Rear-wheel-steering.*

*Rear-wheel-steering is used where high maneuverability is a necessity on a low-speed vehicle, such as forklifts. Rear-wheel-steering is not used on street vehicles because it is unstable at high speeds. The center of rotation for a rear-wheel-steeringe vehicle is always a point on the front axle.*

*Figure 7.11 illustrates a rear-wheel-steering vehicle. The kinematic steering condition (7.1) remains the same for a rear-wheel steering vehicle.*

$$\cot \delta_o - \cot \delta_i = \frac{w}{l} \tag{7.30}$$

**Example 263** ★ *Alternative kinematic steer angles equation.*

*Consider a rear-wheel-drive vehicle with front steerable wheels as shown in Figure 7.12. Assume that the front and rear tracks of the vehicle are equal and the drive wheels are turning without slip. If we show the angular velocities of the inner and outer drive wheels by $\omega_i$ and $\omega_o$, respectively, the kinematical steer angles of the front wheels can be expressed by*

$$\delta_i = \tan^{-1}\left(\frac{l}{w}\left(\frac{\omega_o}{\omega_i} - 1\right)\right) \tag{7.31}$$

$$\delta_o = \tan^{-1}\left(\frac{l}{w}\left(1 - \frac{\omega_i}{\omega_o}\right)\right). \tag{7.32}$$
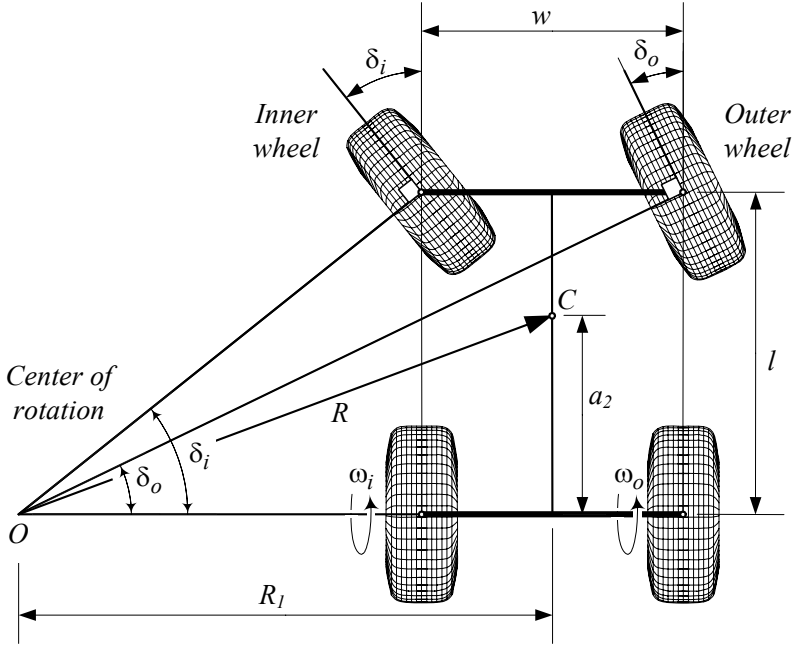
FIGURE 7.12. Kinematic condition of a $FWS$ vehicle using the angular velocity of the inner and outer wheels.

To prove these equations, we may start from the following equation, which is the non-slipping condition for the drive wheels:

$$\frac{R_w\,\omega_o}{R_1 + \dfrac{w}{2}} = \frac{R_w\,\omega_i}{R_1 - \dfrac{w}{2}}. \tag{7.33}$$

Equation (7.33) can be rearranged to

$$\frac{\omega_o}{\omega_i} = \frac{R_1 + \dfrac{w}{2}}{R_1 - \dfrac{w}{2}} \tag{7.34}$$

and substituted in Equations (7.31) and (7.32) to reduce them to Equations (7.4) and (7.5).

The equality (7.33) is the yaw rate of the vehicle, which is the vehicle's angular velocity about the center of rotation.

$$r = \frac{R_w\,\omega_o}{R_1 + \dfrac{w}{2}} = \frac{R_w\,\omega_i}{R_1 - \dfrac{w}{2}} \tag{7.35}$$
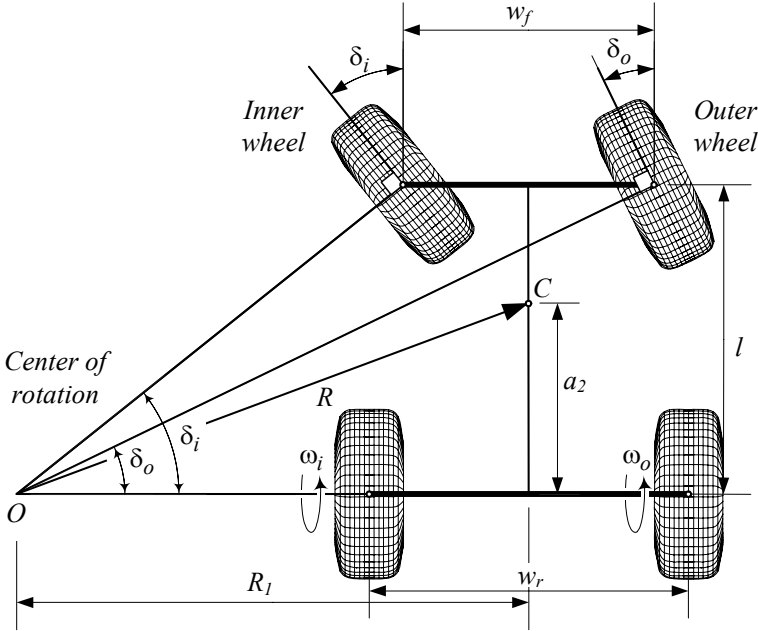
FIGURE 7.13. Kinematic steering condition for a vehicle with different tracks in the front and in the back.

**Example 264 ★** *Unequal front and rear tracks.*

It is possible to design a vehicle with different tracks in the front and rear. It is a common design for race cars, which are usually equipped with wider and larger rear tires to increase traction and stability. For street cars we use the same tires in the front and rear, however, it is common to have a few centimeters of larger track in the back. Such a vehicle is illustrated in Figure 7.13.

The angular velocity of the vehicle is

$$r = \frac{R_w\,\omega_o}{R_1 + \dfrac{w_r}{2}} = \frac{R_w\,\omega_i}{R_1 - \dfrac{w_r}{2}} \tag{7.36}$$

and the kinematic steer angles of the front wheels are

$$\delta_i = \tan^{-1}\frac{2l\,(\omega_o + \omega_i)}{w_f\,(\omega_o - \omega_i) + w_r\,(\omega_o + \omega_i)} \tag{7.37}$$

$$\delta_o = \tan^{-1}\frac{2l\,(\omega_o - \omega_i)}{w_f\,(\omega_o - \omega_i) + w_r\,(\omega_o + \omega_i)}. \tag{7.38}$$

To show these equations, we should find $R_1$ from Equation (7.36)

$$R_1 = \frac{w_r}{2}\frac{\omega_o + \omega_i}{\omega_o - \omega_i} \tag{7.39}$$

*and substitute it in the following equations.*

$$\tan \delta_i = \frac{l}{R_1 - \dfrac{w_f}{2}} \tag{7.40}$$

$$\tan \delta_o = \frac{l}{R_1 + \dfrac{w_f}{2}} \tag{7.41}$$

*In the above equations, $w_f$ is the front track, $w_r$ is the rear track, and $R_w$ is the wheel radius.*

**Example 265** ★ *Independent rear-wheel-drive.*
    *For some special-purpose vehicles, such as moon rovers and autonomous mobile robots, we may attach each drive wheel to an independently controlled motor to apply any desired angular velocity. Furthermore, the steerable wheels of such vehicles are able to turn more than $90 \deg$ to the left and right. Such a vehicle is highly maneuverable at a low speed.*
    *Figure 7.14 illustrates the advantages of such a steerable vehicle and its possible turnings. Figures 7.14 (a)-(c) illustrate forward maneuvering. The arrows by the rear wheels, illustrate the magnitude of the angular velocity of the wheel, and the arrows on the front wheels illustrate the direction of their motion. The maneuvering in backward motion is illustrated in Figures 7.14(d)-(f). Having such a vehicle allows us to turn the vehicle about any point on the rear axle including the inner points. In Figure 7.14(g) the vehicle is turning about the center of the rear right wheel, and in Figure 7.14(h) about the center of the rear left wheel. Figure 7.14(i) illustrates a rotation about the center point of the rear axle.*
    *In any of the above scenarios, the steer angle of the front wheels should be determined using a proper equation, such as (7.40) and (7.41). The ratio of the outer to inner angular velocities of the drive wheels $\omega_o/\omega_i$ may be determined using either the outer or inner steer angles.*

$$\frac{\omega_o}{\omega_i} = \frac{\delta_o \left(w_f - w_r\right) - 2l}{\delta_o \left(w_f + w_r\right) - 2l} \tag{7.42}$$

$$\frac{\omega_o}{\omega_i} = \frac{\delta_i \left(w_f + w_r\right) + 2l}{\delta_i \left(w_f - w_r\right) + 2l} \tag{7.43}$$

**Example 266** ★ *Race car steering.*
    *The Ackerman or kinematic steering is a correct condition when the turning speed of the vehicle is slow. When the vehicle turns fast, significant lateral acceleration is needed, and therefore, the wheels operate at high slip angles. Furthermore, the loads on the inner wheels will be much lower than the outer wheels. Tire performance curves show that by increasing the wheel load, less slip angle is required to reach the peak of the lateral force. Under these conditions the inner front wheel of a kinematic steering vehicle would be at a higher slip angle than required for maximum lateral force.*
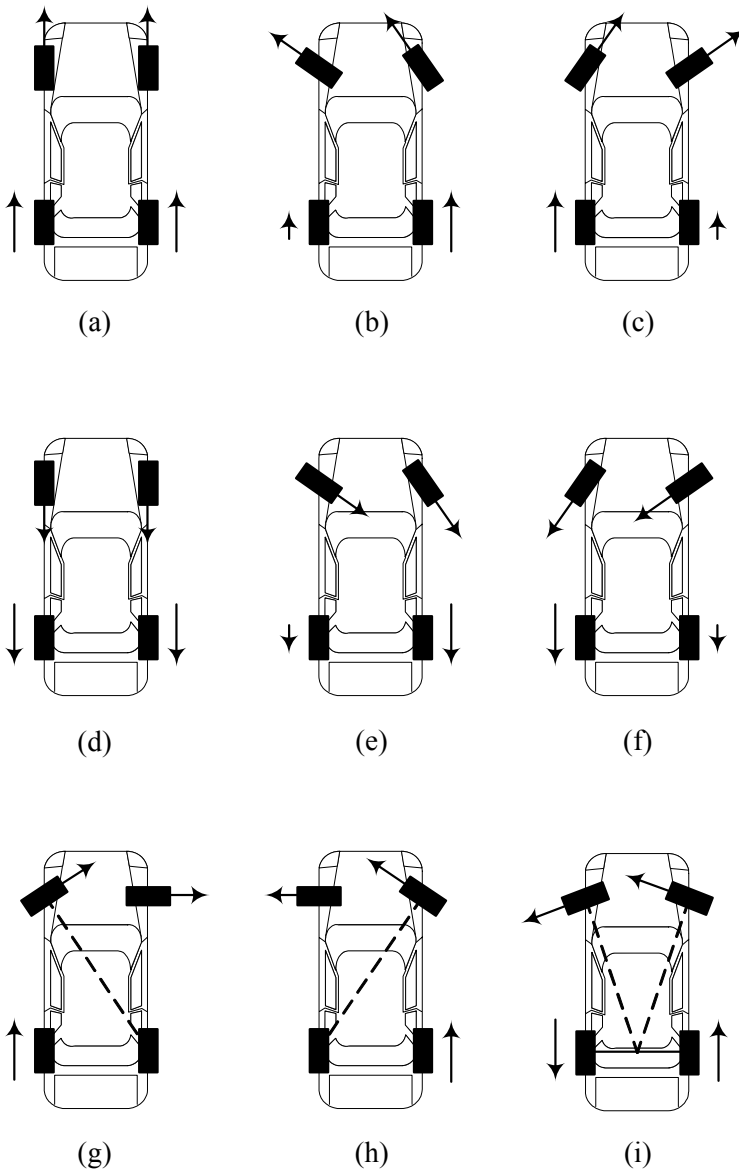
FIGURE 7.14. A highly steerable vehicle.

Ackerman          Parallel          Reverse
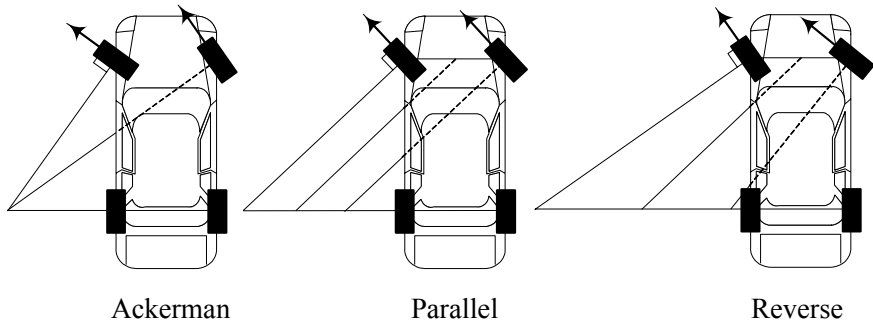
FIGURE 7.15. By increasing the speed at a turn, parallel or reverse steering is needed instead of Ackerman steering.

*Therefore, the inner wheel of a vehicle in a high speed turn must operate at a lower steer angle than kinematic steering. Reducing the steer angle of the inner wheel reduces the difference between steer angles of the inner and outer wheels.*

*For race cars, it is common to use parallel or reverse steering. Ackerman, parallel, and reverse Ackerman steering are illustrated in Figure 7.15.*

*The correct steer angle is a function of the instant wheel load, road condition, speed, and tire characteristics. Furthermore, the vehicle must also be able to turn at a low speed under an Ackerman steering condition. Hence, there is no ideal steering mechanism unless we control the steer angle of each steerable wheel independently using a smart system.*

**Example 267** ★ *Speed dependent steering system.*

*There is a speed adjustment idea that says it is better to have a harder steering system at high speeds. This idea can be applied in power steering systems to make them speed dependent, such that the steering be heavily assisted at low speeds and lightly assisted at high speeds. The idea is supported by this fact that the drivers might need large steering for parking, and small steering when traveling at high speeds.*

**Example 268** ★ *Ackerman condition history.*

*Correct steering geometry was a major problem in the early days of carriages, horse-drawn vehicles, and cars. Four- or six-wheel cars and carriages always left rubber marks behind. This is why there were so many three-wheeled cars and carriages in the past. The problem was making a mechanism to give the inner wheel a smaller turning radius than the outside wheel when the vehicle was driven in a circle.*

*The required geometric condition for a front-wheel-steering four-wheel-carriage was introduced in 1816 by George Langensperger in Munich, Germany. Langensperger's mechanism is illustrated in Figure 7.16.*

*Rudolf Ackerman met Langensperger and saw his invention. Ackerman*
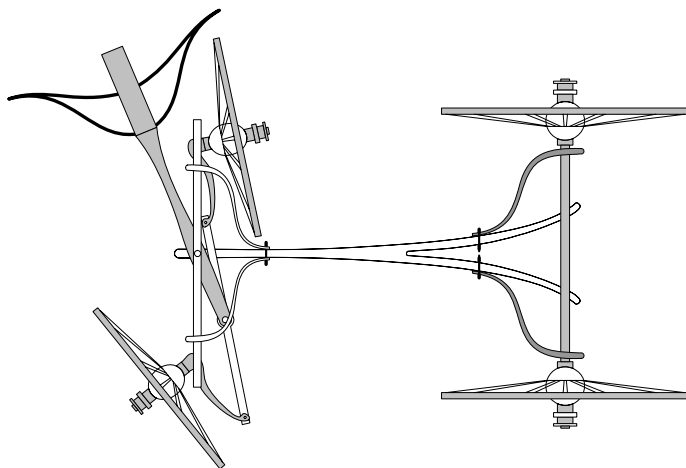
FIGURE 7.16. Langensperger invention for the steering geometry condition.

*acted as Langensperger's patent agent in London and introduced the invention to British carriage builders. Car manufacturers have been adopting and improving the Ackerman geometry for their steering mechanisms since 1881.*

*The basic design of vehicle steering systems has changed little since the invention of the steering mechanism. The driver's steering input is transmitted by a shaft through some type of gear reduction mechanism to generate steering motion at the front wheels.*

## 7.2   Vehicles with More Than Two Axles

If a vehicle has more than two axles, all the axles, except one, must be steerable to provide slip-free turning at zero velocity. When an $n$-axle vehicle has only one non-steerable axle, there are $n - 1$ geometric steering conditions. A three-axle vehicle with two steerable axles is shown in Figure 7.17.

To indicate the geometry of a multi-axle vehicle, we start from the front axle and measure the longitudinal distance $a_i$ between axle $i$ and the mass center $C$. Hence, $a_1$ is the distance between the front axle and $C$, and $a_2$ is the distance between the second axle and $C$. Furthermore, we number the wheels in a clockwise rotation starting from the driver's wheel as number 1.

For the three-axle vehicle shown in Figure 7.17, there are two indepen-
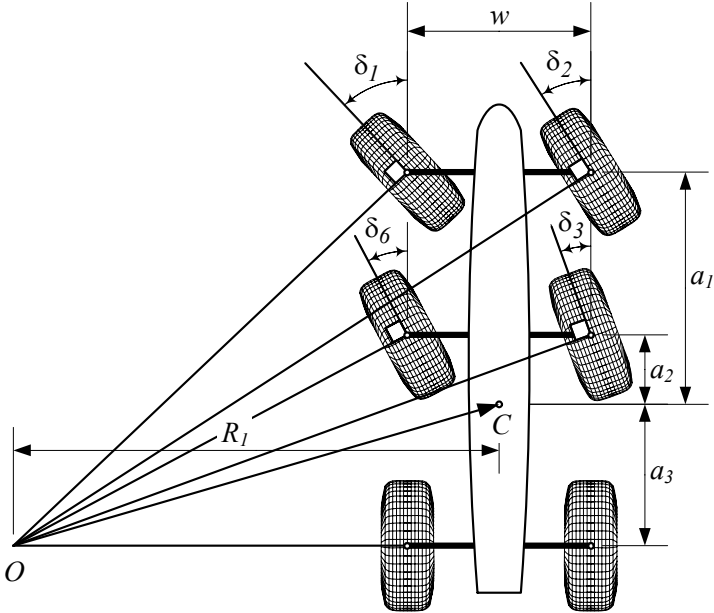
FIGURE 7.17. Steering of a three-axle vehicle.

dent Ackerman conditions:

$$\cot \delta_2 - \cot \delta_1 = \frac{w}{a_1 + a_3} \tag{7.44}$$

$$\cot \delta_3 - \cot \delta_6 = \frac{w}{a_2 + a_3}. \tag{7.45}$$

**Example 269** *A six-wheel vehicle with one steerable axle.*

*When a multi-axle vehicle has only one steerable axle, slip-free rotation is impossible for the non-steering wheels. The kinematic length or wheelbase of the vehicle is not clear, and it is not possible to define an Ackerman condition. Strong wear occurs for the tires, especially at low speeds and large steer angles. Hence, such a combination is not recommended. However, in case of a long three-axle vehicle with two nonsteerable axles close to each other, an approximated analysis is possible for low-speed steering.*

*Figure 7.18 illustrates a six-wheel vehicle with only one steerable axle in front. We design the steering mechanism such that the center of rotation $O$ is on a lateral line, called the **midline**, between the couple rear axles. The kinematic length of the vehicle, l, is the distance between the front axle and the midline. For this design we have*

$$\cot \delta_o - \cot \delta_i = \frac{w}{l} \tag{7.46}$$
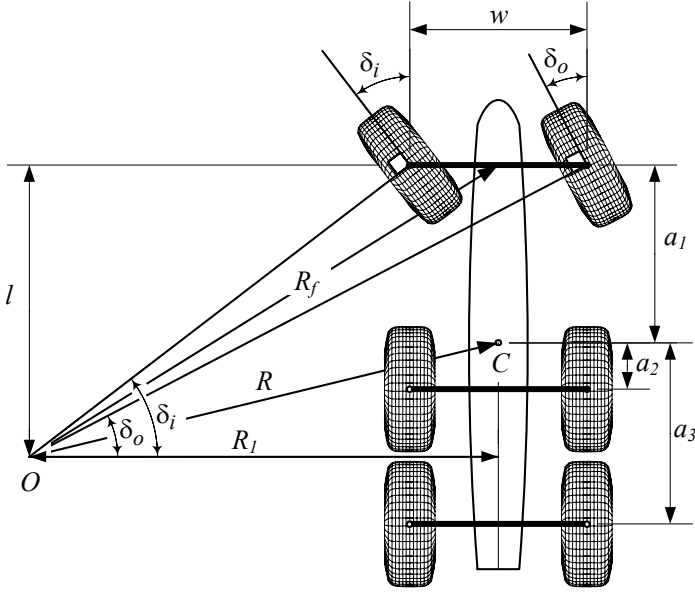
FIGURE 7.18. A six-wheel vehicle with one steerable axle in front.

*and*

$$R_1 = l \cot \delta_o - \frac{w}{2}$$
$$= l \cot \delta_i + \frac{w}{2}. \tag{7.47}$$

*The center of the front axle and the mass center of the vehicle are turning about $O$ by radii $R_f$ and $R$.*

$$R_f = \frac{R_1}{\cos\left(\tan^{-1}\dfrac{l}{R_1}\right)} \tag{7.48}$$

$$R = \frac{R_1}{\cos\left(\tan^{-1}\dfrac{a_3 - a_2}{2R_1}\right)} \tag{7.49}$$

*If the radius of rotation is large compared to the wheelbase, we may approximate Equations (7.48) and (7.49).*

$$R_f \approx \frac{R_1}{\cos\left(\dfrac{l}{R_1}\right)} \tag{7.50}$$
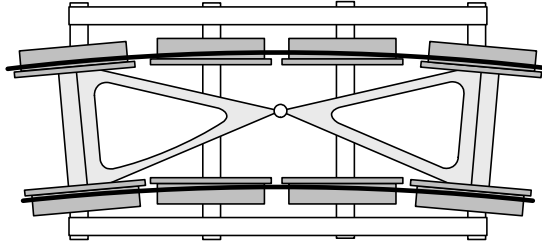
FIGURE 7.19. A self-steering axle mechanism for locomotive wagons.

$$R \approx \frac{R_1}{\cos\left(\dfrac{a_3 - a_2}{2R_1}\right)} \tag{7.51}$$

$$R_1 = \frac{l}{2}\left(\cot\delta_o + \cot\delta_i\right) \tag{7.52}$$

*To avoid strong wear, it is possible to lift an axle when the vehicle is not carrying heavy loads. For such a vehicle, we may design the steering mechanism to follow an Ackerman condition based on a wheelbase for the non-lifted axle. However, when this vehicle is carrying a heavy load and using all the axles, the liftable axle encounters huge wear in large steer angles.*

*Another option for multi-axle vehicles is to use **self-steering** wheels that can adjust themselves to minimize sideslip. Such wheels cannot provide lateral force, and hence, cannot help in maneuvers very much. Self-steering wheels may be installed on buggies and trailers. Such a self-steering axle mechanism for locomotive wagons is shown in Figure 7.19.*

## 7.3 ★ Vehicle with Trailer

If a four-wheel vehicle has a trailer with one axle, it is possible to derive a kinematic condition for slip-free steering. Figure 7.20 illustrates a vehicle with a one-axle trailer. The mass center of the vehicle is turning on a circle with radius $R$, while the trailer is turning on a circle with radius $R_t$.

$$R_t = \sqrt{\left(l\cot\delta_i + \frac{1}{2}w\right)^2 + b_1^2 - b_2^2} \tag{7.53}$$

$$R_t = \sqrt{\left(l\cot\delta_o - \frac{1}{2}w\right)^2 + b_1^2 - b_2^2} \tag{7.54}$$

At a steady-state condition, the angle between the trailer and the vehicle
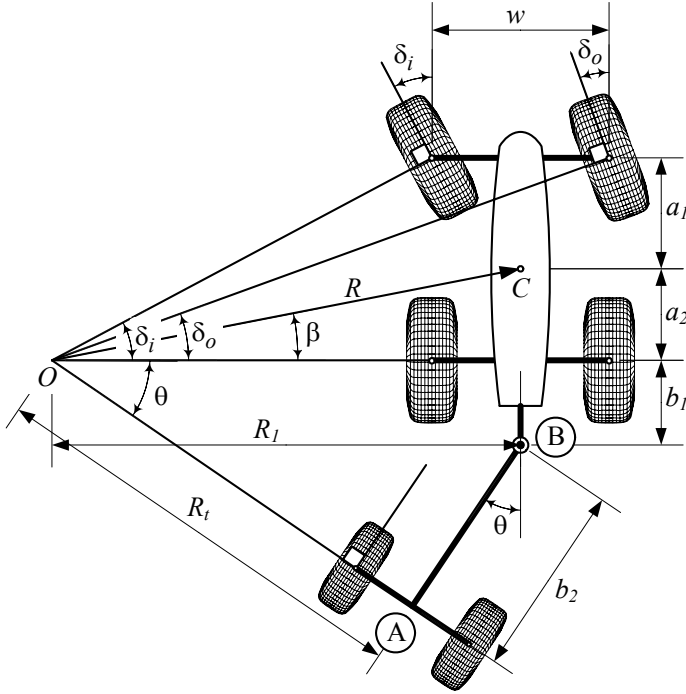
FIGURE 7.20. A vehicle with a one-axle trailer.

is

$$
\theta = \begin{cases} 2\tan^{-1}\left[\dfrac{1}{b_1 - b_2}\left(R_t - \sqrt{R_t^2 - b_1^2 + b_2^2}\right)\right] & b_1 - b_2 \neq 0 \\[4mm] 2\tan^{-1}\dfrac{1}{2R_t}\left(b_1 + b_2\right) & b_1 - b_2 = 0 \end{cases}
\tag{7.55}
$$

**Proof.** Using the right triangle $\triangle OAB$ in Figure 7.20, we may write the trailer's radius of rotation as

$$
R_t = \sqrt{R_1^2 + b_1^2 - b_2^2}
\tag{7.56}
$$

because the length $\overline{OB}$ is

$$
\begin{aligned}
\overline{OB}^2 &= R_t^2 + b_2^2 \\
&= R_1^2 + b_1^2.
\end{aligned}
\tag{7.57}
$$

Substituting $R_1$ from Equation (7.6) shows that the trailer's radius of ro-
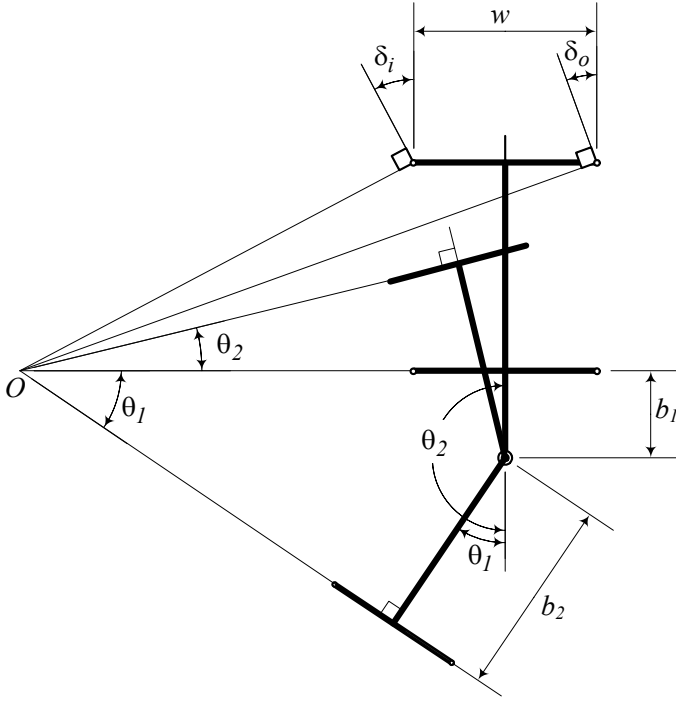
FIGURE 7.21. Two possible angle $\theta$ for a set of $(R_t, b_1, b_2)$.

tation is related to the vehicle's geometry by

$$R_t = \sqrt{\left(l\cot\delta_i + \frac{1}{2}w\right)^2 + b_1^2 - b_2^2} \tag{7.58}$$

$$R_t = \sqrt{\left(l\cot\delta_o - \frac{1}{2}w\right)^2 + b_1^2 - b_2^2} \tag{7.59}$$

$$R_t = \sqrt{R^2 - a_2^2 + b_1^2 - b_2^2}. \tag{7.60}$$

Using the equation

$$R_t \sin\theta = b_1 + b_2 \cos\theta \tag{7.61}$$

and employing trigonometry, we may calculate the angle $\theta$ between the trailer and the vehicle as (7.55).

The minus sign, in case $b_1 - b_2 \neq 0$, is the usual case in forward motion, and the plus sign is a solution associated with a backward motion. Both possible configuration $\theta$ for a set of $(R_t, b_1, b_2)$ are shown in Figure 7.21. The $\theta_2$ is called a **jackknifing** configuration. ∎

**Example 270 ★** *Two possible trailer-vehicle angles.*
    *Consider a four-wheel vehicle that is pulling a one-axle trailer with the following dimensions:*

$$
\begin{aligned}
l &= 103.1\,\text{in} \approx 2.619\,\text{m} \\
w &= 61.6\,\text{in} \approx 1.565\,\text{m} \\
b_1 &= 24\,\text{in} \approx 0.61\,\text{m} \\
b_2 &= 90\,\text{in} \approx 2.286\,\text{m} \\
\delta_i &= 12\,\text{deg} \approx 0.209\,\text{rad}
\end{aligned}
\tag{7.62}
$$

*The kinematic steering characteristics of the vehicle would be*

$$
\begin{aligned}
\delta_o &= \cot^{-1}\left(\frac{w}{l} + \cot\delta_i\right) \\
&= 0.186\,\text{rad} \approx 10.661\,\text{deg}
\end{aligned}
\tag{7.63}
$$

$$
\begin{aligned}
R_t &= \sqrt{\left(l\cot\delta_i + \frac{1}{2}w\right)^2 + b_1^2 - b_2^2} \\
&= 509.57\,\text{in} \approx 12.943\,\text{m}
\end{aligned}
\tag{7.64}
$$

$$
\begin{aligned}
R_1 &= l\cot\delta_i + \frac{1}{2}w \\
&= 516.9\,\text{in} \approx 13.129\,\text{m}
\end{aligned}
\tag{7.65}
$$

$$
\begin{aligned}
\delta &= \cot^{-1}\left(\frac{\cot\delta_o + \cot\delta_i}{2}\right) \\
&= 0.19684\,\text{rad} \approx 11.278\,\text{deg}
\end{aligned}
\tag{7.66}
$$

$$
\begin{aligned}
R &= \sqrt{a_2^2 + l^2\cot^2\delta} \\
&= 520.46\,\text{in} \approx 13.219\,\text{m}
\end{aligned}
\tag{7.67}
$$

$$
\begin{aligned}
\theta &= 2\tan^{-1}\left[\frac{1}{b_1 - b_2}\left(R_t \pm \sqrt{R_t^2 - b_1^2 + b_2^2}\right)\right] \\
&= \begin{cases} -3.0132\,\text{rad} \approx -172.64\,\text{deg} \\ \phantom{-}0.22121\,\text{rad} \approx 12.674\,\text{deg} \end{cases}
\end{aligned}
\tag{7.68}
$$

**Example 271 ★** *Space requirement.*
    *The kinematic steering condition can be used to calculate the space requirement of a vehicle with a trailer during a turn. Consider that the front wheels of a two-axle vehicle with a trailer are steered according to the Ackerman geometry, as shown in Figure 7.22.*
    *The outer point of the front of the vehicle will run on the maximum radius $R_{Max}$, whereas a point on the inner side of the wheel at the trailer's rear*
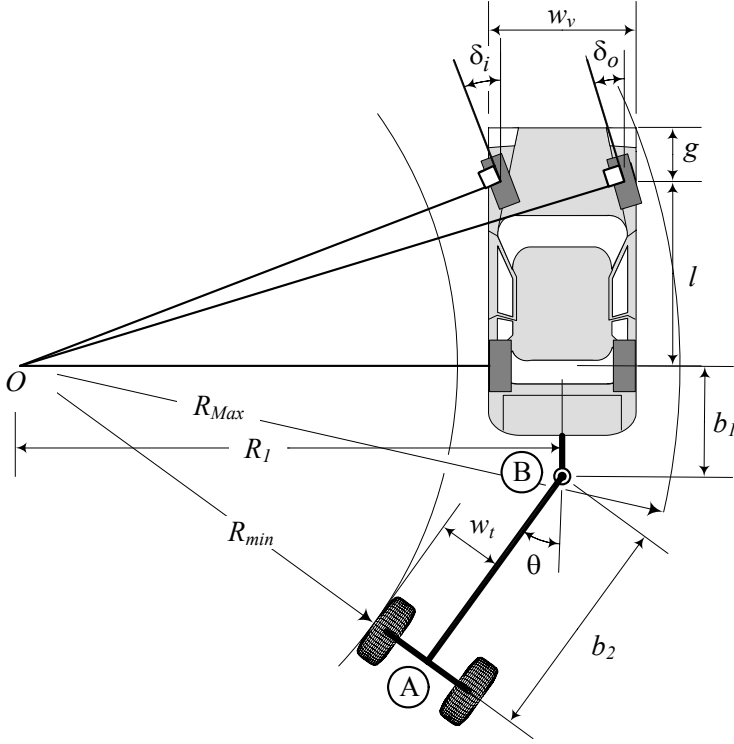
FIGURE 7.22. A two-axle vehicle with a trailer is steered according to the Ackerman condition.

axle will run on the minimum radius $R_{min}$. The maximum radius $R_{Max}$ is

$$R_{Max} = \sqrt{\left(R_1 + \frac{w_v}{2}\right)^2 + (l+g)^2} \qquad (7.69)$$

where

$$R_1 = \sqrt{(R_{min} + w_t)^2 + b_2^2 - b_1^2}. \qquad (7.70)$$

and the width of the vehicle is shown by $w_v$.

The required space for turning the vehicle and trailer is a ring with a width $\triangle R$, which is a function of the vehicle and trailer geometry.

$$\triangle R = R_{Max} - R_{min} \qquad (7.71)$$

The required space $\triangle R$ can be calculated based on the steer angle by

*substituting $R_{min}$*

$$
\begin{aligned}
R_{min} &= R_t - \frac{1}{2}w_t \\
&= \sqrt{\left(l\cot\delta_i + \frac{1}{2}w\right)^2 + b_1^2 - b_2^2} - \frac{1}{2}w_t \\
&= \sqrt{\left(l\cot\delta_o - \frac{1}{2}w\right)^2 + b_1^2 - b_2^2} - \frac{1}{2}w_t \\
&= \sqrt{R^2 - a_2^2 + b_1^2 - b_2^2} - \frac{1}{2}w_t.
\end{aligned}
\tag{7.72}
$$

## 7.4  Steering Mechanisms

A steering system begins with the *steering wheel* or *steering handle*. The driver's steering input is transmitted by a shaft through a gear reduction system, usually rack-and-pinion or recirculating ball bearings. The steering gear output goes to steerable wheels to generate motion through a *steering mechanism*. The lever, which transmits the steering force from the steering gear to the steering linkage, is called *Pitman arm*.

The direction of each wheel is controlled by one steering arm. The steering arm is attached to the steerable wheel hub by a keyway, locking taper, and a hub. In some vehicles, it is an integral part of a one-piece hub and steering knuckle.

To achieve good maneuverability, a minimum steering angle of approximately 35 deg must be provided at the front wheels of passenger cars.

A sample parallelogram steering mechanism and its components are shown in Figure 7.23. The parallelogram steering linkage is common on independent front-wheel vehicles. There are many varieties of steering mechanisms each with some advantages and disadvantages.

**Example 272** *Steering ratio.*

The **Steering ratio** *is the rotation angle of a steering wheel divided by the steer angle of the front wheels. The steering ratio of street cars is around* $10 : 1$ *steering ratio of race cars varies between* $5 : 1$ *to* $20 : 1$.

*The steering ratio of Ackerman steering is different for inner and outer wheels. Furthermore, it has a nonlinear behavior and is a function of the wheel angle.*

**Example 273** *Rack-and-pinion steering.*

*Rack-and-pinion is the most common steering system of passenger cars. Figure 7.24 illustrates a sample rack-and-pinion steering system. The rack is either in front or behind the steering axle. The driver's rotary steering command* $\delta_S$ *is transformed by a steering box to translation* $u_R = u_R(\delta_S)$
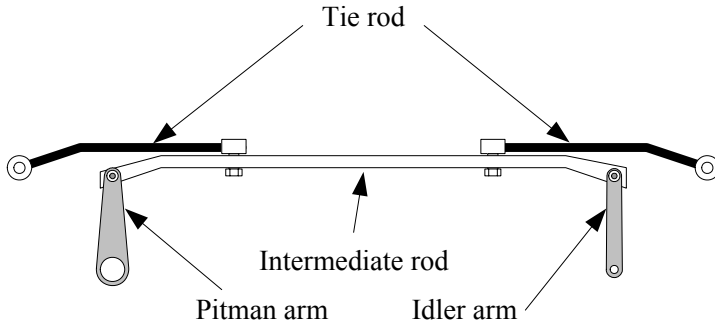
FIGURE 7.23. A sample parallelogram steering linkage and its components.
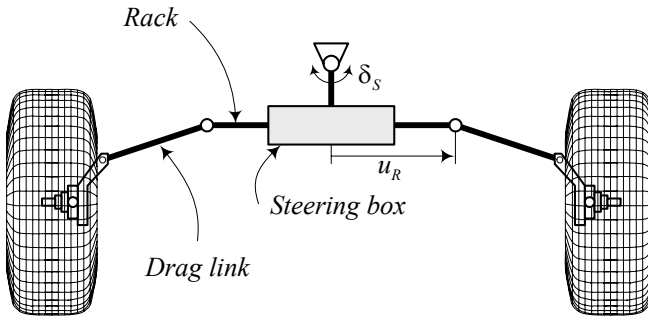


FIGURE 7.24. A rack-and-pinion steering system.

of the racks, and then by the **drag links** to the wheel steering $\delta_i = \delta_i(u_R)$, $\delta_o = \delta_o(u_R)$. The drag link is also called the **tie rod**.

The overall steering ratio depends on the ratio of the steering box and on the kinematics of the steering linkage.

**Example 274** *Lever arm steering system.*

*Figure 7.25 illustrates a steering linkage that sometimes is called a lever arm steering system. Using a lever arm steering system, large steering angles at the wheels are possible. This steering system is used on trucks with large wheel bases and independent wheel suspension at the front axle. The steering box and triangle can also be placed outside of the axle's center.*

**Example 275** *Drag link steering system.*

*It is sometimes better to send the steering command to only one wheel and connect the other one to the first wheel by a drag link, as shown in Figure 7.26. Such steering linkages are usually used for trucks and busses with a front solid axle. The rotations of the steering wheel are transformed by a steering box to the rotation of the steering arm and then to the rotation*
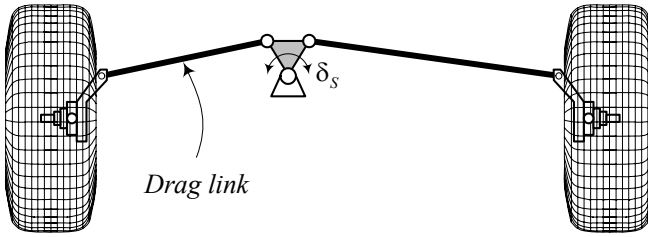
FIGURE 7.25. A lever arm steering system.
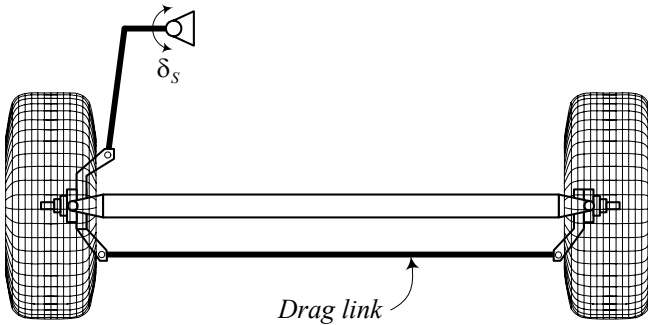


FIGURE 7.26. A drag link steering system.

of the left wheel. A drag link transmits the rotation of the left wheel to the right wheel.

Figure 7.27 shows a sample for connecting a steering mechanism to the Pitman arm of the left wheel and using a trapezoidal linkage to connect the right wheel to the left wheel.

**Example 276** *Multi-link steering mechanism.*

In busses and big trucks, the driver may sit more than $2\,\mathrm{m} \approx 7\,\mathrm{ft}$ *in front of the front axle. These vehicles need large steering angles at the front wheels to achieve good maneuverability. So a more sophisticated multi-link steering mechanism needed. A sample multi-link steering mechanism is shown in Figure 7.28.*

The rotations of the steering wheel are transformed by the steering box to a steering lever arm. The lever arm is connected to a distributing linkage, which turns the left and right wheels by a long tire rod.

**Example 277 ★** *Reverse efficiency.*

The ability of the steering mechanism to feedback the road inputs to the driver is called **reverse efficiency**. Feeling the applied steering torque or aligning moment helps the driver to make smoother turn.

Rack-and-pinion and recirculating ball steering gears have a feedback of
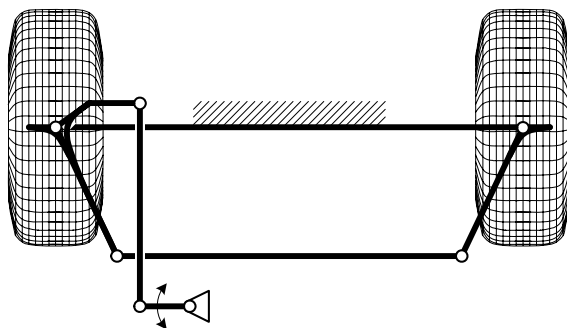
FIGURE 7.27. Connection of the Pitman arm to a trapezoidal steering mechanism.
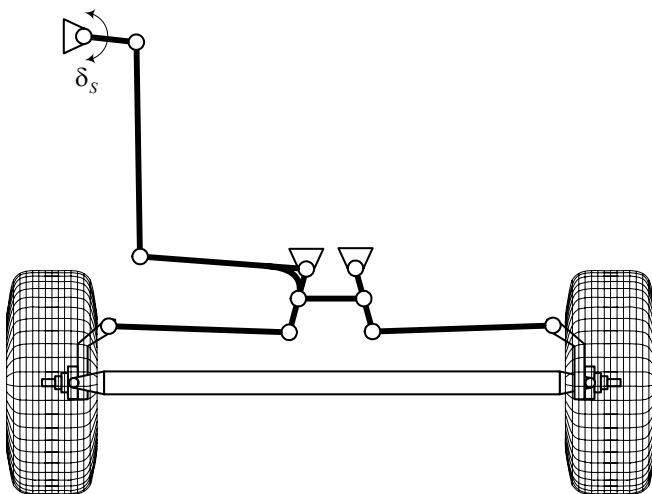


FIGURE 7.28. A multi-link steering mechanism.

the wheels steering torque to the driver. However, worm and sector steering gears have very weak feedback. Low feedback may be desirable for off-road vehicles, to reduce the driver's fatigue.

Because of safety, the steering torque feedback should be proportional to the speed of the vehicle. In this way, the required torque to steer the vehicle is higher at higher speeds. Such steering prevents a sharp and high steer angle. A steering damper with a damping coefficient increasing with speed is the mechanism that provides such behavior. A steering damper can also reduce shimmy vibrations.

**Example 278** ★ *Power steering.*

Power steering has been developed in the 1950s when a hydraulic power steering assist was first introduced. Since then, power assist has become a standard component in automotive steering systems. Using hydraulic pressure, supplied by an engine-driven pump, amplifies the driver-applied torque at the steering wheel. As a result, the steering effort is reduced.

In recent years, electric torque amplifiers were introduced in automotive steering systems as a substitute for hydraulic amplifiers. Electrical steering eliminates the need for the hydraulic pump. Electric power steering is more efficient than conventional power steering, because the electric power steering motor needs to provide assistance when only the steering wheel is turned, whereas the hydraulic pump runs constantly. The assist level is also tunable by vehicle type, road speed, and driver preference.

**Example 279** *Bump steering.*

The steer angle generated by the vertical motion of the wheel with respect to the body is called **bump steering**. Bump steering is usually an undesirable phenomenon and is a function of the suspension and steering mechanisms. If the vehicle has a bump steering character, then the wheel steers when it runs over a bump or when the vehicle rolls in a turn. As a result, the vehicle will travel in a path not selected by the driver.

Bump steering occurs when the end of the tie rod is not at the instant center of the suspension mechanism. Hence, in a suspension deflection, the suspension and steering mechanisms will rotate about different centers.

**Example 280** ★ *Offset steering axis.*

Theoretically, the steering axis of each steerable wheel must vertically go through the center of the wheel at the tire-plane to minimize the required steering torque. Figure 7.27 is an example of matching the center of a wheel with the steering axis. However, it is possible to attach the wheels to the steering mechanism, using an offset design, as shown in Figure 7.29.

Figure 7.30 depicts a steered trapezoidal mechanism with an offset wheel attachment. The path of motion for the center of the tireprint for an offset design is a circle with radius e equal to the value of the offset arm. Such a design is not recommended for street vehicles, especially because of the huge steering torque in stationary vehicle. However, the steering torque
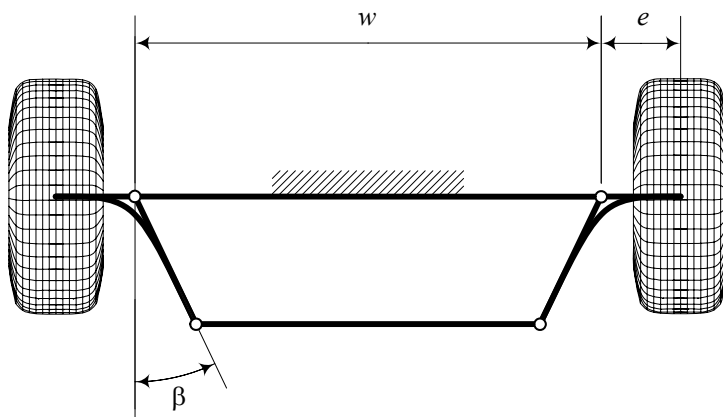
FIGURE 7.29. An offset design for wheel attachment to an steering mechanism.



*Path of motion for the center*
*of the tireprint*
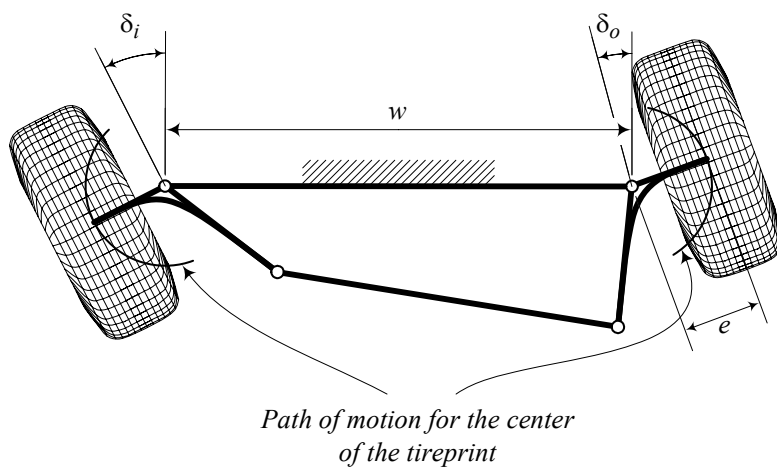
FIGURE 7.30. Offset attachment of steerable wheels to a trapezoidal steering mechanism.
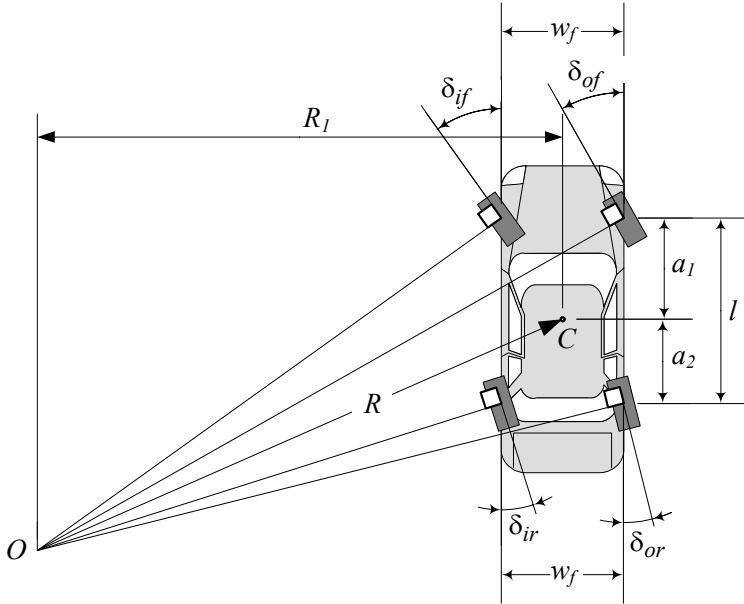
FIGURE 7.31. A positive four-wheel steering vehicle.

*reduces dramatically to an acceptable value when the vehicle is moving. Furthermore, an offset design sometimes makes more room to attach the other devices, and simplifies manufacturing. So, it may be used for small off-road vehicles, such as a mini Baja, and toy vehicles.*

## 7.5  ★ Four wheel steering.

At very low speeds, the kinematic steering condition that the perpendicular lines to each tire meet at one point, must be applied. The intersection point is the *turning center* of the vehicle.

Figure 7.31 illustrates a *positive* four-wheel steering vehicle, and Figure 7.32 illustrates a *negative* $4WS$ vehicle. In a *positive* $4WS$ situation the front and rear wheels steer in the same direction, and in a *negative* $4WS$ situation the front and rear wheels steer opposite to each other. The kinematic condition between the steer angles of a $4WS$ vehicle is

$$\cot \delta_{of} - \cot \delta_{if} = \frac{w_f}{l} - \frac{w_r}{l} \frac{\cot \delta_{of} - \cot \delta_{if}}{\cot \delta_{or} - \cot \delta_{ir}} \tag{7.73}$$

where, $w_f$ and $w_r$ are the front and rear tracks, $\delta_{if}$ and $\delta_{of}$ are the steer angles of the front inner and outer wheels, $\delta_{ir}$ and $\delta_{or}$ are the steer angles of the rear inner and outer wheels, and $l$ is the wheelbase of the vehicle.
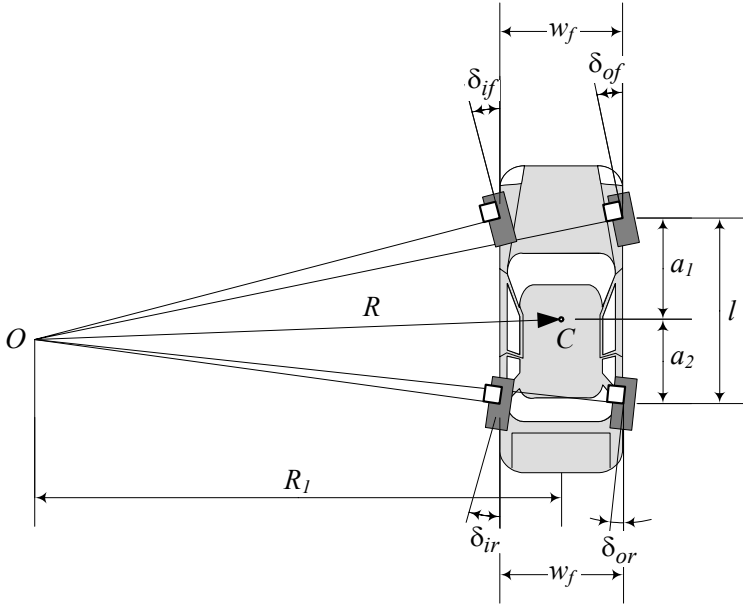
FIGURE 7.32. A negative four-wheel steering vehicle.

We may also use the following more general equation for the kinematic condition between the steer angles of a $4WS$ vehicle

$$\cot \delta_{fr} - \cot \delta_{fl} = \frac{w_f}{l} - \frac{w_r}{l} \frac{\cot \delta_{fr} - \cot \delta_{fl}}{\cot \delta_{rr} - \cot \delta_{rl}} \qquad (7.74)$$

where, $\delta_{fl}$ and $\delta_{fr}$ are the steer angles of the front left and front right wheels, and $\delta_{rl}$ and $\delta_{rr}$ are the steer angles of the rear left and rear right wheels.

If we define the steer angles according to the sign convention shown in Figure 7.33 then, Equation (7.73) expresses the kinematic condition for both, positive and negative $4WS$ systems. Employing the wheel coordinate frame $(x_w, y_w, z_w)$, we define the steer angle as the angle between the vehicle $x$-axis and the wheel $x_w$-axis, measured about the $z$-axis. Therefore, a steer angle is positive when the wheel is turned to the left, and it is negative when the wheel is turned to the right.

**Proof.** The slip-free condition for wheels of a $4WS$ in a turn requires that the normal lines to the center of each tire-plane intersect at a common point. This is the kinematic steering condition.

Figure 7.34 illustrates a positive $4WS$ vehicle in a left turn. The turning center $O$ is on the left, and the inner wheels are the left wheels that are closer to the turning center. The longitudinal distance between point $O$ and the axles of the car are indicated by $c_1$, and $c_2$ measured in the body

(*Positive steer angle*)                    (*Negative steer angle*)
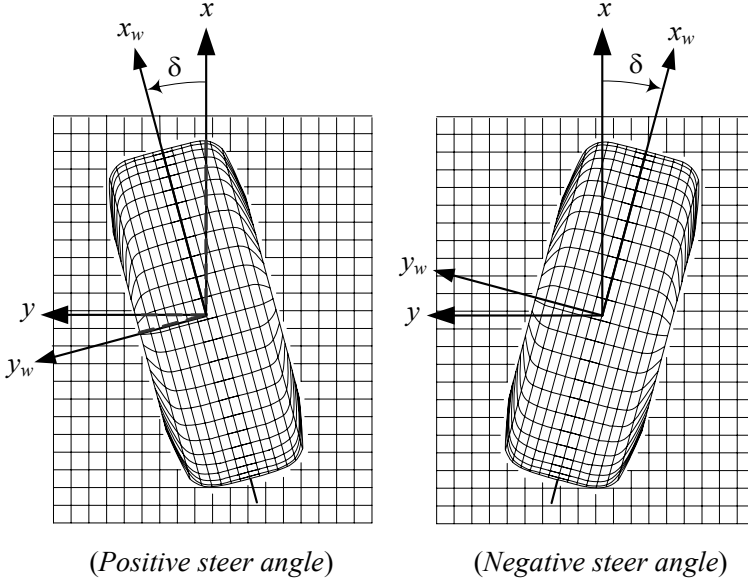
FIGURE 7.33. Sign convention for steer angles.

coordinate frame.

The front inner and outer steer angles $\delta_{if}$, $\delta_{of}$ may be calculated from the triangles $\triangle OAE$ and $\triangle OBF$, while the rear inner and outer steer angles $\delta_{ir}$, $\delta_{or}$ may be calculated from the triangles $\triangle ODG$ and $\triangle OCH$ as follows.

$$\tan \delta_{if} = \frac{c_1}{R_1 - \dfrac{w_f}{2}} \tag{7.75}$$

$$\tan \delta_{of} = \frac{c_1}{R_1 + \dfrac{w_f}{2}} \tag{7.76}$$

$$\tan \delta_{ir} = \frac{c_2}{R_1 - \dfrac{w_r}{2}} \tag{7.77}$$

$$\tan \delta_{or} = \frac{c_2}{R_1 + \dfrac{w_r}{2}} \tag{7.78}$$

Eliminating $R_1$

$$R_1 = \frac{1}{2} w_f + \frac{c_1}{\tan \delta_{if}} \tag{7.79}$$

$$= -\frac{1}{2} w_f + \frac{c_1}{\tan \delta_{of}} \tag{7.80}$$
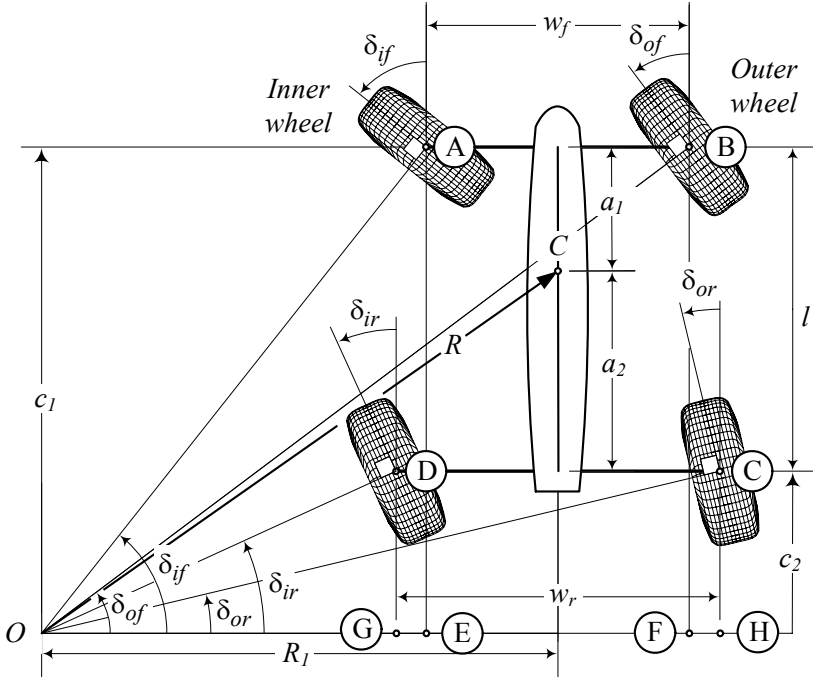
FIGURE 7.34. Illustration of a negative four-wheel steering vehicle in a left turn.

between (7.75) and (7.76) provides the kinematic condition between the front steering angles $\delta_{if}$ and $\delta_{of}$.

$$\cot \delta_{of} - \cot \delta_{if} = \frac{w_f}{c_1} \tag{7.81}$$

Similarly, we may eliminate $R_1$

$$R_1 = \frac{1}{2}w_r + \frac{c_2}{\tan \delta_{ir}} \tag{7.82}$$

$$= -\frac{1}{2}w_r + \frac{c_2}{\tan \delta_{or}} \tag{7.83}$$

between (7.77) and (7.78) to provide the kinematic condition between the rear steering angles $\delta_{ir}$ and $\delta_{or}$.

$$\cot \delta_{or} - \cot \delta_{ir} = \frac{w_r}{c_2} \tag{7.84}$$

Using the following constraint

$$c_1 - c_2 = l \tag{7.85}$$
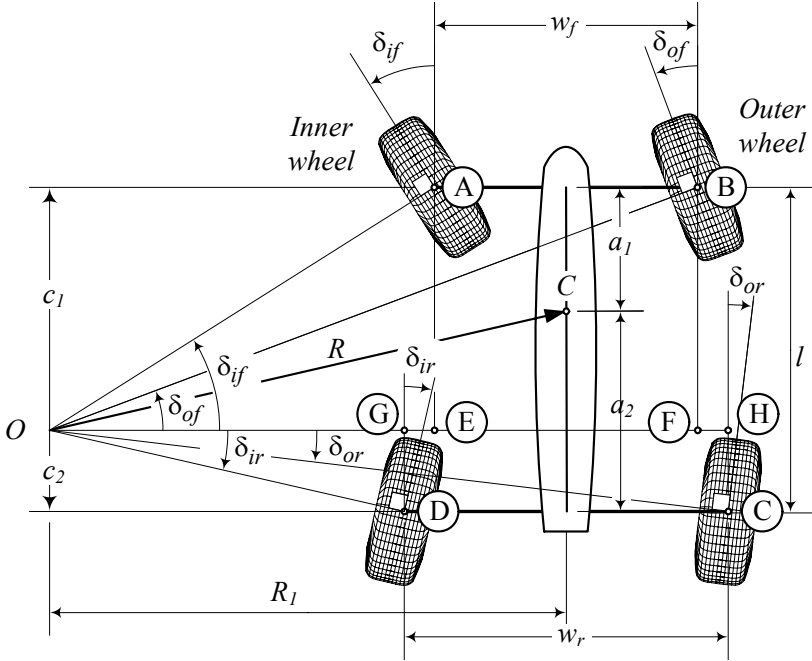
FIGURE 7.35. Illustration of a positive four-wheel steering vehicle in a left turn.

we may combine Equations (7.81) and (7.84)

$$\frac{w_f}{\cot \delta_{of} - \cot \delta_{if}} - \frac{w_r}{\cot \delta_{or} - \cot \delta_{ir}} = l \tag{7.86}$$

to find the kinematic condition (7.73) between the steer angles of the front and rear wheels for a positive $4WS$ vehicle.

Figure 7.35 illustrates a negative $4WS$ vehicle in a left turn. The turning center $O$ is on the left, and the inner wheels are the left wheels that are closer to the turning center. The front inner and outer steer angles $\delta_{if}$, $\delta_{of}$ may be calculated from the triangles $\triangle OAE$ and $\triangle OBF$, while the rear inner and outer steer angles $\delta_{ir}$, $\delta_{or}$ may be calculated from the triangles $\triangle ODG$ and $\triangle OCH$ as follows.

$$\tan \delta_{if} = \frac{c_1}{R_1 - \dfrac{w_f}{2}} \tag{7.87}$$

$$\tan \delta_{of} = \frac{c_1}{R_1 + \dfrac{w_f}{2}} \tag{7.88}$$

$$-\tan \delta_{ir} \;=\; \frac{-c_2}{R_1 - \dfrac{w_r}{2}} \tag{7.89}$$

$$-\tan \delta_{or} \;=\; \frac{-c_2}{R_1 + \dfrac{w_r}{2}} \tag{7.90}$$

Eliminating $R_1$

$$R_1 \;=\; \frac{1}{2}w_f + \frac{c_1}{\tan \delta_{if}} \tag{7.91}$$

$$\;=\; -\frac{1}{2}w_f + \frac{c_1}{\tan \delta_{of}} \tag{7.92}$$

between (7.87) and (7.88) provides the kinematic condition between the front steering angles $\delta_{if}$ and $\delta_{of}$.

$$\cot \delta_{of} - \cot \delta_{if} = \frac{w_f}{c_1} \tag{7.93}$$

Similarly, we may eliminate $R_1$

$$R_1 \;=\; \frac{1}{2}w_r + \frac{c_2}{\tan \delta_{ir}} \tag{7.94}$$

$$\;=\; -\frac{1}{2}w_r + \frac{c_2}{\tan \delta_{or}} \tag{7.95}$$

between (7.89) and (7.90) to provide the kinematic condition between the rear steering angles $\delta_{ir}$ and $\delta_{or}$.

$$\cot \delta_{or} - \cot \delta_{ir} = \frac{w_r}{c_2} \tag{7.96}$$

Using the following constraint

$$c_1 - c_2 = l \tag{7.97}$$

we may combine Equations (7.93) and (7.96)

$$\frac{w_f}{\cot \delta_{of} - \cot \delta_{if}} - \frac{w_r}{\cot \delta_{or} - \cot \delta_{ir}} = l \tag{7.98}$$

to find the kinematic condition (7.73) between the steer angles of the front and rear wheels for a negative $4WS$ vehicle.

Using the sign convention shown in Figure 7.33, we may re-examine Figures 7.35 and 7.34. When the steer angle of the front wheels are positive then, the steer angle of the rear wheels are negative in a negative $4WS$ system, and are positive in a positive $4WS$ system. Therefore, Equation (7.74)

$$\cot \delta_{fr} - \cot \delta_{fl} = \frac{w_f}{l} - \frac{w_r}{l}\frac{\cot \delta_{fr} - \cot \delta_{fl}}{\cot \delta_{rr} - \cot \delta_{rl}} \tag{7.99}$$

can express the kinematic condition for both, positive and negative $4WS$ systems. Similarly, the following equations can uniquely determine $c_1$ and $c_2$ regardless of the positive or negative $4WS$ system.

$$c_1 = \frac{w_f}{\cot \delta_{fr} - \cot \delta_{fl}} \qquad (7.100)$$

$$c_2 = \frac{w_r}{\cot \delta_{rr} - \cot \delta_{rl}} \qquad (7.101)$$

Four-wheel steering or all wheel steering $AWS$ may be applied on vehicles to improve steering response, increase the stability at high speeds maneuvering, or decrease turning radius at low speeds. A negative $4WS$ has shorter turning radius $R$ than a front-wheel steering $FWS$ vehicle.

For a $FWS$ vehicle, the perpendicular to the front wheels meet at a point on the extension of the rear axle. However, for a $4WS$ vehicle, the intersection point can be any point in the $xy$ plane. The point is the *turning center* of the car and its position depends on the steer angles of the wheels. Positive steering is also called *same steer*, and a negative steering is also called *counter steer*.  ∎

**Example 281 ★** *Steering angles relationship.*
   *Consider a car with the following dimensions.*

$$l = 2.8\,\mathrm{m}$$
$$w_f = 1.35\,\mathrm{m}$$
$$w_r = 1.4\,\mathrm{m} \qquad (7.102)$$

*The set of equations (7.75)-(7.78) which are the same as (7.87)-(7.90) must be used to find the kinematic steer angles of the tires. Assume one of the angles, such as*

$$\delta_{if} = 15 \deg \qquad (7.103)$$

*is a known input steer angle. To find the other steer angles, we need to know the position of the turning center $O$. The position of the turning center can be determined if we have one of the three parameters $c_1$, $c_2$, $R_1$. To clarify this fact, let's assume that the car is turning left and we know the value of $\delta_{if}$. Therefore, the perpendicular line to the front left wheel is known. The turning center can be any point on this line. When we pick a point, the other wheels can be adjusted accordingly.*

*The steer angles for a $4WS$ system is a set of four equations, each with two variables.*

$$\delta_{if} = \delta_{if}(c_1, R_1) \qquad (7.104)$$
$$\delta_{of} = \delta_{of}(c_1, R_1) \qquad (7.105)$$
$$\delta_{ir} = \delta_{ir}(c_2, R_1) \qquad (7.106)$$
$$\delta_{or} = \delta_{or}(c_2, R_1) \qquad (7.107)$$

*If $c_1$ and $R_1$ are known, we will be able to determine the steer angles $\delta_{if}$, $\delta_{of}$, $\delta_{ir}$, and $\delta_{or}$ uniquely. However, a practical situation is when we have one of the steer angles, such as $\delta_{if}$, and we need to determine the required steer angle of the other wheels, $\delta_{of}$, $\delta_{ir}$, $\delta_{or}$. It can be done if we know $c_1$ or $R_1$.*

*The turning center is the curvature center of the path of motion. If the path of motion is known, then at any point of the road, the turning center can be found in the vehicle coordinate frame.*

*In this example, let's assume*

$$R_1 = 50\,\mathrm{m} \tag{7.108}$$

*therefore, from Equation (7.75), we have*

$$
\begin{aligned}
c_1 &= \left(R_1 - \frac{w_f}{2}\right)\tan\delta_{if} \\
&= \left(50 - \frac{1.35}{2}\right)\tan\frac{\pi}{12} = 13.217\,\mathrm{m} \tag{7.109}
\end{aligned}
$$

*Because $c_1 > l$ and $\delta_{if} > 0$ the vehicle is in a positive $4WS$ configuration and the turning center is behind the car.*

$$
\begin{aligned}
c_2 &= c_1 - l \\
&= 13.217 - 2.8 = 10.417\,\mathrm{m}. \tag{7.110}
\end{aligned}
$$

*Now, employing Equations (7.76)-(7.78) provides the other steer angles.*

$$
\begin{aligned}
\delta_{of} &= \tan^{-1}\frac{c_1}{R_1 + \dfrac{w_f}{2}} = \tan^{-1}\frac{13.217}{50 + \dfrac{1.35}{2}} \\
&= 0.25513\,\mathrm{rad} \approx 14.618\,\mathrm{deg} \tag{7.111}
\end{aligned}
$$

$$
\begin{aligned}
\delta_{ir} &= \tan^{-1}\frac{c_2}{R_1 - \dfrac{w_r}{2}} = \tan^{-1}\frac{10.417}{50 - \dfrac{1.4}{2}} \\
&= 0.20824\,\mathrm{rad} \approx 11.931\,\mathrm{deg} \tag{7.112}
\end{aligned}
$$

$$
\begin{aligned}
\delta_{or} &= \tan^{-1}\frac{c_2}{R_1 + \dfrac{w_r}{2}} = \tan^{-1}\frac{10.417}{50 + \dfrac{1.4}{2}} \\
&= 0.202\,64\,\mathrm{rad} \approx 11.61\,\mathrm{deg} \tag{7.113}
\end{aligned}
$$

**Example 282 ★** *Position of the turning center.*
*The turning center of a vehicle, in the vehicle body coordinate frame, is at a point with coordinates $(x_O, y_O)$. The coordinates of the turning center*

*are*

$$
\begin{aligned}
x_O &= -a_2 - c_2 \\
&= -a_2 - \frac{w_r}{\cot \delta_{or} - \cot \delta_{ir}} & (7.114) \\
y_O &= R_1 \\
&= \frac{l + \dfrac{1}{2}\left(w_f \tan \delta_{if} - w_r \tan \delta_{ir}\right)}{\tan \delta_{if} - \tan \delta_{ir}}. & (7.115)
\end{aligned}
$$

*Equation (7.115) is found by substituting $c_1$ and $c_2$ from (7.91) and (7.94) in (7.97), and define $y_O$ in terms of $\delta_{if}$ and $\delta_{ir}$. It is also possible to define $y_O$ in terms of $\delta_{of}$ and $\delta_{or}$.*

*Equations (7.114) and (7.115) can be used to define the coordinates of the turning center for both positive and negative 4WS systems.*

*As an example, let's examine a car with the following data.*

$$
\begin{aligned}
l &= 2.8 \,\mathrm{m} \\
w_f &= 1.35 \,\mathrm{m} \\
w_r &= 1.4 \,\mathrm{m} \\
a_1 &= a_2 & (7.116)
\end{aligned}
$$

$$
\begin{aligned}
\delta_{if} &= 0.26180 \,\mathrm{rad} \approx 15 \,\mathrm{deg} \\
\delta_{of} &= 0.25513 \,\mathrm{rad} \approx 14.618 \,\mathrm{deg} \\
\delta_{ir} &= 0.20824 \,\mathrm{rad} \approx 11.931 \,\mathrm{deg} \\
\delta_{or} &= 0.20264 \,\mathrm{rad} \approx 11.61 \,\mathrm{deg} & (7.117)
\end{aligned}
$$

*and find the position of the turning center.*

$$
\begin{aligned}
x_O &= -a_2 - \frac{w_r}{\cot \delta_{or} - \cot \delta_{ir}} \\
&= -\frac{2.8}{2} - \frac{1.4}{\cot 0.20264 - \cot 0.20824} = -11.802 \,\mathrm{m} & (7.118) \\
y_O &= \frac{l + \dfrac{1}{2}\left(w_f \tan \delta_{if} - w_r \tan \delta_{ir}\right)}{\tan \delta_{if} - \tan \delta_{ir}} \\
&= \frac{2.8 + \dfrac{1}{2}\left(1.35 \tan 0.26180 - 1.4 \tan 0.20824\right)}{\tan 0.26180 - \tan 0.20824} = 50.011 \,\mathrm{m} \ (7.119)
\end{aligned}
$$

*The position of turning center for a $FWS$ vehicle is at*

$$
\begin{aligned}
x_O &= -a_2 \\
y_O &= \frac{1}{2}w_f + \frac{l}{\tan \delta_{if}} & (7.120)
\end{aligned}
$$
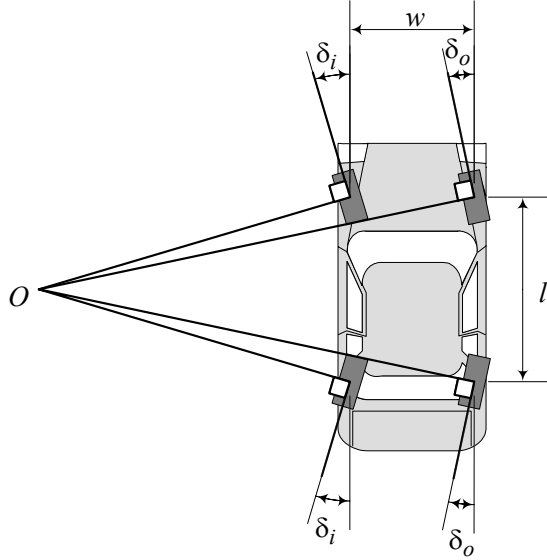
FIGURE 7.36. A symmetric four-wheel steering vehicle.

and for a $RWS$ vehicle is at

$$
\begin{aligned}
x_O &= a_1 \\
y_O &= \frac{1}{2}w_r + \frac{l}{\tan \delta_{ir}}.
\end{aligned}
\tag{7.121}
$$

**Example 283 ★** *Curvature.*

Consider a road as a path of motion that is expressed mathematically by a function $Y = f(X)$, in a global coordinate frame. The radius of curvature $R_\kappa$ of such a road at point $X$ is

$$
R_\kappa = \frac{\left(1 + Y'^2\right)^{3/2}}{Y''}
\tag{7.122}
$$

where

$$
Y' = \frac{dY}{dX}
\tag{7.123}
$$

$$
Y'' = \frac{d^2 Y}{dX^2}.
\tag{7.124}
$$

**Example 284 ★** *Symmetric four-wheel steering system.*

Figure 7.36 illustrates a symmetric $4WS$ vehicle that the front and rear wheels steer opposite to each other equally. The kinematic steering condition for a symmetric steering is simplified to

$$
\cot \delta_o - \cot \delta_i = \frac{w_f}{l} + \frac{w_r}{l}
\tag{7.125}
$$

and $c_1$ and $c_2$ are reduced to

$$c_1 = \frac{1}{2}l \tag{7.126}$$

$$c_2 = -\frac{1}{2}l. \tag{7.127}$$

**Example 285** ★ $c_2/c_1$ *ratio.*

Longitudinal distance of the turning center of a vehicle from the front axle is $c_1$ and from the rear axle is $c_2$. We show the ratio of these distances by $c_s$ and call it the $4WS$ **factor**.

$$
\begin{aligned}
c_s &= \frac{c_2}{c_1} \\
&= \frac{w_r}{w_f} \frac{\cot \delta_{fr} - \cot \delta_{fl}}{\cot \delta_{rr} - \cot \delta_{rl}}
\end{aligned} \tag{7.128}
$$

$c_s$ is negative for a negative $4WS$ vehicle and is positive for a positive $4WS$ vehicle. When $c_s = 0$, the car is $FWS$, and when $c_s = -\infty$, the car is $RWS$. A symmetric $4WS$ system has $c_s = -\frac{1}{2}$.

**Example 286** ★ *Steering length $l_s$.*

For a $4WS$ vehicle, we may define a **steering length** $l_s$ as

$$
\begin{aligned}
l_s &= \frac{c_1 + c_2}{l} = \frac{l}{c_1} + 2c_s \\
&= \frac{1}{l} \left( \frac{w_f}{\cot \delta_{fr} - \cot \delta_{fl}} + \frac{w_r}{\cot \delta_{rr} - \cot \delta_{rl}} \right)
\end{aligned} \tag{7.129}
$$

Steering length $l_s$ is 1 for a $FWS$ car, zero for a symmetric car, and $-1$ for a $RWS$ car. When a car has a negative $4WS$ system then, $-1 < l_s < 1$, and when the car has a positive $4WS$ system then, $1 < l_s$ or $l_s < -1$. The case $1 < l_s$ happens when the turning center is behind the car, and the case $l_s < -1$ happens when the turning center is ahead of the car.

**Example 287** ★ *FWS and Ackerman condition.*

When a car is $FWS$ vehicle, then the Ackerman condition (7.1) can be written as the following equation.

$$\cot \delta_{fr} - \cot \delta_{fl} = \frac{w}{l} \tag{7.130}$$

Writing the Ackerman condition as this equation frees us from checking the inner and outer wheels.

**Example 288** ★ *Turning radius.*

To find the vehicle's turning radius $R$, we may define equivalent bicycle models as shown in Figure 7.37 and 7.38 for positive and negative $4WS$
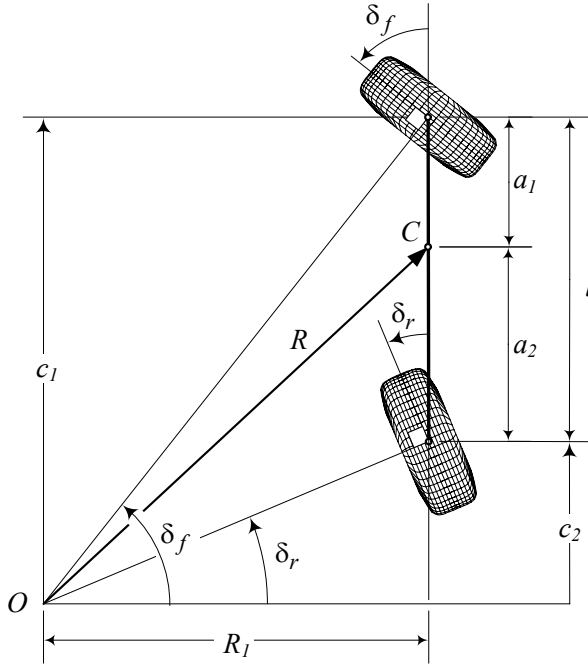
FIGURE 7.37. Bicycle model for a positive $4WS$ vehicle.

*vehicles. The radius of rotation $R$ is perpendicular to the vehicle's velocity vector $\mathbf{v}$ at the mass center $C$.*

*Let's examine the positive $4WS$ situation in Figure 7.37. Using the geometry shown in the bicycle model, we have*

$$
\begin{aligned}
R^2 &= \left(a_2 + c_2\right)^2 + R_1^2 & (7.131)\\
\cot \delta_f &= \frac{R_1}{c_1} \\
&= \frac{1}{2}\left(\cot \delta_{if} + \cot \delta_{of}\right) & (7.132)
\end{aligned}
$$

*and therefore,*

$$
R = \sqrt{\left(a_2 + c_2\right)^2 + c_1^2 \cot^2 \delta_f}. \tag{7.133}
$$

*Examining Figure 7.38 shows that the turning radius of a negative $4WS$ vehicle can be determined from the same equation (7.133).*

**Example 289 ★** *FWS and $4WS$ comparison.*

*The turning center of a FWS car is always on the extension of the rear axel, and its steering length $l_s$ is always equal to 1. However, the turning center of a $4WS$ car can be:*
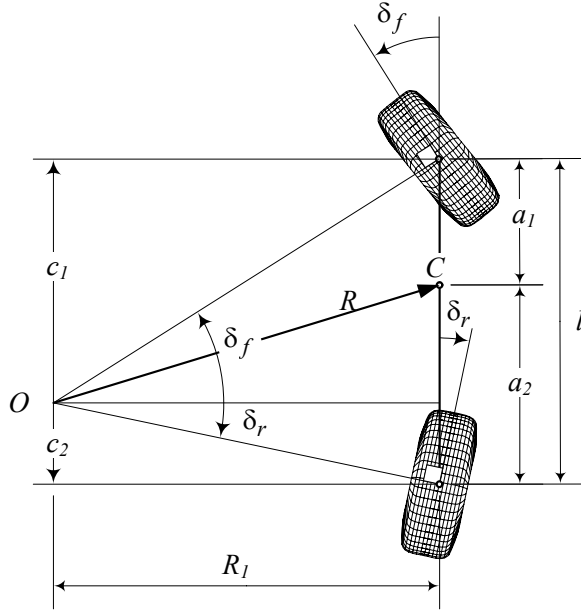
FIGURE 7.38. Bicycle model for a negative $4WS$ vehicle.

1— *ahead of the front axle, if $l_s < -1$*
2— *for a FWS car, if $-1 < l_s < 1$ or*
3— *behind the rear axle, if $1 < l_s$*

*A comparison among the different steering lengths is illustrated in Figure 7.39. A FWS car is shown in Figure 7.39(a), while the 4WS systems with $l_s < -1$, $-1 < l_s < 1$, and $1 < l_s$ are shown in Figures 7.39(b)-(d) respectively.*

**Example 290** ★ *Passive and active four-wheel steering.*
   *The negative $4WS$ is not recommended at high speeds because of high yaw rates, and the positive steering is not recommended at low speeds because of increasing radius of turning. Therefore, to maximize the advantages of a 4WS system, we need a smart system to allow the wheels to change the mode of steering depending on the speed of the vehicle and adjust the steer angles for different purposes. A **smart steering** is also called **active steering** system.*
   *An active system may provide a negative steering at low speeds and a positive steering at high speeds. In a negative steering, the rear wheels are steered in the opposite direction as the front wheels to turn in a significantly smaller radius, while in positive steering, the rear wheels are steered in the same direction as the front wheels to increase the lateral force.*
   *When the 4WS system is passive, there is a constant proportional ratio*
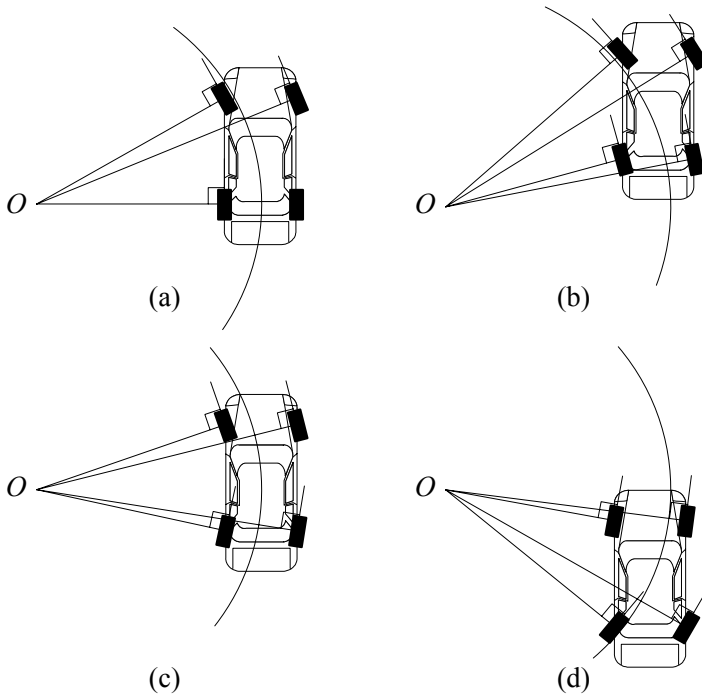
FIGURE 7.39. A comparison among the different steering lengths.

between the front and rear steer angles which is equivalent to have a constant $c_s$.

A passive steering may be applied in vehicles to compensate some vehicle tendencies. As an example, in a $FWS$ system, the rear wheels tend to steer slightly to the outside of a turn. Such tendency can reduce stability.

**Example 291 ★** *Autodriver.*

Consider a car that is moving on a road, as shown in Figure 7.40. Point $O$ indicates the center of curvature of the road at the car's position. Center of curvature of the road is supposed to be the turning center of the car at the instant of consideration.

There is a global coordinate frame $G$ attached to the ground, and a vehicle coordinate frame $B$ attached to the car at its mass center $C$. The $z$ and $Z$ axes are parallel and the angle $\psi$ indicates the angle between $X$ and $x$ axes. If $(X_O, Y_O)$ are the coordinates of $O$ in the global coordinate frame $G$ then,
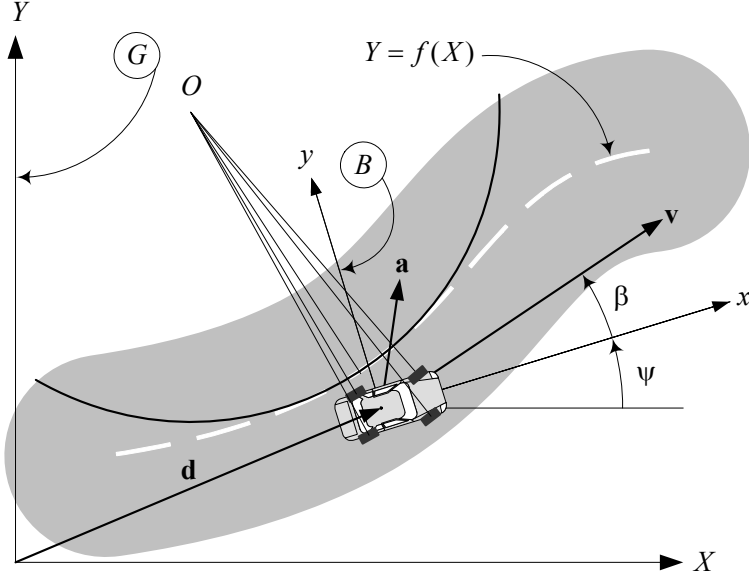
FIGURE 7.40. Illustration of a car that is moving on a road at the point that $O$ is the center of curvature.

*the coordinates of $O$ in $B$ would be*

$$
\begin{aligned}
{}^{B}\mathbf{r}_O &= R_{z,\psi}\, {}^{G}\mathbf{r}_O \\
\begin{bmatrix} x \\ y \\ 0 \end{bmatrix} &= 
\begin{bmatrix} \cos\psi & \sin\psi & 0 \\ -\sin\psi & \cos\psi & 0 \\ 0 & 0 & 1 \end{bmatrix}
\begin{bmatrix} X \\ Y \\ 0 \end{bmatrix} \\
&= \begin{bmatrix} X\cos\psi + Y\sin\psi \\ Y\cos\psi - X\sin\psi \\ 0 \end{bmatrix}.
\end{aligned}
\tag{7.134}
$$

*Having coordinates of $O$ in the vehicle coordinate frame is enough to determine $R_1$, $c_1$, and $c_2$.*

$$
\begin{aligned}
R_1 &= y_O \\
&= Y\cos\psi - X\sin\psi \tag{7.135} \\
c_2 &= -a_2 - x_O \\
&= X\cos\psi + Y\sin\psi - a_2 \tag{7.136} \\
c_1 &= c_2 + l \\
&= X\cos\psi + Y\sin\psi + a_1 \tag{7.137}
\end{aligned}
$$

*Then, the required steer angles of the wheels can be uniquely determined by Equations (7.75)-(7.78).*

It is possible to define a road by a mathematical function $Y = f(X)$ in a global coordinate frame. At any point $X$ of the road, the position of the vehicle and the position of the turning center in the vehicle coordinate frame can be determined. The required steer angles can accordingly be set to keep the vehicle on the road and run the vehicle in the correct direction. This principle may be used to design an **autodriver**.

**Example 292 ★** *Curvature equation.*
    Consider a vehicle that is moving on a path $Y = f(X)$ with velocity **v** and acceleration **a**. The curvature $\kappa = 1/R$ of the path that the vehicle is moving on is

$$\kappa = \frac{1}{R} = \frac{a_n}{v^2} \tag{7.138}$$

where, $a_n$ is the normal component of the acceleration **a**. The normal component $a_n$ is toward the rotation center and is equal to

$$
\begin{aligned}
a_n &= \left| \frac{\mathbf{v}}{v} \times \mathbf{a} \right| = \frac{1}{v} |\mathbf{v} \times \mathbf{a}| \\
&= \frac{1}{v} (a_Y v_X - a_X v_Y) = \frac{\ddot{Y}\dot{X} - \ddot{X}\dot{Y}}{\sqrt{\dot{X}^2 + \dot{Y}^2}}
\end{aligned} \tag{7.139}
$$

and therefore,

$$\kappa = \frac{\ddot{Y}\dot{X} - \ddot{X}\dot{Y}}{\left(\dot{X}^2 + \dot{Y}^2\right)^{3/2}} = \frac{\ddot{Y}\dot{X} - \ddot{X}\dot{Y}}{\dot{X}^3} \frac{1}{\left(1 + \dfrac{\dot{Y}^2}{\dot{Y}^2}\right)^{3/2}}. \tag{7.140}$$

However,

$$Y' = \frac{dY}{dX} = \frac{\dot{Y}}{\dot{X}} \tag{7.141}$$

$$Y'' = \frac{d^2Y}{dX^2} = \frac{d}{dx}\left(\frac{\dot{Y}}{\dot{X}}\right) = \frac{d}{dt}\left(\frac{\dot{Y}}{\dot{X}}\right)\frac{1}{\dot{X}} = \frac{\ddot{Y}\dot{X} - \ddot{X}\dot{Y}}{\dot{X}^3} \tag{7.142}$$

and we find the following equation for the curvature of the path based on the equation of the path.

$$\kappa = \frac{Y''}{(1 + Y'^2)^{3/2}} \tag{7.143}$$

## 7.6   ★ Steering Mechanism Optimization

Optimization means steering mechanism is the design of a system that works as closely as possible to a desired function. Assume the Ackerman

kinematic condition is the desired function for a steering system. Comparing the function of the designed steering mechanism to the Ackerman condition, we may define an error function $e$ to compare the two functions. An example for the $e$ function can be the difference between the outer steer angles of the designed mechanism $\delta_{D_o}$ and the Ackerman $\delta_{A_o}$ for the same inner angle $\delta_i$.

The error function may be the absolute value of the maximum difference,

$$e = \max |\delta_{D_o} - \delta_{A_o}| \tag{7.144}$$

or the root mean square $(RMS)$ of the difference between the two functions

$$e = \sqrt{\int (\delta_{D_o} - \delta_{A_o})^2 \, d\delta_i} \tag{7.145}$$

in a specific range of the inner steer angle $\delta_i$.

The error $e$, would be a function of a set of parameters. Minimization of the error function for a parameter, over the working range of the steer angle $\delta_i$, generates the optimized value of the parameter.

The $RMS$ function (7.145) is defined for continuous variables $\delta_{D_o}$ and $\delta_{A_o}$. However, depending on the designed mechanism, it is not always possible to find a closed-form equation for $e$. In this case, the error function cannot be defined explicitly, and hence, the error function should be evaluated for $n$ different values of the inner steer angle $\delta_i$ numerically. The error function for a set of discrete values of $e$ is define by

$$e = \sqrt{\frac{1}{n} \sum_{i=1}^{n} (\delta_{D_o} - \delta_{A_o})^2}. \tag{7.146}$$

The error function (7.145) or (7.146) must be evaluated for different values of a parameter. Then a plot for $e = e(parameter)$ can show the trend of variation of $e$ as a function of the parameter. If there is a minimum for $e$, then the optimal value for the parameter can be found. Otherwise, the trend of the $e$ function can show the direction for minimum searching.

**Example 293 ★** *Optimized trapezoidal steering mechanism.*

*The inner-outer angles relationship for a trapezoidal steering mechanism, shown in Figure 7.6, is*

$$\sin(\beta + \delta_i) + \sin(\beta - \delta_o)$$
$$= \frac{w}{d} + \sqrt{\left(\frac{w}{d} - 2\sin\beta\right)^2 - (\cos(\beta - \delta_o) - \cos(\beta + \delta_i))^2}. \tag{7.147}$$

*Comparing Equation (7.147) with the Ackerman condition,*

$$\cot\delta_o - \cot\delta_i = \frac{w}{l} \tag{7.148}$$

*we may define an error function*

$$e = \sqrt{\frac{1}{n} \sum_{i=1}^{n} (\delta_{D_o} - \delta_{A_o})^2} \qquad (7.149)$$

*and search for its minimum to optimize the trapezoidal steering mechanism.*

Consider a vehicle with the dimensions

$$w = 2.4\,\mathrm{m}$$
$$l = 4.8\,\mathrm{m}. \qquad (7.150)$$

*Let's optimize a trapezoidal steering mechanism for*

$$d = 0.4\,\mathrm{m} \qquad (7.151)$$

*and use $\beta$ as a parameter.*

A plot of comparison between such a mechanism and the Ackerman condition, for a set of different $\beta$, is shown in Figure 7.9, and their difference $\Delta\delta_o = \delta_{D_o} - \delta_{A_o}$ is shown in Figure 7.10.

We may set a value for $\beta$, say $\beta = 6\deg$, and evaluate $\delta_{D_o}$ and $\delta_{A_o}$ at $n = 100$ different values of $\delta_i$ for a working range such as $-40\deg \leq \delta_i \leq 40\deg$. Then, we calculate the associated error function $e$

$$e = \sqrt{\frac{1}{100} \sum_{i=1}^{100} (\delta_{D_o} - \delta_{A_o})^2} \qquad (7.152)$$

*for the specific $\beta$. Now we conduct our calculation again for new values of $\beta$, such as $\beta = 8\deg, 9\deg, \cdots$. Figure 7.41 depicts the function $e = e(\beta)$ with a minimum at $\beta \approx 12\deg$.*

The geometry of the optimal trapezoidal steering mechanism is shown in Figure 7.42(a). The two side arms intersect at point $G$ on their extensions. For an optimal mechanism, the intersection of point $G$ is at the outer side of the rear axle. However, it is recommended to put the intersection point at the center of the rear axle and design a near optimal trapezoidal steering mechanism. Using the recommendation, it is possible to eliminate the optimization process and get a good enough design. Such an estimated design is shown in Figure 7.42(b). The angle $\beta$ for the optimal design is $\beta = 12.6\deg$, and for the estimated design is $\beta = 13.9\deg$.

**Example 294 ★** *There is no exact Ackerman mechanism.*

It is not possible to make a simple steering linkage to work exactly based on the Ackerman steering condition. However, it is possible to optimize various steering linkages for a working range, to work closely to the Ackerman condition, and be exact at a few points. An isosceles trapezoidal linkage is
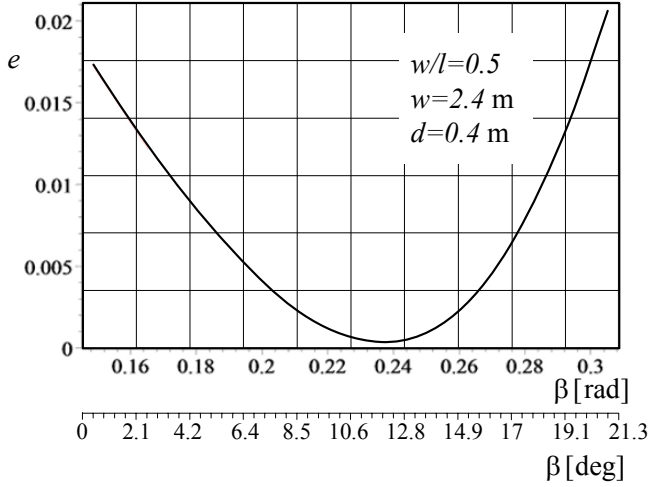
FIGURE 7.41. Error function $e = e(\beta)$ for a specific trapezoidal steering mechanism, with a minimum at $\beta \approx 12\,\mathrm{deg}$.

*not as exact as the Ackerman steering at every arbitrary turning radius, however, it is simple enough to be mass produced, and exact enough work in street cars.*

**Example 295** ★ *Optimization of a multi-link steering mechanism.*
*Assume that we want to design a multi-link steering mechanism for a vehicle with the following dimensions.*

$$
\begin{aligned}
w &= 2.4\,\mathrm{m} \\
l &= 4.8\,\mathrm{m} \\
a_2 &= 0.45l
\end{aligned}
\tag{7.153}
$$

*Due to space constraints, the position of some joints of the mechanism are determined as shown in Figure 7.43. However, we may vary the length $x$ to design the best mechanism according to the Ackerman condition.*

$$
\cot \delta_2 - \cot \delta_1 = \frac{w}{l} = \frac{1}{2}
\tag{7.154}
$$

*The steering wheel input $\delta_s$ turns the triangle $PBC$ which turns both the left and the right wheels.*
*The vehicle must be able to turn in a circle with radius $R_m$.*

$$
R_m = 10\,\mathrm{m}
\tag{7.155}
$$

*(a)*                                    *(b)*
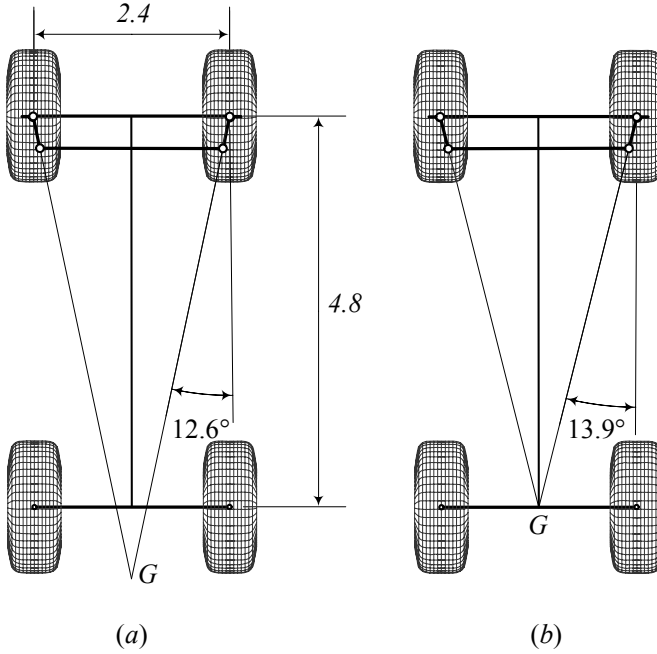
FIGURE 7.42. The geometry of the optimal trapezoidal steering mechanism and the estimated design.

*The minimum turning radius determines the maximum steer angle $\delta$*

$$
\begin{aligned}
R_m &= \sqrt{a_2^2 + l^2 \cot^2 \delta_M} \\
10 &= \sqrt{(0.45 \times 4.8)^2 + 4.8^2 \cot^2 \delta_M} \\
\delta_M &= 0.23713 \, \text{rad} \approx 13.587 \, \text{deg} \qquad\qquad (7.156)
\end{aligned}
$$

*where $\delta$ is the cot-average of the inner and outer steer angles. Having $R$ and $\delta$ is enough to determine $\delta_o$ and $\delta_i$.*

$$
\begin{aligned}
R_1 &= l \cot \delta_M \\
&= 4.8 \cot 0.23713 = 19.861 \, \text{m} \qquad\qquad (7.157) \\
\delta_i &= \tan^{-1} \frac{l}{R_1 - \dfrac{w}{2}} = 0.25176 \, \text{rad} \approx 14.425 \, \text{deg} \qquad (7.158) \\
\delta_o &= \tan^{-1} \frac{l}{R_1 + \dfrac{w}{2}} = 0.22408 \, \text{rad} \approx 12.839 \, \text{deg} \qquad (7.159)
\end{aligned}
$$

*Because the mechanism is symmetric, each wheel of the steering mechanism*
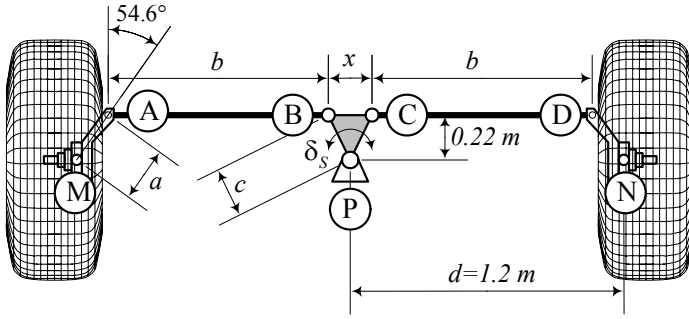
FIGURE 7.43. A multi-link steering mechanism that must be optimized by varying $x$.
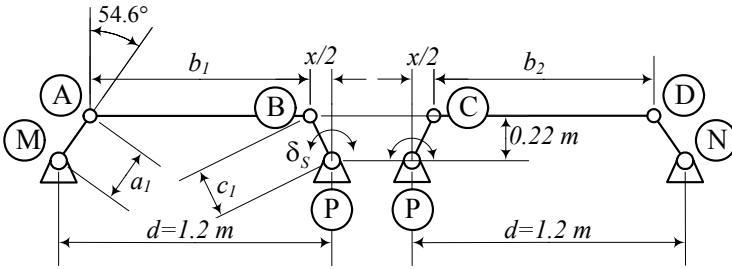


FIGURE 7.44. The multi-link steering is a 6-link mechanism that may be treeted as two combined 4-bar linkages.

*in Figure 7.43 must be able to turn at least* $14.425\,\mathrm{deg}$. *To be safe, we try to optimize the mechanism for* $\delta = \pm 15\,\mathrm{deg}$.

*The multi-link steering mechanism is a six-link Watt linkage. Let us divide the mechanism into two four-bar linkages. The linkage* 1 *is on the left and the linkage* 2 *is on the right, as shown in Figure 7.44. We may assume that* $MA$ *is the input link of the left linkage and* $PB$ *is its output link. Link* $PB$ *is rigidly attached to* $PC$, *which is the input of the right linkage. The output of the right linkage is* $ND$. *To find the inner-outer steer angles relationship, we need to find the angle of* $ND$ *as a function of the angle of* $MA$. *The steer angles can be calculated based on the angle of these two links.*

$$\delta_1 = \theta_2 - (90 - 54.6)\,\mathrm{deg} \qquad (7.160)$$
$$\delta_2 = \varphi_4 - (90 + 54.6)\,\mathrm{deg} \qquad (7.161)$$

*Figure 7.44 illustrates the link numbers, and the input-output angles of the four-bar linkages. The length of the links for the mechanisms are collected in Table 7.1.*
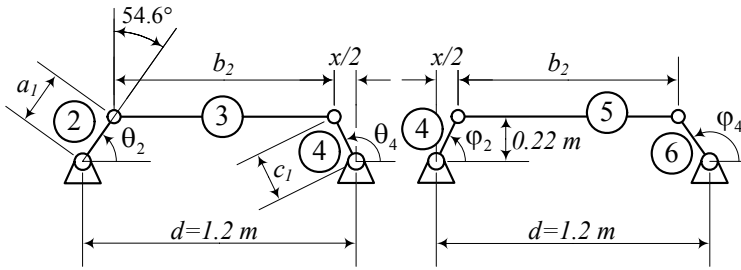
FIGURE 7.45. The input and output angles of the two 4-bar linkages.

Table 7.1 - Link numbers, and the input-output angles
for the multi-link steering mechanism

| Link | Length | angle |
|---|---|---|
| | Left linkage | |
| 1 | $d_1 = 1.2$ | 180 |
| 2 | $a_1 = 0.22/\cos 54.6 = 0.37978$ | $\theta_2$ |
| 3 | $b_1 = 1.2 - 0.22 \tan 54.6 - \frac{x}{2}$ $= 0.89043 - \frac{x}{2}$ | $\theta_3$ |
| 4 | $c_1 = \sqrt{0.22^2 + x^2/4}$ | $\theta_4$ |
| | | |
| | Right linkage | |
| Link | Length | angle |
| 1 | $d_1 = 1.2$ | 180 |
| 4 | $a_1 = \sqrt{0.22^2 + x^2/4}$ | $\varphi_2 = \theta_4 - 2\tan^{-1}\frac{x}{0.44}$ |
| 5 | $b_1 = 0.89043 - \frac{x}{2}$ | $\varphi_3$ |
| 6 | $c_1 = 0.22/\cos 54.6 = 0.37978$ | $\varphi_4$ |

Equation (6.1) that is repeated below, provides the angle $\theta_4$ as a function of $\theta_2$.

$$\theta_4 = 2\tan^{-1}\left(\frac{-B \pm \sqrt{B^2 - 4AC}}{2A}\right) \tag{7.162}$$

$$
\begin{aligned}
A &= J_3 - J_1 + (1 - J_2)\cos\theta_2 & (7.163)\\
B &= -2\sin\theta_2 & (7.164)\\
C &= J_1 + J_3 - (1 + J_2)\cos\theta_2 & (7.165)
\end{aligned}
$$

$$J_1 = \frac{d_1}{a_1} \tag{7.166}$$

$$J_2 = \frac{d_1}{c_1} \tag{7.167}$$

$$J_3 = \frac{a_1^2 - b_1^2 + c_1^2 + d_1^2}{2a_1c_1} \tag{7.168}$$

$$J_4 = \frac{d_1}{b_1} \tag{7.169}$$

$$J_5 = \frac{c_1^2 - d_1^2 - a_1^2 - b_1^2}{2a_1b_1} \tag{7.170}$$

The same equation (7.162) can be used to connect the input-output angles of the right four-bar linkage.

$$\varphi_4 = 2\tan^{-1}\left(\frac{-B \pm \sqrt{B^2 - 4AC}}{2A}\right) \tag{7.171}$$

$$A = J_3 - J_1 + (1 - J_2)\cos\varphi_2 \tag{7.172}$$
$$B = -2\sin\varphi_2 \tag{7.173}$$
$$C = J_1 + J_3 - (1 + J_2)\cos\varphi_2 \tag{7.174}$$

$$J_1 = \frac{d_2}{a_2} \tag{7.175}$$

$$J_2 = \frac{d_2}{c_2} \tag{7.176}$$

$$J_3 = \frac{a_2^2 - b_2^2 + c_2^2 + d_2^2}{2a_2c_2} \tag{7.177}$$

$$J_4 = \frac{d_2}{b_2} \tag{7.178}$$

$$J_5 = \frac{c_2^2 - d_2^2 - a_2^2 - b_2^2}{2a_2b_2} \tag{7.179}$$

Starting with a guess value for $x$, we are able to calculate the length of the links. Using Equations (7.162) and (7.171), along with (7.160) and (7.161), we calculate $\delta_2$ for a given value of $\delta_1$.

Let's start with $x = 0$, then

$$\begin{aligned} a_1 &= 0.37978\,\text{m} \\ b_1 &= 0.89043\,\text{m} \\ c_1 &= 0.22\,\text{m} \end{aligned} \tag{7.180}$$

$$\begin{aligned} a_2 &= 0.22\,\text{m} \\ b_2 &= 0.89043\,\text{m} \\ c_2 &= 0.37978\,\text{m}. \end{aligned} \tag{7.181}$$
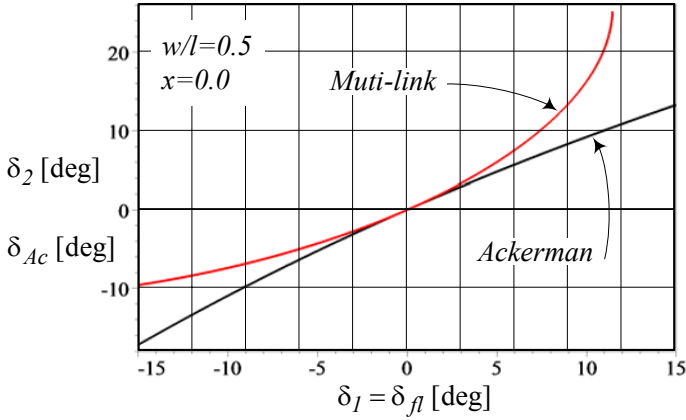
FIGURE 7.46. Steer angles $\delta_2$ and $\delta_{Ac}$ versus $\delta_1$.

*Using Equations (7.160) and (7.162), we may calculate the output of the first four-bar linkage, $\theta_4$, for a range of the left steer angle $-15\deg < \delta_1 < 15\deg$. The following constraint, provides the numerical values for $\varphi_2$ to be used as the input of the right four-bar linkage.*

$$\varphi_2 = \theta_4 - 2\tan^{-1}\frac{x}{0.44} \tag{7.182}$$

*Then, using Equations (7.171) and (7.162), we can calculate the steer angle $\delta_2$ for the right wheel.*

*Figure 7.46 depicts the numerical values of the steer angles $\delta_2$ and $\delta_{Ac}$ versus $\delta_1$. The angle $\delta_{Ac}$ is the steer angle of the right wheel based on the Ackerman equation (7.154).*

*Having $\delta_2$ and $\delta_{Ac}$, we calculate the difference $\Delta$*

$$\Delta = \delta_2 - \delta_{Ac} \tag{7.183}$$

*for $n$ different values of $\delta_1$ in the working range angle $-15\deg < \delta_1 < 15\deg$. Based on the $n$ numbers for $\Delta$, we may find the error $e$.*

$$e = \sqrt{\frac{\Delta^2}{n}} \tag{7.184}$$

*Changing the value of $x$ and recalculating $e$, results an error function $e = e(x)$.*

*Figure 7.47 illustrates the result of the calculation. It shows that the error is minimum for $x = -0.824\,\mathrm{m}$, which is the best length for the base of the triangle $PBC$.*

*The behavior of the multi-link steering mechanism for different values of $x$, is shown in Figure 7.48. The Ackerman condition is also plotted to*
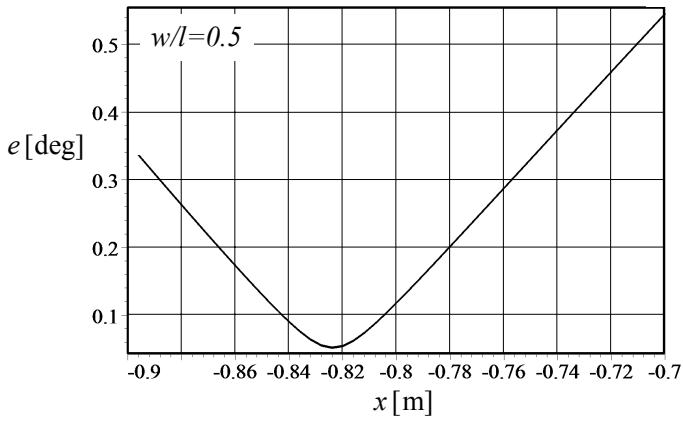
FIGURE 7.47. Illustration of the error function $e = e(x)$.
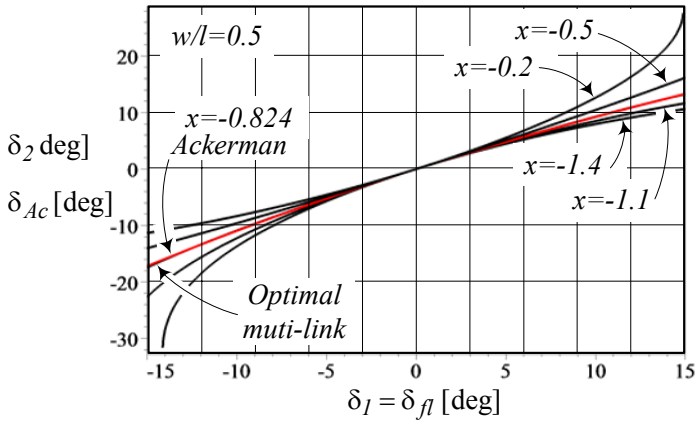


FIGURE 7.48. The behavior of the multi-link steering mechanism for different values of $x$.
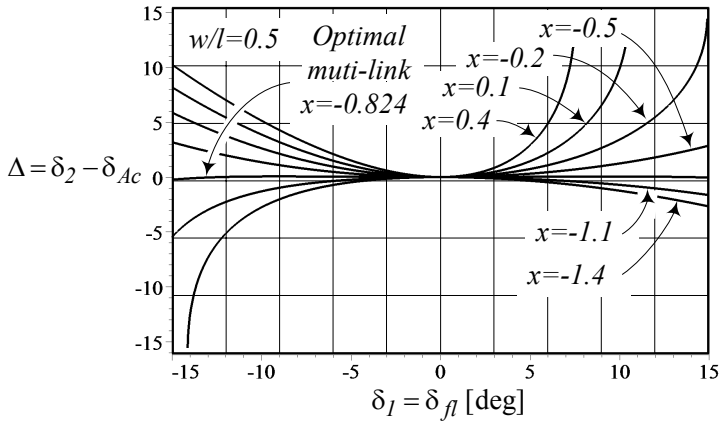
FIGURE 7.49. Illustration of the difference $\Delta = \delta_2 - \delta_{Ac}$ for different values of $x$.
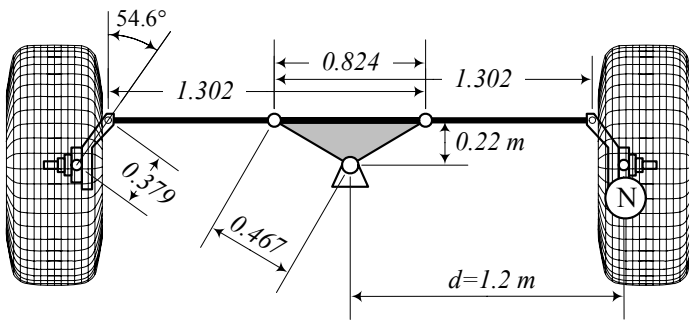


FIGURE 7.50. The optimal multi-link steering mechanism along with the length of its links.

compare with the optimal multi-link mechanism. The optimality of $x = -0.824$ m *may be more clear in Figure 7.49 that shows the difference $\Delta = \delta_2 - \delta_{Ac}$ for different values of $x$.*

*The optimal multi-link steering mechanism along with the length of its links is shown in Figure 7.50. The mechanism and the meaning of negative value for $x$ are shown in Figure 7.51 where the mechanism is in a positive turning position.*

## 7.7  ★ Trailer-Truck Kinematics

Consider a car pulling a one-axle trailer, as shown in Figure 7.52. We may normalize the dimensions such that the length of the trailer is 1. The
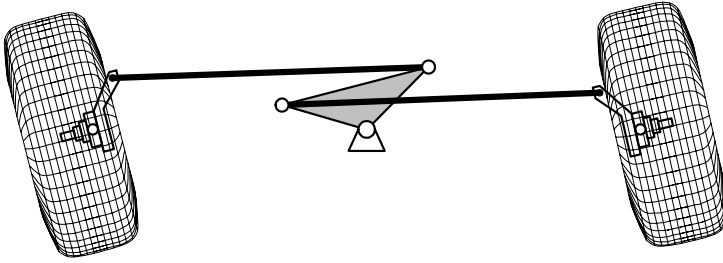
FIGURE 7.51. The optimal multi-link steering mechanism in a positive turning position.
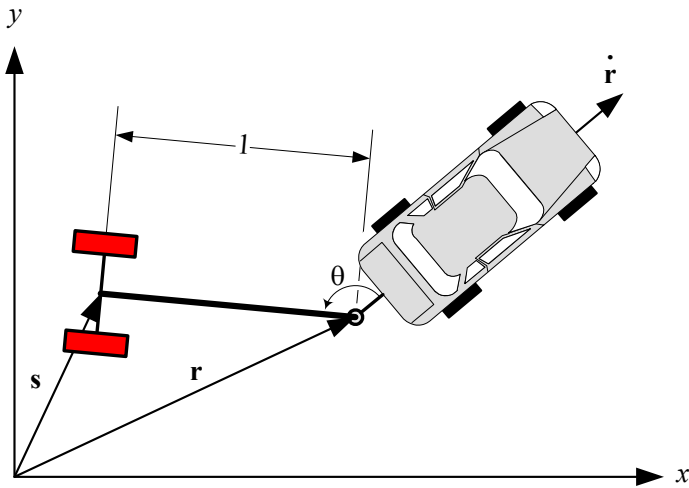


FIGURE 7.52. A car pulling a one-axle trailer.

positions of the car at the hinge point and the trailer at the center of its axle are shown by vectors $\mathbf{r}$ and $\mathbf{s}$.

Assuming $\mathbf{r}$ is a given differentiable function of time $t$, we would like to examine the behavior of the trailer by calculating $\mathbf{s}$, and predict jackknifing. When the car is moving forward, we say the car and trailer are *jackknifed* if

$$\dot{\mathbf{r}} \cdot \mathbf{z} < 0 \qquad (7.185)$$

where

$$\mathbf{z} = \mathbf{r} - \mathbf{s}. \qquad (7.186)$$

A jackknifed configuration is shown in Figure 7.53, while Figure 7.52 is showing an *unjackknifed* configuration.

Mathematically, we want to know if the truck-trailer will jackknife for a
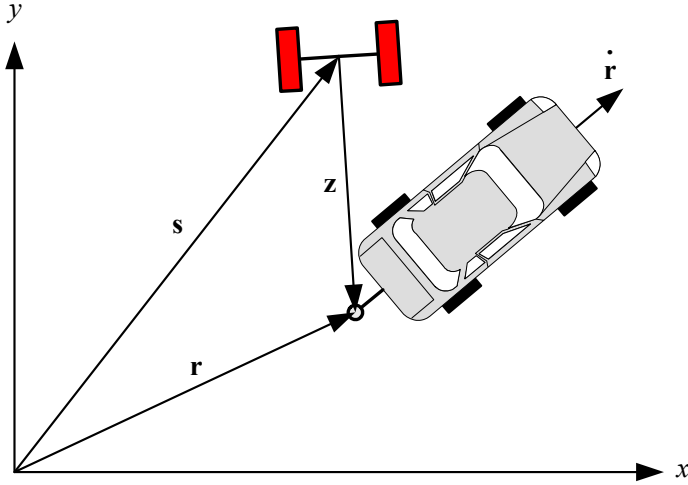
FIGURE 7.53. A jackknifed configuration of a car pulling a one-axle trailer.

given path of motion $\mathbf{r} = \mathbf{r}(t)$ and what conditions we must impose on $\mathbf{r}(t)$ to prevent jackknifing.

The velocity of the trailer can be expressed by

$$\dot{\mathbf{s}} = c\,(\mathbf{r} - \mathbf{s}) \qquad (7.187)$$

where

$$c = \dot{\mathbf{r}} \cdot \mathbf{z} \qquad (7.188)$$

and the unjackknifing condition is

$$c > 0. \qquad (7.189)$$

Assume the twice continuously differentiable function $\mathbf{r}$ is the path of car motion. If $|\mathbf{z}| = 1$, and $\mathbf{r}$ has a radius of curvature $R(t) > 1$, and

$$\dot{\mathbf{r}}(0) \cdot \mathbf{z}(0) > 0 \qquad (7.190)$$

then

$$\dot{\mathbf{r}}(t) \cdot \mathbf{z}(t) > 0 \qquad (7.191)$$

for all $t > 0$.

Therefore, if the car is moving forward and the car-trailer combination is not originally jackknifed, then it will remain unjackknifed.

**Proof.** The normalized trailer length is 1 and is constant, therefore, $\mathbf{z}$ is a unit vector

$$\begin{aligned} |\mathbf{z}| &= |\mathbf{r} - \mathbf{s}| \\ &= 1 \end{aligned} \qquad (7.192)$$

and

$$(\mathbf{r} - \mathbf{s}) \cdot (\mathbf{r} - \mathbf{s}) = 1. \tag{7.193}$$

The nonslip wheels of the trailer constrain the vector $\mathbf{s}$ such that its velocity vector $\dot{\mathbf{s}}$ must be directed along the trailer axis indicated by $\mathbf{z}$.

$$\begin{aligned} \dot{\mathbf{s}} &= c\,(\mathbf{r} - \mathbf{s}) \\ &= c\mathbf{z} \end{aligned} \tag{7.194}$$

Differentiating (7.193) yields

$$2\,(\dot{\mathbf{r}} - \dot{\mathbf{s}}) \cdot (\mathbf{r} - \mathbf{s}) = 0 \tag{7.195}$$
$$\dot{\mathbf{r}} \cdot (\mathbf{r} - \mathbf{s}) = \dot{\mathbf{s}} \cdot (\mathbf{r} - \mathbf{s}) \tag{7.196}$$

and therefore,

$$\dot{\mathbf{r}} \cdot (\mathbf{r} - \mathbf{s}) = c\,(\mathbf{r} - \mathbf{s}) \cdot (\mathbf{r} - \mathbf{s}) \tag{7.197}$$

$$\begin{aligned} c &= \dot{\mathbf{r}} \cdot (\mathbf{r} - \mathbf{s}) \\ &= \dot{\mathbf{r}} \cdot \mathbf{z}. \end{aligned} \tag{7.198}$$

Having $c$ enables us to write Equation (7.194) as

$$\begin{aligned} \dot{\mathbf{s}} &= [\dot{\mathbf{r}} \cdot (\mathbf{r} - \mathbf{s})]\,(\mathbf{r} - \mathbf{s}) \\ &= (\dot{\mathbf{r}} \cdot \mathbf{z})\,\mathbf{z}. \end{aligned} \tag{7.199}$$

There are three situations

1. When $c > 0$, the velocity vector of the trailer $\dot{\mathbf{s}}$ is along the trailer axis $\mathbf{z}$. The trailer follows the car and the system is stable.

2. When $c = 0$, the velocity vector of the trailer $\dot{\mathbf{s}}$ is zero. In this case, the trailer spins about the center of its axle and the system is neutral-stable.

3. When $c < 0$, the velocity vector of the trailer $\dot{\mathbf{s}}$ is along the trailer axis $-\mathbf{z}$. The trailer does not follow the car and the system is unstable.

Using a Cartesian coordinate expression, we may show the car and trailer position vectors by

$$\mathbf{r} = \begin{bmatrix} x_c \\ y_c \end{bmatrix} \tag{7.200}$$

$$\mathbf{s} = \begin{bmatrix} x_t \\ y_t \end{bmatrix} \tag{7.201}$$

and therefore,

$$
\dot{\mathbf{s}} = \begin{bmatrix} \dot{x}_t \\ \dot{y}_t \end{bmatrix} = [\dot{\mathbf{r}} \cdot (\mathbf{r} - \mathbf{s})] (\mathbf{r} - \mathbf{s})
$$

$$
= \begin{bmatrix} \dot{x}_c (x_c - x_t)^2 + (x_c - x_t)(y_c - y_t)\,\dot{y}_c \\ \dot{x}_c (x_c - x_t)(y_c - y_t) + (y_c - y_t)^2\,\dot{y}_c \end{bmatrix} \tag{7.202}
$$

$$
c = (x_c - x_t)\,\dot{x}_c + (y_c - y_t)\,\dot{y}_c
$$

$$
= \dot{x}_c x_c + \dot{y}_c y_c - (\dot{x}_c x_t + \dot{y}_c y_t). \tag{7.203}
$$

Let's define a function $f(t) = \dot{\mathbf{r}} \cdot \mathbf{z}$ and assume that conclusion (7.191) is wrong while assumption (7.190) is correct. Then there exists a time $t_1 > 0$ such that $f(t_1) = 0$ and $f'(t_1) \leq 0$. Using $|\mathbf{z}| = 1$ and $\dot{\mathbf{r}} \neq 0$, we have $\dot{\mathbf{r}}(t_1) \cdot \mathbf{z}(t_1) = 0$ and therefore, $\dot{\mathbf{r}}(t_1)$ is perpendicular to $\mathbf{z}(t_1)$. The derivative $f'(t)$ would be

$$
\begin{aligned}
f'(t) &= \ddot{\mathbf{r}} \cdot \mathbf{z} + \dot{\mathbf{r}} \cdot \dot{\mathbf{z}} \\
&= \ddot{\mathbf{r}} \cdot \mathbf{z} + \dot{\mathbf{r}} \cdot (\dot{\mathbf{r}} - \dot{\mathbf{s}}) \\
&= \ddot{\mathbf{r}} \cdot \mathbf{z} + |\dot{\mathbf{r}}|^2 - \dot{\mathbf{r}} \cdot \dot{\mathbf{s}} \\
&= \ddot{\mathbf{r}} \cdot \mathbf{z} + |\dot{\mathbf{r}}|^2 - \dot{\mathbf{r}} \cdot ((\dot{\mathbf{r}} \cdot \mathbf{z})\,\mathbf{z}) \\
&= \ddot{\mathbf{r}} \cdot \mathbf{z} + |\dot{\mathbf{r}}|^2 - (\dot{\mathbf{r}} \cdot \mathbf{z})^2 \\
&= \ddot{\mathbf{r}} \cdot \mathbf{z} + |\dot{\mathbf{r}}|^2 - f^2(t) \tag{7.204}
\end{aligned}
$$

and therefore,

$$
f'(t_1) = \ddot{\mathbf{r}} \cdot \mathbf{z} + |\dot{\mathbf{r}}|^2. \tag{7.205}
$$

The acceleration $\ddot{\mathbf{r}}$ in a normal-tangential coordinate frame $(\hat{e}_n, \hat{e}_t)$ is

$$
\ddot{\mathbf{r}} = \frac{d\,|\dot{\mathbf{r}}|}{dt}\hat{e}_t + \kappa\,|\dot{\mathbf{r}}|^2\,\hat{e}_n \tag{7.206}
$$

$$
\kappa = \frac{1}{R} \tag{7.207}
$$

where $\hat{e}_n$ and $\hat{e}_t$ are the unit normal and tangential vectors. $\hat{e}_t$ is parallel to $\dot{\mathbf{r}}(t_1)$, and $\hat{e}_n$ is parallel to $\mathbf{z}(t_1)$. Hence,

$$
\ddot{\mathbf{r}} \cdot \mathbf{z} = \pm\kappa(t_1)\,|\dot{\mathbf{r}}(t_1)|^2 \tag{7.208}
$$

and

$$
\begin{aligned}
f'(t_1) &= |\dot{\mathbf{r}}(t_1)|^2 \pm \kappa(t_1)\,|\dot{\mathbf{r}}(t_1)|^2 \\
&= [1 \pm \kappa(t_1)]\,|\dot{\mathbf{r}}(t_1)|^2. \tag{7.209}
\end{aligned}
$$

Because $\kappa(t_1) = 1/R(t) > 0$, we conclude that $f'(t_1) > 0$, and it is not possible to have $f'(t_1) \leq 0$. ∎
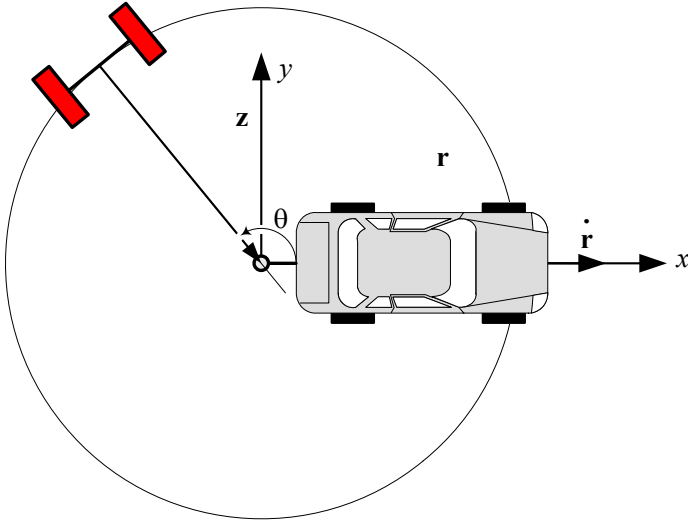
FIGURE 7.54. The initial position of a one-axle trailer pulled by a car moving forward in a straight line with a constant velocity is a circle about the hinge point.

**Example 296** ★ *Straight motion of the car with constant velocity.*

*Consider a car moving forward in a straight line with a constant velocity. We may use a normalization and set the speed of the car as 1 moving in positive x direction starting from $x = 0$. Using a two-dimensional vector expression we have*

$$\mathbf{r} = \left[ \begin{array}{c} x_c \\ y_c \end{array} \right] = \left[ \begin{array}{c} t \\ 0 \end{array} \right]. \tag{7.210}$$

*Because of (7.192), we get*

$$\begin{aligned} \mathbf{z}(0) &= \mathbf{r}(0) - \mathbf{s}(0) \\ &= -\mathbf{s}(0) \end{aligned} \tag{7.211}$$

*and therefore, the initial position of the trailer must lie on a unit circle as shown in Figure 7.54.*

*Using two dimensional vectors, we may express $\mathbf{z}(0)$ as a function of $\theta$*

$$\begin{aligned} \mathbf{z}(0) &= -\mathbf{s}(0) \\ &= \left[ \begin{array}{c} x_t(0) \\ y_t(0) \end{array} \right] = \left[ \begin{array}{c} \cos\theta \\ \sin\theta \end{array} \right] \end{aligned} \tag{7.212}$$

*and simplify Equation (7.202) as*

$$\dot{\mathbf{s}} = \left[ \begin{array}{c} \dot{x}_t \\ \dot{y}_t \end{array} \right] = \left[ \begin{array}{c} (t - x_t)^2 \\ -y_t(t - x_t) \end{array} \right]. \tag{7.213}$$

*Equation (7.213) is a set of two coupled first-order ordinary differential equations with the solution*

$$\mathbf{s} = \begin{bmatrix} x_t \\ y_t \end{bmatrix} = \begin{bmatrix} t + \dfrac{e^{-2t} - C_1}{e^{-2t} + C_1} \\ \dfrac{C_2 e^{-t}}{e^{-2t} + C_1} \end{bmatrix}. \qquad (7.214)$$

*Applying the initial conditions (7.212) we find*

$$C_1 = \frac{\cos\theta - 1}{\cos\theta + 1} \qquad (7.215)$$

$$C_2 = \frac{2\sin\theta}{\cos\theta + 1}. \qquad (7.216)$$

*If $\theta \neq k\pi$, then the solution depends on time, and when time goes to infinity, the solution leads to the following limits asymptotically:*

$$\lim_{t\to\infty} x_t = t - 1$$
$$\lim_{t\to\infty} y_t = 0 \qquad (7.217)$$

*When the car is moving with a constant velocity, this solution shows that the trailer will approach the position of straight forward moving, following the car.*

*We may also consider that the car is backing up. In this situation, the solution shows that, except for the unstable initial condition $\theta = \pi$, all solutions ultimately approach the jackknifed position.*

*If $\theta = 0$, then*

$$\begin{aligned} C_1 &= 0 \\ C_2 &= 0 \\ x_t &= t + 1 \\ y_t &= 0 \end{aligned} \qquad (7.218)$$

*and the trailer moves in an unstable configuration. Any deviation from $\theta = 0$ ends up to change the situation and leads to the stable limiting solution (7.217).*

*If $\theta = \pi$, then*

$$\begin{aligned} C_1 &= \infty \\ C_2 &= \infty \\ x_t &= t - 1 \\ y_t &= 0 \end{aligned} \qquad (7.219)$$

*and the trailer follows the car in an stable configuration. Any deviation from $\theta = 0$ will disappear after a while.*

**Example 297 ★** *Straight car motion with different initial θ.*

Consider a car moving on an $x$-axis with constant speed. The car is pulling a trailer, which is initially at $\theta$ such as shown in Figure 7.52. Using a normalized length, we assume the distance between the center of the trailer axle and the hinge is the length of trailer, and is equal to 1.

If we show the absolute position of the car at hinge by $\mathbf{r} = \begin{bmatrix} x_c & y_c \end{bmatrix}^T$ and the absolute position of the trailer by $\mathbf{s} = \begin{bmatrix} x_t & y_t \end{bmatrix}^T$ then the position of the trailer is a function of the car's motion. When the position of the car is given by a time-dependent vector function

$$\mathbf{r} = \begin{bmatrix} x_c(t) \\ y_c(t) \end{bmatrix} \tag{7.220}$$

the trailer position can be found by solving two coupled differential equation.

$$\dot{x}_t = (x_c - x_t)^2 \, \dot{x}_c + (x_c - x_t)(y_c - y_t) \, \dot{y}_c \tag{7.221}$$

$$\dot{y}_t = (x_c - x_t)(y_c - y_t) \, \dot{x}_c + (y_c - y_t)^2 \, \dot{y}_c \tag{7.222}$$

For a constantly uniform car motion $\mathbf{r} = \begin{bmatrix} t & 0 \end{bmatrix}^T$, Equations (7.221) and (7.222) reduce to

$$\dot{x}_t = (t - x_t)^2 \tag{7.223}$$

$$\dot{y}_t = -y_t (t - x_t) \tag{7.224}$$

The first equation (7.223) is independent of the second equation (7.224) and can be solved independently.

$$x_t = \frac{C_1 e^{2t} (t - 1) - t - 1}{C_1 e^{2t} - 1}$$

$$= t + \frac{e^{-2t} - C_1}{e^{-2t} + C_1} \tag{7.225}$$

Substituting Equation (7.225) in (7.224) generates the following differential equation:

$$\dot{y}_t = \frac{e^{-2t} - C_1}{e^{-2t} + C_1} \, y_t \tag{7.226}$$

with the solution

$$y_t = \frac{C_2 e^{-t}}{e^{-2t} + C_1}. \tag{7.227}$$

When the trailer starts from $\mathbf{s} = \begin{bmatrix} \cos\theta & \sin\theta \end{bmatrix}^T$, the constants of integral would be equal to Equations (7.215) and (7.216) and therefore,

$$x_t = t + \frac{e^{-2t} (\cos\theta + 1) - \cos\theta + 1}{e^{-2t} (\cos\theta + 1) + \cos\theta - 1} \tag{7.228}$$

$$y_t = \frac{2e^{-t} \sin\theta}{e^{-2t} (\cos\theta + 1) + \cos\theta - 1}. \tag{7.229}$$
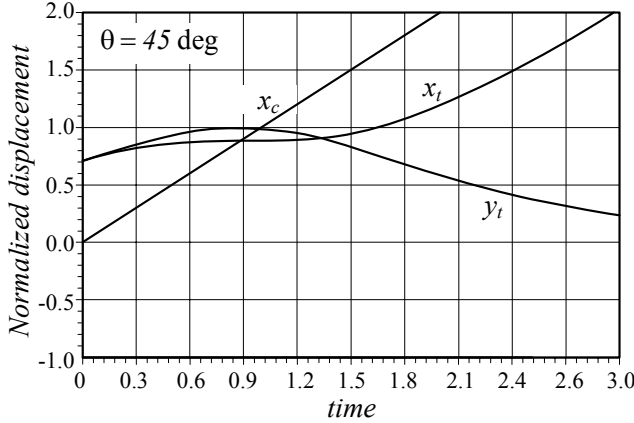
FIGURE 7.55. Trailer kinematics for a $\theta = 45$ deg starting position.

*Figures 7.55, 7.56, and 7.57 illustrate the behavior of the trailer starting from $\theta = 45$ deg, $\theta = 90$ deg, $\theta = 135$ deg.*

**Example 298 ★** *Circular motion of the car with constant velocity.*

*Consider a car pulling a trailer such as Figure 7.52 shows. The car is traveling along a circle of radius $R > 1$, based on a normalized length in which the length of the trailer is $1$. In a circular motion with a normalized angular velocity $\omega = 1$ and period $T = 2\pi$, the position of the car is given by the following time-dependent vector function:*

$$\mathbf{r} = \begin{bmatrix} x_c(t) \\ y_c(t) \end{bmatrix}$$
$$= \begin{bmatrix} R\cos(t) \\ R\sin(t) \end{bmatrix}. \qquad (7.230)$$

*The initial position of the trailer must lie on a unit circle with a center at $\mathbf{r}(0) = \begin{bmatrix} x_c(0) & y_c(0) \end{bmatrix}^T$.*

$$\mathbf{s}(0) = \begin{bmatrix} x_t(0) \\ y_t(0) \end{bmatrix}$$
$$= \begin{bmatrix} x_c(0) \\ y_c(0) \end{bmatrix} + \begin{bmatrix} \cos\theta \\ \sin\theta \end{bmatrix} \qquad (7.231)$$

*The car-trailer combination approaches a steady-state configuration as shown in Figure 7.58.*

*Substituting*

$$\dot{\mathbf{r}} = \begin{bmatrix} -R\sin(t) \\ R\cos(t) \end{bmatrix}. \qquad (7.232)$$
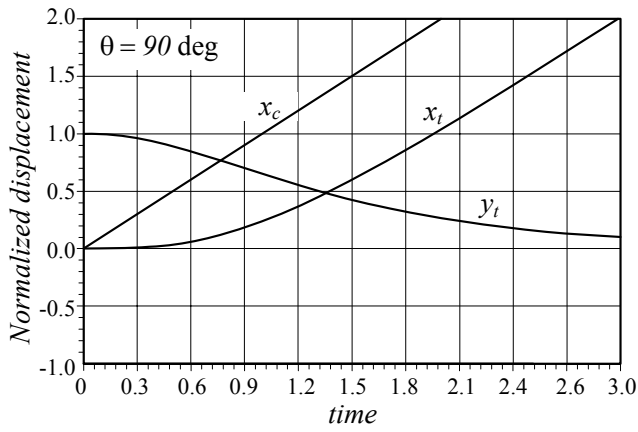
FIGURE 7.56. Trailer kinematics for a $\theta = 90\,\mathrm{deg}$ starting position.
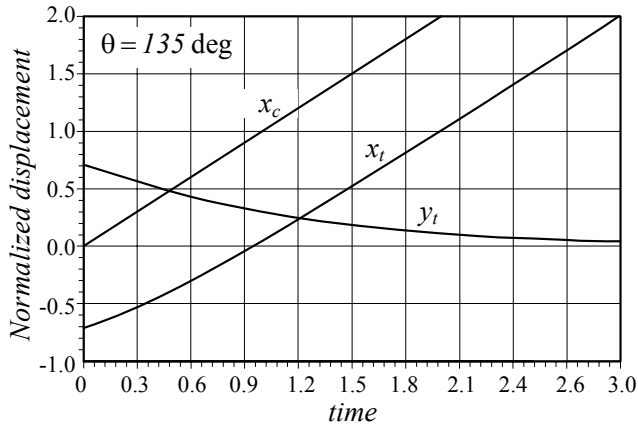


FIGURE 7.57. Trailer kinematics for a $\theta = 135\,\mathrm{deg}$ starting position.
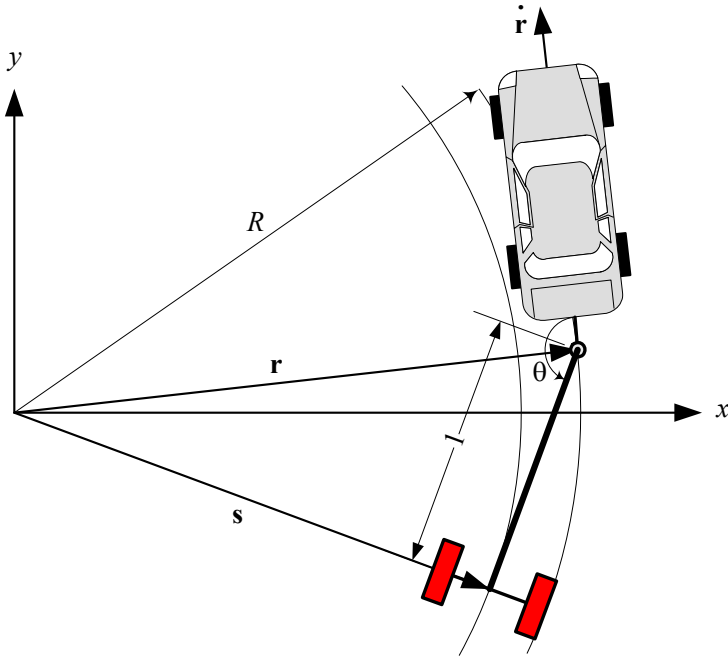
FIGURE 7.58. Steady state configuration of a car-trailer combination.

*and the initial conditions (7.231) in (7.202) will generate two differential equations for trailer position.*

$$\dot{x}_t = R\left(R\cos t - x_t\right)\left(x_t \sin t - y_t \cos t\right) \qquad (7.233)$$
$$\dot{y}_t = R\left(R\sin t - y_t\right)\left(x_t \sin t - y_t \cos t\right) \qquad (7.234)$$

*Assuming $\mathbf{r}(0) = \begin{bmatrix} 0 & 0 \end{bmatrix}^T$ the steady-state solutions of these equations are*

$$x_t = c\cos(t - \alpha) \qquad (7.235)$$
$$y_t = c\sin(t - \alpha) \qquad (7.236)$$

*where $c$ is the trailer's radius of rotation, and $\alpha$ is the angular position of the trailer behind the car.*

$$c = \sqrt{R^2 - 1} \qquad (7.237)$$
$$\sin\alpha = \frac{1}{R} \qquad (7.238)$$
$$\cos\alpha = \frac{c}{R} \qquad (7.239)$$

*We may check the solution by employing two new variables, u and v, such that*

$$u = x_t \sin t - y_t \cos t \qquad (7.240)$$
$$v = x_t \cos t + y_t \sin t \qquad (7.241)$$

*and*

$$\dot{u} = v. \qquad (7.242)$$

*Using the new variables we find*

$$x_t = u \sin t + v \cos t \qquad (7.243)$$
$$y_t = -u \cos t + v \sin t \qquad (7.244)$$

$$\dot{x}_t = Ru(R \cos t - u \sin t - v \cos t) \qquad (7.245)$$
$$\dot{y}_t = Ru(R \sin t + u \cos(t) - v \sin t). \qquad (7.246)$$

*Direct differentiating from (7.240), (7.241), (7.243), and (7.244) shows that*

$$\dot{u} = x_t \cos t + y_t \sin t + \dot{x}_t (\sin t) - \dot{y}_t (\cos t) \qquad (7.247)$$
$$\dot{v} = -x_t \sin t + y_t \cos t + \dot{x}_t \cos t + \dot{y}_t \sin t \qquad (7.248)$$

$$\dot{x}_t = \dot{u} \sin t + \dot{v} \cos t + u \cos t - v \sin t \qquad (7.249)$$
$$\dot{y}_t = \dot{u} \cos t - \dot{v} \sin t - u \sin t - v \cos t \qquad (7.250)$$

*and therefore, the problem can be expressed in a new set of equations.*

$$\dot{u} = v - Ru^2 \qquad (7.251)$$
$$\dot{v} = u \left( R^2 - Rv - 1 \right) \qquad (7.252)$$

*At the steady-state condition the time differentials must be zero, and therefore, the steady-state solutions would be the answers to the following algebraic equations:*

$$v - Ru^2 = 0 \qquad (7.253)$$
$$u \left( R^2 - Rv - 1 \right) = 0 \qquad (7.254)$$

*There are three sets of solutions.*

$$\{u = 0, v = 0\} \qquad (7.255)$$
$$\left\{u = \frac{c}{R}, v = \frac{c^2}{R}\right\} \qquad (7.256)$$
$$\left\{u = -\frac{c}{R}, v = \frac{c^2}{R}\right\} \qquad (7.257)$$

*The first solution is associated with* $\mathbf{s} = 0$,

$$x_t = 0 \tag{7.258}$$
$$y_t = 0 \tag{7.259}$$

*which shows that the center of the trailer's axle remains at the origin and the car is turning on a circle* $R = 1$. *This is a stable motion.*

*The second solution is associated with*

$$x_t = \frac{c}{R} \sin t + \frac{c^2}{R} \cos t \tag{7.260}$$

$$y_t = -\frac{c}{R} \cos t + \frac{c^2}{R} \sin t \tag{7.261}$$

*which are equivalent to (7.235) and (7.236).*

*To examine the stability of the second solution, we may substitute a perturbed solution*

$$u = \frac{c}{R} + p \tag{7.262}$$

$$v = \frac{c^2}{R} + q \tag{7.263}$$

*in the linearized equations of motion (7.251) and (7.252) at the second set of solutions*

$$\dot{u} = v - 2cu \tag{7.264}$$
$$\dot{v} = -cv \tag{7.265}$$

*to get two equations for the perturbed functions* $p$ *and* $q$.

$$\dot{p} = q - 2cp \tag{7.266}$$
$$\dot{q} = cq \tag{7.267}$$

*The set of linear perturbed equations can be set in a matrix form*

$$\begin{bmatrix} \dot{p} \\ \dot{q} \end{bmatrix} = \begin{bmatrix} -2c & 1 \\ 0 & -c \end{bmatrix} \begin{bmatrix} p \\ q \end{bmatrix}. \tag{7.268}$$

*The stability of Equation (7.268) is determined by the eigenvalues* $\lambda_i$ *of the coefficient matrix, which are*

$$\lambda_1 = -c$$
$$\lambda_2 = -2c.$$

*Because both eigenvalues* $\lambda_1$ *and* $\lambda_2$ *are negative, the solution of the perturbed equations symptomatically goes to zero. Therefore, the second set of*

*solutions (7.256) is stable and it absorbs any near path that starts close to it.*

*The third solution is associated with*

$$x_t = -\frac{c}{R}\sin t + \frac{c^2}{R}\cos t \tag{7.269}$$

$$y_t = \frac{c}{R}\cos t + \frac{c^2}{R}\sin t. \tag{7.270}$$

*The linearized equations of motion at the third set of solutions (7.257) are*

$$\dot{u} = v + 2cu \tag{7.271}$$

$$\dot{v} = cv. \tag{7.272}$$

*The perturbed equations would then be*

$$\begin{bmatrix} \dot{p} \\ \dot{q} \end{bmatrix} = \begin{bmatrix} 2c & 1 \\ 0 & c \end{bmatrix}\begin{bmatrix} p \\ q \end{bmatrix} \tag{7.273}$$

*with two positive eigenvalues*

$$\lambda_1 = c$$

$$\lambda_2 = 2c$$

*Positive eigenvalues show that the solution of the perturbed equations diverges and goes to infinity. Therefore, the third set of solutions (7.257) is unstable and repels any near path that starts close to it.*

## 7.8    Summary

Steering is required to guide a vehicle in a desired direction. When a vehicle turns, the wheels closer to the center of rotation are called the inner wheels, and the wheels further from the center of rotation are called the outer wheels. If the speed of a vehicle is very slow, there is a kinematic condition between the inner and outer steerable wheels, called the Ackerman condition.

Street cars are four-wheel vehicles and usually have front-wheel-steering. The kinematic condition between the inner and outer steered wheels is

$$\cot\delta_o - \cot\delta_i = \frac{w}{l} \tag{7.274}$$

where $\delta_i$ is the steer angle of the inner wheel, $\delta_o$ is the steer angle of the outer wheel, $w$ is the track, and $l$ is the wheelbase of the vehicle. Track $w$ and wheel base $l$ are considered the kinematic width and length of the vehicle.

The mass center of a steered vehicle will turn on a circle with radius $R$,

$$R = \sqrt{a_2^2 + l^2 \cot^2 \delta} \qquad (7.275)$$

where $\delta$ is the cot-average of the inner and outer steer angles.

$$\cot \delta = \frac{\cot \delta_o + \cot \delta_i}{2}. \qquad (7.276)$$

The angle $\delta$ is the equivalent steer angle of a bicycle having the same wheelbase $l$ and radius of rotation $R$.

## 7.9   Key Symbols

| | |
|---|---|
| $4WS$ | four-wheel-steering |
| $a, b, c, d$ | lengths of the links of a four-bar linkage |
| $a_i$ | distance of the axle number $i$ from the mass center |
| $A, B, C$ | input angle parameters of a four-bar linkage |
| $AWS$ | all-wheel-steering |
| $b_1$ | distance of the hinge point from rear axle |
| $b_2$ | distance of trailer axle from the hinge point |
| $c$ | stability index of a trailer motion |
| $c$ | trailer's radius of rotation |
| $c_1$ | longitudinal distance of turn center and front axle of a $4WS$ car |
| $c_2$ | longitudinal distance of turn center and rear axle of a $4WS$ car |
| $C$ | mass center |
| $C_1, C_2, \cdots$ | constants of integration |
| $d$ | arm length in trapezoidal steering mechanism |
| $e$ | error |
| $e$ | length of the offset arm |
| $FWS$ | front-wheel-steering |
| $g$ | overhang distance |
| $J$ | link parameters of a four-bar linkage |
| $l$ | wheelbase |
| $n$ | number of increments |
| $O$ | center of rotation in a turn |
| $r$ | yaw velocity of a turning vehicle |
| $\mathbf{r}$ | position vector of a car at the hinge |
| $R$ | radius of rotation at mass center |
| $R_1$ | radius of rotation at the center of the rear axle for $FWS$ |
| $R_1$ | horizontal distance of $O$ and the center of axles |
| $R_t$ | radius of rotation at the center of the trailer axle |
| $R_w$ | radius of the rear wheel |
| $RWS$ | rear wheel steering |
| $\mathbf{s}$ | position vector of a trailer at the axle center |
| $t$ | time |
| $u_R$ | steering rack translation |
| $v \equiv \dot{x},\ \mathbf{v}$ | vehicle velocity |
| $v_{ri}$ | speed of the inner rear wheel |
| $v_{ro}$ | speed of the outer rear wheel |
| $w$ | track |
| $w_f$ | front track |
| $w_r$ | rear track |
| $x, y, z,\ \mathbf{x}$ | displacement |
| $\mathbf{z} = \mathbf{r} - \mathbf{s}$ | position vector of a trailer relative to the car |

| | |
|---|---|
| $\beta$ | arm angle in trapezoidal steering mechanism |
| $\delta$ | cot-average of the inner and outer steer angles |
| $\delta_1 = \delta_{fl}$ | front left wheel steer angle |
| $\delta_2 = \delta_{fr}$ | front right wheel steer angle |
| $\delta_{Ac}$ | steer angle based on Ackerman condition |
| $\delta_{fl}$ | front left wheel steer angle |
| $\delta_{fr}$ | front right wheel steer angle |
| $\delta_i$ | inner wheel |
| $\delta_{rl}$ | rear left wheel steer angle |
| $\delta_{rr}$ | rear right wheel steer angle |
| $\delta_o$ | outer wheel |
| $\delta_S$ | steer command |
| $\Delta = \delta_2 - \delta_{Ac}$ | steer angle difference |
| $\theta$ | angle between trailer and vehicle longitudinal axes |
| $\omega$ | angular velocity |
| $\omega_i = \omega_{ri}$ | angular velocity of the rear inner wheel |
| $\omega_o = \omega_{ro}$ | angular velocity of the rear outer wheel |

# Exercises

1. Bicycle model and radius of rotation.

   Mercedes-Benz $GL450^{TM}$ has the following dimensions.

$$
\begin{aligned}
l &= 121.1\,\text{in} \\
w_f &= 65.0\,\text{in} \\
w_r &= 65.1\,\text{in} \\
R &= 39.7\,\text{ft}
\end{aligned}
$$

   Assume $a_1 = a_2$ and use an average track to determine the maximum steer angle $\delta$ for a bicycle model of the car.

2. Radius of rotation.

   Consider a two-axle truck that is offered in different wheelbases.

$$
\begin{aligned}
l &= 109\,\text{in} \\
l &= 132.5\,\text{in} \\
l &= 150.0\,\text{in} \\
l &= 176.0\,\text{in}
\end{aligned}
$$

   If the front track of the vehicles is

$$
w = 70\,\text{in}
$$

   and $a_1 = a_2$, calculate the radius of rotations if $\delta = 30\,\text{deg}$.

3. Required space.

   Consider a two-axle vehicle with the following dimensions.

$$
\begin{aligned}
l &= 4\,\text{m} \\
w &= 1.3\,\text{m} \\
g &= 1.2\,\text{m}
\end{aligned}
$$

   Determine $R_{min}$, $R_{Max}$, and $\Delta R$ for $\delta = 30\,\text{deg}$.

4. Rear wheel steering lift truck.

   A battery powered lift truck has the following dimensions.

$$
\begin{aligned}
l &= 55\,\text{in} \\
w &= 30\,\text{in}
\end{aligned}
$$

   Calculate the radius of rotations if $\delta = 55\,\text{deg}$ for $a_1 = a_2$.

5. Wheel angular velocity.

   Consider a two-axle vehicle with the following dimensions.

   $$l \;=\; 2.7 \,\text{m}$$
   $$w \;=\; 1.36 \,\text{m}$$

   What is the angular velocity ratio of $\omega_o/\omega_i$?

6. A three-axle vehicle.

   A three-axle vehicle is shown in Figure 7.17. Find the relationship between $\delta_2$ and $\delta_3$, and also between $\delta_1$ and $\delta_6$.

7. A three-axle truck.

   Consider a three-axle truck that has only one steerable axle in front. The dimensions of the truck are

   $$a_1 \;=\; 5300 \,\text{mm}$$
   $$a_2 \;=\; 300 \,\text{mm}$$
   $$a_3 \;=\; 1500 \,\text{mm}$$
   $$w \;=\; 1800 \,\text{mm}.$$

   Determine maximum steer angles of the front wheels if the truck is supposed to be able to turn with $R = 11\,\text{m}$.

8. A vehicle with a one-axle trailer.

   Determine the angle between the trailer and vehicle with the following dimensions.

   $$a_1 \;=\; 1000 \,\text{mm}$$
   $$a_2 \;=\; 1300 \,\text{mm}$$
   $$w_v \;=\; 1500 \,\text{mm}$$
   $$b_1 \;=\; 1200 \,\text{mm}$$
   $$b_2 \;=\; 1800 \,\text{mm}$$
   $$w_t \;=\; 1100 \,\text{mm}$$
   $$g \;=\; 800 \,\text{mm}$$
   $$\delta_i \;=\; 12 \,\text{deg}.$$

   What is the rotation radius of the trailer $R_t$, and the vehicle $R$? Determine minimum radius $R_{\min}$, maximum $R_{Max}$, and difference radius $\Delta R$?

9. ★ Turning radius of a $4WS$ vehicle.

   Consider a $FWS$ vehicle with the following dimensions.

$$
\begin{aligned}
l &= 2300\,\text{mm} \\
w_f &= 1457\,\text{mm} \\
w_r &= 1607\,\text{mm} \\
\frac{a_1}{a_2} &= \frac{38}{62}
\end{aligned}
$$

   Determine the turning radius of the vehicle for $\delta_{fl} = 5\,\text{deg}$.

   What should be the steer angles of the front and rear wheels to de-crease 10% of the turning radius, if we make the vehicle $4WS$?

10. ★ Coordinates of the turning center.

   Determine the coordinates of the turning center for the vehicle in Exercise 9 if $\delta_{fl} = 5\,\text{deg}$ and $c_1 = 1300\,\text{mm}$.

11. ★ Different front and rear tracks.

   Lotus 2-Eleven$^{TM}$ is a $RWD$ sportscar with the following specifica-tions.

$$
\begin{aligned}
l &= 2300\,\text{mm} \\
w_f &= 1457\,\text{mm} \\
w_r &= 1607\,\text{mm} \\
Front\ tire &= 195/50R16 \\
Rear\ tire &= 225/45R17 \\
\frac{F_{z_1}}{F_{z_2}} &= \frac{38}{62}
\end{aligned}
$$

   Determine the angular velocity ratio of $\omega_o/\omega_i$, $R$, $\delta_i$, and $\delta_o$ for $\delta = 5\,\text{deg}$.

12. ★ Coordinates of turning center.

   Determine the coordinates of turning center of a $4WS$ vehicle in terms of outer steer angles $\delta_{of}$ and $\delta_{or}$.

13. ★ Turning radius.

   Determine the turning radius of a $4WS$ vehicle in terms of $\delta_r$.

$$
\cot \delta_r = \frac{1}{2} \left( \cot \delta_{ir} + \cot \delta_{or} \right)
$$

14. ★ A three-axle car.

Consider a three-axle off-road pick-up car. Assume

$$
\begin{aligned}
a_1 &= 1100\,\text{mm} \\
a_2 &= 1240\,\text{mm} \\
a_3 &= 1500\,\text{mm} \\
w &= 1457\,\text{mm}
\end{aligned}
$$

and determine $\delta_o$, $R_1$, $R_f$, and $R$ if $\delta_i = 10\,\text{deg}$.

15. ★ Steering mechanism optimization.

Find the optimum length $x$ for the multi-link steering mechanism shown in Figure 7.59 to operate as close as possible to the kinematic steering condition. The vehicle has a track $w = 2.64\,\text{m}$ and a wheelbase $l = 3.84\,\text{m}$, and must be able to turn the front wheels within a working range equal to $-22\,\text{deg} \le \delta \le 22\,\text{deg}$.
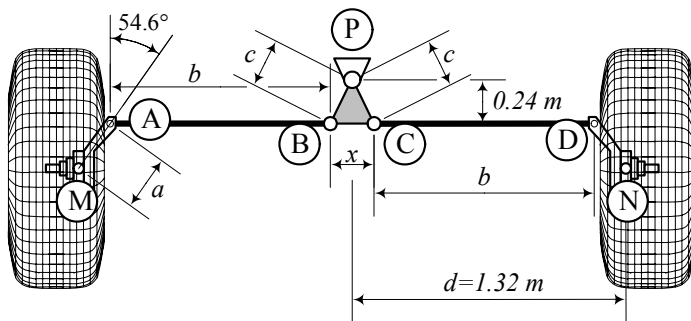


FIGURE 7.59. A multi-link steering mechanism tha must be optimized by varying $x$.

# 8

# Suspension Mechanisms

The suspension is what links the wheels to the vehicle body and allows relative motion. This chapter covers the suspension mechanisms, and discusses the possible relative motions between the wheel and the vehicle body. The wheels, through the suspension linkage, must propel, steer, and stop the vehicle, and support the associated forces.

## 8.1   Solid Axle Suspension

The simplest way to attach a pair of wheels to a vehicle is to mount them at opposite ends of a *solid axle*, such as the one that is shown in Figure 8.1.
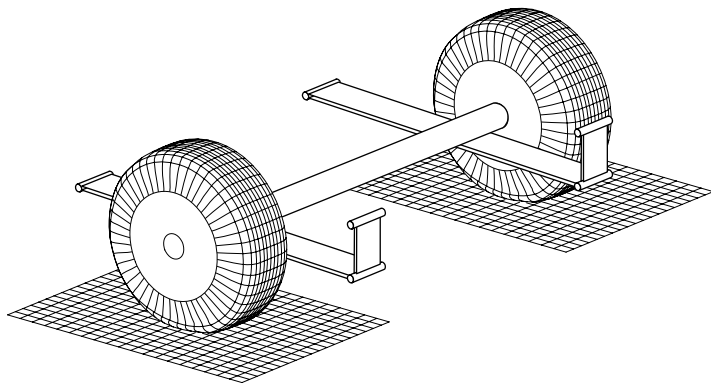


FIGURE 8.1. A solid axle with leaf spring suspension.

The solid axle must be attached to the body such that an up and down motion in the $z$-direction, as well as a roll rotation about the $x$-axis, is possible. So, no forward and lateral translation, and also no rotation about the axle and the $z$-axis, is allowed. There are many combinations of links and springs that can provide the kinematic and dynamic requirements. The simplest design is to clamp the axle to the middle of two leaf springs with their ends tied or shackled to the vehicle frame as shown schematically in Figure 8.1. A side view of a multi-leaf spring and solid axle is shown in Figure 8.2. A suspension with a solid connection between the left and right wheels is called *dependent suspension*.
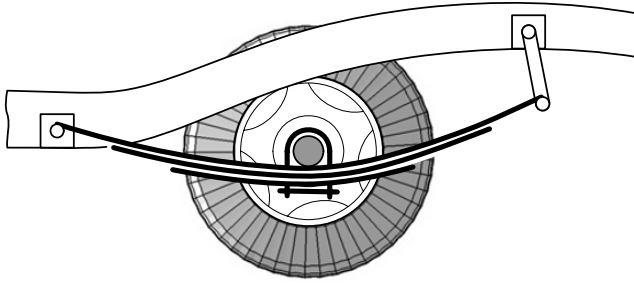
FIGURE 8.2. A side view of a multi-leaf spring and solid axle suspension.

The performance of a solid axle with leaf springs suspension can be improved by adding a linkage to guide the axle kinematically and provide dynamic support to carry the non $z$-direction forces.

The solid axle with leaf spring combination came to vehicle industry from horse-drawn vehicles.

**Example 299** *Hotchkiss drive.*

*When a live solid axle is connected to the body with nothing but two leaf springs, it is called the* **Hotchkiss drive***, which is the name of the car that used it first. The main problems of a Hotchkiss drive, which is shown in Figure 8.2, are locating the axle under lateral and longitudinal forces, and having a low mass ratio $\varepsilon = m_s/m_u$, where $m_s$ is the sprung mass and $m_u$ is the unsprung mass.*

*Sprung mass refers to all masses that are supported by the spring, such as vehicle body. Unsprung mass refers to all masses that are attached to and not supported by the spring, such as wheel, axle, or brakes.*

**Example 300** *Leaf spring suspension and flexibility problem.*

*The solid axle suspension systems with longitudinal leaf springs have many drawbacks. The main problem lies in the fact that springs themselves act as locating members. Springs are supposed to flex under load, but their flexibility is needed in only one direction. However, it is the nature of leaf springs to twist and bend laterally and hence, flex also in planes other than the tireplane. Leaf springs are not suited for taking up the driving and braking traction forces. These forces tend to push the springs into an S-shaped profile, as shown in Figure 8.3. The driving and braking flexibility of leaf springs, generates a negative caster and increases instability.*

*Long springs provide better ride. However, long sprigs exaggerate their bending and twisting under different load conditions.*

**Example 301** *Leaf spring suspension and flexibility solution.*

*To reduce the effect of a horizontal force and S-shaped profile appearance in a solid axle with leaf springs, the axle may be attached to the chassis by a longitudinal bar as Figure 8.4(a) shows. Such a bar is called an* **anti-tramp**

(*a*) Acceleration
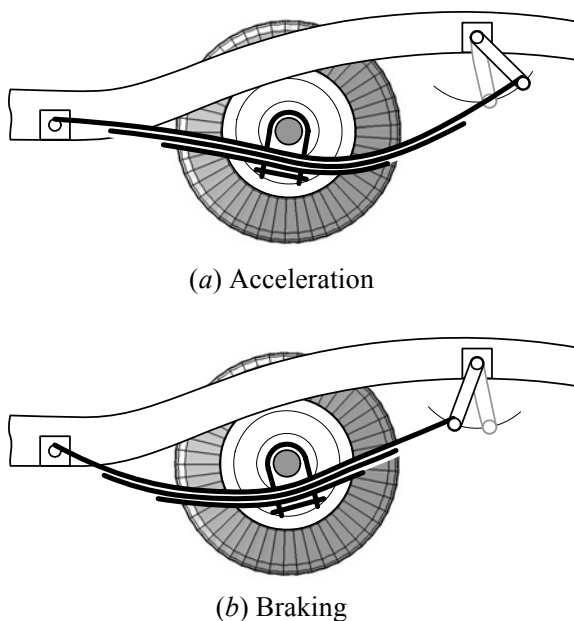


(*b*) Braking

FIGURE 8.3. A driving and braking trust, force leaf springs into an *S* shaped profile.

bar, and the suspension is the simplest cure for longitudinal problems of a Hotchkiss drive.

A solid axle with an anti-tramp bar may be kinematically approximated by a four-bar linkage, as shown in Figure 8.4(b). Although an anti-tramp bar may control the shape of the leaf spring, it introduces a twisting angle problem when the axle is moving up and down, as shown in Figure 8.5. Twisting the axle and the wheel about the axle is called caster.

The solid axle is frequently used to help keeping the wheels perpendicular to the road.

**Example 302** *Leaf spring location problem.*

The front wheels need room to steer left and right. Therefore, leaf springs cannot be attached close to the wheel hubs, and must be placed closer to the middle of the axle. That gives a narrow spring-base, which means that a small side force can sway or tilt the body relative to the axle through a considerable roll angle due to weight transfer. This is uncomfortable for the vehicle passengers, and may also produce unwanted steering.

The solid axle positively prevents the camber change by body roll. The wheels remain upright and hence, do not roll on a side. However, a solid axle shifts laterally from its static plane and its center does not remain on the vehicle's longitudinal axis under a lateral force.

(a)



(b)
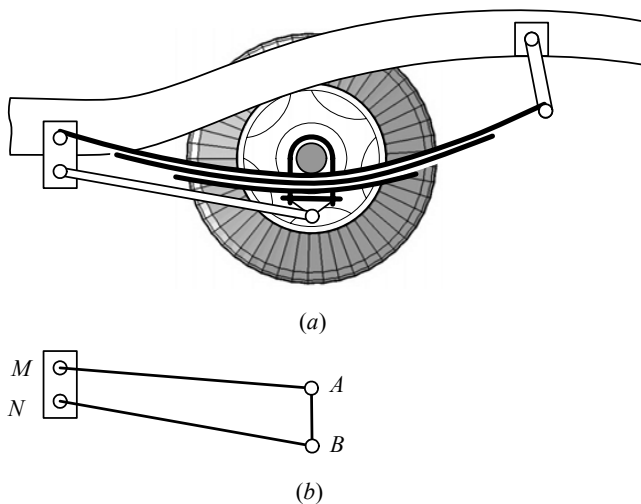
FIGURE 8.4. (a) Adding an anti-tramp bar to guide a solid axle. (b) Equivalent kinematic model.



(a)                              (b)
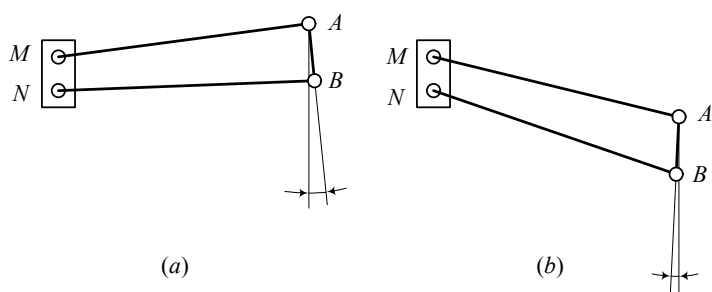
FIGURE 8.5. An anti-tramp bar introduces a twistng angle problem. (a) The wheel moves up and (b) The wheel moves down.
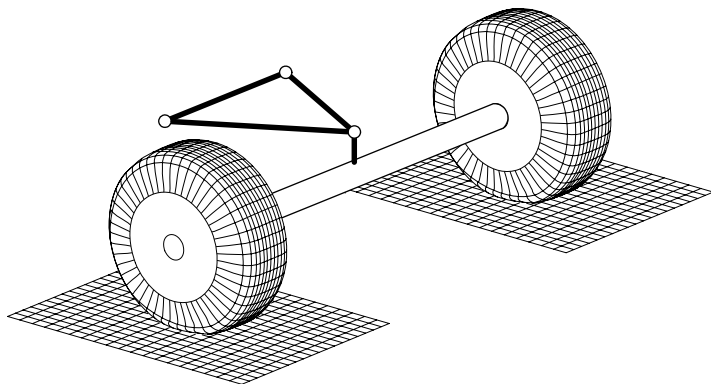
FIGURE 8.6. A solid axle suspension with a triangulated linkage.

*A solid axle produces bump-camber when single-wheel bump occurs. If the right wheel goes over a bump, the axle is raised at its right end, and that tilts the left wheel hub, putting the left wheel at a camber angle for the duration of deflection.*

**Example 303** *Triangular linkage.*
*A triangulated linkage, as shown in Figure 8.6, may be attached to a solid axle to provide lateral and twist resistance during acceleration and braking.*

**Example 304** *Panhard arm.*
*High spring rate is a problem of leaf springs. Reducing their stiffness by narrowing them and using fewer leaves, reduces the lateral stiffness and increases the directional stability of the suspension significantly. A Panhard arm is a bar that attaches a solid axle suspension to the chassis laterally. Figure 8.7 illustrates a solid axle and a Panhard arm to guide the axle. Figure 8.8 shows a triangular linkage and a Panhard arm combination for guiding a solid axle.*
*A double triangle mechanism, as shown in Figure 8.9, is an alternative design to guide the axle and support it laterally.*

**Example 305** *Straight line linkages.*
*There are many mechanisms that can provide a straight line motion. The simplest mechanisms are four-bar linkages with a coupler point moving straight. Some of the most applied and famous linkages are shown in Figure 8.10. By having proper lengths, the Watt, Robert, Chebyshev, and Evance linkages can make the coupler point C move on a straight line vertically. Such a mechanism and straight motion may be used to guide a solid axle.*
*Two Watt suspension mechanisms with a Panhard arm are shown in Figures 8.11 and 8.12.*
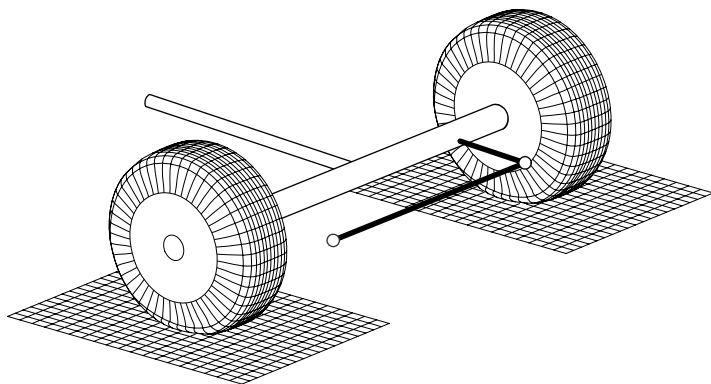
FIGURE 8.7. A solid axle and a Panhard arm to guide the axle.
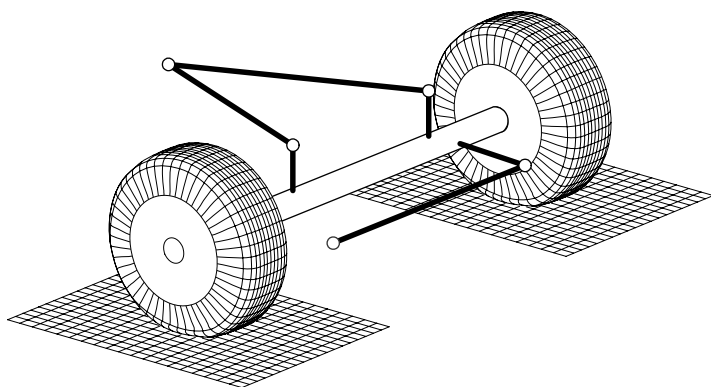


FIGURE 8.8. A triangle mechanism and a Panhard arm to guide a solid axle.
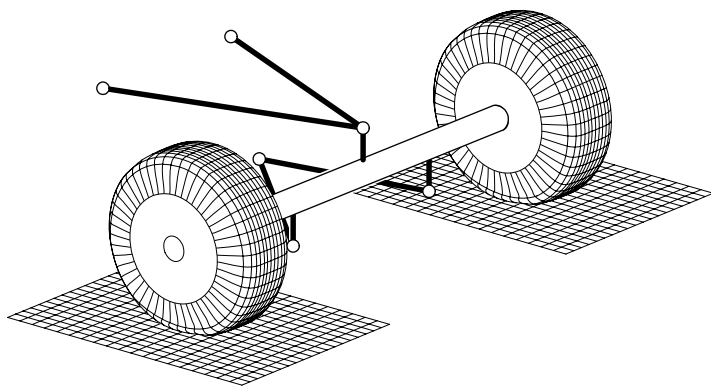


FIGURE 8.9. Double triangle suspension mechanism.

($a$) – Watt linkage              ($b$) – Robert linkage

($b$) – Chebyshev linkage       ($d$) – Evans linkage
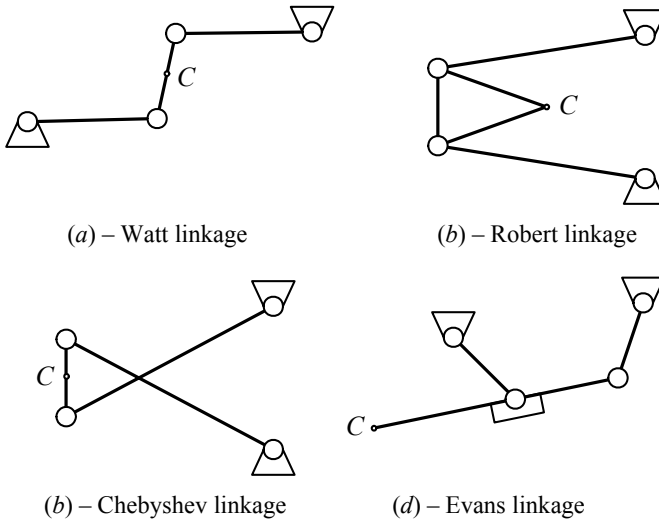
FIGURE 8.10. Some linkages with straight line motion.
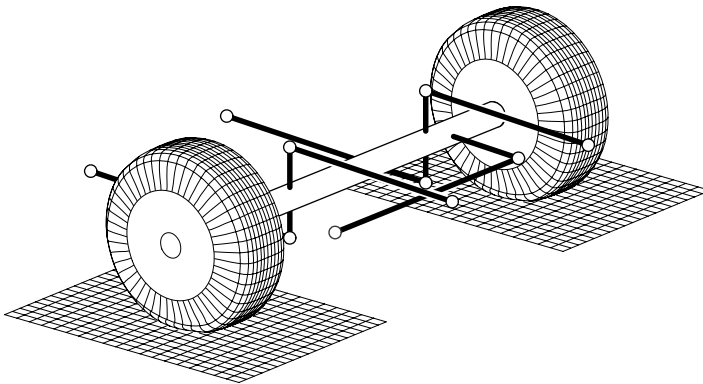


FIGURE 8.11. A Watt suspension mechanisms with a Panhard arm.
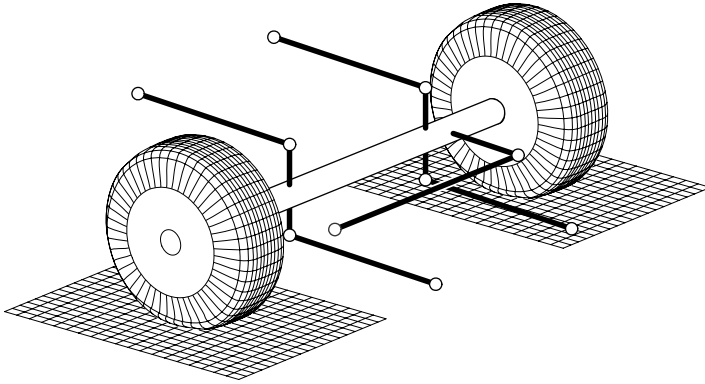
FIGURE 8.12. A Watt suspension mechanisms with a Panhard arm.
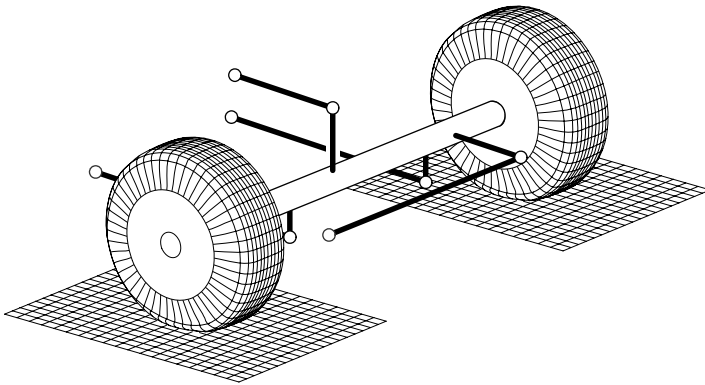


FIGURE 8.13. A Robert suspension mechanism with a Panhard arm.

*Figures 8.13, 8.14, and 8.15 illustrate three combinations of Robert suspension linkages equipped with a Panhard arm.*

**Example 306** *Solid axle suspension and unsprung mass problem.*
*A solid axle is counted as an unsprung member, and hence, the unsprung mass is increased where using solid axle suspension. A heavy unsprung mass ruins both, the ride and handling of a vehicle. Lightening the solid axle makes it weaker and increases the most dangerous problem in vehicles: axle breakage. The solid axle must be strong enough to make sure it will not break under any loading conditions at any age. As a rough estimate, 90% of the leaf spring mass may also be counted as unsprung mass, which makes the problem worse.*

*The unsprung mass problem is worse in front, and it is the main reason that they are no longer used in street cars. However, front solid axles are still common on trucks and buses. These are heavy vehicles and solid axle*
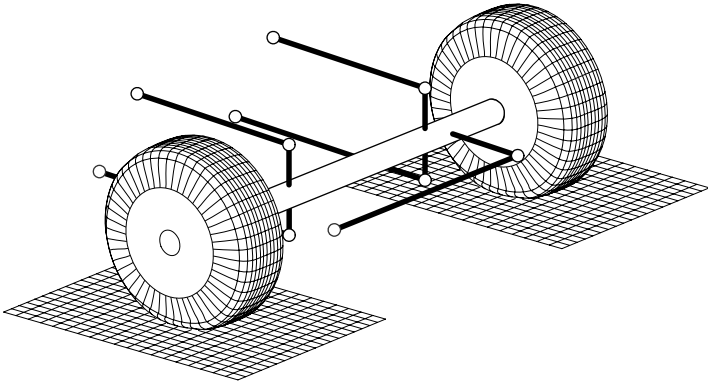
FIGURE 8.14. A Robert suspension mechanism with a Panhard arm.
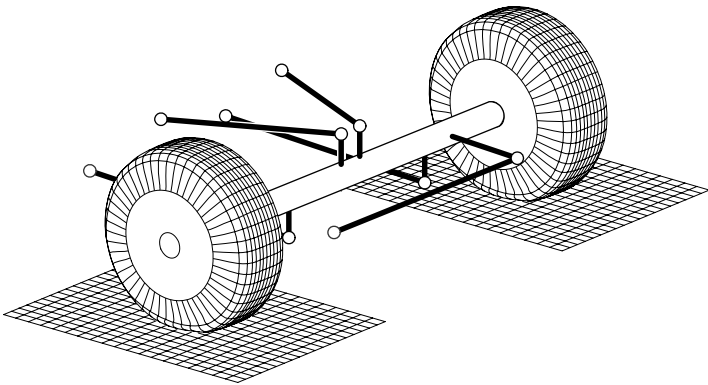


FIGURE 8.15. A Robert suspension mechanism with a Panhard arm.
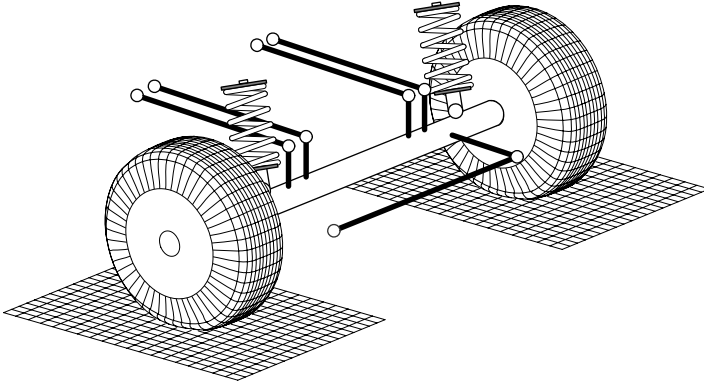
FIGURE 8.16. A solid axle suspension with coil springs.

suspension does not reduce the mass ratio $\varepsilon = m_s/m_u$ very much.

When a vehicle is rear-wheel-drive and a solid axle suspension is used in the back, the suspension is called **live axle**. A live axle is a casing that contains a differential, and two drive shafts. The drive shafts are connected to the wheel hubs. A live axle can be three to four times heavier than a dead I-beam axle. It is called live axle because of rotating gears and shafts inside the axle.

**Example 307** *Solid axle and coil spring.*

To decrease the unsprung mass and increase vertical flexibility of solid axle suspensions, it is possible to equip them with coil springs. A sample of a solid axle suspension with coil spring is shown in Figure 8.16. The suspension mechanism is made of four longitudinal bars between the axle and chassis. The springs may have some lateral or longitudinal angle to introduce some lateral or longitudinal compliance.

**Example 308** *De Dion axle.*

When a solid axle is a dead axle with no driving wheels, the connecting beam between the left and right wheels may have different shapes to do different jobs, usually to give the wheels independent flexibility. We may also modify the shape of a live axle to attach the differential to the chassis and reduce the unsprung mass.

De Dion design is a modification of a beam axle that may be used as a dead axle or to attach the differential to the chassis and transfer the driving power to the drive wheels by employing universal joints and split shafts. Figure 8.17 illustrates a De Dion suspension.
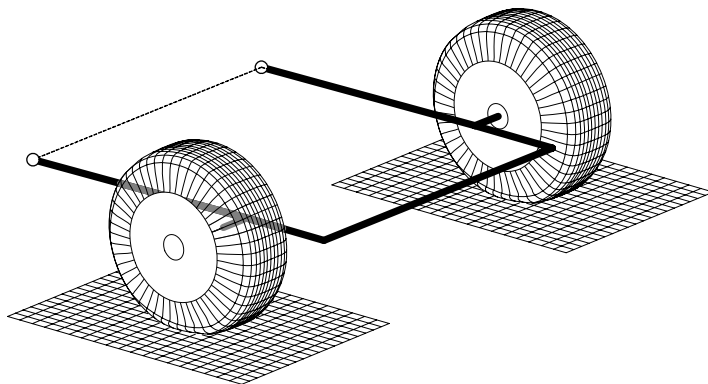
FIGURE 8.17. Illustration of a De Dion suspension.

## 8.2 Independent Suspension

Independent suspensions is introduced to let a wheel to move up and down without affecting the opposite wheel. There are many forms and designs of independent suspensions. However, *double A-arm* and *McPherson strut* suspensions are the simplest and the most common designs. Figure 8.18 illustrates a sample of a double $A$-arm and Figure 8.19 shows a McPherson suspension.

Kinematically, a double $A$-arm suspension mechanism is a four-bar linkage with the chassis as the ground link, and coupler as the wheel carrying link. A McPherson suspension is an inverted slider mechanism that has the chassis as the ground link and the coupler as the wheel carrying link. A double $A$-arm and a McPherson suspension mechanism on the left and right wheels are schematically shown in Figures 8.20 and 8.21 respectively.

Double $A$-arm, is also called *double wishbone*, or *short/long arm* suspension. McPherson also may be written as MacPherson.

**Example 309** *Double A-arm suspension and spring position.*

*Consider a double A-arm suspension mechanism. The coil spring may be between the lower arm and the chassis, as shown in Figure 8.18. It is also possible to install the spring between the upper arm and the chassis, or between the upper and lower arms. In either case, the lower or the upper arm, which supports the spring, is made stronger and the other arm acts as a connecting arm.*

**Example 310** *Multi-link suspension mechanism.*

*When the two side bars of an A-arm are attached to each other with a joint, as shown in Figure 8.22, then the double A-arm is called a multi-link mechanism. A multi-link mechanism is a six-bar mechanism that may have a better coupler motion than a double A-arm mechanism. However, multi-*
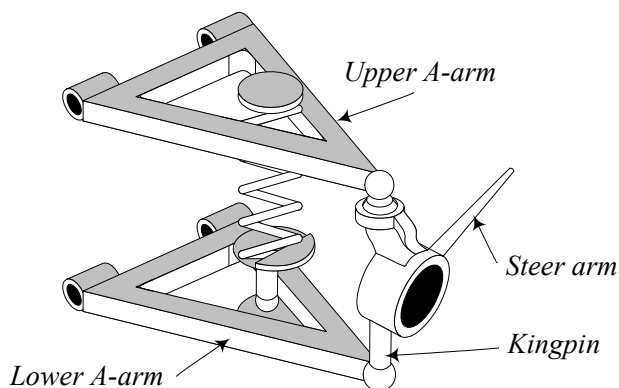
FIGURE 8.18. A double *A*-arm suspension.
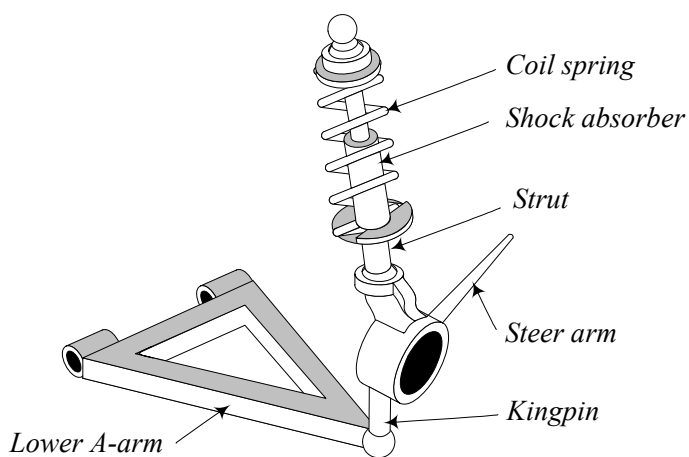


FIGURE 8.19. A McPherson suspension.
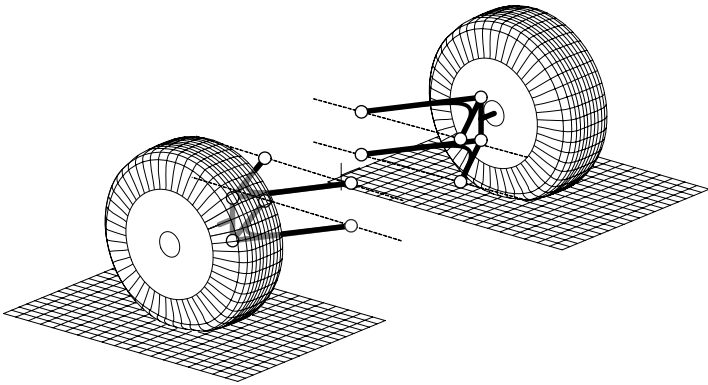
FIGURE 8.20. A double $A$-arm suspension mechanism on the left and right wheels
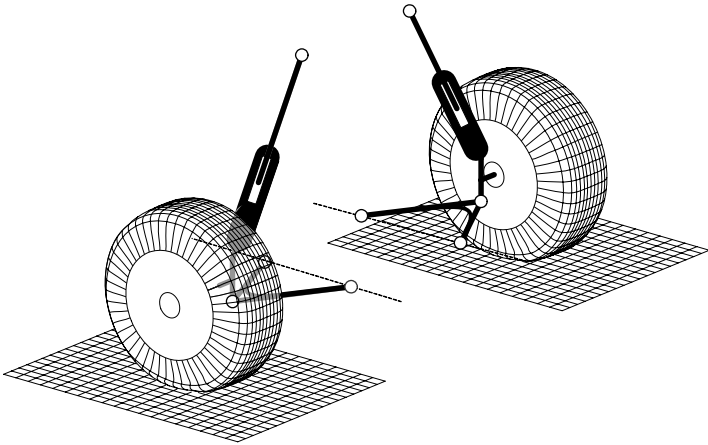


FIGURE 8.21. A McPherson suspension mechanism on the left and right wheels.
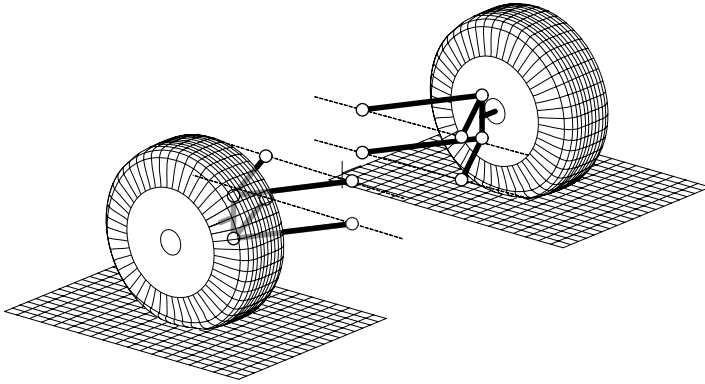
FIGURE 8.22. A multi-link suspension mechanism.
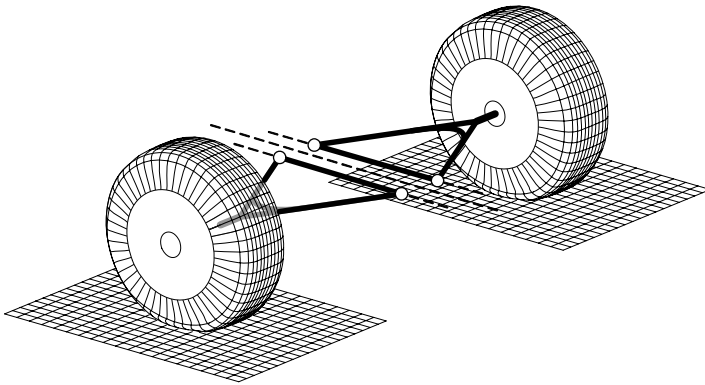


FIGURE 8.23. A swing arm suspension.

link suspensions are more expensive, less reliable, and more complicated compare to a double A-arm four-bar linkage. There are vehicles with more than six-link suspension with possibly better kinematic performance.

**Example 311** *Swing arm suspension.*

An independent suspension may be as simple as a triangle shown in Figure 8.23. The base of the triangle is jointed to the chassis and the wheel to the tip point. The base of the triangle is aligned with the longitudinal axis of the vehicle. Such a suspension mechanism is called a **swing axle** or **swing arm**.

The variation in camber angle for a swing arm suspension is maximum, compared to the other suspension mechanisms.

**Example 312** *Trailing arm suspension.*

Figure 8.24 illustrates a trailing arm suspension that is a longitudinal
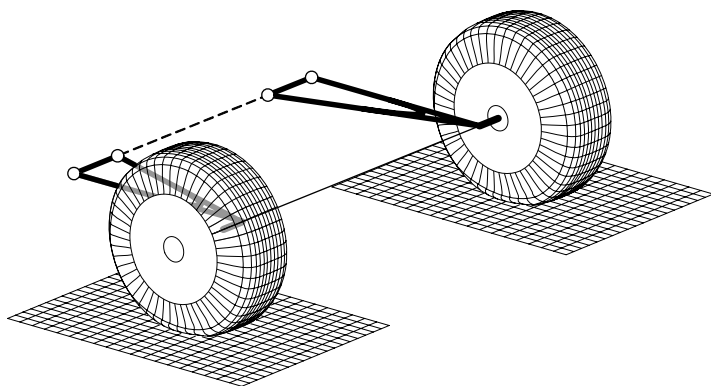
FIGURE 8.24. A trailing arm suspension.
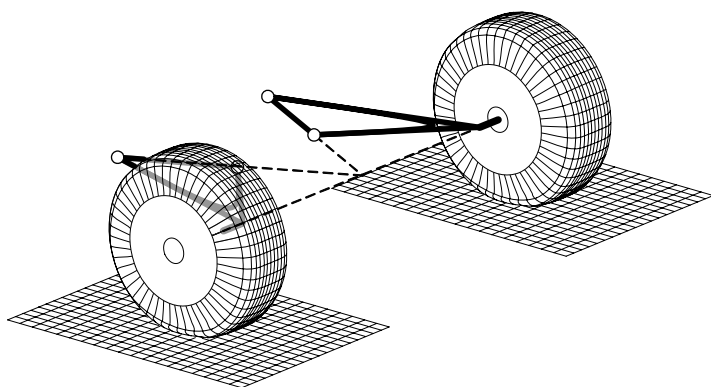
FIGURE 8.25. A semi-trailing arm suspension.

*arm with a lateral axis of rotation. The camber angle of the wheel, supported by a trailing arm, will not change during the up and down motion.*

*Trailing arm suspension has been successfully using in a variety of front-wheel-drive vehicles, to suspend their rear wheels.*

**Example 313** *Semi-trailing arm*

*Semi-trailing arm suspension, as shown in Figure 8.25, is a compromise between the swing arm and trailing arm suspensions. The joint axis may have any angle, however an angle not too far from 45 deg is more applied. Such suspensions have acceptable camber angle change, while they can handle both, the lateral and longitudinal forces. Semi-trailing design has successfully applied to a series of rear-wheel-drive cars for several decades.*

**Example 314** *Antiroll bar and roll stiffness.*

*Coil springs are used in vehicles because they are less stiff with better*
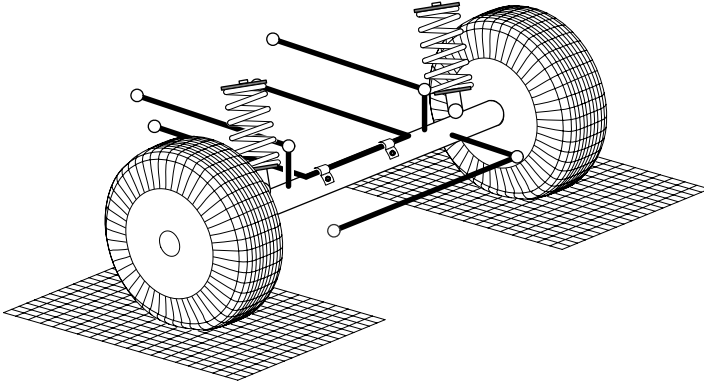
FIGURE 8.26. An anti-roll bar attached to a solid axle with coil springs.

*ride comfort compared to leaf springs. Therefore, the roll stiffness of the vehicle with coil springs is usually less than in vehicles with leaf springs. To increase the roll stiffness of such suspensions, an **antiroll bar** must be used. Leaf springs with reduced layers, uni-leaf, trapezoidal, or nonuniform thickness may also need an antiroll bar to compensate for their reduced roll stiffness. The antiroll bar is also called a **stabilizer**. Figure 8.26 illustrates an anti-roll bare attached to a solid axle with coil springs.*

**Example 315** *Need for longitudinal compliance.*

*A bump is an obstacle on the road that opposes the forward motion of a wheel. When a vehicle goes over a bump, the first action is a force that tends to push the wheel backward relative to the rest of the vehicle. So, the lifting force has a longitudinal component, which will be felt inside the vehicle unless the suspension system has horizontal compliance.*

*There are situations in which the horizontal component of the force is even higher than the vertical component. Leaf springs can somewhat absorb this horizontal force by flattening out and stretching the distance from the forward spring anchor and the axle. Such a stretch is usually less than $1/2 \, \text{in} \approx 1 \, \text{cm}$.*

## 8.3   Roll Center and Roll Axis

The *roll axis* is the instantaneous line about which the body of a vehicle rolls. Roll axis is found by connecting the *roll center* of the front and rear suspensions of the vehicle. Assume we cut a vehicle laterally to disconnect the front and rear half of the vehicle. Then, the roll center of the front or rear suspension is the instantaneous center of rotation of the body with respect to the ground.
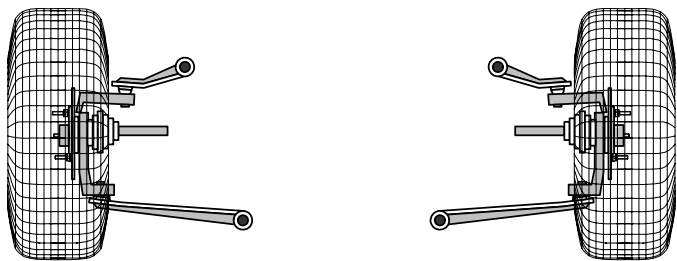
FIGURE 8.27. An example of a double A-arm front suspensions.
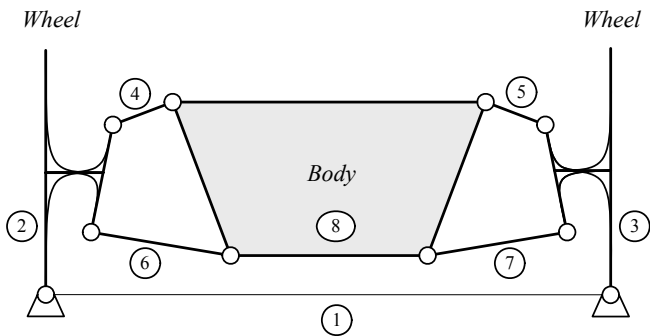


FIGURE 8.28. Kinematically equivalent mechanism for the front half of the double A-arm suspension shown in Figure 8.27.
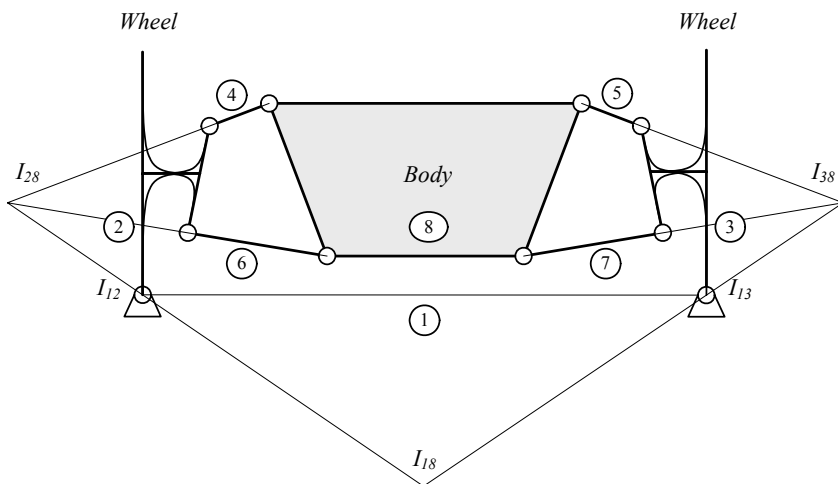
FIGURE 8.29. The roll center $I_{18}$ is at the intersection of lines $\overline{I_{12}I_{28}}$ and $\overline{I_{13}I_{38}}$.

Figure 8.27 illustrates a sample of the front suspensions of a car with a double $A$-arm mechanism. To find the roll center of the body with respect to the ground, we analyze the two-dimensional kinematically equivalent mechanism shown in Figure 8.28. The center of tireprint is the instant center of rotation of the wheel with respect to the ground, so the wheels are jointed links to the ground at their center of tireprints.

The instant center $I_{18}$ is the roll center of the body with respect to the ground. To find $I_{18}$, we apply the Kennedy theorem and find the intersection of the line $\overline{I_{12}I_{28}}$ and $\overline{I_{13}I_{38}}$ as shown in Figure 8.29.

The point $I_{28}$ and $I_{38}$ are the instant center of rotation for the wheels with respect to the body. The instant center of rotation of a wheel with respect to the body is called *suspension roll center*. So, to find the roll center of the front or rear half of a car, we should determine the suspension roll centers, and find the intersection of the lines connecting the suspension roll centers to the center of their associated tireprints.

The *Kennedy theorem* states that the instant center of every three relatively moving objects are colinear.

**Example 316** *McPherson suspension roll center.*

*A McPherson suspension is an inverted slider crank mechanism. The instant centers of an example of inverted slider crank mechanism are shown in Figure 8.30. In this figure, the point $I_{12}$ is the suspension roll center, which is the instant center of rotation for the wheel link number 2 with respect to the chassis link number 1.*

*A car with a McPherson suspension system is shown in Figure 8.31. The kinematic equivalent mechanism is depicted in Figure 8.32. Suspension roll centers along with the body roll center are shown in Figure 8.33. To*
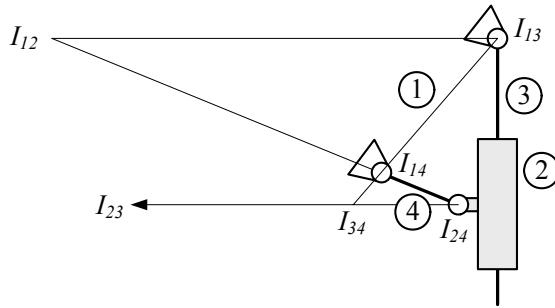
FIGURE 8.30. Instant center or rotation for an example of inverted slider crank mechanism.
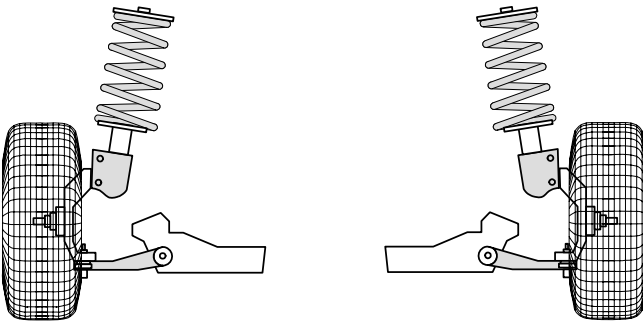


FIGURE 8.31. A car with a McPherson suspension system.

*find the roll center of the front or rear half of a car, we determine each suspension roll center and then find the intersection of the lines connecting the suspension roll centers to the center of the associated tireprint.*

**Example 317** *Roll center of double A-arm suspension.*

*The roll center of an independent suspension such as a double A-arm can be internal or external. The kinematic model of a double A-arm suspension for the front left wheel of a car is illustrated in Figure 8.34. The suspension roll center in Figure 8.34(a) is internal, and in Figure 8.34(b) is external. An internal suspension roll center is toward the vehicle body, while an external suspension roll center goes away from the vehicle body.*

*A suspension roll center may be on, above, or below the road surface, as shown in Figure 8.35(a)-(c) for an external suspension roll center. When the suspension roll center is on the ground, above the ground, or below the ground, the vehicle roll center would be on the ground, below the ground, and above the ground, respectively.*

**Example 318** ★ *Camber variation of double A-arm suspension.*

*When a wheel moves up and down with respect to the vehicle body, de-*
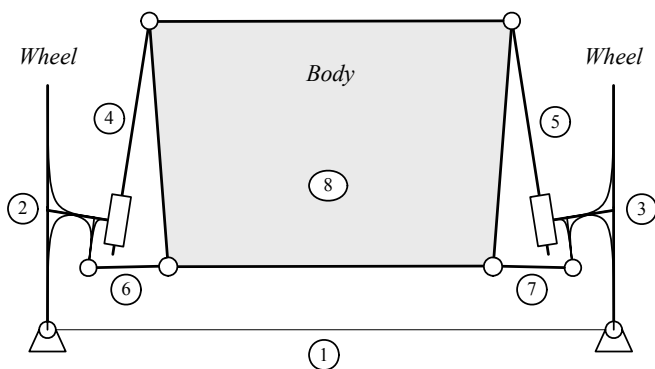
FIGURE 8.32. Kinematics model of a car with a McPherson suspension system.
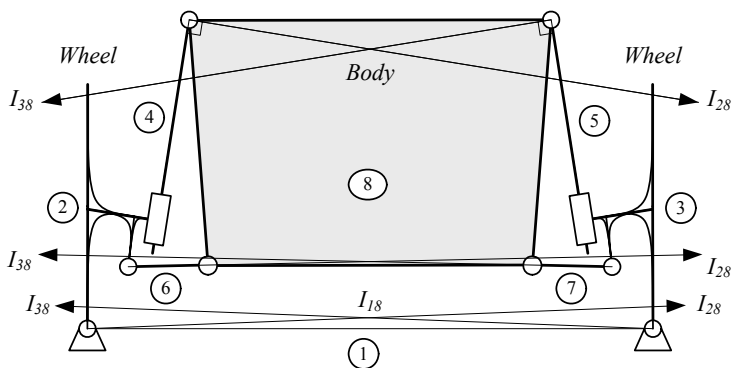


FIGURE 8.33. Roll center of a car with a McPherson suspension system.
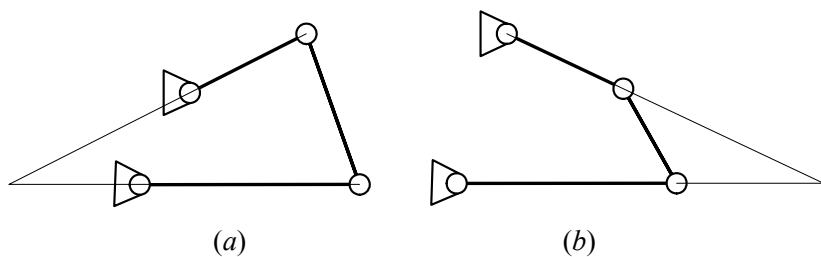


FIGURE 8.34. The kinematic model of the suspension of a front left wheel: (a) an internal roll center, and (b) an external roll center.
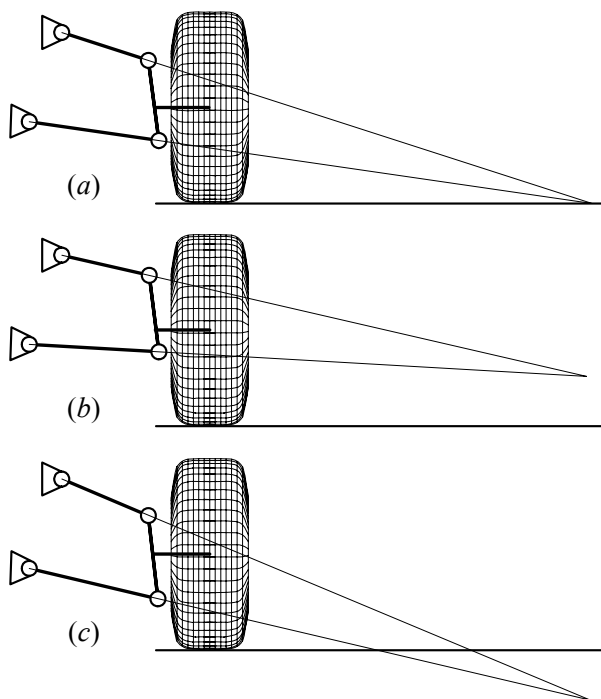
FIGURE 8.35. A suspension roll center at (a) on, (b) above, and (c) below the road surface.

pending on the suspension mechanism, the wheel may camber. Figure 8.36 illustrates the kinematic model for a double A-arm suspension mechanism.

The mechanism is equivalent to a four-bar linkage with the ground link as the vehicle chasis. The wheel is always attached to a coupler point $C$ of the mechanism. We set a local suspension coordinate frame $(x, y)$ with the $x$-axis indicating the ground link $MN$. The $x$-axis makes a constant angle $\theta_0$ with the vertical direction. The suspension machanism has a length $a$ for the upper A-arm, $b$ for the coupler link, $c$ for the lower A-arm, and $d$ for the ground link. The configuration of the suspension is determined by the angles $\theta_2$, $\theta_3$, and $\theta_4$, all measured from the positive direction of the $x$-axis. When the suspension is at its equilibrium position, the links of the double A-arm suspension make initial angles $\theta_{20}$ $\theta_{30}$, and $\theta_{40}$ with the $x$-axis.

The equilibrium position of a suspension is called the **rest position**.

To determine the camber angle during the fluctuation of the wheel, we should determine the variation of the coupler angle $\theta_3$, as a function of vertical motion $z$ of the coupler point $C$.

Using $\theta_2$ as a parameter, we can find the coordinates $(x_C, y_C)$ of the
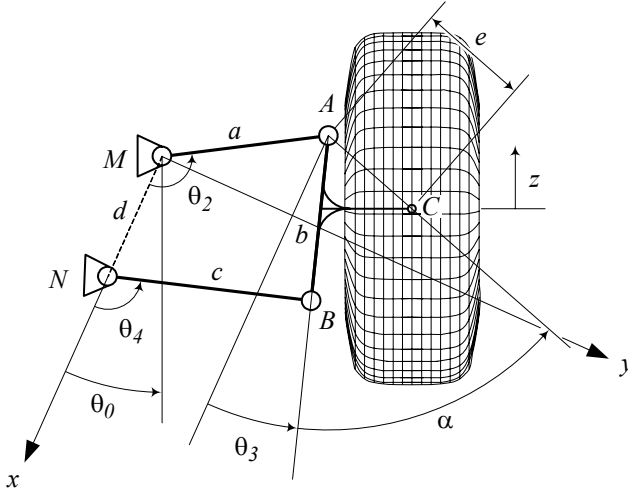
FIGURE 8.36. The kinematic model for a double A-arm suspension mechanism.

*coupler point $C$ in the suspension coordinate frame $(x, y)$ as*

$$
\begin{align}
x_C &= a\cos\theta_2 + e\cos(p - q + \alpha) \tag{8.1}\\
y_C &= a\sin\theta_2 + e\sin(p - q + \alpha) \tag{8.2}
\end{align}
$$

*where,*

$$
q = \tan^{-1}\frac{a\sin\theta_2}{d - a\cos\theta_2} \tag{8.3}
$$

$$
p = \tan^{-1}\frac{\sqrt{4b^2 f^2 - (b^2 + f^2 - c^2)^2}}{b^2 + f^2 - c^2} \tag{8.4}
$$

$$
f = \sqrt{a^2 + d^2 - 2ad\cos\theta_2}. \tag{8.5}
$$

*The position vector of the coupler point is $\mathbf{u}_C$*

$$
\mathbf{u}_C = x_C\hat{\imath} + y_C\hat{\jmath} \tag{8.6}
$$

*and the unit vector in the z-direction is*

$$
\hat{u}_z = -\cos\theta_0\hat{\imath} - \sin\theta_0\hat{\jmath}. \tag{8.7}
$$

*Therefore, the displacement $z$ in terms of $x_C$ and $y_C$ is:*

$$
\begin{align}
z &= \mathbf{u}_C \cdot \hat{u}_z\\
&= -x_C\cos\theta_0 - y_C\sin\theta_0 \tag{8.8}
\end{align}
$$

*The initial coordinates of the coupler point $C$ and the initial value of $z$ are:*

$$x_{C0} = a\cos\theta_{20} + e\cos(p_0 - q_0 + \alpha) \tag{8.9}$$

$$y_{C0} = a\sin\theta_{20} + e\sin(p_0 - q_0 + \alpha) \tag{8.10}$$

$$z_0 = -x_{C0}\cos\theta_0 - y_{C0}\sin\theta_0 \tag{8.11}$$

*and hence, the vertical displacement of the wheel center can be calculated by*

$$h = z - z_0 \tag{8.12}$$

*The initial angle of the coupler link with the vertical direction is $\theta_0 - \theta_{30}$. Therefore, the camber angle of the wheel would be*

$$\gamma = (\theta_0 - \theta_3) - (\theta_0 - \theta_{30})$$
$$= \theta_{30} - \theta_3 \tag{8.13}$$

*The angle of the coupler link with the $x$-direction is equal to*

$$\theta_3 = 2\tan^{-1}\left(\frac{-E \pm \sqrt{E^2 - 4DF}}{2D}\right) \tag{8.14}$$

*where,*

$$D = J_5 - J_1 + (1 + J_4)\cos\theta_2 \tag{8.15}$$

$$E = -2\sin\theta_2 \tag{8.16}$$

$$F = J_5 + J_1 - (1 - J_4)\cos\theta_2 \tag{8.17}$$

*and*

$$J_1 = \frac{d}{a} \tag{8.18}$$

$$J_2 = \frac{d}{c} \tag{8.19}$$

$$J_3 = \frac{a^2 - b^2 + c^2 + d^2}{2ac} \tag{8.20}$$

$$J_4 = \frac{d}{b} \tag{8.21}$$

$$J_5 = \frac{c^2 - d^2 - a^2 - b^2}{2ab}. \tag{8.22}$$

*Substituting (8.14) and (8.13), and then, eliminating $\theta_2$ between (8.13) and (8.8) provides the relationship between the vertical motion of the wheel, $z$, and the camber angle $\gamma$.*

**Example 319 ★** *Camber angle and wheel fluctuations.*

Consider the double A-arm suspension that is shown in Figure 8.36. The dimensions of the equivalent kinematic model are:

$$
\begin{aligned}
a &= 22.4\,\text{cm} \\
b &= 22.1\,\text{cm} \\
c &= 27.3\,\text{cm} \\
d &= 17.4\,\text{cm} \\
\theta_0 &= 24.3\,\text{deg}
\end{aligned}
\tag{8.23}
$$

*The coupler point C is at:*

$$
\begin{aligned}
e &= 14.8\,\text{cm} \\
\alpha &= 54.8\,\text{deg}
\end{aligned}
\tag{8.24}
$$

*If the angle $\theta_2$ at the rest position is at*

$$
\theta_{20} = 121.5\,\text{deg}
\tag{8.25}
$$

*then the initial angle of the other links are:*

$$
\begin{aligned}
\theta_{30} &= 18.36\,\text{deg} \\
\theta_{40} &= 107.32\,\text{deg}
\end{aligned}
\tag{8.26}
$$

*At the rest position, the coupler point is at:*

$$
\begin{aligned}
x_{C0} &= -22.73\,\text{cm} \\
y_{C0} &= 9.23\,\text{cm} \\
z_0 &= 16.92\,\text{cm}
\end{aligned}
\tag{8.27}
$$

We may calculate $h$ and $\gamma$ by varying the parameter $\theta_2$. Figure 8.37 illustrates $h$ as a function of the camber angle $\gamma$. For this suspension mechanism, the wheel gains a positive camber when the wheel moves up, and gains a negative camber when the it moves down. The mechanism is shown in Figure 8.38, when the wheel is at the rest position and has a positive or a negative displacement.

# 8.4   ★ Car Tire Relative Angles

There are four major wheel alignment parameters that affect vehicle dynamics: *toe, camber, caster,* and *trust angle.*

The figure shows a curve with the following annotations:

a=22.4 cm
b=22.1 cm
c=27.3 cm
d=17.4 cm
e=14.8 cm

$\theta_0 = 24.3°$
$\theta_{20} = 121.5°$
$\alpha = 58.8°$

Vertical axis: $h[cm]$ with values 8, 6, 4, 2, 0, -2, -4, -6, -8

Horizontal axis: $\gamma[\deg]$ with values -8, -6, -4, -2, 0, 2, 4, 6
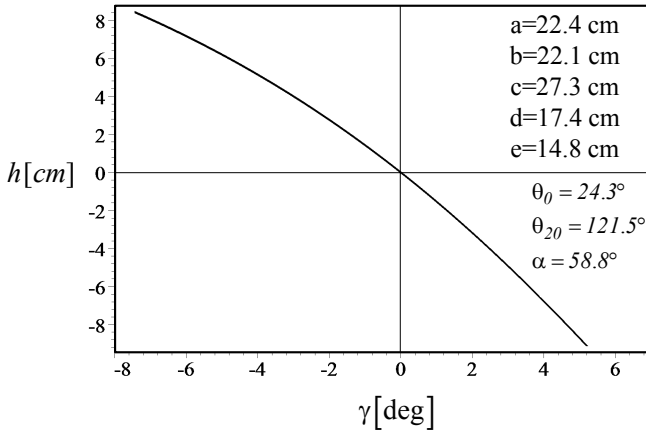
FIGURE 8.37. $h$ as a function of the camber angle $\gamma$.

## 8.4.1  ★ Toe

When a pair of wheels is set so that their leading edges are pointed toward each other, the wheel pair is said to have *toe-in*. If the leading edges point away from each other, the pair is said to have *toe-out*. Toe-in and toe-out front wheel configurations of a car are illustrated in Figure 8.39.

The amount of toe can be expressed in degrees of the angle to which the wheels are not parallel. However, it is more common to express the toe-in and toe-out as the difference between the track widths as measured at the leading and trailing edges of the tires. Toe settings affect three major performances: tire wear, straight-line stability, and corner entry handling.

For minimum tire wear and power loss, the wheels on a given axle of a car should point directly ahead when the car is running in a straight line. Excessive toe-in causes accelerated wear at the outboard edges of the tires, while too much toe-out causes wear at the inboard edges.

Toe-in increases the directional stability of the vehicle, and toe-out increases the steering response. Hence, a toe-in setting makes the steering function lazy, while a toe-out makes the vehicle unstable.

With four wheel independent suspensions, the toe may also be set at the rear of the car. Toe settings at the rear have the same effect on wear, directional stability, and turn-in as they do on the front. However, we usually do not set up a rear-drive race car toed out in the rear, because of excessive instability.

When driving torque is applied to the wheels, they pull themselves forward and try to create toe-in. Furthermore, when pushed down the road, a non-driven wheel or a braking wheel will tend to toe-out.

**Example 320** *Toe-in and directional stability.*
*Toe settings have an impact on directional stability. When the steering*
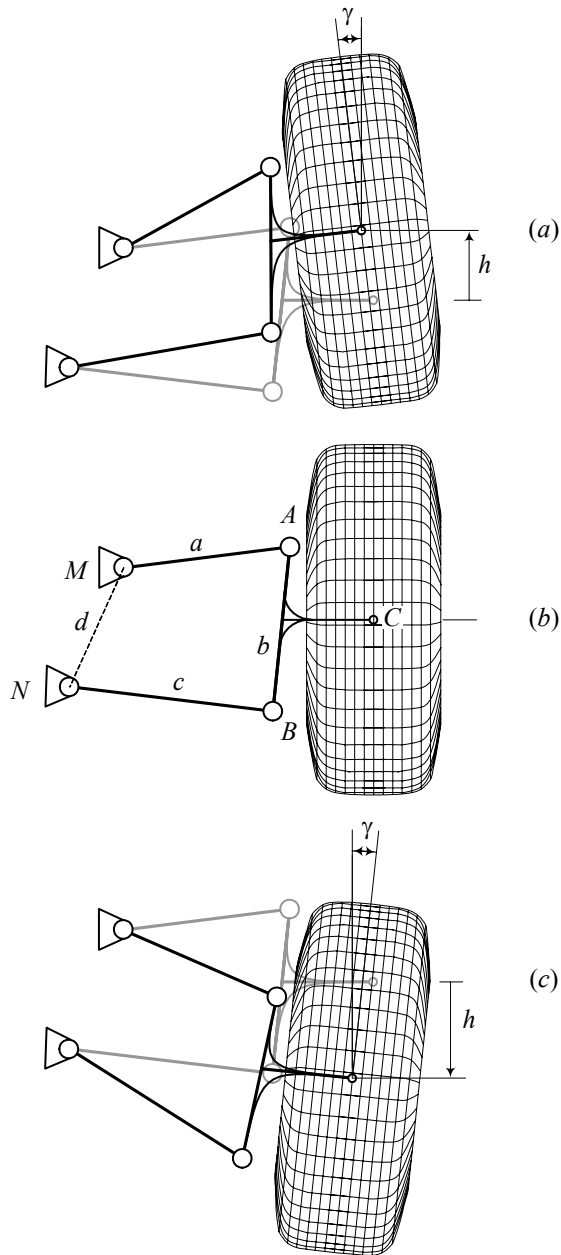
FIGURE 8.38. A double A-arm suspension mechanism when the wheel is at: (a) a positive displacement, (b) rest position, and (c) a negative displacement.
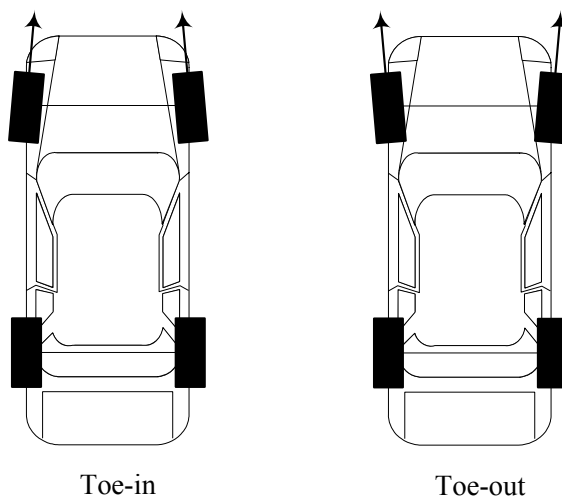
FIGURE 8.39. Toe-in and toe-out configuration on the front wheels of a car.

wheel is centered, toe-in causes the wheels to tent to move along paths that intersect each other in front of the vehicle. However, the wheels are in balance and no turn results. Toe-in setup can increase the directional stability caused by little steering fluctuations and keep the car moving straight. Steering fluctuations may be a result of road disturbances.

If a car is set up with toe-out, the front wheels are aligned so that slight disturbances cause the wheel pair to assume rolling directions that approach a turn. Therefore, toe-out encourages the initiation of a turn, while toe-in discourages it. Toe-out makes the steering quicker. So, it may be used in vehicles for a faster response. The toe setting on a particular car becomes a trade-off between the straight-line stability afforded by toe-in and the quick steering response by toe-out. Toe-out is not desirable for street cars, however, race car drivers are willing to drive a car with a little directional instability, for sharper turn-in to the corners. So street cars are generally set up with toe-in, while race cars are often set up with toe-out.

**Example 321** *Toe-in and toe-out in the front and rear axles.*

Front toe-in: slower steering response, more straight-line stability, greater wear at the outboard edges of the tires.

Front toe-zero: medium steering response, minimum power loss, minimum tire wear.

Front toe-out: quicker steering response, less straight-line stability, greater wear at the inboard edges of the tires.

Rear toe-in: straight-line stability, traction out of the corner, more steerability, higher top speed.
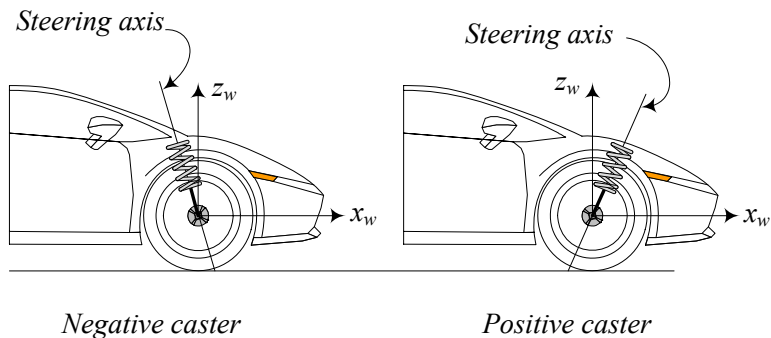
FIGURE 8.40. A positive and negative caster configuration on front wheel of a car.

## 8.4.2 ★ Caster Angle

Caster is the angle to which the steering pivot axis is tilted forward or rearward from vertical, as viewed from the side. Assume the wheel is straight to have the body frame and the wheel frame coincident. If the steering axis is turned about the wheel $y_w$-axis then the wheel has *positive caster*. If the steering axis is turned about the wheel $-y_w$-axis, then the wheel has *negative caster*. Positive and negative caster configurations on the front wheel of a car are shown in Figure 8.40.

Negative caster aids in centering the steering wheel after a turn and makes the front tires straighten quicker. Most street cars are made with $4 - 6$ deg negative caster. Negative caster tends to straighten the wheel when the vehicle is traveling forward, and thus is used to enhance straight-line stability.

**Example 322** *Negative caster of shopping carts.*

*The steering axis of a shopping cart wheel is set forward of where the wheel contacts the ground. As the cart is pushed forward, the steering axis pulls the wheel along, and because the wheel drags along the ground, it falls directly in line behind the steering axis. The force that causes the wheel to follow the steering axis is proportional to the distance between the steering axis and the wheel-to-ground contact point, if the caster is small. This distance is referred to as trail. The cars' steering axis intersects the ground at a point in front of the tireprint, and thus the same effect as seen in the shopping cart casters is achieved.*

*While greater caster angles improves straight-line stability, they also cause an increase in steering effort.*

**Example 323** *Characteristics of caster in front axle.*

*Zero castor provides: easy steering into the corner, low steering out of the corner, low straight-line stability.*

*Negative caster provides: low steering into the corner, easy steering out of the corner, more straight-line stability, high tireprint area during turn, good turn-in response, good directional stability, good steering feel.*

*When a castered wheel rotates about the steering axis, the wheel gains camber. This camber is generally favorable for cornering.*

### 8.4.3 ★ Camber

Camber is the angle of the wheel relative to vertical line to the road, as viewed from the front or the rear of the car. Figure 8.41 illustrates the wheel number 1 of a vehicle. If the wheel leans in toward the chassis, it is called negative camber and if it leans away from the car, it is called positive camber.

The cornering force that a tire can develop is highly dependent on its angle relative to the road surface, and so wheel camber has a major effect on the road holding of a car. A tire develops its maximum lateral force at a small camber angle. This fact is due to the contribution of camber thrust, which is an additional lateral force generated by elastic deformation as the tread rubber pulls through the tire/road interface.

To optimize a tire's performance in a turn, the suspension should provide a slight camber angle in the direction of rotation. As the body rolls in a turn, the suspension deflects vertically. The wheel is connected to the chassis by suspension mechanism, which must rotate to allow for the wheel deflection. Therefore, the wheel can be subject to large camber changes as the suspension moves up and down. So, the more the wheel must deflect from its static position, the more difficult it is to maintain an ideal camber angle. Thus, the relatively large wheel travel and soft roll stiffness needed to provide a smooth ride in passenger cars presents a difficult design challenge, while the small wheel travel and high roll stiffness inherent in racing cars reduces the problem.

**Example 324** *Castor versus camber.*
*Camber doesn't improve turn-in as the positive caster does. Camber is not generally good for tire wear. Camber in one wheel does not improve directional stability. Camber adversely affects braking and acceleration efforts.*

### 8.4.4 ★ Trust Angle

The *trust angle v* is the angle between vehicle's centerline and perpendicular to the rear axle. It compares the direction that the rear axle is aimed with the centerline of the vehicle. A nonzero angle configuration is shown in Figure 8.42.

Zero angle confirms that the rear axle is parallel to the front axle, and the wheelbase on both sides of the vehicle are the same. A reason for nonzero
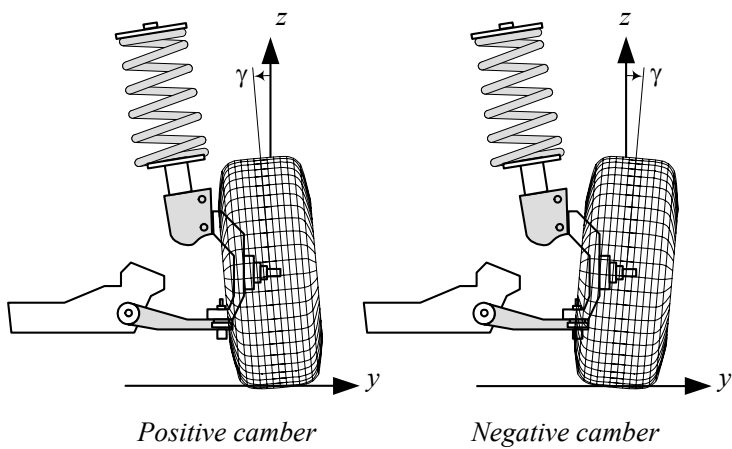
FIGURE 8.41. A positive and negative camber on the front wheel of a car.
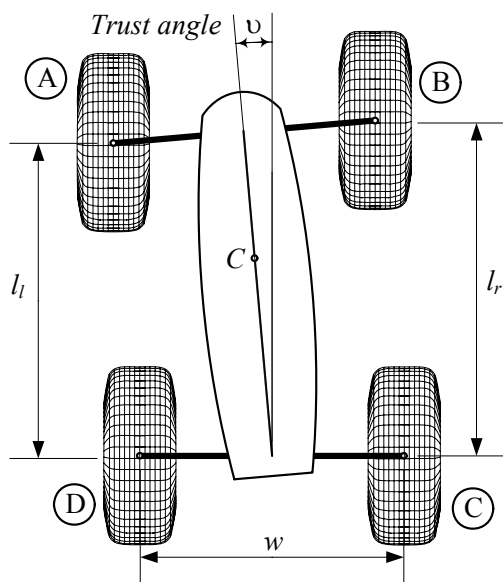


FIGURE 8.42. Illustration of trust angle.

$z_w$

$\delta$ *Steer angle*

*Tire axis*    $y_w$

$\varphi$ *Spin angle*

$x_w$

$\gamma$ *Camber angle*

*Ground surface*
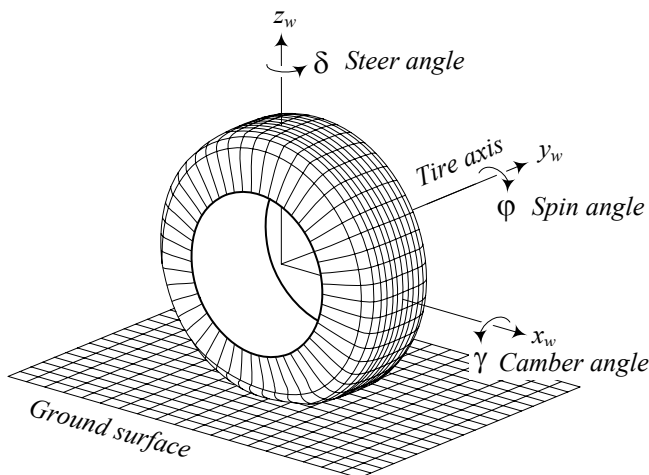
FIGURE 8.43. *Six* degrees of freedom of a wheel with respect to a vehicle body.

trust angle would have unequal toe-in or toe-out on both sides of the axle.

**Example 325** *Torque reaction.*

There are two kinds of torque reactions in rear-whel-drive: 1− the re-
action of the axle housing to rotate in the opposite direction of the crown
wheel rotation, and 2− the reaction of axle housing to spin about its own
center, opposite to the direction of pinion's rotation.

The first reaction leads to a lifting force in the differential causing a
wind-up in springs. The second reaction leads to a lifting force on the right
wheels.

## 8.5   Suspension Requirements and Coordinate Frames

The suspension mechanism should allow a relative motion between the
wheel and the vehicle body. The relative motions are needed to pass the
road irregularities and steering. To function properly, a suspension mecha-
nism should have some kinematic and dynamics requirements.

### 8.5.1   Kinematic Requirements

To express the motions of a wheel, we attach a wheel coordinate system
$W\,(ox_w y_w z_w)$ to the center of the wheel. A wheel, as a rigid body, has *six*
degrees-of-freedom with respect to the vehicle body: three translations and
three rotations, as shown in Figure 8.43.
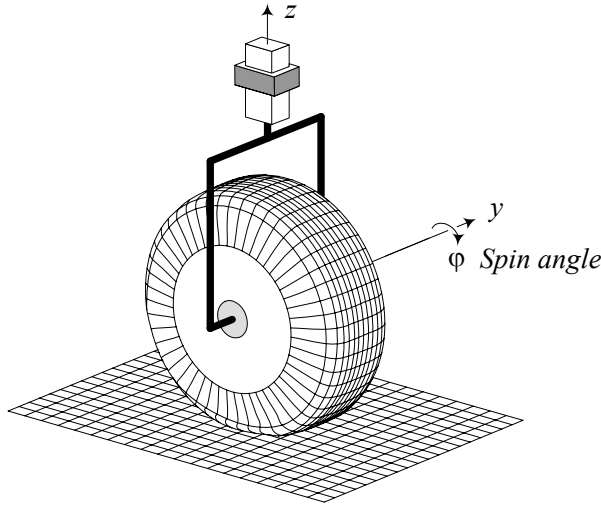
FIGURE 8.44. A non-steerable wheel must have *two* DOF.

The axes $x_w$, $y_w$, and $z_w$ indicate the direction of forward, lateral, and vertical translations and rotations. In the position shown in the figure, the rotation about the $x_w$-axis is the *camber* angle, about the $y_w$-axis is the *spin*, and about the $z_w$-axis is the *steer* angle.

Consider a non-steerable wheel. Translation in $z_w$-direction and spin about the $y_w$-axis are the only *two* DOF allowed for such a wheel. So, we need to take four DOF. If the wheel is steerable, then translation in the $z_w$-direction, spin about the $y_w$-axis, and steer rotation about the $z_w$-axis are the three DOF allowed. So, we must take three DOF of a steerable wheel.

Kinematically, non-steerable and steerable wheels should be supported as shown in Figures 8.44 and 8.45 respectively. Providing the required freedom, as well as eliminating the taken DOF, are the *kinematic requirements* of a suspension mechanism.

## 8.5.2 Dynamic Requirements

Wheels should be able to propel, steer, and stop the vehicle. So, the suspension system must transmit the driving traction and deceleration braking forces between the vehicle body and the ground. The suspension members must also resist lateral forces acting on the vehicle. Hence, the wheel suspension system must make the wheel rigid for the taken DOF. However, there must also be some compliance members to limit the untaken DOF. The most important compliant members are spring and dampers to provide returning and resistance forces in the $z$-direction.
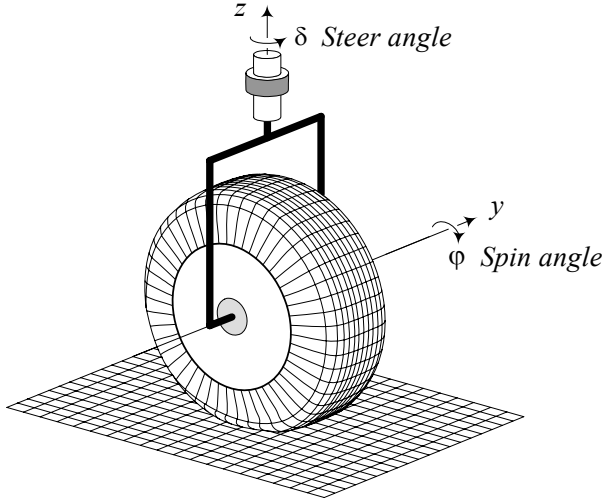
FIGURE 8.45. A steerable wheel must have *three* DOF.

### 8.5.3   *Wheel, wheel-body, and tire Coordinate Frames*

Three coordinate frames are employed to express the orientation of a tire and wheel with respect to the vehicle: the wheel frame $W$, wheel-body frame $C$, and tire frame $T$. A wheel coordinate frame $W\,(x_w, y_w, z_w)$ is attached to the center of a wheel. It follows every translation and rotation of the wheel except the spin. Hence, the $x_w$ and $z_w$ axes are always in the tire-plane, while the $y_w$-axis is always along the spin axis. A wheel coordinate frame is shown in Figure 8.43.

When the wheel is straight and the $W$ frame is parallel to the vehicle coordinate frame, we attach a wheel-body coordinate frame $C\,(x_c, y_c, z_c)$ at the center of the wheel parallel to the vehicle coordinate axes. The wheel-body frame $C$ is motionless with respect to the vehicle coordinate and does not follow any motion of the wheel.

The tire coordinate frame $T\,(x_t, y_t, z_t)$ is set at the center of the tireprint. The $z_t$-axis is always perpendicular to the ground. The $x_t$-axis is along the intersection line of the tire-plane and the ground. The tire frame does not follows the spin and camber rotations of the tire however, it follows the steer angle rotation about the $z_c$-axis.

Figure 8.46 illustrates a tire and a wheel coordinate frames.

**Example 326** *Visualization of the wheel, tire, and wheel-body frames.*
*Figure 8.47 illustrates the relative configuration of a wheel-body frame $C$, a tire frame $T$, and a wheel frame $W$. If the steering axis is along the $z_c$-axis then, the rotation of the wheel about the $z_c$-axis is the steer angle $\delta$. Rotation about the $x_t$-axis is the camber angle $\gamma$.*
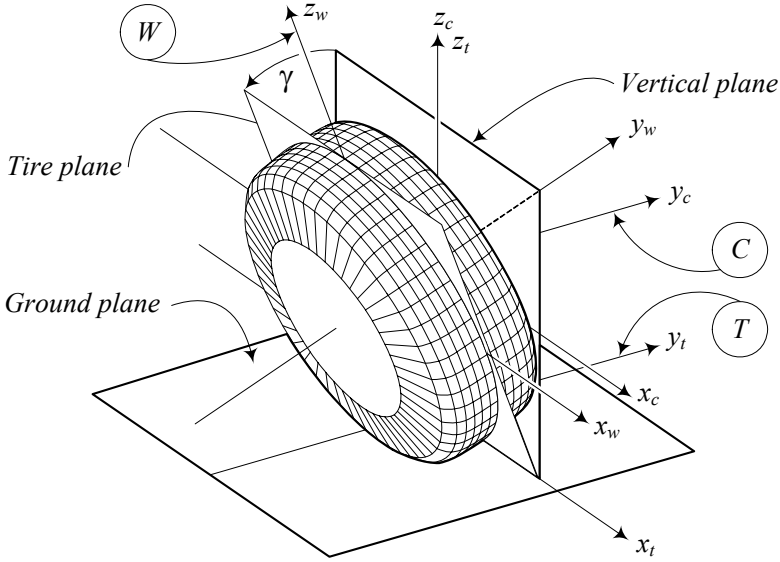
FIGURE 8.46. Illustration of tire and wheel coordinate frames.

*Generally speaking, the steering axis may have any angle and may go through any point of the ground plane.*

**Example 327** *Wheel to tire coordinate frame transformation.*
If $^T\mathbf{d}_W$ indicates the $T$-expression of the position vector of the wheel frame origin relative to the tire frame origin, then having the coordinates of a point $P$ in the wheel frame, we can find its coordinates in the tire frame using the following equation.

$$^T\mathbf{r}_P = {}^TR_W\,{}^W\mathbf{r}_P + {}^T\mathbf{d}_W \tag{8.28}$$

If $^W\mathbf{r}_P$ indicates the position vector of a point $P$ in the wheel frame,

$$^W\mathbf{r}_P = \begin{bmatrix} x_P \\ y_P \\ z_P \end{bmatrix} \tag{8.29}$$

then the coordinates of the point $P$ in the tire frame $^T\mathbf{r}_P$ are

$$
\begin{aligned}
^T\mathbf{r}_P &= {}^TR_W\,{}^W\mathbf{r}_P + {}^T\mathbf{d} \\
&= {}^TR_W\,{}^W\mathbf{r}_P + {}^TR_W\,{}^W_T\mathbf{d}_W \\
&= \begin{bmatrix} x_P \\ y_P\cos\gamma - R_w\sin\gamma - z_P\sin\gamma \\ R_w\cos\gamma + z_P\cos\gamma + y_P\sin\gamma \end{bmatrix}
\end{aligned} \tag{8.30}
$$
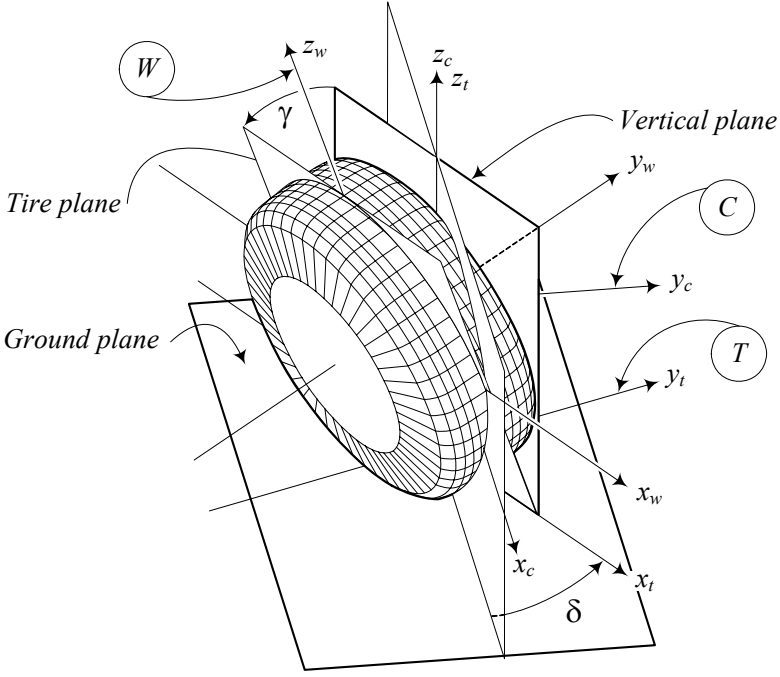
FIGURE 8.47. Illustration of tire, wheel, and body coordinate frames.

where, $^W_T\mathbf{d}_W$ is the $W$-expression of the position vector of the wheel frame in the tire frame, $R_w$ is the radius of the tire, and $^TR_W$ is the rotation matrix to go from the wheel frame $W$ to the tire frame $T$.

$$^TR_W = \begin{bmatrix} 1 & 0 & 0 \\ 0 & \cos\gamma & -\sin\gamma \\ 0 & \sin\gamma & \cos\gamma \end{bmatrix} \tag{8.31}$$

$$^W_T\mathbf{d}_W = \begin{bmatrix} 0 \\ 0 \\ R_w \end{bmatrix}. \tag{8.32}$$

As an example, the center of the wheel $^W\mathbf{r}_P = {}^W\mathbf{r}_o = \mathbf{0}$ is the origin of the wheel frame $W$, that is at

$$
\begin{aligned}
^T\mathbf{r}_o &= {}^T\mathbf{d}_W = {}^TR_W \,{}^W_T\mathbf{d}_W \\
&= \begin{bmatrix} 0 \\ -R_w\sin\gamma \\ R_w\cos\gamma \end{bmatrix}
\end{aligned} \tag{8.33}
$$

in the tire coordinate frame $T$.

**Example 328** ★ *Tire to wheel coordinate frame transformation.*
    *If $\mathbf{r}_P$ indicates the position vector of a point $P$ in the tire coordinate frame,*

$$^T\mathbf{r}_P = \begin{bmatrix} x_P \\ y_P \\ z_P \end{bmatrix} \tag{8.34}$$

*then the position vector $^W\mathbf{r}_P$ of the point $P$ in the wheel coordinate frame is*

$$
\begin{aligned}
^W\mathbf{r}_P &= {}^W R_T \, {}^T\mathbf{r}_P - {}^W_T\mathbf{d}_W \\
&= \begin{bmatrix} x_P \\ y_P \cos\gamma + z_P \sin\gamma \\ z_P \cos\gamma - R_w - y_P \sin\gamma \end{bmatrix}
\end{aligned}
\tag{8.35}
$$

*because*

$$^W R_T = \begin{bmatrix} 1 & 0 & 0 \\ 0 & \cos\gamma & \sin\gamma \\ 0 & -\sin\gamma & \cos\gamma \end{bmatrix} \tag{8.36}$$

$$^W\mathbf{d}_T = \begin{bmatrix} 0 \\ 0 \\ R_w \end{bmatrix} \tag{8.37}$$

*and we may multiply both sides of Equation (8.28) by $^T R_W^T$ to get*

$$
\begin{aligned}
^T R_W^T \, {}^T\mathbf{r}_P &= {}^W\mathbf{r}_P + {}^T R_W^T \, {}^T\mathbf{d}_W \tag{8.38} \\
&= {}^W\mathbf{r}_P + {}^W_T\mathbf{d}_W \\
^W\mathbf{r}_P &= {}^W R_T \, {}^T\mathbf{r}_P - {}^W_T\mathbf{d}_W. \tag{8.39}
\end{aligned}
$$

*As an example, the center of tireprint in the wheel frame is at*

$$
^W\mathbf{r}_P = \begin{bmatrix} 1 & 0 & 0 \\ 0 & \cos\gamma & -\sin\gamma \\ 0 & \sin\gamma & \cos\gamma \end{bmatrix}^T \begin{bmatrix} 0 \\ 0 \\ 0 \end{bmatrix} - \begin{bmatrix} 0 \\ 0 \\ R_w \end{bmatrix} = \begin{bmatrix} 0 \\ 0 \\ -R_w \end{bmatrix}.
\tag{8.40}
$$

**Example 329** ★ *Wheel to tire homogeneous transformation matrices.*
    *The transformation from the wheel to tire coordinate frame may also be expressed by a $4 \times 4$ homogeneous transformation matrix $^T T_W$,*

$$
\begin{aligned}
^T\mathbf{r}_P &= {}^T T_W \, {}^W\mathbf{r}_P \\
&= \begin{bmatrix} ^T R_W & ^T\mathbf{d}_W \\ 0 & 1 \end{bmatrix} {}^W\mathbf{r}_P \tag{8.41}
\end{aligned}
$$

*where*

$$
^T T_W = \begin{bmatrix} 1 & 0 & 0 & 0 \\ 0 & \cos\gamma & -\sin\gamma & -R_w \sin\gamma \\ 0 & \sin\gamma & \cos\gamma & R_w \cos\gamma \\ 0 & 0 & 0 & 1 \end{bmatrix}.
\tag{8.42}
$$

*The corresponding homogeneous transformation matrix $^W T_T$ from the tire to wheel frame would be*

$$
\begin{aligned}
^W T_T &= \begin{bmatrix} ^W R_T & ^W \mathbf{d}_T \\ 0 & 1 \end{bmatrix} \\[2mm]
&= \begin{bmatrix}
1 & 0 & 0 & 0 \\
0 & \cos\gamma & -\sin\gamma & 0 \\
0 & \sin\gamma & \cos\gamma & -R_w \\
0 & 0 & 0 & 1
\end{bmatrix}.
\end{aligned} \tag{8.43}
$$

*It can be checked that $^W T_T = {^T T_W^{-1}}$, using the inverse of a homogeneous transformation matrix rule.*

$$
\begin{aligned}
^T T_W^{-1} &= \begin{bmatrix} ^T R_W & ^T \mathbf{d}_W \\ 0 & 1 \end{bmatrix}^{-1} = \begin{bmatrix} ^T R_W^T & -^T R_W^T {}^T \mathbf{d}_W \\ 0 & 1 \end{bmatrix} \\[2mm]
&= \begin{bmatrix} ^W R_T & -^W R_T {}^T \mathbf{d}_W \\ 0 & 1 \end{bmatrix}
\end{aligned} \tag{8.44}
$$

**Example 330 ★** *Tire to wheel-body frame transformation.*
   *The origin of the tire frame is at $^C \mathbf{d}_T$ in the wheel-body frame.*

$$
^C \mathbf{d}_T = \begin{bmatrix} 0 \\ 0 \\ -R_w \end{bmatrix} \tag{8.45}
$$

*The tire frame can steer about the $z_c$-axis with respect to the wheel-body frame. The associated rotation matrix is*

$$
^C R_T = \begin{bmatrix}
\cos\delta & -\sin\delta & 0 \\
\sin\delta & \cos\delta & 0 \\
0 & 0 & 1
\end{bmatrix} \tag{8.46}
$$

*Therefore, the transformation between the tire and wheel-body frames can be expressed by*

$$
^C \mathbf{r} = {^C R_T} \, {^T \mathbf{r}} + {^C \mathbf{d}_T} \tag{8.47}
$$

*or equivalently, by a homogeneous transformation matrix $^C T_T$.*

$$
\begin{aligned}
^C T_T &= \begin{bmatrix} ^C R_T & ^C \mathbf{d}_T \\ 0 & 1 \end{bmatrix} \\[2mm]
&= \begin{bmatrix}
\cos\delta & -\sin\delta & 0 & 0 \\
\sin\delta & \cos\delta & 0 & 0 \\
0 & 0 & 1 & -R_w \\
0 & 0 & 0 & 1
\end{bmatrix}
\end{aligned} \tag{8.48}
$$

*As an example, the wheel-body coordinates of the point $P$ on the tread of a*
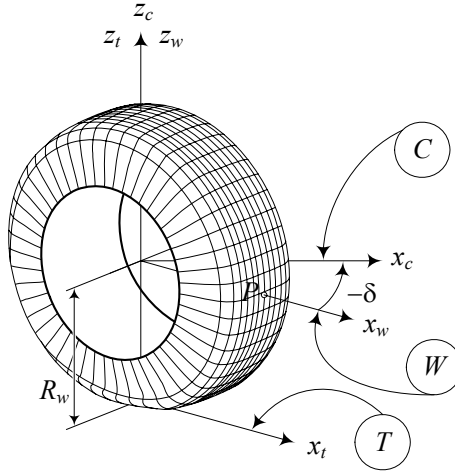
FIGURE 8.48. The tire, wheel, and wheel body frames of a steered wheel.

negatively steered tire at the position shown in Figure 8.48, are:

$$
\begin{aligned}
{}^C\mathbf{r} &= {}^CT_T\,{}^T\mathbf{r}_P \\
&= \begin{bmatrix} \cos-\delta & -\sin-\delta & 0 & 0 \\ \sin-\delta & \cos-\delta & 0 & 0 \\ 0 & 0 & 1 & -R_w \\ 0 & 0 & 0 & 1 \end{bmatrix} \begin{bmatrix} R_w \\ 0 \\ R_w \\ 1 \end{bmatrix} \\
&= \begin{bmatrix} R_w\cos\delta \\ -R_w\sin\delta \\ 0 \\ 1 \end{bmatrix}
\end{aligned}
\tag{8.49}
$$

The homogeneous transformation matrix for tire to wheel-body frame $^TT_C$ is:

$$
\begin{aligned}
{}^TT_C &= {}^CT_T^{-1} = \begin{bmatrix} {}^CR_T & {}^C\mathbf{d}_T \\ 0 & 1 \end{bmatrix}^{-1} = \begin{bmatrix} {}^CR_T^T & -{}^CR_T^T\,{}^C\mathbf{d}_T \\ 0 & 1 \end{bmatrix} \\
&= \begin{bmatrix} {}^CR_T^T & -{}^T_C\mathbf{d}_T \\ 0 & 1 \end{bmatrix} = \begin{bmatrix} \cos\delta & \sin\delta & 0 & 0 \\ -\sin\delta & \cos\delta & 0 & 0 \\ 0 & 0 & 1 & R_w \\ 0 & 0 & 0 & 1 \end{bmatrix}
\end{aligned}
\tag{8.50}
$$

**Example 331 ★** *Cycloid.*
   *Assume that the wheel in Figure 8.48 is turning with angular velocity $\omega$ and has no slip on the ground. If the point $P$ is at the center of the tireprint*

*when $t = 0$,*

$$^M\mathbf{r}_P = \begin{bmatrix} 0 \\ 0 \\ -R_w \end{bmatrix} \qquad (8.51)$$

*then we can find its position in the wheel frame at a time $t$ by employing another coordinate frame $M$. The frame $M$ is called the rim frame and is stuck to the wheel at its center. Because of spin, the $M$ frame turns about the $y_w$-axis, and therefore, the rotation matrix to go from the rim frame to the wheel frame is:*

$$^W R_M = \begin{bmatrix} \cos \omega t & 0 & \sin \omega t \\ 0 & 1 & 0 \\ -\sin \omega t & 0 & \cos \omega t \end{bmatrix} \qquad (8.52)$$

*So the coordinates of $P$ in the wheel frame are:*

$$\begin{aligned} ^W\mathbf{r}_P &= {}^W R_M \, {}^M\mathbf{r}_P \\ &= \begin{bmatrix} -R_w \sin t\omega \\ 0 \\ -R_w \cos t\omega \end{bmatrix} \end{aligned} \qquad (8.53)$$

*The center of the wheel is moving with speed $v_x = R_w\omega$ and it is at $^G\mathbf{r} = \begin{bmatrix} v_x t & 0 & R_w \end{bmatrix}$ in the global coordinate frame $G$ on the ground. Hence, the coordinates of point $P$ in the global frame $G$, would be*

$$^G\mathbf{r}_P = {}^W\mathbf{r}_P + \begin{bmatrix} v_x t \\ 0 \\ R_w \end{bmatrix} = \begin{bmatrix} R_w \left( \omega t - \sin t\omega \right) \\ 0 \\ R_w \left( 1 - \cos t\omega \right) \end{bmatrix}. \qquad (8.54)$$

*The path of motion of point $P$ in the $(X, Z)$-plane can be found by eliminating $t$ between $X$ and $Z$ coordinates. However, it is easier to expressed the path by using $\omega t$ as a parameter. Such a path is called **cycloid**.*

*In general case, point $P$ can be at any distance from the center of the rim frame. If the point is at a distance $d \neq R_w$, then its path of motion is called the **trochoid**. A trochoid is called a **curtate cycloid** when $d < R_w$ and a **prolate cycloid** when $d > R_w$. Figure 8.49(a)-(c) illustrate a cycloid, curtate cycloid, and prolate cycloid respectively.*

**Example 332 ★** *Wheel to wheel-body frame transformation.*
   *The homogeneous transformation matrix $^C T_W$ to go from the wheel frame*
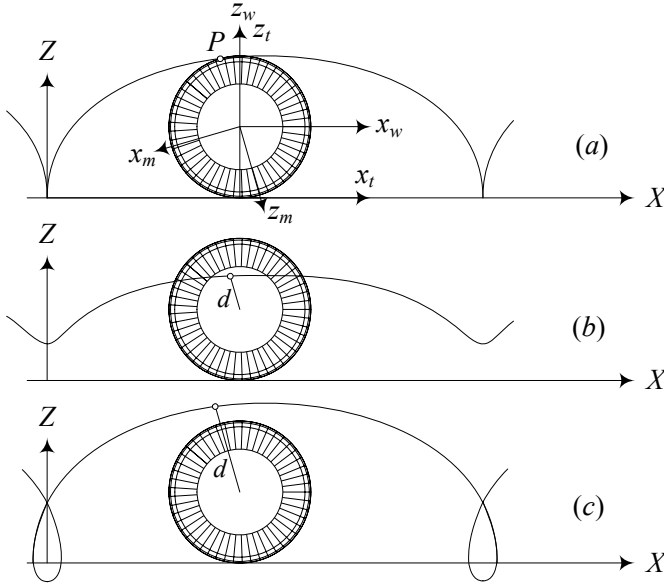
FIGURE 8.49. A cycloid (a), curtate cycloid (b), and prolate cycloid (c).

*to the wheel-body frame can be found by combined transformation.*

$$
\begin{aligned}
{}^{C}T_{W} &= {}^{C}T_{T}\,{}^{T}T_{W} \hspace{4cm} (8.55) \\[2mm]
&= \begin{bmatrix} c\delta & -s\delta & 0 & 0 \\ s\delta & c\delta & 0 & 0 \\ 0 & 0 & 1 & -R_{w} \\ 0 & 0 & 0 & 1 \end{bmatrix}
\begin{bmatrix} 1 & 0 & 0 & 0 \\ 0 & c\gamma & -s\gamma & -R_{w}\sin\gamma \\ 0 & s\gamma & c\gamma & R_{w}\cos\gamma \\ 0 & 0 & 0 & 1 \end{bmatrix} \\[2mm]
&= \begin{bmatrix} \cos\delta & -\cos\gamma\sin\delta & \sin\gamma\sin\delta & R_{w}\sin\gamma\sin\delta \\ \sin\delta & \cos\gamma\cos\delta & -\cos\delta\sin\gamma & -R_{w}\cos\delta\sin\gamma \\ 0 & \sin\gamma & \cos\gamma & R_{w}\cos\gamma - R_{w} \\ 0 & 0 & 0 & 1 \end{bmatrix}
\end{aligned}
$$

*If $\mathbf{r}_{P}$ indicates the position vector of a point $P$ in the wheel coordinate frame,*

$$
{}^{W}\mathbf{r}_{P} = \begin{bmatrix} x_{P} \\ y_{P} \\ z_{P} \end{bmatrix} \hspace{3cm} (8.56)
$$

*then the homogeneous position vector ${}^{C}\mathbf{r}_{P}$ of the point $P$ in the wheel-body*

*coordinate frame is:*

$$
\begin{aligned}
{}^C\mathbf{r}_P &= {}^C T_W \, {}^W\mathbf{r}_P \\
&= \begin{bmatrix} x_P \cos\delta - y_P \cos\gamma \sin\delta + (R_w + z_P)\sin\gamma \sin\delta \\ x_P \sin\delta + y_P \cos\gamma \cos\delta - (R_w + z_P)\cos\delta \sin\gamma \\ -R_w + (R_w + z_P)\cos\gamma + y_P \sin\gamma \\ 1 \end{bmatrix}
\end{aligned}
\tag{8.57}
$$

The position of the wheel center ${}^W\mathbf{r} = \mathbf{0}$, for a cambered and steered wheel is at

$$
\begin{aligned}
{}^C\mathbf{r} &= {}^C T_W \, {}^W\mathbf{r} \\
&= \begin{bmatrix} R_w \sin\gamma \sin\delta \\ -R_w \cos\delta \sin\gamma \\ -R_w(1 - \cos\gamma) \\ 1 \end{bmatrix}
\end{aligned}
\tag{8.58}
$$

The $z_c = R_w(\cos\gamma - 1)$ indicates how much the center of the wheel comes down when the wheel cambers.

If the wheel is not steerable, then $\delta = 0$ and the transformation matrix ${}^C T_W$ reduces to

$$
{}^C T_W = \begin{bmatrix} 1 & 0 & 0 & 0 \\ 0 & \cos\gamma & -\sin\gamma & -R_w \sin\gamma \\ 0 & \sin\gamma & \cos\gamma & R_w(\cos\gamma - 1) \\ 0 & 0 & 0 & 1 \end{bmatrix}
\tag{8.59}
$$

*that shows*

$$
\begin{aligned}
{}^C\mathbf{r}_P &= {}^C T_W \, {}^W\mathbf{r}_P \\
&= \begin{bmatrix} x_P \\ y_P \cos\gamma - R_w \sin\gamma - z_P \sin\gamma \\ z_P \cos\gamma + y_P \sin\gamma + R_w(\cos\gamma - 1) \\ 1 \end{bmatrix}
\end{aligned}
\tag{8.60}
$$

**Example 333 ★** *Tire to vehicle coordinate frame transformation.*

Figure 8.50 illustrates the first and fourth tires of a 4-wheel vehicle. There is a body coordinate frame $B(x, y, z)$ attached to the mass center $C$ of the vehicle. There are also two tire coordinate frames $T_1(x_{t_1}, y_{t_1}, z_{t_1})$ and $T_4(x_{t_4}, y_{t_4}, z_{t_4})$ attached to the tires 1 and 4 at the center of their tireprints.

The origin of the tire coordinate frame $T_1$ is at ${}^B\mathbf{d}_1$

$$
{}^B\mathbf{d}_{T_1} = \begin{bmatrix} a_1 \\ -b_1 \\ -h \end{bmatrix}
\tag{8.61}
$$
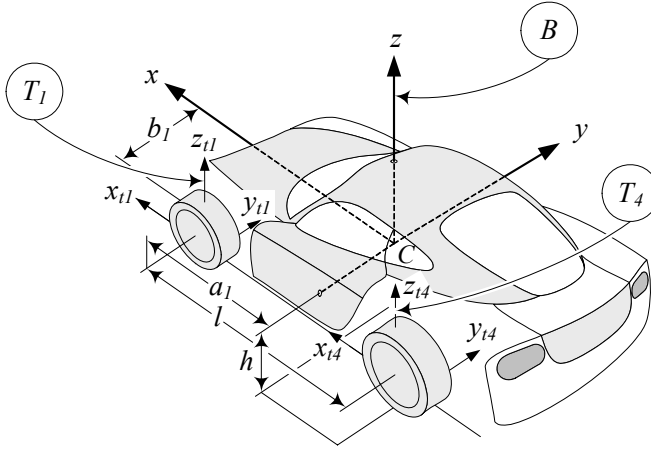
FIGURE 8.50. The coordinate frames of the first and fourth tires of a 4-wheel vehicle with respect to the body frame.

*where, $a_1$ is the longitudinal distance between $C$ and the front axle, $b_1$ is the lateral distance between $C$ and the tireprint of the tire $1$, and $h$ is the height of $C$ from the ground level. If $P$ is a point in the tire frame at $^{T_1}\mathbf{r}_P$*

$$
^{T_1}\mathbf{r}_P = \begin{bmatrix} x_P \\ y_P \\ z_P \end{bmatrix}. \tag{8.62}
$$

*then its coordinates in the body frame are*

$$
\begin{aligned}
^{B}\mathbf{r}_P &= {}^{B}R_{T_1}\,{}^{T_1}\mathbf{r}_P + {}^{B}\mathbf{d}_{T_1} \\
&= \begin{bmatrix} a_1 + x_P \cos \delta_1 - y_P \sin \delta_1 \\ y_P \cos \delta_1 - b_1 + x_P \sin \delta_1 \\ z_P - h \end{bmatrix}.
\end{aligned} \tag{8.63}
$$

*The rotation matrix $^{B}R_{T_1}$ is a result of steering about the z-axis.*

$$
^{B}R_{T_1} = \begin{bmatrix} \cos \delta_1 & -\sin \delta_1 & 0 \\ \sin \delta_1 & \cos \delta_1 & 0 \\ 0 & 0 & 1 \end{bmatrix} \tag{8.64}
$$

*Employing Equation (8.28), we may examine a wheel point $P$ at $^{W}\mathbf{r}_P$*

$$
^{W}\mathbf{r}_P = \begin{bmatrix} x_P \\ y_P \\ z_P \end{bmatrix} \tag{8.65}
$$

*and find the body coordinates of the point*

$$
\begin{aligned}
{}^{B}\mathbf{r}_P &= {}^{B}R_{T_1}\,{}^{T_1}\mathbf{r}_P + {}^{B}\mathbf{d}_{T_1} \\
&= {}^{B}R_{T_1}\left({}^{T_1}R_W\,{}^{W}\mathbf{r}_P + {}^{T_1}\mathbf{d}_W\right) + {}^{B}\mathbf{d}_{T_1} \\
&= {}^{B}R_{T_1}\,{}^{T_1}R_W\,{}^{W}\mathbf{r}_P + {}^{B}R_{T_1}\,{}^{T_1}\mathbf{d}_W + {}^{B}\mathbf{d}_{T_1} \\
&= {}^{B}R_W\,{}^{W}\mathbf{r}_P + {}^{B}R_{T_1}\,{}^{T_1}\mathbf{d}_W + {}^{B}\mathbf{d}_{T_1} \qquad (8.66)
\end{aligned}
$$

$$
{}^{B}\mathbf{r}_P = \begin{bmatrix}
a_1 + x_P \cos\delta_1 - y_P \cos\gamma\sin\delta_1 + (R_w + z_P)\sin\gamma\sin\delta_1 \\
x_P \sin\delta_1 - b_1 + y_P \cos\gamma\cos\delta_1 - (R_w + z_P)\cos\delta_1\sin\gamma \\
(R_w + z_P)\cos\gamma + y_P\sin\gamma - h
\end{bmatrix}
$$
$$(8.67)$$

*where,*

$$
\begin{aligned}
{}^{B}R_W &= {}^{B}R_{T_1}\,{}^{T_1}R_W \\
&= \begin{bmatrix}
\cos\delta_1 & -\cos\gamma\sin\delta_1 & \sin\gamma\sin\delta_1 \\
\sin\delta_1 & \cos\gamma\cos\delta_1 & -\cos\delta_1\sin\gamma \\
0 & \sin\gamma & \cos\gamma
\end{bmatrix} \qquad (8.68)
\end{aligned}
$$

$$
{}^{T_1}\mathbf{d}_W = \begin{bmatrix}
0 \\
-R_w\sin\gamma \\
R_w\cos\gamma
\end{bmatrix}. \qquad (8.69)
$$

**Example 334 ★** *Wheel-body to vehicle transformation.*
    *The wheel-body coordinate frames are always parallel to the vehicle frame. The origin of the wheel-body coordinate frame of the wheel number* 1 *is at*

$$
{}^{B}\mathbf{d}_{W_1} = \begin{bmatrix}
a_1 \\
-b_1 \\
-h + R_w
\end{bmatrix}. \qquad (8.70)
$$

*Hence the transformation between the two frames is only a displacement.*

$$
{}^{B}\mathbf{r} = {}^{B}\mathbf{I}_{W_1}\,{}^{W_1}\mathbf{r} + {}^{B}\mathbf{d}_{W_1} \qquad (8.71)
$$

## 8.6   ★ Caster Theory

The steer axis may have any angle and any location with respect to the wheel-body coordinate frame. The wheel-body frame $C\left(x_c, y_c, z_c\right)$ is a frame at the center of the wheel at its rest position, parallel to the vehicle coordinate frame. The frame $C$ does not follow any motion of the wheel. The steer axis is the kingpin axis of rotation.

    Figure 8.51 illustrates the front and side views of a wheel and its steering axis. The steering axis has angle $\varphi$ with $(y_c, z_c)$ plane, and angle $\theta$ with $(x_c, z_c)$ plane. The angles $\varphi$ and $\theta$ are measured about the $y_c$ and $x_c$ axes,
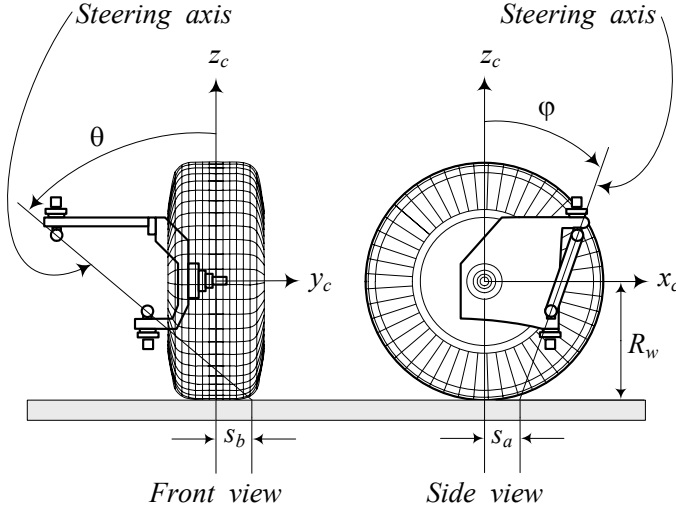
FIGURE 8.51. The front and side views of a wheel and its steering axis.

respectively. The angle $\varphi$ is the *caster angle* of the wheel, while the angle $\theta$ is the *lean angle*. The steering axis of the wheel, as shown in Figure 8.51, is at a positive caster and lean angles. The steering axis intersect the ground plane at a point that has coordinates $(s_a, s_b, -R_w)$ in the wheel-body coordinate frame.

If we indicate the steering axis by the unit vector $\hat{u}$, then the components of $\hat{u}$ are functions of the caster and lean angles.

$$
{}^C\hat{u} = \begin{bmatrix} u_1 \\ u_2 \\ u_3 \end{bmatrix} = \frac{1}{\sqrt{\cos^2\varphi + \cos^2\theta\sin^2\varphi}} \begin{bmatrix} \cos\theta\sin\varphi \\ -\cos\varphi\sin\theta \\ \cos\theta\cos\varphi \end{bmatrix} \tag{8.72}
$$

The position vector of the point that $\hat{u}$ intersects the ground plane, is called the *location vector* $\mathbf{s}$ that in the wheel-body frame has the following coordinates:

$$
{}^C\mathbf{s} = \begin{bmatrix} s_a \\ s_b \\ -R_w \end{bmatrix} \tag{8.73}
$$

We express the rotation of the wheel about the steering axis $\hat{u}$ by a zero pitch screw motion $\check{s}$.

$$
\begin{aligned}
{}^C T_W &= {}^C\check{s}_W(0, \delta, \hat{u}, \mathbf{s}) \\
&= \begin{bmatrix} {}^C R_W & {}^C\mathbf{s} - {}^C R_W\,{}^C\mathbf{s} \\ 0 & 1 \end{bmatrix} = \begin{bmatrix} {}^C R_W & {}^C\mathbf{d}_W \\ 0 & 1 \end{bmatrix}
\end{aligned} \tag{8.74}
$$

**Proof.** The steering axis is at the intersection of the *caster plane* $\boldsymbol{\pi}_C$ and the *lean plane* $\boldsymbol{\pi}_L$, both expressed in the wheel-body coordinate frame. The

two planes can be indicated by their normal unit vectors $\hat{n}_1$ and $\hat{n}_2$.

$$
{}^C\hat{n}_1 = \begin{bmatrix} 0 \\ \cos\theta \\ \sin\theta \end{bmatrix} \tag{8.75}
$$

$$
{}^C\hat{n}_2 = \begin{bmatrix} -\cos\varphi \\ 0 \\ \sin\varphi \end{bmatrix} \tag{8.76}
$$

The unit vector $\hat{u}$ on the intersection of the caster and lean planes can be found by

$$
\hat{u} = \frac{\hat{n}_1 \times \hat{n}_2}{|\hat{n}_1 \times \hat{n}_2|} \tag{8.77}
$$

where,

$$
\hat{n}_1 \times \hat{n}_2 = \begin{bmatrix} \cos\theta\sin\varphi \\ -\cos\varphi\sin\theta \\ \cos\theta\cos\varphi \end{bmatrix} \tag{8.78}
$$

$$
|\hat{n}_1 \times \hat{n}_2| = \sqrt{\cos^2\varphi + \cos^2\theta\sin^2\varphi} \tag{8.79}
$$

and therefore,

$$
{}^C\hat{u} = \begin{bmatrix} u_1 \\ u_2 \\ u_3 \end{bmatrix} = \begin{bmatrix} \dfrac{\cos\theta\sin\varphi}{\sqrt{\cos^2\varphi + \cos^2\theta\sin^2\varphi}} \\ \dfrac{-\cos\varphi\sin\theta}{\sqrt{\cos^2\varphi + \cos^2\theta\sin^2\varphi}} \\ \dfrac{\cos\theta\cos\varphi}{\sqrt{\cos^2\varphi + \cos^2\theta\sin^2\varphi}} \end{bmatrix}. \tag{8.80}
$$

Steering axis does not follow any motion of the wheel except the wheel hop in the $z$-direction. We assume that the steering axis is a fixed line with respect to the vehicle, and the steer angle $\delta$ is the rotation angle about $\hat{u}$.

The intersection point of the steering axis and the ground plane defines the *location vector* $\mathbf{s}$.

$$
{}^C\mathbf{s} = \begin{bmatrix} s_a \\ s_b \\ -R_w \end{bmatrix} \tag{8.81}
$$

The components $s_a$ and $s_b$ are called the *forward* and *lateral locations* respectively.

Using the axis-angle rotation $(\hat{u}, \delta)$, and the location vector $\mathbf{s}$, we can define the steering process as a screw motion $\check{s}$ with zero pitch. Employing Equations (5.473)-(5.477), we find the transformation screw for wheel frame $W$ to wheel-body frame $C$.

$$
\begin{aligned}
{}^C T_W &= {}^C\check{s}_W(0, \delta, \hat{u}, \mathbf{s}) \\
&= \begin{bmatrix} {}^C R_W & {}^C\mathbf{s} - {}^C R_W\,{}^C\mathbf{s} \\ 0 & 1 \end{bmatrix} = \begin{bmatrix} {}^C R_W & {}^C\mathbf{d} \\ 0 & 1 \end{bmatrix}
\end{aligned} \tag{8.82}
$$

$$^CR_W = \mathbf{I}\cos\delta + \hat{u}\hat{u}^T \text{ vers }\delta + \tilde{u}\sin\delta \tag{8.83}$$

$$^C\mathbf{d}_W = \left(\left(\mathbf{I} - \hat{u}\hat{u}^T\right)\text{ vers }\delta - \tilde{u}\sin\delta\right)\,{}^C\mathbf{s}. \tag{8.84}$$

$$\tilde{u} = \begin{bmatrix} 0 & -u_3 & u_2 \\ u_3 & 0 & -u_1 \\ -u_2 & u_1 & 0 \end{bmatrix} \tag{8.85}$$

$$\text{vers }\delta = 1 - \cos\delta \tag{8.86}$$

Direct substitution shows that $^CR_W$ and $^C\mathbf{d}_W$ are:

$$^CR_W = \begin{bmatrix} u_1^2 \text{ vers }\delta + c\delta & u_1u_2 \text{ vers }\delta - u_3 s\delta & u_1u_3 \text{ vers }\delta + u_2 s\delta \\ u_1u_2 \text{ vers }\delta + u_3 s\delta & u_2^2 \text{ vers }\delta + c\delta & u_2u_3 \text{ vers }\delta - u_1 s\delta \\ u_1u_3 \text{ vers }\delta - u_2 s\delta & u_2u_3 \text{ vers }\delta + u_1 s\delta & u_3^2 \text{ vers }\delta + c\delta \end{bmatrix} \tag{8.87}$$

$$^C\mathbf{d}_W = \begin{bmatrix} (s_1 - u_1(s_3u_3 + s_2u_2 + s_1u_1))\text{ vers }\delta + (s_2u_3 - s_3u_2)\sin\delta \\ (s_2 - u_2(s_3u_3 + s_2u_2 + s_1u_1))\text{ vers }\delta + (s_3u_1 - s_1u_3)\sin\delta \\ (s_3 - u_3(s_3u_3 + s_2u_2 + s_1u_1))\text{ vers }\delta + (s_1u_2 - s_2u_1)\sin\delta \end{bmatrix} \tag{8.88}$$

The vector $^C\mathbf{d}_W$ indicates the position of the wheel center with respect to the wheel-body frame.

The matrix $^CT_W$ is the homogeneous transformation from wheel frame $W$ to wheel-body frame $C$, when the wheel is steered by the angle $\delta$ about the steering axis $\hat{u}$. ∎

**Example 335 ★** *Zero steer angle.*

*To examine the screw transformation, we check the zero steering. Substituting $\delta = 0$ simplifies the rotation matrix $^CR_W$ and the position vector $^C\mathbf{d}_W$ to $\mathbf{I}$ and $\mathbf{0}$*

$$^CR_W = \begin{bmatrix} 1 & 0 & 0 \\ 0 & 1 & 0 \\ 0 & 0 & 1 \end{bmatrix} \tag{8.89}$$

$$^C\mathbf{d}_W = \begin{bmatrix} 0 \\ 0 \\ 0 \end{bmatrix} \tag{8.90}$$

*indicating that at zero steering, the wheel frame $W$ and wheel-body frame $C$ are coincident.*

**Example 336 ★** *Steer angle transformation for zero lean and caster.*

*Consider a wheel with a steer axis coincident with $z_w$. Such a wheel has no lean or caster angle. When the wheel is steered by the angle $\delta$, we can find the coordinates of a wheel point $P$ in the wheel-body coordinate frame using transformation method. Figure 8.52 illustrates a 3D view, and Figure 8.53 a top view of such a wheel.*
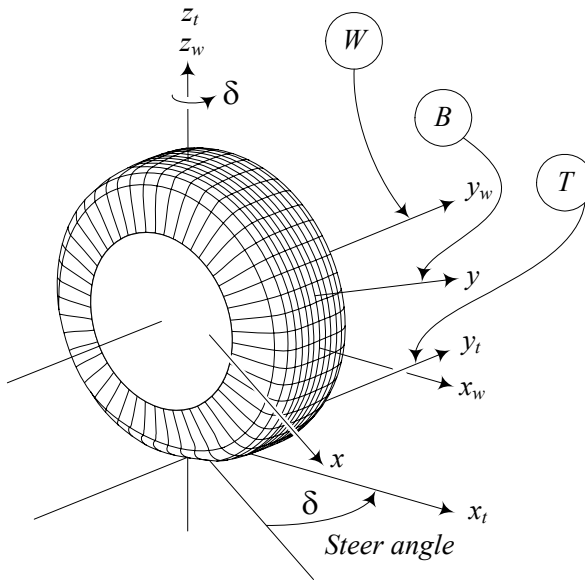
FIGURE 8.52. A $3D$ illustration of a steered wheel with a steer axis coincident with $z_w$.
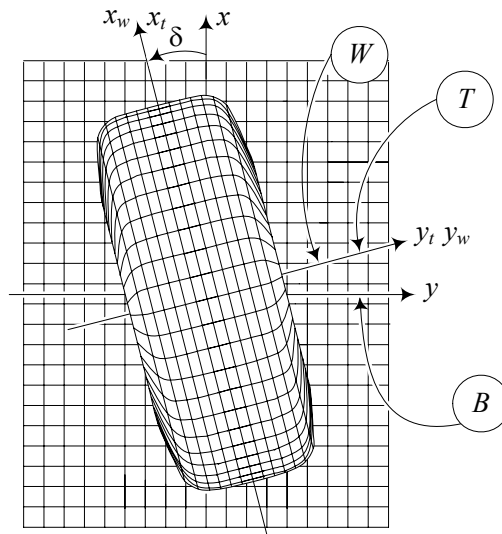


FIGURE 8.53. Top view of a steered wheel with a steer axis coincident with $z_w$.

*Assume* $^W\mathbf{r}_P = [x_w, y_w, z_w]^T$ *is the position vector of a wheel point, then its position vector in the wheel-body coordinate frame $C$ is*

$$
\begin{aligned}
{}^C\mathbf{r}_P \quad &= \quad {}^C R_W \,{}^W\mathbf{r}_P = R_{z,\delta}\,{}^W\mathbf{r}_P \\[4pt]
&= \quad \begin{bmatrix} \cos\delta & -\sin\delta & 0 \\ \sin\delta & \cos\delta & 0 \\ 0 & 0 & 1 \end{bmatrix} \begin{bmatrix} x_w \\ y_w \\ z_w \end{bmatrix} \\[4pt]
&= \quad \begin{bmatrix} x_w \cos\delta - y_w \sin\delta \\ y_w \cos\delta + x_w \sin\delta \\ z_w \end{bmatrix}.
\end{aligned} \qquad (8.91)
$$

*We assumed that the wheel-body coordinate is installed at the center of the wheel and is parallel to the vehicle coordinate frame. Therefore, the transformation from the frame $W$ to the frame $C$ is a rotation $\delta$ about the wheel-body $z$-axis. There would be no camber angle when the lean and caster angles are zero and steer axis is on the $z_w$-axis.*

**Example 337 ★** *Zero lean, zero lateral location.*
   *The case of zero lean, $\theta = 0$, and zero lateral location, $s_b = 0$, is important in caster dynamics of bicycle model. The screw transformation for this case will be simplified to*

$$
{}^C\hat{u} = \begin{bmatrix} u_1 \\ u_2 \\ u_3 \end{bmatrix} = \begin{bmatrix} \sin\varphi \\ 0 \\ \cos\varphi \end{bmatrix} \qquad (8.92)
$$

$$
{}^C\mathbf{s} = \begin{bmatrix} s_a \\ 0 \\ -R_w \end{bmatrix} \qquad (8.93)
$$

$$
{}^C R_W = \begin{bmatrix} \sin^2\varphi\,\text{vers}\,\delta + \cos\delta & -\cos\varphi \sin\delta & \sin\varphi \cos\varphi\,\text{vers}\,\delta \\ \cos\varphi \sin\delta & \cos\delta & -\sin\varphi \sin\delta \\ \sin\varphi \cos\varphi\,\text{vers}\,\delta & \sin\varphi \sin\delta & \cos^2\varphi\,\text{vers}\,\delta + \cos\delta \end{bmatrix} \qquad (8.94)
$$

$$
{}^C\mathbf{d} = \begin{bmatrix} \cos\varphi\,(s_a \cos\varphi + R_w \sin\varphi)\,\text{vers}\,\delta \\ -(s_a \cos\varphi + R_w \sin\varphi)\sin\delta \\ -\dfrac{1}{2}(R_w - R_w \cos 2\varphi + s_a \sin 2\varphi)\,\text{vers}\,\delta \end{bmatrix}. \qquad (8.95)
$$

**Example 338 ★** *Position of the tireprint.*
   *The center of tireprint in the wheel coordinate frame is at $\mathbf{r}_T$*

$$
{}^W\mathbf{r}_T = \begin{bmatrix} 0 \\ 0 \\ -R_w \end{bmatrix}. \qquad (8.96)
$$

*If we assume the width of the tire is zero and the wheel is steered, the center of tireprint would be at*

$$^C\mathbf{r}_T = {}^C T_W \, {}^W\mathbf{r}_T = \begin{bmatrix} x_T \\ y_T \\ z_T \end{bmatrix} \tag{8.97}$$

*where*

$$x_T = \left(1 - u_1^2\right)\left(1 - \cos\delta\right)s_a + \left(u_3\sin\delta - u_1 u_2\left(1 - \cos\delta\right)\right)s_b \tag{8.98}$$

$$y_T = -\left(u_3\sin\delta + u_1 u_2\left(1 - \cos\delta\right)\right)s_a + \left(1 - u_2^2\right)\left(1 - \cos\delta\right)s_b \tag{8.99}$$

$$z_T = \left(u_2\sin\delta - u_1 u_3\left(1 - \cos\delta\right)\right)s_a$$
$$- \left(u_1\sin\delta + u_2 u_3\left(1 - \cos\delta\right)\right)s_b - R_w \tag{8.100}$$

*or*

$$x_T = s_b\left(\frac{\cos\theta\cos\varphi\sin\delta}{\sqrt{\cos^2\theta\sin^2\varphi + \cos^2\varphi}} + \frac{1}{4}\frac{\sin 2\theta\sin 2\varphi\left(1 - \cos\delta\right)}{\cos^2\theta\sin^2\varphi + \cos^2\varphi}\right)$$
$$+ s_a\left(1 - \frac{\cos^2\theta\sin^2\varphi}{\cos^2\theta\sin^2\varphi + \cos^2\varphi}\right)\left(1 - \cos\delta\right) \tag{8.101}$$

$$y_T = -s_a\left(\frac{\cos\theta\cos\varphi\sin\delta}{\sqrt{\cos^2\theta\sin^2\varphi + \cos^2\varphi}} - \frac{1}{4}\frac{\sin 2\theta\sin 2\varphi\left(1 - \cos\delta\right)}{\cos^2\theta\sin^2\varphi + \cos^2\varphi}\right)$$
$$+ s_b\left(1 - \frac{\cos^2\varphi\sin^2\theta}{\cos^2\theta\sin^2\varphi + \cos^2\varphi}\right)\left(1 - \cos\delta\right) \tag{8.102}$$

$$z_T = -R_w - \frac{s_b\cos\theta\sin\varphi + s_a\cos\varphi\sin\theta}{\sqrt{\cos^2\theta\sin^2\varphi + \cos^2\varphi}}\sin\delta$$
$$+ \frac{1}{2}\frac{s_b\cos^2\varphi\sin 2\theta - s_a\cos^2\theta\sin 2\varphi}{\cos^2\theta\sin^2\varphi + \cos^2\varphi}\left(1 - \cos\delta\right) \tag{8.103}$$

**Example 339 ★** *Wheel center drop.*
   The $z_T$ coordinate in (8.100) or (8.103) indicates the amount that the center of the tireprint will move in the vertical direction with respect to the wheel-body frame when the wheel is steering. If the steer angle is zero, $\delta = 0$, then $z_T$ is at

$$z_T = -R_w. \tag{8.104}$$

Because the center of tireprint must be on the ground, $H = -R_w - z_T$ indicated the height that the center of the wheel will drop during steering.

$$H = -R_w - z_T \tag{8.105}$$
$$= \frac{s_b\cos\theta\sin\varphi + s_a\cos\varphi\sin\theta}{\sqrt{\cos^2\theta\sin^2\varphi + \cos^2\varphi}}\sin\delta$$
$$- \frac{1}{2}\frac{s_b\cos^2\varphi\sin 2\theta - s_a\cos^2\theta\sin 2\varphi}{\cos^2\theta\sin^2\varphi + \cos^2\varphi}\left(1 - \cos\delta\right)$$
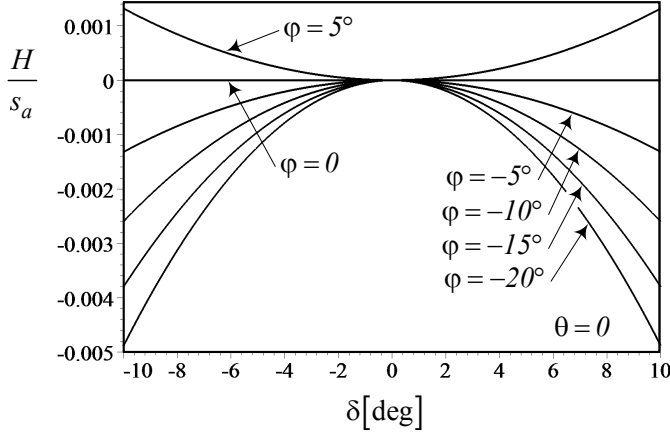
FIGURE 8.54. $H/s_a$ for the caster angle $\varphi = 5 \deg 0$, $-5 \deg$, $-10 \deg$, $-15 \deg$, $-20 \deg$ and the steer angle in the range $-10 \deg < \delta < 10 \deg$.

*The $z_T$ coordinate of the tireprint may be simplifie for different designs:*
*1− If the lean angle is zero, $\theta = 0$, then $z_T$ is at*

$$z_T = -R_w - \frac{1}{2} s_a \sin 2\varphi \left(1 - \cos \delta\right) - s_b \sin \varphi \sin \delta. \qquad (8.106)$$

*2− If the lean angle and lateral location are zero, $\theta = 0$, $s_b = 0$, then $z_T$ is at*

$$z_T = -R_w - \frac{1}{2} s_a \sin 2\varphi \left(1 - \cos \delta\right). \qquad (8.107)$$

*In this case, the wheel center drop may be expressed by a dimensionless equation.*

$$\frac{H}{s_a} = \frac{1}{2} \sin 2\varphi \left(1 - \cos \delta\right) \qquad (8.108)$$

*Figure 8.54 illustrates $H/s_a$ for the caster angle $\varphi = 5 \deg$, $0 \deg$, $-5 \deg$, $-10 \deg$, $-15 \deg$, $-20 \deg$, and the steer angle $\delta$ in the range $-10 \deg < \delta < 10 \deg$. In street cars, we set the steering axis with a positive longitudinal location $s_a > 0$, and a few degrees negative caster angle $\varphi < 0$. In this case the wheel center drops as is shown in the figure.*
*3− If the caster angle is zero, $\varphi = 0$, then $z_T$ is at*

$$z_T = -R_w + \frac{1}{2} s_b \sin 2\theta \left(1 - \cos \delta\right) - s_a \sin \theta \sin \delta. \qquad (8.109)$$

*4− If the caster angle and lateral location are zero, $\varphi = 0$, $s_b = 0$, then $z_T$ is at*

$$z_T = -R_w - s_a \sin \theta \sin \delta. \qquad (8.110)$$
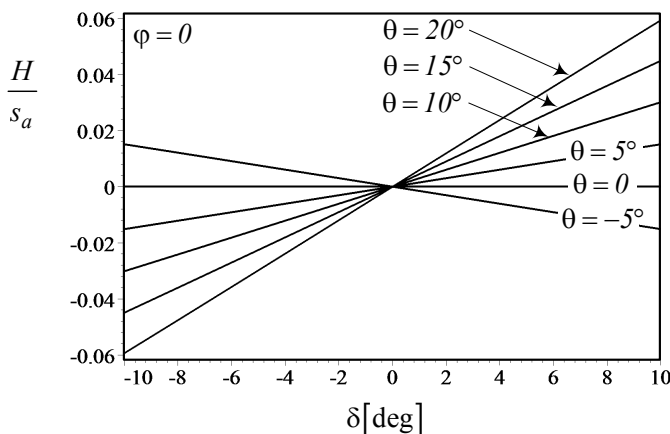
FIGURE 8.55. $H/s_a$ for the lean angle $\theta = 5\deg 0$, $-5\deg$, $-10\deg$, $-15\deg$, $-20\deg$ and the steer angle in the range $-10\deg < \delta < 10\deg$.

In this case, the wheel center drop may be expressed by a dimensionless equation.

$$\frac{H}{s_a} = -\sin\theta\sin\delta \qquad (8.111)$$

Figure 8.55 illustrates $H/s_a$ for the lean angle $\theta = 5\deg$, $0$, $-5\deg$, $-10\deg$, $-15\deg$, $-20\deg$ and the steer angle $\delta$ in the range $-10\deg < \delta < 10\deg$. The steering axis of street cars is usually set with a positive longitudinal location $s_a > 0$, and a few degrees positive lean angle $\theta > 0$. In this case the wheel center lowers when the wheel number 1 turns to the right, and elevates when the wheel turns to the left.

Comparison of Figures 8.54 and 8.55 shows that the lean angle has much more affect on the wheel center drop than the caster angle.

5— If the lateral location is zero, $s_b = 0$, then $z_T$ is at

$$z_T = -R_w - s_a \frac{\cos\varphi\sin\theta}{\sqrt{\cos^2\theta\sin^2\varphi + \cos^2\varphi}}\sin\delta$$
$$-\frac{1}{2}s_a\frac{\cos^2\theta\sin 2\varphi}{\cos^2\theta\sin^2\varphi + \cos^2\varphi}(1 - \cos\delta) \qquad (8.112)$$

and the wheel center drop, $H$, may be expressed by a dimensionless equation.

$$\frac{H}{s_a} = -\frac{1}{2}\frac{\cos^2\theta\sin^2\varphi(1 - \cos\delta)}{\cos^2\theta\sin^2\varphi + \cos^2\varphi} - \frac{\cos\varphi\sin\theta\sin\delta}{\sqrt{\cos^2\theta\sin^2\varphi + \cos^2\varphi}} \qquad (8.113)$$

**Example 340 ★** *Position of the wheel center.*
As given in Equation (8.88), the wheel center is at $^C\mathbf{d}_W$ with respect to

*the wheel-body frame.*

$$^C\mathbf{d}_W = \begin{bmatrix} x_W \\ y_W \\ z_W \end{bmatrix} \tag{8.114}$$

*Substituting for $\hat{u}$ and $\mathbf{s}$ from (8.72) and (8.73) in (8.88) provides the coordinates of the wheel center in the wheel-body frame as*

$$
\begin{aligned}
x_W &= (s_a - u_1(-R_w u_3 + s_b u_2 + s_a u_1))(1 - \cos\delta) \\
&\quad + (s_b u_3 + R_w u_2)\sin\delta
\end{aligned} \tag{8.115}
$$

$$
\begin{aligned}
y_W &= (s_b - u_2(-R_w u_3 + s_b u_2 + s_a u_1))(1 - \cos\delta) \\
&\quad - (R_w u_1 + s_a u_3)\sin\delta
\end{aligned} \tag{8.116}
$$

$$
\begin{aligned}
z_W &= (-R_w - u_3(-R_w u_3 + s_b u_2 + s_a u_1))(1 - \cos\delta) \\
&\quad + (s_a u_2 - s_b u_1)\sin\delta
\end{aligned} \tag{8.117}
$$

*or*

$$
\begin{aligned}
x_W &= s_a(1 - \cos\delta) \\
&\quad + \frac{\left(\frac{1}{2}R_w\sin 2\varphi - s_a\sin^2\varphi\right)\cos^2\theta + \frac{1}{4}s_b\sin 2\theta\sin 2\varphi}{\cos^2\varphi + \cos^2\theta\sin^2\varphi}(1 - \cos\delta) \\
&\quad + \frac{(s_b\cos\theta - R_w\sin\theta)}{\sqrt{\cos^2\varphi + \cos^2\theta\sin^2\varphi}}\cos\varphi\sin\delta
\end{aligned} \tag{8.118}
$$

$$
\begin{aligned}
y_W &= s_b(1 - \cos\delta) \\
&\quad - \frac{\frac{1}{2}\left(R_w\sin 2\theta + s_b\sin^2\theta\right)\cos^2\varphi - \frac{1}{4}s_a\sin 2\theta\sin 2\varphi}{\cos^2\varphi + \cos^2\theta\sin^2\varphi}(1 - \cos\delta) \\
&\quad - \frac{R_w\sin\varphi + s_a\cos\varphi}{\sqrt{\cos^2\varphi + \cos^2\theta\sin^2\varphi}}\cos\theta\sin\delta
\end{aligned} \tag{8.119}
$$

$$
\begin{aligned}
z_W &= -R_w(1 - \cos\delta) \\
&\quad + \frac{\left(R_w\cos^2\theta + \frac{1}{2}s_b\sin 2\theta\right)\cos^2\varphi - \frac{1}{2}s_a\cos^2\theta\sin 2\varphi}{\cos^2\varphi + \cos^2\theta\sin^2\varphi}(1 - \cos\delta) \\
&\quad - \frac{s_a\cos\varphi\sin\theta + s_b\cos\theta\sin\varphi}{\sqrt{\cos^2\varphi + \cos^2\theta\sin^2\varphi}}\sin\delta
\end{aligned} \tag{8.120}
$$

The $z_W$ coordinate indicates how the center of the wheel will move in the vertical direction with respect to the wheel-body frame, when the wheel is steering. It shows that $z_W = 0$, as long as $\delta = 0$.

*The $z_W$ coordinate of the wheel center may be simplified for different designs:*

*1— If the lean angle is zero, $\theta = 0$, then $z_W$ is at*

$$
\begin{aligned}
z_W \;=\; & -R_w \left(1 - \cos^2 \varphi\right) \left(1 - \cos \delta\right) - s_b \sin \varphi \sin \delta \\
& -\frac{1}{2} s_a \sin 2\varphi \left(1 - \cos \delta\right).
\end{aligned}
\tag{8.121}
$$

*2— If the lean angle and lateral location are zero, $\theta = 0$, $s_b = 0$, then $z_W$ is at*

$$
z_W = -R_w \left(1 - \cos^2 \varphi\right) \left(1 - \cos \delta\right) - \frac{1}{2} s_a \sin 2\varphi \left(1 - \cos \delta\right).
\tag{8.122}
$$

*3— If the caster angle is zero, $\varphi = 0$, then $z_W$ is at*

$$
\begin{aligned}
z_W \;=\; & -R_w \left(1 - \cos^2 \theta\right) \left(1 - \cos \delta\right) - s_a \sin \theta \sin \delta \\
& +\frac{1}{2} s_b \sin 2\theta \left(1 - \cos \delta\right).
\end{aligned}
\tag{8.123}
$$

*4— If the caster angle and lateral location are zero, $\varphi = 0$, $s_b = 0$, then $z_W$ is at*

$$
z_W = -R_w \left(1 - \cos^2 \theta\right) \left(1 - \cos \delta\right) - s_a \sin \theta \sin \delta.
\tag{8.124}
$$

*5— If the lateral location is zero, $s_b = 0$, then $z_T$ is at*

$$
\begin{aligned}
z_W \;=\; & -R_w \left(1 - \cos \delta\right) - \frac{s_a \cos \varphi \sin \theta}{\sqrt{\cos^2 \varphi + \cos^2 \theta \sin^2 \varphi}} \sin \delta \\
& +\frac{R_w \cos^2 \theta \cos^2 \varphi - \frac{1}{2} s_a \cos^2 \theta \sin 2\varphi}{\cos^2 \varphi + \cos^2 \theta \sin^2 \varphi} \left(1 - \cos \delta\right)
\end{aligned}
\tag{8.125}
$$

*In each case of the above designs, the height of the wheel center with respect to the ground level can be found by adding $H$ to $z_W$. The equations for calculating $H$ are found in Example 340.*

**Example 341 ★** *Camber theory.*

*Having a non-zero lean and caster angles causes a camber angle $\gamma$ for a steered wheel. To find the camber angle of an steered wheel, we may determine the angle between the camber line and the vertical direction $z_c$. The* **camber line** *is the line connecting the wheel center and the center of tireprint.*

*The coordinates of the center of tireprint $(x_T, y_T, z_T)$ are given in Equations (8.101)-(8.103), and the coordinates of the wheel center $(x_W, y_W, z_W)$ are given in Equations (8.118)-(8.120). The line connecting $(x_T, y_T, z_T)$ to $(x_W, y_W, z_W)$ may be indicated by the unit vector $\hat{l}_c$*

$$
\hat{l}_c = \frac{(x_W - x_T)\,\hat{I} + (y_W - y_T)\,\hat{J} + (z_W - z_T)\,\hat{K}}{\sqrt{(x_W - x_T)^2 + (y_W - y_T)^2 + (z_W - z_T)^2}}
\tag{8.126}
$$

*in which $\hat{I}, \hat{J}, \hat{K}$, are the unit vectors of the wheel-body coordinate frame $C$.*

*The camber angle is the angle between $\hat{l}_c$ and $\hat{K}$, which can be found by the inner vector product.*

$$\gamma = \cos^{-1}\left(\hat{l}_c \cdot \hat{K}\right)$$

$$= \cos^{-1} \frac{(z_W - z_T)}{\sqrt{(x_W - x_T)^2 + (y_W - y_T)^2 + (z_W - z_T)^2}} \quad (8.127)$$

*As an special case, let us determine the camber angle when the lean angle and lateral location are zero, $\theta = 0$, $s_b = 0$. In this case, we have*

$$x_T = s_a \left(1 - \sin^2 \varphi\right)(\cos \delta - 1) \quad (8.128)$$

$$y_T = -s_a \cos \varphi \sin \delta \quad (8.129)$$

$$z_T = z_T = -R_w - \frac{1}{2} s_a \sin 2\varphi \left(1 - \cos \delta\right) \quad (8.130)$$

$$x_W = \left(s_a + \frac{1}{2} R_w \sin 2\varphi - s_a \sin^2 \varphi\right)(1 - \cos \delta) \quad (8.131)$$

$$y_W = s_b (1 - \cos \delta) - R_w \sin \varphi + s_a \cos \varphi \sin \delta \quad (8.132)$$

$$z_W = \left(R_w \left(\cos^2 \varphi - 1\right) - \frac{1}{2} s_a \sin 2\varphi\right)(1 - \cos \delta). \quad (8.133)$$

## 8.7  Summary

There are two general types of suspensions: *dependent*, in which the left and right wheels on an axle are rigidly connected, and *independent*, in which the left and right wheels are disconnected. Solid axle is the most common dependent suspension, while McPherson and double $A$-arm are the most common independent suspensions.

The *roll axis* is the instantaneous line about which the body of a vehicle rolls. Roll axis is found by connecting the *roll center* of the front and rear suspensions of the vehicle. The instant center of rotation of a wheel with respect to the body is called *suspension roll center*. So, to find the roll center of the front or rear half of a car, we should determine the suspension roll centers, and find the intersection of the lines connecting the suspension roll centers to the center of their associated tireprints.

Three coordinate frames are employed to express the orientation of a tire and wheel with respect to the vehicle: the wheel frame $W$, wheel-body frame $C$, and tire frame $T$. A wheel coordinate frame $W (x_w, y_w, z_w)$ is attached to the center of a wheel. It follows every translation and rotation of the wheel except the spin. Hence, the $x_w$ and $z_w$ axes are always in the tire-plane, while the $y_w$-axis is always along the spin axis. When the wheel

is straight and the $W$ frame is parallel to the vehicle coordinate frame, we attach a wheel-body coordinate frame $C\,(x_c, y_c, z_c)$ at the center of the wheel parallel to the vehicle coordinate axes. The wheel-body frame $C$ is motionless with respect to the vehicle coordinate and does not follow any motion of the wheel. The tire coordinate frame $T\,(x_t, y_t, z_t)$ is set at the center of the tireprint. The $z_t$-axis is always perpendicular to the ground. The $x_t$-axis is along the intersection line of the tire-plane and the ground. The tire frame does not follows the spin and camber rotations of the tire however, it follows the steer angle rotation about the $z_c$-axis.

We define the orientation and position of a steering axis by the caster angle $\varphi$, lean angle $\theta$, and the intersection point of the axis with the ground surface at $(s_a, s_b)$ with respect to the center of tireprint. Because of these parameters, a steered wheel will camber and generates a lateral force. This is called the caster theory. The camber angle $\gamma$ of a steered wheel for $\theta = 0$, and $s_b = 0$ is:

$$
\begin{aligned}
\gamma &= \cos^{-1}\left(\hat{l}_c \cdot \hat{K}\right) \\
&= \cos^{-1} \frac{(z_W - z_T)}{\sqrt{(x_W - x_T)^2 + (y_W - y_T)^2 + (z_W - z_T)^2}}
\end{aligned}
\tag{8.134}
$$

where

$$
x_T = s_a\left(1 - \sin^2\varphi\right)\left(\cos\delta - 1\right)
\tag{8.135}
$$

$$
y_T = -s_a \cos\varphi \sin\delta
\tag{8.136}
$$

$$
z_T = z_T = -R_w - \frac{1}{2}s_a \sin 2\varphi\left(1 - \cos\delta\right)
\tag{8.137}
$$

$$
x_W = \left(s_a + \frac{1}{2}R_w \sin 2\varphi - s_a \sin^2\varphi\right)\left(1 - \cos\delta\right)
\tag{8.138}
$$

$$
y_W = s_b\left(1 - \cos\delta\right) - R_w \sin\varphi + s_a \cos\varphi \sin\delta
\tag{8.139}
$$

$$
z_W = \left(R_w\left(\cos^2\varphi - 1\right) - \frac{1}{2}s_a \sin 2\varphi\right)\left(1 - \cos\delta\right).
\tag{8.140}
$$

## 8.8   Key Symbols

| | |
|---|---|
| $a, b, c, d$ | lengths of the links of a four-bar linkage |
| $a_i$ | distance of the axle number $i$ from the mass center |
| $A, B, \cdots$ | coefficients in equation for calculating $\theta_3$ |
| $b_1$ | distance of left wheels from mass center |
| $B(x, y, z)$ | vehicle coordinate frame |
| $C$ | mass center |
| $C$ | coupler point |
| $C(x_c, y_c, z_c)$ | wheel-body coordinate frame |
| $_T^C \mathbf{d}_W$ | $C$ expression of the position of $W$ with respect to $T$ |
| $e, \alpha$ | polar coordinates of a coupler point |
| $g$ | overhang |
| $h = z - z_0$ | vertical displacement of the wheel center |
| $H$ | wheel center drop |
| $I_{ij}$ | instant center of rotation between link $i$ and link $j$ |
| $\overline{I_{ij}I_{mn}}$ | a line connecting $I_{ij}$ and $I_{mn}$ |
| $\hat{I}, \hat{J}, \hat{K}$ | unit vectors of the wheel-body frame $C$ |
| $\mathbf{I}$ | identity matrix |
| $J_1, J_2, \cdots$ | length function for calculating $\theta_3$ |
| $\hat{l}_c$ | unit vector on the line $(x_T, y_T, z_T)$ to $(x_W, y_W, z_W)$ |
| $m_s$ | sprung mass |
| $m_u$ | unsprung mass |
| $\hat{n}_1$ | normal unit vectors to $\boldsymbol{\pi}_L$ |
| $\hat{n}_2$ | normal unit vectors to $\boldsymbol{\pi}_C$ |
| $P$ | point |
| $q, p, f$ | parameters for calculating couple point coordinate |
| $\mathbf{r}$ | position vector |
| $R_w$ | tire radius |
| $^T R_W$ | rotation matrix to go from $W$ frame to $T$ frame |
| $\mathbf{s}$ | position vector of the steer axis |
| $s_a$ | forward location of the steer axis |
| $s_b$ | lateral location of the steer axis |
| $\check{s}_W(0, \delta, \hat{u}, \mathbf{s})$ | zero pitch screw about the steer axis |
| $T(x_t, y_t, z_t)$ | tire coordinate system |
| $^T T_W$ | homogeneous transformation to go from $W$ to $T$ |
| $\hat{u}$ | steer axis unit vector |
| $\tilde{u}$ | skew symmetrix matrix associated to $\hat{u}$ |
| $\mathbf{u}_C$ | position vector of the coupler point |
| $\hat{u}_z$ | unit vector in the $z$-direction |
| $v_x$ | forward speed |
| $x, y$ | suspension coordinate frame |
| $x_C, y_C$ | coordinate of a couple point |
| $(x_T, y_T, z_T)$ | wheel-body coordinates of the origin of $T$ frame |

| | |
|---|---|
| $(x_W, y_W, z_W)$ | wheel-body coordinates of the origin of $W$ frame |
| vers $\delta$ | $1 - \cos\delta$ |
| $W\,(x_w y_w z_w)$ | wheel coordinate system |
| $z$ | vertical position of the wheel center |
| $z_0$ | initial vertical position of the wheel center |
| | |
| | |
| $\alpha$ | angle of a coupler point with upper $A$-arm |
| $\gamma$ | camber angle |
| $\delta$ | steer angle |
| $\varepsilon = m_s/m_u$ | sprung to unsprung mass ratio |
| $\theta$ | lean angle |
| $\theta_0$ | angle between the ground link and the $z$-direction |
| $\theta_i$ | angular position of link number $i$ |
| $\theta_2$ | angular position of the upper $A$-arm |
| $\theta_3$ | angular position of the coupler link |
| $\theta_4$ | angular position of link lower $A$-arm |
| $\theta_{i0}$ | initial angular position of $\theta_i$ |
| $\boldsymbol{\pi}_C$ | caster plane |
| $\boldsymbol{\pi}_L$ | lean plane |
| $\upsilon$ | trust angle |
| $\varphi$ | caster angle |
| $\omega$ | angular velocity |

# Exercises

1. Roll center.

   Determine the roll ceneter of the kinematic models of vehicles shown in Figures 8.56 to 8.59.
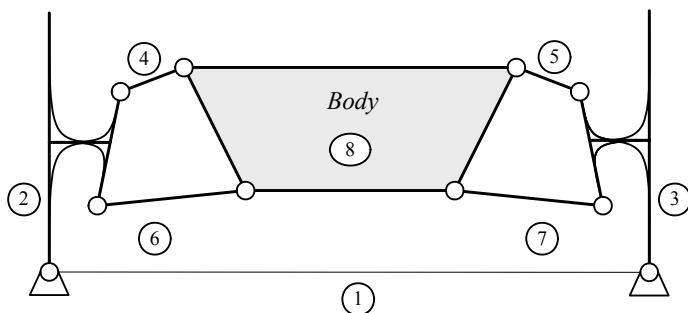


FIGURE 8.56.
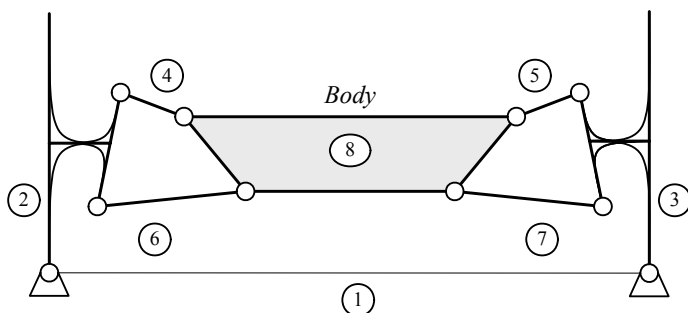


FIGURE 8.57.

2. Upper $A$-arm and roll center.

   Design the upper $A$-arm for the suspensions that are shown in Figures 8.60 to 8.62, such that the roll center of the vehicle is at point $P$.

3. Lower arm and roll center.

   Design the lower arm for the McPherson suspensions that are shown in Figures 8.63 to 8.65, such that the roll center of the vehicle is at point $P$.
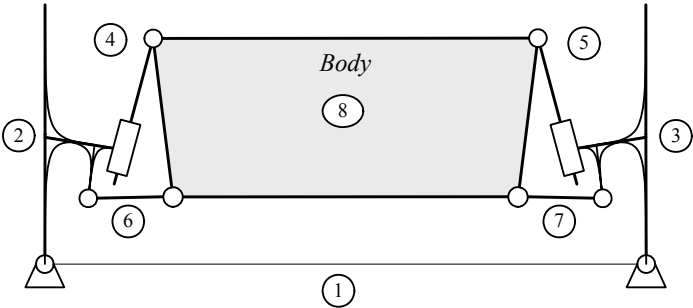
FIGURE 8.58.
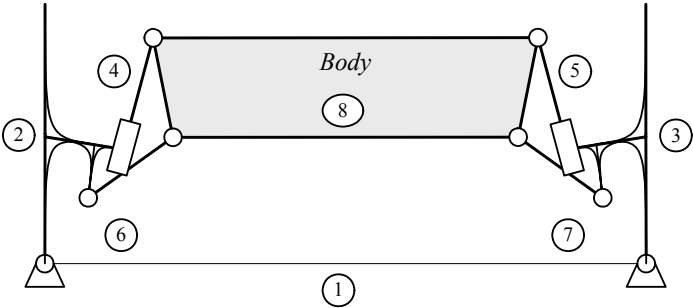


FIGURE 8.59.
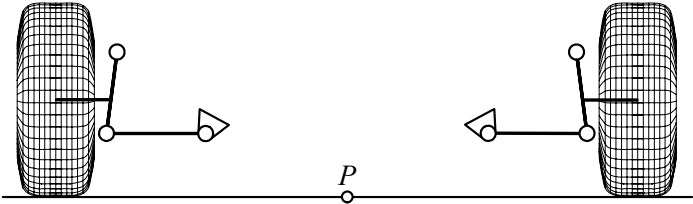


FIGURE 8.60.
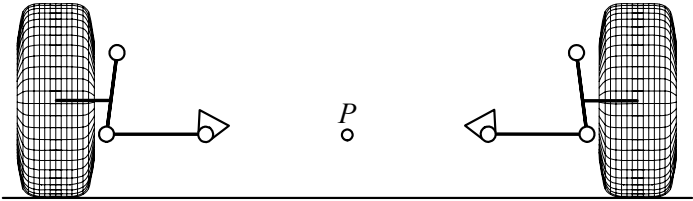


FIGURE 8.61.
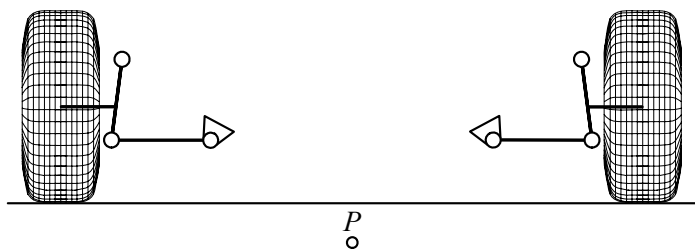
FIGURE 8.62.
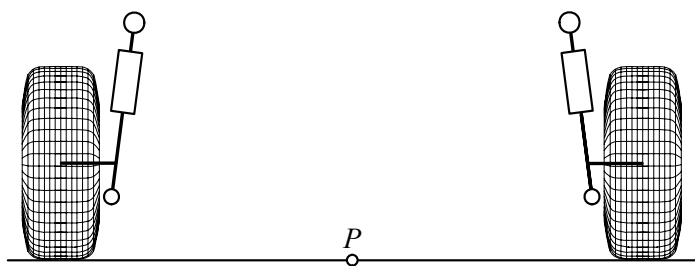


FIGURE 8.63.
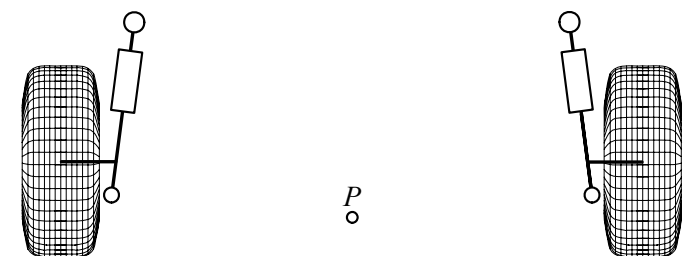


FIGURE 8.64.
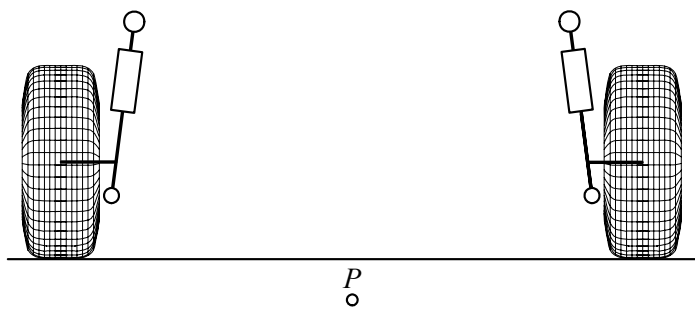


FIGURE 8.65.

4. ★ Position of the roll center and mass ceneter.

Figure 8.66 illustrates the wheels and mass center $C$ of a vehicle. Design a double $A$-arm suspension such that the roll center of the
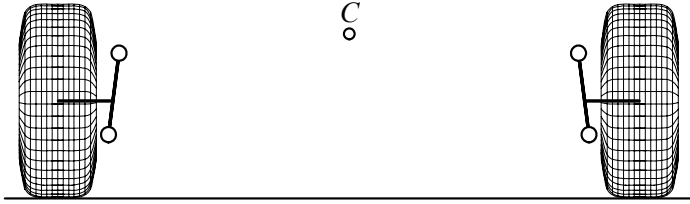
FIGURE 8.66.

vehicle is

(a) above $C$.

(b) on $C$.

(c) below $C$.

(d) Is it possible to make street cars with a roll center on or above $C$?

(e) What would be the advantages or disadvantages of a roll center on or above $C$.

5. ★ Asymmetric position of the roll center.

Design a double $A$-arm suspension for the vehicle shown in 8.67, such that the roll center of the vehicle is at point $P$. What would be the advantages or disadvantages of an asymmetric roll center?

FIGURE 8.67.

6. ★ Camber angle variation.

Consider a double $A$-arm suspension such that is shown in Figure 8.68. Assume that the dimensions of the equivalent kinematic model
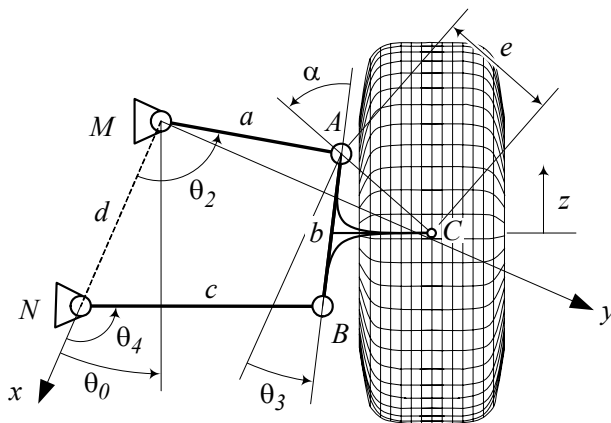
FIGURE 8.68.

are:

$$
\begin{aligned}
a &= 22.57\,\text{cm} \\
b &= 18.88\,\text{cm} \\
c &= 29.8\,\text{cm} \\
d &= 24.8\,\text{cm} \\
\theta_0 &= 23.5\,\text{deg}
\end{aligned}
$$

and the coupler point $C$ is at:

$$
\begin{aligned}
e &= 14.8\,\text{cm} \\
\alpha &= 56.2\,\text{deg}
\end{aligned}
$$

Draw a graph to show the variation of the camber angle, when the wheel is moving up and down.

7. ★ Steer axis unit vector.

   Determine the $C$ expression of the unit vector $\hat{u}$ on the steer axis, for a caster angle $\varphi = 15\,\text{deg}$, and a lean angle $\theta = 8\,\text{deg}$.

8. ★ Location vector and steer axis.

   Determine the location vector $\mathbf{s}$, if the steer axis is going through the wheel center. The caster and lean angles are $\varphi = 10\,\text{deg}$ and $\theta = 0\,\text{deg}$.

9. ★ Homogeneous transformation matrix $^{C}T_{W}$.

Determine $^C T_W$ for $\varphi = 8\,\text{deg}$, $\theta = 12\,\text{deg}$, and the location vector $^C\mathbf{s}$

$$^C\mathbf{s} = \begin{bmatrix} 3.8\,\text{cm} \\ 1.8\,\text{cm} \\ -R_w \end{bmatrix}.$$

(a) The vehicle uses a tire $235/35ZR19$.

(b) The vehicle uses a tire $P215/65R15\ 96H$.

10. ★ Wheel drop.

Find the coordinates of the tireprint for

$$\varphi = 10\,\text{deg}$$
$$\theta = 10\,\text{deg}$$
$$^C\mathbf{s} = \begin{bmatrix} 3.8\,\text{cm} \\ 1.8\,\text{cm} \\ 38\,\text{cm} \end{bmatrix}$$

if $\delta = 18\,\text{deg}$. How much is the wheel drop $H$.

11. ★ Wheel drop and steer angle.

Draw a plot to show the wheel drop $H$ at different steer angle $\delta$ for the given data in Exercise 10.

12. ★ Camber and steering.

Draw a plot to show the camber angle $\gamma$ at different steer angle $\delta$ for the following characteristics:

$$\varphi = 10\,\text{deg}$$
$$\theta = 0\,\text{deg}$$
$$^C\mathbf{s} = \begin{bmatrix} 3.8\,\text{cm} \\ 0\,\text{cm} \\ 38\,\text{cm} \end{bmatrix}$$

# Part III

# Vehicle Dynamics

# 9

# Applied Dynamics

Dynamics of a rigid vehicle may be considered as the motion of a rigid body with respect to a fixed global coordinate frame. The principles of Newton and Euler equations of motion that describe the translational and rotational motion of the rigid body are reviewed in this chapter.

## 9.1   Force and Moment

In Newtonian dynamics, the forces acting on a system of connected rigid bodied can be divided into *internal* and *external forces*. Internal forces are acting between connected bodies, and external forces are acting from outside of the system. An external force can be a *contact force*, such as the traction force at the tireprint of a driving wheel, or a *body force*, such as the gravitational force on the vehicle's body.
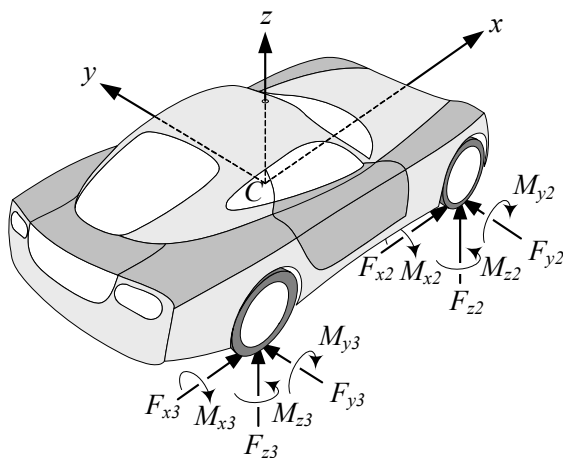


FIGURE 9.1. The force system of a vehicle is the applied forces and moments at the tireprints.

External forces and moments are called *load*, and a set of forces and moments acting on a rigid body, such as forces and moments on the vehicle shown in Figure 9.1, is called a *force system*. The *resultant* or *total force* **F** is the sum of all the external forces acting on a body, and the *resultant* or

*total moment* $\mathbf{M}$ is the sum of all the moments of the external forces.

$$\mathbf{F} = \sum_i \mathbf{F}_i \tag{9.1}$$

$$\mathbf{M} = \sum_i \mathbf{M}_i \tag{9.2}$$

Consider a force $\mathbf{F}$ acting on a point $P$ at $\mathbf{r}_P$. The *moment of the force* about a directional line $l$ passing through the origin is

$$\mathbf{M}_l = l\hat{u} \cdot (\mathbf{r}_P \times \mathbf{F}) \tag{9.3}$$

where $\hat{u}$ is a unit vector on $l$. The moment of the force $\mathbf{F}$, about a point $Q$ at $\mathbf{r}_Q$ is

$$\mathbf{M}_Q = (\mathbf{r}_P - \mathbf{r}_Q) \times \mathbf{F} \tag{9.4}$$

so, the moment of $\mathbf{F}$ about the origin is

$$\mathbf{M} = \mathbf{r}_P \times \mathbf{F}. \tag{9.5}$$

The moment of a force may also be called *torque* or *moment*.

The effect of a force system is equivalent to the effect of the resultant force and resultant moment of the force system. Any two force systems are equivalent if their resultant forces and resultant moments are equal. If the resultant force of a force system is zero, the resultant moment of the force system is independent of the origin of the coordinate frame. Such a resultant moment is called *couple*.

When a force system is reduced to a resultant $\mathbf{F}_P$ and $\mathbf{M}_P$ with respect to a reference point $P$, we may change the reference point to another point $Q$ and find the new resultants as

$$\mathbf{F}_Q = \mathbf{F}_P \tag{9.6}$$
$$\mathbf{M}_Q = \mathbf{M}_P + (\mathbf{r}_P - \mathbf{r}_Q) \times \mathbf{F}_P$$
$$= \mathbf{M}_P + {}_Q\mathbf{r}_P \times \mathbf{F}_P. \tag{9.7}$$

The *momentum* of a moving rigid body is a vector quantity equal to the total mass of the body times the translational velocity of the mass center of the body.

$$\mathbf{p} = m\mathbf{v} \tag{9.8}$$

The momentum $\mathbf{p}$ is also called *translational momentum* or *linear momentum*.

Consider a rigid body with momentum $\mathbf{p}$. The *moment of momentum*, $\mathbf{L}$, about a directional line $l$ passing through the origin is

$$\mathbf{L}_l = l\hat{u} \cdot (\mathbf{r}_C \times \mathbf{p}) \tag{9.9}$$

where $\hat{u}$ is a unit vector indicating the direction of the line, and $\mathbf{r}_C$ is the position vector of the mass center $C$. The moment of momentum about the origin is

$$\mathbf{L} = \mathbf{r}_C \times \mathbf{p}. \tag{9.10}$$

The moment of momentum $\mathbf{L}$ is also called *angular momentum*.

A *bounded vector* is a vector fixed at a point in space. A *sliding* or *line vector* is a vector free to slide on its *line of action*. A *free vector* is a vector that may move to any point as long as it keeps its direction. Force is a sliding vector and couple is a free vector. However, the moment of a force is dependent on the distance between the origin of the coordinate frame and the line of action.

The application of a force system is emphasized by *Newton's second and third laws of motion*. The second law of motion, also called the *Newton's equation of motion*, states that the global rate of change of *linear momentum* is proportional to the global *applied force*.

$$^G\mathbf{F} = \frac{^Gd}{dt}\,^G\mathbf{p} = \frac{^Gd}{dt}\left(m\,^G\mathbf{v}\right) \tag{9.11}$$

The third law of motion states that the action and reaction forces acting between two bodies are equal and opposite.

The second law of motion can be expanded to include rotational motions. Hence, the second law of motion also states that the global rate of change of *angular momentum* is proportional to the global *applied moment*.

$$^G\mathbf{M} = \frac{^Gd}{dt}\,^G\mathbf{L} \tag{9.12}$$

**Proof.** Differentiating from angular momentum (9.10) shows that

$$
\begin{aligned}
\frac{^Gd}{dt}\,^G\mathbf{L} &= \frac{^Gd}{dt}\left(\mathbf{r}_C \times \mathbf{p}\right) \\
&= \left(\frac{^Gd\mathbf{r}_C}{dt} \times \mathbf{p} + \mathbf{r}_C \times \frac{^Gd\mathbf{p}}{dt}\right) \\
&= {}^G\mathbf{r}_C \times \frac{^Gd\mathbf{p}}{dt} \\
&= {}^G\mathbf{r}_C \times {}^G\mathbf{F} \\
&= {}^G\mathbf{M}. \tag{9.13}
\end{aligned}
$$

∎

*Kinetic energy* $K$ of a moving body point $P$ with mass $m$ at a position $^G\mathbf{r}_P$, and having a velocity $^G\mathbf{v}_P$, is

$$
\begin{aligned}
K &= \frac{1}{2}m\,^G\mathbf{v}_P^2 \\
&= \frac{1}{2}m\left(^G\dot{\mathbf{d}}_B + {}^B\mathbf{v}_P + {}^B_G\boldsymbol{\omega}_B \times {}^B\mathbf{r}_P\right)^2. \tag{9.14}
\end{aligned}
$$

The work done by the applied force $^G\mathbf{F}$ on $m$ in moving from point 1 to point 2 on a path, indicated by a vector $^G\mathbf{r}$, is

$$_1W_2 = \int_1^2 {}^G\mathbf{F} \cdot d\,{}^G\mathbf{r}. \tag{9.15}$$

However,

$$
\begin{aligned}
\int_1^2 {}^G\mathbf{F} \cdot d\,{}^G\mathbf{r} &= m \int_1^2 \frac{{}^G d}{dt} {}^G\mathbf{v} \cdot {}^G\mathbf{v} dt \\
&= \frac{1}{2} m \int_1^2 \frac{d}{dt} v^2 dt \\
&= \frac{1}{2} m \left( v_2^2 - v_1^2 \right) \\
&= K_2 - K_1 \tag{9.16}
\end{aligned}
$$

that shows $_1W_2$ is equal to the difference of the kinetic energy between terminal and initial points.

$$_1W_2 = K_2 - K_1 \tag{9.17}$$

Equation (9.17) is called *principle of work and energy*.

**Example 342** *Position of center of mass.*
   *The position of the mass center of a rigid body in a coordinate frame is indicated by $^B\mathbf{r}_C$ and is usually measured in the body coordinate frame.*

$$^B\mathbf{r}_C = \frac{1}{m} \int_B {}^B\mathbf{r}\, dm \tag{9.18}$$

$$
\begin{bmatrix} x_C \\ y_C \\ z_C \end{bmatrix} =
\begin{bmatrix} \frac{1}{m} \int_B x\, dm \\ \frac{1}{m} \int_B y\, dm \\ \frac{1}{m} \int_B z\, dm \end{bmatrix} \tag{9.19}
$$

*Applying the mass center integral on the symmetric and uniform L-section rigid body with $\rho = 1$ shown in Figure 9.2 provides the position of mass center $C$ of the section. The $x$ position of $C$ is*

$$
\begin{aligned}
x_C &= \frac{1}{m} \int_B x\, dm \\
&= \frac{1}{A} \int_B x\, dA \\
&= -\frac{b^2 + ab - a^2}{4ab + 2a^2} \tag{9.20}
\end{aligned}
$$

*and because of symmetry, we have*

$$y_C = -x_C = \frac{b^2 + ab - a^2}{4ab + 2a^2}. \tag{9.21}$$
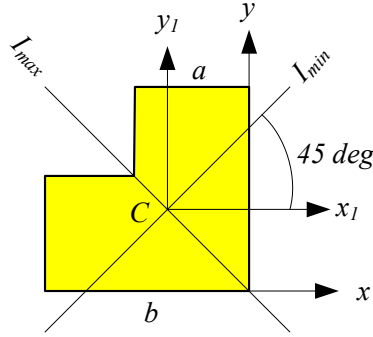
FIGURE 9.2. Principal coordinate frame for a symmetric L-section.

When $a = b$, the position of $C$ reduces to

$$y_C = -x_C = \frac{1}{2}b. \tag{9.22}$$

**Example 343** ★ *Every force system is equivalent to a wrench.*

The Poinsot theorem states: Every force system is equivalent to a single force, plus a moment parallel to the force. Let $\mathbf{F}$ and $\mathbf{M}$ be the resultant force and moment of a force system. We decompose the moment into parallel and perpendicular components, $\mathbf{M}_\parallel$ and $\mathbf{M}_\perp$, to the force axis. The force $\mathbf{F}$ and the perpendicular moment $\mathbf{M}_\perp$ can be replaced by a single force $\mathbf{F}'$ parallel to $\mathbf{F}$. Therefore, the force system is reduced to a force $\mathbf{F}'$ and a moment $\mathbf{M}_\parallel$ parallel to each other. A force and a moment about the force axis is called a **wrench**.

The Poinsot theorem is similar to the Chasles theorem that states: Every rigid body motion is equivalent to a screw, which is a translation plus a rotation about the axis of translation.

**Example 344** ★ *Motion of a moving point in a moving body frame.*

The velocity and acceleration of a moving point $P$ as shown in Figure 5.12 are found in Example 200.

$$^G\mathbf{v}_P = {^G\dot{\mathbf{d}}_B} + {^GR_B}\left({^B\mathbf{v}_P} + {^B_G\boldsymbol{\omega}_B} \times {^B\mathbf{r}_P}\right) \tag{9.23}$$

$$
\begin{aligned}
^G\mathbf{a}_P &= {^G\ddot{\mathbf{d}}_B} + {^GR_B}\left({^B\mathbf{a}_P} + 2\,{^B_G\boldsymbol{\omega}_B} \times {^B\mathbf{v}_P} + {^B_G\dot{\boldsymbol{\omega}}_B} \times {^B\mathbf{r}_P}\right) \\
&\quad + {^GR_B}\left({^B_G\boldsymbol{\omega}_B} \times \left({^B_G\boldsymbol{\omega}_B} \times {^B\mathbf{r}_P}\right)\right)
\end{aligned}
\tag{9.24}
$$

Therefore, the equation of motion for the point mass $P$ is

$$
\begin{aligned}
^G\mathbf{F} &= m\,{^G\mathbf{a}_P} \\
&= m\left({^G\ddot{\mathbf{d}}_B} + {^GR_B}\left({^B\mathbf{a}_P} + 2\,{^B_G\boldsymbol{\omega}_B} \times {^B\mathbf{v}_P} + {^B_G\dot{\boldsymbol{\omega}}_B} \times {^B\mathbf{r}_P}\right)\right) \\
&\quad + m\,{^GR_B}\left({^B_G\boldsymbol{\omega}_B} \times \left({^B_G\boldsymbol{\omega}_B} \times {^B\mathbf{r}_P}\right)\right).
\end{aligned}
\tag{9.25}
$$

**Example 345** *Newton's equation in a rotating frame.*

Consider a spherical rigid body, such as Earth, with a fixed point that is rotating with a constant angular velocity. The equation of motion for a moving point vehicle $P$ on the rigid body is found by setting ${}^{G}\ddot{\mathbf{d}}_{B} = {}^{B}_{G}\dot{\boldsymbol{\omega}}_{B} = 0$ in the equation of motion of a moving point in a moving body frame (9.25)

$$
\begin{aligned}
{}^{B}\mathbf{F} \;&=\; m\,{}^{B}\mathbf{a}_{P} + m\,{}^{B}_{G}\boldsymbol{\omega}_{B} \times \left({}^{B}_{G}\boldsymbol{\omega}_{B} \times {}^{B}\mathbf{r}_{P}\right) + 2m\,{}^{B}_{G}\boldsymbol{\omega}_{B} \times {}^{B}\dot{\mathbf{r}}_{P} \quad (9.26)\\
&\neq\; m\,{}^{B}\mathbf{a}_{P}
\end{aligned}
$$

which shows that the Newton's equation of motion $\mathbf{F} = m\,\mathbf{a}$ must be modified for rotating frames.

**Example 346** *Coriolis force.*

The equation of motion of a moving vehicle point on the surface of the Earth is

$$
{}^{B}\mathbf{F} = m\,{}^{B}\mathbf{a}_{P} + m\,{}^{B}_{G}\boldsymbol{\omega}_{B} \times \left({}^{B}_{G}\boldsymbol{\omega}_{B} \times {}^{B}\mathbf{r}_{P}\right) + 2m\,{}^{B}_{G}\boldsymbol{\omega}_{B} \times {}^{B}\mathbf{v}_{P} \qquad (9.27)
$$

which can be rearranged to

$$
{}^{B}\mathbf{F} - m\,{}^{B}_{G}\boldsymbol{\omega}_{B} \times \left({}^{B}_{G}\boldsymbol{\omega}_{B} \times {}^{B}\mathbf{r}_{P}\right) - 2m\,{}^{B}_{G}\boldsymbol{\omega}_{B} \times {}^{B}\mathbf{v}_{P} = m\,{}^{B}\mathbf{a}_{P}. \qquad (9.28)
$$

Equation (9.28) is the equation of motion for an observer in the rotating frame, which in this case is an observer on the Earth. The left-hand side of this equation is called the **effective force** $\mathbf{F}_{eff}$,

$$
\mathbf{F}_{eff} = {}^{B}\mathbf{F} - m\,{}^{B}_{G}\boldsymbol{\omega}_{B} \times \left({}^{B}_{G}\boldsymbol{\omega}_{B} \times {}^{B}\mathbf{r}_{P}\right) - 2m\,{}^{B}_{G}\boldsymbol{\omega}_{B} \times {}^{B}\mathbf{v}_{P} \qquad (9.29)
$$

because it seems that the particle is moving under the influence of this force.

The second term is negative of the centrifugal force and pointing outward. The maximum value of this force on the Earth is on the equator

$$
\begin{aligned}
r\omega^{2} \;&=\; 6378.388 \times 10^{3} \times \left(\frac{2\pi}{24 \times 3600}\frac{366.25}{365.25}\right)^{2}\\
&=\; 3.3917 \times 10^{-2}\,\mathrm{m/s^{2}} \qquad (9.30)
\end{aligned}
$$

which is about 0.3% of the acceleration of gravity. If we add the variation of the gravitational acceleration because of a change of radius from $R = 6356912\,\mathrm{m}$ at the pole to $R = 6378388\,\mathrm{m}$ on the equator, then the variation of the acceleration of gravity becomes 0.53%. So, generally speaking, a sportsman such as a pole-vaulter who has practiced in the north pole can show a better record in a competition held on the equator.

The third term is called the **Coriolis force** or **Coriolis effect**, $F_{C}$, which is perpendicular to both $\boldsymbol{\omega}$ and ${}^{B}\mathbf{v}_{P}$. For a mass $m$ moving on the north hemisphere at a latitude $\theta$ towards the equator, we should provide a

*lateral eastward force equal to the Coriolis effect to force the mass, keeping its direction relative to the ground.*

$$
\begin{aligned}
F_C &= 2m\,{}_G^B\boldsymbol{\omega}_B \times {}^B\mathbf{v}_m \\
&= 1.4584 \times 10^{-4}\,{}^B\mathbf{p}_m \cos\theta \;\; \mathrm{kg\,m/s^2}
\end{aligned}
\tag{9.31}
$$

*The Coriolis effect is the reason why the west side of railways, roads, and rivers wears. The lack of providing the Coriolis force is the reason for turning the direction of winds, projectiles, flood, and falling objects westward.*

**Example 347** *Work, force, and kinetic energy in a unidirectional motion.*

*A vehicle with mass $m = 1200\,\mathrm{kg}$ has an initial kinetic energy $K = 6000\,\mathrm{J}$. The mass is under a constant force $\mathbf{F} = F\hat{I} = 4000\hat{I}$ and moves from $X(0) = 0$ to $X(t_f) = 1000\,\mathrm{m}$ at a terminal time $t_f$. The work done by the force during this motion is*

$$
\begin{aligned}
W &= \int_{\mathbf{r}(0)}^{\mathbf{r}(t_f)} \mathbf{F} \cdot d\mathbf{r} \\
&= \int_0^{1000} 4000\,dX \\
&= 4 \times 10^6\,\mathrm{N\,m} \\
&= 4\,\mathrm{MJ}
\end{aligned}
\tag{9.32}
$$

*The kinetic energy at the terminal time is*

$$
K(t_f) = W + K(0) = 4006000\,\mathrm{J}
\tag{9.33}
$$

*which shows that the terminal speed of the mass is*

$$
v_2 = \sqrt{\frac{2K(t_f)}{m}} \approx 81.7\,\mathrm{m/s}.
\tag{9.34}
$$

**Example 348** *Direct dynamics.*
*When the applied force is time varying and is a known function, then,*

$$
\mathbf{F}(t) = m\,\ddot{\mathbf{r}}.
\tag{9.35}
$$

*The general solution for the equation of motion can be found by integration.*

$$
\dot{\mathbf{r}}(t) = \dot{\mathbf{r}}(t_0) + \frac{1}{m}\int_{t_0}^{t} \mathbf{F}(t)dt
\tag{9.36}
$$

$$
\mathbf{r}(t) = \mathbf{r}(t_0) + \dot{\mathbf{r}}(t_0)(t - t_0) + \frac{1}{m}\int_{t_0}^{t}\int_{t_0}^{t} \mathbf{F}(t)dt\,dt
\tag{9.37}
$$

*This kind of problem is called direct or forward dynamics.*
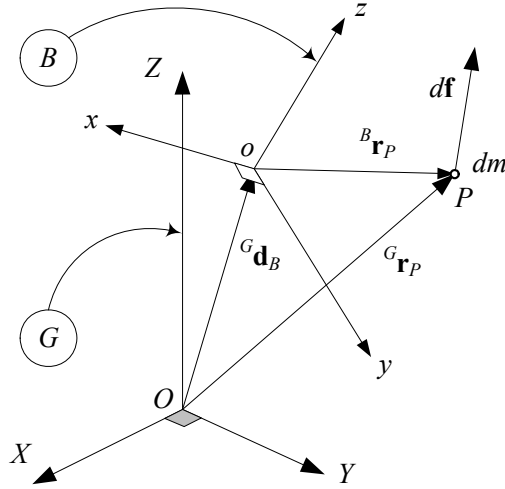
FIGURE 9.3. A body point mass moving with velocity $^G\mathbf{v}_P$ and acted on by force $d\mathbf{f}$.

## 9.2    Rigid Body Translational Dynamics

Figure 9.3 depicts a moving body $B$ in a global coordinate frame $G$. Assume that the body frame is attached at the mass center of the body. Point $P$ indicates an infinitesimal sphere of the body, which has a very small mass $dm$. The point mass $dm$ is acted on by an infinitesimal force $d\mathbf{f}$ and has a global velocity $^G\mathbf{v}_P$.

According to Newton's law of motion we have

$$d\mathbf{f} = {}^G\mathbf{a}_P \, dm. \tag{9.38}$$

However, the equation of motion for the whole body in a global coordinate frame is

$$^G\mathbf{F} = m \, {}^G\mathbf{a}_B \tag{9.39}$$

which can be expressed in the body coordinate frame as

$$^B\mathbf{F} = m \, {}^B_G\mathbf{a}_B + m \, {}^B_G\boldsymbol{\omega}_B \times {}^B\mathbf{v}_B \tag{9.40}$$

$$\begin{bmatrix} F_x \\ F_y \\ F_z \end{bmatrix} = \begin{bmatrix} ma_x + m\left(\omega_y v_z - \omega_z v_y\right) \\ ma_y - m\left(\omega_x v_z - \omega_z v_x\right) \\ ma_z + m\left(\omega_x v_y - \omega_y v_x\right) \end{bmatrix}. \tag{9.41}$$

In these equations, $^G\mathbf{a}_B$ is the acceleration vector of the body mass center $C$ in the global frame, $m$ is the total mass of the body, and $\mathbf{F}$ is the resultant of the external forces acted on the body at $C$.

**Proof.** A body coordinate frame at the mass center is called a *central frame*. If frame $B$ is a central frame, then the *center of mass*, $C$, is defined such that

$$\int_B {}^B\mathbf{r}_{dm} \, dm = 0. \tag{9.42}$$

The global position vector of $dm$ is related to its local position vector by

$$^G\mathbf{r}_{dm} = {}^G\mathbf{d}_B + {}^G R_B \, {}^B\mathbf{r}_{dm} \tag{9.43}$$

where ${}^G\mathbf{d}_B$ is the global position vector of the central body frame, and therefore,

$$\begin{aligned}
\int_B {}^G\mathbf{r}_{dm} \, dm &= \int_B {}^G\mathbf{d}_B \, dm + {}^G R_B \int_m {}^B\mathbf{r}_{dm} \, dm \\
&= \int_B {}^G\mathbf{d}_B \, dm \\
&= {}^G\mathbf{d}_B \int_B dm \\
&= m \, {}^G\mathbf{d}_B. \tag{9.44}
\end{aligned}$$

A time derivative of both sides shows that

$$m \, {}^G\dot{\mathbf{d}}_B = m \, {}^G\mathbf{v}_B = \int_B {}^G\dot{\mathbf{r}}_{dm} \, dm = \int_B {}^G\mathbf{v}_{dm} \, dm \tag{9.45}$$

and another derivative is

$$m \, {}^G\dot{\mathbf{v}}_B = m \, {}^G\mathbf{a}_B = \int_B {}^G\dot{\mathbf{v}}_{dm} \, dm. \tag{9.46}$$

However, we have $d\mathbf{f} = {}^G\dot{\mathbf{v}}_P \, dm$ and therefore,

$$m \, {}^G\mathbf{a}_B = \int_B d\mathbf{f}. \tag{9.47}$$

The integral on the right-hand side accounts for all the forces acting on the body. The internal forces cancel one another out, so the net result is the vector sum of all the externally applied forces, $\mathbf{F}$, and therefore,

$$^G\mathbf{F} = m \, {}^G\mathbf{a}_B = m \, {}^G\dot{\mathbf{v}}_B. \tag{9.48}$$

In the body coordinate frame we have

$$\begin{aligned}
^B\mathbf{F} &= {}^B R_G \, {}^G\mathbf{F} \\
&= m \, {}^B R_G \, {}^G\mathbf{a}_B \\
&= m \, {}^B_G\mathbf{a}_B \\
&= m \, {}^B\mathbf{a}_B + m \, {}^B_G\boldsymbol{\omega}_B \times {}^B\mathbf{v}_B. \tag{9.49}
\end{aligned}$$

The expanded form of the Newton's equation in the body coordinate frame is then equal to

$$
\begin{aligned}
{}^{B}\mathbf{F} &= m\,{}^{B}\mathbf{a}_B + m\,{}^{B}_{G}\boldsymbol{\omega}_B \times {}^{B}\mathbf{v}_B \\[4pt]
\begin{bmatrix} F_x \\ F_y \\ F_z \end{bmatrix} &= m \begin{bmatrix} a_x \\ a_y \\ a_z \end{bmatrix} + m \begin{bmatrix} \omega_x \\ \omega_y \\ \omega_z \end{bmatrix} \times \begin{bmatrix} v_x \\ v_y \\ v_z \end{bmatrix} \\[6pt]
&= \begin{bmatrix} ma_x + m\,(\omega_y v_z - \omega_z v_y) \\ ma_y - m\,(\omega_x v_z - \omega_z v_x) \\ ma_z + m\,(\omega_x v_y - \omega_y v_x) \end{bmatrix}.
\end{aligned}
\tag{9.50}
$$

∎

## 9.3   Rigid Body Rotational Dynamics

The rigid body rotational equation of motion is the *Euler equation*

$$
\begin{aligned}
{}^{B}\mathbf{M} &= \frac{{}^{G}d}{dt}\,{}^{B}\mathbf{L} \\[4pt]
&= {}^{B}\dot{\mathbf{L}} + {}^{B}_{G}\boldsymbol{\omega}_B \times {}^{B}\mathbf{L} \\[4pt]
&= {}^{B}I\,{}^{B}_{G}\dot{\boldsymbol{\omega}}_B + {}^{B}_{G}\boldsymbol{\omega}_B \times \left( {}^{B}I\,{}^{B}_{G}\boldsymbol{\omega}_B \right)
\end{aligned}
\tag{9.51}
$$

where $\mathbf{L}$ is the *angular momentum*

$$
{}^{B}\mathbf{L} = {}^{B}I\,{}^{B}_{G}\boldsymbol{\omega}_B
\tag{9.52}
$$

and $I$ is the *moment of inertia* of the rigid body.

$$
I = \begin{bmatrix} I_{xx} & I_{xy} & I_{xz} \\ I_{yx} & I_{yy} & I_{yz} \\ I_{zx} & I_{zy} & I_{zz} \end{bmatrix}
\tag{9.53}
$$

The elements of $I$ are functions of the mass distribution of the rigid body and may be defined by

$$
I_{ij} = \int_{B} \left( r_i^2 \delta_{mn} - x_{im} x_{jn} \right) dm \quad , \quad i,j = 1,2,3
\tag{9.54}
$$

where $\delta_{ij}$ is Kronecker's delta.

$$
\delta_{mn} = \begin{cases} 1 & if \quad m = n \\ 0 & if \quad m \neq n \end{cases}
\tag{9.55}
$$

The expanded form of the Euler equation (9.51) is

$$
\begin{aligned}
M_x &= I_{xx}\dot{\omega}_x + I_{xy}\dot{\omega}_y + I_{xz}\dot{\omega}_z - (I_{yy} - I_{zz})\,\omega_y \omega_z \\
&\quad - I_{yz}\left(\omega_z^2 - \omega_y^2\right) - \omega_x\,(\omega_z I_{xy} - \omega_y I_{xz})
\end{aligned}
\tag{9.56}
$$

$$
\begin{aligned}
M_y \;=\; & I_{yx}\dot{\omega}_x + I_{yy}\dot{\omega}_y + I_{yz}\dot{\omega}_z - (I_{zz} - I_{xx})\,\omega_z\omega_x \\
& - I_{xz}\left(\omega_x^2 - \omega_z^2\right) - \omega_y\left(\omega_x I_{yz} - \omega_z I_{xy}\right)
\end{aligned}
\tag{9.57}
$$

$$
\begin{aligned}
M_z \;=\; & I_{zx}\dot{\omega}_x + I_{zy}\dot{\omega}_y + I_{zz}\dot{\omega}_z - (I_{xx} - I_{yy})\,\omega_x\omega_y \\
& - I_{xy}\left(\omega_y^2 - \omega_x^2\right) - \omega_z\left(\omega_y I_{xz} - \omega_x I_{yz}\right).
\end{aligned}
\tag{9.58}
$$

which can be reduced to

$$
\begin{aligned}
M_1 &= I_1\dot{\omega}_1 - (I_2 - I_2)\,\omega_2\omega_3 \\
M_2 &= I_2\dot{\omega}_2 - (I_3 - I_1)\,\omega_3\omega_1 \\
M_3 &= I_3\dot{\omega}_3 - (I_1 - I_2)\,\omega_1\omega_2
\end{aligned}
\tag{9.59}
$$

in a special Cartesian coordinate frame called the *principal coordinate frame*. The principal coordinate frame is denoted by numbers 123 to indicate the first, second, and third *principal axes*. The parameters $I_{ij}$, $i \neq j$ are zero in the principal frame. The body and principal coordinate frame sit at the mass center $C$.

Kinetic energy of a rotating rigid body is

$$
\begin{aligned}
K \;=\;& \frac{1}{2}\left(I_{xx}\omega_x^2 + I_{yy}\omega_y^2 + I_{zz}\omega_z^2\right) \\
& - I_{xy}\omega_x\omega_y - I_{yz}\omega_y\omega_z - I_{zx}\omega_z\omega_x
\end{aligned}
\tag{9.60}
$$

$$
=\; \frac{1}{2}\boldsymbol{\omega}\cdot\mathbf{L}
\tag{9.61}
$$

$$
=\; \frac{1}{2}\boldsymbol{\omega}^T I\,\boldsymbol{\omega}
\tag{9.62}
$$

that in the principal coordinate frame reduces to

$$
K = \frac{1}{2}\left(I_1\omega_1^2 + I_2\omega_2^2 + I_3\omega_3^2\right).
\tag{9.63}
$$

**Proof.** Let $m_i$ be the mass of the $i$th particle of a rigid body $B$, which is made of $n$ particles and let

$$
\mathbf{r}_i = {}^B\mathbf{r}_i = \begin{bmatrix} x_i & y_i & z_i \end{bmatrix}^T
\tag{9.64}
$$

be the Cartesian position vector of $m_i$ in a central body fixed coordinate frame $Oxyz$. Assume that

$$
\boldsymbol{\omega} = {}^B_G\boldsymbol{\omega}_B = \begin{bmatrix} \omega_x & \omega_y & \omega_z \end{bmatrix}^T
\tag{9.65}
$$

is the angular velocity of the rigid body with respect to the ground, expressed in the body coordinate frame.

The angular momentum of $m_i$ is

$$
\begin{aligned}
\mathbf{L}_i &= \mathbf{r}_i \times m_i \dot{\mathbf{r}}_i \\
&= m_i \left[ \mathbf{r}_i \times (\boldsymbol{\omega} \times \mathbf{r}_i) \right] \\
&= m_i \left[ (\mathbf{r}_i \cdot \mathbf{r}_i) \boldsymbol{\omega} - (\mathbf{r}_i \cdot \boldsymbol{\omega}) \mathbf{r}_i \right] \\
&= m_i r_i^2 \boldsymbol{\omega} - m_i (\mathbf{r}_i \cdot \boldsymbol{\omega}) \mathbf{r}_i.
\end{aligned}
\tag{9.66}
$$

Hence, the angular momentum of the rigid body would be

$$
\mathbf{L} = \boldsymbol{\omega} \sum_{i=1}^{n} m_i r_i^2 - \sum_{i=1}^{n} m_i (\mathbf{r}_i \cdot \boldsymbol{\omega}) \mathbf{r}_i.
\tag{9.67}
$$

Substitution for $\mathbf{r}_i$ and $\boldsymbol{\omega}$ gives us

$$
\begin{aligned}
\mathbf{L} &= \left( \omega_x \hat{\imath} + \omega_y \hat{\jmath} + \omega_z \hat{k} \right) \sum_{i=1}^{n} m_i \left( x_i^2 + y_i^2 + z_i^2 \right) \\
&\quad - \sum_{i=1}^{n} m_i \left( x_i \omega_x + y_i \omega_y + z_i \omega_z \right) \cdot \left( x_i \hat{\imath} + y_i \hat{\jmath} + z_i \hat{k} \right)
\end{aligned}
\tag{9.68}
$$

and therefore,

$$
\begin{aligned}
\mathbf{L} &= \sum_{i=1}^{n} m_i \left( x_i^2 + y_i^2 + z_i^2 \right) \omega_x \hat{\imath} \\
&\quad + \sum_{i=1}^{n} m_i \left( x_i^2 + y_i^2 + z_i^2 \right) \omega_y \hat{\jmath} \\
&\quad + \sum_{i=1}^{n} m_i \left( x_i^2 + y_i^2 + z_i^2 \right) \omega_z \hat{k} \\
&\quad - \sum_{i=1}^{n} m_i \left( x_i \omega_x + y_i \omega_y + z_i \omega_z \right) x_i \hat{\imath} \\
&\quad - \sum_{i=1}^{n} m_i \left( x_i \omega_x + y_i \omega_y + z_i \omega_z \right) y_i \hat{\jmath} \\
&\quad - \sum_{i=1}^{n} m_i \left( x_i \omega_x + y_i \omega_y + z_i \omega_z \right) z_i \hat{k}
\end{aligned}
\tag{9.69}
$$

or

$$
\begin{aligned}
\mathbf{L} &= \sum_{i=1}^{n} m_i \left[ \left( x_i^2 + y_i^2 + z_i^2 \right) \omega_x - \left( x_i \omega_x + y_i \omega_y + z_i \omega_z \right) x_i \right] \hat{\imath} \\
&\quad + \sum_{i=1}^{n} m_i \left[ \left( x_i^2 + y_i^2 + z_i^2 \right) \omega_y - \left( x_i \omega_x + y_i \omega_y + z_i \omega_z \right) y_i \right] \hat{\jmath} \\
&\quad + \sum_{i=1}^{n} m_i \left[ \left( x_i^2 + y_i^2 + z_i^2 \right) \omega_z - \left( x_i \omega_x + y_i \omega_y + z_i \omega_z \right) z_i \right] \hat{k}
\end{aligned}
\tag{9.70}
$$

which can be rearranged as

$$
\begin{aligned}
\mathbf{L} \;=\; & \sum_{i=1}^{n} \left[ m_i \left( y_i^2 + z_i^2 \right) \right] \omega_x \hat{\imath} \\[4pt]
& + \sum_{i=1}^{n} \left[ m_i \left( z_i^2 + x_i^2 \right) \right] \omega_y \hat{\jmath} \\[4pt]
& + \sum_{i=1}^{n} \left[ m_i \left( x_i^2 + y_i^2 \right) \right] \omega_z \hat{k} \\[4pt]
& - \left( \sum_{i=1}^{n} \left( m_i x_i y_i \right) \omega_y + \sum_{i=1}^{n} \left( m_i x_i z_i \right) \omega_z \right) \hat{\imath} \\[4pt]
& - \left( \sum_{i=1}^{n} \left( m_i y_i z_i \right) \omega_z + \sum_{i=1}^{n} \left( m_i y_i x_i \right) \omega_x \right) \hat{\jmath} \\[4pt]
& - \left( \sum_{i=1}^{n} \left( m_i z_i x_i \right) \omega_x + \sum_{i=1}^{n} \left( m_i z_i y_i \right) \omega_y \right) \hat{k}. \qquad (9.71)
\end{aligned}
$$

By introducing the moment of inertia matrix $I$ with the following elements,

$$
I_{xx} \;=\; \sum_{i=1}^{n} \left[ m_i \left( y_i^2 + z_i^2 \right) \right] \tag{9.72}
$$

$$
I_{yy} \;=\; \sum_{i=1}^{n} \left[ m_i \left( z_i^2 + x_i^2 \right) \right] \tag{9.73}
$$

$$
I_{zz} \;=\; \sum_{i=1}^{n} \left[ m_i \left( x_i^2 + y_i^2 \right) \right] \tag{9.74}
$$

$$
I_{xy} \;=\; I_{yx} = - \sum_{i=1}^{n} \left( m_i x_i y_i \right) \tag{9.75}
$$

$$
I_{yz} \;=\; I_{zy} = - \sum_{i=1}^{n} \left( m_i y_i z_i \right) \tag{9.76}
$$

$$
I_{zx} \;=\; I_{xz} = - \sum_{i=1}^{n} \left( m_i z_i x_i \right). \tag{9.77}
$$

we may write the angular momentum $\mathbf{L}$ in a concise form

$$
\begin{aligned}
L_x &= I_{xx}\omega_x + I_{xy}\omega_y + I_{xz}\omega_z & (9.78) \\
L_y &= I_{yx}\omega_x + I_{yy}\omega_y + I_{yz}\omega_z & (9.79) \\
L_z &= I_{zx}\omega_x + I_{zy}\omega_y + I_{zz}\omega_z & (9.80)
\end{aligned}
$$

or in a matrix form

$$\mathbf{L} = I \cdot \boldsymbol{\omega} \tag{9.81}$$

$$\begin{bmatrix} L_x \\ L_y \\ L_z \end{bmatrix} = \begin{bmatrix} I_{xx} & I_{xy} & I_{xz} \\ I_{yx} & I_{yy} & I_{yz} \\ I_{zx} & I_{zy} & I_{zz} \end{bmatrix} \begin{bmatrix} \omega_x \\ \omega_y \\ \omega_z \end{bmatrix}. \tag{9.82}$$

For a rigid body that is a continuous solid, the summations must be replaced by integrations over the volume of the body as in Equation (9.54).

The Euler equation of motion for a rigid body is

$$^{B}\mathbf{M} = \frac{^{G}d}{dt} \, ^{B}\mathbf{L} \tag{9.83}$$

where $^{B}\mathbf{M}$ is the resultant of the external moments applied on the rigid body. The angular momentum $^{B}\mathbf{L}$ is a vector defined in the body coordinate frame. Hence, its time derivative in the global coordinate frame is

$$\frac{^{G}d \, ^{B}\mathbf{L}}{dt} = \,^{B}\dot{\mathbf{L}} + \,^{B}_{G}\boldsymbol{\omega}_B \times \,^{B}\mathbf{L}. \tag{9.84}$$

Therefore,

$$\begin{aligned} ^{B}\mathbf{M} &= \frac{d\mathbf{L}}{dt} = \dot{\mathbf{L}} + \boldsymbol{\omega} \times \mathbf{L} \\ &= I\dot{\boldsymbol{\omega}} + \boldsymbol{\omega} \times (I\boldsymbol{\omega}) \end{aligned} \tag{9.85}$$

or in expanded form

$$\begin{aligned} ^{B}\mathbf{M} &= (I_{xx}\dot{\omega}_x + I_{xy}\dot{\omega}_y + I_{xz}\dot{\omega}_z)\,\hat{\imath} \\ &+ (I_{yx}\dot{\omega}_x + I_{yy}\dot{\omega}_y + I_{yz}\dot{\omega}_z)\,\hat{\jmath} \\ &+ (I_{zx}\dot{\omega}_x + I_{zy}\dot{\omega}_y + I_{zz}\dot{\omega}_z)\,\hat{k} \\ &+ \omega_y (I_{xz}\omega_x + I_{yz}\omega_y + I_{zz}\omega_z)\,\hat{\imath} \\ &- \omega_z (I_{xy}\omega_x + I_{yy}\omega_y + I_{yz}\omega_z)\,\hat{\imath} \\ &+ \omega_z (I_{xx}\omega_x + I_{xy}\omega_y + I_{xz}\omega_z)\,\hat{\jmath} \\ &- \omega_x (I_{xz}\omega_x + I_{yz}\omega_y + I_{zz}\omega_z)\,\hat{\jmath} \\ &+ \omega_x (I_{xy}\omega_x + I_{yy}\omega_y + I_{yz}\omega_z)\,\hat{k} \\ &- \omega_y (I_{xx}\omega_x + I_{xy}\omega_y + I_{xz}\omega_z)\,\hat{k} \end{aligned} \tag{9.86}$$

and therefore, the most general form of the Euler equations of motion for a rigid body in a body frame attached to $C$ are

$$\begin{aligned} M_x &= I_{xx}\dot{\omega}_x + I_{xy}\dot{\omega}_y + I_{xz}\dot{\omega}_z - (I_{yy} - I_{zz})\,\omega_y\omega_z \\ &- I_{yz}\left(\omega_z^2 - \omega_y^2\right) - \omega_x\left(\omega_z I_{xy} - \omega_y I_{xz}\right) \end{aligned} \tag{9.87}$$

$$\begin{aligned} M_y &= I_{yx}\dot{\omega}_x + I_{yy}\dot{\omega}_y + I_{yz}\dot{\omega}_z - (I_{zz} - I_{xx})\,\omega_z\omega_x \\ &- I_{xz}\left(\omega_x^2 - \omega_z^2\right) - \omega_y\left(\omega_x I_{yz} - \omega_z I_{xy}\right) \end{aligned} \tag{9.88}$$

$$\begin{aligned} M_z &= I_{zx}\dot{\omega}_x + I_{zy}\dot{\omega}_y + I_{zz}\dot{\omega}_z - (I_{xx} - I_{yy})\,\omega_x\omega_y \\ &- I_{xy}\left(\omega_y^2 - \omega_x^2\right) - \omega_z\left(\omega_y I_{xz} - \omega_x I_{yz}\right). \end{aligned} \tag{9.89}$$

Assume that we are able to rotate the body frame about its origin to find an orientation that makes $I_{ij} = 0$, for $i \neq j$. In such a coordinate frame, which is called a principal frame, the Euler equations reduce to

$$
\begin{align}
M_1 &= I_1 \dot{\omega}_1 - (I_2 - I_2) \, \omega_2 \omega_3 \tag{9.90}\\
M_2 &= I_2 \dot{\omega}_2 - (I_3 - I_1) \, \omega_3 \omega_1 \tag{9.91}\\
M_3 &= I_3 \dot{\omega}_3 - (I_1 - I_2) \, \omega_1 \omega_2. \tag{9.92}
\end{align}
$$

The kinetic energy of a rigid body may be found by the integral of the kinetic energy of a mass element $dm$, over the whole body.

$$
\begin{align}
K &= \frac{1}{2} \int_B \dot{\mathbf{v}}^2 dm \\
&= \frac{1}{2} \int_B (\boldsymbol{\omega} \times \mathbf{r}) \cdot (\boldsymbol{\omega} \times \mathbf{r}) \, dm \\
&= \frac{\omega_x^2}{2} \int_B \left(y^2 + z^2\right) dm + \frac{\omega_y^2}{2} \int_B \left(z^2 + x^2\right) dm + \frac{\omega_z^2}{2} \int_B \left(x^2 + y^2\right) dm \\
&\quad - \omega_x \omega_y \int_B xy \, dm - \omega_y \omega_z \int_B yz \, dm - \omega_z \omega_x \int_B zx \, dm \\
&= \frac{1}{2} \left(I_{xx} \omega_x^2 + I_{yy} \omega_y^2 + I_{zz} \omega_z^2\right) \\
&\quad - I_{xy} \omega_x \omega_y - I_{yz} \omega_y \omega_z - I_{zx} \omega_z \omega_x \tag{9.93}
\end{align}
$$

The kinetic energy can be rearranged to a matrix multiplication form

$$
\begin{align}
K &= \frac{1}{2} \boldsymbol{\omega}^T I \, \boldsymbol{\omega} \tag{9.94}\\
&= \frac{1}{2} \boldsymbol{\omega} \cdot \mathbf{L}. \tag{9.95}
\end{align}
$$

When the body frame is principal, the kinetic energy will simplify to

$$
K = \frac{1}{2} \left(I_1 \omega_1^2 + I_2 \omega_2^2 + I_3 \omega_3^2\right). \tag{9.96}
$$

∎

**Example 349** *A tilted disc on a massless shaft.*

*Figure 9.4 illustrates a disc with mass m and radius r, mounted on a massless shaft. The shaft is turning with a constant angular speed ω. The disc is attached to the shaft at an angle θ. Because of θ, the bearings at A and B must support a rotating force.*

*We attach a principal body coordinate frame at the disc center as shown in the figure. The angular velocity vector in the body frame is*

$$
{}^B_G \boldsymbol{\omega}_B = \omega \cos \theta \, \hat{\imath} + \omega \sin \theta \, \hat{\jmath} \tag{9.97}
$$
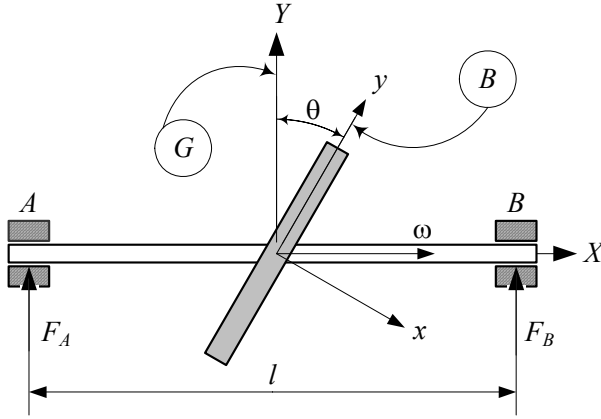
FIGURE 9.4. A disc with mass $m$ and radius $r$, mounted on a massless turning shaft.

and the mass moment of inertia matrix is

$$
{}^B I = \begin{bmatrix} \dfrac{mr^2}{2} & 0 & 0 \\ 0 & \dfrac{mr^2}{4} & 0 \\ 0 & 0 & \dfrac{mr^2}{4} \end{bmatrix}. \tag{9.98}
$$

Substituting (9.97) and (9.98) in (9.90)-(9.92), with $1 \equiv x$, $2 \equiv y$, $3 \equiv z$, provides that

$$
\begin{align}
M_x &= 0 \tag{9.99} \\
M_y &= 0 \tag{9.100} \\
M_z &= \frac{mr^2}{4} \omega \cos\theta \sin\theta. \tag{9.101}
\end{align}
$$

Therefore, the bearing reaction forces $F_A$ and $F_B$ are

$$
\begin{align}
F_A &= -F_B \\
&= -\frac{M_z}{l} \\
&= -\frac{mr^2}{4l} \omega \cos\theta \sin\theta. \tag{9.102}
\end{align}
$$

**Example 350** *Steady rotation of a freely rotating rigid body.*
   *The Newton-Euler equations of motion for a rigid body are*

$$
\begin{align}
{}^G\mathbf{F} &= m\, {}^G\dot{\mathbf{v}} \tag{9.103} \\
{}^B\mathbf{M} &= I\, {}^B_G\dot{\boldsymbol{\omega}}_B + {}^B_G\boldsymbol{\omega}_B \times {}^B\mathbf{L}. \tag{9.104}
\end{align}
$$

*Consider a situation in which the resultant applied force and moment on the body are zero.*

$$^G\mathbf{F} = {}^B\mathbf{F} = 0 \tag{9.105}$$

$$^G\mathbf{M} = {}^B\mathbf{M} = 0 \tag{9.106}$$

*Based on the Newton's equation, the velocity of the mass center will be constant in the global coordinate frame. However, the Euler equation reduces to*

$$\dot{\omega}_1 = \frac{I_2 - I_3}{I_1}\omega_2\omega_3 \tag{9.107}$$

$$\dot{\omega}_2 = \frac{I_3 - I_1}{I_{22}}\omega_3\omega_1 \tag{9.108}$$

$$\dot{\omega}_3 = \frac{I_1 - I_2}{I_3}\omega_1\omega_2 \tag{9.109}$$

*that show the angular velocity can be constant if*

$$I_1 = I_2 = I_3 \tag{9.110}$$

*or if two principal moments of inertia, say $I_1$ and $I_2$, are zero and the third angular velocity, in this case $\omega_3$, is initially zero, or if the angular velocity vector is initially parallel to a principal axis.*

**Example 351** *Angular momentum of a two-link manipulator.*
    *A two-link manipulator is shown in Figure 9.5. Link A rotates with angular velocity $\dot{\varphi}$ about the z-axis of its local coordinate frame. Link B is attached to link A and has angular velocity $\dot{\psi}$ with respect to A about the $x_A$-axis. We assume that A and G were coincident at $\varphi = 0$, therefore, the rotation matrix between A and G is*

$$^G R_A = \begin{bmatrix} \cos\varphi(t) & -\sin\varphi(t) & 0 \\ \sin\varphi(t) & \cos\varphi(t) & 0 \\ 0 & 0 & 1 \end{bmatrix}. \tag{9.111}$$

*Frame B is related to frame A by Euler angles $\varphi = 90\deg$, $\theta = 90\deg$, and $\psi$, hence,*

$$^A R_B = \begin{bmatrix} c\pi c\psi - c\pi s\pi s\psi & -c\pi s\psi - c\pi c\psi s\pi & s\pi s\pi \\ c\psi s\pi + c\pi c\pi s\psi & -s\pi s\psi + c\pi c\pi c\psi & -c\pi s\pi \\ s\pi s\psi & s\pi c\psi & c\pi \end{bmatrix}$$
$$= \begin{bmatrix} -\cos\psi & \sin\psi & 0 \\ \sin\psi & \cos\psi & 0 \\ 0 & 0 & -1 \end{bmatrix} \tag{9.112}$$
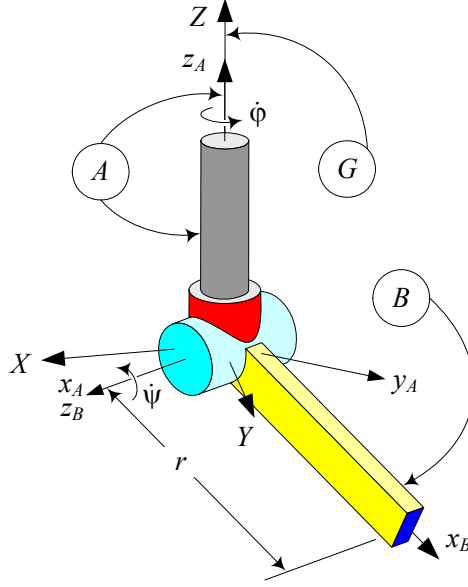
FIGURE 9.5. A two-link manipulator.

*and therefore,*

$$
\begin{aligned}
{}^{G}R_{B} &= {}^{G}R_{A}\ {}^{A}R_{B} \tag{9.113} \\
&= \begin{bmatrix} -\cos\varphi\cos\psi - \sin\varphi\sin\psi & \cos\varphi\sin\psi - \cos\psi\sin\varphi & 0 \\ \cos\varphi\sin\psi - \cos\psi\sin\varphi & \cos\varphi\cos\psi + \sin\varphi\sin\psi & 0 \\ 0 & 0 & -1 \end{bmatrix}.
\end{aligned}
$$

*The angular velocity of $A$ in $G$, and $B$ in $A$ are*

$$
{}_{G}\boldsymbol{\omega}_{A} = \dot{\varphi}\hat{K} \tag{9.114}
$$

$$
{}_{A}\boldsymbol{\omega}_{B} = \dot{\psi}\hat{\imath}_{A}. \tag{9.115}
$$

*Moment of inertia matrices for the arms $A$ and $B$ can be defined as*

$$
{}^{A}I_{A} = \begin{bmatrix} I_{A1} & 0 & 0 \\ 0 & I_{A2} & 0 \\ 0 & 0 & I_{A3} \end{bmatrix} \tag{9.116}
$$

$$
{}^{B}I_{B} = \begin{bmatrix} I_{B1} & 0 & 0 \\ 0 & I_{B2} & 0 \\ 0 & 0 & I_{B3} \end{bmatrix}. \tag{9.117}
$$

*These moments of inertia must be transformed to the global frame*

$$
{}^{G}I_{A} = {}^{G}R_{B}\ {}^{A}I_{A}\ {}^{G}R_{A}^{T} \tag{9.118}
$$

$$
{}^{G}I_{B} = {}^{G}R_{B}\ {}^{B}I_{B}\ {}^{G}R_{B}^{T}. \tag{9.119}
$$

*The total angular momentum of the manipulator is*

$$^{G}\mathbf{L} = {}^{G}\mathbf{L}_A + {}^{G}\mathbf{L}_B \tag{9.120}$$

*where*

$$
\begin{aligned}
^{G}\mathbf{L}_A &= {}^{G}I_{A\ G}\boldsymbol{\omega}_A & (9.121)\\
^{G}\mathbf{L}_B &= {}^{G}I_{B\ G}\boldsymbol{\omega}_B \\
&= {}^{G}I_B \left( {}^{G}_{A}\boldsymbol{\omega}_B + {}_{G}\boldsymbol{\omega}_A \right). & (9.122)
\end{aligned}
$$

**Example 352** *Poinsot's construction.*

*Consider a freely rotating rigid body with an attached principal coordinate frame. Having* $\mathbf{M} = 0$ *provides a motion under constant angular momentum and constant kinetic energy*

$$
\begin{aligned}
\mathbf{L} &= I\,\boldsymbol{\omega} = cte & (9.123)\\
K &= \frac{1}{2}\boldsymbol{\omega}^T I\,\boldsymbol{\omega} = cte. & (9.124)
\end{aligned}
$$

*Because the length of the angular momentum* $\mathbf{L}$ *is constant, the equation*

$$
\begin{aligned}
L^2 &= \mathbf{L} \cdot \mathbf{L} \\
&= L_x^2 + L_y^2 + L_z^2 \\
&= I_1^2\omega_1^2 + I_2^2\omega_2^2 + I_3^2\omega_3^2 & (9.125)
\end{aligned}
$$

*introduces an ellipsoid in the* $(\omega_1, \omega_2, \omega_3)$ *coordinate frame, called the* **momentum ellipsoid***. The tip of all possible angular velocity vectors must lie on the surface of the momentum ellipsoid. The kinetic energy also defines an* **energy ellipsoid** *in the same coordinate frame so that the tip of the angular velocity vectors must also lie on its surface.*

$$K = \frac{1}{2}\left(I_1\omega_1^2 + I_2\omega_2^2 + I_3\omega_3^2\right) \tag{9.126}$$

*In other words, the dynamics of moment-free motion of a rigid body requires that the corresponding angular velocity* $\boldsymbol{\omega}(t)$ *satisfy both Equations (9.125) and (9.126) and therefore lie on the intersection of the momentum and energy ellipsoids.*

*For clarity, we may define the ellipsoids in the* $(L_x, L_y, L_z)$ *coordinate system as*

$$
\begin{aligned}
L_x^2 + L_y^2 + L_z^2 &= L^2 & (9.127)\\
\frac{L_x^2}{2I_1 K} + \frac{L_y^2}{2I_2 K} + \frac{L_z^2}{2I_3 K} &= 1. & (9.128)
\end{aligned}
$$

*Equation (9.127) is a sphere and Equation (9.128) defines an ellipsoid with* $\sqrt{2I_i K}$ *as semi-axes. To have a meaningful motion, these two shapes must intersect. The intersection may form a trajectory, as shown in Figure 9.6.*
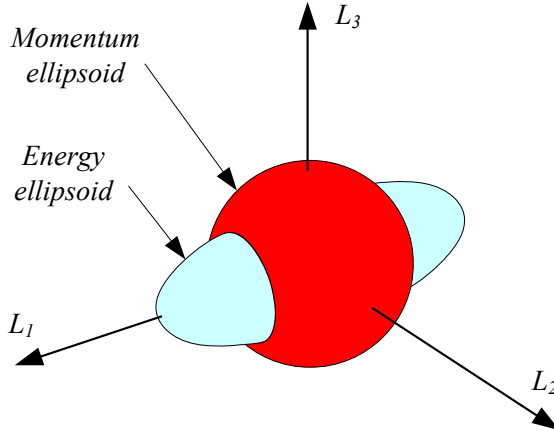
FIGURE 9.6. Intersection of the momentum and energy ellipsoids.

*It can be deduced that for a certain value of angular momentum there are maximum and minimum limit values for acceptable kinetic energy. Assuming*

$$I_1 > I_3 > I_3 \tag{9.129}$$

*the limits of possible kinetic energy are*

$$K_{\min} = \frac{L^2}{2I_1} \tag{9.130}$$

$$K_{\max} = \frac{L^2}{2I_3} \tag{9.131}$$

*and the corresponding motions are turning about the axes $I_1$ and $I_3$ respectively.*

**Example 353 ★** *Alternative derivation of Euler equations of motion.*
*Assume that the moment of the small force $d\mathbf{f}$ is shown by $d\mathbf{m}$ and a mass element is shown by $dm$, then,*

$$
\begin{aligned}
d\mathbf{m} &= {}^G\mathbf{r}_{dm} \times d\mathbf{f} \\
&= {}^G\mathbf{r}_{dm} \times {}^G\dot{\mathbf{v}}_{dm}\, dm.
\end{aligned} \tag{9.132}
$$

*The global angular momentum $d\mathbf{l}$ of $dm$ is equal to*

$$d\mathbf{l} = {}^G\mathbf{r}_{dm} \times {}^G\mathbf{v}_{dm}\, dm \tag{9.133}$$

*and according to (9.12) we have*

$$d\mathbf{m} = \frac{{}^G d}{dt} d\mathbf{l} \tag{9.134}$$

$$
{}^G\mathbf{r}_{dm} \times d\mathbf{f} = \frac{{}^G d}{dt}\left({}^G\mathbf{r}_{dm} \times {}^G\mathbf{v}_{dm}\, dm\right). \tag{9.135}
$$

*Integrating over the body results in*

$$\int_B {}^G\mathbf{r}_{dm} \times d\mathbf{f} = \int_B \frac{{}^Gd}{dt} \left( {}^G\mathbf{r}_{dm} \times {}^G\mathbf{v}_{dm}\, dm \right)$$

$$= \frac{{}^Gd}{dt} \int_B \left( {}^G\mathbf{r}_{dm} \times {}^G\mathbf{v}_{dm}\, dm \right). \qquad (9.136)$$

*However, utilizing*

$$^G\mathbf{r}_{dm} = {}^G\mathbf{d}_B + {}^GR_B\, {}^B\mathbf{r}_{dm} \qquad (9.137)$$

*where ${}^G\mathbf{d}_B$ is the global position vector of the central body frame, can simplify the left-hand side of the integral to*

$$\int_B {}^G\mathbf{r}_{dm} \times d\mathbf{f} = \int_B \left( {}^G\mathbf{d}_B + {}^GR_B\, {}^B\mathbf{r}_{dm} \right) \times d\mathbf{f}$$

$$= \int_B {}^G\mathbf{d}_B \times d\mathbf{f} + \int_B {}^G_B\mathbf{r}_{dm} \times d\mathbf{f}$$

$$= {}^G\mathbf{d}_B \times {}^G\mathbf{F} + {}^G\mathbf{M}_C \qquad (9.138)$$

*where $\mathbf{M}_C$ is the resultant external moment about the body mass center $C$. The right-hand side of Equation (9.136) is*

$$\frac{{}^Gd}{dt} \int_B \left( {}^G\mathbf{r}_{dm} \times {}^G\mathbf{v}_{dm}\, dm \right)$$

$$= \frac{{}^Gd}{dt} \int_B \left( \left( {}^G\mathbf{d}_B + {}^GR_B\, {}^B\mathbf{r}_{dm} \right) \times {}^G\mathbf{v}_{dm}\, dm \right)$$

$$= \frac{{}^Gd}{dt} \int_B \left( {}^G\mathbf{d}_B \times {}^G\mathbf{v}_{dm} \right) dm + \frac{{}^Gd}{dt} \int_B \left( {}^G_B\mathbf{r}_{dm} \times {}^G\mathbf{v}_{dm} \right) dm$$

$$= \frac{{}^Gd}{dt} \left( {}^G\mathbf{d}_B \times \int_B {}^G\mathbf{v}_{dm}\, dm \right) + \frac{{}^Gd}{dt} \mathbf{L}_C$$

$$= {}^G\dot{\mathbf{d}}_B \times \int_B {}^G\mathbf{v}_{dm}\, dm + {}^G\mathbf{d}_B \times \int_B {}^G\dot{\mathbf{v}}_{dm}\, dm + \frac{d}{dt} \mathbf{L}_C. \qquad (9.139)$$

*We use $\mathbf{L}_C$ for angular momentum about the body mass center. Because the body frame is at the mass center, we have*

$$\int_B {}^G\mathbf{r}_{dm}\, dm = m\, {}^G\mathbf{d}_B = m\, {}^G\mathbf{r}_C \qquad (9.140)$$

$$\int_B {}^G\mathbf{v}_{dm}\, dm = m\, {}^G\dot{\mathbf{d}}_B = m\, {}^G\mathbf{v}_C \qquad (9.141)$$

$$\int_B {}^G\dot{\mathbf{v}}_{dm}\, dm = m\, {}^G\ddot{\mathbf{d}}_B = m\, {}^G\mathbf{a}_C \qquad (9.142)$$

*and therefore,*

$$\frac{{}^Gd}{dt} \int_B \left( {}^G\mathbf{r}_{dm} \times {}^G\mathbf{v}_{dm}\, dm \right) = {}^G\mathbf{d}_B \times {}^G\mathbf{F} + \frac{{}^Gd}{dt} {}^G\mathbf{L}_C. \qquad (9.143)$$

*Substituting (9.138) and (9.143) in (9.136) provides the Euler equation of motion in the global frame, indicating that the resultant of externally applied moments about $C$ is equal to the global derivative of angular momentum about $C$.*

$$^{G}\mathbf{M}_C = \frac{^{G}d}{dt}\,^{G}\mathbf{L}_C. \tag{9.144}$$

*The Euler equation in the body coordinate can be found by transforming (9.144)*

$$
\begin{aligned}
^{B}\mathbf{M}_C &= \; ^{G}R_B^T\,^{G}\mathbf{M}_C \\
&= \; ^{G}R_B^T\,\frac{^{G}d}{dt}\mathbf{L}_C \\
&= \; \frac{^{G}d}{dt}\,^{G}R_B^T\,\mathbf{L}_C \\
&= \; \frac{^{G}d}{dt}\,^{B}\mathbf{L}_C \\
&= \; ^{B}\dot{\mathbf{L}}_C + {}_{G}^{B}\boldsymbol{\omega}_B \times \,^{B}\mathbf{L}_C. \tag{9.145}
\end{aligned}
$$

## 9.4   Mass Moment of Inertia Matrix

In analyzing the motion of rigid bodies, two types of integrals arise that belong to the geometry of the body. The first type defines the center of mass and is important when the translation motion of the body is considered. The second is the *moment of inertia* that appears when the rotational motion of the body is considered. The moment of inertia is also called *centrifugal moments*, or *deviation moments*. Every rigid body has a $3 \times 3$ moment of inertia matrix $I$, which is denoted by

$$I = \begin{bmatrix} I_{xx} & I_{xy} & I_{xz} \\ I_{yx} & I_{yy} & I_{yz} \\ I_{zx} & I_{zy} & I_{zz} \end{bmatrix}. \tag{9.146}$$

The diagonal elements $I_{ij}$, $i = j$ are called *polar moments of inertia*

$$I_{xx} = I_x = \int_B \left(y^2 + z^2\right) dm \tag{9.147}$$

$$I_{yy} = I_y = \int_B \left(z^2 + x^2\right) dm \tag{9.148}$$

$$I_{zz} = I_z = \int_B \left(x^2 + y^2\right) dm \tag{9.149}$$

and the off-diagonal elements $I_{ij}$, $i \neq j$ are called *products of inertia*

$$I_{xy} = I_{yx} = -\int_B xy\, dm \tag{9.150}$$

$$I_{yz} = I_{zy} = -\int_B yz \, dm \qquad (9.151)$$

$$I_{zx} = I_{xz} = -\int_B zx \, dm. \qquad (9.152)$$

The elements of $I$ for a rigid body, made of discrete point masses, are defined in Equation (9.54).

The elements of $I$ are calculated about a body coordinate frame attached to the mass center $C$ of the body. Therefore, $I$ is a frame-dependent quantity and must be written like ${}^B I$ to show the frame it is computed in.

$$
\begin{aligned}
{}^B I &= \int_B \begin{bmatrix} y^2 + z^2 & -xy & -zx \\ -xy & z^2 + x^2 & -yz \\ -zx & -yz & x^2 + y^2 \end{bmatrix} dm & (9.153) \\
&= \int_B \left( r^2 \mathbf{I} - \mathbf{r}\,\mathbf{r}^T \right) dm & (9.154) \\
&= \int_B -\tilde{r}\,\tilde{r} \, dm. & (9.155)
\end{aligned}
$$

Moments of inertia can be transformed from a coordinate frame $B_1$ to another coordinate frame $B_2$, both installed at the mass center of the body, according to the rule of the *rotated-axes theorem*

$$^{B_2}I = {}^{B_2}R_{B_1} \; {}^{B_1}I \; {}^{B_2}R_{B_1}^T. \qquad (9.156)$$

Transformation of the moment of inertia from a central frame $B_1$ located at ${}^{B_2}\mathbf{r}_C$ to another frame $B_2$, which is parallel to $B_1$, is, according to the rule of *parallel-axes theorem,*

$$^{B_2}I = {}^{B_1}I + m\,\tilde{r}_C\,\tilde{r}_C^T. \qquad (9.157)$$

If the local coordinate frame $Oxyz$ is located such that the products of inertia vanish, the local coordinate frame is called the *principal coordinate frame* and the associated moments of inertia are called *principal moments of inertia*. Principal axes and principal moments of inertia can be found by solving the following equation for $I$:

$$
\begin{vmatrix} I_{xx} - I & I_{xy} & I_{xz} \\ I_{yx} & I_{yy} - I & I_{yz} \\ I_{zx} & I_{zy} & I_{zz} - I \end{vmatrix} = 0 \qquad (9.158)
$$

$$\det\left( [I_{ij}] - I\,[\delta_{ij}] \right) = 0. \qquad (9.159)$$

Since Equation (9.159) is a cubic equation in $I$, we obtain three eigenvalues

$$I_1 = I_x \qquad I_2 = I_y \qquad I_3 = I_z \qquad (9.160)$$
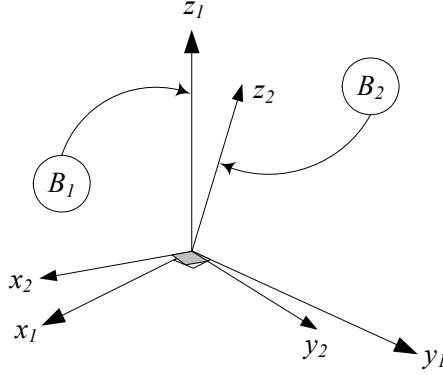
FIGURE 9.7. Two coordinate frames with a common origin at the mass center of a rigid body.

that are the principal moments of inertia.

**Proof.** Two coordinate frames with a common origin at the mass center of a rigid body are shown in Figure 9.7. The angular velocity and angular momentum of a rigid body transform from the frame $B_1$ to the frame $B_2$ by vector transformation rule

$$
\begin{align}
{}^{B_2}\boldsymbol{\omega} &= {}^{B_2}R_{B_1}\,{}^{B_1}\boldsymbol{\omega} \tag{9.161}\\
{}^{B_2}\mathbf{L} &= {}^{B_2}R_{B_1}\,{}^{B_1}\mathbf{L}. \tag{9.162}
\end{align}
$$

However, $\mathbf{L}$ and $\boldsymbol{\omega}$ are related according to Equation (9.52)

$$
{}^{B_1}\mathbf{L} = {}^{B_1}I\,{}^{B_1}\boldsymbol{\omega} \tag{9.163}
$$

and therefore,

$$
\begin{align}
{}^{B_2}\mathbf{L} &= {}^{B_2}R_{B_1}\,{}^{B_1}I\,{}^{B_2}R_{B_1}^T\,{}^{B_2}\boldsymbol{\omega} \\
&= {}^{B_2}I\,{}^{B_2}\boldsymbol{\omega} \tag{9.164}
\end{align}
$$

which shows how to transfer the moment of inertia from the coordinate frame $B_1$ to a rotated frame $B_2$

$$
{}^{B_2}I = {}^{B_2}R_{B_1}\,{}^{B_1}I\,{}^{B_2}R_{B_1}^T. \tag{9.165}
$$

Now consider a central frame $B_1$, shown in Figure 9.8, at ${}^{B_2}\mathbf{r}_C$, which rotates about the origin of a fixed frame $B_2$ such that their axes remain parallel. The angular velocity and angular momentum of the rigid body transform from frame $B_1$ to frame $B_2$ by

$$
\begin{align}
{}^{B_2}\boldsymbol{\omega} &= {}^{B_1}\boldsymbol{\omega} \tag{9.166}\\
{}^{B_2}\mathbf{L} &= {}^{B_1}\mathbf{L} + (\mathbf{r}_C \times m\mathbf{v}_C). \tag{9.167}
\end{align}
$$
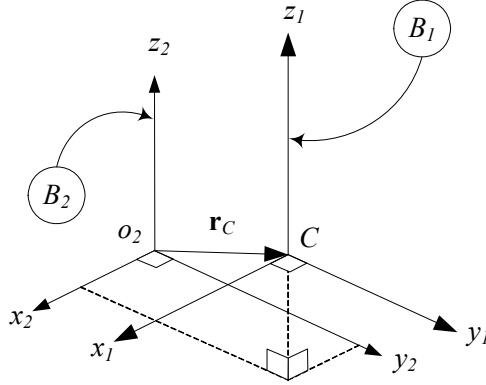
FIGURE 9.8. A central coordinate frame $B_1$ and a translated frame $B_2$.

Therefore,

$$
\begin{aligned}
{}^{B_2}\mathbf{L} &= {}^{B_1}\mathbf{L} + m\,{}^{B_2}\mathbf{r}_C \times \left({}^{B_2}\boldsymbol{\omega} \times {}^{B_2}\mathbf{r}_C\right) \\
&= {}^{B_1}\mathbf{L} + \left(m\,{}^{B_2}\tilde{r}_C\,{}^{B_2}\tilde{r}_C^T\right){}^{B_2}\boldsymbol{\omega} \\
&= \left({}^{B_1}I + m\,{}^{B_2}\tilde{r}_C\,{}^{B_2}\tilde{r}_C^T\right){}^{B_2}\boldsymbol{\omega}
\end{aligned}
\tag{9.168}
$$

which shows how to transfer the moment of inertia from frame $B_1$ to a parallel frame $B_2$

$$
{}^{B_2}I = {}^{B_1}I + m\,\tilde{r}_C\,\tilde{r}_C^T.
\tag{9.169}
$$

The parallel-axes theorem is also called the *Huygens-Steiner theorem*.

Referring to Equation (9.165) for transformation of the moment of inertia to a rotated frame, we can always find a frame in which ${}^{B_2}I$ is diagonal. In such a frame, we have

$$
{}^{B_2}R_{B_1}\,{}^{B_1}I = {}^{B_2}I\,{}^{B_2}R_{B_1}
\tag{9.170}
$$

or

$$
\begin{aligned}
&\begin{bmatrix} r_{11} & r_{12} & r_{13} \\ r_{21} & r_{22} & r_{23} \\ r_{31} & r_{32} & r_{33} \end{bmatrix}
\begin{bmatrix} I_{xx} & I_{xy} & I_{xz} \\ I_{yx} & I_{yy} & I_{yz} \\ I_{zx} & I_{zy} & I_{zz} \end{bmatrix} \\
&= \begin{bmatrix} I_1 & 0 & 0 \\ 0 & I_2 & 0 \\ 0 & 0 & I_3 \end{bmatrix}
\begin{bmatrix} r_{11} & r_{12} & r_{13} \\ r_{21} & r_{22} & r_{23} \\ r_{31} & r_{32} & r_{33} \end{bmatrix}
\end{aligned}
\tag{9.171}
$$

which shows that $I_1$, $I_2$, and $I_3$ are eigenvalues of ${}^{B_1}I$. These eigenvalues can be found by solving the following equation for $\lambda$:

$$
\begin{vmatrix} I_{xx} - \lambda & I_{xy} & I_{xz} \\ I_{yx} & I_{yy} - \lambda & I_{yz} \\ I_{zx} & I_{zy} & I_{zz} - \lambda \end{vmatrix} = 0.
\tag{9.172}
$$

The eigenvalues $I_1$, $I_2$, and $I_3$ are *principal moments of inertia,* and their associated eigenvectors are called *principal directions.* The coordinate frame made by the eigenvectors is the *principal body coordinate frame.* In the principal coordinate frame, the rigid body angular momentum is

$$\begin{bmatrix} L_1 \\ L_2 \\ L_3 \end{bmatrix} = \begin{bmatrix} I_1 & 0 & 0 \\ 0 & I_2 & 0 \\ 0 & 0 & I_3 \end{bmatrix} \begin{bmatrix} \omega_1 \\ \omega_2 \\ \omega_3 \end{bmatrix}. \tag{9.173}$$

■

**Example 354** *Principal moments of inertia.*
  *Consider the inertia matrix I*

$$I = \begin{bmatrix} 20 & -2 & 0 \\ -2 & 30 & 0 \\ 0 & 0 & 40 \end{bmatrix}. \tag{9.174}$$

*We set up the determinant (9.159)*

$$\begin{vmatrix} 20 - \lambda & -2 & 0 \\ -2 & 30 - \lambda & 0 \\ 0 & 0 & 40 - \lambda \end{vmatrix} = 0 \tag{9.175}$$

*which leads to the following characteristic equation.*

$$(20 - \lambda)(30 - \lambda)(40 - \lambda) - 4(40 - \lambda) = 0 \tag{9.176}$$

  *Three roots of Equation (9.176) are*

$$I_1 = 30.385, \qquad I_2 = 19.615, \qquad I_3 = 40 \tag{9.177}$$

*and therefore, the principal moment of inertia matrix is*

$$I = \begin{bmatrix} 30.385 & 0 & 0 \\ 0 & 19.615 & 0 \\ 0 & 0 & 40 \end{bmatrix}. \tag{9.178}$$

**Example 355** *Principal coordinate frame.*
  *Consider the inertia matrix I*

$$I = \begin{bmatrix} 20 & -2 & 0 \\ -2 & 30 & 0 \\ 0 & 0 & 40 \end{bmatrix} \tag{9.179}$$

*the direction of a principal axis $x_i$ is established by solving*

$$\begin{bmatrix} I_{xx} - I_i & I_{xy} & I_{xz} \\ I_{yx} & I_{yy} - I_i & I_{yz} \\ I_{zx} & I_{zy} & I_{zz} - I_i \end{bmatrix} \begin{bmatrix} \cos \alpha_i \\ \cos \beta_i \\ \cos \gamma_i \end{bmatrix} = \begin{bmatrix} 0 \\ 0 \\ 0 \end{bmatrix} \tag{9.180}$$

*for direction cosines, which must also satisfy*

$$\cos^2 \alpha_i + \cos^2 \beta_i + \cos^2 \gamma_i = 1. \tag{9.181}$$

*For the first principal moment of inertia $I_1 = 30.385$ we have*

$$\begin{bmatrix} 20 - 30.385 & -2 & 0 \\ -2 & 30 - 30.385 & 0 \\ 0 & 0 & 40 - 30.385 \end{bmatrix} \begin{bmatrix} \cos \alpha_1 \\ \cos \beta_1 \\ \cos \gamma_1 \end{bmatrix} = \begin{bmatrix} 0 \\ 0 \\ 0 \end{bmatrix} \tag{9.182}$$

*or*

$$\begin{array}{rcl} -10.385 \cos \alpha_1 - 2 \cos \beta_1 + 0 &=& 0 \\ -2 \cos \alpha_1 - 0.385 \cos \beta_1 + 0 &=& 0 \\ 0 + 0 + 9.615 \cos \gamma_1 &=& 0 \end{array} \qquad \begin{array}{c} (9.183) \\ (9.184) \\ (9.185) \end{array}$$

*and we obtain*

$$\begin{array}{rcl} \alpha_1 &=& 79.1 \deg \\ \beta_1 &=& 169.1 \deg \\ \gamma_1 &=& 90.0 \deg . \end{array} \qquad \begin{array}{c} (9.186) \\ (9.187) \\ (9.188) \end{array}$$

*Using $I_2 = 19.615$ for the second principal axis*

$$\begin{bmatrix} 20 - 19.62 & -2 & 0 \\ -2 & 30 - 19.62 & 0 \\ 0 & 0 & 40 - 19.62 \end{bmatrix} \begin{bmatrix} \cos \alpha_2 \\ \cos \beta_2 \\ \cos \gamma_2 \end{bmatrix} = \begin{bmatrix} 0 \\ 0 \\ 0 \end{bmatrix} \tag{9.189}$$

*we obtain*

$$\begin{array}{rcl} \alpha_2 &=& 10.9 \deg \\ \beta_2 &=& 79.1 \deg \\ \gamma_2 &=& 90.0 \deg . \end{array} \qquad \begin{array}{c} (9.190) \\ (9.191) \\ (9.192) \end{array}$$

*The third principal axis is for $I_3 = 40$*

$$\begin{bmatrix} 20 - 40 & -2 & 0 \\ -2 & 30 - 40 & 0 \\ 0 & 0 & 40 - 40 \end{bmatrix} \begin{bmatrix} \cos \alpha_3 \\ \cos \beta_3 \\ \cos \gamma_3 \end{bmatrix} = \begin{bmatrix} 0 \\ 0 \\ 0 \end{bmatrix} \tag{9.193}$$

*which leads to*

$$\begin{array}{rcl} \alpha_3 &=& 90.0 \deg \\ \beta_3 &=& 90.0 \deg \\ \gamma_3 &=& 0.0 \deg . \end{array} \qquad \begin{array}{c} (9.194) \\ (9.195) \\ (9.196) \end{array}$$
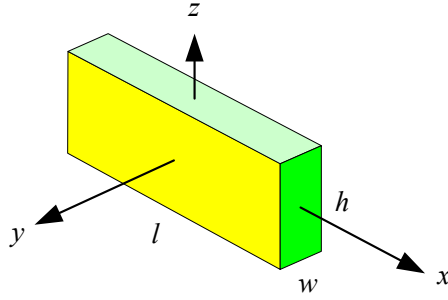
FIGURE 9.9. A homogeneous rectangular link.

**Example 356** *Moment of inertia of a rigid rectangular bar.*

*Consider a homogeneous rectangular link with mass m, length l, width w, and height h, as shown in Figure 9.9.*

*The local central coordinate frame is attached to the link at its mass center. The moments of inertia matrix of the link can be found by the integral method. We begin with calculating $I_{xx}$*

$$
\begin{aligned}
I_{xx} &= \int_B \left(y^2 + z^2\right) dm = \int_v \left(y^2 + z^2\right) \rho dv \\
&= \frac{m}{lwh} \int_v \left(y^2 + z^2\right) dv \\
&= \frac{m}{lwh} \int_{-h/2}^{h/2} \int_{-w/2}^{w/2} \int_{-l/2}^{l/2} \left(y^2 + z^2\right) dx\, dy\, dz \\
&= \frac{m}{12} \left(w^2 + h^2\right)
\end{aligned}
\tag{9.197}
$$

*which shows $I_{yy}$ and $I_{zz}$ can be calculated similarly*

$$
I_{yy} = \frac{m}{12} \left(h^2 + l^2\right) \tag{9.198}
$$

$$
I_{zz} = \frac{m}{12} \left(l^2 + w^2\right). \tag{9.199}
$$

*Since the coordinate frame is central, the products of inertia must be zero. To show this, we examine $I_{xy}$.*

$$
\begin{aligned}
I_{xy} &= I_{yx} = -\int_B xy\, dm = \int_v xy \rho dv \\
&= \frac{m}{lwh} \int_{-h/2}^{h/2} \int_{-w/2}^{w/2} \int_{-l/2}^{l/2} xy\, dx\, dy\, dz \\
&= 0
\end{aligned}
\tag{9.200}
$$
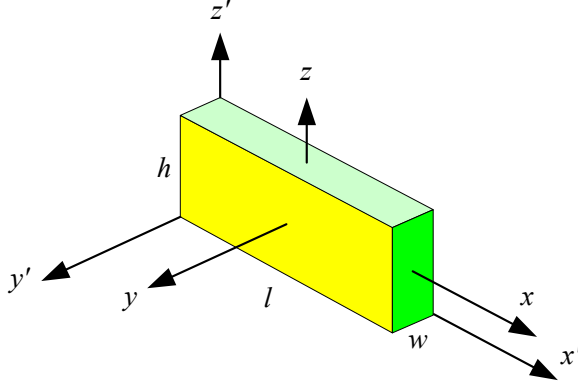
FIGURE 9.10. A rigid rectangular link in the principal and non principal frames.

*Therefore, the moment of inertia matrix for the rigid rectangular bar in its central frame is*

$$I = \begin{bmatrix} \frac{m}{12}\left(w^2 + h^2\right) & 0 & 0 \\ 0 & \frac{m}{12}\left(h^2 + l^2\right) & 0 \\ 0 & 0 & \frac{m}{12}\left(l^2 + w^2\right) \end{bmatrix}. \tag{9.201}$$

**Example 357** *Translation of the inertia matrix.*

*The moment of inertia matrix of the rigid body shown in Figure 9.10, in the principal frame $B(oxyz)$ is given in Equation (9.201). The moment of inertia matrix in the non-principal frame $B'(ox'y'z')$ can be found by applying the parallel-axes transformation formula (9.169).*

$$^{B'}I = \,^{B}I + m \,^{B'}\tilde{r}_C \,^{B'}\tilde{r}_C^T \tag{9.202}$$

*The mass center is at*

$$^{B'}\mathbf{r}_C = \frac{1}{2}\begin{bmatrix} l \\ w \\ h \end{bmatrix} \tag{9.203}$$

*and therefore,*

$$^{B'}\tilde{r}_C = \frac{1}{2}\begin{bmatrix} 0 & -h & w \\ h & 0 & -l \\ -w & l & 0 \end{bmatrix} \tag{9.204}$$

*that provides*

$$^{B'}I = \begin{bmatrix} \frac{1}{3}h^2m + \frac{1}{3}mw^2 & -\frac{1}{4}lmw & -\frac{1}{4}hlm \\ -\frac{1}{4}lmw & \frac{1}{3}h^2m + \frac{1}{3}l^2m & -\frac{1}{4}hmw \\ -\frac{1}{4}hlm & -\frac{1}{4}hmw & \frac{1}{3}l^2m + \frac{1}{3}mw^2 \end{bmatrix}. \tag{9.205}$$

**Example 358** *Principal rotation matrix.*
    *Consider a body inertia matrix as*

$$I = \begin{bmatrix} 2/3 & -1/2 & -1/2 \\ -1/2 & 5/3 & -1/4 \\ -1/2 & -1/4 & 5/3 \end{bmatrix}. \tag{9.206}$$

*The eigenvalues and eigenvectors of $I$ are*

$$I_1 = 0.2413 , \quad \begin{bmatrix} 2.351 \\ 1 \\ 1 \end{bmatrix} \tag{9.207}$$

$$I_2 = 1.8421 , \quad \begin{bmatrix} -0.851 \\ 1 \\ 1 \end{bmatrix} \tag{9.208}$$

$$I_3 = 1.9167 , \quad \begin{bmatrix} 0 \\ -1 \\ 1 \end{bmatrix}. \tag{9.209}$$

*The normalized eigenvector matrix $W$ is equal to the transpose of the required transformation matrix to make the inertia matrix diagonal*

$$W = \begin{bmatrix} | & | & | \\ \mathbf{w}_1 & \mathbf{w}_2 & \mathbf{w}_3 \\ | & | & | \end{bmatrix} = {}^2R_1^T$$

$$= \begin{bmatrix} 0.856\,9 & -0.515\,6 & 0.0 \\ 0.364\,48 & 0.605\,88 & -0.707\,11 \\ 0.364\,48 & 0.605\,88 & 0.707\,11 \end{bmatrix}. \tag{9.210}$$

*We may verify that*

$${}^2I \approx {}^2R_1 \, {}^1I \, {}^2R_1^T = W^T \, {}^1I \, W$$

$$= \begin{bmatrix} 0.2413 & -1 \times 10^{-4} & 0.0 \\ -1 \times 10^{-4} & 1.842\,1 & -1 \times 10^{-19} \\ 0.0 & 0.0 & 1.916\,7 \end{bmatrix}. \tag{9.211}$$

**Example 359** ★ *Relative diagonal moments of inertia.*
    *Using the definitions for moments of inertia (9.147), (9.148), and (9.149) it is seen that the inertia matrix is symmetric, and*

$$\int_B \left( x^2 + y^2 + z^2 \right) dm = \frac{1}{2} \left( I_{xx} + I_{yy} + I_{zz} \right) \tag{9.212}$$

*and also*

$$I_{xx} + I_{yy} \geq I_{zz} \tag{9.213}$$
$$I_{yy} + I_{zz} \geq I_{xx} \tag{9.214}$$
$$I_{zz} + I_{xx} \geq I_{yy}. \tag{9.215}$$

*Noting that*

$$(y - z)^2 \geq 0$$

*it is evident that*

$$\left(y^2 + z^2\right) \geq 2yz$$

*and therefore*

$$I_{xx} \geq 2I_{yz} \tag{9.216}$$

*and similarly*

$$I_{yy} \geq 2I_{zx} \tag{9.217}$$

$$I_{zz} \geq 2I_{xy}. \tag{9.218}$$

**Example 360 ★** *Coefficients of the characteristic equation.*
*The determinant (9.172)*

$$\begin{vmatrix} I_{xx} - \lambda & I_{xy} & I_{xz} \\ I_{yx} & I_{yy} - \lambda & I_{yz} \\ I_{zx} & I_{zy} & I_{zz} - \lambda \end{vmatrix} = 0 \tag{9.219}$$

*for calculating the principal moments of inertia, leads to a third-degree equation for λ, called the **characteristic equation**.*

$$\lambda^3 - a_1 \lambda^2 + a_2 \lambda - a_3 = 0 \tag{9.220}$$

*The coefficients of the characteristic equation are called the **principal invariants** of [I]. The coefficients of the characteristic equation can directly be found from the following equations:*

$$\begin{aligned} a_1 &= I_{xx} + I_{yy} + I_{zz} \\ &= \operatorname{tr}[I] \end{aligned} \tag{9.221}$$

$$\begin{aligned} a_2 &= I_{xx}I_{yy} + I_{yy}I_{zz} + I_{zz}I_{xx} - I_{xy}^2 - I_{yz}^2 - I_{zx}^2 \\ &= \begin{vmatrix} I_{xx} & I_{xy} \\ I_{yx} & I_{yy} \end{vmatrix} + \begin{vmatrix} I_{yy} & I_{yz} \\ I_{zy} & I_{zz} \end{vmatrix} + \begin{vmatrix} I_{xx} & I_{xz} \\ I_{zx} & I_{zz} \end{vmatrix} \\ &= \frac{1}{2}\left(a_1^2 - \operatorname{tr}\left[I^2\right]\right) \end{aligned} \tag{9.222}$$

$$\begin{aligned} a_3 &= I_{xx}I_{yy}I_{zz} + I_{xy}I_{yz}I_{zx} + I_{zy}I_{yx}I_{xz} \\ &\quad - \left(I_{xx}I_{yz}I_{zy} + I_{yy}I_{zx}I_{xz} + I_{zz}I_{xy}I_{yx}\right) \\ &= I_{xx}I_{yy}I_{zz} + 2I_{xy}I_{yz}I_{zx} - \left(I_{xx}I_{yz}^2 + I_{yy}I_{zx}^2 + I_{zz}I_{xy}^2\right) \\ &= \det[I] \end{aligned} \tag{9.223}$$

**Example 361** ★ *The principal moments of inertia are coordinate invariants.*

The roots of the inertia characteristic equation are the principal moments of inertia. They are all real but not necessarily different. The principal moments of inertia are extreme. That is, the principal moments of inertia determine the smallest and the largest values of $I_{ii}$. Since the smallest and largest values of $I_{ii}$ do not depend on the choice of the body coordinate frame, the solution of the characteristic equation is not dependent of the coordinate frame.

In other words, if $I_1$, $I_2$, and $I_3$ are the principal moments of inertia for $^{B_1}I$, the principal moments of inertia for $^{B_2}I$ are also $I_1$, $I_2$, and $I_3$ when

$$^{B_2}I = {}^{B_2}R_{B_1} \, {}^{B_1}I \, {}^{B_2}R_{B_1}^T.$$

We conclude that $I_1$, $I_2$, and $I_3$ are coordinate invariants of the matrix $[I]$, and therefore any quantity that depends on $I_1$, $I_2$, and $I_3$ is also coordinate invariant. The matrix $[I]$ has only three independent invariants and every other invariant can be expressed in terms of $I_1$, $I_2$, and $I_3$.

Since $I_1$, $I_2$, and $I_3$ are the solutions of the characteristic equation of $[I]$ given in (9.220), we may write the determinant (9.172) in the form

$$(\lambda - I_1)(\lambda - I_2)(\lambda - I_3) = 0. \tag{9.224}$$

The expanded form of this equation is

$$\lambda^3 - (I_1 + I_2 + I_3)\lambda^2 + (I_1 I_2 + I_2 I_3 + I_3 I_1) a_2 \lambda - I_1 I_2 I_3 = 0. \tag{9.225}$$

By comparing (9.225) and (9.220) we conclude that

$$
\begin{aligned}
a_1 &= I_{xx} + I_{yy} + I_{zz} = I_1 + I_2 + I_3 & (9.226)\\
a_2 &= I_{xx}I_{yy} + I_{yy}I_{zz} + I_{zz}I_{xx} - I_{xy}^2 - I_{yz}^2 - I_{zx}^2 \\
&= I_1 I_2 + I_2 I_3 + I_3 I_1 & (9.227)\\
a_3 &= I_{xx}I_{yy}I_{zz} + 2I_{xy}I_{yz}I_{zx} - \left(I_{xx}I_{yz}^2 + I_{yy}I_{zx}^2 + I_{zz}I_{xy}^2\right) \\
&= I_1 I_2 I_3. & (9.228)
\end{aligned}
$$

Being able to express the coefficients $a_1$, $a_2$, and $a_3$ as functions of $I_1$, $I_2$, and $I_3$ determines that the coefficients of the characteristic equation are coordinate-invariant.

**Example 362** ★ *Short notation for the elements of inertia matrix.*

Taking advantage of the Kronecker's delta (5.138) we may write the el-

ements of the moment of inertia matrix $I_{ij}$ in short notation forms

$$I_{ij} \quad = \quad \int_B \left( \left(x_1^2 + x_2^2 + x_3^2\right) \delta_{ij} - x_i x_j \right) dm \qquad (9.229)$$

$$I_{ij} \quad = \quad \int_B \left( r^2 \delta_{ij} - x_i x_j \right) dm \qquad (9.230)$$

$$I_{ij} \quad = \quad \int_B \left( \sum_{k=1}^{3} x_k x_k \delta_{ij} - x_i x_j \right) dm \qquad (9.231)$$

where we utilized the following notations:

$$x_1 = x \qquad x_2 = y \qquad x_3 = z. \qquad (9.232)$$

**Example 363 ★** *Moment of inertia with respect to a plane, a line, and a point.*

The moment of inertia of a system of particles may be defined with respect to a plane, a line, or a point as the sum of the products of the mass of the particles into the square of the perpendicular distance from the particle to the plane, line, or point. For a continuous body, the sum would be definite integral over the volume of the body.

The moments of inertia with respect to the $xy$, $yz$, and $zx$-plane are

$$I_{z^2} \quad = \quad \int_B z^2 dm \qquad (9.233)$$

$$I_{y^2} \quad = \quad \int_B y^2 dm \qquad (9.234)$$

$$I_{x^2} \quad = \quad \int_B x^2 dm. \qquad (9.235)$$

The moments of inertia with respect to the $x$, $y$, and $z$ axes are

$$I_x \quad = \quad \int_B \left( y^2 + z^2 \right) dm \qquad (9.236)$$

$$I_y \quad = \quad \int_B \left( z^2 + x^2 \right) dm \qquad (9.237)$$

$$I_z \quad = \quad \int_B \left( x^2 + y^2 \right) dm \qquad (9.238)$$

and therefore,

$$I_x \quad = \quad I_{y^2} + I_{z^2} \qquad (9.239)$$
$$I_y \quad = \quad I_{z^2} + I_{x^2} \qquad (9.240)$$
$$I_z \quad = \quad I_{x^2} + I_{y^2}. \qquad (9.241)$$

*The moment of inertia with respect to the origin is*

$$
\begin{aligned}
I_o &= \int_B \left(x^2 + y^2 + z^2\right) dm \\
&= I_{x^2} + I_{y^2} + I_{z^2} \\
&= \frac{1}{2}\left(I_x + I_y + I_z\right).
\end{aligned}
\tag{9.242}
$$

*Because the choice of the coordinate frame is arbitrary, we can say that the moment of inertia with respect to a line is the sum of the moments of inertia with respect to any two mutually orthogonal planes that pass through the line. The moment of inertia with respect to a point has similar meaning for three mutually orthogonal planes intersecting at the point.*

## 9.5  Lagrange's Form of Newton's Equations of Motion

Newton's equation of motion can be transformed to

$$
\frac{d}{dt}\left(\frac{\partial K}{\partial \dot{q}_r}\right) - \frac{\partial K}{\partial q_r} = F_r \qquad r = 1, 2, \cdots n
\tag{9.243}
$$

where

$$
F_r = \sum_{i=1}^{n}\left(F_{ix}\frac{\partial f_i}{\partial q_1} + F_{iy}\frac{\partial g_i}{\partial q_2} + F_{iz}\frac{\partial h_i}{\partial q_n}\right).
\tag{9.244}
$$

Equation (9.243) is called the *Lagrange equation of motion*, where $K$ is the kinetic energy of the $n$ degree-of-freedom $(DOF)$ system, $q_r, r = 1, 2, \cdots, n$ are the generalized coordinates of the system, $\mathbf{F} = \begin{bmatrix} F_{ix} & F_{iy} & F_{iz} \end{bmatrix}^T$ is the external force acting on the $i$th particle of the system, and $F_r$ is the generalized force associated to $q_r$.

**Proof.** Let $m_i$ be the mass of one of the particles of a system and let $(x_i, y_i, z_i)$ be its Cartesian coordinates in a globally fixed coordinate frame. Assume that the coordinates of every individual particle are functions of another set of coordinates $q_1, q_2, q_3, \cdots, q_n$, and possibly time $t$.

$$
\begin{aligned}
x_i &= f_i(q_1, q_2, q_3, \cdots, q_n, t) \tag{9.245} \\
y_i &= g_i(q_1, q_2, q_3, \cdots, q_n, t) \tag{9.246} \\
z_i &= h_i(q_1, q_2, q_3, \cdots, q_n, t) \tag{9.247}
\end{aligned}
$$

If $F_{xi}, F_{yi}, F_{zi}$ are components of the total force acting on the particle $m_i$, then the Newton equations of motion for the particle would be

$$
\begin{aligned}
F_{xi} &= m_i\ddot{x}_i \tag{9.248} \\
F_{yi} &= m_i\ddot{y}_i \tag{9.249} \\
F_{zi} &= m_i\ddot{z}_i. \tag{9.250}
\end{aligned}
$$

We multiply both sides of these equations by

$$\frac{\partial f_i}{\partial q_r}$$

$$\frac{\partial g_i}{\partial q_r}$$

$$\frac{\partial h_i}{\partial q_r}$$

respectively, and add them up for all the particles to have

$$\sum_{i=1}^{n} m_i \left( \ddot{x}_i \frac{\partial f_i}{\partial q_r} + \ddot{y}_i \frac{\partial g_i}{\partial q_r} + \ddot{z}_i \frac{\partial h_i}{\partial q_r} \right) = \sum_{i=1}^{n} \left( F_{xi} \frac{\partial f_i}{\partial q_r} + F_{yi} \frac{\partial g_i}{\partial q_r} + F_{zi} \frac{\partial h_i}{\partial q_r} \right)$$

(9.251)

where $n$ is the total number of particles.

Taking a time derivative of Equation (9.245),

$$\dot{x}_i = \frac{\partial f_i}{\partial q_1} \dot{q}_1 + \frac{\partial f_i}{\partial q_2} \dot{q}_2 + \frac{\partial f_i}{\partial q_3} \dot{q}_3 + \cdots + \frac{\partial f_i}{\partial q_n} \dot{q}_n + \frac{\partial f_i}{\partial t}$$

(9.252)

we find

$$\frac{\partial \dot{x}_i}{\partial \dot{q}_r} = \frac{\partial}{\partial \dot{q}_r} \left( \frac{\partial f_i}{\partial q_1} \dot{q}_1 + \frac{\partial f_i}{\partial q_2} \dot{q}_2 + \cdots + \frac{\partial f_i}{\partial q_n} \dot{q}_n + \frac{\partial f_i}{\partial t} \right)$$

$$= \frac{\partial f_i}{\partial q_r}.$$

(9.253)

and therefore,

$$\ddot{x}_i \frac{\partial f_i}{\partial q_r} = \ddot{x}_i \frac{\partial \dot{x}_i}{\partial \dot{q}_r}$$

$$= \frac{d}{dt} \left( \dot{x}_i \frac{\partial \dot{x}_i}{\partial \dot{q}_r} \right) - \dot{x}_i \frac{d}{dt} \left( \frac{\partial \dot{x}_i}{\partial \dot{q}_r} \right).$$

(9.254)

However,

$$\dot{x}_i \frac{d}{dt} \left( \frac{\partial \dot{x}_i}{\partial \dot{q}_r} \right) = \dot{x}_i \frac{d}{dt} \left( \frac{\partial f_i}{\partial q_r} \right)$$

$$= \dot{x}_i \left( \frac{\partial^2 f_i}{\partial q_1 \partial q_r} \dot{q}_1 + \cdots + \frac{\partial^2 f_i}{\partial q_n \partial q_r} \dot{q}_n + \frac{\partial^2 f_i}{\partial t \partial q_r} \right)$$

$$= \dot{x}_i \frac{\partial}{\partial q_r} \left( \frac{\partial f_i}{\partial q_1} \dot{q}_1 + \frac{\partial f_i}{\partial q_2} \dot{q}_2 + \cdots + \frac{\partial f_i}{\partial q_n} \dot{q}_n + \frac{\partial f_i}{\partial t} \right)$$

$$= \dot{x}_i \frac{\partial \dot{x}_i}{\partial q_r}$$

(9.255)

and we have

$$\ddot{x}_i \frac{\partial \dot{x}_i}{\partial \dot{q}_r} = \frac{d}{dt} \left( \dot{x}_i \frac{\partial \dot{x}_i}{\partial \dot{q}_r} \right) - \dot{x}_i \frac{\partial \dot{x}_i}{\partial q_r}$$

(9.256)

which is equal to

$$\ddot{x}_i \frac{\dot{x}_i}{\dot{q}_r} = \frac{d}{dt}\left[\frac{\partial}{\partial \dot{q}_r}\left(\frac{1}{2}\dot{x}_i^2\right)\right] - \frac{\partial}{\partial q_r}\left(\frac{1}{2}\dot{x}_i^2\right). \tag{9.257}$$

Now substituting (9.254) and (9.257) in the left-hand side of (9.251) leads to

$$\sum_{i=1}^{n} m_i \left(\ddot{x}_i \frac{\partial f_i}{\partial q_r} + \ddot{y}_i \frac{\partial g_i}{\partial q_r} + \ddot{z}_i \frac{\partial h_i}{\partial q_r}\right)$$

$$= \sum_{i=1}^{n} m_i \frac{d}{dt}\left[\frac{\partial}{\partial \dot{q}_r}\left(\frac{1}{2}\dot{x}_i^2 + \frac{1}{2}\dot{y}_i^2 + \frac{1}{2}\dot{z}_i^2\right)\right]$$

$$-\sum_{i=1}^{n} m_i \frac{\partial}{\partial q_r}\left(\frac{1}{2}\dot{x}_i^2 + \frac{1}{2}\dot{y}_i^2 + \frac{1}{2}\dot{z}_i^2\right)$$

$$= \frac{1}{2}\sum_{i=1}^{n} m_i \frac{d}{dt}\left[\frac{\partial}{\partial \dot{q}_r}\left(\dot{x}_i^2 + \dot{y}_i^2 + \dot{z}_i^2\right)\right]$$

$$-\frac{1}{2}\sum_{i=1}^{n} m_i \frac{\partial}{\partial q_r}\left(\dot{x}_i^2 + \dot{y}_i^2 + \dot{z}_i^2\right). \tag{9.258}$$

where

$$\frac{1}{2}\sum_{i=1}^{n} m_i \left(\dot{x}_i^2 + \dot{y}_i^2 + \dot{z}_i^2\right) = K \tag{9.259}$$

is the *kinetic energy* of the system. Therefore, the Newton equations of motion (9.248), (9.249), and (9.250) are converted to

$$\frac{d}{dt}\left(\frac{\partial K}{\partial \dot{q}_r}\right) - \frac{\partial K}{\partial q_r} = \sum_{i=1}^{n}\left(F_{xi}\frac{\partial f_i}{\partial q_r} + F_{yi}\frac{\partial g_i}{\partial q_r} + F_{zi}\frac{\partial h_i}{\partial q_r}\right). \tag{9.260}$$

Because of (9.245), (9.246), and (9.247), the kinetic energy is a function of $q_1, q_2, q_3, \cdots, q_n$ and time $t$. The left-hand side of Equation (9.260) includes the kinetic energy of the whole system and the right-hand side is a generalized force and shows the effect of changing coordinates from $x_i$ to $q_j$ on the external forces. Let us assume that the coordinate $q_r$ alters to $q_r + \delta q_r$ while the other coordinates $q_1, q_2, q_3, \cdots, q_{r-1}, q_{r+1}, \cdots, q_n$ and time $t$ are unaltered. So, the coordinates of $m_i$ are changed to

$$x_i + \frac{\partial f_i}{\partial q_r}\delta q_r \tag{9.261}$$

$$y_i + \frac{\partial g_i}{\partial q_r}\delta q_r \tag{9.262}$$

$$z_i + \frac{\partial h_i}{\partial q_r}\delta q_r \tag{9.263}$$

Such a displacement is called virtual displacement. The work done in this virtual displacement by all forces acting on the particles of the system is

$$\delta W = \sum_{i=1}^{n} \left( F_{xi}\frac{\partial f_i}{\partial q_r} + F_{yi}\frac{\partial g_i}{\partial q_r} + F_{zi}\frac{\partial h_i}{\partial q_r} \right) \delta q_r. \qquad (9.264)$$

Because the work done by internal forces appears in opposite pairs, only the work done by external forces remains in Equation (9.264). Let's denote the virtual work by

$$\delta W = F_r \left( q_1, q_2, q_3, \cdots, q_n, t \right) \delta q_r. \qquad (9.265)$$

Then we have

$$\frac{d}{dt}\left( \frac{\partial K}{\partial \dot{q}_r} \right) - \frac{\partial K}{\partial q_r} = F_r \qquad (9.266)$$

where

$$F_r = \sum_{i=1}^{n} \left( F_{xi}\frac{\partial f_i}{\partial q_r} + F_{yi}\frac{\partial g_i}{\partial q_r} + F_{zi}\frac{\partial h_i}{\partial q_r} \right). \qquad (9.267)$$

Equation (9.266) is the Lagrange form of equations of motion. This equation is true for all values of $r$ from 1 to $n$. We thus have $n$ second-order ordinary differential equations in which $q_1$, $q_2$, $q_3$, $\cdots$, $q_n$ are the dependent variables and $t$ is the independent variable. The coordinates $q_1, q_2, q_3, \cdots, q_n$ are called *generalized coordinates* and can be any measurable parameters to provide the configuration of the system. The number of equations and the number of dependent variables are equal, therefore, the equations are theoretically sufficient to determine the motion of all $m_i$. ∎

**Example 364** *Equation of motion for a simple pendulum.*
*A pendulum is shown in Figure 9.11. Using $x$ and $y$ for the Cartesian position of $m$, and using $\theta = q$ as the generalized coordinate, we have*

$$x = f(\theta) = l \sin\theta \qquad (9.268)$$
$$y = g(\theta) = l \cos\theta \qquad (9.269)$$
$$K = \frac{1}{2}m\left( \dot{x}^2 + \dot{y}^2 \right) = \frac{1}{2}ml^2\dot{\theta}^2 \qquad (9.270)$$

*and therefore,*

$$\frac{d}{dt}\left( \frac{\partial K}{\partial \dot{\theta}} \right) - \frac{\partial K}{\partial \theta} = \frac{d}{dt}(ml^2\dot{\theta}) = ml^2\ddot{\theta}. \qquad (9.271)$$

*The external force components, acting on $m$, are*

$$F_x = 0 \qquad (9.272)$$
$$F_y = mg \qquad (9.273)$$
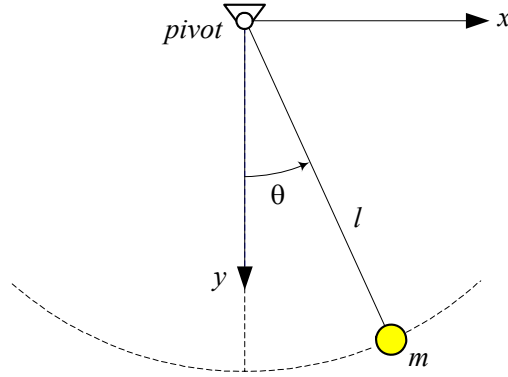
FIGURE 9.11. A simple pendulum.

*and therefore,*

$$F_\theta = F_x \frac{\partial f}{\partial \theta} + F_y \frac{\partial g}{\partial \theta} = -mgl \sin \theta. \qquad (9.274)$$

*Hence, the equation of motion for the pendulum is*

$$ml^2 \ddot{\theta} = -mgl \sin \theta. \qquad (9.275)$$

**Example 365** *A pendulum attached to an oscillating mass.*

*Figure 9.12 illustrates a vibrating mass with a hanging pendulum. The pendulum can act as a vibration absorber if designed properly.*

*Starting with coordinate relationships*

$$
\begin{array}{rcll}
x_M &=& f_M = x & (9.276) \\
y_M &=& g_M = 0 & (9.277) \\
x_m &=& f_m = x + l \sin \theta & (9.278) \\
y_m &=& g_m = l \cos \theta & (9.279)
\end{array}
$$

*we may find the kinetic energy in terms of the generalized coordinates $x$ and $\theta$.*

$$
\begin{aligned}
K &= \frac{1}{2} M \left( \dot{x}_M^2 + \dot{y}_M^2 \right) + \frac{1}{2} m \left( \dot{x}_m^2 + \dot{y}_m^2 \right) \\
&= \frac{1}{2} M \dot{x}^2 + \frac{1}{2} m \left( \dot{x}^2 + l^2 \dot{\theta}^2 + 2 l \dot{x} \dot{\theta} \cos \theta \right) \qquad (9.280)
\end{aligned}
$$

*Then, the left-hand side of the Lagrange equations are*

$$\frac{d}{dt} \left( \frac{\partial K}{\partial \dot{x}} \right) - \frac{\partial K}{\partial x} = (M + m) \ddot{x} + ml \ddot{\theta} \cos \theta - ml \dot{\theta}^2 \sin \theta \qquad (9.281)$$

$$\frac{d}{dt} \left( \frac{\partial K}{\partial \dot{\theta}} \right) - \frac{\partial K}{\partial \theta} = ml^2 \ddot{\theta} + ml \ddot{x} \cos \theta. \qquad (9.282)$$
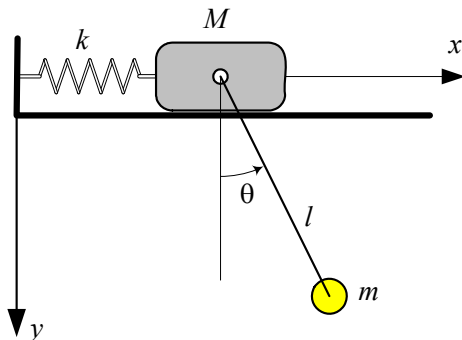
FIGURE 9.12. A vibrating mass with a hanging pendulum.

The external forces acting on $M$ and $m$ are

$$F_{x_M} = -kx \qquad (9.283)$$
$$F_{y_M} = 0 \qquad (9.284)$$
$$F_{x_m} = 0 \qquad (9.285)$$
$$F_{y_m} = mg. \qquad (9.286)$$

Therefore, the generalized forces are

$$
\begin{aligned}
F_x &= F_{x_M}\frac{\partial f_M}{\partial x} + F_{y_M}\frac{\partial g_M}{\partial x} + F_{x_m}\frac{\partial f_m}{\partial x} + F_{y_m}\frac{\partial g_m}{\partial x} \\
&= -kx \qquad (9.287)
\end{aligned}
$$

$$
\begin{aligned}
F_\theta &= F_{x_M}\frac{\partial f_M}{\partial \theta} + F_{y_M}\frac{\partial g_M}{\partial \theta} + F_{x_m}\frac{\partial f_m}{\partial \theta} + F_{y_m}\frac{\partial g_m}{\partial \theta} \\
&= -mgl\sin\theta \qquad (9.288)
\end{aligned}
$$

and finally the Lagrange equations of motion are

$$(M+m)\ddot{x} + ml\ddot{\theta}\cos\theta - ml\dot{\theta}^2\sin\theta = -kx \qquad (9.289)$$
$$ml^2\ddot{\theta} + ml\ddot{x}\cos\theta = -mgl\sin\theta. \qquad (9.290)$$

**Example 366** *Kinetic energy of the Earth.*
    *Earth is approximately a rotating rigid body about a fixed axis. The two motions of the Earth are called **revolution** about the sun, and **rotation** about an axis approximately fixed in the Earth. The kinetic energy of the Earth due to its rotation is*

$$
\begin{aligned}
K_1 &= \frac{1}{2}I\omega_1^2 \\
&= \frac{1}{2}\frac{2}{5}\left(5.9742\times 10^{24}\right)\left(\frac{6356912 + 6378388}{2}\right)^2 \left(\frac{2\pi}{24\times 3600}\frac{366.25}{365.25}\right)^2 \\
&= 2.5762\times 10^{29}\ \text{J}
\end{aligned}
$$

and the kinetic energy of the Earth due to its revolution is

$$
\begin{aligned}
K_2 &= \frac{1}{2} M r^2 \omega_2^2 \\
&= \frac{1}{2} \left(5.9742 \times 10^{24}\right) \left(1.49475 \times 10^{11}\right)^2 \left(\frac{2\pi}{24 \times 3600} \frac{1}{365.25}\right)^2 \\
&= 2.6457 \times 10^{33} \text{ J}
\end{aligned}
$$

where $r$ is the distance from the sun and $\omega_2$ is the angular speed about the sun. The total kinetic energy of the Earth is $K = K_1 + K_2$. However, the ratio of the revolutionary to rotational kinetic energies is

$$
\frac{K_2}{K_1} = \frac{2.6457 \times 10^{33}}{2.5762 \times 10^{29}} \approx 10000.
$$

**Example 367 ★** *Explicit form of Lagrange equations.*
   Assume the coordinates of every particle are functions of the coordinates $q_1, q_2, q_3, \cdots, q_n$ but not the time $t$. The kinetic energy of the system made of $n$ massive particles can be written as

$$
\begin{aligned}
K &= \frac{1}{2} \sum_{i=1}^{n} m_i \left(\dot{x}_i^2 + \dot{y}_i^2 + \dot{z}_i^2\right) \\
&= \frac{1}{2} \sum_{j=1}^{n} \sum_{k=1}^{n} a_{jk} \dot{q}_j \dot{q}_k
\end{aligned} \tag{9.291}
$$

where the coefficients $a_{jk}$ are functions of $q_1, q_2, q_3, \cdots, q_n$ and

$$
a_{jk} = a_{kj}. \tag{9.292}
$$

The Lagrange equations of motion

$$
\frac{d}{dt}\left(\frac{\partial K}{\partial \dot{q}_r}\right) - \frac{\partial K}{\partial q_r} = F_r \qquad r = 1, 2, \cdots n \tag{9.293}
$$

are then equal to

$$
\frac{d}{dt} \sum_{m=1}^{n} a_{mr} \dot{q}_m - \frac{1}{2} \sum_{j=1}^{n} \sum_{k=1}^{n} \frac{a_{jk}}{\partial q_r} \dot{q}_j \dot{q}_k = F_r \tag{9.294}
$$

or

$$
\sum_{m=1}^{n} a_{mr} \ddot{q}_m + \sum_{k=1}^{n} \sum_{n=1}^{n} \Gamma_{k,n}^{r} \dot{q}_k \dot{q}_n = F_r \tag{9.295}
$$

where $\Gamma_{j,k}^{i}$ is called the **Christoffel operator**

$$
\Gamma_{j,k}^{i} = \frac{1}{2}\left(\frac{\partial a_{ij}}{\partial q_k} + \frac{\partial a_{ik}}{\partial q_j} - \frac{\partial a_{kj}}{\partial q_i}\right). \tag{9.296}
$$

## 9.6  Lagrangian Mechanics

Assume for some forces $\mathbf{F} = \begin{bmatrix} F_{ix} & F_{iy} & F_{iz} \end{bmatrix}^T$ there is a function $V$, called *potential energy*, such that the force is derivable from $V$

$$\mathbf{F} = -\nabla V. \tag{9.297}$$

Such a force is called *potential* or *conservative force*. Then, the Lagrange equation of motion can be written as

$$\frac{d}{dt}\left(\frac{\partial \mathcal{L}}{\partial \dot{q}_r}\right) - \frac{\partial \mathcal{L}}{\partial q_r} = Q_r \qquad r = 1, 2, \cdots n \tag{9.298}$$

where

$$\mathcal{L} = K - V \tag{9.299}$$

is the *Lagrangean* of the system and $Q_r$ is the nonpotential generalized force.

**Proof.** Assume the external forces $\mathbf{F} = \begin{bmatrix} F_{xi} & F_{yi} & F_{zi} \end{bmatrix}^T$ acting on the system are conservative.

$$\mathbf{F} = -\nabla V \tag{9.300}$$

The work done by these forces in an arbitrary virtual displacement $\delta q_1$, $\delta q_2$, $\delta q_3$, $\cdots$, $\delta q_n$ is

$$\partial W = -\frac{\partial V}{\partial q_1}\delta q_1 - \frac{\partial V}{\partial q_2}\delta q_2 - \cdots \frac{\partial V}{\partial q_n}\delta q_n \tag{9.301}$$

then the Lagrange equation becomes

$$\frac{d}{dt}\left(\frac{\partial K}{\partial \dot{q}_r}\right) - \frac{\partial K}{\partial q_r} = -\frac{\partial V}{\partial q_1} \qquad r = 1, 2, \cdots n. \tag{9.302}$$

Introducing the Lagrangean function $\mathcal{L} = K - V$ converts the Lagrange equation to

$$\frac{d}{dt}\left(\frac{\partial \mathcal{L}}{\partial \dot{q}_r}\right) - \frac{\partial \mathcal{L}}{\partial q_r} = 0 \qquad r = 1, 2, \cdots n \tag{9.303}$$

for a conservative system. The Lagrangean is also called *kinetic potential*.

If a force is not conservative, then the virtual work done by the force is

$$
\begin{aligned}
\delta W &= \sum_{i=1}^{n}\left(F_{xi}\frac{\partial f_i}{\partial q_r} + F_{yi}\frac{\partial g_i}{\partial q_r} + F_{zi}\frac{\partial h_i}{\partial q_r}\right)\delta q_r \\
&= Q_r\,\delta q_r
\end{aligned}
\tag{9.304}
$$

and the equation of motion would be

$$\frac{d}{dt}\left(\frac{\partial \mathcal{L}}{\partial \dot{q}_r}\right) - \frac{\partial \mathcal{L}}{\partial q_r} = Q_r \qquad r = 1, 2, \cdots n \tag{9.305}$$

where $Q_r$ is the nonpotential generalized force doing work in a virtual displacement of the $r$th generalized coordinate $q_r$. ∎
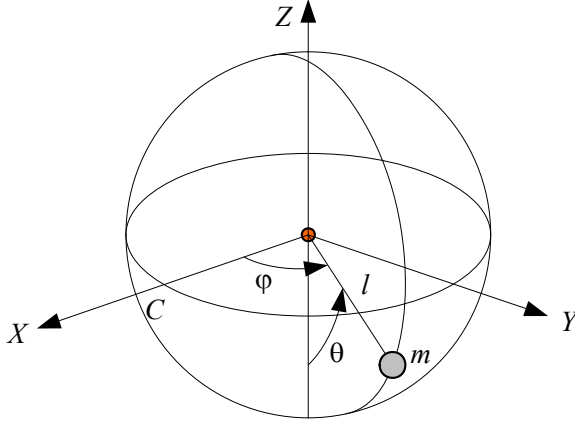
FIGURE 9.13. A spherical pendulum.

**Example 368** *Spherical pendulum.*

A pendulum analogy is utilized in modeling of many dynamical problems. Figure 9.13 illustrates a spherical pendulum with mass $m$ and length $l$. The angles $\varphi$ and $\theta$ may be used as describing coordinates of the system.

The Cartesian coordinates of the mass as a function of the generalized coordinates are

$$\begin{bmatrix} X \\ Y \\ Z \end{bmatrix} = \begin{bmatrix} r\cos\varphi\sin\theta \\ r\sin\theta\sin\varphi \\ -r\cos\theta \end{bmatrix} \tag{9.306}$$

and therefore, the kinetic and potential energies of the pendulum are

$$K = \frac{1}{2}m\left(l^2\dot\theta^2 + l^2\dot\varphi^2\sin^2\theta\right) \tag{9.307}$$

$$V = -mgl\cos\theta. \tag{9.308}$$

The kinetic potential function of this system is then equal to

$$\mathcal{L} = \frac{1}{2}m\left(l^2\dot\theta^2 + l^2\dot\varphi^2\sin^2\theta\right) + mgl\cos\theta \tag{9.309}$$

which leads to the following equations of motion:

$$\ddot\theta - \dot\varphi^2\sin\theta\cos\theta + \frac{g}{l}\sin\theta = 0 \tag{9.310}$$

$$\ddot\varphi\sin^2\theta + 2\dot\varphi\dot\theta\sin\theta\cos\theta = 0. \tag{9.311}$$

**Example 369** *Controlled compound pendulum.*

A massive arm is attached to a ceiling at a pin joint $O$ as illustrated in Figure 9.14. Assume that there is viscous friction in the joint where an ideal motor can apply a torque $Q$ to move the arm. The rotor of an ideal motor has no moment of inertia by assumption.
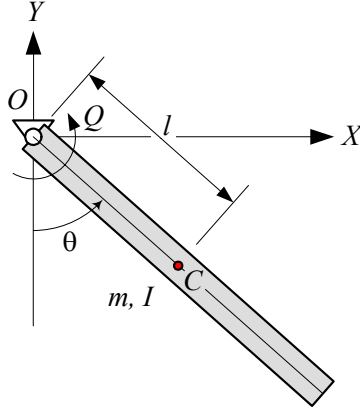
FIGURE 9.14. A controlled compound pendulum.

*The kinetic and potential energies of the manipulator are*

$$K = \frac{1}{2}I\dot\theta^2$$

$$= \frac{1}{2}\left(I_C + ml^2\right)\dot\theta^2 \tag{9.312}$$

$$V = -mg\cos\theta \tag{9.313}$$

*where $m$ is the mass and $I$ is the moment of inertia of the pendulum about $O$. The Lagrangean of the manipulator is*

$$\mathcal{L} = K - V$$

$$= \frac{1}{2}I\dot\theta^2 + mg\cos\theta \tag{9.314}$$

*and therefore, the equation of motion of the pendulum is*

$$M = \frac{d}{dt}\left(\frac{\partial\mathcal{L}}{\partial\dot\theta}\right) - \frac{\partial\mathcal{L}}{\partial\theta}$$

$$= I\ddot\theta + mgl\sin\theta. \tag{9.315}$$

*The generalized force $M$ is the contribution of the motor torque $Q$ and the viscous friction torque $-c\dot\theta$. Hence, the equation of motion of the manipulator is*

$$Q = I\ddot\theta + c\dot\theta + mgl\sin\theta. \tag{9.316}$$

**Example 370** *An ideal 2R planar manipulator dynamics.*

*An ideal model of a 2R planar manipulator is illustrated in Figure 9.15. It is called ideal because we assume the links are massless and there is no friction. The masses $m_1$ and $m_2$ are the mass of the second motor to run*
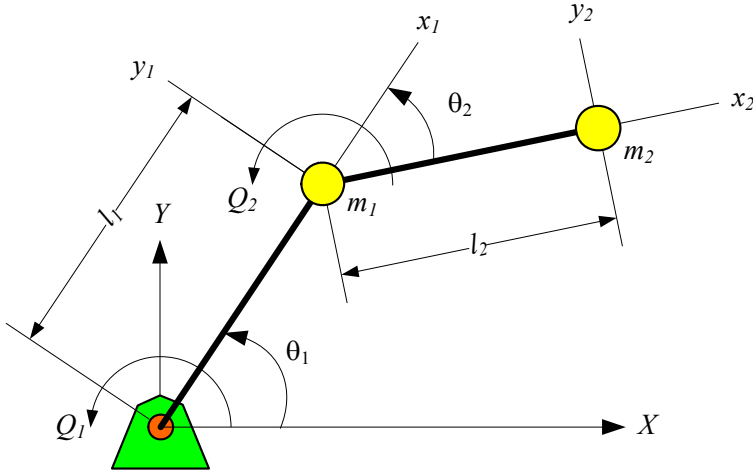
FIGURE 9.15. A model for a 2R planar manipulator.

the second link and the load at the endpoint. We take the absolute angle $\theta_1$ and the relative angle $\theta_2$ as the generalized coordinates to express the configuration of the manipulator.

The global positions of $m_1$ and $m_2$ are

$$
\begin{bmatrix} X_1 \\ Y_2 \end{bmatrix} = \begin{bmatrix} l_1 \cos \theta_1 \\ l_1 \sin \theta_1 \end{bmatrix} \tag{9.317}
$$

$$
\begin{bmatrix} X_2 \\ Y_2 \end{bmatrix} = \begin{bmatrix} l_1 \cos \theta_1 + l_2 \cos (\theta_1 + \theta_2) \\ l_1 \sin \theta_1 + l_2 \sin (\theta_1 + \theta_2) \end{bmatrix} \tag{9.318}
$$

and therefore, the global velocity of the masses are

$$
\begin{bmatrix} \dot{X}_1 \\ \dot{Y}_1 \end{bmatrix} = \begin{bmatrix} -l_1 \dot{\theta}_1 \sin \theta_1 \\ l_1 \dot{\theta}_1 \cos \theta_1 \end{bmatrix} \tag{9.319}
$$

$$
\begin{bmatrix} \dot{X}_2 \\ \dot{Y}_2 \end{bmatrix} = \begin{bmatrix} -l_1 \dot{\theta}_1 \sin \theta_1 - l_2 \left( \dot{\theta}_1 + \dot{\theta}_2 \right) \sin (\theta_1 + \theta_2) \\ l_1 \dot{\theta}_1 \cos \theta_1 + l_2 \left( \dot{\theta}_1 + \dot{\theta}_2 \right) \cos (\theta_1 + \theta_2) \end{bmatrix}. \tag{9.320}
$$

The kinetic energy of this manipulator is made of kinetic energy of the masses and is equal to

$$
\begin{aligned}
K &= K_1 + K_2 \\
&= \frac{1}{2} m_1 \left( \dot{X}_1^2 + \dot{Y}_1^2 \right) + \frac{1}{2} m_2 \left( \dot{X}_2^2 + \dot{Y}_2^2 \right) \\
&= \frac{1}{2} m_1 l_1^2 \dot{\theta}_1^2 \\
&\quad + \frac{1}{2} m_2 \left( l_1^2 \dot{\theta}_1^2 + l_2^2 \left( \dot{\theta}_1 + \dot{\theta}_2 \right)^2 + 2 l_1 l_2 \dot{\theta}_1 \left( \dot{\theta}_1 + \dot{\theta}_2 \right) \cos \theta_2 \right).
\end{aligned} \tag{9.321}
$$

*The potential energy of the manipulator is*

$$
\begin{aligned}
V &= V_1 + V_2 \\
&= m_1 g Y_1 + m_2 g Y_2 \\
&= m_1 g l_1 \sin \theta_1 + m_2 g \left( l_1 \sin \theta_1 + l_2 \sin (\theta_1 + \theta_2) \right). \quad (9.322)
\end{aligned}
$$

*The Lagrangean is then obtained from Equations (9.321) and (9.322)*

$$
\begin{aligned}
\mathcal{L} &= K - V \quad (9.323) \\
&= \frac{1}{2} m_1 l_1^2 \dot{\theta}_1^2 \\
&\quad + \frac{1}{2} m_2 \left( l_1^2 \dot{\theta}_1^2 + l_2^2 \left( \dot{\theta}_1 + \dot{\theta}_2 \right)^2 + 2 l_1 l_2 \dot{\theta}_1 \left( \dot{\theta}_1 + \dot{\theta}_2 \right) \cos \theta_2 \right) \\
&\quad - \left( m_1 g l_1 \sin \theta_1 + m_2 g \left( l_1 \sin \theta_1 + l_2 \sin (\theta_1 + \theta_2) \right) \right).
\end{aligned}
$$

*which provides the required partial derivatives as follows:*

$$
\frac{\partial \mathcal{L}}{\partial \theta_1} = -\left( m_1 + m_2 \right) g l_1 \cos \theta_1 - m_2 g l_2 \cos (\theta_1 + \theta_2) \quad (9.324)
$$

$$
\begin{aligned}
\frac{\partial \mathcal{L}}{\partial \dot{\theta}_1} &= \left( m_1 + m_2 \right) l_1^2 \dot{\theta}_1 + m_2 l_2^2 \left( \dot{\theta}_1 + \dot{\theta}_2 \right) \\
&\quad + m_2 l_1 l_2 \left( 2 \dot{\theta}_1 + \dot{\theta}_2 \right) \cos \theta_2 \quad (9.325)
\end{aligned}
$$

$$
\begin{aligned}
\frac{d}{dt} \left( \frac{\partial \mathcal{L}}{\partial \dot{\theta}_1} \right) &= \left( m_1 + m_2 \right) l_1^2 \ddot{\theta}_1 + m_2 l_2^2 \left( \ddot{\theta}_1 + \ddot{\theta}_2 \right) \\
&\quad + m_2 l_1 l_2 \left( 2 \ddot{\theta}_1 + \ddot{\theta}_2 \right) \cos \theta_2 \\
&\quad - m_2 l_1 l_2 \dot{\theta}_2 \left( 2 \dot{\theta}_1 + \dot{\theta}_2 \right) \sin \theta_2 \quad (9.326)
\end{aligned}
$$

$$
\frac{\partial \mathcal{L}}{\partial \theta_2} = -m_2 l_1 l_2 \dot{\theta}_1 \left( \dot{\theta}_1 + \dot{\theta}_2 \right) \sin \theta_2 - m_2 g l_2 \cos (\theta_1 + \theta_2) \quad (9.327)
$$

$$
\frac{\partial \mathcal{L}}{\partial \dot{\theta}_2} = m_2 l_2^2 \left( \dot{\theta}_1 + \dot{\theta}_2 \right) + m_2 l_1 l_2 \dot{\theta}_1 \cos \theta_2 \quad (9.328)
$$

$$
\frac{d}{dt} \left( \frac{\partial \mathcal{L}}{\partial \dot{\theta}_2} \right) = m_2 l_2^2 \left( \ddot{\theta}_1 + \ddot{\theta}_2 \right) + m_2 l_1 l_2 \ddot{\theta}_1 \cos \theta_2 - m_2 l_1 l_2 \dot{\theta}_1 \dot{\theta}_2 \sin \theta_2 \quad (9.329)
$$

*Therefore, the equations of motion for the 2R manipulator are*

$$
\begin{aligned}
Q_1 &= \frac{d}{dt} \left( \frac{\partial \mathcal{L}}{\partial \dot{\theta}_1} \right) - \frac{\partial \mathcal{L}}{\partial \theta_1} \\
&= \left( m_1 + m_2 \right) l_1^2 \ddot{\theta}_1 + m_2 l_2^2 \left( \ddot{\theta}_1 + \ddot{\theta}_2 \right) \\
&\quad + m_2 l_1 l_2 \left( 2 \ddot{\theta}_1 + \ddot{\theta}_2 \right) \cos \theta_2 - m_2 l_1 l_2 \dot{\theta}_2 \left( 2 \dot{\theta}_1 + \dot{\theta}_2 \right) \sin \theta_2 \\
&\quad + \left( m_1 + m_2 \right) g l_1 \cos \theta_1 + m_2 g l_2 \cos (\theta_1 + \theta_2) \quad (9.330)
\end{aligned}
$$

$$Q_2 = \frac{d}{dt}\left(\frac{\partial \mathcal{L}}{\partial \dot{\theta}_2}\right) - \frac{\partial \mathcal{L}}{\partial \theta_2}$$

$$= m_2 l_2^2 \left(\ddot{\theta}_1 + \ddot{\theta}_2\right) + m_2 l_1 l_2 \ddot{\theta}_1 \cos\theta_2 - m_2 l_1 l_2 \dot{\theta}_1 \dot{\theta}_2 \sin\theta_2$$

$$+ m_2 l_1 l_2 \dot{\theta}_1 \left(\dot{\theta}_1 + \dot{\theta}_2\right)\sin\theta_2 + m_2 g l_2 \cos\left(\theta_1 + \theta_2\right). \quad (9.331)$$

The generalized forces $Q_1$ and $Q_2$ are the required forces to drive the generalized coordinates. In this case, $Q_1$ is the torque at the base motor and $Q_2$ is the torque of the motor at $m_1$.

The equations of motion can be rearranged to have a more systematic form

$$Q_1 = \left((m_1 + m_2)\, l_1^2 + m_2 l_2 \left(l_2 + 2l_1 \cos\theta_2\right)\right)\ddot{\theta}_1$$

$$+ m_2 l_2 \left(l_2 + l_1 \cos\theta_2\right)\ddot{\theta}_2$$

$$- 2m_2 l_1 l_2 \sin\theta_2\, \dot{\theta}_1 \dot{\theta}_2 - m_2 l_1 l_2 \sin\theta_2\, \dot{\theta}_2^2$$

$$+ (m_1 + m_2)\, g l_1 \cos\theta_1 + m_2 g l_2 \cos\left(\theta_1 + \theta_2\right) \quad (9.332)$$

$$Q_2 = m_2 l_2 \left(l_2 + l_1 \cos\theta_2\right)\ddot{\theta}_1 + m_2 l_2^2 \ddot{\theta}_2$$

$$+ m_2 l_1 l_2 \sin\theta_2\, \dot{\theta}_1^2 + m_2 g l_2 \cos\left(\theta_1 + \theta_2\right). \quad (9.333)$$

**Example 371** *Mechanical energy.*

If a system of masses $m_i$ are moving in a potential force field

$$\mathbf{F}_{m_i} = -\nabla_i V \quad (9.334)$$

*their Newton equations of motion will be*

$$m_i \ddot{\mathbf{r}}_i = -\nabla_i V \qquad i = 1, 2, \cdots n. \quad (9.335)$$

*The inner product of equations of motion with $\dot{\mathbf{r}}_i$ and adding the equations*

$$\sum_{i=1}^{n} m_i \dot{\mathbf{r}}_i \cdot \ddot{\mathbf{r}}_i = -\sum_{i=1}^{n} \dot{\mathbf{r}}_i \cdot \nabla_i V \quad (9.336)$$

*and then, integrating over time*

$$\frac{1}{2}\sum_{i=1}^{n} m_i \dot{\mathbf{r}}_i \cdot \dot{\mathbf{r}}_i = -\int \sum_{i=1}^{n} \mathbf{r}_i \cdot \nabla_i V \quad (9.337)$$

*shows that*

$$K = -\int \sum_{i=1}^{n} \left(\frac{\partial V}{\partial x_i} x_i + \frac{\partial V}{\partial y_i} y_i + \frac{\partial V}{\partial z_i} z_i\right)$$

$$= -V + E \quad (9.338)$$
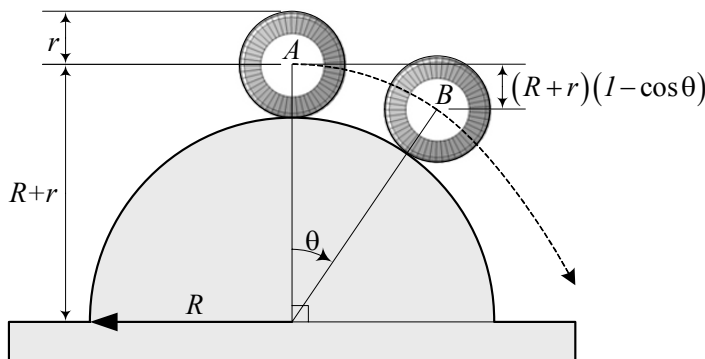
FIGURE 9.16. A wheel turning, without slip, over a cylindrical hill.

where $E$ is the constant of integration. $E$ is called the **mechanical energy** of the system and is equal to kinetic plus potential energies.

$$E = K + V \qquad (9.339)$$

**Example 372** *Falling wheel.*

Figure 9.16 illustrates a wheel turning, without slip, over a cylindrical hill. We may use the conservation of mechanical energy to find the angle at which the wheel leaves the hill.

At the initial instant of time, the wheel is at point $A$. We assume the initial kinetic and potential, and hence, the mechanical energies are zero. When the wheel is turning over the hill, its angular velocity, $\omega$, is

$$\omega = \frac{v}{r} \qquad (9.340)$$

where $v$ is the speed at the center of the wheel. At any other point $B$, the wheel achieves some kinetic energy and loses some potential energy. At a certain angle, where the normal component of the weight cannot provide more centripetal force,

$$mg \cos \theta = \frac{mv^2}{R+r}. \qquad (9.341)$$

the wheel separates from the surface. Employing the conservation of energy, we have

$$E_A \;=\; E_B \qquad (9.342)$$
$$K_A + V_A \;=\; K_B + V_B. \qquad (9.343)$$

The kinetic and potential energy at the separation point $B$ are

$$K_B \;=\; \frac{1}{2}mv^2 + \frac{1}{2}I_C\omega^2 \qquad (9.344)$$
$$V_B \;=\; -mg\,(R+r)\,(1 - \cos\theta) \qquad (9.345)$$
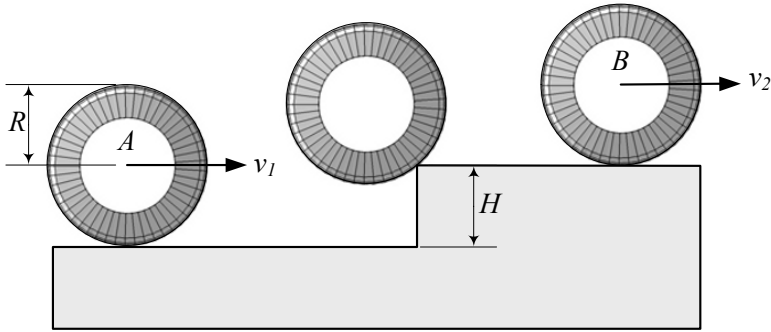
FIGURE 9.17. A turning wheel moving up a step.

where $I_C$ is the mass moment of inertia for the wheel about its center. Therefore,

$$\frac{1}{2}mv^2 + \frac{1}{2}I_C\omega^2 = mg\,(R+r)\,(1-\cos\theta) \qquad (9.346)$$

and substituting (9.340) and (9.341) provides

$$\left(1 + \frac{I_C}{mr^2}\right)(R+r)\,g\cos\theta = 2g\,(R+r)\,(1-\cos\theta) \qquad (9.347)$$

and therefore, the separation angle is

$$\theta = \cos^{-1}\frac{2mr^2}{I_C + 3mr^2}. \qquad (9.348)$$

Let's examine the equation for a disc wheel with

$$I_C = \frac{1}{2}mr^2. \qquad (9.349)$$

and find the separation angle.

$$\begin{aligned} \theta &= \cos^{-1}\frac{4}{7} \\ &\approx 0.96\,\text{rad} \\ &\approx 55.15\,\text{deg} \end{aligned} \qquad (9.350)$$

**Example 373** *Turning wheel over a step.*
   *Figure 9.17 illustrates a wheel of radius $R$ turning with speed $v$ to go over a step with height $H < R$.*
   *We may use the principle of energy conservation and find the speed of the wheel after getting across the step. Employing the conservation of energy,*

*we have*

$$E_A = E_B \tag{9.351}$$

$$K_A + V_A = K_B + V_B \tag{9.352}$$

$$\frac{1}{2}mv_1^2 + \frac{1}{2}I_C\omega_1^2 + 0 = \frac{1}{2}mv_2^2 + \frac{1}{2}I_C\omega_2^2 + mgH \tag{9.353}$$

$$\left(m + \frac{I_C}{R^2}\right)v_1^2 = \left(m + \frac{I_C}{R^2}\right)v_2^2 + 2mgH \tag{9.354}$$

*and therefore,*

$$v_2 = \sqrt{v_1^2 - \frac{2gH}{1 + \dfrac{I_C}{mR^2}}}. \tag{9.355}$$

*The condition for having a real $v_2$ is*

$$v_1 > \sqrt{\frac{2gH}{1 + \dfrac{I_C}{mR^2}}}. \tag{9.356}$$

*The second speed (9.355) and the condition (9.356) for a solid disc are*

$$v_2 = \sqrt{v_1^2 - \frac{4}{3}Hg} \tag{9.357}$$

$$v_1 > \sqrt{\frac{4}{3}Hg} \tag{9.358}$$

*because we assumed that*

$$I_C = \frac{1}{2}mR^2. \tag{9.359}$$

**Example 374** *Trebuchet.*

*A **trebuchet**, shown schematically in Figure 9.18, is a shooting weapon of war powered by a falling massive counterweight $m_1$. A beam $AB$ is pivoted to the chassis with two unequal sections $a$ and $b$.*

*The figure shows a trebuchet at its initial configuration. The origin of a global coordinate frame is set at the pivot point. The counterweight $m_1$ is at $(x_1, y_1)$ and is hinged at the shorter arm of the beam at a distance $c$ from the end $B$. The mass of the projectile is $m_2$ and it is at the end of a massless sling with a length $l$ attached to the end of the longer arm of the beam. The three independent variable angles $\alpha$, $\theta$, and $\gamma$ describe the motion of the device. We consider the parameters $a$, $b$, $c$, $d$, $l$, $m_1$, and $m_2$ constant, and determine the equations of motion by the Lagrange method.*

*Figure 9.19 illustrates the trebuchet when it is in motion. The position coordinates of masses $m_1$ and $m_2$ are*

$$x_1 = b\sin\theta - c\sin(\theta + \gamma) \tag{9.360}$$

$$y_1 = -b\cos\theta + c\cos(\theta + \gamma) \tag{9.361}$$
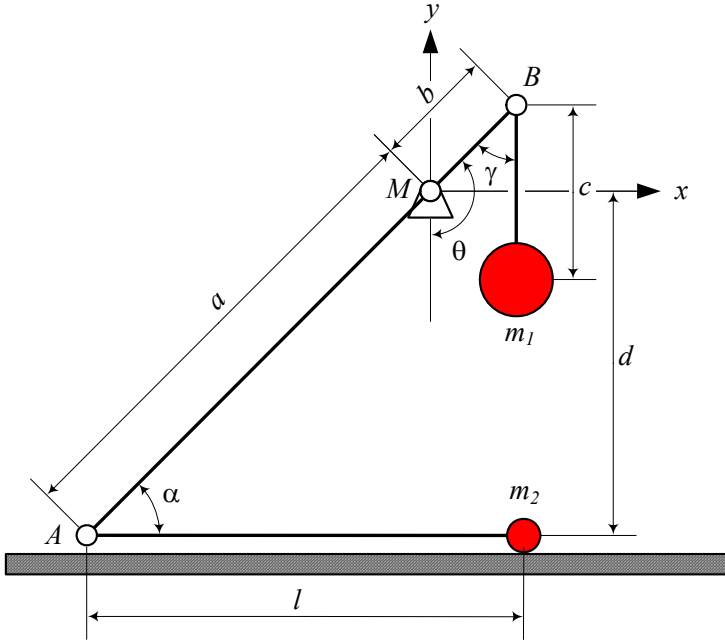
FIGURE 9.18. A trebuchet at starting position.

*and*

$$x_2 = -a\sin\theta - l\sin(-\theta + \alpha) \qquad (9.362)$$
$$y_2 = -a\cos\theta - l\cos(-\theta + \alpha). \qquad (9.363)$$

*Taking a time derivative provides the velocity components*

$$\dot{x}_1 = b\dot{\theta}\cos\theta - c\left(\dot{\theta} + \dot{\gamma}\right)\cos(\theta + \gamma) \qquad (9.364)$$
$$\dot{y}_1 = b\dot{\theta}\sin\theta - c\left(\dot{\theta} + \dot{\gamma}\right)\sin(\theta + \gamma) \qquad (9.365)$$

$$\dot{x}_2 = l\left(c - \dot{\alpha}\right)\cos(\alpha - \theta) - a\dot{\theta}\cos(\theta) \qquad (9.366)$$
$$\dot{y}_2 = a\dot{\theta}\sin\theta - l\left(\dot{\theta} - \dot{\alpha}\right)\sin(\alpha - \theta). \qquad (9.367)$$

*which shows that the kinetic energy of the system is*

$$
\begin{aligned}
K &= \frac{1}{2}m_1 v_1^2 + \frac{1}{2}m_2 v_2^2 = \frac{1}{2}m_1\left(\dot{x}_1^2 + \dot{y}_1^2\right) + \frac{1}{2}m_2\left(\dot{x}_2^2 + \dot{y}_2^2\right) \\
&= \frac{1}{2}m_1\left(\left(b^2 + c^2\right)\dot{\theta}^2 + c^2\dot{\gamma}^2 + 2c^2\dot{\theta}\dot{\gamma}\right) \\
&\quad - m_1 bc\dot{\theta}\left(\dot{\theta} + \dot{\gamma}\right)\cos\gamma \\
&\quad + \frac{1}{2}m_2\left(\left(a^2 + l^2\right)\dot{\theta}^2 + l^2\dot{\alpha}^2 - 2l^2\dot{\theta}\dot{\alpha}\right) \\
&\quad - m_2 al\dot{\theta}\left(\dot{\theta} - \dot{\alpha}\right)\cos\left(2\theta - \alpha\right).
\end{aligned}
\tag{9.368}
$$

*The potential energy of the system can be calculated by y-position of the masses.*

$$
\begin{aligned}
V &= m_1 g y_1 + m_2 g y_2 \\
&= m_1 g\left(-b\cos\theta + c\cos\left(\theta + \gamma\right)\right) \\
&\quad + m_2 g\left(-a\cos\theta - l\cos\left(-\theta + \alpha\right)\right)
\end{aligned}
\tag{9.369}
$$

*Having the energies $K$ and $V$, we can set up the Lagrangean $\mathcal{L}$.*

$$
\mathcal{L} = K - V
\tag{9.370}
$$

*Using the Lagrangean, we are able to find the three equations of motion.*

$$
\frac{d}{dt}\left(\frac{\partial\mathcal{L}}{\partial\dot{\theta}}\right) - \frac{\partial\mathcal{L}}{\partial\theta} = 0
\tag{9.371}
$$

$$
\frac{d}{dt}\left(\frac{\partial\mathcal{L}}{\partial\dot{\alpha}}\right) - \frac{\partial\mathcal{L}}{\partial\alpha} = 0
\tag{9.372}
$$

$$
\frac{d}{dt}\left(\frac{\partial\mathcal{L}}{\partial\dot{\gamma}}\right) - \frac{\partial\mathcal{L}}{\partial\gamma} = 0.
\tag{9.373}
$$

The trebuchet appeared in 500 to 400 B.C. China and was developed by Persian armies around 300 B.C. It was used by the Arabs against the Romans during 600 to 1200 A.D. The trebuchet is also called the **manjaniq**, **catapults**, or **onager**. The "Manjaniq" is the root of the words "machine" and "mechanic".

## 9.7 Summary

The translational and rotational equations of motion for a rigid body, expressed in the global coordinate frame, are

$$
{}^G\mathbf{F} = \frac{{}^G d}{dt}{}^G\mathbf{p}
\tag{9.374}
$$

$$
{}^G\mathbf{M} = \frac{{}^G d}{dt}{}^G\mathbf{L}
\tag{9.375}
$$
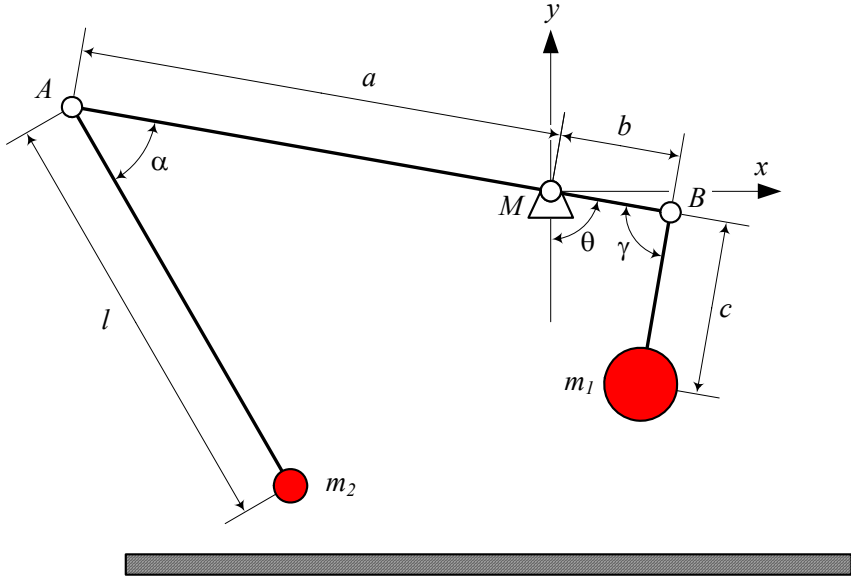
FIGURE 9.19. A trebuchet in motion.

where $^G\mathbf{F}$ and $^G\mathbf{M}$ indicate the resultant of the external forces and moments applied on the rigid body, measured at the mass center $C$. The vector $^G\mathbf{p}$ is the momentum and $^G\mathbf{L}$ is the moment of momentum for the rigid body at $C$

$$\mathbf{p} = m\,\mathbf{v} \tag{9.376}$$

$$\mathbf{L} = \mathbf{r}_C \times \mathbf{p}. \tag{9.377}$$

The expression of the equations of motion in the body coordinate frame are

$$
\begin{aligned}
^B\mathbf{F} &= {}^G\dot{\mathbf{p}} + {}^B_G\boldsymbol{\omega}_B \times {}^B\mathbf{p} \\
&= m\,{}^B\mathbf{a}_B + m\,{}^B_G\boldsymbol{\omega}_B \times {}^B\mathbf{v}_B
\end{aligned} \tag{9.378}
$$

$$
\begin{aligned}
^B\mathbf{M} &= {}^B\dot{\mathbf{L}} + {}^B_G\boldsymbol{\omega}_B \times {}^B\mathbf{L} \\
&= {}^BI\,{}^B_G\dot{\boldsymbol{\omega}}_B + {}^B_G\boldsymbol{\omega}_B \times \left({}^BI\,{}^B_G\boldsymbol{\omega}_B\right)
\end{aligned} \tag{9.379}
$$

where $I$ is the moment of inertia for the rigid body.

$$
I = \begin{bmatrix}
I_{xx} & I_{xy} & I_{xz} \\
I_{yx} & I_{yy} & I_{yz} \\
I_{zx} & I_{zy} & I_{zz}
\end{bmatrix}. \tag{9.380}
$$

The elements of $I$ are functions of the mass distribution of the rigid body and are defined by

$$I_{ij} = \int_B \left(r_i^2 \delta_{mn} - x_{im} x_{jn}\right) dm \quad , \quad i, j = 1, 2, 3 \tag{9.381}$$

where $\delta_{ij}$ is Kronecker's delta.

Every rigid body has a principal body coordinate frame in which the moment of inertia is in the form

$$^B I = \begin{bmatrix} I_1 & 0 & 0 \\ 0 & I_2 & 0 \\ 0 & 0 & I_3 \end{bmatrix}. \tag{9.382}$$

The rotational equation of motion in the principal coordinate frame simplifies to

$$\begin{aligned} M_1 &= I_1 \dot{\omega}_1 - (I_2 - I_2)\,\omega_2 \omega_3 \\ M_2 &= I_2 \dot{\omega}_2 - (I_3 - I_1)\,\omega_3 \omega_1 \\ M_3 &= I_3 \dot{\omega}_3 - (I_1 - I_2)\,\omega_1 \omega_2. \end{aligned} \tag{9.383}$$

The equations of motion for a mechanical system having $n$ DOF can also be found by the Lagrange equation

$$\frac{d}{dt}\left(\frac{\partial \mathcal{L}}{\partial \dot{q}_r}\right) - \frac{\partial \mathcal{L}}{\partial q_r} = Q_r \qquad r = 1, 2, \cdots n \tag{9.384}$$

$$\mathcal{L} = K - V \tag{9.385}$$

where $\mathcal{L}$ is the *Lagrangean* of the system, $K$ is the kinetic energy, $V$ is the potential energy, and $Q_r$ is the nonpotential generalized force.

$$Q_r = \sum_{i=1}^{n} \left( Q_{ix}\frac{\partial f_i}{\partial q_1} + Q_{iy}\frac{\partial g_i}{\partial q_2} + Q_{iz}\frac{\partial h_i}{\partial q_n} \right) \tag{9.386}$$

The parameters $q_r$, $r = 1, 2, \cdots, n$ are the generalized coordinates of the system, $\mathbf{Q} = \begin{bmatrix} Q_{ix} & Q_{iy} & Q_{iz} \end{bmatrix}^T$ is the external force acting on the $i$th particle of the system, and $Q_r$ is the generalized force associated to $q_r$. When $(x_i, y_i, z_i)$ are Cartesian coordinates in a globally fixed coordinate frame for the particle $m_i$, then its coordinates may be functions of another set of generalized coordinates $q_1, q_2, q_3, \cdots, q_n$ and possibly time $t$.

$$\begin{aligned} x_i &= f_i(q_1, q_2, q_3, \cdots, q_n, t) \tag{9.387} \\ y_i &= g_i(q_1, q_2, q_3, \cdots, q_n, t) \tag{9.388} \\ z_i &= h_i(q_1, q_2, q_3, \cdots, q_n, t) \tag{9.389} \end{aligned}$$

## 9.8   Key Symbols

| | |
|---|---|
| $a, b, w, h$ | length |
| $\mathbf{a}$ | acceleration |
| $C$ | mass center |
| $\mathbf{d}$ | position vector of the body coordinate frame |
| $d\mathbf{f}$ | infinitesimal force |
| $dm$ | infinitesimal mass |
| $d\mathbf{m}$ | infinitesimal moment |
| $E$ | mechanical energy |
| $\mathbf{F}$ | force |
| $F_C$ | Coriolis force |
| $g$ | gravitational acceleration |
| $H$ | height |
| $I$ | moment of inertia matrix |
| $I_1, I_2, I_3$ | principal moment of inertia |
| $K$ | kinetic energy |
| $l$ | directional line |
| $\mathbf{L}$ | moment of momentum |
| $\mathcal{L} = K - V$ | Lagrangean |
| $m$ | mass |
| $\mathbf{M}$ | moment |
| $\mathbf{p}$ | momentum |
| $P, Q$ | points in rigid body |
| $r$ | radius of disc |
| $\mathbf{r}$ | position vector |
| $R$ | radius |
| $R$ | rotation matrix |
| $t$ | time |
| $\hat{u}$ | unit vector to show the directional line |
| $v \equiv \dot{x}, \ \mathbf{v}$ | velocity |
| $V$ | potential energy |
| $\mathbf{w}$ | eigenvector |
| $W$ | work |
| $W$ | eigenvector matrix |
| $x, y, z, \ \mathbf{x}$ | displacement |
| | |
| $\delta_{ij}$ | Kronecker's delta |
| $\Gamma^i_{j,k}$ | Christoffel operator |
| $\lambda$ | eigenvalue |
| $\varphi, \theta, \psi$ | Euler angles |
| $\omega, \boldsymbol{\omega}$ | angular velocity |
| $\parallel$ | parallel |
| $\perp$ | orthogonal |

# Exercises

1. Kinetic energy of a rigid link.

   Consider a straight and uniform bar as a rigid bar. The bar has a mass $m$. Show that the kinetic energy of the bar can be expressed as

   $$K = \frac{1}{6}m\left(\mathbf{v}_1 \cdot \mathbf{v}_1 + \mathbf{v}_1 \cdot \mathbf{v}_2 + \mathbf{v}_2 \cdot \mathbf{v}_2\right)$$

   where $\mathbf{v}_1$ and $\mathbf{v}_2$ are the velocity vectors of the endpoints of the bar.

2. Discrete particles.

   There are three particles $m_1 = 10\,\text{kg}$, $m_2 = 20\,\text{kg}$, $m_3 = 30\,\text{kg}$, at

   $$\mathbf{r}_1 = \begin{bmatrix} 1 \\ -1 \\ 1 \end{bmatrix} \quad \mathbf{r}_1 = \begin{bmatrix} -1 \\ -3 \\ 2 \end{bmatrix} \quad \mathbf{r}_1 = \begin{bmatrix} 2 \\ -1 \\ -3 \end{bmatrix}.$$

   Their velocities are

   $$\mathbf{v}_1 = \begin{bmatrix} 2 \\ 1 \\ 1 \end{bmatrix} \quad \mathbf{v}_1 = \begin{bmatrix} -1 \\ 0 \\ 2 \end{bmatrix} \quad \mathbf{v}_1 = \begin{bmatrix} 3 \\ -2 \\ -1 \end{bmatrix}.$$

   Find the position and velocity of the system at $C$. Calculate the system's momentum and moment of momentum. Calculate the system's kinetic energy and determine the rotational and translational parts of the kinetic energy.

3. Newton's equation of motion in the body frame.

   Show that Newton's equation of motion in the body frame is

   $$\begin{bmatrix} F_x \\ F_y \\ F_z \end{bmatrix} = m \begin{bmatrix} a_x \\ a_y \\ a_z \end{bmatrix} + \begin{bmatrix} 0 & -\omega_z & \omega_y \\ \omega_z & 0 & -\omega_x \\ -\omega_y & \omega_x & 0 \end{bmatrix} \begin{bmatrix} v_x \\ v_y \\ v_z \end{bmatrix}.$$

4. Work on a curved path.

   A particle of mass $m$ is moving on a circular path given by

   $$^{G}\mathbf{r}_P = \cos\theta\,\hat{I} + \sin\theta\,\hat{J} + 4\,\hat{K}.$$

   Calculate the work done by a force $^{G}\mathbf{F}$ when the particle moves from $\theta = 0$ to $\theta = \frac{\pi}{2}$.

   (a)
   $$^{G}\mathbf{F} = \frac{z^2 - y^2}{(x+y)^2}\,\hat{I} + \frac{y^2 - x^2}{(x+y)^2}\,\hat{J} + \frac{x^2 - y^2}{(x+z)^2}\,\hat{K}$$

(b)

$$^{G}\mathbf{F} = \frac{z^2 - y^2}{(x + y)^2}\,\hat{I} + \frac{2y}{x + y}\,\hat{J} + \frac{x^2 - y^2}{(x + z)^2}\,\hat{K}$$

5. Principal moments of inertia.

Find the principal moments of inertia and directions for the following inertia matrices:

(a)

$$[I] = \begin{bmatrix} 3 & 2 & 2 \\ 2 & 2 & 0 \\ 2 & 0 & 4 \end{bmatrix}$$

(b)

$$[I] = \begin{bmatrix} 3 & 2 & 4 \\ 2 & 0 & 2 \\ 4 & 2 & 3 \end{bmatrix}$$

(c)

$$[I] = \begin{bmatrix} 100 & 20\sqrt{3} & 0 \\ 20\sqrt{3} & 60 & 0 \\ 0 & 0 & 10 \end{bmatrix}$$

6. Rotated moment of inertia matrix.

A principal moment of inertia matrix $^{B_2}I$ is given as

$$[I] = \begin{bmatrix} 3 & 0 & 0 \\ 0 & 5 & 0 \\ 0 & 0 & 4 \end{bmatrix}.$$

The principal frame was achieved by rotating the initial body coordinate frame $30\deg$ about the $x$-axis, followed by $45\deg$ about the $z$-axis. Find the initial moment of inertia matrix $^{B_1}I$.

7. Rotation of moment of inertia matrix.

Find the required rotation matrix that transforms the moment of inertia matrix $[I]$ to an diagonal matrix.

$$[I] = \begin{bmatrix} 3 & 2 & 2 \\ 2 & 2 & 0.1 \\ 2 & 0.1 & 4 \end{bmatrix}$$

8. ★ Cubic equations.

The solution of a cubic equation

$$ax^3 + bx^2 + cx + d = 0$$

where $a \neq 0$, can be found in a systematic way.

Transform the equation to a new form with discriminant $4p^3 + q^2$,

$$y^3 + 3py + q = 0$$

using the transformation $x = y - \frac{b}{3a}$, where,

$$p = \frac{3ac - b^2}{9a^2}$$

$$q = \frac{2b^3 - 9abc + 27a^2d}{27a^3}.$$

The solutions are then

$$y_1 = \sqrt[3]{\alpha} - \sqrt[3]{\beta}$$
$$y_2 = e^{\frac{2\pi i}{3}} \sqrt[3]{\alpha} - e^{\frac{4\pi i}{3}} \sqrt[3]{\beta}$$
$$y_3 = e^{\frac{4\pi i}{3}} \sqrt[3]{\alpha} - e^{\frac{2\pi i}{3}} \sqrt[3]{\beta}$$

where,

$$\alpha = \frac{-q + \sqrt{q^2 + 4p^3}}{2}$$

$$\beta = \frac{-q + \sqrt{q^2 + 4p^3}}{2}.$$

For real values of $p$ and $q$, if the discriminant is positive, then one root is real, and two roots are complex conjugates. If the discriminant is zero, then there are three real roots, of which at least two are equal. If the discriminant is negative, then there are three unequal real roots.

Apply this theory for the characteristic equation of the matrix $[I]$ and show that the principal moments of inertia are real.

9. **Kinematics of a moving car on the Earth.**

The location of a vehicle on the Earth is described by its longitude $\varphi$ from a fixed meridian, say, the Greenwich meridian, and its latitude $\theta$ from the equator, as shown in Figure 9.20. We attach a coordinate frame $B$ at the center of the Earth with the $x$-axis on the equator's plane and the $y$-axis pointing to the vehicle. There are also two coordinate frames $E$ and $G$ where $E$ is attached to the Earth and $G$ is the global coordinate frame. Show that the angular velocity of $B$ and the velocity of the vehicle are

$$\begin{aligned}
{}^B_G\boldsymbol{\omega}_B &= \dot{\theta}\,\hat{\imath}_B + (\omega_E + \dot{\varphi})\sin\theta\,\hat{\jmath}_B + (\omega_E + \dot{\varphi})\cos\theta\,\hat{k} \\
{}^B_G\mathbf{v}_P &= -r(\omega_E + \dot{\varphi})\cos\theta\,\hat{\imath}_B + r\dot{\theta}\,\hat{k}.
\end{aligned}$$

Calculate the acceleration of the vehicle.
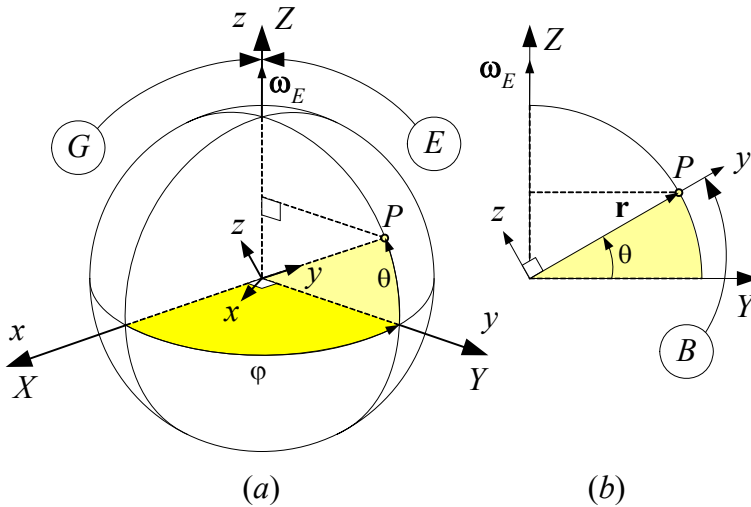
FIGURE 9.20. The location on the Earth is defined by longitude $\varphi$ and latitude $\theta$.

10. Global differential of angular momentum.

    Convert the moment of inertia $^{B}I$ and the angular velocity $^{B}_{G}\boldsymbol{\omega}_{B}$ to the global coordinate frame and then find the differential of angular momentum. It is an alternative method to show that

    $$\frac{^{G}d}{dt}\,{^{B}\mathbf{L}} = \frac{^{G}d}{dt}\left(^{B}I\,{^{B}_{G}\boldsymbol{\omega}_{B}}\right)$$
    $$= {^{B}\dot{\mathbf{L}}} + {^{B}_{G}\boldsymbol{\omega}_{B}} \times {^{B}\mathbf{L}}$$
    $$= I\dot{\boldsymbol{\omega}} + \boldsymbol{\omega} \times (I\boldsymbol{\omega}).$$

11. Lagrange method and nonlinear vibrating system.

    Use the Lagrange method and find the equation of motion for the pendulum shown in Figure 9.21. The stiffness of the linear spring is $k$.

12. Forced vibration of a pendulum.

    Figure 9.22 illustrates a simple pendulum having a length $l$ and a bob with mass $m$. Find the equation of motion if

    (a) the pivot $O$ has a dictated motion in $X$ direction

    $$X_{O} = a\sin\omega t$$

    (b) the pivot $O$ has a dictated motion in $Y$ direction

    $$Y_{O} = b\sin\omega t$$
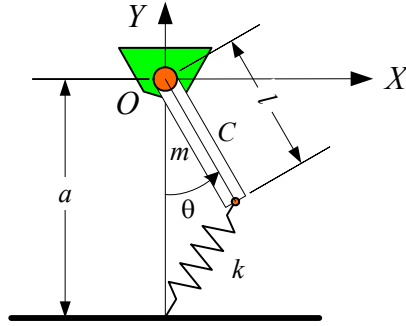
FIGURE 9.21. A compound pendulum attached with a linear spring at the tip point.
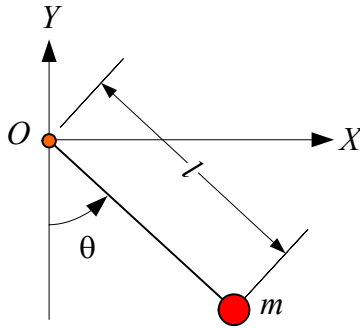


FIGURE 9.22. A pendulum with a vibrating pivot.

(c) the pivot $O$ has a uniform motion on a circle

$$\mathbf{r}_O = R\cos\omega t \ \hat{I} + R\sin\omega t \ \hat{J}.$$

13. Equations of motion from Lagrangean.

    Consider a physical system with a Lagrangean as

    $$\mathcal{L} = \frac{1}{2}m\left(a\dot{x} + b\dot{y}\right)^2 - \frac{1}{2}k\left(ax + by\right)^2.$$

    and find the equations of motion. The coefficients $m$, $k$, $a$, and $b$ are constant.

14. Lagrangean from equation of motion.

    Find the Lagrangean associated to the following equations of motions:

    (a)
    $$mr^2\ddot{\theta} + k_1 l_1\theta + k_2 l_2\theta + mgl = 0$$
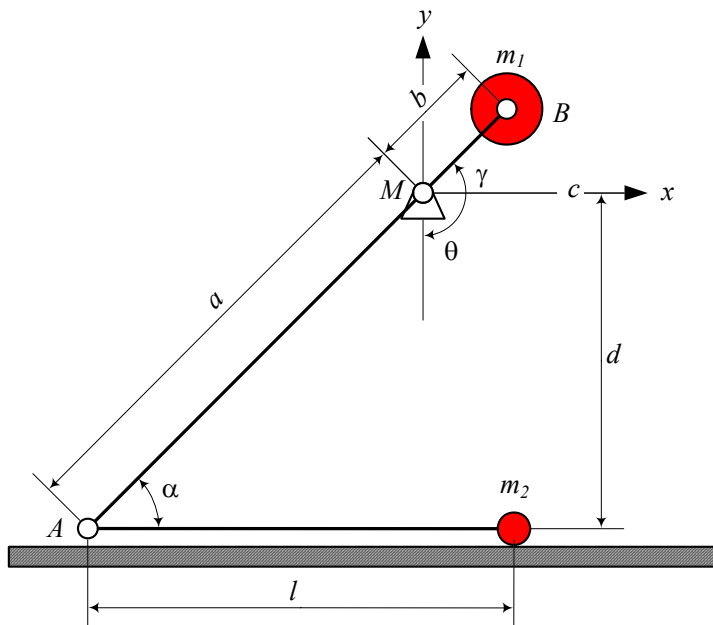
FIGURE 9.23. A simplified models of a trebuchet.

(b)

$$\ddot{r} - r\,\dot{\theta}^2 = 0$$
$$r^2\,\ddot{\theta} + 2r\,\dot{r}\,\dot{\theta} = 0$$

15. Trebuchet.

Derive the equations of motion for the trebuchet shown in Figure 9.18.

16. Simplified trebuchet.

Three simplified models of a trebuchet are shown in Figures 9.23 to 9.25. Derive and compare their equations of motion.
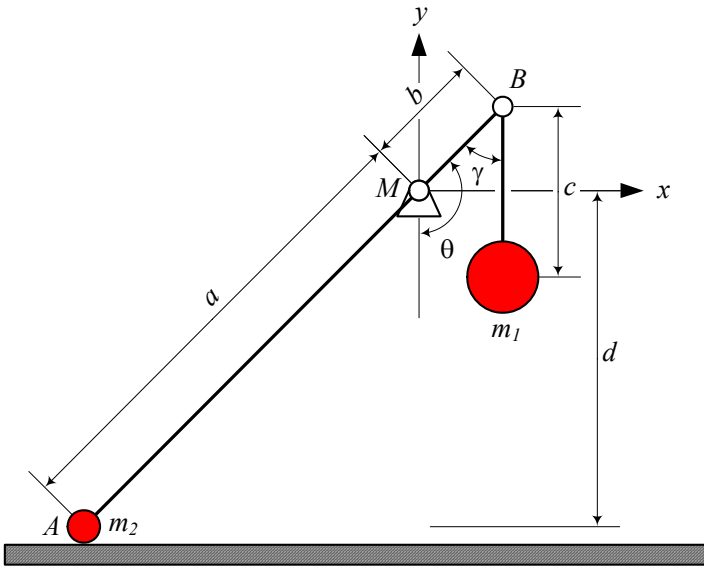
FIGURE 9.24. A simplified models of a trebuchet.
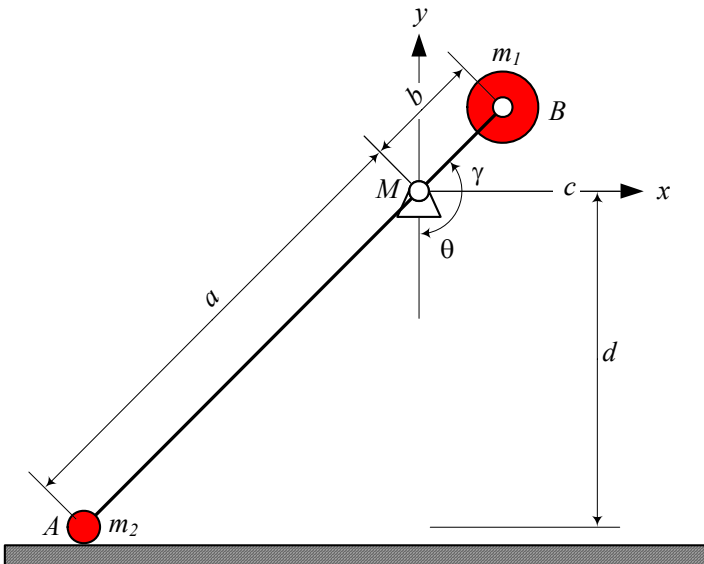


FIGURE 9.25. A simplified models of a trebuchet.

# 10

# Vehicle Planar Dynamics

In this chapter we develop a dynamic model for a rigid vehicle in a planar motion. When the forward, lateral and yaw velocities are important and are enough to examine the behavior of a vehicle, the planar model is applicable.

## 10.1 Vehicle Coordinate Frame

The equations of motion in vehicle dynamics are usually expressed in a set of vehicle coordinate frame $B(Cxyz)$, attached to the vehicle at the mass center $C$, as shown in Figure 10.1. The $x$-axis is a longitudinal axis passing through $C$ and directed forward. The $y$-axis goes laterally to the left from the driver's viewpoint. The $z$-axis makes the coordinate system a right-hand triad. When the car is parked on a flat horizontal road, the $z$-axis is perpendicular to the ground, opposite to the gravitational acceleration $\mathbf{g}$.
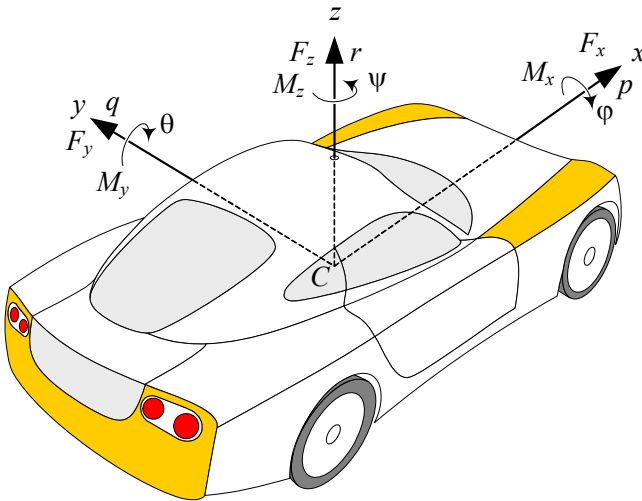


FIGURE 10.1. Vehicle body coordinate frame $B(Cxyz)$.

To show the vehicle orientation, we use three angles: *roll angle* $\varphi$ about the $x$-axis, *pitch angle* $\theta$ about the $y$-axis, and *yaw angle* $\psi$ about the $z$-axis. Because the rate of the orientation angles are important in vehicle

dynamics, we usually show them by a special character and call them *roll rate*, *pitch rate*, and *yaw rate* respectively.

$$\dot{\varphi} = p \tag{10.1}$$
$$\dot{\theta} = q \tag{10.2}$$
$$\dot{\psi} = r \tag{10.3}$$

The resultant of external forces and moments, that the vehicle receives from the ground and environment, makes the *vehicle force system* $(\mathbf{F}, \mathbf{M})$. This force system will be expressed in the body coordinate frame.

$$^{B}\mathbf{F} = F_x\hat{\imath} + F_y\hat{\jmath} + F_z\hat{k} \tag{10.4}$$
$$^{B}\mathbf{M} = M_x\hat{\imath} + M_y\hat{\jmath} + M_z\hat{k} \tag{10.5}$$

The individual components of the 3D vehicle force system are shown in Figure 10.2. These components have special names and importance.

1. *Longitudinal force $F_x$*. It is a force acting along the $x$-axis. The resultant $F_x > 0$ if the vehicle is accelerating, and $F_x < 0$ if the vehicle is braking. Longitudinal force is also called *forward force*, or *traction force*.

2. *Lateral force $F_y$*. It is an orthogonal force to both $F_x$ and $F_z$. The resultant $F_y > 0$ if it is leftward from the driver's viewpoint. Lateral force is usually a result of steering and is the main reason to generate a yaw moment and turn a vehicle.

3. *Normal force $F_z$*. It is a vertical force, normal to the ground plane. The resultant $F_z > 0$ if it is upward. Normal force is also called *vertical force* or *vehicle load*.

4. *Roll moment $M_x$*. It is a longitudinal moment about the $x$-axis. The resultant $M_x > 0$ if the vehicle tends to turn about the $x$-axis. The roll moment is also called the *bank moment*, *tilting torque*, or *overturning moment*.

5. *Pitch moment $M_y$*. It is a lateral moment about the $y$-axis. The resultant $M_y > 0$ if the vehicle tends to turn about the $y$-axis and move the head down.

6. *Yaw moment $M_z$*. It is an upward moment about the $z$-axis. The resultant $M_z > 0$ if the tire tends to turn about the $z$-axis. The yaw moment is also called the *aligning moment*.

The position and orientation of the vehicle coordinate frame $B(Cxyz)$ is measured with respect to a grounded fixed coordinate frame $G(OXYZ)$.
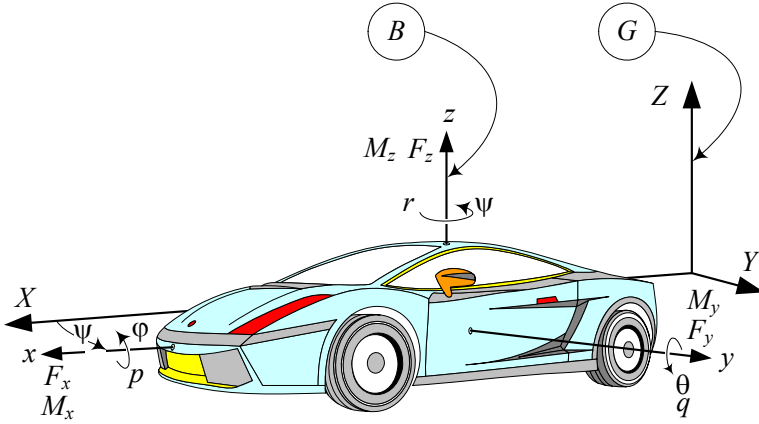
FIGURE 10.2. Illustration of a moving vehicle, indicated by its body coordinate frame $B$ in a global coordinate frame $G$.

The vehicle coordinate frame is called the *body frame* or *vehicle frame*, and the grounded frame is called the *global coordinate frame*. Analysis of the vehicle motion is equivalent to expressing the position and orientation of $B(Cxyz)$ in $G(OXYZ)$. Figure 10.2 shows how a moving vehicle is indicated by a body frame $B$ in a global frame $G$.

The angle between the $x$ and $X$ axes is the yaw angle $\psi$ and is called the *heading angle*. The velocity vector $\mathbf{v}$ of the vehicle makes an angle $\beta$ with the body $x$-axis which is called *sideslip angle* or *attitude angle*. The vehicle's velocity vector $\mathbf{v}$ makes an angle $\beta + \psi$ with the global $X$-axis that is called the *cruise angle*. These angles are shown in the top view of a moving vehicle in Figure 10.3.

There are many situations in which we need to number the wheels of a vehicle. We start numbering from the front left wheel as number 1, and then the front right wheel would be number 2. Numbering increases sequentially on the right wheels going to the back of the vehicle up to the rear right wheel. Then, we go to the left of the vehicle and continue numbering the wheels from the rear left toward the front. Each wheel is indicated by a position vector $\mathbf{r}_i$

$$^{B}\mathbf{r}_i = x_i i + y_i j + z_i k \tag{10.6}$$

expressed in the body coordinate frame $B$. Numbering of a four wheel vehicle is shown in Figure 10.3.

**Example 375** *Wheel numbers and their position vectors.*

*Figure 10.4 depicts a six-wheel passenger car. The wheel numbers are indicated besides each wheel. The front left wheel is wheel number 1, and the front right wheel is number 2. Moving to the back on the right side, we count the wheels numbered 3 and 4. The back left wheel gets number 5,*
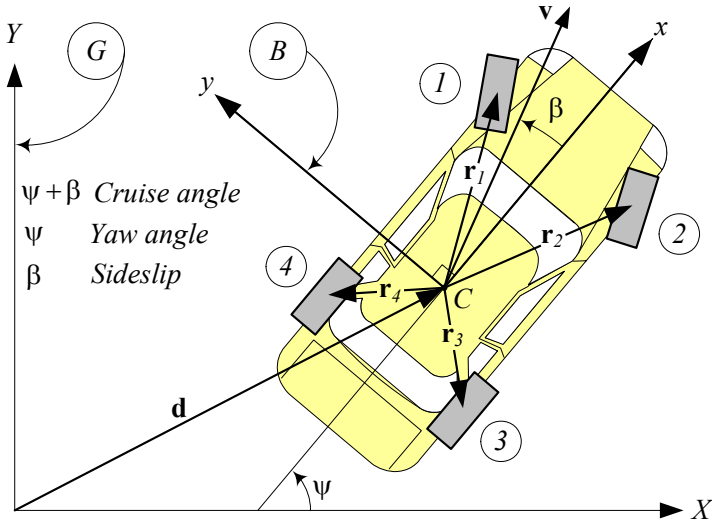
FIGURE 10.3. Top view of a moving vehicle to show the yaw angle $\psi$ between the $x$ and $X$ axes, the sideslip angle $\beta$ between the velocity vector $v$ and the $x$-axis, and the crouse angle $\beta + \psi$ between with the velocity vector $v$ and the $X$-axis.

*and then moving forward on the left side, the only unnumbered wheel is the wheel number 6.*

*If the global position vector of the car's mass center is given by*

$$^G\mathbf{d} = \begin{bmatrix} X_C \\ Y_C \end{bmatrix} \tag{10.7}$$

*and the body position vectors of the wheels are*

$$^B\mathbf{r}_1 = \begin{bmatrix} a_1 \\ w/2 \end{bmatrix} \tag{10.8}$$

$$^B\mathbf{r}_2 = \begin{bmatrix} a_1 \\ -w/2 \end{bmatrix} \tag{10.9}$$

$$^B\mathbf{r}_3 = \begin{bmatrix} -a_2 \\ -w/2 \end{bmatrix} \tag{10.10}$$

$$^B\mathbf{r}_4 = \begin{bmatrix} -a_3 \\ -w/2 \end{bmatrix} \tag{10.11}$$

$$^B\mathbf{r}_5 = \begin{bmatrix} -a_3 \\ w/2 \end{bmatrix} \tag{10.12}$$
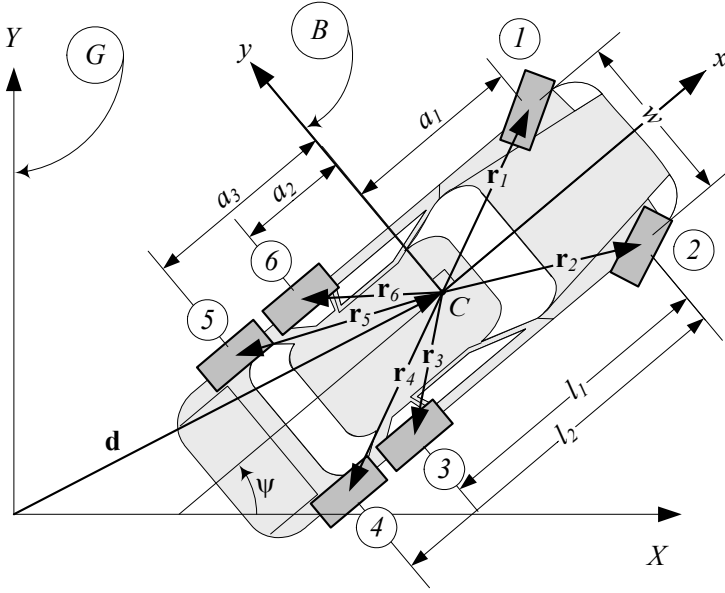
FIGURE 10.4. A six-wheel passenger car and its wheel numbering.

$$
{}^{B}\mathbf{r}_6 = \begin{bmatrix} -a_2 \\ w/2 \end{bmatrix} \tag{10.13}
$$

then the global position of the wheels are

$$
\begin{aligned}
{}^{G}\mathbf{r}_1 &= {}^{G}\mathbf{d} + {}^{G}R_B \, {}^{B}\mathbf{r}_1 \\
&= \begin{bmatrix} X_C - \dfrac{1}{2}w\sin\psi + a_1\cos\psi \\[2mm] Y_C + \dfrac{1}{2}w\cos\psi + a_1\sin\psi \end{bmatrix}
\end{aligned} \tag{10.14}
$$

$$
\begin{aligned}
{}^{G}\mathbf{r}_2 &= {}^{G}\mathbf{d} + {}^{G}R_B \, {}^{B}\mathbf{r}_2 \\
&= \begin{bmatrix} X_C + \dfrac{1}{2}w\sin\psi + a_1\cos\psi \\[2mm] Y_C - \dfrac{1}{2}w\cos\psi + a_1\sin\psi \end{bmatrix}
\end{aligned} \tag{10.15}
$$

$$
\begin{aligned}
{}^{G}\mathbf{r}_3 &= {}^{G}\mathbf{d} + {}^{G}R_B \, {}^{B}\mathbf{r}_3 \\
&= \begin{bmatrix} X_C + \dfrac{1}{2}w\sin\psi - a_2\cos\psi \\[2mm] Y_C - \dfrac{1}{2}w\cos\psi - a_2\sin\psi \end{bmatrix}
\end{aligned} \tag{10.16}
$$

$$
\begin{aligned}
{}^G\mathbf{r}_4 &= {}^G\mathbf{d} + {}^G R_B \, {}^B\mathbf{r}_4 \\
&= \begin{bmatrix} X_C + \dfrac{1}{2} w \sin\psi - a_3 \cos\psi \\[2mm] Y_C - \dfrac{1}{2} w \cos\psi - a_3 \sin\psi \end{bmatrix}
\end{aligned}
\tag{10.17}
$$

$$
\begin{aligned}
{}^G\mathbf{r}_5 &= {}^G\mathbf{d} + {}^G R_B \, {}^B\mathbf{r}_5 \\
&= \begin{bmatrix} X_C - \dfrac{1}{2} w \sin\psi - a_3 \cos\psi \\[2mm] Y_C + \dfrac{1}{2} w \cos\psi - a_3 \sin\psi \end{bmatrix}
\end{aligned}
\tag{10.18}
$$

$$
\begin{aligned}
{}^G\mathbf{r}_6 &= {}^G\mathbf{d} + {}^G R_B \, {}^B\mathbf{r}_6 \\
&= \begin{bmatrix} X_C - \dfrac{1}{2} w \sin\psi - a_2 \cos\psi \\[2mm] Y_C + \dfrac{1}{2} w \cos\psi - a_2 \sin\psi \end{bmatrix} .
\end{aligned}
\tag{10.19}
$$

The rotation matrix between the global $G$ and body coordinate $B$ is

$$
{}^G R_B = \begin{bmatrix} \cos\psi & -\sin\psi \\ \sin\psi & \cos\psi \end{bmatrix} .
\tag{10.20}
$$

**Example 376** *Crouse angle, attitude angle, and heading angle.*

*Figure 10.5 illustrates a car moving on a road with the angles*

$$
\begin{aligned}
\psi &= 15 \deg \tag{10.21} \\
\beta &= 16 \deg . \tag{10.22}
\end{aligned}
$$

*The heading angle of the car is*

$$
\begin{aligned}
Heading\ angle &= \psi \\
&= 15 \deg \tag{10.23}
\end{aligned}
$$

*which is the angle between the car's longitudinal $x$-axis and a reference $X$-axis on the road. The attitude angle of the car is*

$$
\begin{aligned}
Attitude\ angle &= \beta \\
&= 16 \deg \tag{10.24}
\end{aligned}
$$

*which is the angle between the direction of the car's motion and its longitudinal axis. The cruise angle of the car is*

$$
\begin{aligned}
Heading\ angle &= \beta + \psi \\
&= 31 \deg \tag{10.25}
\end{aligned}
$$

*which is the angle between the car's direction of motion and the reference $X$-axis on the road.*
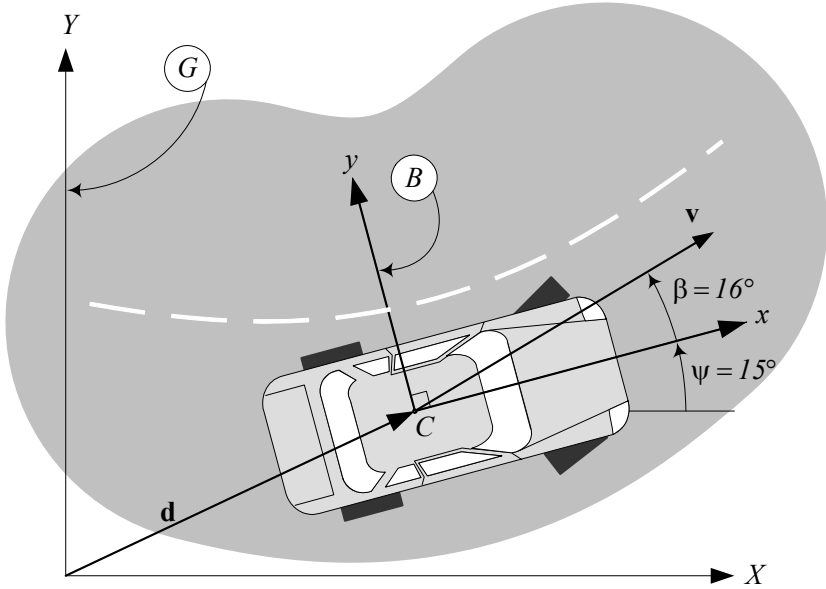
FIGURE 10.5. A car moving on a road with sideslip angle $\beta$ and heading angle $\psi$.

## 10.2   Rigid Vehicle Newton-Euler Dynamics

A rigid vehicle is assumed to act similar to a flat box moving on a horizontal surface. A rigid vehicle has a planar motion with three degrees of freedom that are: translation in the $x$ and $y$ directions, and a rotation about the $z$-axis. The *Newton-Euler equations of motion* for a rigid vehicle in the body coordinate frame $B$, attached to the vehicle at its mass center $C$ are:

$$F_x = m\,\dot{v}_x - m\omega_z\,v_y \tag{10.26}$$
$$F_y = m\,\dot{v}_y + m\omega_z\,v_x \tag{10.27}$$
$$M_z = \dot{\omega}_z\,I_z. \tag{10.28}$$

**Proof.** Figure 10.6 illustrates a rigid vehicle in a planar motion. A global coordinate frame $G$ is attached to the ground and a local coordinate frame $B$ is attached to the vehicle at the mass center $C$. The $Z$ and $z$ axes are parallel, and the orientation of the frame $B$ is indicated by the heading angle $\psi$ between the $x$ and $X$ axes. The global position vector of the mass center is denoted by $^G\mathbf{d}$.
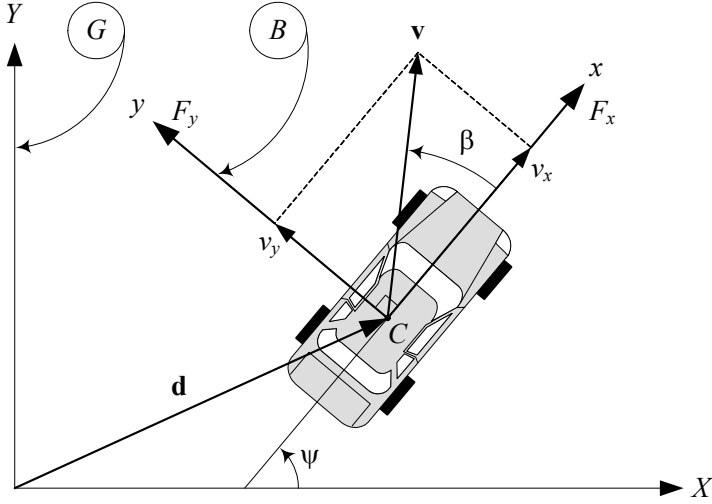
FIGURE 10.6. A rigid vehicle in a planar motion.

The velocity vector of the vehicle, expressed in the body frame, is

$$
{}^B\mathbf{v}_C = \begin{bmatrix} v_x \\ v_y \\ 0 \end{bmatrix} \tag{10.29}
$$

where $v_x$ is the forward component and $v_y$ is the lateral component of $\mathbf{v}$. The rigid body equations of motion in the body coordinate frame are:

$$
\begin{aligned}
{}^B\mathbf{F} &= {}^B R_G\, {}^G\mathbf{F} \\
&= {}^B R_G \left( m\, {}^G\mathbf{a}_B \right) \\
&= m\, {}^B_G\mathbf{a}_B \\
&= m\, {}^B\dot{\mathbf{v}}_B + m\, {}^B_G\boldsymbol{\omega}_B \times {}^B\mathbf{v}_B.
\end{aligned} \tag{10.30}
$$

$$
\begin{aligned}
{}^B\mathbf{M} &= \frac{{}^G d}{dt}\, {}^B\mathbf{L} \\
&= {}^B_G\dot{\mathbf{L}}_B \\
&= {}^B\dot{\mathbf{L}} + {}^B_G\boldsymbol{\omega}_B \times {}^B\mathbf{L} \\
&= {}^B I\, {}^B_G\dot{\boldsymbol{\omega}}_B + {}^B_G\boldsymbol{\omega}_B \times \left( {}^B I\, {}^B_G\boldsymbol{\omega}_B \right).
\end{aligned} \tag{10.31}
$$

The force, moment, and kinematic vectors for the rigid vehicle are:

$$
{}^B\mathbf{F}_C = \begin{bmatrix} F_x \\ F_y \\ 0 \end{bmatrix} \tag{10.32}
$$

$$
{}^B\mathbf{M}_C = \begin{bmatrix} 0 \\ 0 \\ M_z \end{bmatrix} \tag{10.33}
$$

$$
{}^B\dot{\mathbf{v}}_C = \begin{bmatrix} \dot{v}_x \\ \dot{v}_y \\ 0 \end{bmatrix} \tag{10.34}
$$

$$
{}^B_G\boldsymbol{\omega}_B = \begin{bmatrix} 0 \\ 0 \\ \omega_z \end{bmatrix} \tag{10.35}
$$

$$
{}^B_G\dot{\boldsymbol{\omega}}_B = \begin{bmatrix} 0 \\ 0 \\ \dot{\omega}_z \end{bmatrix}. \tag{10.36}
$$

We may assume that the body coordinate is the principal coordinate frame of the vehicle to have a diagonal moment of inertia matrix.

$$
{}^BI = \begin{bmatrix} I_1 & 0 & 0 \\ 0 & I_2 & 0 \\ 0 & 0 & I_3 \end{bmatrix} \tag{10.37}
$$

Substituting the above vectors and matrices in the equations of motion (10.30)-(10.31) provides the following equations:

$$
\begin{aligned}
{}^B\mathbf{F} &= m\,{}^B\dot{\mathbf{v}}_B + m\,{}^B_G\boldsymbol{\omega}_B \times {}^B\mathbf{v}_B \\
&= m \begin{bmatrix} \dot{v}_x \\ \dot{v}_y \\ 0 \end{bmatrix} + m \begin{bmatrix} 0 \\ 0 \\ \omega_z \end{bmatrix} \times \begin{bmatrix} v_x \\ v_y \\ 0 \end{bmatrix} \\
&= \begin{bmatrix} m\dot{v}_x - m\omega_z v_y \\ m\dot{v}_y + m\omega_z v_x \\ 0 \end{bmatrix} \tag{10.38}
\end{aligned}
$$

$$
\begin{aligned}
{}^B\mathbf{M} &= {}^BI\,{}^B_G\dot{\boldsymbol{\omega}}_B + {}^B_G\boldsymbol{\omega}_B \times \left( {}^BI\,{}^B_G\boldsymbol{\omega}_B \right) \\
&= \begin{bmatrix} I_1 & 0 & 0 \\ 0 & I_2 & 0 \\ 0 & 0 & I_3 \end{bmatrix} \begin{bmatrix} 0 \\ 0 \\ \dot{\omega}_z \end{bmatrix} \\
&\quad + \begin{bmatrix} 0 \\ 0 \\ \omega_z \end{bmatrix} \times \left( \begin{bmatrix} I_1 & 0 & 0 \\ 0 & I_2 & 0 \\ 0 & 0 & I_3 \end{bmatrix} \begin{bmatrix} 0 \\ 0 \\ \omega_z \end{bmatrix} \right) \\
&= \begin{bmatrix} 0 \\ 0 \\ I_3\dot{\omega}_z \end{bmatrix} \tag{10.39}
\end{aligned}
$$

The first two Newton equations (10.38) and the third Euler equation (10.39) are the only nonzero equations that make up the set of equations of motion (10.26)-(10.28) for the planar rigid vehicle. ∎

**Example 377** *Rigid vehicle and Lagrange method.*
   *The kinetic energy of a rigid vehicle in a planar motion is,*

$$
\begin{aligned}
K &= \frac{1}{2} {}^G\mathbf{v}_B^T \, m \, {}^G\mathbf{v}_B + \frac{1}{2} {}^G\boldsymbol{\omega}_B^T \, {}^G I \, {}^G\boldsymbol{\omega}_B \\[2mm]
&= \frac{1}{2}
\begin{bmatrix} v_X \\ v_Y \\ 0 \end{bmatrix}^T
m
\begin{bmatrix} v_X \\ v_Y \\ 0 \end{bmatrix}
+ \frac{1}{2}
\begin{bmatrix} 0 \\ 0 \\ \omega_Z \end{bmatrix}^T
{}^G I
\begin{bmatrix} 0 \\ 0 \\ \omega_Z \end{bmatrix} \\[2mm]
&= \frac{1}{2} m v_X^2 + \frac{1}{2} m v_Y^2 + \frac{1}{2} I_3 \omega_Z^2 \\[2mm]
&= \frac{1}{2} m \left( \dot{X}^2 + \dot{Y}^2 \right) + \frac{1}{2} I_z \, \dot{\psi}^2 \qquad\qquad (10.40)
\end{aligned}
$$

*where,*

$$
\begin{aligned}
{}^G I &= {}^G R_B \, {}^B I \, {}^G R_B^T \\[2mm]
&=
\begin{bmatrix}
\cos\psi & -\sin\psi & 0 \\
\sin\psi & \cos\psi & 0 \\
0 & 0 & 1
\end{bmatrix}
\begin{bmatrix}
I_1 & 0 & 0 \\
0 & I_2 & 0 \\
0 & 0 & I_3
\end{bmatrix}
\begin{bmatrix}
\cos\psi & -\sin\psi & 0 \\
\sin\psi & \cos\psi & 0 \\
0 & 0 & 1
\end{bmatrix}^T \\[2mm]
&=
\begin{bmatrix}
I_1 \cos^2\psi + I_2 \sin^2\psi & (I_1 - I_2)\sin\psi\cos\psi & 0 \\
(I_1 - I_2)\sin\psi\cos\psi & I_2 \cos^2\psi + I_1 \sin^2\psi & 0 \\
0 & 0 & I_3
\end{bmatrix} \qquad (10.41)
\end{aligned}
$$

*and*

$$
{}^G\mathbf{v}_B =
\begin{bmatrix} v_X \\ v_Y \\ 0 \end{bmatrix}
=
\begin{bmatrix} \dot{X} \\ \dot{Y} \\ 0 \end{bmatrix}
\qquad\qquad (10.42)
$$

$$
{}^G\boldsymbol{\omega}_B =
\begin{bmatrix} 0 \\ 0 \\ \omega_Z \end{bmatrix}
=
\begin{bmatrix} 0 \\ 0 \\ r \end{bmatrix}
=
\begin{bmatrix} 0 \\ 0 \\ \dot{\psi} \end{bmatrix} .
\qquad\qquad (10.43)
$$

   *The resultant external force system are:*

$$
{}^G\mathbf{F}_C =
\begin{bmatrix} F_X \\ F_Y \\ 0 \end{bmatrix}
\qquad\qquad (10.44)
$$

$$
{}^G\mathbf{M}_C =
\begin{bmatrix} 0 \\ 0 \\ M_Z \end{bmatrix} .
\qquad\qquad (10.45)
$$

*Applying the Lagrange method*

$$
\frac{d}{dt}\left( \frac{\partial K}{\partial \dot{q}_i} \right) - \frac{\partial K}{\partial q_i} = F_i \qquad i = 1, 2, \cdots n
\qquad\qquad (10.46)
$$

*and using the coordinates $X$, $Y$, and $\psi$ for $q_i$, generates the following equations of motion in the global coordinate frame:*

$$m \frac{d}{dt}\dot{X} = F_X \tag{10.47}$$

$$m \frac{d}{dt}\dot{Y} = F_Y \tag{10.48}$$

$$I_z \frac{d}{dt}\dot{\psi} = M_Z \tag{10.49}$$

**Example 378** *Transforming to the body coordinate frame.*

*We may find the rigid vehicle's equations of motion in the body coordinate frame by expressing the global equations of motion (10.47)-(10.49) in the vehicle's body coordinate $B$, using the transformation matrix $^G R_B$.*

$$^G R_B = \begin{bmatrix} \cos\psi & -\sin\psi & 0 \\ \sin\psi & \cos\psi & 0 \\ 0 & 0 & 1 \end{bmatrix} \tag{10.50}$$

*The velocity vector is equal to*

$$^G\mathbf{v}_C = {}^G R_B \, {}^B\mathbf{v}_C \tag{10.51}$$

$$\begin{bmatrix} v_X \\ v_Y \\ 0 \end{bmatrix} = \begin{bmatrix} \cos\psi & -\sin\psi & 0 \\ \sin\psi & \cos\psi & 0 \\ 0 & 0 & 1 \end{bmatrix} \begin{bmatrix} v_x \\ v_y \\ 0 \end{bmatrix}$$

$$= \begin{bmatrix} v_x \cos\psi - v_y \sin\psi \\ v_y \cos\psi + v_x \sin\psi \\ 0 \end{bmatrix} \tag{10.52}$$

*and therefore, the global acceleration components are*

$$\begin{bmatrix} \dot{v}_X \\ \dot{v}_Y \\ 0 \end{bmatrix} = \begin{bmatrix} \left(\dot{v}_x - \dot{\psi}\, v_y\right)\cos\psi - \left(\dot{v}_y + \dot{\psi}\, v_x\right)\sin\psi \\ \left(\dot{v}_y + \dot{\psi}\, v_x\right)\cos\psi + \left(\dot{v}_x - \dot{\psi}\, v_y\right)\sin\psi \\ 0 \end{bmatrix}. \tag{10.53}$$

*The global Newton's equation of motion is*

$$^G\mathbf{F}_C = m \, {}^G\dot{\mathbf{v}}_C$$

*and the force vector transformation is*

$$^G\mathbf{F}_C = {}^G R_B \, {}^B\mathbf{F}_C \tag{10.54}$$

*therefore, the body coordinate expression for the equations of motion is*

$$^B\mathbf{F}_C = {}^G R_B^T \, {}^G\mathbf{F}_C$$
$$= m \, {}^G R_B^T \, {}^G\dot{\mathbf{v}}_C. \tag{10.55}$$

*Substituting the associated vectors generates the Newton equations of motion in the body coordinate frame.*

$$\begin{bmatrix} F_x \\ F_y \\ 0 \end{bmatrix} = m\,{}^G R_B^T \begin{bmatrix} \left(\dot{v}_x - \dot{\psi}\,v_y\right)\cos\psi - \left(\dot{v}_y + \dot{\psi}\,v_x\right)\sin\psi \\ \left(\dot{v}_y + \dot{\psi}\,v_x\right)\cos\psi + \left(\dot{v}_x - \dot{\psi}\,v_y\right)\sin\psi \\ 0 \end{bmatrix}$$

$$= m\begin{bmatrix} \dot{v}_x - \dot{\psi}\,v_y \\ \dot{v}_y + \dot{\psi}\,v_x \\ 0 \end{bmatrix} \tag{10.56}$$

*Applying the same procedure for moment transformation,*

$$\begin{aligned} {}^G\mathbf{M}_C &= {}^G R_B\,{}^B\mathbf{M}_C \\ \begin{bmatrix} 0 \\ 0 \\ M_Z \end{bmatrix} &= \begin{bmatrix} \cos\psi & -\sin\psi & 0 \\ \sin\psi & \cos\psi & 0 \\ 0 & 0 & 1 \end{bmatrix}\begin{bmatrix} 0 \\ 0 \\ M_z \end{bmatrix} \\ &= \begin{bmatrix} 0 \\ 0 \\ M_z \end{bmatrix} \end{aligned} \tag{10.57}$$

*we find the Euler equation in the body coordinate frame.*

$$M_z = \dot{\omega}_z\,I_z \tag{10.58}$$

**Example 379** *Vehicle path.*
    *When we find the translational and rotational velocities of a rigid vehicle, $v_x$, $v_y$, $r$, we may find the path of motion for the vehicle by integration.*

$$\psi = \psi_0 + \int r\,dt \tag{10.59}$$

$$x = \int \left(v_x\cos\psi - v_y\sin\psi\right)dt \tag{10.60}$$

$$y = \int \left(v_x\sin\psi + v_y\cos\psi\right)dt \tag{10.61}$$

**Example 380** ★ *Equations of motion using principal method.*
    *The equations of motion for a rigid vehicle in a planar motion may also be found by principle of differential calculus. Consider a vehicle at time $t = 0$ that has a lateral velocity $v_y$, a yaw rate $r$, and a forward velocity $v_x$. The longitudinal x-axis makes angle $\psi$ with a fixed X-axis as shown in Figure 10.7. Point $P(x, y)$ indicates a general point of the vehicle. The velocity components of point $P$ are*

$$v_{Px} = v_x - y\,r \tag{10.62}$$

$$v_{Py} = v_y + x\,r \tag{10.63}$$
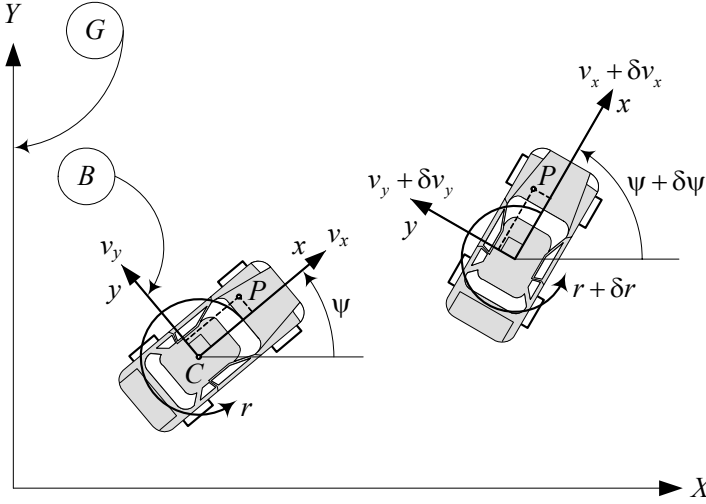
FIGURE 10.7. A vehicle at time $t = 0$ and $t = dt$ moving with a lateral velocity $v_y$, a yaw rate $r$, and a forward velocity $v_x$ at a heading angle $\psi$.

*because*

$$
\begin{aligned}
{}^B\mathbf{v}_P &= {}^B\mathbf{v}_C + {}^B_G\boldsymbol{\omega}_B \times {}^B\mathbf{r}_P \\
&= \begin{bmatrix} v_x \\ v_y \\ 0 \end{bmatrix} + \begin{bmatrix} 0 \\ 0 \\ r \end{bmatrix} \times \begin{bmatrix} x \\ y \\ 0 \end{bmatrix}. 
\end{aligned} \tag{10.64}
$$

*After an increment of time, at $t = dt$, the vehicle has moved to a new position. The velocity components of point $P$ at the second position are*

$$
\begin{aligned}
v'_{Px} &= (v_x + dv_x) - y(r + dr) & (10.65) \\
v'_{Py} &= (v_y + dv_y) + x(r + dr). & (10.66)
\end{aligned}
$$

*However,*

$$
\begin{aligned}
v_{Px} + dv_{Px} &= v'_{Px}\cos d\psi - v'_{Py}\sin d\psi & (10.67) \\
v_{Py} + dv_{Py} &= v'_{Px}\sin d\psi + v'_{Py}\cos d\psi. & (10.68)
\end{aligned}
$$

*and therefore,*

$$
\begin{aligned}
dv_{Px} &= [(v_x + dv_x) - y(r + dr)]\cos d\psi \\
&\quad - [(v_y + dv_y) + x(r + dr)]\sin d\psi - (v_x - y\,r) \quad (10.69) \\
dv_{Py} &= [(v_x + dv_x) - y(r + dr)]\sin d\psi \\
&\quad + [(v_y + dv_y) + x(r + dr)]\cos d\psi - (v_y + x\,r). \quad (10.70)
\end{aligned}
$$

*We simplify Equations (10.69) and (10.70) and divide them by dt.*

$$\frac{dv_{Px}}{dt} = \frac{1}{dt}\left([dv_x - y\,dr]\cos d\psi\right)$$
$$-\frac{1}{dt}\left([(v_y + dv_y) + x\,(r + dr)]\sin d\psi\right) \qquad (10.71)$$

$$\frac{dv_{Py}}{dt} = \frac{1}{dt}\left([dv_y + x\,dr]\cos d\psi\right)$$
$$+\frac{1}{dt}\left([(v_x + dv_x) - y\,(r + dr)]\sin d\psi\right). \qquad (10.72)$$

*When dt → 0, then* $\sin d\psi \to \psi$ *and* $\cos d\psi \to 1$, *and we may substitute* $\dot\psi = r$ *to get the acceleration components of point P.*

$$\dot v_{Px} = a_{Px} = \dot v_x - v_y\,r - y\,\dot r + x\,r^2 \qquad (10.73)$$
$$\dot v_{Py} = a_{Py} = \dot v_y + v_x\,r + x\,\dot r - y\,r^2 \qquad (10.74)$$

*Let's assume point P has a small mass dm. Multiplying dm by the acceleration components of point P and integrating over the whole rigid vehicle must be equal to the applied external force system.*

$$F_x = \int_m a_{Px}\,dm \qquad (10.75)$$

$$F_y = \int_m a_{Py}\,dm \qquad (10.76)$$

$$M_z = \int_m (x\,a_{Py} - y\,a_{Px})\,dm \qquad (10.77)$$

*Substituting for accelerations and assuming the body coordinate frame is the principal frame at the mass center C, we find*

$$F_x = \int_m \left(\dot v_x - v_y\,r - y\,\dot r + x\,r^2\right) dm$$
$$= m\,(\dot v_x - v_y\,r) - \dot r \int_m y\,dm + r^2 \int_m x\,dm$$
$$= m\,(\dot v_x - v_y\,r) \qquad (10.78)$$

$$F_y = \int_m \left(\dot v_y + v_x\,r + x\,\dot r - y\,r^2\right) dm$$
$$= m\,(\dot v_y + v_x\,r) + \dot r \int_m x\,dm - r^2 \int_m y\,dm$$
$$= m\,(\dot v_y + v_x\,r) \qquad (10.79)$$

$$M_z = \int_m \left( x \left( \dot{v}_y + v_x\, r + x\, \dot{r} - y\, r^2 \right) - y \left( \dot{v}_x - v_y\, r - y\, \dot{r} + x\, r^2 \right) \right)\, dm$$

$$= \dot{r} \int_m \left( x^2 + y^2 \right)\, dm + \left( \dot{v}_y + v_x\, r \right) \int_m x\, dm$$

$$- \left( \dot{v}_x - v_y\, r \right) \int_m y\, dm - 2 r^2 \int_m xy\, dm$$

$$= I_z\, \dot{r} \tag{10.80}$$

*because for a principal coordinate frame we have*

$$\int_m x\, dm = 0 \tag{10.81}$$

$$\int_m y\, dm = 0 \tag{10.82}$$

$$\int_m xy\, dm = 0. \tag{10.83}$$

## 10.3 Force System Acting on a Rigid Vehicle

To determine the force system on a rigid vehicle, first we define the force system at the tireprint of a wheel. The lateral force at the tireprint depends on the sideslip angle. Then, we transform and apply the tire force system on the body of the vehicle.

### 10.3.1 Tire Force and Body Force Systems

Figure 10.8 depicts wheel number 1 of a vehicle. The components of the force system in the $xy$-plane applied on a rigid vehicle, because of the generated forces at the tireprint of the wheel number $i$, are

$$F_{x_i} = F_{x_{w_i}} \cos \delta_i - F_{y_{w_i}} \sin \delta_i \tag{10.84}$$

$$F_{y_i} = F_{y_{w_i}} \cos \delta_i + F_{x_{w_i}} \sin \delta_i \tag{10.85}$$

$$M_{z_i} = M_{z_{w_i}} + x_i F_{y_i} - y_i F_{x_i}. \tag{10.86}$$

Therefore, the total planar force system on the rigid vehicle in the body coordinate frame is

$$^B F_x = \sum_i F_{x_i}$$
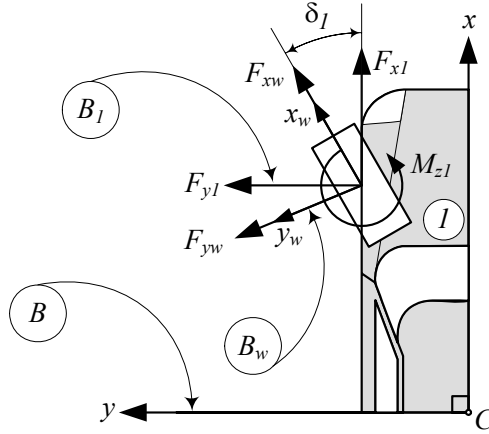
$$= \sum_i F_{x_w} \cos \delta_i - \sum_i F_{y_w} \sin \delta_i \tag{10.87}$$

FIGURE 10.8. The force system at the tireprint of tire number 1.

$$^{B}F_y = \sum_i F_{y_i}$$

$$= \sum_i F_{y_w} \cos \delta_i + \sum_i F_{x_w} \sin \delta_i \qquad (10.88)$$

$$^{B}M_z = \sum_i M_{z_i} + \sum_i x_i F_{y_i} - \sum_i y_i F_{x_i}. \qquad (10.89)$$

**Proof.** The coordinate frame of the wheel is a local coordinate called the *wheel frame* shown by $T(x_w, y_w, z_w)$ or $B_w$. For simplicity, we ignore the difference between the tire frame at the center of tireprint and wheel frame at the wheel center. The force system generated at the tireprint in the wheel frame is

$$^{B_w}\mathbf{F}_w = F_{x_w}\hat{\imath}_1 + F_{y_w}\hat{\jmath}_1 \qquad (10.90)$$

$$^{B_w}\mathbf{M}_w = M_{z_w}\hat{k}_1 \qquad (10.91)$$

where

$$F_{x_w} = F_{x_{w_1}} - F_{r_1}\cos\alpha \qquad (10.92)$$

$$F_{y_w} = F_{y_{w_1}} - F_{r_1}\sin\alpha \qquad (10.93)$$

$$M_{z_w} = M_{z_{w_1}} \qquad (10.94)$$

The wheel force in the $x_w$-direction, $F_{x_w}$, is a combination of the longitudinal force $F_{x_{w_1}}$, defined by (3.96) or (4.59), and the tire roll resistance $F_{r_1}$ defined in (3.64). The wheel force in the $y_w$-direction, $F_{y_w}$, is a combination of the lateral force $F_{y_{w_1}}$ defined by (3.130) and (3.153), and the tire roll resistance $F_{r_1}$ defined in (3.64). The wheel moment in the $z_w$-direction,

$M_{z_w}$, is a combination of the aligning moment $M_{z_{w_1}}$ defined by (3.133) and (3.160).

The rotation matrix between the wheel frame $B_w$ and the wheel-body coordinate frame $B_1$, parallel to the vehicle coordinate frame $B$, is

$$^{B_1}R_{B_w} = \begin{bmatrix} \cos\delta_1 & -\sin\delta_1 \\ \sin\delta_1 & \cos\delta_1 \end{bmatrix} \tag{10.95}$$

and therefore, the force system at the tireprint of the wheel, parallel to the vehicle coordinate frame, is

$$
\begin{aligned}
{}^{B_1}\mathbf{F}_w &= {}^{B}R_{B_w}{}^{B_w}\mathbf{F}_w \\
\begin{bmatrix} F_{x_1} \\ F_{y_1} \end{bmatrix} &= \begin{bmatrix} \cos\delta_1 & -\sin\delta_1 \\ \sin\delta_1 & \cos\delta_1 \end{bmatrix} \begin{bmatrix} F_{x_w} \\ F_{y_w} \end{bmatrix} \\
&= \begin{bmatrix} F_{x_w}\cos\delta_1 - F_{y_w}\sin\delta_1 \\ F_{y_w}\cos\delta_1 + F_{x_w}\sin\delta_1 \end{bmatrix}
\end{aligned} \tag{10.96}
$$

$$
\begin{aligned}
{}^{B_1}\mathbf{M}_w &= {}^{B_1}R_{B_w}{}^{B_w}\mathbf{M}_w \\
M_{z_1} &= M_{z_w}.
\end{aligned} \tag{10.97}
$$

Transforming the force system of each tire to the body coordinate frame $B$, located at the body mass center $C$, generates the total force system applied on the vehicle

$$^{B}\mathbf{F} = \sum_i F_{x_i}\,\hat{\imath} + \sum_i F_{y_i}\,\hat{\jmath} \tag{10.98}$$

$$^{B}\mathbf{M} = \sum_i M_{z_i}\,\hat{k} + \sum_i {}^{B}\mathbf{r}_i \times {}^{B}\mathbf{F}_{w_i} \tag{10.99}$$

where, $^{B}\mathbf{r}_i$ is the position vector of the wheel number $i$.

$$^{B}\mathbf{r}_i = x_i\hat{\imath} + y_i\hat{\jmath} + z_i\hat{k} \tag{10.100}$$

Expanding Equations (10.98) and (10.99) provides the total planar force system.

$$^{B}F_x = \sum_i F_{x_w}\cos\delta_i - \sum_i F_{y_w}\sin\delta_i \tag{10.101}$$

$$^{B}F_y = \sum_i F_{y_w}\cos\delta_i + \sum_i F_{x_w}\sin\delta_i \tag{10.102}$$

$$^{B}M_z = \sum_i M_{z_i} + \sum_i x_i F_{y_i} - \sum_i y_i F_{x_i} \tag{10.103}$$

∎
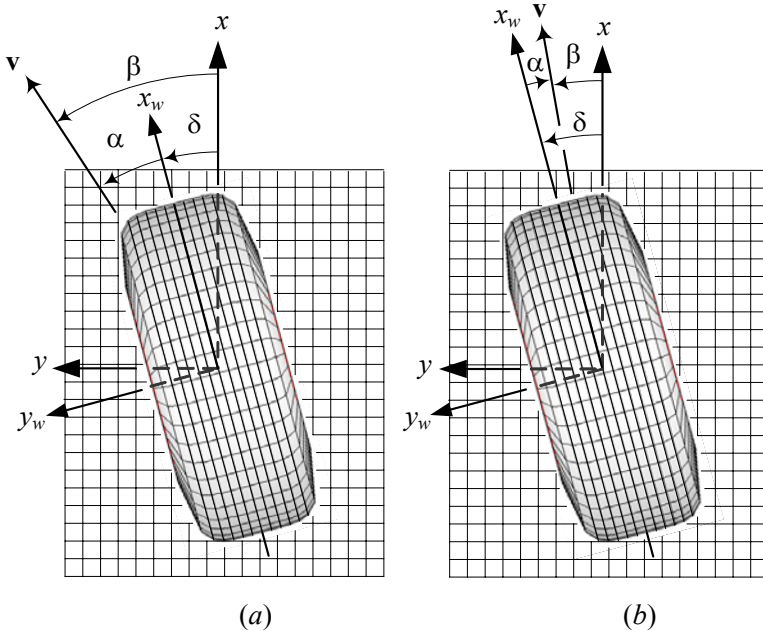
FIGURE 10.9. Angular orientation of a moving tire along the velocity vector $\mathbf{v}$ at a sideslip angle $\alpha$ and a steer angle $\delta$.

## 10.3.2   Tire Lateral Force

Figure 10.9(a) illustrates a tire, moving along the velocity vector $\mathbf{v}$ at a sideslip angle $\alpha$. The tire is steered by the steer angle $\delta$. If the angle between the velocity vector $\mathbf{v}$ and the vehicle $x$-axis is shown by $\beta$, then

$$\alpha = \beta - \delta. \tag{10.104}$$

The lateral force, generated by a tire, is dependent on sideslip angle $\alpha$ that is proportional to the sideslip for small $\alpha$.

$$
\begin{aligned}
F_y &= -C_\alpha\,\alpha \\
&= -C_\alpha\,(\beta - \delta)
\end{aligned}
\tag{10.105}
$$

**Proof.** A tire coordinate frame $B_w(x_w, y_w)$ is attached to the tire at the center of tireprint as shown in Figure 10.9(a). The orientation of the tire frame is measured with respect to another coordinate frame, parallel to the vehicle frame $B(x, y)$. The angle between the $x$ and $x_w$ axes is the tire steer angle $\delta$, measured about the $z$-axis. The tire is moving along the tire velocity vector $\mathbf{v}$. The angle between the $x_w$-axis and $\mathbf{v}$ is the sideslip angle

$\alpha$, and the angle between the body $x$-axis is the *global sideslip angle* $\beta$. The angles $\alpha$, $\beta$, and $\delta$ in Figure 10.9(a) are positive. The Figure shows that

$$\alpha = \beta - \delta. \tag{10.106}$$

Practically, when a steered tire is moving forward, the relationship between the angles $\alpha$, $\beta$, and $\delta$ are such that the velocity vector sits between the $x$ and $x_w$ axes. A practical situation is shown in Figure 10.9(b). A steer angle will turn the heading of the tire by a $\delta$ angle. However, because of tire flexibility, the velocity vector of the tire is lazier than the heading and turns by a $\beta$ angle, where $\beta < \delta$. So, a positive steer angle generates a negative sideslip angle. Analysis of Figure 10.9(b) and using the definition for positive direction of the angles, shows that under a practical situation we have the same relation (10.104).

According to (3.131), the existence of a sideslip angle is sufficient to generate a lateral force $F_y$, which is proportional to $\alpha$ when the angle is small.

$$F_y = -C_\alpha \, \alpha \tag{10.107}$$

∎

## 10.3.3  Two-wheel Model and Body Force Components

Figure 10.10 illustrates the forces in the $xy$-plane acting at the tireprints of a front-wheel-steering four-wheel vehicle. When we ignore the roll motion of the vehicle, the $xy$-plane remains parallel to the road's $XY$-plane, and we may use a *two-wheel model* for the vehicle. Figure 10.11 illustrates a two-wheel model for a vehicle with no roll motion. The two-wheel model is also called a *bicycle model*, although a two-wheel model does not act similar to a bicycle.

The force system applied on a two-wheel vehicle, in which only the front wheel is steerable, is

$$\begin{align}
F_x &= F_{x_f} \cos \delta + F_{x_r} - F_{y_f} \sin \delta \tag{10.108}\\
F_y &= F_{y_f} \cos \delta + F_{y_r} + F_{x_f} \sin \delta \tag{10.109}\\
M_z &= a_1 F_{y_f} - a_2 F_{y_r} \tag{10.110}
\end{align}$$

where, $\left( F_{x_f}, F_{x_r} \right)$ and $\left( F_{y_f}, F_{y_r} \right)$ are the planar forces on the tireprint of the front and rear wheels. The force system may be approximated by the following equations, if the steer angle $\delta$ is assumed small:

$$\begin{align}
F_x &\approx F_{x_f} + F_{x_r} \tag{10.111}\\
F_y &\approx F_{y_f} + F_{y_r} \tag{10.112}\\
M_z &\approx a_1 F_{y_f} - a_2 F_{y_r} \tag{10.113}
\end{align}$$
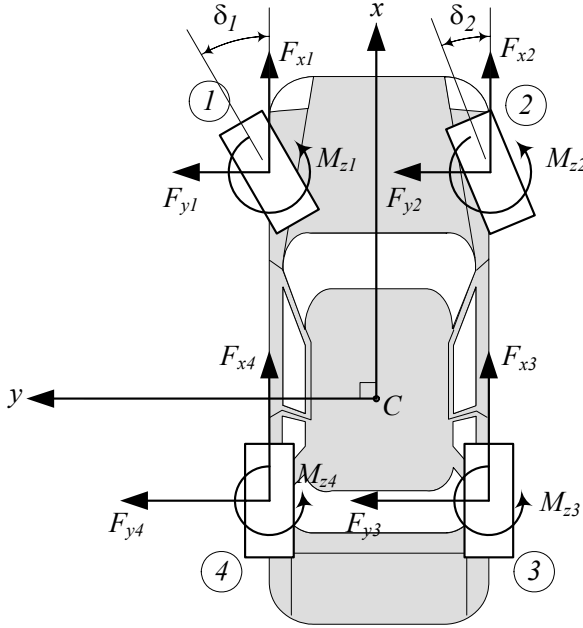
FIGURE 10.10. A front-wheel-steering four-wheel vehicle and the forces in the $xy$-plane acting at the trireprints.

The vehicle lateral force $F_y$ and moment $M_z$ depend on only the front and rear wheels' lateral forces $F_{y_f}$ and $F_{y_r}$, which are functions of the wheels sideslip angles $\alpha_f$ and $\alpha_r$. They can be approximated by the following equations:

$$F_y = \left(-\frac{a_1}{v_x}C_{\alpha f} + \frac{a_2}{v_x}C_{\alpha r}\right)r - (C_{\alpha f} + C_{\alpha r})\beta + C_{\alpha f}\delta \tag{10.114}$$

$$M_z = \left(-\frac{a_1^2}{v_x}C_{\alpha f} - \frac{a_2^2}{v_x}C_{\alpha r}\right)r - (a_1 C_{\alpha f} - a_2 C_{\alpha r})\beta + a_1 C_{\alpha f}\delta \tag{10.115}$$

where $C_{\alpha f} = C_{\alpha f_L} + C_{\alpha f_R}$ and $C_{\alpha r} = C_{\alpha r_L} + C_{\alpha r_R}$ are equal to the sideslip coefficients of the left and right wheels in front and rear, respectively.

$$C_{\alpha f} = C_{\alpha f_L} + C_{\alpha f_R} \tag{10.116}$$

$$C_{\alpha r} = C_{\alpha r_L} + C_{\alpha r_R} \tag{10.117}$$

**Proof.** For the two-wheel vehicle, we use the cot-average (7.3) of the outer and inner steer angles as the only steer angle $\delta$.

$$\cot\delta = \frac{\cot\delta_o + \cot\delta_i}{2} \tag{10.118}$$
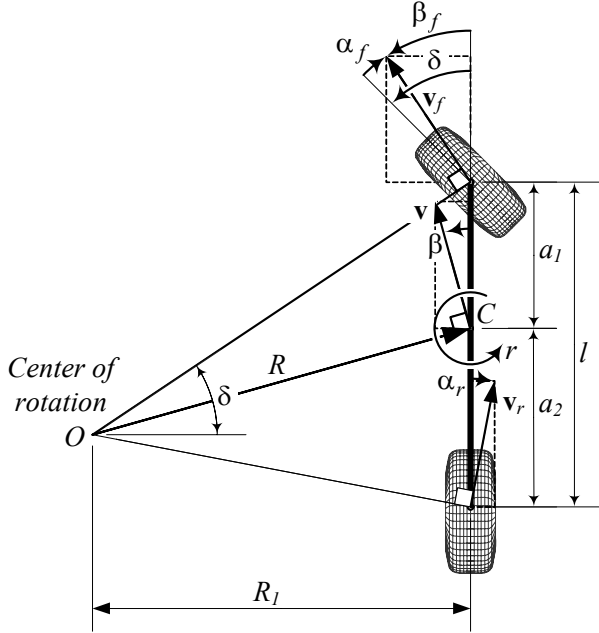
FIGURE 10.11. A two-wheel model for a vehicle moving with no roll.

Furthermore, we define a single sideslip coefficient $C_{\alpha f}$ and $C_{\alpha r}$ as (10.116) and (10.117) for the front and rear wheels. The coefficient $C_{\alpha f}$ and $C_{\alpha r}$ are equal to the sum of the left and right wheels' sideslip coefficients.

Employing Equations (10.87)-(10.89) and ignoring the aligning moments $M_{z_i}$, the applied forces on the two-wheel vehicle are:

$$
\begin{aligned}
F_x &= F_{x_1}\cos\delta_1 + F_{x_2}\cos\delta_2 - F_{y_1}\sin\delta_1 - F_{y_2}\sin\delta_2 \\
&= F_{x_f}\cos\delta + F_{x_r} - F_{y_f}\sin\delta & (10.119) \\
F_y &= F_{y_1}\cos\delta_1 + F_{y_2}\cos\delta_2 + F_{x_1}\sin\delta_1 + F_{x_2}\sin\delta_2 \\
&= F_{y_f}\cos\delta + F_{y_r} + F_{x_f}\sin\delta & (10.120) \\
M_z &= a_1 F_{y_f} - a_2 F_{y_r} & (10.121)
\end{aligned}
$$

The force equations can be approximated by the following equations, if we assume $\delta$ small.

$$
\begin{aligned}
F_x &\approx F_{x_f} + F_{x_r} & (10.122) \\
F_y &\approx F_{y_r} + F_{y_r} & (10.123) \\
M_z &\approx a_1 F_{y_f} - a_2 F_{y_r} & (10.124)
\end{aligned}
$$

Assume the wheel number $i$ of a rigid vehicle is located at $(x_i, y_i)$ in the

body coordinate frame. The velocity of the wheel number $i$ is

$$^B\mathbf{v}_i = {}^B\mathbf{v} + {}^B\dot{\boldsymbol{\psi}} \times {}^B\mathbf{r}_i \tag{10.125}$$

in which $^B\mathbf{r}_i$ is the position vector of the wheel number $i$, $^B\mathbf{v}$ is the velocity vector of the vehicle at its mass center $C$, and $^B\dot{\boldsymbol{\psi}} = r\hat{k}$ is the yaw rate of the vehicle. Expanding Equation (10.125) provides the following velocity vector for the wheel number $i$ expressed in the vehicle coordinate frame at $C$.

$$
\begin{bmatrix} v_{x_i} \\ v_{y_i} \\ 0 \end{bmatrix} = \begin{bmatrix} v_x \\ v_y \\ 0 \end{bmatrix} + \begin{bmatrix} 0 \\ 0 \\ \dot{\psi} \end{bmatrix} \times \begin{bmatrix} x_i \\ y_i \\ 0 \end{bmatrix}
$$

$$
= \begin{bmatrix} v_x - y_i\,\dot{\psi} \\ v_y + x_i\,\dot{\psi} \\ 0 \end{bmatrix} \tag{10.126}
$$

The global sideslip $\beta_i$ for the wheel $i$, is the angle between the wheel velocity vector $\mathbf{v}_i$ and the vehicle body $x$-axis.

$$\beta_i = \tan^{-1}\left(\frac{v_{y_i}}{v_{x_i}}\right) \tag{10.127}$$

$$= \tan^{-1}\left(\frac{v_y + x_i\,\dot{\psi}}{v_x - y_i\,\dot{\psi}}\right) \tag{10.128}$$

If the wheel number $i$ has a steer angle $\delta_i$ then, its local sideslip angle $\alpha_i$, that generates a lateral force $F_{y_w}$ on the tire, is

$$\alpha_i = \beta_i - \delta_i$$

$$= \tan^{-1}\left(\frac{v_y + x_i\dot{\psi}}{v_x - y_i\dot{\psi}}\right) - \delta_i. \tag{10.129}$$

The global sideslip angles $\beta_i$ for the front and rear wheels of a two-wheel vehicle, $\beta_f$ and $\beta_r$, are

$$\beta_f = \tan^{-1}\left(\frac{v_{y_f}}{v_{x_f}}\right)$$

$$= \tan^{-1}\left(\frac{v_y + a_1\,r}{v_x}\right) \tag{10.130}$$

$$\beta_r = \tan^{-1}\left(\frac{v_{y_r}}{v_{x_r}}\right)$$

$$= \tan^{-1}\left(\frac{v_y - a_2\,r}{v_x}\right) \tag{10.131}$$

and the vehicle sideslip angle $\beta$ is

$$\beta = \tan^{-1}\left(\frac{v_y}{v_x}\right). \tag{10.132}$$

Assuming small angles for global sideslips $\beta_f$, $\beta$, and $\beta_r$, the local sideslip angles for the front and rear wheels, $\alpha_f$ and $\alpha_r$, may be approximated as

$$\begin{aligned}
\alpha_f &= \beta_f - \delta \\
&= \frac{1}{v_x}(v_y + a_1 r) - \delta \\
&= \beta + \frac{a_1 r}{v_x} - \delta \tag{10.133} \\
\alpha_r &= \frac{1}{v_x}(v_y - a_2 r) \\
&= \beta - \frac{a_2 r}{v_x}. \tag{10.134}
\end{aligned}$$

When the sideslip angles are small, the associated lateral forces are

$$\begin{aligned}
F_{yf} &= -C_{\alpha f}\,\alpha_f \tag{10.135} \\
F_{yr} &= -C_{\alpha r}\,\alpha_r \tag{10.136}
\end{aligned}$$

and therefore, the second and third equations of motion (10.112) and (10.113) can be written as

$$\begin{aligned}
F_y &= F_{yf} + F_{yr} \\
&= -C_{\alpha f}\,\alpha_f - C_{\alpha r}\,\alpha_r \\
&= -C_{\alpha f}\left(\frac{1}{v_x}(v_y + a_1 r) - \delta\right) - C_{\alpha r}\left(\beta - \frac{a_2 r}{v_x}\right) \tag{10.137} \\
M_z &= a_1 F_{yf} - a_2 F_{yr} \\
&= -C_{\alpha f}\,\alpha_f - C_{\alpha r}\,\alpha_r \\
&= -C_{\alpha f}\,\alpha_f\left(\frac{1}{v_x}(v_y + a_1 r) - \delta\right) - C_{\alpha r}\,\alpha_r\left(\beta - \frac{a_2 r}{v_x}\right) \tag{10.138}
\end{aligned}$$

which reduce to the force system

$$F_y = \left(-\frac{a_1}{v_x}C_{\alpha f} + \frac{a_2}{v_x}C_{\alpha r}\right)r - (C_{\alpha f} + C_{\alpha r})\beta + C_{\alpha f}\delta \tag{10.139}$$

$$M_z = \left(-\frac{a_1^2}{v_x}C_{\alpha f} - \frac{a_2^2}{v_x}C_{\alpha r}\right)r - (a_1 C_{\alpha f} - a_2 C_{\alpha r})\beta + a_1 C_{\alpha f}\delta. \tag{10.140}$$

The parameters $C_{\alpha f}$, $C_{\alpha r}$ are the sideslip stiffness for the front and rear wheels, $r$ is the yaw rate, $\delta$ is the steer angle, and $\beta$ is the sideslip angle of the vehicle.

These equations are dependent on three parameters, $r$, $\beta$, $\delta$, and may be written as

$$
\begin{aligned}
F_y &= F_y\left(r, \beta, \delta\right) \\
&= \frac{\partial F_y}{\partial r} r + \frac{\partial F_y}{\partial \beta} \beta + \frac{\partial F_y}{\partial \delta} \delta \\
&= C_r\, r + C_\beta\, \beta + C_\delta\, \delta
\end{aligned}
\tag{10.141}
$$

$$
\begin{aligned}
M_z &= M_z\left(r, \beta, \delta\right) \\
&= \frac{\partial M_z}{\partial r} r + \frac{\partial M_z}{\partial \beta} \beta + \frac{\partial M_z}{\partial \delta} \delta \\
&= D_r\, r + D_\beta\, \beta + D_\delta\, \delta
\end{aligned}
\tag{10.142}
$$

where the *force system coefficients* are

$$
C_r = \frac{\partial F_y}{\partial r} = -\frac{a_1}{v_x} C_{\alpha f} + \frac{a_2}{v_x} C_{\alpha r}
\tag{10.143}
$$

$$
C_\beta = \frac{\partial F_y}{\partial \beta} = -\left(C_{\alpha f} + C_{\alpha r}\right)
\tag{10.144}
$$

$$
C_\delta = \frac{\partial F_y}{\partial \delta} = C_{\alpha f}
\tag{10.145}
$$

$$
D_r = \frac{\partial M_z}{\partial r} = -\frac{a_1^2}{v_x} C_{\alpha f} - \frac{a_2^2}{v_x} C_{\alpha r}
\tag{10.146}
$$

$$
D_\beta = \frac{\partial M_z}{\partial \beta} = -\left(a_1 C_{\alpha f} - a_2 C_{\alpha r}\right)
\tag{10.147}
$$

$$
D_\delta = \frac{\partial M_z}{\partial \delta} = a_1 C_{\alpha f}.
\tag{10.148}
$$

The coefficients $C_r$, $C_\beta$, $C_\delta$, $D_r$, $D_\beta$, and $D_\delta$ are slopes of the curves for lateral force $F_y$ and yaw moment $M_z$ as a function of $r$, $\beta$, and $\delta$ respectively.
■

**Example 381** *Physical significance of the coefficients $C_r$, $C_\beta$, $C_\delta$, $D_r$, $D_\beta$, and $D_\delta$.*

*Assuming a steady-state condition and constant values for $r$, $\beta$, $\delta$, $C_{\alpha f}$, and $C_{\alpha r}$, the lateral force $F_y$ and the yaw moment $M_z$ can be written as a superposition of three independent forces proportional to $r$, $\beta$, and $\delta$.*

$$
F_y = C_r\, r + C_\beta\, \beta + C_\delta\, \delta
\tag{10.149}
$$
$$
M_z = D_r\, r + D_\beta\, \beta + D_\delta\, \delta
\tag{10.150}
$$

*$C_r$ indicates the proportionality between the lateral force $F_y$ and the yaw rate $r$. The value of $C_r$ decreases by increasing the forward velocity of the vehicle, $v_x$. The sign of $C_r$ is the same as the sign of $D_\beta$.*

$C_\beta$ indicates the proportionality between the lateral force $F_y$ and the vehicle sideslip angle $\beta$. It is the lateral stiffness for the whole vehicle and acts similarly to the lateral stiffness of tires $C_\alpha$. $C_\beta$ is always negative.

$C_\delta$ indicates the proportionality between the lateral force $F_y$ and the steer angle $\delta$. $C_\delta$ is always negative and generates greater lateral force by increasing the steer angle.

$D_r$ indicates the proportionality between the yaw moment $M_z$ and the yaw rate $r$. $D_\delta$ is a negative number and is called the yaw damping coefficient because it always tries to reduce the yaw moment. The value of $D_\delta$ increases with $a_1^2 C_{\alpha f}$ and $a_2^2 C_{\alpha r}$ and decreases with the forward velocity of the vehicle, $v_x$. When $C_{\alpha f} = C_{\alpha r}$, it is maximum if $a_1 = a_2$.

$D_\beta$ indicates the proportionality between the yaw moment $M_z$ and the vehicle sideslip angle $\beta$. $D_\beta$ indicates the under/oversteer behavior and hence, indicates the directional stability of a vehicle. If the rear wheel produces greater moment than the front wheel, the vehicle is stable and tries to reduce the effect of $\beta$. A negative $D_\beta$ tries to align the vehicle with the velocity vector.

$D_\delta$ indicates the proportionality between the yaw moment $M_z$ and the steer angle $\delta$. Because $\delta$ is the input command to control the maneuvering of a vehicle, $D_\delta$ is called the control moment coefficient. $D_\delta$ is a positive number and increases with $a_1$ and $C_{\alpha f}$.

**Example 382 ★** *Load transfer effect and rigid vehicle assumption.*

If a vehicle has more than three wheels, the normal forces acting on the wheels, $F_{z_i}$, are indeterminate. The normal force on each tire of a symmetric vehicle is

$$F_{z_1} = \frac{1}{2} F_{z_f} + \Delta F_z \tag{10.151}$$

$$F_{z_2} = \frac{1}{2} F_{z_f} - \Delta F_z \tag{10.152}$$

$$F_{z_3} = \frac{1}{2} F_{z_r} - \Delta F_z \tag{10.153}$$

$$F_{z_4} = \frac{1}{2} F_{z_r} + \Delta F_z \tag{10.154}$$

where $\Delta F_z$ is a change in wheel load due to an asymmetric reason such as the engine torque $T$.

The rigid vehicle assumption must be linked with the compliance suspensions to keep road contact through road irregularities and any asymmetric load transfer.

Load transfer also occurs because of acceleration, however, assuming a linear relationship between the wheel load $F_z$ and the cornering stiffness $C_\alpha$ makes the two-wheel model valid, because any increase in cornering stiffness for the more loaded wheel compensates for the decrease in the cornering stiffness of the unloaded wheel. However, when the acceleration is high,
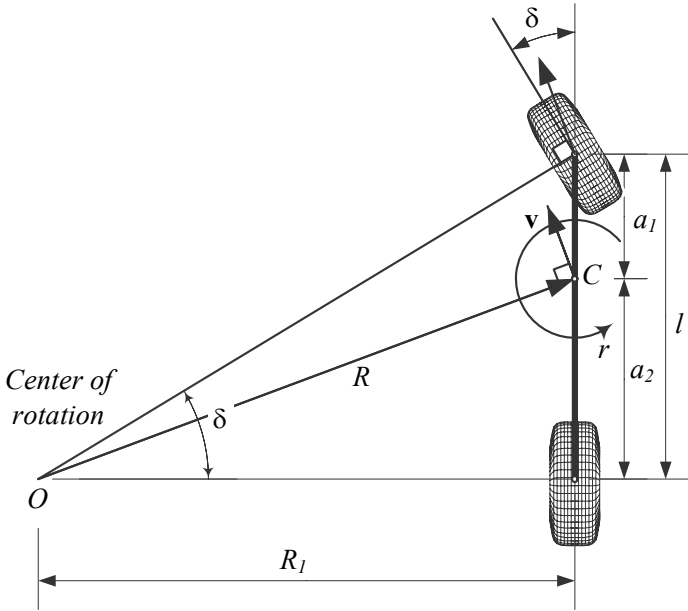
FIGURE 10.12. A two-wheel model for a vehicle moving with no roll.

the load transfer is higher than the linear limit and $C_\alpha$ is a descending nonlinear function of $F_z$. Hence, at high acceleration, the load transfer causes a decrease in cornering stiffness.

**Example 383** *Kinematic steering of a two-wheel vehicle.*

*For the two-wheel vehicle shown in Figure 10.12, we use the* cot*-average (7.3) of the outer and inner steer angles as the input steer angle,*

$$\cot \delta = \frac{\cot \delta_o + \cot \delta_i}{2}. \tag{10.155}$$

*where,*

$$\tan \delta_i \quad = \quad \frac{l}{R_1 - \dfrac{w}{2}} \tag{10.156}$$

$$\tan \delta_o \quad = \quad \frac{l}{R_1 + \dfrac{w}{2}}. \tag{10.157}$$

*The radius of rotation $R$ for the two-wheel vehicle is given by (7.2)*

$$R = \sqrt{a_2^2 + l^2 \cot^2 \delta}. \tag{10.158}$$

*and is measured at the mass center of the steered vehicle.*

## 10.4   Two-wheel Rigid Vehicle Dynamics

We can approximate the planar equations of motion (10.26)-(10.28) along with (10.111)-(10.113) for a two-wheel rigid vehicle with no roll motion, and express its motion by the following set of equations:

$$\dot{v}_x = \frac{1}{m} F_x + r\, v_y \tag{10.159}$$

$$= \frac{1}{m}\left(F_{x_f} + F_{x_r}\right) + r\, v_y$$

$$
\begin{bmatrix} \dot{v}_y \\ \dot{r} \end{bmatrix}
=
\begin{bmatrix}
\dfrac{C_\beta}{mv_x} & \dfrac{C_r}{m} - v_x \\[2mm]
\dfrac{D_\beta}{I_z v_x} & \dfrac{D_r}{I_z}
\end{bmatrix}
\begin{bmatrix} v_y \\ r \end{bmatrix}
+
\begin{bmatrix}
\dfrac{C_\delta}{m} \\[2mm]
\dfrac{D_\delta}{I_z}
\end{bmatrix}\delta
$$

$$
=
\begin{bmatrix}
-\dfrac{C_{\alpha f} + C_{\alpha r}}{mv_x} & \dfrac{-a_1 C_{\alpha f} + a_2 C_{\alpha r}}{mv_x} - v_x \\[3mm]
-\dfrac{a_1 C_{\alpha f} - a_2 C_{\alpha r}}{I_z v_x} & -\dfrac{a_1^2 C_{\alpha f} + a_2^2 C_{\alpha r}}{I_z v_x}
\end{bmatrix}
\begin{bmatrix} v_y \\ r \end{bmatrix}
$$

$$
+
\begin{bmatrix}
\dfrac{C_{\alpha f}}{m} \\[3mm]
\dfrac{a_1 C_{\alpha f}}{I_z}
\end{bmatrix}\delta
\tag{10.160}
$$

These sets of equations are good enough to analyze a vehicle that is moving at a constant forward speed. Having $\dot{v}_x = 0$, the first equation (10.159) becomes independent, and the lateral velocity $v_y$ and yaw rate $r$ of the vehicle will change according to the two coupled equations (10.160).

Assuming the steer angle $\delta$ is the input command, the lateral velocity $v_y$ and the yaw rate $r$ may be assumed as the output. Hence, we may consider Equation (10.160) as a linear control system, and write them as

$$\dot{\mathbf{q}} = [A]\,\mathbf{q} + \mathbf{u} \tag{10.161}$$

in which $[A]$ is a coefficient matrix, $\mathbf{q}$ is the vector of control variables, and $\mathbf{u}$ is the vector of inputs.

$$
[A] =
\begin{bmatrix}
-\dfrac{C_{\alpha f} + C_{\alpha r}}{mv_x} & \dfrac{-a_1 C_{\alpha f} + a_2 C_{\alpha r}}{mv_x} - v_x \\[3mm]
-\dfrac{a_1 C_{\alpha f} - a_2 C_{\alpha r}}{I_z v_x} & -\dfrac{a_1^2 C_{\alpha f} + a_2^2 C_{\alpha r}}{I_z v_x}
\end{bmatrix}
$$

$$\mathbf{q} = \begin{bmatrix} v_y \\ r \end{bmatrix} \tag{10.162}$$

$$\mathbf{u} = \begin{bmatrix} \dfrac{C_{\alpha f}}{m} \\ \dfrac{a_1 C_{\alpha f}}{I_z} \end{bmatrix} \delta \tag{10.163}$$

**Proof.** The Newton-Euler equations of motion for a rigid vehicle in the local coordinate frame $B$, attached to the vehicle at its mass center $C$, are given in Equations (10.26)–(10.28) as

$$F_x = m\dot{v}_x - mr\,v_y \tag{10.164}$$
$$F_y = m\dot{v}_y + mr\,v_x \tag{10.165}$$
$$M_z = \dot{r}\,I_z. \tag{10.166}$$

The approximate force system applied on a two-wheel rigid vehicle is found in Equations (10.111)–(10.113)

$$F_x \approx F_{x_f} + F_{x_r} \tag{10.167}$$
$$F_y \approx F_{y_f} + F_{y_r} \tag{10.168}$$
$$M_z \approx a_1 F_{y_f} - a_2 F_{y_r} \tag{10.169}$$

and in terms of tire characteristics, in (10.114) and (10.115).

$$F_x = \frac{T_w}{R_w} \tag{10.170}$$

$$F_y = \left(-\frac{a_1}{v_x}C_{\alpha f} + \frac{a_2}{v_x}C_{\alpha r}\right) r - (C_{\alpha f} + C_{\alpha r})\beta + C_{\alpha f}\delta \tag{10.171}$$

$$M_z = \left(-\frac{a_1^2}{v_x}C_{\alpha f} - \frac{a_2^2}{v_x}C_{\alpha r}\right) r - (a_1 C_{\alpha f} - a_2 C_{\alpha r})\beta + a_1 C_{\alpha f}\delta \tag{10.172}$$

Substituting (10.170)–(10.172) in (10.164)–(10.166) produces the following equations of motion:

$$m\dot{v}_x - mr\,v_y = F_x \tag{10.173}$$

$$m\dot{v}_y + mr\,v_x = \left(-\frac{a_1}{v_x}C_{\alpha f} + \frac{a_2}{v_x}C_{\alpha r}\right) r$$
$$- (C_{\alpha f} + C_{\alpha r})\beta + C_{\alpha f}\delta \tag{10.174}$$

$$\dot{r}\,I_z = \left(-\frac{a_1^2}{v_x}C_{\alpha f} - \frac{a_2^2}{v_x}C_{\alpha r}\right) r$$
$$- (a_1 C_{\alpha f} - a_2 C_{\alpha r})\beta + a_1 C_{\alpha f}\delta \tag{10.175}$$

These equations can be transformed to a set of differential equations for

$v_x$, $v_y$, and $r$.

$$\dot{v}_x = \frac{F_x}{m} + r\,v_y \tag{10.176}$$

$$\dot{v}_y = \frac{1}{m}\left(-\frac{a_1}{v_x}C_{\alpha f} + \frac{a_2}{v_x}C_{\alpha r}\right)r$$
$$-\frac{1}{m}\left(C_{\alpha f} + C_{\alpha r}\right)\beta + \frac{1}{m}C_{\alpha f}\delta - r\,v_x \tag{10.177}$$

$$\dot{r} = \frac{1}{I_z}\left(-\frac{a_1^2}{v_x}C_{\alpha f} - \frac{a_2^2}{v_x}C_{\alpha r}\right)r$$
$$-\frac{1}{I_z}\left(a_1 C_{\alpha f} - a_2 C_{\alpha r}\right)\beta + \frac{1}{I_z}a_1 C_{\alpha f}\delta. \tag{10.178}$$

The vehicle sideslip angle can be substituted by vehicle velocity components

$$\beta = \frac{v_y}{v_x} \tag{10.179}$$

and we can find a new form for the equations.

$$\dot{v}_x = \frac{F_x}{m} + r\,v_y \tag{10.180}$$

$$\dot{v}_y = \frac{1}{mv_x}\left(-a_1 C_{\alpha f} + a_2 C_{\alpha r}\right)r$$
$$-\frac{1}{mv_x}\left(C_{\alpha f} + C_{\alpha r}\right)v_y + \frac{1}{m}C_{\alpha f}\delta - r\,v_x \tag{10.181}$$

$$\dot{r} = \frac{1}{I_z v_x}\left(-a_1^2 C_{\alpha f} - a_2^2 C_{\alpha r}\right)r$$
$$-\frac{1}{I_z v_x}\left(a_1 C_{\alpha f} - a_2 C_{\alpha r}\right)v_y + \frac{1}{I_z}a_1 C_{\alpha f}\delta. \tag{10.182}$$

The first equation (10.180) depends on the yaw rate $r$ and the lateral velocity $v_y$, which are the output of the second and third equations, (10.181) and (10.182). However, if we assume the vehicle is moving with a constant forward speed,

$$v_x = cte. \tag{10.183}$$

then Equation (10.180) becomes an algebraic equation and then Equations (10.181) and (10.182) become independent with (10.180). So, the second and third equations may be treated independently of the first one.

Equations (10.181) and (10.182) may be considered as two coupled differential equations describing the behavior of a dynamic system. The dynamic system receives the steering angle $\delta$ as the input, and uses $v_x$ as a parameter

to generate two outputs, $v_y$ and $r$.

$$
\begin{bmatrix} \dot{v}_y \\ \dot{r} \end{bmatrix} = \begin{bmatrix} -\dfrac{C_{\alpha f} + C_{\alpha r}}{m v_x} & \dfrac{-a_1 C_{\alpha f} + a_2 C_{\alpha r}}{m v_x} - v_x \\[3mm] -\dfrac{a_1 C_{\alpha f} - a_2 C_{\alpha r}}{I_z v_x} & -\dfrac{a_1^2 C_{\alpha f} + a_2^2 C_{\alpha r}}{I_z v_x} \end{bmatrix} \begin{bmatrix} v_y \\ r \end{bmatrix}
$$

$$
+ \begin{bmatrix} \dfrac{C_{\alpha f}}{m} \\[3mm] \dfrac{a_1 C_{\alpha f}}{I_z} \end{bmatrix} \delta \tag{10.184}
$$

Equation (10.184) may be rearranged in the following form to show the input-output relationship:

$$
\dot{\mathbf{q}} = [A]\,\mathbf{q} + \mathbf{u} \tag{10.185}
$$

The vector $\mathbf{q}$ is called the *control variables vector*, and $\mathbf{u}$ is called the *inputs vector*. The matrix $[A]$ is the control variable coefficients matrix.

Employing the force system coefficients $C_r$, $C_\beta$, $C_\delta$, $D_r$, $D_\beta$, and $D_\delta$ for a front-wheel steering vehicle, we may write the set of Equations (10.184) as

$$
\begin{bmatrix} \dot{v}_y \\ \dot{r} \end{bmatrix} = \begin{bmatrix} \dfrac{C_\beta}{m v_x} & \dfrac{C_r}{m} - v_x \\[3mm] \dfrac{D_\beta}{I_z v_x} & \dfrac{D_r}{I_z} \end{bmatrix} \begin{bmatrix} v_y \\ r \end{bmatrix} + \begin{bmatrix} \dfrac{C_\delta}{m} \\[3mm] \dfrac{D_\delta}{I_z} \end{bmatrix} \delta. \tag{10.186}
$$

∎

**Example 384** *Equations of motion based on kinematic angles.*

*The equations of motion (10.160) can be expressed based on only the angles $\beta$, $r$, and $\delta$, by employing (10.179).*

*Taking a time derivative from Equation (10.179) for constant $v_x$*

$$
\dot{\beta} = \frac{\dot{v}_y}{v_x} \tag{10.187}
$$

*and substituting it in Equations (10.177) shows that we can transform the equation for $\dot{\beta}$ to:*

$$
\begin{aligned}
v_x \dot{\beta} &= \frac{1}{m}\left( -\frac{a_1}{v_x} C_{\alpha f} + \frac{a_2}{v_x} C_{\alpha r} \right) r \\
&\quad - \frac{1}{m}\left( C_{\alpha f} + C_{\alpha r} \right)\beta + \frac{1}{m} C_{\alpha f}\delta - r\,v_x.
\end{aligned} \tag{10.188}
$$

*Therefore, the set of equations of motion can be expressed in terms of the*

*vehicle's angular variables $\beta$, $r$, and $\delta$.*

$$
\begin{bmatrix} \dot{\beta} \\ \dot{r} \end{bmatrix} = \begin{bmatrix} -\dfrac{C_{\alpha f} + C_{\alpha r}}{mv_x} & \dfrac{-a_1 C_{\alpha f} + a_2 C_{\alpha r}}{mv_x^2} - 1 \\[3mm] -\dfrac{a_1 C_{\alpha f} - a_2 C_{\alpha r}}{I_z} & -\dfrac{a_1^2 C_{\alpha f} + a_2^2 C_{\alpha r}}{I_z v_x} \end{bmatrix} \begin{bmatrix} \beta \\ r \end{bmatrix}
$$
$$
+ \begin{bmatrix} \dfrac{C_{\alpha f}}{mv_x} \\[3mm] \dfrac{a_1 C_{\alpha f}}{I_z} \end{bmatrix} \delta \tag{10.189}
$$

*Employing the force system coefficients $C_r$, $C_\beta$, $C_\delta$, $D_r$, $D_\beta$, and $D_\delta$ for a front-wheel steering vehicle, we may write the set of Equations (10.189) as*

$$
\begin{bmatrix} \dot{\beta} \\ \dot{r} \end{bmatrix} = \begin{bmatrix} \dfrac{C_\beta}{mv_x} & \dfrac{C_r}{mv_x} - 1 \\[3mm] \dfrac{D_\beta}{I_z} & \dfrac{D_r}{I_z} \end{bmatrix} \begin{bmatrix} \beta \\ r \end{bmatrix} + \begin{bmatrix} \dfrac{C_\delta}{mv_x} \\[3mm] \dfrac{D_\delta}{I_z} \end{bmatrix} \delta. \tag{10.190}
$$

**Example 385** *Four-wheel-steering vehicles.*

*Consider a vehicle with steerable wheels in both the front and rear. Let's indicate the steer angle in the front and rear by $\delta_f$ and $\delta_r$ respectively. To find the planar equations of motion we start from Equation (10.104) for the relationship between $\alpha$, $\beta$, and $\delta$*

$$
\alpha = \beta - \delta \tag{10.191}
$$

*and apply the equation to the front and rear wheels.*

$$
\begin{aligned}
\alpha_f &= \beta_f - \delta_f = \frac{1}{v_x}(v_y + a_1 r) - \delta_f \\
&= \beta + \frac{a_1 r}{v_x} - \delta_f \tag{10.192}
\end{aligned}
$$

$$
\begin{aligned}
\alpha_r &= \beta_r - \delta_r = \frac{1}{v_x}(v_y - a_2 r) - \delta_r \\
&= \beta - \frac{a_2 r}{v_x} - \delta_r \tag{10.193}
\end{aligned}
$$

*When the sideslip angles are small, the associated lateral forces are*

$$
\begin{aligned}
F_{yf} &= -C_{\alpha f}\, \alpha_f \tag{10.194} \\
F_{yr} &= -C_{\alpha r}\, \alpha_r \tag{10.195}
\end{aligned}
$$

*Substituting these equations in the second and third equations of motion (10.112) and (10.113) results in the force system*

$$
\begin{aligned}
F_y &= F_{yf} + F_{yr} \\
&= \left(-\frac{a_1}{v_x}C_{\alpha f} + \frac{a_2}{v_x}C_{\alpha r}\right)r \\
&\quad - (C_{\alpha f} + C_{\alpha r})\beta + C_{\alpha f}\delta_f + C_{\alpha r}\delta_r \qquad (10.196) \\
M_z &= a_1 F_{yf} - a_2 F_{yr} \\
&= \left(-\frac{a_1^2}{v_x}C_{\alpha f} - \frac{a_2^2}{v_x}C_{\alpha r}\right)r \\
&\quad - (a_1 C_{\alpha f} - a_2 C_{\alpha r})\beta + a_1 C_{\alpha f}\delta_f - a_2 C_{\alpha r}\delta_r. \qquad (10.197)
\end{aligned}
$$

*The Newton-Euler equations of motion for a rigid vehicle are given in Equations (10.26)–(10.28) as*

$$
\begin{aligned}
F_x &= m\,\dot{v}_x - m r\,v_y \qquad (10.198) \\
F_y &= m\,\dot{v}_y + m r\,v_x \qquad (10.199) \\
M_z &= \dot{r}\,I_z. \qquad (10.200)
\end{aligned}
$$

*and therefore, the equations of motion for a four-wheel-steering vehicle are*

$$
m\,\dot{v}_x - m r\,v_y = F_x \qquad (10.201)
$$

$$
\begin{aligned}
m\,\dot{v}_y + m r\,v_x &= \left(-\frac{a_1}{v_x}C_{\alpha f} + \frac{a_2}{v_x}C_{\alpha r}\right)r \\
&\quad - (C_{\alpha f} + C_{\alpha r})\beta + C_{\alpha f}\delta_f + C_{\alpha r}\delta_r \qquad (10.202)
\end{aligned}
$$

$$
\begin{aligned}
\dot{r}\,I_z &= \left(-\frac{a_1^2}{v_x}C_{\alpha f} - \frac{a_2^2}{v_x}C_{\alpha r}\right)r \\
&\quad - (a_1 C_{\alpha f} - a_2 C_{\alpha r})\beta + a_1 C_{\alpha f}\delta_f - a_2 C_{\alpha r}\delta_r. \qquad (10.203)
\end{aligned}
$$

*These equations can be transformed to a set of differential equations for $v_x$, $v_y$, and $r$.*

$$
\dot{v}_x = \frac{F_x}{m} + r\,v_y \qquad (10.204)
$$

$$
\begin{aligned}
\dot{v}_y &= \frac{1}{m}\left(-\frac{a_1}{v_x}C_{\alpha f} + \frac{a_2}{v_x}C_{\alpha r}\right)r \\
&\quad - \frac{1}{m}(C_{\alpha f} + C_{\alpha r})\beta + \frac{1}{m}C_{\alpha f}\delta_f + \frac{1}{m}C_{\alpha r}\delta_r - r\,v_x \qquad (10.205)
\end{aligned}
$$

$$
\begin{aligned}
\dot{r} &= \frac{1}{I_z}\left(-\frac{a_1^2}{v_x}C_{\alpha f} - \frac{a_2^2}{v_x}C_{\alpha r}\right)r \\
&\quad - \frac{1}{I_z}(a_1 C_{\alpha f} - a_2 C_{\alpha r})\beta + \frac{1}{I_z}a_1 C_{\alpha f}\delta_f - \frac{1}{I_z}a_2 C_{\alpha r}\delta_r \qquad (10.206)
\end{aligned}
$$

*Using the vehicle sideslip angle*

$$\beta = \frac{v_y}{v_x} \tag{10.207}$$

*we may transform the equations to the following set of three coupled first order ordinary differential equations:*

$$\dot{v}_x = \frac{F_x}{m} + r\,v_y \tag{10.208}$$

$$\dot{v}_y = \frac{1}{mv_x}\left(-a_1 C_{\alpha f} + a_2 C_{\alpha r}\right) r$$
$$-\frac{1}{mv_x}\left(C_{\alpha f} + C_{\alpha r}\right) v_y + \frac{1}{m}C_{\alpha f}\delta_f + \frac{1}{m}C_{\alpha r}\delta_r - r\,v_x \tag{10.209}$$

$$\dot{r} = \frac{1}{I_z v_x}\left(-a_1^2 C_{\alpha f} - a_2^2 C_{\alpha r}\right) r$$
$$-\frac{1}{I_z v_x}\left(a_1 C_{\alpha f} - a_2 C_{\alpha r}\right) v_y + \frac{1}{I_z}a_1 C_{\alpha f}\delta_f - \frac{1}{I_z}a_2 C_{\alpha r}\delta_r \tag{10.210}$$

*The second and third equations may be cast in the following matrix form for $\begin{bmatrix} v_y & r \end{bmatrix}^T$:*

$$\begin{bmatrix} \dot{v}_y \\ \dot{r} \end{bmatrix} = \begin{bmatrix} -\dfrac{C_{\alpha f} + C_{\alpha r}}{mv_x} & \dfrac{-a_1 C_{\alpha f} + a_2 C_{\alpha r}}{mv_x} - v_x \\ -\dfrac{a_1 C_{\alpha f} - a_2 C_{\alpha r}}{I_z v_x} & -\dfrac{a_1^2 C_{\alpha f} + a_2^2 C_{\alpha r}}{I_z v_x} \end{bmatrix} \begin{bmatrix} v_y \\ r \end{bmatrix}$$
$$+ \begin{bmatrix} \dfrac{1}{m}C_{\alpha f} & \dfrac{1}{m}C_{\alpha r} \\ \dfrac{1}{I_z}a_1 C_{\alpha f} & -\dfrac{1}{I_z}a_2 C_{\alpha r} \end{bmatrix} \begin{bmatrix} \delta_f \\ \delta_r \end{bmatrix} \tag{10.211}$$

*or to the following form for $\begin{bmatrix} \beta & r \end{bmatrix}^T$:*

$$\begin{bmatrix} \dot{\beta} \\ \dot{r} \end{bmatrix} = \begin{bmatrix} -\dfrac{C_{\alpha f} + C_{\alpha r}}{mv_x} & \dfrac{-a_1 C_{\alpha f} + a_2 C_{\alpha r}}{mv_x^2} - 1 \\ -\dfrac{a_1 C_{\alpha f} - a_2 C_{\alpha r}}{I_z} & -\dfrac{a_1^2 C_{\alpha f} + a_2^2 C_{\alpha r}}{I_z v_x} \end{bmatrix} \begin{bmatrix} \beta \\ r \end{bmatrix}$$
$$+ \begin{bmatrix} \dfrac{1}{mv_x}C_{\alpha f} & \dfrac{1}{mv_x}C_{\alpha r} \\ \dfrac{1}{I_z}a_1 C_{\alpha f} & -\dfrac{1}{I_z}a_2 C_{\alpha r} \end{bmatrix} \begin{bmatrix} \delta_f \\ \delta_r \end{bmatrix} \tag{10.212}$$

*For computerization of the equations of motion, it is better to write them*

*as*

$$\begin{bmatrix} \dot{v}_y \\ \dot{r} \end{bmatrix} = \begin{bmatrix} \dfrac{C_\beta}{mv_x} & \dfrac{C_r}{m} - v_x \\[2ex] \dfrac{D_\beta}{I_z v_x} & \dfrac{D_r}{I_z} \end{bmatrix} \begin{bmatrix} v_y \\ r \end{bmatrix} + \begin{bmatrix} \dfrac{C_{\delta_f}}{m} & \dfrac{C_{\delta_r}}{m} \\[2ex] \dfrac{D_{\delta_f}}{I_z} & \dfrac{D_{\delta_r}}{I_z} \end{bmatrix} \delta \qquad (10.213)$$

*or*

$$\begin{bmatrix} \dot{\beta} \\ \dot{r} \end{bmatrix} = \begin{bmatrix} \dfrac{C_\beta}{mv_x} & \dfrac{C_r}{mv_x} - 1 \\[2ex] \dfrac{D_\beta}{I_z} & \dfrac{D_r}{I_z} \end{bmatrix} \begin{bmatrix} \beta \\ r \end{bmatrix} + \begin{bmatrix} \dfrac{C_{\delta_f}}{mv_x} & \dfrac{C_{\delta_r}}{mv_x} \\[2ex] \dfrac{D_{\delta_f}}{I_z} & \dfrac{D_{\delta_r}}{I_z} \end{bmatrix} \delta \qquad (10.214)$$

*where*

$$C_r = \frac{\partial F_y}{\partial r} = -\frac{a_1}{v_x}C_{\alpha f} + \frac{a_2}{v_x}C_{\alpha r} \qquad (10.215)$$

$$C_\beta = \frac{\partial F_y}{\partial \beta} = -(C_{\alpha f} + C_{\alpha r}) \qquad (10.216)$$

$$C_{\delta_f} = \frac{\partial F_y}{\partial \delta_f} = C_{\alpha f} \qquad (10.217)$$

$$C_{\delta_r} = \frac{\partial F_y}{\partial \delta_r} = C_{\alpha r} \qquad (10.218)$$

$$D_r = \frac{\partial M_z}{\partial r} = -\frac{a_1^2}{v_x}C_{\alpha f} - \frac{a_2^2}{v_x}C_{\alpha r} \qquad (10.219)$$

$$D_\beta = \frac{\partial M_z}{\partial \beta} = -(a_1 C_{\alpha f} - a_2 C_{\alpha r}) \qquad (10.220)$$

$$D_{\delta_f} = \frac{\partial M_z}{\partial \delta_f} = a_1 C_{\alpha r} \qquad (10.221)$$

$$D_{\delta_r} = \frac{\partial M_z}{\partial \delta_r} = -a_2 C_{\alpha r}. \qquad (10.222)$$

*Equation (10.211) may be rearranged in the following form to show the input-output relationship:*

$$\dot{\mathbf{q}} = [A]\,\mathbf{q} + [B]\,\mathbf{u} \qquad (10.223)$$

*The vector* **q** *is called the control variables vector,*

$$\mathbf{q} = \begin{bmatrix} v_y \\ r \end{bmatrix} \qquad (10.224)$$

*and* **u** *is called the inputs vector.*

$$\mathbf{u} = \begin{bmatrix} \delta_f \\ \delta_r \end{bmatrix} \qquad (10.225)$$

*The matrix $[A]$ is the control variable coefficients matrix and the matrix $[B]$ is the input coefficient matrix.*

*To double check, we may substitute $\delta_r = 0$, and $\delta_f = \delta$ to reduce Equations (10.211) to (10.184) for a front-wheel-steering vehicle.*

**Example 386** *Rear-wheel-steering vehicle.*

*Rear wheel steering is frequently employed in lift trucks and construction vehicles. The equations of motion for rear steering vehicles are similar to those in front steering. To find the equations of motion, we substitute $\delta_f = 0$ in Equations (10.211) to find these equations*

$$
\begin{bmatrix} \dot{v}_y \\ \dot{r} \end{bmatrix} = \begin{bmatrix} -\dfrac{C_{\alpha f} + C_{\alpha r}}{m v_x} & \dfrac{-a_1 C_{\alpha f} + a_2 C_{\alpha r}}{m v_x} - v_x \\ -\dfrac{a_1 C_{\alpha f} - a_2 C_{\alpha r}}{I_z v_x} & -\dfrac{a_1^2 C_{\alpha f} + a_2^2 C_{\alpha r}}{I_z v_x} \end{bmatrix} \begin{bmatrix} v_y \\ r \end{bmatrix}
$$
$$
+ \begin{bmatrix} \dfrac{1}{m} C_{\alpha r} \\ -\dfrac{1}{I_z} a_2 C_{\alpha r} \end{bmatrix} \delta_r. \tag{10.226}
$$

*These equations are valid as long as the angles are very small. However, most of the rear steering construction vehicles work at a big steer angle. Therefore, these equations cannot predict the behavior of the construction vehicles very well.*

**Example 387** ★ *Better model for two-wheel vehicles.*

*Because of the steer angle, a reaction moment appears at the tireprints of the front and rear wheels, which act as external moments $M_1$ and $M_2$ on the wheels. So the total steering reaction moment on the front and rear wheels are*

$$
\begin{align}
M_1 &\approx 2 D_{\delta_f} M_z \tag{10.227} \\
M_2 &\approx 2 D_{\delta_r} M_z \tag{10.228}
\end{align}
$$

*where*

$$
D_{\delta_f} = \frac{dM_z}{d\delta_f} \tag{10.229}
$$

$$
D_{\delta_r} = \frac{dM_z}{d\delta_r}. \tag{10.230}
$$

*Figure 10.13 illustrates a two-wheel vehicle model. The force system on the vehicle is*

$$
\begin{align}
F_x &\approx F_{x_f} + F_{x_r} \tag{10.231} \\
F_y &\approx F_{y_f} + F_{y_r} \tag{10.232} \\
M_z &\approx a_1 F_{y_f} - a_2 F_{y_r} + M_1 + M_2. \tag{10.233}
\end{align}
$$
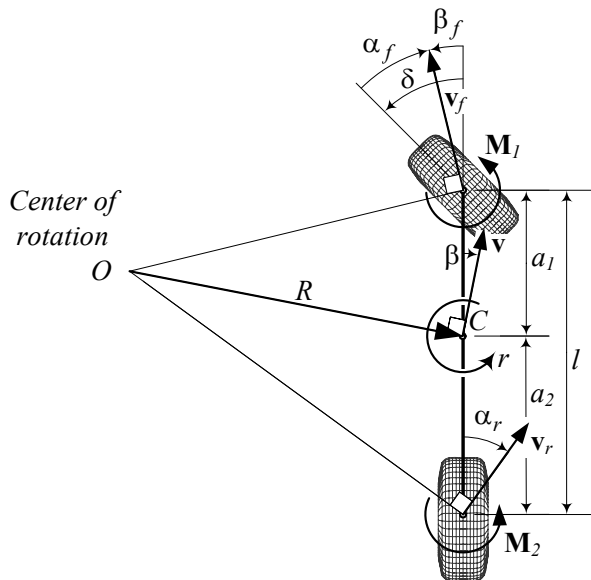
FIGURE 10.13. A two-wheel vehicle and its force system, including the steer moment reactions.

**Example 388 ★** *The race care* 180 deg *quick turn from reverse.*

You have seen that race car drivers can turn a 180 deg *quickly when the car is moving backward. Here is how they do this. The driver moves backward when the car is in reverse gear. To make a fast* 180 deg *turn without stopping, the driver may follow these steps:* 1− *The driver should push the gas pedal to gain enough speed,* 2− *free the gas pedal and put the gear in neutral,* 3− *cut the steering wheel sharply around* 90 deg, 4− *change the gear to drive, and* 5− *push the gas pedal and return the steering wheel to* 0 deg *after the car has completed the* 180 deg *turn.*

The backward speed before step 2 *may be around* 20 m/s ≈ 70 km/h ≈ 45 mi/h. *Steps* 2 to 4 *should be done fast and almost simultaneously. Figure* 10.14(a) *illustrates the* 180 deg *fast turning maneuver from reverse.*

This example should never be performed by the reader of this book.

**Example 389 ★** *The race care* 180 deg *quick turn from forward.*

You have seen that race car drivers can turn a 180 deg *quickly when the car is moving forward. Here is how they do this. The driver moves forward when the car is in drive or a forward gear. To make a fast* 180 deg *turn without stopping, the driver may follow these steps:* 1− *The driver should push the gas pedal to gain enough speed,* 2− *free the gas pedal and put the gear in neutral,* 3− *cut the steering wheel sharply around* 90 deg *while*
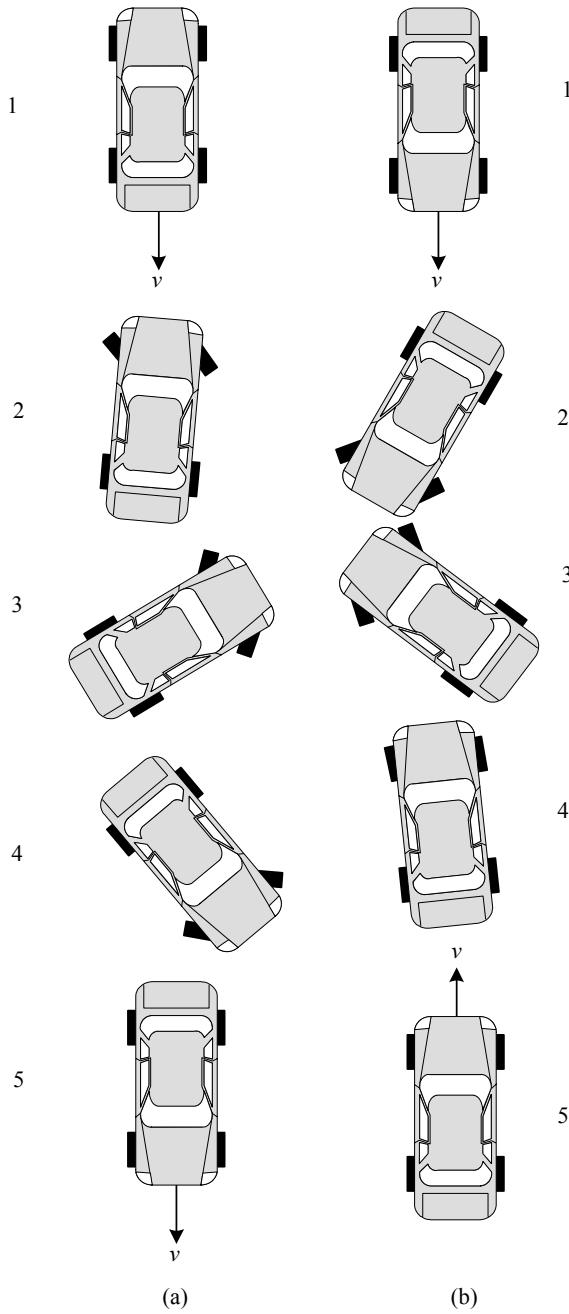
FIGURE 10.14. (a)- A 180 deg, fast turning maneuver from reverse. (b)- A 180 deg, fast turning maneuver from forward.

*you pull hard the hand brake, 4— while the rear swings around, return the steering wheel to 0 deg and put the gear into drive, and 5— push the gas pedal after the car has completed the 180 deg turn. Figure 10.14(b) illustrates this maneuver.*

*The forward speed before step 2 may be around 20 m/s ≈ 70 km/h ≈ 45 mi/h. Steps 2 to 4 should be done fast and almost simultaneously. The 180 deg fast turning from forward is more difficult than backward and can be done because the hand brakes are connected to the rear wheels. It can be done better when the rear of a car is lighter than the front to slides easier. Road condition, nonuniform friction, slippery surface can cause flipping the car and spinning out of control.*

*This example should never be performed by the reader of this book.*

## 10.5 Steady-State Turning

The turning of a front-wheel-steering, two-wheel rigid vehicle at its steady-state condition is governed by the following equations:

$$F_x = -mr\, v_y \tag{10.234}$$

$$C_r\, r + C_\beta\, \beta + C_\delta\, \delta = mr\, v_x \tag{10.235}$$

$$D_r\, r + D_\beta\, \beta + D_\delta\, \delta = 0 \tag{10.236}$$

or equivalently, by the following equations:

$$F_x = -\frac{m}{R} v_x\, v_y \tag{10.237}$$

$$C_\beta\, \beta + \left(C_r\, v_x - m\, v_x^2\right) \frac{1}{R} = -C_\delta\, \delta \tag{10.238}$$

$$D_\beta\, \beta + D_r\, v_x \frac{1}{R} = -D_\delta\, \delta. \tag{10.239}$$

The first equation determines the required forward force to keep $v_x$ constant. The second and third equations show the steady-state values of the output variables, vehicle slip angle $\beta$, and path curvature $\kappa$,

$$\kappa = \frac{1}{R} \tag{10.240}$$

$$= \frac{r}{v_x} \tag{10.241}$$

for a constant steering input $\delta$ at a constant forward speed $v_x$. The output-input relationships are defined by the following responses:

1− *Curvature response,* $S_\kappa$

$$
\begin{aligned}
S_\kappa &= \frac{\kappa}{\delta} \\
&= \frac{1}{R\delta} \\
&= \frac{C_\delta D_\beta - C_\beta D_\delta}{v_x \left( D_r C_\beta - C_r D_\beta + m v_x D_\beta \right)}
\end{aligned}
\tag{10.242}
$$

2− *Sideslip response,* $S_\beta$

$$
\begin{aligned}
S_\beta &= \frac{\beta}{\delta} \\
&= \frac{D_\delta \left( C_r - m v_x \right) - D_r C_\delta}{D_r C_\beta - C_r D_\beta + m v_x D_\beta}
\end{aligned}
\tag{10.243}
$$

3− *Yaw rate response,* $S_r$

$$
\begin{aligned}
S_r &= \frac{r}{\delta} \\
&= \frac{\kappa}{\delta} v_x \\
&= S_\kappa v_x \\
&= \frac{C_\delta D_\beta - C_\beta D_\delta}{D_r C_\beta - C_r D_\beta + m v_x D_\beta}
\end{aligned}
\tag{10.244}
$$

4− *Lateral acceleration response,* $S_a$

$$
\begin{aligned}
S_a &= \frac{v_x^2 / R}{\delta} \\
&= \frac{\kappa}{\delta} v_x^2 \\
&= S_\kappa v_x^2 \\
&= \frac{\left( C_\delta D_\beta - C_\beta D_\delta \right) v_x}{D_r C_\beta - C_r D_\beta + m v_x D_\beta}
\end{aligned}
\tag{10.245}
$$

**Proof.** In steady-state conditions, all the variables are constant, and hence, their derivatives are zero. Therefore, the equations of motion (10.173)–(10.175) reduce to

$$
\begin{aligned}
F_x &= -m r\, v_y & (10.246) \\
F_y &= m r\, v_x & (10.247) \\
M_z &= 0 & (10.248)
\end{aligned}
$$

where the lateral force $F_y$ and yaw moment $M_z$ from (10.141) and (10.142) are

$$
\begin{aligned}
F_y &= C_r\, r + C_\beta\, \beta + C_\delta\, \delta & (10.249) \\
M_z &= D_r\, r + D_\beta\, \beta + D_\delta\, \delta. & (10.250)
\end{aligned}
$$

Therefore, the equations describing the steady-state turning of a two-wheel rigid vehicle are equal to

$$F_x = -mr\,v_y \tag{10.251}$$

$$C_r\,r + C_\beta\,\beta + C_\delta\,\delta = mr\,v_x \tag{10.252}$$

$$D_r\,r + D_\beta\,\beta + D_\delta\,\delta = 0. \tag{10.253}$$

At steady-state turning, the vehicle will move on a circle with radius $R$ at a speed $v_x$ and angular velocity $r$, so

$$v_x = R\,r. \tag{10.254}$$

Substituting (10.254) in Equations (10.251)-(10.253) shows that we may write the equations as (10.237)-(10.239). Equation (10.237) may be used to calculate the required traction force to keep the motion steady. However, Equations (10.238) and (10.239) can be used to determine the steady-state responses of the vehicle. We use the curvature definition (10.240) and write the equations in matrix form

$$\begin{bmatrix} C_\beta & C_r\,v_x - m\,v_x^2 \\ D_\beta & D_r\,v_x \end{bmatrix}\begin{bmatrix} \beta \\ \kappa \end{bmatrix} = \begin{bmatrix} -C_\delta \\ -D_\delta \end{bmatrix}\delta. \tag{10.255}$$

Solving the equations for $\beta$ and $\kappa$ shows that

$$\begin{bmatrix} \beta \\ \kappa \end{bmatrix} = \begin{bmatrix} C_\beta & C_r\,v_x - m\,v_x^2 \\ D_\beta & D_r\,v_x \end{bmatrix}^{-1}\begin{bmatrix} -C_\delta \\ -D_\delta \end{bmatrix}\delta$$

$$= \begin{bmatrix} \dfrac{D_\delta\,(C_r - mv_x) - D_r C_\delta}{D_r C_\beta - C_r D_\beta + mv_x D_\beta} \\[3mm] \dfrac{C_\delta D_\beta - C_\beta D_\delta}{v_x\,(D_r C_\beta - C_r D_\beta + mv_x D_\beta)} \end{bmatrix}\delta. \tag{10.256}$$

Using the solutions in (10.256) and Equation (10.254), we are able to define different output-input relationships as (10.242)-(10.245). ∎

**Example 390** *Force system coefficients for a car.*
   *Consider a front-wheel-steering, four-wheel-car with the following characteristics.*

$$\begin{aligned} C_{\alpha f_L} = C_{\alpha f_R} \quad &= 500\,\mathrm{N/\,deg} \\ &\approx 112.4\,\mathrm{lb/\,deg} \\ &\approx 28648\,\mathrm{N/\,rad} \\ &\approx 6440\,\mathrm{lb/\,rad} \end{aligned} \tag{10.257}$$

$$\begin{aligned} C_{\alpha r_L} = C_{\alpha r_R} \quad &= 460\,\mathrm{N/\,deg} \\ &\approx 103.4\,\mathrm{lb/\,deg} \\ &\approx 26356\,\mathrm{N/\,rad} \\ &\approx 5924.4\,\mathrm{lb/\,rad} \end{aligned} \tag{10.258}$$

$$mg = 9000\,\text{N} \approx 2023\,\text{lb} \qquad (10.259)$$
$$m = 917\,\text{kg} \approx 62.8\,\text{slug} \qquad (10.260)$$
$$I_z = 1128\,\text{kg}\,\text{m}^2 \approx 832\,\text{slug}\,\text{ft}^2 \qquad (10.261)$$
$$a_1 = 91\,\text{cm} \approx 2.98\,\text{ft} \qquad (10.262)$$
$$a_2 = 164\,\text{cm} \approx 5.38\,\text{ft} \qquad (10.263)$$

The sideslip coefficient of an equivalent bicycle model are

$$C_{\alpha f} = C_{\alpha f_L} + C_{\alpha f_R} = 57296\,\text{N}/\,\text{rad} \qquad (10.264)$$
$$C_{\alpha r} = C_{\alpha r_L} + C_{\alpha r_R} = 52712\,\text{N}/\,\text{rad}. \qquad (10.265)$$

The force system coefficients $C_r$, $C_\beta$, $C_\delta$, $D_r$, $D_\beta$, and $D_\delta$ are then equal to the following if $v_x$ is measured in $[\,\text{m}/\,\text{s}\,]$.

$$C_r = -\frac{a_1}{v_x}C_{\alpha f} + \frac{a_2}{v_x}C_{\alpha r} = \frac{34308}{v_x}\,\text{N}\,\text{s}/\,\text{rad} \qquad (10.266)$$
$$C_\beta = -(C_{\alpha f} + C_{\alpha r}) = -1.1001 \times 10^5\,\text{N}/\,\text{rad} \qquad (10.267)$$
$$C_\delta = C_{\alpha f} = 57296\,\text{N}/\,\text{rad} \qquad (10.268)$$

$$D_r = -\frac{a_1^2}{v_x}C_{\alpha f} - \frac{a_2^2}{v_x}C_{\alpha r} = -\frac{1.8922 \times 10^5}{v_x}\,\text{N}\,\text{m}\,\text{s}/\,\text{rad} \qquad (10.269)$$
$$D_\beta = -(a_1 C_{\alpha f} - a_2 C_{\alpha r}) = 34308\,\text{N}\,\text{m}/\,\text{rad} \qquad (10.270)$$
$$D_\delta = a_1 C_{\alpha f} = 52139\,\text{N}\,\text{m}/\,\text{rad}. \qquad (10.271)$$

The coefficients $C_r$ and $D_r$ are functions of the forward speed $v_x$. As an example $C_r$ and $D_r$ at

$$v_x = 10\,\text{m}/\,\text{s} = 36\,\text{km}/\,\text{h} \qquad (10.272)$$
$$\approx 32.81\,\text{ft}/\,\text{s} \approx 22.37\,\text{mi}/\,\text{h}$$

are

$$C_r = 3430.8\,\text{N}\,\text{s}/\,\text{rad} \qquad (10.273)$$
$$D_r = -18922\,\text{N}\,\text{m}\,\text{s}/\,\text{rad} \qquad (10.274)$$

and at

$$v_x = 30\,\text{m}/\,\text{s} = 108\,\text{km}/\,\text{h} \qquad (10.275)$$
$$\approx 98.43\,\text{ft}/\,\text{s} \approx 67.11\,\text{mi}/\,\text{h}$$

are

$$C_r = 1143.6\,\text{N}\,\text{s}/\,\text{rad} \qquad (10.276)$$
$$D_r = -6307.3\,\text{N}\,\text{m}\,\text{s}/\,\text{rad}. \qquad (10.277)$$

**Example 391** *Steady state responses and forward velocity.*

The steady-state responses are function of the forward velocity of a vehicle. To visualize how these steady-state parameters vary when the speed of a vehicle increases, we calculate $S_\kappa$, $S_\beta$, $S_r$, and $S_a$ for a vehicle with the following values.

$$C_{\alpha f_L} = C_{\alpha f_R} \approx 3000\,\mathrm{N/\,rad} \tag{10.278}$$
$$C_{\alpha r_L} = C_{\alpha r_R} \approx 3000\,\mathrm{N/\,rad} \tag{10.279}$$

$$m = 1000\,\mathrm{kg} \tag{10.280}$$
$$I_z = 1650\,\mathrm{kg\,m^2} \tag{10.281}$$
$$a_1 = 1.0\,\mathrm{m} \tag{10.282}$$
$$a_2 = 1.5\,\mathrm{m} \tag{10.283}$$

$$S_\kappa = \frac{0.9 \times 10^{10}}{v_x\left(\dfrac{2.25 \times 10^{10}}{v_x} + 3 \times 10^7 v_x\right)} \tag{10.284}$$

$$S_\beta = \frac{\dfrac{1.35 \times 10^{10}}{v_x} - 6 \times 10^7 v_x}{\dfrac{2.25 \times 10^{10}}{v_x} + 3 \times 10^7 v_x} \tag{10.285}$$

$$S_r = S_\kappa v_x = \frac{0.9 \times 10^{10}}{\dfrac{2.25 \times 10^{10}}{v_x} + 3 \times 10^7 v_x)} \tag{10.286}$$

$$S_a = S_\kappa v_x^2 = \frac{0.9 \times 10^{10} v_x}{\dfrac{2.25 \times 10^{10}}{v_x} + 3 \times 10^7 v_x)} \tag{10.287}$$

*Figures 10.15-10.18 illustrates how the steady-states vary by increasing the forward velocity.*

**Example 392** *Under steering, over steering, neutral steering.*

Curvature response $S_\kappa$ indicates how the radius of turning will change with a change in steer angle. $S_\kappa$ can be expressed as

$$S_\kappa = \frac{\kappa}{\delta} = \frac{1/R}{\delta} = \frac{1}{l}\frac{1}{1 + Kv_x^2} \tag{10.288}$$

$$K = \frac{m}{l^2}\left(\frac{a_2}{C_{\alpha f}} - \frac{a_1}{C_{\alpha r}}\right) \tag{10.289}$$

*where $K$ is called the **stability factor**. It determine that the vehicle is*

$$\begin{array}{lll} 1 - Understeer & if & K > 0 \\ 2 - Neutral & if & K = 0 \\ 3 - Oversteer & if & K < 0. \end{array} \tag{10.290}$$
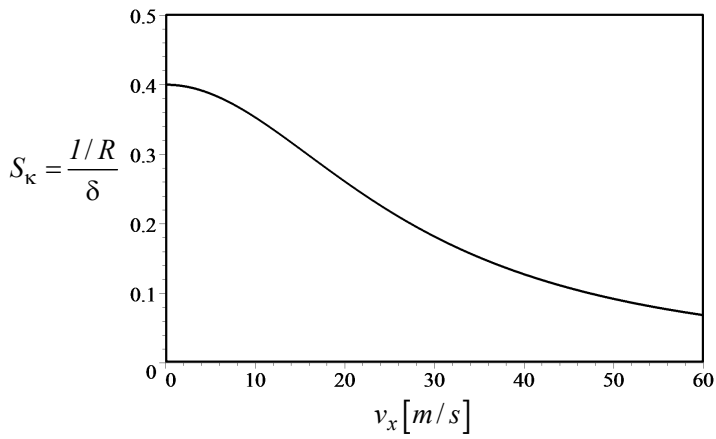
FIGURE 10.15. Curvature response, $S_\kappa$, as a function of forward velocity $v_x$.
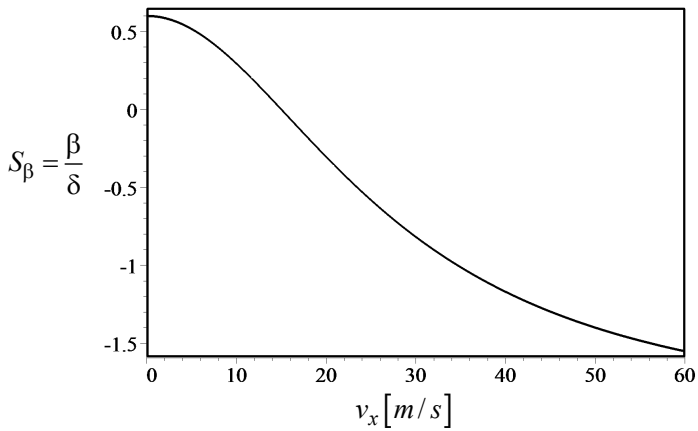


FIGURE 10.16. Sideslip response, $S_\beta$, as a function of forward velocity $v_x$.
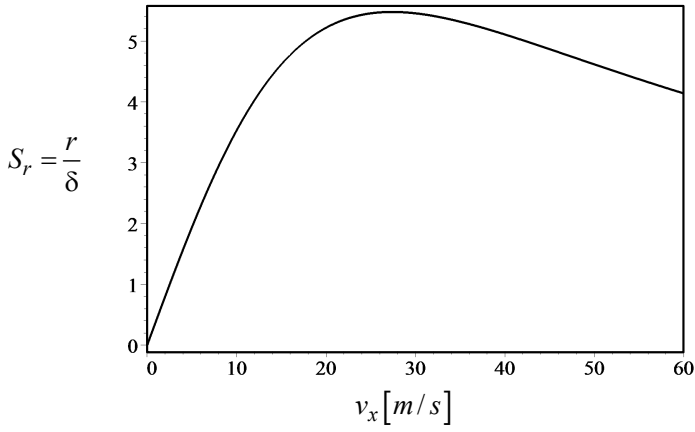
FIGURE 10.17. Yaw rate response, $S_r$, as a function of forward velocity $v_x$.
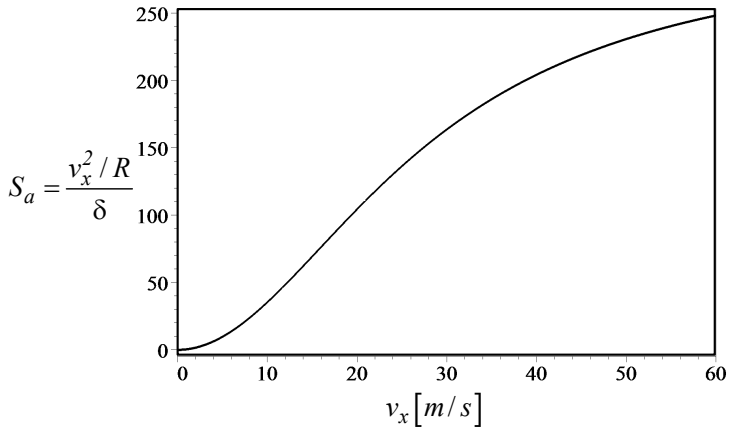


FIGURE 10.18. Lateral acceleration response, $S_a$, as a function of forward velocity $v_x$.

*To find $K$ we may rewrite $S_\kappa$ as*

$$\begin{aligned}
S_\kappa &= \frac{\kappa}{\delta} = \frac{1/R}{\delta} = \frac{C_\delta D_\beta - C_\beta D_\delta}{v_x\left(D_r C_\beta - C_r D_\beta + mv_x D_\beta\right)} \\
&= \frac{1}{v_x\left(\dfrac{D_r C_\beta - C_r D_\beta}{C_\delta D_\beta - C_\beta D_\delta} + \dfrac{mv_x D_\beta}{C_\delta D_\beta - C_\beta D_\delta}\right)} \\
&= \frac{1}{l + \dfrac{mv_x^2 D_\beta}{C_\delta D_\beta - C_\beta D_\delta}} = \frac{1}{l}\frac{1}{1 + \dfrac{m}{l}\dfrac{D_\beta}{C_\delta D_\beta - C_\beta D_\delta}v_x^2} \\
&= \frac{1}{l}\frac{1}{1 + Kv_x^2}. 
\end{aligned} \qquad (10.291)$$

*Therefore,*

$$K = \frac{m}{l}\frac{D_\beta}{C_\delta D_\beta - C_\beta D_\delta} \qquad (10.292)$$

*which, after substituting the force system coefficients, $K$ will be equal to*

$$K = \frac{m}{l^2}\left(\frac{a_2}{C_{\alpha f}} - \frac{a_1}{C_{\alpha r}}\right). \qquad (10.293)$$

*The sign of stability factor $K$ determines if $S_\kappa$ is an increasing or decreasing function of velocity $v_x$. The sign of $K$ depends on the weight of $\frac{a_2}{C_{\alpha f}}$ and $\frac{a_1}{C_{\alpha r}}$, which are dependent on the position of mass center $a_1$, $a_2$, and sideslip coefficients of the front and rear wheels $C_{\alpha f}$, $C_{\alpha r}$.*

*If $K > 0$ and*

$$\frac{a_2}{C_{\alpha f}} > \frac{a_1}{C_{\alpha r}} \qquad (10.294)$$

*then $S_\kappa = \frac{\kappa}{\delta}$ is a decreasing function of $v_x$ and hence, the curvature of the path $\kappa = 1/R$ decreases for a constant $\delta$. Decreasing $\kappa$ indicates that the radius of the steady-state circle, $R$, increases by increasing speed $v_x$. A positive stability factor is desirable and a vehicle with $K > 0$ is stable and is called **understeer**. We need to increase the steering angle if we increase the speed of the vehicle, to keep the same turning circle if the vehicle is understeer.*

*If $K < 0$ and*

$$\frac{a_2}{C_{\alpha f}} < \frac{a_1}{C_{\alpha r}} \qquad (10.295)$$

*then $S_\kappa = \frac{\kappa}{\delta}$ is an increasing function of $v_x$ and hence, the curvature of the path $\kappa = 1/R$ increases for a constant $\delta$. Increasing $\kappa$ indicates that the radius of the steady-state circle, $R$, decreases by increasing speed $v_x$. A negative stability factor is undesirable and a vehicle with $K < 0$ is unstable and is called **oversteer**. We need to decrease the steering angle if we increase the speed of the vehicle, to keep the same turning circle of an oversteer vehicle.*

*If $K = 0$ and*

$$\frac{a_2}{C_{\alpha f}} = \frac{a_1}{C_{\alpha r}} \tag{10.296}$$

*then $S_\kappa = \frac{\kappa}{\delta}$ is not a function of $v_x$ and hence, the curvature of the path, $\kappa = 1/R$ remains constant for a constant $\delta$. Having a constant $\kappa$ indicates that the radius of the steady-state circle, $R$, will not change by changing the speed $v_x$. A zero stability factor is neutral and a vehicle with $K = 0$ is on the border of stability and is called a **neutral steer**. When driving a neutral steer vehicle, we do not need to change the steering angle if we increase or decrease the speed of the vehicle, to keep the same turning circle.*

*As an example, consider a car with the following characteristics:*

$$
\begin{align}
C_{\alpha f} &= 57296\,\mathrm{N/\,rad} \tag{10.297}\\
C_{\alpha r} &= 52712\,\mathrm{N/\,rad} \tag{10.298}\\
m &= 917\,\mathrm{kg} \approx 62.8\,\mathrm{slug} \tag{10.299}\\
a_1 &= 91\,\mathrm{cm} \approx 2.98\,\mathrm{ft} \tag{10.300}\\
a_2 &= 164\,\mathrm{cm} \approx 5.38\,\mathrm{ft} \tag{10.301}
\end{align}
$$

*This car has a stability factor $K$ and a curvature response $S_\kappa$ equal to*

$$
\begin{align}
K &= \frac{m}{l^2}\left(\frac{a_2}{C_{\alpha f}} - \frac{a_1}{C_{\alpha r}}\right) = 1.602 \times 10^{-3} \tag{10.302}\\
S_\kappa &= \frac{1}{l}\frac{1}{1 + Kv_x^2} = \frac{0.392\,16}{1 + 1.602 \times 10^{-3}v_x^2}. \tag{10.303}
\end{align}
$$

*Now assume we fill the trunk and change the car's characteristics to a new set.*

$$
\begin{align}
m &= 1400\,\mathrm{kg} \approx 95.9\,\mathrm{slug} \tag{10.304}\\
a_1 &= 125\,\mathrm{cm} \approx 4.1\,\mathrm{ft} \tag{10.305}\\
a_2 &= 130\,\mathrm{cm} \approx 4.26\,\mathrm{ft} \tag{10.306}
\end{align}
$$

*The new stability factor $K$ and curvature response $S_\kappa$ are*

$$
\begin{align}
K &= -2.21 \times 10^{-4} \tag{10.307}\\
S_\kappa &= -\frac{0.392\,16}{2.21 \times 10^{-4}v_x^2 - 1}. \tag{10.308}
\end{align}
$$

*Figure 10.19 compares the curvature response $S_\kappa$ for two situations of a neutral steering. We assumed that increasing weight did not change the tire characteristics, and we kept same sideslip coefficients.*

**Example 393** *Critical speed $v_c$.*
*If $K < 0$ then $S_\kappa = \frac{\kappa}{\delta} = \frac{1}{l}\frac{1}{1+Kv_x^2}$ increases with increasing $v_x$. The steering angle must be decreased to maintain a constant radius path. When*
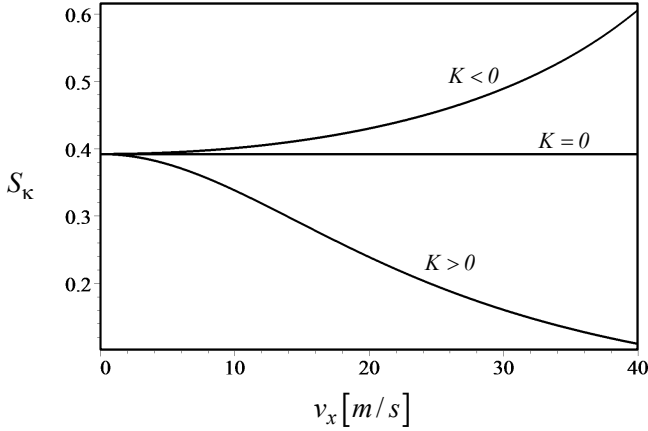
FIGURE 10.19. Comarison of the curvature response $S_\kappa$ for a car with $K = 1.602 \times 10^{-3}$, $K = -2.21 \times 10^{-4}$, and $K = 0$.

the speed $v_x$ is equal to the following critical value

$$v_c = \sqrt{-\frac{1}{K}} \tag{10.309}$$

then

$$S_\kappa \to \infty \tag{10.310}$$

and any decrease in steering angle cannot keep the path. When $v_x = v_c$, the curvature $\kappa$ is not a function of steering angle $\delta$, and any radius of rotation is possible for a constant $\delta$. The critical speed makes the system unstable. Controlling an oversteer vehicle gets harder by $v_x \to v_c$ and becomes uncontrollable when $v_x = v_c$.

The critical speed of an oversteer car with the characteristics

$$
\begin{align}
C_{\alpha f} &= 57296\,\mathrm{N/rad} \tag{10.311}\\
C_{\alpha r} &= 52712\,\mathrm{N/rad} \tag{10.312}\\
m &= 1400\,\mathrm{kg} \approx 95.9\,\mathrm{slug} \tag{10.313}\\
a_1 &= 125\,\mathrm{cm} \approx 4.1\,\mathrm{ft} \tag{10.314}\\
a_2 &= 130\,\mathrm{cm} \approx 4.26\,\mathrm{ft} \tag{10.315}
\end{align}
$$

is

$$v_c = \sqrt{-\frac{1}{K}} = 67.33\,\mathrm{m/s} \tag{10.316}$$

because

$$K = \frac{m}{l^2}\left(\frac{a_2}{C_{\alpha f}} - \frac{a_1}{C_{\alpha r}}\right) = -2.2059 \times 10^{-4}. \tag{10.317}$$

**Example 394** *Neutral steer point.*

The **neutral steer point** of a bicycle vehicle is the point along the lon-gitudinal axis at which the mass center allows neutral steering. To find the neutral steer point $P_N$ we defined a distance $a_N$ from the front axle to have $K = 0$

$$\frac{l - a_N}{C_{\alpha f}} - \frac{a_N}{C_{\alpha r}} = 0 \qquad (10.318)$$

*therefore,*

$$a_N = \frac{C_{\alpha r}}{C_{\alpha f} + C_{\alpha r}} l. \qquad (10.319)$$

The **neutral distance** $d_N$

$$d_N = a_N - a_1 \qquad (10.320)$$

indicates how much the mass center can move to have neutral steering.

For example, the neutral steer point $P_N$ for a car with the characteristics

$$
\begin{aligned}
C_{\alpha f} &= 57296\,\mathrm{N/\,rad} & (10.321) \\
C_{\alpha r} &= 52712\,\mathrm{N/\,rad} & (10.322) \\
a_1 &= 91\,\mathrm{cm} \approx 2.98\,\mathrm{ft} & (10.323) \\
a_2 &= 164\,\mathrm{cm} \approx 5.38\,\mathrm{ft} & (10.324)
\end{aligned}
$$

*is at*

$$a_N = 1.2219\,\mathrm{m}. \qquad (10.325)$$

*Therefore, the mass center can move a distance $d_N$ forward and still have an understeer car.*

$$
\begin{aligned}
d_N &= a_N - a_1 \\
&\approx 31.2\,\mathrm{cm} & (10.326)
\end{aligned}
$$

**Example 395** ★ *Constant lateral force and steady-state response.*

Consider a situation in which there is a constant lateral force $F_y$ on a vehicle and there is no steering angle. At steady-state conditions, the following equations describe the motion of the vehicle.

$$
\begin{aligned}
F_y &= mr\,v_x & (10.327) \\
M_z &= 0 & (10.328) \\
F_y &= C_r\,r + C_\beta\,\beta & (10.329) \\
M_z &= D_r\,r + D_\beta\,\beta & (10.330)
\end{aligned}
$$

Equation (10.329) and (10.330) may be used to define these steady-state responses

$$S_{y1} = \frac{\kappa}{F_y} = \frac{1/R}{F_y} = \frac{D_\beta}{v_x\,(C_r D_\beta - C_\beta D_r)} \qquad (10.331)$$

$$S_{y_2} = \frac{r}{F_y} = \frac{D_\beta}{C_r D_\beta - C_\beta D_r} \tag{10.332}$$

A constant lateral force can be a result of driving straight on a banked road, or having a side wind. A nonzero lateral rotation response $S_{y_1}$ indicates that the vehicle will turn with $\delta = 0$ and $F_y \neq 0$. The lateral rotation response $S_{y_1}$ may be transformed to the following equation to be a function of the stability factor $K$:

$$S_{y_1} = \frac{1}{v_x \left( C_r - C_\beta \dfrac{D_r}{D_\beta} \right)} = \frac{a_1 C_{\alpha f} - a_2 C_{\alpha r}}{v_x C_{\alpha f} C_{\alpha r} l^2}$$

$$= -\frac{1}{v_x l^2} \left( \frac{a_2}{C_{\alpha f}} - \frac{a_1}{C_{\alpha r}} \right) = -\frac{1}{m v_x} K \tag{10.333}$$

To drain the rain and water from roads, we build the roads on flat ground, a little banked from the center to the shoulder. Consider a moving car on a straight banked road. There is a lateral gravitational force for the bank angle $\theta$

$$F_y = -mg \sin \theta$$

$$\approx -mg\theta \tag{10.334}$$

to pull the car downhill. If the car is an understeer and $K > 0$ then the car will turn downhill, while an oversteer car with $K < 0$ will turn uphill.

**Example 396 ★** *SAE steering definition.*

SAE steer definitions for under and oversteer behaviors are as follows:

$US-$ A vehicle is understeer if the ratio of the steering wheel angle gradient to the overall steering ratio is greater than the Ackerman steer gradient.

$OS-$ A vehicle is oversteer if the ratio of the steering wheel angle gradient to the overall steering ratio is less than the Ackerman steer gradient.

$AS-$ Ackerman steering gradient is

$$S_A = \frac{l}{v_x^2} = \frac{d\,(l/R)}{d\,(v_x^2/R)} \tag{10.335}$$

## 10.6 ★ Linearized Model for a Two-Wheel Vehicle

When the sideslip angle $\beta$ is very small, the equations of motion of bicycle reduce to the following set of equations:

$$F_x = m\dot{v} - mrv\beta \tag{10.336}$$

$$F_y = mv\left(r + \dot{\beta}\right) + m\beta\dot{v} \tag{10.337}$$

$$M_z = I_z \dot{r} \tag{10.338}$$

$$
\begin{aligned}
F_y &= (-C_{\alpha f} - C_{\alpha r})\beta + \frac{1}{v}(a_2 C_{\alpha r} - a_1 C_{\alpha f})r \\
&\quad + \delta_f C_{\alpha f} + \delta_r C_{\alpha r} \tag{10.339}
\end{aligned}
$$

$$
\begin{aligned}
M_z &= (a_2 C_{\alpha r} - a_1 C_{\alpha f})\beta - \frac{1}{v}(a_1^2 C_{\alpha f} + a_2^2 C_{\alpha r})r \\
&\quad + a_1 C_{\alpha f}\delta_f - a_2 C_{\alpha r}\delta_r. \tag{10.340}
\end{aligned}
$$

Although these equations are not linear, because of assumption $\beta \ll 1$, they are called linearized equations of motion.

When the speed of the vehicle is constant, then the equations are

$$
\begin{aligned}
F_x &= -mrv\beta \tag{10.341} \\
F_y &= mv\left(r + \dot{\beta}\right) \tag{10.342} \\
M_z &= I_z \dot{r}. \tag{10.343}
\end{aligned}
$$

**Proof.** For a small sideslip, $\beta$, we may assume that,

$$
\begin{aligned}
v_x &= v\cos\beta \approx v \tag{10.344} \\
v_y &= v\sin\beta \approx v\beta. \tag{10.345}
\end{aligned}
$$

Therefore, the equations of motion (10.164)–(10.166) will be simplified to

$$
\begin{aligned}
F_x &= m\dot{v}_x - mrv_y \\
&= m\dot{v} - mrv\beta \tag{10.346} \\
F_y &= m\dot{v}_y + mrv_x \\
&= m\left(\dot{v}\beta + v\dot{\beta}\right) + mrv \tag{10.347} \\
M_z &= \dot{r}I_z. \tag{10.348}
\end{aligned}
$$

Substitute $\dot{v} = 0$ for a constant velocity, and these equations will be equal to (10.341)-(10.343).

The sideslip angle $\alpha_f$ and $\alpha_r$ can also be linearized to

$$
\begin{aligned}
\alpha_f &= \beta_f - \delta_f \\
&= \frac{1}{v_x}(v_y + a_1 r) - \delta_f \\
&= \beta + \frac{a_1 r}{v} - \delta_f \tag{10.349} \\
\alpha_r &= \beta_r - \delta_r \\
&= \frac{1}{v_x}(v_y - a_2 r) - \delta_r \\
&= \beta - \frac{a_2 r}{v} - \delta_r. \tag{10.350}
\end{aligned}
$$

The front and rear lateral forces are

$$
\begin{aligned}
F_{yf} &= -C_{\alpha f}\alpha_f \tag{10.351} \\
F_{yr} &= -C_{\alpha r}\alpha_r \tag{10.352}
\end{aligned}
$$

Substituting these equations in (10.346)-(10.348) and using the definitions

$$F_x \approx F_{x_f} + F_{x_r} \tag{10.353}$$
$$F_y \approx F_{y_f} + F_{y_r} \tag{10.354}$$
$$M_z \approx a_1 F_{y_f} - a_2 F_{y_r} \tag{10.355}$$

results in the force system

$$
\begin{aligned}
F_y &= F_{yf} + F_{yr} \\
&= (-C_{\alpha f} - C_{\alpha r})\beta + \frac{1}{v}(a_2 C_{\alpha r} - a_1 C_{\alpha f})r \\
&\quad + \delta_f C_{\alpha f} + \delta_r C_{\alpha r}
\end{aligned}
\tag{10.356}
$$

$$
\begin{aligned}
M_z &= a_1 F_{yf} - a_2 F_{yr} \\
&= (a_2 C_{\alpha r} - a_1 C_{\alpha f})\beta - \frac{1}{v}\left(a_1^2 C_{\alpha f} + a_2^2 C_{\alpha r}\right)r \\
&\quad + a_1 C_{\alpha f}\delta_f - a_2 C_{\alpha r}\delta_r
\end{aligned}
\tag{10.357}
$$

Factorization can transform the force system to (10.339)-(10.340). ■

**Example 397 ★** *Front-wheel-steering and constant velocity.*
*In most cases, the front wheel is the only steerable wheel, hence $\delta_f = \delta$ and $\delta_r = 0$. This simplifies the equations of motion for a front steering vehicle at constant velocity to*

$$F_x = -mrv\beta \tag{10.358}$$

$$
\begin{aligned}
mv\dot{\beta} &= (-C_{\alpha f} - C_{\alpha r})\beta \\
&\quad + \left(-\frac{1}{v}(a_1 C_{\alpha f} - a_2 C_{\alpha r}) - mv\right)r + C_{\alpha f}\delta
\end{aligned}
\tag{10.359}
$$

$$
\begin{aligned}
I_z \dot{r} &= (a_2 C_{\alpha r} - a_1 C_{\alpha f})\beta \\
&\quad + \left(-\frac{1}{v}\left(C_{\alpha f}a_1^2 + C_{\alpha r}a_2^2\right)\right)r + (a_1 C_{\alpha f})\delta.
\end{aligned}
\tag{10.360}
$$

*The second and third equations may be written in a matrix form for simpler calculation.*

$$
\begin{bmatrix} \dot{\beta} \\ \dot{r} \end{bmatrix} =
\begin{bmatrix}
\dfrac{-(C_{\alpha f} + C_{\alpha r})}{mv} & \dfrac{a_2 C_{\alpha r} - a_1 C_{\alpha f}}{mv^2} - 1 \\[2ex]
\dfrac{a_2 C_{\alpha r} - a_1 C_{\alpha f}}{I_z} & \dfrac{-\left(C_{\alpha f}a_1^2 + C_{\alpha r}a_2^2\right)}{vI_z}
\end{bmatrix}
\begin{bmatrix} \beta \\ r \end{bmatrix}
$$
$$
+ \begin{bmatrix} \dfrac{C_{\alpha f}}{mv} \\[2ex] \dfrac{a_1 C_{\alpha f}}{I_z} \end{bmatrix} \delta
\tag{10.361}
$$

**Example 398** ★ *Steady state conditions and a linearized system.*

*The equations of motion for a front steering, two-wheel model of four-wheel vehicles are given in equation (10.361) for linearized angle $\beta$. At a steady-state condition we have*

$$\begin{bmatrix} \dot{\beta} \\ \dot{r} \end{bmatrix} = 0 \tag{10.362}$$

*and therefore,*

$$\begin{bmatrix} \beta \\ r \end{bmatrix} = \begin{bmatrix} \dfrac{-C_{\alpha f} - C_{\alpha r}}{mv} & \dfrac{a_2 C_{\alpha r} - a_1 C_{\alpha f}}{mv^2} - 1 \\[3mm] \dfrac{a_2 C_{\alpha r} - a_1 C_{\alpha f}}{I_z} & \dfrac{-C_{\alpha f} a_1^2 - C_{\alpha r} a_2^2}{v I_z} \end{bmatrix}^{-1} \begin{bmatrix} \dfrac{C_{\alpha f}}{mv}\delta \\[3mm] \dfrac{a_1 C_{\alpha f}}{I_z}\delta \end{bmatrix}$$

$$= \begin{bmatrix} \dfrac{-\left(a_2^2 C_{\alpha r} + a_1 a_2 C_{\alpha r} - mv^2 a_1\right) C_{\alpha f}\delta}{C_{\alpha f} C_{\alpha r} (a_1 + a_2)^2 - mv^2 (a_1 C_{\alpha f} - a_2 C_{\alpha r})} \\[5mm] \dfrac{-(a_1 + a_2) v C_{\alpha f} C_{\alpha r}\delta}{C_{\alpha f} C_{\alpha r} (a_1 + a_2)^2 - mv^2 (a_1 C_{\alpha f} - a_2 C_{\alpha r})} \end{bmatrix}. \tag{10.363}$$

*Using Equation (10.363) we can define the following steady-state responses:*

2− *Sideslip response, $S_\beta$*

$$S_\beta = \frac{\beta}{\delta} = \frac{-\left(a_2^2 C_{\alpha r} + a_1 a_2 C_{\alpha r} - mv^2 a_1\right) C_{\alpha f}}{C_{\alpha f} C_{\alpha r} l^2 - mv^2 (a_1 C_{\alpha f} - a_2 C_{\alpha r})} \tag{10.364}$$

3− *Yaw rate response, $S_r$*

$$S_r = \frac{r}{\delta} = \frac{-C_{\alpha f} C_{\alpha r} l v}{C_{\alpha f} C_{\alpha r} l^2 - mv^2 (a_1 C_{\alpha f} - a_2 C_{\alpha r})} \tag{10.365}$$

*At steady-state conditions we have*

$$r = \frac{v}{R} \tag{10.366}$$

*where $R$ is the radius of the circular path of the vehicle. Employing Equation (10.366) we are able to define two more steady-state responses as follows:*

1− *Curvature response, $S_\kappa$*

$$\begin{aligned} S_\kappa &= \frac{\kappa}{\delta} = \frac{1}{R\delta} = \frac{r}{v\delta} = \frac{1}{v}S_r \\ &= \frac{-l C_{\alpha f} C_{\alpha r}}{C_{\alpha f} C_{\alpha r} l^2 - mv^2 (a_1 C_{\alpha f} - a_2 C_{\alpha r})} \end{aligned} \tag{10.367}$$

4− *Lateral acceleration response, $S_a$*

$$\begin{aligned} S_a &= \frac{v^2/R}{\delta} = \frac{\kappa}{\delta} v^2 = S_\kappa v^2 \\ &= \frac{-l C_{\alpha f} C_{\alpha r} v^2}{C_{\alpha f} C_{\alpha r} l^2 - mv^2 (a_1 C_{\alpha f} - a_2 C_{\alpha r})} \end{aligned} \tag{10.368}$$

*The above steady-state responses are comparable to the steady-states numbered 1 to 4 given in Equations (10.242)-(10.245) for a more general case.*

**Example 399 ★** *Understeer and oversteer for a linearized model.*
   *Employing the curvature response $S_\kappa$ in Equation (10.367) we may define*

$$
\begin{aligned}
S_\kappa &= \frac{\kappa}{\delta} = \frac{1/R}{\delta} = \frac{-lC_{\alpha f}C_{\alpha r}}{C_{\alpha f}C_{\alpha r}l^2 - mv^2\left(a_1C_{\alpha f} - a_2C_{\alpha r}\right)} \\
&= \frac{1}{l + \dfrac{mv^2\left(a_1C_{\alpha f} - a_2C_{\alpha r}\right)}{-lC_{\alpha f}C_{\alpha r}}} \\
&= \frac{1}{l}\frac{1}{1 + \dfrac{mv^2\left(a_1C_{\alpha f} - a_2C_{\alpha r}\right)}{-l^2C_{\alpha f}C_{\alpha r}}} = \frac{1}{l}\frac{1}{1 + Kv_x^2}
\end{aligned}
\qquad (10.369)
$$

*where*

$$
K = \frac{m}{l^2}\left(\frac{a_2}{C_{\alpha f}} - \frac{a_1}{C_{\alpha r}}\right).
\qquad (10.370)
$$

*This $K$ is the same as the stability factor given in Equation (10.293). Therefore, the stability factor remains the same if we use the linearized equations.*

**Example 400 ★** *Source of nonlinearities.*
   *There are three main reasons for nonlinearity in rigid vehicle equations of motion: product of variables, trigonometric functions, and nonlinear nature of forces. When the steer angle $\delta$ and sideslip angles $\alpha_i$ and $\beta$ are very small, it is reasonable to ignore all kinds of nonlinearities. This is called* **low angles condition** *driving, and is correct for low turn and normal speed driving.*

## 10.7   ★ Time Response

To analyze the time response of a vehicle and examine how the vehicle will respond to a steering input, the following set of coupled ordinary differential equations must be solved.

$$
\dot{v}_x = \frac{1}{m}F_x + r\,v_y
\qquad (10.371)
$$

$$\begin{bmatrix} \dot{v}_y \\ \dot{r} \end{bmatrix} = \begin{bmatrix} -\dfrac{C_{\alpha f} + C_{\alpha r}}{m v_x} & \dfrac{-a_1 C_{\alpha f} + a_2 C_{\alpha r}}{m v_x} - v_x \\ -\dfrac{a_1 C_{\alpha f} - a_2 C_{\alpha r}}{I_z v_x} & -\dfrac{a_1^2 C_{\alpha f} + a_2^2 C_{\alpha r}}{I_z v_x} \end{bmatrix} \begin{bmatrix} v_y \\ r \end{bmatrix}$$

$$+ \begin{bmatrix} \dfrac{C_{\alpha f}}{m} \\ \dfrac{a_1 C_{\alpha f}}{I_z} \end{bmatrix} \delta(t) \tag{10.372}$$

The answers to this set of equations to a given time dependent steer angle are

$$v_x = v_x(t) \tag{10.373}$$
$$v_y = v_y(t) \tag{10.374}$$
$$r = r(t). \tag{10.375}$$

Such a solution is called *time response* or *transient response*.

Assuming a constant forward velocity, the first equation (10.371) simplifies to

$$F_x = -mr\, v_y \tag{10.376}$$

and Equations (10.372) become independent from the first one. The set of Equations (10.372) can be written in the following form:

$$\dot{\mathbf{q}} = [A]\, \mathbf{q} + \mathbf{u} \tag{10.377}$$

in which $[A]$ is a constant coefficient matrix, $\mathbf{q}$ is the vector of control variables, and $\mathbf{u}$ is the vector of inputs.

$$[A] = \begin{bmatrix} -\dfrac{C_{\alpha f} + C_{\alpha r}}{m v_x} & \dfrac{-a_1 C_{\alpha f} + a_2 C_{\alpha r}}{m v_x} - v_x \\ -\dfrac{a_1 C_{\alpha f} - a_2 C_{\alpha r}}{I_z v_x} & -\dfrac{a_1^2 C_{\alpha f} + a_2^2 C_{\alpha r}}{I_z v_x} \end{bmatrix}$$

$$\mathbf{q} = \begin{bmatrix} v_y \\ r \end{bmatrix} \tag{10.378}$$

$$\mathbf{u} = \begin{bmatrix} \dfrac{C_{\alpha f}}{m} \\ \dfrac{a_1 C_{\alpha f}}{I_z} \end{bmatrix} \delta(t) \tag{10.379}$$

To solve the inverse dynamic problem and find the vehicle response, the steering function $\delta(t)$ must be given.

**Example 401 ★** *Direct and indirect, or forward and inverse dynamic problem.*

*Two types of dynamic problems may be defined:* $1-$*direct or forward and,* $2-$*indirect or inverse. In forward dynamics a set of desired functions* $v_x = v_x(t)$, $v_y = v_y(t)$, $r = r(t)$ *are given and the required* $\delta(t)$ *is asked for. In the inverse dynamic problem, an input function* $\delta = \delta(t)$ *is given and the output functions* $v_x = v_x(t)$, $v_y = v_y(t)$, $r = r(t)$ *are asked for.*

*The forward dynamic problem needs differentiation and the inverse dynamic problem needs integration. Generally speaking, solving an inverse dynamic problem is more complicated than a forward dynamic problem.*

**Example 402 ★** *Analytic solution to a step steer input.*

*Consider a vehicle with the following characteristics*

$$C_{\alpha f} = 60000\,\mathrm{N/rad} \tag{10.380}$$
$$C_{\alpha r} = 60000\,\mathrm{N/rad} \tag{10.381}$$
$$m = 1000\,\mathrm{kg} \tag{10.382}$$
$$I_z = 1650\,\mathrm{kg\,m^2} \tag{10.383}$$
$$a_1 = 1.0\,\mathrm{m} \tag{10.384}$$
$$a_2 = 1.5\,\mathrm{cm} \tag{10.385}$$
$$v_x = 20\,\mathrm{m/s.} \tag{10.386}$$

*The force system coefficients for the vehicle from (10.143)-(10.148) are*

$$C_r = 1500\,\mathrm{N\,s/rad} \tag{10.387}$$
$$C_\beta = -120000\,\mathrm{N/rad} \tag{10.388}$$
$$C_\delta = 60000\,\mathrm{N/rad} \tag{10.389}$$
$$D_r = -9750\,\mathrm{N\,m\,s/rad} \tag{10.390}$$
$$D_\beta = 30000\,\mathrm{N\,m/rad} \tag{10.391}$$
$$D_\delta = 60000\,\mathrm{N\,m/rad.} \tag{10.392}$$

*Let's assume the steering input is*

$$\delta(t) = \begin{cases} 0.2\,\mathrm{rad} \approx 11.5\,\mathrm{deg} & t > 0 \\ 0 & t \le 0 \end{cases}. \tag{10.393}$$

*The equations of motion for a zero initial condition*

$$\mathbf{q}_0 = \begin{bmatrix} v_y(0) \\ r(0) \end{bmatrix} = \begin{bmatrix} 0 \\ 0 \end{bmatrix} \tag{10.394}$$

*are*

$$\dot{v}_y + 6v_y + 18.5r = 60\delta(t)$$
$$= 12 \tag{10.395}$$
$$\dot{r} + .909v_y + 5.909r = 36.363\delta(t)$$
$$= 7.272. \tag{10.396}$$
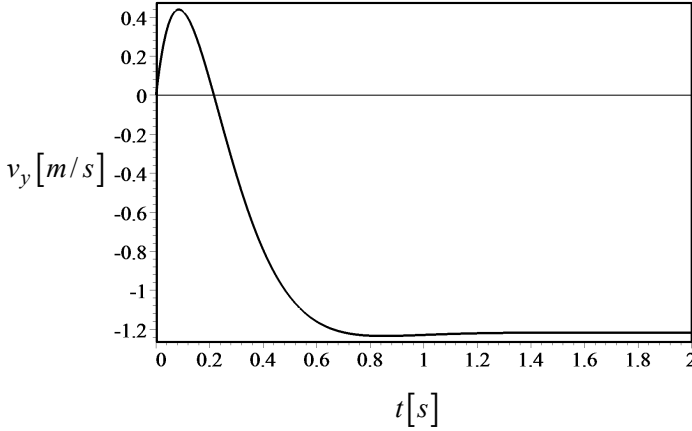
FIGURE 10.20. Lateral velocity response to a sudden change in steer angle.

*The solution of the equations of motion are*

$$\begin{bmatrix} v_y(t) \\ r(t) \end{bmatrix} = \begin{bmatrix} -1.217 + e^{-5.95t} \left( 4.69 \sin 4.1t + 1.21 \cos 4.1t \right) \\ 1.043 + e^{-5.95t} \left( 0.258 \sin 4.1t - 1.043 \cos 4.1t \right) \end{bmatrix}.$$
$$(10.397)$$

*To examine the response of the vehicle to a sudden change in steer angle while going straight at a constant speed, we plot the kinematic variables of the vehicle. Figures 10.20 and 10.21 depict the solutions $v_y(t)$ and $r(t)$ respectively.*

*The steering input is positive and therefore, the vehicle must turn left, in a positive direction of the y-axis. The yaw rate in Figure 10.21 is positive and correctly shows that the vehicle is turning about the z-axis. We can find the lateral velocity of the front and rear wheels,*

$$v_{y_1} = v_y + a_1 r \qquad (10.398)$$
$$v_{y_2} = v_y - a_2 r \qquad (10.399)$$

*by having $v_y$ and $r$. The lateral speed of the front and rear wheels are shown in Figures 10.22 and 10.23. The sideslip angle $\beta = v_y/v_x$ and the radius of rotation $R = v_x/r$ are also shown in Figures 10.24 and 10.25.*

*Figure 10.26 illustrates the vehicle at a steady-state condition when it is turning on a circle. The steer angle $\delta$ is shown, however, the angles $\alpha$ and $\beta$ are too small to be shown.*

**Example 403 ★** *Time series and free response.*
*The response of a vehicle to zero steer angle*

$$\delta(t) = 0 \qquad (10.400)$$
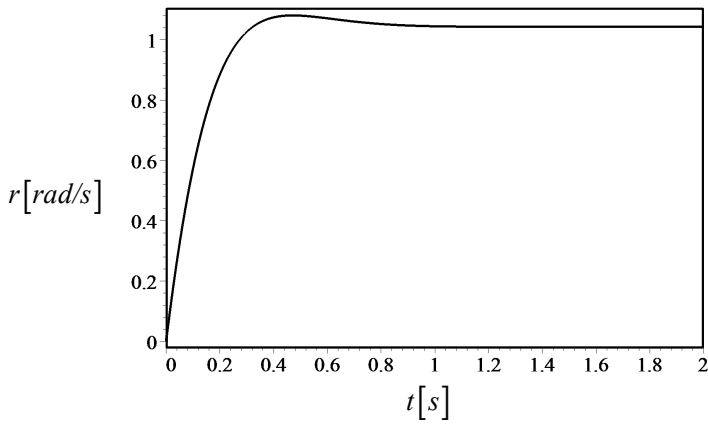
FIGURE 10.21. Yaw velocity response to a sudden change in steer angle.
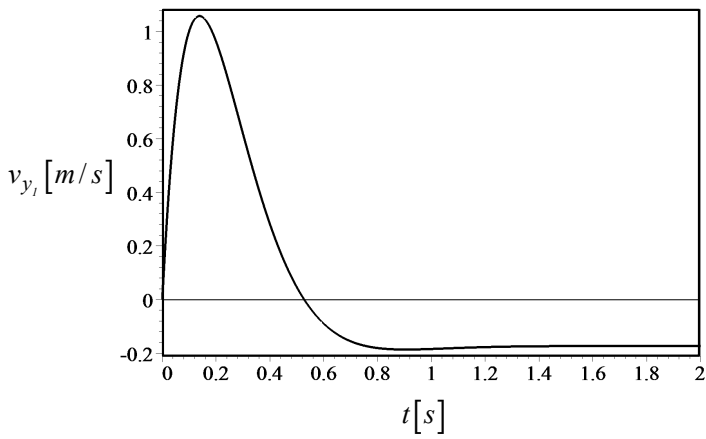


FIGURE 10.22. Lateral velocity response of the front wheel to a sudden change in steer angle.
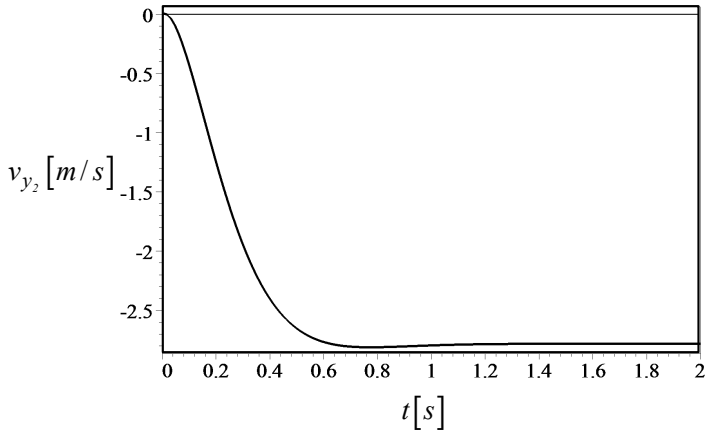
FIGURE 10.23. Lateral velocity response of the rear wheel to a sudden change in steer angle.
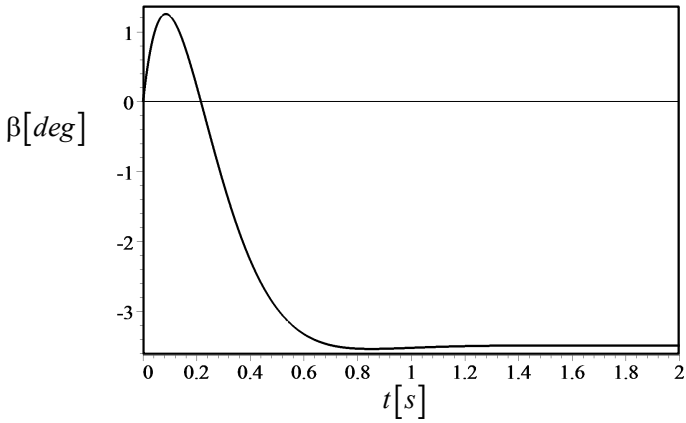


FIGURE 10.24. Sideslip response to a sudden change in steer angle.
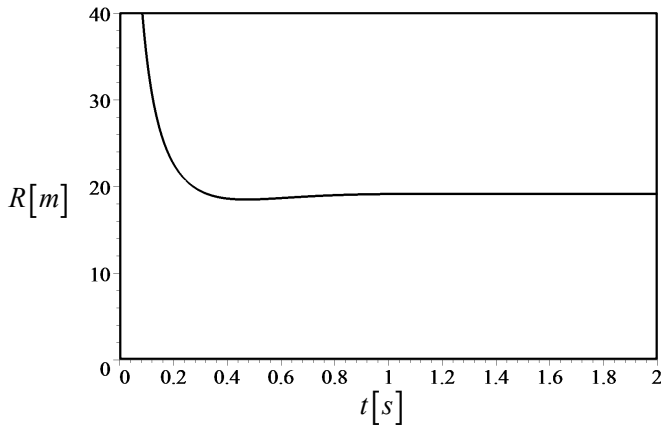
FIGURE 10.25. Radius of rotation response to a sudden change in steer angle.
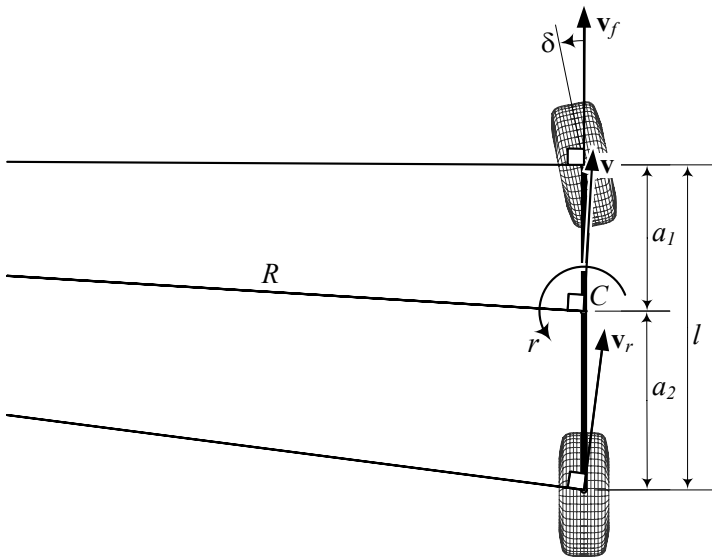


FIGURE 10.26. A vehicle in a steady state condition when it is turning in a circle.

*at constant speed is called free response. The equation of motion under free dynamics is*

$$\dot{\mathbf{q}} = [A]\,\mathbf{q}. \tag{10.401}$$

*To solve the equations, let's assume*

$$[A] = \begin{bmatrix} a & b \\ c & d \end{bmatrix} \tag{10.402}$$

*and therefore, the equations of motion are*

$$\begin{bmatrix} \dot{v}_y \\ \dot{r} \end{bmatrix} = \begin{bmatrix} a & b \\ c & d \end{bmatrix} \begin{bmatrix} v_y \\ r \end{bmatrix} \tag{10.403}$$

*Because the equations are linear, the solutions are an exponential function*

$$v_y = Ae^{\lambda t} \tag{10.404}$$

$$r = Be^{\lambda t}. \tag{10.405}$$

*Substituting the solutions*

$$\begin{bmatrix} A\lambda e^{\lambda t} \\ B\lambda e^{\lambda t} \end{bmatrix} = \begin{bmatrix} a & b \\ c & d \end{bmatrix} \begin{bmatrix} Aee^{\lambda t} \\ Be^{\lambda t} \end{bmatrix} \tag{10.406}$$

*shows that*

$$\begin{bmatrix} a - \lambda & b \\ c & d - \lambda \end{bmatrix} \begin{bmatrix} Ae^{st} \\ Be^{\lambda t} \end{bmatrix} = 0. \tag{10.407}$$

*Therefore, the condition to for functions (10.404) and (10.405) to be the solution of the equation (10.403) is that the exponent $\lambda$ is the eigenvalue of $[A]$. To find $\lambda$, we may expand the determinant of the above coefficient matrix*

$$\det \begin{bmatrix} a - \lambda & b \\ c & d - \lambda \end{bmatrix} = \lambda^2 - (a + d)\,\lambda + (ad - bc) \tag{10.408}$$

*and find the characteristic equation*

$$\lambda^2 - (a + d)\,\lambda + (ad - bc) = 0. \tag{10.409}$$

*The solution of the characteristic equations is*

$$\lambda = \frac{1}{2}\,(a + d) \pm \frac{1}{2}\sqrt{(a - d)^2 + 4bc}. \tag{10.410}$$

*Having the eigenvalues $\lambda_{1,2}$ provides the following general solution for the free dynamics of a bicycle vehicle.*

$$v_y = A_1 e^{\lambda_1 t} + A_2 e^{\lambda_2 t} \tag{10.411}$$

$$r = B_1 e^{\lambda_1 t} + B_2 e^{\lambda_2 t}. \tag{10.412}$$

*The coefficients $A_1$, $A_2$, $B_1$, and $B_2$, must be found from initial conditions:
As an example, consider a vehicle with the following characteristics*

$$C_{\alpha f} = 57296 \, \text{N}/\text{rad} \tag{10.413}$$

$$C_{\alpha r} = 52712 \, \text{N}/\text{rad} \tag{10.414}$$

$$m = 1400 \, \text{kg} \approx 95.9 \, \text{slug} \tag{10.415}$$

$$I_z = 1128 \, \text{kg m}^2 \approx 832 \, \text{slug ft}^2 \tag{10.416}$$

$$a_1 = 125 \, \text{cm} \approx 4.1 \, \text{ft} \tag{10.417}$$

$$a_2 = 130 \, \text{cm} \approx 4.26 \, \text{ft} \tag{10.418}$$

$$v_x = 20 \, \text{m}/\text{s} \tag{10.419}$$

*which start from*

$$\mathbf{q}_0 = \left[ \begin{array}{c} v_y(0) \\ r(0) \end{array} \right] = \left[ \begin{array}{c} 1 \\ 0 \end{array} \right]. \tag{10.420}$$

*Substituting these values provide the following equations of motion:*

$$\left[ \begin{array}{c} \dot{v}_y \\ \dot{r} \end{array} \right] = \left[ \begin{array}{cc} -3.929 & -31.051 \\ -13.716 & -79170.337 \end{array} \right] \left[ \begin{array}{c} v_y \\ r \end{array} \right] \tag{10.421}$$

*and their solutions are*

$$v_y = -0.173 \times 10^{-3} \left( e^{-3.92t} - e^{-79170.34t} \right) \tag{10.422}$$

$$r = e^{-3.92t} + 0.68 \times 10 \times 10^{-7} e^{-79170.34t}. \tag{10.423}$$

*Figures 10.27 and 10.28 illustrate the time response. Figure 10.29 is a
magnification of Figure 10.28 to show that $r$ does not jump to a negative
point but decreases rapidly and then approaches zero gradually.*

**Example 404** ★ *Matrix exponentiation.*
   *The exponential function $e^{[A]t}$ is called matrix exponentiation. This func-
tion is defined as a matrix time series.*

$$e^{[A]t} = I + [A]\, t + \frac{[A]^2}{2!} t^2 + \frac{[A]^3}{3!} t^3 + \cdots \tag{10.424}$$

*This series always converges. As an example assume*

$$[A] = \left[ \begin{array}{cc} 0.1 & 0.2 \\ -0.3 & 0.4 \end{array} \right] \tag{10.425}$$

*then*

$$e^{[A]t} \approx \left[ \begin{array}{cc} 1 & 0 \\ 0 & 1 \end{array} \right] + \left[ \begin{array}{cc} 0.1 & 0.2 \\ -0.3 & 0.4 \end{array} \right] t + \frac{1}{2} \left[ \begin{array}{cc} 0.1 & 0.2 \\ -0.3 & 0.4 \end{array} \right]^2 t^2 + \cdots$$

$$\approx \left[ \begin{array}{cc} 1 + 0.1t - 0.025\, t^2 + \cdots & 0.2t + 0.05t^2 + \cdots \\ -0.3t - 0.075\, t^2 + \cdots & 1 + 0.4t + 0.05t^2 + \cdots \end{array} \right]. \tag{10.426}$$
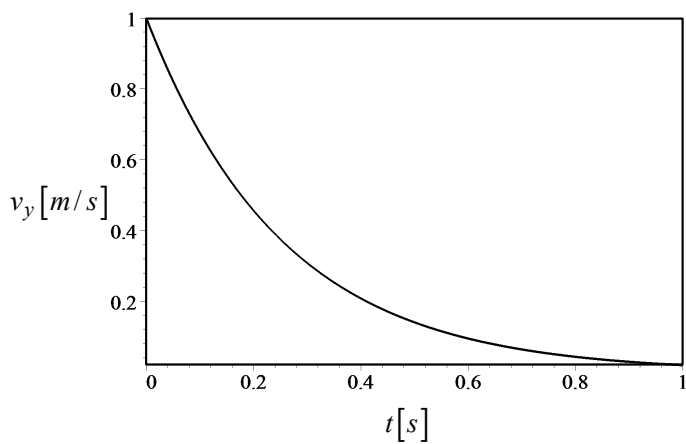
FIGURE 10.27. Lateral velocity response in example 403.
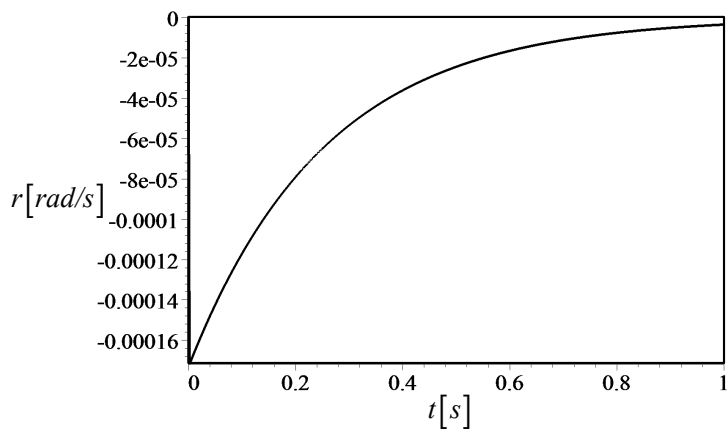


FIGURE 10.28. Yaw velocity response in example 403.
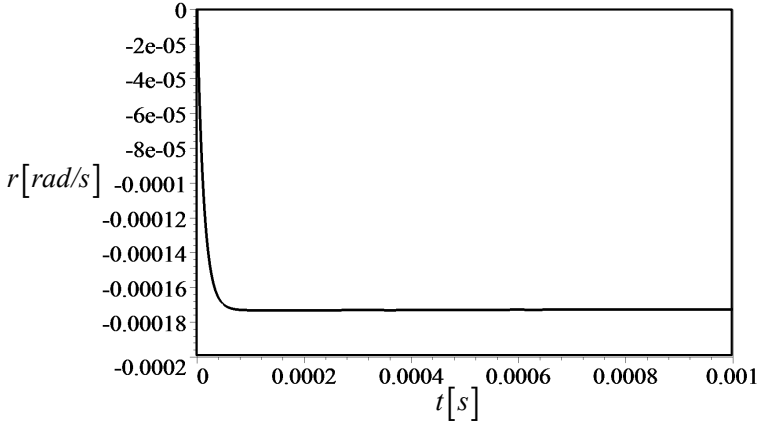
FIGURE 10.29. Yaw velocity response in example 403.

**Example 405 ★** *Time series and free response.*
*The response of a vehicle to zero steer angle*

$$\delta\left(t\right) = 0 \tag{10.427}$$

*at constant speed is called free response. The equation of motion under free dynamics is*

$$\dot{\mathbf{q}} = [A]\,\mathbf{q}. \tag{10.428}$$

*The solution of this differential equation with the initial conditions*

$$\mathbf{q}\left(0\right) = \mathbf{q}_0 \tag{10.429}$$

*is*

$$\mathbf{q}\left(t\right) = e^{[A]t}\mathbf{q}_0. \tag{10.430}$$

$\mathbf{q}\left(t\right) \to \mathbf{0}$ *for* $\forall \mathbf{q}_0$, *if the eigenvalues of* $[A]$ *are negative.*
*The free dynamic in a series can be expressed as*

$$
\begin{aligned}
\mathbf{q}\left(t\right) \;&=\; e^{[A]t}\mathbf{q}_0 \\
&=\; \left( I + [A]\,t + \frac{[A]^2}{2!}t^2 + \frac{[A]^3}{3!}t^3 + \cdots \right)\mathbf{q}_0. 
\end{aligned}
\tag{10.431}
$$

*For example, consider a vehicle with the following characteristics:*

$$C_{\alpha f} = 57296 \, \text{N}/\text{rad} \tag{10.432}$$
$$C_{\alpha r} = 52712 \, \text{N}/\text{rad} \tag{10.433}$$
$$m = 1400 \, \text{kg} \approx 95.9 \, \text{slug} \tag{10.434}$$
$$I_z = 1128 \, \text{kg} \, \text{m}^2 \approx 832 \, \text{slug} \, \text{ft}^2 \tag{10.435}$$
$$a_1 = 125 \, \text{cm} \approx 4.1 \, \text{ft} \tag{10.436}$$
$$a_2 = 130 \, \text{cm} \approx 4.26 \, \text{ft} \tag{10.437}$$
$$v_x = 20 \, \text{m}/\text{s} \tag{10.438}$$

*which start from*

$$\mathbf{q}_0 = \begin{bmatrix} v_y(0) \\ r(0) \end{bmatrix} = \begin{bmatrix} 1 \\ 0 \end{bmatrix}. \tag{10.439}$$

*Employing the vehicle's characteristics, we have*

$$[A] = \begin{bmatrix} -3.929 & -31.051 \\ -13.716 & -79170.337 \end{bmatrix} \tag{10.440}$$

*and therefore, the time response of the vehicle is*

$$\begin{bmatrix} v_y(t) \\ r(t) \end{bmatrix} = \begin{bmatrix} 1 & 0 \\ 0 & 1 \end{bmatrix} \begin{bmatrix} 1 \\ 0 \end{bmatrix}$$
$$+ \begin{bmatrix} -3.929 & -31.051 \\ -13.716 & -79170.337 \end{bmatrix} t \begin{bmatrix} 1 \\ 0 \end{bmatrix}$$
$$+ \frac{1}{2} \begin{bmatrix} -3.929 & -31.051 \\ -13.716 & -79170.337 \end{bmatrix}^2 t^2 \begin{bmatrix} 1 \\ 0 \end{bmatrix}$$
$$+ \frac{1}{6} \begin{bmatrix} -3.929 & -31.051 \\ -13.716 & -79170.337 \end{bmatrix}^3 t^3 \begin{bmatrix} 1 \\ 0 \end{bmatrix} \cdots . \tag{10.441}$$

*Accepting an approximate solution up to cubic degree provides the following approximate solution:*

$$\begin{bmatrix} v_y(t) \\ r(t) \end{bmatrix} \approx \begin{bmatrix} -5.620\,3 \times 10^6 t^3 + 220.67 t^2 - 3.929t + 1 \\ -1.432\,9 \times 10^{10} t^3 + 5.4298 \times 10^5 t^2 - 13.716t \end{bmatrix} \tag{10.442}$$

**Example 406 ★** *Response of an understeer vehicle to a step input.*
   *The response of dynamic systems to a step input is a traditional method to examine the behavior of dynamic systems. A step input for vehicle dynamics is a sudden change in steer angle from zero to a nonzero constant value.*

*Consider a vehicle with the following characteristics:*

$$C_{\alpha f} = 57296 \, \text{N}/\text{rad} \tag{10.443}$$
$$C_{\alpha r} = 52712 \, \text{N}/\text{rad} \tag{10.444}$$
$$m = 917 \, \text{kg} \approx 62.8 \, \text{slug} \tag{10.445}$$
$$I_z = 1128 \, \text{kg} \, \text{m}^2 \approx 832 \, \text{slug} \, \text{ft}^2 \tag{10.446}$$
$$a_1 = 0.91 \, \text{m} \approx 2.98 \, \text{ft} \tag{10.447}$$
$$a_2 = 1.64 \, \text{m} \approx 5.38 \, \text{ft} \tag{10.448}$$
$$v_x = 20 \, \text{m}/\text{s}. \tag{10.449}$$

*and a sudden change in the steering input to a constant value*

$$\delta\left(t\right) = \begin{cases} 0.1 \, \text{rad} \approx 5.7296 \, \text{deg} & t > 0 \\ 0 & t \leq 0 \end{cases}. \tag{10.450}$$

*The equations of motion for a zero initial condition*

$$\mathbf{q}_0 = \begin{bmatrix} v_y\left(0\right) \\ r\left(0\right) \end{bmatrix} = \begin{bmatrix} 0 \\ 0 \end{bmatrix} \tag{10.451}$$

*are*

$$\dot{v}_y + 5.998\,3 v_y + 18.12931734 r = 62.48200654 \delta\left(t\right)$$
$$= 6.248200654 \tag{10.452}$$
$$\dot{r} - 1.520758865 v_y - 4.181178085 r = 46.22283688 \delta\left(t\right)$$
$$= 4.622283688. \tag{10.453}$$

*The force system coefficients for the vehicle from (10.143)-(10.148) are*

$$C_r = -\frac{a_1}{v_x} C_{\alpha f} + \frac{a_2}{v_x} C_{\alpha r} = 1715.416 \, \text{N s}/\text{rad} \tag{10.454}$$
$$C_\beta = -\left(C_{\alpha f} + C_{\alpha r}\right) = -110008 \, \text{N}/\text{rad} \tag{10.455}$$
$$C_\delta = C_{\alpha f} = 57296 \, \text{N}/\text{rad} \tag{10.456}$$

$$D_r = -\frac{a_1^2}{v_x} C_{\alpha f} - \frac{a_2^2}{v_x} C_{\alpha r} = -9461.05064 \, \text{N m s}/\text{rad} \tag{10.457}$$
$$D_\beta = -\left(a_1 C_{\alpha f} - a_2 C_{\alpha r}\right) = 34308.32 \, \text{N m}/\text{rad} \tag{10.458}$$
$$D_\delta = a_1 C_{\alpha f} = 52139.36 \, \text{N m}/\text{rad}. \tag{10.459}$$

*Equations (10.242)-(10.245) indicate that the steady-state response of the*
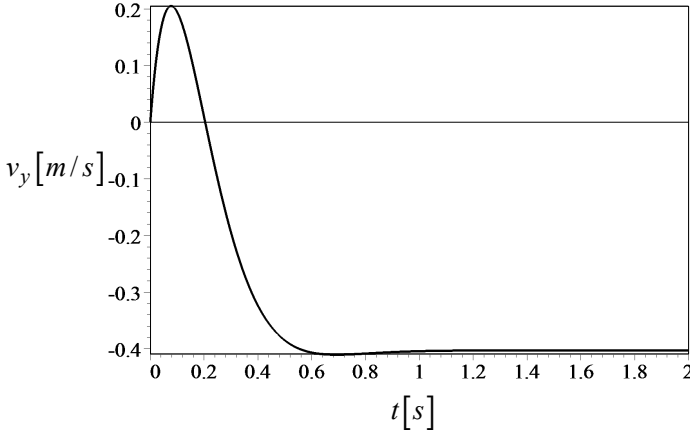
FIGURE 10.30. Lateral velocity response in example 406.

*vehicle, when* $t \to \infty$, *are*

$$S_\kappa = \frac{\kappa}{\delta} = \frac{1}{R\delta} = 0.2390051454 \tag{10.460}$$

$$S_\beta = \frac{\beta}{\delta} = -0.2015419091 \tag{10.461}$$

$$S_r = \frac{r}{\delta} = \frac{\kappa}{\delta}v_x = S_\kappa v_x = 4.780102908 \tag{10.462}$$

$$S_a = \frac{v_x^2/R}{\delta} = \frac{\kappa}{\delta}v_x^2 = S_\kappa v_x^2 = 95.60205816. \tag{10.463}$$

*Therefore, the steady-state characteristics of the vehicle with* $\delta = 0.1$ *must be*

$$R = 41.84010341 \,\text{m} \tag{10.464}$$

$$\beta = -0.02015 \,\text{rad} \approx -1.1545 \,\text{deg} \tag{10.465}$$

$$r = 0.4780102908 \,\text{rad/s} \tag{10.466}$$

$$\frac{v_x^2}{R} = 9.560205816 \,\text{m/s}^2 \tag{10.467}$$

*Substituting the input function (10.470) and solving the equations provides the following solutions:*

$$\begin{bmatrix} v_y(t) \\ r(t) \end{bmatrix} = \begin{bmatrix} -0.4 + e^{-7.193t}(1.789\sin 5.113t + 0.403\cos 5.113t) \\ 0.478 + e^{-7.193t}(0.232\sin 5.113t + 0.478\cos 5.113t) \end{bmatrix} \tag{10.468}$$

*Figures 10.30 and 10.31 depict the solutions.*

*Having* $v_y(t)$ *and* $r(t)$ *are enough to calculate the other kinematic variables as well as the required forward force* $F_x$ *to maintain the constant*
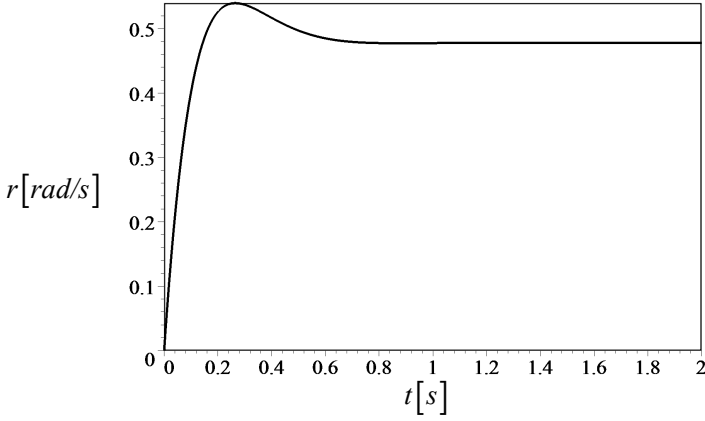
FIGURE 10.31. Yaw rate response in example 406.

*speed.*

$$F_x = -mr\,v_y \tag{10.469}$$

*Figures 10.32 and 10.33 show the kinematics variables of the vehicle, and Figure 10.34 depicts how the require $F_x$ is changing as a function of time.*

**Example 407** ★ *Response of an oversteer vehicle to a step input.*
*Let's assume the steering input is*

$$\delta\left(t\right) = \begin{cases} 0.1\,\mathrm{rad} \approx 5.7296\,\mathrm{deg} & t > 0 \\ 0 & t \leq 0 \end{cases} \tag{10.470}$$

*and the vehicle characteristics are*

$$
\begin{aligned}
C_{\alpha f} &= 57296\,\mathrm{N/\,rad} & (10.471)\\
C_{\alpha r} &= 52712\,\mathrm{N/\,rad} & (10.472)\\
m &= 1400\,\mathrm{kg} \approx 95.9\,\mathrm{slug} & (10.473)\\
I_z &= 1128\,\mathrm{kg\,m}^2 \approx 832\,\mathrm{slug\,ft}^2 & (10.474)\\
a_1 &= 1.25\,\mathrm{m} \approx 4.1\,\mathrm{ft} & (10.475)\\
a_2 &= 1.30\,\mathrm{m} \approx 4.26\,\mathrm{ft} & (10.476)\\
v_x &= 20\,\mathrm{m/\,s}. & (10.477)
\end{aligned}
$$

*The equations of motion for a zero initial conditions*

$$\mathbf{q}_0 = \begin{bmatrix} v_y\left(0\right) \\ r\left(0\right) \end{bmatrix} = \begin{bmatrix} 0 \\ 0 \end{bmatrix} \tag{10.478}$$
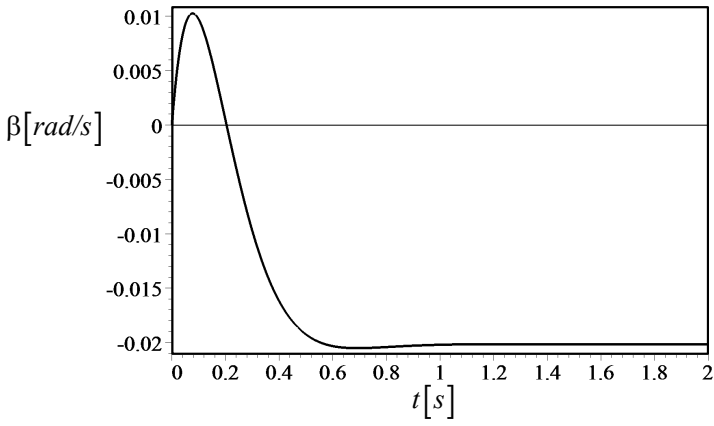
FIGURE 10.32. Sideslip angle response in example 406.
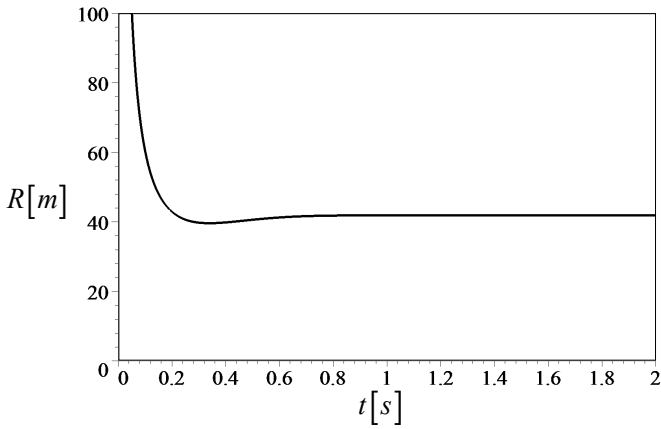


FIGURE 10.33. Radius of rotation response in example 406.
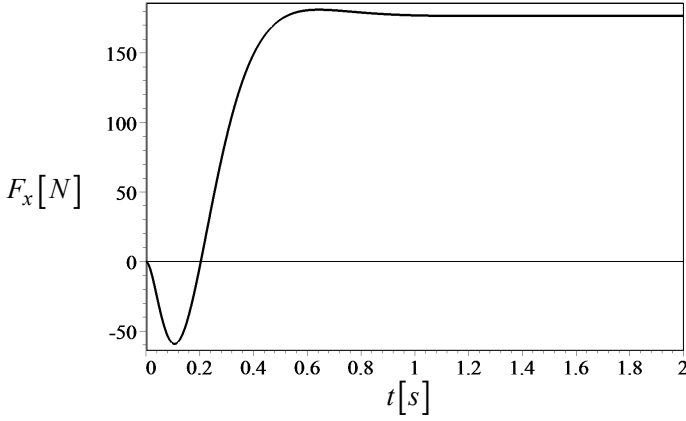
FIGURE 10.34. The required forward force $F_x$ to keep the speed constant, in example 406.

are

$$\dot{v}_y + 3.928857143v_y + 20.11051429r \; = \; 40.92571429\delta\left(t\right)$$
$$= \; 4.092571429 \qquad (10.479)$$
$$\dot{r} + 0.1371631206v_y + 7.917033690r \; = \; 63.4929078\delta\left(t\right)$$
$$= \; 6.34929078. \qquad (10.480)$$

*Substituting the input function (10.470) and solving the equations provides the following solutions:*

$$\left[\begin{array}{c} v_y\left(t\right) \\ r\left(t\right) \end{array}\right] = \left[\begin{array}{c} 6.3e^{-3.328t} - 2.943e^{-8.518t} - 3.361 \\ -0.188e^{-3.328t} - 0.672e^{-8.518t} + 0.188 \end{array}\right] \qquad (10.481)$$

*Figures 10.35 and 10.36 depict the solutions.*

**Example 408 ★** *Standard steer inputs.*
    *Step and sinusoidal excitation inputs are the most general input to examine the behavior of a vehicle. Furthermore, some other transient inputs may also be used to analyze the dynamic behavior of a vehicle. Single sine steering, linearly increasing steering, and half sine lane change steering are the most common transient steering inputs.*

**Example 409 ★** *Position of the rotation center.*
    *The position of the center of rotation O in the vehicle body coordinate is at*

$$x \; = \; -R\sin\beta \qquad (10.482)$$
$$y \; = \; R\cos\beta \qquad (10.483)$$
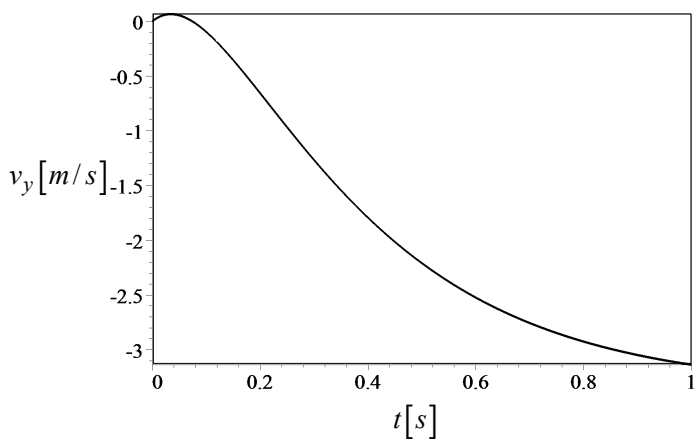
FIGURE 10.35. Lateral velocity response for example 407.
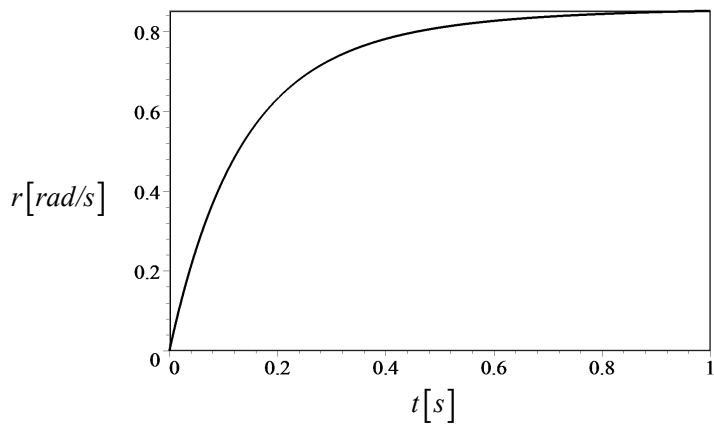


FIGURE 10.36. Yaw velocity response for example 407.
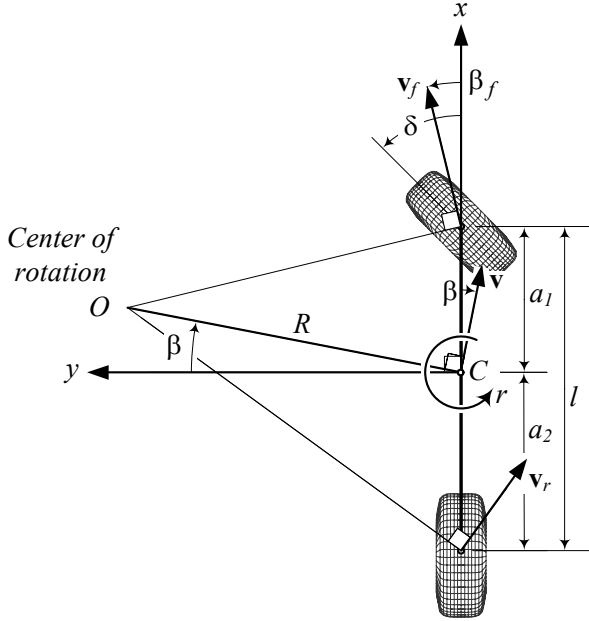
FIGURE 10.37. A two-wheel vehicle model with the vehicle body coordinate frame and the center of rotation $O$.

*because $\beta$ is positive when it is about a positive direction of the z-axis. Figure 10.37 illustrates a two-wheel vehicle model, the vehicle body coordinate frame, and the center of rotation O.*

*At the steady-state condition the radius of rotation can be found from the curvature response $S_\kappa$, and the angle $\beta$ can be found from the sideslip response $S_\beta$.*

$$R = \frac{1}{\delta S_\kappa} = \frac{v_x \left( D_r C_\beta - C_r D_\beta + m v_x D_\beta \right)}{\left( C_\delta D_\beta - C_\beta D_\delta \right) \delta} \tag{10.484}$$

$$\beta = \delta S_\beta = \frac{D_\delta \left( C_r - m v_x \right) - D_r C_\delta}{D_r C_\beta - C_r D_\beta + m v_x D_\beta} \delta \tag{10.485}$$

*Therefore, the position of the center point O is at*

$$x = -\frac{v_x \left( D_r C_\beta - C_r D_\beta + m v_x D_\beta \right)}{\left( C_\delta D_\beta - C_\beta D_\delta \right) \delta}$$
$$\times \sin \frac{D_\delta \left( C_r - m v_x \right) - D_r C_\delta}{D_r C_\beta - C_r D_\beta + m v_x D_\beta} \delta \tag{10.486}$$

$$y = \frac{v_x \left(D_r C_\beta - C_r D_\beta + mv_x D_\beta\right)}{\left(C_\delta D_\beta - C_\beta D_\delta\right)\delta}$$

$$\times \cos\frac{D_\delta\left(C_r - mv_x\right) - D_r C_\delta}{D_r C_\beta - C_r D_\beta + mv_x D_\beta}\delta. \tag{10.487}$$

*Assuming a small $\beta$, we may find the position of $O$ approximately.*

$$x \approx -\frac{D_\delta\left(C_r - mv_x\right) - D_r C_\delta}{C_\delta D_\beta - C_\beta D_\delta}v_x \tag{10.488}$$

$$y \approx \frac{D_r C_\beta - C_r D_\beta + mv_x D_\beta}{\left(C_\delta D_\beta - C_\beta D_\delta\right)\delta}v_x. \tag{10.489}$$

**Example 410** ★ *Second-order equations.*

*The coupled equations of motion (10.160) may be modified to a second-order differential equation of only one variable. To do this, let's rewrite the equations.*

$$\dot{v}_y = \frac{1}{mv_x}\left(v_y C_\beta + rC_r v_x - mrv_x^2 + \delta v_x C_\delta\right) \tag{10.490}$$

$$\dot{r} = \frac{1}{I_z v_x}\left(v_y D_\beta + rD_r v_x + \delta v_x D_\delta\right) \tag{10.491}$$

*Assuming a constant forward speed*

$$v_x = cte \tag{10.492}$$

*and taking a derivative from Equation (10.491) provides the equation.*

$$\ddot{r} = \frac{1}{I_z v_x}\left(\dot{v}_y D_\beta + \dot{r} D_r v_x\right) \tag{10.493}$$

*We substitute Equation (10.490) in (10.493)*

$$\ddot{r} = \frac{1}{I_z v_x}\left(\frac{1}{mv_x}\left(v_y C_\beta + rC_r v_x - mrv_x^2 + \delta v_x C_\delta\right)\right)D_\beta$$

$$+\frac{1}{I_z v_x}\dot{r} D_r v_x + \dot{\delta} v_x D_\delta \tag{10.494}$$

*and then substitute for $v_y$ from (10.491) and get the following equation:*

$$mI_z v_x \ddot{r} - \left(I_z C_\beta + mD_r v_x\right)\dot{r} + \left(D_r C_\beta - C_r F_\beta + mv_x D_\beta\right)r$$

$$= -\left(\delta C_\delta D_\beta - \delta C_\beta D_\delta + m\dot{\delta}v_x D_\delta\right) \tag{10.495}$$

*This equation is similar to the equation of motion for a force vibration single DOF system*

$$m_{eq}\ddot{x} + c_{eq}\dot{x} + k_{eq}x = f_{eq}\left(t\right) \tag{10.496}$$

*where the equivalent mass $m_{eq}$, damping $c_{eq}$, stiffness $k_{eq}$, and force $f_{eq}(t)$
are*

$$m_{eq} = mI_z v_x \tag{10.497}$$

$$c_{eq} = -(I_z C_\beta + mD_r v_x) \tag{10.498}$$

$$k_{eq} = D_r C_\beta - C_r F_\beta + mv_x D_\beta \tag{10.499}$$

$$f_e(t) = -m\frac{d\delta(t)}{dt}v_x D_\delta + (C_\delta D_\beta - C_\beta D_\delta+)\delta(t). \tag{10.500}$$

*We may use Equation (10.495) and determine the behavior of a vehicle
similar to analysis of a vibrating system. The response of the equation to
a step steering input may be expressed by rise time, peak time, overshoot,
and settling time.*

## 10.8 Summary

A vehicle may be effectively modeled as a rigid bicycle in a planar motion
by ignoring the roll of the vehicle. Such a vehicle has three DOF in a body
coordinate frame attached to the vehicle at $C$: forward motion, lateral
motion, and yaw motion. The dynamic equations of such a vehicle are can
be expressed in $(v_x, v_y, r)$ variables in the following set of three coupled
first order ordinary differential equations.

$$\dot{v}_x = \frac{F_x}{m} + r\,v_y \tag{10.501}$$

$$\dot{v}_y = \frac{1}{mv_x}(-a_1 C_{\alpha f} + a_2 C_{\alpha r})r$$
$$-\frac{1}{mv_x}(C_{\alpha f} + C_{\alpha r})v_y + \frac{1}{m}C_{\alpha f}\delta_f + \frac{1}{m}C_{\alpha r}\delta_r - r\,v_x \tag{10.502}$$

$$\dot{r} = \frac{1}{I_z v_x}(-a_1^2 C_{\alpha f} - a_2^2 C_{\alpha r})r$$
$$-\frac{1}{I_z v_x}(a_1 C_{\alpha f} - a_2 C_{\alpha r})v_y + \frac{1}{I_z}a_1 C_{\alpha f}\delta_f - \frac{1}{I_z}a_2 C_{\alpha r}\delta_r. \tag{10.503}$$

The second and third equations may be written in a matrix form for
$\begin{bmatrix} v_y & r \end{bmatrix}^T$

$$\begin{bmatrix} \dot{v}_y \\ \dot{r} \end{bmatrix} = \begin{bmatrix} -\dfrac{C_{\alpha f} + C_{\alpha r}}{mv_x} & \dfrac{-a_1 C_{\alpha f} + a_2 C_{\alpha r}}{mv_x} - v_x \\ -\dfrac{a_1 C_{\alpha f} - a_2 C_{\alpha r}}{I_z v_x} & -\dfrac{a_1^2 C_{\alpha f} + a_2^2 C_{\alpha r}}{I_z v_x} \end{bmatrix}\begin{bmatrix} v_y \\ r \end{bmatrix}$$
$$+ \begin{bmatrix} \dfrac{1}{m}C_{\alpha f} & \dfrac{1}{m}C_{\alpha r} \\ \dfrac{1}{I_z}a_1 C_{\alpha f} & -\dfrac{1}{I_z}a_2 C_{\alpha r} \end{bmatrix}\begin{bmatrix} \delta_f \\ \delta_r \end{bmatrix} \tag{10.504}$$

or in a matrix form for $\begin{bmatrix} \beta & r \end{bmatrix}^T$.

$$
\begin{bmatrix} \dot{\beta} \\ \dot{r} \end{bmatrix} =
\begin{bmatrix}
-\dfrac{C_{\alpha f} + C_{\alpha r}}{m v_x} & \dfrac{-a_1 C_{\alpha f} + a_2 C_{\alpha r}}{m v_x^2} - 1 \\
-\dfrac{a_1 C_{\alpha f} - a_2 C_{\alpha r}}{I_z} & -\dfrac{a_1^2 C_{\alpha f} + a_2^2 C_{\alpha r}}{I_z v_x}
\end{bmatrix}
\begin{bmatrix} \beta \\ r \end{bmatrix}
$$

$$
+
\begin{bmatrix}
\dfrac{1}{m} C_{\alpha f} & \dfrac{1}{m} C_{\alpha r} \\
\dfrac{1}{I_z} a_1 C_{\alpha f} & -\dfrac{1}{I_z} a_2 C_{\alpha r}
\end{bmatrix}
\begin{bmatrix} \delta_f \\ \delta_r \end{bmatrix}
\qquad (10.505)
$$

# 10.9   Key Symbols

| | |
|---|---|
| $a \equiv \ddot{x}$ | acceleration |
| $a_i$ | distance of the axle number $i$ from the mass center |
| $[A]$ | force coefficient matrix |
| $b_1$ | distance of the hinge point from rear axle |
| $b_2$ | distance of trailer axle from the hinge point |
| $B(Cxyz)$ | vehicle coordinate frame |
| $C$ | mass center |
| $C_\alpha$ | sideslip coefficient |
| $C_{\alpha f}$ | front sideslip coefficient |
| $C_{\alpha f_L}$ | front left sideslip coefficient |
| $C_{\alpha f_R}$ | front right sideslip coefficient |
| $C_{\alpha r}$ | rear sideslip coefficient |
| $C_{\alpha r_L}$ | rear left sideslip coefficient |
| $C_{\alpha r_R}$ | rear right sideslip coefficient |
| $C_r, \cdots, D_\delta$ | force system coefficients |
| $C_r$ | proportionality coefficient between $F_y$ and $r$ |
| $C_\beta$ | proportionality coefficient between $F_y$ and $\beta$ |
| $C_\delta$ | proportionality coefficient between $F_y$ and $\delta$ |
| $D_r$ | proportionality coefficient between $M_z$ and $r$ |
| $D_\beta$ | proportionality coefficient between $M_z$ and $\beta$ |
| $D_\delta$ | proportionality coefficient between $M_z$ and $\delta$ |
| $\mathbf{d}$ | frame position vector |
| $d_N$ | neutral distance |
| $dm$ | mass element |
| $F_i$ | generalized force |
| $F_x$ | longitudinal force, forward force, traction force |
| $F_y$ | lateral force |
| $F_{yf}$ | front lateral force |
| $F_{yr}$ | rear lateral force |
| $F_z$ | normal force, vertical force, vehicle load |
| $\mathbf{F}, \mathbf{M}$ | vehicle force system |
| $\mathbf{g}, g$ | gravitational acceleration |
| $G(OXYZ)$ | global coordinate frame |
| $I$ | mass moment of inertia |
| $K$ | kinetic energy |
| $K$ | stability factor |
| $\mathbf{L}$ | moment of momentum |
| $\mathcal{L}$ | Lagrangean |
| $m$ | mass |
| $M_x$ | roll moment, bank moment, tilting torque |
| $M_y$ | pitch moment |
| $M_z$ | yaw moment, aligning moment |

$p = \dot{\varphi}$ ⟶ roll rate

$\mathbf{p}$ ⟶ momentum

$P_N$ ⟶ neutral steer point

$q = \dot{\theta}$ ⟶ pitch rate

$\mathbf{q}$ ⟶ control variable vector

$q_i$ ⟶ generalized coordinate

$r = \dot{\psi}$ ⟶ yaw rate

$\mathbf{r}$ ⟶ position vector

$R$ ⟶ radius of rotation

$R_w$ ⟶ tire radius

$^G R_B$ ⟶ rotation matrix to go from $B$ frame to $G$ frame

$S_\kappa = \kappa/\delta$ ⟶ curvature response

$S_\beta = \beta/\delta$ ⟶ sideslip response

$S_r = r/\delta$ ⟶ yaw rate response

$S_a = v_x^2/R/\delta$ ⟶ lateral acceleration response

$S_{y_1}, S_{y_2}$ ⟶ steady-state responses

$S_A = 1/v_x^2$ ⟶ Ackerman steering gradient

$t$ ⟶ time

$T$ ⟶ tire coordinate frame

$T_w$ ⟶ wheel torque

$\mathbf{u}$ ⟶ input vector

$v \equiv \dot{x},\ \mathbf{v}$ ⟶ velocity

$V$ ⟶ potential energy

$w$ ⟶ wheelbase

$x, y, z,\ \mathbf{x}$ ⟶ displacement

$\alpha$ ⟶ sideslip angle

$\beta$ ⟶ global sideslip angle

$\beta$ ⟶ vehicle sideslip angle, attitude angle

$\beta$ ⟶ attitude angle

$\beta + \psi$ ⟶ cruise angle

$\delta$ ⟶ steer angle

$\delta_f$ ⟶ front steer angle

$\delta_r$ ⟶ rear steer angle

$\theta$ ⟶ pitch angle

$\dot{\theta} = q$ ⟶ pitch rate

$\kappa = 1/R$ ⟶ curvature

$\lambda$ ⟶ eigenvalue

$\varphi$ ⟶ roll angle

$\dot{\varphi} = p$ ⟶ roll rate

$\psi$ ⟶ yaw angle

$\dot{\psi} = r$ ⟶ yaw rate

$\psi$ ⟶ heading angle

$\boldsymbol{\omega}$ ⟶ angular velocity

$\dot{\boldsymbol{\omega}}$ ⟶ angular acceleration

# Exercises

1. Force system coefficients.

   Consider a front-wheel-steering car with the following characteristics and determine the force system coefficients $C_r$, $C_\beta$, $C_\delta$, $D_r$, $D_\beta$, and $D_\delta$.

$$
\begin{aligned}
C_{\alpha f_L} &= C_{\alpha f_R} = 500\,\mathrm{N/\,deg} \\
C_{\alpha r_L} &= C_{\alpha r_R} = 460\,\mathrm{N/\,deg} \\
m &= 1245\,\mathrm{kg} \\
I_z &= 1328\,\mathrm{kg\,m^2} \\
a_1 &= 110\,\mathrm{cm} \\
a_2 &= 132\,\mathrm{cm} \\
v_x &= 30\,\mathrm{m/\,s}
\end{aligned}
$$

2. Force system and two-wheel model of a car.

   Consider a front-wheel-steering car with the following characteristics

$$
\begin{aligned}
C_{\alpha r_L} &= C_{\alpha r_R} = C_{\alpha f_L} = C_{\alpha f_R} = 500\,\mathrm{N/\,deg} \\
a_1 &= 110\,\mathrm{cm} \\
a_2 &= 132\,\mathrm{cm} \\
m &= 1205\,\mathrm{kg} \\
I_z &= 1300\,\mathrm{kg\,m^2}
\end{aligned}
$$

   and determine the force system that applies on the two-wheel model of the car.

$$
\begin{aligned}
F_y &= C_r\,r + C_\beta\,\beta + C_\delta\,\delta \\
M_z &= D_r\,r + D_\beta\,\beta + D_\delta\,\delta
\end{aligned}
$$

   Then, write the equations of motion of the car as

$$
\begin{aligned}
F_x &= m\,\dot v_x - m\,r\,v_y \\
F_y &= m\,\dot v_y + m\,r\,v_x \\
M_z &= \dot r\,I_z.
\end{aligned}
$$

3. Equations of motion for a front-wheel-steering car.

   Consider a front-wheel-steering car with the following characteristics

$$
C_{\alpha r_L} = C_{\alpha r_R} = C_{\alpha f_L} = C_{\alpha f_R} = 500\,\mathrm{N/\,deg}
$$

$$
\begin{aligned}
a_1 &= 110\,\text{cm} \\
a_2 &= 132\,\text{cm} \\
m &= 1245\,\text{kg} \\
I_z &= 1328\,\text{kg}\,\text{m}^2 \\
v_x &= 40\,\text{m/s}
\end{aligned}
$$

and develop the equations of motion

$$
\dot{\mathbf{q}} = [A]\,\mathbf{q} + \mathbf{u}.
$$

4. Equations of motion in different variables.

   Consider a car with the following characteristics

$$
\begin{aligned}
C_{\alpha r_L} &= C_{\alpha r_R} = C_{\alpha f_L} = C_{\alpha f_R} = 500\,\text{N/deg} \\
a_1 &= 100\,\text{cm} \\
a_2 &= 120\,\text{cm} \\
m &= 1000\,\text{kg} \\
I_z &= 1008\,\text{kg}\,\text{m}^2 \\
v_x &= 40\,\text{m/s}
\end{aligned}
$$

   and develop the equations of motion

   (a) in terms of $(\dot{v}_x, \dot{v}_y, \dot{r})$, if the car is front-wheel steering.
   (b) in terms of $(\dot{v}_x, \dot{v}_y, \dot{r})$, if the car is four-wheel steering.
   (c) in terms of $\left(\dot{v}_x, \dot{\beta}, \dot{r}\right)$, if the car is front-wheel steering.
   (d) in terms of $\left(\dot{v}_x, \dot{\beta}, \dot{r}\right)$, if the car is four-wheel steering.

5. Steady state response parameters.

   Consider a car with the following characteristics

$$
\begin{aligned}
C_{\alpha f_L} &= C_{\alpha f_R} = 500\,\text{N/deg} \\
C_{\alpha r_L} &= C_{\alpha r_R} = 520\,\text{N/deg} \\
m &= 1245\,\text{kg} \\
I_z &= 1328\,\text{kg}\,\text{m}^2 \\
a_1 &= 110\,\text{cm} \\
a_2 &= 132\,\text{cm} \\
v_x &= 40\,\text{m/s}
\end{aligned}
$$

   and determine the steady-state curvature response $S_\kappa$, sideslip response $S_\beta$, yaw rate response, $S_r$, and lateral acceleration response $S_a$.

6. Steady state motion parameters.

   Consider a car with the following characteristics

$$
\begin{aligned}
C_{\alpha f_L} &= C_{\alpha f_R} = 600\,\mathrm{N/\,deg} \\
C_{\alpha r_L} &= C_{\alpha r_R} = 550\,\mathrm{N/\,deg} \\
m &= 1245\,\mathrm{kg} \\
I_z &= 1128\,\mathrm{kg\,m^2} \\
a_1 &= 120\,\mathrm{cm} \\
a_2 &= 138\,\mathrm{cm} \\
v_x &= 20\,\mathrm{m/\,s} \\
\delta &= 3\,\mathrm{deg}
\end{aligned}
$$

   and determine the steady state values of $r$, $R$, $\beta$, and $v_x^2/R$.

7. ★ Inertia and steady state parameters.

   Consider a car that is made up of a uniform solid box with dimensions $260\,\mathrm{cm} \times 140\,\mathrm{cm} \times 40\,\mathrm{cm}$. If the density of the box is $\rho = 1000\,\mathrm{kg/\,m^3}$, and the other characteristics are

$$
\begin{aligned}
C_{\alpha f_L} &= C_{\alpha f_R} = 600\,\mathrm{N/\,deg} \\
C_{\alpha r_L} &= C_{\alpha r_R} = 550\,\mathrm{N/\,deg} \\
a_1 &= a_2 = \frac{l}{2}
\end{aligned}
$$

   then,

   (a) determine $m$, $I_z$.

   (b) determine the steady-state responses $S_\kappa$, $S_\beta$, $S_r$, and $S_a$ as functions of $v_x$.

   (c) determine the velocity $v_x$ at which the car has a radius of turning equal to
   $$R = 35\,\mathrm{m}$$
   when
   $$\delta = 4\,\mathrm{deg}\,.$$

   (d) determine the steady state parameters $r$, $R$, $\beta$, and $v_x^2/R$ at that speed.

   (e) set the speed of the car at
   $$v_x = 20\,\mathrm{m/\,s}$$
   and plot the steady-state responses $S_\kappa$, $S_\beta$, $S_r$, and $S_a$ for variable $\rho$.

8. Stability factor and understeer behavior.

   Examine the stability factor $K$ and

   (a) determine the condition to have an understeer car, if $a_1 = a_2$.

   (b) determine the condition to have an understeer car, if $C_{\alpha f} = C_{\alpha r}$.

   (c) do the results show that if we use the same type of tires in front and rear with $C_{\alpha f} = C_{\alpha r}$, then the front of the car must be heavier?

   (d) do the results show that if we have a car with $a_1 = a_2$, then we must use different tires in the front and rear such that $C_{\alpha r} > C_{\alpha f}$?

9. Stability factor and mass of the car.

   Find $a_1$ and $a_2$ in terms of $F_{z_1}$, $F_{z_2}$, and $mg$ to rewrite the stability factor $K$ to see the effect of a car's mass distribution.

10. Stability factor and car behavior.

    Examine the stability factor of a car with the parameters

$$\begin{aligned}
C_{\alpha f_L} &= C_{\alpha f_R} = 500\,\mathrm{N/\,deg} \\
C_{\alpha r_L} &= C_{\alpha r_R} = 460\,\mathrm{N/\,deg} \\
m &= 1245\,\mathrm{kg} \\
I_z &= 1328\,\mathrm{kg\,m^2} \\
a_1 &= 110\,\mathrm{cm} \\
a_2 &= 132\,\mathrm{cm} \\
v_x &= 30\,\mathrm{m/\,s}
\end{aligned}$$

    and

    (a) determine if the car is understeer, neutral, or oversteer?

    (b) determine the neutral distance $d_N$.

11. Critical speed of a car.

    Consider a car with the characteristics

$$\begin{aligned}
C_{\alpha f_L} &= C_{\alpha f_R} = 700\,\mathrm{N/\,deg} \\
C_{\alpha r_L} &= C_{\alpha r_R} = 520\,\mathrm{N/\,deg} \\
m &= 1245\,\mathrm{kg} \\
I_z &= 1328\,\mathrm{kg\,m^2} \\
a_1 &= 118\,\mathrm{cm} \\
a_2 &= 122\,\mathrm{cm}.
\end{aligned}$$

    (a) determine if the car is understeer, neutral, or oversteer?

    (b) in case of an oversteer situation, determine the neutral distance $d_N$ and the critical speed $v_c$ of the car.

12. ★ Step input response at different speed.

    Consider a car with the characteristics

$$
\begin{aligned}
C_{\alpha f_L} &= C_{\alpha f_R} = 600 \, \mathrm{N/deg} \\
C_{\alpha r_L} &= C_{\alpha r_R} = 750 \, \mathrm{N/deg} \\
m &= 1245 \, \mathrm{kg} \\
I_z &= 1328 \, \mathrm{kg\,m^2} \\
a_1 &= 110 \, \mathrm{cm} \\
a_2 &= 132 \, \mathrm{cm}
\end{aligned}
$$

and a step input

$$
\delta(t) = \begin{cases} 5 \, \mathrm{deg} & t > 0 \\ 0 & t \le 0 \end{cases}.
$$

Determine the time response of the car at

    (a) $v_x = 10 \, \mathrm{m/s}$.

    (b) $v_x = 20 \, \mathrm{m/s}$.

    (c) $v_x = 30 \, \mathrm{m/s}$.

    (d) $v_x = 40 \, \mathrm{m/s}$.

13. ★ Step input response for different steer angle.

    Consider a car with the characteristics

$$
\begin{aligned}
C_{\alpha f_L} &= C_{\alpha f_R} = 600 \, \mathrm{N/deg} \\
C_{\alpha r_L} &= C_{\alpha r_R} = 750 \, \mathrm{N/deg} \\
m &= 1245 \, \mathrm{kg} \\
I_z &= 1328 \, \mathrm{kg\,m^2} \\
a_1 &= 110 \, \mathrm{cm} \\
a_2 &= 132 \, \mathrm{cm} \\
v_x &= 20 \, \mathrm{m/s}.
\end{aligned}
$$

Determine the time response of the car to a step input

$$
\delta(t) = \begin{cases} \delta & t > 0 \\ 0 & t \le 0 \end{cases}
$$

when

(a) $\delta = 3 \deg.$

(b) $\delta = 5 \deg.$

(c) $\delta = 10 \deg.$

14. ★ Eigenvalues and free response.

Consider a car with the characteristics

$$
\begin{aligned}
C_{\alpha f_L} &= C_{\alpha f_R} = 600 \,\mathrm{N/deg} \\
C_{\alpha r_L} &= C_{\alpha r_R} = 750 \,\mathrm{N/deg} \\
m &= 1245 \,\mathrm{kg} \\
I_z &= 1328 \,\mathrm{kg\,m}^2 \\
a_1 &= 110 \,\mathrm{cm} \\
a_2 &= 132 \,\mathrm{cm} \\
v_x &= 20 \,\mathrm{m/s.}
\end{aligned}
$$

(a) Determine the eigenvalues of the coefficient matrix $[A]$ and find out if the car is stable at zero steer angle.

(b) In either case, determine the weight distribution ratio, $a_1/a_2$, such that the car is neutral stable.

(c) Recommend a condition for the weight distribution ratio, $a_1/a_2$, such that the car is stable.

15. ★ Time response to different steer functions.

Consider a car with the characteristics

$$
\begin{aligned}
C_{\alpha f_L} &= C_{\alpha f_R} = 600 \,\mathrm{N/deg} \\
C_{\alpha r_L} &= C_{\alpha r_R} = 750 \,\mathrm{N/deg} \\
m &= 1245 \,\mathrm{kg} \\
I_z &= 1328 \,\mathrm{kg\,m}^2 \\
a_1 &= 110 \,\mathrm{cm} \\
a_2 &= 132 \,\mathrm{cm} \\
v_x &= 20 \,\mathrm{m/s}
\end{aligned}
$$

and a step input

$$
\delta(t) = \begin{cases} 5 \deg & t > 0 \\ 0 & t \le 0 \end{cases}.
$$

Determine the time response of the car to

(a) $\delta(t) = \sin 0.1t$ for $0 < t < 10\pi$ and $\delta(t) = 0$ for $t \le 0$ and $t \ge 10\pi$.

(b) $\delta(t) = \sin 0.5t$ for $0 < t < 2\pi$ and $\delta(t) = 0$ for $t \le 0$ and $t \ge 2\pi$.

(c) $\delta(t) = \sin t$ for $0 < t < \pi$ and $\delta(t) = 0$ for $t \le 0$ and $t \ge \pi$.

# 11

# ★ Vehicle Roll Dynamics

In this chapter, we develop a dynamic model for a rigid vehicle having forward, lateral, yaw, and roll velocities. The model of a rollable rigid vehicle is more exact and more effective compared to the rigid vehicle planar model. Using this model, we are able to analyze the roll behavior of a vehicle as well as its maneuvering.

## 11.1 ★ Vehicle Coordinate and DOF

Figure 11.1 illustrates a vehicle with a body coordinate $B(Cxyz)$ at the mass center $C$. The $x$-axis is a longitudinal axis passing through $C$ and directed forward. The $y$-axis goes laterally to the left from the driver's viewpoint. The $z$-axis makes the coordinate system a right-hand triad. When the car is parked on a flat horizontal road, the $z$-axis is perpendicular to the ground, opposite to the gravitational acceleration $\mathbf{g}$. The equations of motion of the vehicle are expressed in $B(Cxyz)$.
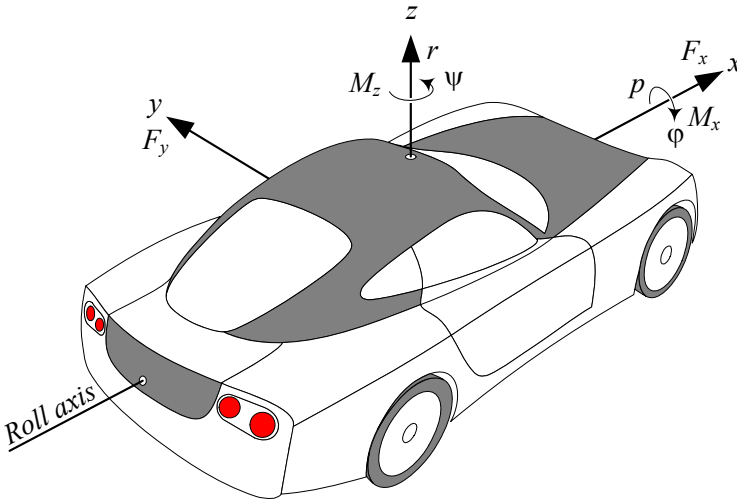


FIGURE 11.1. The DOF of a roll model of rigid vehicles are: $x, y, \varphi, \psi$.

Angular orientation and angular velocity of a vehicle are expressed by three angles: *roll* $\varphi$, *pitch* $\theta$, *yaw* $\psi$, and their rates: *roll rate p, pitch rate*

*q, yaw rate r.*

$$p = \dot{\varphi} \tag{11.1}$$
$$q = \dot{\theta} \tag{11.2}$$
$$r = \dot{\psi} \tag{11.3}$$

The vehicle force system $(\mathbf{F}, \mathbf{M})$ is the resultant of external forces and moments that the vehicle receives from the ground and environment. The force system may be expressed in the body coordinate frame as:

$$^B\mathbf{F} = F_x\hat{\imath} + F_y\hat{\jmath} + F_z\hat{k} \tag{11.4}$$
$$^B\mathbf{M} = M_x\hat{\imath} + M_y\hat{\jmath} + M_z\hat{k} \tag{11.5}$$

The roll model vehicle dynamics can be expressed by *four* kinematic variables: the forward motion $x$, the lateral motion $y$, the roll angle $\varphi$, and the roll angle $\psi$. In this model, we do not consider vertical movement $z$, and pitch motion $\theta$.

## 11.2    ★ Equations of Motion

A rolling rigid vehicle has a motion with four degrees of freedom, which are translation in $x$ and $y$ directions, and rotation about the $x$ and $z$ axes. The *Newton-Euler equations of motion* for such a rolling rigid vehicle in the body coordinate frame $B$ are:

$$F_x = m\dot{v}_x - mr\,v_y \tag{11.6}$$
$$F_y = m\dot{v}_y + mr\,v_x \tag{11.7}$$
$$M_z = I_z\dot{\omega}_z = I_z\dot{r} \tag{11.8}$$
$$M_x = I_x\dot{\omega}_x = I_x\dot{p}. \tag{11.9}$$

**Proof.** Consider the vehicle shown in Figure 11.2. A global coordinate frame $G$ is fixed on the ground, and a local coordinate frame $B$ is attached to the vehicle at the mass center $C$. The orientation of the frame $B$ can be expressed by the heading angle $\psi$ between the $x$ and $X$ axes, and the roll angle $\varphi$ between the $z$ and $Z$ axes. The global position vector of the mass center is denoted by $^G\mathbf{d}$.

The rigid body equations of motion in the body coordinate frame are:

$$\begin{aligned}
^B\mathbf{F} &= {}^B R_G\,{}^G\mathbf{F} \\
&= {}^B R_G \left(m\,{}^G\mathbf{a}_B\right) \\
&= m\,{}^B_G\mathbf{a}_B \\
&= m\,{}^B\dot{\mathbf{v}}_B + m\,{}^B_G\boldsymbol{\omega}_B \times {}^B\mathbf{v}_B. \tag{11.10}
\end{aligned}$$
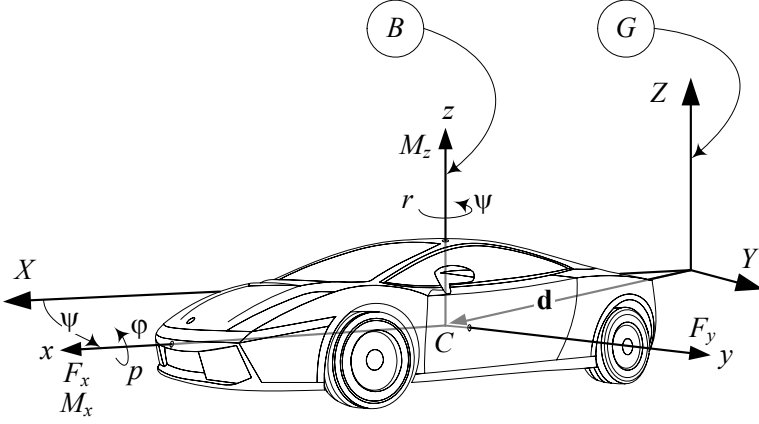
FIGURE 11.2. A vehicle with roll, and yaw rotations.

$$^B\mathbf{M} = \frac{^Gd}{dt} {}^B\mathbf{L}$$

$$= {}^B_G\dot{\mathbf{L}}_B$$

$$= {}^B\dot{\mathbf{L}} + {}^B_G\boldsymbol{\omega}_B \times {}^B\mathbf{L}$$

$$= {}^BI\,{}^B_G\dot{\boldsymbol{\omega}}_B + {}^B_G\boldsymbol{\omega}_B \times \left({}^BI\,{}^B_G\boldsymbol{\omega}_B\right). \tag{11.11}$$

The velocity vector of the vehicle, expressed in the body frame, is

$$^B\mathbf{v}_C = \begin{bmatrix} v_x \\ v_y \\ 0 \end{bmatrix} \tag{11.12}$$

where $v_x$ is the forward component and $v_y$ is the lateral component of $\mathbf{v}$. The other kinematic vectors for the rigid vehicle are:

$$^B\dot{\mathbf{v}}_C = \begin{bmatrix} \dot{v}_x \\ \dot{v}_y \\ 0 \end{bmatrix} \tag{11.13}$$

$$^B_G\boldsymbol{\omega}_B = \begin{bmatrix} \omega_x \\ 0 \\ \omega_z \end{bmatrix} = \begin{bmatrix} p \\ 0 \\ r \end{bmatrix} \tag{11.14}$$

$$^B_G\dot{\boldsymbol{\omega}}_B = \begin{bmatrix} \dot{\omega}_x \\ 0 \\ \dot{\omega}_z \end{bmatrix} = \begin{bmatrix} \dot{p} \\ 0 \\ \dot{r} \end{bmatrix}. \tag{11.15}$$

We may assume that the body coordinate is the principal coordinate frame

of the vehicle to have a diagonal moment of inertia matrix.

$$^B I = \begin{bmatrix} I_1 & 0 & 0 \\ 0 & I_2 & 0 \\ 0 & 0 & I_3 \end{bmatrix} \tag{11.16}$$

Substituting the above vectors and matrices in the equations of motion (11.10) and (11.11) provides the following equations:

$$^B \mathbf{F} = m\, ^B\dot{\mathbf{v}}_B + m\, ^B_G \boldsymbol{\omega}_B \times\, ^B \mathbf{v}_B \tag{11.17}$$

$$\begin{bmatrix} F_x \\ F_y \\ 0 \end{bmatrix} = m \begin{bmatrix} \dot{v}_x \\ \dot{v}_y \\ 0 \end{bmatrix} + m \begin{bmatrix} \omega_x \\ 0 \\ \omega_z \end{bmatrix} \times \begin{bmatrix} v_x \\ v_y \\ 0 \end{bmatrix}$$

$$= \begin{bmatrix} m\dot{v}_x - m\omega_z v_y \\ m\dot{v}_y + m\omega_z v_x \\ m\omega_x v_y \end{bmatrix} \tag{11.18}$$

$$^B \mathbf{M} = {}^B I\, ^B_G \dot{\boldsymbol{\omega}}_B + {}^B_G \boldsymbol{\omega}_B \times \left( {}^B I\, ^B_G \boldsymbol{\omega}_B \right) \tag{11.19}$$

$$\begin{bmatrix} M_x \\ 0 \\ M_z \end{bmatrix} = \begin{bmatrix} I_1 & 0 & 0 \\ 0 & I_2 & 0 \\ 0 & 0 & I_3 \end{bmatrix} \begin{bmatrix} \dot{\omega}_x \\ 0 \\ \dot{\omega}_z \end{bmatrix}$$

$$+ \begin{bmatrix} \omega_x \\ 0 \\ \omega_z \end{bmatrix} \times \left( \begin{bmatrix} I_1 & 0 & 0 \\ 0 & I_2 & 0 \\ 0 & 0 & I_3 \end{bmatrix} \begin{bmatrix} \omega_x \\ 0 \\ \omega_z \end{bmatrix} \right)$$

$$= \begin{bmatrix} I_1 \dot{\omega}_x \\ I_1 \omega_x \omega_z - I_3 \omega_x \omega_z \\ I_3 \dot{\omega}_z \end{bmatrix} \tag{11.20}$$

The first two Newton equations (11.18) are the equations of motion in the $x$ and $y$ directions.

$$\begin{bmatrix} F_x \\ F_y \end{bmatrix} = \begin{bmatrix} m\dot{v}_x - m\omega_z v_y \\ m\dot{v}_y + m\omega_z v_x \end{bmatrix} \tag{11.21}$$

The third Newton's equation

$$m\omega_x v_y = 0 \tag{11.22}$$

is static equation. It provides a compatibility condition to keep the vehicle on the road.

The first and third Euler equations (11.20) are the equations of motion about the $x$ and $z$ axes.

$$\begin{bmatrix} M_x \\ M_z \end{bmatrix} = \begin{bmatrix} I_1 \dot{\omega}_x \\ I_3 \dot{\omega}_z \end{bmatrix} \tag{11.23}$$

The second Euler equation

$$I_1 \omega_x \omega_z - I_3 \omega_x \omega_z = 0 \tag{11.24}$$

is another static equation. It provides the required pitch moment condition to keep the vehicle on the road. ■

**Example 411 ★** *Motion of a six DOF vehicle.*

   *Consider a vehicle that moves in space. Such a vehicle has six DOF. To develop the equations of motion of such a vehicle, we need to define the kinematic characteristics as follows:*

$$^B\mathbf{v}_C = \begin{bmatrix} v_x \\ v_y \\ v_z \end{bmatrix} \tag{11.25}$$

$$^B\dot{\mathbf{v}}_C = \begin{bmatrix} \dot{v}_x \\ \dot{v}_y \\ \dot{v}_z \end{bmatrix} \tag{11.26}$$

$$^B_G\boldsymbol{\omega}_B = \begin{bmatrix} \omega_x \\ \omega_y \\ \omega_z \end{bmatrix} \tag{11.27}$$

$$^B_G\dot{\boldsymbol{\omega}}_B = \begin{bmatrix} \dot{\omega}_x \\ \dot{\omega}_y \\ \dot{\omega}_z \end{bmatrix} \tag{11.28}$$

*The acceleration vector of the vehicle in the body coordinate is*

$$
\begin{aligned}
^B\mathbf{a} &= {}^B\dot{\mathbf{v}}_B + {}^B_G\boldsymbol{\omega}_B \times {}^B\mathbf{v}_B \\
&= \begin{bmatrix} \dot{v}_x + \omega_y v_z - \omega_z v_y \\ \dot{v}_y + \omega_z v_x - \omega_x v_z \\ \dot{v}_z + \omega_x v_y - \omega_y v_x \end{bmatrix}
\end{aligned} \tag{11.29}
$$

*and therefore, the Newton equations of motion for the vehicle are*

$$\begin{bmatrix} F_x \\ F_y \\ F_z \end{bmatrix} = m \begin{bmatrix} \dot{v}_x + \omega_y v_z - \omega_z v_y \\ \dot{v}_y + \omega_z v_x - \omega_x v_z \\ \dot{v}_z + \omega_x v_y - \omega_y v_x \end{bmatrix}. \tag{11.30}$$

   *To find the Euler equations of motion,*

$$^B\mathbf{M} = {}^BI \, {}^B_G\dot{\boldsymbol{\omega}}_B + {}^B_G\boldsymbol{\omega}_B \times \left( {}^BI \, {}^B_G\boldsymbol{\omega}_B \right) \tag{11.31}$$

*we need to define the moment of inertia matrix and perform the required matrix calculations. Assume the body coordinate system is the principal*

*coordinate frame. So,*

$$
^{B}I\,{}^{B}_{G}\dot{\boldsymbol{\omega}}_{B} + {}^{B}_{G}\boldsymbol{\omega}_{B} \times \left( {}^{B}I\,{}^{B}_{G}\boldsymbol{\omega}_{B} \right)
$$

$$
\begin{bmatrix} I_1 & 0 & 0 \\ 0 & I_2 & 0 \\ 0 & 0 & I_3 \end{bmatrix} \begin{bmatrix} \dot{\omega}_x \\ \dot{\omega}_y \\ \dot{\omega}_z \end{bmatrix} + \begin{bmatrix} \omega_x \\ \omega_y \\ \omega_z \end{bmatrix} \times \left( \begin{bmatrix} I_1 & 0 & 0 \\ 0 & I_2 & 0 \\ 0 & 0 & I_3 \end{bmatrix} \begin{bmatrix} \omega_x \\ \omega_y \\ \omega_z \end{bmatrix} \right)
$$

$$
= \begin{bmatrix} \dot{\omega}_x I_1 - \omega_y \omega_z I_2 + \omega_y \omega_z I_3 \\ \dot{\omega}_y I_2 + \omega_x \omega_z I_1 - \omega_x \omega_z I_3 \\ \dot{\omega}_z I_3 - \omega_x \omega_y I_1 + \omega_x \omega_y I_2 \end{bmatrix} \tag{11.32}
$$

*and therefore, the Euler equations of motion for the vehicle are*

$$
\begin{bmatrix} M_x \\ M_y \\ M_z \end{bmatrix} = \begin{bmatrix} \dot{\omega}_x I_1 - \omega_y \omega_z I_2 + \omega_y \omega_z I_3 \\ \dot{\omega}_y I_2 + \omega_x \omega_z I_1 - \omega_x \omega_z I_3 \\ \dot{\omega}_z I_3 - \omega_x \omega_y I_1 + \omega_x \omega_y I_2 \end{bmatrix}. \tag{11.33}
$$

**Example 412 ★** *Roll rigid vehicle from general motion.*

We may derive the equations of motion for a roll rigid vehicle from the general equations of motion for a vehicle with six DOF (11.30) and (11.33).

Consider a bicycle model of a four-wheel vehicle moving on a road. Because the vehicle cannot move in z-direction and cannot turn about the y-axis, we have

$$
\begin{align}
v_z &= 0 \tag{11.34} \\
\dot{v}_z &= 0 \tag{11.35} \\
\omega_y &= 0 \tag{11.36} \\
\dot{\omega}_y &= 0. \tag{11.37}
\end{align}
$$

Furthermore, the overall force in the z-direction and overall moment in y-direction for such a bicycle must be zero,

$$
\begin{align}
F_z &= 0 \tag{11.38} \\
M_y &= 0 \tag{11.39}
\end{align}
$$

Substitution Equations (11.34)-(11.39) in (11.30) and (11.33) results in the force system.

$$
\begin{bmatrix} F_x \\ F_y \\ 0 \end{bmatrix} = m \begin{bmatrix} \dot{v}_x - \omega_z v_y \\ \dot{v}_y + \omega_z v_x \\ \omega_x v_y \end{bmatrix} \tag{11.40}
$$

$$
\begin{bmatrix} M_x \\ 0 \\ M_z \end{bmatrix} = \begin{bmatrix} \dot{\omega}_x I_1 \\ \omega_x \omega_z I_1 - \omega_x \omega_z I_3 \\ \dot{\omega}_z I_3 \end{bmatrix} \tag{11.41}
$$
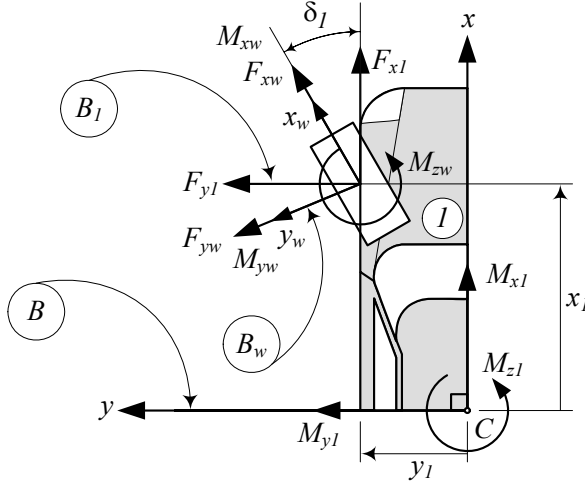
FIGURE 11.3. The force system at the tireprint of tire number 1, and their resultant force system at $C$.

## 11.3   ★ Vehicle Force System

To determine the force system on a rigid vehicle, we define the force system at the tireprint of a wheel. The lateral force at the tireprint depends on the sideslip angle. Then, we transform and apply the tire force system on the rollable model of the vehicle.

### 11.3.1   ★ Tire and Body Force Systems

Figure 11.3 depicts wheel number 1 of a vehicle. The components of the applied force system on the rigid vehicle, because of the generated forces at the tireprint of the wheel number $i$, are

$$
\begin{align}
F_{x_i} &= F_{x_{w_i}} \cos \delta_i - F_{y_{w_i}} \sin \delta_i \tag{11.42} \\
F_{y_i} &= F_{y_{w_i}} \cos \delta_i + F_{x_{w_i}} \sin \delta_i \tag{11.43} \\
M_{x_i} &= M_{x_{w_i}} + y_i F_{z_i} - z_i F_{y_i} \tag{11.44} \\
M_{y_i} &= M_{y_{w_i}} + z_i F_{x_i} - x_i F_{z_i} \tag{11.45} \\
M_{z_i} &= M_{z_{w_i}} + x_i F_{y_i} - y_i F_{x_i} \tag{11.46}
\end{align}
$$

where $(x_i, y_i, z_i)$ are body coordinates of the wheel number $i$. It is possible to ignore the components of the tire moment at the tireprint, $M_{x_{w_i}}$, $M_{y_{w_i}}$, $M_{z_{w_i}}$, and simplify the equations.

The total planar force system on the rigid vehicle in the body coordinate

frame is

$$
\begin{aligned}
{}^{B}F_x &= \sum_i F_{x_i} \\
&= \sum_i F_{x_w} \cos \delta_i - \sum_i F_{y_w} \sin \delta_i \tag{11.47}
\end{aligned}
$$

$$
\begin{aligned}
{}^{B}F_y &= \sum_i F_{y_i} \\
&= \sum_i F_{y_w} \cos \delta_i + \sum_i F_{x_w} \sin \delta_i \tag{11.48}
\end{aligned}
$$

$$
{}^{B}F_z = \sum_i F_{z_i} = mg \tag{11.49}
$$

$$
{}^{B}M_x = \sum_i M_{x_i} + \sum_i y_i F_{z_i} - \sum_i z_i F_{y_i} \tag{11.50}
$$

$$
{}^{B}M_y = \sum_i M_{y_i} + \sum_i z_i F_{x_i} - \sum_i x_i F_{z_i} \tag{11.51}
$$

$$
{}^{B}M_z = \sum_i M_{z_i} + \sum_i x_i F_{y_i} - \sum_i y_i F_{x_i} . \tag{11.52}
$$

**Proof.** To simplify the roll model of vehicle dynamics, we ignore the difference between the tire frame at the center of tireprint and wheel frame at the wheel center for small roll angles.

Ignoring the lateral moment at the tireprint $M_{y_w}$, the force system generated at the tireprint of the wheel in the wheel frame $B_w$ is

$$
{}^{B_w}\mathbf{F}_w = F_{x_w} \hat{\imath}_1 + F_{y_w} \hat{\jmath}_1 + F_{z_w} \hat{k}_1 \tag{11.53}
$$

$$
{}^{B_w}\mathbf{M}_w = M_{x_w} \hat{\imath}_1 + M_{z_w} \hat{k}_1 \tag{11.54}
$$

The rotation matrix between the wheel frame $B_w$ and the wheel-frame coordinate frame $B_1$, parallel to the vehicle body coordinate frame $B$, is

$$
{}^{B_1}R_{B_w} = \begin{bmatrix} \cos \delta_1 & -\sin \delta_1 & 0 \\ \sin \delta_1 & \cos \delta_1 & 0 \\ 0 & 0 & 1 \end{bmatrix} \tag{11.55}
$$

and therefore, the force system at the tireprint of the wheel, parallel to the vehicle coordinate frame, is

$$
\begin{aligned}
{}^{B_1}\mathbf{F}_w &= {}^{B}R_{B_w} {}^{B_w}\mathbf{F}_w \tag{11.56} \\
\begin{bmatrix} F_{x_1} \\ F_{y_1} \\ F_{z_1} \end{bmatrix} &= \begin{bmatrix} \cos \delta_1 & -\sin \delta_1 & 0 \\ \sin \delta_1 & \cos \delta_1 & 0 \\ 0 & 0 & 1 \end{bmatrix} \begin{bmatrix} F_{x_w} \\ F_{y_w} \\ F_{z_w} \end{bmatrix} \\
&= \begin{bmatrix} F_{x_w} \cos \delta_1 - F_{y_w} \sin \delta_1 \\ F_{y_w} \cos \delta_1 + F_{x_w} \sin \delta_1 \\ F_{z_w} \end{bmatrix} \tag{11.57}
\end{aligned}
$$

$$^{B_1}\mathbf{M}_w = {}^{B_1}R_{B_w}{}^{B_w}\mathbf{M}_w \tag{11.58}$$

$$\begin{bmatrix} M_{x_1} \\ M_{y_1} \\ M_{z_1} \end{bmatrix} = \begin{bmatrix} \cos\delta_1 & -\sin\delta_1 & 0 \\ \sin\delta_1 & \cos\delta_1 & 0 \\ 0 & 0 & 1 \end{bmatrix} \begin{bmatrix} M_{x_w} \\ 0 \\ M_{z_w} \end{bmatrix}$$

$$= \begin{bmatrix} M_{x_w}\cos\delta_1 \\ M_{x_w}\sin\delta_1 \\ M_{z_w} \end{bmatrix} \tag{11.59}$$

Transforming the force system of each tire to the body coordinate frame $B$, located at the vehicle mass center $C$, generates the total force system applied on the vehicle

$$^B\mathbf{F} = \sum_i {}^{B_i}\mathbf{F}_w$$

$$= \sum_i F_{x_i}\,\hat{\imath} + \sum_i F_{y_i}\,\hat{\jmath} \tag{11.60}$$

$$^B\mathbf{M} = \sum_i {}^{B_i}\mathbf{M}_w$$

$$= \sum_i M_{x_i}\,\hat{\imath} + \sum_i M_{y_i}\,\hat{\jmath} + \sum_i M_{z_i}\,\hat{k} + \sum_i {}^B\mathbf{r}_i \times {}^B\mathbf{F}_{w_i} \tag{11.61}$$

where $^B\mathbf{r}_i$ is the position vector of the wheel number $i$.

$$^B\mathbf{r}_i = x_i\hat{\imath} + y_i\hat{\jmath} + z_i\hat{k} \tag{11.62}$$

In deriving Equation (11.60), we have used the equation $\sum_i F_{z_i} - mg = 0$. Expanding Equations (11.60) and (11.61) provides the total vehicle force system.

$$^B F_x = \sum_i F_{x_w}\cos\delta_i - \sum_i F_{y_w}\sin\delta_i \tag{11.63}$$

$$^B F_y = \sum_i F_{y_w}\cos\delta_i + \sum_i F_{x_w}\sin\delta_i \tag{11.64}$$

$$^B M_x = \sum_i M_{x_i} + \sum_i y_i F_{z_i} - \sum_i z_i F_{y_i} \tag{11.65}$$

$$^B M_y = \sum_i M_{y_i} + \sum_i z_i F_{x_i} - \sum_i x_i F_{z_i} \tag{11.66}$$

$$^B M_z = \sum_i M_{z_i} + \sum_i x_i F_{y_i} - \sum_i y_i F_{x_i} \tag{11.67}$$

For a two-wheel vehicle model we have

$$\begin{aligned} x_1 &= a_1 \\ x_2 &= -a_2 \\ y_1 &= y_2 = 0. \end{aligned} \tag{11.68}$$

For such a vehicle, the force system reduces to

$$
\begin{aligned}
{}^{B}F_x &= F_{x_1}\cos\delta_1 + F_{x_2}\cos\delta_2 - F_{y_1}\sin\delta_1 - F_{y_2}\sin\delta_2 & (11.69)\\
{}^{B}F_y &= F_{y_1}\cos\delta_1 + F_{y_2}\cos\delta_2 + F_{x_1}\sin\delta_1 + F_{x_2}\sin\delta_2 & (11.70)\\
{}^{B}M_x &= M_{x_1} + M_{x_2} - z_1 F_{y_1} - z_2 F_{y_2} & (11.71)\\
{}^{B}M_y &= M_{y_1} + M_{y_2} + z_2 F_{x_2} + z_1 F_{x_1} - a_1 F_{z_1} - a_2 F_{z_2} & (11.72)\\
{}^{B}M_z &= M_{z_1} + M_{z_2} + a_1 F_{y_1} + a_2 F_{y_2}. & (11.73)
\end{aligned}
$$

It is common to assume

$$
M_{z_i} = 0 \tag{11.74}
$$

and therefore,

$$
{}^{B}M_z = a_1 F_{y_f} - a_2 F_{y_r}. \tag{11.75}
$$

∎

### 11.3.2   ★ Tire Lateral Force

If the steer angle of the steering mechanism is denoted by $\delta$, then the actual steer angle $\delta_a$ of a rollable vehicle is

$$
\delta_a = \delta + \delta_\varphi \tag{11.76}
$$

where, $\delta_\varphi$ is the *roll-steering* angle.

$$
\delta_\varphi = C_{\delta\varphi}\varphi \tag{11.77}
$$

The roll-steering angle $\delta_\varphi$ is proportional to the roll angle $\varphi$ and the coefficient $C_{\delta\varphi}$ is called the *roll-steering* coefficient. The roll-steering happens because of the suspension mechanisms that generate some steer angle when deflected. The *tire sideslip angle* of each tire of a rollable vehicle is

$$
\begin{aligned}
\alpha_i &= \beta_i - \delta_a\\
&= \beta_i - \delta_i - \delta_\varphi. \tag{11.78}
\end{aligned}
$$

where $\beta_i$ is the angle between the velocity vector $\mathbf{v}$ and the vehicle body $x$-axis, and is called the *tire slip angle*.

The generated lateral force by such a tire for a small sideslip angle, is

$$
\begin{aligned}
F_y &= -C_\alpha\,\alpha_i - C_\varphi\varphi_i\\
&= -C_\alpha\,(\beta_i - \delta_i - C_{\delta\varphi}\varphi_i) - C_\varphi\varphi \tag{11.79}
\end{aligned}
$$

and $C_\varphi$ is the *tire camber trust coefficient*, because of the vehicle's roll. The tire slip angle $\beta_i$ can be approximated by

$$
\beta_i = \frac{v_y + x_i\,r - C_{\beta_i}p}{v_x} \tag{11.80}
$$

to find the tire lateral force $F_y$ in terms of the vehicle kinematic variables.

$$F_y = -x_i\frac{C_\alpha}{v_x}r + \frac{C_\alpha C_\beta}{v_x}p - C_\alpha\beta + (C_\alpha C_{\delta\varphi} - C_\varphi)\varphi + C_\alpha\delta_i \quad (11.81)$$

$$\beta = \frac{v_y}{v_x}. \quad (11.82)$$

$C_{\beta_i}$ is *tire slip coefficient*.

**Proof.** When a vehicle rolls, there are some new reactions in the tires that introduce new dynamic terms in the behavior of the tire. The most important reactions are:

1−Tire camber trust $F_{y\varphi}$, which is a lateral force because of the vehicle roll. Tire camber trust may be assumed proportional to the vehicle roll angle $\varphi$.

$$F_{y\varphi} = -C_\varphi\varphi \quad (11.83)$$

$$C_\varphi = \frac{dF_y}{d\varphi}. \quad (11.84)$$

2−Tire roll steering angle $\delta_\varphi$, which is the tire steer angle because of the vehicle roll. Most suspension mechanisms provide some steer angle when the vehicle rolls and the mechanism deflects. The tire roll steering may be assumed proportional to the roll angle.

$$\delta_\varphi = C_{\delta\varphi}\varphi \quad (11.85)$$

$$C_{\delta\varphi} = \frac{d\delta}{d\varphi} \quad (11.86)$$

Therefore, the actual steer angle $\delta_a$ of such a tire is

$$\delta_a = \delta + \delta_\varphi. \quad (11.87)$$

Assume the wheel number $i$ of a rigid vehicle is located at

$$^B\mathbf{r}_i = \begin{bmatrix} x_i & y_i & z_i \end{bmatrix}^T. \quad (11.88)$$

The velocity of the wheel number $i$ is

$$^B\mathbf{v}_i = {}^B\mathbf{v} + {}^B\boldsymbol{\omega} \times {}^B\mathbf{r}_i \quad (11.89)$$

in which $^B\mathbf{v}$ is the velocity vector of the vehicle at its mass center $C$, and $^B\boldsymbol{\omega} = \dot\varphi\hat\imath + \dot\psi\hat k = p\hat\imath + r\hat k$ is the angular velocity of the vehicle. Expanding Equation (11.89) provides the following velocity vector for the wheel number $i$ expressed in the vehicle coordinate frame at $C$.

$$\begin{bmatrix} v_{x_i} \\ v_{y_i} \\ v_{z_i} \end{bmatrix} = \begin{bmatrix} v_x \\ v_y \\ 0 \end{bmatrix} + \begin{bmatrix} \dot\varphi \\ 0 \\ \dot\psi \end{bmatrix} \times \begin{bmatrix} x_i \\ y_i \\ z_i \end{bmatrix}$$

$$= \begin{bmatrix} v_x - \dot\psi y_i \\ v_y - \dot\varphi z_i + \dot\psi x_i \\ \dot\varphi y_i \end{bmatrix} \quad (11.90)$$

Consider a bicycle model for the rollable vehicle to have

$$y_i = 0 \tag{11.91}$$

$$x_1 = a_1 \tag{11.92}$$

$$x_2 = -a_2. \tag{11.93}$$

The tire slip angle $\beta_i$ for the wheel $i$, is defined as the angle between the wheel velocity vector $\mathbf{v}_i$ and the vehicle body $x$-axis. When the roll angle is very small, $\beta_i$ is

$$\beta_i = \tan^{-1}\left(\frac{v_{y_i}}{v_{x_i}}\right) \tag{11.94}$$

$$\approx \frac{v_{y_i}}{v_{x_i}} \approx \frac{v_y - \dot{\varphi}z_i + \dot{\psi}x_i}{v_x} \tag{11.95}$$

If the wheel number $i$ has a steer angle $\delta_i$ then, its sideslip angle $\alpha_i$, that generates a lateral force $F_{y_w}$ on the tire, is

$$\alpha_i = \beta_i - \delta_i$$

$$\approx \frac{v_y - \dot{\varphi}z_i + \dot{\psi}x_i}{v_x} - \delta_i + \delta_{\varphi_i}. \tag{11.96}$$

The tire slip angle $\beta_i$ for the front and rear wheels of a two-wheel vehicle, $\beta_f$ and $\beta_r$, are

$$\beta_f = \tan^{-1}\left(\frac{v_{y_f}}{v_{x_f}}\right)$$

$$\approx \frac{v_{y_f}}{v_{x_f}} \approx \frac{v_y + a_1 r - z_f p}{v_x} \tag{11.97}$$

$$\beta_r = \tan^{-1}\left(\frac{v_{y_r}}{v_{x_r}}\right)$$

$$\approx \frac{v_{y_r}}{v_{x_r}} \approx \frac{v_y - a_2 r - z_r p}{v_x} \tag{11.98}$$

and the *vehicle slip angle* $\beta$ is

$$\beta = \tan^{-1}\left(\frac{v_y}{v_x}\right) \approx \frac{v_y}{v_x}. \tag{11.99}$$

The $z_i$ coordinate of the wheels is not constant however, its variation is small. To show the effect of $z_i$, we may substitute it by coefficient $C_{\beta_i}$ called the *tire roll rate coefficient*, and define coefficients $C_{\beta_f}$ and $C_{\beta_r}$ to express the change in $\beta_i$ because of roll rate $p$.

$$\beta_i = C_{\beta_i} p \tag{11.100}$$

$$C_{\beta_i} = \frac{d\beta_i}{dp} \tag{11.101}$$

Therefore,

$$\beta_f = \tan^{-1}\left(\frac{v_y + a_1 r - C_{\beta_f} p}{v_x}\right) \tag{11.102}$$

$$\beta_r = \tan^{-1}\left(\frac{v_y - a_2 r - C_{\beta_r} p}{v_x}\right). \tag{11.103}$$

Assuming small angles for slip angles $\beta_f$, $\beta$, and $\beta_r$, the tire sideslip angles for the front and rear wheels, $\alpha_f$ and $\alpha_r$, may be approximated as

$$\alpha_f = \frac{1}{v_x}(v_y + a_1 r - z_f p) - \delta - \delta_{\varphi_f}$$
$$= \beta + a_1\frac{r}{v_x} - C_{\beta_f}\frac{p}{v_x} - \delta - C_{\delta\varphi_f}\varphi \tag{11.104}$$

$$\alpha_r = \frac{1}{v_x}(v_y - a_2 r - z_r p) - \delta_{\varphi_r}$$
$$= \beta - a_2\frac{r}{v_x} - C_{\beta_r}\frac{p}{v_x} - C_{\delta\varphi_r}\varphi. \tag{11.105}$$

∎

### 11.3.3  ★ *Body Force Components on a Two-wheel Model*

Figure 11.4 illustrates a top view of a car and the force systems acting at the tireprints of a front-wheel-steering four-wheel vehicle. When we consider the roll motion of the vehicle, the $xy$-plane does not remain parallel to the road's $XY$-plane, however, we may still use a *two-wheel model* for the vehicle.

Figure 11.5 illustrates the force system and Figure 11.6 illustrates the kinematics of a two-wheel model for a vehicle with roll and yaw rotations. The rolling two-wheel model is also called the *bicycle model.*

The force system applied on the bicycle vehicle, having only the front wheel steerable, is

$$F_x = \sum_{i=1}^{2}(F_{x_i}\cos\delta - F_{y_i}\sin\delta) \tag{11.106}$$

$$F_y = \sum_{i=1}^{2}F_{y_i} \tag{11.107}$$

$$M_x = M_{x_f} + M_{x_r} - wc_f\dot\varphi - wk_f\varphi \tag{11.108}$$
$$M_z = a_1 F_{y_f} - a_2 F_{y_r} \tag{11.109}$$

where $\left(F_{x_f}, F_{x_r}\right)$ and $\left(F_{y_f}, F_{y_r}\right)$ are the planar forces on the tireprint of the front and rear wheels. The force system may be approximated by the
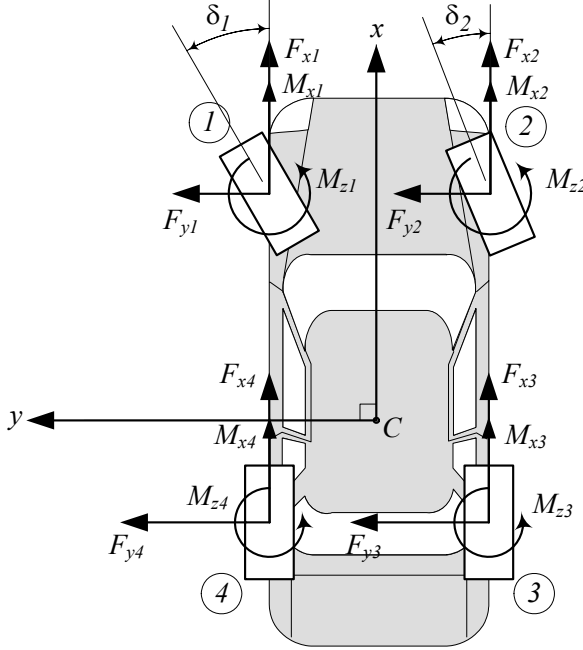
FIGURE 11.4. Top view of a car and the forces system acting at the tireprints.

following equations, if the steer angle $\delta$ is assumed small:

$$F_x \approx F_{x_f} + F_{x_r} \tag{11.110}$$

$$F_y \approx F_{y_f} + F_{y_r} \tag{11.111}$$

$$M_x \approx C_{T_f} F_{y_f} + C_{T_r} F_{y_r} - k_\varphi \varphi - c_\varphi \dot{\varphi} \tag{11.112}$$

$$M_z \approx a_1 F_{y_f} - a_2 F_{y_r} \tag{11.113}$$

The vehicle's lateral force $F_y$ and moment $M_z$ depend only on the front and rear wheels' lateral forces $F_{y_f}$ and $F_{y_r}$, which are functions of the wheels sideslip angles $\alpha_f$ and $\alpha_r$. They can be approximated by the following equations:

$$
\begin{aligned}
F_y &= \left( \frac{a_2}{v_x} C_{\alpha r} - \frac{a_1}{v_x} C_{\alpha f} \right) r + \left( \frac{C_{\alpha f} C_{\beta_f}}{v_x} + \frac{C_{\alpha r} C_{\beta_r}}{v_x} \right) p \\
&\quad + (-C_{\alpha f} - C_{\alpha r}) \beta + \left( C_{\alpha f} C_{\delta \varphi_f} - C_{\varphi_r} - C_{\varphi_f} + C_{\alpha r} C_{\delta \varphi_r} \right) \varphi \\
&\quad + C_{\alpha f} \delta
\end{aligned}
\tag{11.114}
$$
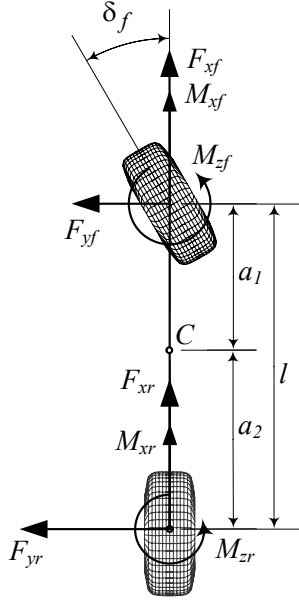
FIGURE 11.5. A two-wheel model for a vehicle with roll and yaw rotations.

$$
\begin{aligned}
M_x \;=\;& \left( \frac{a_2}{v_x} C_{T_r} C_{\alpha r} - \frac{a_1}{v_x} C_{T_f} C_{\alpha f} \right) r \\
&+ \left( \frac{1}{v_x} C_{\beta_f} C_{T_f} C_{\alpha f} + \frac{1}{v_x} C_{\beta_r} C_{T_r} C_{\alpha r} - c_\varphi \right) p \\
&+ \left( -C_{T_f} \left( C_{\varphi_f} - C_{\alpha f} C_{\delta \varphi_f} \right) - C_{T_r} \left( C_{\varphi_r} - C_{\alpha r} C_{\delta \varphi_r} \right) - k_\varphi \right) \varphi \\
&+ C_{T_f} C_{\alpha f} \delta \qquad\qquad\qquad\qquad\qquad\qquad\qquad\qquad (11.115)
\end{aligned}
$$

$$
\begin{aligned}
M_z \;=\;& \left( -\frac{a_1^2}{v_x} C_{\alpha f} - \frac{a_2^2}{v_x} C_{\alpha r} \right) r + \left( \frac{a_1}{v_x} C_{\beta_f} C_{\alpha f} - \frac{a_2}{v_x} C_{\beta_r} C_{\alpha r} \right) p \\
&+ \left( a_2 C_{\alpha r} - a_1 C_{\alpha f} \right) \beta \\
&+ \left( a_2 \left( C_{\varphi_r} - C_{\alpha r} C_{\delta \varphi_r} \right) - a_1 \left( C_{\varphi_f} - C_{\alpha f} C_{\delta \varphi_f} \right) \right) \varphi \\
&+ a_1 C_{\alpha f} \delta \qquad\qquad\qquad\qquad\qquad\qquad\qquad\qquad (11.116)
\end{aligned}
$$

where $C_{\alpha f} = C_{\alpha f_L} + C_{\alpha f_R}$ and $C_{\alpha r} = C_{\alpha r_L} + C_{\alpha r_R}$ are equal to the sideslip coefficients of the left and right wheels in front and rear, respectively.

$$
\begin{aligned}
C_{\alpha f} &= C_{\alpha f_L} + C_{\alpha f_R} & (11.117) \\
C_{\alpha r} &= C_{\alpha r_L} + C_{\alpha r_R} & (11.118)
\end{aligned}
$$
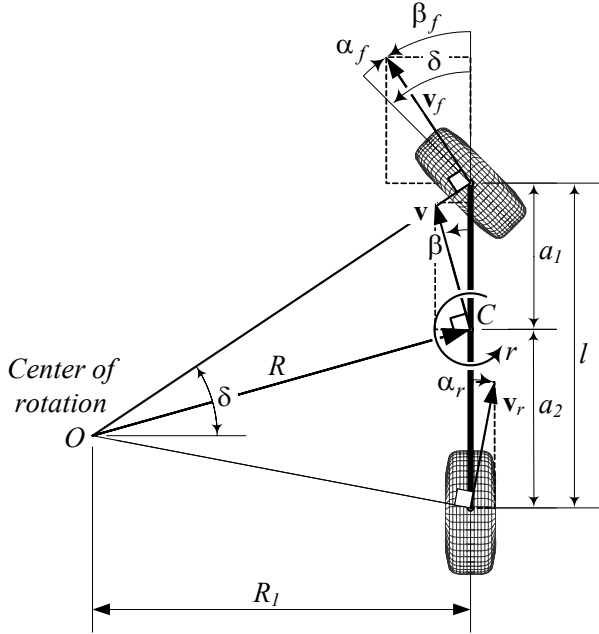
FIGURE 11.6. Kinematics of a two-wheel model for a vehicle with roll and yaw rotations.

**Proof.** For a two-wheel vehicle, we use the cot-average (7.3) of the outer and inner steer angles as the only steer angle $\delta$.

$$\cot \delta = \frac{\cot \delta_o + \cot \delta_i}{2} \tag{11.119}$$

Furthermore, we define a single sideslip coefficient $C_{\alpha f}$ and $C_{\alpha r}$ for the front and rear wheels. The coefficient $C_{\alpha f}$ and $C_{\alpha r}$ are equal to sum of the left and right wheels' sideslip coefficients.

Employing Equations (11.47)-(11.52) the forward and lateral forces on the rollable bicycle would be

$$
\begin{aligned}
F_x &= F_{x_f} \cos \delta + F_{x_r} - F_{y_f} \sin \delta & (11.120) \\
F_y &= F_{y_f} + F_{y_r}. & (11.121)
\end{aligned}
$$

The yaw moment equation does not interact with the vehicle roll. We may also ignore the moments $M_{z_i}$ and assume that the forward forces on the front left and right wheels are equal, as well as the forward forces on the rear left and right wheels. So, the terms $\sum_i y_i F_{x_i}$ cancel each other and the yaw moment reduces to

$$M_z = a_1 F_{y_f} - a_2 F_{y_r}. \tag{11.122}$$

The vehicle roll moment $M_x$ is a summation of the slip and camber moments on the front and rear wheels, $M_{x_f}$, $M_{x_r}$, and the moment because of change in normal loads of the left and right wheels $y_i F_{z_i}$. Let's assume that the slip and camber moments are proportional to the wheels' lateral force and write them as

$$M_{x_f} = C_{T_f} F_{y_f} \tag{11.123}$$

$$M_{x_r} = C_{T_r} F_{y_r} \tag{11.124}$$

where $C_{T_f}$ and $C_{T_r}$ are the overall *torque coefficient* of the front and rear wheels respectively.

$$C_{T_f} = \frac{dM_{x_f}}{dF_{y_f}} \tag{11.125}$$

$$C_{T_r} = \frac{dM_{x_r}}{dF_{y_r}} \tag{11.126}$$

Roll moment because of change in normal force of the left and right wheels is a result of force change in springs and dampers. These unbalanced forces generate a roll stiffness moment that is proportional to the vehicle's roll angle

$$M_{x_k} = -k_\varphi \varphi \tag{11.127}$$

$$M_{x_c} = -c_\varphi \dot{\varphi} \tag{11.128}$$

where $k_\varphi$ and $c_\varphi$ are the roll stiffness and roll damping of the vehicle.

$$
\begin{aligned}
k_\varphi &= wk \\
&= w\left(k_f + k_r\right) \tag{11.129}
\end{aligned}
$$

$$
\begin{aligned}
c_\varphi &= wc \\
&= w\left(c_f + c_r\right) \tag{11.130}
\end{aligned}
$$

$w$ is the track of the vehicle and $k$ and $c$ are sum of the front and rear springs' stuffiness and shock absorbers damping. The coefficients $k_\varphi$ and $c_\varphi$ are called the *roll stiffness* and *roll damping*, respectively.

$$k = k_f + k_r \tag{11.131}$$

$$c = c_f + c_r \tag{11.132}$$

Therefore, the applied roll moment on the vehicle can be summarized as

$$
\begin{aligned}
M_x &= M_{x_f} + M_{x_r} + M_{x_c} + M_{x_k} \\
&= C_{T_f} F_{y_f} + C_{T_r} F_{y_r} - w\left(c_f + c_r\right)\dot{\varphi} - w\left(k_f + k_r\right)\varphi. \tag{11.133}
\end{aligned}
$$

If we assume a small steer angle $\delta$, the vehicle force system can be approximated by the following equations:

$$F_x \approx F_{x_f} + F_{x_r} \tag{11.134}$$

$$F_y \approx F_{y_f} + F_{y_r} \tag{11.135}$$

$$M_x \approx C_{T_f}F_{y_f} + C_{T_r}F_{y_r} - k_\varphi \varphi - c_\varphi \dot{\varphi} \tag{11.136}$$

$$M_z \approx a_1 F_{y_f} - a_2 F_{y_r}. \tag{11.137}$$

Substituting for the lateral forces from (11.81), and expanding Equations (11.134)-(11.137) provides the following force system.

$$
\begin{aligned}
F_x &= F_{x_f} + F_{x_r} \tag{11.138}\\
F_y &= F_{y_f} + F_{y_r}\\
&= -C_{\alpha f}\alpha_f - C_{\varphi_f}\varphi - C_{\alpha r}\alpha_r - C_{\varphi_r}\varphi\\
&= -C_{\alpha f}\left(\beta + a_1\frac{r}{v_x} - C_{\beta_f}\frac{p}{v_x} - \delta - C_{\delta\varphi_f}\varphi\right) - C_{\varphi_f}\varphi\\
&\quad -C_{\alpha r}\left(\beta - a_2\frac{r}{v_x} - C_{\beta_r}\frac{p}{v_x} - C_{\delta\varphi_r}\varphi\right) - C_{\varphi_r}\varphi\\
&= \left(\frac{a_2}{v_x}C_{\alpha r} - \frac{a_1}{v_x}C_{\alpha f}\right)r + \left(\frac{C_{\alpha f}C_{\beta_f}}{v_x} + \frac{C_{\alpha r}C_{\beta_r}}{v_x}\right)p\\
&\quad + (-C_{\alpha f} - C_{\alpha r})\beta + \left(C_{\alpha f}C_{\delta\varphi_f} - C_{\varphi_r} - C_{\varphi_f} + C_{\alpha r}C_{\delta\varphi_r}\right)\varphi\\
&\quad + C_{\alpha f}\delta \tag{11.139}
\end{aligned}
$$

$$
\begin{aligned}
M_x &= C_{T_f}F_{y_f} + C_{T_r}F_{y_r} - k_\varphi \varphi - c_\varphi p\\
&= -C_{T_f}\left(C_{\alpha f}\left(\beta + a_1\frac{r}{v_x} - C_{\beta_f}\frac{p}{v_x} - \delta - C_{\delta\varphi_f}\varphi\right) + C_{\varphi_f}\varphi\right)\\
&\quad -C_{T_r}\left(C_{\alpha r}\left(\beta - a_2\frac{r}{v_x} - C_{\beta_r}\frac{p}{v_x} - C_{\delta\varphi_r}\varphi\right) + C_{\varphi_r}\varphi\right)\\
&\quad -k_\varphi \varphi - c_\varphi p\\
&= \left(\frac{a_2}{v_x}C_{T_r}C_{\alpha r} - \frac{a_1}{v_x}C_{T_f}C_{\alpha f}\right)r\\
&\quad + \left(\frac{1}{v_x}C_{\beta_f}C_{T_f}C_{\alpha f} + \frac{1}{v_x}C_{\beta_r}C_{T_r}C_{\alpha r} - c_\varphi\right)p\\
&\quad + \left(-C_{T_f}C_{\alpha f} - C_{T_r}C_{\alpha r}\right)\beta\\
&\quad + \left(-C_{T_f}\left(C_{\varphi_f} - C_{\alpha f}C_{\delta\varphi_f}\right) - C_{T_r}\left(C_{\varphi_r} - C_{\alpha r}C_{\delta\varphi_r}\right) - k_\varphi\right)\varphi\\
&\quad + C_{T_f}C_{\alpha f}\delta \tag{11.140}
\end{aligned}
$$

$$M_z = a_1 F_{y_f} - a_2 F_{y_r}$$

$$= -a_1 \left( C_{\alpha f} \left( \beta + a_1 \frac{r}{v_x} - C_{\beta_f} \frac{p}{v_x} - \delta - C_{\delta \varphi_f} \varphi \right) + C_{\varphi_f} \varphi \right)$$

$$+ a_2 \left( C_{\alpha r} \left( \beta - a_2 \frac{r}{v_x} - C_{\beta_r} \frac{p}{v_x} - C_{\delta \varphi_r} \varphi \right) + C_{\varphi_r} \varphi \right)$$

$$= \left( -\frac{a_1^2}{v_x} C_{\alpha f} - \frac{a_2^2}{v_x} C_{\alpha r} \right) r + \left( \frac{a_1}{v_x} C_{\beta_f} C_{\alpha f} - \frac{a_2}{v_x} C_{\beta_r} C_{\alpha r} \right) p$$

$$+ (a_2 C_{\alpha r} - a_1 C_{\alpha f}) \beta$$

$$+ \left( a_2 \left( C_{\varphi_r} - C_{\alpha r} C_{\delta \varphi_r} \right) - a_1 \left( C_{\varphi_f} - C_{\alpha f} C_{\delta \varphi_f} \right) \right) \varphi$$

$$+ a_1 C_{\alpha f} \delta \tag{11.141}$$

The parameters $C_{\alpha f}$ and $C_{\alpha r}$ are the sideslip stiffness for the front and rear wheels, $r$ is the yaw rate, $p$ is the roll rate, $\varphi$ is the roll angle, $\delta$ is the steer angle, and $\beta$ is the slip angle of the vehicle.

These equations are dependent on five parameters: $r$, $p$, $\beta$, $\varphi$, $\delta$, and may be written as

$$\begin{aligned} F_y &= F_y (r, p, \beta, \varphi, \delta) \\ &= \frac{\partial F_y}{\partial r} r + \frac{\partial F_y}{\partial p} p + \frac{\partial F_y}{\partial \beta} \beta + \frac{\partial F_y}{\partial \varphi} \varphi + \frac{\partial F_y}{\partial \delta} \delta \\ &= C_r r + C_p p + C_\beta \beta + C_\varphi \varphi + C_\delta \delta \end{aligned} \tag{11.142}$$

$$\begin{aligned} M_x &= M_x (r, p, \beta, \varphi, \delta) \\ &= \frac{\partial M_x}{\partial r} r + \frac{\partial M_x}{\partial p} p + \frac{\partial M_x}{\partial \beta} \beta + \frac{\partial M_x}{\partial \varphi} \varphi + \frac{\partial M_x}{\partial \delta} \delta \\ &= E_r r + E_p p + E_\beta \beta + E_\varphi \varphi + E_\delta \delta \end{aligned} \tag{11.143}$$

$$\begin{aligned} M_z &= M_z (r, p, \beta, \varphi, \delta) \\ &= \frac{\partial M_z}{\partial r} r + \frac{\partial M_z}{\partial p} p + \frac{\partial M_z}{\partial \beta} \beta + \frac{\partial M_z}{\partial \varphi} \varphi + \frac{\partial M_z}{\partial \delta} \delta \\ &= D_r r + D_p p + D_\beta \beta + D_\varphi \varphi + D_\delta \delta \end{aligned} \tag{11.144}$$

where the *force system coefficients* are

$$C_r = \frac{\partial F_y}{\partial r} = -\frac{a_1}{v_x} C_{\alpha f} + \frac{a_2}{v_x} C_{\alpha r} \tag{11.145}$$

$$C_p = \frac{\partial F_y}{\partial p} = \frac{C_{\alpha f} C_{\beta_f}}{v_x} + \frac{C_{\alpha r} C_{\beta_r}}{v_x} \tag{11.146}$$

$$C_\beta = \frac{\partial F_y}{\partial \beta} = - (C_{\alpha f} + C_{\alpha r}) \tag{11.147}$$

$$C_\varphi = \frac{\partial F_y}{\partial \varphi} = C_{\alpha r} C_{\delta \varphi_r} + C_{\alpha f} C_{\delta \varphi_f} - C_{\varphi_f} - C_{\varphi_r} \tag{11.148}$$

$$C_\delta = \frac{\partial F_y}{\partial \delta} = C_{\alpha f} \tag{11.149}$$

$$E_r = \frac{\partial M_x}{\partial r} = -\frac{a_1}{v_x} C_{T_f} C_{\alpha f} + \frac{a_2}{v_x} C_{T_r} C_{\alpha r} \tag{11.150}$$

$$E_p = \frac{\partial M_x}{\partial p} = \frac{1}{v_x} C_{\beta_f} C_{T_f} C_{\alpha f} + \frac{1}{v_x} C_{\beta_r} C_{T_r} C_{\alpha r} - c_\varphi \tag{11.151}$$

$$E_\beta = \frac{\partial M_x}{\partial \beta} = -C_{T_f} C_{\alpha f} - C_{T_r} C_{\alpha r} \tag{11.152}$$

$$E_\varphi = \frac{\partial M_x}{\partial \varphi} = -C_{T_f} \left( C_{\varphi_f} - C_{\alpha f} C_{\delta \varphi_f} \right) - k_\varphi$$
$$-C_{T_r} \left( C_{\varphi_r} - C_{\alpha r} C_{\delta \varphi_r} \right) \tag{11.153}$$

$$E_\delta = \frac{\partial M_x}{\partial \delta} = C_{T_f} C_{\alpha f}. \tag{11.154}$$

$$D_r = \frac{\partial M_z}{\partial r} = -\frac{a_1^2}{v_x} C_{\alpha f} - \frac{a_2^2}{v_x} C_{\alpha r} \tag{11.155}$$

$$D_p = \frac{\partial M_z}{\partial p} = \frac{a_1}{v_x} C_{\beta_f} C_{\alpha f} - \frac{a_2}{v_x} C_{\beta_r} C_{\alpha r} \tag{11.156}$$

$$D_\beta = \frac{\partial M_z}{\partial \beta} = -\left( a_1 C_{\alpha f} - a_2 C_{\alpha r} \right) \tag{11.157}$$

$$D_\varphi = \frac{\partial M_z}{\partial \varphi} = -a_1 \left( C_{\varphi_f} - C_{\alpha f} C_{\delta \varphi_f} \right) + a_2 \left( C_{\varphi_r} - C_{\alpha r} C_{\delta \varphi_r} \right) \tag{11.158}$$

$$D_\delta = \frac{\partial M_z}{\partial \delta} = a_1 C_{\alpha f}. \tag{11.159}$$

The force system coefficients are slopes of the curves for lateral force $F_y$, roll moment $M_x$, and yaw moment $M_z$ as a function of $r$, $p$, $\beta$, $\varphi$, and $\delta$ respectively. ■

## 11.4   ★ Two-wheel Rigid Vehicle Dynamics

We may combine the equations of motion (11.6)-(11.9) along with (11.110)-(11.116) for a two-wheel rollable rigid vehicle, and express its motion by the following set of equations:

$$\dot{v}_x = \frac{1}{m} F_x + r v_y \tag{11.160}$$
$$= \frac{1}{m} \left( F_{x_f} + F_{x_r} \right) + r v_y$$

$$
\begin{bmatrix} \dot{v}_y \\ \dot{p} \\ \dot{\varphi} \\ \dot{r} \end{bmatrix} = \begin{bmatrix} \dfrac{C_\beta}{mv_x} & \dfrac{C_p}{m} & \dfrac{C_\varphi}{m} & \dfrac{C_r}{m} - v_x \\[2ex] \dfrac{E_\beta}{I_x v_x} & \dfrac{E_p}{I_x} & \dfrac{E_\varphi}{I_x} & \dfrac{E_r}{I_x} \\[2ex] 0 & 1 & 0 & 0 \\[2ex] \dfrac{D_\beta}{I_z v_x} & \dfrac{D_p}{I_z} & \dfrac{D_\varphi}{I_z} & \dfrac{D_r}{I_z} \end{bmatrix} \begin{bmatrix} v_y \\ p \\ \varphi \\ r \end{bmatrix} + \begin{bmatrix} \dfrac{C_\delta}{m} \\[2ex] \dfrac{E_\delta}{I_x} \\[2ex] 0 \\[2ex] \dfrac{D_\delta}{I_z} \end{bmatrix} \delta \quad (11.161)
$$

These sets of equations are very useful to analyze vehicle motions, especially when they move at a constant forward speed.

Assuming $\dot{v}_x = 0$, the first equation (11.160) becomes an independent algebraic equation, while the lateral velocity $v_y$, roll rate $p$, roll angle $\varphi$, and yaw rate $r$ of the vehicle will change according to the four coupled equations (11.161).

Assuming the steer angle $\delta$ is the input command, the other variables $v_y$, $p$, $\varphi$, and $r$ may be assumed as the outputs. Hence, we may consider Equation (11.161) as a linear control system, and write the equations as

$$
\dot{\mathbf{q}} = [A]\,\mathbf{q} + \mathbf{u} \tag{11.162}
$$

in which $[A]$ is the coefficient matrix, $\mathbf{q}$ is the vector of control variables, and $\mathbf{u}$ is the vector of inputs.

$$
[A] = \begin{bmatrix} \dfrac{C_\beta}{mv_x} & \dfrac{C_p}{m} & \dfrac{C_\varphi}{m} & \dfrac{C_r}{m} - v_x \\[2ex] \dfrac{E_\beta}{I_x v_x} & \dfrac{E_p}{I_x} & \dfrac{E_\varphi}{I_x} & \dfrac{E_r}{I_x} \\[2ex] 0 & 1 & 0 & 0 \\[2ex] \dfrac{D_\beta}{I_z v_x} & \dfrac{D_p}{I_z} & \dfrac{D_\varphi}{I_z} & \dfrac{D_r}{I_z} \end{bmatrix} \tag{11.163}
$$

$$
\mathbf{q} = \begin{bmatrix} v_y \\ p \\ \varphi \\ r \end{bmatrix} \tag{11.164}
$$

$$
\mathbf{u} = \begin{bmatrix} \dfrac{C_\delta}{m} \\[2ex] \dfrac{E_\delta}{I_x} \\[2ex] 0 \\[2ex] \dfrac{D_\delta}{I_z} \end{bmatrix} \delta \tag{11.165}
$$

**Proof.** The Newton-Euler equations of motion for a rigid vehicle in the local coordinate frame $B$, attached to the vehicle at its mass center $C$, are

given in Equations (11.6)-(11.9) as

$$F_x = m\,\dot{v}_x - mr\,v_y \qquad (11.166)$$
$$F_y = m\,\dot{v}_y + mr\,v_x \qquad (11.167)$$
$$M_z = I_z\dot{\omega}_z = I_z\dot{r} \qquad (11.168)$$
$$M_x = I_x\dot{\omega}_x = I_x\dot{p}. \qquad (11.169)$$

The approximate force system applied on a two-wheel vehicle is found in Equations (11.110)-(11.113)

$$F_x \approx F_{x_f} + F_{x_r} \qquad (11.170)$$
$$F_y \approx F_{y_f} + F_{y_r} \qquad (11.171)$$
$$M_x \approx C_{T_f}F_{y_f} + C_{T_r}F_{y_r} - k_\varphi\varphi - c_\varphi\dot{\varphi} \qquad (11.172)$$
$$M_z \approx a_1 F_{y_f} - a_2 F_{y_r} \qquad (11.173)$$

and in terms of tire characteristics, in (11.114)-(11.116). These equations could be summarized in (11.142)-(11.144) as follows:

$$F_y = C_r\,r + C_p\,p + C_\beta\,\beta + C_\varphi\,\varphi + C_\delta\,\delta \qquad (11.174)$$
$$M_x = E_r\,r + E_p\,p + E_\beta\,\beta + E_\varphi\,\varphi + E_\delta\,\delta \qquad (11.175)$$
$$M_z = D_r\,r + D_p\,p + D_\beta\,\beta + D_\varphi\,\varphi + D_\delta\,\delta \qquad (11.176)$$

Substituting (11.174)–(11.176) in (11.166)–(11.169) produces the following set of equations of motion:

$$m\,\dot{v}_x - mr\,v_y = F_x \qquad (11.177)$$
$$m\,\dot{v}_y + mr\,v_x = C_r\,r + C_p\,p + C_\beta\,\beta + C_\varphi\,\varphi + C_\delta\,\delta \qquad (11.178)$$
$$I_x\dot{p} = E_r\,r + E_p\,p + E_\beta\,\beta + E_\varphi\,\varphi + E_\delta\,\delta \qquad (11.179)$$
$$\dot{r}\,I_z = D_r\,r + D_p\,p + D_\beta\,\beta + D_\varphi\,\varphi + D_\delta\,\delta \qquad (11.180)$$

Employing

$$\beta = \frac{v_y}{v_x} \qquad (11.181)$$

we are able to transform these equations to a set of differential equations for $v_x$, $v_y$, $p$, and $r$.

$$\dot{v}_x = \frac{F_x}{m} + r\,v_y \qquad (11.182)$$
$$\dot{v}_y = \left(\frac{C_r}{m} - v_x\right)r + \frac{C_p}{m}p + \frac{C_\beta}{m}\frac{v_y}{v_x} + \frac{C_\varphi}{m}\varphi + \frac{C_\delta}{m}\delta \qquad (11.183)$$
$$\dot{p} = \frac{1}{I_x}\left(E_r\,r + E_p\,p + E_\beta\frac{v_y}{v_x} + E_\varphi\,\varphi + E_\delta\,\delta\right) \qquad (11.184)$$
$$\dot{r} = \frac{1}{I_z}\left(D_r\,r + D_p\,p + D_\beta\frac{v_y}{v_x} + D_\varphi\,\varphi + D_\delta\,\delta\right). \qquad (11.185)$$

The first equation (11.182) depends on the yaw rate $r$ and the lateral velocity $v_y$, which are the outputs of the other equations, (11.183)-(11.185). However, if we assume the vehicle is moving with a constant forward speed,

$$v_x = cte. \tag{11.186}$$

then Equations (11.183)-(11.185) become independent with (11.182), and may be treated independent of the first equation.

Equations (11.183)-(11.185) may be considered as three coupled differential equations describing the behavior of a dynamic system. The dynamic system receives the steering angle $\delta$ as an input, and uses $v_x$ as a parameter to generates four outputs: $v_y$, $p$, $\varphi$, and $r$.

$$
\begin{bmatrix} \dot{v}_y \\ \dot{p} \\ \dot{\varphi} \\ \dot{r} \end{bmatrix}
=
\begin{bmatrix}
\dfrac{C_\beta}{mv_x} & \dfrac{C_p}{m} & \dfrac{C_\varphi}{m} & \dfrac{C_r}{m} - v_x \\[2mm]
\dfrac{E_\beta}{I_x v_x} & \dfrac{E_p}{I_x} & \dfrac{E_\varphi}{I_x} & \dfrac{E_r}{I_x} \\[2mm]
0 & 1 & 0 & 0 \\[2mm]
\dfrac{D_\beta}{I_z v_x} & \dfrac{D_p}{I_z} & \dfrac{D_\varphi}{I_z} & \dfrac{D_r}{I_z}
\end{bmatrix}
\begin{bmatrix} v_y \\ p \\ \varphi \\ r \end{bmatrix}
+
\begin{bmatrix} \dfrac{C_\delta}{m} \\[2mm] \dfrac{E_\delta}{I_x} \\[2mm] 0 \\[2mm] \dfrac{D_\delta}{I_z} \end{bmatrix}
\delta \tag{11.187}
$$

Equation (11.187) may be rearranged to show the input-output relationship.

$$\dot{\mathbf{q}} = [A]\,\mathbf{q} + \mathbf{u} \tag{11.188}$$

The vector $\mathbf{q}$ is called the *control variables vector*, and $\mathbf{u}$ is called the *inputs vector*. The matrix $[A]$ is the control variable coefficients matrix.  ■

**Example 413** *Equations of motion based on kinematic angles.*
*The equations of motion (11.187) can be expressed based on the angles $\beta$, $p$, $\varphi$, $r$, and $\delta$, by employing (11.181).*
*Taking a derivative from Equation (11.181) for constant $v_x$*

$$\dot{\beta} = \frac{\dot{v}_y}{v_x} \tag{11.189}$$

*and substituting in Equations (11.178) shows that we can transform the equation for $\dot{\beta}$.*

$$mv_x\dot{\beta} + mr\,v_x = C_r\,r + C_p\,p + C_\beta\,\beta + C_\varphi\,\varphi + C_\delta\,\delta \tag{11.190}$$

*Therefore, the set of equations of motion can be expressed in terms of the*

*vehicle's angular variables.*

$$
\begin{bmatrix} \dot{\beta} \\ \dot{p} \\ \dot{\varphi} \\ \dot{r} \end{bmatrix} =
\begin{bmatrix}
\dfrac{C_\beta}{mv_x} & \dfrac{C_p}{mv_x} & \dfrac{C_\varphi}{mv_x} & \dfrac{C_r}{mv_x} - 1 \\[2mm]
\dfrac{E_\beta}{I_x} & \dfrac{E_p}{I_x} & \dfrac{E_\varphi}{I_x} & \dfrac{E_r}{I_x} \\[2mm]
0 & 1 & 0 & 0 \\[2mm]
\dfrac{D_\beta}{I_z} & \dfrac{D_p}{I_z} & \dfrac{D_\varphi}{I_z} & \dfrac{D_r}{I_z}
\end{bmatrix}
\begin{bmatrix} \beta \\ p \\ \varphi \\ r \end{bmatrix} +
\begin{bmatrix} \dfrac{C_\delta}{m} \\[2mm] \dfrac{E_\delta}{I_x} \\[2mm] 0 \\[2mm] \dfrac{D_\delta}{I_z} \end{bmatrix} \delta
\tag{11.191}
$$

## 11.5   ★ Steady-State Motion

Turning of a front steering, two-wheel, rollable rigid vehicle at steady-state condition is governed by the following equations:

$$
\begin{aligned}
F_x &= -mr\,v_y & (11.192) \\
C_r\,r + C_p\,p + C_\beta\,\beta + C_\varphi\,\varphi + C_\delta\,\delta &= mr\,v_x & (11.193) \\
E_r\,r + E_p\,p + E_\beta\,\beta + E_\varphi\,\varphi + E_\delta\,\delta &= 0 & (11.194) \\
D_r\,r + D_p\,p + D_\beta\,\beta + D_\varphi\,\varphi + D_\delta\,\delta &= 0 & (11.195)
\end{aligned}
$$

or equivalently, by the following equations

$$
\begin{aligned}
F_x &= -\frac{m}{R}v_x\,v_y & (11.196) \\
\left(C_r\,v_x - m\,v_x^2\right)\frac{1}{R} + C_\beta\,\beta + C_p\,p + C_\varphi\,\varphi &= -C_\delta\,\delta & (11.197) \\
E_r\,v_x\frac{1}{R} + E_\beta\,\beta + E_p\,p + E_\varphi\,\varphi &= -E_\delta\,\delta & (11.198) \\
D_r\,v_x\frac{1}{R} + D_\beta\,\beta + D_p\,p + D_\varphi\,\varphi &= -D_\delta\,\delta. & (11.199)
\end{aligned}
$$

The first equation determines the required forward force to keep $v_x$ constant. The next three equations show the steady-state values of the output variables, which are: path curvature $\kappa$,

$$
\begin{aligned}
\kappa &= \frac{1}{R} \\
&= \frac{r}{v_x} & (11.200)
\end{aligned}
$$

vehicle slip angle $\beta$, vehicle roll rate $p$, and vehicle roll angle $\varphi$ for a constant steering input $\delta$ at a constant forward speed $v_x$. The output-input relationships are defined by the following responses:

1− *Curvature response, $S_\kappa$*

$$S_\kappa = \frac{\kappa}{\delta} = \frac{1}{R\delta}$$

$$= -\frac{Z_1}{v_x Z_0} \tag{11.201}$$

2− *Slip response, $S_\beta$*

$$S_\beta = \frac{\beta}{\delta}$$

$$= \frac{Z_2}{Z_0} \tag{11.202}$$

3− *Yaw rate response, $S_r$*

$$S_r = \frac{r}{\delta} = \frac{\kappa}{\delta} v_x = S_\kappa v_x$$

$$= -\frac{Z_1}{Z_0} \tag{11.203}$$

4− *Lateral acceleration response, $S_a$*

$$S_a = \frac{v_x^2 / R}{\delta} = \frac{\kappa}{\delta} v_x^2 = S_\kappa v_x^2$$

$$= \frac{v_x Z_1}{Z_0} \tag{11.204}$$

5− *Roll angle response, $S_\varphi$*

$$S_\varphi = \frac{\varphi}{\delta}$$

$$= -\frac{Z_3}{Z_0} \tag{11.205}$$

$$
\begin{aligned}
Z_0 =\ & E_\beta \left( D_r C_\varphi - C_r D_\varphi + m v_x D_\varphi \right) + \\
& E_\varphi \left( C_r D_\beta - D_r C_\beta - m v_x D_\beta \right) + E_r \left( C_\beta D_\varphi - D_\beta C_\varphi \right) \quad (11.206) \\
Z_1 =\ & E_\beta \left( C_\varphi D_\delta - v_x C_\delta D_\varphi \right) - E_\varphi \left( C_\beta D_\delta - v_x C_\delta D_\beta \right) \\
& + E_\delta \left( C_\beta D_\varphi - D_\beta C_\varphi \right) \quad (11.207) \\
Z_2 =\ & E_\varphi \left( m v_x D_\delta - C_r D_\delta + D_r v_x C_\delta \right) + E_r \left( C_\varphi D_\delta - v_x C_\delta D_\varphi \right) \\
& - E_\delta \left( D_r C_\varphi - C_r D_\varphi + m v_x D_\varphi \right) \quad (11.208) \\
Z_3 =\ & E_\beta \left( m v_x D_\delta - C_r D_\delta + D_r v_x C_\delta \right) + E_r \left( C_\beta D_\delta - v_x C_\delta D_\beta \right) \\
& - E_\delta \left( D_r C_\beta - C_r D_\beta + m v_x D_\beta \right) \quad (11.209)
\end{aligned}
$$

**Proof.** In steady-state conditions, all the variables are constant and hence, their derivatives are zero. Therefore, the equations of motion (11.166)–(11.169) reduce to

$$F_x = -mr\,v_y \tag{11.210}$$
$$F_y = mr\,v_x \tag{11.211}$$
$$M_x = 0 \tag{11.212}$$
$$M_z = 0 \tag{11.213}$$

where the lateral force $F_y$, roll moment $M_x$, and yaw moment $M_z$ from (11.174)–(11.176) would be

$$F_y = C_r\,r + C_\beta\,\beta + C_\varphi\,\varphi + C_\delta\,\delta \tag{11.214}$$
$$M_x = E_r\,r + E_\beta\,\beta + E_\varphi\,\varphi + E_\delta\,\delta \tag{11.215}$$
$$M_z = D_r\,r + D_\beta\,\beta + D_\varphi\,\varphi + D_\delta\,\delta \tag{11.216}$$

Therefore, the equations describing the steady-state turning of a two-wheel rigid vehicle are equal to

$$F_x = -mr\,v_y \tag{11.217}$$
$$C_r\,r + C_\beta\,\beta + C_\varphi\,\varphi + C_\delta\,\delta = mr\,v_x \tag{11.218}$$
$$E_r\,r + E_\beta\,\beta + E_\varphi\,\varphi + E_\delta\,\delta = 0 \tag{11.219}$$
$$D_r\,r + D_\beta\,\beta + D_\varphi\,\varphi + D_\delta\,\delta = 0. \tag{11.220}$$

Equation (11.217) may be used to calculate the required traction force to keep the motion steady. However, Equations (11.218) and (11.220) can be used to determine the steady-state responses of the vehicle.

$$C_r\,\frac{v_x}{R} + C_\beta\,\beta + C_\varphi\,\varphi + C_\delta\,\delta = m\frac{v_x}{R}\,v_x \tag{11.221}$$
$$E_r\,\frac{v_x}{R} + E_\beta\,\beta + E_\varphi\,\varphi + E_\delta\,\delta = 0 \tag{11.222}$$
$$D_r\,\frac{v_x}{R} + D_\beta\,\beta + D_\varphi\,\varphi + D_\delta\,\delta = 0. \tag{11.223}$$

At steady-state turning, the vehicle will move on a circle with radius $R$ at a speed $v_x$ and angular velocity $r$, so

$$v_x = R\,r. \tag{11.224}$$

By substituting (11.224) in Equations (11.218)-(11.220) and employing the curvature definition (11.200), we may write the equations in matrix form

$$\begin{bmatrix} C_\beta & C_r\,v_x - m\,v_x^2 & C_\varphi \\ E_\beta & E_r\,v_x & E_\varphi \\ D_\beta & D_r\,v_x & D_\varphi \end{bmatrix} \begin{bmatrix} \beta \\ \kappa \\ \varphi \end{bmatrix} = \begin{bmatrix} -C_\delta \\ -E_\delta \\ -D_\delta \end{bmatrix} \delta. \tag{11.225}$$

Solving the equations for $\beta$, $\kappa$, and $\varphi$ enables us to define different output-input relationships as (11.201)-(11.205). ∎

**Example 414** *Force system coefficients for a car.*
   *Consider a front steering, four-wheel car with the following characteristics:*

$$C_{\alpha f_L} = C_{\alpha f_R} \approx 26000\,\text{N}/\text{rad} \qquad (11.226)$$
$$C_{\alpha r_L} = C_{\alpha r_R} \approx 32000\,\text{N}/\text{rad} \qquad (11.227)$$

$$
\begin{aligned}
m &= 838.7\,\text{kg} \\
I_x &= 300\,\text{kg}\,\text{m}^2 \\
I_z &= 1391\,\text{kg}\,\text{m}^2 \\
a_1 &= 0.859\,\text{m} \\
a_2 &= 1.486\,\text{m} \\
k_\varphi &= 26612\,\text{N}/\text{rad} \\
c_\varphi &= 1700\,\text{N}\,\text{s}/\text{rad} \qquad (11.228)
\end{aligned}
$$

$$
\begin{aligned}
C_{\beta_f} &= -0.4 \\
C_{\beta_r} &= -0.1 \\
C_{T_f} &= -0.4 \\
C_{T_r} &= -0.2 \\
C_{\delta\varphi_f} &= 0.01 \\
C_{\delta\varphi_r} &= 0 \\
C_{\varphi_f} &= -3200 \\
C_{\varphi_r} &= 0 \qquad (11.229)
\end{aligned}
$$

$$
\begin{aligned}
v_x &= 16.6\,\text{m}/\text{s} \qquad (11.230) \\
\delta &= 0.1\,\text{rad} \qquad (11.231)
\end{aligned}
$$

*The sideslip coefficients of an equivalent bicycle model are*

$$C_{\alpha f} = C_{\alpha f_L} + C_{\alpha f_R} = 52000\,\text{N}/\text{rad} \qquad (11.232)$$
$$C_{\alpha r} = C_{\alpha r_L} + C_{\alpha r_R} = 64000\,\text{N}/\text{rad} \qquad (11.233)$$

*The force system coefficients are equal to the following if $v_x$ is measured in* $[\text{m}/\text{s}]$*:*

$$
\begin{aligned}
C_r &= 2521.8 \\
C_p &= -1360 \\
C_\beta &= -116000 \\
C_\varphi &= 8400 \\
C_\delta &= 52000 \qquad (11.234)
\end{aligned}
$$

$$
\begin{aligned}
E_r &= -57.68 \\
E_p &= -1220 \\
E_\beta &= 33600 \\
E_\varphi &= -29972 \\
E_\delta &= -20800
\end{aligned}
\tag{11.235}
$$

$$
\begin{aligned}
D_r &= -8984.7178 \\
D_p &= -417.84 \\
D_\beta &= 50436 \\
D_\varphi &= 7215.6 \\
D_\delta &= 44668.
\end{aligned}
\tag{11.236}
$$

*The $Z_i$ parameters and the steady-state responses of the vehicle are as follows:*

$$
\begin{aligned}
Z_0 &= 0.5377445876 \times 10^{14} \\
Z_1 &= -0.1940746914 \times 10^{16} \\
Z_2 &= .02619612932 \times 10^{15} \\
Z_3 &= -0.2526173904 \times 10^{15}
\end{aligned}
\tag{11.237}
$$

$$
\begin{aligned}
S_\kappa &= \frac{\kappa}{\delta} = \frac{1/R}{\delta} = 1.804524824 \\
S_\beta &= \frac{\beta}{\delta} = 4.871481726 \\
S_r &= \frac{r}{\delta} = 36.09049647 \\
S_a &= \frac{v_x^2/R}{\delta} = -721.8099294 \\
S_\varphi &= \frac{\varphi}{\delta} = 4.697720744
\end{aligned}
\tag{11.238}
$$

*Having the steady-state responses, we are able to calculate the steady-state characteristic of the motion.*

$$
\begin{aligned}
R &= 5.54\,\mathrm{m} & (11.239) \\
\beta &= .487\,\mathrm{rad} \approx 27.9\,\mathrm{deg} & (11.240) \\
r &= 3.61\,\mathrm{rad/s} & (11.241) \\
\frac{v_x^2}{R} &= -72.18\,\mathrm{m/s^2} & (11.242)
\end{aligned}
$$

**Example 415 ★** *Camber trust.*
  *When a vehicle rolls, the road wheels of almost all types of suspensions take up a camber angle in the same sense as the roll. The wheel camber is*

*always less than the roll angle. The camber angle in independent suspensions is higher than in dependent suspensions.*

*At steady-state conditions, camber at the front wheels increases the understeer characteristic of the vehicle, while camber at the rear increases the oversteer characteristic of the vehicle. Most road vehicles are made such that in a turn, the rear wheels remain upright and the front wheels camber. These vehicles have an increasing understeer behavior with roll and are more stable.*

**Example 416 ★** *Roll steer.*

*Positive roll steer means the wheel steers about the z-axis when the vehicle rolls about the x-axis. So, when the vehicle turns to the right, a positive roll steer wheel will steer to the left.*

*Positive roll steer at the front wheels increases the understeer characteristic of the vehicle, while roll steer at the rear increases the oversteer characteristic of the vehicle. Most road vehicles' suspension is made such that in a turn the front wheels have positive roll steering. These vehicles have an increasing understeer behavior with roll and are more stable.*

## 11.6  ★ Time Response

The equations of motion must analytically or numerically be integrated to analyze the time response of a vehicle and examine how the vehicle will respond to a steering input. The equations of motion are a set of coupled ordinary differential equations as expressed here.

$$\dot{v}_x = \frac{1}{m}F_x + r\,v_y \tag{11.243}$$

$$
\begin{bmatrix} \dot{v}_y \\ \dot{p} \\ \dot{\varphi} \\ \dot{r} \end{bmatrix} =
\begin{bmatrix}
\dfrac{C_\beta}{mv_x} & \dfrac{C_p}{m} & \dfrac{C_\varphi}{m} & \dfrac{C_r}{m}-v_x \\[2mm]
\dfrac{E_\beta}{I_x v_x} & \dfrac{E_p}{I_x} & \dfrac{E_\varphi}{I_x} & \dfrac{E_r}{I_x} \\[2mm]
0 & 1 & 0 & 0 \\[2mm]
\dfrac{D_\beta}{I_z v_x} & \dfrac{D_p}{I_z} & \dfrac{D_\varphi}{I_z} & \dfrac{D_r}{I_z}
\end{bmatrix}
\begin{bmatrix} v_y \\ p \\ \varphi \\ r \end{bmatrix}
+
\begin{bmatrix}
\dfrac{C_\delta}{m} \\[2mm]
\dfrac{E_\delta}{I_x} \\[2mm]
0 \\[2mm]
\dfrac{D_\delta}{I_z}
\end{bmatrix}
\delta\left(t\right) \tag{11.244}
$$

Their answers to a given time-dependent steer angle $\delta\left(t\right)$ are

$$v_x = v_x\left(t\right) \tag{11.245}$$
$$v_y = v_y\left(t\right) \tag{11.246}$$
$$p = p\left(t\right) \tag{11.247}$$
$$\varphi = \varphi\left(t\right) \tag{11.248}$$
$$r = r\left(t\right). \tag{11.249}$$

Such a solution is called the *time response* or *transient response* of the vehicle.

Assuming a constant forward velocity, the first equation (11.243) simplifies to

$$F_x = -mr\, v_y \tag{11.250}$$

and Equation (11.244) becomes independent from the first one. The set of Equations (11.244) can be written in the form

$$\dot{\mathbf{q}} = [A]\,\mathbf{q} + \mathbf{u} \tag{11.251}$$

in which $[A]$ is a constant coefficient matrix, $\mathbf{q}$ is the vector of control variables, and $\mathbf{u}$ is the vector of inputs.

To solve the inverse dynamics problem and find the vehicle response, the steering function $\delta(t)$ must be given.

**Example 417 ★** *Free dynamics and free response.*
*The response of a vehicle to zero steer angle $\delta(t) = 0$ at constant speed is called **free response**. The equation of motion under a **free dynamics** is*

$$\dot{\mathbf{q}} = [A]\,\mathbf{q}. \tag{11.252}$$

*To solve the equation, let's assume*

$$[A] = \begin{bmatrix} a_{11} & a_{12} & a_{13} & a_{14} \\ a_{21} & a_{22} & a_{23} & a_{24} \\ a_{31} & a_{32} & a_{33} & a_{34} \\ a_{41} & a_{42} & a_{43} & a_{44} \end{bmatrix} \tag{11.253}$$

*and therefore, the equations of motion are*

$$\begin{bmatrix} \dot{v}_y \\ \dot{p} \\ \dot{\varphi} \\ \dot{r} \end{bmatrix} = \begin{bmatrix} a_{11} & a_{12} & a_{13} & a_{14} \\ a_{21} & a_{22} & a_{23} & a_{24} \\ a_{31} & a_{32} & a_{33} & a_{34} \\ a_{41} & a_{42} & a_{43} & a_{44} \end{bmatrix} \begin{bmatrix} v_y \\ p \\ \varphi \\ r \end{bmatrix} \tag{11.254}$$

*Because the equations are linear, the solutions are an exponential function*

$$v_y = A_1 e^{\lambda t} \tag{11.255}$$
$$p = A_2 e^{\lambda t} \tag{11.256}$$
$$\varphi = A_3 e^{\lambda t} \tag{11.257}$$
$$r = A_4 e^{\lambda t}. \tag{11.258}$$

*Substituting the solutions shows that the condition for functions (11.255)-(11.258) to be the solution of the equations (11.254) is that the exponent $\lambda$ is the eigenvalue of $[A]$. To find $\lambda$, we may expand the determinant of the above coefficient matrix and find the characteristic equation*

$$\det [A] = 0. \tag{11.259}$$

*Having the eigenvalues $\lambda_{1,2,3,4}$ provides the following general solution for the free dynamics of the vehicle:*

$$
\begin{aligned}
v_y &= A_{11}e^{\lambda_1 t} + A_{12}e^{\lambda_2 t} + A_{13}e^{\lambda_3 t} + A_{14}e^{\lambda_4 t} & (11.260) \\
p &= A_{21}e^{\lambda_1 t} + A_{22}e^{\lambda_2 t} + A_{23}e^{\lambda_3 t} + A_{24}e^{\lambda_4 t} & (11.261) \\
\varphi &= A_{31}e^{\lambda_1 t} + A_{32}e^{\lambda_2 t} + A_{33}e^{\lambda_3 t} + A_{34}e^{\lambda_4 t} & (11.262) \\
r &= A_{41}e^{\lambda_1 t} + A_{42}e^{\lambda_2 t} + A_{43}e^{\lambda_3 t} + A_{44}e^{\lambda_4 t}. & (11.263)
\end{aligned}
$$

*The coefficients $A_{ij}$ must be found from initial conditions. The free dynamics and hence the vehicle, is stable as long as the eigenvalues have negative real part.*

*As an example, consider a vehicle with the characteristics given in (11.226)-(11.229), and the following steer angle and forward velocity.*

$$
\begin{aligned}
v_x &= 20\,\mathrm{m/s} & (11.264) \\
\delta &= 0.1\,\mathrm{rad} & (11.265)
\end{aligned}
$$

*Substituting those values provide the following equations of motion for free dynamics.*

$$
\begin{bmatrix} \dot{v}_y \\ \dot{p} \\ \dot{\varphi} \\ \dot{r} \end{bmatrix} =
\begin{bmatrix}
-6.91 & -1.62 & 10.01 & -16.99 \\
5.6 & -4.067 & -99.9 & -.192 \\
0 & 1 & 0 & 0 \\
1.81 & -0.3 & 5.19 & -6.46
\end{bmatrix}
\begin{bmatrix} v_y \\ p \\ \varphi \\ r \end{bmatrix}
\qquad (11.266)
$$

*The eigenvalues of the coefficient matrix are*

$$
\begin{aligned}
\lambda_1 &= -2.503 + 9.6154i \\
\lambda_2 &= -2.503 - 9.6154i \\
\lambda_3 &= -6.2155 + 6.2528i \\
\lambda_4 &= -6.2155 - 6.2528i & (11.267)
\end{aligned}
$$

*which shows the vehicle is stable because all of the eigenvalues have real negative parts.*

*Substituting the eigenvalues in Equations (11.260)-(11.263) provides the solution with unknown coefficients. Let's examine the free dynamics behavior of the vehicle for a nonzero initial condition.*

$$
\mathbf{q}_0 = \begin{bmatrix} v_y(0) \\ p(0) \\ \varphi(0) \\ r(0) \end{bmatrix} = \begin{bmatrix} 0 \\ 0.1 \\ 0 \\ 0 \end{bmatrix}
\qquad (11.268)
$$

*Figures 11.7 to 11.10 illustrate the time responses of the vehicle.*
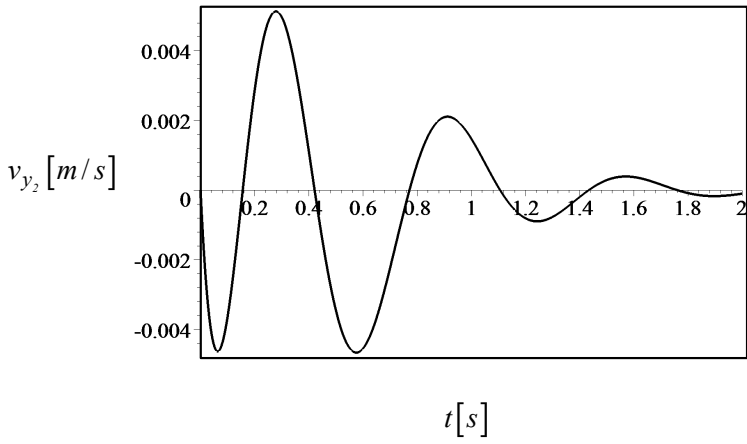
FIGURE 11.7. Lateral velocity response over time.
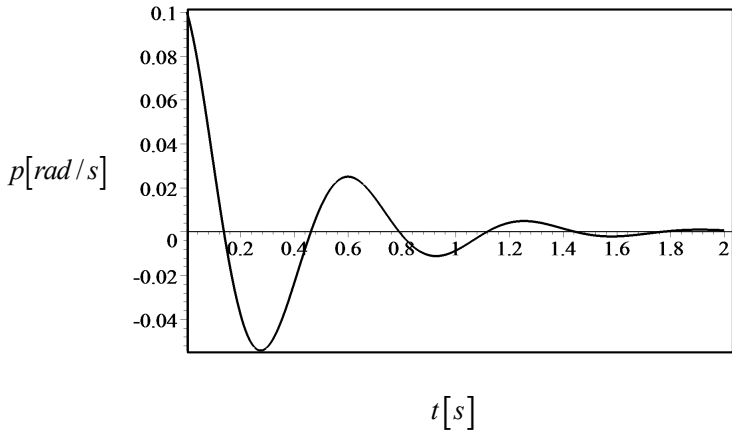


FIGURE 11.8. Roll rate response over time.
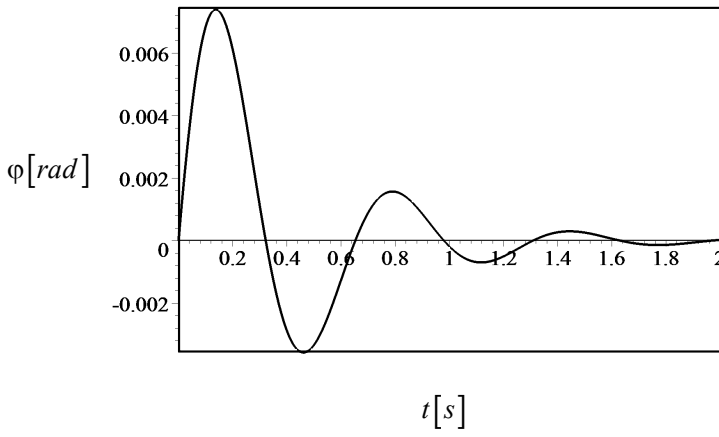
FIGURE 11.9. Roll angle response over time.
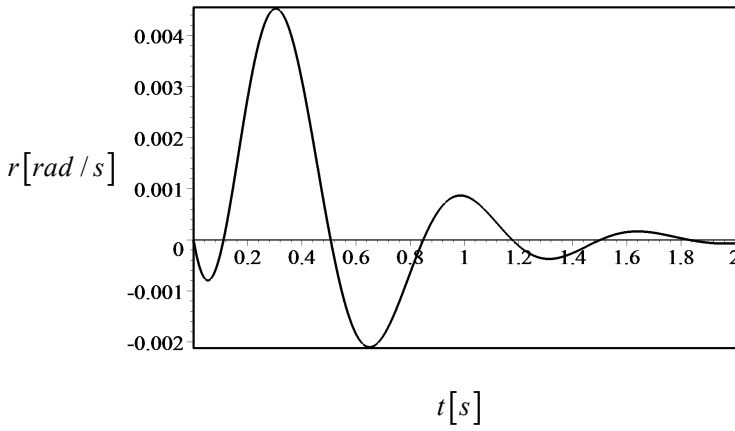


FIGURE 11.10. Yaw rate response over time.
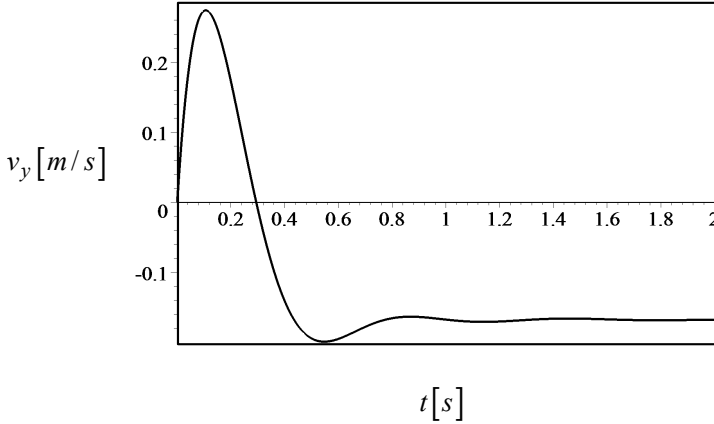
FIGURE 11.11. Lateral velocity response for a step steer angle.

**Example 418 ★** *Response to a step input.*
   *The response of dynamic systems to a step input is a standard test to examine the behavior of dynamic systems. Step input for vehicle dynamics is a sudden change in steer angle from zero to a nonzero constant value.*
   *Consider a vehicle with the characteristics given in (11.226)-(11.229) and a sudden change in the steering input to a constant value*

$$\delta\left(t\right) = \begin{cases} 0.2\,\text{rad} \approx 11.459\,\text{deg} & t > 0 \\ 0 & t \leq 0 \end{cases}. \tag{11.269}$$

*The equations of motion for non-zero initial conditions*

$$\mathbf{q}_0 = \left[\begin{bmatrix} v_y\left(0\right) \\ p\left(0\right) \\ \varphi\left(0\right) \\ r\left(0\right) \end{bmatrix}\right] = \begin{bmatrix} 0 \\ 0.1 \\ 0 \\ 0 \end{bmatrix} \tag{11.270}$$

*are*

$$\dot{v}_y + 6.91v_y + 1.62p - 10.01\varphi + 16.99r \;=\; 62\delta\left(t\right) \tag{11.271}$$

$$\dot{p} - 5.6v_y + 4.06p + 99.91\varphi + .192r \;=\; -69.33\left(t\right) \tag{11.272}$$

$$\dot{\varphi} - p \;=\; 0 \tag{11.273}$$

$$\dot{r} - 1.81v_y + 0.3p - 5.19\varphi + 6.46r \;=\; 32.11\delta\left(t\right) \tag{11.274}$$

   *Figures 11.11 to 11.14 depict the solutions.*
   *Having $v_y\left(t\right)$, $p(t)$, $\varphi(t)$, and $r\left(t\right)$ are enough to calculate any other kinematic variables as well as the required forward force $F_x$ to maintain a constant speed.*

$$F_x = -mr\,v_y \tag{11.275}$$

*Figure 11.15 illustrates the required forward force $F_x(t)$.*
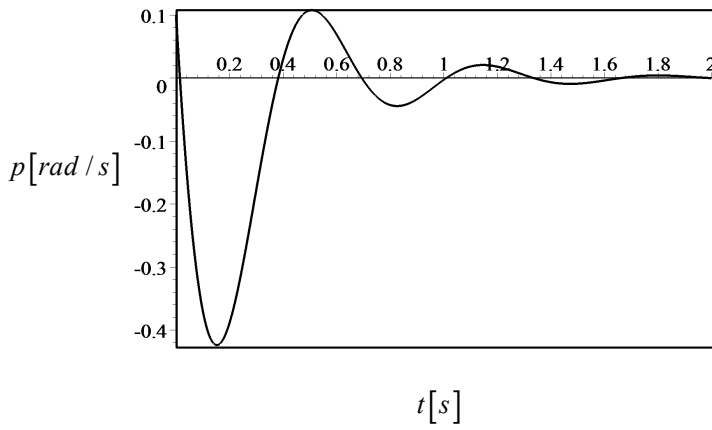
FIGURE 11.12. Roll rate response for a step steer angle.
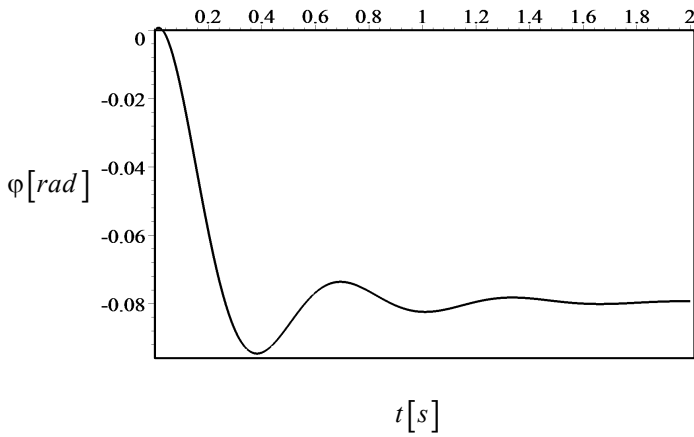


FIGURE 11.13. Roll angle response for a step steer angle.
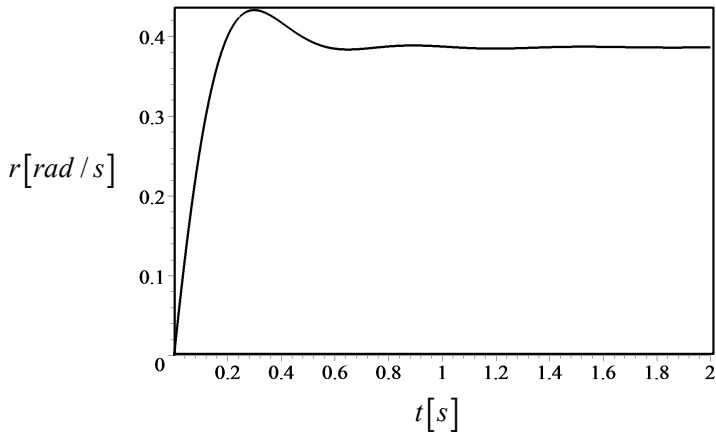
FIGURE 11.14. Yaw rate response for a step steer angle.
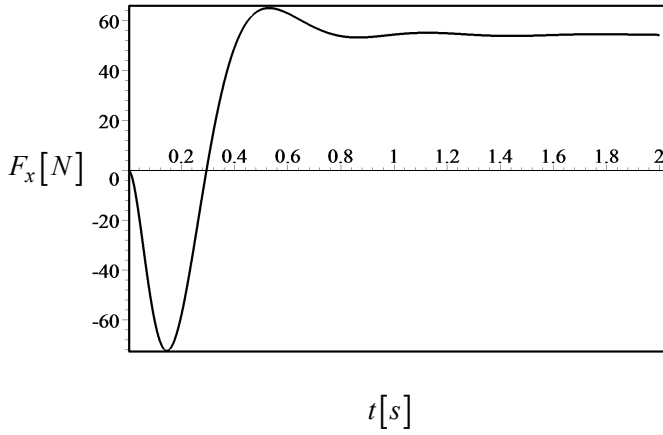


FIGURE 11.15. The required forward force $F_x$ to maintain the speed constant.

**Example 419 ★** *Passing maneuver.*

   *Passing and lane-change maneuvers are two other standard tests to examine a vehicle's dynamic responses. Passing can be expressed by a half-sine or a sine-squared function for steering input. Two examples of such functions are*

$$\delta(t) = \begin{cases} \delta_0 \sin \omega t & t_1 < t < \dfrac{\pi}{\omega} \\ 0 & \dfrac{\pi}{\omega} < t < t_1 \end{cases} \text{ rad} \qquad (11.276)$$

$$\delta(t) = \begin{cases} \delta_0 \sin^2 \omega t & t_1 < t < \dfrac{\pi}{\omega} \\ 0 & \dfrac{\pi}{\omega} < t < t_1 \end{cases} \text{ rad} \qquad (11.277)$$

$$\omega = \dfrac{\pi L}{v_x}. \qquad (11.278)$$

*where $L$ is the moving length during the passing and $v_x$ is the forward speed of the vehicle. The path of a passing car would be similar to Figure 11.16.*

   *Let's examine a vehicle with the characteristics given in (11.226)-(11.229) and a change in half-sine steering input $\delta(t)$.*

$$\delta(t) = \begin{cases} 0.2 \sin \dfrac{\pi L}{v_x} t & 0 < t < \dfrac{v_x}{L} \\ 0 & \dfrac{v_x}{L} < t < 0 \end{cases} \text{ rad} \qquad (11.279)$$

$$L = 100 \,\mathrm{m} \qquad (11.280)$$

$$v_x = 30 \,\mathrm{m/s}. \qquad (11.281)$$

*The equations of motion for zero initial conditions are as given in (11.271)-(11.274).*

   *Figures 11.17 to 11.20 show the time responses of the vehicle for the steering function (11.279).*

**Example 420 ★** *Passing with a sine-square steer function.*

   *A good driver should change the steer angle as smoothly as possible to minimize undesired roll angle and roll fluctuation. A sine-square steer function*

$$\delta(t) = \begin{cases} \delta_0 \sin^2 \omega t & t_1 < t < \dfrac{\pi}{\omega} \\ 0 & \dfrac{\pi}{\omega} < t < t_1 \end{cases} \text{ rad} \qquad (11.282)$$

$$\omega = \dfrac{\pi L}{v_x}. \qquad (11.283)$$

*which is introduced in Equation (11.277), makes for smoother passing steering. The responses of the vehicle in Example 419 to the steering (11.282) are illustrated in Figures 11.21 to 11.24.*
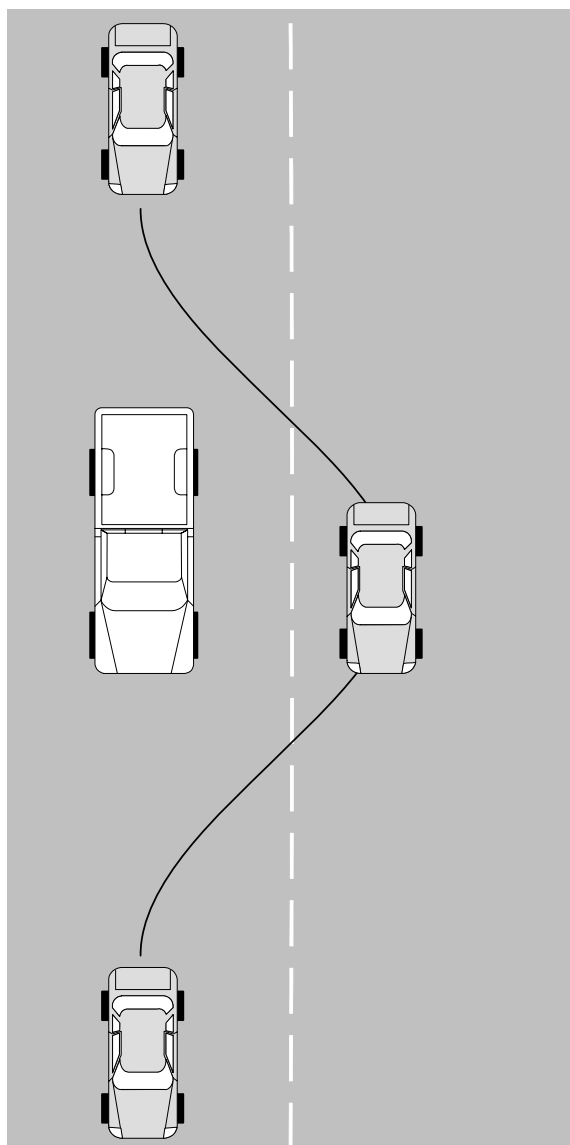
FIGURE 11.16. A passing maneuver.
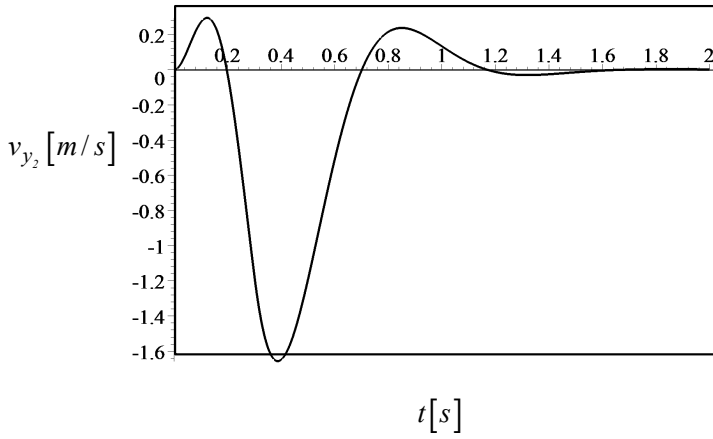
FIGURE 11.17. Lateral velocity response for the steering function (11.279).
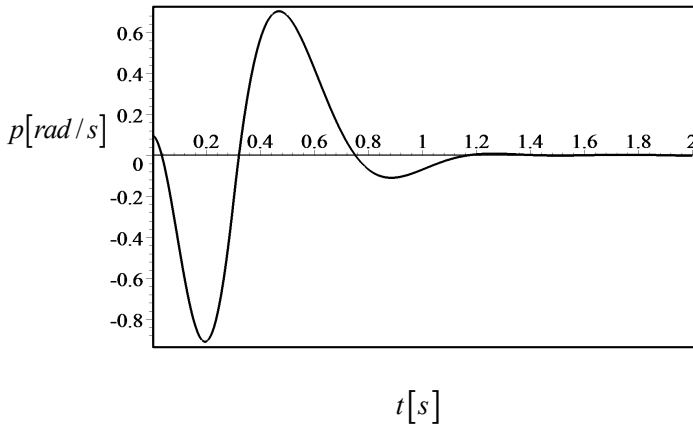


FIGURE 11.18. Roll rate response for the steering function (11.279).
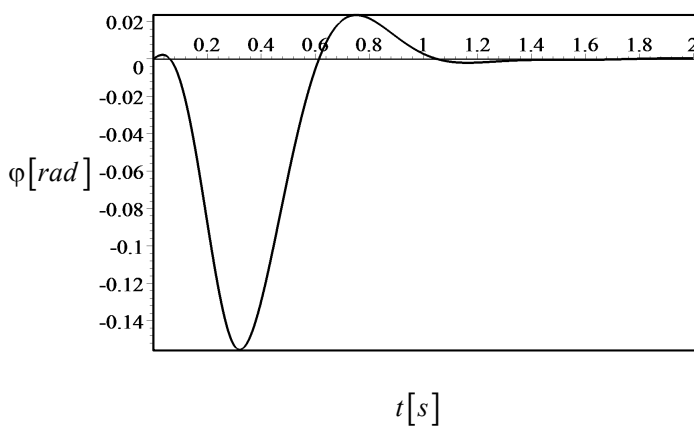
FIGURE 11.19. Roll angle response for the steering function (11.279).
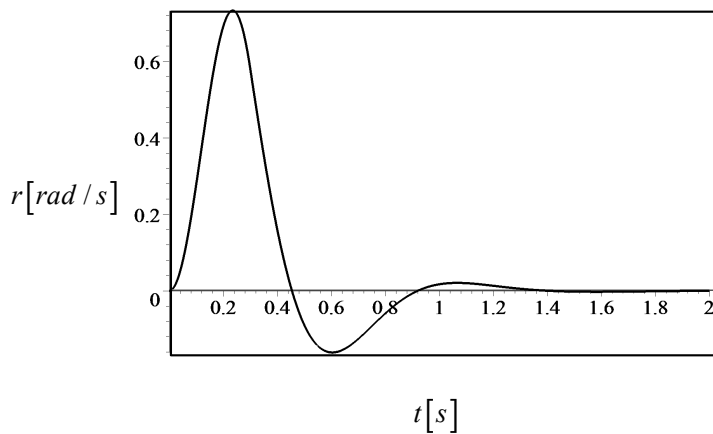


FIGURE 11.20. Yaw rate response for the steering function (11.279).
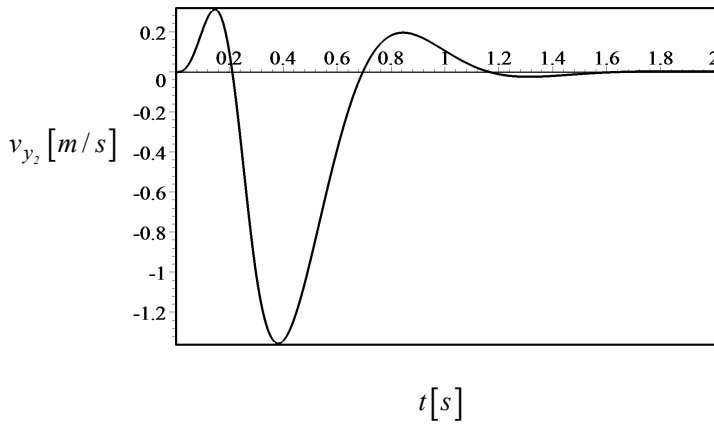
FIGURE 11.21. Lateral velocity response for the steering function (11.282).
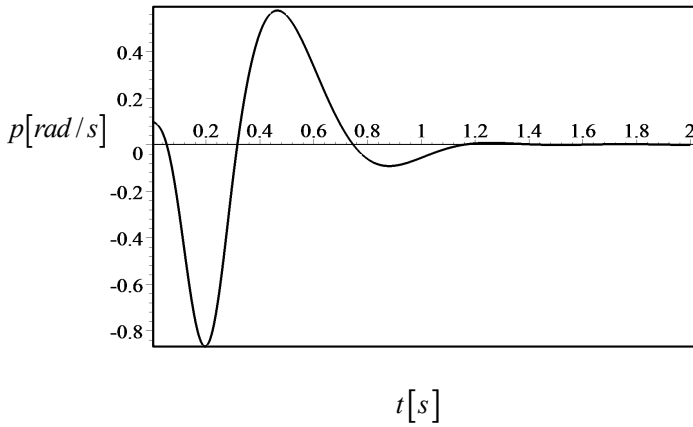


FIGURE 11.22. Roll rate response for the steering function (11.282).
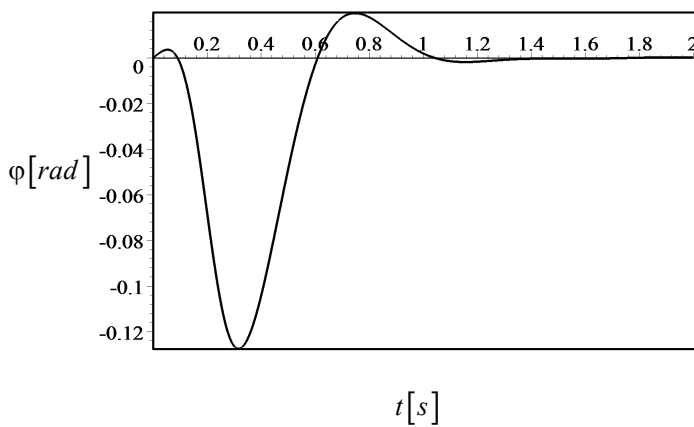
FIGURE 11.23. Roll angle response for the steering function (11.282).
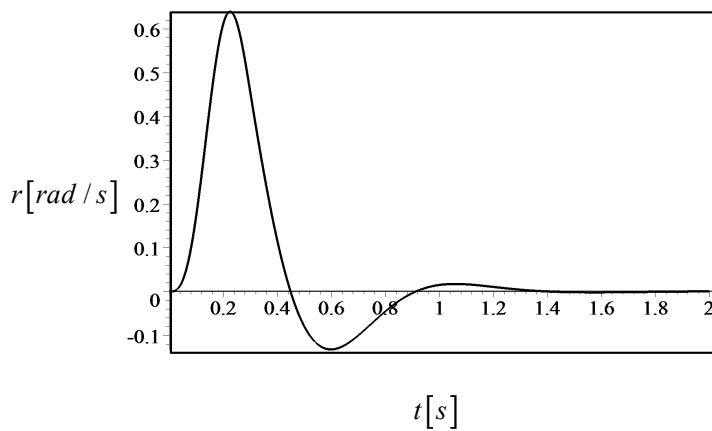


FIGURE 11.24. Yaw rate response for the steering function (11.282).

**Example 421 ★** *Vehicle driving and classical feedback control.*

Driving a car is a problem in feedback control. The driver compares desired direction, speed, and acceleration with actual direction, speed, and acceleration. The driver uses the cars's indicator and measuring devices, as well as human sensors to sense actual direction, speed, and acceleration. When the actual data differs from the desired values, the driver uses the control devices such as gas pedal, brake, steering, and gear selection to improve the actual.

**Example 422 ★** *Hatchback, notchback, and station models of a platform.*

It is common in vehicle manufacturing companies to install different bodies on the same chassis and platform to make different models easier. Consider a hatchback, notchback, and station models of a car that use the same platform. To compare the dynamic behavior of the three models, we may examine their response to a step input.

The common characteristics of the cars are

$$C_{\alpha f_L} = C_{\alpha f_R} \approx 26000 \, \text{N}/\,\text{rad} \tag{11.284}$$
$$C_{\alpha r_L} = C_{\alpha r_R} \approx 32000 \, \text{N}/\,\text{rad} \tag{11.285}$$

$$
\begin{aligned}
l &= 2.345 \, \text{m} \\
C_{\beta_f} &= -0.4 \\
C_{\beta_r} &= -0.1 \\
C_{T_f} &= -0.4 \\
C_{T_r} &= -0.4 \\
C_{\delta\varphi_f} &= 0.01 \\
C_{\delta\varphi_r} &= 0.01 \\
C_{\varphi_f} &= -3200 \\
C_{\varphi_r} &= 0 \\
k_\varphi &= 26612 \, \text{N}/\,\text{rad} \\
c_\varphi &= 1700 \, \text{N}\,\text{s}/\,\text{rad}.
\end{aligned}
\tag{11.286}
$$

For the hatchback, we use

$$
\begin{aligned}
m &= 838.7 \, \text{kg} \\
I_x &= 300 \, \text{kg}\,\text{m}^2 \\
I_z &= 1391 \, \text{kg}\,\text{m}^2 \\
a_1 &= 0.859 \, \text{m} \\
a_2 &= 1.486 \, \text{m}
\end{aligned}
\tag{11.287}
$$
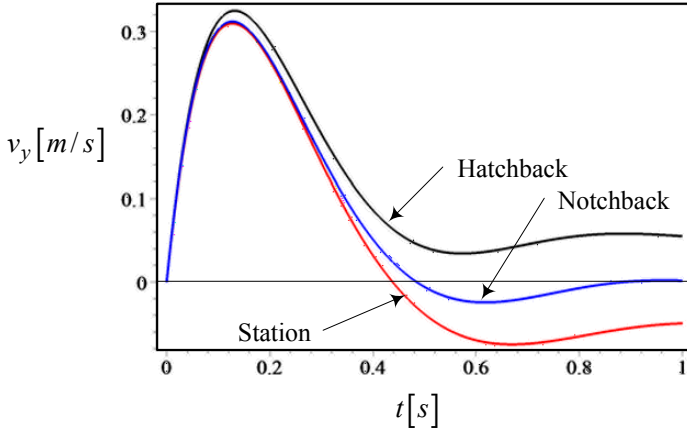
FIGURE 11.25. Lateral velocity response for hatchback, notchback, and station models of a car to a step steer angle.

*and for the notchback we have*

$$
\begin{aligned}
m &= 845.4\,\text{kg} \\
I_x &= 350\,\text{kg}\,\text{m}^2 \\
I_z &= 1490\,\text{kg}\,\text{m}^2 \\
a_1 &= 0.909\,\text{m} \\
a_2 &= 1.436\,\text{m}
\end{aligned}
\tag{11.288}
$$

*and finally for the station model we use the following data.*

$$
\begin{aligned}
m &= 859\,\text{kg} \\
I_x &= 400\,\text{kg}\,\text{m}^2 \\
I_z &= 1680\,\text{kg}\,\text{m}^2 \\
a_1 &= 0.945\,\text{m} \\
a_2 &= 1.4\,\text{m}
\end{aligned}
\tag{11.289}
$$

*Assume the cars are moving at*

$$
v_x = 16.6\,\text{m/s}
\tag{11.290}
$$

*and the step input of the steer angle is*

$$
\delta = 0.1\,\text{rad.}
\tag{11.291}
$$

   *Figure 11.25 compares the lateral velocity responses of the three models. It shows that the steady-state lateral velocity of the station model is a negative, while the hatchback's is a positive. When the lateral velocity is zero, the*
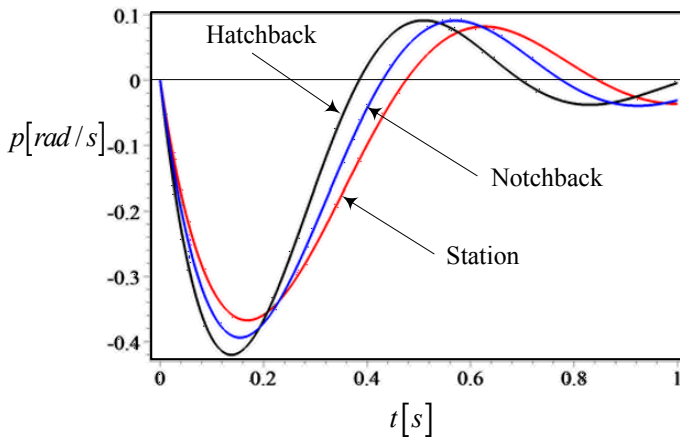
FIGURE 11.26. Roll rate response for hatchback, notchback, and station models of a car to a step steer angle.
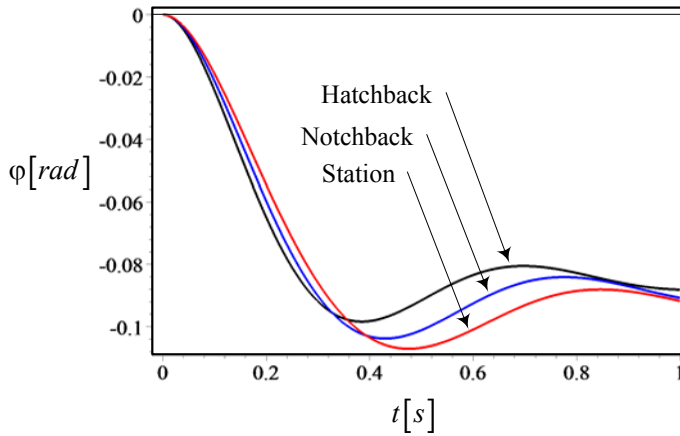


FIGURE 11.27. Roll angle response for hatchback, notchback, and station models of a car to a step steer angle.
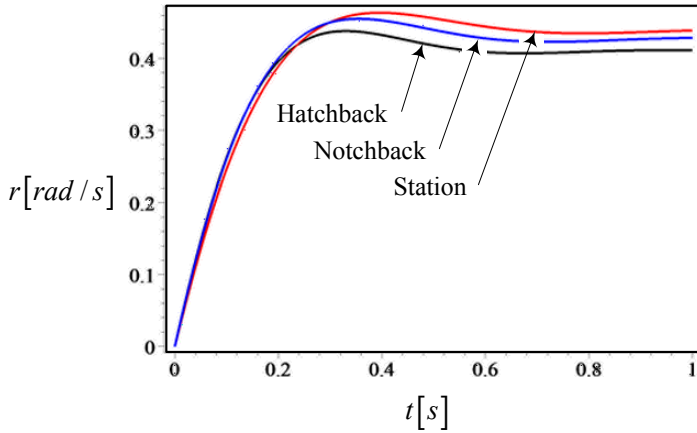
FIGURE 11.28. Yaw rate response for hatchback, notchback, and station models of a car to a step steer angle.

*velocity vector of the car,* **v**, *is perpendicular to the turning radius $R$ at $C$. A positive $v_y$ indicates that $R$ is perpendicular to a point behind $C$, and a negative $v_y$ indicates that $R$ is perpendicular to a point in front of $C$.*

*Figure 11.26 compares the roll rate responses of the three models. The hatchback model has the least longitudinal moment of inertia and hence shows the fastest roll rate response. It will also reach to the zero steady-state value faster than the other models.*

*Figure 11.27 compares the roll angle responses of the three models. The station model has the largest roll angle because of the highest longitudinal moment of inertia. It will also reach to the steady-state roll angle later than the other models.*

*Figure 11.28 compares the yaw rate responses of the three models. The station model has the highest yaw rate because of the highest vertical moment of inertia. It will also reach to the steady-state yaw rate later than the other models.*

## 11.7  Summary

The most applied dynamic model for vehicle motion shows the yaw and roll DOF as well as the $x$ and $y$ motions. Such a model is called the rigid vehicle roll model and can be expressed by the following *five* differential

equations.

$$\dot{v}_x \;=\; \frac{1}{m}F_x + r\,v_y$$

$$
\begin{bmatrix} \dot{v}_y \\ \dot{p} \\ \dot{\varphi} \\ \dot{r} \end{bmatrix}
=
\begin{bmatrix}
\dfrac{C_\beta}{mv_x} & \dfrac{C_p}{m} & \dfrac{C_\varphi}{m} & \dfrac{C_r}{m} - v_x \\[2mm]
\dfrac{E_\beta}{I_x v_x} & \dfrac{E_p}{I_x} & \dfrac{E_\varphi}{I_x} & \dfrac{E_r}{I_x} \\[2mm]
0 & 1 & 0 & 0 \\[2mm]
\dfrac{D_\beta}{I_z v_x} & \dfrac{D_p}{I_z} & \dfrac{D_\varphi}{I_z} & \dfrac{D_r}{I_z}
\end{bmatrix}
\begin{bmatrix} v_y \\ p \\ \varphi \\ r \end{bmatrix}
+
\begin{bmatrix}
\dfrac{C_\delta}{m} \\[2mm]
\dfrac{E_\delta}{I_x} \\[2mm]
0 \\[2mm]
\dfrac{D_\delta}{I_z}
\end{bmatrix}
\delta
$$

The vehicle receives the steering angle $\delta$ as an input to generate *five* outputs $v_x$, $v_y$, $p$, $\varphi$, and $r$. However, keeping the forward speed constant, $v_x = cte$, and using it as a parameter, can uncouple the first equation the others. So, a constant forward speed is used in many of the vehicle dynamic examinations of vehicles.

## 11.8   Key Symbols

| | |
|---|---|
| $a, \ddot{x}, \mathbf{a}, \dot{\mathbf{v}}$ | acceleration |
| $a_{fwd}$ | front wheel drive acceleration |
| $a_{rwd}$ | rear wheel drive acceleration |
| $a_1 = x_1$ | distance of first axle from mass center |
| $a_2 = -x_2$ | distance of second axle from mass center |
| $A, B, C$ | constant parameters |
| $[A]$ | control variable coefficient matrix |
| $b_1$ | distance of left wheels from mass center |
| $b_2$ | distance of right wheels from mass center |
| $c$ | damping |
| $c_f$ | damping of front suspension |
| $c_r$ | damping of rear suspension |
| $c_\varphi = dM_{x_k}/d\dot{\varphi}$ | vehicle roll damping |
| $C$ | mass center of vehicle |
| $C_{\alpha_i} = dF_y/d\alpha_i$ | tire sideslip coefficient |
| $C_{\beta_i} = v_x \, d\beta_i/dp$ | tire roll rate coefficient |
| $C_{\delta_{\varphi_i}} = d\delta/d\varphi_i$ | tire roll steering coefficient |
| $C_{\varphi_i} = dF_y/d\varphi_i$ | tire camber trust coefficient |
| $C_{T_i} = dM_x/dF_y$ | tire torque coefficient |
| $C_r = \partial F_y/\partial r$ | vehicle yaw-rate lateral-force coefficient |
| $C_p = \partial F_y/\partial p$ | vehicle roll-rate lateral-force coefficient |
| $C_\beta = \partial F_y/\partial\beta$ | vehicle slip-angle lateral-force coefficient |
| $C_\varphi = \partial F_y/\partial\varphi$ | vehicle yaw-angle lateral-force coefficient |
| $C_\delta = \partial F_y/\partial\delta$ | vehicle steer-angle lateral-force coefficient |
| $D_r = \partial M_z/\partial r$ | vehicle yaw-rate yaw-moment coefficient |
| $D_p = \partial M_z/\partial p$ | vehicle roll-rate yaw-moment coefficient |
| $D_\beta = \partial M_z/\partial\beta$ | vehicle slip-angle yaw-moment coefficient |
| $D_\varphi = \partial M_z/\partial\varphi$ | vehicle yaw-angle yaw-moment coefficient |
| $D_\delta = \partial M_z/\partial\delta$ | vehicle steer-angle yaw-moment coefficient |
| $E_r = \partial M_x/\partial r$ | vehicle yaw-rate roll-moment coefficient |
| $E_p = \partial M_x/\partial p$ | vehicle roll-rate roll-moment coefficient |
| $E_\beta = \partial M_x/\partial\beta$ | vehicle slip-angle roll-moment coefficient |
| $E_\varphi = \partial M_x/\partial\varphi$ | vehicle yaw-angle roll-moment coefficient |
| $E_\delta = \partial M_x/\partial\delta$ | vehicle steer-angle roll-moment coefficient |
| $F, \mathbf{F}$ | force |
| $F_x$ | traction or brake force under a wheel |
| $F_{x_1}$ | traction or brake force under front wheels |
| $F_{x_2}$ | traction or brake force under rear wheels |
| $F_{x_t}$ | horizontal force at hinge |
| $F_z$ | normal force under a wheel |
| $F_{z_1}$ | normal force under front wheels |
| $F_{z_2}$ | normal force under rear wheels |
| $F_{z_3}$ | normal force under trailer wheels |

| $F_{z_t}$ | normal force at hinge |
| $g$, $\mathbf{g}$ | gravitational acceleration |
| $h$ | height of $C$ |
| $H$ | height |
| $I$ | mass moment of inertia |
| $I_1, I_2, I_3$ | principal mass moment of inertia |
| $k$ | stiffness |
| $k_f$ | stiffness of front suspension |
| $k_r$ | stiffness of rear suspension |
| $k_\varphi = dM_{x_k}/d\varphi$ | vehicle roll stiffness |
| $l$ | wheel base |
| $L$ | road wave length |
| $\mathbf{L}$ | angular momentum |
| $m$ | car mass |
| $M, \mathbf{M}$ | moment |
| $p = \dot{\varphi}$ | roll rate |
| $\mathbf{p}$ | translational momentum |
| $q = \dot{\theta}$ | pitch rate |
| $\mathbf{q}$ | control variable vector |
| $\mathbf{q}_0$ | initial condition vector |
| $\mathbf{u}$ | control input vector |
| $r = \dot{\psi}$ | yaw rate |
| $\mathbf{r}$ | position vector |
| $R$ | tire radius |
| $R$ | rotation matrix |
| $R_f$ | front tire radius |
| $R_H$ | radius of curvature |
| $R_r$ | rear tire radius |
| $S_a = v_x^2/R/\delta$ | lateral acceleration response |
| $S_r = r/\delta$ | yaw rate response |
| $S_\beta = \beta/\delta$ | sideslip response |
| $S_\kappa = \kappa/\delta$ | curvature response |
| $S_\varphi = \varphi/\delta$ | roll angle response |
| $t$ | time |
| $v, \dot{x}, \mathbf{v}$ | velocity |
| $v_c$ | critical velocity |
| $v_x$ | forward velocity |
| $v_c$ | lateral velocity |
| $w$ | track |
| $z_i$ | deflection of axil number $i$ |
| $x, y, z$ | vehicle coordinate axes |
| $x_i, y_i, z_i$ | coordinates of wheel number $i$ in $B$ |
| $x_w, y_w, z_w$ | axes of a wheel coordinate frame |
| $X, Y, Z$ | global coordinate axes |
| $Z_0, Z_1, Z_2, Z_3$ | steady-state response parameters |

| | |
|---|---|
| $\alpha$ | tire sideslip angle between $\mathbf{v}_w$ and $x_w$-axis |
| $\beta = v_y/v_x$ | vehicle slip angle between $\mathbf{v}$ and $x$-axis |
| $\beta_f$ | front tire slip angle |
| $\beta_i$ | tire slip angle between $\mathbf{v}$ and $x$-axis |
| $\beta_r$ | rear tire slip angle |
| $\delta$ | vehicle steer angle |
| $\delta_0$ | a constant steer angle value |
| $\delta_w$ | tire steer angle between $x_w$-axis and $x$-axis |
| $\delta_1, \delta_f$ | steer angle of front wheels |
| $\delta_2, \delta_r$ | steer angle of rear wheels |
| $\delta_a$ | actual steer angle |
| $\delta_\varphi$ | roll-steer angle |
| $\eta$ | $atan2\,(a, b)$ |
| $\theta$ | pitch angle |
| $\kappa = 1/R$ | path curvature |
| $\lambda$ | eigenvalue |
| $\mu$ | friction coefficient |
| $\phi$ | slope angle |
| $\phi_M$ | maximum slope angle |
| $\varphi$ | roll angle |
| $\psi$ | yaw angle |
| $\omega$ | angular frequency |
| $\omega, \boldsymbol{\omega}$ | angular velocity |
| $\dot{\omega}, \dot{\boldsymbol{\omega}}$ | angular acceleration |

Subscriptions

| | |
|---|---|
| $dyn$ | dynamic |
| $f$ | front |
| $fwd$ | front-wheel-drive |
| $i$ | wheel number |
| $L$ | left |
| $M$ | maximum |
| $r$ | rear |
| $R$ | right |
| $rwd$ | rear-wheel-drive |
| $st$ | statics |
| $w$ | wheel |

## Exercises

1. ★ Force system coefficients.

   Consider a front-wheel-steering car with the following characteristics and determine the force system coefficients $C_r$, $C_p$, $C_\beta$, $C_\varphi$, $C_\delta$, $E_r$, $E_p$, $E_\beta$, $E_\varphi$, $E_\delta$, $D_r$, $D_p$, $D_\beta$, $D_\varphi$, and $D_\delta$.

$$
\begin{aligned}
C_{\alpha f_L} &= C_{\alpha f_R} = 600\,\text{N}/\deg \\
C_{\alpha r_L} &= C_{\alpha r_R} = 560\,\text{N}/\deg \\
m &= 1245\,\text{kg} \\
I_x &= 300\,\text{kg}\,\text{m}^2 \\
I_z &= 1328\,\text{kg}\,\text{m}^2 \\
a_1 &= 110\,\text{cm} \\
a_2 &= 132\,\text{cm} \\
k_\varphi &= 26612\,\text{N}/\text{rad} \\
c_\varphi &= 1700\,\text{N}\,\text{s}/\text{rad} \\
v_x &= 30\,\text{m}/\text{s}
\end{aligned}
$$

$$
\begin{aligned}
C_{\beta_f} &= -0.4 \\
C_{\beta_r} &= -0.1 \\
C_{T_f} &= -0.4 \\
C_{T_r} &= -0.2 \\
C_{\delta\varphi_f} &= 0.01 \\
C_{\delta\varphi_r} &= 0.01 \\
C_{\varphi_f} &= -3200 \\
C_{\varphi_r} &= -300
\end{aligned}
$$

2. ★ Force system and two-wheel model of a car.

   Consider a front-wheel-steering car with the following characteristics

$$
\begin{aligned}
C_{\alpha r_L} &= C_{\alpha r_R} = C_{\alpha f_L} = C_{\alpha f_R} = 500\,\text{N}/\deg \\
a_1 &= 110\,\text{cm} \\
a_2 &= 132\,\text{cm} \\
m &= 1205\,\text{kg}
\end{aligned}
$$

$$
\begin{aligned}
I_x &= 300\,\text{kg}\,\text{m}^2 \\
I_z &= 1328\,\text{kg}\,\text{m}^2
\end{aligned}
$$

$$k_\varphi \quad = \quad 26612\,\mathrm{N/rad}$$
$$c_\varphi \quad = \quad 1700\,\mathrm{N\,s/rad}$$
$$v_x \quad = \quad 30\,\mathrm{m/s}$$

$$C_{\beta_f} \quad = \quad -0.4$$
$$C_{\beta_r} \quad = \quad -0.1$$
$$C_{T_f} \quad = \quad -0.4$$
$$C_{T_r} \quad = \quad -0.2$$

$$C_{\delta\varphi_f} \quad = \quad 0.01$$
$$C_{\delta\varphi_r} \quad = \quad 0.01$$
$$C_{\varphi_f} \quad = \quad -3200$$
$$C_{\varphi_r} \quad = \quad -300$$

and determine the force system that applies on the two-wheel model of the car.

$$F_y \quad = \quad C_r\,r + C_p\,p + C_\beta\,\beta + C_\varphi\,\varphi + C_\delta\,\delta$$
$$M_x \quad = \quad E_r\,r + E_p\,p + E_\beta\,\beta + E_\varphi\,\varphi + E_\delta\,\delta$$
$$M_z \quad = \quad D_r\,r + D_p\,p + D_\beta\,\beta + D_\varphi\,\varphi + D_\delta\,\delta$$

Then, write the equations of motion of the car as

$$F_x \quad = \quad m\,\dot{v}_x - mr\,v_y$$
$$F_y \quad = \quad m\,\dot{v}_y + mr\,v_x$$
$$M_z \quad = \quad I_z\dot{r}$$
$$M_x \quad = \quad I_x\dot{p}.$$

3. ★ Equations of motion for a front-wheel-steering car.

Consider a front-wheel-steering car with the following characteristics

$$C_{\alpha r_L} = C_{\alpha r_R} = C_{\alpha f_L} = C_{\alpha f_R} = 500\,\mathrm{N/deg}$$

$$a_1 \quad = \quad 110\,\mathrm{cm}$$
$$a_2 \quad = \quad 132\,\mathrm{cm}$$
$$m \quad = \quad 1245\,\mathrm{kg}$$
$$I_z \quad = \quad 1328\,\mathrm{kg\,m}^2$$
$$v_x \quad = \quad 40\,\mathrm{m/s}$$

$$I_x = 300 \,\mathrm{kg\,m^2}$$
$$k_\varphi = 26612 \,\mathrm{N/\,rad}$$
$$c_\varphi = 1700 \,\mathrm{N\,s/\,rad}$$

$$C_{\beta_f} = -0.4$$
$$C_{\beta_r} = -0.1$$
$$C_{T_f} = -0.4$$
$$C_{T_r} = -0.2$$

$$C_{\delta\varphi_f} = 0.01$$
$$C_{\delta\varphi_r} = 0.01$$
$$C_{\varphi_f} = -3200$$
$$C_{\varphi_r} = -300$$

and develop the equations of motion

$$\dot{\mathbf{q}} = [A]\,\mathbf{q} + \mathbf{u}.$$

4. ★ Equations of motion in different variables.

Consider a car with the following characteristics

$$C_{\alpha r_L} = C_{\alpha r_R} = C_{\alpha f_L} = C_{\alpha f_R} = 500 \,\mathrm{N/\,deg}$$
$$a_1 = 100 \,\mathrm{cm}$$
$$a_2 = 120 \,\mathrm{cm}$$
$$m = 1000 \,\mathrm{kg}$$
$$I_z = 1008 \,\mathrm{kg\,m^2}$$
$$v_x = 40 \,\mathrm{m/\,s}$$

$$I_x = 300 \,\mathrm{kg\,m^2}$$
$$k_\varphi = 26612 \,\mathrm{N/\,rad}$$
$$c_\varphi = 1700 \,\mathrm{N\,s/\,rad}$$

$$C_{\beta_f} = -0.4$$
$$C_{\beta_r} = -0.1$$
$$C_{T_f} = -0.4$$
$$C_{T_r} = -0.2$$

$$C_{\delta\varphi_f} = 0.01$$
$$C_{\delta\varphi_r} = 0.01$$
$$C_{\varphi_f} = -3200$$
$$C_{\varphi_r} = -300$$

and develop the equations of motion

(a) in terms of $(\dot{v}_x, \dot{v}_y, \dot{p}, \dot{\varphi}, \dot{r})$, if the car is front-wheel steering.

(b) in terms of $\left(\dot{v}_x, \dot{\beta}, \dot{p}, \dot{\varphi}, \dot{r}\right)$, if the car is front-wheel steering.

5. ★ Steady state response parameters.

Consider a car with the following characteristics

$$
\begin{aligned}
C_{\alpha f_L} &= C_{\alpha f_R} = 500\,\text{N}/\deg \\
C_{\alpha r_L} &= C_{\alpha r_R} = 520\,\text{N}/\deg
\end{aligned}
$$

$$
\begin{aligned}
m &= 1245\,\text{kg} \\
I_z &= 1328\,\text{kg}\,\text{m}^2 \\
a_1 &= 110\,\text{cm} \\
a_2 &= 132\,\text{cm} \\
v_x &= 40\,\text{m}/\text{s}
\end{aligned}
$$

$$
\begin{aligned}
I_x &= 300\,\text{kg}\,\text{m}^2 \\
k_\varphi &= 26612\,\text{N}/\text{rad} \\
c_\varphi &= 1700\,\text{N}\,\text{s}/\text{rad}
\end{aligned}
$$

$$
\begin{aligned}
C_{\beta_f} &= -0.4 \\
C_{\beta_r} &= -0.1 \\
C_{T_f} &= -0.4 \\
C_{T_r} &= -0.2
\end{aligned}
$$

$$
\begin{aligned}
C_{\delta\varphi_f} &= 0.01 \\
C_{\delta\varphi_r} &= 0.01 \\
C_{\varphi_f} &= -3200 \\
C_{\varphi_r} &= -300
\end{aligned}
$$

and determine the steady-state curvature response $S_\kappa$, sideslip response $S_\beta$, yaw rate response, $S_r$, roll angle response, $S_\varphi$, and lateral acceleration response $S_a$.

6. ★ Steady state motion parameters.

Consider a car with the following characteristics

$$
\begin{aligned}
C_{\alpha f_L} &= C_{\alpha f_R} = 600\,\text{N}/\deg \\
C_{\alpha r_L} &= C_{\alpha r_R} = 550\,\text{N}/\deg
\end{aligned}
$$

$$m = 1245\,\mathrm{kg}$$
$$I_z = 1128\,\mathrm{kg\,m^2}$$

$$a_1 = 120\,\mathrm{cm}$$
$$a_2 = 138\,\mathrm{cm}$$
$$v_x = 20\,\mathrm{m/s}$$
$$\delta = 3\,\mathrm{deg}$$

$$I_x = 300\,\mathrm{kg\,m^2}$$
$$k_\varphi = 26612\,\mathrm{N/rad}$$
$$c_\varphi = 1700\,\mathrm{N\,s/rad}$$

$$C_{\beta_f} = -0.4$$
$$C_{\beta_r} = -0.1$$
$$C_{T_f} = -0.4$$
$$C_{T_r} = -0.2$$

$$C_{\delta\varphi_f} = 0.01$$
$$C_{\delta\varphi_r} = 0.01$$
$$C_{\varphi_f} = -3200$$
$$C_{\varphi_r} = -300$$

and determine the steady state values of $r$, $R$, $\beta$, $\varphi$, and $v_x^2/R$.

7. ★ Inertia and steady state parameters.

Consider a car that is made up of a uniform solid box with dimensions $260\,\mathrm{cm} \times 140\,\mathrm{cm} \times 40\,\mathrm{cm}$. If the density of the box is $\rho = 1000\,\mathrm{kg/m^3}$, and the other characteristics are

$$C_{\alpha f_L} = C_{\alpha f_R} = 600\,\mathrm{N/deg}$$
$$C_{\alpha r_L} = C_{\alpha r_R} = 550\,\mathrm{N/deg}$$
$$a_1 = a_2 = \frac{l}{2}$$

$$k_\varphi = 26612\,\mathrm{N/rad}$$
$$c_\varphi = 1700\,\mathrm{N\,s/rad}$$

$$C_{\beta_f} = -0.4$$
$$C_{\beta_r} = -0.1$$
$$C_{T_f} = -0.4$$
$$C_{T_r} = -0.2$$

$$C_{\delta\varphi_f} = 0.01$$
$$C_{\delta\varphi_r} = 0.01$$
$$C_{\varphi_f} = -3200$$
$$C_{\varphi_r} = -300$$

then,

(a) determine $m$, $I_z$.

(b) determine the steady-state responses $S_\kappa$, $S_\beta$, $S_r$, and $S_a$ as functions of $v_x$.

(c) determine the velocity $v_x$ at which the car has a radius of turning equal to
$$R = 35\,\text{m}$$
when
$$\delta = 4\,\text{deg}\,.$$

(d) determine the steady state parameters $r$, $R$, $\beta$, $\varphi$, and $v_x^2/R$ at that speed.

(e) set the speed of the car at
$$v_x = 20\,\text{m/s}$$
and plot the steady-state responses $S_\kappa$, $S_\beta$, $S_r$, and $S_a$ for variable $\rho$.

8. ★ Stability factor and understeer behavior.

Define a stability factor $K$ for the vehicle roll model.

9. ★ Stability factor and mass of the car.

Find $a_1$ and $a_2$ in terms of $F_{z_1}$, $F_{z_2}$, and $mg$ to rewrite the stability factor $K$ to see the effect of a car's mass distribution.

10. ★ Stability factor and car behavior.

Examine the stability factor of a car with the parameters

$$C_{\alpha f_L} = C_{\alpha f_R} = 500\,\text{N/deg}$$
$$C_{\alpha r_L} = C_{\alpha r_R} = 460\,\text{N/deg}$$

$$m = 1245\,\text{kg}$$
$$I_z = 1328\,\text{kg\,m}^2$$
$$a_1 = 110\,\text{cm}$$
$$a_2 = 132\,\text{cm}$$
$$v_x = 30\,\text{m/s}$$

$$I_x = 300 \,\mathrm{kg\,m^2}$$
$$k_\varphi = 26612 \,\mathrm{N/rad}$$
$$c_\varphi = 1700 \,\mathrm{N\,s/rad}$$

$$C_{\beta_f} = -0.4$$
$$C_{\beta_r} = -0.1$$
$$C_{T_f} = -0.4$$
$$C_{T_r} = -0.2$$

$$C_{\delta\varphi_f} = 0.01$$
$$C_{\delta\varphi_r} = 0.01$$
$$C_{\varphi_f} = -3200$$
$$C_{\varphi_r} = -300$$

and determine if the car is understeer, neutral, or oversteer?

11. ★ Critical speed of a car.

Consider a car with the characteristics

$$C_{\alpha f_L} = C_{\alpha f_R} = 700 \,\mathrm{N/deg}$$
$$C_{\alpha r_L} = C_{\alpha r_R} = 520 \,\mathrm{N/deg}$$

$$m = 1245 \,\mathrm{kg}$$
$$I_z = 1328 \,\mathrm{kg\,m^2}$$
$$a_1 = 118 \,\mathrm{cm}$$
$$a_2 = 122 \,\mathrm{cm.}$$

$$I_x = 300 \,\mathrm{kg\,m^2}$$
$$k_\varphi = 26612 \,\mathrm{N/rad}$$
$$c_\varphi = 1700 \,\mathrm{N\,s/rad}$$

$$C_{\beta_f} = -0.4$$
$$C_{\beta_r} = -0.1$$
$$C_{T_f} = -0.4$$
$$C_{T_r} = -0.2$$

$$C_{\delta\varphi_f} = 0.01$$
$$C_{\delta\varphi_r} = 0.01$$
$$C_{\varphi_f} = -3200$$
$$C_{\varphi_r} = -300$$

(a) Define a critical speed for oversteer condition.

(b) Determine if the car is understeer, neutral, or oversteer?

12. ★ Step input response at different speed.

Consider a car with the characteristics

$$
\begin{aligned}
C_{\alpha f_L} &= C_{\alpha f_R} = 600 \, \text{N}/ \text{deg} \\
C_{\alpha r_L} &= C_{\alpha r_R} = 750 \, \text{N}/ \text{deg}
\end{aligned}
$$

$$
\begin{aligned}
m &= 1245 \, \text{kg} \\
I_z &= 1328 \, \text{kg m}^2 \\
a_1 &= 110 \, \text{cm} \\
a_2 &= 132 \, \text{cm}
\end{aligned}
$$

$$
\begin{aligned}
I_x &= 300 \, \text{kg m}^2 \\
k_\varphi &= 26612 \, \text{N}/ \text{rad} \\
c_\varphi &= 1700 \, \text{N s}/ \text{rad}
\end{aligned}
$$

$$
\begin{aligned}
C_{\beta_f} &= -0.4 \\
C_{\beta_r} &= -0.1 \\
C_{T_f} &= -0.4 \\
C_{T_r} &= -0.2
\end{aligned}
$$

$$
\begin{aligned}
C_{\delta\varphi_f} &= 0.01 \\
C_{\delta\varphi_r} &= 0.01 \\
C_{\varphi_f} &= -3200 \\
C_{\varphi_r} &= -300
\end{aligned}
$$

and a step input

$$
\delta(t) = \begin{cases} 5 \, \text{deg} & t > 0 \\ 0 & t \leq 0 \end{cases}.
$$

Determine the time response of the car at

(a) $v_x = 10 \, \text{m}/ \text{s}$.

(b) $v_x = 20 \, \text{m}/ \text{s}$.

(c) $v_x = 30 \, \text{m}/ \text{s}$.

(d) $v_x = 40 \, \text{m}/ \text{s}$.

13. ★ Step input response for different steer angle.

Consider a car with the characteristics

$$
\begin{aligned}
C_{\alpha f_L} &= C_{\alpha f_R} = 600\,\text{N/deg} \\
C_{\alpha r_L} &= C_{\alpha r_R} = 750\,\text{N/deg} \\
m &= 1245\,\text{kg} \\
I_z &= 1328\,\text{kg}\,\text{m}^2 \\
a_1 &= 110\,\text{cm} \\
a_2 &= 132\,\text{cm} \\
v_x &= 20\,\text{m/s} \\
I_x &= 300\,\text{kg}\,\text{m}^2 \\
k_\varphi &= 26612\,\text{N/rad} \\
c_\varphi &= 1700\,\text{N}\,\text{s/rad} \\
C_{\beta_f} &= -0.4 \\
C_{\beta_r} &= -0.1 \\
C_{T_f} &= -0.4 \\
C_{T_r} &= -0.2 \\
C_{\delta\varphi_f} &= 0.01 \\
C_{\delta\varphi_r} &= 0.01 \\
C_{\varphi_f} &= -3200 \\
C_{\varphi_r} &= -300
\end{aligned}
$$

Determine the time response of the car to a step input

$$
\delta\left(t\right) = \begin{cases} \delta & t > 0 \\ 0 & t \le 0 \end{cases}
$$

when

(a) $\delta = 3\,\text{deg}$.

(b) $\delta = 5\,\text{deg}$.

(c) $\delta = 10\,\text{deg}$.

14. ★ Eigenvalues and free response.

Consider a car with the characteristics

$$
\begin{aligned}
C_{\alpha f_L} &= C_{\alpha f_R} = 600\,\text{N/deg} \\
C_{\alpha r_L} &= C_{\alpha r_R} = 750\,\text{N/deg}
\end{aligned}
$$

$$
\begin{aligned}
m &= 1245\,\mathrm{kg} \\
I_z &= 1328\,\mathrm{kg\,m^2} \\
a_1 &= 110\,\mathrm{cm} \\
a_2 &= 132\,\mathrm{cm} \\
v_x &= 20\,\mathrm{m/s.}
\end{aligned}
$$

$$
\begin{aligned}
I_x &= 300\,\mathrm{kg\,m^2} \\
k_\varphi &= 26612\,\mathrm{N/rad} \\
c_\varphi &= 1700\,\mathrm{N\,s/rad}
\end{aligned}
$$

$$
\begin{aligned}
C_{\beta_f} &= -0.4 \\
C_{\beta_r} &= -0.1 \\
C_{T_f} &= -0.4 \\
C_{T_r} &= -0.2
\end{aligned}
$$

$$
\begin{aligned}
C_{\delta\varphi_f} &= 0.01 \\
C_{\delta\varphi_r} &= 0.01 \\
C_{\varphi_f} &= -3200 \\
C_{\varphi_r} &= -300
\end{aligned}
$$

(a) Determine the eigenvalues of the coefficient matrix $[A]$ and find out if the car is stable at zero steer angle.

(b) In either case, determine the weight distribution ratio, $a_1/a_2$, such that the car is neutral stable.

(c) Recommend a condition for the weight distribution ratio, $a_1/a_2$, such that the car is stable.

15. ★ Time response to different steer functions.

Consider a car with the characteristics

$$
\begin{aligned}
C_{\alpha f_L} &= C_{\alpha f_R} = 600\,\mathrm{N/deg} \\
C_{\alpha r_L} &= C_{\alpha r_R} = 750\,\mathrm{N/deg}
\end{aligned}
$$

$$
\begin{aligned}
m &= 1245\,\mathrm{kg} \\
I_z &= 1328\,\mathrm{kg\,m^2} \\
a_1 &= 110\,\mathrm{cm} \\
a_2 &= 132\,\mathrm{cm} \\
v_x &= 20\,\mathrm{m/s}
\end{aligned}
$$

$$
\begin{aligned}
I_x &= 300\,\mathrm{kg\,m^2} \\
k_\varphi &= 26612\,\mathrm{N/rad} \\
c_\varphi &= 1700\,\mathrm{N\,s/rad}
\end{aligned}
$$

$$
\begin{aligned}
C_{\beta_f} &= -0.4 \\
C_{\beta_r} &= -0.1 \\
C_{T_f} &= -0.4 \\
C_{T_r} &= -0.2
\end{aligned}
$$

$$
\begin{aligned}
C_{\delta\varphi_f} &= 0.01 \\
C_{\delta\varphi_r} &= 0.01 \\
C_{\varphi_f} &= -3200 \\
C_{\varphi_r} &= -300
\end{aligned}
$$

and a step input

$$
\delta(t) = \begin{cases} 5\deg & t > 0 \\ 0 & t \le 0 \end{cases}.
$$

Determine the time response of the car to

(a) $\delta(t) = \sin 0.1t$ for $0 < t < 10\pi$ and $\delta(t) = 0$ for $t \le 0$ and $t \ge 10\pi$.

(b) $\delta(t) = \sin 0.5t$ for $0 < t < 2\pi$ and $\delta(t) = 0$ for $t \le 0$ and $t \ge 2\pi$.

(c) $\delta(t) = \sin t$ for $0 < t < \pi$ and $\delta(t) = 0$ for $t \le 0$ and $t \ge \pi$.

16. ★ Research exercise 1.

Consider a bicycle model of a car such that tires are always upright and remain perpendicular to the road surface. Develop the equations of motion for the roll model of the car.

17. ★ Research exercise 2.

Employ the tire frame $T$ at the tireprint, wheel frame $W$ at the wheel center, and wheel-body frame $C$ that is at the point corresponding to the wheel center at zero $\delta$ and zero $\gamma$, and remains parallel to the vehicle frame $B$. Develop the $W$, $C$, and $B$ expressions of the generated forces at the tireprint in $T$ frame, and develop a better set of equations for the roll model of a car.

18. ★ Research exercise 3.

Use the caster theory to find the associated camber angle $\gamma$ for a steer angle $\delta$, when the caster angle $\varphi$ and lean angle $\theta$ are given. Then provide a better set of equations for the roll model of vehicles.

# Part IV

# Vehicle Vibration

# 12

# Applied Vibrations

Vibration is an avoidable phenomena in vehicle dynamics. In this chapter, we review the principles of vibrations, analysis methods, and their applications, along with the frequency and time responses of systems. Special attention is devoted to frequency response analysis, because most of the optimization methods for vehicle suspensions and vehicle vibrating components are based on frequency responses.

## 12.1  Mechanical Vibration Elements

Mechanical vibrations is a result of continuous transformation of kinetic energy $K$ to potential energy $V$, back and forth. When the potential energy is at its maximum, the kinetic energy is zero and vice versa. Because a periodic fluctuations of kinetic energy appears as a periodic motion of a massive body, we call this energy transformation *mechanical vibrations*.



Mass                    Spring                    Damper
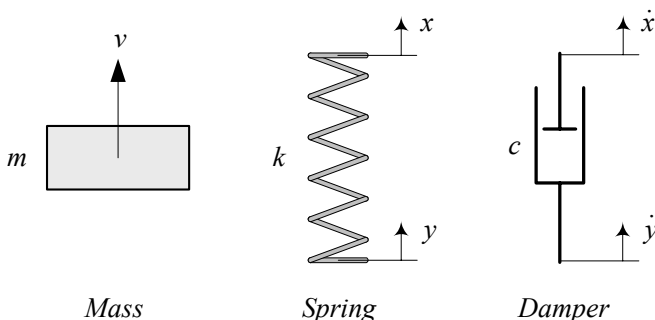
FIGURE 12.1. A mass $m$, spring $k$, and damper $c$.

The mechanical element that stores kinetic energy is called *mass*, and the mechanical element that stores potential energy, is called *spring*. If the total value of mechanical energy $E = K + V$ decreases during a vibration, there is a mechanical element that dissipates energy. The dissipative element is called . A mass, spring, and damper are illustrated as symbols in Figure 12.1.

The amount of stored kinetic energy in a mass $m$ is proportional to the square of its velocity, $v^2$. The velocity $v \equiv \dot{x}$ may be a function of position

and time.

$$K = \frac{1}{2}mv^2 \tag{12.1}$$

The required force $f_m$ to move a mass $m$ is proportional to its acceleration $a \equiv \ddot{x}$.

$$f_m = ma \tag{12.2}$$

A spring is characterized by its *stiffness* $k$. A force $f_k$ to generate a deflection in spring is proportional to relative displacement of its ends. The stiffness $k$ may be a function of position and time.

$$
\begin{aligned}
f_k &= -kz \\
&= -k(x-y) \tag{12.3}
\end{aligned}
$$

If $k$ is constant then, the value of stored potential energy in the spring is equal to the work done by the spring force $f_k$ during the spring deflection.

$$V = -\int f_k \, dz = -\int -kz \, dz \tag{12.4}$$

The spring potential energy is then a function of displacement. If the stiffness of a spring, $k$, is not a function of displacements, it is called *linear spring*. Then, its potential energy is

$$V = \frac{1}{2}kz^2. \tag{12.5}$$

Damping of a damper is measured by the value of mechanical energy loss in one cycle. Equivalently, a damper may be defined by the required force $f_c$ to generate a motion in the damper. If $f_c$ is proportional to the relative velocity of the its ends, it is a *linear damper* with a constant damping $c$.

$$
\begin{aligned}
f_c &= -c\dot{z} \\
&= -c(\dot{x}-\dot{y}) \tag{12.6}
\end{aligned}
$$

Such a damping is also called *viscous damping*.

A vibrating motion $x$ is characterized by *period* $T$, which is the required time for one complete cycle of vibration, starting from and ending at $(\dot{x}=0, \ddot{x}<0)$. *Frequency* $f$ is the number of cycles in one $T$.

$$f = \frac{1}{T} \tag{12.7}$$

In theoretical vibrations, we usually work with *angular frequency* $\omega\,[\mathrm{rad/\,s}]$, and in applied vibrations we use *cyclic frequency* $f\,[\mathrm{Hz}]$.

$$\omega = 2\pi f \tag{12.8}$$
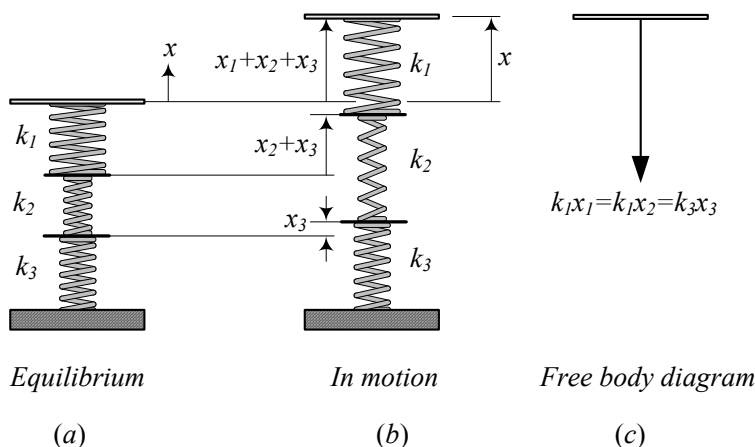
FIGURE 12.2. Three serial springs

When there is no applied external force or *excitation* on a vibrating system, any possible motion of the system is called *free vibration*. A free vibrating system will oscillate if any one of the kinematic states $x$, $\dot{x}$, or $\ddot{x}$ is not zero. If we apply any external force or excitation, a possible motion of the system is called *forced vibration*. There are four types of applied excitations: *harmonic*, *periodic*, *transient*, and *random*. The harmonic and transient excitations are more applied, and more predictable than the periodic and random types. When the excitation is a sinusoidal function of time, it is called *harmonic excitation* and when the excitation disappears after a while or stays steady, it is *transient excitation*. A *random excitation* has no short term pattern, however, we may define some long term averages to characterize a random excitation.

We use $f$ to indicate a harmonically-variable force with amplitude $F$, to be consistent with a harmonic motion $x$ with amplitude $X$. We also use $f$ for cyclic frequency, however, $f$ is a force unless it is indicated that it is a frequency.

**Example 423** *Serial springs and dampers.*

*Serial springs have the same force, and a resultant displacement equal to the sum of individual displacements. Figure 12.2 illustrates three serial springs attached to a massless plate and the ground.*

*The equilibrium position of the springs is the un-stretched configuration in Figure 12.2(a). Applying a displacement $x$ as shown in Figure 12.2(b) generates the free body diagram as shown in Figure 12.2(c). Each spring makes a force $f_i = -k_i x_i$ where $x_i$ is the length change in spring number $i$. The total displacement of the springs, $x$, is the sum of their individual*

displacements, $x = \sum x_i$.

$$x = x_1 + x_2 + x_3. \tag{12.9}$$

We may substitute a set of serial springs with only one equivalent spring, having a stiffness $k_{eq}$, that produces the same displacement $x$ under the same force $f_k$.

$$\begin{aligned} f_k &= -k_1 x_1 \\ &= -k_2 x_2 \\ &= -k_3 x_3 \\ &= -k_{eq} x \end{aligned} \tag{12.10}$$

Substituting (12.10) in (12.9)

$$\frac{f_s}{k_{eq}} = \frac{f_s}{k_1} + \frac{f_s}{k_2} + \frac{f_s}{k_3} \tag{12.11}$$

shows that the inverse of the equivalent stiffness of the serial springs, $1/k_{eq}$, is the sum of their inverse stiffness, $\sum 1/k_i$.

$$\frac{1}{k_{eq}} = \frac{1}{k_1} + \frac{1}{k_2} + \frac{1}{k_3} \tag{12.12}$$

We assume that velocity $\dot{x}$ has no effect on the force of a linear spring.

Serial dampers have the same force, $f_c$, and a resultant velocity $\dot{x}$ equal to the sum of individual velocities, $\sum \dot{x}_i$. We may substitute a set of serial dampers with only one equivalent damping $c_{eq}$ that produces the same velocity $\dot{x}$ under the same force $f_c$. For three parallel dampers, the velocity and force balance

$$\begin{aligned} \dot{x} &= \dot{x}_1 + \dot{x}_2 + \dot{x}_3 \tag{12.13} \\ f_c &= -c_1 \dot{x} \\ &= -c_2 \dot{x} \\ &= -c_3 \dot{x} \\ &= -c_{eq} \dot{x} \end{aligned} \tag{12.14}$$

show that the equivalent damping is

$$\frac{1}{c_{eq}} = \frac{1}{c_1} + \frac{1}{c_2} + \frac{1}{c_3}. \tag{12.15}$$

We assume that displacement $x$ has no effect on the force of a linear damper.
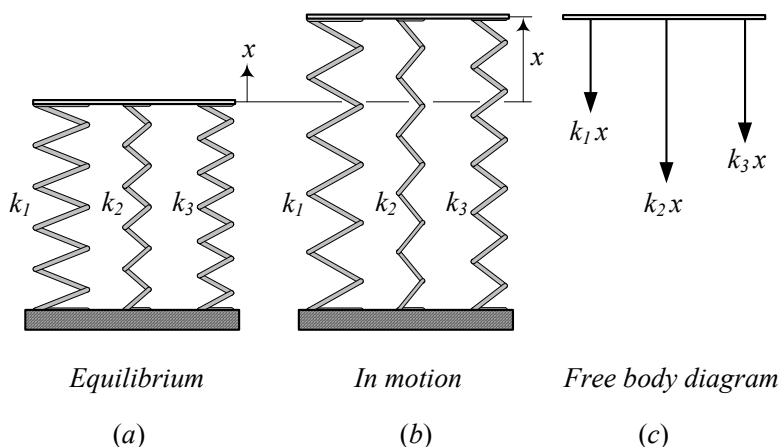
FIGURE 12.3. Three parallel springs.

**Example 424** *Parallel springs and dampers.*

*Parallel springs have the same displacement $x$, with a resultant force, $f_k$, equal to sum of the individual forces $\sum f_i$. Figure 12.3 illustrates three parallel springs between a massless plate and the ground.*

*The equilibrium position of the springs is the un-stretched configuration shown in Figure 12.3(a). Applying a displacement $x$ to all the springs in Figure 12.3(b) generates the free body diagram shown in Figure 12.3(c). Each spring makes a force $-kx$ opposite to the direction of displacement. The resultant force of the springs is*

$$f_k = -k_1 x - k_2 x - k_3 x. \tag{12.16}$$

*We may substitute parallel springs with only one equivalent stiffness $k_{eq}$ that produces the same force $f_k$ under the same displacement.*

$$f_k = -k_{eq} x \tag{12.17}$$

*Therefore, the equivalent stiffness of the parallel springs is sum of their stiffness.*

$$k_{eq} = k_1 + k_2 + k_3 \tag{12.18}$$

*Parallel dampers have the same speed $\dot{x}$, and a resultant force $f_c$ equal to the sum of individual forces. We may substitute parallel dampers with only one equivalent damping $c_{eq}$ that produces the same force $f_c$ under the same velocity. Consider three parallel dampers such as is shown in Figure 12.4. Their force balance and equivalent damping would be*

$$
\begin{aligned}
f_c &= -c_1\dot{x} - c_2\dot{x} - c_3\dot{x} & (12.19)\\
f_c &= -c_{eq}\dot{x} & (12.20)\\
c_{eq} &= c_1 + c_2 + c_3. & (12.21)
\end{aligned}
$$

Equilibrium          In motion          Free body diagram

(a)                (b)                (c)
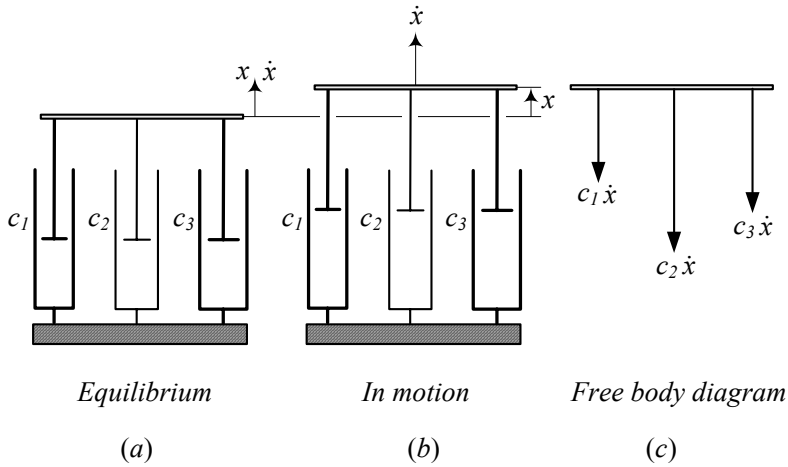
FIGURE 12.4. Three parallel dampers

**Example 425** *Flexible frame.*

Figure 12.5 depicts a mass m hanging from a frame. The frame is flexible, so it can be modeled by some springs attached to each other, as shown in Figure 12.6(a). If we assume that each beam is simply supported, then the equivalent stiffness for a lateral deflection of each beam at their midspan is

$$k_5 \quad = \quad \frac{48E_5I_5}{l_5^3} \tag{12.22}$$

$$k_4 \quad = \quad \frac{48E_4I_4}{l_4^3} \tag{12.23}$$

$$k_3 \quad = \quad \frac{48E_3I_3}{l_3^3}. \tag{12.24}$$

When the mass is vibrating, the elongation of each spring would be similar to Figure 12.6(b). Assume we separate the mass and springs, and then apply a force $f$ at the end of spring $k_1$ as shown in Figure 12.6(c). Because the springs $k_1$, $k_2$, and $k_3$ have the same force, and their resultant displacement is the sum of individual displacements, they are in series.

The springs $k_4$ and $k_5$ are neither in series nor parallel. To find their equivalent, let's assume that springs $k_4$ and $k_5$ support a force equal to $f/2$. Therefore,

$$\delta_4 = \frac{f}{2k_4} \tag{12.25}$$

$$\delta_5 = \frac{f}{2k_5} \tag{12.26}$$
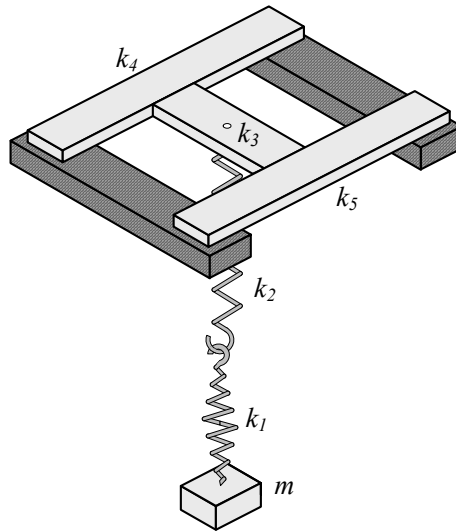
FIGURE 12.5. A mass $m$ hanging from a flexible frame.
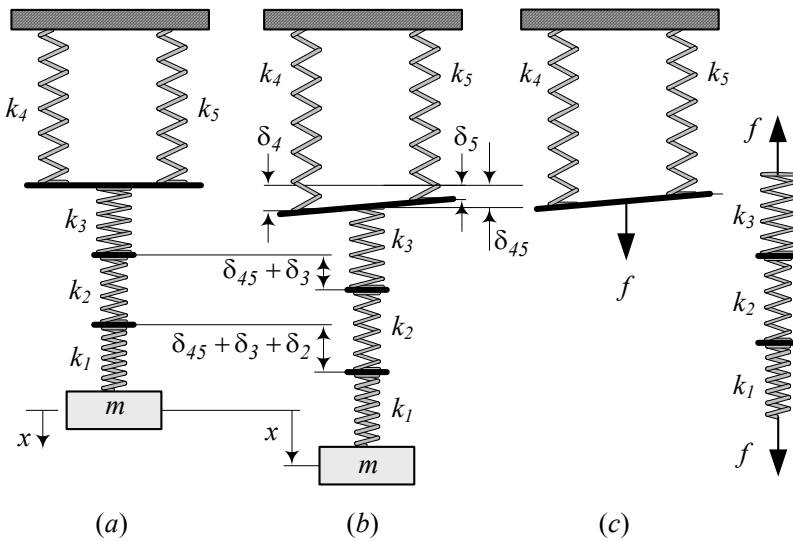


FIGURE 12.6. Equivalent springs model for the flexible frame.
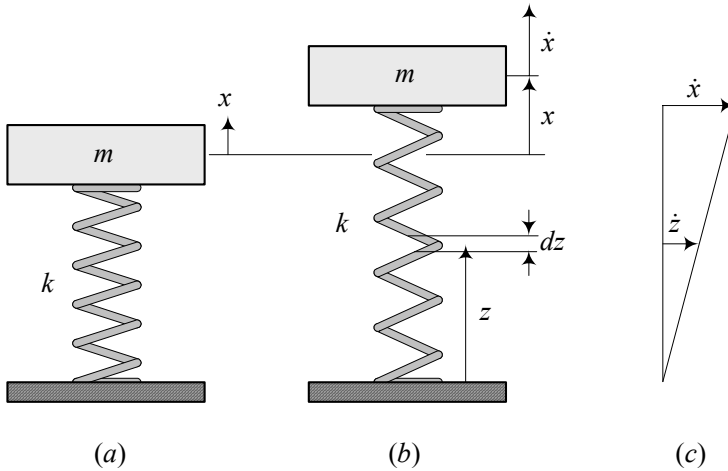
FIGURE 12.7. A vibrating system with a massive spring.

and the displacement at midspan of the lateral beam is

$$\delta_{45} = \frac{\delta_4 + \delta_5}{2}. \qquad (12.27)$$

Assuming

$$\delta_{45} = \frac{f}{k_{45}} \qquad (12.28)$$

we can define an equivalent stiffness $k_{45}$ for $k_4$ and $k_5$ as

$$\frac{1}{k_{45}} = \frac{1}{2}\left(\frac{1}{2k_4} + \frac{1}{2k_5}\right)$$
$$= \frac{1}{4}\left(\frac{1}{k_4} + \frac{1}{k_5}\right). \qquad (12.29)$$

Now the equivalent spring $k_{45}$ is in series with the series of $k_1$, $k_2$, and $k_3$. Hence the overall equivalent spring $k_{eq}$ is

$$\frac{1}{k_{eq}} = \frac{1}{k_1} + \frac{1}{k_2} + \frac{1}{k_3} + \frac{1}{k_{45}}$$
$$= \frac{1}{k_1} + \frac{1}{k_2} + \frac{1}{k_3} + \frac{1}{4k_4} + \frac{1}{4k_5}. \qquad (12.30)$$

**Example 426 ★ Massive spring.**
In modeling of vibrating systems we ignore the mass of springs and dampers. This assumption is valid as long as the mass of springs and dampers are much smaller than the mass of the body they support. However, when the mass of spring $m_s$ or damper $m_d$ is comparable with the

*mass of body m, we may define a new system with an equivalent mass $m_{eq}$*

$$m_{eq} = m + \frac{1}{3}m_s \tag{12.31}$$

*which is supported by massless spring and damper.*

*Consider a vibrating system with a massive spring as shown in Figure 12.7(a). The spring has a mass $m_s$, and a length $l$, when the system is at equilibrium. The mass of spring is uniformly distributed along its length, so, we may define a length density as*

$$\rho = \frac{m}{l}. \tag{12.32}$$

*To show (12.31), we seek for a system with a mass $m_{eq}$ and a massless spring, which can keep the same amount of kinetic energy as the original system. Figure 12.7(b) illustrates the system when the mass $m$ is at position $x$ and has a velocity $\dot{x}$. The spring is between the mass and the ground. So, the base of spring has no velocity, while the other end has the same velocity as $m$. Let's define a coordinate $z$ that goes from the grounded base of the spring to the end point. An element of spring at $z$ has a length $dz$ and a mass $dm$.*

$$dm = \rho \, dz \tag{12.33}$$

*Assuming a linear velocity distribution of the elements of spring, as shown in Figure 12.7(c), we find the velocity $\dot{z}$ of $dm$ as*

$$\dot{z} = \frac{z}{l}\dot{x}. \tag{12.34}$$

*The kinetic energy of the system is a summation of kinetic energy of the mass $m$ and kinetic energy of the spring.*

$$
\begin{aligned}
K &= \frac{1}{2}m\dot{x}^2 + \frac{1}{2}\int_0^l \left(dm\,\dot{z}^2\right) = \frac{1}{2}m\dot{x}^2 + \frac{1}{2}\int_0^l \rho\left(\frac{z}{l}\dot{x}\right)^2 dz \\
&= \frac{1}{2}m\dot{x}^2 + \frac{1}{2}\frac{\rho}{l^2}\dot{x}^2 \int_0^l z^2 \, dz \\
&= \frac{1}{2}m\dot{x}^2 + \frac{1}{2}\frac{\rho}{l^2}\dot{x}^2 \left(\frac{1}{3}l^3\right) \\
&= \frac{1}{2}m\dot{x}^2 + \frac{1}{2}\left(\frac{1}{3}\rho l\right)\dot{x}^2 \\
&= \frac{1}{2}\left(m + \frac{1}{3}m_s\right)\dot{x}^2 \\
&= \frac{1}{2}m_{eq}\dot{x}^2 \tag{12.35}
\end{aligned}
$$

*Therefore, an equivalent system should have a massless spring and a mass $m_{eq} = m + \frac{1}{3}m_s$ to keep the same amount of kinetic energy.*

Equilibrium          In motion          Free body diagram

(a)                   (b)                     (c)
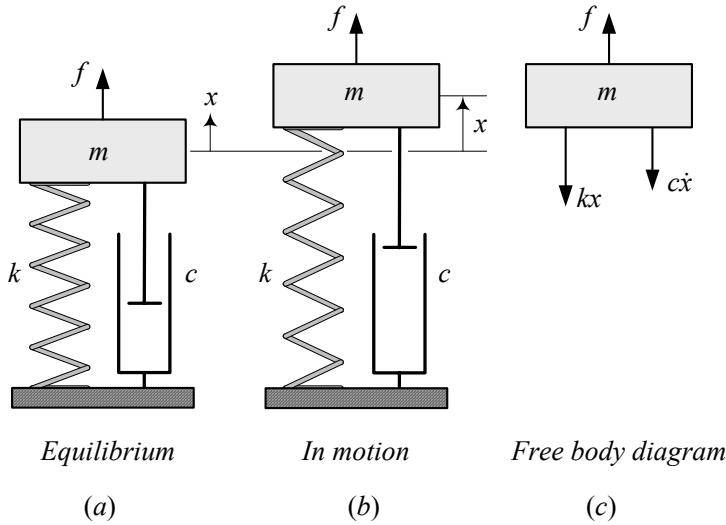
FIGURE 12.8. A one DOF vibrating systems.

## 12.2   Newton's Method and Vibrations

Every vibrating system can be modeled as a combination of masses $m_i$, dampers $c_i$, and springs $k_i$. Such a model is called a *discrete* or *lumped* model of the system. A one DOF vibrating system, with the following equation of motion, is shown in Figure 12.8.

$$ma = -cv - kx + f(x, v, t) \qquad (12.36)$$

To apply Newton's method and find the equations of motion, we assume all the masses $m_i$ are out of the equilibrium at positions $x_i$ with velocities $\dot{x}_i$. Such a situation is shown in Figure 12.8(b) for a *one* DOF system. The free body diagram as shown in Figure 12.8(c), illustrates the applied forces and then, Newton's equation (9.11)

$$ {}^G\mathbf{F} = \frac{{}^G d}{dt} {}^G\mathbf{p} = \frac{{}^G d}{dt} \left( m \, {}^G\mathbf{v} \right) \qquad (12.37) $$

generates the equations of motion.

The *equilibrium position* of a vibrating system is where the potential energy of the system, $V$, is extremum.

$$ \frac{\partial V}{\partial x} = 0 \qquad (12.38) $$

We usually set $V = 0$ at the equilibrium position. Linear systems with constant stiffness have only one equilibrium or infinity equilibria, while
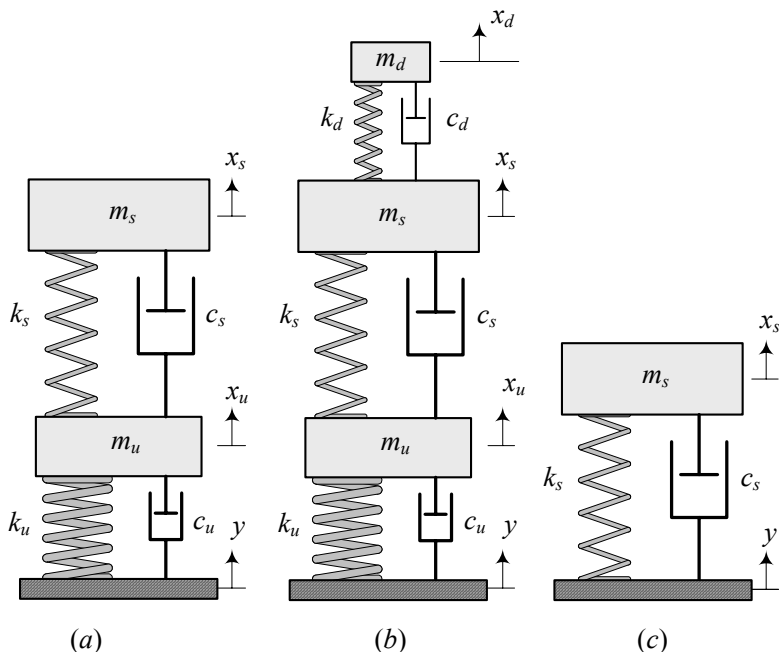
FIGURE 12.9. Two, three, and one DOF models for vertical vibrations of vehicles.

nonlinear systems may have multiple equilibria. An equilibrium is *stable* if

$$\frac{\partial^2 V}{\partial x^2} > 0 \tag{12.39}$$

and is *unstable* if

$$\frac{\partial^2 V}{\partial x^2} < 0. \tag{12.40}$$

The arrangement and the number of employed elements can be used to classify discrete vibrating systems. The number of masses, times the DOF of each mass, makes the total DOF of the vibrating system $n$. The final set of equations would be $n$ second-order differential equations to be solved for $n$ generalized coordinates. When each mass has one DOF, then the system's DOF is equal to the number of masses. The DOF may also be defined as the minimum number of independent coordinates that defines the configuration of a system.

A one, two, and three DOF model for analysis of vertical vibrations of a vehicle are shown in Figure 12.9(a)-(c). The system in Figure 12.9(a) is called the *quarter car* model, which $m_s$ represents a quarter mass of the body, and $m_u$ represents a wheel. The parameters $k_u$ and $c_u$ are models for tire stiffness and damping. Similarly, $k_s$ and $c_u$ are models for the main suspension of the vehicle. Figure 12.9(c) is called the 1/8 car model which
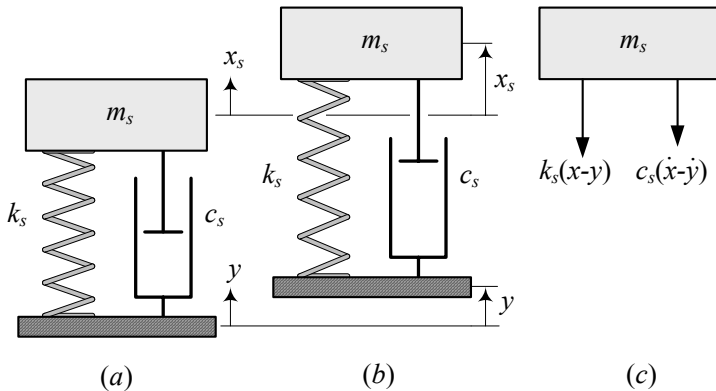
FIGURE 12.10. A 1/8 car model and its free body diagram.

does not show the wheel of the car, and Figure 12.9(b) is a quarter car with a driver $m_d$ and the driver's seat modeled as $k_d$ and $c_d$.

**Example 427** *1/8 car model.*
*Figure 12.9(c) and 12.10(a) show the simplest model for vertical vibrations of a vehicle. This model is sometimes called 1/8 car model. The mass $m_s$ represents one quarter of the car's body, which is mounted on a suspension made of a spring $k_s$ and a damper $c_s$. When $m_s$ is vibrating at a position such as in Figure 12.10(b), its free body diagram is as Figure 12.10(c) shows.*
*Applying Newton's method, the equation of motion would be*

$$m_s \ddot{x} = -k_s \left( x_s - y \right) - c_s \left( \dot{x}_s - \dot{y} \right) \tag{12.41}$$

*which can be simplified to the following equation, when we separate the input $y$ and output $x$ variables.*

$$m_s \ddot{x} + c_s \dot{x}_s + k_s x_s = k_s y + c_s \dot{y}. \tag{12.42}$$

**Example 428** *Equivalent mass and spring.*
*Figure 12.11(a) illustrates a pendulum made by a point mass $m$ attached to a massless bar with length $l$. The coordinate $\theta$ shows the angular position of the bar. The equation of motion for the pendulum can be found by using the Euler equation and employing the free-body-diagram shown in Figure 12.11(b).*

$$ml^2 \ddot{\theta} = -mgl \sin \theta \tag{12.43}$$

*Simplifying the equation of motion and assuming a very small swing angle shows that*

$$l\ddot{\theta} + g\theta = 0. \tag{12.44}$$
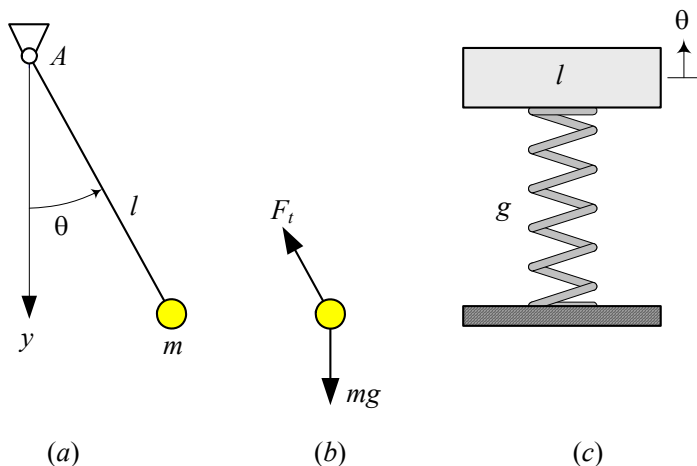
FIGURE 12.11. Equivalent mass-spring vibrator for a pendulum.

*This equation is equivalent to an equation of motion for a mass-spring system made by a mass $m \equiv l$, and a spring with stiffness $k \equiv g$. The displacement of the mass would be $x \equiv \theta$. Figure 12.11(c) depicts such an equivalent mass-spring system.*

**Example 429** *Force proportionality.*
*The equation of motion for a vibrating system is a balance between four different forces. A force proportional to displacement, $-kx$, a force proportional to velocity, $-cv$, a force proportional to acceleration, $ma$, and an applied external force $f(x, v, t)$, which can be a function of displacement, velocity, and time. Based on Newton's method, the force proportional to acceleration, $ma$, is always equal to the sum of all the other forces.*

$$ma = -cv - kx + f(x, v, t) \qquad (12.45)$$

**Example 430** *A two-DOF base excited system.*
*Figure 12.12(a)-(c) illustrate the equilibrium, motion, and free body diagram of the two-DOF system shown in 12.9(a). The free body diagram is plotted based on the assumption*

$$x_s > x_u > y. \qquad (12.46)$$

*Applying Newton's method provides two equations of motion as follows*

$$
\begin{aligned}
m_s \ddot{x}_s &= -k_s(x_s - x_u) - c_s(\dot{x}_s - \dot{x}_u) & (12.47) \\
m_u \ddot{x}_u &= k_s(x_s - x_u) + c_s(\dot{x}_s - \dot{x}_u) \\
&\quad -k_u(x_u - y) - c_u(\dot{x}_u - \dot{y}). & (12.48)
\end{aligned}
$$
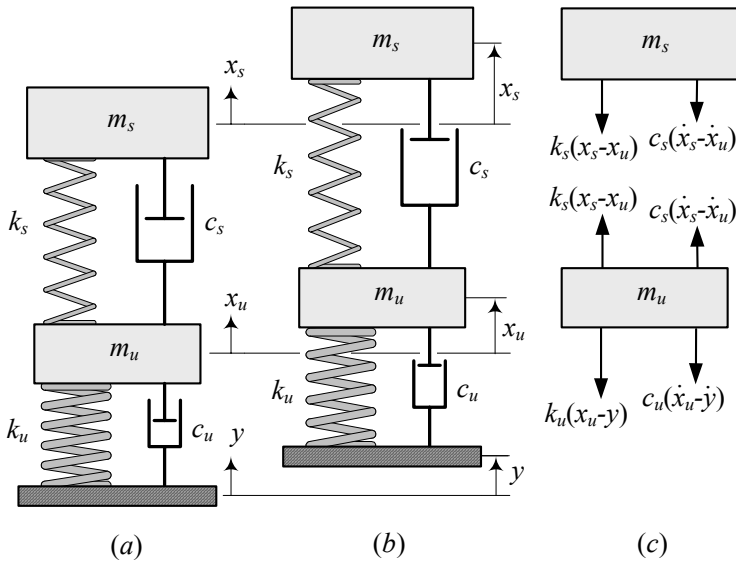
FIGURE 12.12. A 1/4 car model and its free body diagram.

*The assumption (12.46) is not necessarily fulfilled. We can find the same Equations (12.47) and (12.48) using any other assumption, such as $x_s < x_u > y$, $x_s > x_u < y$, or $x_s < x_u < y$. However, having an assumption helps to make a consistent free body diagram.*

*We usually rearrange the equations of motion for a linear system in a matrix form*

$$[M]\,\ddot{\mathbf{x}} + [c]\,\dot{\mathbf{x}} + [k]\,\mathbf{x} = \mathbf{F} \qquad (12.49)$$

*to take advantage of matrix calculus. Rearrangement of Equations (12.47) and (12.48) results in the following set of equations:*

$$
\begin{bmatrix} m_s & 0 \\ 0 & m_u \end{bmatrix} \begin{bmatrix} \ddot{x}_s \\ \ddot{x}_u \end{bmatrix} + \begin{bmatrix} c_s & -c_s \\ -c_s & c_s + c_u \end{bmatrix} \begin{bmatrix} \dot{x}_s \\ \dot{x}_u \end{bmatrix} +
$$
$$
\begin{bmatrix} k_s & -k_s \\ -k_s & k_s + k_u \end{bmatrix} \begin{bmatrix} x_s \\ x_u \end{bmatrix} = \begin{bmatrix} 0 \\ k_u y + c_u \dot{y} \end{bmatrix} \qquad (12.50)
$$

**Example 431 ★** *Inverted pendulum.*

*Figure 12.13(a) illustrates an inverted pendulum with a tip mass m and a length l. The pendulum is supported by two identical springs attached to point B at a distance a < l from the pivot A. A free body diagram of the pendulum is shown in Figure 12.13(b). The equation of motion may be found by taking a moment about A.*

$$
\sum M_A \;=\; I_A \ddot{\theta} \qquad (12.51)
$$
$$
mg\,(l \sin\theta) - 2ka\theta\,(a \cos\theta) \;=\; ml^2 \ddot{\theta} \qquad (12.52)
$$
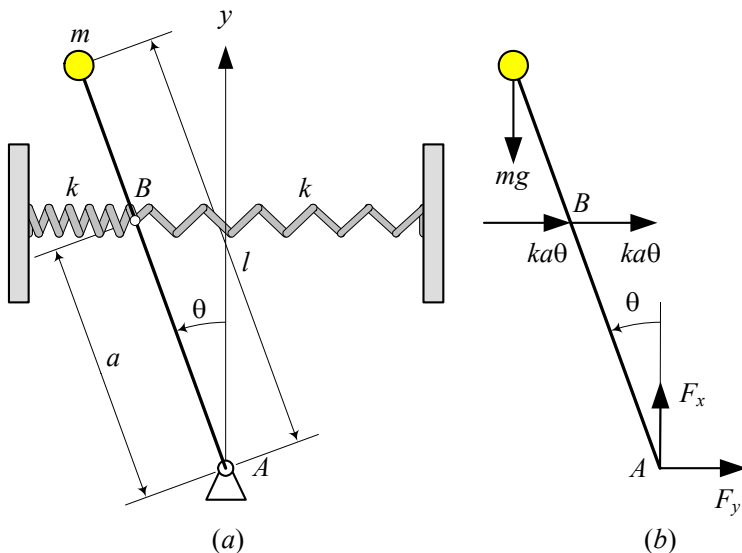
FIGURE 12.13. An inverted pendulum with a tip mass $m$ and two supportive springs.

*To derive Equation (12.52) we assumed that the springs are long enough to remain almost straight when the pendulum oscillates. Rearrangement and assuming a very small $\theta$ shows that the nonlinear equation of motion (12.52) can be approximated by*

$$ml^2\ddot{\theta} + \left(mgl - 2ka^2\right)\theta = 0 \qquad (12.53)$$

*which is equivalent to a linear oscillator*

$$m_{eq}\ddot{\theta} + k_{eq}\theta = 0 \qquad (12.54)$$

*with an equivalent mass $m_{eq}$ and and equivalent $k_{eq}$.*

$$
\begin{aligned}
m_{eq} &= ml^2 & (12.55)\\
k_{eq} &= mgl - 2ka^2 & (12.56)
\end{aligned}
$$

*The potential energy of the inverted pendulum can be expressed as*

$$V = -mgl\left(1 - \cos\theta\right) + ka^2\theta^2 \qquad (12.57)$$

*which has a zero value at $\theta = 0$. The potential energy $V$ is approximately equal to the following equation if $\theta$ is very small*

$$V \approx -\frac{1}{2}mgl\theta^2 + ka^2\theta^2 \qquad (12.58)$$

*because*

$$\cos \theta \approx 1 - \frac{1}{2}\theta^2 + O\left(\theta^4\right).\tag{12.59}$$

*To find the equilibrium positions of the system, we should solve the following equation for any possible $\theta$.*

$$\frac{\partial V}{\partial x} = -2mgl\theta + 2ka^2\theta = 0 \tag{12.60}$$

*The solution of the equation is*

$$\theta = 0 \tag{12.61}$$

*that shows the upright vertical position is the only equilibrium of the inverted pendulum as long as $\theta$ is very small. However, if*

$$mgl = ka^2 \tag{12.62}$$

*then any $\theta$ around $\theta = 0$ can be an equilibrium position and hence, the inverted pendulum would have infinity equilibria.*

*A second derivative of the potential energy*

$$\frac{\partial^2 V}{\partial x^2} = -2mgl + 2ka^2 \tag{12.63}$$

*indicates that the equilibrium position $\theta = 0$ is stable if*

$$ka^2 > mgl. \tag{12.64}$$

*A stable equilibrium pulls the system back, if it deviates from the equilibrium, while an unstable equilibrium repels the system. Vibration happens when the equilibrium is stable.*

## 12.3 Frequency Response of Vibrating Systems

Frequency response is the *steady-state* solution of equations of motion, when the system is *harmonically excited*. Steady-state response refers to a constant amplitude oscillation, after the effect of initial conditions dies out. A harmonic excitation is any combination of *sinusoidal functions* that applies on a vibrating system. If the system is linear, then a harmonic excitation generates a harmonic response with a frequency-dependent amplitude. In frequency response analysis, we are looking for the steady-state amplitude of oscillation as a function of the excitation frequency.

A vast amount of vibrating systems in vehicle dynamics can be modeled by a *one*-DOF system. Consider a *one*-DOF mass-spring-damper system. There are four types of *one*-DOF harmonically excited systems:

1— base excitation,
2— eccentric excitation,
3— eccentric base excitation,
4— forced excitation.

These four systems are shown in Figure 12.14 symbolically.

*Base excitation* is the most practical model for vertical vibration of vehicles. *Eccentric excitation* is a model for every type of rotary motor on a suspension, such as engine on engine mounts. *Eccentric base excitation* is a model for vibration of any equipment mounted on an engine or vehicle. *Forced excitation*, has almost no practical application, however, it is the simplest model for forced vibrations, with good pedagogical use.

For simplicity, we first examine the frequency response of a harmonically forced vibrating system.

### 12.3.1   Forced Excitation

Figure 12.15 illustrates a *one* DOF vibrating mass $m$ supported by spring $k$ and a damper $c$. The absolute motion of $m$ with respect to its equilibrium position is measured by the coordinate $x$. A sinusoidal excitation force

$$f = F \sin \omega t \tag{12.65}$$

is applied on $m$ and makes the system vibrate.

The equation of motion for the system is

$$m\ddot{x} + c\dot{x} + kx = F \sin \omega t \tag{12.66}$$

which generates a frequency response equal to either of the following functions:

$$
\begin{aligned}
x &= A_1 \sin \omega t + B_1 \cos \omega t \tag{12.67}\\
&= X \sin (\omega t - \varphi_x) \tag{12.68}
\end{aligned}
$$

The steady-state response has an *amplitude $X$*

$$\frac{X}{F/k} = \frac{1}{\sqrt{(1 - r^2)^2 + (2\xi r)^2}} \tag{12.69}$$

and a *phase $\varphi_x$*

$$\varphi_x = \tan^{-1} \frac{2\xi r}{1 - r^2} \tag{12.70}$$

where we use the *frequency ratio $r$*, $\omega_n$, and *damping ratio $\xi$*.

$$
\begin{aligned}
r &= \frac{\omega}{\omega_n} \tag{12.71}\\
\xi &= \frac{c}{2\sqrt{km}} \tag{12.72}\\
\omega_n &= \sqrt{\frac{k}{m}} \tag{12.73}
\end{aligned}
$$
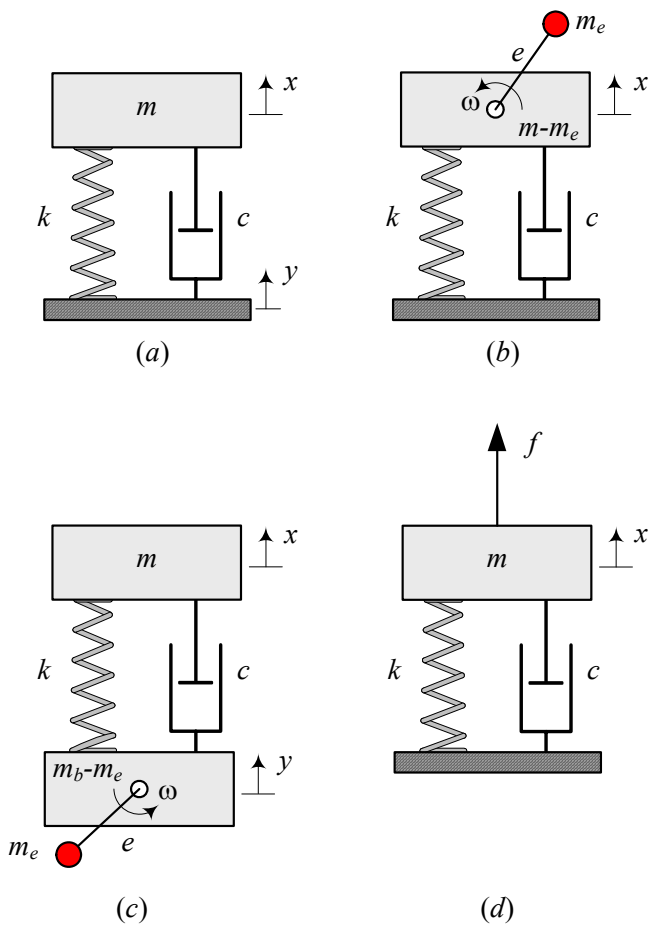
FIGURE 12.14. The four practical types of *one*-DOF harmonically excited systems: *a*−base excitation, *b*−eccentric excitation, *c*−eccentric base excitation, *d*−forced excitation.
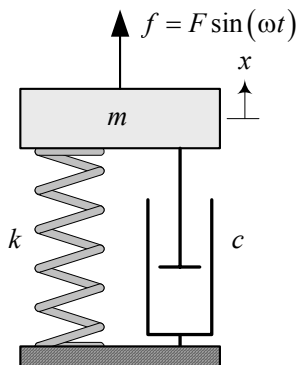
FIGURE 12.15. A harmonically forced excitated, single-DOF system.

Phase $\varphi_x$ indicates the *angular lag* of the response $x$ with respect to the excitation $f$. Because of the importance of the function $X = X(\omega)$, it is common to call this function the *frequency response* of the system. Furthermore, we may use frequency response to every characteristic of the system that is a function of excitation frequency, such as velocity frequency response $\dot{X} = \dot{X}(\omega)$ and transmitted force frequency response $f_T = f_T(\omega)$.

The frequency responses for $X$ and $\varphi_x$ as a function of $r$ and $\xi$ are plotted in Figures 12.16 and 12.17.

**Proof.** Applying Newton's method and using the free body diagram of the system, as shown in Figure 12.18, generates the equation of motion (12.66), which is a linear differential equation.

The steady-state solution of the linear equation is the same function as the excitation with an unknown amplitude and phase. Therefore, the solution can be (12.67), or (12.68). The solution should be substituted in the equation of motion to find the amplitude and phase of the response. We examine the solution (12.67) and find the following equation:

$$
\begin{aligned}
&-m\omega^2 \left(A_1 \sin \omega t + B_1 \cos \omega t\right) \\
&+c\omega \left(A_1 \cos \omega t - B_1 \sin \omega t\right) \\
&+k \left(A_1 \sin \omega t + B_1 \cos \omega t\right) \\
&= \quad F \sin \omega t
\end{aligned}
\tag{12.74}
$$

The functions $\sin \omega t$ and $\cos \omega t$ are orthogonal, therefore, their coefficient must be balanced on both sides of the equal sign. Balancing the coefficients of $\sin \omega t$ and $\cos \omega t$ provides a set of two equations for $A_1$ and $B_1$.

$$
\begin{bmatrix} k - m\omega^2 & -c\omega \\ c\omega & k - m\omega^2 \end{bmatrix} \begin{bmatrix} A_1 \\ B_1 \end{bmatrix} = \begin{bmatrix} F \\ 0 \end{bmatrix}
\tag{12.75}
$$
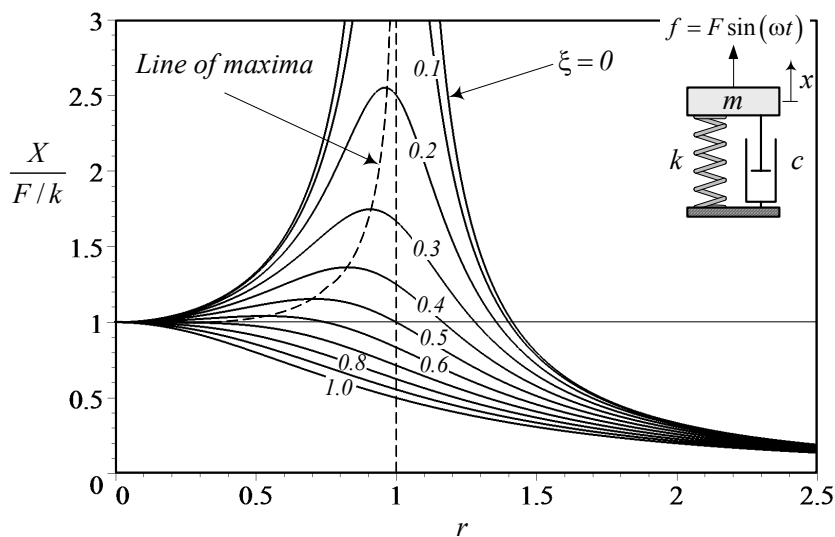
FIGURE 12.16. The position frequency response for $\dfrac{X}{F/k}$.
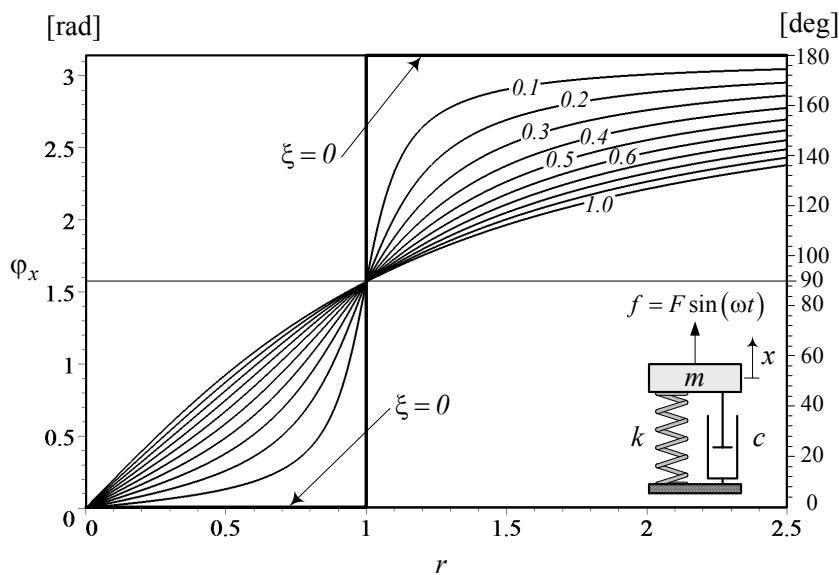


FIGURE 12.17. The frequency response for $\varphi_x$.
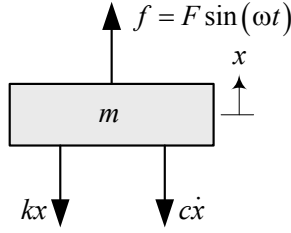
FIGURE 12.18. Free body diagram of the harmonically forced excitated, single-DOF system shown in Figure 12.15.

Solving for coefficients $A_1$ and $B_1$

$$
\begin{bmatrix} A_1 \\ B_1 \end{bmatrix} = \begin{bmatrix} k - m\omega^2 & -c\omega \\ c\omega & k - m\omega^2 \end{bmatrix}^{-1} \begin{bmatrix} F \\ 0 \end{bmatrix}
$$

$$
= \begin{bmatrix} \dfrac{k - m\omega^2}{\left(k - m\omega^2\right)^2 + c^2\omega^2} F \\[3mm] \dfrac{-c\omega}{\left(k - m\omega^2\right)^2 + c^2\omega^2} F \end{bmatrix} \tag{12.76}
$$

provides the steady-state solution (12.67).

Amplitude $X$ and phase $\varphi_x$ can be found by equating Equations (12.67) and (12.68).

$$
\begin{aligned}
A_1 \sin \omega t + B_1 \cos \omega t &= X \sin (\omega t - \varphi_x) \\
&= X \cos \varphi_x \sin \omega t - X \sin \varphi_x \cos \omega t \tag{12.77}
\end{aligned}
$$

It shows that,

$$
\begin{aligned}
A_1 &= X \cos \varphi_x \tag{12.78} \\
B_1 &= -X \sin \varphi_x \tag{12.79}
\end{aligned}
$$

and therefore,

$$
X = \sqrt{A_1^2 + B_1^2} \tag{12.80}
$$

$$
\tan \varphi_x = \frac{-B_1}{A_1}. \tag{12.81}
$$

Substituting $A_1$ and $B_1$ from (12.76) results in the following solutions.

$$
X = \frac{1}{\sqrt{\left(k - m\omega^2\right)^2 + c^2\omega^2}} F \tag{12.82}
$$

$$
\tan \varphi_x = \frac{c\omega}{k - m\omega^2} \tag{12.83}
$$

However, we may use more practical expressions (12.69) and (12.70) for amplitude $X$ and phase $\varphi_x$ by employing $r$ and $\xi$.

When we apply a constant force $f = F$ on $m$, a displacement, $\delta_s$, appears.

$$\delta_s = \frac{F}{k} \qquad (12.84)$$

If we call $\delta_s$ "*static amplitude*" and $X$ "*dynamic amplitude*," then, $X/\delta_s$ is the ratio of dynamic to static amplitudes. The dynamic amplitude is equal to the static amplitude, $X = \delta_s$, at $r = 0$, and approaches zero, $X \to 0$, when $r \to \infty$. However, $X$ gets a high value when $r \to 1$ and $\omega \to \omega_n$. Theoretically, $X \to \infty$ if $\xi = 0$ and $r = 1$. Frequency domains around the natural frequency is called *resonance zone*. The amplitude of vibration in resonance zone can be reduces by introducing damping. ■

**Example 432** *A forced vibrating system*
  *Consider a mass-spring-damper system with*

$$\begin{aligned} m &= 2\,\mathrm{kg} \\ k &= 100000\,\mathrm{N/m} \\ c &= 100\,\mathrm{N\,s/m}. \end{aligned} \qquad (12.85)$$

*The natural frequency frequency and damping ratio of the system are*

$$\omega_n = \sqrt{\frac{k}{m}} = \sqrt{\frac{100000}{2}} = 223.61\,\mathrm{rad/s} \approx 35.6\,\mathrm{Hz} \qquad (12.86)$$

$$\xi = \frac{c}{2\sqrt{km}} = \frac{100}{2\sqrt{100000 \times 2}} = 0.1118. \qquad (12.87)$$

*If a harmonic force $f$*

$$f = 100 \sin 100t \qquad (12.88)$$

*is applied on $m$, then the steady-state amplitude of vibrations of the mass, $X$, would be*

$$X = \frac{F/k}{\sqrt{(1 - r^2)^2 + (2\xi r)^2}} = 1.24 \times 10^{-3}\,\mathrm{m} \qquad (12.89)$$

*because*

$$r = \frac{\omega}{\omega_n} = 0.44721. \qquad (12.90)$$

*The phase $\varphi_x$ of the vibration is*

$$\varphi_x = \tan^{-1} \frac{2\xi r}{1 - r^2} = 0.124\,\mathrm{rad} \approx 7.12\,\mathrm{deg}. \qquad (12.91)$$

*Therefore, the steady-state vibrations of the mass $m$ can be expressed by the following function.*

$$x = 1.24 \times 10^{-3} \sin(100t - 0.124) \qquad (12.92)$$

*The value of $X$ and $\varphi_x$ may also be found from Figures 12.16 and 12.17 approximately.*

**Example 433** *Velocity and acceleration frequency responses.*
   *When we calculate the position frequency response*

$$
\begin{aligned}
x &= A_1 \sin \omega t + B_1 \cos \omega t \\
&= X \sin (\omega t - \varphi_x)
\end{aligned}
\tag{12.93}
$$

*we are able to calculate the velocity and acceleration frequency responses by derivative.*

$$
\begin{aligned}
\dot{x} &= A_1 \omega \cos \omega t - B_1 \omega \sin \omega t \\
&= X \omega \cos (\omega t - \varphi_x) \\
&= \dot{X} \cos (\omega t - \varphi_x)
\end{aligned}
\tag{12.94}
$$

$$
\begin{aligned}
\ddot{x} &= -A_1 \omega^2 \sin \omega t - B_1 \omega^2 \cos \omega t \\
&= -X \omega^2 \sin (\omega t - \varphi_x) \\
&= \ddot{X} \sin (\omega t - \varphi_x)
\end{aligned}
\tag{12.95}
$$

*The amplitude of velocity and acceleration frequency responses are shown by $\dot{X}$, $\ddot{X}$*

$$
\dot{X} = \frac{\omega}{\sqrt{(k - m\omega^2)^2 + c^2 \omega^2}} F
\tag{12.96}
$$

$$
\ddot{X} = \frac{\omega^2}{\sqrt{(k - m\omega^2)^2 + c^2 \omega^2}} F
\tag{12.97}
$$

*which can be written as*

$$
\frac{\dot{X}}{F/\sqrt{km}} = \frac{r}{\sqrt{(1 - r^2)^2 + (2\xi r)^2}}
\tag{12.98}
$$

$$
\frac{\ddot{X}}{F/m} = \frac{r^2}{\sqrt{(1 - r^2)^2 + (2\xi r)^2}}.
\tag{12.99}
$$

*The velocity and acceleration frequency responses (12.98) and (12.99) are plotted in Figures 12.19 and 12.20.*

**Example 434** *Transmitted force to the base.*
   *A forced excited system, such as the one in Figure 12.15, transmits a force, $f_T$, to the ground. The transmitted force is equal to the sum of forces in spring and damper.*

$$
\begin{aligned}
f_T &= f_k + f_c \\
&= kx + c\dot{x}
\end{aligned}
\tag{12.100}
$$
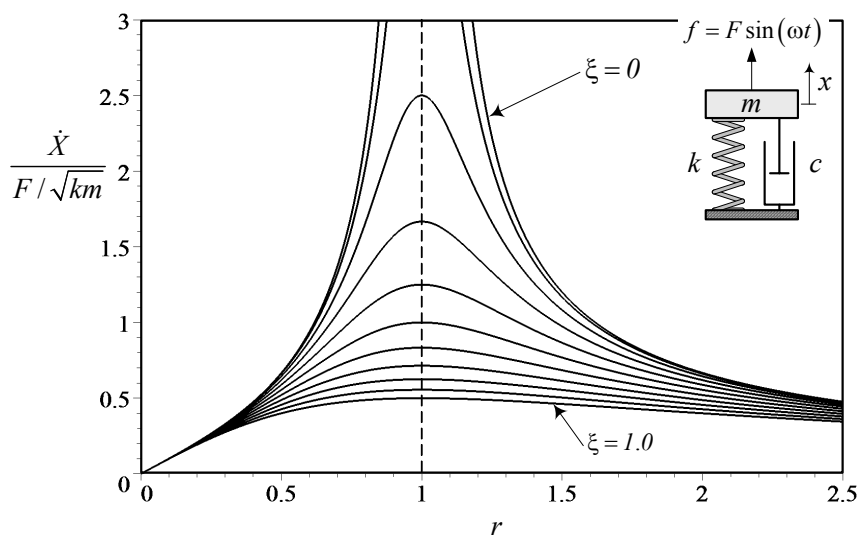
FIGURE 12.19. The velocity frequency response for $\dfrac{\dot{X}}{F/\sqrt{km}}$.
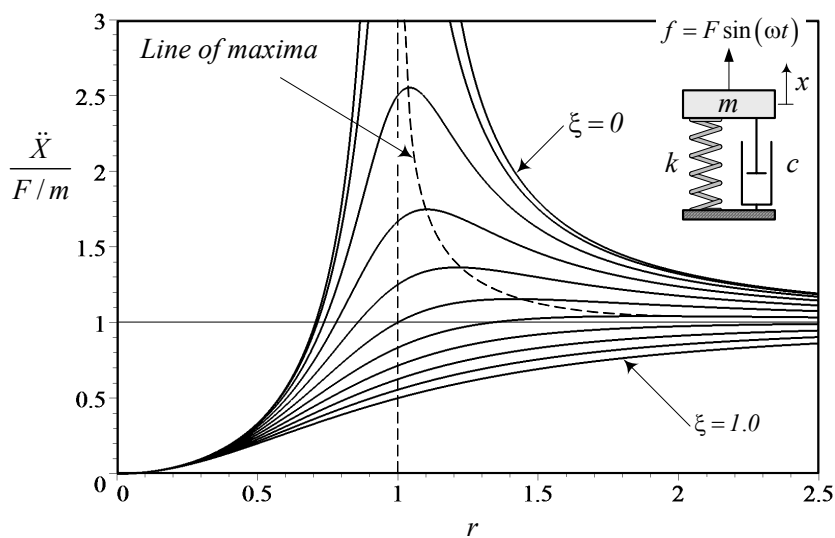


FIGURE 12.20. The acceleration frequency response for $\dfrac{\ddot{X}}{F/m}$.

*Substituting $x$ from (12.67), and $A_1$, $B_1$ from (12.76), shows that the frequency response of the transmitted force is*

$$
\begin{aligned}
f_T &= k\left(A_1 \sin\omega t + B_1 \cos\omega t\right) + c\omega\left(A_1 \cos\omega t - B_1 \sin\omega t\right) \\
&= \left(kA_1 - c\omega B_1\right)\sin t\omega + \left(kB_1 + c\omega A_1\right)\cos t\omega \\
&= F_T \sin\left(\omega t - \varphi_{F_T}\right). \tag{12.101}
\end{aligned}
$$

*The amplitude $F_T$ and phase $\varphi_{F_T}$ of $f_T$ are*

$$
\frac{F_T}{F} = \frac{\sqrt{k + c^2\omega^2}}{\sqrt{\left(k - m\omega^2\right)^2 + c^2\omega^2}} \tag{12.102}
$$

$$
= \frac{\sqrt{1 + (2\xi r)^2}}{\sqrt{\left(1 - r^2\right)^2 + (2\xi r)^2}} \tag{12.103}
$$

$$
\tan\varphi_{F_T} = \frac{c\omega}{k - m\omega^2} = \frac{2\xi r}{1 - r^2} \tag{12.104}
$$

*because*

$$
F_T = \sqrt{\left(kA_1 - c\omega B_1\right)^2 + \left(kB_1 + c\omega A_1\right)^2} \tag{12.105}
$$

$$
\tan\varphi_{F_T} = \frac{-\left(kB_1 + c\omega A_1\right)}{kA_1 - c\omega B_1} \tag{12.106}
$$

*The transmitted force frequency response $F_T/F$ is plotted in Figure 12.21, and because $\varphi_{F_T}$ is the same as Equation (12.70), a graph for $\varphi_{F_T}$ is the same as the one in Figure 12.17.*

**Example 435** *Alternative method to find transmitted force $f_T$.*

*It is possible to use the equation of motion and substitute $x$ from (12.67), to find the transmitted force frequency response of $f_T$ as*

$$
\begin{aligned}
f_T &= F \sin\omega t - m\ddot{x} \\
&= F \sin\omega t + m\omega^2\left(A_1 \sin\omega t + B_1 \cos\omega t\right) \\
&= \left(mA_1\omega^2 + F\right)\sin t\omega + m\omega^2 B_1 \cos t\omega \\
&= F_T \sin\left(\omega t - \varphi_x\right). \tag{12.107}
\end{aligned}
$$

*Amplitude $F_T$ and phase $\varphi_{F_T}$ would be the same as (12.103) and (12.104), because*

$$
F_T = \sqrt{\left(mA_1\omega^2 + F\right)^2 + \left(m\omega^2 B_1\right)^2}
$$

$$
= \frac{\sqrt{k + c^2\omega^2}}{\sqrt{\left(k - m\omega^2\right)^2 + c^2\omega^2}} \tag{12.108}
$$

$$
\tan\varphi_{F_T} = \frac{-m\omega^2 B_1}{m\omega^2 A_1 + F} = \frac{c\omega}{k - m\omega^2}. \tag{12.109}
$$
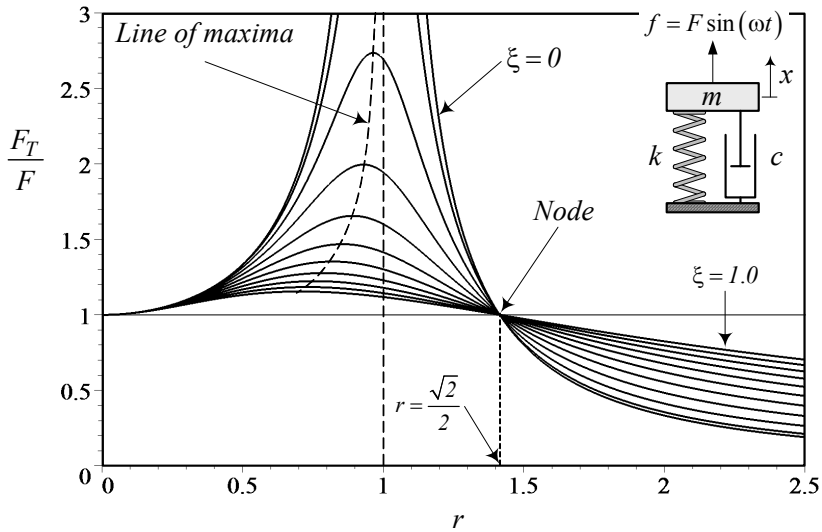
FIGURE 12.21. The frequency response for $\dfrac{F_T}{F}$.

**Example 436** *No mechanical harmonically forced vibration.*

In mechanics, there is no way to apply a periodic force on an object without attaching a mechanical device and applying a displacement. Hence, the forced vibrating system shown in Figure 12.15 has no practical application in mechanics. However, it is possible to make m from a ferromagnetic material to apply an alternative or periodic magnetic force.

**Example 437 ★** *Orthogonality of functions* $\sin \omega t$ *and* $\cos \omega t$.

Two functions $f(t)$ and $g(t)$ are orthogonal in $[a, b]$ if

$$\int_a^b f(t) \; g(t) \; dt = 0. \tag{12.110}$$

The functions $\sin \omega t$ and $\cos \omega t$ are orthogonal in a period $T = [0, 2\pi/\omega]$.

$$\int_0^{2\pi/\omega} \sin \omega t \cos \omega t \; dt = 0 \tag{12.111}$$

**Example 438 ★** *Beating in linear systems.*

Consider a displacement $x(t)$ that is produced by two harmonic forces $f_1$ and $f_2$.

$$\begin{aligned}
f_1 &= F_1 \cos \omega_1 t &\tag{12.112}\\
f_2 &= F_2 \cos \omega_2 t &\tag{12.113}
\end{aligned}$$

Assume that the steady-state response to $f_1$ is

$$x_1(t) = X_1 \cos \left(\omega_1 t + \phi_1\right) \tag{12.114}$$

*and response to $f_2$ is*

$$x_2(t) = X_2 \cos (\omega_2 t + \phi_2) \tag{12.115}$$

*then, because of the linearity of the system, the response to $f_1 + f_2$ would be $x(t) = x_1(t) + x_2(t)$.*

$$
\begin{aligned}
x(t) &= x_1(t) + x_2(t) \\
&= X_1 \cos (\omega_1 t + \phi_1) + X_2 \cos (\omega_2 t + \phi_2)
\end{aligned} \tag{12.116}
$$

*It is convenient to express $x(t)$ in an alternative method*

$$
\begin{aligned}
x(t) =\ & \frac{1}{2} (X_1 + X_2) (\cos (\omega_1 t + \phi_1) + \cos (\omega_2 t + \phi_2)) \\
& + \frac{1}{2} (X_1 - X_2) (\cos (\omega_1 t + \phi_1) - \cos (\omega_2 t + \phi_2))
\end{aligned} \tag{12.117}
$$

*and convert the sums to a product.*

$$
\begin{aligned}
x(t) =\ & (X_1 + X_2) \cos \left( \frac{\omega_1 + \omega_2}{2} t - \frac{\phi_1 + \phi_2}{2} \right) \\
& \times \cos \left( \frac{\omega_1 - \omega_2}{2} t - \frac{\phi_1 - \phi_2}{2} \right) \\
& - (X_1 - X_2) \sin \left( \frac{\omega_1 + \omega_2}{2} t - \frac{\phi_1 + \phi_2}{2} \right) \\
& \times \sin \left( \frac{\omega_1 - \omega_2}{2} t - \frac{\phi_1 - \phi_2}{2} \right)
\end{aligned} \tag{12.118}
$$

*This equation may be expressed better as*

$$
\begin{aligned}
x(t) =\ & (X_1 + X_2) \cos (\Omega_1 t - \Phi_1) \cos (\Omega_2 t - \Phi_2) \\
& - (X_1 - X_2) \sin (\Omega_1 t - \Phi_1) \sin (\Omega_2 t - \Phi_2)
\end{aligned} \tag{12.119}
$$

*if we use the following notations.*

$$\Omega_1 = \frac{\omega_1 + \omega_2}{2} \tag{12.120}$$

$$\Omega_2 = \frac{\omega_1 - \omega_2}{2} \tag{12.121}$$

$$\Phi_1 = \frac{\phi_1 + \phi_2}{2} \tag{12.122}$$

$$\Phi_2 = \frac{\phi_1 - \phi_2}{2}. \tag{12.123}$$

*Figure 12.22 illustrates a sample plot of $x(t)$ for*

$$
\begin{aligned}
\omega_1 &= 10 \\
\omega_2 &= 12 \\
\phi_1 &= \frac{\pi}{4} \\
\phi_2 &= \frac{\pi}{6}
\end{aligned} \tag{12.124}
$$
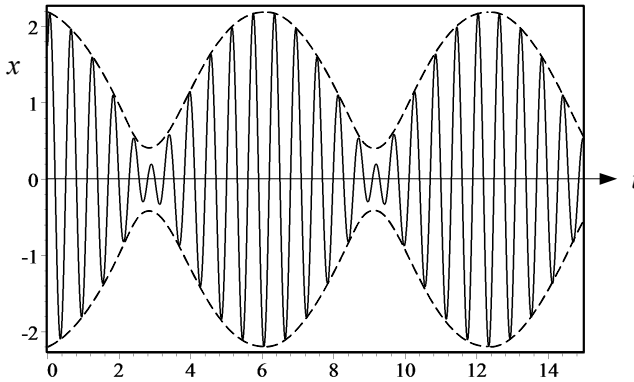
FIGURE 12.22. Beating phenomena.

The displacement $x(t)$ indicates an oscillation between $X_1 + X_2$ and $X_1 - X_2$, with the higher frequency $\Omega_1$ inside an envelope that oscillates, at the lower frequency $\Omega_2$. This behavior is called **beating**.

When $X_1 = X_2 = X$ then

$$x(t) = 2X \cos{(\Omega_1 t - \Phi_1)} \cos{(\Omega_2 t - \Phi_2)} \qquad (12.125)$$

which becomes zero at every half period $T = 2\pi/\Omega_2$.

### 12.3.2   Base Excitation

Figure 12.23 illustrates a *one*-DOF base excited vibrating system with a mass $m$ supported by a spring $k$ and a damper $c$. Base excited system is a good model for vehicle suspension system or any equipment the is mounted on a vibrating base. The absolute motion of $m$ with respect to its equilibrium position is measured by the coordinate $x$. A sinusoidal excitation motion

$$y = Y \sin{\omega t} \qquad (12.126)$$

is applied to the base of the suspension and makes the system vibrate.

The equation of motion for the system can be expressed by either one of the following equations for the absolute displacement $x$

$$m\ddot{x} + c\dot{x} + kx = cY\omega \cos{\omega t} + kY \sin{\omega t} \qquad (12.127)$$

$$\ddot{x} + 2\xi\omega_n \dot{x} + \omega_n^2 x = 2\xi\omega_n \omega Y \cos{\omega t} + \omega_n^2 Y \sin{\omega t} \qquad (12.128)$$

or either one of the following equations for the relative displacement $z$.

$$m\ddot{z} + c\dot{z} + kz = m\omega^2 Y \sin{\omega t} \qquad (12.129)$$

$$\ddot{z} + 2\xi\omega_n \dot{z} + \omega_n^2 z = \omega^2 Y \sin{\omega t} \qquad (12.130)$$

$$z = x - y \qquad (12.131)$$
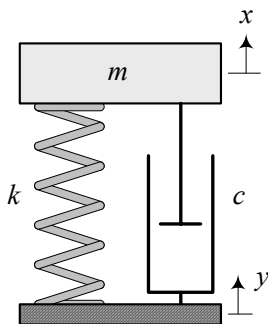
FIGURE 12.23. A harmonically base excitated single DOF system.

The equations of motion generate the following absolute and relative frequency responses.

$$
\begin{aligned}
x &= A_2 \sin \omega t + B_2 \cos \omega t & (12.132) \\
&= X \sin (\omega t - \varphi_x) & (12.133)
\end{aligned}
$$

$$
\begin{aligned}
z &= A_3 \sin \omega t + B_3 \cos \omega t & (12.134) \\
&= Z \sin (\omega t - \varphi_z) & (12.135)
\end{aligned}
$$

The frequency response of $x$ has an amplitude $X$, and the frequency response of $z$ has an amplitude $Z$

$$
\frac{X}{Y} = \frac{\sqrt{1 + (2\xi r)^2}}{\sqrt{(1 - r^2)^2 + (2\xi r)^2}} \tag{12.136}
$$

$$
\frac{Z}{Y} = \frac{r^2}{\sqrt{(1 - r^2)^2 + (2\xi r)^2}} \tag{12.137}
$$

with the following phases $\varphi_x$ and $\varphi_z$ for $x$ and $z$.

$$
\varphi_x = \tan^{-1} \frac{2\xi r^3}{1 - r^2 + (2\xi r)^2} \tag{12.138}
$$

$$
\varphi_z = \tan^{-1} \frac{2\xi r}{1 - r^2} \tag{12.139}
$$

The phase $\varphi_x$ indicates the *angular lag* of the response $x$ with respect to the excitation $y$. The frequency responses for $X$, $Z$, and $\varphi_x$ as a function of $r$ and $\xi$ are plotted in Figures 12.24, 12.25, and 12.26.

**Proof.** Newton's method and the free body diagram of the system, as shown in Figure 12.27, generate the equation of motion

$$
m \ddot{x} = -c (\dot{x} - \dot{y}) - k (x - y) \tag{12.140}
$$
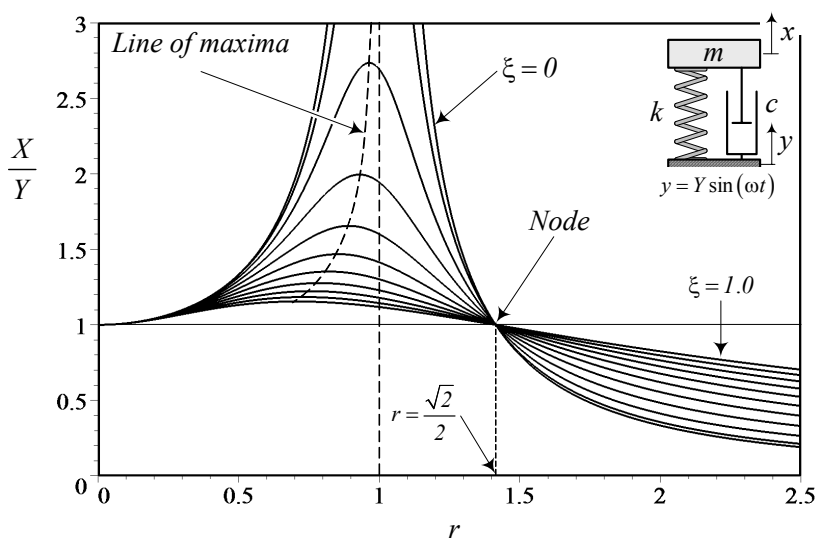
FIGURE 12.24. The position frequency response for $\dfrac{X}{Y}$.
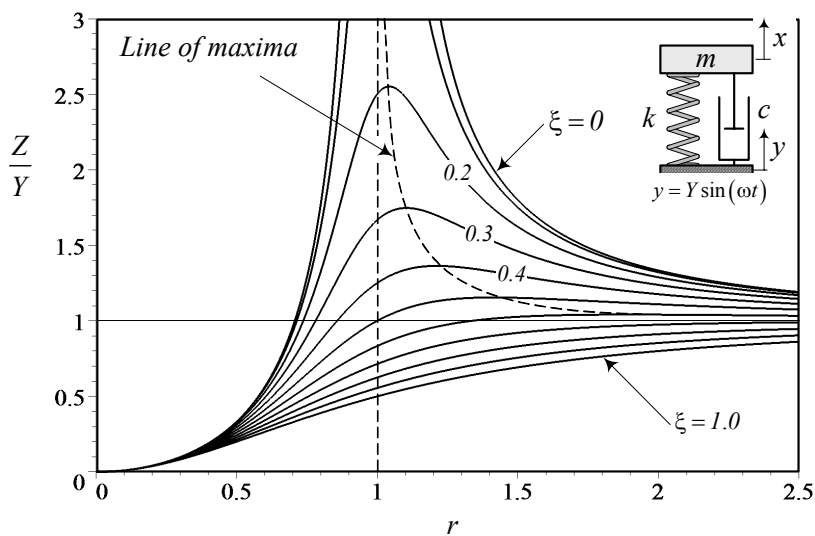


FIGURE 12.25. The frequency response for $\dfrac{Z}{Y}$.
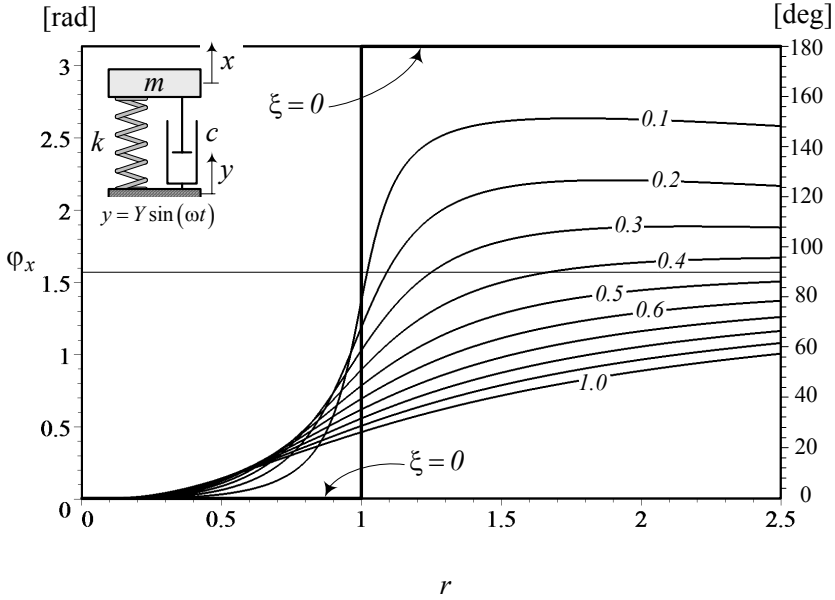
FIGURE 12.26. The frequency response for $\varphi_x$.
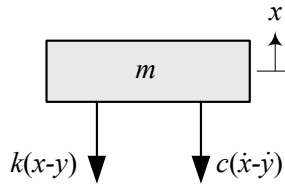


FIGURE 12.27. A harmonically based excitated single-DOF system.

which, after substituting (12.126), makes the equation of motion (12.127). Equation (12.127) can be transformed to (12.128) by dividing over $m$ and using the definition (12.71)-(12.73) for natural frequency and damping ratio.

A practical response for a base excited system is the relative displacement

$$z = x - y. \tag{12.141}$$

Relative displacement is important because for every mechanical device mounted on a suspension such as vehicle body, we need to control the maximum or minimum distance between the base and the device. Taking derivatives from (12.141)

$$\ddot{z} = \ddot{x} - \ddot{y} \tag{12.142}$$

and substituting in (12.140)

$$m\left(\ddot{z}+\ddot{y}\right)=-c\,\dot{z}-kz \tag{12.143}$$

can be transformed to Equations (12.129) and (12.130).

The steady-state solution of Equation (12.127) can be (12.132), or (12.133). To find the amplitude and phase of the response, we substitute the solution (12.132) in the equation of motion.

$$
\begin{aligned}
&-m\omega^2\left(A_2\sin\omega t+B_2\cos\omega t\right)\\
&+c\omega\left(A_2\cos\omega t-B_2\sin\omega t\right)\\
&+k\left(A_2\sin\omega t+B_2\cos\omega t\right)\\
=\ &cY\omega\cos\omega t+kY\sin\omega t
\end{aligned} \tag{12.144}
$$

The coefficients of the functions $\sin\omega t$ and $\cos\omega t$ must balance on both sides of the equation.

$$kA_2-mA_2\omega^2-cB_2\omega = Yk \tag{12.145}$$
$$kB_2-m\omega^2 B_2+c\omega A_2 = Yc\omega \tag{12.146}$$

Therefore, we find two algebraic equations to calculate $A_2$ and $B_2$.

$$
\begin{bmatrix} k-m\omega^2 & -c\omega \\ c\omega & k-m\omega^2 \end{bmatrix}
\begin{bmatrix} A_2 \\ B_2 \end{bmatrix}=
\begin{bmatrix} Yk \\ Yc\omega \end{bmatrix} \tag{12.147}
$$

Solving for the coefficients $A_2$ and $B_2$

$$
\begin{aligned}
\begin{bmatrix} A_2 \\ B_2 \end{bmatrix}
&=\begin{bmatrix} k-m\omega^2 & -c\omega \\ c\omega & k-m\omega^2 \end{bmatrix}^{-1}
\begin{bmatrix} Yk \\ Yc\omega \end{bmatrix}\\[2mm]
&=\begin{bmatrix} \dfrac{k\left(k-m\omega^2\right)+c^2\omega^2}{\left(k-m\omega^2\right)^2+c^2\omega^2}Y \\[4mm] \dfrac{c\omega\left(k-m\omega^2\right)-ck\omega}{\left(k-m\omega^2\right)^2+c^2\omega^2}Y \end{bmatrix}
\end{aligned} \tag{12.148}
$$

provides the steady-state solution (12.132).

The amplitude $X$ and phase $\varphi_x$ can be found by

$$X = \sqrt{A_2^2+B_2^2} \tag{12.149}$$

$$\tan\varphi_x = \frac{-B_2}{A_2} \tag{12.150}$$

which, after substituting $A_2$ and $B_2$ from (12.148), results in the following solutions:

$$X = \frac{\sqrt{k^2+c^2\omega^2}}{\sqrt{\left(k-m\omega^2\right)^2+c^2\omega^2}}Y \tag{12.151}$$

$$\tan\varphi_x = \frac{-cm\omega^3}{k\left(k-m\omega^2\right)+c^2\omega^2} \tag{12.152}$$

A more practical expressions for $X$ and $\varphi_x$ are Equations (12.136) and (12.138), which can be found by employing $r$ and $\xi$.

To find the relative displacement frequency response (12.137), we substitute Equation (12.134) in (12.129).

$$
\begin{aligned}
&-m\omega^2 \left(A_3 \sin\omega t + B_3 \cos\omega t\right) \\
&+c\omega \left(A_3 \cos\omega t - B_3 \sin\omega t\right) \\
&+k \left(A_3 \sin\omega t + B_3 \cos\omega t\right) \\
&= \quad m\omega^2 Y \sin\omega t
\end{aligned}
\tag{12.153}
$$

Balancing the coefficients of the functions $\sin\omega t$ and $\cos\omega t$

$$
\begin{aligned}
kA_2 - mA_2\omega^2 - cB_2\omega &= m\omega^2 Y \tag{12.154} \\
kB_2 - m\omega^2 B_2 + c\omega A_2 &= 0 \tag{12.155}
\end{aligned}
$$

provides two algebraic equations to find $A_3$ and $B_3$.

$$
\begin{bmatrix} k - m\omega^2 & -c\omega \\ c\omega & k - m\omega^2 \end{bmatrix}
\begin{bmatrix} A_3 \\ B_3 \end{bmatrix}
= \begin{bmatrix} m\omega^2 Y \\ 0 \end{bmatrix}
\tag{12.156}
$$

Solving for the coefficients $A_3$ and $B_3$

$$
\begin{aligned}
\begin{bmatrix} A_3 \\ B_3 \end{bmatrix}
&= \begin{bmatrix} k - m\omega^2 & -c\omega \\ c\omega & k - m\omega^2 \end{bmatrix}^{-1}
\begin{bmatrix} m\omega^2 Y \\ 0 \end{bmatrix} \\
&= \begin{bmatrix} \dfrac{m\omega^2 \left(k - m\omega^2\right)}{\left(k - m\omega^2\right)^2 + c^2\omega^2}Y \\[2ex] -\dfrac{mc\omega^3}{\left(k - m\omega^2\right)^2 + c^2\omega^2}Y \end{bmatrix}
\end{aligned}
\tag{12.157}
$$

provides the steady-state solution (12.134). The amplitude $Z$ and phase $\varphi_z$ can be found by

$$
Z = \sqrt{A_3^2 + B_3^2}
\tag{12.158}
$$

$$
\tan\varphi_z = \frac{-B_3}{A_3}
\tag{12.159}
$$

which, after substituting $A_3$ and $B_3$ from (12.157), results in the following solutions.

$$
Z = \frac{m\omega^2}{\sqrt{\left(k - m\omega^2\right)^2 + c^2\omega^2}}Y
\tag{12.160}
$$

$$
\tan\varphi_z = \frac{c\omega}{k - m\omega^2}
\tag{12.161}
$$

A more practical expression for $Z$ and $\varphi_z$ are Equations (12.137) and (12.139). ∎

**Example 439** *A base excited system.*
  *Consider a mass-spring-damper system with*

$$\begin{aligned} m &= 2\,\mathrm{kg} \\ k &= 100000\,\mathrm{N/m} \\ c &= 100\,\mathrm{N\,s/m}. \end{aligned} \tag{12.162}$$

*If a harmonic base excitation* $y$

$$y = 0.002 \sin 350t \tag{12.163}$$

*is applied on the system, then the absolute and relative steady-state ampli-
tude of vibrations of the mass,* $X$ *and* $Z$ *would be*

$$X = \frac{Y\sqrt{1 + (2\xi r)^2}}{\sqrt{(1 - r^2)^2 + (2\xi r)^2}} = 1.9573 \times 10^{-3}\,\mathrm{m} \tag{12.164}$$

$$Z = \frac{Yr^2}{\sqrt{(1 - r^2)^2 + (2\xi r)^2}} = 9.589 \times 10^{-4}\,\mathrm{m} \tag{12.165}$$

*because*

$$\begin{aligned} \omega_n &= \sqrt{\frac{k}{m}} = 223.61\,\mathrm{rad/s} \approx 35.6\,\mathrm{Hz} \tag{12.166} \\ \xi &= \frac{c}{2\sqrt{km}} = 0.1118 \tag{12.167} \\ r &= \frac{\omega}{\omega_n} = 1.5652. \tag{12.168} \end{aligned}$$

*The phases* $\varphi_x$ *and* $\varphi_z$ *for* $x$ *and* $z$ *are*

$$\begin{aligned} \varphi_x &= \tan^{-1}\frac{2\xi r^3}{1 - r^2 + (2\xi r)^2} = 0.489\,\mathrm{rad} \approx 28.02\,\mathrm{deg} \tag{12.169} \\ \varphi_z &= \tan^{-1}\frac{2\xi r}{1 - r^2} = 1.8585\,\mathrm{rad} \approx 106.48\,\mathrm{deg} \tag{12.170} \end{aligned}$$

*Therefore, the steady-state vibrations of the mass* $m$ *can be expressed by the
following functions.*

$$\begin{aligned} x &= 1.9573 \times 10^{-3} \sin(350t - 0.489) \tag{12.171} \\ z &= 9.589 \times 10^{-4} \sin(350t - 1.8585) \tag{12.172} \end{aligned}$$

**Example 440** *Comparison between frequency responses.*
  *A comparison shows that Equation (12.137) is equal to Equation (12.98),
and therefore the relative frequency response* $\frac{Z}{Y}$ *for a base excited system,*

*is the same as acceleration frequency response $\frac{\ddot{X}}{F/m}$ for a forces excited system. Also a graph for $\varphi_z$ would be the same as Figure 12.17.*

*Comparing Equations (12.136) and (12.103) indicates that the amplitude frequency response of a base excited system, $\frac{X}{Y}$ is the same as the transmitted force frequency response of a harmonically force excited system $\frac{F_T}{F}$. However, the phase of these two responses are different.*

**Example 441** *Absolute velocity and acceleration of a base excited system.*

*Having the position frequency response of a base excited system*

$$
\begin{aligned}
x &= A_2 \sin \omega t + B_2 \cos \omega t \\
&= X \sin (\omega t - \varphi_x)
\end{aligned} \tag{12.173}
$$

*we are able to calculate the velocity and acceleration frequency responses.*

$$
\begin{aligned}
\dot{x} &= A_2 \omega \cos \omega t - B_2 \omega \sin \omega t \\
&= X \omega \cos (\omega t - \varphi_x) \\
&= \dot{X} \cos (\omega t - \varphi_x)
\end{aligned} \tag{12.174}
$$

$$
\begin{aligned}
\ddot{x} &= -A_2 \omega^2 \sin \omega t - B_2 \omega^2 \cos \omega t \\
&= -X \omega^2 \sin (\omega t - \varphi_x) \\
&= \ddot{X} \sin (\omega t - \varphi_x)
\end{aligned} \tag{12.175}
$$

*The amplitude of velocity and acceleration frequency responses, $\dot{X}$, $\ddot{X}$ are*

$$
\dot{X} = \frac{\omega \sqrt{k^2 + c^2 \omega^2}}{\sqrt{(k - m\omega^2)^2 + c^2 \omega^2}} Y \tag{12.176}
$$

$$
\ddot{X} = \frac{\omega^2 \sqrt{k^2 + c^2 \omega^2}}{\sqrt{(k - m\omega^2)^2 + c^2 \omega^2}} Y \tag{12.177}
$$

*which can be written as*

$$
\frac{\dot{X}}{\omega_n Y} = \frac{r \sqrt{1 + (2\xi r)^2}}{\sqrt{(1 - r^2)^2 + (2\xi r)^2}} \tag{12.178}
$$

$$
\frac{\ddot{X}}{\omega_n^2 Y} = \frac{r^2 \sqrt{1 + (2\xi r)^2}}{\sqrt{(1 - r^2)^2 + (2\xi r)^2}}. \tag{12.179}
$$

*The velocity and acceleration frequency responses (12.178) and (12.179) are plotted in Figures 12.28 and 12.29.*
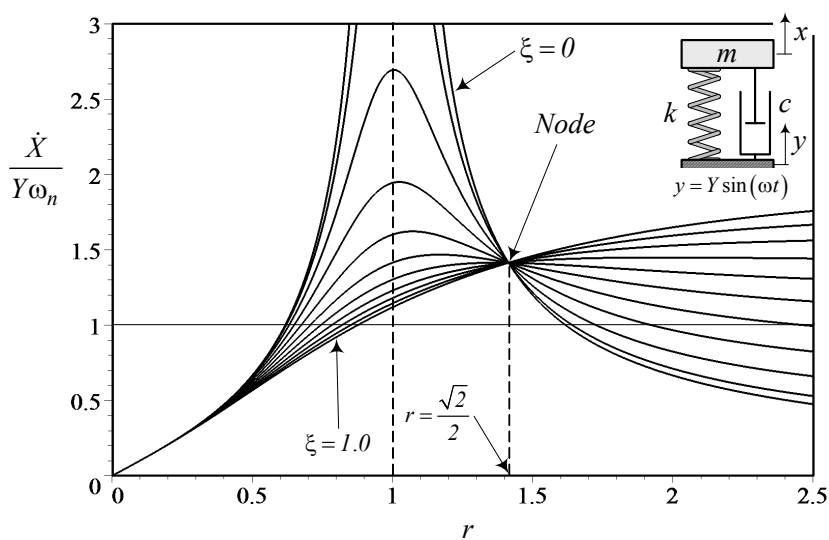
FIGURE 12.28.
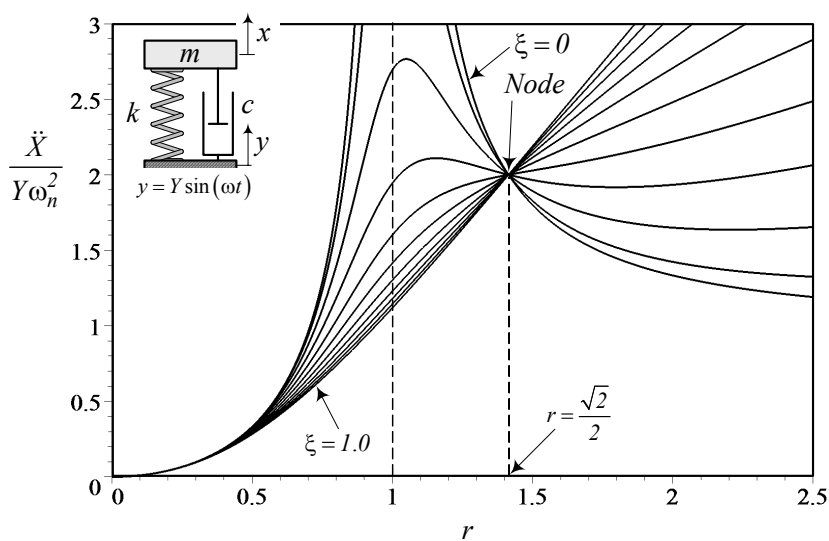


FIGURE 12.29.

*There is a point in both figures, called the **switching point** or **node**, at which the behavior of $\dot{X}$ and $\ddot{X}$ as a function of $\xi$ switches. Before the node, $\dot{X}$ and $\ddot{X}$ increase by increasing $\xi$, while they decrease after the node. To find the node, we may find the intersection between frequency response curves for $\xi = 0$ and $\xi = \infty$. We apply this method to the acceleration frequency response.*

$$\lim_{\xi \to 0} \frac{\ddot{X}}{\omega_n^2 Y} = \pm \frac{r^2}{(1 - r^2)} \tag{12.180}$$

$$\lim_{\xi \to \infty} \frac{\ddot{X}}{\omega_n^2 Y} = \pm r^2 \tag{12.181}$$

*Therefore, the frequency ratio $r$ at the intersection of these two limits is the solution of the equation*

$$r^2 \left( r^2 - 2 \right) = 0. \tag{12.182}$$

*The nodal frequency response is then equal to*

$$r = \frac{\sqrt{2}}{2}. \tag{12.183}$$

*The value of acceleration frequency response at the node is a function of $\xi$.*

$$\lim_{r \to \frac{\sqrt{2}}{2}} \frac{\ddot{X}}{\omega_n^2 Y} = \frac{\sqrt{2\xi^2 + 1}}{\sqrt{8\xi^2 + 1}} \tag{12.184}$$

*Applying the same method for the velocity frequency response results in the same nodal frequency ratio $r = \frac{\sqrt{2}}{2}$. However, the value of the frequency response at the node is different.*

$$\lim_{r \to \frac{\sqrt{2}}{2}} \frac{\dot{X}}{\omega_n Y} = \sqrt{2} \frac{\sqrt{2\xi^2 + 1}}{\sqrt{8\xi^2 + 1}} \tag{12.185}$$

**Example 442** *Relative velocity and acceleration of a base excited system.*

*We may use the relative displacement frequency response of a base excited system*

$$\begin{aligned} z &= A_3 \sin \omega t + B_3 \cos \omega t \\ &= Z \sin (\omega t - \varphi_z) \end{aligned} \tag{12.186}$$

*and calculate the relative velocity and acceleration frequency responses.*

$$\begin{aligned} \dot{z} &= A_3 \omega \cos \omega t - B_3 \omega \sin \omega t \\ &= Z \omega \cos (\omega t - \varphi_z) \\ &= \dot{Z} \cos (\omega t - \varphi_z) \end{aligned} \tag{12.187}$$

$$\begin{aligned}
\ddot{z} &= -A_3\omega^2 \sin \omega t - B_3\omega^2 \cos \omega t \\
&= -Z\omega^2 \sin (\omega t - \varphi_z) \\
&= \ddot{Z} \sin (\omega t - \varphi_z)
\end{aligned} \tag{12.188}$$

The amplitude of velocity and acceleration frequency responses, $\dot{Z}$, $\ddot{Z}$

$$\dot{Z} = \frac{m\omega^3}{\sqrt{(k - m\omega^2)^2 + c^2\omega^2}} Y \tag{12.189}$$

$$\ddot{Z} = \frac{m\omega^4}{\sqrt{(k - m\omega^2)^2 + c^2\omega^2}} Y \tag{12.190}$$

can be written as

$$\frac{\dot{Z}}{\omega_n Y} = \frac{r^3}{\sqrt{(1 - r^2)^2 + (2\xi r)^2}} \tag{12.191}$$

$$\frac{\ddot{Z}}{\omega_n^2 Y} = \frac{r^4}{\sqrt{(1 - r^2)^2 + (2\xi r)^2}}. \tag{12.192}$$

**Example 443** *Transmitted force to the base of a base excited system.*

The transmitted force $f_T$ to the ground by a base excited system, such as is shown in Figure 12.23, is equal to the sum of forces in the spring and damper.

$$\begin{aligned}
f_T &= f_k + f_c \\
&= k(x - y) + c(\dot{x} - \dot{y})
\end{aligned} \tag{12.193}$$

which based on the equation of motion (12.140) is also equal to

$$f_T = -m\ddot{x}. \tag{12.194}$$

Substituting $\ddot{x}$ from (12.175) and (12.179) shows that the frequency response of the transmitted force can be written as

$$\frac{F_T}{kY} = \frac{\omega^2 \sqrt{k^2 + c^2\omega^2}}{\sqrt{(k - m\omega^2)^2 + c^2\omega^2}} \tag{12.195}$$

$$= \frac{r^2 \sqrt{1 + (2\xi r)^2}}{\sqrt{(1 - r^2)^2 + (2\xi r)^2}}. \tag{12.196}$$

The frequency response of $\frac{F_T}{kY}$ is the same as is shown in Figure 12.29.
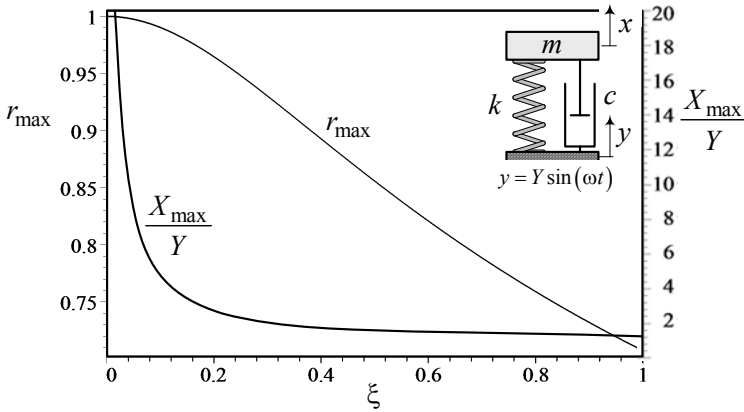
FIGURE 12.30. The peak amplitude $X_{\max}$ and the associated frequency $r_{\max}$, as a function of $\xi$.

**Example 444 ★** *Line of maxima in $X/Y$.*

*The peak value of the absolute displacement frequency response $X/Y$ happens at different $r$ depending on $\xi$. To find this relationship, we take a derivative of $X/Y$, given in Equation (12.136), with respect to $r$ and solve the equation.*

$$\frac{d}{dr}\frac{X}{Y} = \frac{2r\left(1 - r^2 - 2r^4\xi^2\right)}{\sqrt{1 + 4r^2\xi^2}\left(\left(1 - r^2\right)^2 + \left(2\xi r\right)^2\right)^{\frac{3}{2}}} = 0 \qquad (12.197)$$

*Let's indicate the peak amplitude by $X_{\max}$ and the associated frequency by $r_{\max}$. The value of $r_{\max}^2$ is*

$$r_{\max}^2 = \frac{1}{4\xi^2}\left(-1 \pm \sqrt{1 + 8\xi^2}\right) \qquad (12.198)$$

*which is only a function of $\xi$.*

*Substituting the positive sign of (12.198) in (12.136) determines the peak amplitude $X_{\max}$.*

$$\frac{X_{\max}}{Y} = \frac{2\sqrt{2}\xi^2 \sqrt[4]{8\xi^2 + 1}}{\sqrt{8\xi^2 + \left(8\xi^4 - 4\xi^2 - 1\right)\sqrt{8\xi^2 + 1} + 1}} \qquad (12.199)$$

*Figure 12.30 shows $X_{\max}$ and $r_{\max}$ as a function of $\xi$.*

**Example 445 ★** *Line of maxima in $Z/Y$.*

*The peak value of the relative displacement frequency response $Z/Y$ happens at $r > 1$ depending on $\xi$. To find this relationship, we take a derivative*

of $Z/Y$, given in Equation (12.137), with respect to $r$ and solve the equation.

$$\frac{d}{dr}\frac{Z}{Y} = \frac{2r\left(1 - r^2 - 2r^4\xi^2\right)}{\left((1-r^2)^2 + (2\xi r)^2\right)^{\frac{3}{2}}} = 0 \qquad (12.200)$$

Let's indicate the peak amplitude by $Z_{\max}$ and the associated frequency by $r_{\max}$. The value of $r_{\max}^2$ is

$$r_{\max}^2 = \frac{1}{\sqrt{1 - 2\xi^2}} \qquad (12.201)$$

which has a real value for

$$\xi < \frac{\sqrt{2}}{2}. \qquad (12.202)$$

Substituting (12.201) in (12.137) determines the peak amplitude $Z_{\max}$.

$$\frac{Z_{\max}}{Y} = \frac{1}{2\xi\sqrt{1 - 2\xi^2}} \qquad (12.203)$$

As an example, the maximum amplitude of a system with

$$
\begin{aligned}
m &= 2\,\mathrm{kg} \\
k &= 100000\,\mathrm{N/m} \\
c &= 100\,\mathrm{N\,s/m} \\
\omega_n &= 223.61\,\mathrm{rad/s} \\
\xi &= 0.1118 \\
Y &= 0.002\,\mathrm{m} \qquad (12.204)
\end{aligned}
$$

is

$$Z_{\max} = \frac{Y}{2\xi\sqrt{1 - 2\xi^2}} = 9.0585 \times 10^{-3}\,\mathrm{m} \qquad (12.205)$$

that occurs at

$$r_{\max} = \frac{1}{\sqrt[4]{1 - 2\xi^2}} = 1.0063. \qquad (12.206)$$

### 12.3.3  Eccentric Excitation

Figure 12.31 illustrates a *one*-DOF eccentric excited vibrating system with a mass $m$ supported by a suspension made of a spring $k$ and a damper $c$. There is an unbalance mass $m_e$ at a distance $e$ that is rotating with an angular velocity $\omega$. An eccentric excited vibrating system is a good model for vibration analysis of the engine of a vehicle, or any rotary motor that is mounted on a stationary base with a flexible suspension.
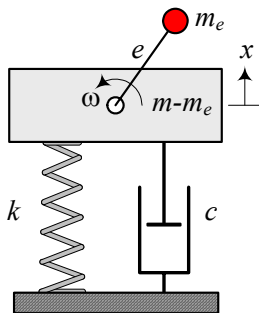
FIGURE 12.31. An eccentric excitated single-DOF system.

The absolute motion of $m$ with respect to its equilibrium position is measured by the coordinate $x$. When the lateral motion of $m$ is protected, a harmonic excitation force

$$f_x = m_e e \omega^2 \sin \omega t \tag{12.207}$$

is applied on $m$ and makes the system vibrate. The distance $e$ is called the *eccentricity* and $m_e$ is called the *eccentric mass*.

The equation of motion for the system can be expressed by

$$m\ddot{x} + c\dot{x} + kx = m_e e \omega^2 \sin \omega t \tag{12.208}$$

or

$$\ddot{x} + 2\xi \omega_n \dot{x} + \omega_n^2 x = \varepsilon e \omega^2 \sin \omega t \tag{12.209}$$

$$\varepsilon = \frac{m_e}{m}. \tag{12.210}$$

The absolute displacement responses of the system is

$$x = A_4 \sin \omega t + B_4 \cos \omega t \tag{12.211}$$

$$= X \sin (\omega t - \varphi_e) \tag{12.212}$$

which has an amplitude $X$, and phases $\varphi_e$

$$\frac{X}{e\varepsilon} = \frac{r^2}{\sqrt{(1 - r^2)^2 + (2\xi r)^2}} \tag{12.213}$$

$$\varphi_e = \tan^{-1} \frac{2\xi r}{1 - r^2} \tag{12.214}$$

Phase $\varphi_e$ indicates the angular lag of the response $x$ with respect to the excitation $m_e e \omega^2 \sin \omega t$. The frequency responses for $X$ and $\varphi_e$ as a function of $r$ and $\xi$ are plotted in Figures 12.32 and 12.33.
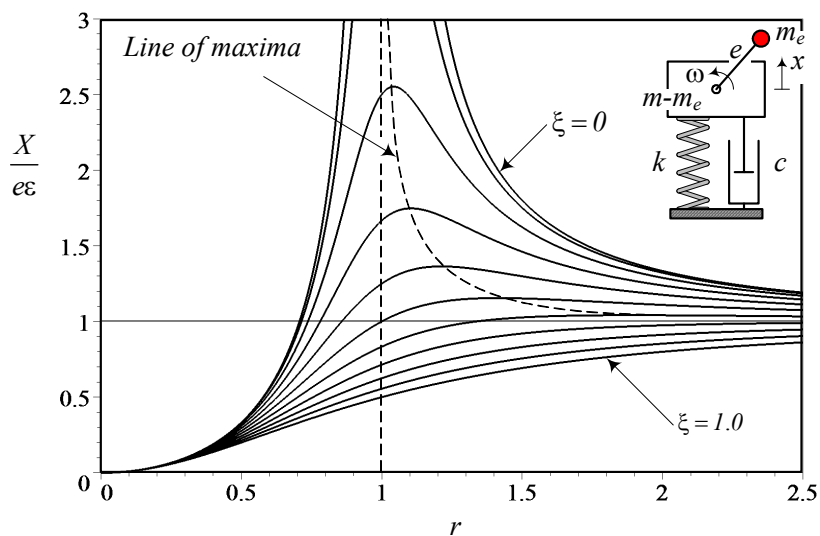
FIGURE 12.32. The position frequency response for $\dfrac{X}{e\varepsilon}$.
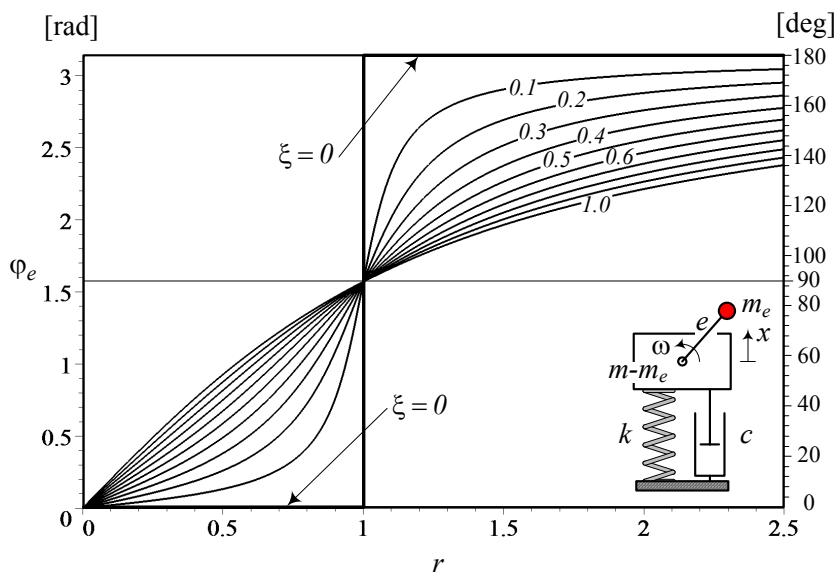


FIGURE 12.33. The frequency response for $\varphi_e$.
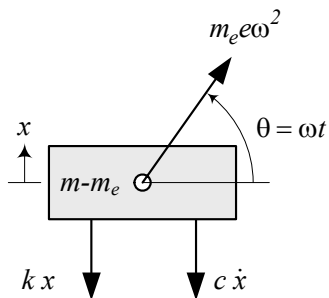
FIGURE 12.34. Free body diagram of an eccentric excited single-DOF system.

**Proof.** Employing the free body diagram of the system, as shown in Figure 12.34, and applying Newton's method in the $x$-direction generate the equation of motion

$$m\ddot{x} = -c\dot{x} - kx + m_e e\omega^2 \sin\omega t. \tag{12.215}$$

Equation (12.208) can be transformed to (12.209) by dividing over $m$ and using the following definitions for natural frequency, damping ratio, and frequency ratio.

$$\omega_n = \sqrt{\frac{k}{m}} \tag{12.216}$$

$$\xi = \frac{c}{2\sqrt{km}} \tag{12.217}$$

$$r = \frac{\omega}{\omega_n} \tag{12.218}$$

The parameter $\varepsilon = \frac{m_e}{m}$ is called the *mass ratio* and indicates the ratio between the eccentric mass $m_e$ and the total mass $m$.

The steady-state solution of Equations (12.208) can be (12.211), or (12.212). To find the amplitude and phase of the response, we substitute the solution (12.211) in the equation of motion.

$$-m\omega^2 \left( A_4 \sin\omega t + B_4 \cos\omega t \right)$$
$$+c\omega \left( A_4 \cos\omega t - B_4 \sin\omega t \right)$$
$$+k \left( A_4 \sin\omega t + B_4 \cos\omega t \right)$$
$$= m_e e\omega^2 \sin\omega t \tag{12.219}$$

The coefficients of the functions $\sin\omega t$ and $\cos\omega t$ must balance on both sides of the equation.

$$kA_4 - mA_4\omega^2 - cB_4\omega = m_e e\omega^2 \tag{12.220}$$
$$kB_4 - m\omega^2 B_4 + c\omega A_4 = 0 \tag{12.221}$$

Therefore, we find two algebraic equations to calculate $A_4$ and $B_4$.

$$\begin{bmatrix} k - \omega^2 m & -c\omega \\ c\omega & k - \omega^2 m \end{bmatrix} \begin{bmatrix} A_4 \\ B_4 \end{bmatrix} = \begin{bmatrix} e\omega^2 m_e \\ 0 \end{bmatrix} \tag{12.222}$$

Solving for the coefficients $A_4$ and $B_4$

$$\begin{aligned} \begin{bmatrix} A_4 \\ B_4 \end{bmatrix} &= \begin{bmatrix} k - \omega^2 m & -c\omega \\ c\omega & k - \omega^2 m \end{bmatrix}^{-1} \begin{bmatrix} e\omega^2 m_e \\ 0 \end{bmatrix} \\[2mm] &= \begin{bmatrix} \dfrac{k - m\omega^2 - \omega^2 m_e}{\left(k - \omega^2 m\right)^2 + c^2\omega^2} e\omega^2 m_e \\[4mm] \dfrac{-c\omega}{\left(k - \omega^2 m\right)^2 + c^2\omega^2} e\omega^2 m_e \end{bmatrix} \end{aligned} \tag{12.223}$$

provides the steady-state solution (12.211).

The amplitude $X$ and phase $\varphi_e$ can be found by

$$X = \sqrt{A_4^2 + B_4^2} \tag{12.224}$$

$$\tan \varphi_e = \frac{-B_4}{A_4} \tag{12.225}$$

which, after substituting $A_4$ and $B_4$ from (12.223), results in the following solutions.

$$X = \frac{\omega^2 e m_e}{\sqrt{\left(k - m\omega^2\right)^2 + c^2\omega^2}} \tag{12.226}$$

$$\tan \varphi_e = \frac{c\omega}{k - m\omega^2} \tag{12.227}$$

A more practical expression for $X$ and $\varphi_e$ is Equation (12.213) and (12.214), which can be found by employing $r$ and $\xi$. ∎

**Example 446** *An eccentric excited system.*
*Consider an engine with a mass $m$*

$$m = 110 \, \text{kg} \tag{12.228}$$

*that is supported by four engine mounts, each with the following equivalent stiffness and damping.*

$$k = 100000 \, \text{N/m} \tag{12.229}$$

$$c = 1000 \, \text{N s/m}. \tag{12.230}$$

*The engine is running at*

$$\omega = 5000 \, rpm \approx 523.60 \, \text{rad/s} \approx 83.333 \, \text{Hz} \tag{12.231}$$

*with the following eccentric parameters.*

$$m_e = 0.001 \,\text{kg} \tag{12.232}$$

$$e = 0.12 \,\text{m} \tag{12.233}$$

*The natural frequency $\omega_n$, damping ratio $\xi$, and mass ratio $\varepsilon$ of the system, and frequency ratio $r$ are*

$$\omega_n = \sqrt{\frac{k}{m}} = \sqrt{\frac{400000}{110}} = 60.302 \,\text{rad/s} \approx 9.6 \,\text{Hz} \tag{12.234}$$

$$\xi = \frac{c}{2\sqrt{km}} = 0.30151 \tag{12.235}$$

$$\varepsilon = \frac{m_e}{m} = \frac{0.001}{110} = 9.0909 \times 10^{-6} \tag{12.236}$$

$$r = \frac{\omega}{\omega_n} = \frac{523.60}{60.302} = 8.683 \tag{12.237}$$

*The engine's amplitude of vibration is*

$$\begin{aligned} X &= \frac{r^2 e \varepsilon}{\sqrt{(1-r^2)^2 + (2\xi r)^2}} \\ &= 1.1028 \times 10^{-6} \,\text{m.} \end{aligned} \tag{12.238}$$

*However, if the speed of the engine is at the natural frequency of the system,*

$$\omega = 576.0 \; rpm \approx 60.302 \,\text{rad/s} \approx 9.6 \,\text{Hz} \tag{12.239}$$

*then the amplitude of the engine's vibration increases to*

$$\begin{aligned} X &= \frac{r^2 e \varepsilon}{\sqrt{(1-r^2)^2 + (2\xi r)^2}} \\ &= 1.8091 \times 10^{-6} \,\text{m.} \end{aligned} \tag{12.240}$$

**Example 447** *Eccentric exciting systems.*
   *All rotating machines such as engines, turbines, generators, and turning machines can have imperfections in their rotating components or have irregular mass distribution, which creates dynamic imbalances. When the unbalanced components rotate, an eccentric load applies to the structure. The load can be decomposed into two perpendicular harmonic forces in the plane of rotation in lateral and normal directions of the suspension. If the lateral force component is balanced by a reaction, the normal component provides a harmonically variable force with an amplitude depending on the eccentricity $m_e e$. Unbalanced rotating machines are a common source of vibration excitation.*

**Example 448** *Absolute velocity and acceleration of an eccentric excited system.*

Using the position frequency response of an eccentric excited system

$$
\begin{aligned}
x &= A_4 \sin \omega t + B_4 \cos \omega t \\
&= X \sin \left( \omega t - \varphi_e \right)
\end{aligned}
\tag{12.241}
$$

we can find the velocity and acceleration frequency responses.

$$
\begin{aligned}
\dot{x} &= A_4 \omega \cos \omega t - B_4 \omega \sin \omega t \\
&= X \omega \cos \left( \omega t - \varphi_e \right) \\
&= \dot{X} \cos \left( \omega t - \varphi_e \right)
\end{aligned}
\tag{12.242}
$$

$$
\begin{aligned}
\ddot{x} &= -A_4 \omega^2 \sin \omega t - B_4 \omega^2 \cos \omega t \\
&= -X \omega^2 \sin \left( \omega t - \varphi_e \right) \\
&= \ddot{X} \sin \left( \omega t - \varphi_e \right)
\end{aligned}
\tag{12.243}
$$

The amplitude of velocity and acceleration frequency responses, $\dot{X}$, $\ddot{X}$ are

$$
\frac{\dot{X}}{e \varepsilon} = \frac{\omega^3 e m_e}{\sqrt{\left( k - m \omega^2 \right)^2 + c^2 \omega^2}}
\tag{12.244}
$$

$$
\frac{\ddot{X}}{e \varepsilon} = \frac{\omega^4 e m_e}{\sqrt{\left( k - m \omega^2 \right)^2 + c^2 \omega^2}}
\tag{12.245}
$$

which can be written as

$$
\frac{\dot{X}}{e \varepsilon \omega_n} = \frac{r^3}{\sqrt{\left( 1 - r^2 \right)^2 + \left( 2 \xi r \right)^2}}
\tag{12.246}
$$

$$
\frac{\ddot{X}}{e \varepsilon \omega_n^2} = \frac{r^4}{\sqrt{\left( 1 - r^2 \right)^2 + \left( 2 \xi r \right)^2}}.
\tag{12.247}
$$

**Example 449** *Transmitted force to the base of an eccentric excited system.*

The transmitted force

$$
f_T = F_T \sin \left( \omega t - \varphi_T \right)
\tag{12.248}
$$

to the ground by an eccentric excited system is equal to the sum of forces in the spring and damper.

$$
\begin{aligned}
f_T &= f_k + f_c \\
&= kx + c\dot{x}
\end{aligned}
\tag{12.249}
$$
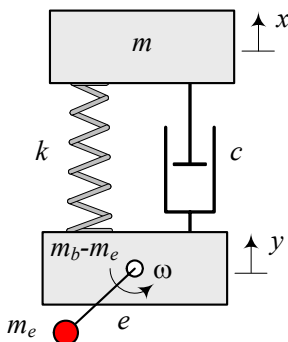
FIGURE 12.35. An eccentric base excited single-DOF system.

*Substituting $x$ and $\dot{x}$ from (12.211) shows that*

$$f_T = (kA_4 - c\omega B_4)\sin t\omega + (kB_4 + c\omega A_4)\cos t\omega \tag{12.250}$$

*therefore the amplitude of the transmitted force is*

$$
\begin{aligned}
F_T &= \sqrt{(kA_4 - c\omega B_4)^2 + (kB_4 + c\omega A_4)^2} \\
&= e\omega^2 m_e \sqrt{\frac{c^2\omega^2 + k^2}{(k - m\omega^2)^2 + c^2\omega^2}}.
\end{aligned}
\tag{12.251}
$$

*The frequency response of the transmitted force can be simplified to the following applied equation.*

$$\frac{F_T}{e\omega^2 m_e} = \frac{\sqrt{1 + (2\xi r)^2}}{\sqrt{(1 - r^2)^2 + (2\xi r)^2}} \tag{12.252}$$

## 12.3.4 ★ Eccentric Base Excitation

Figure 12.35 illustrates a *one*-DOF eccentric base excited vibrating system with a mass $m$ suspended by a spring $k$ and a damper $c$ on a base with mass $m_b$. The base has an unbalance mass $m_e$ at a distance $e$ that is rotating with angular velocity $\omega$. The eccentric base excited system is a good model for vibration analysis of different equipment that are attached to the engine of a vehicle, or any equipment mounted on a rotary motor.

Using the relative motion of $m$ with respect to the base

$$z = x - y \tag{12.253}$$

we may develop the equation of motion as

$$\frac{mm_b}{m_b + m}\ddot{z} + c\dot{z} + kz = \frac{mm_e}{m_b + m}e\omega^2 \sin \omega t \tag{12.254}$$
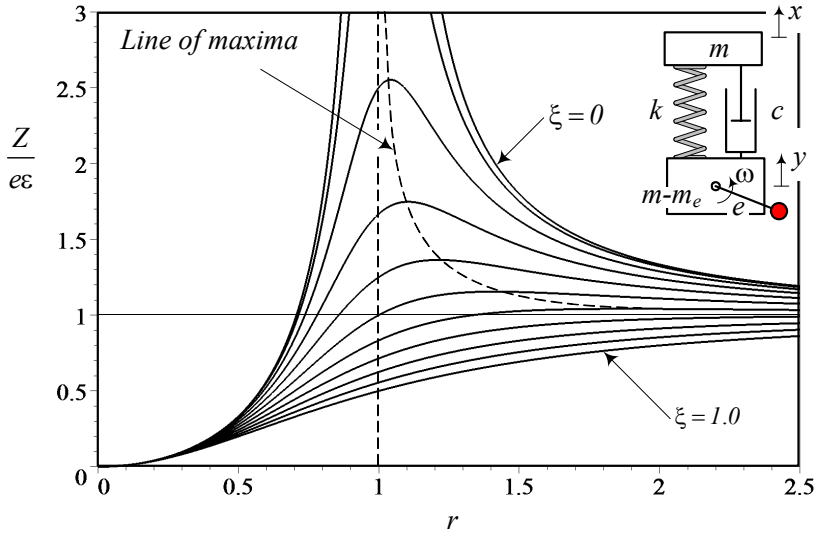
FIGURE 12.36. The position frequency response for $\dfrac{Z}{e\varepsilon}$.

or

$$\ddot{z} + 2\xi\omega_n\,\dot{z} + \omega_n^2\,z \quad = \quad \varepsilon e\omega^2 \sin\omega t \qquad (12.255)$$

$$\varepsilon \quad = \quad \frac{m_e}{m_b}. \qquad (12.256)$$

The relative displacement response of the system is

$$z \quad = \quad A_5 \sin\omega t + B_5 \cos\omega t \qquad (12.257)$$

$$\quad = \quad Z \sin\left(\omega t - \varphi_b\right) \qquad (12.258)$$

which has an amplitude $Z$ and phases $\varphi_b$.

$$\frac{Z}{e\varepsilon} \quad = \quad \frac{r^2}{\sqrt{\left(1 - r^2\right)^2 + \left(2\xi r\right)^2}} \qquad (12.259)$$

$$\varphi_b \quad = \quad \tan^{-1}\frac{2\xi r}{1 - r^2} \qquad (12.260)$$

The frequency responses for $Z$, and $\varphi_b$ as a function of $r$ and $\xi$ are plotted in Figures 12.36 and 12.37.

**Proof.** The free body diagram shown in Figure 12.38, along with Newton's method in the $x$-direction, may be used to find the equation of motion.

$$m\ddot{x} \quad = \quad -c\left(\dot{x} - \dot{y}\right) - k\left(x - y\right) \qquad (12.261)$$

$$m_b\ddot{y} \quad = \quad c\left(\dot{x} - \dot{y}\right) + k\left(x - y\right) - m_e e\omega^2 \sin\omega t \qquad (12.262)$$
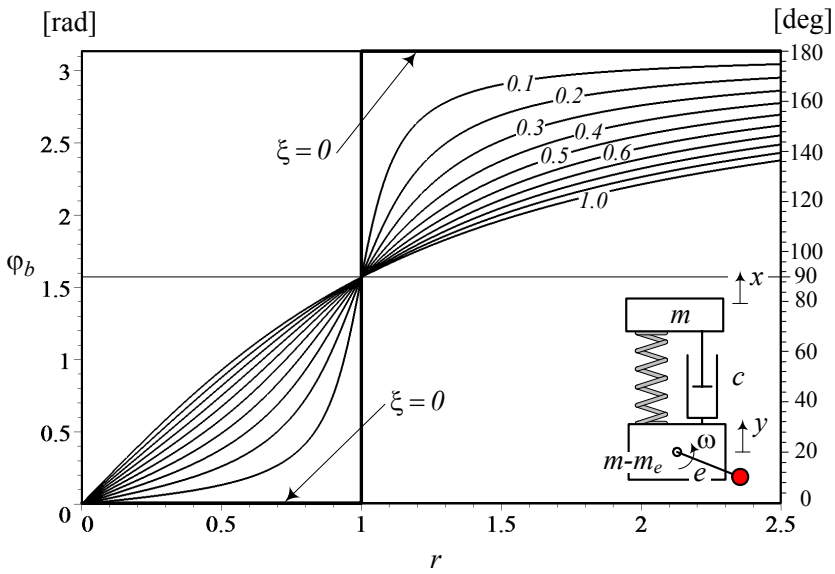
FIGURE 12.37. The frequency response for $\varphi_b$.
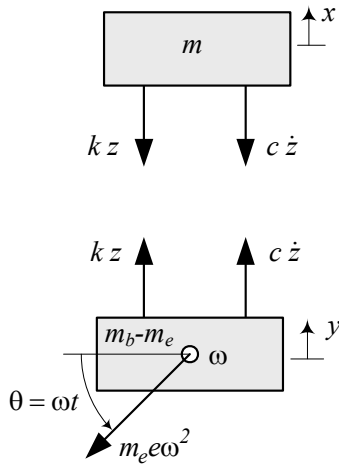


FIGURE 12.38. Free body diagram of an eccentric base excited single DOF system.

Using $z = x - y$, and
$$\ddot{z} = \ddot{x} - \ddot{y} \tag{12.263}$$
we may combine Equations (12.261) and (12.262) to find the equation of relative motion.
$$\frac{mm_b}{m_b + m}\ddot{z} + c\dot{z} + kz = \frac{mm_e}{m_b + m}e\omega^2 \sin\omega t \tag{12.264}$$

Equation (12.264) can be transformed to (12.255) if we divide it by $\frac{mm_b}{m_b+m}$ and use the following definitions:
$$\xi = \frac{c}{2\sqrt{k\dfrac{mm_b}{m_b + m}}} \tag{12.265}$$
$$\omega_n = \sqrt{k\frac{m_b + m}{mm_b}}. \tag{12.266}$$

The parameter $\varepsilon = \frac{m_e}{m_b}$ is called the *mass ratio* and indicates the ratio between the eccentric mass $m_e$ and the total base mass $m_b$.

The steady-state solution of Equation (12.255) can be (12.257). To find the amplitude and phase of the response, we substitute the solution in the equation of motion.

$$
\begin{aligned}
&-\omega^2 (A_5 \sin\omega t + B_5 \cos\omega t) \\
&+2\xi\omega_n\omega (A_5 \cos\omega t - B_5 \sin\omega t) \\
&+\omega_n^2 (A_5 \sin\omega t + B_5 \cos\omega t) \\
=\quad &\varepsilon e\omega^2 \sin\omega t
\end{aligned} \tag{12.267}
$$

The coefficients of the functions $\sin\omega t$ and $\cos\omega t$ must balance on both sides of the equation.
$$\omega_n^2 A_5 - \omega^2 A_5 - 2\xi\omega\omega_n B_5 = \varepsilon\omega^2 e \tag{12.268}$$
$$2\xi A_5\omega\omega_n - B_5\omega^2 + B_5\omega_n^2 = 0 \tag{12.269}$$

Therefore, we find two algebraic equations to calculate $A_5$ and $B_5$.
$$\begin{bmatrix} \omega_n^2 - \omega^2 & -2\xi\omega\omega_n \\ 2\xi\omega\omega_n & \omega_n^2 - \omega^2 \end{bmatrix}\begin{bmatrix} A_5 \\ B_5 \end{bmatrix} = \begin{bmatrix} \varepsilon\omega^2 e \\ 0 \end{bmatrix} \tag{12.270}$$
Solving for the coefficients $A_5$ and $B_5$

$$
\begin{aligned}
\begin{bmatrix} A_5 \\ B_5 \end{bmatrix} &= \begin{bmatrix} \omega_n^2 - \omega^2 & -2\xi\omega\omega_n \\ 2\xi\omega\omega_n & \omega_n^2 - \omega^2 \end{bmatrix}^{-1}\begin{bmatrix} \varepsilon\omega^2 e \\ 0 \end{bmatrix} \\
&= \begin{bmatrix} \dfrac{\omega_n^2 - \omega^2}{(\omega_n^2 - \omega^2)^2 + (2\xi\omega\omega_n)^2}\varepsilon\omega^2 e \\[4mm] \dfrac{-2\xi\omega\omega_n}{(\omega_n^2 - \omega^2)^2 + (2\xi\omega\omega_n)^2}\varepsilon\omega^2 e \end{bmatrix}
\end{aligned} \tag{12.271}
$$

provides the steady-state solution (12.255).

The amplitude $Z$ and phase $\varphi_b$ can be found by

$$X = \sqrt{A_5^2 + B_5^2} \tag{12.272}$$

$$\tan \varphi_b = \frac{-B_5}{A_5} \tag{12.273}$$

which, after substituting $A_5$ and $B_5$ from (12.271), results in the following solutions:

$$Z = \frac{\omega^2 e \varepsilon}{\sqrt{(\omega_n^2 - \omega^2)^2 + (2\xi\omega\omega_n)^2}} \tag{12.274}$$

$$\tan \varphi_b = \frac{2\xi\omega\omega_n}{\omega_n^2 - \omega^2} \tag{12.275}$$

Equations (12.274) and (12.275) can be simplified to more practical expressions (12.259) and (12.260) by employing $r = \frac{\omega}{\omega_n}$. ∎

**Example 450 ★** *A base eccentric excited system.*
*Consider an engine with a mass $m_b$*

$$m_b = 110\,\mathrm{kg} \tag{12.276}$$

*and an air intake device with a mass*

$$m = 2\,\mathrm{kg} \tag{12.277}$$

*that is mounted on the engine using an elastic mounts, with the following equivalent stiffness and damping.*

$$k = 10000\,\mathrm{N/m} \tag{12.278}$$
$$c = 100\,\mathrm{N\,s/m.} \tag{12.279}$$

*The engine is running at*

$$\omega = 576.0\ rpm \approx 60.302\,\mathrm{rad/s} \approx 9.6\,\mathrm{Hz} \tag{12.280}$$

*with the following eccentric parameters.*

$$m_e = 0.001\,\mathrm{kg} \tag{12.281}$$
$$e = 0.12\,\mathrm{m} \tag{12.282}$$

*The natural frequency $\omega_n$, damping ratio $\xi$, and mass ratio $\varepsilon$ of the system,*

*and frequency ratio $r$ are*

$$\omega_n = \sqrt{k \frac{m_b + m}{m m_b}} = 100 \, \text{rad/s} \approx 15.9 \, \text{Hz} \qquad (12.283)$$

$$\xi = \frac{c}{2\sqrt{k \frac{m m_b}{m_b + m}}} = 0.49995 \qquad (12.284)$$

$$\varepsilon = \frac{m_e}{m_b} = 9.0909 \times 10^{-6} \qquad (12.285)$$

$$r = \frac{\omega}{\omega_n} = 0.60302. \qquad (12.286)$$

*The relative amplitude of the device's vibration is*

$$Z = \frac{e\varepsilon r^2}{\sqrt{(1 - r^2)^2 + (2\xi r)^2}} = 4.525 \times 10^{-7} \, \text{m}. \qquad (12.287)$$

**Example 451 ★** *Absolute displacement of the upper mass in an eccentric base excited system.*
   *Equation (12.261)*

$$\ddot{x} = -\frac{c}{m}(\dot{x} - \dot{y}) - \frac{k}{m}(x - y)$$

$$= -\frac{c}{m}\dot{z} - \frac{k}{m}z \qquad (12.288)$$

*along with the solution (12.257) may be used to calculate the displacement frequency response of the upper mass $m$ in the eccentric base excited system shown in Figure 12.35. Assuming a steady-state displacement*

$$x = A_6 \sin \omega t + B_6 \cos \omega t \qquad (12.289)$$

$$= X \sin(\omega t - \varphi_{bx}) \qquad (12.290)$$

*we have*

$$-\omega^2 (A_6 \sin \omega t + B_6 \cos \omega t) = -\frac{c}{m}\dot{z} - \frac{k}{m}z$$

$$= -\frac{c}{m}\omega (A_5 \cos \omega t - B_5 \sin \omega t)$$

$$-\frac{k}{m}(A_5 \sin \omega t + B_5 \cos \omega t)$$

$$= \left(\frac{c}{m}\omega B_5 - \frac{k}{m}A_5\right) \sin t\omega$$

$$+ \left(-\frac{k}{m}B_5 - \frac{c}{m}\omega A_5\right) \cos t\omega \qquad (12.291)$$

*and therefore,*

$$-\omega^2 A_6 \;=\; \frac{c}{m}\omega B_5 - \frac{k}{m}A_5 \tag{12.292}$$

$$-\omega^2 B_6 \;=\; -\frac{k}{m}B_5 - \frac{c}{m}\omega A_5. \tag{12.293}$$

*Substituting $A_5$ and $B_5$ from (12.271) and using*

$$X \;=\; \sqrt{A_6^2 + B_6^2} \tag{12.294}$$

$$\tan\varphi_{bx} \;=\; \frac{-B_6}{A_6} \tag{12.295}$$

*shows that*

$$A_6 \;=\; -\frac{2c\xi\omega^2\omega_n + k\left(\omega_n^2 - \omega^2\right)}{\left(\omega_n^2 - \omega^2\right)^2 + \left(2\xi\omega\omega_n\right)^2}\frac{1}{m}\varepsilon e \tag{12.296}$$

$$B_6 \;=\; \frac{-c\left(\omega_n^2 - \omega^2\right) + 2k\xi\omega_n}{\left(\omega_n^2 - \omega^2\right)^2 + \left(2\xi\omega\omega_n\right)^2}\frac{1}{m}\varepsilon\omega e \tag{12.297}$$

*the amplitude $X$ of steady-state vibration of the upper mass in an eccentric base excited system is*

$$X = \frac{\sqrt{c^2\omega^2 + k^2}}{\sqrt{\left(\omega_n^2 - \omega^2\right)^2 + \left(2\xi\omega\omega_n\right)^2}}\frac{\varepsilon}{m}e. \tag{12.298}$$

## 12.3.5   ★ *Classification for the Frequency Responses of One-DOF Forced Vibration Systems*

A harmonically excited *one*-DOF systems can be one of the four systems shown in Figure 12.39 as a concise version of Figure 12.14. The dimensionless amplitude of different applied steady-state responses of these systems is equal to one of the following equations (12.299)-(12.306), and the phase of the motion is equal to one of the equations (12.307)-(12.310).

$$S_0 \;=\; \frac{1}{\sqrt{\left(1 - r^2\right)^2 + \left(2\xi r\right)^2}} \tag{12.299}$$

$$S_1 \;=\; \frac{r}{\sqrt{\left(1 - r^2\right)^2 + \left(2\xi r\right)^2}} \tag{12.300}$$

$$S_2 \;=\; \frac{r^2}{\sqrt{\left(1 - r^2\right)^2 + \left(2\xi r\right)^2}} \tag{12.301}$$

$$S_3 \;=\; \frac{r^3}{\sqrt{\left(1 - r^2\right)^2 + \left(2\xi r\right)^2}} \tag{12.302}$$

| Base excitation | Eccentric excitation | Eccentric base excitation | Forced excitation |
|:---:|:---:|:---:|:---:|
| (a) | (b) | (c) | (d) |
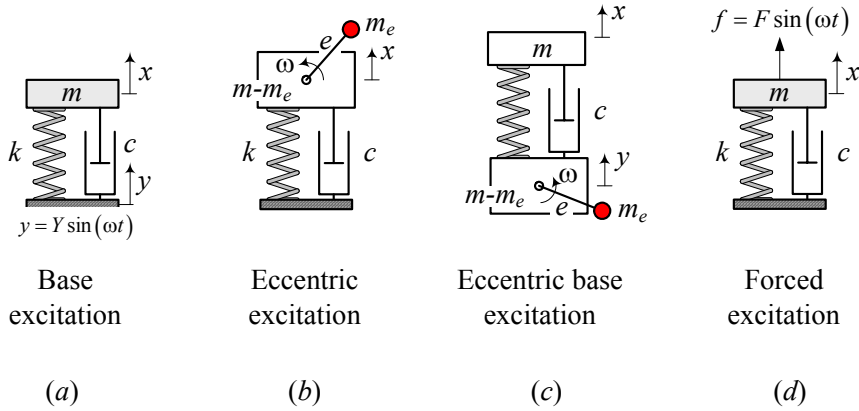
FIGURE 12.39. The four practical types of *one* DOF harmonically excited systems: *a*−base excitation, *b*−eccentric excitation, *c*−eccentric base excitation, *d*−forced excitation.

$$S_4 = \frac{r^4}{\sqrt{(1-r^2)^2 + (2\xi r)^2}} \tag{12.303}$$

$$G_0 = \frac{\sqrt{1+(2\xi r)^2}}{\sqrt{(1-r^2)^2 + (2\xi r)^2}} \tag{12.304}$$

$$G_1 = \frac{r\sqrt{1+(2\xi r)^2}}{\sqrt{(1-r^2)^2 + (2\xi r)^2}} \tag{12.305}$$

$$G_2 = \frac{r^2\sqrt{1+(2\xi r)^2}}{\sqrt{(1-r^2)^2 + (2\xi r)^2}} \tag{12.306}$$

$$\Phi_0 = \tan^{-1}\frac{2\xi r}{1-r^2} \tag{12.307}$$

$$\Phi_1 = \tan^{-1}\frac{1-r^2}{-2\xi r} \tag{12.308}$$

$$\Phi_2 = \tan^{-1}\frac{-2\xi r}{1-r^2} \tag{12.309}$$

$$\Phi_3 = \tan^{-1}\frac{2\xi r^3}{(1-r^2)^2 + (2\xi r)^2} \tag{12.310}$$

The function $S_0$ and $G_0$ are the main parts in all the amplitude frequency responses. To have a sense about the behavior of different responses, we use

plot them as a function of $r$ and using $\xi$ as a parameter. Mass $m$, stiffness $k$, and damper $c$ of the system are fixed and hence, the excitation frequency $\omega$ is the only variable. We combine $m$, $k$, $c$, $\omega$ and define two parameters $r$ and $\xi$ to express frequency responses by two variable functions.

To develop a clear classification let's indicate the frequency responses related to the systems shown in Figure 12.39 by adding a subscript and express their different responses as follow:

1— For a *base excitation system*, we usually use the frequency responses of the relative and absolute kinematics $Z_B$, $\dot{Z}_B$, $\ddot{Z}_B$, $X_B$, $\dot{X}_B$, $\ddot{X}_B$, along with the transmitted force frequency response $F_{T_B}$.

2— For an *eccentric excitation system*, we usually use the frequency responses of the absolute kinematics $X_E$, $\dot{X}_E$, $\ddot{X}_E$, along with the transmitted force frequency response $F_{T_E}$.

3— For an *eccentric base excitation system*, we usually use the frequency responses of the relative and absolute kinematics $Z_R$, $\dot{Z}_R$, $\ddot{Z}_R$, $X_R$, $\dot{X}_R$, $\ddot{X}_R$, $Y_R$, $\dot{Y}_R$, $\ddot{Y}_R$, along with the transmitted force frequency response $F_{T_R}$.

4— For a *forced excitation system*, we usually use the frequency responses of the absolute kinematics $X_F$, $\dot{X}_F$, $\ddot{X}_F$, along with the transmitted force frequency response $F_{T_F}$

The frequency response of different features of the four systems in Figure 12.39 may be summarized and labeled as follows:

$$S_0 = \frac{X_F}{F/k} \tag{12.311}$$

$$S_1 = \frac{\dot{X}_F}{F/\sqrt{km}} \tag{12.312}$$

$$S_2 = \frac{\ddot{X}_F}{F/m} = \frac{Z_B}{Y} = \frac{X_E}{e\varepsilon_E} = \frac{Z_R}{e\varepsilon_R} \tag{12.313}$$

$$S_3 = \frac{\dot{Z}_B}{\omega_n Y} = \frac{\dot{X}_E}{e\varepsilon_E \omega_n} = \frac{\dot{Z}_R}{e\varepsilon_R \omega_n} \tag{12.314}$$

$$S_4 = \frac{\ddot{Z}_B}{\omega_n^2 Y} = \frac{\ddot{X}_E}{e\varepsilon_E \omega_n^2} = \frac{\ddot{Z}_R}{e\varepsilon_R \omega_n^2} \tag{12.315}$$

$$G_0 = \frac{F_{T_F}}{F} = \frac{X_B}{Y} \tag{12.316}$$

$$G_1 = \frac{\dot{X}_B}{\omega_n Y} \tag{12.317}$$

$$G_2 = \frac{\ddot{X}_B}{\omega_n^2 Y} = \frac{F_{T_B}}{kY} = \frac{F_{T_E}}{e\omega_n^2 m_e} = \frac{F_{T_R}}{e\omega_n^2 m_e}\left(1 + \frac{m_b}{m}\right) \tag{12.318}$$

Figures A.1-A.8 in Appendix A visualize the frequency responses used in analysis and designing of the systems. However, the exact value of the responses should be found from the associated equations.

**Proof.** The equations of motion for a harmonically forced vibrating *one* DOF system is always equal to

$$m\ddot{q} + c\dot{q} + kq = f(q, \dot{q}, t) \qquad (12.319)$$

where, the variable $q$ is a general coordinate to show the absolute displacement $x$, or relative displacement $z = x - y$. The forcing term $f(x, \dot{x}, t)$ is a harmonic function which in the general case can be a combination of $\sin \omega t$ and $\cos \omega t$, where $\omega$ is the excitation frequency.

$$f(q, \dot{q}, t) = a \sin \omega t + b \cos \omega t. \qquad (12.320)$$

Depending on the system and the frequency response we are looking for, the coefficients $a$ and $b$ are zero, constant, or proportional to $\omega$, $\omega^2$, $\omega^3$, $\omega^4$, $\cdots$, $\omega^n$. To cover every practical harmonically forced vibrating systems, let's assume

$$a = a_0 + a_1\omega + a_2\omega^2 \qquad (12.321)$$
$$b = b_0 + b_1\omega + b_2\omega^2. \qquad (12.322)$$

We usually divide the equation of motion (12.319) by $m$ to express that with $\xi$ and $\omega_n$

$$\ddot{q} + 2\xi\omega_n\dot{q} + \omega_n^2 q = \left(A_0 + A_1\omega + A_2\omega^2\right)\sin \omega t$$
$$+ \left(B_0 + B_1\omega + B_2\omega^2\right)\cos \omega t \qquad (12.323)$$

where,

$$A_0 + A_1\omega + A_2\omega^2 = \frac{1}{m}\left(a_0 + a_1\omega + a_2\omega^2\right) \qquad (12.324)$$

$$B_0 + B_1\omega + B_2\omega^2 = \frac{1}{m}\left(b_0 + b_1\omega + b_2\omega^2\right). \qquad (12.325)$$

The solution of the equation of motion would be a harmonic response with unknown coefficients.

$$q = A \sin \omega t + B \cos \omega t \qquad (12.326)$$
$$= Q \sin(\omega t - \varphi) \qquad (12.327)$$

To find the steady-state amplitude of the response $Q$

$$Q = \sqrt{A^2 + B^2} \qquad (12.328)$$

$$\varphi = \tan^{-1}\frac{-B}{A} \qquad (12.329)$$

we should substitute the solution in the equation of motion.

$$-\omega^2 \left(A \sin \omega t + B \cos \omega t\right) + 2\xi \omega_n \omega \left(A \cos \omega t - B \sin \omega t\right)$$
$$+\omega_n^2 \left(A \sin \omega t + B \cos \omega t\right)$$
$$= \left(A_0 + A_1\omega + A_2\omega^2\right) \sin \omega t + \left(B_0 + B_1\omega + B_2\omega^2\right) \cos \omega t \quad (12.330)$$

The coefficients of the functions $\sin \omega t$ and $\cos \omega t$ must balance on both sides of the equation.

$$\omega_n^2 A - \omega^2 A - 2\xi \omega \omega_n B = A_0 + A_1\omega + A_2\omega^2 \quad (12.331)$$
$$2\xi A\omega\omega_n - B\omega^2 + B\omega_n^2 = B_0 + B_1\omega + B_2\omega^2 \quad (12.332)$$

Therefore, we find two algebraic equations to calculate $A$ and $B$.

$$\begin{bmatrix} \omega_n^2 - \omega^2 & -2\xi\omega\omega_n \\ 2\xi\omega\omega_n & \omega_n^2 - \omega^2 \end{bmatrix} \begin{bmatrix} A \\ B \end{bmatrix} = \begin{bmatrix} A_0 + A_1\omega + A_2\omega^2 \\ B_0 + B_1\omega + B_2\omega^2 \end{bmatrix} \quad (12.333)$$

Solving for the coefficients $A$ and $B$

$$\begin{bmatrix} A \\ B \end{bmatrix} = \begin{bmatrix} \omega_n^2 - \omega^2 & -2\xi\omega\omega_n \\ 2\xi\omega\omega_n & \omega_n^2 - \omega^2 \end{bmatrix}^{-1} \begin{bmatrix} A_0 + A_1\omega + A_2\omega^2 \\ B_0 + B_1\omega + B_2\omega^2 \end{bmatrix}$$
$$= \begin{bmatrix} \dfrac{Z_1}{\left(1 - r^2\right)^2 + \left(2\xi r\right)^2} \\[4mm] \dfrac{Z_2}{\left(1 - r^2\right)^2 + \left(2\xi r\right)^2} \end{bmatrix} \quad (12.334)$$

$$Z_1 = 2\xi r \frac{1}{\omega_n^2} \left(B_2\omega^2 + B_1\omega + B_0\right)$$
$$+ \frac{1}{\omega_n^2} \left(1 - r^2\right) \left(A_2\omega^2 + A_1\omega + A_0\right) \quad (12.335)$$

$$Z_2 = \frac{1}{\omega_n^2} \left(1 - r^2\right) \left(B_2\omega^2 + B_1\omega + B_0\right)$$
$$- 2\xi r \frac{1}{\omega_n^2} \left(A_2\omega^2 + A_1\omega + A_0\right) \quad (12.336)$$

provides the steady-state solution amplitude $Q$ and phase $\varphi$

$$Q = \sqrt{A^2 + B^2} \quad (12.337)$$
$$\tan \varphi = \frac{-B}{A}. \quad (12.338)$$

We are able to reproduce any of the steady-state responses $S_i$ and $G_i$ by setting the coefficients $A_0$, $A_1$, $A_2$, $B_0$, $B_1$, and $B_2$ properly. ∎

**Example 452 ★** *Base excited frequency responses.*

   A one DOF base excited vibrating system is shown in Figure 12.23. The equation of relative motion $z = x - y$ with a harmonic excitation $y = Y \sin \omega t$ is

$$\ddot{z} + 2\xi\omega_n \dot{z} + \omega_n^2 z = \omega^2 Y \sin \omega t. \tag{12.339}$$

*This equation can be found from Equation (12.323) if*

$$
\begin{aligned}
A_0 &= 0 \\
A_1 &= 0 \\
A_2 &= Y \\
B_0 &= 0 \\
B_1 &= 0 \\
B_2 &= 0.
\end{aligned}
\tag{12.340}
$$

*So, the frequency response of the system would be*

$$
\begin{aligned}
Z &= Q = \sqrt{A^2 + B^2} \\
&= \frac{r^2}{\sqrt{(1 - r^2)^2 + (2\xi r)^2}} Y
\end{aligned}
\tag{12.341}
$$

*because,*

$$
\begin{bmatrix} A \\ B \end{bmatrix} = 
\begin{bmatrix} \dfrac{Z_1}{(1 - r^2)^2 + (2\xi r)^2} \\[3mm] \dfrac{Z_2}{(1 - r^2)^2 + (2\xi r)^2} \end{bmatrix}
\tag{12.342}
$$

$$
\begin{aligned}
Z_1 &= r^2 \left(1 - r^2\right) Y \tag{12.343} \\
Z_2 &= 2\xi r^3 Y. \tag{12.344}
\end{aligned}
$$

## 12.4   Time Response of Vibrating Systems

Linear vibrating systems have a general equation of motion as the set of differential equations,

$$[m]\ddot{\mathbf{x}} + [c]\dot{\mathbf{x}} + [k]\mathbf{x} = \mathbf{F} \tag{12.345}$$

with the following initial conditions.

$$
\begin{aligned}
\mathbf{x}(0) &= \mathbf{x}_0 \tag{12.346} \\
\dot{\mathbf{x}}(0) &= \dot{\mathbf{x}}_0 \tag{12.347}
\end{aligned}
$$

The time response of the system is the solution $\mathbf{x} = \mathbf{x}(t), t > 0$ for a set of coupled ordinary differential equations. Such a problem is called an *initial-value problem.*

Consider a *one*-DOF vibrating system

$$m\ddot{x} + c\dot{x} + kx = f(x, \dot{x}, t) \tag{12.348}$$

with the initial conditions

$$x(0) = x_0 \tag{12.349}$$
$$\dot{x}(0) = \dot{x}_0. \tag{12.350}$$

The coefficients $m, c, k$ are assumed constant, although, they may be functions of time in more general problems. The solution of such a problem, $x = x(t), t > 0$, is unique.

The *order* of an equation is the highest number of derivatives. In mechanical vibrations of lumped models, we work with a set of second-order differential equations. If $x_1(t)$, $x_2(t)$, $\cdots$, $x_n(t)$, are solutions of an $n$-order equation, then its general solution is

$$x(t) = a_1 x_1(t) + a_2 x_2(t) + \cdots + a_n x_n(t). \tag{12.351}$$

When $f = 0$, the equation is called *homogeneous,*

$$m\ddot{x} + c\dot{x} + kx = 0 \tag{12.352}$$

otherwise it is *non-homogeneous.* The solution of the non-homogeneous equation (12.348) is equal to

$$x(t) = x_h(t) + x_p(t) \tag{12.353}$$

where, $x_h(t)$ is the *homogeneous solution,* and $x_p(t)$ is the *particular solution.* In mechanical vibration, the homogeneous equation is called *free vibration* and its solution is called *free vibration response.* The non-homogeneous equation is called *forced vibration* and its solution is called *forced vibration response.*

An exponential function

$$x = e^{\lambda t} \tag{12.354}$$

satisfies every homogeneous linear differential equation. Therefore, the homogeneous response of the second order equation (12.352) is

$$x_h(t) = a_1 e^{\lambda_1 t} + a_2 e^{\lambda_2 t} \tag{12.355}$$

where the constants $a_1$ and $a_2$ depend on the initial conditions. The parameters $\lambda_1$ and $\lambda_2$ are called *characteristic parameters* or *eigenvalues* of the system The eigenvalues are the solution of an algebraic equation, called a *characteristic equation,* which is the result of substituting the solution

(12.354) in Equation (12.352). The characteristic equation is the condition to make the solution (12.354) satisfy the equation of motion (12.352).

A general particular solution of a forced equation is hard to find, however, we know that the forcing function $f = f(t)$ is a combination of the following functions:

1− a constant, such as $f = a$
2− a polynomial in $t$, such as $f = a_0 + a_1 t + a_2 t^2 + \cdots + a_n t^n$
3− an exponential function, such as $f = e^{at}$
4− a harmonic function, such as $f = F_1 \sin at + F_2 \cos at$

if the particular solution $x_p(t)$ has the same form as a forcing term.

1− $x_p(t) =$ a constant, such as $x_p(t) = C$
2− $x_p(t) =$ a polynomial of the same degree, such as $x_p(t) = C_0 + C_1 t + C_2 t^2 + \cdots + C_n t^n$
3− $x_p(t) =$ an exponential function, such as $x_p(t) = C e^{at}$
4− $x_p(t) =$ a harmonic function, such as $x_p(t) = A \sin at + B \cos at$.

If the system is force free, or the forcing term disappears after a while, the solution of the equation is called *time response* or *transient response*. The initial conditions are important in transient response.

When the system has some damping, the effect of initial conditions disappears after a while, in both transient and forced vibration responses, and a steady-state response remains. If the forcing term is harmonic, then the steady-state solution is called frequency response.

**Example 453** *A homogeneous solution of a second-order linear equation.*
*Consider a system with the following equation of motion:*

$$\ddot{x} + \dot{x} - 2x \;=\; 0 \tag{12.356}$$
$$x_0 \;=\; 1 \tag{12.357}$$
$$\dot{x}_0 \;=\; 7 \tag{12.358}$$

*To find the solution, we substitute an exponential solution $x = e^{\lambda t}$ in the equation of motion and find the characteristic equation.*

$$\lambda^2 + \lambda - 2 = 0 \tag{12.359}$$

*The eigenvalues are*
$$\lambda_{1,2} = 1, -2 \tag{12.360}$$

*and therefore, the solution is*
$$x = a_1 e^t + a_2 e^{-2t}. \tag{12.361}$$

*Taking a derivative*
$$\dot{x} = a_1 e^t - 2a_2 e^{-2t} \tag{12.362}$$
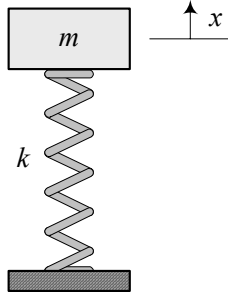
FIGURE 12.40. A mass-spring, single degree-of-freedom vibrating system.

*and employing the initial conditions*

$$1 = a_1 + a_2 \tag{12.363}$$
$$7 = a_1 - 2a_2 \tag{12.364}$$

*provides the constants $a_1$, $a_2$, and the solution $x = x(t)$.*

$$a_1 = 3 \tag{12.365}$$
$$a_2 = -2 \tag{12.366}$$
$$x = 3e^t - 2e^{-2t} \tag{12.367}$$

**Example 454** *Natural frequency.*

*Consider a free mass-spring system such as the one shown in Figure 12.40. The system is undamped and free of excitation forces, so its equation of motion is*

$$m\ddot{x} + kx = 0. \tag{12.368}$$

*To find the solution, let's try a harmonic solution with an unknown frequency.*

$$x = A \sin \Omega t + B \cos \Omega t \tag{12.369}$$

*Substituting (12.369) in (12.368) provides*

$$-\Omega^2 m \left( A \sin \Omega t + B \cos \Omega t \right) + k \left( A \sin \Omega t + B \cos \Omega t \right) = 0 \tag{12.370}$$

*which can be collected as*

$$\left( Bk - Bm\Omega^2 \right) \cos \Omega t + \left( Ak - Am\Omega^2 \right) \sin \Omega t = 0. \tag{12.371}$$

*The coefficients of $\sin \Omega t$ and $\cos \Omega t$ must be zero, and hence,*

$$\Omega = \sqrt{\frac{k}{m}} \tag{12.372}$$
$$x = A \sin \sqrt{\frac{k}{m}} t + B \cos \sqrt{\frac{k}{m}} t. \tag{12.373}$$

The frequency $\Omega = \sqrt{k/m}$ is the frequency of vibration of a free and un-damped mass-spring system. It is called **natural frequency** and is shown by a special character $\omega_n$.

$$\omega_n = \sqrt{\frac{k}{m}} \tag{12.374}$$

A system has as many natural frequencies as its degrees of freedom.

**Example 455** *Free vibration of a single-DOF system.*
   *The simplest free vibration equation of motion is*

$$m\ddot{x} + c\dot{x} + kx = 0 \tag{12.375}$$

*which is equivalent to*

$$\ddot{x} + 2\xi\omega_n\dot{x} + \omega_n^2 x = 0. \tag{12.376}$$

*The response of a system to free vibration is called **transient response** and depends solely on the initial conditions $x_0 = x(0)$ and $\dot{x}_0 = \dot{x}(0)$.*
   *To determine the solution of the linear equation (12.375), we may search for a solution in an exponential form.*

$$x = A e^{\lambda t} \tag{12.377}$$

*Substituting (12.377) in (12.376) provides the characteristic equation*

$$\lambda^2 + 2\xi\omega_n\lambda + \omega_n^2 = 0 \tag{12.378}$$

*to find the eigenvalues $\lambda_{1,2}$.*

$$\lambda_{1,2} = -\xi\omega_n \pm \omega_n\sqrt{\xi^2 - 1} \tag{12.379}$$

*Therefore, the general solution for Equation (12.376) is*

$$\begin{aligned}
x &= A_1 e^{\lambda_1 t} + A_2 e^{\lambda_2 t} \\
&= A_1 e^{\left(-\xi\omega_n + \omega_n\sqrt{\xi^2-1}\right)t} + A_2 e^{\left(-\xi\omega_n - \omega_n\sqrt{\xi^2-1}\right)t} \\
&= e^{-\xi\omega_n t}\left(A_1 e^{i\omega_d t} + A_2 e^{-i\omega_d t}\right) \tag{12.380}
\end{aligned}$$
$$\omega_d = \omega_n\sqrt{1 - \xi^2} \tag{12.381}$$

*where $\omega_d$ is called **damped natural frequency**.*
   *By using the Euler equation*

$$e^{i\alpha} = \cos\alpha + i\sin\alpha \tag{12.382}$$

*we may modify solution (12.380) to the following forms:*

$$\begin{aligned}
x &= e^{-\xi\omega_n t}\left(B_1 \sin\omega_d t + B_2 \cos\omega_d t\right) \tag{12.383} \\
x &= B e^{-\xi\omega_n t}\sin\left(\omega_d t + \phi\right) \tag{12.384}
\end{aligned}$$

*where*

$$B_1 = i(A_1 - A_2) \tag{12.385}$$

$$B_2 = A_1 + A_2 \tag{12.386}$$

$$B = \sqrt{B_1^2 + B_2^2} \tag{12.387}$$

$$\phi = \tan^{-1}\frac{B_2}{B_1}. \tag{12.388}$$

*Because the displacement $x$ is a real physical quantity, coefficients $B_1$ and $B_2$ in Equation (12.383) must also be real. This requires that $A_1$ and $A_2$ be complex conjugates. The motion described by Equation (12.384) consists of a harmonic motion of frequency $\omega_d = \omega_n\sqrt{1-\xi^2}$ and a decreasing amplitude $Be^{-\xi\omega_n t}$.*

**Example 456** *Under-damped, critically-damped, and over-damped systems.*

*The time response of a damped one-DOF system is given by Equation (12.380). The solution can be transformed to Equation (12.383) as long as $\xi < 1$.*

*The value of a damping ratio controls the type of time response of a one-DOF system. Depending on the value of damping, there are three major solution categories:*

1— *under-damped,*
2— *critically-damped, and*
3— *over-damped.*

*An **under damped** system is when $\xi < 1$. For such a system, the characteristic parameters (12.379) are a complex conjugate*

$$\lambda_{1,2} = -\xi\omega_n \pm i\omega_n\sqrt{1-\xi^2} \tag{12.389}$$

*and therefore, the general solution (12.380)*

$$x = A_1\,e^{\lambda_1 t} + A_2\,e^{\lambda_2 t} \tag{12.390}$$

*can be transformed to (12.383)*

$$x = e^{-\xi\omega_n t}\left(B_1\sin\omega_d t + B_2\cos\omega_d t\right). \tag{12.391}$$

*An under-damped system has an oscillatory time response with a decaying amplitude as shown in Figure 12.41 for $\xi = 0.15$, $\omega_n = 20\pi$ rad, $x_0 = 1$, and $\dot{x}_0 = 0$. The exponential function $e^{\pm\xi\omega_n t}$ is an envelope for the curve of response.*

*A **critically damped** system is when $\xi = 1$. For such a system, the characteristic parameters (12.379) are equal.*

$$\lambda = \lambda_{1,2} = -\omega_n \tag{12.392}$$
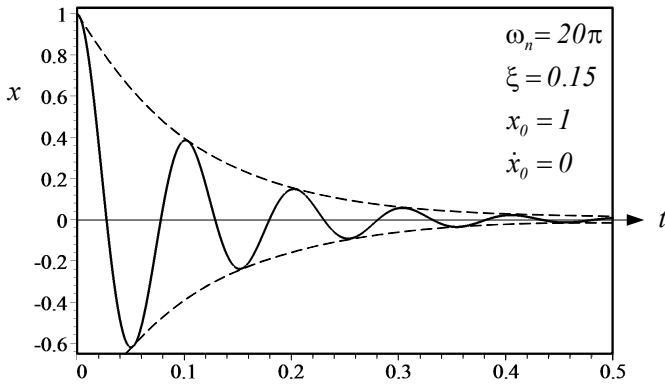
FIGURE 12.41. A sample time response for an under-damped system.
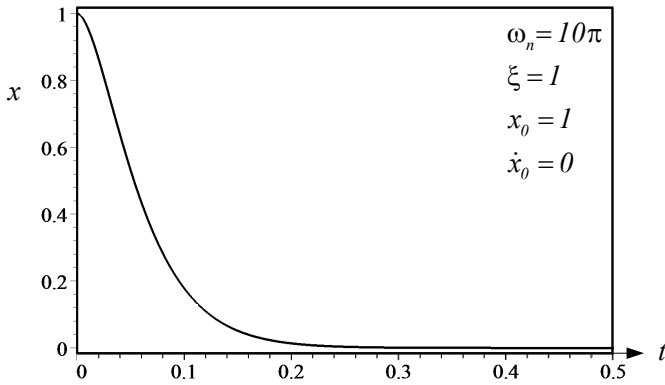


FIGURE 12.42. A sample time response for an critically-damped system.

*When the characteristic values are equal, the time response of the system is*

$$x = A_1 e^{\lambda t} + A_2 t e^{\lambda t} \tag{12.393}$$

*which is equal to*

$$x = e^{-\xi \omega_n t} (A_1 + A_2 t). \tag{12.394}$$

*Figure 12.42 shows a critically-damped response for $\xi = 1$, $\omega_n = 10\pi$ rad, $x_0 = 1$, and $\dot{x}_0 = 0$.*

*An **over damped** system is when $\xi > 1$. The characteristic parameters (12.379) for an over-damped system are two real numbers*

$$\lambda_{1,2} = -\xi \omega_n \pm \omega_n \sqrt{\xi^2 - 1} \tag{12.395}$$

*and therefore, the exponential solution cannot be converted to harmonic*
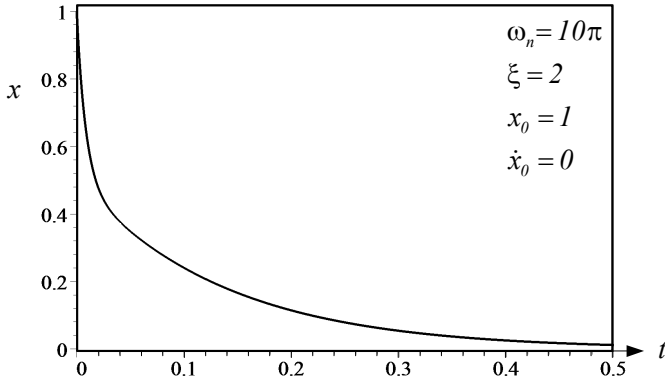
FIGURE 12.43. A sample time response for an over-damped system.

*functions.*

$$x = A_1\, e^{\lambda_1 t} + A_2\, e^{\lambda_2 t} \tag{12.396}$$

*Starting from any set of initial conditions, the time response of an over-damped system goes to zero exponentially. Figure 12.43 shows an over-damped response for $\xi = 2$, $\omega_n = 10\pi$ rad, $x_0 = 1$, and $\dot{x}_0 = 0$.*

**Example 457** *Free vibration and initial conditions.*
   *Consider a one DOF mass-spring-damper in a free vibration. The general motion of the system, given in Equation (12.383), is*

$$x = e^{-\xi \omega_n t}\left(B_1 \sin \omega_d t + B_2 \cos \omega_d t\right). \tag{12.397}$$

*If the initial conditions of the system are*

$$
\begin{aligned}
x(0) &= x_0 & (12.398)\\
\dot{x}(0) &= \dot{x}_0 & (12.399)
\end{aligned}
$$

*then,*

$$
\begin{aligned}
x_0 &= B_2 & (12.400)\\
\dot{x}_0 &= -\xi \omega_n B_2 + B_1 \omega_d & (12.401)
\end{aligned}
$$

*and hence,*

$$
\begin{aligned}
B_1 &= \frac{\dot{x}_0 + \xi \omega_n x_0}{\omega_d} & (12.402)\\
B_2 &= x_0. & (12.403)
\end{aligned}
$$

*Substituting $B_1$ and $B_2$ in solution (12.397) generates the general solution for free vibration of a single-DOF system.*

$$x = e^{-\xi \omega_n t}\left(\frac{\dot{x}_0 + \xi \omega_n x_0}{\omega_d} \sin \omega_d t + x_0 \cos \omega_d t\right) \tag{12.404}$$

*The solution can also be written as*

$$x = e^{-\xi\omega_n t}\left(x_0\left(\cos\omega_d t + \frac{\xi}{\omega_d}\omega_n\sin\omega_d t\right) + \frac{\dot{x}_0}{\omega_d}\sin\omega_d t\right). \qquad (12.405)$$

*If the initial conditions of the system are substituted in solution (12.384)*

$$x = Be^{-\xi\omega_n t}\sin\left(\omega_d t + \phi\right) \qquad (12.406)$$

*then,*

$$x_0 \quad = \quad B\sin\phi \qquad (12.407)$$
$$\dot{x}_0 \quad = \quad -B\xi\omega_n\sin\phi + B\omega_d\cos\phi. \qquad (12.408)$$

*To solve for B and $\phi$, we may write*

$$B \quad = \quad \frac{x_0}{\sin\phi} \qquad (12.409)$$

$$\tan\phi \quad = \quad \frac{\omega_d x_0}{\dot{x}_0 + \xi\omega_n x_0} \qquad (12.410)$$

*and therefore,*

$$B = \frac{1}{\omega_d}\sqrt{(\omega_d x_0)^2 + (\dot{x}_0 + \xi\omega_n x_0)^2}. \qquad (12.411)$$

*Now the solution (12.406) becomes*

$$
\begin{aligned}
x \quad = \quad & \frac{e^{-\xi\omega_n t}}{\omega_d}\sqrt{(\omega_d x_0)^2 + (\dot{x}_0 + \xi\omega_n x_0)^2} \\
& \times\sin\left(\omega_d t + \tan^{-1}\frac{\omega_d x_0}{\dot{x}_0 + \xi\omega_n x_0}\right). \qquad (12.412)
\end{aligned}
$$

**Example 458** *Free vibration, initial conditions, and critically damping.*
*If the system is critically damped, then the time response to free vibrations is*

$$x = e^{-\xi\omega_n t}\left(A_1 + A_2 t\right). \qquad (12.413)$$

*Using the initial conditions, $x(0) = x_0$, $\dot{x}(0) = \dot{x}_0$, we can find the coefficients $A_1$ and $A_2$ as*

$$A_1 \quad = \quad x_0 \qquad (12.414)$$
$$A_2 \quad = \quad \dot{x}_0 + \xi\omega_n x_0 \qquad (12.415)$$

*and therefore the general critically-damped response is*

$$x = e^{-\xi\omega_n t}\left(x_0 + (\dot{x}_0 + \xi\omega_n x_0)\,t\right). \qquad (12.416)$$

**Example 459** *Free vibration, initial conditions, and over damping.*
   *If the system is over-damped, then the characteristic parameters $\lambda_{1,2}$ are real and the time response to free vibrations is a real exponential function.*

$$x = A_1\, e^{\lambda_1 t} + A_2\, e^{\lambda_2 t} \qquad (12.417)$$

*Using the initial conditions, $x(0) = x_0$, $\dot{x}(0) = \dot{x}_0$,*

$$\begin{aligned}
x_0 &= A_1 + A_2 & (12.418)\\
\dot{x}_0 &= \lambda_1 A_1 + \lambda_2 A_2 & (12.419)
\end{aligned}$$

*we can find the coefficients $A_1$ and $A_2$ as*

$$A_1 = \frac{\dot{x}_0 - \lambda_2 x_0}{\lambda_1 - \lambda_2} \qquad (12.420)$$

$$A_2 = \frac{\lambda_1 x_0 - \dot{x}_0}{\lambda_1 - \lambda_2}. \qquad (12.421)$$

*Hence, the general over-damped response is*

$$x = \frac{\dot{x}_0 - \lambda_2 x_0}{\lambda_1 - \lambda_2}\, e^{\lambda_1 t} + \frac{\lambda_1 x_0 - \dot{x}_0}{\lambda_1 - \lambda_2}\, e^{\lambda_2 t}. \qquad (12.422)$$

**Example 460** *Work done by a harmonic force.*
   *The work done by a harmonic force*

$$f(t) = F \sin(\omega t + \varphi) \qquad (12.423)$$

*acting on a body with a harmonic displacement*

$$x(t) = X \sin(\omega t) \qquad (12.424)$$

*during one period*

$$T = \frac{2\pi}{\omega} \qquad (12.425)$$

*is equal to*

$$\begin{aligned}
W &= \int_0^{2\pi/\omega} f(t)\,dx \\
&= \int_0^{2\pi/\omega} f(t)\frac{dx}{dt}\,dt \\
&= FX\omega \int_0^{2\pi/\omega} \sin(\omega t + \varphi)\cos(\omega t)\,dt \\
&= FX \int_0^{2\pi} \sin(\omega t + \varphi)\cos(\omega t)\,d(\omega t) \\
&= FX \int_0^{2\pi} \left(\sin\varphi \cos^2\omega t + \cos\varphi \sin\omega t \cos\omega t\right)d(\omega t) \\
&= \pi FX \sin\varphi. & (12.426)
\end{aligned}$$

The work $W$ is a function of the phase $\varphi$ between $f$ and $x$. When $\varphi = \frac{\pi}{2}$ then the work is maximum

$$W_{Max} = \pi F_0 X_0 \tag{12.427}$$

and when $\varphi = 0$, the work is minimum.

$$W_{min} = 0 \tag{12.428}$$

**Example 461** ★ *Response to a step input.*

Step input is an standard and the most important transient excitation by which we examine and compare vibrating systems. Consider a linear second order system with the following equation of motion.

$$\ddot{x} + 2\xi\omega_n\dot{x} + \omega_n^2 x = f(t) \tag{12.429}$$
$$\xi < 1 \tag{12.430}$$

A step input, is a sudden change of the forcing function $f(t)$ from zero to a constant and steady value. If the value is unity then,

$$f(t) = \begin{cases} 1\,\mathrm{N/kg} & t > 0 \\ 0 & t \le 0 \end{cases}. \tag{12.431}$$

This excitation is called **unit step input**, and the response of the system is called the **unit step response**. Linearity of the equation of motion guarantees that the response to a non-unit step input is proportional to the unit step response.

Consider a force function as

$$f(t) = \begin{cases} F_0\,\mathrm{N/kg} & t > 0 \\ 0 & t \le 0 \end{cases}. \tag{12.432}$$

The general solution of Equation (12.429) along with (12.432) is equal to sum of the homogeneous and particular solutions, $x = x_h + x_p$. The homogeneous solution was given by Equation (12.380) in Example 455. The particular solution would be constant $x_p = C$ because the input is constant $f(t) = F_0$. Substituting $x_p = C$ in Equation (12.429) provides

$$C = \frac{F_0}{\omega_n^2}. \tag{12.433}$$

Therefore, the general solution of Equation (12.429) is

$$\begin{aligned} x &= x_h + x_p \\ &= \frac{F_0}{\omega_n^2} + e^{-\xi\omega_n t}\left(A\cos\omega_d t + B\sin\omega_d t\right) \qquad t \ge 0 \tag{12.434} \\ \omega_d &= \omega_n\sqrt{1-\xi^2}. \tag{12.435} \end{aligned}$$
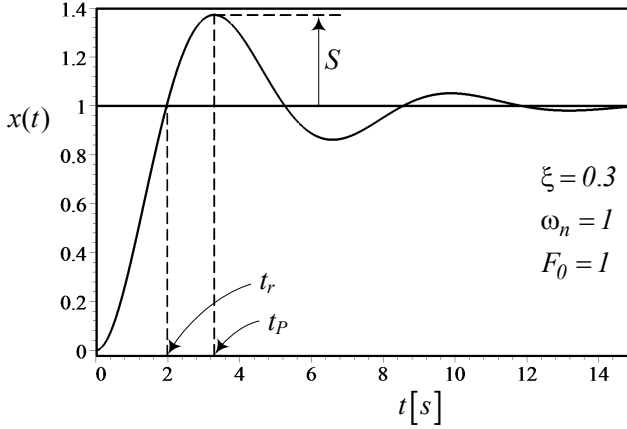
FIGURE 12.44. Response of a *one* DOF vibrating system to a step input.

*The zero initial conditions are the best to explore the natural behavior of the system. Applying a zero initial condition*

$$x(0) \quad = \quad 0 \tag{12.436}$$
$$\dot{x}(0) \quad = \quad 0 \tag{12.437}$$

*provides two equations for A and B*

$$\frac{F_0}{\omega_n^2} + A \quad = \quad 0 \tag{12.438}$$
$$\xi \omega_n A + \omega_d B \quad = \quad 0 \tag{12.439}$$

*with the following solutions.*

$$A \quad = \quad -\frac{F_0}{\omega_n^2} \tag{12.440}$$

$$B \quad = \quad -\frac{\xi F_0}{\omega_d \omega_n} \tag{12.441}$$

*Therefore, the step response is*

$$x = \frac{F_0}{\omega_n^2} \left( 1 - e^{-\xi \omega_n t} \left( \cos \omega_d t + \frac{\xi \omega_n}{\omega_d} \sin \omega_d t \right) \right). \tag{12.442}$$

*Figure 12.44 depicts a step input for the following numerical values.*

$$\xi \quad = \quad 0.3$$
$$\omega_n \quad = \quad 1$$
$$F_0 \quad = \quad 1 \tag{12.443}$$

*There are some characteristics for a step response: **rise time** $t_r$, **peak time** $t_P$, **peak value** $x_P$, **overshoot** $S = x_P - \frac{F_0}{\omega_n^2}$, and **settling time** $t_s$.*

*Rise time $t_r$ is the first time that the response $x(t)$ reaches the value of the step input $\frac{F_0}{\omega_n^2}$.*

$$t_r = \frac{2}{\omega_d} \tan^{-1} \frac{\xi + 1}{\sqrt{1 - \xi^2}} \tag{12.444}$$

*Rise time may also be defines as the inverse of the largest slope of the step response, or as the time it takes to pass from $10\%$ to $90\%$ of the steady-state value.*

*Peak time $t_P$ is the first time that the response $x(t)$ reaches its maximum value.*

$$t_P = \frac{\pi}{\omega_d} \tag{12.445}$$

*Peak value $x_P$ is the value of $x(t)$ when $t = t_P$.*

$$x_P = \frac{F_0}{\omega_n^2}\left(1 + e^{-\xi \omega_n \frac{\pi}{\omega_d}}\right) = \frac{F_0}{\omega_n^2}\left(1 + e^{-\xi \frac{\pi}{\sqrt{1-\xi^2}}}\right) \tag{12.446}$$

*Overshoot $S$ indicates how much the response $x(t)$ exceeds the step input.*

$$S = x_P - \frac{F_0}{\omega_n^2} = \frac{F_0}{\omega_n^2}e^{-\xi\frac{\pi}{\sqrt{1-\xi^2}}} \tag{12.447}$$

*Settling time $t_s$ is, by definition, four times of the time constant of the exponential function $e^{-\xi\omega_n t}$.*

$$t_s = \frac{4}{\xi \omega_n} \tag{12.448}$$

*Settling time may also be defines as the required time that the step response $x(t)$ needs to settles within a $\pm p\%$ window of the step input. The value $p = 2$ is commonly used.*

$$t_s \approx \frac{\ln\left(p\sqrt{1 - \xi^2}\right)}{\xi \omega_n} \tag{12.449}$$

*For the given data in (12.443) we find the following characteristic values.*

$$
\begin{aligned}
t_r &= 1.966 \\
t_P &= 3.2933 \\
x_P &= 1.3723 \\
S &= 0.3723 \\
t_s &= 13.333
\end{aligned} \tag{12.450}
$$
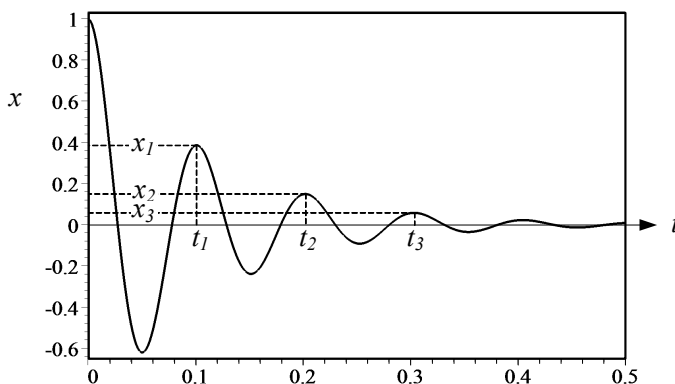
FIGURE 12.45. An $x$-response for the free vibration of an under-damped *one*-DOF system.

## 12.5   Vibration Application and Measurement

The measurable vibration parameters, such as period $T$ and amplitude $X$, may be used to identify mechanical characteristics of the vibrating system. In most vibration measurement and test methods, a transient or harmonically steady-state vibration will be examined. Using time and kinematic measurement devices, we measure amplitude and period of response, and use the analytic equations to find the required data.

**Example 462** *Damping ratio determination.*
   *Damping ratio of an under-damped one-DOF system can be found by*

$$\xi \quad = \quad \frac{1}{\sqrt{4\left(n-1\right)^2 \pi^2 + \ln^2 \frac{x_1}{x_n}}} \ln \frac{x_1}{x_n} \qquad (12.451)$$

$$\approx \quad \frac{1}{2\left(n-1\right)\pi} \ln \frac{x_1}{x_n} \qquad (12.452)$$

*which is based on a plot of $x = x\left(t\right)$ and peak amplitudes $x_i$.*
   *To show this equation, consider the free vibration of an under-damped one-DOF system with the following equation of motion:*

$$\ddot{x} + 2\xi\omega_n \dot{x} + \omega_n^2 x = 0. \qquad (12.453)$$

*The time response of the system is given in Equation (12.383) as*

$$x = X\, e^{-\xi\omega_n t} \cos\left(\omega_d t + \phi\right) \qquad (12.454)$$

*where the constants $X$ and $\phi$ are dependent on initial conditions.*

*Figure 12.45 illustrates a sample of the x-response. The peak amplitudes $x_i$ are*

$$
\begin{align}
x_1 &= e^{-\xi\omega_n t_1}\left(X\cos\left(\omega_d t_1 + \phi\right)\right) \tag{12.455}\\
x_2 &= e^{-\xi\omega_n t_2}\left(X\cos\left(\omega_d t_2 + \phi\right)\right) \tag{12.456}\\
&\vdots \\
x_n &= e^{-\xi\omega_n t_n}\left(X\cos\left(\omega_d t_n + \phi\right)\right). \tag{12.457}
\end{align}
$$

*The ratio of the first two peaks is*

$$
\frac{x_1}{x_2} = e^{-\xi\omega_n(t_1-t_2)}\frac{\cos\left(\omega_d t_1 + \phi\right)}{\cos\left(\omega_d t_2 + \phi\right)} \tag{12.458}
$$

*Because the time difference between $t_1$ and $t_2$ is the period of oscillation*

$$
\begin{align}
T_d &= t_2 - t_1 \\
&= \frac{2\pi}{\omega_d} \\
&= \frac{2\pi}{\omega_n\sqrt{1-\xi^2}} \tag{12.459}
\end{align}
$$

*we may simplify Equation (12.458) to*

$$
\begin{align}
\frac{x_1}{x_2} &= e^{\xi\omega_n T_d}\frac{\cos\left(\omega_d t_1 + \phi\right)}{\cos\left(\omega_d\left(t_1 + T_d\right) + \phi\right)} \\
&= e^{\xi\omega_n T_d}\frac{\cos\left(\omega_d t_1 + \phi\right)}{\cos\left(\omega_d t_1 + 2\pi + \phi\right)} \\
&= e^{\xi\omega_n T_d}. \tag{12.460}
\end{align}
$$

*This equation shows that,*

$$
\ln\frac{x_1}{x_2} = \xi\omega_n T_d = \frac{2\pi\xi}{\sqrt{1-\xi^2}} \tag{12.461}
$$

*which can be used to evaluate the damping ratio $\xi$.*

$$
\xi \approx \frac{1}{\sqrt{4\pi^2 + \ln^2\frac{x_1}{x_2}}}\ln\frac{x_1}{x_2} \tag{12.462}
$$

*For a better evaluation we may measure the ratio between $x_1$ and any other $x_n$, and use the following equation:*

$$
\xi \approx \frac{1}{\sqrt{4\left(n-1\right)^2\pi^2 + \ln^2\frac{x_1}{x_n}}}\ln\frac{x_1}{x_n} \tag{12.463}
$$
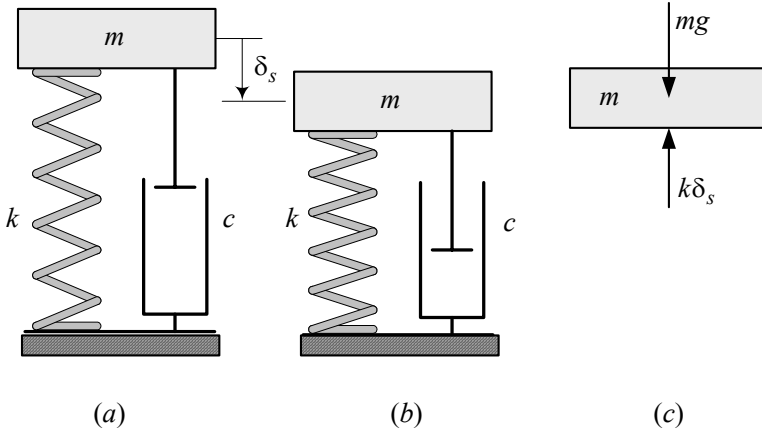
FIGURE 12.46. Static deflection and natural frequency determination.

*If $\xi << 1$, then $\sqrt{1 - \xi^2} \approx 1$, and we may evaluate $\xi$ from (12.461) with a simpler equation.*

$$\xi \approx \frac{1}{2\,(n-1)\,\pi} \ln \frac{x_1}{x_n} \tag{12.464}$$

**Example 463** *Natural frequency determination.*

*Natural frequency of a mass-spring-damper system can be found by measuring the static deflection of the system. Consider a one-DOF system shown in Figure 12.46(a) that barely touches the ground. Assume that the spring has no tension or compression. When the system rests on the ground as shown in Figure 12.46(b), the spring is compressed by a static deflection $\delta_s = mg/k$ because of gravity. We may determine the natural frequency of the system by measuring $\delta_s$*

$$\omega_n = \sqrt{\frac{g}{\delta_s}} \tag{12.465}$$

*because*

$$\delta_s = \frac{mg}{k} = \frac{g}{\omega_n^2}. \tag{12.466}$$

**Example 464** *Moments of inertia determination.*

*Mass moments of inertia are important characteristics of a vehicle that affect its dynamic behavior. The main moments of inertia $I_x$, $I_y$, and $I_z$ can be calculated by an experiment.*

*Figure 12.47 illustrates an oscillating platform hung from point A. Assume the platform has a mass $M$ and a moment of inertia $I_0$ about the pivot point A. Ignoring the mass of cables, we can write the Euler equation about point A*

$$\sum M_y = I_0\, \ddot{\theta} = -Mgh_1 \sin\theta \tag{12.467}$$
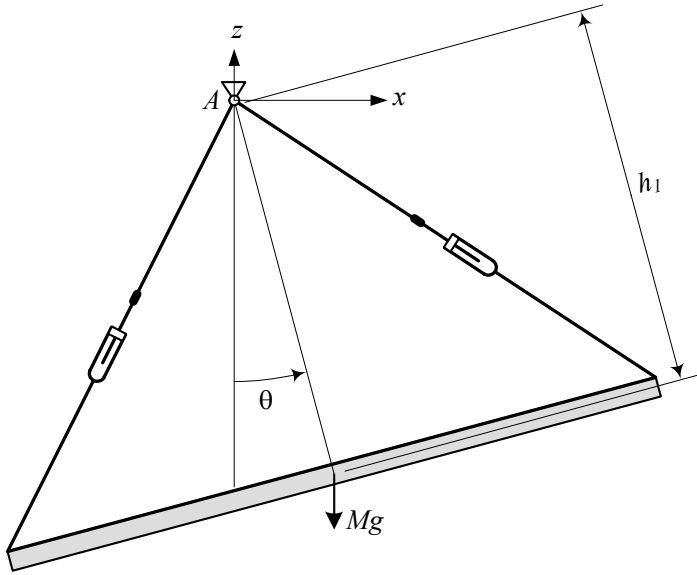
FIGURE 12.47. An oscillating platform hung from point $A$.

and derive the equation of motion.

$$I_0 \ddot{\theta} + Mgh_1 \sin \theta = 0 \qquad (12.468)$$

If the angle of oscillation $\theta$ is very small, then $\sin \theta \approx \theta$ and therefore, Equation (12.468) reduces to a linear equation

$$\ddot{\theta} + \omega_n^2 \, \theta \;\; = \;\; 0 \qquad (12.469)$$

$$\omega_n \;\; = \;\; \sqrt{\frac{Mgh_1}{I_0}} \qquad (12.470)$$

where $\omega_n$ is the natural frequency of the oscillation.

$\omega_n$ can be assumed as the frequency of small oscillation about the point $A$ when the platform is set free after a small deviation from equilibrium position. The natural period of oscillation $T_n = 2\pi/\omega_n$ is what we can measure, and therefore, the moment of inertia $I_0$ is equal to

$$I_0 = \frac{1}{4\pi^2} Mgh_1 T_n^2. \qquad (12.471)$$

The natural period $T_n$ may be measured by an average period of a few cycles, or more accurately, by an accelerometer.

Now consider the swing shown in Figure 12.48. A car with mass $m$ at $C$ is on the platform such that $C$ is exactly above the mass center of the platform. Because the location of the mass center $C$ is known, the distance between $C$ and the fulcrum $A$ is also known as $h_2$.
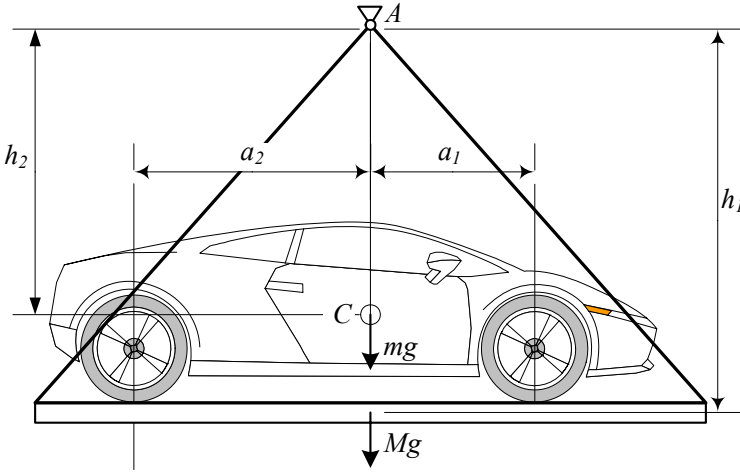
FIGURE 12.48. A car with mass $m$ on an oscillating platform hung from point $A$.

To find the car's pitch mass moment of inertia $I_y$ about $C$, we apply the Euler equation about point $A$, when the oscillator is deviated from the equilibrium condition.

$$\sum M_y = I_A \ddot{\theta} \qquad (12.472)$$

$$-Mgh_1 \sin\theta - mgh_2 \sin\theta = I_0 + I_y + mh_2^2 \qquad (12.473)$$

Assuming very small oscillation, we may use $\sin\theta \approx \theta$ and then Equation (12.473) reduces to a linear oscillator

$$\ddot{\theta} + \omega_n^2 \theta = 0 \qquad (12.474)$$

$$\omega_n = \sqrt{\frac{(Mh_1 + mh_2)\, g}{I_0 + I_y + mh_2^2}}. \qquad (12.475)$$

Therefore, the pitch moment of inertia $I_y$ can be calculated by measuring the natural period of oscillation $T_n = 2\pi/\omega_n$ from the following equation.

$$I_y = \frac{1}{4\pi^2} (Mh_1 + mh_2)\, g T_n^2 - I_0 - mh_2^2. \qquad (12.476)$$

To determine the roll moment of inertia, we may put the car on the platform as shown in Figure 12.49.

Having $I_x$ and $I_y$ we may put the car on the platform, at an angle $\alpha$, to find its moment of inertia about the axis passing through $C$ and parallel to the swing axis. Then, the product moment of inertia $I_{xy}$ can be calculated by transformation calculus.
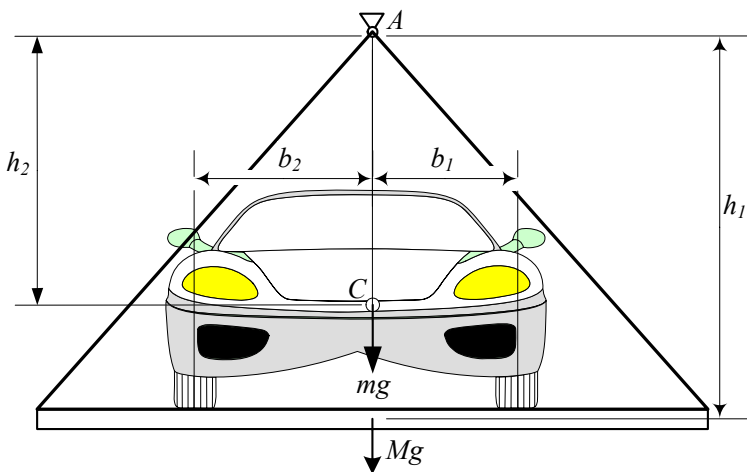
FIGURE 12.49. Roll moment of inertia measurement, using a swinging platform.

**Example 465** *Sample data.*

   *Tables* 12.1 *indicates an example of data for the mass center position, moment of inertia, and geometry of street cars, that are close to a Mercedes-Benz A-Class.*

Table 12.1 - *Sample data close to a Mercedes-Benz A-Class.*

| | |
|---|---|
| *wheelbase* | 2424 mm |
| *front track* | 1492 mm |
| *rear track* | 1426 mm |
| *mass* | 1245 kg |
| $a_1$ | 1100 mm |
| $a_2$ | 1323 mm |
| $h$ | 580 mm |
| $I_x$ | 335 kg m$^2$ |
| $I_y$ | 1095 kg m$^2$ |
| $I_z$ | 1200 kg m$^2$ |

# 12.6   ★ Vibration Optimization Theory

The first goal in vibration optimization is to reduce the vibration amplitude of a primary mass to zero, when the system is under a forced vibration. There are two principal methods for decreasing the vibration amplitude of a primary mass: *vibration absorber*, and *vibration isolator*.

   When the suspension of a *primary system* is not easy to change, we add another vibrating system, known as the *vibration absorber* or *secondary*
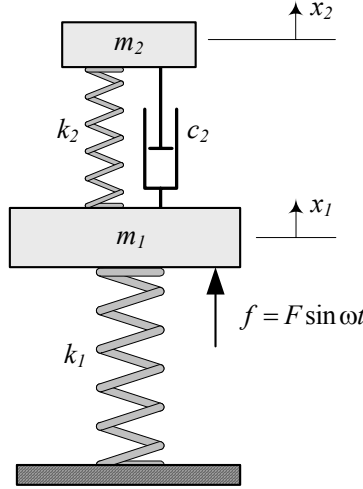
FIGURE 12.50. A secondary vibration absorber system $(m_2, c_2, k_2)$ added to a primary vibrating system $(m_1, k_1)$.

*system*, to absorb the vibrations of the primary system. The vibration absorber increases the DOF of the system, and is an applied method for vibration reduction in frequency domain. It can work very well in a few specific frequencies, and may be designed to work well in a range of frequencies.

Consider a mass $m_1$ supported by a suspension made of only a spring $k_1$, as shown in Figure 12.50. There is a harmonic force $f = F \sin \omega t$ applied on $m_1$. We add a secondary system $(m_2, c_2, k_2)$ to the primary mass $m_1$ and make a two-DOF vibrating system. Such a system is sometimes called *Frahm absorber*, or *Frahm damper*.

It is possible to design the suspension of the secondary system $(c_2, k_2)$ to reduce the amplitude of vibration $m_1$ to zero at any specific excitation frequency $\omega$. However, if the excitation frequency is variable, we can adjust $k_2$ at the optimal value $k_2^{\star}$,

$$k_2^{\star} = \frac{m_1 m_2}{(m_1 + m_2)^2} k_1 \qquad (12.477)$$

and select $c_2$ within the range

$$2 m_2 \omega_1 \xi_1^{\star} < c_2 < 2 m_2 \omega_1 \xi_2^{\star}$$

to minimize the amplitude of $m_1$ over the whole frequency range. The

optimal $\xi_1^{\star}$ and $\xi_2^{\star}$ are the positive values of

$$\xi_1^{\star} = \sqrt{\frac{-B - \sqrt{B^2 - 4AC}}{2A}} \tag{12.478}$$

$$\xi_2^{\star} = \sqrt{\frac{-B + \sqrt{B^2 - 4AC}}{2A}} \tag{12.479}$$

where

$$\begin{align}
A &= 16Z_8 - 4r^2 \left(4Z_4 + 8Z_5\right) \tag{12.480} \\
B &= 4Z_9 - 4Z_6 r^2 - Z_7 \left(4Z_4 + 8Z_5\right) + 4Z_3 Z_8 \tag{12.481} \\
C &= Z_3 Z_9 - Z_6 Z_7. \tag{12.482}
\end{align}$$

and

$$\begin{align}
Z_3 &= 2\left(r^2 - \alpha^2\right) \tag{12.483} \\
Z_4 &= \left[r^2\left(1 + \varepsilon\right) - 1\right]^2 \tag{12.484} \\
Z_5 &= r^2\left(1 + \varepsilon\right)\left[r^2\left(1 + \varepsilon\right) - 1\right] \tag{12.485} \\
Z_6 &= 2\left[\varepsilon\alpha^2 r^2 - \left(r^2 - \alpha^2\right)\left(r^2 - 1\right)\right] \\
&\quad \times \left[\varepsilon\alpha^2 - \left(r^2 - \alpha^2\right) - \left(r^2 - 1\right)\right] \tag{12.486} \\
Z_7 &= \left(r^2 - \alpha^2\right)^2 \tag{12.487} \\
Z_8 &= r^2\left[r^2\left(1 + \varepsilon\right) - 1\right]^2 \tag{12.488} \\
Z_9 &= \left[\varepsilon\alpha^2 r^2 - \left(r^2 - 1\right)\left(r^2 - \alpha^2\right)\right]^2. \tag{12.489}
\end{align}$$

**Proof.** The equations of motion for the system shown in Figure 12.50 are:

$$\begin{align}
m_1\ddot{x}_1 + c_2\left(\dot{x}_1 - \dot{x}_2\right) + k_1 x_1 + k_2\left(x_1 - x_2\right) &= F\sin\omega t \tag{12.490} \\
m_2\ddot{x}_2 - c_2\left(\dot{x}_1 - \dot{x}_2\right) - k_2\left(x_1 - x_2\right) &= 0. \tag{12.491}
\end{align}$$

To find the frequency response of the system, we substitute the following solutions in the equations of motion:

$$\begin{align}
x_1 &= A_1\cos\omega t + B_1\sin\omega t \tag{12.492} \\
x_2 &= A_2\cos\omega t + B_2\sin\omega t \tag{12.493}
\end{align}$$

Assuming a steady-state condition, we find the following set of equations for $A_1$, $B_1$, $A_2$, $B_2$

$$\begin{bmatrix} a_{11} & c_2\omega & -k_2 & -c_2\omega \\ -c_2\omega & a_{22} & c_2\omega & -k_2 \\ -k_2 & -c_2\omega & a_{33} & c_2\omega \\ c_2\omega & -k_2 & -c_2\omega & a_{44} \end{bmatrix} \begin{bmatrix} A_1 \\ B_1 \\ A_2 \\ B_2 \end{bmatrix} = \begin{bmatrix} 0 \\ F \\ 0 \\ 0 \end{bmatrix} \tag{12.494}$$

where,

$$a_{11} \;=\; a_{22} = k_1 + k_2 - m_1\omega^2 \tag{12.495}$$
$$a_{33} \;=\; a_{44} = k_2 - m_2\omega^2. \tag{12.496}$$

The steady-state amplitude $X_1$ for vibration of the primary mass $m_1$ is found by

$$X_1 = \sqrt{A_1^2 + B_1^2} \tag{12.497}$$

and is equal to

$$\left(\frac{X_1}{F}\right)^2 = \frac{\left(k_2 - \omega^2 m_2\right)^2 + \omega^2 c_2^2}{Z_1^2 + \omega^2 c_2^2 Z_2^2} \tag{12.498}$$

where,

$$Z_1 \;=\; \left(k_1 - \omega^2 m_1\right)\left(k_2 - \omega^2 m_2\right) - \omega^2 m_2 k_2 \tag{12.499}$$
$$Z_2 \;=\; k_1 - \omega^2 m_1 - \omega^2 m_2. \tag{12.500}$$

Introducing the parameters

$$\varepsilon \;=\; \frac{m_2}{m_1} \tag{12.501}$$

$$\omega_1 \;=\; \sqrt{\frac{k_1}{m_1}} \tag{12.502}$$

$$\omega_2 \;=\; \sqrt{\frac{k_2}{m_2}} \tag{12.503}$$

$$\alpha \;=\; \frac{\omega_2}{\omega_1} \tag{12.504}$$

$$r \;=\; \frac{\omega}{\omega_1} \tag{12.505}$$

$$\xi \;=\; \frac{c_2}{2m_2\omega_1} \tag{12.506}$$

$$\mu \;=\; \frac{X_1}{F/k_1} \tag{12.507}$$

we may rearrange the frequency response (12.498) to the following equation.

$$\mu^2 = \frac{4\xi^2 r^2 + \left(r^2 - \alpha^2\right)^2}{4\xi^2 r^2 \left[r^2\left(1+\varepsilon\right) - 1\right]^2 + \left[\varepsilon\alpha^2 r^2 - \left(r^2 - 1\right)\left(r^2 - \alpha^2\right)\right]^2} \tag{12.508}$$

The parameter $\varepsilon$ is the *mass ratio* between $m_2$ and the $m_1$, $\omega_1$ is the angular natural frequency of the main system, $\omega_2$ is the angular natural frequency of the vibration absorber system, $\alpha$ is the natural frequency ratio, $r$ is the excitation frequency ratio, $\xi$ is the damping ratio, and $\mu$ is the amplitude ratio between dynamic amplitude $X_1$ and the static deflection $F/k_1$.
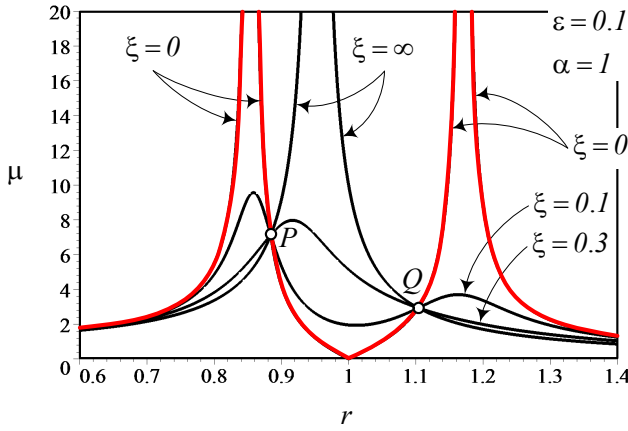
FIGURE 12.51. Behavior of ferquency response $\mu$ for a set of parameters and different damping ratios.

Figure 12.51 illustrates the behavior of frequency response $\mu$ for

$$\varepsilon = 0.1 \tag{12.509}$$
$$\alpha = 1 \tag{12.510}$$

and

$$\xi = 0 \tag{12.511}$$
$$\xi = 0.2 \tag{12.512}$$
$$\xi = 0.3 \tag{12.513}$$
$$\xi = \infty. \tag{12.514}$$

All the curves pass through two nodes $P$ and $Q$, independent of the damping ratio $\xi$. To find the parameters that control the position of the nodes, we find the intersection points of the curves for $\xi = 0$ and $\xi = \infty$. Setting $\xi = 0$ and $\xi = \infty$ results in the following equations:

$$\mu^2 = \frac{\left(r^2 - \alpha^2\right)^2}{\left[\varepsilon\alpha^2 r^2 - (r^2 - 1)\left(r^2 - \alpha^2\right)\right]^2} \tag{12.515}$$

$$\mu^2 = \frac{1}{\left[r^2(1 + \varepsilon) - 1\right]^2} \tag{12.516}$$

When $\xi = 0$, the system is an undamped, linear two-DOF system with *two* natural frequencies. The vibration amplitude of the system approaches infinity $\mu \to \infty$ when the excitation frequency approaches either of the natural frequencies. When $\xi = \infty$, there would be no relative motion between

$m_1$ and $m_2$. The system reduces to an undamped, linear *one*-DOF system with *one* natural frequency

$$\omega_n = \sqrt{\frac{k_1}{m_1 + m_2}} \tag{12.517}$$

or

$$r_n = \frac{1}{\sqrt{1 + \varepsilon}}. \tag{12.518}$$

The vibration amplitude of the system approaches infinity $\mu \to \infty$ when the excitation frequency approaches the natural frequency $\omega \to \omega_{n_i}$ or $r \to 1/(1 + \varepsilon)$.

Using Equations (12.515) and (12.516), we find

$$\frac{\left(r^2 - \alpha^2\right)^2}{\left(\varepsilon \alpha^2 r^2 - \left(r^2 - 1\right)\left(r^2 - \alpha^2\right)\right)^2} = \frac{1}{\left[r^2\left(1 + \varepsilon\right) - 1\right]^2} \tag{12.519}$$

which can be simplified to

$$\varepsilon \alpha^2 r^2 - \left(r^2 - 1\right)\left(r^2 - \alpha^2\right) = \pm\left(r^2 - \alpha^2\right)\left[r^2\left(1 + \varepsilon\right) - 1\right]. \tag{12.520}$$

The negative sign is equivalent to

$$r^4 \varepsilon = 0$$

which indicates that there is a common point at $r = 0$. The plus sign produces a quadratic equation for $r^2$

$$\left(2 + \varepsilon\right) r^4 - r^2\left(2 + 2\alpha^2\left(1 + \varepsilon\right)\right) + 2\alpha^2 = 0 \tag{12.521}$$

with two positive solutions $r_1$ and $r_2$ corresponding to nodes $P$ and $Q$.

$$r_{1,2}^2 = \frac{1}{\varepsilon + 2}\left(\alpha^2 \pm \sqrt{\left(\varepsilon^2 + 2\varepsilon + 1\right)\alpha^4 - 2\alpha^2 + 1} + \alpha^2 \varepsilon + 1\right) \tag{12.522}$$

$$r_1 \quad < \quad r_n < r_2 \tag{12.523}$$

Because the frequency response curves always pass through $P$ and $Q$, the optimal situation would be when the nodes $P$ and $Q$ have equal height.

$$\mu\left(P\right) = \mu\left(Q\right) \tag{12.524}$$

Because the value of $\mu^2$ at $P$ and $Q$ are independent of $\xi$, we may substitute $r_1$ and $r_2$ in Equation (12.516) for $\mu$ corresponding to $\xi = \infty$. However, $\mu$ from Equation (12.516)

$$\mu = \frac{1}{\left[r^2\left(1 + \varepsilon\right) - 1\right]} \tag{12.525}$$

produces a positive number for $r < r_n$ and a negative number for $r > r_n$. Therefore,

$$\mu(r_1) = -\mu(r_2) \tag{12.526}$$

generates the equality

$$\frac{1}{1 - r_1^2(1+\varepsilon)} = \frac{-1}{1 - r_2^2(1+\varepsilon)} \tag{12.527}$$

which can be simplified to

$$r_1^2 + r_2^2 = \frac{2}{1+\varepsilon}. \tag{12.528}$$

The sum of the roots from Equation (12.521) is

$$r_1^2 + r_2^2 = \frac{2 + 2\alpha^2(1+\varepsilon)}{1+\varepsilon} \tag{12.529}$$

and therefore,

$$\frac{2}{1+\varepsilon} = \frac{[2 + 2\alpha^2(1+\varepsilon)]}{1+\varepsilon} \tag{12.530}$$

which provides

$$\alpha = \frac{1}{1+\varepsilon}. \tag{12.531}$$

Equation (12.531) is the required condition to make the height of the nodes $P$ and $Q$ equal, and hence, provides the optimal value of $\alpha$. Having an optimal value for $\alpha$ is equivalent to designing the optimal stiffness $k_2$ for the secondary suspension, because,

$$
\begin{aligned}
\alpha &= \frac{\omega_2}{\omega_1} \\
&= \sqrt{\frac{m_1}{m_2}}\sqrt{\frac{k_2}{k_1}} \tag{12.532}
\end{aligned}
$$

and Equation (12.531) simplifies to

$$\alpha = \frac{m_1}{m_1 + m_2} \tag{12.533}$$

to provide the following condition for optimal $k_2^\star$:

$$k_2^\star = k_1 \frac{m_1 m_2}{(m_1 + m_2)^2} \tag{12.534}$$

To determine the optimal damping ratio $\xi$, we force $\mu$ to have its maximum at $P$ or $Q$. Having $\mu_{Max}$ at $P$ guarantees that $\mu(r_1)$ is the highest value in a frequency domain around $r_1$, and having $\mu_{Max}$ at $Q$, guarantees
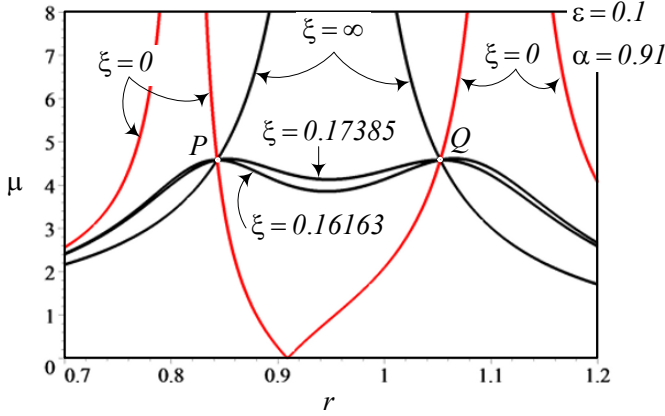
FIGURE 12.52. Optimal damping ratio $\xi$ to have maximum of $\mu$ at $P$ or $Q$.

that $\mu(r_2)$ is the highest value in a frequency domain around $r_2$. The position of $\mu_{Max}$ is controlled by $\xi$, so we may determine two optimal $\xi$ at which $\mu_{Max}$ is at $\mu(r_1)$ and $\mu(r_2)$. An example of this situation is shown in Figure 12.52.

Using the optimal $\alpha$ from (12.531), the nodal frequencies are

$$r_{1,2}^2 = \frac{1}{1+\varepsilon}\left(1 \pm \sqrt{\frac{\varepsilon}{2+\varepsilon}}\right). \tag{12.535}$$

To set the partial derivative $\partial\mu^2/\partial r^2$ equal to zero at the nodal frequencies

$$\left.\frac{\partial\mu^2}{\partial r^2}\right|_{r_1^2} = 0 \tag{12.536}$$

$$\left.\frac{\partial\mu^2}{\partial r^2}\right|_{r_2^2} = 0 \tag{12.537}$$

we write $\mu^2$ by numerator $N(r)$ divided by denominator $D(r)$

$$\mu^2 = \frac{N(r)}{D(r)} \tag{12.538}$$

which helps to find the derivative easier.

$$\begin{aligned}
\frac{\partial\mu^2}{\partial r^2} &= \frac{1}{D^2}\left(D\frac{\partial N}{\partial r^2} - N\frac{\partial D}{\partial r^2}\right) \\
&= \frac{1}{D}\left(\frac{\partial N}{\partial r^2} - \frac{N}{D}\frac{\partial D}{\partial r^2}\right) \tag{12.539}
\end{aligned}$$

Differentiating gives

$$\frac{\partial N}{\partial r^2} = \frac{\partial N}{\partial r^2} = 4\xi^2 + Z_3 \tag{12.540}$$

$$\frac{\partial D}{\partial r^2} = 4\xi^2 Z_4 + 8\xi^2 Z_5 + Z_6. \tag{12.541}$$

Equations (12.540) and (12.541), along with (12.535), must be substituted in (12.539) to be solved for $\xi$. After substitution, the equation $\partial \mu^2 / \partial r^2 = 0$ would be

$$\begin{aligned}
\frac{\partial N}{\partial r^2} - \frac{N}{D}\frac{\partial D}{\partial r^2} &= \left(4\xi^2 + Z_3\right)\left(4\xi^2 Z_8 + Z_9\right) \\
&\quad - \left(4\xi^2 r^2 + Z_7\right)\left(4\xi^2 Z_4 + 8\xi^2 Z_5 + Z_6\right) \\
&= 0 \tag{12.542}
\end{aligned}$$

because of

$$\frac{N}{D} = \frac{4\xi^2 r^2 + Z_7}{4\xi^2 Z_8 + Z_9}. \tag{12.543}$$

Equation (12.542) is a quadratic for $\xi^2$

$$\begin{aligned}
&\left(16Z_8 - 4r^2\left(4Z_4 + 8Z_5\right)\right)\xi^4 \\
&+ \left(4Z_9 - 4Z_6 r^2 - Z_7\left(4Z_4 + 8Z_5\right) + 4Z_3 Z_8\right)\xi^2 \\
&+ \left(Z_3 Z_9 - Z_6 Z_7\right) \\
&= A\left(\xi^2\right)^2 + B\xi^2 + C = 0 \tag{12.544}
\end{aligned}$$

with the solution

$$\xi^2 = \frac{-B \pm \sqrt{B^2 - 4AC}}{2A}. \tag{12.545}$$

The positive value of $\xi$ from (12.545) for $r = r_1$ and $r = r_2$ provides the limiting values for $\xi_1^\star$ and $\xi_2^\star$. Figure 12.52 shows the behavior of $\mu$ for optimal $\alpha$ and $\xi = 0, \xi_1^\star, \xi_2^\star, \infty$.   ∎

**Example 466 ★** *Optimal spring and damper for $\varepsilon = 0.1$.*
  *Consider a Frahm vibration absorber with*

$$\varepsilon = \frac{m_2}{m_1} = 0.1. \tag{12.546}$$

*We adjust the optimal frequency ratio $\alpha$ form Equation (12.531).*

$$\alpha^\star = \frac{1}{1 + \varepsilon} \approx 0.9091 \tag{12.547}$$

*and find the nodal frequencies $r_{1,2}^2$ from (12.535).*

$$\begin{aligned}
r_{1,2}^2 &= \frac{1}{1 + \varepsilon}\left(1 \pm \sqrt{\frac{\varepsilon}{2 + \varepsilon}}\right) \\
&= 0.71071, 1.1075. \tag{12.548}
\end{aligned}$$

*Now, we set* $r = r_1 = \sqrt{0.71071} \approx 0.843$ *and evaluate the parameters* $Z_3$
*to* $Z_9$ *from (12.483)-(12.489)*

$$
\begin{aligned}
Z_3 &= -0.231470544 \\
Z_4 &= 0.0476190476 \\
Z_5 &= -0.1705988426 \\
Z_6 &= 0.0246326501 \\
Z_7 &= 0.01339465321 \\
Z_8 &= 0.03384338136 \\
Z_9 &= 0.0006378406298
\end{aligned}
\tag{12.549}
$$

*and the coefficients A, B, and C from (12.480)-(12.482)*

$$
\begin{aligned}
A &= 3.879887219 \\
B &= -0.08308086729 \\
C &= -0.0004775871233
\end{aligned}
\tag{12.550}
$$

*to find the first optimal damping ratio* $\xi_1$.

$$
\xi_1^{\star} = 0.1616320694
\tag{12.551}
$$

*Using* $r = r_2 = \sqrt{1.1075} \approx 1.05236$ *we find the following numbers*

$$
\begin{aligned}
Z_3 &= 0.562049056 \\
Z_4 &= 0.04761904752 \\
Z_5 &= 0.2658369375 \\
Z_6 &= -0.375123324 \\
Z_7 &= 0.07897478534 \\
Z_8 &= 0.05273670508 \\
Z_9 &= 0.003760704084
\end{aligned}
\tag{12.552}
$$

$$
\begin{aligned}
A &= -9.421012739 \\
B &= 0.1167823931 \\
C &= 0.005076228579
\end{aligned}
\tag{12.553}
$$

*to find the second optimal damping ratio* $\xi_1$.

$$
\xi_2^{\star} = 0.1738496023
\tag{12.554}
$$

*Therefore, the optimal* $\alpha$ *is* $\alpha^{\star} = 0.9091$, *and the optimal* $\xi$ *is between*
$0.1616320694 < \xi^{\star} < 0.1738496023$.
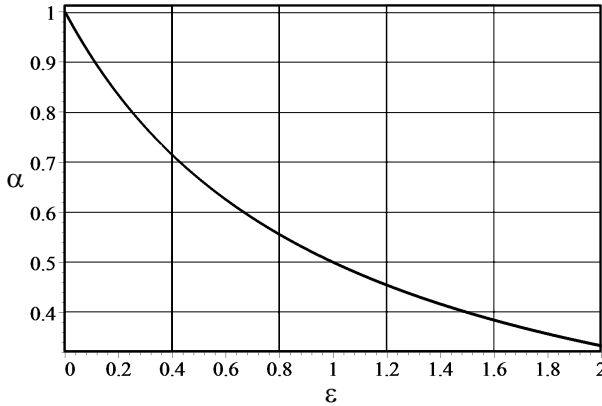
FIGURE 12.53. Optimal value of the natural frequency ratio, $\alpha$, as a function of mass ratio $\varepsilon$.

**Example 467 ★** *The vibration absorber is most effective when $r = \alpha = 1$.*
   *When $\xi = 0$, then $\mu = 0$ at $r = 1$, which shows the amplitude of the primary mass reduces to zero if the natural frequency of the primary and secondary systems are equal to the excitation frequency $r = \alpha = 1$.*

**Example 468 ★** *The optimal nodal amplitude.*
   *Substituting the optimal $\alpha$ from (12.531) in Equation (12.521),*

$$r^4 - \frac{2}{2+\varepsilon}r^2 + \frac{2}{(2+\varepsilon)(1+\varepsilon)^2} = 0 \qquad (12.555)$$

*provides the following nodal frequencies:*

$$r_{1,2}^2 = \frac{1}{1+\varepsilon}\left(1 \pm \sqrt{\frac{\varepsilon}{2+\varepsilon}}\right) \qquad (12.556)$$

*Applying $r_{1,2}$ in Equation (12.525) shows that the common nodal amplitude $\mu(r_{1,2})$ is*

$$\mu = \sqrt{\frac{2+\varepsilon}{\varepsilon}}. \qquad (12.557)$$

**Example 469 ★** *Optimal $\alpha$ and mass ratio $\varepsilon$.*
   *The optimal value of the natural frequency ratio, $\alpha$, is only a function of mass ratio $\varepsilon$, as determined in Equation (12.531). Figure 12.53 depicts the behavior of $\alpha$ as a function of $\varepsilon$. The value of optimal $\alpha$, and hence, the value of optimal $k_2$, decreases by increasing $\varepsilon = m_2/m_1$. Therefore, a smaller mass for the vibration absorber needs a stiffer spring.*
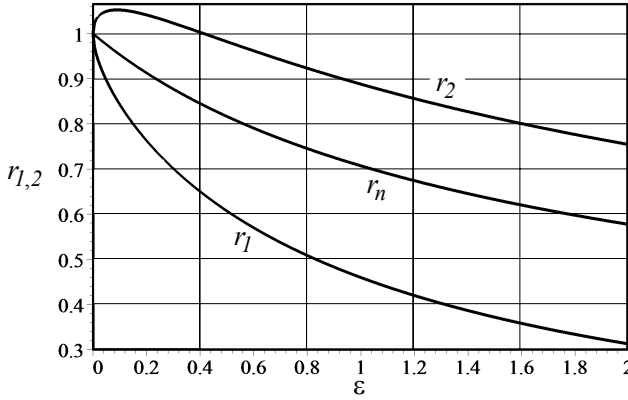
FIGURE 12.54. Behavior of nodal frequencies $r_{1,2}$ as a function of mass ratio $\varepsilon$.

**Example 470** ★ *Nodal frequencies $r_{1,2}$ and mass ratio $\varepsilon$.*

*As shown in Equation (12.535), the nodal frequencies $r_{1,2}$ for optimal $\alpha$ (12.531), are only a function of the mass ratio $\varepsilon$.*

$$r_{1,2}^2 = \frac{1}{1+\varepsilon}\left(1 \pm \sqrt{\frac{\varepsilon}{2+\varepsilon}}\right) \qquad (12.558)$$

*Figure 12.54 illustrates the behavior of $r_{1,2}$ as a function of $\varepsilon$. When, $\varepsilon \to 0$, the vibration absorber $m_2$ vanishes, and hence, the system becomes a one-DOF primary oscillator. Such a system has only one natural frequency $r_n = 1$ as given by Equation (12.518). It is the frequency that $r_{1,2}$ will approach by vanishing $m_2$.*

*The nodal frequencies $r_{1,2}$ are always on both sides of the singe-DOF natural frequency $r_n$*

$$r_1 < r_n < r_2 \qquad (12.559)$$

*while all of them are decreasing functions of the mass ratio $\varepsilon$.*

**Example 471** ★ *Natural frequencies for extreme values of damping.*

*By setting $\xi = 0$ for $\varepsilon = 0.1$, we find*

$$\mu = \left|\frac{r^2 - 1}{0.1r^2 - (r^2 - 1)^2}\right| \qquad (12.560)$$

*and by setting $\xi = \infty$, we find*

$$\mu = \left|\frac{1}{1.1r^2 - 1}\right|. \qquad (12.561)$$

*Having $\xi = 0$ is equivalent to no damping. When there is no damping, $\mu$ approaches infinity at the real roots of its denominator, $r_{n_1}$ and $r_{n_2}$,*

*which are the natural frequencies of the system. As an example, the natural frequencies $r_{n_1}$ and $r_{n_2}$ for $\varepsilon = 0.1$, are*

$$0.1r^2 - \left(r^2 - 1\right)^2 = 0 \tag{12.562}$$

$$r_{n_1} = 0.854\,31 \tag{12.563}$$

$$r_{n_2} = 1.170\,5. \tag{12.564}$$

*Having $\xi = \infty$ is equivalent to a rigid connection between $m_1$ and $m_2$. The system would have only one DOF and therefore, $\mu$ approaches infinity at the only roots of the denominator, $r_n$*

$$1.1r^2 - 1 = 0 \tag{12.565}$$

$$r_n = 0.953 \tag{12.566}$$

*where, $r_n$ is always between $r_{n_1}$ and $r_{n_2}$.*

$$r_{n_1} < r_n < r_{n_2} \tag{12.567}$$

## 12.7 Summary

Generally speaking, vibration is a harmful and unwanted phenomenon. Vibration is important when a non-vibrating system is connected to a vibrating system. To minimize the effects of vibration, we connect the systems by a damping elastic isolator. For simplicity, we model the isolator by a spring and damper parallel to each other. Such an isolator is called suspension.

Vibration can be physically expressed as a result of energy conversion. It can mathematically be expressed by solutions of a set of differential equations. If the system is linear, then its equations of motion can always be arranged in the following matrix form:

$$[M]\,\ddot{\mathbf{x}} + [c]\,\dot{\mathbf{x}} + [k]\,\mathbf{x} = \mathbf{F}\left(\mathbf{x}, \dot{\mathbf{x}}, t\right) \tag{12.568}$$

Vibration can be separated into *free vibrations*, when $\mathbf{F} = 0$, and *forced vibrations*, when $\mathbf{F} \neq 0$. However, in applied vibrations, we usually separate the solution of the equations of motion into *transient* and *steady-state*. Transient response is the solution of the equations of motion when $\mathbf{F} = 0$ or $\mathbf{F}$ is active for a short period of time. Because most industrial machines are equipped with a rotating motor, periodic and harmonic excitation is very common. Frequency response is the steady-state solution of equations of motion when the system is harmonically excited. In frequency analysis we seek the steady-state response of the system, after the effect of initial conditions dies out.

Frequency response of mechanical systems, such as vehicles, is dominated by the natural frequencies of the system and by excitation frequencies. The

amplitude of vibration increases when an excitation frequency approaches one of the natural frequencies of the system. Frequency domains around the natural frequencies are called the *resonance zone*. The amplitude of vibration in resonance zones can be reduced by introducing damping.

*One*-DOF, harmonically excited systems may be classified as *base excitation, eccentric excitation, eccentric base excitation,* and *forced excitation.* Every frequency response these systems can be expressed by one of the functions $S_i$, $G_i$, and $\Phi_i$, each with a specific characteristic. We usually use a graphical illustration to see the frequency response of the system as a function of frequency ratio $r = \omega/\omega_n$ and damping ratio $\xi = c/\sqrt{4km}$.

## 12.8   Key Symbols

| | |
|---|---|
| $a \equiv \ddot{x}$ | acceleration |
| $a_1$ | distance from mass center to front axle |
| $a_2$ | distance from mass center to rear axle |
| $[a], [A]$ | coefficient matrix |
| $A, B, C$ | unknown coefficients for frequency responses |
| $b_1$ | distance from mass center to left wheel |
| $b_2$ | distance from mass center to right wheel |
| $c$ | damping |
| $c^{\star}$ | optimum damping |
| $c_{eq}$ | equivalent damping |
| $c_{ij}$ | element of row $i$ and column $j$ of a damping matrix |
| $[c]$ | damping matrix |
| $D$ | denominator |
| $e$ | eccentricity arm |
| $e$ | exponential function |
| $E$ | mechanical energy |
| $E$ | Young modulus of elasticity |
| $f = 1/T$ | cyclic frequency [ Hz] |
| $f, \mathbf{F}$ | force |
| $f_c$ | damper force |
| $f_{eq}$ | equivalent force |
| $f_k$ | spring force |
| $f_m$ | required force to move a mass $m$ |
| $F$ | amplitude of a harmonic force $f = F \sin \omega t$ |
| $F_0$ | constant force |
| $F_t$ | tension force |
| $F_T$ | transmitted force |
| $g$ | gravitational acceleration |
| $G_0, G_1, G_2$ | amplitude frequency response |
| $I$ | area moment of inertia for beams |
| $I$ | mass moment of inertia for vehicles |
| $\mathbf{I}$ | identity matrix |
| $k$ | stiffness |
| $k^{\star}$ | optimum stiffness |
| $k_{eq}$ | equivalent stiffness |
| $k_{ij}$ | element of row $i$ and column $j$ of a stiffness matrix |
| $k_R$ | antiroll bar torsional stiffness |
| $[k]$ | stiffness matrix |
| $K$ | kinetic energy |
| $l$ | length |
| $m$ | mass |
| $m_b$ | device mass |

| | |
|---|---|
| $m_e$ | eccentric mass |
| $m_{ij}$ | element of row $i$ and column $j$ of a mass matrix |
| $m_s$ | sprung mass |
| $m_s$ | mass of spring |
| $m_u$ | unsprung mass |
| $[m]$ | mass matrix |
| $M$ | mass of platform |
| $N$ | numerator |
| $\mathbf{p}$ | momentum |
| $Q$ | general amplitude |
| $r = \omega/\omega_n$ | frequency ratio |
| $r,\ R$ | radius |
| $r_1, r_2$ | frequency ratio at nodes |
| $r_n = \omega_n/\omega_1$ | dimensionless natural frequency |
| $S$ | overshoot |
| $S$ | quadrature |
| $S_0, S_1, \cdots, S_4$ | amplitude frequency response |
| $t$ | time |
| $t_p$ | peak time |
| $t_r$ | rise time |
| $t_s$ | settling time |
| $T$ | period |
| $T_n$ | natural period |
| $v \equiv \dot{x},\ \mathbf{v}$ | velocity |
| $V$ | potential energy |
| $w$ | track of a car |
| $w_f$ | front track of a car |
| $w_r$ | rear track of a car |
| $x, y, z,\ \mathbf{x}$ | displacement |
| $x_0$ | initial displacement |
| $x_h$ | homogeneous solution |
| $x_p$ | particular solution |
| $x_P$ | peak displacement |
| $\dot{x}_0$ | initial velocity |
| $X, Y, Z,$ | amplitude |
| $Z_i, i = 1, 2, \cdots$ | short notation parameters |
| | |
| $\alpha = \omega_2/\omega_1$ | natural frequency ratio |
| $\delta$ | deflection |
| $\delta_s$ | static deflection |
| $\varepsilon$ | mass ratio |
| $\theta$ | angular motion |
| $\Theta$ | amplitude of angular vibration |
| $\lambda$ | eigenvalue |
| $\mu$ | amplitude frequency response |

| | |
|---|---|
| $\varphi$ | phase angle |
| $\Phi_0, \Phi_1, \cdots, \Phi_3$ | phase frequency response |
| $\omega = 2\pi f$ | angular frequency $[\,\mathrm{rad/\,s}]$ |
| $\omega_n$ | natural frequency |
| $\xi$ | damping ratio |
| $\xi^{\star}$ | optimum damping ratio |

Subscriptions

| | |
|---|---|
| $d$ | driver |
| $f$ | front |
| $M$ | maximum |
| $r$ | rear |
| $s$ | sprung mass |
| $u$ | unsprung mass |

## Exercises

1. Natural frequency and damping ratio.

   A *one* DOF mass-spring-damper has $m = 1\,\text{kg}$, $k = 1000\,\text{N/m}$ and $c = 100\,\text{N s/m}$. Determine the natural frequency, and damping ratio of the system.

2. Equivalent spring.

   Determine the equivalent spring for the vibrating system that is shown in Figure 12.55.
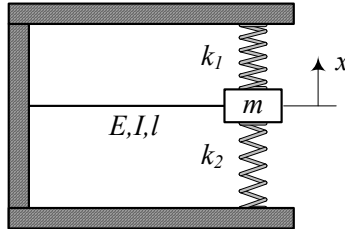


FIGURE 12.55. Spring connected cantilever beam.

3. ★ Equivalent mass for massive spring.

   Figure 12.56 illustrates an elastic cantilever beam with a tip mass $m$. The beam has characteristics: elasticity $E$, area moment of inertia $I$, mass $m_s$. Assume that when the tip mass $m$ oscillates laterally, the beam gets a harmonic shape.

   $$y = Y \sin \frac{\pi x}{2l}$$

4. Ideal spring connected pendulum.

   Determine the kinetic and potential energies of the pendulum in Figure 12.57, at an arbitrary angle $\theta$. The free length of the spring is $l = a - b$.

5. ★ General spring connected pendulum.

   Determine the potential energy of the pendulum in Figure 12.57, at an angle $\theta$, if:

   (a) The free length of the spring is $l = a - 1.2b$.
   (b) The free length of the spring is $l = a - 0.8b$.
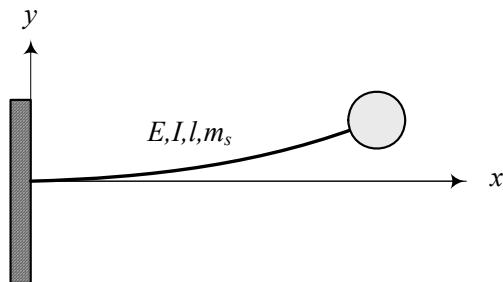
FIGURE 12.56. An elastic and massive cantilever beam with a tip mass $m$.
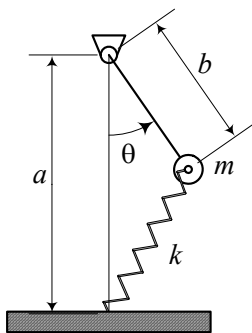


FIGURE 12.57. Spring connected pendulum.

6. ★ Spring connected rectilinear oscillator.

   Determine the kinetic and potential energies of the oscillator shown in Figure 12.58. The free length of the spring is $a$.

   (a) Express your answers in terms of the variable angle $\theta$.
   (b) Express your answers in terms of the variable distance $x$.
   (c) Determine the equation of motion for large and small $\theta$.
   (d) Determine the equation of motion for large and small $x$.

7. ★ Cushion mathematical model.

   Figure 12.59 illustrates a mathematical model for cushion suspension. Such a model can be used to analyze the driver's seat, or a rubbery pad suspension.

   (a) Derive the equations of motion for the variables $x$ and $z$ and using $y$ as a known input function.
   (b) Eliminate $z$ and derive a third-order equation for $x$.
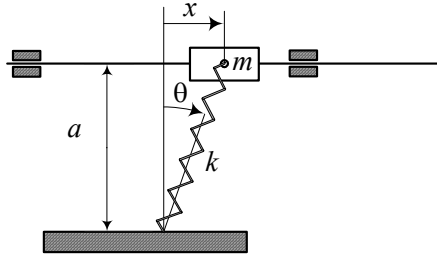
FIGURE 12.58. Spring connected rectilinear oscillator.
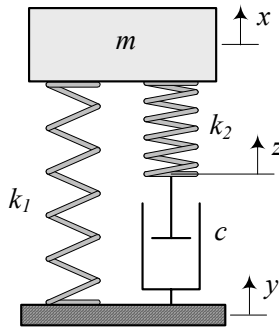


FIGURE 12.59. Mathematical model for cushion suspension.

8. Forced excitation and spring stiffness.

A forced excited mass-spring-damper system has

$$m = 200 \, \text{kg}$$
$$c = 1000 \, \text{N s}/\,\text{m}.$$

Determine the stiffness of the spring, $k$, such that the natural frequency of the system is *one* Hz. What would be the amplitude of displacement, velocity and acceleration of $m$ if a force $F$ is applied on the mass $m$.

$$F = 100 \sin 10t$$

9. Forced excitation and system parameters.

A forced excited *m-k-c* system is under a force $f$.

$$F = 100 \sin 10t$$

If the mass $m = 200 \, \text{kg}$ should not have a dimensionless steady-state amplitude higher than *two* when it is excited at the natural frequency, determine $m$, $c$, $k$, $X$, $\varphi_x$, and $F_T$.

10. Base excited system and spring stiffness.

    A base excited $m$-$k$-$c$ system has

    $$m = 200\,\text{kg}$$
    $$c = 1000\,\text{N\,s/m}.$$

    Determine the stiffness of the spring, $k$, such that the steady-state amplitude of $m$ is lass than $0.07\,\text{m}$ when the base is excited as

    $$y = 0.05\sin 2\pi t$$

    at the natural frequency of the system.

11. Base excited system and absolute acceleration.

    Assume a base excited $m$-$k$-$c$ system is vibrating at the node of its absolute acceleration frequency response. If the base is excited according to
    $$y = 0.05\sin 2\pi t$$
    determine $\omega_n$, $\ddot{X}$, $X$.

12. Eccentric excitation and transmitted force.

    An engine with mass $m = 175\,\text{kg}$ and eccentricity $m_e e = 0.4\times 0.1\,\text{kg\,m}$ is turning at $\omega_e = 4000$ $rpm$.

    (a) Determine the steady-state amplitude of its vibration, if there are four engine mounts, each with $k = 10000\,\text{N/m}$ and $c = 100\,\text{N\,s/m}$.

    (b) Determine the transmitted force to the base.

13. ★ Eccentric base excitation and absolute displacement.

    An eccentric base excited system has $m = 3\,\text{kg}$, $m_b = 175\,\text{kg}$, $m_e e = 0.4\times 0.1\,\text{kg\,m}$, and $\omega = 4000$ $rpm$. If $Z/(e\varepsilon) = 2$ at $r = 1$, calculate $X$ and $Y$.

14. Characteristic values and free vibrations.

    An $m$-$k$-$c$ system has

    $$m = 250\,\text{kg}$$
    $$k = 8000\,\text{N/m}$$
    $$c = 1000\,\text{N\,s/m}.$$

    Determine the characteristic values of the system and its free vibration response, for zero initial conditions.

15. ★ Response to the step input.

Consider an *m-k-c* system with

$$
\begin{aligned}
m &= 250\,\text{kg} \\
k &= 8000\,\text{N/m} \\
c &= 1000\,\text{N s/m}.
\end{aligned}
$$

Determine the step input parameters, $t_r$, $t_P$, $x_P$, $S$, and $t_s$ for 2% window.

16. Damping ratio determination.

Consider a vibrating system that after $n = 100$ times oscillation, the peak amplitude drops by 2%. Determine the exact and approximate values of $\xi$.

17. The car lateral moment of inertia.

Consider a car with the following characteristics:

| | |
|---|---|
| $b_1$ | 746 mm |
| $b_2$ | 740 mm |
| mass | 1245 kg |
| $a_1$ | 1100 mm |
| $a_2$ | 1323 mm |
| $h$ | 580 mm |
| $I_x$ | 335 kg m$^2$ |
| $I_y$ | 1095 kg m$^2$ |

Determine the period of oscillation when the car is on a solid steel platform with dimension 2000 mm × 3800 mm × 35 mm,

(a) laterally

(b) longitudinally.

18. ★ Optimal vibration absorber.

Consider a primary system with $m_1 = 250\,\text{kg}$ and $k = 8000\,\text{N/m}$.

(a) Determine the best suspension for the secondary system with $m_2 = 1\,\text{kg}$ to act as a vibration absorber.

(b) Determine the natural frequencies of the two system for the optimized vibration absorber.

(c) Determine the nodal frequencies and amplitudes of the primary system.

19. ★ Frequency response.

Prove the following equations:

$$G_2 = \frac{F_{T_B}}{kY}$$

$$G_2 = \frac{F_{T_E}}{e\omega_n^2 m_e}$$

$$G_2 = \frac{F_{T_R}}{e\omega_n^2 m_e}\left(1 + \frac{m_b}{m}\right)$$

# 13

# Vehicle Vibrations

Vehicles are multiple-DOF systems as the one that is shown in Figure 13.1. The vibration behavior of a vehicle, which is called *ride* or *ride comfort*, is highly dependent on the natural frequencies and mode shapes of the vehicle. In this chapter, we review and examine the applied methods of determining the equations of motion, natural frequencies, and mode shapes of different models of vehicles.
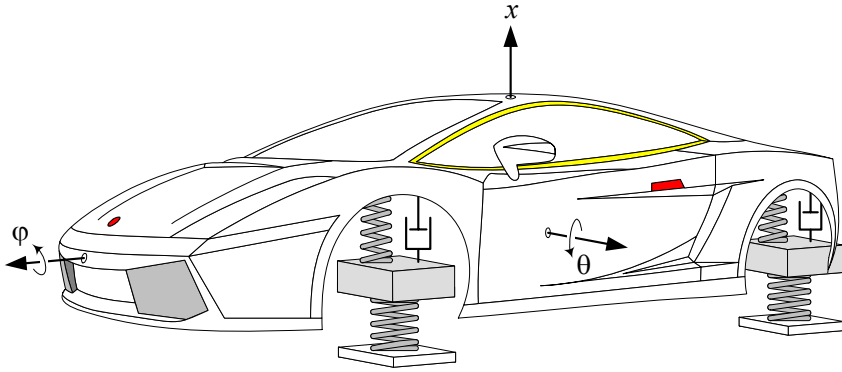


FIGURE 13.1. A full car vibrating model of a vehicle.

## 13.1 Lagrange Method and Dissipation Function

Lagrange equation,

$$\frac{d}{dt}\left(\frac{\partial K}{\partial \dot{q}_r}\right) - \frac{\partial K}{\partial q_r} = F_r \qquad r = 1, 2, \cdots n \qquad (13.1)$$

or,

$$\frac{d}{dt}\left(\frac{\partial \mathcal{L}}{\partial \dot{q}_r}\right) - \frac{\partial \mathcal{L}}{\partial q_r} = Q_r \qquad r = 1, 2, \cdots n \qquad (13.2)$$

as introduced in Equations (9.243) and (9.298), can both be applied to find the equations of motion for a vibrating system. However, for small and linear vibrations, we may use a simpler and more practical Lagrange

equation such as

$$\frac{d}{dt}\left(\frac{\partial K}{\partial \dot{q}_r}\right) - \frac{\partial K}{\partial q_r} + \frac{\partial D}{\partial \dot{q}_r} + \frac{\partial V}{\partial q_r} = f_r \qquad r = 1, 2, \cdots n \qquad (13.3)$$

where $K$ is the kinetic energy, $V$ is the potential energy, and $D$ is the *dissipation function* of the system

$$
\begin{aligned}
K &= \frac{1}{2}\dot{\mathbf{x}}^T [m] \dot{\mathbf{x}} \\
&= \frac{1}{2}\sum_{i=1}^{n}\sum_{j=1}^{n} \dot{x}_i m_{ij} \dot{x}_j \qquad (13.4)
\end{aligned}
$$

$$
\begin{aligned}
V &= \frac{1}{2}\mathbf{x}^T [k] \mathbf{x} \\
&= \frac{1}{2}\sum_{i=1}^{n}\sum_{j=1}^{n} x_i k_{ij} x_j \qquad (13.5)
\end{aligned}
$$

$$
\begin{aligned}
D &= \frac{1}{2}\dot{\mathbf{x}}^T [c] \dot{\mathbf{x}} \\
&= \frac{1}{2}\sum_{i=1}^{n}\sum_{j=1}^{n} \dot{x}_i c_{ij} \dot{x}_j \qquad (13.6)
\end{aligned}
$$

and $f_r$ is the applied force on the mass $m_r$.

**Proof.** Consider a one-DOF mass-spring-damper vibrating system. When viscous damping is the only type of damping in the system, we may employ a function known as *Rayleigh dissipation function*

$$D = \frac{1}{2}c\dot{x}^2 \qquad (13.7)$$

to find the damping force $f_c$ by differentiation.

$$f_c = -\frac{\partial D}{\partial \dot{x}}. \qquad (13.8)$$

Remembering the elastic force $f_k$ can be found from a potential energy $V$

$$f_k = -\frac{\partial V}{\partial x}$$

then, the generalized force $F$ can be separated to

$$
\begin{aligned}
F &= f_c + f_k + f \\
&= -\frac{\partial D}{\partial \dot{x}} - \frac{\partial V}{\partial x} + f \qquad (13.9)
\end{aligned}
$$
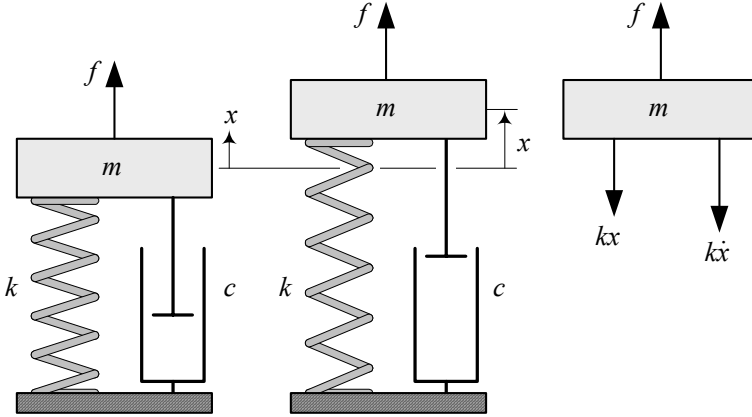
FIGURE 13.2. A one DOF forced mass-spring-damper system.

where $f$ is the non-conservative applied force on mass $m$. Substituting (13.9) in (13.1)

$$\frac{d}{dt}\left(\frac{\partial K}{\partial \dot{x}}\right) - \frac{\partial K}{\partial x} = -\frac{\partial D}{\partial \dot{x}} - \frac{\partial V}{\partial x} + f \qquad (13.10)$$

gives us the Lagrange equation for a viscous damped vibrating system.

$$\frac{d}{dt}\left(\frac{\partial K}{\partial \dot{x}}\right) - \frac{\partial K}{\partial x} + \frac{\partial D}{\partial \dot{x}} + \frac{\partial V}{\partial x} = f \qquad (13.11)$$

When the vibrating system has $n$ DOF, then the kinetic energy $K$, potential energy $V$, and dissipating function $D$ are as (13.4)-(13.6). Applying the Lagrange equation to the $n$-DOF system would result $n$ second-order differential equations (13.3). ∎

**Example 472** *A one-DOF forced mass-spring-damper system.*
*Figure 13.2 illustrates a single DOF mass-spring-damper system with an external force $f$ applied on the mass $m$. The kinetic and potential energies of the system, when it is in motion, are*

$$K = \frac{1}{2}m\dot{x}^2 \qquad (13.12)$$

$$V = \frac{1}{2}kx^2 \qquad (13.13)$$

*and its dissipation function is*

$$D = \frac{1}{2}c\dot{x}^2. \qquad (13.14)$$
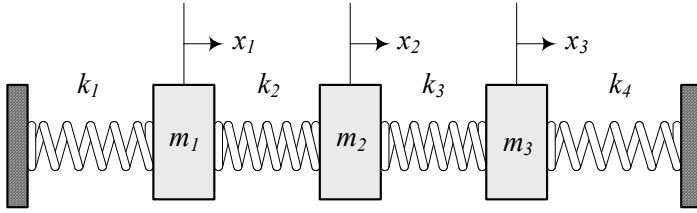
FIGURE 13.3. An undamped three-DOF system.

*Substituting (13.12)-(13.14) in Lagrange equation (13.3), generates the following equation of motion:*

$$\frac{d}{dt}(m\dot{x}) + c\dot{x} + kx = f, \tag{13.15}$$

*because*

$$\frac{\partial K}{\partial \dot{x}} = m\dot{x} \tag{13.16}$$

$$\frac{\partial K}{\partial x} = 0 \tag{13.17}$$

$$\frac{\partial D}{\partial \dot{x}} = c\dot{x} \tag{13.18}$$

$$\frac{\partial V}{\partial x} = kx. \tag{13.19}$$

**Example 473** *An undamped three-DOF system.*

*Figure 13.3 illustrates an undamped three-DOF linear vibrating system. The kinetic and potential energies of the system are:*

$$K = \frac{1}{2}m_1\dot{x}_1^2 + \frac{1}{2}m_2\dot{x}_2^2 + \frac{1}{2}m_3\dot{x}_3^2 \tag{13.20}$$

$$V = \frac{1}{2}k_1x_1^2 + \frac{1}{2}k_2(x_1 - x_2)^2 + \frac{1}{2}k_3(x_2 - x_3)^2 + \frac{1}{2}k_4x_3^2 \tag{13.21}$$

*Because there is no damping in the system, we may find the Lagrangean $\mathcal{L}$*

$$\mathcal{L} = K - V \tag{13.22}$$

*and use Equation (13.2) with $Q_r = 0$*

$$\frac{\partial \mathcal{L}}{\partial x_1} = -k_1x_1 - k_2(x_1 - x_2) \tag{13.23}$$

$$\frac{\partial \mathcal{L}}{\partial x_2} = k_2(x_1 - x_2) - k_3(x_2 - x_3) \tag{13.24}$$

$$\frac{\partial \mathcal{L}}{\partial x_3} = k_3(x_2 - x_3) - k_4x_3 \tag{13.25}$$

$$\frac{\partial \mathcal{L}}{\partial \dot{x}_1} = m_1 \dot{x}_1 \tag{13.26}$$

$$\frac{\partial \mathcal{L}}{\partial \dot{x}_2} = m_2 \dot{x}_2 \tag{13.27}$$

$$\frac{\partial \mathcal{L}}{\partial \dot{x}_3} = m_3 \dot{x}_3 \tag{13.28}$$

to find the equations of motion:

$$m_1 \ddot{x}_1 + k_1 x_1 + k_2 (x_1 - x_2) = 0 \tag{13.29}$$
$$m_2 \ddot{x}_2 - k_2 (x_1 - x_2) + k_3 (x_2 - x_3) = 0 \tag{13.30}$$
$$m_3 \ddot{x}_3 - k_3 (x_2 - x_3) + k_4 x_3 = 0 \tag{13.31}$$

These equations can be rewritten in matrix form for simpler calculation.

$$\begin{bmatrix} m_1 & 0 & 0 \\ 0 & m_2 & 0 \\ 0 & 0 & m_3 \end{bmatrix} \begin{bmatrix} \ddot{x}_1 \\ \ddot{x}_2 \\ \ddot{x}_3 \end{bmatrix}$$
$$+ \begin{bmatrix} k_1 + k_2 & -k_2 & 0 \\ -k_2 & k_2 + k_3 & -k_3 \\ 0 & -k_3 & k_3 + k_4 \end{bmatrix} \begin{bmatrix} x_1 \\ x_2 \\ x_3 \end{bmatrix} = 0 \tag{13.32}$$

**Example 474** *An eccentric excited one-DOF system.*
*An eccentric excited one-DOF system is shown in Figure 12.31 with mass $m$ supported by a suspension made up of a spring $k$ and a damper $c$. There is also a mass $m_e$ at a distance $e$ that is rotating with an angular velocity $\omega$. We may find the equation of motion by applying the Lagrange method.*
*The kinetic energy of the system is*

$$K = \frac{1}{2}(m - m_e)\dot{x}^2 + \frac{1}{2}m_e(\dot{x} + e\omega\cos\omega t)^2 + \frac{1}{2}m_e(-e\omega\sin\omega t)^2 \tag{13.33}$$

*because the velocity of the main vibrating mass $m - m_e$ is $\dot{x}$, and the velocity of the eccentric mass $m_e$ has two components $\dot{x} + e\omega\cos\omega t$ and $-e\omega\sin\omega t$. The potential energy and dissipation function of the system are:*

$$V = \frac{1}{2}kx^2 \tag{13.34}$$

$$D = \frac{1}{2}c\dot{x}^2. \tag{13.35}$$

*Applying the Lagrange equation (13.3),*

$$\frac{\partial K}{\partial \dot{x}} = m\dot{x} + m_e e\omega \cos \omega t \tag{13.36}$$

$$\frac{d}{dt}\left(\frac{\partial K}{\partial \dot{x}}\right) = m\ddot{x} - m_e e\omega^2 \sin \omega t \tag{13.37}$$

$$\frac{\partial D}{\partial \dot{x}} = c\dot{x} \tag{13.38}$$

$$\frac{\partial V}{\partial x} = kx \tag{13.39}$$

*provides the equation of motion*

$$m\ddot{x} + c\dot{x} + kx = m_e e\omega^2 \sin \omega t \tag{13.40}$$

*that is the same as Equation (12.208).*

**Example 475** *An eccentric base excited vibrating system.*
   *Figure 12.35 illustrates a one DOF eccentric base excited vibrating system. A mass m is mounted on an eccentric excited base by a spring k and a damper c. The base has a mass $m_b$ with an attached unbalance mass $m_e$ at a distance e. The mass $m_e$ is rotating with an angular velocity $\omega$.*
   *We may derive the equation of motion of the system by applying Lagrange method. The required functions are:*

$$K = \frac{1}{2}m\dot{x}^2 + \frac{1}{2}(m_b - m_e)\dot{y}^2$$
$$+\frac{1}{2}m_e(\dot{y} - e\omega \cos \omega t)^2 + \frac{1}{2}m_e(e\omega \sin \omega t)^2 \tag{13.41}$$

$$V = \frac{1}{2}k(x - y)^2 \tag{13.42}$$

$$D = \frac{1}{2}c(\dot{x} - \dot{y})^2. \tag{13.43}$$

*Applying the Lagrange method (13.3), provides the equations*

$$m\ddot{x} + c(\dot{x} - \dot{y}) + k(x - y) = 0 \tag{13.44}$$
$$m_b\ddot{y} + m_e e\omega^2 \sin \omega t - c(\dot{x} - \dot{y}) - k(x - y) = 0 \tag{13.45}$$

*because*

$$\frac{\partial K}{\partial \dot{x}} = m\dot{x} \tag{13.46}$$

$$\frac{d}{dt}\left(\frac{\partial K}{\partial \dot{x}}\right) = m\ddot{x} \tag{13.47}$$

$$\frac{\partial D}{\partial \dot{x}} = c(\dot{x} - \dot{y}) \tag{13.48}$$

$$\frac{\partial V}{\partial x} = k(x - y) \tag{13.49}$$
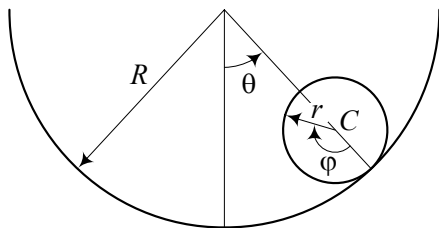
FIGURE 13.4. A uniform disc, rolling in a circular path.

$$\frac{\partial K}{\partial \dot{y}} = m_b \dot{y} - m_e e\omega \cos \omega t \tag{13.50}$$

$$\frac{d}{dt}\left(\frac{\partial K}{\partial \dot{y}}\right) = m_b \ddot{y} + m_e e\omega^2 \sin \omega t \tag{13.51}$$

$$\frac{\partial D}{\partial \dot{y}} = -c\left(\dot{x} - \dot{y}\right) \tag{13.52}$$

$$\frac{\partial V}{\partial y} = -k\left(x - y\right). \tag{13.53}$$

*Using $z = x - y$, we may combine Equations (13.44) and (13.45) to find the equation of relative motion*

$$\frac{mm_b}{m_b + m}\ddot{z} + c\dot{z} + kz = \frac{mm_e}{m_b + m}e\omega^2 \sin \omega t \tag{13.54}$$

*that is equal to*

$$\ddot{z} + 2\xi\omega_n \dot{z} + \omega_n^2 z = \varepsilon e\omega^2 \sin \omega t \tag{13.55}$$

$$\varepsilon = \frac{m_e}{m_b}. \tag{13.56}$$

**Example 476 ★** *A rolling disc in a circular path.*

*Figure 13.4 illustrates a uniform disc with mass m and radius r. The disc is rolling without slip in a circular path with radius R. The disc may have a free oscillation around $\theta = 0$.*

*When the oscillation is very small, we may substitute the oscillating disc with an equivalent mass-spring system. To find the equation of motion, we employ the Lagrange method. The energies of the system are*

$$K = \frac{1}{2}mv_C^2 + \frac{1}{2}I_c\omega^2$$

$$= \frac{1}{2}m(R - r)^2\dot{\theta}^2 + \frac{1}{2}\left(\frac{1}{2}mr^2\right)\left(\dot{\varphi} - \dot{\theta}\right)^2 \tag{13.57}$$

$$V = -mg(R - r)\cos\theta. \tag{13.58}$$

*When there is no slip, there is a constraint between $\theta$ and $\varphi$*

$$R\theta = r\varphi \tag{13.59}$$
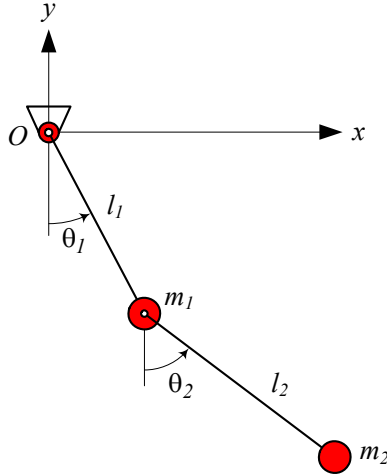
FIGURE 13.5. A double pendulum.

*which can be used to eliminate $\varphi$ from $K$.*

$$K = \frac{3}{4}m\,(R-r)^2\,\dot{\theta}^2 \tag{13.60}$$

*Based on the following partial derivatives:*

$$\frac{d}{dt}\left(\frac{\partial \mathcal{L}}{\partial \dot{\theta}}\right) = \frac{3}{2}m\,(R-r)^2\,\ddot{\theta} \tag{13.61}$$

$$\frac{\partial \mathcal{L}}{\partial \theta} = -mg(R-r)\sin\theta \tag{13.62}$$

*we find the equation of motion for the oscillating disc.*

$$\frac{3}{2}\,(R-r)\,\ddot{\theta} + g\sin\theta = 0 \tag{13.63}$$

*When $\theta$ is very small, this equation is equivalent to a mass-spring system with $m_{eq} = 3\,(R-r)$ and $k_{eq} = 2g$.*

**Example 477 ★** *A double pendulum.*

*Figure 13.5 illustrates a double pendulum made by a series of two pendulums. There are two massless rods with lengths $l_1$ and $l_2$, and two point masses $m_1$ and $m_2$. The variables $\theta_1$ and $\theta_2$ can be used as the generalized coordinates to express the system configuration. To calculate the Lagrangean of the system and find the equations of motion, we start by defining the global position of the masses.*

$$x_1 = l_1 \sin \theta_1 \tag{13.64}$$
$$y_1 = -l_1 \cos \theta_1 \tag{13.65}$$
$$x_2 = l_1 \sin \theta_1 + l_2 \sin \theta_2 \tag{13.66}$$
$$y_2 = -l_1 \cos \theta_1 - l_2 \cos \theta_2 \tag{13.67}$$

*Time derivatives of the coordinates are*

$$\dot{x}_1 = l_1 \dot{\theta}_1 \cos \theta_1 \tag{13.68}$$
$$\dot{y}_1 = l_1 \dot{\theta}_1 \sin \theta_1 \tag{13.69}$$
$$\dot{x}_2 = l_1 \dot{\theta}_1 \cos \theta_1 + l_2 \dot{\theta}_2 \cos \theta_2 \tag{13.70}$$
$$\dot{y}_2 = l_1 \dot{\theta}_1 \sin \theta_1 + l_2 \dot{\theta}_2 \sin \theta_2 \tag{13.71}$$

*and therefore, the squares of the masses' velocities are*

$$
\begin{aligned}
v_1^2 &= \dot{x}_1^2 + \dot{y}_1^2 \\
&= l_1^2 \dot{\theta}_1^2 \tag{13.72} \\
v_2^2 &= \dot{x}_2^2 + \dot{y}_2^2 \\
&= l_1^2 \dot{\theta}_1^2 + l_2^2 \dot{\theta}_2^2 + 2 l_1 l_2 \dot{\theta}_1 \dot{\theta}_2 \cos(\theta_1 - \theta_2). \tag{13.73}
\end{aligned}
$$

*The kinetic energy of the pendulum is then equal to*

$$
\begin{aligned}
K &= \frac{1}{2} m_1 v_1^2 + \frac{1}{2} m_2 v_2^2 \\
&= \frac{1}{2} m_1 l_1^2 \dot{\theta}_1^2 + \frac{1}{2} m_2 \left( l_1^2 \dot{\theta}_1^2 + l_2^2 \dot{\theta}_2^2 + 2 l_1 l_2 \dot{\theta}_1 \dot{\theta}_2 \cos(\theta_1 - \theta_2) \right). \tag{13.74}
\end{aligned}
$$

*The potential energy of the pendulum is equal to sum of the potentials of each mass.*

$$
\begin{aligned}
V &= m_1 g y_1 + m_2 g y_2 \\
&= -m_1 g l_1 \cos \theta_1 - m_2 g \left( l_1 \cos \theta_1 + l_2 \cos \theta_2 \right) \tag{13.75}
\end{aligned}
$$

*The kinetic and potential energies make the following Lagrangean:*

$$
\begin{aligned}
\mathcal{L} &= K - V \\
&= \frac{1}{2} m_1 l_1^2 \dot{\theta}_1^2 + \frac{1}{2} m_2 \left( l_1^2 \dot{\theta}_1^2 + l_2^2 \dot{\theta}_2^2 + 2 l_1 l_2 \dot{\theta}_1 \dot{\theta}_2 \cos(\theta_1 - \theta_2) \right) \\
&\quad + m_1 g l_1 \cos \theta_1 + m_2 g \left( l_1 \cos \theta_1 + l_2 \cos \theta_2 \right) \tag{13.76}
\end{aligned}
$$

*Employing Lagrange method (13.2) we find the following equations of motion:*

$$
\begin{aligned}
\frac{d}{dt} \left( \frac{\partial \mathcal{L}}{\partial \dot{\theta}_1} \right) - \frac{\partial \mathcal{L}}{\partial \theta_1} &= (m_1 + m_2) l_1^2 \ddot{\theta}_1 + m_2 l_1 l_2 \ddot{\theta}_2 \cos(\theta_1 - \theta_2) \\
&\quad - m_2 l_1 l_2 \dot{\theta}_2^2 \sin(\theta_1 - \theta_2) + (m_1 + m_2) l_1 g \sin \theta_1 \\
&= 0 \tag{13.77}
\end{aligned}
$$
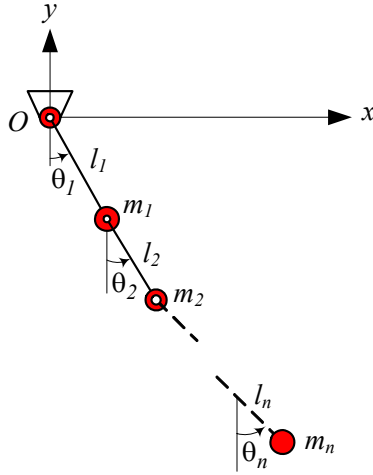
FIGURE 13.6. A chain pendulum.

$$\frac{d}{dt}\left(\frac{\partial \mathcal{L}}{\partial \dot{\theta}_2}\right) - \frac{\partial \mathcal{L}}{\partial \theta_2} = m_2 l_2^2 \ddot{\theta}_2 + m_2 l_1 l_2 \ddot{\theta}_1 \cos(\theta_1 - \theta_2)$$

$$+ m_2 l_1 l_2 \dot{\theta}_1^2 \sin(\theta_1 - \theta_2) + m_2 l_2 g \sin \theta_2$$

$$= 0 \qquad (13.78)$$

**Example 478 ★** *Chain pendulum.*

*Consider an n-chain-pendulum as shown in Figure 13.6. Each pendulum has a massless length $l_i$ with a concentrated point mass $m_i$, and a generalized angular coordinate $\theta_i$ measured from the vertical direction.*

*The $x_i$ and $y_i$ components of the mass $m_i$ are*

$$x_i = \sum_{j=1}^{i} l_j \sin \theta_j \qquad (13.79)$$

$$y_i = -\sum_{j=1}^{i} l_j \cos \theta_j. \qquad (13.80)$$

*We find their time derivatives*

$$\dot{x}_i = \sum_{j=1}^{i} l_j \dot{\theta}_j \cos \theta_j \qquad (13.81)$$

$$\dot{y}_i = \sum_{j=1}^{i} l_j \dot{\theta}_j \sin \theta_j \qquad (13.82)$$

*and the square of $\dot{x}_i$ and $\dot{y}_i$*

$$
\begin{aligned}
\dot{x}_i^2 &= \left( \sum_{j=1}^{i} l_j \dot{\theta}_j \cos \theta_j \right) \left( \sum_{k=1}^{i} l_k \dot{\theta}_k \cos \theta_k \right) \\
&= \sum_{j=1}^{n} \sum_{k=1}^{n} l_j l_k \dot{\theta}_j \dot{\theta}_k \cos \theta_j \cos \theta_k
\end{aligned}
\tag{13.83}
$$

$$
\begin{aligned}
\dot{y}_i^2 &= \left( \sum_{j=1}^{i} l_j \dot{\theta}_j \sin \theta_j \right) \left( \sum_{k=1}^{i} l_k \dot{\theta}_k \sin \theta_k \right) \\
&= \sum_{j=1}^{i} \sum_{k=1}^{i} l_j l_k \dot{\theta}_j \dot{\theta}_k \sin \theta_j \sin \theta_k
\end{aligned}
\tag{13.84}
$$

*to calculate the velocity $v_i$ of the mass $m_i$.*

$$
\begin{aligned}
v_i^2 &= \dot{x}_i^2 + \dot{y}_i^2 \\
&= \sum_{j=1}^{i} \sum_{k=1}^{i} l_j l_k \dot{\theta}_j \dot{\theta}_k \left( \cos \theta_j \cos \theta_k + \sin \theta_j \sin \theta_k \right) \\
&= \sum_{j=1}^{i} \sum_{k=1}^{i} l_j l_k \dot{\theta}_j \dot{\theta}_k \cos \left( \theta_j - \theta_k \right) \\
&= \sum_{r=1}^{i} l_r^2 \dot{\theta}_r^2 + 2 \sum_{j=1}^{i} \sum_{k=j+1}^{i} l_j l_k \dot{\theta}_j \dot{\theta}_k \cos \left( \theta_j - \theta_k \right)
\end{aligned}
\tag{13.85}
$$

*Now, we may calculate the kinetic energy, $K$, of the chain.*

$$
\begin{aligned}
K &= \frac{1}{2} \sum_{i=1}^{n} m_i v_i^2 \\
&= \frac{1}{2} \sum_{i=1}^{n} m_i \left( \sum_{r=1}^{i} l_r^2 \dot{\theta}_r^2 + 2 \sum_{j=1}^{i} \sum_{k=j+1}^{i} l_j l_k \dot{\theta}_j \dot{\theta}_k \cos \left( \theta_j - \theta_k \right) \right) \\
&= \frac{1}{2} \sum_{i=1}^{n} \sum_{r=1}^{i} m_i l_r^2 \dot{\theta}_r^2 + \sum_{i=1}^{n} \sum_{j=1}^{i} \sum_{k=j+1}^{i} m_i l_j l_k \dot{\theta}_j \dot{\theta}_k \cos \left( \theta_j - \theta_k \right)
\end{aligned}
\tag{13.86}
$$

*The potential energy of the ith pendulum is related to $m_i$*

$$
\begin{aligned}
V_i &= m_i g y_i \\
&= -m_i g \sum_{j=1}^{i} l_j \cos \theta_j
\end{aligned}
\tag{13.87}
$$

*and therefore, the potential energy of the chain is*

$$V = \sum_{i=1}^{n} m_i g y_i$$

$$= -\sum_{i=1}^{n}\sum_{j=1}^{i} m_i g l_j \cos\theta_j \tag{13.88}$$

*To find the equations of motion for the chain, we may use the Lagrangean* $\mathcal{L}$

$$\mathcal{L} = K - V \tag{13.89}$$

*and apply the Lagrange equation*

$$\frac{d}{dt}\left(\frac{\partial\mathcal{L}}{\partial\dot{q}_s}\right) - \frac{\partial\mathcal{L}}{\partial q_s} = 0 \qquad s = 1, 2, \cdots n \tag{13.90}$$

*or*

$$\frac{d}{dt}\left(\frac{\partial K}{\partial\dot{q}_s}\right) - \frac{\partial K}{\partial q_s} + \frac{\partial V}{\partial q_s} = 0 \qquad s = 1, 2, \cdots n. \tag{13.91}$$

## 13.2   ★ Quadratures

If $[m]$ is an $n \times n$ square matrix and $\mathbf{x}$ is an $n \times 1$ vector, then $S$ is a scalar function called *quadrature* and is defined by

$$S = \mathbf{x}^T [m] \mathbf{x}. \tag{13.92}$$

The derivative of the quadrature $S$ with respect to the vector $\mathbf{x}$ is

$$\frac{\partial S}{\partial\mathbf{x}} = \left([m] + [m]^T\right)\mathbf{x}. \tag{13.93}$$

Kinetic energy $K$, potential energy $V$, and dissipation function $D$, are quadratures

$$K = \frac{1}{2}\dot{\mathbf{x}}^T [m]\dot{\mathbf{x}} \tag{13.94}$$

$$V = \frac{1}{2}\mathbf{x}^T [k]\mathbf{x} \tag{13.95}$$

$$D = \frac{1}{2}\dot{\mathbf{x}}^T [c]\dot{\mathbf{x}} \tag{13.96}$$

and therefore,

$$\frac{\partial K}{\partial\dot{\mathbf{x}}} = \frac{1}{2}\left([m] + [m]^T\right)\dot{\mathbf{x}} \tag{13.97}$$

$$\frac{\partial V}{\partial\mathbf{x}} = \frac{1}{2}\left([k] + [k]^T\right)\mathbf{x} \tag{13.98}$$

$$\frac{\partial D}{\partial\dot{\mathbf{x}}} = \frac{1}{2}\left([c] + [c]^T\right)\dot{\mathbf{x}}. \tag{13.99}$$

Employing quadrature derivatives and the Lagrange method,

$$\frac{d}{dt}\frac{\partial K}{\partial \dot{\mathbf{x}}} + \frac{\partial K}{\partial \mathbf{x}} + \frac{\partial D}{\partial \dot{\mathbf{x}}} + \frac{\partial V}{\partial \mathbf{x}} = \mathbf{F} \qquad (13.100)$$

the equation of motion for a linear $n$ degree-of-freedom vibrating system becomes

$$[\underline{m}]\,\ddot{\mathbf{x}} + [\underline{c}]\,\dot{\mathbf{x}} + [\underline{k}]\,\mathbf{x} = \mathbf{F} \qquad (13.101)$$

where, $[\underline{m}]$, $[\underline{c}]$, $[\underline{k}]$ are symmetric matrices.

$$[\underline{m}] \;=\; \frac{1}{2}\left([m] + [m]^T\right) \qquad (13.102)$$

$$[\underline{c}] \;=\; \frac{1}{2}\left([c] + [c]^T\right) \qquad (13.103)$$

$$[\underline{k}] \;=\; \frac{1}{2}\left([k] + [k]^T\right) \qquad (13.104)$$

Quadratures are also called *Hermitian form*.

**Proof.** Let's define a general asymmetric quadrature as

$$\begin{aligned}
S \;&=\; \mathbf{x}^T\,[a]\,\mathbf{y} \\
&=\; \sum_i \sum_j x_i a_{ij} y_j.
\end{aligned} \qquad (13.105)$$

If the quadrature is symmetric, then $\mathbf{x} = \mathbf{y}$ and

$$\begin{aligned}
S \;&=\; \mathbf{x}^T\,[a]\,\mathbf{x} \\
&=\; \sum_i \sum_j x_i a_{ij} x_j.
\end{aligned} \qquad (13.106)$$

The vectors $\mathbf{x}$ and $\mathbf{y}$ may be functions of $n$ generalized coordinates $q_i$ and time $t$.

$$\mathbf{x} \;=\; \mathbf{x}\,(q_1, q_2, \cdots, q_n, t) \qquad (13.107)$$

$$\mathbf{y} \;=\; \mathbf{y}\,(q_1, q_2, \cdots, q_n, t) \qquad (13.108)$$

$$\mathbf{q} \;=\; \begin{bmatrix} q_1 & q_2 & \cdots & q_n \end{bmatrix}^T \qquad (13.109)$$

The derivative of $\mathbf{x}$ with respect to $\mathbf{q}$ is a square matrix

$$\frac{\partial \mathbf{x}}{\partial \mathbf{q}} = \begin{bmatrix}
\dfrac{\partial x_1}{\partial q_1} & \dfrac{\partial x_2}{\partial q_1} & \cdots & \dfrac{\partial x_n}{\partial q_1} \\[2mm]
\dfrac{\partial x_1}{\partial q_2} & \dfrac{\partial x_2}{\partial q_2} & \cdots & \cdots \\[2mm]
\cdots & \cdots & \cdots & \cdots \\[2mm]
\dfrac{\partial x_1}{\partial q_n} & \cdots & \cdots & \dfrac{\partial x_n}{\partial q_n}
\end{bmatrix} \qquad (13.110)$$

that can also be expressed by

$$
\frac{\partial \mathbf{x}}{\partial \mathbf{q}} = \begin{bmatrix} \dfrac{\partial \mathbf{x}}{\partial q_1} \\ \dfrac{\partial \mathbf{x}}{\partial q_2} \\ \cdots \\ \dfrac{\partial \mathbf{x}}{\partial q_n} \end{bmatrix} \tag{13.111}
$$

or

$$
\frac{\partial \mathbf{x}}{\partial \mathbf{q}} = \begin{bmatrix} \dfrac{\partial x_1}{\partial \mathbf{q}} & \dfrac{\partial x_2}{\partial \mathbf{q}} & \cdots & \dfrac{\partial x_n}{\partial \mathbf{q}} \end{bmatrix}. \tag{13.112}
$$

Now a derivative of $S$ with respect to an element of $q_k$ is

$$
\begin{aligned}
\frac{\partial S}{\partial q_k} &= \frac{\partial}{\partial q_k} \sum_i \sum_j x_i a_{ij} y_j \\
&= \sum_i \sum_j \frac{\partial x_i}{\partial q_k} a_{ij} y_j + \sum_i \sum_j x_i a_{ij} \frac{\partial y_j}{\partial q_k} \\
&= \sum_j \sum_i \frac{\partial x_i}{\partial q_k} a_{ij} y_j + \sum_i \sum_j \frac{\partial y_j}{\partial q_k} a_{ij} x_i \\
&= \sum_j \sum_i \frac{\partial x_i}{\partial q_k} a_{ij} y_j + \sum_j \sum_i \frac{\partial y_i}{\partial q_k} a_{ji} x_j
\end{aligned} \tag{13.113}
$$

and hence, the derivative of $S$ with respect to $\mathbf{q}$ is

$$
\frac{\partial S}{\partial \mathbf{q}} = \frac{\partial \mathbf{x}}{\partial \mathbf{q}} [a] \, \mathbf{y} + \frac{\partial \mathbf{y}}{\partial \mathbf{q}} [a]^T \mathbf{x}. \tag{13.114}
$$

If $S$ is a symmetric quadrature then,

$$
\begin{aligned}
\frac{\partial S}{\partial \mathbf{q}} &= \frac{\partial}{\partial \mathbf{q}} \left( \mathbf{x}^T [a] \, \mathbf{x} \right) \\
&= \frac{\partial \mathbf{x}}{\partial \mathbf{q}} [a] \, \mathbf{x} + \frac{\partial \mathbf{x}}{\partial \mathbf{q}} [a]^T \mathbf{x}.
\end{aligned} \tag{13.115}
$$

and if $\mathbf{q} = \mathbf{x}$, then the derivative of a symmetric $S$ with respect to $\mathbf{x}$ is

$$
\begin{aligned}
\frac{\partial S}{\partial \mathbf{x}} &= \frac{\partial}{\partial \mathbf{x}} \left( \mathbf{x}^T [a] \, \mathbf{x} \right) \\
&= \frac{\partial \mathbf{x}}{\partial \mathbf{x}} [a] \, \mathbf{x} + \frac{\partial \mathbf{x}}{\partial \mathbf{x}} [a]^T \mathbf{x} \\
&= [a] \, \mathbf{x} + [a]^T \mathbf{x} \\
&= \left( [a] + [a]^T \right) \mathbf{x}.
\end{aligned} \tag{13.116}
$$

If $[a]$ is a symmetric matrix, then

$$[a] + [a]^T = 2\,[a] \tag{13.117}$$

however, if $[a]$ is not a symmetric matrix, then $[\underline{a}] = [a]+[a]^T$ is a symmetric matrix because

$$
\begin{aligned}
\underline{a}_{ij} &= a_{ij} + a_{ji} \\
&= a_{ji} + a_{ij} \\
&= \underline{a}_{ji}
\end{aligned}
\tag{13.118}
$$

and therefore,

$$[\underline{a}] = [\underline{a}]^T . \tag{13.119}$$

Kinetic energy $K$, potential energy $V$, and dissipation function $D$ can be expressed by quadratures.

$$K = \frac{1}{2}\dot{\mathbf{x}}^T\,[m]\,\dot{\mathbf{x}} \tag{13.120}$$

$$V = \frac{1}{2}\mathbf{x}^T\,[k]\,\mathbf{x} \tag{13.121}$$

$$D = \frac{1}{2}\dot{\mathbf{x}}^T\,[c]\,\dot{\mathbf{x}} \tag{13.122}$$

Substituting $K$, $V$, and $D$ in the Lagrange equation provides the equations of motion:

$$
\begin{aligned}
\mathbf{F} &= \frac{d}{dt}\frac{\partial K}{\partial \dot{\mathbf{x}}} + \frac{\partial K}{\partial \mathbf{x}} + \frac{\partial D}{\partial \dot{\mathbf{x}}} + \frac{\partial V}{\partial \mathbf{x}} \\
&= \frac{1}{2}\frac{d}{dt}\frac{\partial}{\partial \dot{\mathbf{x}}}\left(\dot{\mathbf{x}}^T\,[m]\,\dot{\mathbf{x}}\right) + \frac{1}{2}\frac{\partial}{\partial \dot{\mathbf{x}}}\left(\dot{\mathbf{x}}^T\,[c]\,\dot{\mathbf{x}}\right) + \frac{1}{2}\frac{\partial}{\partial \mathbf{x}}\left(\mathbf{x}^T\,[k]\,\mathbf{x}\right) \\
&= \frac{1}{2}\left[\frac{d}{dt}\left(\left([m]+[m]^T\right)\dot{\mathbf{x}}\right) + \left([c]+[c]^T\right)\dot{\mathbf{x}} + \left([k]+[k]^T\right)\mathbf{x}\right] \\
&= \frac{1}{2}\left([m]+[m]^T\right)\ddot{\mathbf{x}} + \frac{1}{2}\left([c]+[c]^T\right)\dot{\mathbf{x}} + \frac{1}{2}\left([k]+[k]^T\right)\mathbf{x} \\
&= [\underline{m}]\,\ddot{\mathbf{x}} + [\underline{c}]\,\dot{\mathbf{x}} + [\underline{k}]\,\mathbf{x}
\end{aligned}
\tag{13.123}
$$

where

$$[\underline{m}] = \frac{1}{2}\left([m]+[m]^T\right) \tag{13.124}$$

$$[\underline{c}] = \frac{1}{2}\left([k]+[k]^T\right) \tag{13.125}$$

$$[\underline{k}] = \frac{1}{2}\left([c]+[c]^T\right) . \tag{13.126}$$

From now on, we assume that every equation of motion is found from the Lagrange method to have symmetric coefficient matrices. Hence, we show the equations of motion as,

$$[m]\,\ddot{\mathbf{x}} + [c]\,\dot{\mathbf{x}} + [k]\,\mathbf{x} = \mathbf{F} \tag{13.127}$$
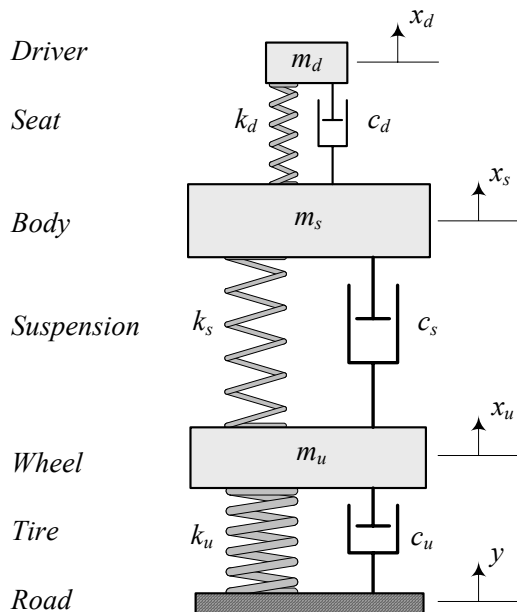
FIGURE 13.7. A quarter car model with driver.

and use $[m]$, $[c]$, $[k]$ as a substitute for $[\underline{m}]$, $[\underline{c}]$, $[\underline{k}]$

$$[m] \equiv [\underline{m}] \tag{13.128}$$
$$[c] \equiv [\underline{c}] \tag{13.129}$$
$$[k] \equiv [\underline{k}]. \tag{13.130}$$

∎

**Example 479 ★** *A quarter car model with driver's chair.*
*Figure 13.7 illustrates a quarter car model plus a driver, which is modeled by a mass $m_d$ over a linear cushion above the sprung mass $m_s$.*
*Assuming*

$$y = 0 \tag{13.131}$$

*we can find the free vibration equations of motion by the Lagrange method and quadrature derivative.*

*The kinetic energy $K$ of the system can be expressed by*

$$
\begin{aligned}
K &= \frac{1}{2}m_u \dot{x}_u^2 + \frac{1}{2}m_s \dot{x}_s^2 + \frac{1}{2}m_d \dot{x}_d^2 \\
&= \frac{1}{2}\begin{bmatrix} \dot{x}_u & \dot{x}_s & \dot{x}_d \end{bmatrix}
\begin{bmatrix} m_u & 0 & 0 \\ 0 & m_s & 0 \\ 0 & 0 & m_d \end{bmatrix}
\begin{bmatrix} \dot{x}_u \\ \dot{x}_s \\ \dot{x}_d \end{bmatrix} \\
&= \frac{1}{2}\dot{\mathbf{x}}^T \left[ m \right] \dot{\mathbf{x}}
\end{aligned}
\tag{13.132}
$$

*and the potential energy $V$ can be expressed as*

$$
\begin{aligned}
V &= \frac{1}{2}k_u \left( x_u \right)^2 + \frac{1}{2}k_s \left( x_s - x_u \right)^2 + \frac{1}{2}k_d \left( x_d - x_s \right)^2 \\
&= \frac{1}{2}\begin{bmatrix} x_u & x_s & x_d \end{bmatrix}
\begin{bmatrix} k_u + k_s & -k_s & 0 \\ -k_s & k_s + k_d & -k_d \\ 0 & -k_d & k_d \end{bmatrix}
\begin{bmatrix} x_u \\ x_s \\ x_d \end{bmatrix} \\
&= \frac{1}{2}\mathbf{x}^T \left[ k \right] \mathbf{x}.
\end{aligned}
\tag{13.133}
$$

*Similarly, the dissipation function $D$ can be expressed by*

$$
\begin{aligned}
D &= \frac{1}{2}k_u \left( \dot{x}_u \right)^2 + \frac{1}{2}k_s \left( \dot{x}_s - \dot{x}_u \right)^2 + \frac{1}{2}k_d \left( \dot{x}_d - \dot{x}_s \right)^2 \\
&= \frac{1}{2}\begin{bmatrix} \dot{x}_u & \dot{x}_s & \dot{x}_d \end{bmatrix}
\begin{bmatrix} c_u + c_s & -c_s & 0 \\ -c_s & c_s + c_d & -c_d \\ 0 & -c_d & c_d \end{bmatrix}
\begin{bmatrix} \dot{x}_u \\ \dot{x}_s \\ \dot{x}_d \end{bmatrix} \\
&= \frac{1}{2}\dot{\mathbf{x}}^T \left[ c \right] \dot{\mathbf{x}}.
\end{aligned}
\tag{13.134}
$$

*Employing the quadrature derivative method, we may find derivatives of $K$, $V$, and $D$ with respect to their variable vectors as follow:*

$$
\begin{aligned}
\frac{\partial K}{\partial \dot{\mathbf{x}}} &= \frac{1}{2}\left( \left[ m \right] + \left[ m \right]^T \right) \dot{\mathbf{x}} \\
&= \frac{1}{2}\left( \left[ k \right] + \left[ k \right]^T \right)
\begin{bmatrix} \dot{x}_u \\ \dot{x}_s \\ \dot{x}_d \end{bmatrix} \\
&= \begin{bmatrix} m_u & 0 & 0 \\ 0 & m_s & 0 \\ 0 & 0 & m_d \end{bmatrix}
\begin{bmatrix} \dot{x}_u \\ \dot{x}_s \\ \dot{x}_d \end{bmatrix}
\end{aligned}
\tag{13.135}
$$

$$\frac{\partial V}{\partial \mathbf{x}} = \frac{1}{2}\left([k] + [k]^T\right)\mathbf{x}$$

$$= \frac{1}{2}\left([k] + [k]^T\right)\begin{bmatrix} x_u \\ x_s \\ x_d \end{bmatrix}$$

$$= \begin{bmatrix} k_u + k_s & -k_s & 0 \\ -k_s & k_s + k_d & -k_d \\ 0 & -k_d & k_d \end{bmatrix}\begin{bmatrix} x_u \\ x_s \\ x_d \end{bmatrix} \qquad (13.136)$$

$$\frac{\partial D}{\partial \dot{\mathbf{x}}} = \frac{1}{2}\left([c] + [c]^T\right)\dot{\mathbf{x}}$$

$$= \frac{1}{2}\left([c] + [c]^T\right)\begin{bmatrix} \dot{x}_u \\ \dot{x}_s \\ \dot{x}_d \end{bmatrix}$$

$$= \begin{bmatrix} c_u + c_s & -c_s & 0 \\ -c_s & c_s + c_d & -c_d \\ 0 & -c_d & c_d \end{bmatrix}\begin{bmatrix} \dot{x}_u \\ \dot{x}_s \\ \dot{x}_d \end{bmatrix} \qquad (13.137)$$

*Therefore, we find the system's free vibration equations of motion.*

$$[m]\,\ddot{\mathbf{x}} + [c]\,\dot{\mathbf{x}} + [k]\,\mathbf{x} = 0 \qquad (13.138)$$

$$\begin{bmatrix} m_u & 0 & 0 \\ 0 & m_s & 0 \\ 0 & 0 & m_d \end{bmatrix}\begin{bmatrix} \ddot{x}_u \\ \ddot{x}_s \\ \ddot{x}_d \end{bmatrix} + \begin{bmatrix} c_u + c_s & -c_s & 0 \\ -c_s & c_s + c_d & -c_d \\ 0 & -c_d & c_d \end{bmatrix}\begin{bmatrix} \dot{x}_u \\ \dot{x}_s \\ \dot{x}_d \end{bmatrix}$$

$$+ \begin{bmatrix} k_u + k_s & -k_s & 0 \\ -k_s & k_s + k_d & -k_d \\ 0 & -k_d & k_d \end{bmatrix}\begin{bmatrix} x_u \\ x_s \\ x_d \end{bmatrix} = 0 \qquad (13.139)$$

**Example 480 ★** *Different* $[m]$, $[c]$, *and* $[k]$ *arrangements.*

*Mass, damping, and stiffness matrices* $[m]$, $[c]$, $[k]$ *for a vibrating system may be arranged in different forms with the same overall kinetic energy* $K$, *potential energy* $V$, *and dissipation function* $D$. *As an example, the potential energy* $V$ *for the quarter car model that is shown in Figure 13.7 may be expressed by different* $[k]$.

$$V = \frac{1}{2}k_u\left(x_u\right)^2 + \frac{1}{2}k_s\left(x_s - x_u\right)^2 + \frac{1}{2}k_d\left(x_d - x_s\right)^2 \qquad (13.140)$$

$$V = \frac{1}{2}\mathbf{x}^T\begin{bmatrix} k_u + k_s & -k_s & 0 \\ -k_s & k_s + k_d & -k_d \\ 0 & -k_d & k_d \end{bmatrix}\mathbf{x} \qquad (13.141)$$

$$V = \frac{1}{2}\mathbf{x}^T \begin{bmatrix} k_u + k_s & -2k_s & 0 \\ 0 & k_s + k_d & -2k_d \\ 0 & 0 & k_d \end{bmatrix} \mathbf{x} \qquad (13.142)$$

$$V = \frac{1}{2}\mathbf{x}^T \begin{bmatrix} k_u + k_s & 0 & 0 \\ -2k_s & k_s + k_d & 0 \\ 0 & -2k_d & k_d \end{bmatrix} \mathbf{x} \qquad (13.143)$$

*The matrices $[m]$, $[c]$, and $[k]$, in $K$, $D$, and $V$, may not be symmetric however, the matrices $[\underline{m}]$, $[\underline{c}]$, and $[\underline{k}]$ in $\partial K/\partial \dot{\mathbf{x}}$, $\partial D/\partial \dot{\mathbf{x}}$, $\partial V/\partial \mathbf{x}$ are symmetric.*

*When a matrix $[a]$ is diagonal, it is symmetric and*

$$[a] = [\underline{a}]. \qquad (13.144)$$

*A diagonal matrix cannot be written in different forms. The matrix $[m]$ in Example 479 is diagonal and hence, $K$ has only one form (13.132).*

**Example 481 ★** *Positive definite matrix.*
*A matrix $[a]$ is called **positive definite** if $\mathbf{x}^T [a] \mathbf{x} > 0$ for all $\mathbf{x} \neq 0$. A matrix $[a]$ is called **positive semidefinite** if $\mathbf{x}^T [a] \mathbf{x} \geq 0$ for all $\mathbf{x}$. Kinetic energy is positive definite and it means we cannot have $K = 0$ unless $\dot{\mathbf{x}} = 0$. Potential energy is positive semidefinite and it means we have $V \geq 0$ as long as $\mathbf{x} > 0$, however, it is possible to have a especial $\mathbf{x}_0 > 0$ at which $V = 0$.*

## 13.3 Natural Frequencies and Mode Shapes

Unforced and undamped vibrations of a system is a basic response of the system which expresses its natural behavior. We call a system with no damping and no external excitation, a *free system*. A free system is governed by the following set of differential equations.

$$[m]\ddot{\mathbf{x}} + [k]\mathbf{x} = \mathbf{0} \qquad (13.145)$$

The response of the free system is harmonic

$$\mathbf{x} = \sum_{i=1}^{n} \mathbf{u}_i \left( A_i \sin \omega_i t + B_i \cos \omega_i t \right) \qquad i = 1, 2, 3, \cdots n$$

$$= \sum_{i=1}^{n} C_i \mathbf{u}_i \sin \left( \omega_i t - \varphi_i \right) \qquad i = 1, 2, 3, \cdots n \qquad (13.146)$$

where, $\omega_i$ are the *natural frequencies* and $\mathbf{u}_i$ are the *mode shapes* of the system.

The natural frequencies $\omega_i$ are solutions of the characteristic equation of the system

$$\det\left[[k] - \omega^2\,[m]\right] = 0 \tag{13.147}$$

and the mode shapes $\mathbf{u}_i$, corresponding to $\omega_i$, are solutions of the following equation.

$$\left[[k] - \omega_i^2\,[m]\right]\mathbf{u}_i = 0 \tag{13.148}$$

The unknown coefficients $A_i$ and $B_i$, or $C_i$ and $\varphi_i$, must be determined from the initial conditions.

**Proof.** By eliminating the force and damping terms from the general equations of motion

$$[m]\,\ddot{\mathbf{x}} + [c]\,\dot{\mathbf{x}} + [k]\,\mathbf{x} = \mathbf{F} \tag{13.149}$$

we find the equations for free systems.

$$[m]\,\ddot{\mathbf{x}} + [k]\,\mathbf{x} = \mathbf{0} \tag{13.150}$$

Let's search for a possible solution of the following form

$$\mathbf{x} = \mathbf{u}\,q(t) \tag{13.151}$$
$$x_i = u_i\,q(t) \qquad i = 1, 2, 3, \cdots n. \tag{13.152}$$

This solution implies that the amplitude ratio of two coordinates during motion does not depend on time. Substituting (13.151) in Equation (13.150)

$$[m]\,\mathbf{u}\,\ddot{q}(t) + [k]\,\mathbf{u}\,q(t) = \mathbf{0} \tag{13.153}$$

and separating the time dependent terms, ends up with the following equation.

$$\begin{aligned}
-\frac{\ddot{q}(t)}{q(t)} &= [[m]\,\mathbf{u}]^{-1}\,[[k]\,\mathbf{u}] \\
&= \frac{\sum_{j=1}^{n} k_{ij}u_j}{\sum_{j=1}^{n} m_{ij}u_j} \qquad i = 1, 2, 3, \cdots n
\end{aligned} \tag{13.154}$$

Because the right hand side of this equation is time independent and the left hand side is independent of the index $i$, both sides must be equal to a constant. Let's assume the constant be a positive number $\omega^2$. Hence, Equation (13.154) can be separated into two equations

$$\ddot{q}(t) + \omega^2 q(t) = 0 \tag{13.155}$$

and

$$\left[[k] - \omega^2\,[m]\right]\mathbf{u} = 0 \tag{13.156}$$

or

$$\sum_{j=1}^{n}\left(k_{ij} - \omega^2 m_{ij}\right)u_j = 0 \qquad i = 1, 2, 3, \cdots n. \tag{13.157}$$

The solution of (13.155) is

$$
\begin{aligned}
q(t) &= \sin \omega t + \cos \omega t \\
&= \sin (\omega t - \varphi)
\end{aligned}
\tag{13.158}
$$

which shows that all the coordinates of the system, $x_i$, have harmonic motion with identical frequency $\omega$ and identical phase angle $\varphi$. The frequency $\omega$ can be determined from Equation (13.156) which is a set of homogeneous equations for the unknown $\mathbf{u}$.

The set of equations (13.156) has a solution $\mathbf{u} = \mathbf{0}$, which is the *rest position* of the system and shows no motion. This solution is called *trivial solution* and is unimportant. To have a *nontrivial solution*, the determinant of the coefficient matrix must be zero.

$$
\det \left[ [k] - \omega^2 [m] \right] = 0
\tag{13.159}
$$

Determining the constant $\omega$, such that the set of equations (13.156) provide a nontrivial solution, is called *eigenvalue problem*. Expanding the determinant (13.159) provides an algebraic equation that is called the *characteristic equation*. The characteristic equation is an $n$th order equation in $\omega^2$, and provides $n$ natural frequencies $\omega_i$. The natural frequencies $\omega_i$ can be set in the following order.

$$
\omega_1 \leq \omega_2 \leq \omega_3 \leq \cdots \leq \omega_n
\tag{13.160}
$$

Having $n$ values for $\omega$ indicates that the solution (13.158) is possible with $n$ different frequencies $\omega_i$, $i = 1, 2, 3, \cdots n$.

We may multiply the Equation (13.150) by $[m]^{-1}$

$$
\ddot{\mathbf{x}} + [m]^{-1} [k] \mathbf{x} = \mathbf{0}
\tag{13.161}
$$

and find the the characteristic equation (13.159) as

$$
\det \left[ [A] - \lambda \mathbf{I} \right] = 0
\tag{13.162}
$$

where

$$
[A] = [m]^{-1} [k] \, .
\tag{13.163}
$$

So, determination of the natural frequencies $\omega_i$ would be equivalent to determining the eigenvalues $\lambda_i$ of the matrix $[A] = [m]^{-1} [k]$.

$$
\lambda_i = \omega_i^2
\tag{13.164}
$$

Determining the vectors $\mathbf{u}_i$ to satisfy Equation (13.156) is called the *eigenvector problem*. To determine $\mathbf{u}_i$, we may solve Equation (13.156) for every $\omega_i$

$$
\left[ [k] - \omega_i^2 [m] \right] \mathbf{u}_i = 0
\tag{13.165}
$$

and find $n$ different $\mathbf{u}_i$. In vibrations and vehicle dynamics, the eigenvector $\mathbf{u}_i$ corresponding to the eigenvalue $\omega_i$ is called the *mode shape*.

Alternatively, we may find the eigenvectors of matrix $[A] = [m]^{-1}[k]$

$$[[A] - \lambda_i \mathbf{I}] \mathbf{u}_i = 0 \qquad (13.166)$$

instead of finding the mode shapes from ((13.165)).

Equations (13.165) are homogeneous so, if $\mathbf{u}_i$ is a solution, then $a\mathbf{u}_i$ is also a solution. Hence, the eigenvectors are not unique and may be expressed with any length. However, the ratio of any two elements of an eigenvector is unique and therefore, $\mathbf{u}_i$ has a unique shape. If one of the elements of $\mathbf{u}_i$ is assigned, the remaining $n-1$ elements are uniquely determined. The shape of an eigenvector indicates the relative amplitudes of the coordinates of the system in vibration.

Because the length of an eigenvector is not uniquely defined, there are many options to express $\mathbf{u}_i$. The most common expressions are:

1− normalization,
2− normal form,
3− high-unit,
4− first-unit,
5− last-unit.

In the *normalization* expression, we may adjust the length of $\mathbf{u}_i$ such that

$$\mathbf{u}_i^T [m] \mathbf{u}_i = 1 \qquad (13.167)$$

or

$$\mathbf{u}_i^T [k] \mathbf{u}_i = 1 \qquad (13.168)$$

and call $\mathbf{u}_i$ a *normal mode* with respect to $[m]$ or $[k]$ respectively.

In the *normal form* expression, we adjust $\mathbf{u}_i$ such that its length has a unity value.

In the *high-unit* expression, we adjust the length of $\mathbf{u}_i$ such that the largest element has a unity value.

In the *first-unit* expression, we adjust the length of $\mathbf{u}_i$ such that the first element has a unity value.

In the *last-unit* expression, we adjust the length of $\mathbf{u}_i$ such that the last element has a unity value. ∎

**Example 482** *Eigenvalues and eigenvectors of a $2 \times 2$ matrix.*

*Consider a $2 \times 2$ matrix is given as*

$$[A] = \begin{bmatrix} 5 & 3 \\ 3 & 6 \end{bmatrix}. \qquad (13.169)$$

*To find the eigenvalues $\lambda_i$ of $[A]$, we find the characteristic equation of the matrix by subtracting an unknown $\lambda$ from the main diagonal, and taking*

*the determinant.*

$$\det\left[[A] - \lambda \mathbf{I}\right] = \det\left[\begin{bmatrix} 5 & 3 \\ 3 & 6 \end{bmatrix} - \lambda \begin{bmatrix} 1 & 0 \\ 0 & 1 \end{bmatrix}\right]$$

$$= \det\begin{bmatrix} 5 - \lambda & 3 \\ 3 & 6 - \lambda \end{bmatrix}$$

$$= \lambda^2 - 11\lambda + 21 \qquad (13.170)$$

*The solution of the characteristic equation (13.170) are*

$$\lambda_1 = 8.5414 \qquad (13.171)$$

$$\lambda_2 = 2.4586. \qquad (13.172)$$

*To find the corresponding eigenvectors $\mathbf{u}_1$ and $\mathbf{u}_2$ we solve the following equations.*

$$[[A] - \lambda_1 \mathbf{I}] \mathbf{u}_1 = 0 \qquad (13.173)$$

$$[[A] - \lambda_2 \mathbf{I}] \mathbf{u}_2 = 0 \qquad (13.174)$$

*Let's denote the eigenvectors by*

$$\mathbf{u}_1 = \begin{bmatrix} u_{11} \\ u_{12} \end{bmatrix} \qquad (13.175)$$

$$\mathbf{u}_2 = \begin{bmatrix} u_{21} \\ u_{22} \end{bmatrix} \qquad (13.176)$$

*therefore,*

$$[[A] - \lambda_1 \mathbf{I}] \mathbf{u}_1 = \left[\begin{bmatrix} 5 & 3 \\ 3 & 6 \end{bmatrix} - 8.5414 \begin{bmatrix} 1 & 0 \\ 0 & 1 \end{bmatrix}\right] \begin{bmatrix} u_{11} \\ u_{12} \end{bmatrix}$$

$$= \begin{bmatrix} 3u_{12} - 3.5414u_{11} \\ 3u_{11} - 2.5414u_{12} \end{bmatrix} = 0 \qquad (13.177)$$

$$[[A] - \lambda_2 \mathbf{I}] \mathbf{u}_2 = \left[\begin{bmatrix} 5 & 3 \\ 3 & 6 \end{bmatrix} - 2.4586 \begin{bmatrix} 1 & 0 \\ 0 & 1 \end{bmatrix}\right] \begin{bmatrix} u_{21} \\ u_{22} \end{bmatrix}$$

$$= \begin{bmatrix} 2.5414u_{21} + 3u_{22} \\ 3u_{21} + 3.5414u_{22} \end{bmatrix} = 0. \qquad (13.178)$$

*Assigning last-unit eigenvectors*

$$u_{12} = 1 \qquad (13.179)$$

$$u_{22} = 1 \qquad (13.180)$$

*provides*

$$\mathbf{u}_1 = \begin{bmatrix} -1.1805 \\ 1.0 \end{bmatrix} \qquad (13.181)$$

$$\mathbf{u}_2 = \begin{bmatrix} 0.84713 \\ 1.0 \end{bmatrix}. \qquad (13.182)$$

**Example 483 ★** *Unique ratio of the eigenvectors' elements.*

To show an example that the ratio of the elements of eigenvectors is unique, we examine the eigenvectors $\mathbf{u}_1$ and $\mathbf{u}_2$ in Example 482.

$$\mathbf{u}_1 = \begin{bmatrix} 3u_{12} - 3.5414u_{11} \\ 3u_{11} - 2.5414u_{12} \end{bmatrix} \tag{13.183}$$

$$\mathbf{u}_2 = \begin{bmatrix} 2.5414u_{21} + 3u_{22} \\ 3u_{21} + 3.5414u_{22} \end{bmatrix} \tag{13.184}$$

The ratio $u_{11}/u_{12}$ may be found from the first row of $\mathbf{u}_1$ in (13.183)

$$\frac{u_{11}}{u_{12}} = \frac{3}{3.5414} = 0.84712 \tag{13.185}$$

or from the second row

$$\frac{u_{11}}{u_{12}} = \frac{2.5414}{3} = 0.84713 \tag{13.186}$$

to examine their equality.

The ratio $u_{21}/u_{22}$ may also be found from the first or second row of $\mathbf{u}_2$ in (13.184) to check their equality.

$$\frac{u_{21}}{u_{22}} = -\frac{3}{2.5414} = -\frac{3.5414}{3} = -1.1805 \tag{13.187}$$

**Example 484 ★** *Characteristics of free systems.*

Free systems have two characteristics: $1-$natural frequencies, and $2-$mode shapes. An $n$ DOF vibrating system will have $n$ natural frequencies $\omega_i$ and $n$ mode shapes $\mathbf{u}_i$. The natural frequencies $\omega_i$ are cores for the system's resonance zones, and the eigenvectors $\mathbf{u}_i$ show the relative vibration of different coordinates of the system at the resonance $\omega_i$. The highest element of each mode shape $\mathbf{u}_i$, indicates the coordinate or the component of the system which is most willing to vibrate at $\omega_i$.

**Example 485** *Importance of free systems.*

The response of free systems is the core for all other responses of the vibrating system. When there is damping, then the response of the system is bounded by the free undamped solution. When there is a forcing function, the natural frequencies of the free response indicate the resonance zones at which the amplitude of the response may go to infinity if an excitation frequency of the force function matches.

**Example 486 ★** *Sign of the separation constant $\omega^2$.*

Both, left and right sides of Equation (13.154) must be equal to a constant. The sign of the constant is dictated by physical considerations. A free and undamped vibrating system is conservative and as a constant mechanical energy, so the amplitude of vibration must remain finite when $t \to \infty$.
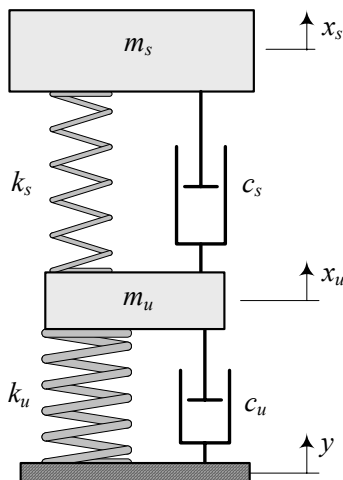
FIGURE 13.8. A quarter car model.

*If the constant is positive, then the response is harmonic with a constant amplitude, however, if the constant is negative, the response is hyperbolic with an exponentially increasing amplitude.*

**Example 487 ★** *Quarter car natural frequencies and mode shapes.*

*Figure 13.8 illustrates a quarter car model which is made of two solid masses $m_s$ and $m_u$ denoted as sprung and unsprung masses, respectively. The sprung mass $m_s$ represents $1/4$ of the body of the vehicle, and the unsprung mass $m_u$ represents one wheel of the vehicle. A spring of stiffness $k_s$, and a shock absorber with viscous damping coefficient $c_s$ support the sprung mass. The unsprung mass $m_u$ is in direct contact with the ground through a spring $k_u$, and a damper $c_u$ representing the tire stiffness and damping.*

*The governing differential equations of motion for the quarter car model are*

$$m_s \ddot{x}_s = -k_s (x_s - x_u) - c_s (\dot{x}_s - \dot{x}_u) \qquad (13.188)$$

$$m_u \ddot{x}_u = k_s (x_s - x_u) + c_s (\dot{x}_s - \dot{x}_u)$$
$$-k_u (x_u - y) - c_u (\dot{x}_u - \dot{y}) \qquad (13.189)$$

*which can be expressed in a matrix form*

$$[M]\,\ddot{\mathbf{x}} + [c]\,\dot{\mathbf{x}} + [k]\,\mathbf{x} = \mathbf{F} \qquad (13.190)$$

$$\begin{bmatrix} m_s & 0 \\ 0 & m_u \end{bmatrix} \begin{bmatrix} \ddot{x}_s \\ \ddot{x}_u \end{bmatrix} + \begin{bmatrix} c_s & -c_s \\ -c_s & c_s + c_u \end{bmatrix} \begin{bmatrix} \dot{x}_s \\ \dot{x}_u \end{bmatrix} +$$
$$\begin{bmatrix} k_s & -k_s \\ -k_s & k_s + k_u \end{bmatrix} \begin{bmatrix} x_s \\ x_u \end{bmatrix} = \begin{bmatrix} 0 \\ k_u y + c_u \dot{y} \end{bmatrix}. \qquad (13.191)$$

*To find the natural frequencies and mode shapes of the quarter car model, we have to drop the damping and forcing terms and analyze the following set of equations.*

$$\begin{bmatrix} m_s & 0 \\ 0 & m_u \end{bmatrix}\begin{bmatrix} \ddot{x}_s \\ \ddot{x}_u \end{bmatrix} + \begin{bmatrix} k_s & -k_s \\ -k_s & k_s + k_u \end{bmatrix}\begin{bmatrix} x_s \\ x_u \end{bmatrix} = 0 \qquad (13.192)$$

*Consider a vehicle with the following characteristics.*

$$\begin{aligned} m_s &= 375\,\text{kg} \\ m_u &= 75\,\text{kg} \\ k_u &= 193000\,\text{N}/\text{m} \\ k_s &= 35000\,\text{N}/\text{m}. \end{aligned} \qquad (13.193)$$

*The equations of motion for this vehicle are*

$$\begin{bmatrix} 375 & 0 \\ 0 & 75 \end{bmatrix}\begin{bmatrix} \ddot{x}_s \\ \ddot{x}_u \end{bmatrix} + \begin{bmatrix} 35000 & -35000 \\ -35000 & 2.28 \times 10^5 \end{bmatrix}\begin{bmatrix} x_s \\ x_u \end{bmatrix} = 0.$$
$$(13.194)$$

*The natural frequencies of the vehicle can be found by solving its characteristic equation.*

$$\begin{aligned} \det\left[[k] - \omega^2 [m]\right] &= \det\begin{bmatrix} 35000 & -35000 \\ -35000 & 2.28 \times 10^5 \end{bmatrix} - \omega^2 \begin{bmatrix} 375 & 0 \\ 0 & 75 \end{bmatrix} \\ &= \det\begin{bmatrix} 35\,000 - 375\omega^2 & -35\,000 \\ -35\,000 & 2.28 \times 10^5 - 75\omega^2 \end{bmatrix} \\ &= 28125\omega^4 - 8.8125 \times 10^7 \omega^2 + 6.755 \times 10^9 \qquad (13.195) \end{aligned}$$

$$\begin{aligned} \omega_1 &= 8.8671\,\text{rad}/\text{s} \\ &\approx 1.41\,\text{Hz} \qquad\qquad (13.196) \\ \omega_2 &= 55.269\,\text{rad}/\text{s} \\ &\approx 8.79\,\text{Hz} \qquad\qquad (13.197) \end{aligned}$$

*To find the corresponding mode shapes, we use Equation (13.165).*

$$\begin{aligned} &\left[[k] - \omega_1^2 [m]\right]\mathbf{u}_1 \\ &= \left[\begin{bmatrix} 35000 & -35000 \\ -35000 & 2.28 \times 10^5 \end{bmatrix} - 3054.7\begin{bmatrix} 375 & 0 \\ 0 & 75 \end{bmatrix}\right]\begin{bmatrix} u_{11} \\ u_{12} \end{bmatrix} \\ &= \begin{bmatrix} -1.1105 \times 10^6 u_{11} - 35000u_{12} \\ -35000u_{11} - 1102.5u_{12} \end{bmatrix} = 0 \qquad (13.198) \end{aligned}$$

$$\begin{aligned} &\left[[k] - \omega_2^2 [m]\right]\mathbf{u}_2 \\ &= \left[\begin{bmatrix} 35000 & -35000 \\ -35000 & 2.28 \times 10^5 \end{bmatrix} - 78.625\begin{bmatrix} 375 & 0 \\ 0 & 75 \end{bmatrix}\right]\begin{bmatrix} u_{21} \\ u_{22} \end{bmatrix} \\ &= \begin{bmatrix} 5515.6u_{21} - 35000u_{22} \\ 2.221 \times 10^5 u_{22} - 35000u_{21} \end{bmatrix} = 0 \qquad (13.199) \end{aligned}$$
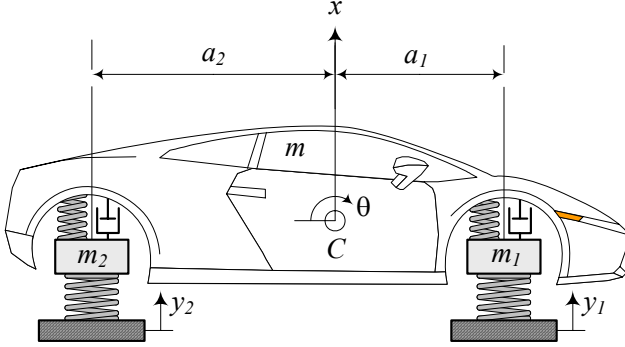
FIGURE 13.9. A bicycle vibrating model of a vehicle.

*Searching for the first-unit expression of* $\mathbf{u}_1$ *and* $\mathbf{u}_2$ *provides the following mode shapes.*

$$\mathbf{u}_1 = \begin{bmatrix} 1 \\ -3.1729 \times 10^{-3} \end{bmatrix} \tag{13.200}$$

$$\mathbf{u}_2 = \begin{bmatrix} 1 \\ 0.157\,58 \end{bmatrix} \tag{13.201}$$

*Therefore, the free vibrations of the quarter car is*

$$\mathbf{x} = \sum_{i=1}^{n} \mathbf{u}_i \left( A_i \sin \omega_i t + B_i \cos \omega_i t \right) \qquad i = 1, 2 \tag{13.202}$$

$$\begin{bmatrix} x_s \\ x_u \end{bmatrix} = \begin{bmatrix} 1 \\ -3.1729 \times 10^{-3} \end{bmatrix} \left( A_1 \sin 8.8671t + B_1 \cos 8.8671t \right)$$

$$+ \begin{bmatrix} 1 \\ 0.157\,58 \end{bmatrix} \left( A_2 \sin 55.269t + B_2 \cos 55.269t \right) \tag{13.203}$$

## 13.4 Bicycle Car and Body Pitch Mode

Quarter car model is excellent to examine and optimize the body bounce mode of vibrations. However, we may expand the vibrating model of a vehicle to include pitch and other modes of vibrations as well. Figure 13.9 illustrates a bicycle vibrating model of a vehicle. This model includes the body bounce $x$, body pitch $\theta$, wheels hop $x_1$ and $x_2$ and independent road excitations $y_1$ and $y_2$.

The equations of motion for the bicycle vibrating model of a vehicle are

as follow.

$$m\ddot{x} + c_1\left(\dot{x} - \dot{x}_1 - a_1\dot{\theta}\right) + c_2\left(\dot{x} - \dot{x}_2 + a_2\dot{\theta}\right)$$
$$+k_1\left(x - x_1 - a_1\theta\right) + k_2\left(x - x_2 + a_2\theta\right) \quad = \quad 0 \quad (13.204)$$
$$I_z\ddot{\theta} - a_1c_1\left(\dot{x} - \dot{x}_1 - a_1\dot{\theta}\right) + a_2c_2\left(\dot{x} - \dot{x}_2 + a_2\dot{\theta}\right)$$
$$-a_1k_1\left(x - x_1 - a_1\theta\right) + a_2k_2\left(x - x_2 + a_2\theta\right) \quad = \quad 0 \quad (13.205)$$

$$m_1\ddot{x}_1 - c_1\left(\dot{x} - \dot{x}_1 - a_1\dot{\theta}\right) + k_{t_1}\left(x_1 - y_1\right)$$
$$-k_1\left(x - x_1 - a_1\theta\right) \quad = \quad 0 \quad (13.206)$$
$$m_2\ddot{x}_2 - c_2\left(\dot{x} - \dot{x}_2 + a_2\dot{\theta}\right) + k_{t_2}\left(x_2 - y_2\right)$$
$$-k_2\left(x - x_2 + a_2\theta\right) \quad = \quad 0 \quad (13.207)$$

As a reminder, the definition of the employed parameters are indicated in Table 13.1.

Table 13.1 - Parameters of a bicycle vibrating vehicle.

| Parameter | Meaning |
|---|---|
| $m$ | half of body mass |
| $m_1$ | mass of a front wheel |
| $m_2$ | mass of a rear wheel |
| $x$ | body vertical motion coordinate |
| $x_1$ | front wheel vertical motion coordinate |
| $x_2$ | rear wheel vertical motion coordinate |
| $\theta$ | body pitch motion coordinate |
| $y_1$ | road excitation at the front wheel |
| $y_2$ | road excitation at the rear wheel |
| $I_y$ | half of body lateral mass moment of inertia |
| $a_1$ | distance of $C$ from front axle |
| $a_2$ | distance of $C$ from rear axle |

**Proof.** Figure 13.10 shows a better vibrating model of the system. The body of the vehicle is assumed to be a rigid bar. This bar has a mass $m$, which is half of the total body mass, and a lateral mass moment of inertia $I_y$, which is half of the total body mass moment of inertia. The front and real wheels have a mass $m_1$ and $m_2$ respectively. The tires stiffness are indicated by different parameters $k_{t_1}$ and $k_{t_2}$. It is because the rear tires are usually stiffer than the fronts, although in a simpler model we may assume $k_{t_1} = k_{t_2}$. Damping of tires are much smaller than the damping of shock absorbers so, we may ignore the tire damping for simpler calculation.

To find the equations of motion for the bicycle vibrating model, we use
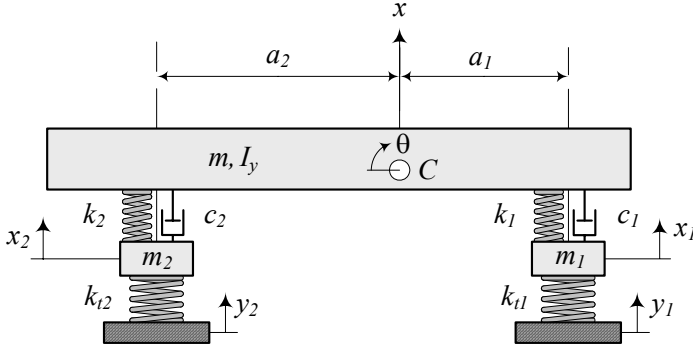
FIGURE 13.10. Bicycle model for a vehicle vibrations.

the Lagrange method. The kinetic and potential energies of the system are

$$K = \frac{1}{2}m\dot{x}^2 + \frac{1}{2}m_1\dot{x}_1^2 + \frac{1}{2}m_2\dot{x}_2^2 + \frac{1}{2}I_z\dot{\theta}^2 \qquad (13.208)$$

$$V = \frac{1}{2}k_{t_1}(x_1 - y_1)^2 + \frac{1}{2}k_{t_2}(x_2 - y_2)^2$$

$$+\frac{1}{2}k_1(x - x_1 - a_1\theta)^2 + \frac{1}{2}k_2(x - x_2 + a_2\theta) \qquad (13.209)$$

and the dissipation function is

$$D = \frac{1}{2}c_1\left(\dot{x} - \dot{x}_1 - a_1\dot{\theta}\right)^2 + \frac{1}{2}c_2\left(\dot{x} - \dot{x}_2 + a_2\dot{\theta}\right). \qquad (13.210)$$

Applying Lagrange method

$$\frac{d}{dt}\left(\frac{\partial K}{\partial \dot{q}_r}\right) - \frac{\partial K}{\partial q_r} + \frac{\partial D}{\partial \dot{q}_r} + \frac{\partial V}{\partial q_r} = f_r \qquad r = 1, 2, \cdots 4 \qquad (13.211)$$

provides the following equations of motion (13.204)-(13.207). These set of equations may be rearranged in a matrix form

$$[m]\ddot{\mathbf{x}} + [c]\dot{\mathbf{x}} + [k]\mathbf{x} = \mathbf{F} \qquad (13.212)$$

where,

$$\mathbf{x} = \begin{bmatrix} x \\ \theta \\ x_1 \\ x_2 \end{bmatrix} \qquad (13.213)$$

$$[m] = \begin{bmatrix} m & 0 & 0 & 0 \\ 0 & I_z & 0 & 0 \\ 0 & 0 & m_1 & 0 \\ 0 & 0 & 0 & m_2 \end{bmatrix} \qquad (13.214)$$

$$[c] = \begin{bmatrix} c_1 + c_2 & a_2 c_2 - a_1 c_1 & -c_1 & -c_2 \\ a_2 c_2 - a_1 c_1 & c_1 a_1^2 + c_2 a_2^2 & a_1 c_1 & -a_2 c_2 \\ -c_1 & a_1 c_1 & c_1 & 0 \\ -c_2 & -a_2 c_2 & 0 & c_2 \end{bmatrix} \qquad (13.215)$$

$$[k] = \begin{bmatrix} k_1 + k_2 & a_2 k_2 - a_1 k_1 & -k_1 & -k_2 \\ a_2 k_2 - a_1 k_1 & k_1 a_1^2 + k_2 a_2^2 & a_1 k_1 & -a_2 k_2 \\ -k_1 & a_1 k_1 & k_1 + k_{t_1} & 0 \\ -k_2 & -a_2 k_2 & 0 & k_2 + k_{t_2} \end{bmatrix} \qquad (13.216)$$

$$\mathbf{F} = \begin{bmatrix} 0 \\ 0 \\ y_1 k_{t_1} \\ y_2 k_{t_2} \end{bmatrix}. \qquad (13.217)$$

■

**Example 488** *Natural frequencies and mode shapes of a bicycle car model.*

*Consider a vehicle with a heavy solid axle in the rear and independent suspensions in front. the vehicle has the following characteristics.*

$$\begin{aligned} m &= \frac{840}{2} \, \text{kg} \\ m_1 &= 53 \, \text{kg} \\ m_2 &= \frac{152}{2} \, \text{kg} \\ I_y &= 1100 \, \text{kg m}^2 \end{aligned} \qquad (13.218)$$

$$\begin{aligned} a_1 &= 1.4 \, \text{m} \\ a_2 &= 1.47 \, \text{m} \end{aligned} \qquad (13.219)$$

$$\begin{aligned} k_1 &= 10000 \, \text{N/m} \\ k_2 &= 13000 \, \text{N/m} \\ k_{t_1} &= k_{t_2} = 200000 \, \text{N/m} \end{aligned} \qquad (13.220)$$

*The natural frequencies of this vehicle can be found by using the undamped and free vibration equations of motion. The characteristic equation of the system is*

$$\begin{aligned} &\det \left[ [k] - \omega^2 [m] \right] = \\ &8609 \times 10^9 \omega^8 - 1.2747 \times 10^{13} \omega^6 \\ &+2.1708 \times 10^{16} \omega^4 - 1.676 \times 10^{18} \omega^2 + 2.9848 \times 10^{19} \qquad (13.221) \end{aligned}$$

*because*

$$[m] = \begin{bmatrix} 420 & 0 & 0 & 0 \\ 0 & 1100 & 0 & 0 \\ 0 & 0 & 53 & 0 \\ 0 & 0 & 0 & 76 \end{bmatrix} \qquad (13.222)$$

$$[k] = \begin{bmatrix} 23000 & 5110 & -10000 & -13000 \\ 5110 & 47692 & 14000 & -19110 \\ -10000 & 14000 & 2.1 \times 10^5 & 0 \\ -13000 & -19110 & 0 & 2.13 \times 10^5 \end{bmatrix}. \qquad (13.223)$$

To find the natural frequencies we may solve the characteristic equation (13.221) or search for eigenvalues of $[A] = [m]^{-1}[k]$.

$$\begin{aligned} [A] &= [m]^{-1}[k] \\ &= \begin{bmatrix} 54.762 & 12.167 & -23.810 & -30.952 \\ 4.6455 & 43.356 & 12.727 & -17.373 \\ -188.68 & 264.15 & 3962.3 & 0 \\ -171.05 & -251.45 & 0 & 2802.6 \end{bmatrix} \end{aligned} \qquad (13.224)$$

The eigenvalues of $[A]$ are

$$\begin{aligned} \lambda_1 &= 37.657 \\ \lambda_2 &= 54.943 \\ \lambda_3 &= 2806.1 \\ \lambda_4 &= 3964.3 \end{aligned} \qquad (13.225)$$

therefore, the natural frequencies of the bicycle car model are

$$\begin{aligned} \omega_1 &= \sqrt{\lambda_1} = 6.1365\,\mathrm{rad/s} \approx 0.97665\,\mathrm{Hz} \\ \omega_2 &= \sqrt{\lambda_2} = 7.4124\,\mathrm{rad/s} \approx 1.1797\,\mathrm{Hz} \\ \omega_3 &= \sqrt{\lambda_3} = 52.973\,\mathrm{rad/s} \approx 8.4309\,\mathrm{Hz} \\ \omega_4 &= \sqrt{\lambda_4} = 62.963\,\mathrm{rad/s} \approx 10.021\,\mathrm{Hz}. \end{aligned} \qquad (13.226)$$

The normal form of the mode shapes of the system are

$$\mathbf{u}_1 = \begin{bmatrix} 0.61258 \\ -0.7854 \\ 8.2312 \times 10^{-2} \\ -3.353 \times 10^{-2} \end{bmatrix} \qquad (13.227)$$

$$\mathbf{u}_2 = \begin{bmatrix} 0.95459 \\ 0.28415 \\ 2.6886 \times 10^{-2} \\ 0.08543 \end{bmatrix} \qquad (13.228)$$

$$\mathbf{u}_3 = \begin{bmatrix} 1.1273 \times 10^{-2} \\ 6.3085 \times 10^{-3} \\ 3.9841 \times 10^{-4} \\ -0.99992 \end{bmatrix} \tag{13.229}$$

$$\mathbf{u}_4 = \begin{bmatrix} 6.0815 \times 10^{-3} \\ -3.2378 \times 10^{-3} \\ -0.99998 \\ -1.9464 \times 10^{-4} \end{bmatrix} \tag{13.230}$$

*The biggest element of the fourth mode shape* $\mathbf{u}_4$ *belongs to* $x_1$. *It shows that in the fourth mode of vibrations at* $\omega_4 \approx 10.021\,\mathrm{Hz}$ *the front wheel will have the largest amplitude, while the amplitude of the other components are*

$$\Theta = \frac{u_{42}}{u_{43}} = \frac{-3.2378 \times 10^{-3}}{-0.99998} X_1 = 3.2379 \times 10^{-3} X_1 \tag{13.231}$$

$$X = \frac{u_{41}}{u_{43}} = \frac{6.0815 \times 10^{-3}}{-0.99998} X_1 = -6.0816 \times 10^{-3} X_1 \tag{13.232}$$

$$X_2 = \frac{u_{44}}{u_{43}} = \frac{-3.2378 \times 10^{-3}}{-0.99998} X_1 = 3.2379 \times 10^{-3} X_1. \tag{13.233}$$

**Example 489** *Comparison of the mode shapes of a bicycle car model.*

*In Example 488, the biggest element of the first mode shape* $\mathbf{u}_1$ *belongs to* $\theta$, *the biggest element of the second mode shape* $\mathbf{u}_2$ *belongs to* $x$, *and the biggest element of the first mode shape* $\mathbf{u}_3$ *belongs to* $x_2$. *Similar to the fourth mode shape* $\mathbf{u}_4$, *we can find the relative amplitude of different coordinates at each mode. Consider a car starts to move on a bumpy road at a very small acceleration. By increasing the speed, the first resonance occurs at* $\omega_1 \approx 0.97665\,\mathrm{Hz}$, *at which the pitch vibration is the most observable vibration. The second resonance occurs at* $\omega_2 \approx 1.1797\,\mathrm{Hz}$ *when the bounce vibration of the body is the most observable vibration. The third and fourth resonances at* $\omega_3 \approx 8.4309\,\mathrm{Hz}$ *and* $\omega_4 \approx 10.021\,\mathrm{Hz}$ *are related to rear and front wheels respectively.*

*When the excitation frequency of a multiple DOF system increases, we will see that observable vibration moves from a coordinate to the others in the order of natural frequencies and associated mode shapes. When the excitation frequency is exactly at a natural frequency, the relative amplitudes of vibration are exactly similar to the associated mode shape. If the excitation frequency is not on a natural frequency, then vibration of the system is a combination of all modes of vibration. However, the weight factor of the closer modes are higher.*

## 13.5   Half Car and Body Roll Mode

To examine and optimize the roll vibration of a vehicle we may use a half car vibrating model. Figure 13.11 illustrates a half car model of a vehicle.
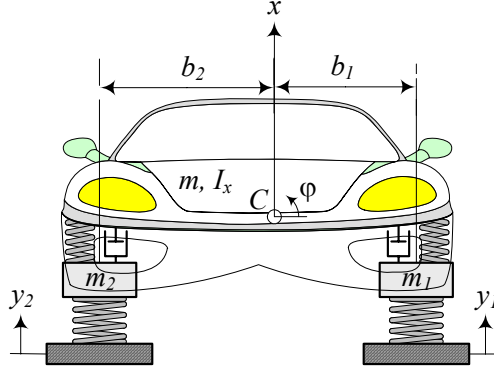
FIGURE 13.11. A half car vibrating model of a vehicle.

This model includes the body bounce $x$, body roll $\varphi$, wheels hop $x_1$ and $x_2$ and independent road excitations $y_1$ and $y_2$.

The equations of motion for the half car vibrating model of a vehicle are as follow.

$$m\ddot{x} + c\left(\dot{x} - \dot{x}_1 + b_1\dot{\varphi}\right) + c\left(\dot{x} - \dot{x}_2 - b_2\dot{\varphi}\right)$$
$$+k\left(x - x_1 + b_1\varphi\right) + k\left(x - x_2 - b_2\varphi\right) \quad = \quad 0 \qquad (13.234)$$
$$I_x\ddot{\varphi} + b_1c\left(\dot{x} - \dot{x}_1 + b_1\dot{\varphi}\right) - b_2c\left(\dot{x} - \dot{x}_2 - b_2\dot{\varphi}\right)$$
$$+b_1k\left(x - x_1 + b_1\varphi\right) - b_2k\left(x - x_2 - b_2\varphi\right) + k_R\varphi \quad = \quad 0 \qquad (13.235)$$

$$m_1\ddot{x}_1 - c\left(\dot{x} - \dot{x}_1 + b_1\dot{\varphi}\right) + k_t\left(x_1 - y_1\right)$$
$$-k\left(x - x_1 + b_1\varphi\right) \quad = \quad 0 \qquad (13.236)$$
$$m_2\ddot{x}_2 - c\left(\dot{x} - \dot{x}_2 - b_2\dot{\varphi}\right) + k_t\left(x_2 - y_2\right)$$
$$-k\left(x - x_2 - b_2\varphi\right) \quad = \quad 0 \qquad (13.237)$$

The half car model may be different for the front half and rear half due to different suspensions and mass distribution. Furthermore, different antiroll bars with different torsional stiffness may be used in the front and rear halves.

**Proof.** Figure 13.12 shows a better vibrating model of the system. The body of the vehicle is assumed to be a rigid bar. This bar has a mass $m$, which is the front or rear half of the total body mass, and a longitudinal mass moment of inertia $I_x$, which is half of the total body mass moment of inertia. The left and right wheels have a mass $m_1$ and $m_2$ respectively, although they are usually equal. The tires stiffness are indicated by $k_t$. Damping of tires are much smaller than the damping of shock absorbers so, we may ignore the tire damping for simpler calculation. The suspension of the car has stiffness $k$ and damping $c$ for the left and right wheels. It
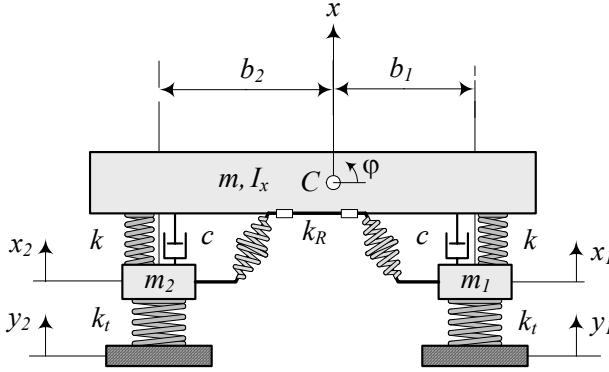
FIGURE 13.12. Half car model for a vehicle vibrations.

is common to make the suspension of the left and right wheels mirror. So, their stiffness and damping are equal. However, the half car model has different $k$, $c$, and $k_t$ for front or rear.

The vehicle may also have an antiroll bar with a torsional stiffness $k_R$ in front and or rear. Using a simple model, the antiroll bar provides a torque $M_R$ proportional to the roll angle $\varphi$.

$$M_R = -k_R\varphi \tag{13.238}$$

However, a better model of the antiroll bar effect is

$$M_R = -k_R\left(\varphi - \frac{x_1 - x_2}{w}\right). \tag{13.239}$$

To find the equations of motion for the half car vibrating model, we use the Lagrange method. The kinetic and potential energies of the system are

$$
K = \frac{1}{2}m\dot{x}^2 + \frac{1}{2}m_1\dot{x}_1^2 + \frac{1}{2}m_2\dot{x}_2^2 + \frac{1}{2}I_x\dot{\varphi}^2 \tag{13.240}
$$

$$
V = \frac{1}{2}k_t(x_1 - y_1)^2 + \frac{1}{2}k_t(x_2 - y_2)^2 + \frac{1}{2}k_R\varphi^2
$$
$$
+\frac{1}{2}k(x - x_1 + b_1\varphi)^2 + \frac{1}{2}k(x - x_2 - b_2\varphi) \tag{13.241}
$$

and the dissipation function is

$$
D = \frac{1}{2}c(\dot{x} - \dot{x}_1 + b_1\dot{\varphi})^2 + \frac{1}{2}c(\dot{x} - \dot{x}_2 - b_2\dot{\varphi}). \tag{13.242}
$$

Applying the Lagrange method

$$
\frac{d}{dt}\left(\frac{\partial K}{\partial \dot{q}_r}\right) - \frac{\partial K}{\partial q_r} + \frac{\partial D}{\partial \dot{q}_r} + \frac{\partial V}{\partial q_r} = f_r \qquad r = 1, 2, \cdots 4 \tag{13.243}
$$

provides the following equations of motion (13.234)-(13.237). The set of equations of motion may be rearranged in a matrix form

$$[m]\,\ddot{\mathbf{x}} + [c]\,\dot{\mathbf{x}} + [k]\,\mathbf{x} = \mathbf{F} \tag{13.244}$$

where,

$$\mathbf{x} = \begin{bmatrix} x \\ \varphi \\ x_1 \\ x_2 \end{bmatrix} \tag{13.245}$$

$$[m] = \begin{bmatrix} m & 0 & 0 & 0 \\ 0 & I_x & 0 & 0 \\ 0 & 0 & m_1 & 0 \\ 0 & 0 & 0 & m_2 \end{bmatrix} \tag{13.246}$$

$$[c] = \begin{bmatrix} 2c & cb_1 - cb_2 & -c & -c \\ cb_1 - cb_2 & cb_1^2 + cb_2^2 & -cb_1 & cb_2 \\ -c & -cb_1 & c & 0 \\ -c & cb_2 & 0 & c \end{bmatrix} \tag{13.247}$$

$$[k] = \begin{bmatrix} 2k & kb_1 - kb_2 & -k & -k \\ kb_1 - kb_2 & kb_1^2 + kb_2^2 + k_R & -kb_1 & kb_2 \\ -k & -kb_1 & k + k_t & 0 \\ -k & kb_2 & 0 & k + k_t \end{bmatrix} \tag{13.248}$$

$$\mathbf{F} = \begin{bmatrix} 0 \\ 0 \\ y_1 k_t \\ y_2 k_t \end{bmatrix}. \tag{13.249}$$

∎

**Example 490** *Natural frequencies and mode shapes of a half car model.*
*Consider a vehicle with the following characteristics.*

$$
\begin{aligned}
m &= \frac{840}{2}\,\mathrm{kg} \\
m_1 &= 53\,\mathrm{kg} \\
m_2 &= 53\,\mathrm{kg} \\
I_x &= 820\,\mathrm{kg\,m^2}
\end{aligned}
\tag{13.250}
$$

$$
\begin{aligned}
b_1 &= 0.7\,\mathrm{m} \\
b_2 &= 0.75\,\mathrm{m}
\end{aligned}
\tag{13.251}
$$

$$
\begin{aligned}
k &= 10000\,\mathrm{N/m} \\
k_t &= k_t = 200000\,\mathrm{N/m} \\
k_R &= 25000\,\mathrm{N\,m/rad}
\end{aligned}
\tag{13.252}
$$

*The natural frequency of this vehicle is found by using the undamped and free vibration equations of motion.*

$$[m]\, \ddot{\mathbf{x}} + [k]\, \mathbf{x} = \mathbf{0} \tag{13.253}$$

*The characteristic equation of the system is*

$$
\begin{aligned}
\det\left[[k] - \omega^2\,[m]\right] \;=\; & 6742 \times 10^8 \omega^8 - 8.192\,0 \times 10^{12} \omega^6 \\
& +1.9363 \times 10^{16} \omega^4 - 8.3728 \times 10^{18} \omega^2 \\
& +3.2287 \times 10^{20}
\end{aligned}
\tag{13.254}
$$

*because*

$$[m] = \begin{bmatrix} 420 & 0 & 0 & 0 \\ 0 & 820 & 0 & 0 \\ 0 & 0 & 53 & 0 \\ 0 & 0 & 0 & 53 \end{bmatrix} \tag{13.255}$$

$$[k] = \begin{bmatrix} 2.1 \times 10^5 & -500 & -10000 & -10000 \\ -500 & 35525 & -7000 & 7500 \\ -10000 & -7000 & 2.1 \times 10^5 & 0 \\ -10000 & 7500 & 0 & 2.1 \times 10^5 \end{bmatrix}. \tag{13.256}$$

*To find the natural frequencies we may solve the characteristic equation (13.221) or search for eigenvalues of $[A] = [m]^{-1}\,[k]$.*

$$
\begin{aligned}
[A] \;=\;& [m]^{-1}\,[k] \\
=\;& \begin{bmatrix} 500.0 & -1.1905 & -23.810 & -23.810 \\ -0.609\,76 & 43.323 & -8.5366 & 9.1463 \\ -188.68 & -132.08 & 3962.3 & 0 \\ -188.68 & 141.51 & 0 & 3962.3 \end{bmatrix}
\end{aligned}
\tag{13.257}
$$

*The eigenvalues of $[A]$ are*

$$
\begin{aligned}
\lambda_1 &= 42.702 \\
\lambda_2 &= 497.32 \\
\lambda_3 &= 3962.9 \\
\lambda_4 &= 3964.9
\end{aligned}
\tag{13.258}
$$

*therefore, the natural frequencies of the half car model are*

$$
\begin{aligned}
\omega_1 &= \sqrt{\lambda_1} = 6.5347\,\mathrm{rad/s} \approx 1.04\,\mathrm{Hz} \\
\omega_2 &= \sqrt{\lambda_2} = 22.301\,\mathrm{rad/s} \approx 3.5493\,\mathrm{Hz} \\
\omega_3 &= \sqrt{\lambda_3} = 62.952\,\mathrm{rad/s} \approx 10.019\,\mathrm{Hz} \\
\omega_4 &= \sqrt{\lambda_4} = 62.967\,\mathrm{rad/s} \approx 10.022\,\mathrm{Hz}.
\end{aligned}
\tag{13.259}
$$

*The normal form of the mode shapes of the system are*

$$\mathbf{u}_1 = \begin{bmatrix} 2.4875 \times 10^{-3} \\ 0.99878 \\ 3.3776 \times 10^{-2} \\ -3.5939 \times 10^{-2} \end{bmatrix} \tag{13.260}$$

$$\mathbf{u}_2 = \begin{bmatrix} 0.99705 \\ -1.264 \times 10^{-3} \\ 5.4246 \times 10^{-2} \\ 5.4346 \times 10^{-2} \end{bmatrix} \tag{13.261}$$

$$\mathbf{u}_3 = \begin{bmatrix} 1.0488 \times 10^{-4} \\ 3.1886 \times 10^{-3} \\ -0.71477 \\ 0.69935 \end{bmatrix} \tag{13.262}$$

$$\mathbf{u}_4 = \begin{bmatrix} 9.7172 \times 10^{-3} \\ -1.462 \times 10^{-4} \\ -0.69932 \\ -0.71474 \end{bmatrix} \tag{13.263}$$

**Example 491** *Comparison of the mode shapes of a half car model.*

*In example 490, the biggest element of the first mode shape $\mathbf{u}_1$ belongs to $\varphi$, the biggest element of the second mode shape $\mathbf{u}_2$ belongs to $x$, the biggest element of the third mode shape $\mathbf{u}_3$ belongs to $x_2$, and the biggest element of the fourth mode shape $\mathbf{u}_4$ belongs to $x_1$. Consider a car that starts to move on a bumpy road at a very small acceleration. By increasing the speed, the first resonance occurs at $\omega_1 \approx 1.04\,\mathrm{Hz}$, at which the roll vibration is the most observable vibration. The second resonance occurs at $\omega_2 \approx 3.5493\,\mathrm{Hz}$ when the bounce vibration of the body is the most observable vibration. The third and fourth resonances at $\omega_3 \approx 10.019\,\mathrm{Hz}$ and $\omega_4 \approx 10.022\,\mathrm{Hz}$ are related to right and left wheels respectively.*

**Example 492** *Antiroll bar affects only the roll mode.*

*If in example 490, we eliminate the antiroll bar by setting $k_R = 0$, the natural frequencies and mode shapes of the half car model would be as follow.*

$$
\begin{aligned}
\lambda_1 &= 12.221 \\
\lambda_2 &= 497.41 \\
\lambda_3 &= 3962.9 \\
\lambda_4 &= 3964.9
\end{aligned}
\tag{13.264}
$$

$$
\begin{aligned}
\omega_1 &= \sqrt{\lambda_1} = 3.4957 \,\mathrm{rad/s} \approx 0.556\,36 \,\mathrm{Hz} \\
\omega_2 &= \sqrt{\lambda_2} = 22.301 \,\mathrm{rad/s} \approx 3.5493 \,\mathrm{Hz} \\
\omega_3 &= \sqrt{\lambda_3} = 62.\,967 \,\mathrm{rad/s} \approx 10.022 \,\mathrm{Hz} \\
\omega_4 &= \sqrt{\lambda_4} = 62.\,967 \,\mathrm{rad/s} \approx 10.022 \,\mathrm{Hz}.
\end{aligned}
\tag{13.265}
$$

$$
\mathbf{u}_1 = \begin{bmatrix} 2.332\,2 \times 10^{-3} \\ 0.998\,80 \\ 3.350\,9 \times 10^{-2} \\ -0.035\,67 \end{bmatrix}
\tag{13.266}
$$

$$
\mathbf{u}_2 = \begin{bmatrix} 0.997\,05 \\ -1.184\,6 \times 10^{-3} \\ 5.424\,9 \times 10^{-2} \\ 5.434\,2 \times 10^{-2} \end{bmatrix}
\tag{13.267}
$$

$$
\mathbf{u}_3 = \begin{bmatrix} 1.038\,2 \times 10^{-4} \\ 3.164 \times 10^{-3} \\ -0.714\,69 \\ 0.699\,43 \end{bmatrix}
\tag{13.268}
$$

$$
\mathbf{u}_4 = \begin{bmatrix} 9.717\,2 \times 10^{-3} \\ -1.447\,2 \times 10^{-4} \\ -0.699\,4 \\ -0.714\,66 \end{bmatrix}
\tag{13.269}
$$

*Comparing these results with the results in example 490, shows the antiroll bar affects only the roll mode of vibration. A half car model needs a proper antiroll bar to increase the roll natural frequency.*

*It is recommended to have the roll mode as close as possible to the body bounce natural frequency to have narrow resonance zone around the body bounce. Avoiding a narrow resonance zone would be simpler.*

## 13.6   Full Car Vibrating Model

A general vibrating model of a vehicle is called the *full car* model. Such a model, that is shown in Figure 13.13, includes the body bounce $x$, body roll $\varphi$, body pitch $\theta$, wheels hop $x_1$, $x_2$, $x_3$, and $x_4$ and independent road excitations $y_1$, $y_2$, $y_3$, and $y_4$.

A full car vibrating model has *seven* DOF with the following equations
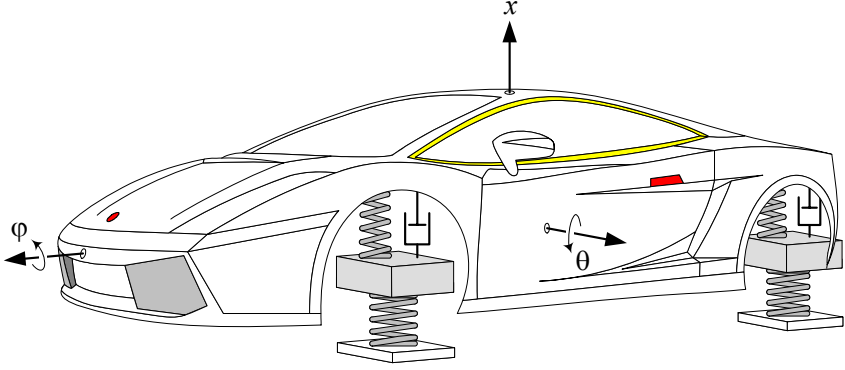
FIGURE 13.13. A full car vibrating model of a vehicle.

of motion.

$$m\ddot{x} + c_f \left( \dot{x} - \dot{x}_1 + b_1\dot{\varphi} - a_1\dot{\theta} \right) + c_f \left( \dot{x} - \dot{x}_2 - b_2\dot{\varphi} - a_1\dot{\theta} \right)$$
$$+ c_r \left( \dot{x} - \dot{x}_3 - b_1\dot{\varphi} + a_2\dot{\theta} \right) + c_r \left( \dot{x} - \dot{x}_4 + b_2\dot{\varphi} + a_2\dot{\theta} \right)$$
$$+ k_f \left( x - x_1 + b_1\varphi - a_1\theta \right) + k_f \left( x - x_2 - b_2\varphi - a_1\theta \right)$$
$$+ k_r \left( x - x_3 - b_1\varphi + a_2\theta \right) + k_r \left( x - x_4 + b_2\varphi + a_2\theta \right)$$
$$= \quad 0 \tag{13.270}$$

$$I_x\ddot{\varphi} + b_1 c_f \left( \dot{x} - \dot{x}_1 + b_1\dot{\varphi} - a_1\dot{\theta} \right) - b_2 c_f \left( \dot{x} - \dot{x}_2 - b_2\dot{\varphi} - a_1\dot{\theta} \right)$$
$$- b_1 c_r \left( \dot{x} - \dot{x}_3 - b_1\dot{\varphi} + a_2\dot{\theta} \right) + b_2 c_r \left( \dot{x} - \dot{x}_4 + b_2\dot{\varphi} + a_2\dot{\theta} \right)$$
$$+ b_1 k_f \left( x - x_1 + b_1\varphi - a_1\theta \right) - b_2 k_f \left( x - x_2 - b_2\varphi - a_1\theta \right)$$
$$- b_1 k_r \left( x - x_3 - b_1\varphi + a_2\theta \right) + b_2 k_r \left( x - x_4 + b_2\varphi + a_2\theta \right)$$
$$+ k_R \left( \varphi - \frac{x_1 - x_2}{w} \right)$$
$$= \quad 0 \tag{13.271}$$

$$I_y\ddot{\theta} - a_1 c_f \left( \dot{x} - \dot{x}_1 + b_1\dot{\varphi} - a_1\dot{\theta} \right) - a_1 c_f \left( \dot{x} - \dot{x}_2 - b_2\dot{\varphi} - a_1\dot{\theta} \right)$$
$$+ a_2 c_r \left( \dot{x} - \dot{x}_3 - b_1\dot{\varphi} + a_2\dot{\theta} \right) + a_2 c_r \left( \dot{x} - \dot{x}_4 + b_2\dot{\varphi} + a_2\dot{\theta} \right)$$
$$- a_1 k_f \left( x - x_1 + b_1\varphi - a_1\theta \right) - a_1 k_f \left( x - x_2 - b_2\varphi - a_1\theta \right)$$
$$+ a_2 k_r \left( x - x_3 - b_1\varphi + a_2\theta \right) + a_2 k_r \left( x - x_4 + b_2\varphi + a_2\theta \right)$$
$$= \quad 0 \tag{13.272}$$

$$m_f \ddot{x}_1 - c_f \left( \dot{x} - \dot{x}_1 + b_1 \dot{\varphi} - a_1 \dot{\theta} \right) - k_f \left( x - x_1 + b_1 \varphi - a_1 \theta \right)$$

$$-k_R \frac{1}{w} \left( \varphi - \frac{x_1 - x_2}{w} \right) + k_{t_f} \left( x_1 - y_1 \right)$$

$$= \quad 0 \tag{13.273}$$

$$m_f \ddot{x}_2 - c_f \left( \dot{x} - \dot{x}_2 - b_2 \dot{\varphi} - a_1 \dot{\theta} \right) - k_f \left( x - x_2 - b_2 \varphi - a_1 \theta \right)$$

$$+k_R \frac{1}{w} \left( \varphi - \frac{x_1 - x_2}{w} \right) + k_{t_f} \left( x_2 - y_2 \right)$$

$$= \quad 0 \tag{13.274}$$

$$m_r \ddot{x}_3 - c_r \left( \dot{x} - \dot{x}_3 - b_1 \dot{\varphi} + a_2 \dot{\theta} \right)$$

$$-k_r \left( x - x_3 - b_1 \varphi + a_2 \theta \right) + k_{t_r} \left( x_3 - y_3 \right) \quad = \quad 0 \tag{13.275}$$

$$m_r \ddot{x}_4 - c_r \left( \dot{x} - \dot{x}_4 + b_2 \dot{\varphi} + a_2 \dot{\theta} \right)$$

$$-k_r \left( x - x_4 + b_2 \varphi + a_2 \theta \right) + k_{t_r} \left( x_4 - y_4 \right) \quad = \quad 0 \tag{13.276}$$

**Proof.** Figure 13.14 shows a better vibrating model of the system. The body of the vehicle is assumed to be a rigid slab. This slab has a mass $m$, which is the total body mass, a longitudinal mass moment of inertia $I_x$, and a lateral mass moment of inertia $I_y$. the moments of inertia are only the body mass moments of inertia not the vehicle's mass moments of inertia. The wheels have a mass $m_1$, $m_2$, $m_3$, and $m_4$ respectively. However, it is common to have

$$m_1 \quad = \quad m_2 = m_f \tag{13.277}$$

$$m_3 \quad = \quad m_4 = m_r. \tag{13.278}$$

The front and rear tires stiffness are indicated by $k_{t_f}$ and $k_{t_r}$ respectively. Because the damping of tires are much smaller than the damping of shock absorbers, we may ignore the tires' damping for simpler calculation.

The suspension of the car has stiffness $k_f$ and damping $c_f$ in the front and stiffness $k_r$ and damping $c_r$ in the rear. It is common to make the suspension of the left and right wheels mirror. So, their stiffness and damping are equal. The vehicle may also have an antiroll bar in front and in the back, with a torsional stiffness $k_{R_f}$ and $k_{R_r}$. Using a simple model, the antiroll bar provides a torque $M_R$ proportional to the roll angle $\varphi$.

$$M_R \quad = \quad - \left( k_{R_f} + k_{R_r} \right) \varphi$$

$$= \quad -k_R \varphi \tag{13.279}$$
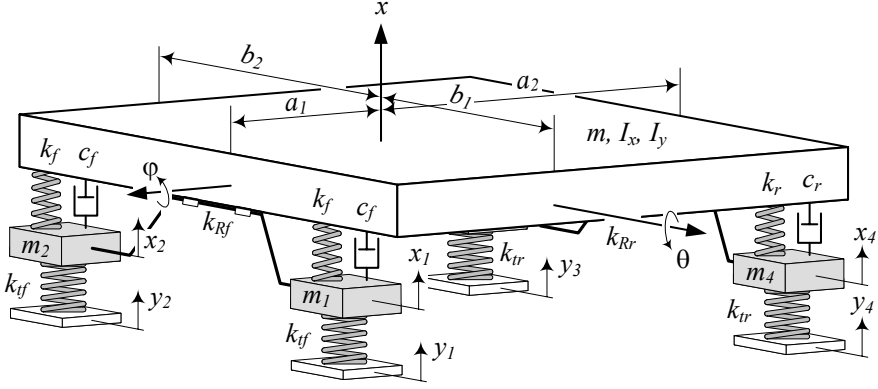
FIGURE 13.14. Full car model for a vehicle vibrations.

However, a better model of the antiroll bar reaction is

$$M_R = -k_{R_f} \left( \varphi - \frac{x_1 - x_2}{w_f} \right) - k_{R_f} \left( \varphi - \frac{x_4 - x_3}{w_r} \right). \tag{13.280}$$

Most cars only have an antiroll bar in front. For these cars, the moment of the antiroll bar simplifies to

$$M_R = -k_R \left( \varphi - \frac{x_1 - x_2}{w} \right) \tag{13.281}$$

if we use

$$w_f \equiv w = b_1 + b_2 \tag{13.282}$$
$$k_{R_f} \equiv k_R. \tag{13.283}$$

To find the equations of motion for the full car vibrating model, we use the Lagrange method. The kinetic and potential energies of the system are

$$
\begin{aligned}
K = {} & \frac{1}{2}m\dot{x}^2 + \frac{1}{2}I_x\dot{\varphi}^2 + \frac{1}{2}I_y\dot{\theta}^2 \\
& + \frac{1}{2}m_f \left( \dot{x}_1^2 + \dot{x}_2^2 \right) + \frac{1}{2}m_r \left( \dot{x}_3^2 + \dot{x}_4^2 \right)
\end{aligned}
\tag{13.284}
$$

$$V = \frac{1}{2}k_f\left(x - x_1 + b_1\varphi - a_1\theta\right)^2 + \frac{1}{2}k_f\left(x - x_2 - b_2\varphi - a_1\theta\right)^2$$

$$+\frac{1}{2}k_r\left(x - x_3 - b_1\varphi + a_2\theta\right)^2 + \frac{1}{2}k_r\left(x - x_4 + b_2\varphi + a_2\theta\right)^2$$

$$+\frac{1}{2}k_R\left(\varphi - \frac{x_1 - x_2}{w}\right)^2$$

$$+\frac{1}{2}k_{t_f}\left(x_1 - y_1\right)^2 + \frac{1}{2}k_{t_f}\left(x_2 - y_2\right)^2$$

$$+\frac{1}{2}k_{t_r}\left(x_3 - y_3\right)^2 + \frac{1}{2}k_{t_r}\left(x_4 - y_4\right)^2 \tag{13.285}$$

and the dissipation function is

$$D = \frac{1}{2}c_f\left(\dot{x} - \dot{x}_1 + b_1\dot{\varphi} - a_1\dot{\theta}\right)^2 + \frac{1}{2}c_f\left(\dot{x} - \dot{x}_2 - b_2\dot{\varphi} - a_1\dot{\theta}\right)^2$$

$$+\frac{1}{2}c_r\left(\dot{x} - \dot{x}_3 - b_1\dot{\varphi} + a_2\dot{\theta}\right)^2$$

$$+\frac{1}{2}c_r\left(\dot{x} - \dot{x}_4 + b_2\dot{\varphi} + a_2\dot{\theta}\right)^2 \tag{13.286}$$

Applying Lagrange method

$$\frac{d}{dt}\left(\frac{\partial K}{\partial \dot{q}_r}\right) - \frac{\partial K}{\partial q_r} + \frac{\partial D}{\partial \dot{q}_r} + \frac{\partial V}{\partial q_r} = f_r \qquad r = 1, 2, \cdots 7 \tag{13.287}$$

provides the following equations of motion (13.270)-(13.276).

The set of equations of motion may be rearranged in a matrix form

$$[m]\ddot{\mathbf{x}} + [c]\dot{\mathbf{x}} + [k]\mathbf{x} = \mathbf{F} \tag{13.288}$$

where,

$$\mathbf{x} = \begin{bmatrix} x \\ \varphi \\ \theta \\ x_1 \\ x_2 \\ x_3 \\ x_4 \end{bmatrix} \tag{13.289}$$

$$[m] = \begin{bmatrix} m & 0 & 0 & 0 & 0 & 0 & 0 \\ 0 & I_x & 0 & 0 & 0 & 0 & 0 \\ 0 & 0 & I_y & 0 & 0 & 0 & 0 \\ 0 & 0 & 0 & m_f & 0 & 0 & 0 \\ 0 & 0 & 0 & 0 & m_f & 0 & 0 \\ 0 & 0 & 0 & 0 & 0 & m_r & 0 \\ 0 & 0 & 0 & 0 & 0 & 0 & m_r \end{bmatrix} \tag{13.290}$$

$$[c] = \begin{bmatrix} c_{11} & c_{12} & c_{13} & -c_f & -c_f & -c_r & -c_r \\ c_{21} & c_{22} & c_{23} & -b_1c_f & b_2c_f & b_1c_r & -b_2c_r \\ c_{31} & c_{32} & c_{33} & a_1c_f & a_1c_f & -a_2c_r & -a_2c_r \\ -c_f & -b_1c_f & a_1c_f & c_f & 0 & 0 & 0 \\ -c_f & b_2c_f & a_1c_f & 0 & c_f & 0 & 0 \\ -c_r & b_1c_r & -a_2c_r & 0 & 0 & c_r & 0 \\ -c_r & -b_2c_r & -a_2c_r & 0 & 0 & 0 & c_r \end{bmatrix}$$

$$(13.291)$$

$$
\begin{aligned}
c_{11} &= 2c_f + 2c_r \\
c_{21} &= c_{12} = b_1c_f - b_2c_f - b_1c_r + b_2c_r \\
c_{31} &= c_{13} = 2a_2c_r - 2a_1c_f \\
c_{22} &= b_1^2c_f + b_2^2c_f + b_1^2c_r + b_2^2c_r \\
c_{32} &= c_{23} = a_1b_2c_f - a_1b_1c_f - a_2b_1c_r + a_2b_2c_r \\
c_{33} &= 2c_f a_1^2 + 2c_r a_2^2
\end{aligned}
$$

$$(13.292)$$

$$[k] = \begin{bmatrix} k_{11} & k_{12} & k_{13} & -k_f & -k_f & -k_r & -k_r \\ k_{21} & k_{22} & k_{23} & k_{24} & k_{25} & b_1k_r & -b_2k_r \\ k_{31} & k_{32} & k_{33} & a_1k_f & a_1k_f & -a_2k_r & -a_2k_r \\ -k_f & k_{42} & a_1k_f & k_{44} & -\dfrac{k_R}{w^2} & 0 & 0 \\ -k_f & k_{52} & a_1k_f & -\dfrac{k_R}{w^2} & k_{55} & 0 & 0 \\ -k_r & b_1k_r & -a_2k_r & 0 & 0 & k_r + k_{t_r} & 0 \\ -k_r & -b_2k_r & -a_2k_r & 0 & 0 & 0 & k_r + k_{t_r} \end{bmatrix}$$

$$(13.293)$$

$$
\begin{aligned}
k_{11} &= 2k_f + 2k_r \\
k_{21} &= k_{12} = b_1k_f - b_2k_f - b_1k_r + b_2k_r \\
k_{31} &= k_{13} = 2a_2k_r - 2a_1k_f \\
k_{22} &= k_R + b_1^2k_f + b_2^2k_f + b_1^2k_r + b_2^2k_r \\
k_{32} &= k_{23} = a_1b_2k_f - a_1b_1k_f - a_2b_1k_r + a_2b_2k_r \\
k_{42} &= k_{24} = -b_1k_f - \frac{1}{w}k_R \\
k_{52} &= k_{25} = b_2k_f + \frac{1}{w}k_R \\
k_{33} &= 2k_f a_1^2 + 2k_r a_2^2 \\
k_{44} &= k_f + k_{t_f} + \frac{1}{w^2}k_R \\
k_{55} &= k_f + k_{t_f} + \frac{1}{w^2}k_R
\end{aligned}
$$

$$(13.294)$$

$$\mathbf{F} = \begin{bmatrix} 0 \\ 0 \\ 0 \\ y_1 k_{t_f} \\ y_2 k_{t_f} \\ y_3 k_{t_r} \\ y_4 k_{t_r} \end{bmatrix}. \tag{13.295}$$

∎

**Example 493** *Natural frequencies and mode shapes of a full car model. Consider a vehicle with a the following characteristics.*

$$\begin{aligned} m &= 840\,\text{kg} \\ m_f &= 53\,\text{kg} \\ m_r &= 76\,\text{kg} \\ I_x &= 820\,\text{kg m}^2 \\ I_y &= 1100\,\text{kg m}^2 \end{aligned} \tag{13.296}$$

$$\begin{aligned} a_1 &= 1.4\,\text{m} \\ a_2 &= 1.47\,\text{m} \\ b_1 &= 0.7\,\text{m} \\ b_2 &= 0.75\,\text{m} \end{aligned} \tag{13.297}$$

$$\begin{aligned} k_f &= 10000\,\text{N}/\text{m} \\ k_r &= 13000\,\text{N}/\text{m} \\ k_{t_f} &= k_{t_r} = 200000\,\text{N}/\text{m} \\ k_R &= 25000\,\text{N m}/\text{rad} \end{aligned} \tag{13.298}$$

*Using the matrix $[A] = [m]^{-1}[k]$ and solving the associated eigenvalue and eigenvector problems, we find the following natural frequencies, and mode shapes for the full car model.*

$$\begin{aligned} \omega_1 &= 1.11274\,\text{Hz} \\ \omega_2 &= 1.15405\,\text{Hz} \\ \omega_3 &= 1.46412\,\text{Hz} \\ \omega_4 &= 8.42729\,\text{Hz} \\ \omega_5 &= 8.43346\,\text{Hz} \\ \omega_6 &= 10.0219\,\text{Hz} \\ \omega_7 &= 10.5779\,\text{Hz}. \end{aligned} \tag{13.299}$$

$$\mathbf{u}_1 = \begin{bmatrix} 1 \\ 0.0871235 \\ -0.257739 \\ 0.0747553 \\ 0.0562862 \\ 0.0347648 \\ 0.0426351 \end{bmatrix} \tag{13.300}$$

$$\mathbf{u}_2 = \begin{bmatrix} -0.0927632 \\ 1 \\ -0.0222029 \\ 0.101837 \\ -0.110205 \\ -0.0514524 \\ 0.0389078 \end{bmatrix} \tag{13.301}$$

$$\mathbf{u}_3 = \begin{bmatrix} .331817 \\ 0.0611334 \\ 1 \\ -0.0453749 \\ -0.0585134 \\ 0.110767 \\ 0.116324 \end{bmatrix} \tag{13.302}$$

$$\mathbf{u}_4 = \begin{bmatrix} -0.0000730868 \\ 0.00826940 \\ -0.0000799890 \\ 0.00233206 \\ -0.00241445 \\ 1 \\ -.986988 \end{bmatrix} \tag{13.303}$$

$$\mathbf{u}_5 = \begin{bmatrix} -0.0111901 \\ -0.000380648 \\ -0.0126628 \\ 0.000965144 \\ 0.00118508 \\ 0.978914 \\ 1 \end{bmatrix} \tag{13.304}$$

$$\mathbf{u}_6 = \begin{bmatrix} -0.00606295e - 2 \\ 0.000156931e - 3 \\ 0.00655247e - 2 \\ 1 \\ 0.99966 \\ -0.000528339e - 3 \\ -0.000566133e - 3 \end{bmatrix} \tag{13.305}$$
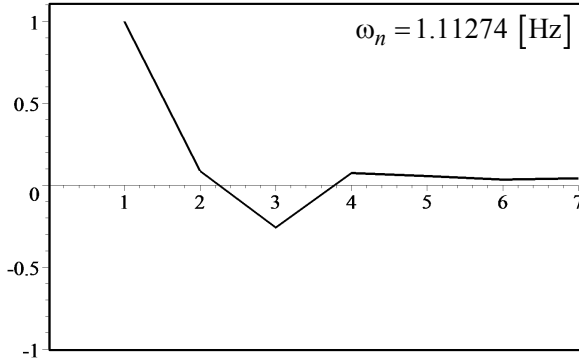
FIGURE 13.15. 1st mode shape of a full car model.
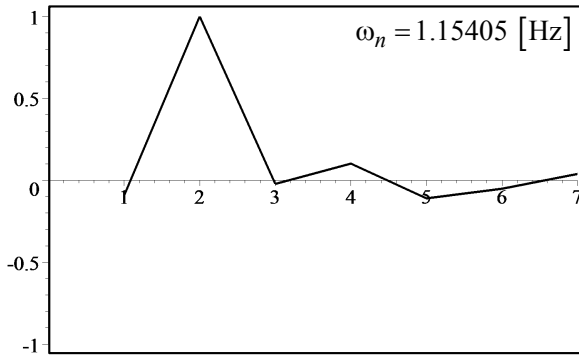


FIGURE 13.16. 2nd mode shape of a full car model.

$$\mathbf{u}_7 = \begin{bmatrix} -0.000000327006 \\ 0.0137130 \\ 0.00000560144 \\ -0.999745 \\ 1 \\ 0.00103530 \\ -0.00107039 \end{bmatrix} \tag{13.306}$$

*A visual illustration of the mode shapes are shown in Figures 13.15 to 13.21. The biggest element of the mode shapes $\mathbf{u}_1$ to $\mathbf{u}_7$ are $x$, $\varphi$, $\theta$, $x_3$, $x_4$, $x_1$, $x_2$ respectively. These figures depict the relative amplitude of each coordinate of the full car model at a resonance frequency.*

*The natural frequencies of a full car can be separated in two classes. The first class is the natural frequencies of the body: body bounce, body roll, and body pitch. Body related natural frequencies are always around 1 Hz. The*
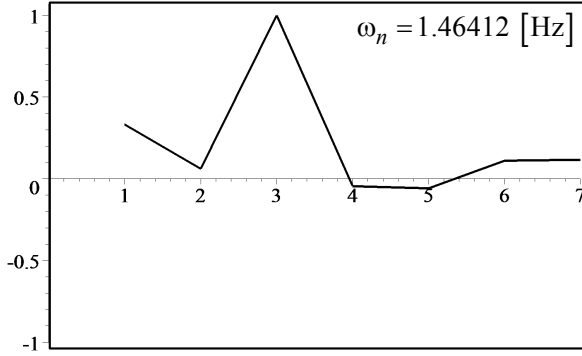
FIGURE 13.17. 3rd mode shape of a full car model.
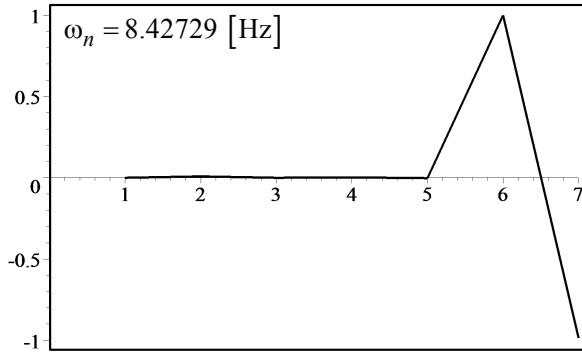


FIGURE 13.18. 4th mode shape of a full car model.
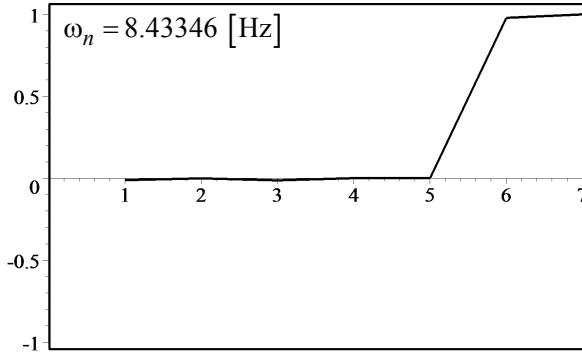


FIGURE 13.19. 5th mode shape of a full car model.
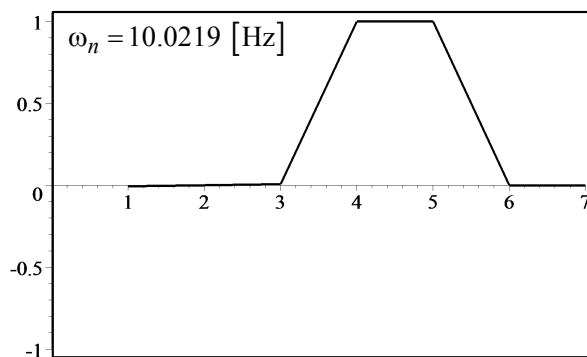
FIGURE 13.20. 6th mode shape of a full car model.
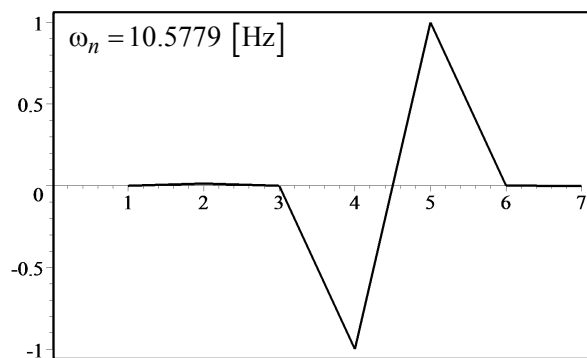


FIGURE 13.21. 7th mode shape of a full car model.

*second class is the natural frequencies of the wheels bounce. Wheel related natural frequencies are always around* 10 Hz.

*In this example, we assumed the car has independent suspension in front and rear. So, each wheel has only vertical displacement. In case of a solid axle, the left and right wheels make a rigid body with a roll and bounce motion. The energies and hence, the equations of motion should be revised accordingly to show the bounce and roll of the solid axle.*

## 13.7   Summary

Vehicles are connected multi-body dynamic systems and hence, their vibrating model has multiple DOF system. The vibrating behavior of multiple DOF systems are very much dependent to their natural frequencies and mode shapes. These characteristics can be determined by solving an eigenvalue and an eigenvector problems.

The most practical vibrating model of vehicles, starting from the simplest to more complex, are the one-eight car, quarter car, bicycle car, half car, and full car models.

Having symmetric mass, stiffness, and damping matrices of multiple DOF system simplifies the calculation of the eigenvalue and eigenvector problems. To have symmetric coefficient matrices, we may define the kinetic energy, potential energy, and dissipation function of the system by quadratures and derive the equations of motion by applying the Lagrange method.

## 13.8   Key Symbols

| | |
|---|---|
| $a, \ddot{x}$ | acceleration |
| $a_1$ | distance from mass center to front axle |
| $a_2$ | distance from mass center to rear axle |
| $[a], [A]$ | coefficient matrix |
| $[A] = [m]^{-1}[k]$ | coefficient matrix of characteristic equation |
| $b_1$ | distance from mass center to left wheel |
| $b_2$ | distance from mass center to right wheel |
| $c$ | damping |
| $c_{eq}$ | equivalent damping |
| $c_{ij}$ | element of row $i$ and column $j$ of $[c]$ |
| $[c]$ | damping matrix |
| $[\underline{c}]$ | symmetric damping matrix |
| $C$ | mass center |
| $D$ | dissipation function |
| $e$ | eccentricity arm |
| $E$ | mechanical energy |
| $f, \mathbf{F}$ | harmonic force |
| $f = \frac{1}{T}$ | cyclic frequency $[\text{Hz}]$ |
| $f_c$ | damper force |
| $f_k$ | spring force |
| $F$ | amplitude of a harmonic force $f$ |
| $F_r, Q_r$ | generalized force |
| $g$ | gravitational acceleration |
| $I$ | mass moment of inertia |
| $\mathbf{I}$ | identity matrix |
| $k$ | stiffness |
| $k_{eq}$ | equivalent stiffness |
| $k_{ij}$ | element of row $i$ and column $j$ of $[k]$ |
| $k_R$ | antiroll bar torsional stiffness |
| $[k]$ | stiffness matrix |
| $[\underline{k}]$ | symmetric stiffness matrix |
| $K$ | kinetic energy |
| $l$ | length |
| $l$ | wheelbase |
| $\mathcal{L}$ | Lagrangean |
| $m$ | mass |
| $m_e$ | eccentric mass |
| $m_{ij}$ | element of row $i$ and column $j$ of $[m]$ |
| $m_s$ | sprung mass |
| $m_u$ | unsprung mass |
| $[m]$ | mass matrix |
| $[\underline{m}]$ | symmetric mass matrix |

| | |
|---|---|
| $n$ | number of DOF |
| $\mathbf{p}$ | momentum |
| $q_i, Q_i$ | generalized force |
| $r = \frac{\omega}{\omega_n}$ | frequency ratio |
| $r, R$ | radius |
| $S$ | quadrature |
| $t$ | time |
| $T$ | period |
| $u_{ij}$ | $j$th element of the $i$th mode shape |
| $\mathbf{u}$ | mode shape, eigenvector |
| $\mathbf{u}_i$ | $i$th eigenvector |
| $v, \mathbf{v}, \dot{x}, \dot{\mathbf{x}}$ | velocity |
| $V$ | potential energy |
| $w$ | track |
| $x$ | absolute displacement |
| $X$ | steady-state amplitude of $x$ |
| $y$ | base excitation displacement |
| $Y$ | steady-state amplitude of $y$ |
| $z$ | relative displacement |
| $Z$ | steady-state amplitude of $z$ |
| $Z_i$ | short notation parameter |

| | |
|---|---|
| $\delta$ | deflection |
| $\xi = \frac{c}{2\sqrt{km}}$ | damping ratio |
| $\lambda$ | eigenvalue |
| $\lambda_i$ | $i$th eigenvalue |
| $\omega = 2\pi f$ | angular frequency $[\,\mathrm{rad/\,s}]$ |
| $\omega_n$ | natural frequency |
| $\omega_i$ | $i$th natural frequency |

Subscript

| | |
|---|---|
| $d$ | driver |
| $f$ | front |
| $r$ | rear |
| $s$ | sprung |
| $u$ | unsprung |

# Exercises

1. Equation of motion of a multiple DOF system.

   Figure 13.22 illustrates a two DOF vibrating system.
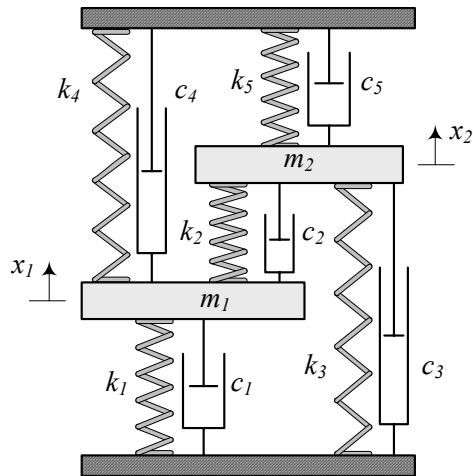


FIGURE 13.22. A two DOF vibrating system.

   (a) Determine $K$, $V$, and $D$ functions.

   (b) Determine the equations of motion using the Lagrange method.

   (c) ★ Rewrite $K$, $V$, and $D$ in quadrature form.

   (d) Determine the natural frequencies and mode shapes of the system.

2. Absolute and relative coordinates.

   Figure 13.23 illustrates two similar double pendulums. We express the motion of the left one using absolute coordinates $\theta_1$ and $\theta_2$, and express the motion of the right one with absolute coordinate $\theta_1$ and relative coordinate $\theta_2$.

   (a) Determine the equation of motion of the absolute coordinate double pendulum.

   (b) Determine the equation of motion of the relative coordinate double pendulum.

   (c) Compare their mass and stiffness matrices.
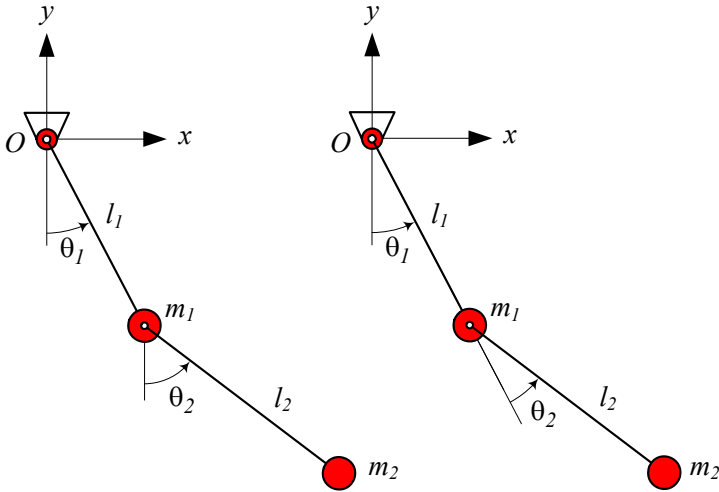
FIGURE 13.23. Two similar double pendulums, expressed by absolute and relative coordinates.

3. One-eight car model.

   Consider a one-eight car model as a base excited one DOF system. Determine its natural $\omega_n$ and damped natural frequencies $\omega_d$ if

$$
\begin{aligned}
m &= 1245\,\text{kg} \\
k &= 60000\,\text{N}/\text{m} \\
c &= 2400\,\text{N s}/\text{m}.
\end{aligned}
$$

4. Quarter car model.

   Consider a quarter car model. Determine its natural frequencies and mode shapes if

$$
\begin{aligned}
m_s &= 1085/4\,\text{kg} \\
m_u &= 40\,\text{kg} \\
k_s &= 10000\,\text{N}/\text{m} \\
k_u &= 150000\,\text{N}/\text{m} \\
c_s &= 800\,\text{N s}/\text{m}.
\end{aligned}
$$

5. Bicycle car model.

Consider a bicycle car model with the following characteristics:

$$
\begin{aligned}
m &= 1085/2 \, \text{kg} \\
m_1 &= 40 \, \text{kg} \\
m_2 &= 40 \, \text{kg} \\
I_y &= 1100 \, \text{kg} \, \text{m}^2
\end{aligned}
$$

$$
\begin{aligned}
a_1 &= 1.4 \, \text{m} \\
a_2 &= 1.47 \, \text{m}
\end{aligned}
$$

$$
\begin{aligned}
k_1 &= 10000 \, \text{N}/\text{m} \\
k_{t_1} &= k_{t_2} = 150000 \, \text{N}/\text{m}
\end{aligned}
$$

Determine its natural frequencies and mode shapes for

(a) $k_2 = 8000 \, \text{N}/\text{m}$
(b) $k_2 = 10000 \, \text{N}/\text{m}$
(c) $k_2 = 12000 \, \text{N}/\text{m}$.
(d) Compare the natural frequencies for different $k_1/k_2$ and express the effect of increasing stiffness ratio on the pitch mode.

6. Half car model.

Consider a bicycle car model with the following characteristics:

$$
\begin{aligned}
m &= 1085/2 \, \text{kg} \\
m_1 &= 40 \, \text{kg} \\
m_2 &= 40 \, \text{kg} \\
I_x &= 820 \, \text{kg} \, \text{m}^2
\end{aligned}
$$

$$
\begin{aligned}
b_1 &= 0.7 \, \text{m} \\
b_2 &= 0.75 \, \text{m}
\end{aligned}
$$

$$
\begin{aligned}
k_1 &= 10000 \, \text{N}/\text{m} \\
k_{t_1} &= k_{t_2} = 150000 \, \text{N}/\text{m}
\end{aligned}
$$

Determine its natural frequencies and mode shapes for

(a) $k_R = 0$
(b) $k_R = 10000 \, \text{N} \, \text{m}/\text{rad}$
(c) $k_R = 50000 \, \text{N} \, \text{m}/\text{rad}$.

(d) Compare the natural frequencies for different $k_R$ and express the effect of increasing roll stiffness on the roll mode.

(e) Determine $k_R$ such that the roll natural frequency be equal to the bounce natural frequency and determine the mode shapes of the half car for that $k_R$.

7. Full car model.

Consider a full car model with the following characteristics:

$$
\begin{aligned}
m &= 1085\,\text{kg} \\
m_f &= 40\,\text{kg} \\
m_r &= 40\,\text{kg} \\
I_x &= 820\,\text{kg}\,\text{m}^2 \\
I_y &= 1100\,\text{kg}\,\text{m}^2
\end{aligned}
\tag{13.307}
$$

$$
\begin{aligned}
a_1 &= 1.4\,\text{m} \\
a_2 &= 1.47\,\text{m} \\
b_1 &= 0.7\,\text{m} \\
b_2 &= 0.75\,\text{m}
\end{aligned}
\tag{13.308}
$$

$$
\begin{aligned}
k_f &= 10000\,\text{N/m} \\
k_r &= 10000\,\text{N/m} \\
k_{t_f} &= k_{t_r} = 150000\,\text{N/m} \\
k_R &= 20000\,\text{N\,m/rad}
\end{aligned}
\tag{13.309}
$$

(a) Determine its natural frequencies and mode shapes.

(b) Change $k_R$ such that the roll mode and pitch modes have the same frequency.

(c) Determine the mode shapes of the car for that $k_R$.

# 14

# Suspension Optimization

In this chapter, we examine a linear, one degree-of-freedom, base excited vibration isolator system as the simplest model for a vibration isolator and vehicle suspension. Based on a root mean square (RMS) optimization method, we develop a design chart to determine the optimal damper and spring for the best vibration isolation and ride comfort.

## 14.1 Mathematical Model

Figure 14.1 illustrates a single-DOF base excited linear vibrating system. It can represent a model for the vertical vibrations of a vehicle.
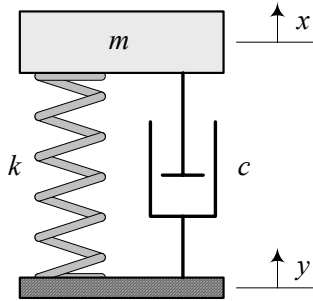


FIGURE 14.1. A base excited linear suspension.

A one-fourth (1/4) of the mass of the body is modeled as a solid mass $m$ denoted as *sprung mass*. A spring of stiffness $k$, and a shock absorber with viscous damping $c$, support the sprung mass and represent the main suspension of the vehicle. The suspension parameters $k$ and $c$ are the equivalent stiffness and damping for one wheel, measured at the center of the wheel. Because we ignore the wheel mass and tire stiffness, this model is sometimes called one-eighth (1/8) car model.

The equation of motion for the system is

$$m\ddot{x} + c\dot{x} + kx = c\dot{y} + ky \tag{14.1}$$

which can be transformed to the equation,

$$m\ddot{z} + c\dot{z} + kz = -m\ddot{y} \tag{14.2}$$

using a relative displacement variable $z$.

$$z = x - y \tag{14.3}$$

The variable $x$ is the absolute displacement of the body, and $y$ is the absolute displacement of the ground.

The equation of motion (14.1) and (14.2), which are dependent on three parameters $(m, c, k)$ can be transformed to the following equations:

$$\ddot{x} + 2\xi\omega_n \dot{x} + \omega_n^2 x = 2\xi\omega_n \dot{y} + \omega_n^2 y \tag{14.4}$$
$$\ddot{z} + 2\xi\omega_n \dot{z} + \omega_n^2 z = -\ddot{y} \tag{14.5}$$

by introducing *natural frequency* $\omega_n$ and *damping ratio* $\xi$.

$$\xi = \frac{c}{2\sqrt{km}} \tag{14.6}$$

$$\omega_n = \sqrt{\frac{k}{m}} = 2\pi f_n \tag{14.7}$$

**Proof.** The kinetic energy, potential energy, and dissipation function of the system are:

$$K = \frac{1}{2}m\dot{x}^2 \tag{14.8}$$

$$V = \frac{1}{2}k(x-y)^2 \tag{14.9}$$

$$D = \frac{1}{2}c(\dot{x}-\dot{y})^2 \tag{14.10}$$

Employing the Lagrange method,

$$\frac{d}{dt}\left(\frac{\partial K}{\partial \dot{x}}\right) - \frac{\partial K}{\partial x} + \frac{\partial D}{\partial \dot{x}} + \frac{\partial V}{\partial x} = 0 \tag{14.11}$$

we find the equation of motion

$$\frac{d}{dt}(m\dot{x}) + c(\dot{x} - \dot{y}) + k(x - y) = 0 \tag{14.12}$$

which can be transformed to Equation (14.1). Introducing a relative position variable, $z = x - y$, we have

$$\dot{z} = \dot{x} - \dot{y} \tag{14.13}$$
$$\ddot{z} = \ddot{x} - \ddot{y} \tag{14.14}$$

to write Equation (14.12) as

$$m\frac{d}{dt}(\ddot{z} + \ddot{y}) + c\dot{z} + kz = 0 \tag{14.15}$$

which is equivalent to (14.2).

Dividing Equations (14.1) and (14.2) by $m$ and using (14.6) and (14.7), generate their equivalent Equations (14.4) and (14.5), respectively. ∎
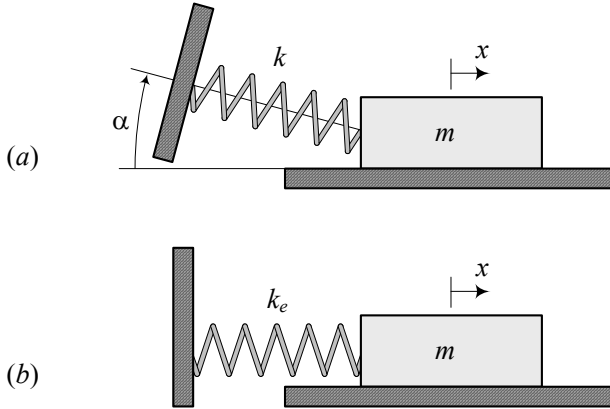
FIGURE 14.2. A tilted spring and its equivalent stiffness.

**Example 494** *Different model for front and rear parts of a vehicle.*
  *Consider a car with the following information:*

$$car\ mass = 1500\,\text{kg} \tag{14.16}$$

$$wheel\ mass = 50\,\text{kg} \tag{14.17}$$

$$F_{z_1} = 3941.78\,\text{N} \tag{14.18}$$

$$F_{z_2} = 3415.6\,\text{N} \tag{14.19}$$

*where $F_{z_1}$ and $F_{z_2}$ are the front and rear tire loads, respectively. The mass $m$ of a 1/8 vibrating model for the front of the car must be*

$$
\begin{aligned}
m &= \frac{F_{z_1}}{F_{z_1} + F_{z_2}} \times (1500 - 4 \times 50) \\
&= 696.49\,\text{kg}
\end{aligned}
\tag{14.20}
$$

*and for the rear of the car must be*

$$
\begin{aligned}
m &= \frac{F_{z_2}}{F_{z_1} + F_{z_2}} \times (1500 - 4 \times 50) \\
&= 603.51\,\text{kg.}
\end{aligned}
\tag{14.21}
$$

**Example 495** *Tilted spring.*
  *Consider a mass-spring system such that the spring makes an angle $\alpha$ with the axis of mass translation, as shown in Figure 14.2(a). We may substitute such a tilted spring with an equivalent spring $k_{eq}$ that is on the same axis of mass translation, as shown in Figure 14.2(b).*

$$k_{eq} \approx k \cos^2 \alpha \tag{14.22}$$

  *When the mass $m$ is in motion, such as is shown in Figure 14.3(a), its free body diagram is as shown in Figure 14.3(b). If the motion of mass $m$ is*
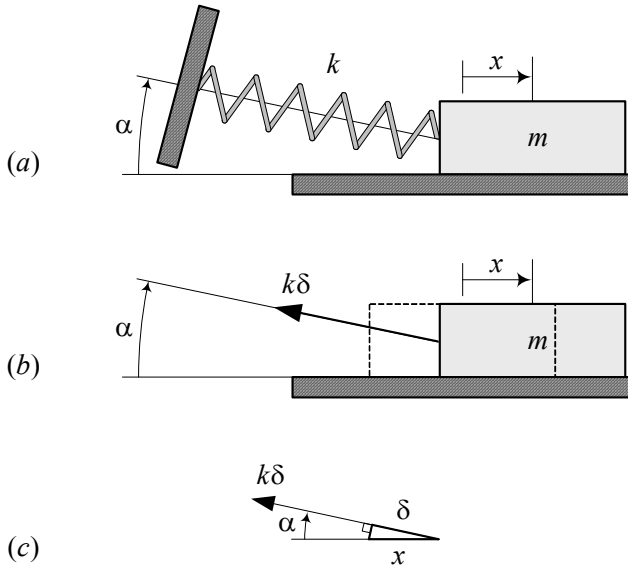
FIGURE 14.3. A mass-spring system such that the spring makes and angle $\alpha$ with directing of mass translation.

$x \ll 1$, we ignore any changes in $\alpha$ and then, as shown in Figure 14.3(c), the spring elongation is

$$\delta \approx x \cos \alpha. \tag{14.23}$$

Therefore, the spring force $f_k$ is

$$f_k = k\delta \approx kx \cos \alpha. \tag{14.24}$$

The spring force may be projected on the $x$-axis to find the $x$ component, $f_x$, that moves the mass $m$.

$$
\begin{aligned}
f_x &= f_k \cos \alpha \\
&\approx \left( k \cos^2 \alpha \right) x
\end{aligned}
\tag{14.25}
$$

The tilted spring can be substituted with an equivalent spring $k_{eq}$ on the $x$-axis that needs the same force $f_x$ to elongate the same amount as the mass moves.

$$
\begin{aligned}
f_x &= k_{eq} x \tag{14.26} \\
k_{eq} &\approx k \cos^2 \alpha \tag{14.27}
\end{aligned}
$$
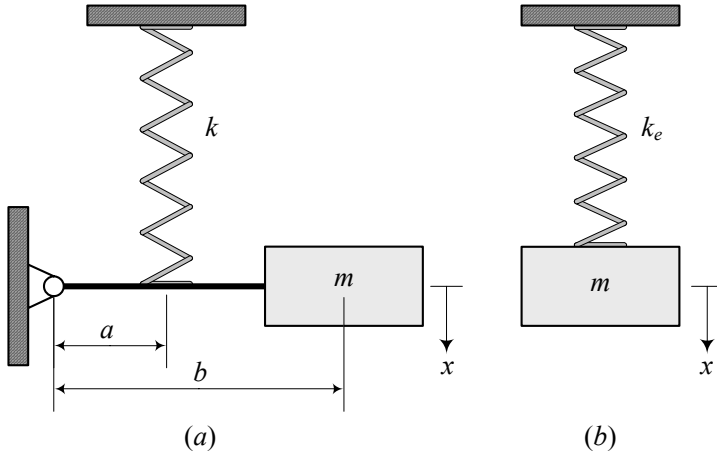
FIGURE 14.4. A mass $m$ attached to the tip of a massless bar with length $b$.

**Example 496** *Alternative proof for a tilted spring.*

Consider a spring that makes an angle $\alpha$ with a direction of motion as shown in Figure 14.2(a). When the moving end translates $x$, the elongation of the spring is

$$\delta \approx x \cos \alpha. \qquad (14.28)$$

The potential energy of such a spring would be

$$V = \frac{1}{2} k \delta^2 = \frac{1}{2} \left( k \cos^2 \alpha \right) x^2. \qquad (14.29)$$

An equivalent spring with stiffness $k_{eq}$ must collect the same amount of potential energy for the same displacement $x$.

$$V = \frac{1}{2} k_{eq} x^2 \qquad (14.30)$$

Therefore, the equivalent stiffness $k_{eq}$ is

$$k_{eq} = k \cos^2 \alpha. \qquad (14.31)$$

**Example 497** *Displaced spring.*

Figure 14.4(a) illustrates a mass $m$ attached to the tip of a massless bar with length $b$. The bar is pivoted to the wall and a spring $k$ is attached to the bar at a distance $a$ from the pivot.

When the mass oscillates with displacement $x \ll 1$, the elongation $\delta$ of the spring is

$$\delta \approx \frac{a}{b} x. \qquad (14.32)$$

We may substitute the system with a translational mass-spring system such as shown in Figure 14.4(b). The new system has the same mass $m$ and an
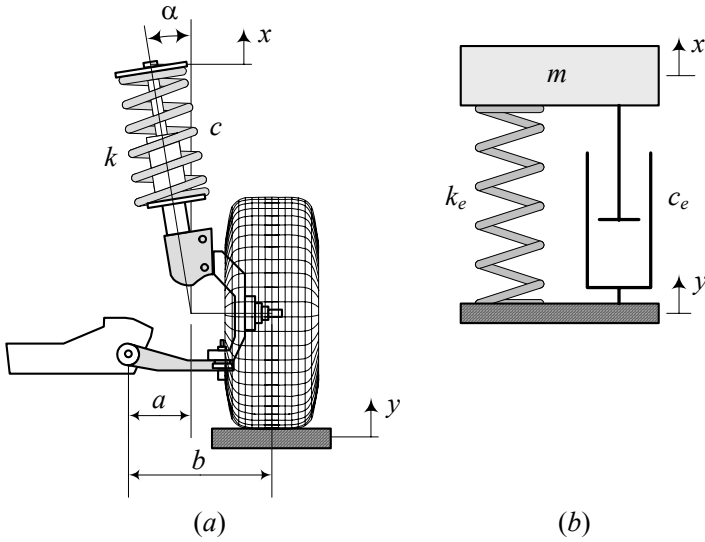
FIGURE 14.5. A MacPherson suspenssion and its equivalent vibrating system.

*equivalent spring $k_{eq}$.*

$$k_{eq} = \left(\frac{a}{b}\right)^2 k \tag{14.33}$$

*The equivalent spring provides the same potential energy as the original spring, when the mass moves.*

$$
\begin{aligned}
V &= \frac{1}{2}k_{eq}x^2 = \frac{1}{2}k\delta^2 = \frac{1}{2}k\left(\frac{a}{b}x\right)^2 \\
&= \frac{1}{2}k\left(\frac{a}{b}\right)^2 x^2
\end{aligned}
\tag{14.34}
$$

**Example 498** *Equivalent spring and damper for a McPherson suspension.*

Figure 14.5 illustrates a McPherson strut mechanism and its equivalent vibrating system.

We assume the tire is stiff and therefore, the wheel center gets the same motion $y$. Furthermore, we assume the wheel and and body of the vehicle move only vertically.

To find the equivalent parameters for a 1/8 vibrating model, we use $m$ equal to 1/4 of the body mass. The spring $k$ and damper $c$ make an angle $\alpha$ with the direction of wheel motion. They are also displaced $b - a$ from the wheel center. So, the equivalent spring $k_{eq}$ and damper $c_{eq}$ are

$$k_{eq} = k\left(\frac{a}{b}\cos\alpha\right)^2 \tag{14.35}$$

$$c_{eq} = c\left(\frac{a}{b}\cos\alpha\right)^2. \tag{14.36}$$
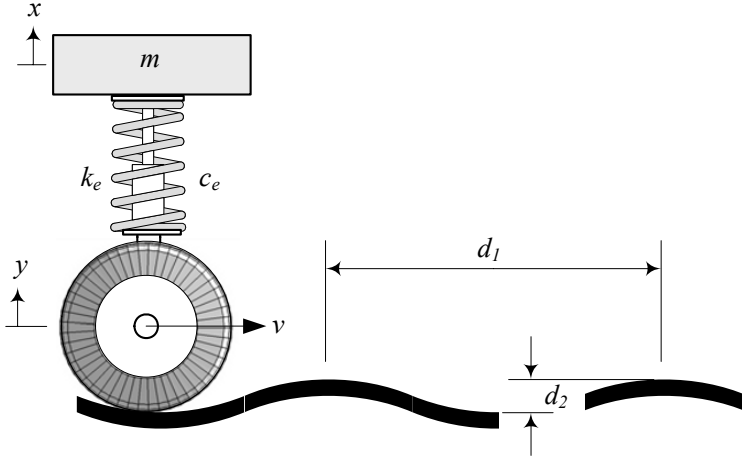
FIGURE 14.6. A 1/8 car model moving with speed $v$ on a wavy road.

*For example assume that we have determined the following stiffness and damping as a result of optimization.*

$$k_{eq} = 9869.6 \, \text{N}/\text{m} \qquad (14.37)$$
$$c_{eq} = 87.965 \, \text{N s}/\text{m}. \qquad (14.38)$$

*The actual $k$ and $c$ for a McPherson suspension with*

$$a = 19 \, \text{cm} \qquad (14.39)$$
$$b = 32 \, \text{cm} \qquad (14.40)$$
$$\alpha = 27 \, \text{deg} \qquad (14.41)$$

*would be*

$$k = 28489 \, \text{N}/\text{m} \qquad (14.42)$$
$$c = 253.9 \, \text{N s}/\text{m}. \qquad (14.43)$$

**Example 499** *Wavy road and excitation frequency.*
    *Figure 14.6 illustrates a 1/8 car model moving with speed $v$ on a wavy road with length $d_1$ and peak-to-peak height $d_2$. Assuming a stiff tire with a small radius compared to the road waves, we may consider $y$ as the fluctuation of the road.*
    *The required time to pass one length $d_1$ is the period of the excitation*

$$T = \frac{d_1}{v} \qquad (14.44)$$

*which can be used to find the frequency of excitation*

$$\omega = \frac{2\pi}{T} = \frac{2\pi v}{d_1}.$$

(14.45)

*Therefore, the excitation $y = Y \sin \omega t$ is*

$$y = \frac{d_2}{2} \sin \frac{2\pi v}{d_1} t.$$

(14.46)

**Example 500** *Function of an isolator*

*The function of an isolator is to reduce the magnitude of motion trans-mitted from a vibrating foundation to the equipment, or to reduce the mag-nitude of force transmitted from the equipment to its foundation, both in time and frequency domain.*

**Example 501** *Rubber mount.*

*In the simplest approach to suspension analysis, the parameters $m$, $k$, and $c$ are considered constant and independent of the excitation frequency or behavior of the foundation. This assumption is equivalent to considering an infinitely stiff and massive foundation. For rubber mounts, the damping coefficient usually decreases, and the stiffness coefficient increases with ex-citation frequency. Moreover, neither the engine nor body can be assumed an infinitely stiff rigid body at high frequencies.*

## 14.2 Frequency Response

The most important frequency responses of a 1/8 car model, shown in Figure 14.1, are: absolute displacement $G_0$, relative displacement $S_2$, and absolute acceleration $G_2$

$$G_0 = \left| \frac{X}{Y} \right| = \frac{\sqrt{1 + (2\xi r)^2}}{\sqrt{(1 - r^2)^2 + (2\xi r)^2}}$$

(14.47)

$$S_2 = \left| \frac{Z}{Y} \right| = \frac{r^2}{\sqrt{(1 - r^2)^2 + (2\xi r)^2}}$$

(14.48)

$$G_2 = \left| \frac{\ddot{X}}{Y\omega_n^2} \right| = \frac{r^2 \sqrt{1 + (2\xi r)^2}}{\sqrt{(1 - r^2)^2 + (2\xi r)^2}}$$

(14.49)

where

$$r = \frac{\omega}{\omega_n} \qquad \xi = \frac{c}{2\sqrt{km}} \qquad \omega_n = \sqrt{\frac{k}{m}}.$$

(14.50)

**Proof.** Applying a harmonic excitation

$$y = Y \sin \omega t \tag{14.51}$$

the equation of motion (14.5) reduces to

$$\ddot{z} + 2\xi\omega_n \dot{z} + \omega_n^2 z = \omega^2 Y \sin \omega t. \tag{14.52}$$

Now, we may consider a harmonic solution such as

$$z = A_3 \sin \omega t + B_3 \cos \omega t \tag{14.53}$$

to substitute in the equation of motion

$$
\begin{aligned}
& -A_3\omega^2 \sin \omega t - B_3\omega^2 \cos \omega t \\
& +2\xi\omega_n \left( A_3\omega \cos \omega t - B_3\omega \sin \omega t \right) \\
& +\omega_n^2 \left( A_3 \sin \omega t + B_3 \cos \omega t \right) \\
= \ & \omega^2 Y \sin \omega t
\end{aligned} \tag{14.54}
$$

and find a set of equations to calculate $A_3$ and $B_3$.

$$\begin{bmatrix} \omega_n^2 - \omega^2 & -2\xi\omega\omega_n \\ 2\xi\omega\omega_n & \omega_n^2 - \omega^2 \end{bmatrix} \begin{bmatrix} A_3 \\ B_3 \end{bmatrix} = \begin{bmatrix} Y\omega^2 \\ 0 \end{bmatrix} \tag{14.55}$$

The first row of the set (14.55) is a balance of the coefficients of $\sin \omega t$ in Equation (14.54), and the second row is a balance of the coefficients of $\cos \omega t$. Therefore, the coefficients $A_3$ and $B_3$ can be found as follow.

$$
\begin{aligned}
\begin{bmatrix} A_3 \\ B_3 \end{bmatrix} &= \begin{bmatrix} \omega_n^2 - \omega^2 & -2\xi\omega\omega_n \\ 2\xi\omega\omega_n & \omega_n^2 - \omega^2 \end{bmatrix}^{-1} \begin{bmatrix} Y\omega^2 \\ 0 \end{bmatrix} \\
&= \begin{bmatrix} -\dfrac{\omega^2 - \omega_n^2}{4\xi^2\omega^2\omega_n^2 + \omega^4 - 2\omega^2\omega_n^2 + \omega_n^4} Y\omega^2 \\ -\dfrac{2\xi\omega\omega_n}{4\xi^2\omega^2\omega_n^2 + \omega^4 - 2\omega^2\omega_n^2 + \omega_n^4} Y\omega^2 \end{bmatrix}
\end{aligned} \tag{14.56}
$$

These equations may be transformed to this simpler form, by using $r$ and $\xi$.

$$\begin{bmatrix} A_3 \\ B_3 \end{bmatrix} = \begin{bmatrix} \dfrac{1 - r^2}{(1 - r^2)^2 + (2\xi r)^2} r^2 Y \\ \dfrac{-2\xi r}{(1 - r^2)^2 + (2\xi r)^2} r^2 Y \end{bmatrix} \tag{14.57}$$

The relative displacement amplitude $Z$ is then equal to

$$
\begin{aligned}
Z &= \sqrt{A_3^2 + B_3^2} \\
&= \frac{r^2}{\sqrt{(1 - r^2)^2 + (2\xi r)^2}} Y
\end{aligned} \tag{14.58}
$$

which provides $S_2 = |Z/Y|$ in Equation (14.48).

To find the absolute frequency response $G_0$, we may assume

$$
\begin{aligned}
x &= A_2 \sin \omega t + B_2 \cos \omega t \\
&= X \sin (\omega t - \varphi_x)
\end{aligned}
\tag{14.59}
$$

and write

$$
z = x - y \tag{14.60}
$$

$$
A_3 \sin \omega t + B_3 \cos \omega t = A_2 \sin \omega t + B_2 \cos \omega t - Y \sin \omega t \tag{14.61}
$$

which shows

$$
A_2 = A_3 + Y \tag{14.62}
$$

$$
B_2 = B_3. \tag{14.63}
$$

The absolute displacement amplitude is then equal to

$$
\begin{aligned}
X &= \sqrt{A_2^2 + B_2^2} \\
&= \sqrt{(A_3 + Y)^2 + B_3^2} \\
&= \frac{\sqrt{1 + (2\xi r)^2}}{\sqrt{(1 - r^2)^2 + (2\xi r)^2}} Y
\end{aligned}
\tag{14.64}
$$

which provides $G_0 = |X/Y|$ in Equation (14.47).

The absolute acceleration frequency response

$$
\begin{aligned}
\ddot{x} &= -X\omega^2 \sin (\omega t - \varphi_x) \\
&= -\ddot{X} \sin (\omega t - \varphi_x)
\end{aligned}
\tag{14.65}
\tag{14.66}
$$

can be found by twice differentiating from the displacement frequency response (14.59). If we show the amplitude of the absolute acceleration by $\ddot{X}$, then we may define $\ddot{X}$ by

$$
\left| \frac{\ddot{X}}{Y\omega_n^2} \right| = \frac{r^2 \sqrt{1 + (2\xi r)^2}}{\sqrt{(1 - r^2)^2 + (2\xi r)^2}}
$$

which provides $G_2 = \left| \ddot{X} / \left( \omega_n^2 Y \right) \right|$ as in Equation (14.49). ∎

**Example 502** *Principal method for absolute motion $X$.*

To find the absolute frequency response $G_0$, we may substitute

$$
y = Y \sin \omega t \tag{14.67}
$$

*and a harmonic solution for x*

$$x = A_2 \sin \omega t + B_2 \cos \omega t \tag{14.68}$$

*in Equation (14.4)*

$$\ddot{x} + 2\xi\omega_n \dot{x} + \omega_n^2 x = 2\xi\omega_n \dot{y} + \omega_n^2 y \tag{14.69}$$

*and solve for* $X = \sqrt{A_2^2 + B_2^2}$.

$$
\begin{aligned}
&-\omega^2 A_2 \sin \omega t - \omega^2 B_2 \cos \omega t \\
&+2\xi\omega_n \omega \left( A_2 \cos \omega t - B_2 \sin \omega t \right) \\
&+\omega_n^2 \left( A_2 \sin \omega t + B_2 \cos \omega t \right) \\
&= \quad 2\xi\omega_n \omega Y \cos \omega t + \omega_n^2 Y \sin \omega t
\end{aligned} \tag{14.70}
$$

*The set of equations for* $A_2$ *and* $B_2$ *from the coefficients of* $\sin$ *and* $\cos$

$$
\begin{bmatrix} \omega_n^2 - \omega^2 & -2\xi\omega\omega_n \\ 2\xi\omega\omega_n & \omega_n^2 - \omega^2 \end{bmatrix}
\begin{bmatrix} A_2 \\ B_2 \end{bmatrix} =
\begin{bmatrix} Y\omega_n^2 \\ 2Y\xi\omega\omega_n \end{bmatrix} \tag{14.71}
$$

*results in the following solution:*

$$
\begin{aligned}
\begin{bmatrix} A_2 \\ B_2 \end{bmatrix} &=
\begin{bmatrix} \omega_n^2 - \omega^2 & -2\xi\omega\omega_n \\ 2\xi\omega\omega_n & \omega_n^2 - \omega^2 \end{bmatrix}^{-1}
\begin{bmatrix} Y\omega_n^2 \\ 2Y\xi\omega\omega_n \end{bmatrix} \\[2mm]
&=
\begin{bmatrix} \dfrac{-\left(\omega^2 - \omega_n^2\right)\omega_n^2 + 4\xi^2\omega^2\omega_n^2}{4\xi^2\omega^2\omega_n^2 + \omega^4 - 2\omega^2\omega_n^2 + \omega_n^4}Y \\[4mm] \dfrac{-2\xi\omega\omega_n^3}{4\xi^2\omega^2\omega_n^2 + \omega^4 - 2\omega^2\omega_n^2 + \omega_n^4}Y \end{bmatrix} \\[2mm]
&=
\begin{bmatrix} \dfrac{(2\xi r)^2 - \left(1 - r^2\right)}{\left(1 - r^2\right)^2 + (2\xi r)^2}Y \\[4mm] \dfrac{-2\xi r^3}{\left(1 - r^2\right)^2 + (2\xi r)^2}Y \end{bmatrix}
\end{aligned} \tag{14.72}
$$

*Therefore, the amplitude of the absolute displacement X would be the same as (14.64).*

**Example 503** $G_0 \neq S_2 + 1$

We may try to find the absolute frequency response $G_0 = |X/Y|$, from the result for $S_2$. The frequency response $S_2$ is

$$S_2 = \frac{Z}{Y} \tag{14.73}$$

*however,*

$$
\begin{aligned}
S_2 &\neq \frac{X}{Y} - 1 \\
&\neq G_0 - 1
\end{aligned} \tag{14.74}
$$
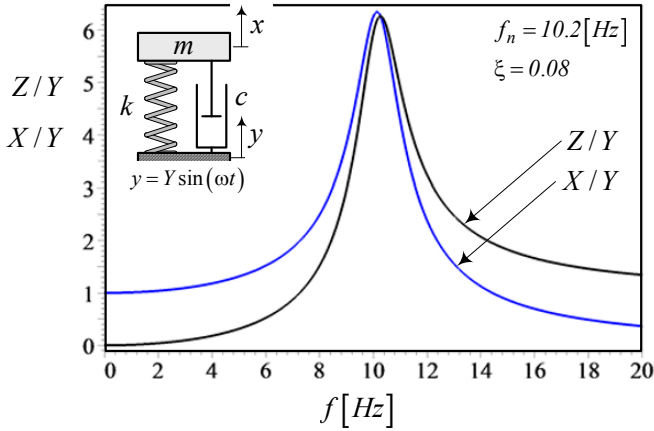
FIGURE 14.7. Absolute and relative displacement frequency responses for a ve-
hicle.

*because the amplitude of the relative displacement Z is not equal to the am-
plitude of absolute displacement X minus the amplitude of road excitation
Y.*

$$Z \neq X - Y \tag{14.75}$$

**Example 504** *A sample of frequency responses.*

*Consider a vehicle with the following natural frequency $f_n$ and damping
ratio $\xi$:*

$$f_n = 10.2 \, \text{Hz} \tag{14.76}$$

$$\xi = 0.08 \tag{14.77}$$

*The absolute and relative displacements frequency responses of the vehicle
are shown in Figure 14.7. The relative displacement starts at zero and
ends up at one, while the absolute displacement starts at one and ends up
at zero.*

## 14.3   RMS Optimization

Figure 14.8 is a design chart for optimal suspension parameters of base
excited systems. The horizontal axis is the root mean square of relative
displacement, $S_Z = RMS(S_2)$, and the vertical axis is the root mean square
of absolute acceleration, $S_{\ddot{X}} = RMS(G_2)$. There are two sets of curves
that make a mesh. The first set, which is almost parallel at the right end,
is constant natural frequency $f_n$, and the second set, which spread from
$S_Z = 1$, is a constant damping ratio $\xi$. There is a curve, called *optimal
design curve*, which indicates the optimal suspension parameters.
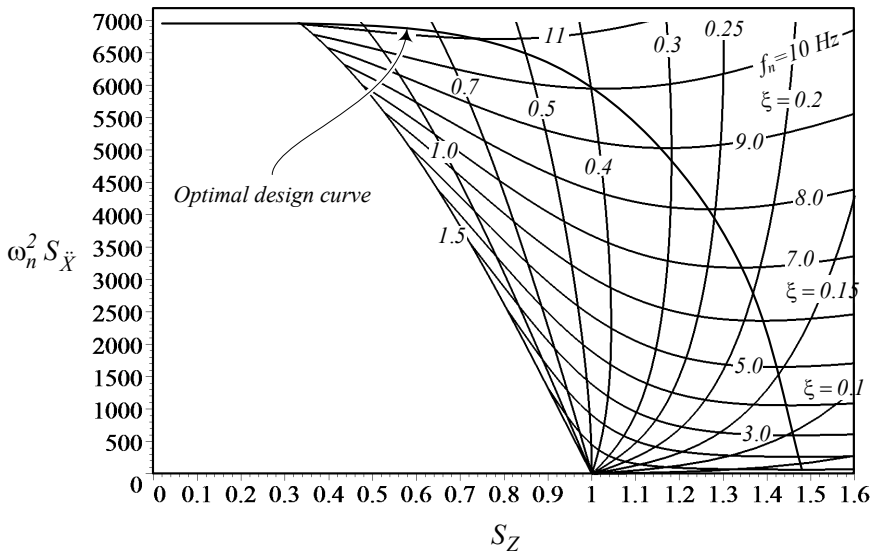
FIGURE 14.8. Design chart for optimal suspension parameters of equipments.
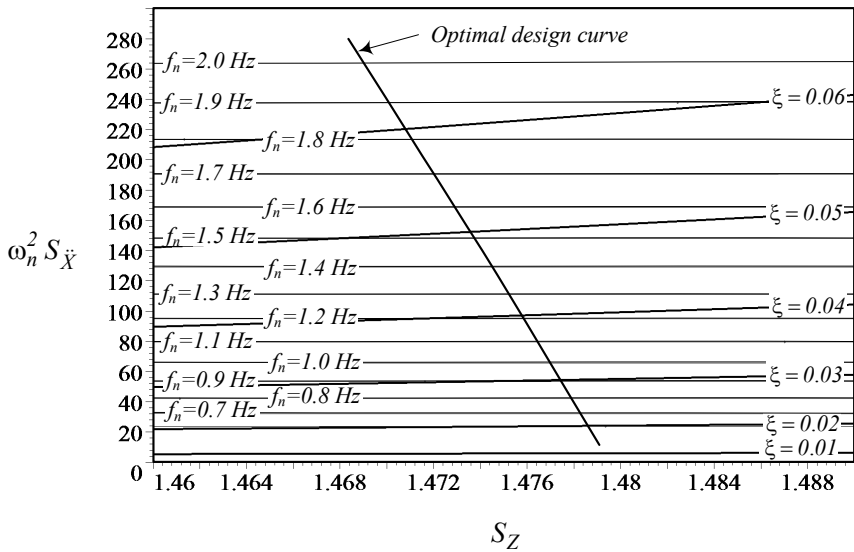


FIGURE 14.9. Design chart for optimal suspension parameters of vehicles.

Most equipment that are mounted on vehicles have natural frequencies around $f_n = 10\,\text{Hz}$, while the main natural frequencies of the vehicle are around $f_n = 1\,\text{Hz}$. So, we use Figure 14.8 to design the suspension of base excited equipment, and use the magnified chart shown in the Figure 14.9 to design vehicle suspensions.

The optimal design curve is the result of the following optimization strategy:

$$Minimize\ S_{\ddot{X}}\ with\ respect\ to\ S_Z \qquad (14.78)$$

which states that the minimum absolute acceleration with respect to the relative displacement, if there is any, makes a suspension optimal. Mathematically it is equivalent to the following minimization problem:

$$\frac{\partial S_{\ddot{X}}}{\partial S_Z} = 0 \qquad (14.79)$$

$$\frac{\partial^2 S_{\ddot{X}}}{\partial S_Z^2} > 0 \qquad (14.80)$$

To determine the optimal stiffness $k$ and damping $c$, we start from an estimated value for $S_X$ on the horizontal axis and draw a vertical line to hit the optimal curve. The intersection point indicates the optimal $f_n$ and $\xi$ for the $S_X$, to have the best vibration isolation.

Figure 14.10 illustrates a sample application for $S_X = 1$, which indicates $\xi \approx 0.4$ and $f_n \approx 10\,\text{Hz}$ make the optimal suspension. $f_n$, $\xi$, and the mass of the equipment determine the optimal value of $k$ and $c$.

**Proof.** Let's define a working frequency range $0 < f < 20\,\text{Hz}$ to include almost all ground vehicles, especially road vehicles, and show the $RMS$ of $S_2$ and $G_2$ by

$$S_Z = RMS(S_2) \qquad (14.81)$$
$$S_{\ddot{X}} = RMS(G_2). \qquad (14.82)$$

In applied vehicle dynamics, we usually measure frequencies in $[\,\text{Hz}\,]$, instead of $[\,\text{rad}/\,\text{s}\,]$, so we perform design calculations based on cyclic frequencies $f$ and $f_n$ in $[\,\text{Hz}\,]$, and analytic calculations based on angular frequencies $\omega$ and $\omega_n$ in $[\,\text{rad}/\,\text{s}\,]$.

To calculate $S_Z$ and $S_{\ddot{X}}$ over the working frequency range

$$S_Z = \sqrt{\frac{1}{40\pi}\int_0^{40\pi} S_2^2 d\omega} \qquad (14.83)$$

$$S_{\ddot{X}} = \sqrt{\frac{1}{40\pi}\int_0^{40\pi} G_2 d\omega} \qquad (14.84)$$

we first find integrals of $S_2^2$ and $G_2$.

$$\int S_2^2 d\omega = Z_1\omega - \frac{Z_2}{Z_3\sqrt{Z_4}}\tan^{-1}\frac{\omega}{\sqrt{Z_4}} + \frac{Z_5}{Z_6\sqrt{Z_7}}\tan^{-1}\frac{\omega}{\sqrt{Z_7}} \qquad (14.85)$$
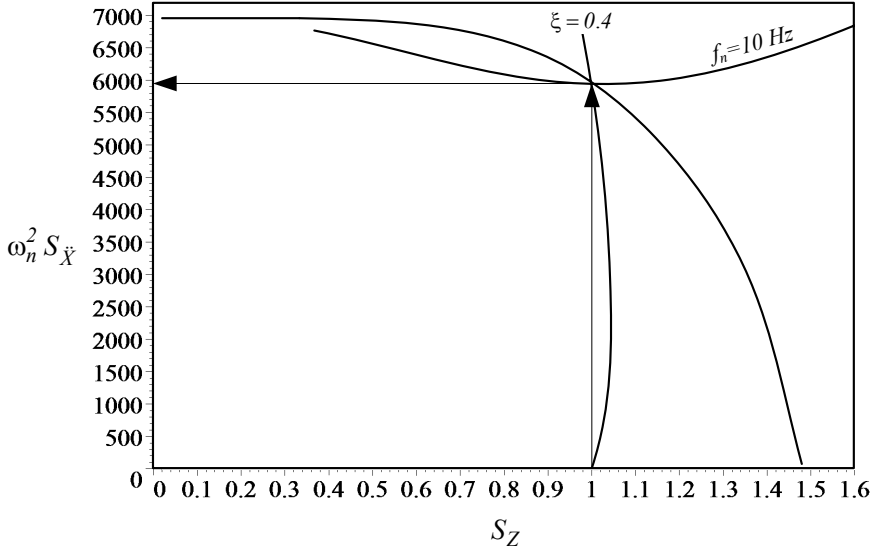
FIGURE 14.10. Application of the design chart for $S_X = 1$, that indicates the optimal values $\xi \approx 0.4$ and $f_n \approx 10\,\text{Hz}$.

$$\omega_n^4 \int G_2 d\omega = Z_8\omega + \frac{1}{3}Z_9\omega^3 + \frac{Z_{10}}{Z_{11}\sqrt{Z_{12}}}\tan^{-1}\frac{\omega}{\sqrt{Z_{12}}}$$
$$+ \frac{Z_{13}}{Z_{14}\sqrt{Z_{15}}}\tan^{-1}\frac{\omega}{\sqrt{Z_{15}}} \qquad (14.86)$$

The parameters $Z_1$ through $Z_{15}$ are as follows:

$$Z_1 = 1 \qquad (14.87)$$

$$Z_2 = \omega_n^2\left(8\xi^6 - 12\xi^4 + 4\xi^2 - \left(-8\xi^4 + 8\xi^2 - 1\right)\xi\sqrt{1-\xi^2}\right) \qquad (14.88)$$

$$Z_3 = -4\xi^2\left(1 - \xi^2\right) \qquad (14.89)$$

$$Z_4 = \omega_n^2\left(-1 + 2\xi^2 + 2\xi\sqrt{1-\xi^2}\right) \qquad (14.90)$$

$$Z_5 = \omega_n^2\left(8\xi^6 - 12\xi^4 + 4\xi^2 - \left(8\xi^4 - 8\xi^2 + 1\right)\xi\sqrt{1-\xi^2}\right) \qquad (14.91)$$

$$Z_6 = -4\xi^2\left(1 - \xi^2\right) \qquad (14.92)$$

$$Z_7 = \omega_n^2\left(-1 + 2\xi^2 - 2\xi\sqrt{1-\xi^2}\right) \qquad (14.93)$$

$$Z_8 = \omega_n^4 \left(-16\xi^4 + 8\xi^2 + 1\right) \tag{14.94}$$

$$Z_9 = 4\omega_n^2 \xi^2 \tag{14.95}$$

$$Z_{10} = \omega_n^6 \left(128\xi^{10} - 256\xi^8 + 144\xi^6 - 12\xi^4 - 4\xi^2\right) \tag{14.96}$$

$$-\omega_n^6 \left(-128\xi^8 + 192\xi^6 - 64\xi^4 - 4\xi^2 + 1\right)\xi\sqrt{1-\xi^2} \tag{14.97}$$

$$Z_{11} = -4\xi^2\left(1-\xi^2\right) \tag{14.98}$$

$$Z_{12} = \omega_n^2\left(-1 + 2\xi^2 + 2\xi\sqrt{1-\xi^2}\right) \tag{14.99}$$

$$Z_{13} = \omega_n^6 \left(128\xi^{10} - 256\xi^8 + 144\xi^6 - 12\xi^4 - 4\xi^2\right) \tag{14.100}$$

$$-\omega_n^6 \left(128\xi^8 - 192\xi^6 + 64\xi^4 + 4\xi^2 - 1\right)\xi\sqrt{1-\xi^2} \tag{14.101}$$

$$Z_{14} = -4\xi^2\left(1-\xi^2\right) \tag{14.102}$$

$$Z_{15} = \omega_n^2\left(-1 + 2\xi^2 - 2\xi\sqrt{1-\xi^2}\right) \tag{14.103}$$

Therefore, $S_Z$ and $S_{\ddot{X}}$ over the frequency range $0 < f < 20\,\mathrm{Hz}$ can be calculated analytically from Equations (14.83) and (14.84).

Equations (14.85) and (14.86) show that both $S_{\ddot{X}}$ and $S_Z$ are functions of only two variables $\omega_n$ and $\xi$.

$$S_{\ddot{X}} = S_{\ddot{X}}(\omega_n, \xi) \tag{14.104}$$

$$S_Z = S_Z(\omega_n, \xi) \tag{14.105}$$

Therefore, any pair of design parameters $(\omega_n, \xi)$ determines $S_{\ddot{X}}$ and $S_Z$ uniquely. It is also possible theoretically to define $\omega_n$ and $\xi$ as two functions of the variables $S_{\ddot{X}}$ and $S_Z$.

$$\omega_n = \omega_n(S_{\ddot{X}}, S_Z) \tag{14.106}$$

$$\xi = \xi(S_{\ddot{X}}, S_Z) \tag{14.107}$$

So, we would be able to determine the required $\omega_n$ and $\xi$ for a specific value of $S_{\ddot{X}}$ and $S_Z$.

Using Equations (14.104) and (14.105), we may draw Figure 14.11 to illustrate how $S_{\ddot{X}}$ behaves with respect to $S_Z$ when $f_n$ and $\xi$ vary. Keeping $f_n$ constant and varying $\xi$, it is possible to minimize $S_{\ddot{X}}$ with respect to $S_Z$. The minimum points make the optimal curve and determine the best $f_n$ and $\xi$. The key to use the optimal design curve is to adjust, determine, or estimate a value for $S_Z$ or $S_{\ddot{X}}$ and find the associated point on the design curve.

To justify the optimization principle (14.78), we plot $\omega_n^2 S_{\ddot{X}}/S_Z$ versus $f_n$ in Figure 14.12 for different values of $\xi$. It shows that increasing either one
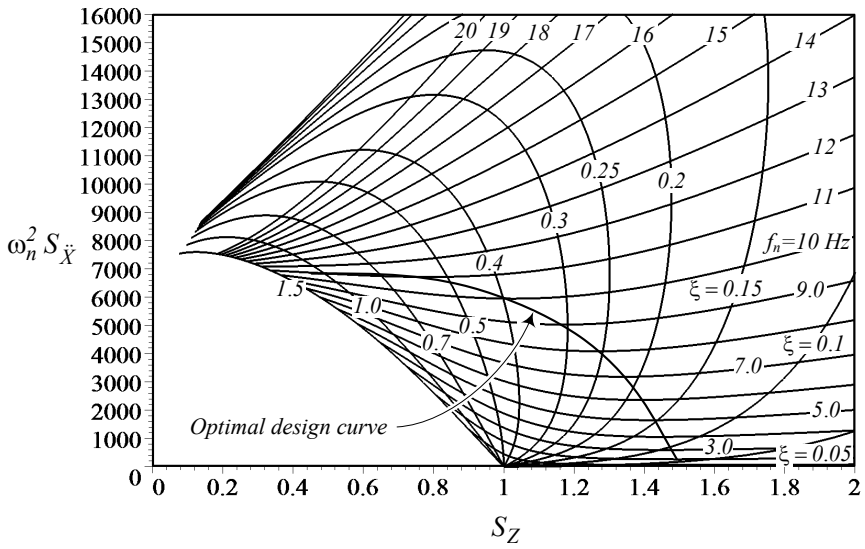
FIGURE 14.11. Behavior of $S_{\ddot{X}}$ with respect to $S_Z$ when $f_n$ and $\xi$ are varied.
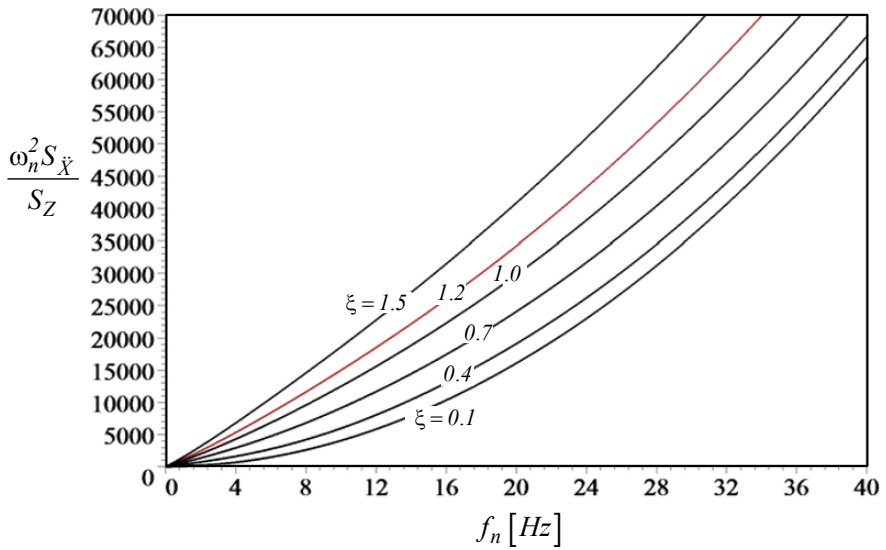


FIGURE 14.12. A plot of ratio $\omega_n^2 S_{\ddot{X}}/S_Z$ versus $f_n$ for different values of $\xi$.

of $\xi$ or $f_n$ increases the value of $\omega_n^2 S_{\ddot{X}}/S_Z$. It is equivalent to making the suspension more rigid, which causes an increase in acceleration or decrease in relative displacement. On the contrary, decreasing $\xi$ or $f_n$ decreases the value of $\omega_n^2 S_{\ddot{X}}/S_Z$, which is equivalent to making the suspension softer.

Softening of a suspension decreases the body acceleration, however it requires a large room for relative displacement. Due to physical constraints the wheel travel is limited and hence, we must design the suspension to use the available suspension travel as much as possible, and decrease the body acceleration as low as possible. Mathematically it is equivalent to (14.79) and (14.80). ■

**Example 505** *Wheel travel calculation.*

*Figure 14.13(a) illustrates a double A-arm suspension mechanism at its equilibrium position. To limit the motion of the wheel with respect to the body, two stoppers must be employed. There are many possible options for the type and position of stoppers. Most stoppers are made of stiff rubber balls and mounted somewhere on the body or suspension mechanism or both. It is also possible that the damper acts as a stopper. Figure 14.13(a) shows an example.*

*The gap sizes $\delta_u$ and $\delta_l$ indicate the upper and lower distances that a mechanism can move. However, the maximum motion of the wheel must be calculated at the center of the wheel. So, we transfer $\delta_u$ and $\delta_l$ to the center of the wheel and show them by $d_u$ and $d_l$.*

$$d_u \approx \frac{b_u}{a_u}\delta_u \tag{14.108}$$

$$d_l \approx \frac{b_l}{a_l}\delta_l \tag{14.109}$$

*Figure 14.13(b) and (c) show the mechanism at the upper and lower limits respectively. The distance $d_u$ is called the **upper wheel travel**, and $d_l$ is called the **lower wheel travel**. The upper wheel travel is important in ride comfort and the lower wheel travel is important for safety. To have better ride comfort, the upper wheel travel should be as high as possible to make the suspension as soft as possible.*

*Although the upper and lower wheel travels may be different, for practical purposes, we may assume $d_l = d_u$ and design the suspension based on a unique wheel travel. Wheel travel is also called suspension travel, suspension room, and suspension clearance.*

**Example 506** *Soft and hard suspensions.*

*Consider two pieces of equipment, A and B, under a base excitation with an average amplitude $Y = 1\,\mathrm{cm} \approx 0.5\,\mathrm{in}$. Equipment A has a suspension travel $d_A = 1.2\,\mathrm{cm} \approx 0.6\,\mathrm{in}$ and equipment B has $d_B = 0.8\,\mathrm{cm} \approx 0.4\,\mathrm{in}$.*
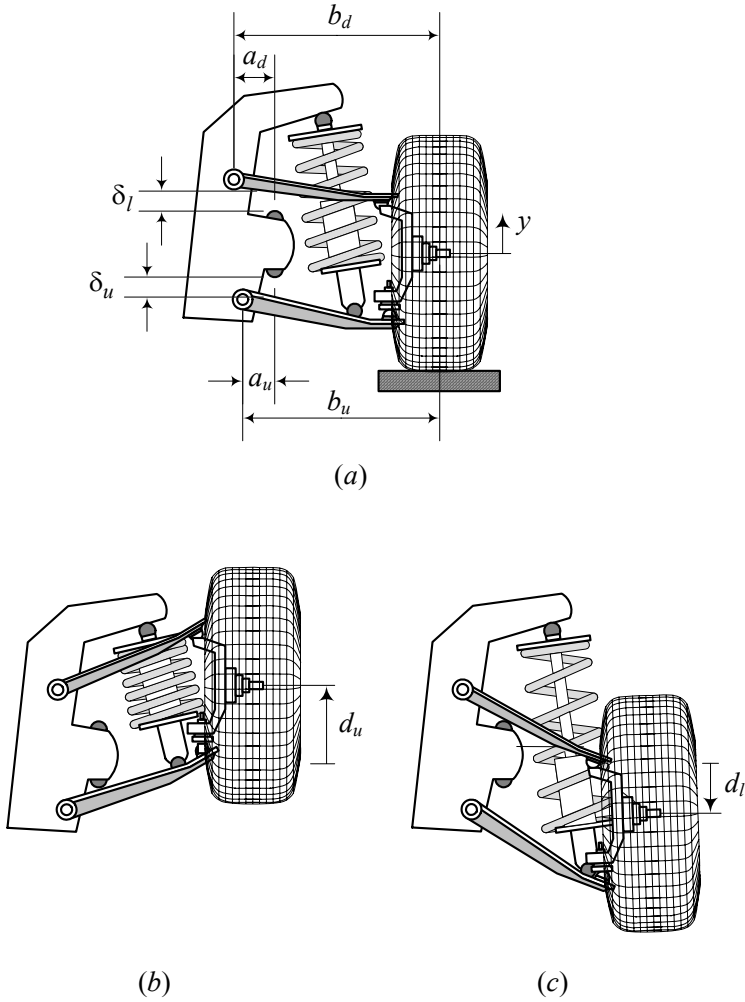
FIGURE 14.13. A double A-arm suspension mechanism at (a)- equilibrium, (b)-upper limit, and (c)- lower limit.
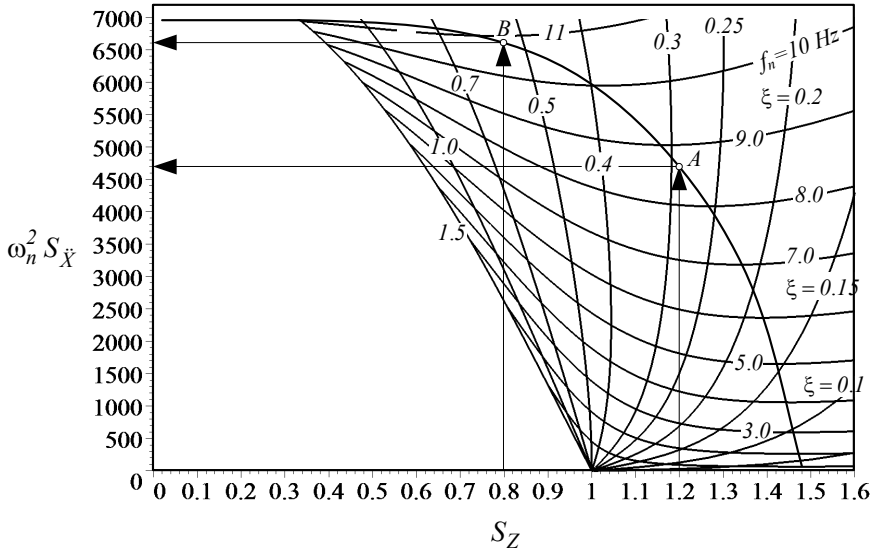
FIGURE 14.14. Comparing two suspensions $A$ and $B$ with $S_{Z_A} = 1.2$ and $S_{Z_B} = 0.8$.

Let's assume $S_Z = d_u/Y$. Therefore,

$$S_{Z_A} = 1.2 \tag{14.110}$$
$$S_{Z_B} = 0.8. \tag{14.111}$$

Using the design chart in Figure 14.14, the optimal suspensions for $A$ and $B$ are

$$f_{n_A} \approx 8.53\,\mathrm{Hz} \tag{14.112}$$
$$\xi_A \approx 0.29 \tag{14.113}$$
$$f_{n_B} \approx 10.8\,\mathrm{Hz} \tag{14.114}$$
$$\xi_B \approx 0.56. \tag{14.115}$$

Assuming a mass $m$

$$m = 300\,\mathrm{kg} \approx 660\,\mathrm{lb} \tag{14.116}$$

we calculate the optimal spring and dampers as follows:

$$k_A = (2\pi f_{n_A})^2\, m = 8.6175 \times 10^5\,\mathrm{N/m} \tag{14.117}$$
$$k_B = (2\pi f_{n_B})^2\, m = 13.814 \times 10^5\,\mathrm{N/m} \tag{14.118}$$

$$c_A = 2\xi_A\sqrt{k_A m} = 9325.7\,\mathrm{N\,s/m} \tag{14.119}$$
$$c_B = 2\xi_B\sqrt{k_B m} = 22800\,\mathrm{N\,s/m} \tag{14.120}$$
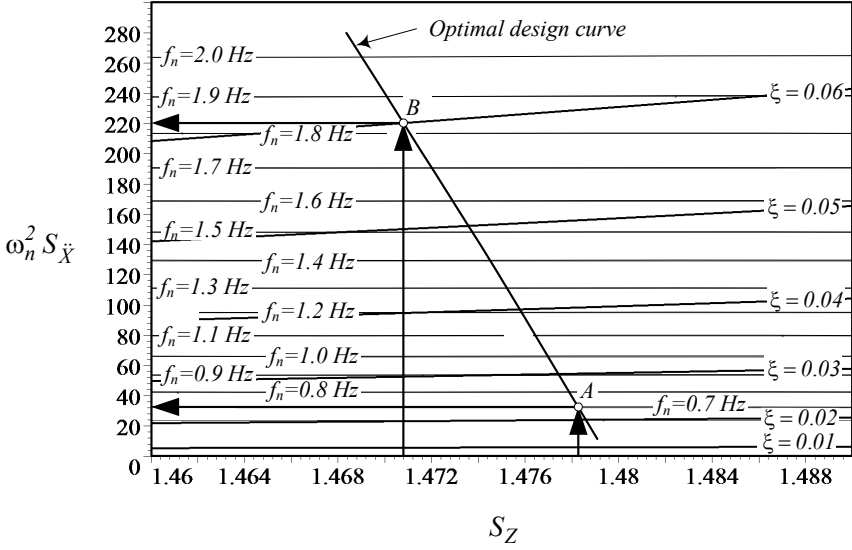
FIGURE 14.15. Comparing two suspensions, $A$ and $B$, with $S_{Z_A} = 1.4772$ and $S_{Z_B} = 1.4714$.

*Equipment B has a harder suspension compared to equipment A. This is because equipment B has less suspension travel, and hence, it has more acceleration level $\omega_n^2 S_{\ddot{X}}$. Figure 14.14 shows that*

$$\omega_n^2 S_{\ddot{X}_A} \approx 4700 \quad 1/\mathrm{s}^2 \tag{14.121}$$
$$\omega_n^2 S_{\ddot{X}_B} \approx 6650 \quad 1/\mathrm{s}^2. \tag{14.122}$$

**Example 507** *Soft and hard vehicle suspensions.*

*Consider two vehicles A and B that are moving on a bumpy road with an average amplitude $Y = 10\,\mathrm{cm} \approx 3.937\,\mathrm{in}$. Vehicle A has a suspension travel $d_A = 14.772\,\mathrm{cm} \approx 5.816\,\mathrm{in}$ and vehicle B has $d_B = 14.714\,\mathrm{cm} \approx 5.793\,\mathrm{in}$. Let's assume $S_Z = d_u/Y$. Therefore,*

$$S_{Z_A} = 1.4772 \tag{14.123}$$
$$S_{Z_B} = 1.4714. \tag{14.124}$$

*Using design chart 14.15, the optimal suspensions for vehicles A and B are:*

$$f_{n_A} \approx 0.7\,\mathrm{Hz} \tag{14.125}$$
$$\xi_A \approx 0.023 \tag{14.126}$$
$$f_{n_B} \approx 1.85\,\mathrm{Hz} \tag{14.127}$$
$$\xi_B \approx 0.06. \tag{14.128}$$

*Assuming a mass m*

$$m = 300\,\text{kg} \approx 660\,\text{lb} \tag{14.129}$$

*we calculate the optimal spring and dampers as follows:*

$$k_A = (2\pi f_{n_A})^2\, m \approx 5803\,\text{N}/\text{m} \tag{14.130}$$
$$k_B = (2\pi f_{n_B})^2\, m \approx 40534\,\text{N}/\text{m} \tag{14.131}$$

$$c_A = 2\xi_A \sqrt{k_A m} \approx 60.7\,\text{N}\,\text{s}/\text{m} \tag{14.132}$$
$$c_B = 2\xi_B \sqrt{k_B m} \approx 418.5\,\text{N}\,\text{s}/\text{m} \tag{14.133}$$

*These are equivalent dampers and springs at the center of the wheel. The actual value of the suspension parameters depends on the geometry of the suspension mechanism and installment of the spring and damper. Because $k_B > k_A$ and $c_B > c_A$, suspension of vehicle B is harder than that of vehicle A. This is because vehicle B has less wheel travel, and hence, it has more acceleration level $\omega_n^2 S_{\ddot{X}}$. Figure 14.15 shows that*

$$\omega_n^2 S_{\ddot{X}_B} \approx 220 \quad 1/\text{s}^2 \tag{14.134}$$
$$\omega_n^2 S_{\ddot{X}_A} \approx 28 \quad 1/\text{s}^2. \tag{14.135}$$

**Example 508** *Average vehicle suspension design.*
   *Most street cars with good ride comfort have a natural frequency equal or less than one Hertz. Optimal suspension characteristics of such a car are*

$$f_n \approx 1\,\text{Hz} \tag{14.136}$$
$$\xi \approx 0.028 \tag{14.137}$$
$$S_Z \approx 1.47644 \tag{14.138}$$
$$\omega_n^2 S_{\ddot{X}_B} \approx 66 \quad 1/\text{s}^2 \tag{14.139}$$

*and therefore,*

$$k = (2\pi f_n)^2\, m \approx 4\pi^2 m \tag{14.140}$$
$$c = 2\xi\sqrt{km} = 4\pi\xi m \approx 0.112\pi m. \tag{14.141}$$

*Both $k$ and $c$ are proportional to the mass of the car, $m$. So, as a good estimate, we may use Figures 14.16 and 14.17 to design a car suspension.*
   *For example, the optimal $k$ and $c$ for a car with $m = 250\,\text{kg}$ and $f_n = 1\,\text{Hz}$ are*

$$k = 9869.6\,\text{N}/\text{m} \tag{14.142}$$
$$c = 87.96\,\text{N}\,\text{s}/\text{m}. \tag{14.143}$$
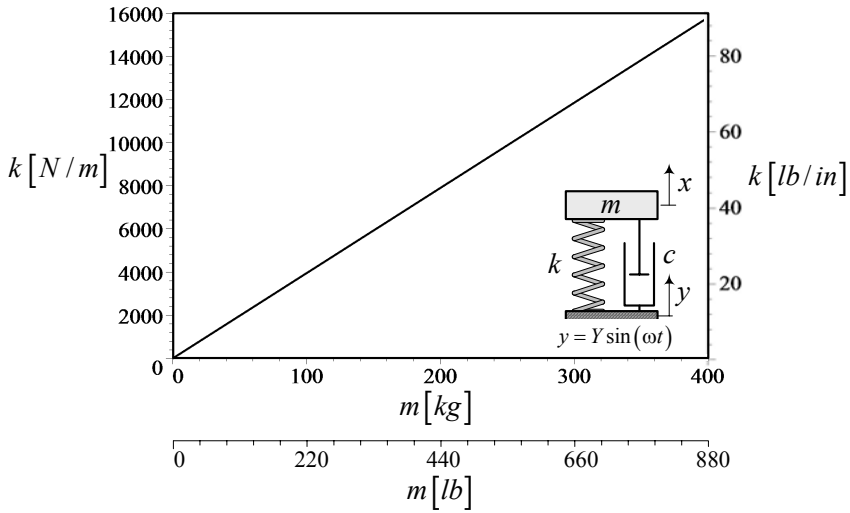
FIGURE 14.16. Optimal $k$ as a function of $m$ for a car with $f_n = 1\,\mathrm{Hz}$.
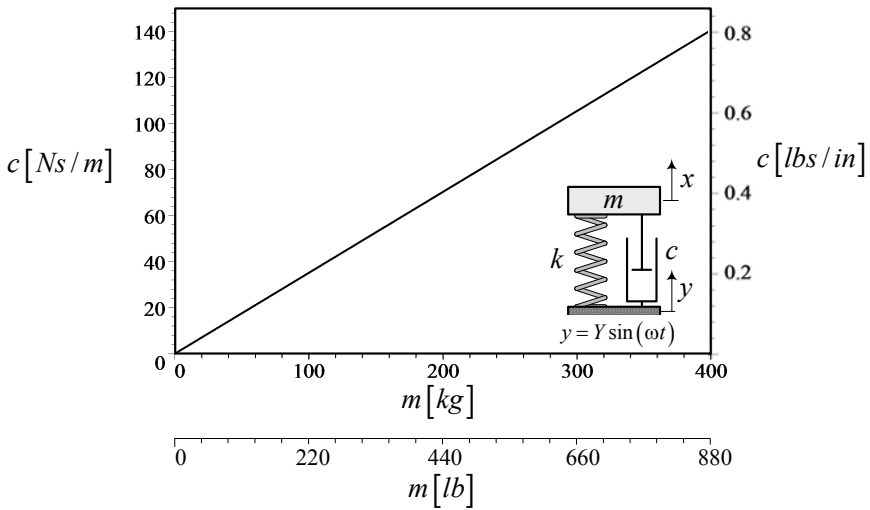


FIGURE 14.17. Optimal $c$ as a function of $m$ for a car with $f_n = 1\,\mathrm{Hz}$.
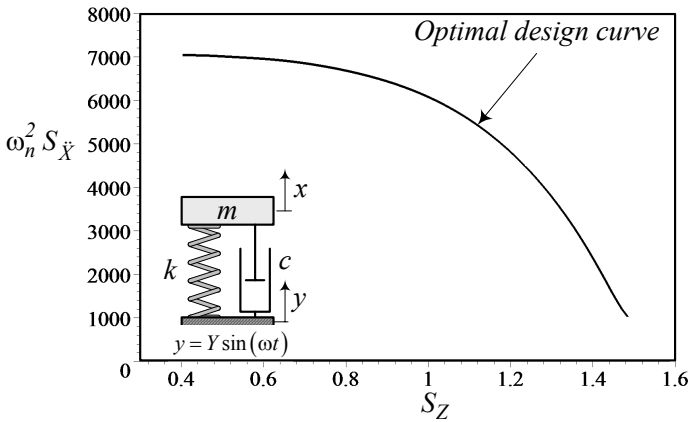
FIGURE 14.18. The optimal design curve in plane $(S_{\ddot{X}}, S_Z)$.

**Example 509** *Graphical representation of optimal characteristics.*

To visualize how the optimal parameters vary with respect to each other, we draw them in different coordinates. Figure 14.18 illustrates the optimal curve in plane $(S_{\ddot{X}}, S_Z)$. Figure 14.19 shows the optimal $f_n$ and $\xi$ versus $S_Z$, and Figure 14.20 shows the optimal $f_n$ and $\xi$ versus each other. The optimal $\xi$ increases slightly with $f_n$ for $f_n \lesssim 10\,\mathrm{Hz}$ and it increases rapidly for $f_n \gtrsim 10\,\mathrm{Hz}$. So, as a general rule, when we change the spring of an optimal suspension with a harder spring, the damper should also be changed for a harder one.

**Example 510** *Examination of the optimization of the design curve.*

To examine the optimal design curve and compare practical ways to make a suspension optimal, we assume that there is equipment with an off-optimal suspension, indicated by point $P_1$ in Figure 14.21.

$$f_n = 10\,\mathrm{Hz} \tag{14.144}$$
$$\xi = 0.15 \tag{14.145}$$

To optimize the suspension practically, we may keep the stiffness constant and change the damper to a corresponding optimal value, or keep the damping constant and change the stiffness to a corresponding optimal value. However, if it is possible, we may change both the stiffness and damping to a point on the optimal curve depending on the physical constraints and requirements.

Point $P_2$ in Figure 14.21 has the same $f_n$ as point $P_1$ with an optimal damping ratio $\xi \approx 0.4$. Point $P_3$ in Figure 14.21 has the same $\xi$ as point $p_1$ with an optimal natural frequency $f_n \approx 5\,\mathrm{Hz}$. Hence, points $P_2$ and $P_3$ are two alternative optimal designs for the off-optimal point $P_1$.
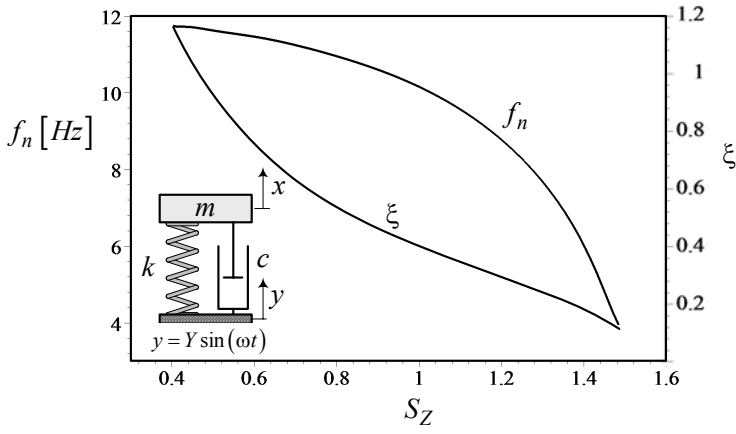
FIGURE 14.19. The optimal $f_n$ and $\xi$ versus $S_Z$.
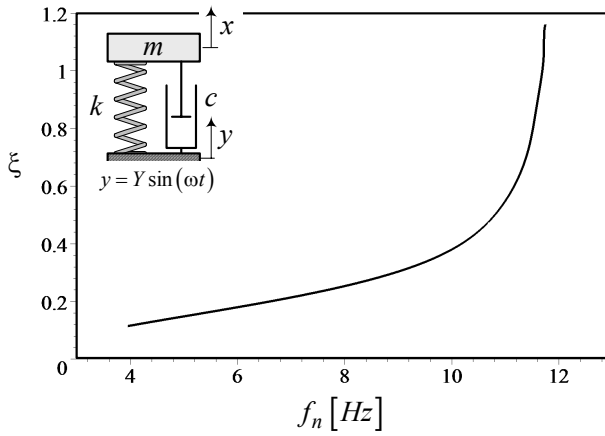


FIGURE 14.20. The optimal $\xi$ versus optimal $f_n$.
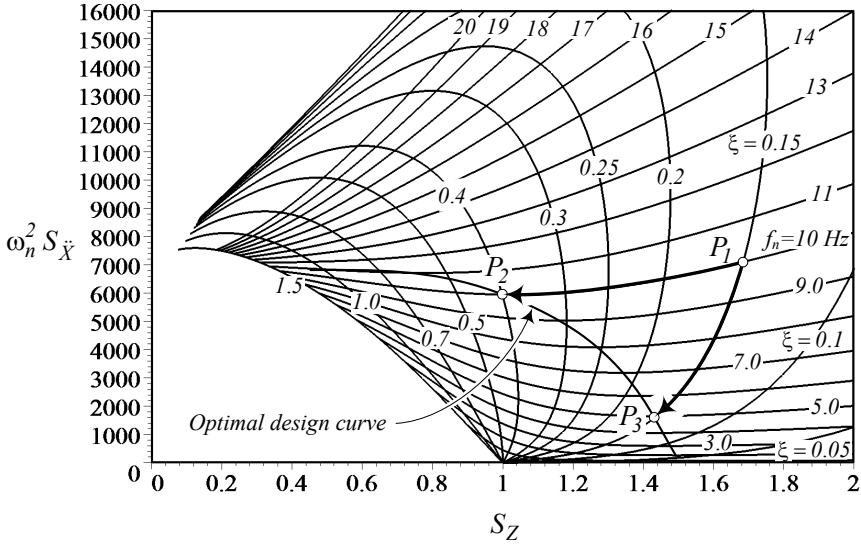
FIGURE 14.21. Two alternative optimal designs at points $P_2$ and $P_3$ for an off-optimal design at point $P_1$.

*Figure 14.22 compares the acceleration frequency response $G_2$ for the three points $P_1$, $P_2$, and $P_3$. Point $P_3$ has the minimum acceleration frequency response. Figure 14.23 depicts the absolute displacement frequency response $G_0$ and Figure 14.24 compares the relative displacement frequency response $S_2$ for points $P_1$, $P_2$, and $P_3$. These Figure show that both points $P_2$ and $P_3$ introduce better suspension than point $P_1$. Suspension $P_2$ has a higher level of acceleration but needs less relative suspension travel. Suspension $P_3$ has a lower acceleration, however it needs more room for suspension travel.*

**Example 511** *Sensitivity of $S_{\ddot{X}}$ with respect to $S_Z$ on the optimal curve.*

*Because $S_{\ddot{X}}$ is minimum on the optimal curve, the sensitivity of acceleration RMS with respect to relative displacement RMS is minimum at any point on the optimal curve. Therefore, an optimal suspension has the least sensitivity to mass variation. If a suspension is optimized for one passenger, it is still near optimal when the number of passengers, and hence the body mass, is changed.*

**Example 512** *Application of the optimal chart.*

*Select a desired value for the relative displacement as a traveling space (or a desired value for the maximum absolute acceleration), and find the associated values for $\omega_n$ and $\xi$ at the intersection of the associated vertical (or horizontal) line with the optimal curve.*
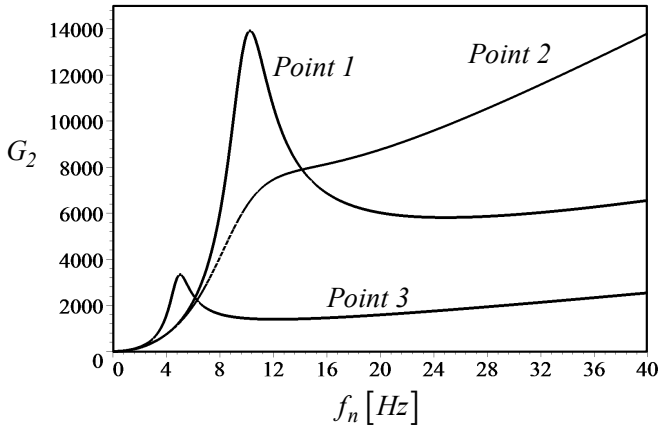
FIGURE 14.22. Acceleration frequency response $G_2$ for points $P_1$, $P_2$, and $P_3$ shown in Figure 14.21.
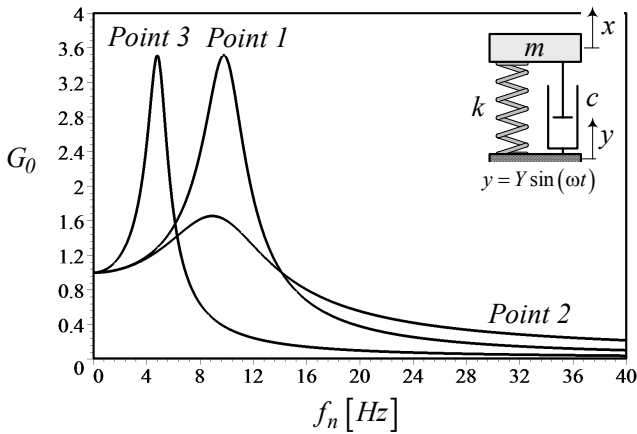


FIGURE 14.23. Absolute displacement frequency response $G_2$ for points $P_1$, $P_2$, and $P_3$ shown in Figure 14.21.
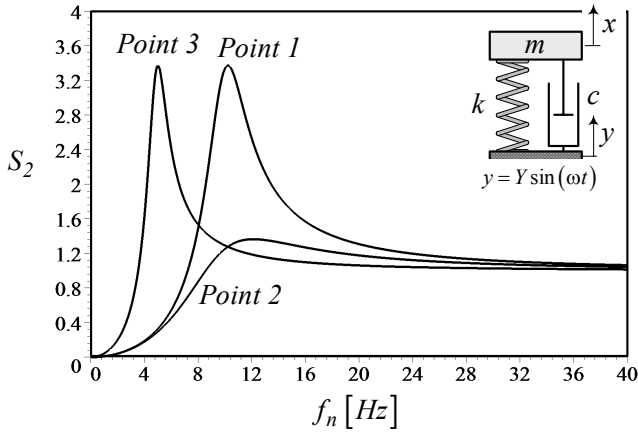
FIGURE 14.24. Relative displacement frequency response $S_2$ for points $P_1$, $P_2$, and $P_3$ shown in Figure 14.21.

**Example 513** ★ *Three-dimensional view of the optimal curve.*

Figure 14.25 illustrates a 3D view of $S_{\ddot{X}}$ for different $S_Z$ and $f_n$, to show the optimal curve in 3D.

Theoretically, we may show the surface by

$$S_{\ddot{X}} = S_{\ddot{X}}(S_Z, f_n) \tag{14.146}$$

and therefore, the optimal curve can be shown by the condition

$$\nabla S_{\ddot{X}} \cdot \hat{e}_{S_Z} = 0 \tag{14.147}$$

where $\hat{e}_{S_Z}$ is the unit vector along the $S_Z$-axis and $\nabla S_{\ddot{X}}$ is the gradient of the surface $S_{\ddot{X}}$.

**Example 514** ★ *Suspension trade-off and trivial optimization.*

Reduction of the absolute acceleration is the main goal in the optimization of suspensions, because it represents the transmitted force to the body. A vibration isolator reduces the absolute acceleration by increasing deflection of the isolator. The relative deflection is a measure of the clearance known as the **working space** of the isolator. The clearance should be minimized due to safety and the physical constraints in the mechanical design.

There is a trade-off between the acceleration and relative motion. The ratio of $\omega_n^4 S_{\ddot{X}}$ to $S_Z$ is a monotonically increasing function of $\omega_n$ and $\xi$. Keeping $S_Z$ constant increases $\omega_n^4 S_{\ddot{X}}$ by increasing both $\omega_n$ and $\xi$. However, keeping $\omega_n^4 S_{\ddot{X}}$ constant, decrease $S_Z$ by increasing $\omega_n$ and $\xi$. Hence, $\omega_n^4 S_{\ddot{X}}$ and $S_Z$ have opposite behaviors. These behaviors show that $\omega_n = 0$ and $\xi = 0$ are the trivial and non practical solutions for the best isolation.
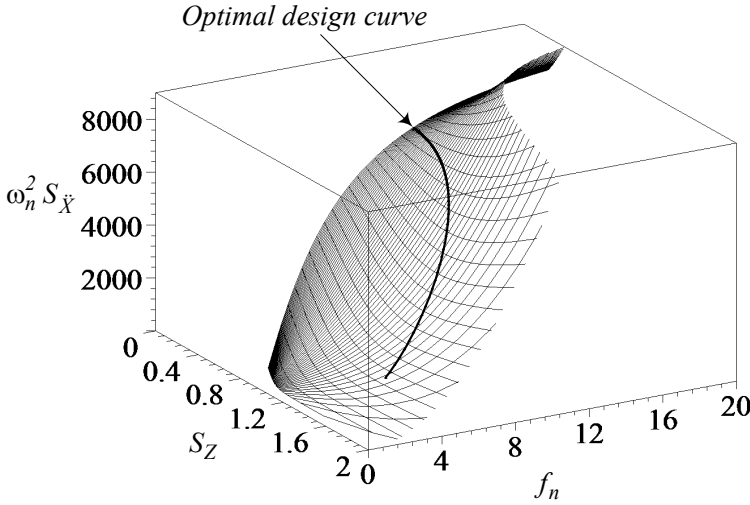
FIGURE 14.25. A three-dimensional view of $S_{\ddot{X}}$ for different $S_Z$ and $f_n$, to show the optimal curve.

**Example 515** ★ *Plot for RMS of absolute acceleration $RMS(G_2) = S_{\ddot{X}}$.*
  *Figures 14.26 and 14.27 illustrate the root mean square of absolute acceleration $RMS(G_2) = S_{\ddot{X}}$ graphically. In Figure 14.26, $S_{\ddot{X}}$ is plotted versus $\xi$ with $f_n$ as a parameter, and in Figure 14.27, $S_{\ddot{X}}$ is plotted versus $f_n$ with $\xi$ as a parameter.*

**Example 516** ★ *Plot for RMS of relative displacement $RMS(S_2) = S_Z$.*
  *Figures 14.28 and 14.29 illustrate the root mean square of relative displacement $RMS(S_2) = S_Z$. In Figure 14.28, $S_Z$ is plotted versus $\xi$ with $f_n$ as a parameter and in Figure 14.29, $S_Z$ is plotted versus $f_n$ with $\xi$ as a parameter.*

**Example 517** ★ $RMS(G_0) \equiv RMS(X/Y)$.
  *RMS of the absolute displacement, $S_X$, needs the integral of $G_0 \equiv (X/Y)^2$, which is determined as follows:*

$$\int G_0 d\omega = \frac{Z_{16}}{Z_{17}\sqrt{Z_{18}}} \tan^{-1} \frac{\omega}{\sqrt{Z_{18}}} + \frac{Z_{19}}{Z_{20}\sqrt{Z_{21}}} \tan^{-1} \frac{\omega}{\sqrt{Z_{21}}} \qquad (14.148)$$

$$Z_{16} = \omega_n^2 \left( -8\xi^6 + 8\xi^4 - \left( 8\xi^4 - 4\xi^2 - 1 \right) \xi \sqrt{1-\xi^2} \right) \quad (14.149)$$

$$Z_{17} = -4\xi^2 \left( 1 - \xi^2 \right) \qquad (14.150)$$

$$Z_{18} = \omega_n^2 \left( 1 - 2\xi^2 - 2\xi\sqrt{1-\xi^2} \right)$$
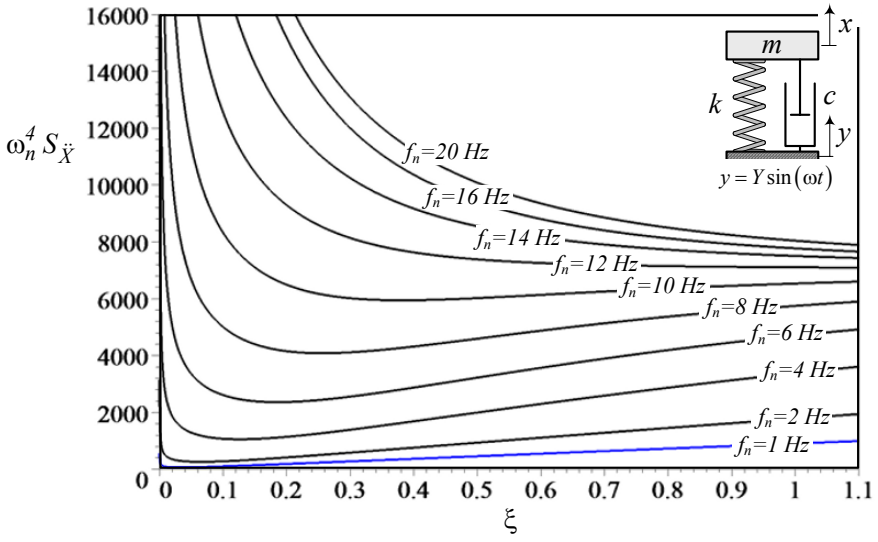
FIGURE 14.26. Plot of root mean square of absolute acceleration $RMS(S_3) = S_{\ddot{X}}$ versus $\xi$ with $f_n$ as a parameter.
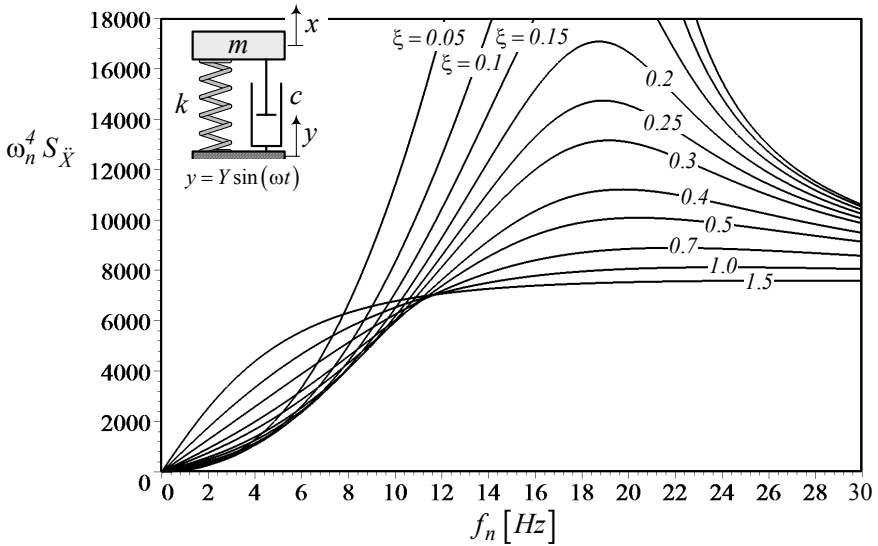


FIGURE 14.27. Plot of root mean square of absolute acceleration $RMS(S_3) = S_{\ddot{X}}$ versus $f_n$ with $\xi$ as a parameter.
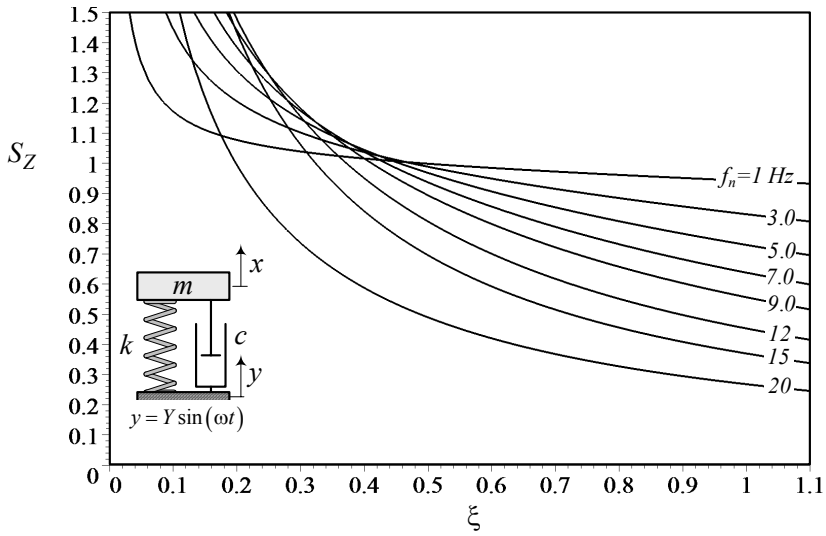
FIGURE 14.28. Plot of root mean square of relative displacement $RMS(S_2) = S_Z$ versus $\xi$ with $f_n$ as a parameter.
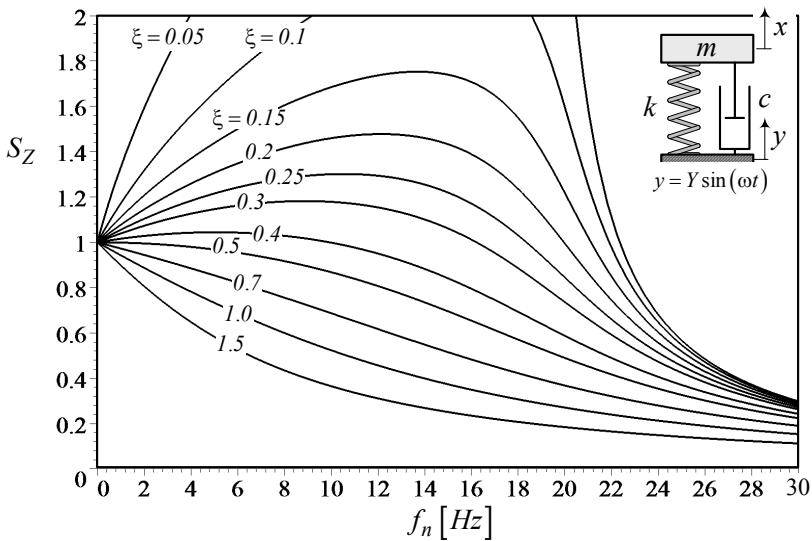


FIGURE 14.29. Plot of root mean square of relative displacement $RMS(S_2) = S_Z$ versus $f_n$ with $\xi$ as a parameter.
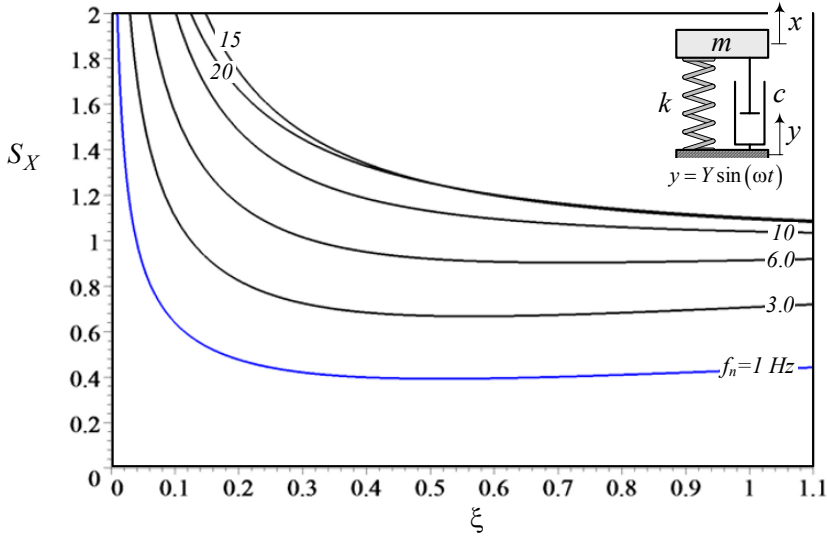
FIGURE 14.30. Plot of root mean square of absolute displacement $RMS(S_1) = S_X$ versus $\xi$ with $f_n$

$$Z_{19} = \omega_n^2 \left( 8\xi^6 - 8\xi^4 - \left( 8\xi^4 - 4\xi^2 - 1 \right) \xi \sqrt{1 - \xi^2} \right) \quad (14.151)$$

$$Z_{20} = Z_{17} = -4\xi^2 \left( 1 - \xi^2 \right) \quad (14.152)$$

$$Z_{21} = -\omega_n^2 \left( 1 - 2\xi^2 - 2\xi \sqrt{1 - \xi^2} \right) \quad (14.153)$$

*Now the RMS of absolute displacement $S_X$ can be determined analytically. Figures 14.30 and 14.31 illustrate the root mean square of relative displacement $RMS(G_0) = S_X$. In Figure 14.30, $S_X$ is plotted versus $\xi$ with $f_n$ as a parameter and in Figure 14.31, $S_X$ is plotted versus $f_n$ with $\xi$ as a parameter.*

**Example 518 ★** *Plot of $RMS(G_2) = S_{\ddot{X}}$ versus $RMS(S_2) = S_Z$.*

*Figures 14.32 and 14.33 show $RMS(G_2) = S_{\ddot{X}}$ versus $RMS(S_2) = S_Z$ graphically. In Figure 14.32, $\omega_n^2 S_{\ddot{X}}$ is plotted for constant natural frequencies $f_n$, and in Figure 14.33 for constant $\xi$. Some of the curves in Figure 14.32 have a minimum, which shows that we may minimize $S_{\ddot{X}}$ versus $S_Z$ for constant $f_n$. Such a minimum is the goal of optimization.*

*Figure 14.33 shows that there is a maximum on some of the constant $\xi$ curves. These maximums indicate the worst suspension design.*

*Figure 14.34 illustrates the behavior of $S_{\ddot{X}}$, instead of $\omega_n^2 S_{\ddot{X}}$, versus $S_Z$. The minimum point on each curve occurs at the same $S_Z$ as in Figure 14.32.*
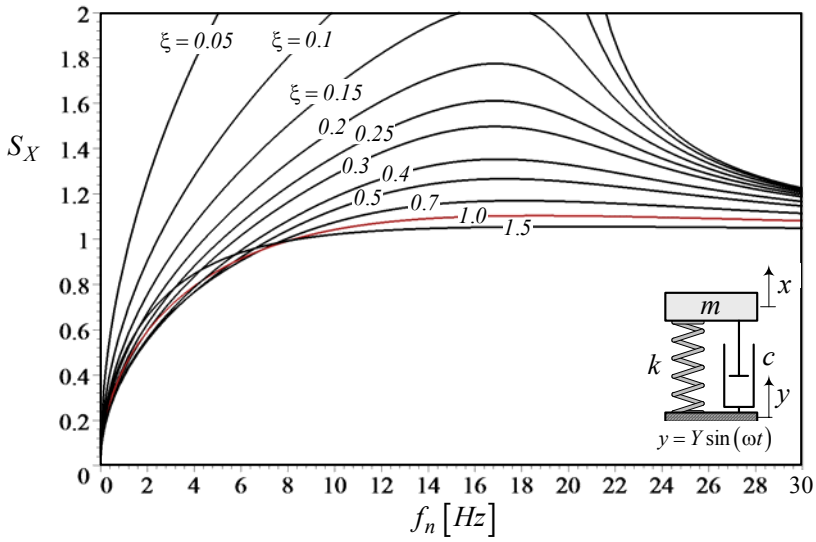
FIGURE 14.31. Plot of root mean square of absolute displacement $RMS(S_1) = S_X$ versus $f_n$ with $\xi$ as a parameter.
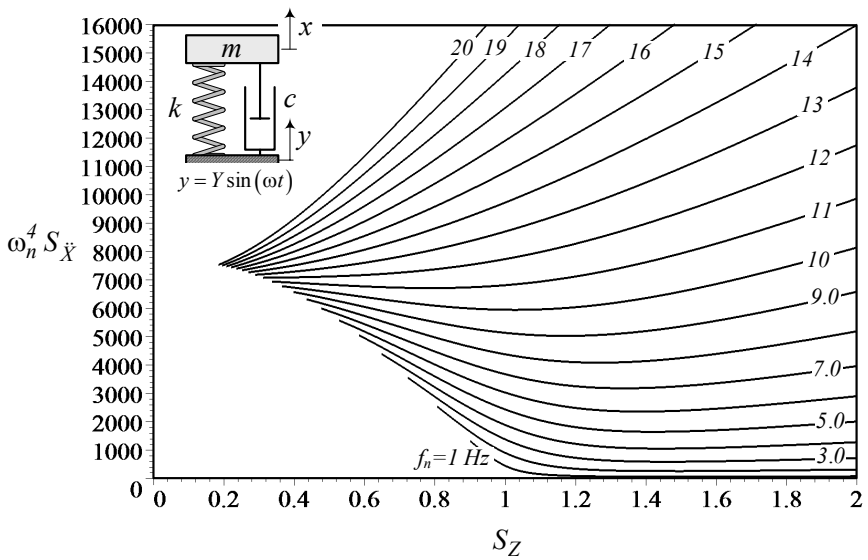


FIGURE 14.32. Plot of $\omega_n^2 RMS(G_2) = \omega_n^2 S_{\ddot{X}}$ versus $RMS(S_2) = S_Z$ for constant natural frequencies $f_n$.
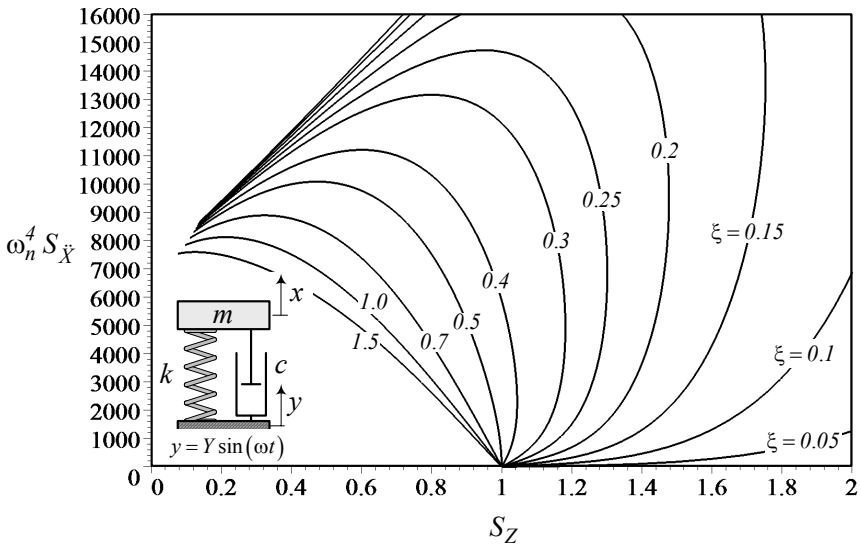
FIGURE 14.33. Plot of $\omega_n^2 RMS(G_2) = \omega_n^2 S_{\ddot{X}}$ versus $RMS(S_2) = S_Z$ for constant damping ratio $\xi$.
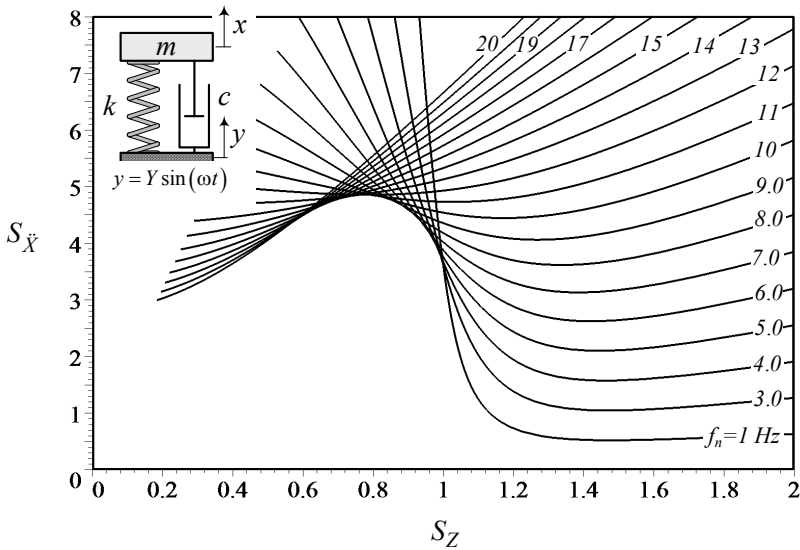


FIGURE 14.34. Plot of $RMS(G_2) = S_{\ddot{X}}$ versus $RMS(S_2) = S_Z$ for constant natural frequencies $f_n$.

**Example 519 ★** *Alternative optimization methods.*

There are various approaches and suggested methods for vibration isolator optimization, depending on the application. However, there is not a universally accepted method applicable to every application. Every optimization strategy can be transformed to a minimization of a function called the **cost function**. Considerable attention has been given to minimization of the absolute displacement, known as the **main transmissibility**. However, for a vibration isolator, the cost function may include any state variables such as absolute and relative displacements, velocities, accelerations, and even jerks.

Constraints may determine the domain of acceptable design parameters by dictating an upper and lower limit for $\omega_n$ and $\xi$. For vehicle suspension, it is generally desired to select $\omega_n$ and $\xi$ such that the absolute acceleration of the system is minimized and the relative displacement does not exceed a prescribed level. The most common optimization strategies are as follow:

**Minimax absolute acceleration** $S_{\ddot{X}}$ **for specified relative displacement** $S_{Z_0}$. Specify the allowable relative displacement, and then find the minimax of absolute acceleration

$$\frac{\partial S_{\ddot{X}}}{\partial \omega_n} = 0 \tag{14.154}$$

$$\frac{\partial S_{\ddot{X}}}{\partial \xi} = 0 \tag{14.155}$$

$$S_Z = S_{Z_0}. \tag{14.156}$$

**Minimax relative displacement** $S_Z$ **for specified absolute acceleration** $S_{\ddot{X}_0}$. Specify the allowable absolute acceleration, and then find the minimax relative displacement.

$$\frac{\partial S_Z}{\partial \omega_n} = 0 \tag{14.157}$$

$$\frac{\partial S_Z}{\partial \xi} = 0 \tag{14.158}$$

$$S_{\ddot{X}} = S_{\ddot{X}_0}. \tag{14.159}$$

**Example 520 ★** *More application of the design chart.*

The optimization criterion

$$\frac{\partial S_{\ddot{X}}}{\partial S_Z} = 0 \tag{14.160}$$

$$\frac{\partial^2 S_{\ddot{X}}}{\partial S_Z^2} > 0 \tag{14.161}$$

is based on the root mean square of $S_2$ and $G_2$ over a working frequency

*range.*

$$S_Z = \sqrt{\frac{1}{40\pi} \int_0^{40\pi} S_2^2 d\omega} \tag{14.162}$$

$$S_{\ddot{X}} = \sqrt{\frac{1}{40\pi} \int_0^{40\pi} G_2 d\omega} \tag{14.163}$$

*The optimal design curve is the optimal condition for suspension of a base excited system using the following functions:*

$$S_2 = \frac{Z_B}{Y}$$

$$G_2 = \frac{\ddot{X}_B}{\omega_n^2 Y}$$

*However, because*

$$S_2 = \frac{\ddot{X}_F}{F/m} = \frac{Z_B}{Y} = \frac{X_E}{e\varepsilon_E} = \frac{Z_R}{e\varepsilon_R} \tag{14.164}$$

$$G_2 = \frac{\ddot{X}_B}{\omega_n^2 Y} = \frac{F_{T_B}}{kY} = \frac{F_{T_E}}{e\omega^2 m_e} = \frac{F_{T_R}}{e\omega^2 m_e}\left(1 + \frac{m_a}{m}\right) \tag{14.165}$$

*the optimal design curve can also be expressed as a minimization condition for any other $G_2$-function with respect to any other $S_2$-function, such as transmitted force to the base $\frac{F_{T_E}}{e\omega^2 m_e}$ for an eccentric excited system $\frac{X_E}{e\varepsilon_E}$. This minimization is equivalent to the optimization of an engine mount.*

## 14.4   ★ Time Response Optimization

Transient response optimization depends on the type of transient excitation, as well as cost function definition. Figure 14.35 illustrates a 1/8 car model and a unit step displacement.

$$y = \begin{cases} 1 & t > 0 \\ 0 & t \leq 0 \end{cases} \tag{14.166}$$

If the transient excitation is a step function, and the optimization criteria is minimization of the peak value of acceleration versus peak value of relative displacement, then there is optimal $\xi^\star$ for any $f_n$ that provides the best transient behavior of a 1/8 car model. This behavior is shown in Figure 14.36.

$$\xi^\star = 0.4 \tag{14.167}$$
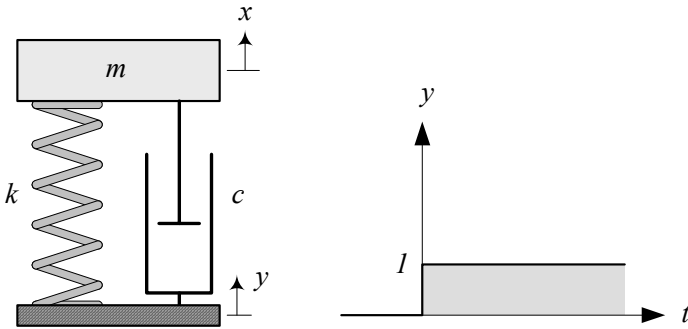
FIGURE 14.35. A 1/8 car model and a unit step displacement base excitation.
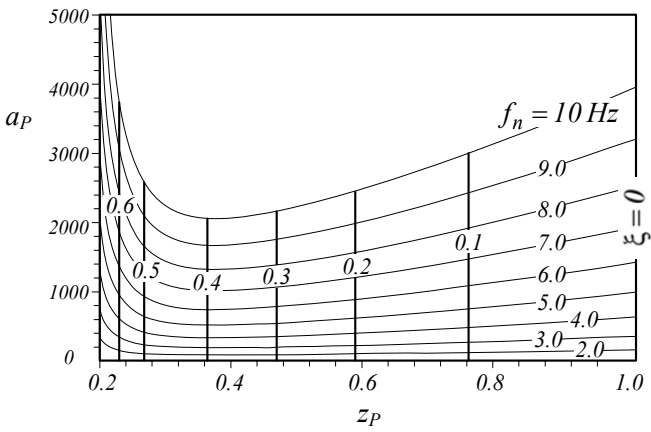


FIGURE 14.36. Peak value of acceleration versus peak value of relative displacement for different $\xi$ and $f_n$.

**Proof.** The equation of motion for the base excited *one*-DOF system shown in Figure 14.35, is

$$\ddot{x} + 2\xi\omega_n\,\dot{x} + \omega_n^2\,x = 2\xi\omega_n\,\dot{y} + \omega_n^2\,y \tag{14.168}$$

Substituting $y = 1$ in Equation (14.168) provides the following initial value problem to determine the absolute outplacement of the mass $m$:

$$\ddot{x} + 2\xi\omega_n\,\dot{x} + \omega_n^2\,x \;=\; \omega_n^2 \tag{14.169}$$
$$y(0) \;=\; 0 \tag{14.170}$$
$$\dot{y}(0) \;=\; 0 \tag{14.171}$$

Solution of the differential equation with zero initial conditions is

$$x = 1 - \frac{1}{2}\frac{A}{ib}e^{-A\omega_n t} + \frac{1}{2}\frac{\overline{A}}{ib}e^{-\overline{A}\omega_n t} \tag{14.172}$$

where $A$ and $\overline{A}$ are two complex conjugate numbers.

$$A \;=\; \xi + i\sqrt{1 - \xi^2} \tag{14.173}$$
$$\overline{A} \;=\; \xi - i\sqrt{1 - \xi^2} \tag{14.174}$$

Having $x$ and $y = 1$ are enough to calculate the relative displacement $z = x - y$.

$$z \;=\; x - y$$
$$\;=\; -\frac{1}{2}\frac{A}{ib}e^{-A\omega_n t} + \frac{1}{2}\frac{\overline{A}}{ib}e^{-\overline{A}\omega_n t} \tag{14.175}$$

The absolute velocity and acceleration of the mass $m$ can be obtained from equation (14.172).

$$\dot{x} \;=\; \frac{1}{2}\frac{A^2\omega_n}{ib}e^{-A\omega_n t} - \frac{1}{2}\frac{\overline{A}^2\omega_n}{ib}e^{-\overline{A}\omega_n t} \tag{14.176}$$
$$\ddot{x} \;=\; -\frac{1}{2}\frac{A^3\omega_n^2}{ib}e^{-A\omega_n t} + \frac{1}{2}\frac{\overline{A}^3\omega_n^2}{ib}e^{-\overline{A}\omega_n t} \tag{14.177}$$

The peak value of the relative displacement is

$$z_P = \exp\left(\frac{\cos^{-1}\left(2\xi^2 - 1\right)}{\omega_n\sqrt{1 - \xi^2}}\right) \tag{14.178}$$

which occurs when $\dot{z} = 0$ at time $t_1$

$$t_1 = \frac{-\xi\cos^{-1}\left(2\xi^2 - 1\right)}{\sqrt{1 - \xi^2}}. \tag{14.179}$$

The peak value of the absolute acceleration is

$$a_P = \omega_n^2 \exp\left(-\xi \frac{2\cos^{-1}\left(2\xi^2 - 1\right) - \pi}{\sqrt{1 - \xi^2}}\right) \tag{14.180}$$

which occurs at the beginning of the excitation, $t = 0$, or at the time instant when $\ddot{x} = 0$ at time $t_2$

$$t_2 = \frac{2\cos^{-1}\left(2\xi^2 - 1\right) - \pi}{\omega_n\sqrt{1 - \xi^2}}. \tag{14.181}$$

Figure 14.36 is a plot for $a_P$ versus $z_P$ for different $\xi$ and $f_n$. The minimum of the curves occur at $\xi = 0.4$ for every $f_n$. The optimal $\xi$ can be found analytically by finding the minimum point of $a_P$ versus $z_P$. The optimal $\xi$ is the solution of the transcendental equation

$$2\xi\cos^{-1}\left(2\xi^2 - 1\right) - \pi - 4\xi\sqrt{1 - \xi^2} = 0 \tag{14.182}$$

which is $\xi = 0.4$. The minimum peak value of the absolute acceleration with respect to relative displacement is independent of the value of natural frequency $f_n$. ∎

**Example 521 ★** *Optimal design curve and time response.*
    *To examine transient response of suspensions on the optimal design curve, we compare a base excited equipment having an off-optimal suspension, at point $P_1$, with optimal suspensions at points $P_2$ and $P_3$ in Figure 14.21. Point $P_1$ is at*

$$f_n \approx 10\,\text{Hz} \tag{14.183}$$
$$\xi \approx 0.15. \tag{14.184}$$

*Points $P_2$ and $P_3$ are two alternative optimizations for point $P_1$. Point $P_2$ has $\xi \approx 0.4$ with the same natural frequency as $P_1$ and point $P_2$ has $f_n \approx 5\,\text{Hz}$ with the same damping as point $P_1$.*
    *Figure 14.37 illustrates a base excited one-DOF system and a sine square bump input.*

$$y = \begin{cases} d_2\sin^2\dfrac{2\pi v}{d_1}t & 0 < t < 0.1 \\ 0 & t \le 0, t \ge 0.1 \end{cases} \tag{14.185}$$
$$d_2 = 0.05\,\text{m} \tag{14.186}$$
$$v = 10\,\text{m/s} \tag{14.187}$$
$$d_1 = 1\,\text{m} \tag{14.188}$$
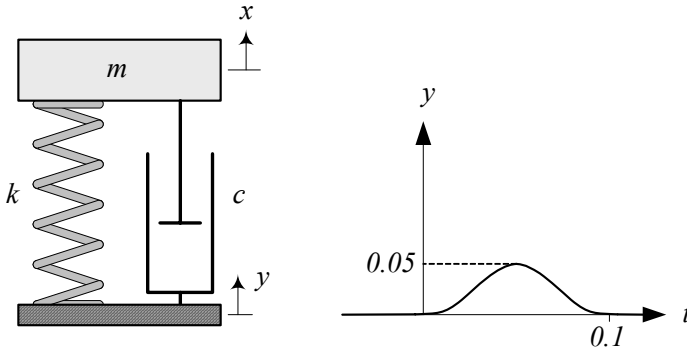
FIGURE 14.37. A base excited *one*-DOF system and a sine square bump input.
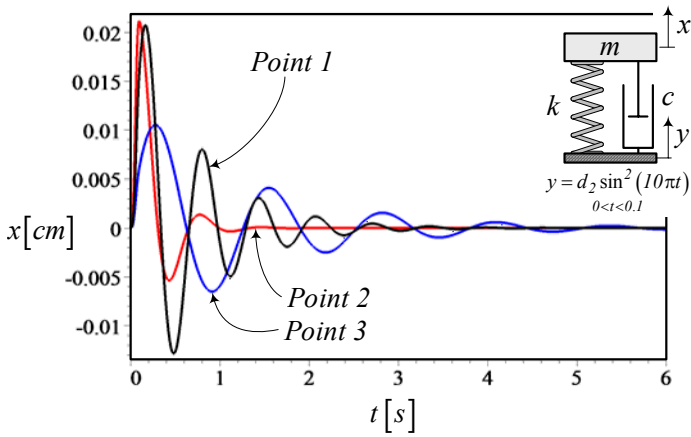


FIGURE 14.38. Absolute displacement time response of the system for three different suspensions.
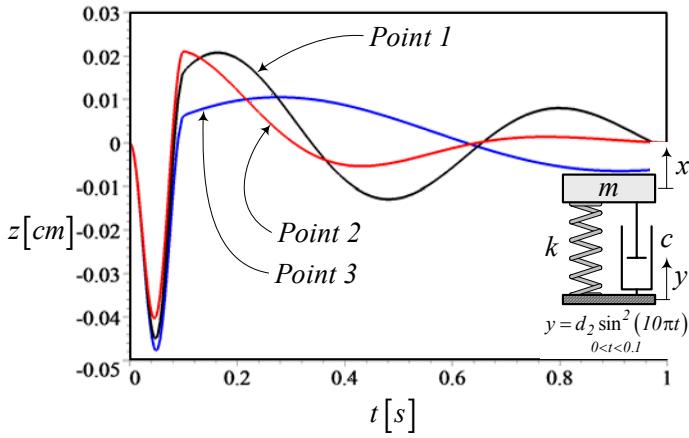
FIGURE 14.39. Relative displacement time response of the system for three different suspensions.
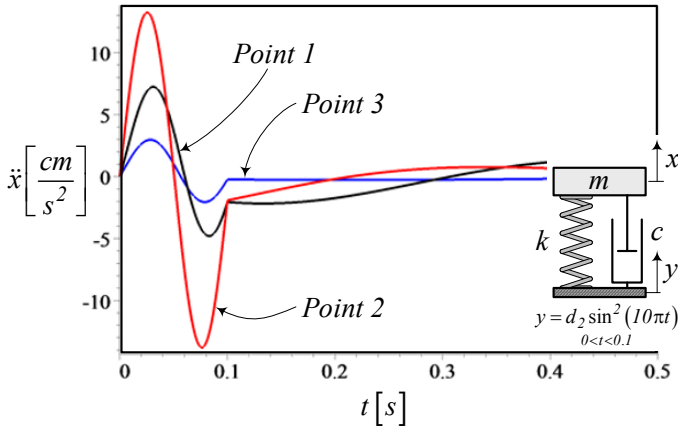


FIGURE 14.40. Absolute acceleration time response of the system for three different suspensions.

*The absolute and relative displacement time responses of the system at points 1, 2, and 3 are shown in Figures 14.38, and 14.39, respectively. The absolute acceleration of m is shown in Figure 14.40.*

*System 3 has a lower relative displacement peak value and a lower absolute acceleration peak value, but it takes more time to settle down.*

## 14.5    Summary

A *one*-DOF base excited system with the equation of motion

$$\ddot{x} + 2\xi\omega_n\,\dot{x} + \omega_n^2\,x = 2\xi\omega_n\,\dot{y} + \omega_n^2\,y \tag{14.189}$$

is an applied model for equipment mounted on a vibrating base, as well as a model for vertical vibration of vehicles. Assuming a variable excitation frequency, we may determine the relative displacement $S_2 = |Z/Y|$ and absolute acceleration $G_2 = \left|\ddot{X}/\left(Y\omega_n^2\right)\right|$ frequency responses to optimize the system. The optimization criterion is

$$\frac{\partial S_{\ddot{X}}}{\partial S_Z} = 0 \tag{14.190}$$

$$\frac{\partial^2 S_{\ddot{X}}}{\partial S_Z^2} > 0 \tag{14.191}$$

where $S_Z$ and $S_{\ddot{X}}$ are the root mean square of $S_2$ and $G_2$ over a working frequency range.

$$S_Z = \sqrt{\frac{1}{40\pi}\int_0^{40\pi} S_2^2 d\omega} \tag{14.192}$$

$$S_{\ddot{X}} = \sqrt{\frac{1}{40\pi}\int_0^{40\pi} G_2 d\omega} \tag{14.193}$$

The optimization criterion states that the minimum absolute acceleration RMS with respect to the relative displacement RMS, makes a suspension optimal. The result of optimization may be cast in a design chart to visualize the relationship of optimal $\xi$ and $\omega_n$.

# 14.6   Key Symbols

| | |
|---|---|
| $a, \ddot{x}$ | acceleration |
| $a, b$ | arm length of displaced spring |
| $c$ | damping |
| $c^{\star}$ | optimum damping |
| $c_{eq}$ | equivalent damping |
| $d_1$ | road wave length |
| $d_2$ | road wave amplitude |
| $D$ | dissipation function |
| $f, \mathbf{F}$ | force |
| $f = \frac{1}{T}$ | cyclic frequency $[\,\mathrm{Hz}\,]$ |
| $f_c$ | damper force |
| $f_k$ | spring force |
| $f_n$ | cyclic natural frequency $[\,\mathrm{Hz}\,]$ |
| $F$ | amplitude of a harmonic force $f$ |
| $g$ | gravitational acceleration |
| $G_0 = \left\vert X/Y \right\vert$ | absolute displacement frequency response |
| $G_2 = \left\vert \ddot{X}/Y\omega_n^2 \right\vert$ | absolute acceleration frequency response |
| $k$ | stiffness |
| $k^{\star}$ | optimum stiffness |
| $k_{eq}$ | equivalent stiffness |
| $K$ | kinetic energy |
| $\mathcal{L}$ | Lagrangean |
| $m$ | mass |
| $r = \frac{\omega}{\omega_n}$ | frequency ratio |
| $S_2 = \left\vert Z/Y \right\vert$ | relative displacement frequency response |
| $S_Z$ | RMS of $S_2$ |
| $S_{\ddot{X}}$ | RMS of $G_2$ |
| $t$ | time |
| $T$ | period |
| $v, \mathbf{v}, \dot{x}, \dot{\mathbf{x}}$ | velocity |
| $V$ | potential energy |
| $x$ | absolute displacement |
| $X$ | steady-state amplitude of $x$ |
| $y$ | base excitation displacement |
| $Y$ | steady-state amplitude of $y$ |
| $z$ | relative displacement |
| $Z$ | steady-state amplitude of $z$ |
| $Z_i$ | short notation parameter |
| | |
| $\alpha$ | tilted spring angle |
| $\delta$ | spring deflection |
| $\delta$ | displacement |

$\xi = \frac{c}{2\sqrt{km}}$     damping ratio

$\omega = 2\pi f$     angular frequency $[\,\mathrm{rad/s}\,]$

$\omega_n$     natural frequency

Subscript

$eq$     equivalent

$f$     front

$l$     low

$r$     rear

$s$     sprung

$u$     unsprung

$u$     up

# Exercises

1. Equivalent McPherson suspension parameters.

   Figure 14.41(a) illustrates a McPherson suspension. Its equivalent vibrating system is shown in Figure 14.41(b).



(a)                                    (b)
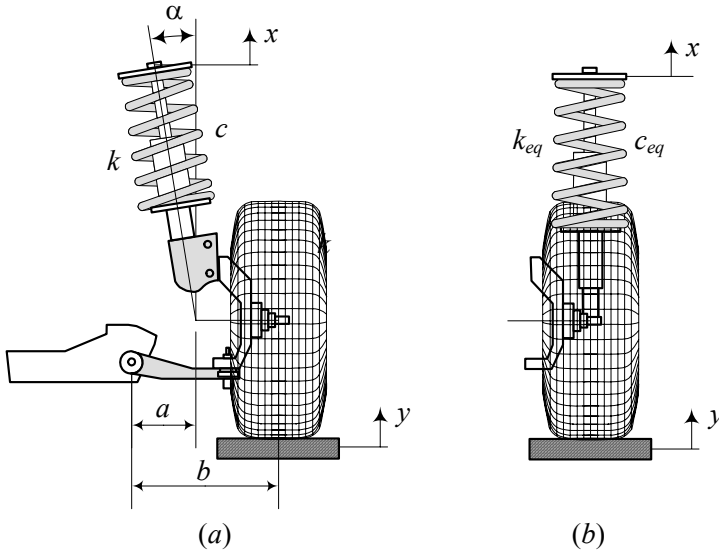
FIGURE 14.41. A McPherson suspension and its equivalent vibrating system.

(a) Determine $k_{eq}$ and $c_{eq}$ if

$$
\begin{aligned}
a &= 22\,\text{cm} \\
b &= 45\,\text{cm} \\
k &= 10000\,\text{N}/\text{m} \\
c &= 1000\,\text{N}\,\text{s}/\text{m} \\
\alpha &= 12\,\text{deg}\,.
\end{aligned}
$$

(b) Determine the stiffness $k$ such that the natural frequency of the vibrating system is $f_n = 1\,\text{Hz}$, if

$$
\begin{aligned}
a &= 22\,\text{cm} \\
b &= 45\,\text{cm} \\
m &= 1000/4\,\text{kg} \\
\alpha &= 12\,\text{deg}\,.
\end{aligned}
$$
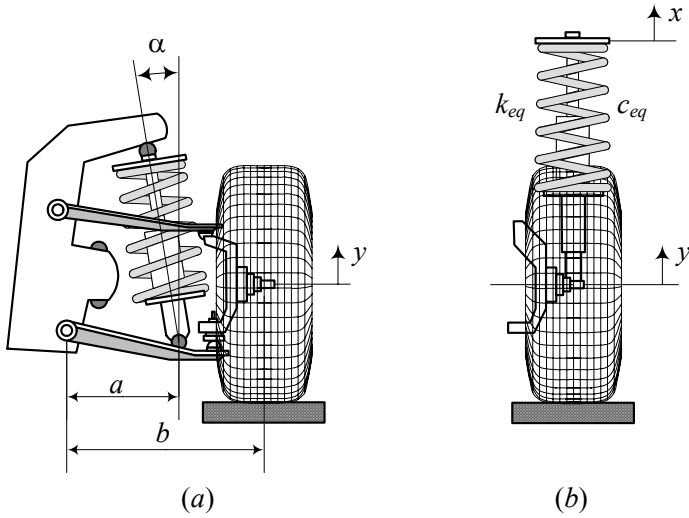
FIGURE 14.42. A double A-arm suspension and its equivalent vibrating system.

    (c) Determine the damping $c$ such that the damping ratio of the vibrating system is $\xi = 0.4$, if

$$
\begin{aligned}
a &= 22\,\text{cm} \\
b &= 45\,\text{cm} \\
m &= 1000/4\,\text{kg} \\
\alpha &= 12\,\text{deg} \\
f_n &= 1\,\text{Hz.}
\end{aligned}
$$

2. Equivalent double A-arm suspension parameters.

   Figure 14.42(a) illustrates a double A-arm suspension. Its equivalent vibrating system is shown in Figure 14.42(b).

    (a) Determine $k_{eq}$ and $c_{eq}$ if

$$
\begin{aligned}
a &= 32\,\text{cm} \\
b &= 45\,\text{cm} \\
k &= 8000\,\text{N}/\,\text{m} \\
c &= 1000\,\text{N s}/\,\text{m} \\
\alpha &= 10\,\text{deg}\,.
\end{aligned}
$$

    (b) Determine the stiffness $k$ such that the natural frequency of the

vibrating system is $f_n = 1\,\text{Hz}$, if

$$
\begin{aligned}
a &= 32\,\text{cm} \\
b &= 45\,\text{cm} \\
m &= 1000/4\,\text{kg} \\
\alpha &= 10\,\text{deg}\,.
\end{aligned}
$$

(c) Determine the damping $c$ such that the damping ratio of the vibrating system is $\xi = 0.4$, if

$$
\begin{aligned}
a &= 32\,\text{cm} \\
b &= 45\,\text{cm} \\
m &= 1000/4\,\text{kg} \\
\alpha &= 10\,\text{deg} \\
f_n &= 1\,\text{Hz}\,.
\end{aligned}
$$

3. Road excitation frequency.

A car is moving on a wavy road. What is the wave length $d_1$ if the excitation frequency is $f_n = 5\,\text{Hz}$ and

(a) $v = 30\,\text{km}/\,\text{h}$
(b) $v = 60\,\text{km}/\,\text{h}$
(c) $v = 100\,\text{km}/\,\text{h}$.

4. ★ Road excitation frequency and wheelbase.

A car is moving on a wavy road.

(a) What is the wave length $d_1$ if the excitation frequency is $f_n = 8\,\text{Hz}$ and $v = 60\,\text{km}/\,\text{h}$?

(b) What is the phase difference between the front and rear wheel excitations if car's wheelbase is $l = 2.82\,\text{m}$?

(c) At what speed the front and rear wheel excitations have no phase difference?

5. ★ Road excitation amplitude.

A car is moving on a wavy road with a wave length $d_1 = 25\,\text{m}$. What is the damping ratio $\xi$ if $S_2 = Z/Y = 1.02$ when the car is moving with $v = 120\,\text{km}/\,\text{h}$?

$$
\begin{aligned}
k &= 10000\,\text{N}/\,\text{m} \\
m &= 1000/4\,\text{kg}
\end{aligned}
$$

6. Optimized suspension comparison.

   A car with $m = 1000/4\,\mathrm{kg}$ is moving on a wavy road with a wave length $d_1 = 45\,\mathrm{m}$ and wave amplitude $d_2 = 8\,\mathrm{cm}$ at $v = 120\,\mathrm{km/h}$. What is the best suspension parameters if the equivalent wheel travel of the car at the wheel center is

   (a) $5\,\mathrm{cm}$?
   (b) $8\,\mathrm{cm}$?
   (c) $12\,\mathrm{cm}$?
   (d) Calculate $G_0$, $G_2$, $S_2$, $S_Z$, $S_{\ddot{X}}$, $X$, $Z$, and $\ddot{X}$ in each case.

7. Suspension optimization and keeping $k$ or $c$.

   Consider a base excited system with

   $$\begin{aligned} k &= 10000\,\mathrm{N/m} \\ m &= 1000/4\,\mathrm{kg} \\ c &= 1000\,\mathrm{N\,s/m}. \end{aligned}$$

   (a) Determine the best $k$ for the same $c$.
   (b) Determine the best $c$ for the same $k$.
   (c) Determine the value of $S_Z$ and $S_{\ddot{X}}$ in each case.

8. Suspension optimization for minimum $S_Z$.

   A base excited system has

   $$\begin{aligned} k &= 250000\,\mathrm{N/m} \\ m &= 2000\,\mathrm{kg} \\ c &= 2000\,\mathrm{N\,s/m}. \end{aligned}$$

   Determine the level of acceleration RMS $S_{\ddot{X}}$ that transfers to the system.

9. Peak values and step input.

   A base excited system has

   $$\begin{aligned} k &= 10000\,\mathrm{N/m} \\ m &= 1000/4\,\mathrm{kg} \\ c &= 1000\,\mathrm{N\,s/m}. \end{aligned}$$

   What is the acceleration and relative displacement peak values for a unit step input?

10. ★ Acceleration peak value and spring stiffness.

    Explain why the $\xi$-constant curves are vertical lines in the plane $(a_P, z_P)$.

# 15

# ★ Quarter Car

The most employed and useful model of a vehicle suspension system is a quarter car model, shown in Figure 15.1. We introduce, examine, and optimize the quarter car model in this chapter.
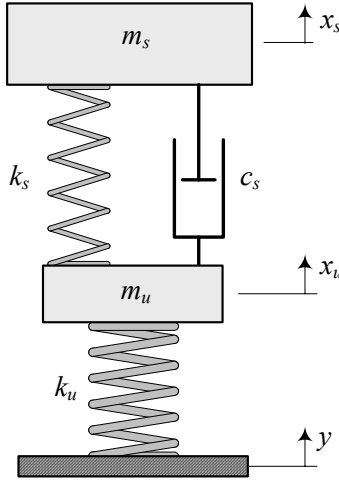


FIGURE 15.1. A quarter car model.

## 15.1    Mathematical Model

We may represent the vertical vibration of a vehicle using a quarter car model made of two solid masses $m_s$ and $m_u$ denoted as *sprung* and *unsprung* masses, respectively. The sprung mass $m_s$ represents 1/4 of the body of the vehicle, and the unsprung mass $m_u$ represents one wheel of the vehicle. A spring of stiffness $k_s$, and a shock absorber with viscous damping coefficient $c_s$, support the sprung mass and are called the *main suspension*. The unsprung mass $m_u$ is in direct contact with the ground through a spring $k_u$, representing the tire stiffness.

The governing differential equations of motion for the quarter car model shown in Figure 15.1, are:

$$m_s\ddot{x}_s + c_s\left(\dot{x}_s - \dot{x}_u\right) + k_s\left(x_s - x_u\right) \;=\; 0 \qquad (15.1)$$

$$m_u\ddot{x}_u + c_s\left(\dot{x}_u - \dot{x}_s\right) + \left(k_u + k_s\right)x_u - k_s x_s \;=\; k_u y. \qquad (15.2)$$

**Proof.** The kinetic energy, potential energy, and dissipation function of the system are as below.

$$K = \frac{1}{2}m_s \dot{x}_s^2 + \frac{1}{2}m_s \dot{x}_s^2 \tag{15.3}$$

$$V = \frac{1}{2}k_s (x_s - x_u)^2 + \frac{1}{2}k_u (x_u - y)^2 \tag{15.4}$$

$$D = \frac{1}{2}c_s (\dot{x}_s - \dot{x}_u)^2 \tag{15.5}$$

Employing the Lagrange method,

$$\frac{d}{dt}\left(\frac{\partial K}{\partial \dot{x}_s}\right) - \frac{\partial K}{\partial x_s} + \frac{\partial D}{\partial \dot{x}_s} + \frac{\partial V}{\partial x_s} = 0 \tag{15.6}$$

$$\frac{d}{dt}\left(\frac{\partial K}{\partial \dot{x}_u}\right) - \frac{\partial K}{\partial x_u} + \frac{\partial D}{\partial \dot{x}_u} + \frac{\partial V}{\partial x_u} = 0 \tag{15.7}$$

we find the equations of motion

$$m_s \ddot{x}_s = -k_s (x_s - x_u) - c_s (\dot{x}_s - \dot{x}_u) \tag{15.8}$$

$$m_u \ddot{x}_u = k_s (x_s - x_u) + c_s (\dot{x}_s - \dot{x}_u) - k_u (x_u - y) \tag{15.9}$$

which can be expressed in a matrix form

$$[m]\,\ddot{\mathbf{x}} + [c]\,\dot{\mathbf{x}} + [k]\,\mathbf{x} = \mathbf{F} \tag{15.10}$$

$$\begin{bmatrix} m_s & 0 \\ 0 & m_u \end{bmatrix}\begin{bmatrix} \ddot{x}_s \\ \ddot{x}_u \end{bmatrix} + \begin{bmatrix} c_s & -c_s \\ -c_s & c_s \end{bmatrix}\begin{bmatrix} \dot{x}_s \\ \dot{x}_u \end{bmatrix} +$$
$$\begin{bmatrix} k_s & -k_s \\ -k_s & k_s + k_u \end{bmatrix}\begin{bmatrix} x_s \\ x_u \end{bmatrix} = \begin{bmatrix} 0 \\ k_u y \end{bmatrix}. \tag{15.11}$$

∎

**Example 522** *Tire damping.*

*We may add a damper $c_u$ in parallel to $k_u$, as shown in Figure, to model any damping in tires. However, the value of $c_u$ for tires, compared to $c_s$, are very small, and hence, we may ignore $c_u$ to simplify the model. Having the damper $c_u$ in parallel to $k_u$, makes the equation of motion the same as Equations (12.47) and (12.48) with a matrix form as Equation (12.50).*

**Example 523** *Mathematical model's limitations.*

*The quarter car model contains no representation of the geometric effects of the full car and offers no possibility of studying longitudinal and lateral interconnections. However, it contains the most basic features of the real problem and includes a proper representation of the problem of controlling wheel and wheel-body load variations.*

In the quarter car model, we assume that the tire is always in contact with the ground, which is true at low frequency but might not be true at high frequency. A better model must be able to include the possibility of separation between the tire and ground.

**Example 524 ★** *History of quarter car model optimization.*
Optimal design of two-DOF vibration systems, including a quarter car model, is the subject of numerous investigations since the invention of the vibration absorber theory by Frahm in 1909. It seems that the first analytical investigation on the damping properties of two-DOF systems is due to Den Hartog (1901 − 1989).

## 15.2   Frequency Response

To find the frequency response, we consider a harmonic excitation,

$$y = Y \cos \omega t \tag{15.12}$$

and look for a harmonic solution in the form

$$
\begin{aligned}
x_s &= A_1 \sin \omega t + B_1 \cos \omega t \\
    &= X_s \sin (\omega t - \varphi_s) \tag{15.13} \\
x_u &= A_2 \sin \omega t + B_2 \cos \omega t \\
    &= X_u \sin (\omega t - \varphi_u) \tag{15.14} \\
z   &= x_s - x_u \\
    &= A_3 \sin \omega t + B_3 \cos \omega t \\
    &= Z \sin (\omega t - \varphi_z) \tag{15.15}
\end{aligned}
$$

where $X_s$, $X_u$, and $Z$ are complex amplitudes.
By introducing the following dimensionless characteristics:

$$
\varepsilon = \frac{m_s}{m_u} \tag{15.16}
$$

$$
\omega_s = \sqrt{\frac{k_s}{m_s}} \tag{15.17}
$$

$$
\omega_u = \sqrt{\frac{k_u}{m_u}} \tag{15.18}
$$

$$
\alpha = \frac{\omega_s}{\omega_u} \tag{15.19}
$$

$$
r = \frac{\omega}{\omega_s} \tag{15.20}
$$

$$
\xi = \frac{c_s}{2 m_s \omega_s} \tag{15.21}
$$

we may search for the following frequency responses:

$$\mu \;\; = \;\; \left| \frac{X_s}{Y} \right| \tag{15.22}$$

$$\tau \;\; = \;\; \left| \frac{X_u}{Y} \right| \tag{15.23}$$

$$\eta \;\; = \;\; \left| \frac{Z}{Y} \right| \tag{15.24}$$

and obtain the following functions:

$$\mu^2 \;\; = \;\; \frac{4\xi^2 r^2 + 1}{Z_1^2 + Z_2^2} \tag{15.25}$$

$$\tau^2 \;\; = \;\; \frac{4\xi^2 r^2 + 1 + r^2 \left( r^2 - 2 \right)}{Z_1^2 + Z_2^2} \tag{15.26}$$

$$\eta^2 \;\; = \;\; \frac{r^4}{Z_1^2 + Z_2^2} \tag{15.27}$$

$$Z_1 \;\; = \;\; \left[ r^2 \left( r^2 \alpha^2 - 1 \right) + \left( 1 - \left( 1 + \varepsilon \right) r^2 \alpha^2 \right) \right] \tag{15.28}$$

$$Z_2 \;\; = \;\; 2\xi r \left( 1 - \left( 1 + \varepsilon \right) r^2 \alpha^2 \right) \tag{15.29}$$

The absolute acceleration of sprung mass and unsprung mass may be defined by the following equations:

$$u \;\; = \;\; \left| \frac{\ddot{X}_s}{Y \omega_u^2} \right| \tag{15.30}$$

$$= \;\; r^2 \alpha^2 \mu \tag{15.31}$$

$$v \;\; = \;\; \left| \frac{\ddot{X}_u}{Y \omega_u^2} \right| \tag{15.32}$$

$$= \;\; r^2 \alpha^2 \tau \tag{15.33}$$

**Proof.** To find the frequency responses, let's apply a harmonic excitation

$$y = Y \cos \omega t \tag{15.34}$$

and assume that the solutions are harmonic functions with unknown coefficients.

$$x_s \;\; = \;\; A_1 \sin \omega t + B_1 \cos \omega t \tag{15.35}$$

$$x_u \;\; = \;\; A_2 \sin \omega t + B_2 \cos \omega t. \tag{15.36}$$

Substituting the solutions in the equations of motion (15.1)-(15.2) and collecting the coefficients of $\sin \omega t$ and $\cos \omega t$ in both equations provides

the following set of algebraic equations for $A_1$, $B_1$, $A_2$, $B_2$ :

$$[A] \begin{bmatrix} A_1 \\ A_2 \\ B_1 \\ B_2 \end{bmatrix} = \begin{bmatrix} 0 \\ 0 \\ k_u Y \\ 0 \end{bmatrix} \tag{15.37}$$

where $[A]$ is the coefficient matrix.

$$[A] = \begin{bmatrix} k_s - m_s\omega^2 & -k_s & -c_s\omega & c_s\omega \\ c_s\omega & -c_s\omega & k_s - m_s\omega^2 & -k_s \\ -k_s & k_s + k_u - m_u\omega^2 & c_s\omega & -c_s\omega \\ -c_s\omega & c_s\omega & -k_s & k_s + k_u - m_u\omega^2 \end{bmatrix} \tag{15.38}$$

The unknowns may be found by matrix inversion

$$\begin{bmatrix} A_1 \\ A_2 \\ B_1 \\ B_2 \end{bmatrix} = [A]^{-1} \begin{bmatrix} 0 \\ 0 \\ k_u Y \\ 0 \end{bmatrix} \tag{15.39}$$

and therefore, the amplitudes $X_s$ and $X_u$ can be found.

$$\begin{aligned} X_s^2 &= A_1^2 + B_1^2 \\ &= \frac{k_u}{k_s} \frac{\left(\omega^2 c_s^2 + k_s^2\right)}{Z_3^2 + Z_4^2} Y^2 \end{aligned} \tag{15.40}$$

$$\begin{aligned} X_u^2 &= A_2^2 + B_2^2 \\ &= \frac{k_u}{k_s} \frac{\left(\omega^4 m_s^2 + \omega^2 c_s^2 - 2\omega^2 k_s m_s + k_s^2\right)}{Z_3^2 + Z_4^2} Y^2 \end{aligned} \tag{15.41}$$

$$Z_3 = -\left(\omega^2 \left(k_s m_s + k_s m_u + k_u m_s\right) - k_s k_u - \omega^4 m_s m_u\right) \tag{15.42}$$

$$Z_4 = -\left(\omega^3 \left(c_s m_s + c_s m_u\right) - \omega c_s k_u\right) \tag{15.43}$$

Having $X_s$ and $X_u$ helps us to calculate $z$ and its amplitude $Z$.

$$\begin{aligned} z &= x_s - x_u \\ &= (A_1 - A_2) \sin \omega t + (B_1 - B_2) \cos \omega t \\ &= A_3 \sin \omega t + B_3 \cos \omega t \\ &= Z \sin (\omega t - \varphi_z) \end{aligned} \tag{15.44}$$

$$\begin{aligned} Z^2 &= A_3^2 + B_3^2 \\ &= \frac{k_u}{k_s} \frac{\omega^4 m_s^2}{Z_3^2 + Z_4^2} Y^2 \end{aligned} \tag{15.45}$$
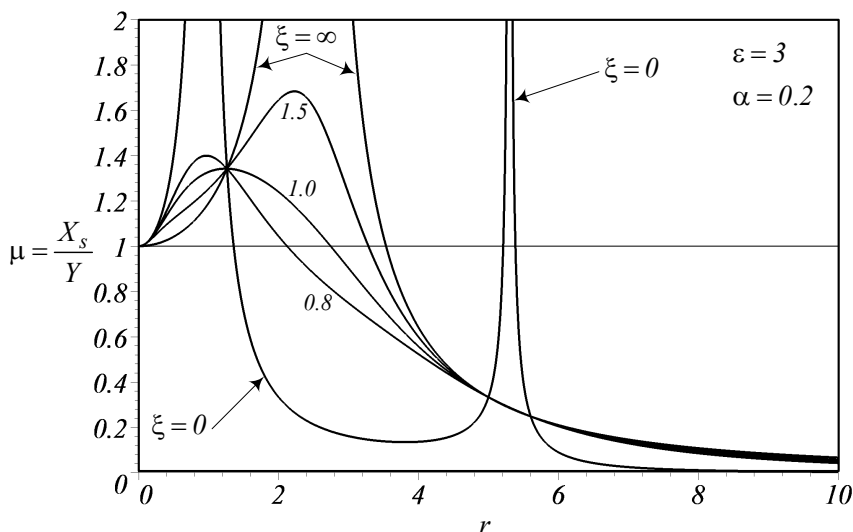
FIGURE 15.2. A sample for the sprung mass displacement frequency response, $\mu = \left| \frac{X_s}{Y} \right|$.

Taking twice the derivative of $\mu$ and $\tau$ ends up the acceleration frequency responses $u$ and $v$ for the unsprung and sprung masses. Equations (15.30)-(15.33) express $u$ and $v$.

Using the definitions (15.16)-(15.21), we may transform Equations (15.40), (15.41), and (15.45) to (15.25), (15.26), and (15.27). Figures 15.2, 15.3, and 15.4, are samples of the frequency responses $\mu$, $\tau$, and $\eta$ for $\varepsilon = 3$, and $\alpha = 0.2$.

∎

**Example 525** *Average value of parameters for street cars.*

*Equations (15.25)-(15.27) indicate that the frequency responses $\mu$, $\tau$, and $\eta$ are functions of four parameters: mass ratio $\varepsilon$, damping ratio $\xi$, natural frequency ratio $\alpha$, and excitation frequency ratio $r$. The average, minimum, and maximum of practical values of the included parameters are indicated in Table 14.1.*

*For a quarter car model, it is known that $m_s > m_u$, and therefore, $\varepsilon > 1$. Typical mass ratio, $\varepsilon$, for vehicles lies in the range 3 to 8, with small cars closer to 8 and large cars near 3. The excitation frequency $\omega$ is equal to $\omega_u$, when $r = 1/\alpha$, and equal to $\omega_s$, when $r = 1$. For a real model, the order of magnitude of the stiffness is $k_u > k_s$, so $\omega_u > \omega_s$, and $\alpha < 1$. Therefore, $r > 1$ at $\omega = \omega_u$. So, we expect to have two resonant frequencies greater*
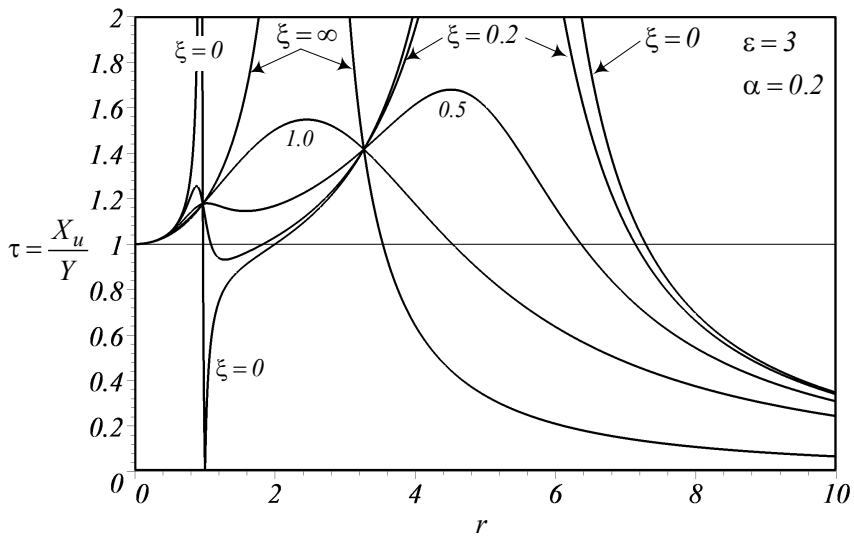
FIGURE 15.3. A sample of the unsprung mass displacement frequency response, $\tau = \left| \frac{X_u}{Y} \right|$.
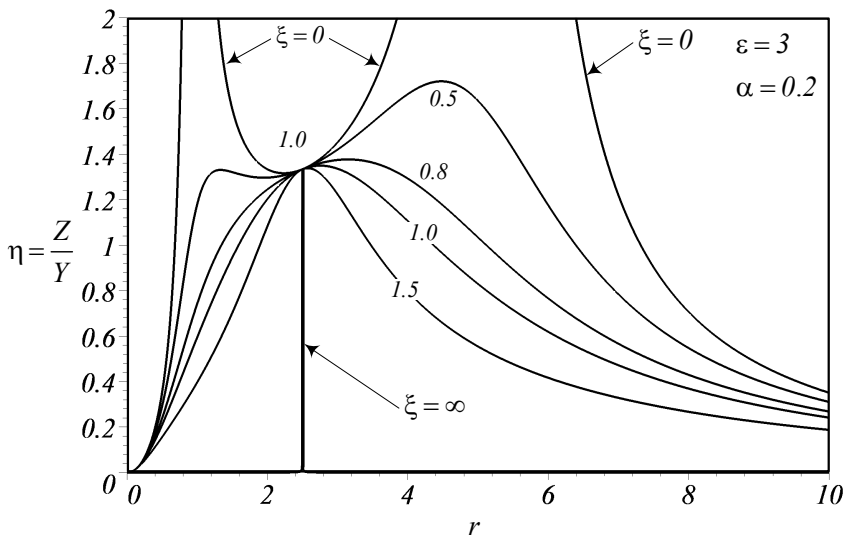


FIGURE 15.4. A sample of the relative displacement frequency response, $\eta = \left| \frac{Z}{Y} \right|$.

*than $r = 1$.*

Table 14.1 - *Average value of quarter car parameters.*

| Parameter | Average | Minimum | Maximum |
|---|---|---|---|
| $\varepsilon = \dfrac{m_s}{m_u}$ | $3 - 8$ | 2 | 20 |
| $\omega_s = \sqrt{\dfrac{k_s}{m_s}}$ | 1 | 0.2 | 1 |
| $\omega_u = \sqrt{\dfrac{k_u}{m_u}}$ | 10 | 2 | 20 |
| $r = \dfrac{\omega}{\omega_s}$ | $0 - 20\,\mathrm{Hz}$ | 0 | $200\,\mathrm{Hz}$ |
| $\alpha = \dfrac{\omega_s}{\omega_u}$ | 0.1 | 0.01 | 1 |
| $\xi = \dfrac{c_s}{2m_s\omega_s}$ | 0.55 | 0 | 2 |

**Example 526 ★** *Three-dimensional visualization for frequency responses.*

To get a sense about the behavior of different frequency responses of a quarter car model, Figures 15.5 to 15.8 are plotted for

$$
\begin{aligned}
m_s &= 375\,\mathrm{kg} \\
m_u &= 75\,\mathrm{kg} \\
k_u &= 193000\,\mathrm{N/m} \\
k_s &= 35000\,\mathrm{N/m.}
\end{aligned}
$$

# 15.3   ★ Natural and Invariant Frequencies

The system is a *two*-DOF system and therefore it has two natural frequencies. The natural frequencies $r_{n_1}$, $r_{n_2}$, of a quarter car are

$$
r_{n_1} = \sqrt{\frac{1}{2\alpha^2}\left(1 + (1+\varepsilon)\,\alpha^2 - \sqrt{\left(1 + (1+\varepsilon)\,\alpha^2\right)^2 - 4\alpha^2}\right)} \tag{15.46}
$$

$$
r_{n_2} = \sqrt{\frac{1}{2\alpha^2}\left(1 + (1+\varepsilon)\,\alpha^2 + \sqrt{\left(1 + (1+\varepsilon)\,\alpha^2\right)^2 - 4\alpha^2}\right)}. \tag{15.47}
$$

The family of response curves for the displacement frequency response of the sprung mass, $\mu$, are obtained by keeping $\varepsilon$ and $\xi$ constant, and varying $\xi$. This family has several points in common, which are at frequencies $r_1$,
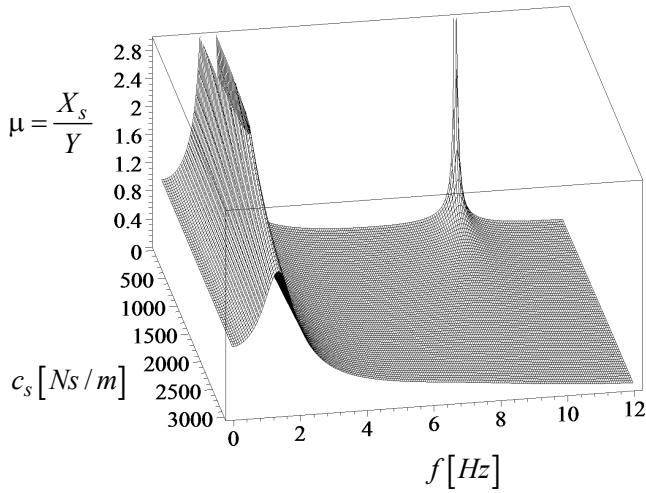
FIGURE 15.5. Three-dimensional view of the frequency response $\mu = \left| \frac{X_s}{Y} \right|$.
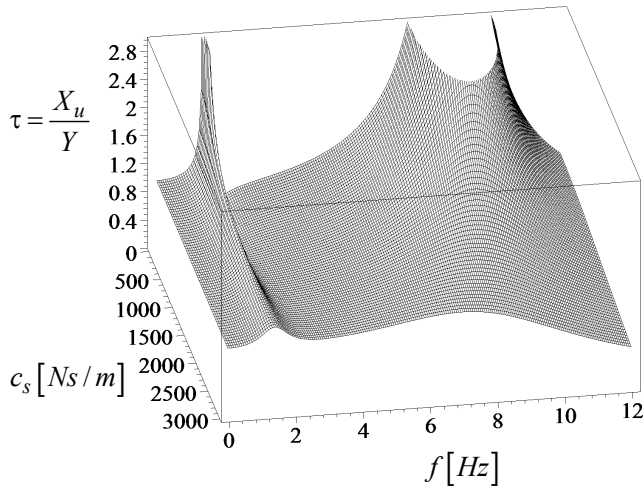


FIGURE 15.6. Three-dimensional view of the frequency response $\tau = \left| \frac{X_u}{Y} \right|$.
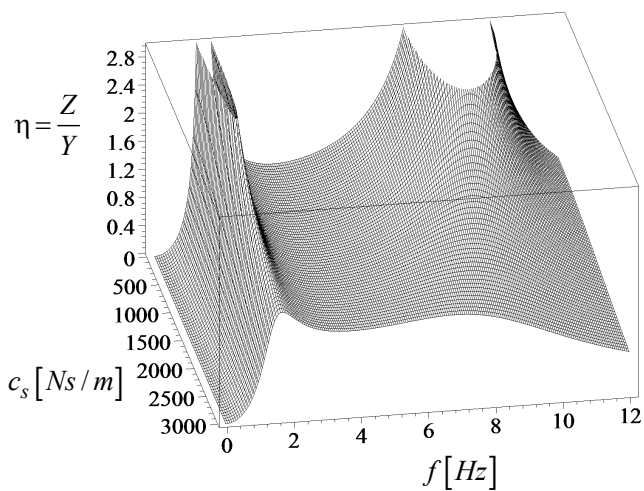
FIGURE 15.7. Three-dimensional view of the frequency response $\eta = \left| \frac{Z}{Y} \right|$.
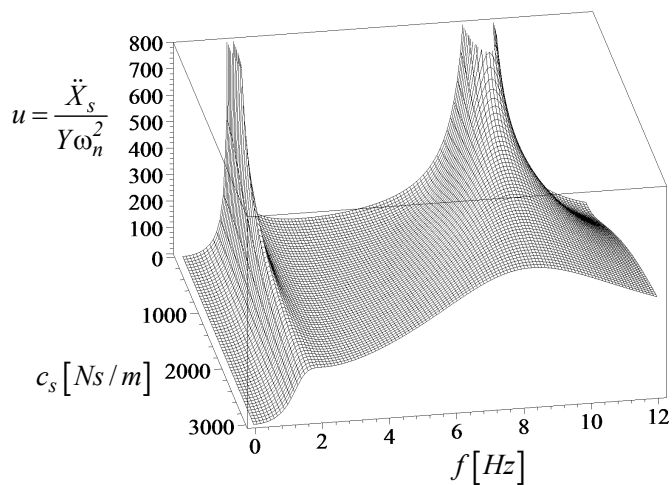


FIGURE 15.8. Three-dimensional view of the frequency response $u = \left| \frac{\ddot{X}_s}{Y \omega_u^2} \right|$.

$r_2$, $r_3$, $r_4$, and $\mu_1$, $\mu_2$, $\mu_3$, $\mu_4$.

$$
\begin{cases}
r_1 = 0 & \mu_1 = 1 \\
r_3 = \dfrac{1}{\alpha} & \mu_3 = \dfrac{1}{\varepsilon} \\
r_2 & \mu_2 = \dfrac{1}{1 - (1+\varepsilon)\, r_2^2 \alpha^2} \\
r_4 & \mu_4 = \dfrac{-1}{1 - (1+\varepsilon)\, r_2^2 \alpha^2}
\end{cases}
\tag{15.48}
$$

$$
r_2 = \sqrt{\frac{1}{2\alpha^2}\left(1 + 2\left(1+\varepsilon\right)\alpha^2 - \sqrt{\left(1 + 2\left(1+\varepsilon\right)\alpha^2\right)^2 - 8\alpha^2}\right)} \tag{15.49}
$$

$$
r_4 = \sqrt{\frac{1}{2\alpha^2}\left(1 + 2\left(1+\varepsilon\right)\alpha^2 + \sqrt{\left(1 + 2\left(1+\varepsilon\right)\alpha^2\right)^2 - 8\alpha^2}\right)} \tag{15.50}
$$

where

$$
r_1\,(= 0) < r_2 < \frac{1}{\alpha\sqrt{1+\varepsilon}} < r_3 \left(= \frac{1}{\alpha}\right) < r_4 \tag{15.51}
$$

the corresponding transmissivities at $r_2$ and $r_4$ are

$$
\mu_2 = \frac{1}{1 - (1+\varepsilon)\, r_2^2 \alpha^2} \tag{15.52}
$$

$$
\mu_4 = \frac{-1}{1 - (1+\varepsilon)\, r_2^2 \alpha^2} \tag{15.53}
$$

The frequencies $r_1$, $r_2$, $r_3$, and $r_4$ are called *invariant frequencies*, and their corresponding amplitudes are called *invariant amplitudes* because they are not dependent on $\xi$. However, they are dependent on the values of $\varepsilon$ and $\alpha$. The order of magnitude of the natural and invariant frequencies are:

$$
r_1\,(= 0) < r_{n_1} < r_2 < \frac{1}{\alpha\sqrt{1+\varepsilon}} < r_3 < \left(= \frac{1}{\alpha^2}\right) < r_{n_2} < r_4 \tag{15.54}
$$

The curves for $\mu$ have no other common points except $r_1$, $r_2$, $r_3$, and $r_4$. The order of frequencies along with the order of corresponding amplitudes can be used to predict the shape of the frequency response curves of the sprung mass $\mu$. Figure 15.9 shows schematically the shape of the amplitude $\mu$ versus excitation frequency ratio $r$.

**Proof.** Natural and resonant frequencies of a system are where the amplitude goes to infinity when damping is zero. Hence, the natural frequencies would be the roots of the denominator of the $\mu$ function.

$$
\begin{aligned}
g\left(r^2\right) &= r^2\left(r^2\alpha^2 - 1\right) + \left(1 - (1+\varepsilon)\, r^2 \alpha^2\right) \\
&= \alpha^2 r^2 - \left(1 + (1+\varepsilon)\,\alpha^2\right) + 1 = 0 \tag{15.55}
\end{aligned}
$$
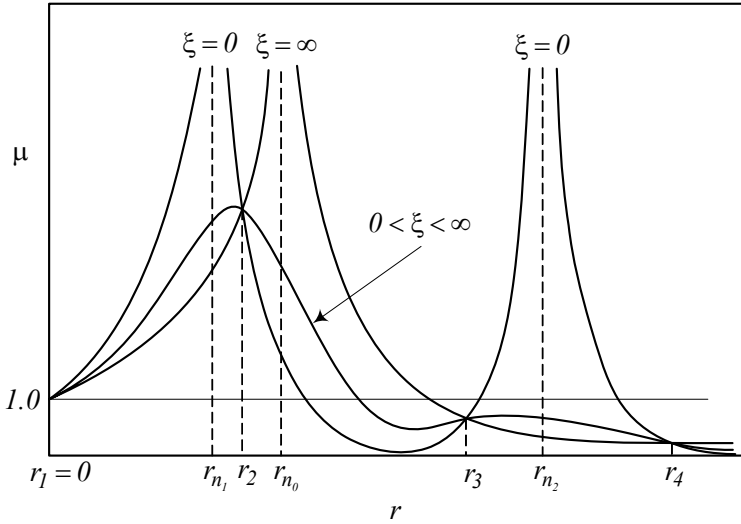
FIGURE 15.9. Schematic illustration of the amplitude $\mu$ versus excitation frequency ratio $r$.

The solution of this equation are the natural frequencies given in Equations (15.46) and (15.47).

$$\mu^2 = \frac{4\xi^2 r^2 + 1}{Z_1^2 + Z_2^2} \tag{15.56}$$

$$\tau^2 = \frac{4\xi^2 r^2 + 1 + r^2 \left(r^2 - 2\right)}{Z_1^2 + Z_2^2} \tag{15.57}$$

$$\eta^2 = \frac{r^4}{Z_1^2 + Z_2^2} \tag{15.58}$$

The invariant frequencies are not dependent $\xi$, so they can be found by intersecting the $\mu$ curves for $\xi = 0$ and $\xi = \infty$.

$$\lim_{\xi \to 0} = \pm\frac{1}{\left(r^2 \left(r^2\alpha^2 - 1\right) - r^2\alpha^2 \left(\varepsilon + 1\right) + 1\right)^2} \tag{15.59}$$

$$\lim_{\xi \to \infty} = \pm\frac{1}{\left(r^2\alpha^2 \left(\varepsilon + 1\right) - 1\right)^2} \tag{15.60}$$

Therefore, the invariant frequencies, $r_i$, can be determined by solving the following equation:

$$r^2 \left(r^2\alpha^2 - 1\right) + \left(1 - (1 + \varepsilon)\,r^2\alpha^2\right) = \pm\left(1 - (1 + \varepsilon)\,r^2\alpha^2\right) \tag{15.61}$$

Using the (+) sign, we find $r_1$ and $r_3$ with their corresponding transmis-

sivities $\mu_1$, and $\mu_3$,

$$r_1 \;=\; 0 \qquad \mu_1 = 1 \tag{15.62}$$

$$r_3 \;=\; \frac{1}{\alpha} \qquad \mu_3 = \frac{1}{\varepsilon} \tag{15.63}$$

and, with the $(-)$ sign, we find the following equation for $r_2$, and $r_4$:

$$\alpha^2 r^4 - \left(1 + 2\left(1 + \varepsilon\right)\alpha^2\right) r^2 + 2 = 0 \tag{15.64}$$

Equation (15.64) has two real positive roots, $r_2$ and $r_4$,

$$r_2 \;=\; \sqrt{\frac{1}{2\alpha^2}\left(1 + 2\left(1 + \varepsilon\right)\alpha^2 - \sqrt{\left(1 + 2\left(1 + \varepsilon\right)\alpha^2\right)^2 - 8\alpha^2}\right)} \tag{15.65}$$

$$r_4 \;=\; \sqrt{\frac{1}{2\alpha^2}\left(1 + 2\left(1 + \varepsilon\right)\alpha^2 + \sqrt{\left(1 + 2\left(1 + \varepsilon\right)\alpha^2\right)^2 - 8\alpha^2}\right)} \tag{15.66}$$

with the following relative order of magnitude:

$$r_1 \left(= 0\right) < r_2 < \frac{1}{\alpha\sqrt{1 + \varepsilon}} < r_3 \left(= \frac{1}{\alpha}\right) < r_4 \tag{15.67}$$

The corresponding amplitudes at $r_2$, and $r_4$ can be found by substituting Equations (15.65) and (15.66) in (15.25).

$$\mu_2 \;=\; \frac{1}{1 - \left(1 + \varepsilon\right) r_2^2 \alpha^2} \tag{15.68}$$

$$\mu_4 \;=\; \frac{-1}{1 - \left(1 + \varepsilon\right) r_4^2 \alpha^2} \tag{15.69}$$

It can be checked that

$$\left(1 + \varepsilon\right)\alpha^2 r_4^2 - 1 > \varepsilon > 1 \tag{15.70}$$

and hence,

$$|r_4| < \frac{1}{\varepsilon} \left(= \mu_3\right) < 1 < |r_2| \tag{15.71}$$

and therefore,

$$\mu_2 \;>\; 1 \tag{15.72}$$

$$\mu_4 \;<\; 1. \tag{15.73}$$

Using Equation (15.55), we can evaluate $g\left(r_2^2\right)$, $g\left(r_4^2\right)$, and $g\left(r_3^2\right)$ as

$$g\left(r_2^2\right) \;=\; \left(1 + \varepsilon\right)\alpha^2 r_2^2 - 1 < 0 \tag{15.74}$$

$$g\left(r_4^2\right) \;=\; \left(1 + \varepsilon\right)\alpha^2 r_4^2 - 1 > 0 \tag{15.75}$$

$$g\left(r_3^2\right) \;=\; g\left(\frac{1}{\alpha^2}\right) \tag{15.76}$$
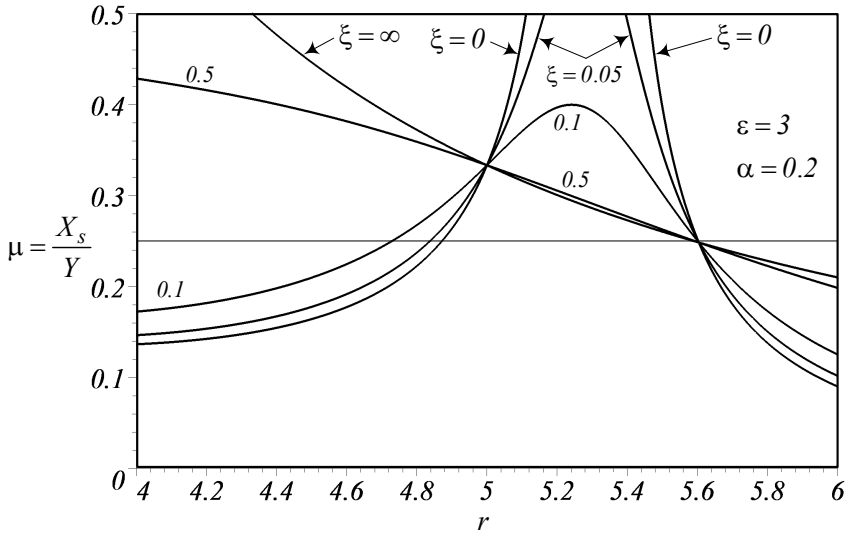
FIGURE 15.10. A magnification around the nodes for the sprung mass displacement frequency response, $\mu = \left|\frac{X_s}{Y}\right|$.

therefore, the two positive roots of Equation (15.55), $r_{n_1}$ and $r_{n_2}$ $(> \sqrt{2} > r_2)$, have the order of magnitudes as follows:

$$r_1 \, (= 0) < r_{n_1} < r_2 < \frac{1}{\alpha\sqrt{1+\varepsilon}} < r_3 < \left(= \frac{1}{\alpha^2}\right) < r_{n_2} < r_4 \qquad (15.77)$$

■

**Example 527 ★** *Nodes of the absolute displacement frequency response* $\mu$.

There are four nodes in the absolute displacement frequency response of a quarter car. The first node is at a trivial point $(r_1 = 0, \mu_1 = 1)$, which shows that $X_s = Y$ when the excitation frequency is zero. The fourth node is at $(r_4, \mu_4 < 1)$. There are also two middle nodes at $(r_2, \mu_2 > 1)$ and $\left(r_3 = \frac{1}{\alpha}, \mu_3 = \frac{1}{\varepsilon}\right)$.

Because $\mu_1 \leq 1$ and $\mu_4 \leq 1$, the middle nodes are important in optimization. To have a better view at the middle nodes, Figure 15.10 illustrates a magnification of the sprung mass displacement frequency response, $\mu = \left|\frac{X_s}{Y}\right|$ around the middle nodes.

**Example 528 ★** *There is no Frahm optimal quarter car.*

Reduction in absolute amplitude is the first attempt at optimization. If the amplitude frequency response $\mu = \mu(r)$ contains fixed points with respect to some parameters, then using the Frahm method, the optimization process is carried out in two steps:
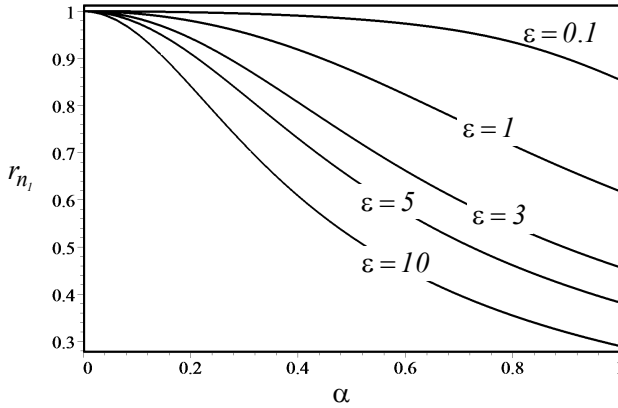
FIGURE 15.11. The natural frequency $r_{n_1}$ as a function of $\varepsilon$ and $\alpha$.

1– *We select the parameters that control the position of the invariant points to equalize the corresponding height at the invariant frequencies, and minimize the height of the fixed points as far as possible.*

2– *We find the remaining parameters such that the maximum amplitude coincides precisely at the invariant points.*

*For a real problem, the values of mass ratio $\varepsilon$, and tire frequency $\omega_u$ are fixed and we are trying to find the optimum values of $\alpha$ and $\xi$. The parameters $\alpha$ and $\xi$ include the unknown stiffness of the main spring and the unknown damping of the main shock absorber, respectively.*

*The amplitude $\mu_i$ at invariant frequencies $r_i$, shows that the first invariant point $(r_1 = 0, \mu_1 = 1)$ is always fixed, and the fourth one $(r_4, \mu_4 < 1)$ happens after the natural frequencies. Therefore, the second and third nodes are the suitable nodes for applying the above optimization steps. However,*

$$\mu_2 \leq 1 \leq \mu_3 \qquad \forall \varepsilon > 1 \tag{15.78}$$

*and hence, we cannot apply the above optimization method. It is because $\mu_2$ and $\mu_3$ can never be equated by varying $\alpha$. Ever so, we can still find the optimum value of $\xi$ by evaluating $\alpha$ based on other constraints.*

**Example 529** *Natural frequency variation.*

*The natural frequencies $r_{n_1}$ and $r_{n_2}$, as given in Equations (15.46) and (15.47), are functions of $\varepsilon$ and $\alpha$. Figures 15.11 and 15.12 illustrate the effect of these two parameters on the variation of the natural frequencies.*

*The first natural frequency $r_{n_1} \leq 1$ decreases by increasing the mass ratio $\varepsilon$. $r_{n_1}$ is close to the natural frequency of a 1/8 car model and indicates the* **principal natural frequency** *of a car. Hence, it is called the* **body bounce natural frequency**. *The second natural frequency, $r_{n_2}$, approaches infinity when $\alpha$ decreases. However, $r_{n_2} \approx 10\,\text{Hz}$ for street cars with acceptable ride*
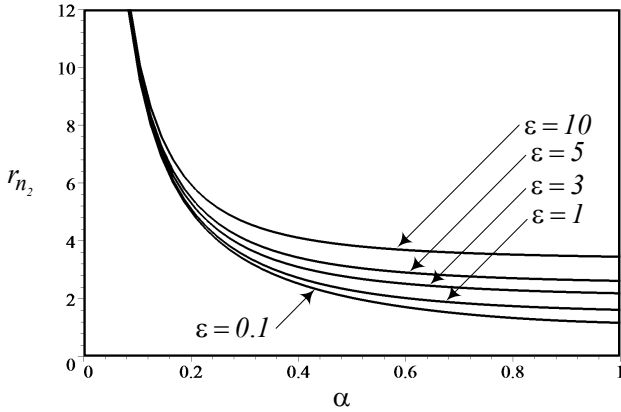
FIGURE 15.12. The natural frequency $r_{n_2}$ as a function of $\varepsilon$ and $\alpha$.

comfort. $r_{n_1}$ relates to the unsprung mass, and is called the **wheel hop natural frequency**.

Figure 15.13 that plots the natural frequency ratio $r_{n_1}/r_{n_2}$ shows their relative behavior better.

**Example 530** *Invariant frequencies variation.*

The invariant frequencies $r_2$, $r_3$, and $r_4$, as given in Equation (15.48), are functions of $\varepsilon$ and $\alpha$. Figures 15.14 to 15.18 illustrate the effect of these two parameters on the invariant frequencies.

The second invariant frequency $r_2$, as shown in Figure 15.14, is always less than $\sqrt{2}$ because

$$\lim_{\alpha \to 0} r_2 = \sqrt{2}. \tag{15.79}$$

So, whatever the value of the mass ratio, $r_2$ cannot be greater than $\sqrt{2}$. Such a behavior may not let us control the position of second node freely.

The third invariant frequency $r_3$ as shown in Figure 15.15 is not a function of the mass ratio and may have any value depending on $\alpha$. The fourth invariant frequency $r_4$ is shown in Figure 15.15. $r_4$ increases when $\alpha$ decreases. However, $r_4$ settles when $\alpha \gtrsim 0.6$.

$$\lim_{\alpha \to 0} r_2 = \infty \tag{15.80}$$

To have a better idea about the behavior of invariant frequencies, Figures 15.17 and 15.18 depict the relative frequency ratio $r_4/r_3$ and $r_3/r_2$.

**Example 531** *Frequency response at invariant frequencies.*

The frequency response $\mu$ is a function of $\alpha$, $\varepsilon$, and $\xi$. Damping always diminishes the amplitude of vibration, so we set $\xi = 0$ and plot the behavior
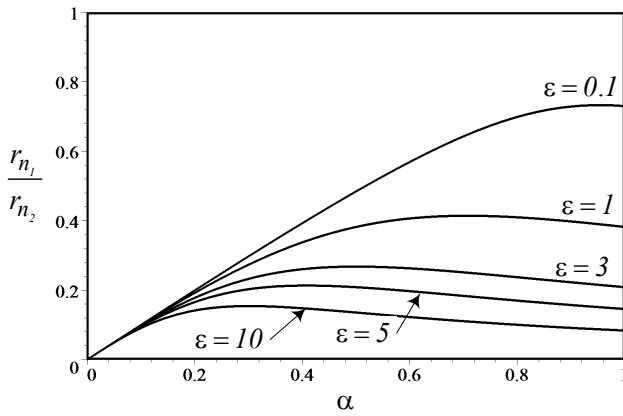
FIGURE 15.13. The natural frequency ratio $r_{n_1}/r_{n_2}$ as a function of $\varepsilon$ and $\alpha$.
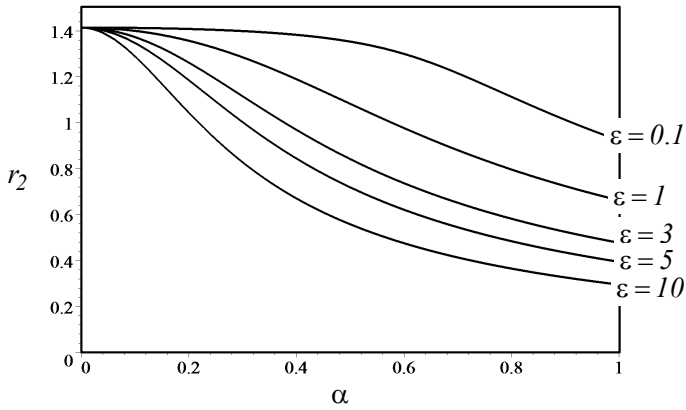


FIGURE 15.14. The second invariant frequency $r_2$ as a function of $\varepsilon$ and $\alpha$.
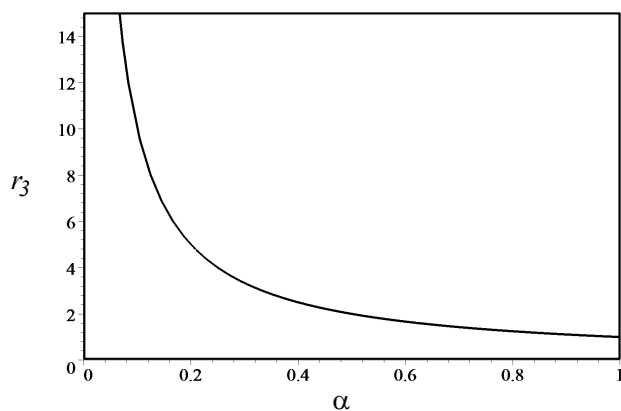
FIGURE 15.15. The third invariant frequency $r_3$ as a function of $\varepsilon$ and $\alpha$.
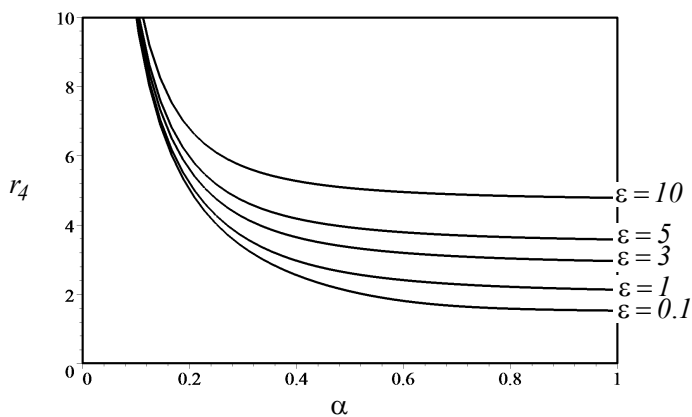


FIGURE 15.16. The fourth invariant frequency $r_4$ as a function of $\varepsilon$ and $\alpha$.
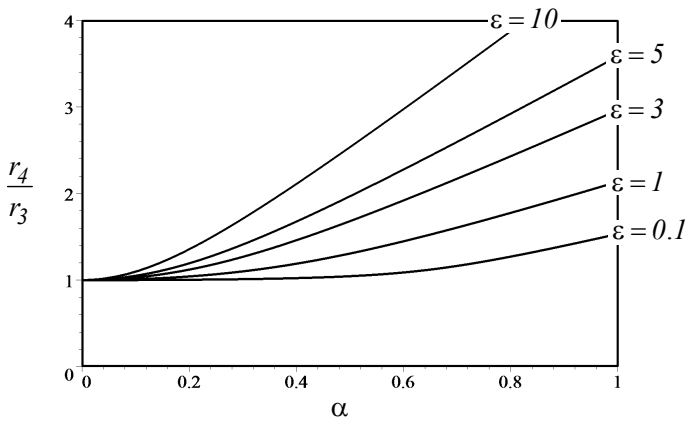
FIGURE 15.17. The ratio of $r_4/r_3$ as a function of $\varepsilon$ and $\alpha$.
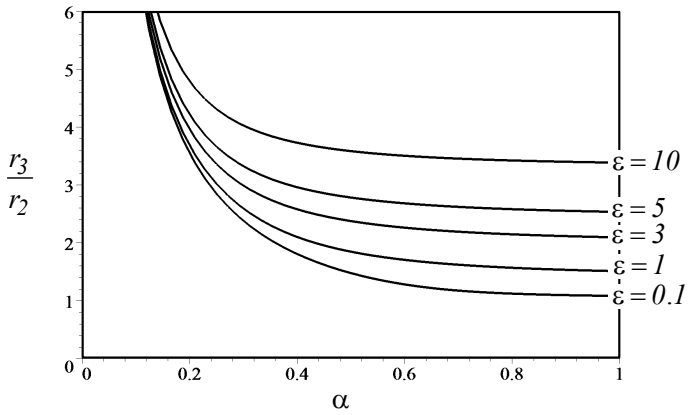


FIGURE 15.18. The ratio of $r_3/r_2$ as a function of $\varepsilon$ and $\alpha$.
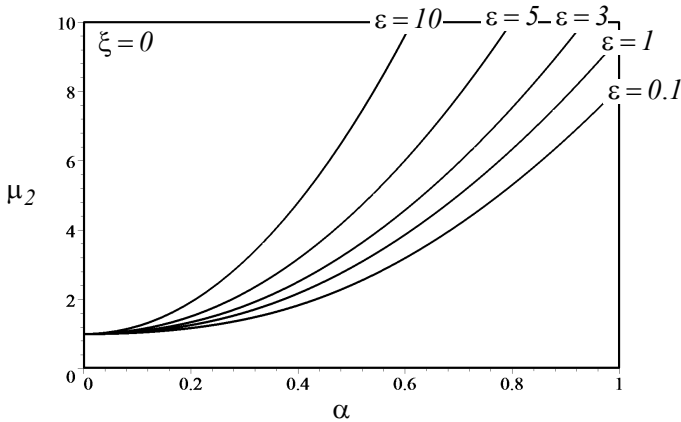
FIGURE 15.19. Behavior of $\mu_2$ as a function of $\alpha$, $\varepsilon$.

*of $\mu$ is a function of $\alpha$, $\varepsilon$. Figure 15.19 illustrates the behavior of $\mu$ at the second invariant frequency $r_2$. Because*

$$\lim_{\alpha \to 0} \mu_2 = 1 \qquad\qquad (15.81)$$

*$\mu_2$ starts at one regardless of the value of $\varepsilon$. The value of $\mu_2$ is always an greater than one and is an increasing function.*

*Figure 15.20 shows that $\mu_3$ is not a function of $\alpha$ and a decreasing function of $\varepsilon$. Figure 15.21 shows that $\mu_4 \le 1$ regardless of the value of $\alpha$ and $\varepsilon$. The relative behavior of $\mu_2$, $\mu_3$, and $\mu_4$ is shown in Figures 15.22 and 15.23.*

**Example 532** *Natural frequencies and vibration isolation of a quarter car.*

*For a modern, typical passenger car, the values of natural frequencies are around 1 Hz and 10 Hz respectively. The former is due to the bounce of sprung mass and the latter belongs to the unsprung mass. At average speed, bumps of wavelengths, which are much greater than the wheelbase of the vehicle, will excite bounce motion of the body, whereas at higher speed, bumps of wavelengths, which become shorter than a wheelbase length, will cause heavy vibrations of the unsprung. Therefore, when the wheels hit a single bump on the road, the impulse will set the wheels into oscillation at the natural frequency of the unsprung mass around 10 Hz. In turn, for the sprung mass, the excitation will be the frequency of vibration of the unsprung around 10 Hz. Because the natural frequency of the sprung is approximately 1 Hz, then the excellent isolation for sprung mass occurs and the frequency range around 10 Hz has no essential influence on the sprung discomfort. When the wheel runs over a rough undulating surface, the excitation will consists of a wide range of frequencies. Again, high excitation frequency at 5 Hz to 20 Hz means high frequency input to the sprung mass,*
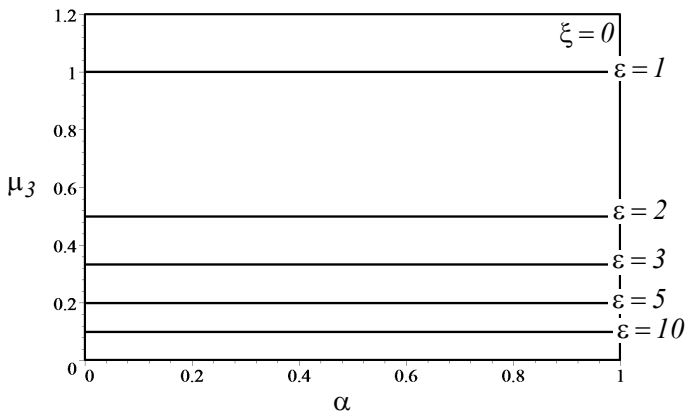
FIGURE 15.20. Behavior of $\mu_3$ as a function of $\varepsilon$.
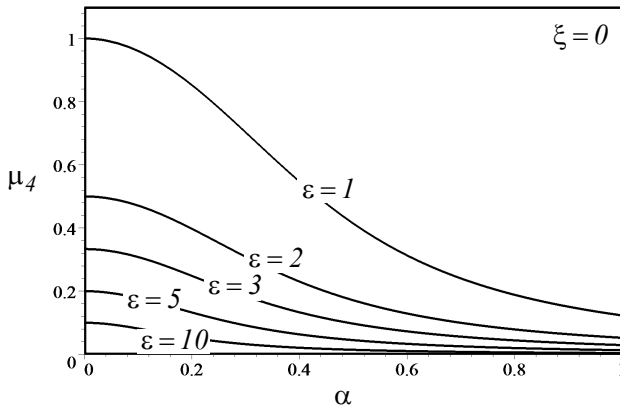


FIGURE 15.21. Behavior of $\mu_4$ as a function of $\alpha$, $\varepsilon$.
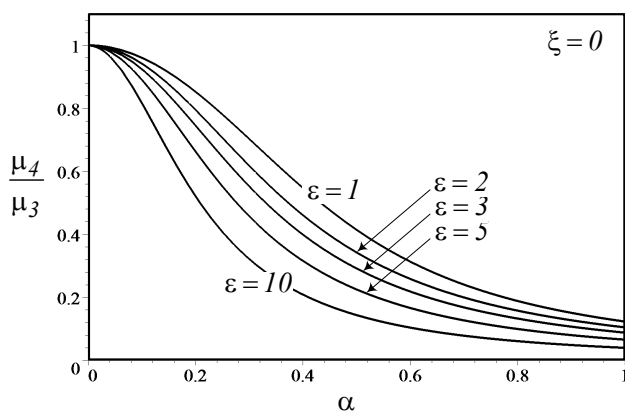
FIGURE 15.22. Behavior of $\dfrac{\mu_4}{\mu_3}$ as a function of $\alpha$, $\varepsilon$.
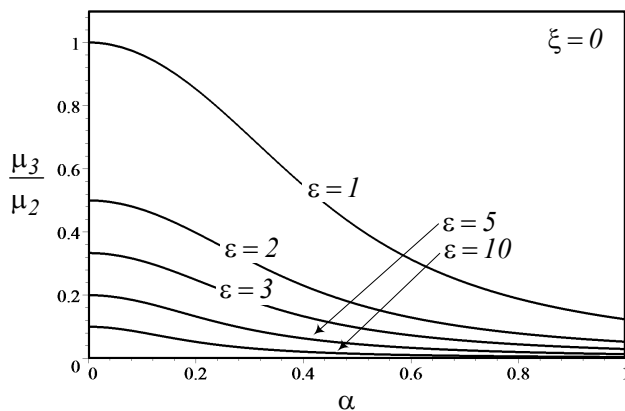


FIGURE 15.23. Behavior of $\dfrac{\mu_3}{\mu_2}$ as a function of $\alpha$, $\varepsilon$.
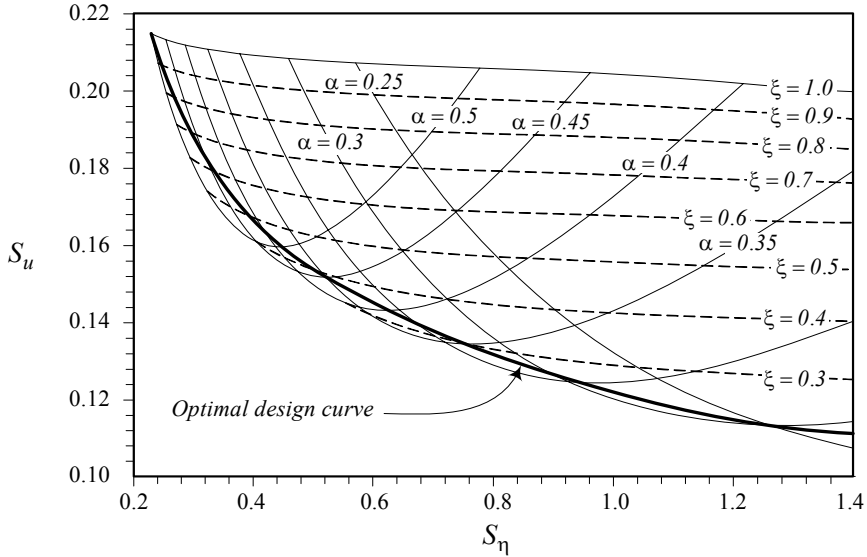
FIGURE 15.24. Root mean square of absolute acceleration, $S_u = RMS(u)$ vreus root mean square of relative displacement $S_\eta = RMS(\eta)$, for a quarter car model and the optimal curve.

*which can effectively be isolated. Low frequency excitation, however, will cause resonance in the sprung mass.*

## 15.4   ★ RMS Optimization

Figure 15.24 is a design chart for optimal suspension parameters of a base excited *two*-DOF system such as a quarter car model. The horizontal axis is the root mean square of relative displacement, $S_\eta = RMS(\eta)$, and the vertical axis is the root mean square of absolute acceleration, $S_u = RMS(u)$.

There are two sets of curves that make a mesh. The first set, which is almost parallel at the right end, are constant damping ratio $\xi$, and the second set is constant natural frequency ratio $\alpha$. There is a curve, called the *optimal design curve*, which indicates the optimal main suspension parameters:

The optimal design curve is the result of the following RMS optimization strategy

$$Minimize\ S_{\ddot{X}}\ with\ respect\ to\ S_Z \qquad (15.82)$$

which states that the minimum absolute acceleration with respect to the relative displacement, if there is any, makes the suspension of a quarter
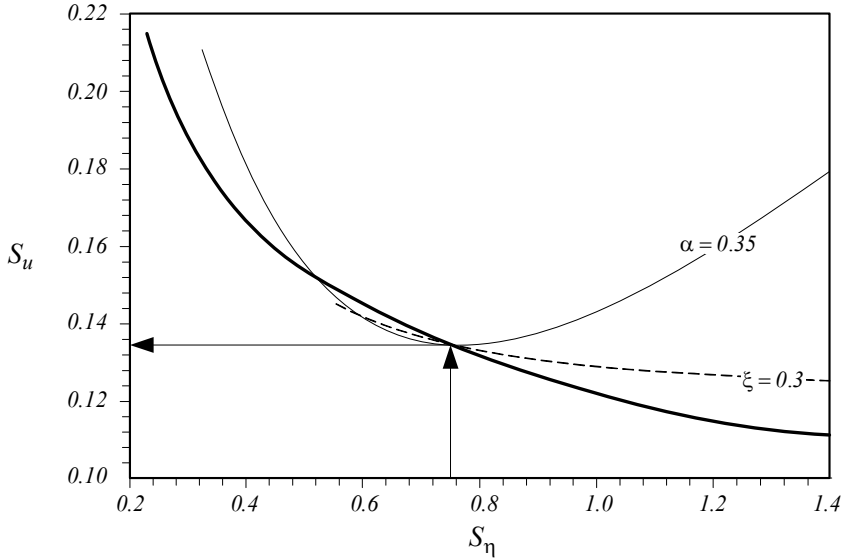
FIGURE 15.25. Application of the design chart for $S_\eta = 1$, which indicates the optimal values $\xi \approx 0.3$ and $\alpha \approx 0.35$.

car optimal. Mathematically, it is equivalent to the following minimization problem:

$$\frac{\partial S_u}{\partial S_\eta} = 0 \tag{15.83}$$

$$\frac{\partial^2 S_u}{\partial S_\eta^2} > 0 \tag{15.84}$$

To use the design curve and determine optimal stiffness $k_s$ and damping $c_s$ for the main suspension of the system, we start from an estimate value for $S_\eta$ on the horizontal axis and draw a vertical line to hit the optimal curve. The intersection point indicates the optimal $\alpha$ and $\xi$ for the $S_\eta$.

Figure 15.25 illustrates a sample application for $S_\eta = 0.75$, which indicates $\xi \approx 0.3$ and $\alpha \approx 0.35$ for optimal suspension. Having $\alpha$, and $\xi$, determines the optimal value of $k_s$ and $c_s$.

$$k_s = \alpha^2 \frac{m_s}{m_u} k_u \tag{15.85}$$

$$c_s = 2\xi \sqrt{k_s m_s} \tag{15.86}$$

**Proof.** The $RMS$ of a function $g(\alpha, \xi, \varepsilon, \omega)$, is defined by

$$RMS(g) = \sqrt{\frac{1}{\omega_2 - \omega_1} \int_{\omega_1}^{\omega_2} g^2(\alpha, \xi, \varepsilon, \omega) \, d\omega}$$

where $\omega_2 \leq \omega \leq \omega_1$ is called the *working frequency range*. Let's consider a working range for the excitation frequency $0 \leq f \left(= \frac{\omega}{2\pi}\right) \leq 20\,\mathrm{Hz}$ to include almost all ground vehicles, especially road vehicles, and show the $RMS$ of $\eta$ and $u$ by

$$S_\eta = RMS(\eta) \tag{15.87}$$
$$S_u = RMS(u). \tag{15.88}$$

In applied vehicle dynamics, we usually measure frequencies in $[\,\mathrm{Hz}\,]$, instead of $[\,\mathrm{rad/\,s}\,]$, we perform design calculations based on cyclic frequencies $f$ and $f_n$ in $[\,\mathrm{Hz}\,]$, and we do analytic calculation based on angular frequencies $\omega$ and $\omega_n$ in $[\,\mathrm{rad/\,s}\,]$.

To calculate $S_\eta$ and $S_u$ over the working frequency range

$$S_\eta = \sqrt{\frac{1}{40\pi} \int_0^{40\pi} \eta^2 dr} \tag{15.89}$$

$$S_u = \sqrt{\frac{1}{40\pi} \int_0^{40\pi} u^2 dr}$$

$$= \alpha^2 \sqrt{\frac{1}{40\pi} \int_0^{40\pi} r^2 \mu^2 dr} \tag{15.90}$$

we first find integrals of $\eta^2$ and $u^2$.

$$
\int u^2 dr = \frac{1}{2Z_6}\left(\frac{1}{Z_1} + Z_1 Z_5\right) \ln\left(\frac{r - Z_1}{r + Z_1}\right)
$$
$$
+ \frac{1}{2Z_7}\left(\frac{1}{Z_2} + Z_2 Z_5\right) \ln\left(\frac{r - Z_2}{r + Z_2}\right)
$$
$$
+ \frac{1}{2Z_8}\left(\frac{1}{Z_3} + Z_3 Z_5\right) \ln\left(\frac{r - Z_3}{r + Z_3}\right)
$$
$$
+ \frac{1}{2Z_9}\left(\frac{1}{Z_4} + Z_4 Z_5\right) \ln\left(\frac{r - Z_4}{r + Z_4}\right) \tag{15.91}
$$

$$
\int \eta^2 dr = \frac{Z_1^3}{2Z_6} \ln\left(\frac{r - Z_1}{r + Z_1}\right) + + \frac{Z_2^3}{2Z_7} \ln\left(\frac{r - Z_2}{r + Z_2}\right)
$$
$$
+ \frac{Z_3^3}{2Z_8} \ln\left(\frac{r - Z_3}{r + Z_3}\right) + \frac{Z_4^3}{2Z_9} \ln\left(\frac{r - Z_4}{r + Z_4}\right) \tag{15.92}
$$

The parameters $Z_1$ through $Z_9$ are as follows:

$$Z_1 = \frac{1}{2}\frac{-Z_{19} + \sqrt{Z_{23}}}{Z_{19}}\frac{1}{4}\frac{Z_{15}}{Z_{14}} \tag{15.93}$$

$$Z_2 = \frac{1}{2}\frac{-Z_{19} - \sqrt{Z_{23}}}{Z_{19}}\frac{1}{4}\frac{Z_{15}}{Z_{14}} \tag{15.94}$$

$$Z_3 = \frac{1}{2}\frac{-Z_{19} + \sqrt{Z_{24}}}{Z_{19}}\frac{1}{4}\frac{Z_{15}}{Z_{14}} \tag{15.95}$$

$$Z_4 = \frac{1}{2}\frac{-Z_{19} - \sqrt{Z_{24}}}{Z_{19}}\frac{1}{4}\frac{Z_{15}}{Z_{14}} \tag{15.96}$$

$$Z_5 = 4\xi^2 \tag{15.97}$$
$$Z_6 = \left(Z_1^2 - Z_2^2\right)\left(Z_1^2 - Z_3^2\right)\left(Z_1^2 - Z_4^2\right) \tag{15.98}$$
$$Z_7 = \left(Z_2^2 - Z_3^2\right)\left(Z_2^2 - Z_3^2\right)\left(Z_2^2 - Z_1^2\right) \tag{15.99}$$
$$Z_8 = \left(Z_3^2 - Z_4^2\right)\left(Z_3^2 - Z_1^2\right)\left(Z_3^2 - Z_2^2\right) \tag{15.100}$$
$$Z_9 = \left(Z_4^2 - Z_1^2\right)\left(Z_4^2 - Z_2^2\right)\left(Z_4^2 - Z_3^2\right) \tag{15.101}$$

$$Z_{10} = \frac{1}{6}\sqrt[3]{Z_{20}} + \frac{8Z_{13} + \frac{2}{3}Z_{11}^2}{\sqrt[3]{Z_{20}}} + \frac{1}{3}Z_{11} \tag{15.102}$$

$$Z_{11} = \frac{8Z_{16}Z_{14} - 3Z_{15}^3}{8Z_{14}^3} \tag{15.103}$$

$$Z_{12} = -\frac{4Z_{16}Z_{14}Z_{15} - Z_{15}^3 - 8Z_{14}^2Z_{17}}{8Z_{14}^3} \tag{15.104}$$

$$Z_{13} = \frac{-64Z_{14}^2Z_{17}Z_{15} + 256Z_{14}^3Z_{18} + 16Z_{14}Z_{15}^2Z_{16} - 3Z_{15}^4}{256Z_{14}^4} \tag{15.105}$$

$$Z_{14} = \alpha^4 \tag{15.106}$$

$$Z_{15} = -2\alpha^4\left(1 + \varepsilon\right) - 2\alpha^2 + 4\left(1 + \varepsilon\right)^2\alpha^4\xi^2 \tag{15.107}$$
$$Z_{16} = -8\alpha^2\xi^2\left(1 + \varepsilon\right) + \left(1 + \varepsilon\right)^2\alpha^4 - 2\alpha^2\left(2 + \varepsilon\right) + 1 \tag{15.108}$$
$$Z_{17} = 4\xi^2 - 2\alpha^2\left(1 + \varepsilon\right) - 2 \tag{15.109}$$
$$Z_{18} = 1 \tag{15.110}$$

$$Z_{19} = Z_{10} - Z_{11} \tag{15.111}$$
$$Z_{20} = Z_{21} + 12\sqrt{Z_{22}} \tag{15.112}$$
$$Z_{21} = -288Z_{11}Z_{13} + 108Z_{12}^2 + 8Z_{11}^3 \tag{15.113}$$

$$Z_{22} = -768Z_{13}^3 + 384Z_{11}^2Z_{13}^2 - 48Z_{13}Z_{11}^4$$
$$-432Z_{11}Z_{12}^2Z_{13} + 81Z_{12}^4 + 12Z_{11}^3Z_{12}^2 \tag{15.114}$$

$$Z_{23} = Z_{19}\left(Z_{11} - Z_{10}\right) - 2Z_{12}Z_{19}^{3/2} \tag{15.115}$$
$$Z_{24} = Z_{19}\left(Z_{11} + Z_{10}\right) + 2Z_{12}Z_{19}^{3/2} \tag{15.116}$$
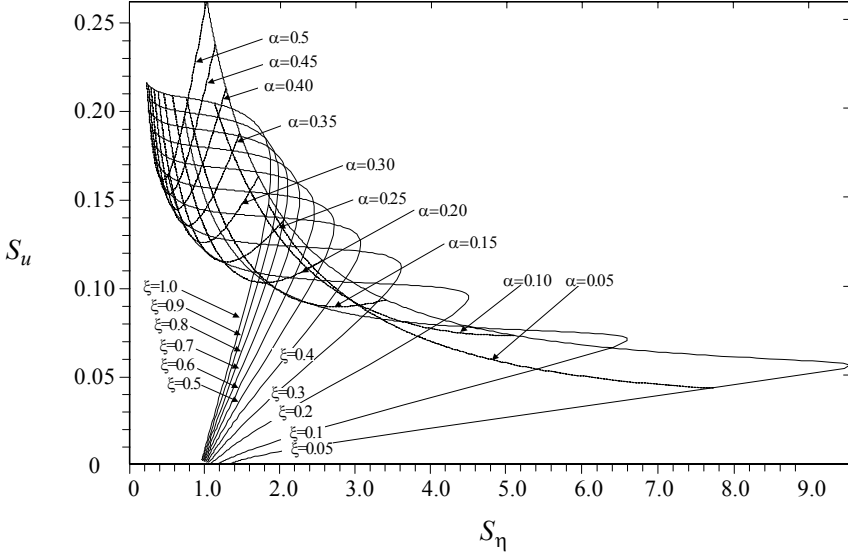
FIGURE 15.26. RMS of absolute acceleration, $S_u = RMS(u)$ vreus RMS of relative displacement $S_\eta = RMS(\eta)$, for a quarter car model.

Now the required RMS, $S_\eta$, and $S_u$, over the frequency range $0 < f < 20\,\mathrm{Hz}$, can be calculated analytically from Equations (15.89) and (15.90).

Equations (15.89) and (15.90) show that both $S_\eta$ and $S_u$ are functions of only three variables: $\varepsilon$, $\alpha$, and $\xi$.

$$S_\eta = S_\eta(\varepsilon, \alpha, \xi) \qquad (15.117)$$
$$S_u = S_u(\varepsilon, \alpha, \xi) \qquad (15.118)$$

In applied vehicle dynamics, $\varepsilon$ is usually a fixed parameter, so, any pair of design parameters $(\alpha, \xi)$ determines $S_\eta$ and $S_u$ uniquely. Let's set

$$\varepsilon = 3 \qquad (15.119)$$

Using Equations (15.89) and (15.90), we may draw Figure 15.26 to illustrate how $S_u$ behaves with respect to $S_\eta$ when $\alpha$ and $\xi$ vary. Keeping $\alpha$ constant and varying $\xi$, it is possible to minimize $S_u$ with respect to $S_\eta$. The minimum points make the optimal curve and determine the best $\alpha$ and $\xi$. The way to use the optimal design curve is to estimate a value for $S_\eta$ or $S_u$ and find the associated point on the design curve. A magnified picture is shown in Figure 15.24.

The horizontal axis is the root mean square of relative displacement, $S_\eta = RMS(\eta)$, and the vertical axis is the root mean square of absolute acceleration, $S_u = RMS(u)$.
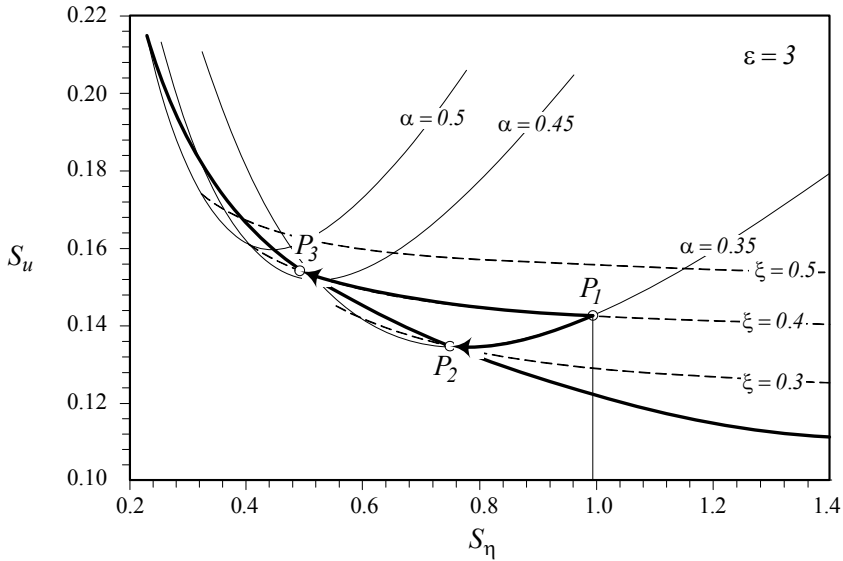
FIGURE 15.27. Two optimal designs at points $P_2$ and $P_3$ for an off-optimal design quarter car at point $P_1$.

The optimal curve indicates that softening a suspension decreases the body acceleration, however, it requires a large room for relative displacement. Due to physical constraints, the wheel travel is limited, and hence, we must design the suspension such that to use the available suspension travel, and decrease the body acceleration as low as possible. Mathematically it is equivalent to (15.83) and (15.84). ■

**Example 533** *Examination of the optimal quarter car model.*
*To examine the optimal design curve and compare practical ways to make a suspension optimal, we assume that there is a quarter car with an off-optimal suspension, indicated by point $P_1$ in Figure 15.27.*

$$\varepsilon = 3 \tag{15.120}$$

$$\alpha = 0.35 \tag{15.121}$$

$$\xi = 0.4 \tag{15.122}$$

*To optimize the suspension practically, we may keep the stiffness constant and change the damper to a corresponding optimal value, or keep the damping constant and change the stiffness to a corresponding optimal value. However, if it is possible, we may change both, stiffness and damping to a point on the optimal curve depending on the physical constraints and requirements.*
*Point $P_2$ in Figure 15.27 has the same $\alpha$ as point $P_1$ with an optimal*
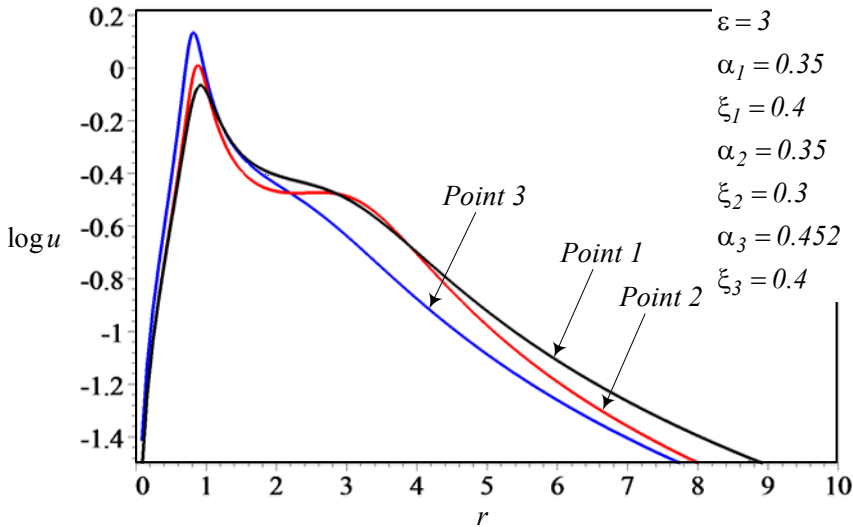
FIGURE 15.28. Absolute displacement frequency response $\mu$ for points $P_1$, $P_2$, and $P_3$ shown in Figure 15.27.

*damping ratio $\xi \approx 0.3$. Point $P_3$ in Figure 15.27 has the same $\xi$ as point $P_1$ with an optimal natural frequency ratio $\alpha \approx 0.452$. Hence, points $P_2$ and $P_3$ are two alternative optimal designs for the off-optimal point $P_1$.*

*Figure 15.28 compares the acceleration frequency response $\log u$ for the three points $P_1$, $P_2$, and $P_3$. Point $P_3$ has the minimum acceleration frequency response. Figure 15.29 depicts the absolute displacement frequency response $\log \mu$ and Figure 15.30 compares the relative displacement frequency response $\log \eta$ for the there points $P_1$, $P_2$, $P_3$. These Figures show that both points $P_2$ and $P_3$ introduce better suspension than point $P_1$. Suspension $P_2$ has a higher level of acceleration but needs less relative suspension travel than suspension $P_3$. Suspension $P_3$ has a lower level of acceleration, but it needs more room for suspension travel than suspension $P_2$.*

**Example 534** *Comparison of an off-optimal quarter car model with two optimal.*

*An alternative method to optimize an off-optimal suspension is to keep the RMS of relative displacement $S_\eta$ or absolute acceleration $S_u$ constant and find the associated point on the optimal design curve. Figure 15.31 illustrates two alternative optimal designs, points $P_2$ and $P_3$, for an off-optimal design at point $P_1$.*

*The mass ratio is assumed to be*

$$\varepsilon = 3 \qquad\qquad (15.123)$$
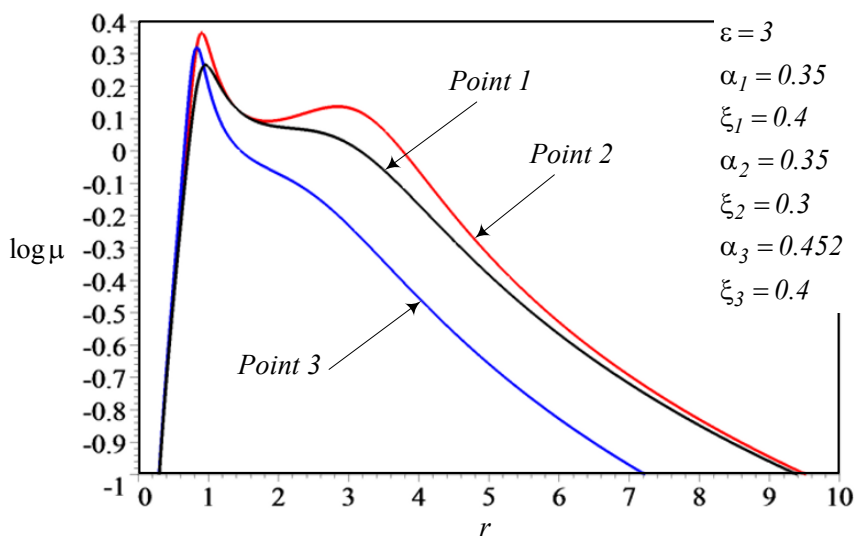
FIGURE 15.29. Relative displacement frequency response $\eta$ for points $P_1$, $P_2$, and $P_3$ shown in Figure 15.27.
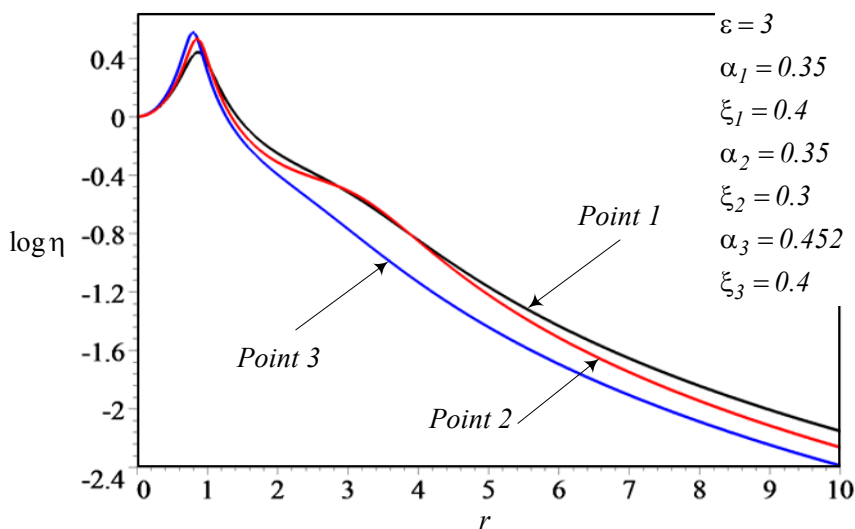


FIGURE 15.30. Absolute acceleration frequency response $u$ for points $P_1$, $P_2$, and $P_3$ shown in Figure 15.27.
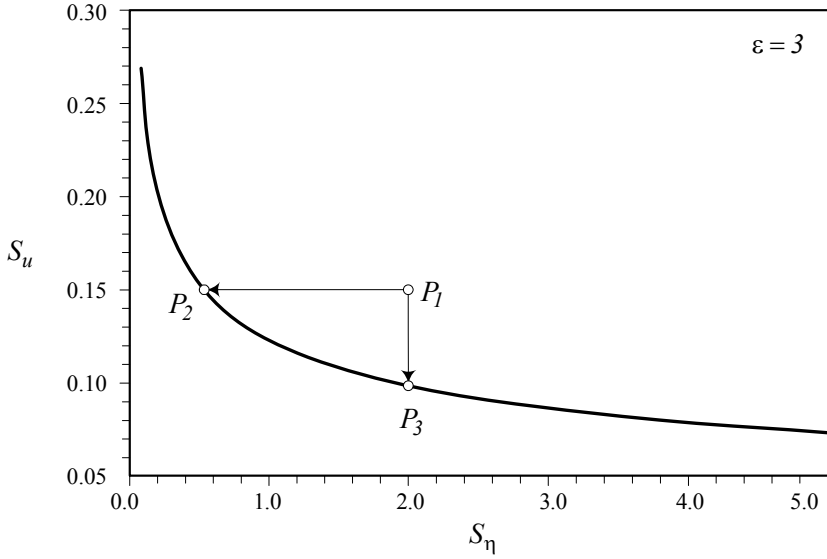
FIGURE 15.31. Two alternative optimal designs at points $P_2$ and $P_3$ for an off-optimal design quarter car at point $P_1$.

and the suspension characteristics at $P_1$ are

$$\xi = 0.0465 \tag{15.124}$$
$$\alpha = 0.265 \tag{15.125}$$
$$S_\eta = 2 \tag{15.126}$$
$$S_u = 0.15. \tag{15.127}$$

The optimal point corresponding to $P_1$ with the same $S_u$ is at $P_2$ with the characteristics

$$\xi = 0.23 \tag{15.128}$$
$$\alpha = 0.45 \tag{15.129}$$
$$S_\eta = 0.543 \tag{15.130}$$
$$S_u = 0.15 \tag{15.131}$$

and the optimal point with the same $S_\eta$ as point $P_1$ is a point at $P_2$ with the characteristics:

$$\xi = 0.0949 \tag{15.132}$$
$$\alpha = 0.1858 \tag{15.133}$$
$$S_\eta = 2 \tag{15.134}$$
$$S_u = 0.0982 \tag{15.135}$$
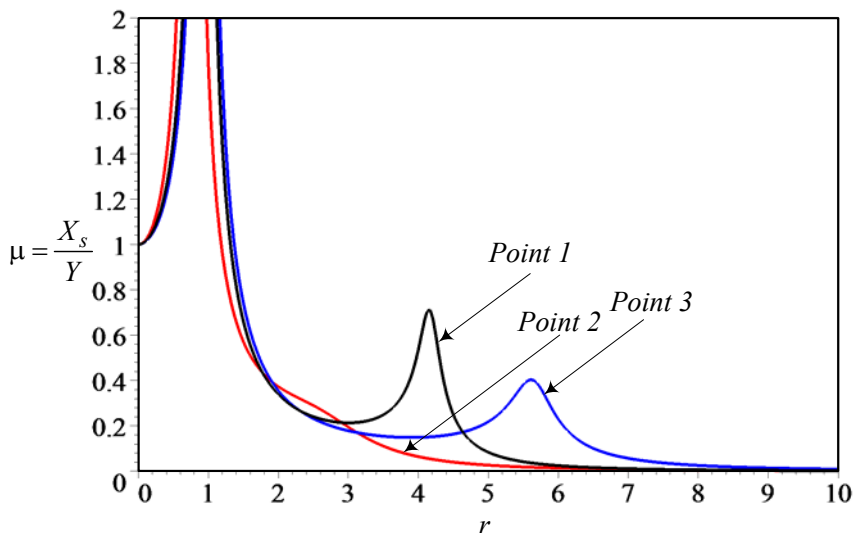
FIGURE 15.32. Absolute displacement frequency response $\mu$ for points $P_1$, $P_2$, and $P_3$ shown in Figure 15.31.

Figure 15.32 depicts the sprung mass vibration amplitude $\mu$, which shows that both points $P_2$ and $P_3$ have lower overall amplitude specially at second resonance. Figure 15.33 shows the amplitude of relative displacement $\eta$ between sprung and unsprung masses. The amplitude of absolute acceleration of the sprung mass $u$ is shown in Figure 15.34.

**Example 535 ★** *Natural frequencies and vibration isolation requirements.*
   Road irregularities are the most common destructive source of excitation for passenger cars. Therefore, the natural frequencies of vehicle system are the primary factors in determining design requirements for conventional isolators. The natural frequency of the vehicle body supported by the primary suspension is usually between $0.2\,\text{Hz}$ and $2\,\text{Hz}$, and the natural frequency of the unsprung mass, called wheel hop frequency, usually is between $2\,\text{Hz}$ and $20\,\text{Hz}$. The higher values generally apply to military vehicles.
   The isolation of sprung mass from the uneven road can be improved by using a soft spring, which reduces the primary natural frequency. Lowering the natural frequency always improves the ride comfort, however it causes a design problem due to the large relative motion between the sprung and unsprung masses. One of the most important constraints that suspension system designers have to consider is the rattle-space constraint, the maximum allowable relative displacement. Additional factors are imposed by the overall stability, reliability, and economic or cost factors.

$$\eta = \frac{Z}{Y}$$
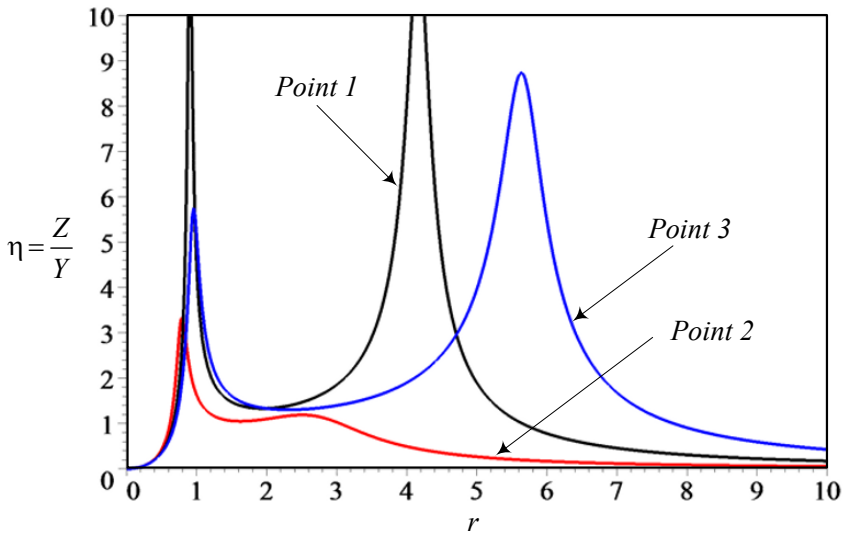
FIGURE 15.33. Relative displacement frequency response $\eta$ for points $P_1$, $P_2$, and $P_3$ shown in Figure 15.31.



$$u = \frac{\ddot{X}_s}{\omega_n^2 Y}$$
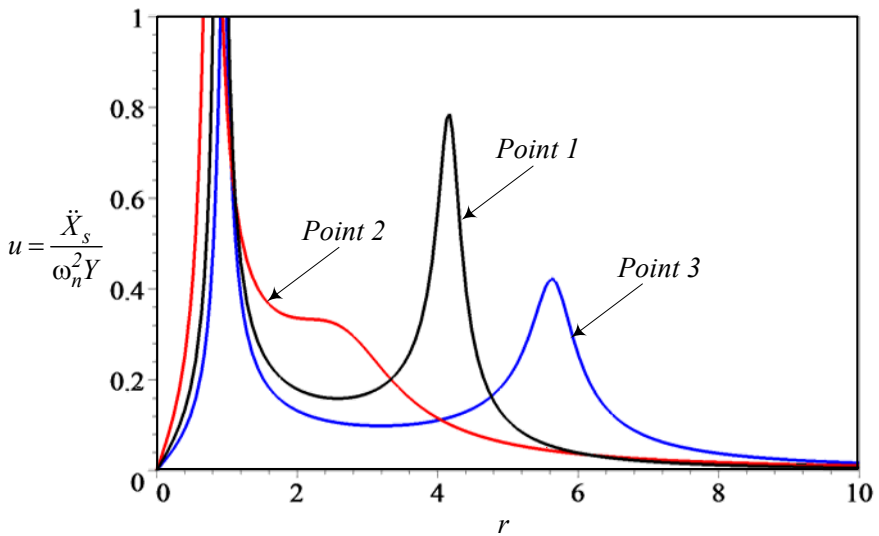
FIGURE 15.34. Absolute acceleration frequency response $u$ for points $P_1$, $P_2$, and $P_3$ shown in Figure 15.31.
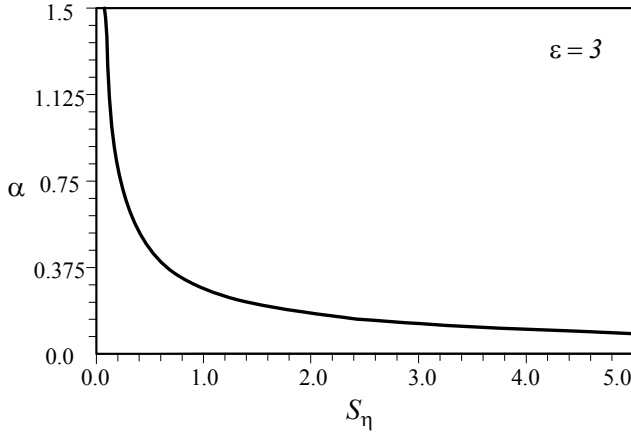
FIGURE 15.35. The optimal value of $\alpha$ as a function of relative displacement RMS $S_\eta$.

**Example 536** *Optimal characteristics variation.*

*We may collect the optimal $\alpha$ and $\xi$ and plot them as shown in Figures 15.35 and 15.36. These figures illustrate the trend of their variation. The optimal value of both $\alpha$ and $\xi$ are decreasing functions of relative displacement RMS $S_\eta$. So, when more room is available, we may reduce $\alpha$ and $\xi$ and have a softer suspension for better ride comfort. Figure 15.37 shows how the optimal $\alpha$ and $\xi$ change with each other.*

## 15.5   ★ Optimization Based on Natural Frequency and Wheel Travel

Assume a fixed value for the mass ratio $\varepsilon$ and natural frequency ratio $\alpha$. So the position of nodes in the frequency response plot are fixed. Then, an optimal value for damping ratio $\xi$ is

$$\xi^\star = \frac{\sqrt{Z_{35}}}{Z_{36}} \sqrt{\sqrt{Z_{37}^2 - 8\alpha^2} + Z_{37} - \frac{8\alpha^2}{Z_{35}}} \qquad (15.136)$$

where

$$Z_{35} = \alpha^2 (1 + \varepsilon) + 1 \qquad (15.137)$$
$$Z_{36} = 4\alpha\sqrt{1 + \varepsilon} \qquad (15.138)$$
$$Z_{37} = \left(2\alpha^2 (1 + \varepsilon) + 1\right). \qquad (15.139)$$

The optimal damping ratio $\xi^\star$ causes the second resonant amplitude $\mu_2$ to occur at the second invariant frequency $r_2$. The value of relative displace-
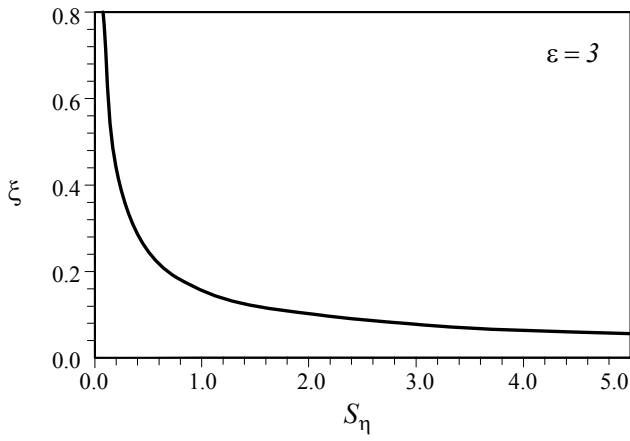
FIGURE 15.36. The optimal value of $\xi$ as a function of relative displacement RMS $S_\eta$.
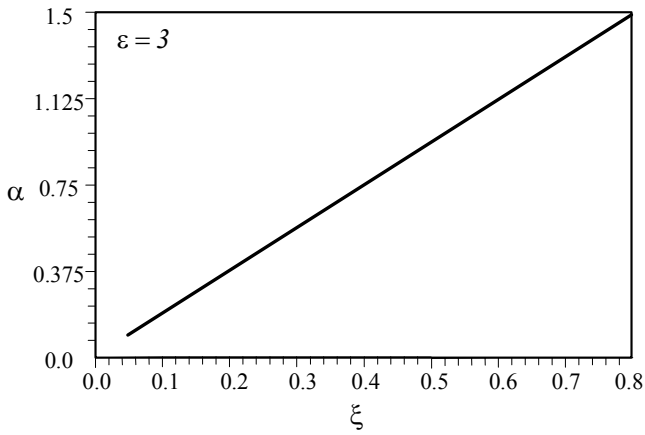


FIGURE 15.37. The optimal $\alpha$ versus optimal $\xi$ for a quarter car with $\varepsilon = 3$.

ment $\eta$ at $r = r_2$ for $\xi = \xi^\star$ is,

$$\eta_2 = \sqrt{\frac{\left(\sqrt{Z_{37}^2 - 8\alpha^2} - Z_{35}\right)\sqrt{1+\varepsilon}}{2\alpha^2\left(Z_{28}\sqrt{Z_{37}^2 - Z_{29}}\right)}} \tag{15.140}$$

where,

$$
\begin{aligned}
Z_{28} &= 4\alpha^4(1+\varepsilon)^4 - 4\alpha^2(1+\varepsilon)^2(1-\varepsilon) + (1+\varepsilon^2) \quad (15.141) \\
Z_{29} &= -8\alpha^6(1+\varepsilon)^5 + 12\alpha^4(1+\varepsilon)^3(1-\varepsilon) \\
&\quad -2\alpha^4(1+\varepsilon)\left(1+3\varepsilon^2 - 2\varepsilon\right) + (1+\varepsilon^2) \quad (15.142)
\end{aligned}
$$

**Proof.** Natural frequencies of the sprung and unsprung masses, as given in Equations (15.46) and (15.47), are related to $\varepsilon$ and $\alpha$. When $\varepsilon$ is set, we can evaluate $\alpha$ by considering the maximum permissible static deflection, which in turn adjusts the value of natural frequencies. If the values of $\alpha$ and $\varepsilon$ are determined and kept fixed, then the value of damping ratio $\xi$ which cause the first resonant amplitude to occur at the second node, can be determined as optimum damping. For a damping ratio less or greater than the optimum, the resonant amplitude would be greater.

The frequencies related to the maximum of $\mu$ are obtained by differentiating $\mu$ with respect to $r$ and setting the result equal to zero

$$
\begin{aligned}
\frac{\partial \mu}{\partial r} &= \frac{1}{2\mu}\frac{\partial \mu^2}{\partial r} \\
&= \frac{1}{Z_{25}^2}\left(8\xi^2 r Z_{25} - Z_{26} - Z_{27}\right) = 0 \quad (15.143)
\end{aligned}
$$

where

$$
\begin{aligned}
Z_{25} &= \left[r^2\left(r^2\alpha^2 - 1\right) + \left(1 - (1+\varepsilon)r^2\alpha^2\right)\right]^2 \\
&\quad + 4\xi^2 r^2\left(1 - (1+\varepsilon)r^2\alpha^2\right)^2 \quad (15.144) \\
Z_{26} &= 8\xi^2 r\left(4\xi^2 r^2 + 1\right)\left(3r^2\alpha^2(1+\varepsilon) - 1\right) \\
&\quad \times \left(r^2\alpha^2(1+\varepsilon) - 1\right) \quad (15.145) \\
Z_{27} &= 4r\left(4\xi^2 r^2 + 1\right)\left[r^2\alpha^2(1+\varepsilon) + r^2\left(1 - r^2\alpha^2\right) - 1\right] \\
&\quad \times \left[\alpha^2(1+\varepsilon) - 2r^2\alpha^2 + 1\right]. \quad (15.146)
\end{aligned}
$$

Now, the optimal value $\xi^\star$ in Equation (15.136) is obtained if the frequency ratio $r$ in Equation (15.143) is replaced with $r_2$ given by Equation (15.65). The optimal damping ratio $\xi^\star$ makes $\mu$ have a maximum at the second invariant frequency $r_2$. Figure 15.38 illustrates an example of frequency response $\mu$ for different $\xi$ including $\xi = \xi^\star$.

Figure 15.39 shows the sensitivity of $\xi^\star$ to $\alpha$ and $\varepsilon$.
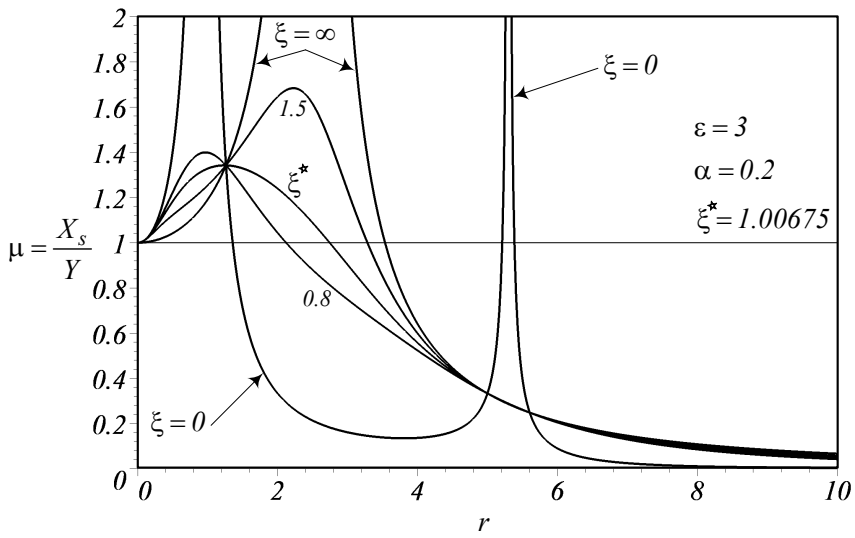
FIGURE 15.38. A sample of frequency response $\mu$ for different $\xi$ including $\xi = \xi^{\star}$.
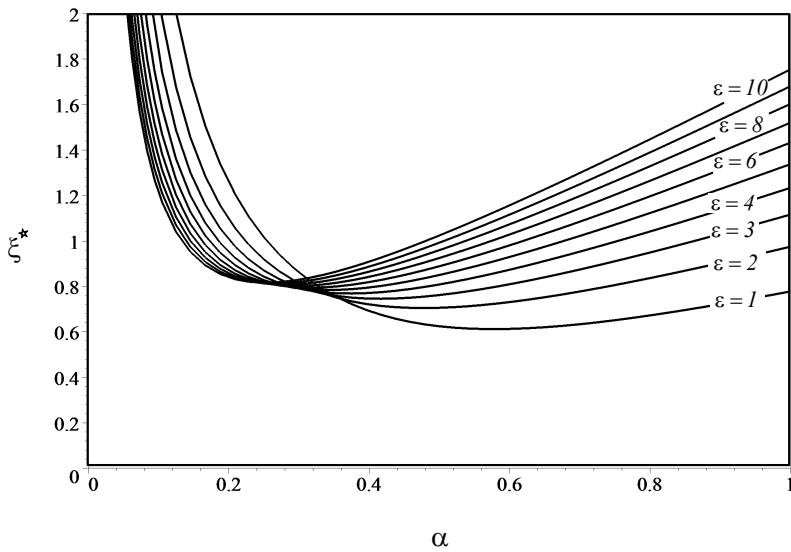


FIGURE 15.39. the optimal value $\xi^{\star}$ as a function of $\alpha$ and $\varepsilon$.
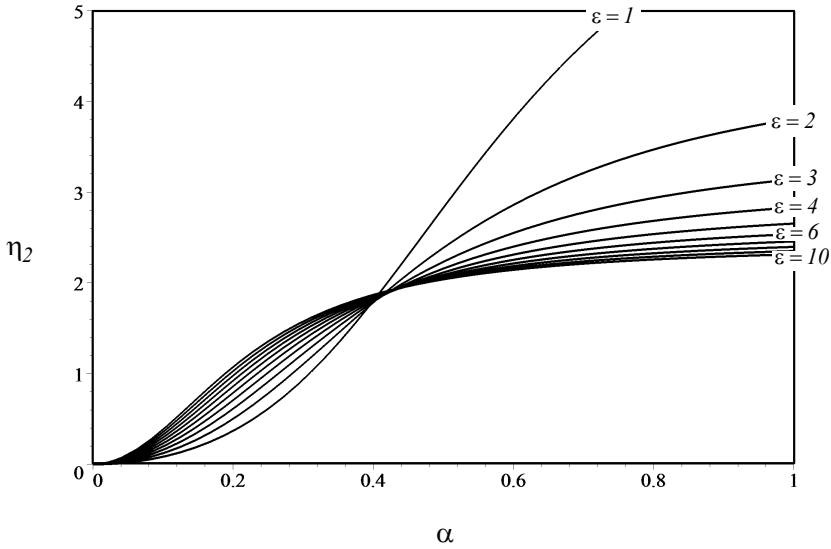
FIGURE 15.40. The behavior of $\eta_2$ for $\xi = \xi^\star$ as a function of $\alpha$ and $\varepsilon$.

Substituting $\xi^\star$ in the general expression of $\mu$, the absolute maximum value of $\mu$ would be equal to $\mu_2$ given by equation (15.52). Substituting $r = r_2$ and $\xi = \xi^\star$ in Equation (15.25) gives us Equation (15.140) for $\eta_2$. The lower the natural frequency of the suspension, the more effective the isolation from road irregularities. So, the stiffness of the main spring must be as low as possible. Figure 15.40 shows the behavior of $\eta_2$ for $\xi = \xi^\star$. ■

**Example 537** *Nodes in $\eta_2$ for $\xi = \xi^\star$.*
*The relative displacement at second node, $\eta_2$, is a monotonically increasing function of $\alpha$, and has two invariant points. The invariant points of $\eta$ may be found from*

$$\pm r^2 \left[ \left( r^2 \alpha^2 - 1 \right) + \left( 1 - (1 + \varepsilon)\,\alpha^2 \right) \right]$$
$$= \left[ r^2 \left( r^2 \alpha^2 - 1 \right) + \left( 1 - (1 + \varepsilon)\,r^2\alpha^2 \right) \right]^2$$
$$+ r^2 \left( 1 - (1 + \varepsilon)\,r^2\alpha^2 \right) \tag{15.147}$$

*that are,*

$$r_1 \;=\; 0 \qquad \eta_1 = 0 \tag{15.148}$$

$$r_{n_0} \;=\; \frac{1}{\alpha\sqrt{1+\varepsilon}} \qquad \eta_{n_0} = 1 + \frac{1}{\varepsilon} \tag{15.149}$$

*The value of $\mu$ at $r_{n_0}$ is,*

$$\mu_{n_0} \;=\; \frac{\alpha^2}{\varepsilon^2}\,(1+\varepsilon)^3 \left[ 4\xi^2 + \alpha^2\,(1+\varepsilon) \right]. \tag{15.150}$$

**Example 538** ★ *Maximum value of $\eta$.*

*Figure 15.4 shows that $\eta$ has a node at the intersection of the curves for $\xi = 0$ and $\xi = \infty$. There might be a specific damping ratio to make $\eta$ have a maximum at the node. To find the maximum value of $\eta$, we have to solve the following equation for $r$:*

$$
\begin{aligned}
\frac{\partial \eta}{\partial r} &= \frac{1}{2\eta} \frac{\partial \eta^2}{\partial r} \\
&= \frac{1}{Z_{23}^2} \left( 4r^3 Z_{23} - Z_{30} - Z_{31} \right) \quad (15.151)
\end{aligned}
$$

*where*

$$
\begin{aligned}
Z_{23} &= \left[ r^2 \left( r^2 \alpha^2 - 1 \right) + \left( 1 - (1+\varepsilon) r^2 \alpha^2 \right) \right]^2 \\
&\quad + 4\xi^2 r^2 \left( 1 - (1+\varepsilon) r^2 \alpha^2 \right)^2 \quad (15.152) \\
Z_{30} &= 8\xi^2 r^5 \left[ 3r^2 \alpha^2 (1+\varepsilon) - 1 \right] \left( r^2 \alpha^2 (1+\varepsilon) - 1 \right) \quad (15.153) \\
Z_{31} &= 4r^5 \left[ r^2 \alpha^2 (1+\varepsilon) + r^2 \left( 1 - r^2 \alpha^2 \right) - 1 \right] \\
&\quad \times \left[ \alpha^2 (1+\varepsilon) - 2r^2 \alpha^2 + 1 \right] \quad (15.154)
\end{aligned}
$$

*Therefore, the maximum $\eta$ occurs at the roots of the equation:*

$$
Z_{32} r^8 + Z_{33} r^6 + Z_{34} r^2 - 1 = 0 \quad (15.155)
$$

*where*

$$
\begin{aligned}
Z_{32} &= \alpha^4 \quad (15.156) \\
Z_{33} &= 2\alpha^4 \xi^2 (1+\varepsilon)^2 + \alpha^4 (1+\varepsilon) - \alpha^2 \quad (15.157) \\
Z_{34} &= \alpha^2 (1+\varepsilon) + 1 - 2\xi^2. \quad (15.158)
\end{aligned}
$$

*Equation (15.155) has two positive roots when $\xi$ is less than a specific value of damping ratio, $\xi_\eta$, and one positive root when $\xi$ is greater than $\xi_\eta$, where,*

$$
\xi_\eta = \xi_\eta (\alpha, \xi, \varepsilon). \quad (15.159)
$$

*The positive roots of Equation (15.155) are $r_5$ and $r_6$, and the corresponding relative displacements are denoted by $\eta_5$ and $\eta_6$, where $r_5 < r_6$. The invariant frequencies $r_5$ and $r_6$ would be equal when $\xi \geq \xi_\eta$, and they approach $r_{n_0}$ when $\xi$ goes to infinity. The invariant frequency $\eta_6$ is greater than $\eta_5$ as long as $\xi \leq \xi_\eta$, and they are equal when $\xi \geq \xi_\eta$. The relative displacements $\eta_5$ and $\eta_6$ are monotonically decreasing functions of $\xi$, and they approach to $\eta_{n_0}$ when $\xi$ goes to infinity.*

*It is seen from (15.149) that the invariant point at $r_{n_0}$, depends on $\alpha$ and $\varepsilon$, but the value of $\eta_{n_0}$ depends only on $\varepsilon$. If $\varepsilon$ is given, then $\eta_{n_0}$ is fixed. Therefore, the maximum value of the relative displacement, $\eta$, cannot be less than $\eta_{n_0}$, and we cannot find any real value for $\xi$ that cause the maximum of $\eta$ to occur at $r_{n_0}$. The optimum value of $\xi$ could be found when we adjust the maximum value of $\eta_6$, and is equated to the allowed wheel travel.*

# 15.6   Summary

The vertical vibration of vehicles may be modeled as a two-DOF linear system called quarter car model. One-fourth of the body mass, known as sprung mass, is suspended by the main suspension of the vehicle $k_s$ and $c_s$. The main suspension $k_s$ and $c_s$ are mounted on a wheel of the vehicle, known as unsprung mass. The wheel is sitting on the road by a tire with stiffness $k_u$.

Assuming the vehicle is running on a harmonically bumped road we are able to find the frequency responses of the sprung and unsprung masses, and relative displacement can be found analytically by taking advantage of the linearity of the system. The frequency response of the sprung mass has four nodes. The first and fourth nodes are usually out of resonance or of working frequency range. The middle nodes sit at different sides of $\mu = 1$, and therefore, they cannot be equated and Frahm optimization cannot be applied.

The root mean square of the absolute acceleration and relative displacement can be found analytically by applying the RMS optimization method. The RMS optimization method is based on minimizing the absolute acceleration RMS with respect to the relative displacement RMS. The result of RMS optimization introduces an optimal design curve for a fixed mass ratio.

# 15.7   Key Symbols

| | |
|---|---|
| $a, \ddot{x}$ | acceleration |
| $c$ | damping |
| $c_s$ | main suspension damper |
| $[c]$ | damping matrix |
| $d_1$ | road wave length |
| $d_2$ | road wave amplitude |
| $D$ | dissipation function |
| $f,\ \mathbf{F}$ | force |
| $f = \frac{1}{T}$ | cyclic frequency $[\,\mathrm{Hz}\,]$ |
| $f_c$ | damper force |
| $f_k$ | spring force |
| $f_n$ | cyclic natural frequency $[\,\mathrm{Hz}\,]$ |
| $g\left(r^2\right)$ | charactristic equation |
| $k$ | stiffness |
| $k_s$ | main suspension spring stiffness |
| $k_u$ | tire stiffness |
| $k_{eq}$ | equivalent stiffness |
| $[k]$ | stiffness matrix |
| $K$ | kinetic energy |
| $\mathcal{L}$ | Lagrangean |
| $m$ | mass |
| $m_s$ | sprung mass |
| $m_u$ | unsprung mass |
| $[m]$ | mass matrix |
| $r = \omega/\omega_s$ | excitation frequency ratio |
| $r_i,\ i \in N$ | nodal frequency ratio |
| $r_n = \omega_n/\omega_s$ | natural frequency ratio |
| $S_u = RMS(u)$ | RMS of $u$ |
| $S_\eta = RMS(\eta)$ | RMS of $\eta$ |
| $t$ | time |
| $T$ | period |
| $u = r^2\alpha^2\mu$ | sprung mass acceleration frequency response |
| $v = r^2\alpha^2\tau$ | unsprung mass acceleration frequency response |
| $V$ | potential energy |
| $x$ | absolute displacement |
| $x_s$ | sprung mass displacement |
| $x_u$ | unsprung mass displacement |
| $X$ | steady-state amplitude of $x$ |
| $X_s$ | steady-state amplitude of $x_s$ |
| $X_u$ | steady-state amplitude of $x_u$ |
| $y$ | base excitation displacement |
| $Y$ | steady-state amplitude of $y$ |

| | |
|---|---|
| $z$ | relative displacement |
| $Z$ | steady-state amplitude of $z$ |
| $Z_i$ | short notation parameter |

| | |
|---|---|
| $\alpha = \omega_s/\omega_u$ | sprung mass ratio |
| $\varepsilon = m_s/m_u$ | sprung mass ratio |
| $\eta = |Z/Y|$ | sprung mass relative frequency response |
| $\mu = |X_s/Y|$ | sprung mass frequency response |
| $\xi = c_s/\left(2\sqrt{k_s m_s}\right)$ | damping ratio |
| $\xi^{\star}$ | optimal damping ratio |
| $\tau = |X_u/Y|$ | unsprung mass frequency response |
| $\omega = 2\pi f$ | angular frequency $[\,\mathrm{rad/\,s}]$ |
| $\omega_s = \sqrt{k_s/m_s}$ | sprung mass frequency |
| $\omega_u = \sqrt{k_u/m_u}$ | unsprung mass frequency |
| $\omega_n$ | natural frequency |

Subscript

| | |
|---|---|
| $i \in N$ | node number |
| $n$ | natural |
| $s$ | sprung |
| $u$ | unsprung |

# Exercises

1. 10Quarter car natural frequencies.

   Determine the natural frequencies of a quarter car with the following characteristics:

   $$\begin{aligned}
   m_s &= 275\,\text{kg} \\
   m_u &= 45\,\text{kg} \\
   k_u &= 200000\,\text{N}/\text{m} \\
   k_s &= 10000\,\text{N}/\text{m}.
   \end{aligned}$$

2. Equations of motion.

   Derive the equations of motion for the quarter car model that is shown in Figure 15.1, using the relative coordinates:

   (a)

   $$\begin{aligned}
   z_s &= x_s - y \\
   z_u &= x_u - y
   \end{aligned}$$

   (b)

   $$\begin{aligned}
   z &= x_s - x_u \\
   z_u &= x_u - y
   \end{aligned}$$

   (c)

   $$\begin{aligned}
   z &= x_s - x_u \\
   z_s &= x_s - y
   \end{aligned}$$

3. ★ Natural frequencies for different coordinates.

   Determine and compare the natural frequencies of the three cases in Exercise 2 and check their equality by employing the numerical data of Exercise 10.

4. Quarter car nodal frequencies.

   Determine the nodal frequencies of a quarter car with the following characteristics:

   $$\begin{aligned}
   m_s &= 275\,\text{kg} \\
   m_u &= 45\,\text{kg} \\
   k_u &= 200000\,\text{N}/\text{m} \\
   k_s &= 10000\,\text{N}/\text{m}.
   \end{aligned}$$

   Check the order of the nodal frequencies with the natural frequencies found in Exercise 10.

5. Frequency responses of a quarter car.

A car is moving on a wavy road with a wave length $d_1 = 20\,\mathrm{m}$ and wave amplitude $d_2 = 0.08\,\mathrm{m}$.

$$
\begin{aligned}
m_s &= 200\,\mathrm{kg} \\
m_u &= 40\,\mathrm{kg} \\
k_u &= 220000\,\mathrm{N/m} \\
k_s &= 8000\,\mathrm{N/m}.
\end{aligned}
$$

Determine the steady-state amplitude $X_s$, $X_u$, and $Z$ if the car is moving at:

(a) $v = 30\,\mathrm{km/h}$
(b) $v = 60\,\mathrm{km/h}$
(c) $v = 120\,\mathrm{km/h}$.

6. Quarter car suspension optimization.

Consider a car with

$$
\begin{aligned}
m_s &= 200\,\mathrm{kg} \\
m_u &= 40\,\mathrm{kg} \\
k_u &= 220000\,\mathrm{N/m} \\
S_\eta &= 0.75
\end{aligned}
$$

and determine the optimal suspension parameters.

A quarter car has $\alpha = 0.45$ and $\xi = 0.4$. What is the required wheel travel if the road excitation has an amplitude $Y = 1\,\mathrm{cm}$?

7. ★ Quarter car and time response.

Find the optimal suspension of a quarter car with the following characteristics:

$$
\begin{aligned}
m_s &= 220\,\mathrm{kg} \\
m_u &= 42\,\mathrm{kg} \\
k_u &= 150000\,\mathrm{N/m} \\
S_\eta &= 0.75
\end{aligned}
$$

and determine the response of the optimal quarter car to a unit step excitation.

8. ★ Quarter car mathematical model.

In the mathematical model of the quarter car, we assumed the tire is always sticking to the road. Determine the condition at which the tire leaves the surface of the road.

9. Optimal damping.

   Consider a quarter car with $\alpha = 0.45$ and $\varepsilon = 0.4$. Determine the optimal damping ratio $\xi^\star$.

# References

## Chapter 1

American Association of State Highway Officials, AASHO, Highway Definitions, June 1968.

American National Standard, Manual on Classification of Motor Vehicle Traffic Accidents, Sixth Edition, National Safety Council, Itasca, Illinois, 1996.

Cossalter, V., 2002, *Motorcycle Dynamics*, Race Dynamic Publishing, Greendale, WI.

National Committee on Uniform Traffic Laws and Ordinances, Uniform Vehicle Code and Model Traffic Ordinance, 1992.

United States Code, Title 23. Highways. Washington: U.S. Government Printing Office.

## Chapter 2

Cossalter, V., 2002, *Motorcycle Dynamics*, Race Dynamic Publishing, Greendale, WI.

Genta, G., 2007, *Motor Vehicle Dynamics, Modeling and Simulation*, World Scientific, Singapore.

Norbe, J. P., 1980, *The Car and its Weels, A Guide to Modern Suspension Systems*, TAB Books Inc.

Wong, J. Y., 2001, *Theory of Ground Vehicles*, John Wiley & Sons, New York.

## Chapter 3

Andrzejewski, R., and Awrejcewicz, J., 2005, *Nonlinear Dynamics of a Wheeled Vehicle*, Springer-Verlag, New York.

Cossalter, V., 2002, *Motorcycle Dynamics*, Race Dynamic Publishing, Greendale, WI.

Ellis, J. R., 1994, *Vehicle Handling Kinematics*, Mechanical Engineering Publications Limited, London.

Genta, G., 2007, *Motor Vehicle Dynamics, Modeling and Simulation*, World Scientific, Singapore.

Haney, P., 2003, *The Racing and High–Performance Tire*, SAE Inc.

Milliken, W. F., and Milliken, D. L., 2002, *Chassis Design*, SAE Inc.

Milliken, W. F., and Milliken, D. L., 1995, *Race Car Vehicle Dynamics*, SAE Inc.

Norbe, J. P., 1980, *The Car and its Wheels, A Guide to Modern Suspension Systems*, TAB Books Inc.

Wong, J. Y., 2001, *Theory of Ground Vehicles*, John Wiley & Sons, New York.

# Chapter 4

Cossalter, V., 2002, *Motorcycle Dynamics*, Race Dynamic Publishing, Greendale, WI.

Genta, G., 2007, *Motor Vehicle Dynamics, Modeling and Simulation*, World Scientific, Singapore.

Milliken, W. F., and Milliken, D. L., 1995, *Race Car Vehicle Dynamics*, SAE Inc.

Wong, J. Y., 2001, *Theory of Ground Vehicles*, John Wiley & Sons, New York.

# Chapter 5

Asada, H., and Slotine, J. J. E., 1986, *Robot Analysis and Control*, John Wiley & Son, New York.

Bottema, O., and Roth, B., 1979, *Theoretical Kinematics*, North-Holland Publication, Amsterdam, The Netherlands.

Goldstein, H., Poole, C., and Safko, J., 2002, *Classical Mechanics*, 3rd ed., Addison Wesley, New York.

Hunt, K. H., 1978, *Kinematic Geometry of Mechanisms*, Oxford University Press, London.

Kane, T. R., Likins, P. W., and Levinson, D. A., 1983, *Spacecraft Dynamics*, McGraw-Hill, New York.

MacMillan, W. D., 1936, *Dynamics of Rigid Bodies*, McGraw-Hill, New York.

Mason, M. T., 2001, *Mechanics of Robotic Manipulation*, MIT Press, Cambridge, Massachusetts.

Murray, R. M., Li, Z., and Sastry, S. S. S., 1994, *A Mathematical Introduction to Robotic Manipulation*, CRC Press, Boca Raton, Florida.

Nikravesh, P., 1988, *Computer-Aided Analysis of Mechanical Systems*, Prentice Hall, New Jersey.

Paul, R. P., 1981, *Robot Manipulators: Mathematics, Programming, and Control*, MIT Press, Cambridge, Massachusetts.

Rosenberg, R. M., 1977, *Analytical Dynamics of Discrete Systems*, Plenum Publishing Co., New York.

Tsai, L. W., 1999, *Robot Analysis*, John Wiley & Sons, New York.

Schaub, H., and Junkins, J. L., 2003, *Analytical Mechanics of Space Systems*, AIAA Educational Series, American Institute of Aeronautics and Astronautics, Inc., Reston, Virginia.

Spong, M. W., Hutchinson, S., and Vidyasagar, M., 2006, *Robot Modeling and Control*, John Wiley & Sons, New York.

# Chapter 6

Beatty, M. F., 1986, *Principles of Engineering Mechanics, Vol. 1, Kinematics-The Geometry of Motion*, Plenum Press, New York.

Jazar, R. N., 2007, *Applied Robotics: Kinematics, Dynamics, and Control*, Springer, New York.

Hartenberg, R. S., and Denavit, J., 1964, *Kinematic Synthesis of Linkages*, McGraw-Hill Book Co.

Hunt, K. H., 1978, *Kinematic Geometry of Mechanisms*, Oxford University Press, London.

Nikravesh, P., 1988, *Computer-Aided Analysis of Mechanical Systems*, Prentice Hall, New Jersey.

Soni, A. H., 1974, *Mechanism Synthesis and Analysis*, McGraw-Hill Book Co.

# Chapter 7

Andrzejewski, R., and Awrejcewicz, J., 2005, *Nonlinear Dynamics of a Wheeled Vehicle*, Springer-Verlag, New York.

Cossalter, V., 2002, *Motorcycle Dynamics*, Race Dynamic Publishing, Greendale, WI.

Ellis, J. R., 1994, *Vehicle Handling Kinematics*, Mechanical Engineering Publications Limited, London.

Genta, G., 2007, *Motor Vehicle Dynamics, Modeling and Simulation*, World Scientific, Singapore.

Haney, P., 2003, *The Racing and High–Performance Tire*, SAE Inc.

Milliken, W. F., and Milliken, D. L., 2002, *Chassis Design*, SAE Inc.

Milliken, W. F., and Milliken, D. L., 1995, *Race Car Vehicle Dynamics*, SAE Inc.

Norbe, J. P., 1980, *The Car and its Wheels, A Guide to Modern Suspension Systems*, TAB Books Inc.

Rajamani, R., 2006, *Vehicle Dynamics and Control*, Springer-Verlag, New York.

Wong, J. Y., 2001, *Theory of Ground Vehicles*, John Wiley & Sons, New York.

# Chapter 8

Andrzejewski, R., and Awrejcewicz, J., 2005, *Nonlinear Dynamics of a Wheeled Vehicle*, Springer-Verlag, New York.

Cossalter, V., 2002, *Motorcycle Dynamics*, Race Dynamic Publishing, Greendale, WI.

Dixon, J. C., 1996, *Tire, Suspension and Handling*, SAE Inc.

Ellis, J. R., 1994, *Vehicle Handling Kinematics*, Mechanical Engineering Publications Limited, London.

Genta, G., 2007, *Motor Vehicle Dynamics, Modeling and Simulation*, World Scientific, Singapore.

Haney, P., 2003, *The Racing and High–Performance Tire*, SAE Inc.

Milliken, W. F., and Milliken, D. L., 2002, *Chassis Design*, SAE Inc.

Milliken, W. F., and Milliken, D. L., 1995, *Race Car Vehicle Dynamics*, SAE Inc.

Norbe, J. P., 1980, *The Car and its Wheels, A Guide to Modern Suspension Systems*, TAB Books Inc.

# Chapter 9

Goldstein, H., Poole, C., and Safko, J., 2002, *Classical Mechanics*, 3rd ed., Addison Wesley, New York.

Jazar, R. N., 2007, *Applied Robotics: Kinematics, Dynamics, and Control*, Springer, New York.

Mason, M. T., 2001, *Mechanics of Robotic Manipulation*, MIT Press, Cambridge, Massachusetts.

Rosenberg, R. M., 1977, *Analytical Dynamics of Discrete Systems*, Plenum Publishing Co., New York.

MacMillan, W. D., 1936, *Dynamics of Rigid Bodies*, McGraw-Hill, New York.

Schaub, H., and Junkins, J. L., 2003, *Analytical Mechanics of Space Systems*, AIAA Educational Series, American Institute of Aeronautics and Astronautics, Inc., Reston, Virginia.

Skalmierski, B., 1991, *Mechanics*, Elsevier, Poland.

Wittacker, E. T., 1947, *A Treatise on the Analytical Dynamics of Particles and Rigid Bodies*, 4th ed., Cambridge University Press, New York.

# Chapter 10

Cossalter, V., 2002, *Motorcycle Dynamics*, Race Dynamic Publishing, Greendale, WI.

Ellis, J. R., 1994, *Vehicle Handling Kinematics*, Mechanical Engineering Publications Limited, London.

Genta, G., 2007, *Motor Vehicle Dynamics, Modeling and Simulation*, World Scientific, Singapore.

Haney, P., 2003, *The Racing and High–Performance Tire*, SAE Inc.

Milliken, W. F., and Milliken, D. L., 2002, *Chassis Design*, SAE Inc.

Milliken, W. F., and Milliken, D. L., 1995, *Race Car Vehicle Dynamics*, SAE Inc.

Rajamani, R., 2006, *Vehicle Dynamics and Control*, Springer-Verlag, New York.

Wong, J. Y., 2001, *Theory of Ground Vehicles*, John Wiley & Sons, New York.

# Chapter 11

Cossalter, V., 2002, *Motorcycle Dynamics*, Race Dynamic Publishing, Greendale, WI.

Ellis, J. R., 1994, *Vehicle Handling Kinematics*, Mechanical Engineering Publications Limited, London.

Genta, G., 2007, *Motor Vehicle Dynamics, Modeling and Simulation*, World Scientific, Singapore.

Milliken, W. F., and Milliken, D. L., 1995, *Race Car Vehicle Dynamics*, SAE Inc.

Rajamani, R., 2006, *Vehicle Dynamics and Control*, Springer-Verlag, New York.

# Chapter 12

Balachandran, B., Magrab, E. B., 2003, *Vibrations*, Brooks/Cole, Pacific Grove, CA.

Benaroya, H., 2004, *Mechaniscal Vibration: Analysis, Uncertainities, and Control*, Marcel Dekker, New York.

Del Pedro, M., and Pahud, P., 1991, *Vibration Mechanics*, Kluwer Academic Publishers, The Netherland.

Den Hartog, J. P., 1934, *Mechanical Vibrations*, McGraw-Hill, New York.

Harris, C. M., and Piersol, A. G., 2002, *Harris' Shock and Vibration Handbook*, McGraw-Hill, New York.

Inman, D., 2007, *Engineering Vibrations*, Prentice Hall, New York.

Meirovitch, L., 2002, *Fundamentals of Vibrations*, McGraw-Hill, New York.

Meirovitch, L., 1967, *Analytical Methods in Vibrations*, Macmillan, New York.

Jazar, R. N., Kazemi, M., and Borhani, S., 1992, *Mechanical Vibrations*, Ettehad Publications, Tehran. (in Persian).

Rao, S. S., 2003, *Mechanical Vibrations*, Prentice Hall, New York.

Roseau, M., 1987, *Vibrations in Mechanical Systems*, Springer-Verlag, Berlin.

Shabana, A. A., 1997, *Vibration of Discrete and Continuous Systems*, Springer-Verlag, New York.

# Chapter 13

Balachandran, B., Magrab, E. B., 2003, *Vibrations*, Brooks/Cole, Pacific Grove, CA.

Benaroya, H., 2004, *Mechaniscal Vibration: Analysis, Uncertainities, and Control*, Marcel Dekker, New York.

Del Pedro, M., and Pahud, P., 1991, *Vibration Mechanics*, Kluwer Academic Publishers, Netherland.

Den Hartog, J. P., 1934, *Mechanical Vibrations*, McGraw-Hill, New York.

Harris, C. M., and Piersol, A. G., 2002, *Harris' Shock and Vibration Handbook*, McGraw-Hill, New York.

Inman, D., 2007, *Engineering Vibrations*, Prentice Hall, New York.

Jazar, R. N., Kazemi, M., and Borhani, S., 1992, *Mechanical Vibrations*, Ettehad Publications, Tehran. (in Persian).

Meirovitch, L., 2002, *Fundamentals of Vibrations*, McGraw-Hill, New York.

Meirovitch, L., 1967, *Analytical Methods in Vibrations*, Macmillan, New York.

Rao, S. S., 2003, *Mechanical Vibrations*, Prentice Hall, New York.

Roseau, M., 1987, *Vibrations in Mechanical Systems*, Springer-Verlag, Berlin.

Shabana, A. A., 1997, *Vibration of Discrete and Continuous Systems*, Springer-Verlag, New York.

# Chapter 14

Alkhatib, R., Jazar, R. N., and Golnaraghi, M. F., Optimal Design of Passive Linear Mounts with Genetic Algorithm Method, *Journal of Sound and Vibration,* ***275****(3-5), 665-691, 2004.*

Asada, H., and Slotine, J. J. E., 1986, *Robot Analysis and Control*, John Wiley & Sons, New York.

Murray, R. M., Li, Z., and Sastry, S. S. S., 1994, *A Mathematical Introduction to Robotic Manipulation*, CRC Press, Boca Raton, Florida.

Jazar, R. N., Alkhatib, R., and Golnaraghi, M. F., Root Mean Square Optimization Criterion for Vibration Behavior of Linear Quarter Car Using Analytical Methods, *Journal of Vehicle System Dynamics,* ***44****(6), 477–512, 2006.*

Jazar, R. N., and Golnaraghi, M. F., Engine Mounts for Automotive Applications: A Survey, *The Shock and Vibration Digest,* ***34****(5), 363-379, 2002.*

Jazar, R. N., Narimani, A., Golnaraghi, M. F., and Swanson, D. A., Practical Frequency and Time Optimal Design of Passive Linear Vibration Isolation Mounts, *Journal of Vehicle System Dynamics,* ***39****(6), 437-466, 2003.*

Roseau, M., 1987, *Vibrations in Mechanical Systems*, Springer-Verlag, Berlin.

Snowdon, J. C., 1968, *Vibration and shock in damped mechanical systems*, John Wiley, New York.

# Chapter 15

Esmailzadeh, E., 1978, Design Synthesis of a Vehicle Suspension System Using Multi-Parameter Optimization, *Vehicle System Dynamics,* ***7****, 83-96.*

Jazar, R. N., Alkhatib, R., and Golnaraghi, M. F., Root Mean Square Optimization Criterion for Vibration Behavior of Linear Quarter Car Using Analytical Methods, *Journal of Vehicle System Dynamics,* ***44****(6), 477–512, 2006.*

Jazar, R. N., Narimani, A., Golnaraghi, M. F., and Swanson, D. A., Practical Frequency and Time Optimal Design of Passive Linear V       ibration Isolation Mounts, *Journal of Vehicle System Dynamics,* ***39****(6), 437-466, 2003.*

Roseau, M., 1987, *Vibrations in Mechanical Systems*, Springer-Verlag, Berlin.

# Appendix A

# Frequency Response Curves

There are four types of *one*-DOF harmonically excited systems as shown in Figure 12.14:

    1− base excitation,
    2− eccentric excitation,
    3− eccentric base excitation,
    4− forced excitation.

The frequency responses of the four systemscan be summarized, labeled and shown as follows:

$$S_0 \quad = \quad \frac{X_F}{F/k} \tag{A.1}$$

$$= \quad \frac{1}{\sqrt{(1-r^2)^2 + (2\xi r)^2}} \tag{A.2}$$

$$S_1 \quad = \quad \frac{\dot{X}_F}{F/\sqrt{km}} \tag{A.3}$$

$$= \quad \frac{r}{\sqrt{(1-r^2)^2 + (2\xi r)^2}} \tag{A.4}$$

$$S_2 \quad = \quad \frac{\ddot{X}_F}{F/m} = \frac{Z_B}{Y} = \frac{X_E}{e\varepsilon_E} = \frac{Z_R}{e\varepsilon_R} \tag{A.5}$$

$$= \quad \frac{r^2}{\sqrt{(1-r^2)^2 + (2\xi r)^2}} \tag{A.6}$$

$$S_3 \quad = \quad \frac{\dot{Z}_B}{\omega_n Y} = \frac{\dot{X}_E}{e\varepsilon_E \omega_n} = \frac{\dot{Z}_R}{e\varepsilon_R \omega_n} \tag{A.7}$$

$$= \quad \frac{r^3}{\sqrt{(1-r^2)^2 + (2\xi r)^2}} \tag{A.8}$$

$$S_4 \quad = \quad \frac{\ddot{Z}_B}{\omega_n^2 Y} = \frac{\ddot{X}_E}{e\varepsilon_E \omega_n^2} = \frac{\ddot{Z}_R}{e\varepsilon_R \omega_n^2} \tag{A.9}$$

$$= \quad \frac{r^4}{\sqrt{(1-r^2)^2 + (2\xi r)^2}} \tag{A.10}$$
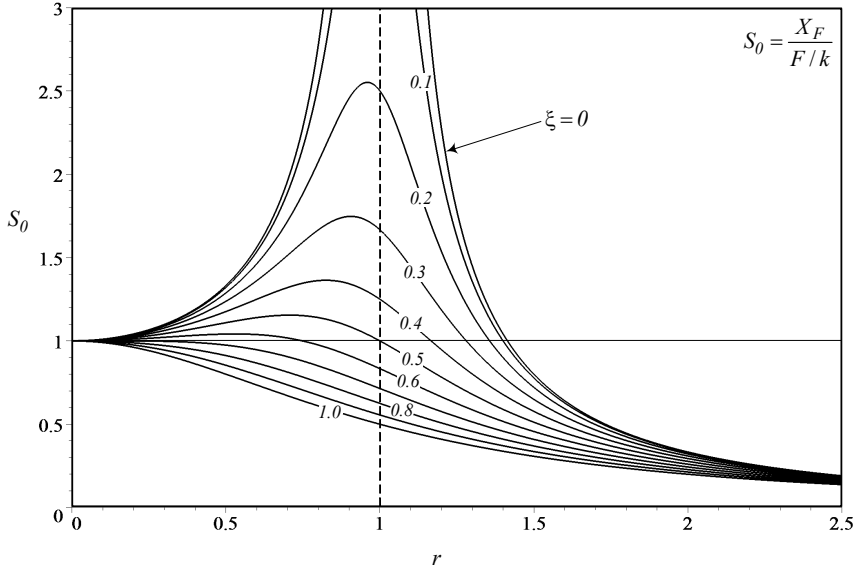
FIGURE A.1. Frequency response for $S_0$.

$$G_0 \quad = \quad \frac{F_{T_F}}{F} = \frac{X_B}{Y} \tag{A.11}$$

$$= \quad \frac{\sqrt{1 + (2\xi r)^2}}{\sqrt{(1 - r^2)^2 + (2\xi r)^2}} \tag{A.12}$$

$$G_1 \quad = \quad \frac{\dot{X}_B}{\omega_n Y} \tag{A.13}$$

$$= \quad \frac{r\sqrt{1 + (2\xi r)^2}}{\sqrt{(1 - r^2)^2 + (2\xi r)^2}} \tag{A.14}$$

$$G_2 \quad = \quad \frac{\ddot{X}_B}{\omega_n^2 Y} = \frac{F_{T_B}}{kY} = \frac{F_{T_E}}{e\omega_n^2 m_e} = \frac{F_{T_R}}{e\omega_n^2 m_e}\left(1 + \frac{m_b}{m}\right) \tag{A.15}$$

$$= \quad \frac{r^2\sqrt{1 + (2\xi r)^2}}{\sqrt{(1 - r^2)^2 + (2\xi r)^2}} \tag{A.16}$$

$$S_1 = \frac{\dot{X}_F}{F / \sqrt{km}}$$
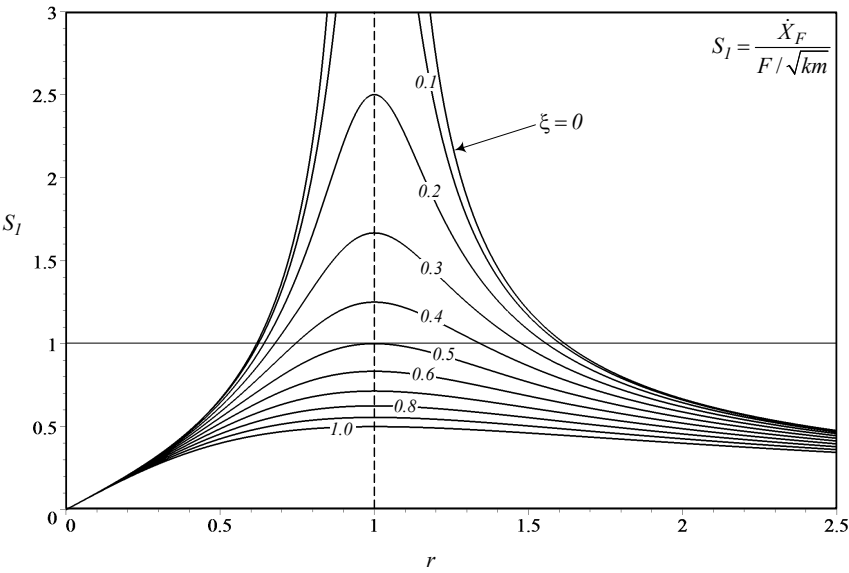
FIGURE A.2. Frequency response for $S_1$.



$$S_2 = \frac{\ddot{X}_F}{F / m} = \frac{Z_B}{Y} = \frac{X_E}{e\varepsilon_E} = \frac{Z_R}{e\varepsilon_R}$$
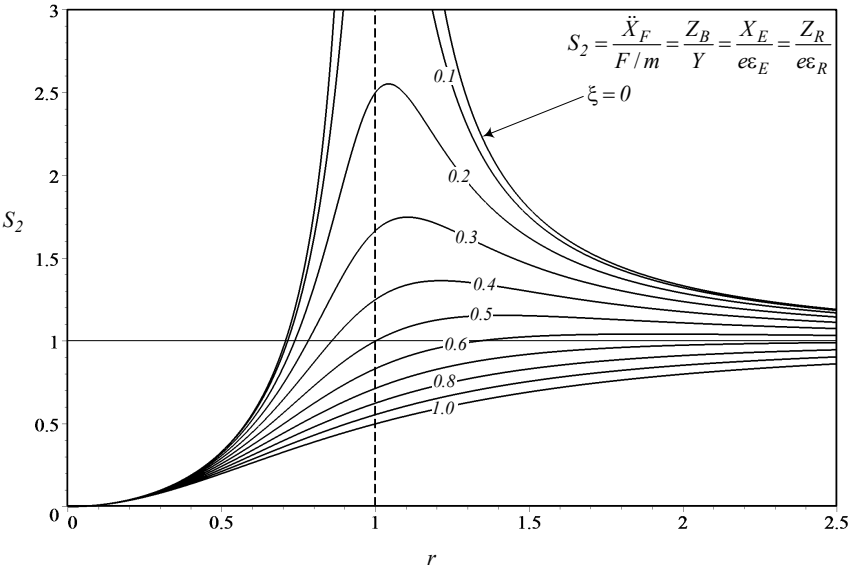
FIGURE A.3. Frequency response for $S_2$.

$$S_3 = \frac{\dot{Z}_B}{\omega_n Y} = \frac{\dot{X}_E}{e\varepsilon_E \omega_n} = \frac{\dot{Z}_R}{e\varepsilon_R \omega_n}$$
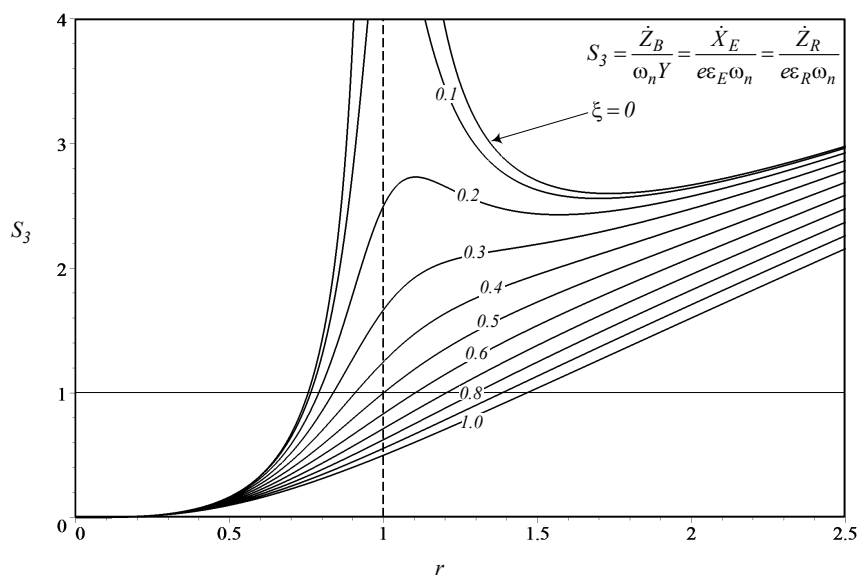
FIGURE A.4. Frequency response for $S_3$.



$$S_4 = \frac{\ddot{Z}_B}{\omega_n^2 Y} = \frac{\ddot{X}_E}{e\varepsilon_E \omega_n^2} = \frac{\ddot{Z}_R}{e\varepsilon_R \omega_n^2}$$
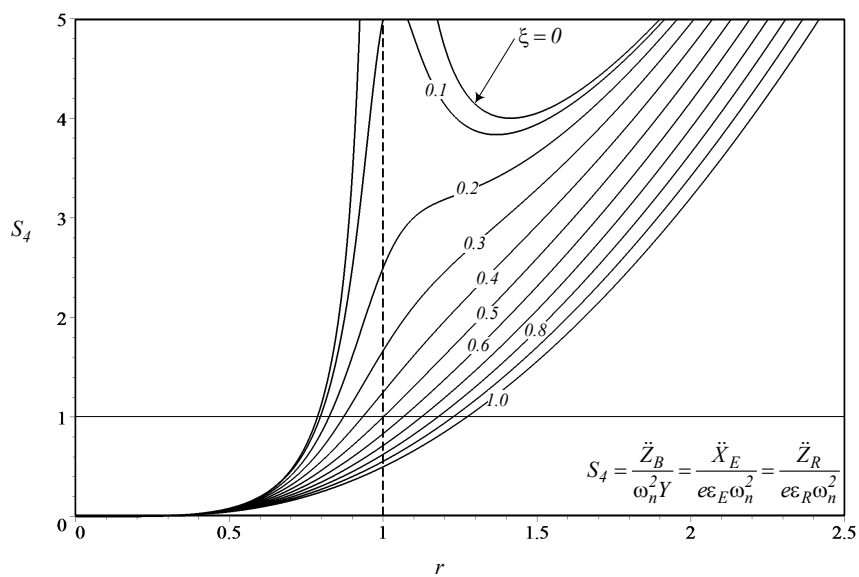
FIGURE A.5. Frequency response for $S_4$.
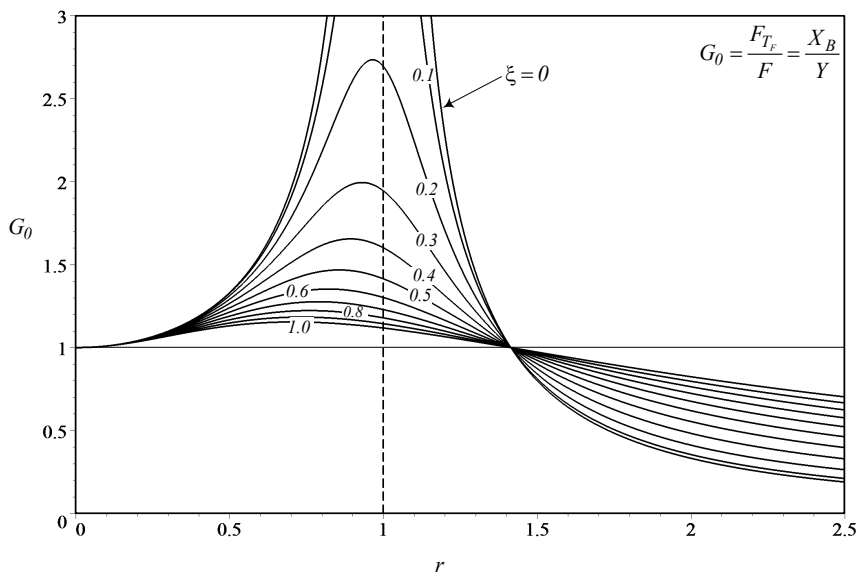
FIGURE A.6. Frequency response for $G_0$.
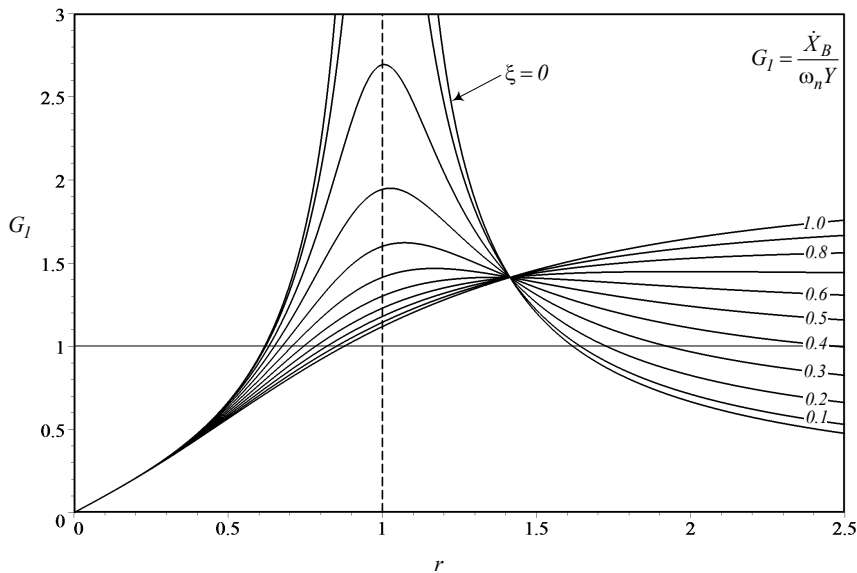


FIGURE A.7. Frequency response for $G_1$.
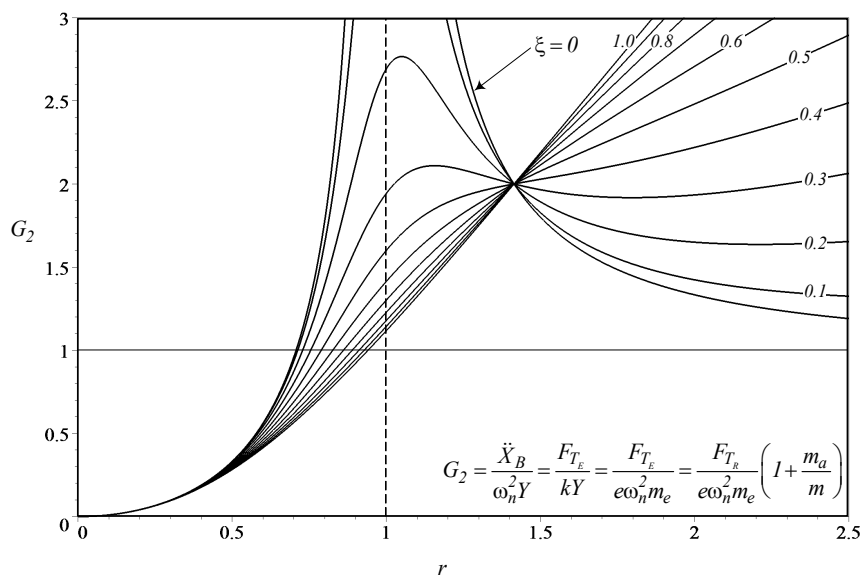
FIGURE A.8. Frequency response for $G_2$.

# Appendix B

# Trigonometric Formulas

Definitions in Terms of Exponentials

$$\cos z = \frac{e^{iz} + e^{-iz}}{2} \tag{B.1}$$

$$\sin z = \frac{e^{iz} - e^{-iz}}{2i} \tag{B.2}$$

$$\tan z = \frac{e^{iz} - e^{-iz}}{i\left(e^{iz} + e^{-iz}\right)} \tag{B.3}$$

$$e^{iz} = \cos z + i \sin z \tag{B.4}$$

$$e^{-iz} = \cos z - i \sin z \tag{B.5}$$

Angle Sum and Difference

$$\sin(\alpha \pm \beta) = \sin\alpha\cos\beta \pm \cos\alpha\sin\beta \tag{B.6}$$

$$\cos(\alpha \pm \beta) = \cos\alpha\cos\beta \mp \sin\alpha\sin\beta \tag{B.7}$$

$$\tan(\alpha \pm \beta) = \frac{\tan\alpha \pm \tan\beta}{1 \mp \tan\alpha\tan\beta} \tag{B.8}$$

$$\cot(\alpha \pm \beta) = \frac{\cot\alpha\cot\beta \mp 1}{\cot\beta \pm \cot\alpha} \tag{B.9}$$

Symmetry

$$\sin(-\alpha) = -\sin\alpha \tag{B.10}$$

$$\cos(-\alpha) = \cos\alpha \tag{B.11}$$

$$\tan(-\alpha) = -\tan\alpha \tag{B.12}$$

Multiple Angles

$$\sin(2\alpha) = 2\sin\alpha\cos\alpha = \frac{2\tan\alpha}{1 + \tan^2\alpha} \tag{B.13}$$

$$\cos(2\alpha) = 2\cos^2\alpha - 1 = 1 - 2\sin^2\alpha = \cos^2\alpha - \sin^2\alpha \tag{B.14}$$

$$\tan(2\alpha) = \frac{2\tan\alpha}{1 - \tan^2\alpha} \tag{B.15}$$

$$\cot(2\alpha) = \frac{\cot^2\alpha - 1}{2\cot\alpha} \tag{B.16}$$

$$\sin(3\alpha) = -4\sin^3\alpha + 3\sin\alpha \tag{B.17}$$

$$\cos(3\alpha) = 4\cos^3\alpha - 3\cos\alpha \tag{B.18}$$

$$\tan(3\alpha) = \frac{-\tan^3\alpha + 3\tan\alpha}{-3\tan^2\alpha + 1} \tag{B.19}$$

$$\sin(4\alpha) = -8\sin^3\alpha\cos\alpha + 4\sin\alpha\cos\alpha \tag{B.20}$$

$$\cos(4\alpha) = 8\cos^4\alpha - 8\cos^2\alpha + 1 \tag{B.21}$$

$$\tan(4\alpha) = \frac{-4\tan^3\alpha + 4\tan\alpha}{\tan^4\alpha - 6\tan^2\alpha + 1} \tag{B.22}$$

$$\sin(5\alpha) = 16\sin^5\alpha - 20\sin^3\alpha + 5\sin\alpha \tag{B.23}$$

$$\cos(5\alpha) = 16\cos^5\alpha - 20\cos^3\alpha + 5\cos\alpha \tag{B.24}$$

$$\sin(n\alpha) = 2\sin((n-1)\alpha)\cos\alpha - \sin((n-2)\alpha) \tag{B.25}$$

$$\cos(n\alpha) = 2\cos((n-1)\alpha)\cos\alpha - \cos((n-2)\alpha) \tag{B.26}$$

$$\tan(n\alpha) = \frac{\tan((n-1)\alpha) + \tan\alpha}{1 - \tan((n-1)\alpha)\tan\alpha} \tag{B.27}$$

## Half Angle

$$\cos\left(\frac{\alpha}{2}\right) = \pm\sqrt{\frac{1+\cos\alpha}{2}} \tag{B.28}$$

$$\sin\left(\frac{\alpha}{2}\right) = \pm\sqrt{\frac{1-\cos\alpha}{2}} \tag{B.29}$$

$$\tan\left(\frac{\alpha}{2}\right) = \frac{1-\cos\alpha}{\sin\alpha} = \frac{\sin\alpha}{1+\cos\alpha} = \pm\sqrt{\frac{1-\cos\alpha}{1+\cos\alpha}} \tag{B.30}$$

$$\sin\alpha = \frac{2\tan\frac{\alpha}{2}}{1+\tan^2\frac{\alpha}{2}} \tag{B.31}$$

$$\cos\alpha = \frac{1-\tan^2\frac{\alpha}{2}}{1+\tan^2\frac{\alpha}{2}} \tag{B.32}$$

## Powers of Functions

$$\sin^2\alpha = \frac{1}{2}\left(1-\cos(2\alpha)\right) \tag{B.33}$$

$$\sin\alpha\cos\alpha = \frac{1}{2}\sin(2\alpha) \tag{B.34}$$

$$\cos^2\alpha = \frac{1}{2}\left(1+\cos(2\alpha)\right) \tag{B.35}$$

$$\sin^3\alpha = \frac{1}{4}\left(3\sin(\alpha)-\sin(3\alpha)\right) \tag{B.36}$$

$$\sin^2 \alpha \cos \alpha = \frac{1}{4} \left( \cos \alpha - 3 \cos(3\alpha) \right) \tag{B.37}$$

$$\sin \alpha \cos^2 \alpha = \frac{1}{4} \left( \sin \alpha + \sin(3\alpha) \right) \tag{B.38}$$

$$\cos^3 \alpha = \frac{1}{4} \left( \cos(3\alpha) + 3 \cos \alpha \right) \tag{B.39}$$

$$\sin^4 \alpha = \frac{1}{8} \left( 3 - 4 \cos(2\alpha) + \cos(4\alpha) \right) \tag{B.40}$$

$$\sin^3 \alpha \cos \alpha = \frac{1}{8} \left( 2 \sin(2\alpha) - \sin(4\alpha) \right) \tag{B.41}$$

$$\sin^2 \alpha \cos^2 \alpha = \frac{1}{8} \left( 1 - \cos(4\alpha) \right) \tag{B.42}$$

$$\sin \alpha \cos^3 \alpha = \frac{1}{8} \left( 2 \sin(2\alpha) + \sin(4\alpha) \right) \tag{B.43}$$

$$\cos^4 \alpha = \frac{1}{8} \left( 3 + 4 \cos(2\alpha) + \cos(4\alpha) \right) \tag{B.44}$$

$$\sin^5 \alpha = \frac{1}{16} \left( 10 \sin \alpha - 5 \sin(3\alpha) + \sin(5\alpha) \right) \tag{B.45}$$

$$\sin^4 \alpha \cos \alpha = \frac{1}{16} \left( 2 \cos \alpha - 3 \cos(3\alpha) + \cos(5\alpha) \right) \tag{B.46}$$

$$\sin^3 \alpha \cos^2 \alpha = \frac{1}{16} \left( 2 \sin \alpha + \sin(3\alpha) - \sin(5\alpha) \right) \tag{B.47}$$

$$\sin^2 \alpha \cos^3 \alpha = \frac{1}{16} \left( 2 \cos \alpha - 3 \cos(3\alpha) - 5 \cos(5\alpha) \right) \tag{B.48}$$

$$\sin \alpha \cos^4 \alpha = \frac{1}{16} \left( 2 \sin \alpha + 3 \sin(3\alpha) + \sin(5\alpha) \right) \tag{B.49}$$

$$\cos^5 \alpha = \frac{1}{16} \left( 10 \cos \alpha + 5 \cos(3\alpha) + \cos(5\alpha) \right) \tag{B.50}$$

$$\tan^2 \alpha = \frac{1 - \cos(2\alpha)}{1 + \cos(2\alpha)} \tag{B.51}$$

Products of sin and cos

$$\cos \alpha \cos \beta = \frac{1}{2} \cos(\alpha - \beta) + \frac{1}{2} \cos(\alpha + \beta) \tag{B.52}$$

$$\sin \alpha \sin \beta = \frac{1}{2} \cos(\alpha - \beta) - \frac{1}{2} \cos(\alpha + \beta) \tag{B.53}$$

$$\sin \alpha \cos \beta = \frac{1}{2} \sin(\alpha - \beta) + \frac{1}{2} \sin(\alpha + \beta) \tag{B.54}$$

$$\cos \alpha \sin \beta = \frac{1}{2} \sin(\alpha + \beta) - \frac{1}{2} \sin(\alpha - \beta) \tag{B.55}$$

$$\sin(\alpha + \beta)\sin(\alpha - \beta) = \cos^2\beta - \cos^2\alpha = \sin^2\alpha - \sin^2\beta \qquad (\text{B.56})$$

$$\cos(\alpha + \beta)\cos(\alpha - \beta) = \cos^2\beta + \sin^2\alpha \qquad (\text{B.57})$$

## Sum of Functions

$$\sin\alpha \pm \sin\beta = 2\sin\frac{\alpha \pm \beta}{2}\cos\frac{\alpha \pm \beta}{2} \qquad (\text{B.58})$$

$$\cos\alpha + \cos\beta = 2\cos\frac{\alpha + \beta}{2}\cos\frac{\alpha - \beta}{2} \qquad (\text{B.59})$$

$$\cos\alpha - \cos\beta = -2\sin\frac{\alpha + \beta}{2}\sin\frac{\alpha - \beta}{2} \qquad (\text{B.60})$$

$$\tan\alpha \pm \tan\beta = \frac{\sin(\alpha \pm \beta)}{\cos\alpha\cos\beta} \qquad (\text{B.61})$$

$$\cot\alpha \pm \cot\beta = \frac{\sin(\beta \pm \alpha)}{\sin\alpha\sin\beta} \qquad (\text{B.62})$$

$$\frac{\sin\alpha + \sin\beta}{\sin\alpha - \sin\beta} = \frac{\tan\frac{\alpha+\beta}{2}}{\tan\frac{\alpha-+\beta}{2}} \qquad (\text{B.63})$$

$$\frac{\sin\alpha + \sin\beta}{\cos\alpha - \cos\beta} = \cot\frac{-\alpha + \beta}{2} \qquad (\text{B.64})$$

$$\frac{\sin\alpha + \sin\beta}{\cos\alpha + \cos\beta} = \tan\frac{\alpha + \beta}{2} \qquad (\text{B.65})$$

$$\frac{\sin\alpha - \sin\beta}{\cos\alpha + \cos\beta} = \tan\frac{\alpha - \beta}{2} \qquad (\text{B.66})$$

## Trigonometric Relations

$$\sin^2\alpha - \sin^2\beta = \sin(\alpha + \beta)\sin(\alpha - \beta) \qquad (\text{B.67})$$

$$\cos^2\alpha - \cos^2\beta = -\sin(\alpha + \beta)\sin(\alpha - \beta) \qquad (\text{B.68})$$

# Appendix C

# Unit Conversions

## General Conversion Formulas

$$
\begin{aligned}
\mathrm{N}^a \, \mathrm{m}^b \, \mathrm{s}^c &\approx 4.448^a \times 0.3048^b \times \mathrm{lb}^a \, \mathrm{ft}^b \, \mathrm{s}^c \\
&\approx 4.448^a \times 0.0254^b \times \mathrm{lb}^a \, \mathrm{in}^b \, \mathrm{s}^c \\
\mathrm{lb}^a \, \mathrm{ft}^b \, \mathrm{s}^c &\approx 0.2248^a \times 3.2808^b \times \mathrm{N}^a \, \mathrm{m}^b \, \mathrm{s}^c \\
\mathrm{lb}^a \, \mathrm{in}^b \, \mathrm{s}^c &\approx 0.2248^a \times 39.37^b \times \mathrm{N}^a \, \mathrm{m}^b \, \mathrm{s}^c
\end{aligned}
$$

## Conversion Factors

### Acceleration

$$1 \, \mathrm{ft/s^2} \approx 0.3048 \, \mathrm{m/s^2} \qquad 1 \, \mathrm{m/s^2} \approx 3.2808 \, \mathrm{ft/s^2}$$

### Angle

$$1 \, \mathrm{deg} \approx 0.01745 \, \mathrm{rad} \qquad 1 \, \mathrm{rad} \approx 57.307 \, \mathrm{deg}$$

### Area

$$1 \, \mathrm{in^2} \approx 6.4516 \, \mathrm{cm^2} \qquad 1 \, \mathrm{cm^2} \approx 0.155 \, \mathrm{in^2}$$
$$1 \, \mathrm{ft^2} \approx 0.09290304 \, \mathrm{m^2} \qquad 1 \, \mathrm{m^2} \approx 10.764 \, \mathrm{ft^2}$$
$$1 \, \mathrm{acre} \approx 4046.86 \, \mathrm{m^2} \qquad 1 \, \mathrm{m^2} \approx 2.471 \times 10^{-4} \, \mathrm{acre}$$
$$1 \, \mathrm{acre} \approx 0.4047 \, \mathrm{hectare} \qquad 1 \, \mathrm{hectare} \approx 2.471 \, \mathrm{acre}$$

### Damping

$$1 \, \mathrm{N\,s/m} \approx 6.85218 \times 10^{-2} \, \mathrm{lb\,s/ft} \qquad 1 \, \mathrm{lb\,s/ft} \approx 14.594 \, \mathrm{N\,s/m}$$
$$1 \, \mathrm{N\,s/m} \approx 5.71015 \times 10^{-3} \, \mathrm{lb\,s/in} \qquad 1 \, \mathrm{lb\,s/in} \approx 175.13 \, \mathrm{N\,s/m}$$

### Energy and Heat

$$1 \, \mathrm{Btu} \approx 1055.056 \, \mathrm{J} \qquad 1 \, \mathrm{J} \approx 9.4782 \times 10^{-4} \, \mathrm{Btu}$$
$$1 \, \mathrm{cal} \approx 4.1868 \, \mathrm{J} \qquad 1 \, \mathrm{J} \approx 0.23885 \, \mathrm{cal}$$
$$1 \, \mathrm{kW\,h} \approx 3600 \, \mathrm{kJ} \qquad 1 \, \mathrm{MJ} \approx 0.27778 \, \mathrm{kW\,h}$$

### Force

$$1 \, \mathrm{lb} \approx 4.448222 \, \mathrm{N} \qquad 1 \, \mathrm{N} \approx 0.22481 \, \mathrm{lb}$$

## Length

$$1\,\text{in} \approx 25.4\,\text{mm} \qquad 1\,\text{cm} \approx 0.3937\,\text{in}$$
$$1\,\text{ft} \approx 30.48\,\text{cm} \qquad 1\,\text{m} \approx 3.28084\,\text{ft}$$
$$1\,\text{mi} \approx 1.609347\,\text{km} \qquad 1\,\text{km} \approx 0.62137\,\text{mi}$$

## Mass.

$$1\,\text{lb} \approx 0.45359\,\text{kg} \qquad 1\,\text{kg} \approx 2.204623\,\text{lb}$$
$$1\,\text{slug} \approx 14.5939\,\text{kg} \qquad 1\,\text{kg} \approx 0.068522\,\text{slug}$$
$$1\,\text{slug} \approx 32.174\,\text{lb} \qquad 1\,\text{lb} \approx 0.03.1081\,\text{slug}$$

## Moment and Torque

$$1\,\text{lb\,ft} \approx 1.35582\,\text{N\,m} \qquad 1\,\text{N\,m} \approx 0.73746\,\text{lb\,ft}$$
$$1\,\text{lb\,in} \approx 8.85075\,\text{N\,m} \qquad 1\,\text{N\,m} \approx 0.11298\,\text{lb\,in}$$

## Moment of Inertia

$$1\,\text{lb\,ft}^2 \approx 0.04214\,\text{kg\,m}^2 \qquad 1\,\text{kg\,m}^2 \approx 23.73\,\text{lb\,ft}^2$$

## Power

$$1\,\text{Btu/\,h} \approx 0.2930711\,\text{W} \qquad 1\,\text{W} \approx 3.4121\,\text{Btu/\,h}$$
$$1\,\text{hp} \approx 745.6999\,\text{W} \qquad 1\,\text{kW} \approx 1.341\,\text{hp}$$
$$1\,\text{hp} \approx 550\,\text{lb\,ft/\,s} \qquad 1\,\text{lb\,ft/\,s} \approx 1.8182 \times 10^{-3}\,\text{hp}$$
$$1\,\text{lb\,ft/\,h} \approx 3.76616 \times 10^{-4}\,\text{W} \qquad 1\,\text{W} \approx 2655.2\,\text{lb\,ft/\,h}$$
$$1\,\text{lb\,ft/\,min} \approx 2.2597 \times 10^{-2}\,\text{W} \qquad 1\,\text{W} \approx 44.254\,\text{lb\,ft/\,min}$$

## Pressure and Stress

$$1\,\text{lb/\,in}^2 \approx 6894.757\,\text{Pa} \qquad 1\,\text{MPa} \approx 145.04\,\text{lb/\,in}^2$$
$$1\,\text{lb/\,ft}^2 \approx 47.88\,\text{Pa} \qquad 1\,\text{Pa} \approx 2.0886 \times 10^{-2}\,\text{lb/\,ft}^2$$

## Stiffness

$$1\,\text{N/\,m} \approx 6.85218 \times 10^{-2}\,\text{lb/\,ft} \qquad 1\,\text{lb/\,ft} \approx 14.594\,\text{N/\,m}$$
$$1\,\text{N/\,m} \approx 5.71015 \times 10^{-3}\,\text{lb/\,in} \qquad 1\,\text{lb/\,in} \approx 175.13\,\text{N/\,m}$$

## Temperature

$$^\circ\text{C} = (\,^\circ\text{F} - 32)/1.8$$
$$^\circ\text{F} = 1.8\,^\circ\text{C} + 32$$

## Velocity

$$1\,\text{mi/\,h} \approx 1.60934\,\text{km/\,h} \qquad 1\,\text{km/\,h} \approx 0.62137\,\text{mi/\,h}$$
$$1\,\text{mi/\,h} \approx 0.44704\,\text{m/\,s} \qquad 1\,\text{m/\,s} \approx 2.2369\,\text{mi/\,h}$$
$$1\,\text{ft/\,s} \approx 0.3048\,\text{m/\,s} \qquad 1\,\text{m/\,s} \approx 3.2808\,\text{ft/\,s}$$
$$1\,\text{ft/\,min} \approx 5.08 \times 10^{-3}\,\text{m/\,s} \qquad 1\,\text{m/\,s} \approx 196.85\,\text{ft/\,min}$$

Volume

$$1\,\text{in}^3 \approx 16.39\,\text{cm}^3 \qquad 1\,\text{cm}^3 \approx 0.0061013\,\text{in}^3$$
$$1\,\text{ft}^3 \approx 0.02831685\,\text{m}^3 \qquad 1\,\text{m}^3 \approx 35.315\,\text{ft}^3$$
$$1\,\text{gal} \approx 3.785\,\text{l} \qquad 1\,\text{l} \approx 0.2642\,\text{gal}$$
$$1\,\text{gal} \approx 3785.41\,\text{cm}^3 \qquad 1\,\text{l} \approx 1000\,\text{cm}^3$$

# Index